CC BY

Noise Temperature in Single Injection Cylindrical Current Flow in Insulator at Low and High Injection Level of Current.

Dr. Shikha Bhardwaj Shrivas[1] , Dr. Uday Patkar[2], Dr . Uday Patil [3], Dr. Neha Shahare[4], Dr. Yogita Sinkar[5], Dr. Reshma Atole[6], Dr. Vipul Vinayak Bag[7], Dinesh Suresh Bhadane[8]

Bharti Vidyapeeth's College of Engineering , Lavale ,Pune(1,2,3,4)
SVPMCOE Malegaon (Bk) Baramati, Pune(5,6)
N K Orchid College Of Engineering And Technology Solapur (7)
Dr. D.Y. Patil Institute Of Technology Pimpari Pune-18 (8)

Abstract

The theoretical and experimental studies are made for the non planner current flow geometry to obtain the information's regarding the space charge current flow in insulators operating under single injection mode. The theoretical investigation has been made in this paper for the cylindrical current flow in an insulator operating under hot career conditions. The suitable metallic electrode is considered for the electron injection in conduction band of the insulator. The path of the injected current careers is decided by the current flow geometry. The modern concept of energy band theory of solid structure may be applied to explain clearly the free movement of the injected free electrons in the conduction band of an insulator. These free electrons interact with the presence of trapping states and space charge inside the insulator to give rise different aspect of the conduction mechanism.

The situation become more complicated due to the presence of hot career conditions inside the insulator which has short length the noise temperature develops to a considerable amount and it is spatial for the cylindrical structure. The hot electron region is considered for this purpose and the noise generated due to the fluctuations of the career velocity governs their diffusion properties under cylindrical structure. Therefore the noise and the Diffusion of hot careers in insulator operating under cylindrical current flow geometry are clearly related properties. The aim of present paper is to develop the theoretical models for the noise temperature with the help of very simple method previously available in Literature. The field dependent mobility is considered their throughout the insulator operating under hot career regime where a significant value of noise temperature is observable. The hot electron effects are observed in a very short device length under cylindrical current flow at low and high injection Label of current separately.

Keywords: Space charge limited, cylindrical structure, mobility Fluctuation, Hot carriers

Introduction

The present theoretical model is developed for the hot career effects in the complete current –voltage and noise temperature characteristics in a steady state single injection cylindrical current flow in insulator at two separate injection level of currents. The model may be developed for the electron injection as well as for hole injection separately with slight change in terminology. The noise temperature

insulator .The above boundary condition is applied to the problem to simplify the equations .The full applied voltage across the cylindrical diode is given by

$$V = \int_{r_c}^{ra} E(r)dr \quad \ldots..(6)$$

Where ra is the anode radius.

COMPLETE CURRENT –VOLTAGE CHARACTERISTIC OF INSULATOR UNDER CYLINDRICAL STRUCTURE AT HIGH FIELD

The single injection mode is considered in the present investigation it is obtained when the current is injected from a cathode by one type of carriers and collected at anode.

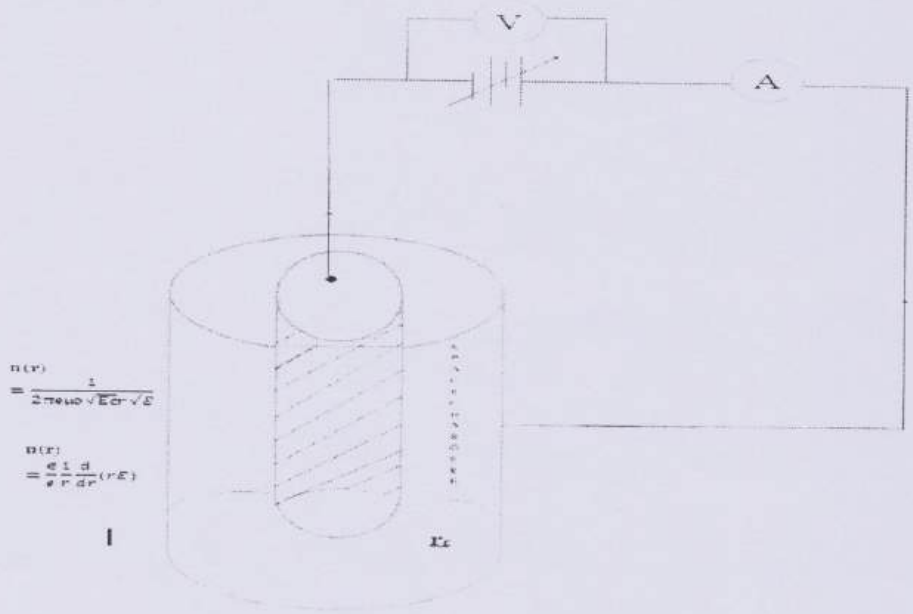
The carriers are either electrons or hole. A space charge is gradually developed inside the insulator which is known as single injection space –charge – limited current flow in the specimen. The current –voltage characteristics are strongly affected by the physical parameters of the specimen and other boundary conditions of the problem. The steady state state single injection contributes to the space –charge –limited current flow in insulator with simple structure.

The complete –voltage characteristics of the steady state single injection current flow in cylindrical structure started at the low injection level where the current is carried by the free carriers and the injected space charge is negligibly small..the experimental arrangements of the ohmic regime inside the cylindrical diode is shown in fig() .the hot carrier conditions are considered in the present problem where the mobility of the carriers is given by

$$E>E_C : \quad \mu = \mu_0 \sqrt{\frac{E_c}{E}} \quad \ldots (7)$$

Where, μ is the high Field carrier mobility, μ_0 is the constant carrier mobility at low field and E_C is the critical field strength across the cylindrical diode at which the high field effect is started. The electric field strength is assumed sufficiently higher than the critical field to gives the high field regime.

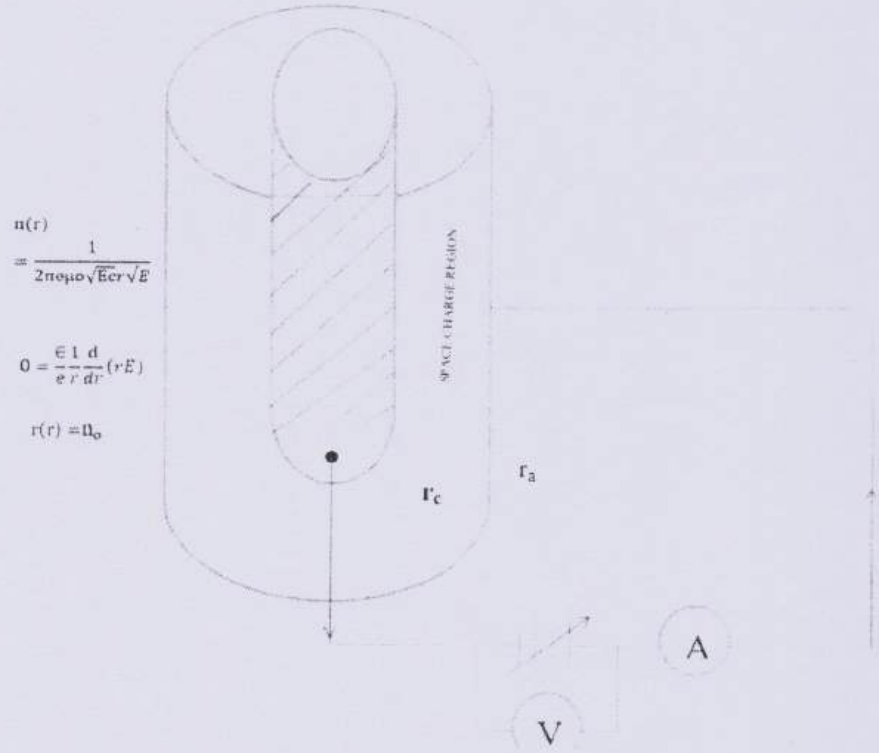
Fig 2.1



space charge regime of the cylindrical structure in which significant amount of free carriers are injected in the insulator at sufficient high injection level of currents. There is a rapid increase IN CURRENT IN SPACE charge regime with increase in the voltage because every injected carrier contributes to the space charge. The high field effect decreases the carrier mobility carrier mobility of the free carriers as evident from the equation (7) .it is now experimentally observed fact that the increase of field strength decrease the mobility above the critical field strength E_C . The effective electron temperature of the heating of electron in solid state cylindrical diode by high fields is represented by the following expression as

$$T_C = T_0\left(1 + \frac{\beta E^2}{{E_C}^2}\right) \quad \ldots.(16)$$

Fig 2



Where T_0 is the lattice temperature ,E is the electric field strength ,E_C is a critical field strength at which high field effect is started and β is a factor that increases with the decrease in the temperature of the fabricating material.

The high field conductivity I/E is considered in the theory of noise of an insulator operating under hot electron effects .the high field conductivity generates the source of noise at the effective electron temperatue T_C and the mean square noise voltage in the open circuit device for a small section Δr inside the insulator in a frequency interval Δf is given by

$$\Delta V^2 = 4k\, T_C\, \Delta R \Delta f = \frac{4k\, T_C\, \Delta r \Delta f}{(I/E)} \quad ..(17)$$

noise e.m.f for a small section or inside the specimen at high field operating under high injection level in a frequency interval Δf is given by

$$\Delta V^2 = 4k\,T_C\,\Delta R\Delta f = \frac{4k\,T_C\,\Delta r\Delta f}{(I/E)} \quad \text{....(28)}$$

here the effective electron temperature is T_C ,I is the total current ,ΔR is the high field resistance of the small section ,Δr at high injection level of current.The equation (18) gives the mean square open circuit total noise voltage across the space –charge-limited cylindrical current flow in insulators as

$$\overline{V_a^{\,2}} = \frac{4K\Delta F}{I}\int_{r_c}^{r_a} T_C E\, dr \quad \text{...(29)}$$

From equation (18) and (19) ,the expression for the mean square noise voltage for the space charge regime is given by

$$\overline{V_a^{\,2}} = \frac{4KT_0\Delta F}{I}\int_{r_c}^{r_a} E\left(1+\frac{\beta E^2}{E_C^{\,2}}\right) dr \quad \text{...(30)}$$

The expression for the electric field strength for high field regime is substituted from the equation (15) and (20),the mean square voltage of pure space charge regime is obtained as

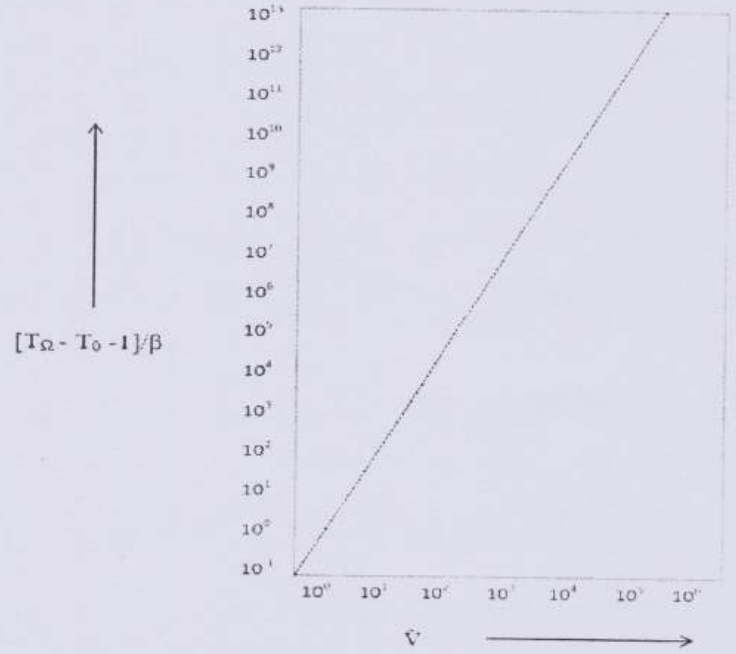
$$\overline{V_a^{\,2}} = \frac{4KT_0\Delta f\, V}{I}\left[1+\frac{\beta V^2}{E_C^{\,2}\, r_a^{\,2}}\right] \quad \text{...(31)}$$

The equation (20) and (21) are compared to give the analytical expression for the noise temperature of a cylindrical diode in hot carrier regime at high injection level as

$$\frac{T_a}{T_0} = 1+\frac{\beta V^2}{E_C^{\,2}\, r_a^{\,2}} \quad \text{...(32)}$$

Which shows that the noise temperature of the space charge regime depends on the applied voltage across the insulator.the fig is drawn on logM-log scale with the help of the equation (22) where the factor /β is varied with the normalized voltage

$$V = (V/\ E_C\ r_a) \quad \text{...(33)}$$



conductivity fluctuations. The equivalent noise temperature may be experimentally measured for the cylindrical structure as described. The practical applications of hot electron system are very useful to develop a new class of solid state electronics devices which may open further various important areas of research field for the scientific and technological development.

References

1. Aas,E.J. An Investigation of Numerical method for Hot carrier problems ELAB Report TE-192,Univ.of Trondheim Norwegian Inst.of Teach., Nov(1972).
2. Bass ,F.G.,Phys.Rev.,B51,7640(1995).
3. Bougalis,D.N.,Noise in SCL Solid State Devices ,Univ.of Minnesota,Minneapolis,U.S.A..,Thesis(1970),121 PP.
4. Burgess ,R.E.(Ed) ,Fluctuation Phenomena in solids ,Academic Press ,New York (1965).
5. Comallonga ,T.,Thesis ,Montpellier ,March(1970).
6. Conwell ,E.M. ,Solid State Physics ,Suppl.9,Academic Press,New York (1967).
7. Dahiya,R.P.and Mathur ,V.k., J. Phys .D.7 1512 (1974).
8. Dahiya,R.P.and Mathur ,V.k., J. Appl. Phys .D.47 3240 (1976).
9. Denda,S., and NICILET, M.A., J. Appl. Phys. 43 4606 (1972).
10 . Devreese ,j.t., And Van Doren,V.E.,(Eds) Linear and Non-Linear Electrron Transport in solids, Plenum Press, New York,PP,491-514 (1976).

Scopus

Sources

ISSN Enter ISSN or ISSNs Find sources

ISSN: 2368-7487 ×

i Improved Citescore

We have updated the CiteScore methodology to ensure a more robust, stable and comprehensive metric which provides an indication of research impact, earlier. The updated methodology will be applied to the calculation of CiteScore, as well as retroactively for all previous CiteScore years (ie. 2018, 2017, 2016...). The previous CiteScore values have been removed and are no longer available.

View CiteScore methodology. >

Filter refine list

Apply Clear filters

Display options

- Display only Open Access journals

Counts for 4-year timeframe

- No minimum selected
- Minimum citations
- Minimum documents

Citescore highest quartile

- Show only titles in top 10 percent
- 1st quartile
- 2nd quartile
- 3rd quartile
- 4th quartile

Source type

- Journals
- Book Series
- Conference Proceedings
- Trade Publications

Apply Clear filters

1 result

Download Scopus Source List | Learn more about Scopus Source List

All | Export to Excel | Save to source list

View metrics for year: 2021

	Source title	CiteScore	Highest percentile	Citations 2018-21	Documents 2018-21	% Cited
1	Journal of Survey in Fisheries Sciences	1.0	38% 11/17 Veterinary (miscellaneous)	79	81	46

Top of page

Scopus

Source details

Journal of Survey in Fisheries Sciences

Scopus coverage years: from 2018 to Present

Publisher: Green Wave Publishing of Canada

E-ISSN: 2368-7487

Subject area: Veterinary: Veterinary (miscellaneous) | Environmental Science: Ecology | Agricultural and Biological Sciences: Ecology, Evolution, Behavior and Systematics | Agricultural and Biological Sciences: Aquatic Science

Source type: Journal

CiteScore 2021
1.0

SJR 2021
0.246

SNIP 2021
0.593

View all documents > | Set document alert | Save to source list | Source Homepage

CiteScore | CiteScore rank & trend | Scopus content coverage

i Improved CiteScore methodology

CiteScore 2021 counts the citations received in 2018-2021 to articles, reviews, conference papers, book chapters and data papers published in 2018-2021, and divides this by the number of publications published in 2018-2021. Learn more >

CiteScore 2021

1.0 = 79 Citations 2018 - 2021 / 81 Documents 2018 - 2021

Calculated on 05 May, 2022

CiteScoreTracker 2022

1.3 = 127 Citations to date / 100 Documents to date

Last updated on 05 March, 2023 • Updated monthly

CiteScore rank 2021

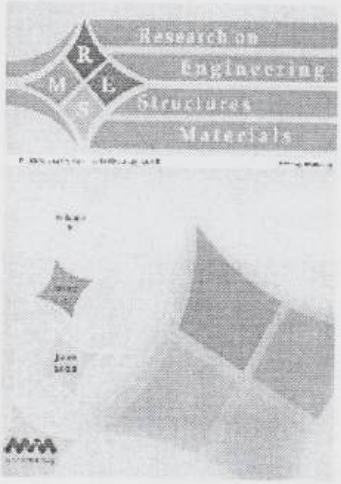
Category	Rank	Percentile
Veterinary └ Veterinary (miscellaneous)	#11/17	38th
Environmental Science └ Ecology	#323/437	26th
Agricultural and		

View CiteScore methodology > | CiteScore FAQ > | Add CiteScore to your site

Research on Engineering Structures & Materials

journal homepage: http://www.jresm.org

Research Group



A Review of fatigue behaviour of resistance spot welds

Amruta Pasarkara, Atish Maneb, Nilesh Singhc, Avinash Datarkard, Nilesh Raut

Online Publication Date: 25 Dec 2022
URL: http://www.jresm.org/archive/resm2022.509me0824tn.html
DOI: http://dx.doi.org/10.17515/resm2022.509me0824tn

Journal Abbreviation: *Res. Eng. Struct. Mater.*

To cite this article

Pasarkara A, Maneb A, Singhc N, DatarkardmA, Raut N. A Review of fatigue behaviour of resistance spot welds. *Res. Eng. Struct. Mater.*, 2023; 9(1): 181-194.

Disclaimer

All the opinions and statements expressed in the papers are on the responsibility of author(s) and are not to be regarded as those of the journal of Research on Engineering Structures and Materials (RESM) organization or related parties. The publishers make no warranty, explicit or implied, or make any representation with respect to the contents of any article will be complete or accurate or up to date. The accuracy of any instructions, equations, or other information should be independently verified. The publisher and related parties shall not be liable for any loss, actions, claims, proceedings, demand or costs or damages whatsoever or howsoever caused arising directly or indirectly in connection with use of the information given in the journal or related means.

Published articles are freely available to users under the terms of Creative Commons Attribution - NonCommercial 4.0 International Public License, as currently displayed at here (the "CC BY - NC").

Research on Engineering Structures & Materials
journal homepage: http://www.jresm.org
MIM Research Group

Technical Note

A Review of fatigue behaviour of resistance spot welds

Amruta Pasarkar[a*], Atish Mane[b], Nilesh Singh[c], Avinash Datarkar[d], Nilesh Raut[e]

Bharati Vidyapeeth's College of Engineering, Lavale, Pune

Article Info

Article history:

Received 24 Aug 2022
Revised 13 Nov 2022
Accepted 20 Dec 2022

Keywords:

Resistance spot welding; Sheet thickness; Material properties; Nugget size; Fatigue; Crack propagation

Abstract

Resistance spot welding (RSW) is a solid-state joining process in which sheet metal parts are joined by applying pressure and heat to the faying surfaces. Spot weld failure can cause severe mishap of any mechanical assemblies and can lead to severe damage. Therefore, robust design of spot welds for proper operation is essential. The cyclic stresses occurring on the spot welds in most of the applications result in fatigue failure of welds and decrease their performance efficiency and fatigue strength. This leads to failure of components at very low loads. Thus, it is essential to design the spot welds for fatigue loading conditions for all structures. This study presents the effects of critical factors affecting the fatigue performance of spot welds. The focus is on parameters, namely, sheet thickness, residual stresses, material properties and nugget size of spot welds.

© 2023 MIM Research Group. All rights reserved.

1. Introduction

Resistance spot welding (RSW) is a widely used joining process in automobiles, aerospace, trucks, furniture, nuclear industries etc. to weld sheet metal components [1,2]. Particularly, 90% of the automobile parts are assembled by resistance spot welding process [3]. Spot welding is done in the automotive industry to transfer structural loads during crash. Around 4000 spot welds are performed in a vehicle for higher safety during a crash [4]. The spot-welding process involves thermal, mechanical and electrical interactions along the faying surfaces. Therefore, it is a complicated process and requires many design parameters like weld current, weld time, weld pressure etc. to be considered [5]. This process is also called thermo-mechanical-electrical coupled process. The ease of automation and robotization is the key feature of RSW process.

RSW is a solid-state joining process where the sheet metal parts are joined by heating at the faying surfaces. The resistance to current at the contact surfaces increases the heat and temperature rises. The metal surfaces begin to melt and localized nuggets are formed at the contact between two surfaces. Pressure is also applied on the copper electrodes to ensure proper contact between the surfaces. The current is then stopped and the pressure continues to be acting on the surfaces, which ensures cooling and solidification of the metal s. Spot weld failure can cause severe mishap of any mechanical assembly and can lead to severe damage. Therefore, robust design of spot welds for proper operation is essential.

There is a need to first understand the reasons as to complexity of spot welds and its factors for failure. There are three different zones formed at the weld nuggets, which have different microstructures. The fusion zone (FZ) shows cast structure with columnar grains. It determines the geometry of weld nugget and hence the strength of the spot weld. The heat-affected zone (HAZ), does not melt but undergoes microstructural deviations during

*Corresponding author: amruta.pasarkar@bharatividyapeeth.edu
[a] orcid.org/0000-0002-8530-2280; [b] orcid.org/0000-0002-4549-8004; [c] orcid.org/0000-0002-8700-3735;
[d] orcid.org/0000-0001-5298-3684; [e] orcid.org/0000-0002-5873-6526
DOI: http://dx.doi.org/10.17515/resm2022.509me0824tn
Res. Eng. Struct. Mat. Vol. 9 Iss. 1 (2023) 181-194

heating. This zone can also affect the quality of spot welds. Base metal (BM) does not undergo any microstructural changes [6–8]. It is required to analyze the sensitization and strain hardening characteristics of all three zones for predicting the failure modes of spot welds. The failure analysis thus becomes more complicated. The failure also depends on the weld geometry and stress acting at the weld [9–12]. The difference in the strength of the zones causes strain concentration at the least strength zone and thus, to understand the mechanism of nugget failure, the strain properties of all zones should be studied [13]. The application of pressure on the electrode leads to the formation of an indent on the nuggets, which causes stress concentration at the weld. This causes reduction in the load-bearing capacity of the spot weld. This failure mode should also be considered during the design process [14].

Vehicle parts experience several vibrations due to rough roads, different driving conditions and road accidents. This causes fatigue loading on the spot welded parts and hence can cause fatigue failure of the spot welds [15–18]. The cyclic loading occurring on the vehicle reduces the performance efficiency of the spot welds and the tensile strength decreases considerably with the formation of fatigue crack. This leads to failure of the vehicle part at very low loads. Thus, it is essential to design the spot welds for fatigue loading conditions for all applications [19]. This critical review presents an understanding of the factors that affect the fatigue performance of spot welds. The focus is placed on parameters like sheet thickness, material properties and nugget size of spot welds.

2. Fatigue Failure Modes for Resistance Spot Welds

Resistance spot welds can fail due to many factors such as mechanical properties of the base material, welding time, welding force, sheet thickness, weld diameter. Interfacial (IF) mode, plug failure and pull-out failure (PF) are the three modes of spot welds failure. Crack propagation in IF mode is through FZ and it has a very high effect on the crashworthiness of the vehicle. In the PF mode, the weld nugget delaminates from one or more sheets and crack propagates from the base metal or heat affected zone. This depends on the sheet material and the geometry of the weld nuggets. Both these failure modes largely affect the energy absorption capacity and load-bearing capacity of spot welds. Due to higher energy absorption in the PF mode, spot welds are preferably designed considering the welding parameters for PF mode [20–23]. Fig. 1 shows the three modes of spot weld fatigue fracture. The PF mode in fatigue is divided into three stages: first, the initiation of fatigue crack, second, crack propagation through sheet thickness and third, crack propagation through sheet width [24]. A detail review of the effects of material properties, sheet thickness and nugget size on the fatigue behavior of spot welds is discussed in this paper.

3. Fatigue Performance of Resistance Spot Welds

3.1 Effect of Nugget Size

A study on the effect of different nugget diameters on the fatigue life of spot welds was done by [26]. Spot welding was performed to join two sheets of galvanized steel and austenitic stainless steel. The welding current was varied to get three different nugget diameters of 4 mm, 5 mm and 6 mm. Fatigue tests were performed on the specimens to get the S-N curve. The tests revealed similar fatigue life for all nugget diameters showing a little higher fatigue life for 6-mm nugget diameter.



(a) (b) (c)

Fig. 1 Fatigue failure modes (a) Pull out failure (b) plug failure (c) Interfacial failure [25]

Banerjee et al. [27] considered two specimens P1 and P2 with different RSW current and weld time parameters. Nuggets formed for P1 samples showed diameter of 5.4 mm and P2 samples predicted diameter of 4.42 mm. The samples were tested for fatigue failure at load range of 7.3 to 6.2 kN. The results predicted that even at larger loads, P1 samples exhibit higher fatigue life as compared to P2. Samples of P2 specimen showed interfacial failure mode and P1 samples showed pull-out failure mode.

Kato et al. [28] performed spot welding on three different material steel sheets of varying tensile strength. The welding parameters were controlled to get two different weld diameters of 5 mm and 3.8 mm. Spot welds with lower nugget diameters showed lower fatigue strength. For 5-mm nugget size, the fatigue strength was almost similar for all the three materials. This is due to dominant fatigue crack propagation life. For nugget size of 3.8 mm, the materials with higher tensile strength showed lower fatigue life.

Heewon Cho et al.[25] studied the fatigue and fracture behavior of Transformation Induced Plasticity Steel (TRIP) steels spot welds using two different electrodes of diameters 8mm and 10 mm. The electrodes with larger diameters gave larger nugget size. The fatigue tests showed that the fatigue life is more for larger nugget size. Fatigue fracture showed pull out, HAZ and plug fracture modes. For both the nugget sizes, the crack initiation occurred at the interface of HAZ region. In pull out fracture mode, the crack propagation occurred around the nugget whereas in the HAZ fracture mode, the crack propagated through the thickness of the sheets. However, the plug fracture occurs having characteristics of both HAZ and pull-out fracture. Fig. 2 shows the S-N curve for fatigue fracture of spot welds of TRIP steels for different electrode diameter.

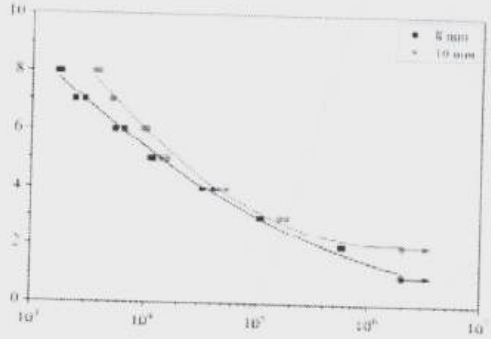


Fig. 2 S-N curve for fatigue fracture of spot welds of TRIP steels for different electrode diameter [25]

A recent study 29] investigated the fatigue life of two sheets of interstitial free steel and high strength niobium micro alloyed steel joined by resistance spot welds. Welding was performed with welding current of 7 kA and 9 kA and an electrode force of 2 kN. The nugget size formed varied due to the different welding currents. Fatigue strength for smaller nugget diameters was found to be high than the larger nugget diameters. This was due to the presence of compressive residual stress in the HAZ and higher micro hardness. The fatigue crack was intergranular, which initiated from interface of HAZ and interstitial free steel side base material.

A study of Akbulut [30] also predicted the influence of nugget size and sheet thickness on the fatigue life of spot welds. Tensile shear specimens of high strength low carbon steel sheets were used for the analysis. Strain-based approach using Coffin Mansion and Morrows mean stress equation was modeled for the specimen analysis. The results show that fatigue life is higher for higher thicknesses because of large elastic and plastic strains. Also, for fatigue life was more for specimens with larger nugget diameter.

Farrahi et al. [31] simulated a finite element model to determine the fatigue damage characteristics of a spotweld on a vehicle body. The results from the FEA model and experimental results were similar. The results showed that the spot welds with small diameters failed in larger number. Approximately 125 spot welds of diameter 2 mm failed due to fatigue. Likewise, spot welds of diameter 4 mm, 6 mm and 8 mm failed in lesser numbers. The comparatively lesser number of spotwelds with 8 mm in diameter failed in fatigue. This can be because the nugget size affects the stiffness of spot welds and thus, the stress concentration at the weld. Thus, the nugget size should be carefully designed to avoid the fatigue failure. Fig. 3 explains the overview of effect of nugget size on fatigue life.

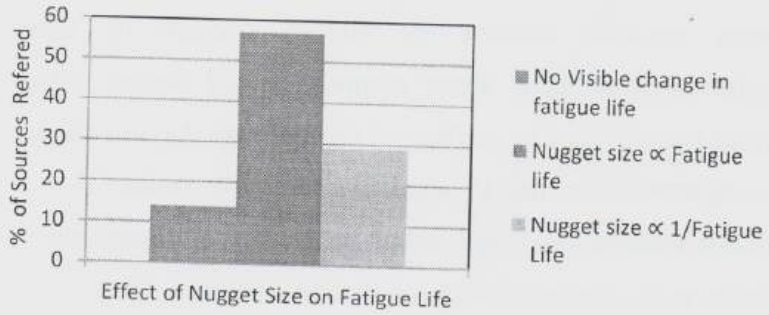


Fig. 3 Overview of effect of nugget size on fatigue life.

3.2 Effects of Sheet Parameters (Geometry/Material)

Bae and Sohn[32] discusses the effect of residual stress, thickness, width and joining the angle of sheet on fatigue life of spot-welds. Fatigue testing was performed for the tensile mode at frequency of 25Hz and stress ratio 0. Variation in fatigue life for different thicknesses is not much significant. However, for smaller loads, the fatigue life increases with an increase in thickness as higher thickness will have higher bending rigidity. Fatigue life decreases as the joint angle increases. However, the effect of sheet width on fatigue life is unpredictable. To consider the effect of residual stress, goodman equation was used to describe a fatigue life equation. It was observed that the there is a significant decrease in fatigue life considering the residual stress at the weld nuggets. Thus, it is essential to consider the residual stress while predicting the fatigue life.

Vural et al. [26] performed fatigue tests on spot welds used to join two similar sheets of austenitic stainless steel and dissimilar sheets of galvanized steel and austenitic stainless steel. Fatigue test results reveal that the spot welds on similar sheets have higher endurance strength than that of dissimilar sheets. This is due to the different expansion properties of different materials. The nugget formed is not symmetrical in the case of dissimilar sheets and thus the fatigue life is lower. Xin Long and Khanna [33] also predicts the fatigue strength of different high strength steel materials. The author mentions that there was no significant change in the fatigue strength of different material spot welds. Fatigue strength depends on loading conditions on spot weld and stress concentration at the weld nugget.

Research shows that with an increase in sheet thickness, the fatigue life decreases. The author modeled the Paris law for determining the effect of sheet thickness on fatigue life of spot weld [34]. In a work of Rahman [35] ,the author considered two specimens of sheet thickness of 1.2 and 0.2 mm for fatigue testing of spot welds. The sheet with 1.2-mm thickness showed larger fatigue life than the other sheet.

Xue, et al. [36] performed fatigue tests to find out the fatigue strength of spot welded dissimilar sheets. AA5754 sheet and high-strength low-alloy (HSLA) steel sheet were welded together with spot welds. The fatigue tests revealed that the fatigue strength of such dissimilar configuration was more than AA5754 welded to itself. Finite element simulation was conducted which enhanced that the larger notch root angle at the weld nugget gives a higher fatigue life as the maximum principal strain is reduced effectively. Fig. 4 explains the overview of effect of sheet material on fatigue life.

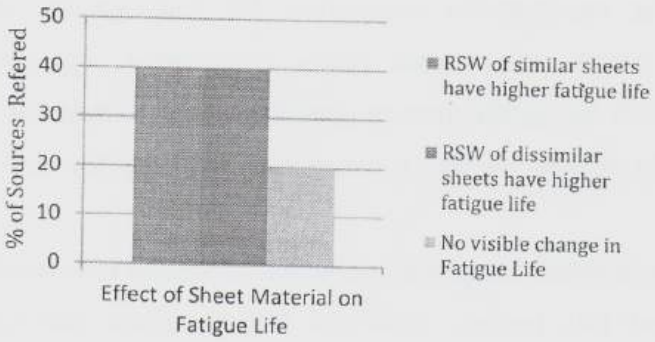


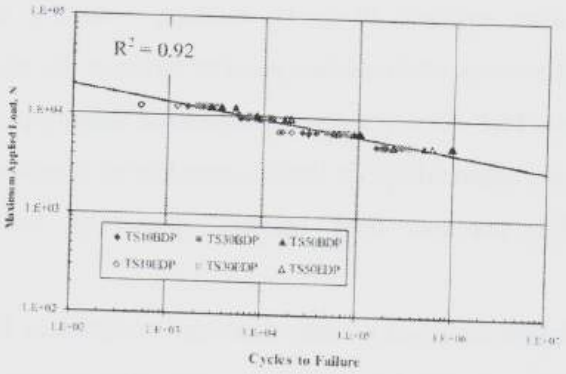
Fig. 4 Overview of effect of sheet material on fatigue life

3.3 Effects of RSW Parameters

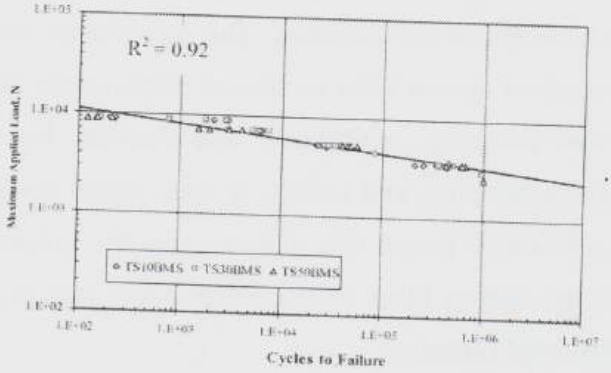
Kang et al. [37] studied the fatigue performance of three sheets of dual phase 600 and mild steel welded separately. Two shapes of electrode tip B nose and E-nose were used for welding. Fatigue tests at a frequency of 10 Hz and stress ratio of 0.01 were performed for both the specimens. Tests were also performed for different indentation levels. The results show that the shape of the electrode tip did not affect the fatigue life of DP600 steel spot welds. Also, fatigue life was not significantly affected by the different indentation levels for both the materials. Dual phase 600 material showed larger fatigue life than mild steel. Fig. 5 shows number of cycles to failure for DP600 and mild steel.

Pal [38] predicted the fatigue behavior of spotwelds used to join sheets of martensitic steels. The welding conditions were varied by changing the welding current, weld time and weld force. Thus, for every specimen, the nugget diameters obtained were different. All the

specimens showed similar fatigue characteristics at lower loads, but showed significant variation at higher loads. At the higher loads, interfacial fracture is observed, which propagates through the weld metal. However, the crack fails to propagate through the weld for lower loads. At the lower loads, plug and hole fracture mode is observed. There is transition in fracture mode at 50% loading of the yield stress.



(a)



(b)

Fig. 5 (a) No. of cycles to failure for DP600, (b) No. of cycles to failure for mild steel [37]

Duan et al. [39] predicted the fatigue life of spot welds used in tensile shear and cross tension specimens of steel. It was seen that the fatigue limit of the tensile shear specimen was more that than that of the cross-tension specimens. Fatigue cracks for both the specimens were initiated in the HAZ region at the notch tip and also at the interface boundaries of the two sheets. The fatigue crack propagation was through the thickness and then into the width of the sheet before the final fracture for tensile shear specimen. However, the crack propagation for cross tension specimen was completely through the thickness only before the final fracture.

Duan et al. [40] compared the fatigue life of spot weld on two materials high strength steel and mild steel. The high strength steel sheet had a thickness of 1.8 mm and M190 steel had a thickness of 1.2 mm. Fatigue strength was more for high strength steel spot welds due to thicker sheets and proper nugget formed which follows the standard nugget size rule. The

crack initiated at the edges of the sheet or at the interface of two sheets and propagated through the HAZ region.

Rao et al. [41] considered two dissimilar sheet stackups of wrought aluminium and interfacial steels and two similar sheets of wrought aluminium. These materials were spot welded in two configurations first, tensile shear and second coach peel. For the tensile shear configuration, the fatigue life of dissimilar stackup was higher than similar aluminium stackup and for coach peel configuration there was not much difference in the fatigue life of spot welds for both the combinations of materials. The dissimilar materials stackups showed better performance due to larger weld nuggets formed. For both configurations of tensile shear and coach peel, the crack growth was seen from the aluminium sheet.

Ordoñez et al. [42] studied the resistance of spot welds used to join dual phase steels by fatigue tests. It was found that due to the stress concentration at the weld nugget at the fusion zone, the fatigue life of weld decreases. Fatigue failure was initiated at the sheet interface. Compressive residual stresses on spot weld increases its fatigue life. A work of Fujimoto et al. [42] also increased the compressive residual stresses in spot weld lap joints of high strength steel sheets by shot blasting process. The work reported that with the compressive residual stress, the fatigue life of spot weld is improved.

Kang et al. [44] also considered the spot weld joining of aluminium and steel sheets. Three specimens were considered, Al-Al weld, Al-steel weld with positive electrode polarity and Al-steel weld with negative electrode polarity. The fatigue analysis was performed to understand the effect of nugget diameter, notch angle and polarity on the fatigue life of spot welds. The research predicted that the nuggets with negative polarity show the largest fatigue life than the nuggets with positive polarity. Also, the Al-Al sheet nuggets showed the least fatigue life. The results were more significant for tensile shear specimens than for the coach peel specimens. Al-Al sheets, had a lesser nugget size of 6.2 mm whereas the Al-Steel sheets had nugget diameter of 8.5 mm approximately. This also shows that the sheets with larger nugget diameters have larger fatigue life as it would take larger energy to fail. Another consideration showed that, as the notch root angle decreased, the tensile stresses increased. This also affects the fatigue life of spot welds. The spot welds with negative polarity have notch root angle of 33 degrees whereas, the welds with positive polarity had a notch root angle of 11 degrees. Thus, owing to increase in the tensile stresses, spot welds with lesser notch root angle failed at had lesser fatigue life.

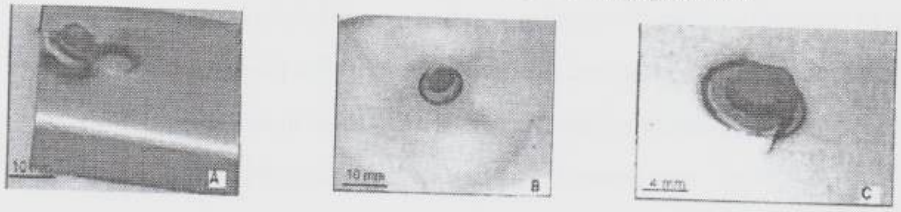
4. Fatigue Failure Characteristics

There is a lot of research where results on fatigue life of spot welds is studied. However, study on the fatigue crack initiation and propagation is very difficult as fatigue cracks occur at a very critical area of spot weld at the sheet interface. This area undergoes several microstructural changes and hence it is very difficult to understand the fatigue mechanism from the point of fracture mechanics. Also, fatigue cracks are not easily visible unless the specimen fails through the thickness. As direct observation was not possible, scientist used instruments to study the crack nucleation and propagation after fatigue loading on spot welds [45].

Hassanifard et al. [46] reported that there is higher stress concentration at the circumference of nugget and hence the crack initiation takes place from such areas. Lanciotti and Polese [45] described the fatigue crack initiation and propagation in spot welded stainless steel. The author mentioned that the crack initiation takes place at a distance of 0.93 mm from the spot weld nugget. The crack initiation took place for 10% of fatigue life. Another research [47] considered the use of half cut tensile shear specimens to study the fatigue fracture mechanism in spot weld. Steel sheets of hot rolled high strength

galvanized alloy were spot welded and tested. The spot welds developed crack of depth 0.25mm at 50% of its fatigue life. The crack was measured after the crack initiated and until the early propagation phase. A study was also done to report the effect of fatigue crack on stiffness of spot welds. The experimental results showed that the stiffness is not affected until a large crack is formed [48].

Pouranvari and Marashi [4] reported that there are various different crack propagation modes for spot welds within low cycle and high cycle region. They mentioned that within the low cycle region, the crack propagates through the base material while within the high cycle region; the crack propagates through the HAZ region. (Xu et al.) [16] found that the kinked angle for the fatigue crack was 80 º. (Newman and Dowling) [49]·also formulated an equation to calculate J integral and stress intensity factor and reported that the kinked angle for fatigue crack was 75º. The crack propagation can be predicted by calculating the stress concentration at the weld nugget area and the crack growth angle. The tensile shear and cross tension configurations can have plug type and interfacial fracture mode [50]. Fig. 6 (a), (b) shows the plug type fracture mode for tensile shear and cross tension specimen. Fig. 6 (c) shows the interfacial fracture mode for cross tension specimen.



(a) (b) (c)

Fig. 6 (a) Plug type fracture mode for tensile shear (b) For cross tension specimen. (c) Interfacial fracture mode for cross tension specimen [50]

Ma et al. [51] reported that the fatigue fracture initiates in the HAZ region showing plastic deformation at higher load levels. The crack initiates at the nugget area, penetrate through the thickness of sheet and propagate through the base metal along the normal to the load at lower load levels. Also, for intermediate load levels, the fractures initiate at the nugget area and propagate along the circumference, and fractures takes place in the base metal. The natural frequency of spot welds significantly changes after the fatigue life reaches more than 50% of the total fatigue life. At 95% of life, the cracks were visible on the surfaces of the joint [52]. First fatigue crack was seen at approximately 50% of total fatigue life of spot welds.

Cooper and Smith [53] tried observing the fatigue crack length of spot welded mild steel sheets. The authors used tensile shear specimens for the test. The potential drop method was used to estimate the crack length. The principal fatigue mechanism was macro crack propagation in the spot welds and the cracks propagation rate was constant throughout the thickness. A work of Swellam et al. [54] also predicted the fatigue crack mechanism in high strength steel spot welds and galvanized steel spot welds. Nucleation of cracks was the major fatigue mechanism for galvanized steel while crack propagation through thickness was that for high strength steel.

A work of Wang and Barkey [55] reported three different fatigue failure modes. In mode A, the crack initiates away from the spot weld nugget, propagates through the base metal and the crack growth was in a straight line. In the mode B, the crack initiation was at the HAZ region and propagated around the spot weld nugget and finally through the base sheet until fracture to partially break the weld at the nugget edge and partially at the base sheets.

Nugget is rotated before fracture. There is no nugget rotation in mode A. In the mode C, the crack is seen to propagate around the spot weld nugget and fracture is seen when half of the nugget is peeled out of the sheet. The nuggets rotated by about 90 before final fracture. Mode A occurs at high cycle tests and mode C occurs at low cycle tests. Mode B occurs between the two. Most cracks propagated in mode C and very few cracks propagated in mode A. For all modes, crack initiated at approximately 50% of the total fatigue life. Fig. 7 shows failure of spot welds due to fatigue in mode A, B, C.

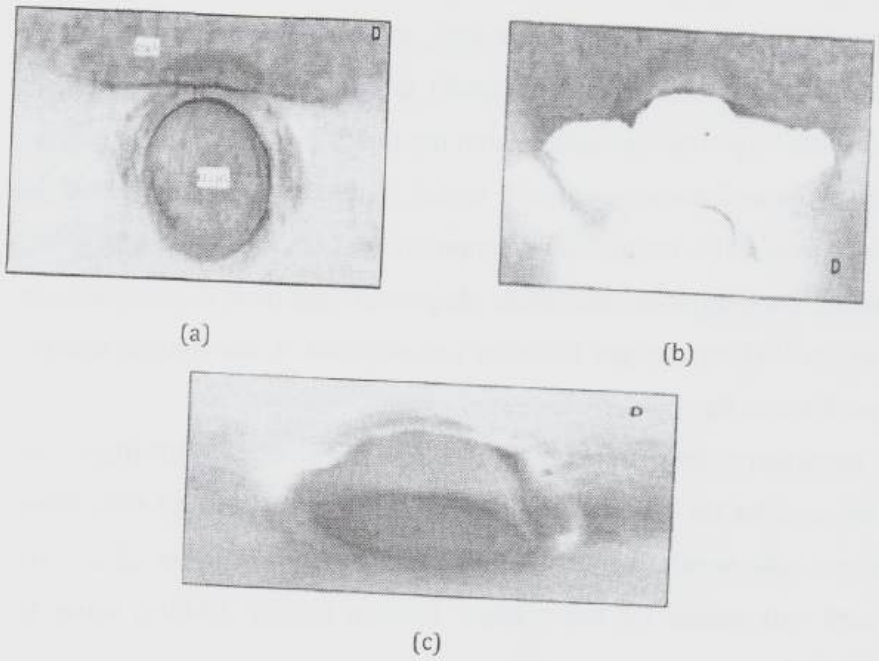


Fig. 7 Fatigue failure of spot welds in modes A, B, C [55]

The fatigue fracture mode of spot welds with positive polarity was observed to be interfacial mode. The weld with negative polarity failed with pull-out fracture mode. The specimen with a smaller notch root angle of 11 degrees exhibited a large shear stress at the notch tip and hence the fatigue crack growth was interfacial. Whereas, specimens with a larger notch root angle of 33 degrees, did not show much stress concentration at the notch tip and hence exhibited a pull-out fracture mode at the weld [44].

Mukhopadhyay et al. [56] studied the fatigue failure of DP600 resistance spot welded steels of thickness 1.4 mm .High cycle fatigue tests were conducted for tensile shear configuration at 3.8kN electrode force. The fatigue crack initiated at the HAZ and propagate through the thickness of sheets till complete fracture. The fatigue failure occurred due to stress concentration at the sheets interference and due to strength of DP600 steel.

Table 1. Summary of the effects of different welding factors on fatigue life of spot welds

	Factors	Effect on fatigue life of spot weld
[27], [28], [25], [30]	Nugget size	Larger nugget sizes exhibited a higher fatigue life.
[29]	Nugget size	Fatigue strength for smaller nugget diameters was found to be higher.
[31]	Nugget size	The spot welds with least diameter failed due to fatigue in large numbers
[26]	Sheet material Nugget size	Spot welds used for joining similar sheets have a higher fatigue limit than that of dissimilar sheets. Similar fatigue life for all nugget sizes.
[33]	Sheet material	Different materials do not significantly affect the fatigue strength of spot weld
[34]	Sheet Thickness	With an increase in sheet thickness, the fatigue life decreases
[32]	Sheet thickness Joint angle Residual Stress Sheet width	Fatigue life increases with an increase in thickness. Fatigue life decreases as the joint angle increases. A significant decrease in fatigue life considering the residual stress at the weld nuggets. The effect of sheet width on fatigue life is not predictable.
[35], [40]	Sheet Thickness	The increase in sheet thickness, the fatigue life increases
[36]	Sheet Material Notch root angle	Fatigue strength of such dissimilar configuration of AA5754 sheet and high-strength low-alloy (HSLA) steel was more . Larger notch root angle is beneficial to achieve longer fatigue life .
[37]	Electrode Tip Indentation levels Sheet material	The shape of the electrode tip did not affect the fatigue life of spot weld Not significantly affected by the different indentation levels for both the materials Dual phase 600 material showed larger fatigue life than mild steel.
[38]	Weld Current Weld Time	All the specimens showed similar fatigue characteristics at lower loads but showed a significant variation at higher loads
[39]	Tensile shear configuration Cross Tension configuration	Fatigue limit for tensile shear specimen was more that than the cross-tension specimen.
[42][43]	Compressive residual stress	Fatigue life improves with induced compressive residual stress in spot welds.
[41]	Sheet material	Fatigue life of dissimilar stackup was higher than similar aluminium stackup.
[44]	Nugget diameter Notch angle Polarity	Sheets with larger nugget diameters have larger fatigue life as it would take larger energy to fail As the notch root angle decrease, fatigue life decreases The nuggets with negative polarity showed largest fatigue life than the nuggets with positive polarity

5. Conclusion

Resistance spot welding is a solid-state joining process wherein sheet metal parts are joined by heating at the faying surfaces. It is a complex thermo-mechanical-electrical coupled process. Mechanical structures that undergo extensive vibrations can cause repetitive loading on the resistance spot welds that leads to fatigue failure. Spot welds have different regions of different microstructures and hence, they are very critical to study for its fatigue failure. It is thus important to consider fatigue parameters while designing the resistance spot welding process. This review presents the study of critical factors affecting the fatigue performance of spot welds. The focus is on RSW parameters and sheet parameters. RSW parameters include weld current, weld time, residual stresses polarity while sheet parameters include sheet materials, sheet thickness and nugget size.The findings of the review are as follows:

- It is observed that with an increase in sheet thickness and nugget size, the fatigue life of spot welds increases. This is due to a decrease in the stress concentration at the nugget area.
- Spot welds used for joining sheets of dissimilar material have lesser fatigue life due to the different thermal expansion coefficients of materials.
- Fatigue life improves with increase in compressive residual stresses at the spot nuggets.
- There is no effective change in fatigue strength with change in weld current or weld time.
- Fatigue cracks occur at the sheet interference and hence it is very difficult to study the fatigue crack characteristics.
- Spot Welds with positive polarity failed in an interfacial mode while welds with negative polarity failed with pull-out fracture mode.
- Crack propagation in IF mode is through the FZ. In the pull-out mode, the weld nugget delaminates from one or more sheets and crack propagates from the base metal or heat affected zone.
- Due to higher energy absorption in the pull-out mode, spot welds are preferably designed for this fracture mode.

References

[1] Akkas N. Welding time effect on tensile-shear loading in resistance spot welding of SPA-H weathering steel sheets used in railway vehicles. Acta Phys Pol A. 2017;131(1):52–4. https://doi.org/10.12693/APhysPolA.131.52

[2] Martín Ó, De Tiedra P, San-Juan M. Combined effect of resistance spot welding and precipitation hardening on tensile shear load bearing capacity of A286 superalloy. Mater Sci Eng A. 2017;688(December 2016):309–14.https://doi.org/10.1016/j.msea.2017.02.015

[3] Li YB, Lin ZQ, Shen Q, Lai XM. Numerical analysis of transport phenomena in resistance spot welding process. J Manuf Sci Eng Trans ASME. 2011;133(3):1–8. https://doi.org/10.1115/1.4004319

[4] Pouranvari M, Marashi SPH. Critical review of automotive steels spot welding: Process, structure and properties. Sci Technol Weld Join. 2013;18(5):361–403. https://doi.org/10.1179/1362171813Y.0000000120

[5] Wan Z, Wang HP, Wang M, Carlson BE, Sigler DR. Numerical simulation of resistance spot welding of Al to zinc-coated steel with improved representation of contact interactions. Int J Heat Mass Transf. 2016;101:749–63.https://doi.org/10.1016/j.ijheatmasstransfer.2016.05.023

[6] Sun X, Stephens E V., Khaleel MA. Effects of fusion zone size and failure mode on peak load and energy absorption of advanced high strength steel spot welds under lap shear

loading conditions. Eng Fail Anal. 2008;15(4):356–67. https://doi.org/10.1016/j.engfailanal.2007.01.018
[7] Lin PC, Lin SH, Pan J. Modeling of failure near spot welds in lap-shear specimens based on a plane stress rigid inclusion analysis. Eng Fract Mech. 2006;73(15):2229–49. https://doi.org/10.1016/j.engfracmech.2006.03.017
[8] Pouranvari M, Asgari HR, Mosavizadch SM, Marashi PH, Goodarzi M. Effect of weld nugget size on overload failure mode of resistance spot welds. Sci Technol Weld Join. 2007;12(3):217–25. https://doi.org/10.1179/174329307X164409
[9] Pouranvari M. Failure mode transition in similar and dissimilar resistance spot welds of HSLA and low carbon steels. Can Metall Q. 2012;51(1):67–74. https://doi.org/10.1179/1879139511Y.0000000020
[10] Tumuluru M. Resistance spot weld performance and weld failure modes for dual phase and TRIP steels [Internet]. Failure Mechanisms of Advanced Welding Processes. Woodhead Publishing Limited; 2010. 43–64 p.https://doi.org/10.1533/9781845699765.43
[11] Yang YP, Babu SS, Orth F, Peterson W. Integrated computational model to predict mechanical behaviour of spot weld. Sci Technol Weld Join. 2008;13(3):232–9. https://doi.org/10.1179/174329308X283901
[12] Yang YP, Gould J, Peterson W, Orth F, Zelenak P, Al-Fakir W. Development of spot weld failure parameters for full vehicle crash modelling. Sci Technol Weld Join. 2013;18(3):222–31.https://doi.org/10.1179/1362171812Y.0000000082
[13] Radakovic DJ, Tumuluru M. Predicting resistance spot weld failure modes in shear tension tests of advanced high-strength automotive steels. Weld J (Miami, Fla). 2008;87(4):96–105.
[14] Pouranvari M, Abedi A, Marashi P, Goodarzi M. Effect of expulsion on peak load and energy absorption of low carbon steel resistance spot welds. Sci Technol Weld Join. 2008;13(1):39–43. https://doi.org/10.1179/174329307X249342
[15] Long X, Khanna SK. Fatigue performance of spot welded and weld bonded advanced high strength steel sheets. Sci Technol Weld Join. 2008;13(3):241–7. https://doi.org/10.1179/174329307X249379
[16] Xu J, Zhang YS, Xinmin L, Chen GL. Experimental investigation of fatigue performance of spot welded dual phase sheet steels. Sci Technol Weld Join. 2008;13(8):726–31. https://doi.org/10.1179/174329307X236841
[17] Daneshpour S, Riekehr S, Koçak M, Gerritsen CHJ. Mechanical and fatigue behaviour of laser and resistance spot welds in advanced high strength steels. Sci Technol Weld Join. 2009;14(1):20–5. https://doi.org/10.1179/136217108X336298
[18] Gaul H, Weber G, Rethmeier M. Influence of HAZ cracks on fatigue resistance of resistance spot welded joints made of advanced high strength steels. Sci Technol Weld Join. 2011;16(5):440–5. https://doi.org/10.1179/1362171810Y.0000000031
[19] Miller KW, Chao YJ, Martinez A, Zhu X, Liu S, Wang PC. Quasi-static and impact strength of fatigue damaged spot welds. SAE Tech Pap. 2003;(724):1–8. https://doi.org/10.4271/2003-01-0610
[20] Mahmood TR, Doos QM, Al-Mukhtar AM. Failure Mechanisms and Modeling of Spot Welded Joints in Low Carbon Mild Sheets Steel and High Strength Low Alloy Steel. Procedia Struct Integr . 2018;9:71–85https://doi.org/10.1016/j.prostr.2018.06.013
[21] Sun X. Resistance spot weld failure mode and weld performance for aluminum alloys. Fail Mech Adv Weld Process. 2010;24–42.https://doi.org/10.1533/9781845699765.24
[22] Pouranvari M. Influence of welding parameters on peak load and energy absorption of dissimilar resistance spot welds of DP600 and AISI 1008 steels. Can Metall Q. 2011;50(4):381–8. https://doi.org/10.1179/1879139511Y.0000000008

[23] Sun X, Stephens E V., Khaleel MA. Effects of fusion zone size and failure mode on peak load and energy absorption of advanced high-strength steel spot welds. Weld J (Miami, Fla). 2007;86(1). https://doi.org/10.4271/2006-01-0531
[24] Hilditch TB, Speer JG, Matlock DK. Effect of susceptibility to interfacial fracture on fatigue properties of spot-welded high strength sheet steel. Mater Des. 2007;28(10):2566–76. https://doi.org/10.1016/j.matdes.2006.10.019
[25] Heewon Cho , Sangwoo Nam IH, Oh JH, Kang M, and Young-Min Kim. Fatigue Behaviors of Resistance Spot Welds for 980 MPa Grade TRIP Steel. Metals (Basel). 2019
[26] Vural M, Akkuş A, Eryürek B. Effect of welding nugget diameter on the fatigue strength of the resistance spot welded joints of different steel sheets. J Mater Process Technol. 2006;176(1–3):127–32. https://doi.org/10.1016/j.jmatprotec.2006.02.026
[27] Banerjee P, Sarkar R, Pal TK, Shome M. Journal of Materials Processing Technology Effect of nugget size and notch geometry on the high cycle fatigue performance of resistance spot welded DP590 steel sheets. J Mater Process Tech .2016;238:226–43.https://doi.org/10.1016/j.jmatprotec.2016.07.023
[28] Kato Y, Kakiuchi T, Okita Y, Matsuda H, Ikeda R, Tagawa T. Fatigue behavior of resistance spot welded high strength steel sheets with different nugget sizes. 8th TSME Int Conf Mech Eng. 2017;(December):1219–23.https://doi.org/10.1299/jsmemm.2017.OS0514
[29] Janardhan G, Kishore K, Mukhopadhyay G, Dutta K. Fatigue Properties of Resistance Spot Welded Dissimilar Interstitial-Free and High Strength Micro-Alloyed Steel Sheets. Met Mater Int . 2020;(0123456789)https://doi.org/10.1007/s12540-020-00678-w
[30] Akbulut M. Parametric investigation into fatigue life behaviour of spot welded tensile shear test samples. Proc IMechE Part C J Mech Eng Sci. 2020;1–10. https://doi.org/10.1177/0954406220966352
[31] Farrahi GH, Ahmadi A, Kasyzadeh KR. Simulation Modelling Practice and Theory Simulation of vehicle body spot weld failures due to fatigue by considering road roughness and vehicle velocity. Simul Model Pract Theory 2020;105(August):102168 https://doi.org/10.1016/j.simpat.2020.102168
[32] D. H. BAE, I. S. SOHN AJKH. Assessing the Effects of Residual Stresses on the Fatigue Strength of Spot Welds. Weld J. 2003;(January).
[33] Long X, Khanna SK. Fatigue properties and failure characterization of spot welded high strength steel sheet. Int Journal of Fatigue. 2007;29:879–86. https://doi.org/10.1016/j.ijfatigue.2006.08.003
[34] Zhang Y, Taylor D. Sheet thickness effect of spot welds based on crack propagation. Eng Fract Mech. 2000;67:55–63. https://doi.org/10.1016/S0013-7944(00)00029-1
[35] Rahman. Effects of Spot Diameter and Sheets Thickness on Fatigue Life of Spot Welded Structure based on FEA Approach. Am J Appl Sci. 2009;6(1):137–42. https://doi.org/10.3844/ajassp.2009.137.142
[36] Shi L, Xue J, Kang J, Haselhuhn AS, Carlson BE. Effect of specimen configuration and notch root angle on fatigue behavior of novel dissimilar resistance spot welds of AA5754 to HSLA steel. Procedia Struct Integr. 2021;37(C):351–8. https://doi.org/10.1016/j.prostr.2022.01.095
[37] Kang H, Accorsi I, Patel B, Pakalnins E. Fatigue performance of resistance spot welds in three sheet stack-ups. Procedia Eng .2010;2(1):129–38. https://doi.org/10.1016/j.proeng.2010.03.014
[38] T. K. PAL KC. Resistance spot weldability and high cycle fatigue behaviour of martensitic (M190) steel sheet. Fatigue Fract Eng Mater Struct. 2010;(June):46–52. https://doi.org/10.1111/j.1460-2695.2010.01489.x
[39] Wang B, Duan QQ, Yao G, Pang JC, Li XW, Wang L, et al. Investigation on fatigue fracture behaviors of spot welded Q & P980 steel. Int J Fatigue. 2014. https://doi.org/10.1016/j.ijfatigue.2014.03.004

[40] Wang B, Duan QQ, Yao G, Pang JC, Zhang ZF, Wang L, et al. Fatigue fracture behaviour of spot welded B1500HS steel under tensile- shear load. Fatigue Fract Engng Mater Struct. 2015;(38):914–22. https://doi.org/10.1111/ffe.12289
[41] Rao HM, Kang J, Shi L, Sigler DR, Carlson BE. Effect of specimen configuration on fatigue properties of dissimilar aluminum to steel resistance spot welds. Int J Fatigue. 2018;116:13–21.https://doi.org/10.1016/j.ijfatigue.2018.06.009
[42] Ordoñez JH, Ambriz RR, García C, Plascencia G, Jaramillo D. Overloading effect on the fatigue strength in resistance spot welding joints of a DP980 steel. Int J Fatigue. 2019;121(November 2018):163–71https://doi.org/10.1016/j.ijfatigue.2018.12.026
[43] Fujimoto H, Ueda H, Ueji R, Fujii H. Improvement of fatigue properties of resistance spot welded joints in high strength steel sheets by shot blast processing. ISIJ Int. 2016;56(7):1276–84. https://doi.org/10.2355/isijinternational.ISIJINT-2016-043
[44] Shi L, Kang J, Gesing M, Chen X, Haselhuhn AS, Carlson BE. E ff ect of notch root angle on fatigue behavior of aluminum to steel resistance spot welds. Int J Fatigue. 2020;141(July):105866.https://doi.org/10.1016/j.ijfatigue.2020.105866
[45] Lanciotti A, Polese C. Fatigue crack propagation in tensile shear stainless steel spot welded specimens. Fatigue Fract Eng Mater Struct. 2008;31(1):76–84. https://doi.org/10.1111/j.1460-2695.2007.01202.x
[46] Hassanifard S, Mohtadi-Bonab MAl, Jabbari G. Investigation of fatigue crack propagation in spot-welded joints based on fracture mechanics approach. J Mater Eng Perform. 2013;22(1):245–50. https://doi.org/10.1007/s11665-012-0220-5
[47] McMahon JC, Smith GA, Lawrence F V. Fatigue Crack Initiation and Growth in Tensile-Shear Spot Weldments. In: Potter JM, McHenry HI, editors. Fatigue and Fracture Testing of Weldments . West Conshohocken, PA: ASTM International; 1990. p. 47–77. https://doi.org/10.1520/STP24090S
[48] Davidson JA. A Review of the Fatigue Properties of Spot-Welded Sheet Steels. SAE Trans . 1983 Aug 20;92:35–47.https://doi.org/10.4271/830033
[49] Newman JA, Dowling NE. A crack growth approach to life prediction of spot-welded lap joints. Fatigue Fract Eng Mater Struct. 1998;21(9):1123–32. https://doi.org/10.1046/j.1460-2695.1998.00099.x
[50] Rathbun RW, Matlock DK, Speer JG. Fatigue behavior of spot welded high-strength sheet steels. Weld J (Miami, Fla). 2003;82(8).
[51] Ma C, Chen DL, Bhole SD, Boudreau G, Lee A, Biro E. Microstructure and fracture characteristics of spot-welded DP600 steel. Mater Sci Eng A. 2008;485(1–2):334–46. https://doi.org/10.1016/j.msea.2007.08.010
[52] Shang D-G, Barkey ME, Wang Y, Lim TC. Fatigue Damage and Dynamic Natural Frequency Response of Spot-Welded Joints. SAE Trans. 2003 Aug 23;112:301–8 https://doi.org/10.4271/2003-01-0695
[53] Cooper JF, Smith RA. The measurement of fatigue cracks at spot-welds. Int J Fatigue. 1985;7(3):137–40. https://doi.org/10.1016/0142-1123(85)90023-4
[54] Swellam MH, Kurath P, Lawrence F V, "Electric-Potential-Drop Studies of Fatigue Crack Development in Tensile-Shear Spot Welds," in Advances in Fatigue Lifetime Predictive Techniques, M. R. Mitchell and R. W. Landgraf, Eds. West Conshohocken, PA: ASTM International, 1992, pp. 383-401. https://doi.org/10.1520/STP24170S
[55] Wang G, Barkey ME. Investigating the spot weld fatigue crack growth process using X-ray imaging. Weld J (Miami, Fla). 2006;85(4).
[56] Janardhan G, Mukhopadhyay G, Dutta K. Failure mechanism of resistance spot-welded DP600 steel under high cycle fatigue. Mater Today Proc. 2022;59:1666–71.. https://doi.org/10.1016/j.matpr.2022.03.332

Source details

Feedback > Compare sources >

Research on Engineering Structures and Materials

Scopus coverage years: from 2019 to Present

Publisher: MIM Research Group

ISSN: 2148-9807 E-ISSN: 2149-4088

Subject area: Engineering: Engineering (miscellaneous) Engineering: Mechanical Engineering Engineering: Mechanics of Materials Engineering: Civil and Structural Engineering

Source type: Journal

View Powered by Scopus Save to source list Source Homepage

CiteScore 2022
1.5

SJR 2022
0.191

SNIP 2022
0.403

CiteScore CiteScore rank & trend Scopus content coverage

Improved CiteScore methodology

CiteScore 2022 counts the citations received in 2019-2022 to articles, reviews, conference papers, book chapters and data papers published in 2019-2022, and divides this by the number of publications published in 2019-2022. Learn more >

CiteScore 2022

1.5 = 231 Citations 2019 - 2022 / 158 Documents 2019 - 2022

Calculated on 05 May, 2023

CiteScoreTracker 2023

1.6 = 304 Citations to date / 187 Documents to date

Last updated on 05 December, 2023 • Updated monthly

CiteScore rank 2022

Category	Rank	Percentile
Engineering — Engineering (miscellaneous)	#94/151	38th
Engineering — Mechanical Engineering	#436/631	30th

A Study Paper: NCPR Reducing Path-Discovery overload in MobileAdhocNetworks(MANET's)

Prof.Ajit R.Patil[1], Prof.Kamlesh V Patil[2], Prof.Sonal M Patil[3], Prof.Parinita J Chate[4], Prof.Pramod G Rahate[5]
[1]Assistant Professor, Bharati Vidyapeeth's College of Engineering Lavale, Pune
[2]Assistant Professor, Bharati Vidyapeeth's College of Engineering For Women, Pune
[3]Assistant Professor, Bharati Vidyapeeth's College of Engineering For Women, Pune
[4]Assistant Professor, Bharati Vidyapeeth's College of Engineering Lavale, Pune
[5]Assistant Professor, Bharati Vidyapeeth's College of Engineering Lavale, Pune
[1]patilajit667@gmail.com,[2]kambpatil@gmail.com, [3]sonalpatil1303@gmail.com, [4]parinitachate@gmail.com, [5]pramodgrahate@gmail.com

Abstract—
In this research manuscript We propose improved NCPR protocol with security mechanism again attack. less broadca traffic than flood broadcast method minimizing congestion and collision with maximum data packet delivery the schem stands in with high density network which is main performance parameter. Due to soaring mobility of nodes in MANET's there exist recurrent connection breakages which direct to recurrent path crash and route Findings. The overhead of path discovery can not be deserted. In a route discovery, broadcasting is a original and successful data distributio method, where a movable node blindly rebroadcasts the first established route appeal packets unless it hasa route to th target, and thus it cause the broadcast tempest difficulty. In this Manuscript we propose a neighbor coverage- base probabilistic rebroadcast protocol (NCPR0 for reducing routing overhead in MANETs. In arrange to successfully explo the neighbor coverage knowledge, we recommend a novel rebroadcast delay to resolve the rebroadcast categorize, an then we can gain the more exact supplementary coverage ratio by sensing neighbor coverage knowledge. We also classif aconnectivity factor to provide the node density adaptation. By combining the additional coverage ratio and connectivit factor, we set a reasonable rebroadcast probability. Our approach combines the advantages of the neighbor coverag knowledge and the probabilistic mechanism, which can appreciably diminish the number of retransmissions so as t reduce the routing overhead, and can also progress the routing performance.

*Keywords—**MobileAdhoc-Networks;AODV,MANET's;Routingoverhead;neighourcoverage.***
DOI Number: 10.14704/nq.2022.20.11.NQ66332 **NeuroQuantology 2022; 20(11): 3226-3234**

I. INTRODUCTION

MANETs is assortment of cellular nodes comprising their individual mobility. The knots exclusive of a permanent transportation can be animatedly self-controlled inside a set of connections. The major confront to employ MANETs is to devise direction- finding practice that have to boost presentation and lessen the direction-finding fixed cost. Presented direction-finding procedures, such as active spring steering i.e.(DSR) [8] and Ad hoc On-demand Distance Vector Routing (AODV)[5] executed for MANETs. These procedures are on stipulate steering procedures and amplify the scalable Value of MANETs by curtailing the direction-finding overload when a fresh direction is required [4]. Because of the mobility of knots in MANETs, there are recurrent corridor shatters causing bond malfunction and influence on path identifications, that influence to amplify the direction-finding over load of steering procedure and which pilots to draw out the container relief fraction and escalating the closing stages container holdup[5]. So,throughout direction finding diminish the direction-finding load up is a vital crisis.

In distribution procedures, if the numeral of knobsin a group amplifies which will influences on deprivation in routine? The neighbor data techniques achieve enhancement in the locale-base ones and the prospect- support ones [7]. The downsides of obtainable scheme in which we necessitate to diminish the direction-

Finding loads in path unearthing, retransmit prospect is not accessible and acknowledged path request as a respond packs except it have a direction to the objective knot which escorts to shape the screen hurricane difficulty.

The suggested technique NCPR [1] is to verify Retransmit remain in the Retransmit sort and acquire the further literal treatment share by sense national experience expertisedata. The procedure in the Retransmit hold up and Retransmit prospect is intended. The projected effort foot on NCPR which successfully enlarge the national reporting facts and compute extra correct added reporting part The retransmit probability is have an extra coverage ratio, which is the ratio of the number of nodes that should be covered by a single broadcast to The tot number of neighbors, which reproduces the network connectivity and the integer of nationals of a known knob connection.

II. LITERATURESUREVYEXAMINATION

The literature survey has been done with research track selection RT's .ten research tracks where been formulated

To generate research issues and challenges in MANET's. A tabular periodic table was formed to study literature survey. The tabular format is as shown.

Author id	Title	Abstract	Methodology	Research Scope

Broadcasting is an effective mechanism for route discovery, but the routing overhead associated with the broadcasting can be quite large, especially in high dynamic networks[9].
Ni

etal.[5]studied the broadcasting protocol analytically and experimentally, and showed that the rebroadcast is very costly and consumes too much network resource. The broadcasting incurs large routing overhead and causes many problems such as redundant retransmissions, contentions, and collisions [5].Thus, optimizing the broad-casting in route discovery is an effective solutionto improve the routing performance. Haasetal. [10] proposed a gossip-based approach, where each node forwards a packet with a probability. They showed that gossip-based approach can save up to 35 percent overhead compared to the flooding. However, when thenetwork density is high or the traffic load is heavy, the improvement of the gossip-based approach is limited [9]. Kim et al. [8] proposed a probabilistic broadcastingscheme based on coverage area and neighbor confirmation. This scheme uses the coverage areato set there broadcast probability, and uses the neighbor con formation to guarantee reachability. Peng and Lu11]proposed a neighbor knowledge scheme named Scalable Broadcast Algorithm(SBA).This scheme determines the rebroadcast of a packet according to the fact whether this rebroadcast would reach additional nodes.Abdulaietal.[12]proposed a Dynamic Probabilistic Route Discovery(DPR)scheme based on neighbor coverage. In this approach, each node determines the forwarding probability according to the number of its neighbors and the set of neighbors which Are covered by the previous broadcast. This scheme only on siders the coverage ratio by the previous node, and it does not consider the neighbors receiving the duplicate RREQpacket. Thus, there is a room off furth optimization and extension for the DPR protocol. Several robust protocols have been proposed in recent years besides the above optimization issues for broad-casting.Chenetal.[13]proposed an AODV protocol with Directional Forward Routing(AODV-DFR) which takes the directional forwarding used in geographic routing into AODV protocol. While a route breaks, this protocol can automatically find the next-hop node for packetforwarding. Keshavarz-Haddadet al.
[14] Proposed two deterministic timer- based broadcast schemes: Dynamic Reflector Broadcast (DRB)and Dynamic Connector-

Performance off looding.In our protocol, we also set a deterministic rebroadcast delay, but the goal is to makethe dissemination of neighbor knowledge much quicker.

III. SYSTEMDESIGN

Connect or Broadcast(DCCB).
They
Point edout that their schemes can achieve full reachability over an idealistic lossless MAC layer, and for the situation o node failure and mobility, their schemes robustness.
Stannetal.
[15] proposed a Robust Broadcast Propagation (RBI protocol to provide near- perfect reliability for flooding i wireless networks, and this protocol also has a goo efficiency. They presented a new perspective fc broadcasting: not to make a single broadcastmore efficier but to make a single broadcast more reliable, which mear by reducing the frequency of upper layer invoking floodir to improve the overall

eISSN 1303-5150

The designed architecture is based on AODV with core mechanism of working as in MANET's. The NCPR system is developed on optimization of AODV algorithm itself.

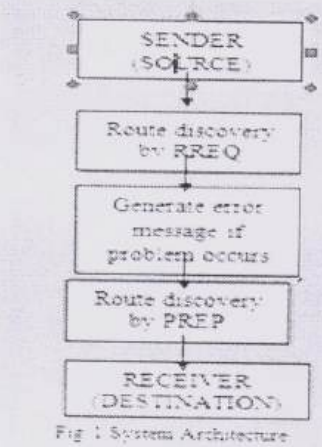


Fig 1 System Architecture

System flow 1 demonstrate the procedure surge in that the system network topological need, the knotsfrom resource to objective are spread and the direction finding is prepared by means of Retransmit hindrance beside through Retransmit prospect worn fort he proposed NCPR[4] where in the position of the knots a rechecked and direction- judgment occasion are allotted and statistics are up linked which call fors to be send to target, router is the chief element now which calculate Retransmit stop page and preserves accumulation on assault sand lastly throws information to target. If he direction- finding in stance beats the allocated nstance the Retran smit have to receive position which now is by default conduit calculates Retransmit wait and the assortment appropriate stoppage is have to and it issolution to victory of that in NCPR as the holdupoccasion influence circulation of national reporting knowledge information, therefore in estimate Retransmit holdup is planned for the complex topology. If the calculate Retransmit wait isfewer than the agreed point it specify that direction-finding point full by NCPR is fewer than allotted time.

IV. PROJECTMODULARDEVELOPMENT

- Structure of network with quantity of cellular node
- Computation of hold up for Retransmitting
- Shaping the Retransmit likelihood

A. Generation of network comprising cellular network nodes

This subsection describes the procedure to implement cellular network system holding huge number of knobs and precisely one source base station. We built in a network environment to supply communication gateway for cellular nodes. In this environment setup every knob sends in network co- ordinates that is NODE SRNO,Port ID that facilitate

transmission which generate known knobs statistics comprising of NODE SRNO ,unique IP co-ordinates and its central port ID that is adjacent to knobsi.e.nodes of implemented system network.

B. Computation of Waiting Time for retransmitting

As that of mobile nature of nodes in MANETs a huge view of path breakup is observed that put forward link loss which impact path finding and increase computation time overload

Of path finding protocols that in turn diminishes information packet destination reaching ratio which sum up to main fold higher time source to target over delay.On user need and demand path-finding procedures for searching pathways, that transmit information packet termed Route REQUEST (RREQ)in the network environment and the transmitting holds tremendous superfluous rebroadcasts of RREQ informationon envelopes and roots the broadcast hurricane crisis in which brings the significant digit of information packet clashes.

C. Finding the Rebroadcast chances of occurrences

This technical subsection I put forward the technical sum up enlightenment on my procedure scheme of rule set as minimizing the groups of rebroadcasts information enveloped that can successfully enhance the transmitting and the adjacent information procedure functioning incomparisons to local mapped ones chances of occurrences based ones in that regard I formulate adjacent neighbor winding on top of probability procedure transmission based probabilistic rebroadcast protocol. Current program module need a retransmission overhead to find the sr no of retransmission following that I would be able to compute précised divisor to dividend wide coverage In order to trace on system network functionalconnectivity and reduce the dummy retransmissions of information data envelopes.

D. Adjacent Neighbor winding up based probability on to pre transmission

In this module of Research I enlighten the novel protocols selected as base which uses HELLO data set to highlights NCPR protocol uses to gain the fellow node facts information and also requires to deem the fellow nodes catalog in the RREQ information packet. The execution in that, some procedures is worn to decrease the superfluous in the clouds of HELLO information packagesand fellow adjacent nod listing in the RREQ sachet. Todiminish the added operating cost of HELLO envelopes, I am not allowing for bulletin HELLO system scheme. Inreference to knob carriage any distributing containers can enlighten to its entire adjacent local that of its subsistence, the spreading sachets that as RREQ and

Fault in route (RRER)can cooperate a function of our HELLO envelopes. Only as soon as the instant outside from the final propagation envelope (RREQ, RRER)is supplementary as the worth of HELLO intermission and the knot requires carriage a HELLO envelope.The significa of HELLO Interval is a like to that in comparison to AODV array to cut the superfluous in the clouds of adjacent neighl knob.



eISSN 1303-5150

register in RREQs a Chet, a piece node require so observing the adjacent counter differences and maintaining hoard information of the adjacent neighbor' s knob list in the acknowledged RREQ container. We striv eto adjust the description of AODV and add superfluous a preset turf Num_Neighbors that symbolizes the exten t of fellow adjacent nodere cordin the RREQ data sachet and in following to the Num_Neighbors is active neighbor node listing

V. PROPOSEDSYSTEM

We proposeanovelapproachtocalculatetherebroadcastdelay. The rebroadcast delay is to determine the forwarding order. The node which has more common neighbors with the previous node has helower delay.If this node rebroadcasts a packet,then more common neighbors will know this fact.There fore, this rebroadcast delay enables the information that the nodes have transmitted the packets read to more neighbors. Rebroadcast probability considers the information a bouttheun covered neighbors(UCN),connectivity metric and local node density to calculateth rebroadcast probability.There broadcast probability is composed of two parts:

a. Additional coverage ratio, which is the ratio of the number of nodes that should be covered by a single broadcast to the total number of neighbors

b. Connectivity factor, which reflects the relationship of network connectivity and the number of neighbors of a given node.

A. Advantages of system

I. Nodes have transmitted the packet spread to more neighbors
II. Delay calculation is done in forwarding order
III. Rebroadcast probability is also available
IV. Broadcasting incurs larger outing overhead and causes many problems such as redundant retransmissions, contentions, and collisions.

B. System Module

1. Network formation with different mobile nodes
2. Rebroadcasting Delay calculation
3. Rebroadcast Probability
4. A neighbor coverage-based probabilistic rebroadcast.

C. Modules description

1. Network formation with different mobile nodes:-

In his module form the mobile network. The network contains number of nodes and one basesta tion.We can construct a topology to provide communication paths for wireless network. Here the node will give the owndetails such as Node ID and port number through which the transmission is done and similarly give the known nodes details such as Node ID, IP address and port number which are neighbors to given node.

2. Rebroadcasting Delay calculation:-

Node mobility available in MANETs, frequent link breakages may lead to frequent path failures and route discoveries, which

eISSN 1303-5150

could increase the overhead of routing protocols and reduce the packet delivery ratio and increasing the end-to-end delay.

Thus, The conventional on- demand routing protocol suseflooding to discover a route. They broadcast a Route REQuest(RREQ)packet to the networks, and the broadcasting in duce excessive redundant retransmissions of RREQ packet and causes the broadcasts to problem, which leads to a consider rable number of packet collisions, especially in dense networks.

3. Rebroadcast Probability:-

We now obtain the initial motivation of our protocol: Since limiting the number of rebroadcasts can effectively optimize the broadcasting, and the neighbor knowledge methods perform better than the area-based ones and the probability- based ones, then we)propose a neighbor coverage- based probabilistic rebroadcast(NCPR)protocol. Therefore, 1) in order to effectively exploit the neighborcoverage knowledge, we need a novel rebroadcast delay to determine there broadcast order, and then we can obtain a more accurate additional coverage ratio; 2)in order to keep the network connectivity and reduce the redundant retransmissions.

A neighbor coverage-based probabilistic rebroadcast:-

The proposed NCPR protocol needs Hello packets to obtain he neighbor information, and also needs to carry theneighbor list in the RREQ packet. Therefore, in our implementation, some techniques are used to reduce the overhead of Hello packets and neighbor list in the RREQ packet. In order to reduce the overhead of Hello packets, we do not use periodical Hello mechanism. Since a node sending any)broadcasting packets can inform its neighbors of it sexistence,the broadcasting packets such as RREQ and route error (RERR)can play a role of Hello packets. Only when the time elapsed from the last broadcasting packet (RREQ, RERR, or some other broadcasting packets) is greaterthan the value of Hello Interval, the node needs to send a Hello packet. The value of Hello Interval is equal to that of the original AODV. In order to reduce the overhead of neighbor list in the RREQ packet, each node needs to monitor the variation of its neighbor table and maintain a cache of the neighbor list in the received RREQ packet. We modify the RREQ header of AODV, and add a fixed field num_neighbors which representsthe size Of neighbor list in the RREQ packet and following the num_neighbors is the dynamic neighbor list.

Algorithm

Definitions:

$RREQ_s$: RREQ packet received from node s

R_id: the unique identifier (id) of $RREQ_s$

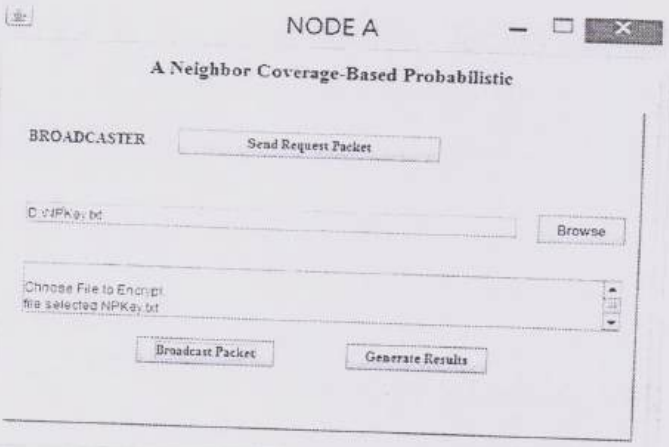
N_s: Neighbor set of node s

$U(s, r)$: Uncovered neighbors set of node s for RREQ whose id is r.

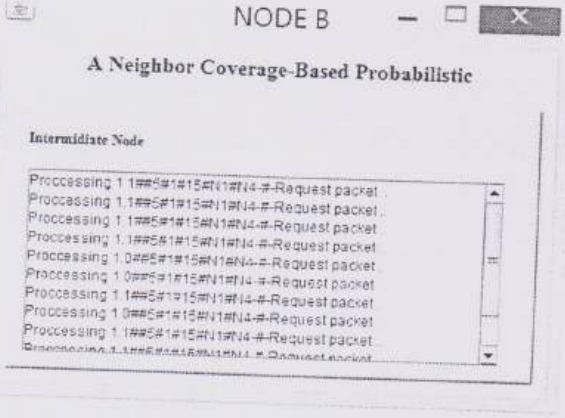
$Timer(s, r)$: Timer of node s for RREQ packet whose id is r.

(Note that, in the actual implementation of NCPR protocol, every different RREQ needs a UCN set and a Timer.)

1: if n_i receives a new $RREQ_s$ from s then
2: {Compute initial uncovered neighbors set $U(n_i, R_id)$ for $RREQ_s$}
3: $U(n_i, R_id) = N(n_i) - N(n_i) \cap N(s) - \{s\}$
4: {Compute the rebroadcast delay $T_d(n_i)$}
5: $T_{DN}(n_i) = 1 - \frac{N_c(n_i)}{N_{max}}$
6: $T_d(n_i) = MaxDelay \cdot T_{DN}(n_i)$
7: Set a Timer(n_i, R_id) according to $T_d(n_i)$
8: end if
9:
10: while n_i receives a duplicate $RREQ_s$ from n_j before Timer(n_i, R_id) expires do
11: {Adjust $U(n_i, R_id)$}
12: $U(n_i, R_id) = U(n_i, R_id) - U(n_i, R_id) \cap N_j$
13: discard($RREQ_s$)
14: end while
15:
16: if Timer(n_i, R_id) expires then
17: {Compute the rebroadcast probability $P_{re}(n_i)$}
18: $R_{DN}(n_i) = \frac{U(n_i, R_id)}{N_{max}}$
19: $F_{DN}(n_i) = \frac{N_c}{N_{max}}$
20: $P_{re}(n_i) = F_{DN}(n_i) \cdot R_{DN}(n_i)$
21: if Random(0,1) $\leq P_{re}(n_i)$ then
22: broadcast($RREQ_s$)
23: else
24: discard($RREQ_s$)
25: end if
26: end if

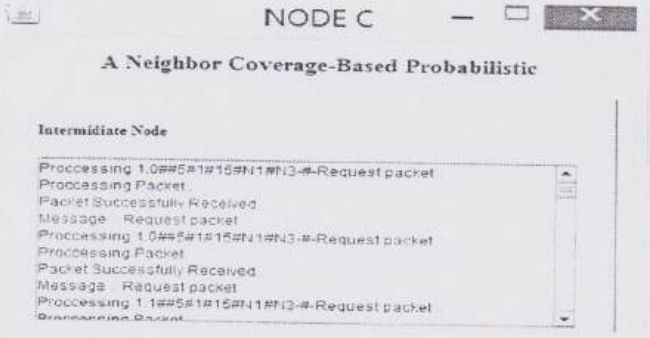


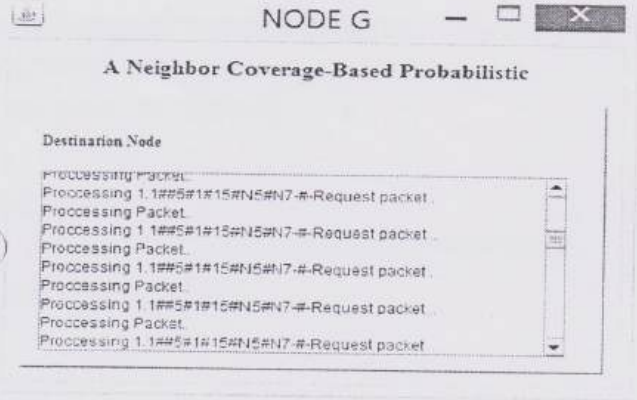
Screen shot 1

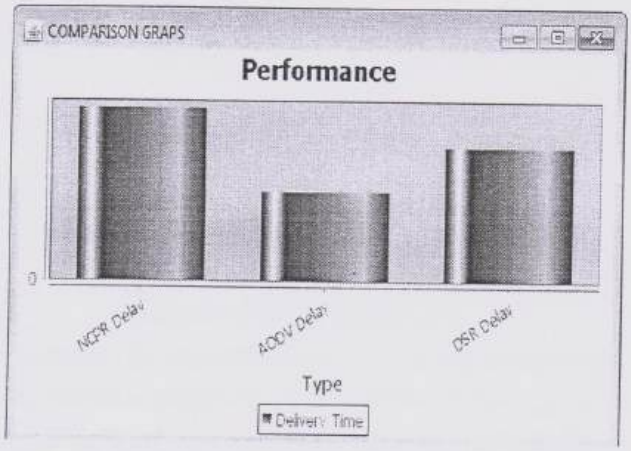


Screen Shot 2

eISSN 1303-5150







Above Graph depicts graphical view of packet deliverance proportion doggerel escalating in system solidity. Because

Of reducing the number of collisions there is increasing the packet delivery ratio in NCPR protocol.by means of the NCPR practice the sachet liberation fraction is amplified in turns to10 percent in comparison to that of in lineto AODV procedure and the NCPR set of rules amplify the envelope liberation share by roughly 3 percent enlarged when evaluated with the presented DSR procedure.

From the investigational consequences I forward in that the scheme labors adequately for boosting the envelope deliverance proportion since it widely cut the digit of envelopeimpacts and cut the middling source to target sachet setback. From gain outcomes we also finish that planned NCPR set of rules has pleasingly routine when the transportable complex isin with towering concentration or the travel is in profound stack.

Acknowledgment

I Express Sincere thanks to my research faculty members without whose support and valuable guide and direction my research work would have not been complete. System designing and architecture has been proposed prof.Kamlesh Patil research Methodology guidance was provided by Prof.P.J Chate.I express my thanks to him also.

VI. CONCLUSIONS AND FUTURE SCOPE

This research article have projected a NCPR protocol worn to lessen the added path finding overload in MANETs.The practice worn to with dynamism work out there transmission wait data information, that is required to settle on the ahead categorize of sachets and supplementary proficiently develop the adjacent neighbor reporting information in order.

eISSN 1303-5150

References

[1] Xin Ming Zhang, Member, IEEE, En Bo Wang, Jing Jing Xia,and DanKeunSung,SeniorMember,IEEE,"A Neighbor Coverage-Based Probabilistic Rebroadcast for Reducing Routing Overhead in Mobile AdHoc Networks" IEEE transactions on mobile computing, VOL. 12,NO.3,March2013.

[2] C.Perkins, E.Belding-Royer, and S.Das, AdHoc On-Demand Distance Vector (AODV)Routing, IETFRFC3561,2003.

[3] D.Johnson, Y.Hu, and D.Maltz,The Dynamic Source Routing Protocol for Mobile Ad Hoc Networks (DSR) for IPv4, IETF RFC 4728,vol. 15,pp.153-181,2007.

[4] H. AlAamri, M. A bolhasan, and T. Wysocki, "On Optimising Route Discovery in Absence of Previous Route Information in MANETs,"Proc.IEEE Vehicular Technology Conf. (VTC),pp.1-5,2009.

[5] X.Wu, H.R.Sadjadpour,andJ.J.Garcia-Luna-Aceves, "Routing Overhead as a Function of Node Mobility: Modeling Framework and Implications on Proactive Routing," Proc. IEEE Int'l Conf. Mobile AdHoc and Sensor Systems(MASS '07), pp.1-9,2007.

[6] S.Y. Ni, Y.C. Tseng, Y.S. Chen, and J.P. Sheu, "The Broadcast Storm Problem ina Mobile AdHoc Network," Proc. ACM/IEEE MobiCom,pp.151-162,1999.

[7] J. Kim, Q. Zhang, and D.P. Agrawal, "Probabilistic Broadcasting Based on Coverage Are a and NeighborConfirmation in Mobile AdHoc Networks," Proc.IEEEGlobeCom, 2004.

[8] A. Keshavarz-Haddady, V. Ribeirox, and R. Riedi, "DRB and DCCB: Efficient and Robust Dynamic Broadcast for AdHoc and Sensor Networks," Proc. IEEE Comm.Soc.Conf. Sensor,Mesh, and AdHoc Comm.and Networks (SECON'07),pp.253-262,2007.

[9] J.D. Abdulai, M. Ould-Khaoua, L.M. Mackenzie, and A. Mohammed,"Neighbour Coverage: A Dynamic Probabilistic Route Discovery for Mobile AdHoc Networks,"Proc. Int'l Symp.Performance Evaluation of Computer and Telecomm. Systems(SPECTS'08),pp.165-172,2008.

[10] H. AlAamri, M. Abolhasan, and T. Wysocki, "On Optimising Route Discovery in Absence of Previous Route Information in MANETs,"Proc.IEEE Vehicular Technology Conf. (VTC),pp.1-5,2009.

[11] X.M.Zhang,E.B.Wang,J.J.Xia,andD.K.Sung,"An Estimated Distance Based Routing Protocol for Mobile Ad Hoc Networks,"IEEETrans.VehicularTechnology,vol.60,no.7,pp.3473-3484,Sept.2011.

[12] W. Peng and X. Lu, "On the Reduction of Broadcast Redundancy in MobileAd HocNetworks,"Proc.ACMMobiHoc,pp.129-130,2000

[13] J. Chen, Y.Z. Lee, H. Zhou, M. Gerla, and Y. Shu, "Robust Ad Hoc Routing for Lossy Wireless Environment, "Proc.IEEE Conf.Military Comm.(MILCOM06)2006.

Scopus

Source details

NeuroQuantology

Scopus coverage years: from 2007 to Present

Publisher: Anka Publishers

SSN: 1303-5150

Subject area: Physics and Astronomy: Atomic and Molecular Physics, and Optics | Neuroscience: Cognitive Neuroscience | Neuroscience: Developmental Neuroscience

Source type: Journal

CiteScore 2021
1.3

SJR 2021
0.285

SNIP 2021
1.038

View all documents > | Set document alert | Save to source list | Source Homepage

CiteScore | CiteScore rank & trend | Scopus content coverage

Improved CiteScore methodology ×

CiteScore 2021 counts the citations received in 2018-2021 to articles, reviews, conference papers, book chapters and data papers published in 2018-2021, and divides this by the number of publications published in 2018-2021. Learn more >

CiteScore 2021

1.3 = 1,044 Citations 2018 - 2021 / 781 Documents 2018 - 2021

Calculated on 05 May, 2022

CiteScoreTracker 2022

1.9 = 800 Citations to date / 419 Documents to date

Last updated on 05 September, 2022 • Updated monthly

CiteScore rank 2021

Category	Rank	Percentile
Physics and Astronomy — Atomic and Molecular Physics, and Optics	#160/205	22nd
Neuroscience — Cognitive Neuroscience	#85/107	21st

View CiteScore methodology > | CiteScore FAQ > | Add CiteScore to your site

About Scopus

What is Scopus

Content coverage

Scopus blog

Scopus API

Privacy matters

Language

日本語版を表示する

查看简体中文版本

查看繁體中文版本

Просмотр версии на русском языке

Customer Service

Help

Tutorials

Contact us

ELSEVIER

Terms and conditions Privacy policy

Copyright © Elsevier B.V. All rights reserved. Scopus® is a registered trademark of Elsevier B.V.

We use cookies to help provide and enhance our service and tailor content. By continuing, you agree to the use of cookies.

RELX

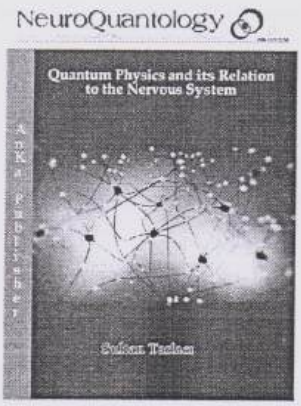
NeuroQuantology
An Interdisciplinary Journal of Neuroscience and Quantum Physics
ISSN 1303 5150

NeuroQuantology

Clarivate Analytics
2017 Journal Citation Reports
Impact Factor: 0.453

Research Databases · Scopus · embase · ProQuest · crossref · GALE CENGAGE Learning

Publisher: AnKa Publisher



Editorial: A Look at the Future and an Open Call for Scientific Community

What we call science is the systematization of information obtained from nature. Nature has had its own laws from the beginning. Some of these laws are easy to express, while others stretch our understanding and even our sense of logic. Our efforts to understand nature and its workings, that is our production of scientific knowledge, will never end. We may never truly understand the workings of nature, or get close to the real truth. Therefore, it is ridiculous to behave as if we knew all of the workings of nature and to say this is not scientific, it is in conflict with the (known) laws of science . The clearest example of this is when we see the workings of quantum physics in biological structures. When nature is working, it does not know the laws of our science and doesn't even take notice of them. Nature even sometimes winks at us with anomalies . We learn from nature but we cannot impose on nature the laws we have learned from it.

Journal Menu

Home
Editorial Board
Archives
Current Archives
Author Guidelines
Call for Submissions
Login

NeuroQuantology
Q3 Atomic and Molecular Physics, and Optics
Best quartile
SJR 2021
0.29
powered by scimagojr.com

0.9 2020 CiteScore
13th percentile
Powered by Scopus

PubMed

twitter

Copyright © 2019 NeuroQuantology - All Rights Reserved

JCST Journal of Data Acquisition and Processing
ISSN: 1004-9037
https://sicivcl.cn/
DOI: 10.5281/zenodo.7691431

A WEB PAGE CLASSIFICATION SURVEY ON TECHNIQUES USING TEXT MINING

Dr. Kalyan D Bamane
D Y Patil College of Engineering, Akurdi Pune (MS), India.
kdbamane@dypcoeakurdi.ac.in

Dr. Preeti Patil
D Y Patil College of Engineering, Akurdi Pune (MS), India.
pspatil@dypcoeakurdi.ac.in

Dr. A. M. Pawar
Bharati Vidayapeeth's College of Engineering for Women, Pune (MS), India.
avinash.m.pawar@bharatividyapeeth.edu

Mrs. S. S. Patil
Bharati Vidyapeeth (Deemed to be University) College of Engineering, Pune, 411043, India.
sspatil@bvucoep.edu.in

Mrs. Anusha Meti
D Y Patil College of Engineering, Akurdi Pune (MS), India.
ammeti@dypcoeakurdi.ac.in

Mrs. Rutuja Vivek Tikait
D Y Patil College of Engineering, Akurdi Pune (MS), India.
rvtikait@dypcoeakurdi.ac.in

Dr. R. B. Jadhav
Bharati Vidyapeeth (Deemed to be University) College of Engineering, Pune, 411043, India.
rbjadhav@bvucoep.edu.in

Dr. Uday C. Patkar
Bharati Vidyapeeth's college of Engineering, lavale, Pune, (MS), India.
uday.patil@bharatividyapeeth.edu

Abstract

The rapid growth of the World Wide Web (www) is demanding for an automated assistance for Web page classification and categorization. In most existing Web page classification tasks, Web pages are classified into topical categories based on their content regardless of the possible relationships among them. In this paper, a comprehensive survey on classification of Web pages is presented. The features for creating tag information, classifiers and datasets used for experimentation are also discussed. It also gives comparative analysis of all Web page

classification techniques. The challenges/Issues involved in developing Web page classification are also discussed. This would help researchers to take up new work on Web page classification and address most of the important challenges/issues.

Keywords— Web page Classification; Web pages; Web content mining; Text mining.

INTRODUCTION

In recent years, the World Wide Web (WWW) has become a global data Centre, which permits people to store and distribute their information. The information in Web pages may be related to be personal, official, commercial and business. The users of Web would like to access such information for their needs. Hence, the Web page classification methods must properly organize Web pages so that the relevant information is supplied for the user queries. Such Web page classification methods use Web content mining, also known as text mining that aims on raw data exists in the Web pages. The Web Content mining is also the scanning and mining of text, pictures and graphs of a Web page to determine the relevance of the content to the search query.

Web content mining is directed toward specific information provided by the customer search information in search engines. This allows for the scanning of the entire Web to retrieve the cluster content triggering the scanning of specific Web pages within those clusters. The results are pages relayed to the search engines through the highest level of relevance to the lowest. Though, the search engines have the ability to provide links to Web pages by the thousands in relation to the search content, this type of web mining enables the reduction of irrelevant information.

Web content mining is very effective when used in relation to a content database dealing with specific topics. For example online universities use a library system to recall articles related to their general areas of study. This specific content database enables to pull only the information within those subjects, providing the most specific results of search queries in search engines.

The main uses for this type of data mining are to gather, categorize, organize and provide the best possible information available on the WWW to the user requesting the information. This approach is imperative to scanning the many HTML documents, images, and text provided on Web pages. The resulting information is provided to the search engines in order of relevance giving more productive results of each search.

In short, the ability to conduct Web content mining allows results of search engines to maximize the flow of customer clicks to a Web site, or particular Web pages of the site, to be accessed

Numerous times in relevance to search queries. The clustering and organization of Web content in a content database enables effective navigation of the pages by the customer and search engines. Images, content, formats and Web structure are examined to produce a higher quality of information to the user based upon the requests made. Businesses can maximize the use of this text mining to improve marketing of their sites as well as the products they offer. The web content mining techniques are very useful for classification web pages. In this paper a comprehensive survey of various web page classification methods is presented.

The rest of the paper is organized in to three sections. Section 2 describes the existing techniques for classification of web pages. Section 3 highlights the challenges involved in developing new methods for web page classification. Section 4 gives the conclusion. Table I gives the comparative study of web page classification.

DESCRIPTION OF EXISTING TECHNIQUES FOR WEB PAGE CLASSIFICATION

Significant amount of work has gone into the research related to development of techniques for web page classification. Some of the important techniques are summarized in the following.

Dou Shen, Qiang Yang, Zheng Chen (2007) proposes a technique to improve the web page classification performance by removing the noise through summarization process. The method uses empirical evidence that ideal web page summaries generated by human editors can indeed improve the performance of web-page classification algorithms. Later, the method put forward a new web-page summarization algorithm; which is based on web page layout and the method is evaluated along with several other state of the art text summarization algorithms on the look smart web directory. Here, around 2 million web pages are used which are crawled from the look smart web directory (i.e http:// search.looksmart.com). The experimental results show that the classification algorithms i.e support vector machine augmented by any summarization approach can achieve an improvement by more than 5.0% as compared to pure text based classification algorithms. To improve the pure text based methods, an ensemble method is introduced to combine the different summarization algorithms. The ensemble summarization method achieves 12.0% improvement over pure text based methods.

Rung-ching chen, Chung-Hsun Hsieh (2005) describe a web page classification based on support vector machine (SVM) using a weighted vote schema for various features. The system uses both latent semantic analysis and web page feature selection training and recognition by the SVM model. The method extracted text features from web page content. The dataset used here is sports news especially to test system performance, sports news was downloaded from udndata website. Data sets include various games such as basketball, baseball, golf, tennis, volley ball, soccer, billiards, football and formula 1 racing. So based upon the output of the support vector machine, a voting schema is used to determine the category of the web page. The weighted vote support vector machine yields a better accuracy even with small data set.

A.J. Shaikh, V. L. Kolhe (2013) reports a framework for Web Content Mining Using Semantic Search and Natural Language Queries. Here the method implements a framework for semantic based web content mining system using semantic ontology and SPARQL. It converts natural language queries into SPARQL quires using NLP query processing module. For testing, the method considers a framework for cricket domain in which it shows a better improvement over traditional keyword based searching. The implemented framework is for cricket domain for ICC World Twenty20, 2012-13 Series. In which OWL API where used for semantic mapping. Protégé is used for ontology design. The performance of keyword based search is than compared with SPARTQL query search. SPAQRL query search gives more precise results compared to keyword based search.

Ali Ahmadi, Mehran Fotouhi, Mahmoud Khaleghi (2010) proposes an Intelligent Classification of Web pages using Contextual and visual features. The method is applied for classification of pornographic Web pages. The filtering of unwanted Web content is achieved based on blocking a specific Web address via searching it in a reference list of black URLs or

by doing a plain contextual analysis on the page by searching special keywords in the text. In this paper, the intelligent approach which is based uses textual, profile and visual features in a hierarchical structure classifier. The ID3 classifier is used for textual and profile features. The Textual features contain information about keywords and black-words. The profile features contains structural information like number of links, meta-tags, pictures etc. The algorithm is applied on a dataset consisting of 1295 web pages as training set which includes 700 porn pages (which includes text, image or both) in both English and Persian and also includes 595 non-porn pages which again includes pages with medical, health and sports. The neural network model is used for skin color and visual features. The model attains 95% accuracy by using test dataset with 290 web-pages.

Chih-Ming Chen, Hahn-Ming Lee, Yu-Jung Chang (2007) employed a two novel feature selection approaches for web page classification. In this model a fuzzy ranking analysis paradigm has been described together with a novel relevance measure and discriminating power measure (DPM) to effectively reduce the input dimensionality from tens of thousands to a few hundred with zero rejection rates and small decrease in accuracy. Thus the result obtained is that the DPM can reduce both redundancy and noise features to set up a better classifier.

Inma Hernandez, Carlos R.Rivero, David Ruiz, Rafael Corchuelo (2013) proposed to automatically generate URL-based web page classifiers which can be used in the context of enterprise web information systems. It builds a number of URL patterns that represent the different classes of pages in a web site, so further pages can be classified by matching their URLs to the patterns. The system is experimented on top 40 alexa websites written in English. And have achieved an average precision of 98% and average recall of 90%.The system is mainly used for real-world web page classification.

Selma Ayse Ozel (2010) describes a web page classification system based on a genetic algorithm using tagged-terms as features. In this method, automatic Web page classification system has been used, which uses both HTML tags and terms as classification features. The system classifies Web pages by simply computing similarity between the learned classifier and the new Web pages. The system is tested on datasets such as conference, course, and student web pages. The classification accuracy is 95%.

R.Etemadi, N.Moghaddam (2010) employs an approach in web content mining for clustering web pages. The algorithm uses data content and new similarity criterion for classification of web pages. For evaluating the accuracy of algorithm some pages with five subjects of software engineering, computerized networks, and architecture of computer, parallel processing and operating system are taken as datasets and have been investigated. The results obtained from simulation show high efficiency of the algorithm in separating web pages and their clustering.

Tarique Anwar, Muhammad Abulaish (2012) proposes a Markov Clustering (MCL) based text mining approach for namesake disambiguation on the web. The technique represents the collection of web pages as a weighted graph and applies MCL to determine different clusters. The system mainly focuses on three broad and realistic aspects to cluster web-pages retrieved through search engines which includes content overlapping, structure overlapping, and local context overlapping. For experimentation, two different datasets are used namely Bekkerman and McCallum. It is found that the computational complexity of the proposed method is quite satisfactory in comparison to other state-of-art techniques.

Aixin Sun,Ying Liu, Ee-Peng Lim (2011) describes Web classification of conceptual entities using co-training. Web pages are described on physical or abstract entity, e.g., company, people, and event. Furthermore, users often like to organize pages into conceptual categories for better search and retrieval. In this work the web pages are categorized into conceptual categories. For experimentation Conf-425 dataset is used. The pre-processing of Conf-425 dataset includes HTML tag removal, stop-word removal, and term stemming. More importantly, the accuracy of EcT was not much worse than classification methods that used a large set of training examples.

Ahmad Pouramini, Shahram Nasiri (2015) proposes a wrapping language supported by a visual tool to create wrappers for extracting the main content from web pages. In this language, various types of features such as syntactical, semantic, visual can be employed in the extraction rules to identify the content of interest. For experimentation the method is tested on websites such as Wikipedia, yahoo news, NY Times, BlogSpot and Word press.

Tao Jiang, Ah-Hwee Tan, Ke Wang (2007) proposes a two-step procedure to mine generalized Associations of semantic relations from textual web content. First, RDF (Resource Description Framework) metadata representing semantic relations are extracted from raw text using natural language processing techniques. Then, a novel generalized association pattern mining algorithm (GP-Close) is applied to discover the underlying association patterns on RDF metadata. The experiments were performed on a desktop PC running Windows XP with a P4-2.6G CPU and 1 G RAM. The GPClose algorithm was implemented using Java (JDK 1.4.2). Two variants of GP-Close with different sizes of tidset buffer were used in the experiments, namely, GP-Close- 0 with a tidset buffer of 0 KB and GP-Close-50000 with a tidset buffer of 50,000 KB. The experimental result shows that the GP-Close algorithm substantially reduce the pattern redundancy and perform much better than the original generalized association rule mining algorithm in terms of time efficiency.

S.Yasodha, S.S.Dhenakaran (2014) presents an Ontology-Based framework for Semantic Web Content Mining. Framework has been implemented for three major domains Education, Medicine and Tourism. The algorithm has been implemented in JAVA with RDF at the back end for storing ontology's. The performance of the framework is evaluated by three metrics: Precision, Average Precision and Relevance Score. The efficiency of the framework is measured in terms of precision, average precision and relevance score.

G.S. Tomar, Shekhar Verma, Ashish Jha (2006) introduces the concept of a classification tool for web pages called Web Classify, which uses modified naïve Bayesian (NB) algorithm with multinomial model to classify pages into various categories. The tool starts the classification from downloading training web text from internet, preparing the hypertext for mining, and then storing web data in a local database. Web pages were taken from web directories, which are pre-classified into various categories and those pages were pre-processed before the words can be sent to training data set. The system has been tested on a very small set of test documents and the vocabulary size of the corpus is also low. The modified approach is measured with a threshold value of 0.4. So NB has a classification accuracy of 42.5% while the approach has a classification accuracy of 55%. This clearly shows the enhancement in performance.

Majid Javid Moayed, A. Hamid Sabery, A. Hamid Sabery (2008) Investigates usage of a swarm intelligence algorithm in the field of the web page classification. Focusing on Persian

web pages Ant Miner II is the used algorithm. It also proposes a simple text preprocessing technique to reduce the large numbers of attributes associated with web content mining. The web pages of news are the most suitable choices for the experimentation because of the solidarity of their contents and being classified. In order to experiment the model, the web pages of Irna news are used. The result shows Ant Miner II and proposed preprocessing technique is efficient in the field of the web page classification.

Vladimir Bartík (2009) describes association based classification for relational data, which can be used for the data extraction from web pages. The method is tested on two Relational Databases NURSERY and ADULT which are taken from the UCI Machine Learning Repository. Next, the experiments with various data is presented, with emphasis on data obtained by extraction and segmentation of web pages. The accuracy showed to be about 80%.

Jiao Lijuan, Feng Liping (2010) presents a method to improve classification accuracy of Web pages by using the hyperlink factor. The Web pages are classified by using KNN classifier. Three hundreds of documents are selected to this experiment, 210 of which are taken as training corpus including sixty on financial, fifty on sports, sixty on culture, forty on military and ninety of which are testing ones. There are 8617 feature items which are extracted. Classification results are evaluated by precision and recall rate which are accepted internationally. The classification accuracy would be increased by 10% or more if hyperlink factor is inducted for web pages by the experiment. Introduction of hyperlink elements of web pages can improve the classification accuracy in feature selection method based on mutual information and correlation by experiment. So the improvement is effective in web page classification.

Vladimir Bartík (2010) describes text-based Web page classification that uses both textual and visual information to find a suitable representation of web page content, based on term frequency (TF) and inverse document frequency (TF-IDF) weighting. The model is experimented on Web KB corpus of web pages to verify the functionality. The first dataset contains 4518 web pages from the computer science department websites. The second dataset was manually created Using web pages taken from several English written news websites (CNN.com, Reuters.com, nytimes.com, boston.com and usatoday.com). The accuracy achieved is approximately 80%.

Lay-Ki Soon, Sang Ho Lee (2010) describes classifying web pages using information extraction patterns – preliminary results and findings. The model uses natural language processing (NLP) techniques such as Naïve Bayesian classifiers, Support Vector Machine (SVM) and association rule mining (ARM). For experimentation the model uses Sundance Sentence Understanding and Concept Extraction (Sundance) to obtain the IE patterns. The experimental results indicate that the existence of a word in different contexts has different impact to the classification task. Thus, the extraction patterns used to represent each document are more semantically meaningful and give better insight to web classification in comparison with keywords.

Hakan Ayral, Sırma Yavuz (2011) describes an automated domain specific stop word generation method for natural language text classification. The model implements a Bayesian Natural language classifier working on web pages. The model is experimented on PASCAL dataset, the results shows that document coverage rank and topic coverage rank of words belonging to natural language corpora follows Zapf's law.

Hu Mingsheng, Jia Zhijuan, Zhang Xiangyu (2012) employees and approach for text extraction from Web news page. The model Uses tree structure of Document Object Model (DOM) when analyzing web page. The model is experimented on some randomly selected websites such as News.qq.com, News.sohu.com, News.163.com, News.tom.com, Cn.msn.com, www.china.com.cn and news.cn.yahoo.com. The results obtained shows that the method is both versatile and a highly accurate. If the web Page is some fairly standard news web pages, the accuracy Rate can reach to 98%. In practice, they have carried out extraction on pages from 150 websites; the accuracy of the sampling rate is 94%.

Wang Zhixing, Chen Shaohong (2011) represents web page classification based on semi-supervised Naive Bayesian EM algorithm. The model uses Hierarchical Clustering EM framework to train Naive Bayesian Classifier iteratively. The model is tested on Look Smart database and most of the selected Web pages contain mainly text, including 2000 pages and 6 chief categories namely: Entertainment, Work, Shopping, Sport, Travel and Society. The result of the experiment proved that the method introduced in the model shows good effect of Web classification.

Dongjin Choi, Byeongkyu Ko, Eunji Lee, Myunggwon Hwang, Pankoo Kim (2012) employed automatic evaluation of document classification using n-gram statistics, which have a great possibility to find similarities between given documents. The proposed method is compared with traditional method suggested by Keselj. The model is tested on bioinformatics data base, computer vision, fuzzy system, mobile and NLP. Each category contains 100 research documents collected from IEEE digital library. The performance using this method is better than the Keel approach.

Hammad Haleem,Pankaj Kumar Sharma,MM Sufyan Beg (2014) describes a novel frequent sequential patterns based probabilistic model for effective classification of web documents. The classification model proposed utilizes the features of naïve bays classifiers and the Pattern discovery model (PTM). The model is experimented on a collection of documents related to predefined categories. The documents were taken from two different sources, firstly they used the Reuters Corpus version 1 (RCV1) and secondly on crawled dataset. After testing the novel approach on RCV1 dataset, 88% accuracy is obtained.

Kolla Bhanu Prakash, M.A. Dorai Rangaswamy, Arun Raja Raman (2013) represents attribute based content mining for regional web documents. The model outlines the use of attributes for content extraction, using basic pixel attributes, pattern matching, statistical model, and Artificial Neural Network training. This preliminary study is focused to bring out the complexities in regional web documents and how to present popular text mining techniques.

Moonis Javed, Aly Akhtar, Akif Khan Yusufzai (2015) describes classification of web pages as evergreen or ephemeral based on content. The approach that has been used is a combination of text classification and other binary classification. The training dataset provided by Stumble Upon was a set of urls with some Meta information like the category of the page, html ratio, is news, along with some boilerplate code (like title and content) of the page. The model is tested on Stumble Upon and an overall accuracy of 88% is reported.

Jia Wu, Shirui Pan, Xingquan Zhu, Zhihua Cai (2015) describes boosting for multi-graph classification. The model uses graph-based learning problem and multi-graph classification (MGC), which aims to learn a classifier from a set of labeled bags each containing a number of graphs inside the bag. The model is experimented on datasets such as DBLP Multi-Graphs;

the DBLP dataset consists of bibliography data in computer science. Experiments and comparisons on real- world multi-graph learning tasks demonstrate the algorithm performance.

Wenlong Ren ,Jianzhuo Yan (2015) represents an improved Cerebellar Model Articulation Controller (CMAC) neural network model for web mining. The CMAC is an excellent classification technique, but when it is applied to deal with high-dimensional dataset such as the data on the Internet, the memory required increase intensively. However, this improved CMAC model requires less memory for processing high-dimensional dataset. The model is tested on datasets such as Syskill & Webert Web pages ratings. Experiments on the four topics show that the improved CMAC model performs a better predicting accuracy rate to identify user interesting Web pages than other well-known classification method.

Aanshi Bhardwaj, Veenu Mangat (2015) represents a novel approach for content extraction from web pages. The model discusses various approaches for extracting informative content from web pages and a new approach for content extraction from web pages using word to leaf ratio and density of links.

Jian Zhu, Hanshi Wang, JinTao Mao (2014) describes sentiment classification using genetic algorithm and conditional random fields. Conditional Random Fields (CRFs) is employed to model the emotional tendency of web pages, which are divided into different types of comments, such as positive comments, negative comments and objective comments. To test the model a corpus of 400 online product reviews from the product: x61. Experimental results on the product reviews and the 1998 People's Daily corpus show that the proposed algorithm works reasonable in the real calculation.

CHALLENGES/ISSUES

The existing web page classification methods have many issues as listed below:

1) Selection of appropriate features
2) Either the HTML tags or terms are considered as the features
3) Tag information representation.
4) It is difficult to classify the unstructured data from web pages.
5) Difficulty in finding relevant information.
6) Extracting new knowledge from the web.

CONCLUSION

In this paper, the techniques for Web page classification techniques are described. The techniques employ Web-page summarization algorithm, support vector machine, Semantic Search, Natural Language Queries, genetic algorithm, Markov Clustering (MCL), Resource Description Framework (RDF), term frequency(TF), inverse document frequency (TF-IDF) etc. which are experimented on datasets such as look smart web directory, Sports news from undated website, Cricket domain for ICC World Twenty20, 2012-13 Series are presented. According to the survey done the classification is done on features such as keywords, visual features, expressions, hyperlink factor, sentiments etc. However still there is a challenge to develop new classification techniques.

COMPARATIVE STUDY

The comparative study of all approaches for Web page classification is summarized below:

TABLE I.COMPARATIVE STUDY

Author	Description of method	Datasets	Accuracy
Dou Shen , Qiang Yang, Zheng Chen (2007) [1]	Noise reduction through summarization for Web-page classification	2 million web pages crawled from the look smart web directory	12.0%
Rung-ching chen, Chung- Hsun Hsieh (2005) [2]	Web page classification based on a support vector machine using a weighted vote schema	Sports news from udndata website	The weighted vote support vector machine yields a better accuracy even with small data set.
A.J.Shaikh, V.L.Kolhe (2013) [3]	Framework for Web Content Mining Using Semantic Search and Natural Language Queries	Cricket domain for ICC World Twenty20,2 012-13 Series.	SPAQRL query search gives more precise results compared to keyword based search.
Ali Ahmadi, Mehran Fotouhi, Mahmoud Khaleghi (2010) [4]	Intelligent classification of web pages using contextual and visual features	1295 web pages as training set which includes 700 porn pages (which includes text, image or both) in both English and Persian and also includes 595 non-porn pages which again includes pages with medical, health, Sports.	Here it attains 95% accuracy by using test dataset with 290 web-pages
Chih-Ming Chen, Hahn- Ming Lee,Yu-Jung Chang(2007) [5]	Two novel feature selection approaches for web page classification	China- Times Web site (http://news .china times. com/) and Reuter- 21578.	DPM can reduce both redundancy and noise features to set up a better classifier.
Inma Hernandez, Carlos R.Rivero, David Ruiz, Rafael Corchuelo (2013) [6]	CALA: An unsupervised URL-based web page classification system	40 websites from Alexa which is written in English.	And have achieved an average precision of 98% and average recall of 90%.
Selma Ayse Ozel (2010) [7]	A Web page classification system based on a genetic algorithm using tagged-terms as features	The course and the student datasets obtained from WebKB project website (http://ww	When there is enough number of negative documents in the training dataset, the classifier

		w.cs.cmu.e du/-webkb)	reaches 95% accuracy.
R.Etemadi, N.Moghaddam (2010)[8]	An Approach in Web Content Mining for Clustering Web Pages	Pages with five subjects of software engineering, computerized networks, architecture of computer, parallel processing and operating system	The results obtained from simulation show high efficiency of the algorithm proposed in separating web pages and their clustering.
Tarique Anwar,Muhammad Abulaish (2012)[9]	An MCL-Based Text Mining Approach for Namesake Disambiguation on the Web	Bekkerman and McCallum.	It is found that the computational complexity of the proposed method is quite satisfactory in comparison to other state-of-art Techniques.
Aixin Sun,Ying Liu,Ee-Peng Lim (2011)[10]	Web classification of conceptual entities using co- training	Conf-425 dataset. The pre- processing of Conf- 425 dataset included HTML tag removal, stop-word removal, and term stemming	The accuracy of EcT was not much worse than classification methods that used a large set of training examples.
Ahmad Pouramini,Shahram Nasiri (2015) [11]	Web content extraction using contextual rules	Websites such as Wikipedia, yahoo news, NY Times, BlogSpot, Word press	Not reported

Tao Jiang, Ah-Hwee Tan, Ke (2007)[12]	Mining Generalized Associations of Semantic Relations from Textual Web Content Relations from Textual Web Content	Desktop PC running Windows XP with a P4-2.6G CPU and 1 G RAM, Two variants of GP-Close with different sizes of tidset buffer, GP- Close-0 with a tidset buffer of 0 KB and GP-Close- 50000 with a tidset buffer of 50.000 KB. P4-2.6G CPU and 1 G RAM, Two variants of GP-Close with different sizes of tidset buffer, GP- Close-0 with a tidset buffer of 0 KB and GP-Close- 50000 with a tides buffer of 50,000 KB.	GP-Close algorithm Substantially reduce the pattern redundancy.
S.Yasodha, S.S.Dhenakaran (2014)[13]	An Ontology- Based Framework for Semantic Web Content Mining	The framework has been implemented d for three major domains, Education, Medicine And Tourism.	The efficiency of the framework is measured in terms of precision, average precision and relevance score.
G.S. Tomar, Shekhar Verma, Ashish Jha (2006) [14]	Web Page Classification using Modified Naïve Bayesian Approach	Web directories, The proposed approach has been tested on a very small set of test documents and the vocabulary size of the corpus is also low	The modified approach is measured With a threshold value of 0.4. So NB has a classification accuracy of 42.5% while our approach has a classification accuracy of 55%.
Majid Javid Moayed, A. Hamid Sabery, A. Hamid Sabery (2008)[15]	Ant Colony Algorithm for Web Page Classification	Web pages of news, the web pages of Iran news are used	The result shows Ant Miner II and proposed preprocessing technique are efficiency in the field

			of the web page classification.
Vladimír Bartík (2009) [16]	Association Based Classification for Relational Data and Its Use in Web Mining	For Experiment s with Relational Databases NURSERY and ADULT datasets taken from the UCI Machine Learning Repository were used	The accuracy showed to be about 80%.
Jiao Lijuan, Feng Liping (2010) [17]	Improvement of Feature Extraction in Web Page Classification	300 documents are selected to this experiment, 210 of hitch are taken as training corpus including sixty on financial, fifty on sports, sixty on culture, forty on military and ninety of which are testing ones. There are 8617 feature items are extracted	The classification accuracy would be increased by 10% or more if hyperlink factor is inducted for web pages by the experiment
Vladimír Bartík (2010) [18]	Text-Based Web Page Classification with Use of 7 Visual Information	4518 web pages from the computer science department websites. The second dataset was manually created. It contains web pages taken from several English written news websites (CNN.com, Reuters.co m, nytimes.com, boston.com and usatoday.com).	The accuracy was approximately 80% for both weightings.

Lay-Ki Soon, Sang Ho Lee (2010)[19]	Classifying Web Pages using Information Extraction Patterns – Preliminary Results and Findings	Four university dataset The dataset consists of 8,282 web pages collected from computer science department s of several universities . 4,162 of the web pages are from Cornel, Texas, Washington and Wisconsin University, while the other . 4,120 are from other universities	The extraction patterns used to represent each document are more semantically meaningful and give better insight to web classification in comparison with keywords.
Hakan Ayral, Sırma Yavuz (2011)[20]	An Automated Domain Specific Stop Word Generation Method for Natural Language Text Classification	PASCAL Dataset	Investigated the distribution of stop-word lists Generated by the model and compared their contents against a Generic stop- word list for English language.
Hu Mingsheng, Jia Zhijuan, Zhang Xiangyu (2012)[21]	An Approach for Text Extraction From Web News Page	Randomly selected from some websites such as News.qq.com, News.sohu.com, News.163.com, News.tom.com, Cn.msn.com, www.china. com.cn, news.cn.yahoo.com.	From the results obtained, this Method is of both versatility and a high accuracy. If the web Page is some fairly standard news web pages, the accuracy Rate can reach to 98%. they have carried out extraction on pages from 150 websites, the accuracy of the sampling rate is 94% or More
Wang Zhixing, Chen Shaohong(2 011)[22]	Web Page Classification based on Semi- supervised Naive Bayesian EM Algorithm	Look Smart (Entertainm ent, Work, Shopping, Sport, Travel, Society) .	The result of the experiment proved that the method introduced in the

			paper shows good effect of Web classification.
Dongjin Choi, Byeongkyu Ko, Eunji Lee, Myunggwo Hwang, Pankoo Kim(2012)[23]	Automatic Evaluation of Document Classification using N-gram Statistics	Training data sets were chosen from bioinformatics data base, 'computer vision,' fuzzy system,' 'mobile', and 'NLP'.	The performance using this method is better than the Keselj approach.
Hammad Haleem,Pankaj Kumar Sharma,M M Sufyan Beg(2014) [24]	Novel Frequent Sequential Patterns based Probabilistic Model for Effective Classification of Web Documents	The documents were taken from two different sources, firstly they used the Reuters Corpus version 1(RCV1), secondly on their own Crawled dataset.	After testing this novel Approach on RCV1 dataset, We were able to obtain classify the test documents with 88% accuracy.
Kolla Bhanu Prakash, M.A. Dorai Rangaswamy, Arun Raja Raman (2013) [25]	Attribute based content mining for regional Web documents	Regional web documents	Not reported
Moonis Javed, Aly Akhtar, Akif Khan Yusufzai (2015) [26]	Classification of 'Web 'Pages as Evergreen or Ephemeral based on content	The training dataset provided by Stumble Up on was a set of urls with some Meta information like the category of the page, html ratio, is news, along with 'some boilerplate code (like title and content) of The page.	Using this we have been able to get an overall accuracy of 88%.
Jia Wu, Shirui Pan, Xingquan Zhu, Zhihua Cai(2015)[27]	Boosting for Multi-Graph Classification	DBLP Multi- Graph Dataset: The DBLP Dataset consists of bibliography data in computer science.	Experiments and comparisons on real-world multi-graph learning tasks demonstrate the algorithm performance.
Wenlong Ren, Jianzhuo Yan(2015) [28]	An Improved CMAC Neural Network Model for Web Mining	The dataset of Syskill & Webert Web pages ratings were used to test the improved CMAC	Experiments on the four topics show that the improved CMAC model performs a

		Model.	better predicting accuracy rate to identify user interesting Web pages than other well-known Classification method.
Aanshi Bhardwaj, Veenu Mangat (2014) [29]	A Novel Approach for Content Extraction from Web Pages	Not reported	Not reported
Jian Zhu, Hanshi Wang, JinTao Mao(2010) [30]	Sentiment Classification Using Genetic Algorithm and Conditional Random Fields	compiled a corpus of 400 online product reviews from this product: x61	Experimental results on both the product reviews and the 1998 People's Daily corpus show that the proposed algorithm works reasonable in the real calculation.

REFERENCES

[1] Chi-Ming Che, Hahn-Ming Lee, Yu-Jung Chang," Two novel feature selection approaches for web page Classification", Expert Systems with Applications 36 (2009) 260–272

[2] Rung-Ching Chen, Chung-Hsun Hsieh, "Web page classification based on a support vector machine using a weighted vote schema", Expert Systems with Applications 31 (2006) 427–435

[3] A. J. Shaikh and V. L. Kolhe, "Framework for web content mining using semantic search and natural language queries," 2013 IEEE International Conference on Computational Intelligence and Computing Research, Enathi, 2013, pp. 1-5.

[4] Ali Ahmadi, Mehran Fotouhi, Mahmoud Khaleghi "Intelligent classification of web pages using contextual and visual features", Applied Soft Computing 11 (2011) 1638–1647

[5] Chih-Ming Chen, Hahn-Ming Lee, Yu-Jung Chang "Two novel feature selection approaches for web page classification", Expert Systems with Applications 36 (2009) 260–272

[6] Inma Hernández, Carlos R. Rivero, David Ruiz, Rafael Corchuelo "CALA: An unsupervised URL-based web page classification system" ,Knowledge-Based Systems 57 (2014) 168–180

[7] Selma Ays_e Ozel "A Web page classification system based on a genetic algorithm using tagged-terms as features", Expert Systems with Applications 38 (2011) 3407–3415

[8] R. Etemadi and N. Moghaddam, "An approach in web content mining for clustering web pages," 2010 Fifth International Conference on Digital Information Management (ICDIM), Thunder Bay, ON, 2010, pp. 279- 284.

[9] T. Anwar and M. Abulaish, "An MCL-Based Text Mining Approach for Namesake Disambiguation on the Web," 2012 IEEE/WIC/ACM International Conferences on Web Intelligence and Intelligent Agent Technology, Macau, 2012, pp. 40-44.

[10] Aixin Sun, Ying Liu, Ee-Peng Lim, "Web classification of conceptual entities using co-training", Expert Systems with Applications 38 (2011) 14367–14375

[11] A. Pouramini and S. Nasiri, "Web content extraction using contextual rules," 2015 2nd International Conference on Knowledge-Based Engineering and Innovation (KBEI), Tehran, 2015, pp.1014-1018.

[12] T. Jiang, A. h. Tan and K. Wang, "Mining Generalized Associations of Semantic Relations from Textual Web Content," in IEEE Transactions on Knowledge and Data Engineering, vol. 19, no. 2, pp. 164-179, Feb. 2007.

[13] S. Yasodha and S. S. Dhenakaran, "An ontology-based framework for Semantic Web Content Mining," 2014 International Conference on Computer Communication and Informatics, Coimbatore, 2014, pp. 1-6.

[14] G. S. Tomar, S. Verma and A. Jha, "Web Page Classification using Modified NaÃve Bayesian Approach," TENCON 2006 - 2006 IEEE Region 10 Conference, Hong Kong, 2006, pp. 1-4.

[15] M. J. Moayed, A. H. Sabery and A. Khanteymoory, "Ant colony algorithm for web page classification," 2008 International Symposium on Information Technology, Kuala Lumpur, 2008, pp.1-8.

[16] V. Bartik, "Association based classification for relational data and its use in web mining," 2009 IEEE Symposium on Computational Intelligence and Data Mining, Nashville, TN, 2009,pp.252-258.

[17] L. Jiao and L. Feng, "Improvement of Feature Extraction in Web Page Classification," 2010 2nd International Conference on E-business and Information System Security, Wuhan, 2010, pp. 1-3.

[18] V. Bartik, "Text-Based Web Page Classification with Use of Visual Information," 2010 International Conference on Advances in Social Networks Analysis and Mining, Odense, 2010, pp.416-420.

[19] L. K. Soon and S. H. Lee, "Classifying Web Pages Using Information Extraction Patterns Preliminary Results and Findings," 2010 Sixth International Conference on Signal-Image Technology and Internet Based Systems, Kuala Lumpur, 2010, pp. 195-202.

[20] H. Ayral and S. Yavuz, "An automated domain specific stop word generation method for natural language text classification," 2011 International Symposium on Innovations in Intelligent Systems and Applications, Istanbul, 2011, pp. 500-503.

[21] H. Mingsheng, J. Zhijuan and Z. Xiangyu, "An approach for text extraction from web news page," 2012 IEEE Symposium on Robotics and Applications (ISRA), Kuala Lumpur, 2012, pp. 562-565.

[22] C. Shaohong and W. Zhixing, "Web page classification based on Semi- supervised Naïve Bayesian EM algorithm," 2011 IEEE 3rd International Conference on Communication Software and Networks, Xi'an, 2011, pp. 242-245.

[23] D. Choi, B. Ko, E. Lee, M. Hwang and P. Kim, "Automatic Evaluation of Document Classification Using N-Gram Statistics," 2012 15th International Conference on Network-Based Information Systems, Melbourne, VIC, 2012, pp. 739-742.

[24] H. Haleem, P. K. Sharma and M. M. Sufyan Beg, "Novel frequent sequential patterns based probabilistic model for effective classification of web documents," 2014 International Conference on Computer and Communication Technology (ICCCT), Allahabad, 2014, pp. 361-371.

[25] K. B. Prakash, M. A. D. Rangaswamy and A. R. Raman, "Attribute based content mining for regional web documents," IET Chennai Fourth International Conference on Sustainable Energy and Intelligent Systems (SEISCON 2013), Chennai, 2013, pp. 368-373.

[26] M. Javed, A. Akhtar and A. K. Yusufzai, "Classification of Web Pages as Evergreen Or Ephemeral Based on Content," 2015 International Conference on Computational Intelligence and Communication Networks (CICN), Jabalpur, 2015, pp. 1381-1385.

[27] J. Wu, S. Pan, X. Zhu and Z. Cai, "Boosting for Multi-Graph Classification," in IEEE Transactions on Cybernetics, vol. 45, no. 3, pp. 416-429, March 2015.

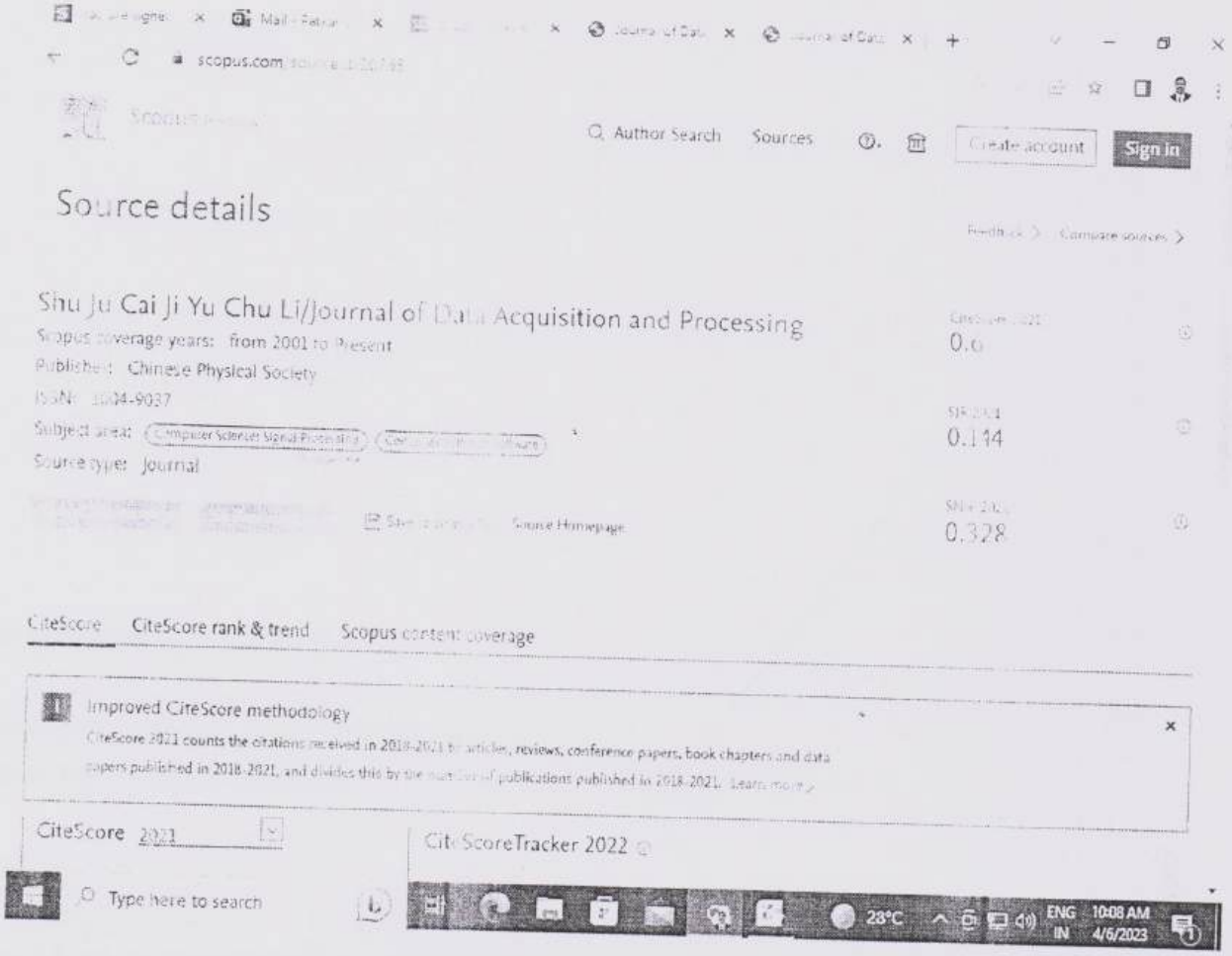
[28] W. Ren and J. Yan, "An Improved CMAC Neural Network Model for Web Mining," 2015 8th International Symposium on Computational Intelligence and Design (ISCID), Hangzhou, 2015, pp. 614-618.

[29] A. Bhardwaj and V. Mangat, "A novel approach for content extraction from web pages," 2014 Recent Advances in Engineering and Computational Sciences (RAECS), Chandigarh, 2014, pp. 1-4.

[30] J. Zhu, H. Wang and J. Mao, "Sentiment classification using genetic algorithm and Conditional Random Fields," 2010 2nd IEEE International Conference on Information Management and Engineering, Chengdu, 2010, pp. 193-196.

[31] PATEL, DHRUVA S., and KETAN SARVAKAR. "Search Engine Optimization Page Rank Algorithm." International Journal of Computer Science Engineering and Information Technology Research 8 (2018): 17-24.

[32] Satyanarayana, K. N. V., et al. "Mobile app & iot based smart weather station." International Journal of Electronics, Communication and Instrumentation Engineering Research and Development (IJECIERD) 7.4 (2017): 1-8.


scopus.com
Author Search
Sources
Create account
Sign in
Source details
Shu Ju Cai Ji Yu Chu Li/Journal of Data Acquisition and Processing
Scopus coverage years: from 2001 to Present
Publisher: Chinese Physical Society
ISSN: 1004-9037
Subject area: Computer Science: Signal Processing
Source type: Journal
Source Homepage
0.6
0.144
0.328
CiteScore
CiteScore rank & trend
Scopus content coverage
Improved CiteScore methodology
CiteScore 2021 counts the citations received in 2018-2021 to articles, reviews, conference papers, book chapters and data papers published in 2018-2021, and divides this by the number of publications published in 2018-2021. Learn more
CiteScore 2021
CiteScoreTracker 2022
Type here to search
28°C
ENG
IN
10:08 AM
4/6/2023

JCST Journal of Data Acquisition and Processing

HOME | ABOUT JCST | AUTHORS | REVIEWERS | PUBLISHED PAPERS

- Current Issue
- Archive

Bimonthly Since 1986
ISSN 1004-9037

Publication Details
Edited by: Editorial Board of Journal of Data Acquisition and Processing
P.O. Box 2704, Beijing 100190, P.R. China
Sponsored by: Institute of Computing Technology, CAS & China Computer Federation
Undertaken by: Institute of Computing Technology, CAS
Published by: SCIENCE PRESS, BEIJING, CHINA
Distributed by:
China: All Local Post Offices

Current Issue

Jan 2023, Volume 38 Issue 1

Article

1. THE STATUS OF [illegible] COLLEGES LIBRARY'S SERVICES: BASIS FOR DEVELOPMENT PLAN

[illegible]

Journal of Data Acquisition and Processing, 2023, 38 (1): 01-16.

2. DETAILED INVESTIGATION ABOUT CYBER SECURITY IN RECENT DIVES ON ARTIFICIAL INTELLIGENCE

[illegible]

Journal of Data Acquisition and Processing, 2023, 38 (1): 17-25.

3. CONTEXT AWARE EXTRACTION OF CONCEPTS FROM UNSTRUCTURED DATA USING MACHINE LEARNING ALGORITHMS

[illegible]

Journal of Data Acquisition and Processing, 2023, 38 (1): 26-43.

Submit Your Manuscript

Shu Ju Cai Ji Yu Chu Li/Journal of Data...

Signal Processing

SJR 2021
0.14

Type here to search
28°C ENG IN 10:08 AM 4/6/2023

57. A NEURAL NETWORK BASED MACHINE TRANSLATION MODEL FOR ENGLISH TO AHIRANI LANGUAGE

[illegible]

Journal of Data Acquisition and Processing, 2023, 38 (1): 741-775

58. CONCEPTUALISING THE SCIENCE OF CRIMINOLOGY: A CONTEMPORARY APPROACH

[illegible]

Journal of Data Acquisition and Processing, 2023, 38 (1): 776-796

59. DEFILING THE DEAD: UNDERSTANDING NECROPHILIA UNDER THE INDIAN LEGAL FRAMEWORK

[illegible]

Journal of Data Acquisition and Processing, 2023, 38 (1): 797-796

60. A WEB PAGE CLASSIFICATION SURVEY ON TECHNIQUES USING TEXT MINING

[illegible]

Journal of Data Acquisition and Processing, 2023, 38 (1): 797-813

61. DYNAMIC BANDWIDTH CONTROL ALGORITHM FOR RELIABLE DATA DISSEMINATION IN WIRELESS SENSOR NETWORKS

[illegible]

Journal of Data Acquisition and Processing, 2023, 38 (1): 814-832

62. MATHEMATICAL AND STATISTICAL STUDY OF STUDENT'S CHOICES ON GETTING ADMISSION IN

Type here to search

28°C ENG IN 10:09 AM 4/6/2023

JCST Journal of Data Acquisition and Processing

Bimonthly Since 1986
ISSN 1004-9037

Publication Details
Edited by: Editorial Board of Journal of Data Acquisition and Processing
P.O. Box 2704, Beijing 100190, P.R. China
Sponsored by: Institute of Computing Technology, CAS & China Computer Federation
Undertaken by: Institute of Computing Technology, CAS
Published by: SCIENCE PRESS, BEIJING, CHINA
Distributed by:
China: All Local Post Offices

1 Jan 2023, Volume 38, Issue 1
Article

Submit Your Manuscript

1. A WEB PAGE CLASSIFICATION SURVEY ON TECHNIQUES USING TEXT MINING

Dr. Rajesh D Bamniya, Dr. A. M. Pawar, Mrs. S. S. Kapil, Mrs. Anusha Vilas Mira Ratuja Jivan Tikait, Dr. [illegible] Jadhav, Dr. Uday K. Kumar

Journal of Data Acquisition and Processing, 2023, 38 (1): 797-813.

Abstract
The rapid growth of the World Wide Web (WWW) is demanding for an automated assistance for Web page classification and categorization. In most existing Web page classification tasks, Web pages are classified into topical categories based on their content regardless of the possible relationships among them. In this paper, a comprehensive survey on classification of Web pages is presented. The features for creating rich information, classifiers and datasets used for experimentation are also discussed. It also gives comparative analysis of all Web page classification techniques. The challenges/issues involved in developing Web page classification are also discussed. This would help researchers to take up new work on Web page classification and address most of the important challenges/issues.

Keyword

Shu Ju Cai Ji Yu Chu Li/Journal of Data...
Q4 Signal Processing
SJR 2021
0.14

Type here to search
28°C ENG IN 10:09 AM 4/6/2023

Mail - Par... Scopus... Journal of... Not secure

JCST Journal of Data Acquisition and Processing

Bimonthly Since 1986
ISSN 1004-9037

Publication Details
Edited by: Editorial Board of Journal of Data Acquisition and Processing
P.O. Box 2704, Beijing 100190, P.R. China
Sponsored by: Institute of Computing Technology, CAS & China Computer Federation
Undertaken by: Institute of Computing Technology, CAS
Published by: SCIENCE PRESS, BEIJING, CHINA
Distributed by:
China: All Local Post Offices

1 Jan 2023, Volume 38 Issue 1
Article

Submit Your Manuscript

1. MACHINE LEARNING AND EASYOCR BASED LANGUAGE RECOGNITION FOR HANDWRITTEN INDIC EXTRACTION AND CLASSIFICATION

Dr. Uday C. Patkar, Mrs. P. [illegible] Tirabade, Mrs. N. S. Patil, Dr. A. M. Pawar, Dr. Uday Patil, Mrs. Gauri Rao, Mrs. S. S. Patil, K. D. Bamane

Journal of Data Acquisition and Processing, 2023, 38 (1): 761-775.

Abstract

Machine Translation is the process of converting one natural language into another through the use of computer-assisted translation. The fundamental goal is to bridge the linguistic gap that exists between two distinct languages spoken by people, communities, or countries. India is a multilingual country, with different territorial languages spoken in different parts of the country. However, not all Indians are polyglots. There are 22 constitutional languages and ten widely used scripts in the world. The majority of the Indians, particularly the residents in distant areas, do not understand, read, or write English, making the use of an efficient language translator necessary and desirable. Machine translation systems that translate content from one language to another will contribute to the advancement of the enlightened

Shu Ju Cai Ji Yu Chu Li/Journal of Data...
Q4 Signal Processing
SJR 2021 0.14

Warning: [illegible]bolmgshare.sercu.com...
Type here to search
28°C ENG IN 10:10 AM 4/6/2023

Advances in Water Science
2022; 33(3)

ISSN: 1001-6791

AWS水科学进展
Advances in Water Science

Accidents Sensing Car Wiper and Location using IoT-Based Notification

Dr. Manisha Ajaykumar Dudhedia*[1], Dr. Aarti Amod Agarkar[2] & Dr. Uday Chandrakant Patkar[3]
*[1]Assistant Professor, Department of Electronics and Telecommunication Engineering, Marathwada Mitra Mandal's College of Engineering, Pune, India Affiliated to Savitribai Phule Pune University, Pune, India
[2]Associate Professor, Department of Computer Engineering, Marathwada Mitra Mandal's College of Engineering, Pune, India Affiliated to Savitribai Phule Pune University, Pune, India
[3]HOD, Department of Computer Engineering, Bharati Vidyapeeth's College of Engineering Lavale Pune

Abstract: *We suggest an Internet of Things-based solution that attempts to increase driving security in wet weather. The system is made up of rain and accident sensors that are connected to a cloud server, together with automobile wipers and position tracking features. When the system senses rain, the wipers begin operating automatically, and the sensors provide real-time data to the server regarding the rain intensity and visibility level. The technology instantly alerts the server in the event of an accident, and the server subsequently notifies the nearby emergency services as well as other linked vehicles. The suggested approach can greatly lower the chance of accidents and increase both the general and personal safety of drivers and passengers in wet weather.*

Keywords: *IoT (Internet of Things), Rain sensing, Car wiper control, Accident detection, Location tracking, Real-time notifications*

1. Introduction

Rainy weather may be dangerous for drivers since it makes it harder to see and makes the roads more likely to be slippery. In the United States, weather is a factor in around 21% of automobile accidents, with rain being the most frequent weather condition, according to a study by the Federal Highway Administration (FHWA). Thus, it is crucial to create technology that can increase driving security in wet weather.[1]

With the help of the Internet of Things (IoT), which connects numerous devices and sensors to the internet, it is now possible to gather and analyse data in real time. In this project, we propose an Internet of Things (IoT)-based system that combines location monitoring, automobile wipers, and collision sensors to increase road safety in wet weather. Rain can be detected, the wiper speed may be changed, and the system can provide the server real-time data regarding the visibility and rain severity. Moreover, the technology may immediately inform the cloud server in the event of an accident, which alerts the nearby emergency services as well as other linked cars. The suggested solution can greatly lower the probability of accidents and increase both the general and personal safety of drivers and passengers in wet weather.[2]

The present vehicle wipers are manual frameworks that work on the standard of manual exchanging. So here we propose a programmed wiper framework that naturally turns on identifying precipitation and stops when downpour stops. Our undertaking presents this framework to mechanize the wiper framework having no requirement for manual mediation. For this reason we use downpour sensor alongside microcontroller and driver IC to drive the wiper engine. Our framework utilizes downpour sensor to identify downpour, this sign is then handled by microcontroller to make the ideal move. The downpour sensor deals with the rule of involving water for finishing its circuit, so when downpour falls on its circuit gets finished and conveys a sign to the microcontroller. The microcontroller now processes this information and drives the engine IC to perform required activity. The engine driver IC presently drives a servomotor to mimic as a vehicle wiper.

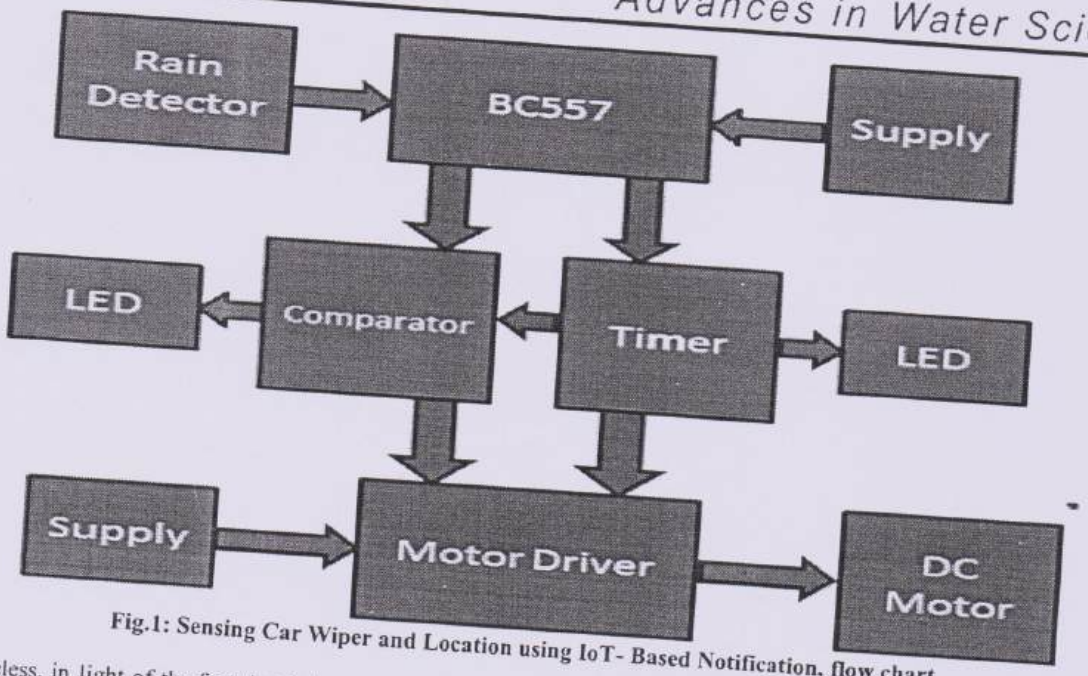


Fig.1: Sensing Car Wiper and Location using IoT- Based Notification, flow chart

Nonetheless, in light of the fact that independent driving alone isn't adequate to perform safe driving, independent agreeable driving utilizing vehicle-to-everything (V2X) correspondence innovation is required. Independent helpful driving isn't decided by just a single vehicle however speaks with neighboring vehicles or side of the road fixed V2X correspondence units (street side unit (RSU)) to make decisions for more secure driving. In any case, security factors should be thought of, on the grounds that V2X correspondence is utilized to speak with different components. As a matter of fact, white programmers penetrated vehicles from an external perspective and showed instances of assaults that controlled different capabilities in the vehicle [5,6]. In such manner, measures for message uprightness confirmation, validation, and individual security ought to be executed. Accordingly, security framework and norms have been laid out.

2. Security Analysis

There are two security weaknesses in independent helpful driving utilizing the SCMSs. The first is the handling velocity of the encryption module. In the Notification of Proposed Rulemaking for Government Engine Vehicle Security Principles [2][3] gave by the Public Parkway Traffic Wellbeing Organization (NHTSA), it is expressed that DSRC gear should perform approval of somewhere around 5500 BSMs each second. Message handling continues in the request for deciphering the substance of the message after its validation. In this manner, in packed circumstances, the OBU should have the option to perform in excess of 5500 BSM signature checks each second. Be that as it may, ECDSA can't process 5500 BSMs each second since it demands more investment to verify than the current RSA [2][4][7]. As per the examination that deliberate the confirmation time in the genuine OBU [1][4], handling pace of OBU is just 35 checks each second on account of the product module. On account of the equipment module, handling rate of OBU is just 163 confirmations each second.

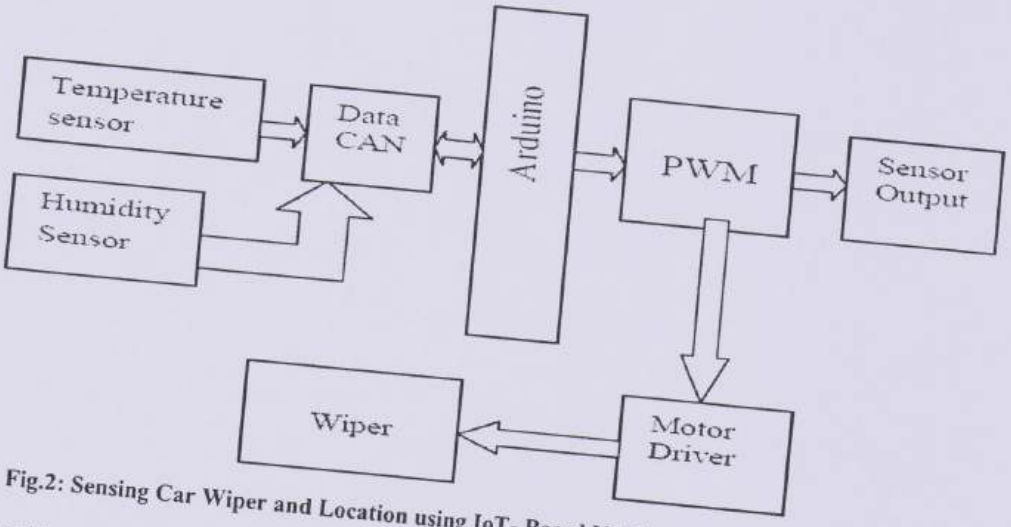


Fig.2: Sensing Car Wiper and Location using IoT- Based Notification, block diagram

In the end, attributable to impediments in the exhibition of equipment and cryptographic modules, numerous BSM validations emerging from blockage circumstances are not performed well. The subsequent weakness is DoS assault. This weakness emerges from the previously mentioned weakness, which forestalls the typical way of behaving of OBUs by sending more BSM messages than they can deal with. These weaknesses can prompt car crashes or blockage during independent agreeable driving utilizing SCMSs. Moreover, assuming validation is excluded to forestall DoS assaults, the gamble of fabrication or it is experienced to alter assaults. In this part, circumstances in which clashes happen in independent helpful driving conditions and security dangers that can emerge in every circumstance are talked about.

Algorithm

A Danger classifier characterizes each got BSM as per relative area with different vehicles and stores it in danger table. Along these lines, when in excess of 5500 danger BSMs happen each second, these BSMs can be ordered into a few kinds. From that point forward, just the primary message of each kind performs signature check and resulting messages are disregarded. The explanation is that the danger to the disregarded message is now producing a caution.

There are three measures for characterizing BSMs in a danger classifier. The first is the wellbeing application to be utilized. The message is grouped by deciding the security application that is utilized to alarm the driver. The following stage is the area of the Distant Vehicle (RV). RV is the source of BSMs. It's anything but a genuine source (assailant). It is the source written in BSMs produced by assailant. Eight spaces are characterized in light of the Host Vehicle (HV) to address the area of the RV. HV is collector of BSMs. As displayed in Figure 5, it is feasible to group the area of the RV from which the message is sent, by isolating it into eight zones, in view of the course in which the HV continues. The third element is the course of movement of the vehicle.

Block diagram: The Architecture diagram

A cloud server, a position GPS sensor, a rain and accident sensor, automobile wipers, an IoT board, and a notification service are some of the parts that make up the system. The IoT board, which is attached to the rain and accident sensors, gathers data from them and transmits it to the cloud server for analysis. The IoT board is also connected to the automobile wiper, which automatically modifies its speed according to the amount of rain falling. The IoT board is attached to the location GPS sensor, which is used to track the vehicle's location.[3]

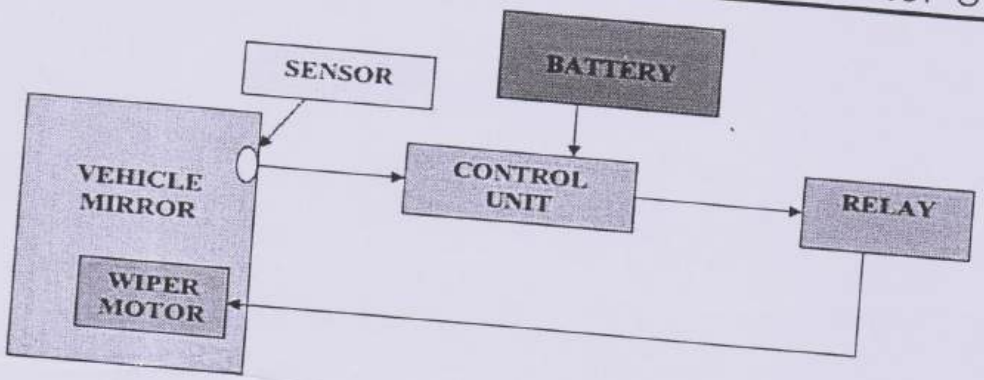


Fig. 3: Automatic rain-sensing wiper block schematic

Data from the IoT board is sent to the cloud server, which then analyses it to look for accidents, accidents with high visibility, and rain. In the event of an accident, the server immediately alerts the notification service, which then notifies the nearby linked vehicles and emergency services. The notification service also notifies the driver interface via notifications of any nearby accidents and the current weather conditions.[4]

The proposed system's overall goal is to increase road safety during rainy weather by giving drivers real-time information on the strength of the rain, the degree of visibility, and accidents so they may alter their driving and avoid possible risks.[5]

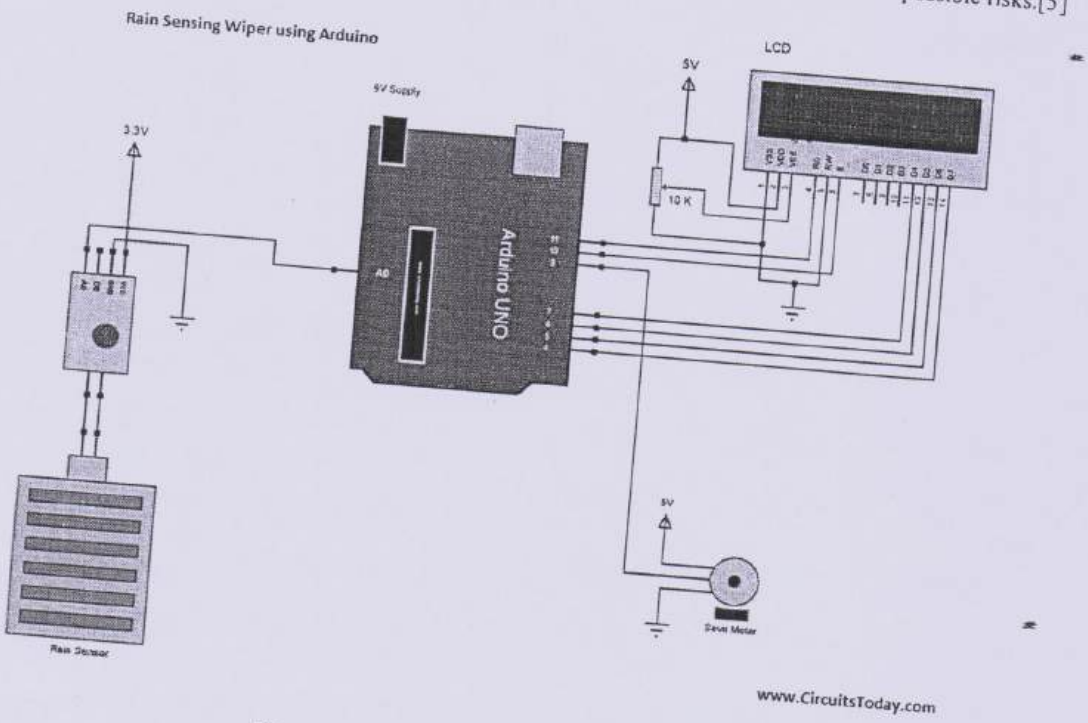


Fig.4: Block diagram of the proposed model

Existing System

There aren't any systems on the market right now that integrate auto wipers, rain and accident sensors, and location monitoring. Depending on the quantity of rain observed, certain automobiles contain rain sensors that may automatically change the wiper speed. The lack of real-time information on visibility and rain severity, however, makes it difficult for drivers to change their

driving style. Also, there are no technologies that can immediately notify nearby linked vehicles and emergency services of accidents and give them notifications.[6]

3. Methodology

The comprises of rain and accident sensors connected to a cloud server, together with auto wipers and position tracking features. Data from the sensors is gathered by the system using an IoT board, which then transmits it to the cloud server for analysis. Based on the amount of rain the rain sensor detects, the IoT board also regulates the wiper speed.[7] When the system senses rain, the wipers begin operating automatically, and the sensors provide real-time data to the server regarding the rain intensity and visibility level. The data is analysed by the cloud server, which then notifies the driver interface about the current weather. In the event of a collision, the server can also transmit alerts to the notification service, which subsequently notifies the nearby connected vehicles and emergency services. The technology tracks the vehicle's location using a GPS sensor and can give information on nearby accidents and perilous road conditions. The driver interface receives messages from the notification service notifying them of any nearby incidents and the safest speed to travel under certain conditions.

The overall goal of the proposed system is to increase traffic safety during wet weather by giving drivers timely information on the amount of rain, the visibility of the road, and accidents so they can adapt their driving and stay clear of possible risks. During wet weather, the technology can considerably lower the probability of accidents and increase overall driver and passenger safety.

Details of components

The system is to increase traffic safety during wet weather by giving drivers timely information on the amount of rain, the visibility of the road, and accidents so they can adapt their driving and stay clear of possible risks. During wet weather, the technology can considerably lower the probability of accidents and increase overall driver and passenger safety.

Rain Sensor: One element that recognises the presence of rain is the rain sensor. In the proposed system, it is utilised to gauge the strength of the downpour and give the cloud server and driver real-time updates on the weather.

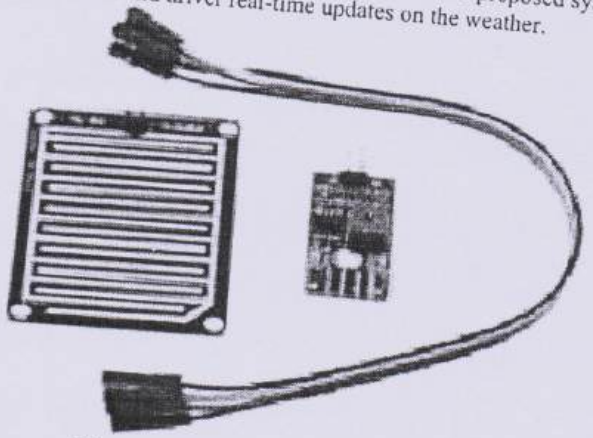


Figure 5-THE RAIN SENSOR

- **Accident Sensor:** The accident detector is a part that recognises any unexpected collision or contact. It is used to identify mishaps in the proposed system and transmit instant notifications to the cloud server and notification service.
- **Car Wiper:** A part of the automobile that is utilised to clean the windscreen is the wiper. With the suggested method, it is wired to an IoT board, which modifies its speed according to the amount of rain the rain sensor detects.
- **IoT Board:** The IoT board is a component that gathers information from the car wiper, GPS position sensor, rain and accident sensors, and other devices. It transmits the information to a cloud server for analysis and regulates the speed of the windscreen wiper based on the amount of rain the rain sensor detects.
- **Cloud Server:** The cloud server is a part that takes information from the IoT board and processes it to identify accidents, the degree of visibility, and rain intensity. In the event of an accident or dangerous weather, it notifies the notification service and driver interface.
- **GPS Location Sensor:** The place Real-time tracking of the vehicle's location is done through a GPS sensor. The suggested system uses it to disseminate information about close-by incidents and perilous driving conditions.

- **Notification Service:** In the event of an accident or dangerous weather circumstances, the notification service is a component that sends notifications to the driver interface, emergency services, and other connected cars nearby.
- **Driver Interface:** The driver interface is a part that shows information about the current weather, the advised speed limit, and neighbouring accidents in real-time. It enables the motorist to make necessary driving adjustments and steer clear of any dangers.

4. Results

The "Rain and Accidents Detecting Vehicle Wiper and Location utilising IoT-Based Notification" prototype was put to the test using these elements. The prototype was fitted in an automobile and put through a series of rainy weather tests. The outcomes demonstrated that the system was capable of precisely detecting rain intensity and adjusting wiper speed. The technology might also recognise accidents and deliver instant notifications to the cloud server and notification service. The GPS sensor's ability to track the location of the car as well as offer details on nearby collisions and perilous road conditions. The driver interface provided real-time data on the weather, suggested speed limit, and close-by accidents, enabling them to alter their driving and prevent any dangers.

5. Conclusion

An innovative strategy for enhancing road safety in wet weather situations is provided by the system "Rain and Accidents Detecting Vehicle Wiper and Location using IoT-Based Notification." The technology gives the driver and emergency services access to real-time information on rain intensity, visibility level, and accidents by fusing rain and accident sensors with vehicle wipers and location tracking capabilities. During wet weather, the system can greatly lower the probability of accidents and increase both the general and personal safety of drivers and passengers. In this review, a strategy to forestall DoS assaults in independent helpful driving utilizing SCMSs is proposed. The proposed strategy orders danger messages to validate just the main messages got inside a similar gathering. Contrasted with VoD, which is a strategy for forestalling DoS assaults, this technique has shown the capacity to handle messages at a speed of 6.3 times to multiple times quicker, contingent upon the circumstance. This ends up being a method that successfully forestalls DoS goes after that send an enormous number of messages. Nonetheless, in the examination, it is challenging to report that a precise outcome was gotten attributable to the presentation distinction in the handling speed between the PC and the OBU while performing it on the PC as opposed to in the genuine OBU. In future exploration, the test is to try different things with the genuine OBU and decide its productivity.

References

1. Goyal, S., Aggarwal, R., & Khanna, A. (2021). Intelligent automobile wiper system for automated rain sensing and wiping. Second IEEE International Conference on Recent Trends in Electronics, Information, and Communication Technologies (RTEICT) was held in 2021; (pp. 1000-1004). IEEE.
2. Almutairi, M. A., Akbar, M. A., Alshahrani, M. A., Almalki, N. M., & (2020). IoT-Based Smart Rain Detecting System for Vehicle Wiper Control the Third Middle East and North Africa Conference on Biomedical Engineering (MENABME), which will be held in 2020, (pp. 1-5). IEEE.
3. J. H. Lee, J. H. Park, & J. H. Kim (2021). An IoT-Based Smart Vehicle Wiper Control System 33(4), 865-876, Journal of Information Science and Engineering.
4. Liu, C., and W. Liu (2019). An Internet of Things-Based Smart Vehicle Wiper System for Rain Detection and Automated Wiping 3rd International Conference on Intelligent Transportation Engineering (ICITE 2019) Proceedings (pp. 67-71).
5. Yang, L., Guo, X., & Zhang (2018). a smart car wiper system for controlling and detecting rain. In the ICRCA 2018 Proceedings: International Conference on Robotics, Control, and Automation (pp. 186-190).
6. Kavitha, G., and D. P. Chakravarthy (2018). IoT-based smart rain sensing system. 7(2), 104–107, International Journal of Engineering and Technology (UAE).
7. Alarie, N., Ahmad, A., Javaid, M., & Imran, N. (2019). IoT-based Smart Vehicle Wiper System for Automatic Rain Detection The 2019 ICCAIS, the Second International Conference on Computer Applications and Information Security (pp. 1-6). IEEE.
8. Zhou, X., and Zhang, H. (2018). Solution for Smart Transportation that Controls Vehicle Wipers Depending on Rain. 2018 International Conference on Advances in Energy, Environment, and Chemical Engineering Proceedings.

9. European Automobile Manufacturers Association, "The automobile industry pocket guide 2020–2021," 2020, https://www.acea.be/uploads/publications/ACEA_Pocket_Guide_2020-2021.pdf.
10. European Automobile Manufacturers Association, "The automobile industry pocket guide 2019–2020," 2019, https://www.acea.be/uploads/publications/ACEA_Pocket_Guide_2019-2020.pdf.
11. C.-Y. Chan, "Advancements, prospects, and impacts of automated driving systems," International Journal of Transportation Science and Technology, vol. 6, no. 3, pp. 208–216, 2017.
12. S. Singh, "Critical reasons for crashes investigated in the national motor Vehicle crash causation survey," Traffic Safety Facts Crash Stats, vol. 812 115, 2015.

Source details

Feedback > Compare sources >

Shuikexue Jinzhan/Advances in Water Science

Scopus coverage years: from 1998 to Present

Publisher: China Water Power Press

ISSN: 1001-6791

Subject area: Earth and Planetary Sciences: General Earth and Planetary Sciences

Source type: Journal

Save to source list Source Homepage

CiteScore 2022
3.1

SJR 2022
0.413

SNIP 2022
0.681

CiteScore | CiteScore rank & trend | Scopus content coverage

Improved CiteScore methodology

CiteScore 2022 counts the citations received in 2019-2022 to articles, reviews, conference papers, book chapters and data papers published in 2019-2022, and divides this by the number of publications published in 2019-2022. Learn more >

CiteScore 2022

3.1 = 963 Citations 2019 - 2022 / 315 Documents 2019 - 2022

Calculated on 05 May, 2023

CiteScoreTracker 2023

3.9 = 1,273 Citations to date / 326 Documents to date

Last updated on 05 December, 2023 • Updated monthly

CiteScore rank 2022

Analysis of Image Parameters in 3D Camera Using Regression Algorithm

Aishwarya Pathak*, Neha Ganvir , Prashant Kadam , Ajinkya Hasabe , Sagar Kale , Shrikant Sutar

Department of Engineering, Bharati Vidyapeeth College of Engineering, Lavale, Pune.

Abstract:

Three dimensional imaging is increasing day by day and many attractive electronicgadgets are available in the market now a days. Three-dimensional imaging finds its applications in the area of image printing, clinical surgery, industry automation etc. Universally compatible fast and morereliable more of acquiring data are the basic requirements today. Thus there is a need to develop an electronic module that can fulfill all the requirements. This paper describes a design of time of flight camera also called as PMD camera. This camera measures the distance between the target device and the camera pixel, also can capture the height width and the depth of an image. Thus, the consequences of 2D cameras are overcome inthis type of 3D camera. This paper focuses on experimental results of the PMD camera using the timeof flight technology and correction of the artifacts that occur during capturing the target scene using deep learning algorithm.

Keywords : CMOS, CW, Time of Flight Technology, Wiggling.

DOI Number: 10.14704/nq.2022.20.9.NQ44661 **Neuro Quantology 2022; 20(9):5671-5677**

Introduction

In recent years, three-dimensional imaging has become important in the industrial, medical, and consumer application areas. The machine vision systems used for capturing images are highly empowered with various types of image processing techniques based upon the light sources used. This allows faster and more accurate inspection of components thereby reducing distortions to a larger extent. Whenever a scene is captured, a two- dimensional type of signal is stored into the device. This data is nothing but the coordinate of the captured scene. Maybe it is height, width, depth, the intensity of the captured scene, or pixel information. These parameters specify whether the capturing device is a two-dimensional device or three dimensional or more. These digital devices provide the intensity level of the screen capture but the depth information is lost. In such a case, three-dimensionalimaging comes into picture. A newly developedimage sensor called as photonic mixer device initiates the property of three dimensions imaging. This type of 3D sensor uses the time of flight technology which is most probably used in the 3D type of cameras. The PMD sensor along with the time of flight technology provides depth information of the target object along with the amplitude distance and phase of the scene which is equal to the 2D image acquired by any standard camera this type of PMD camera differentiate the 2D standard CCD camera only due to the availability of the depth information or the third co-ordinate of the image. The 3D sensors required for capturing images are now replacing the use of conventional cameras due to fast and reliable acquisitions of the target scene which is the main requirement in many areas of industries.

Materials and Methods

Photonic mixer devices are abbreviated as PMD. The PMD chip works on the principle of time of flight technology. As shown in the figure1, the time of flight technology is used to calculate the distance between the target object and the camera.

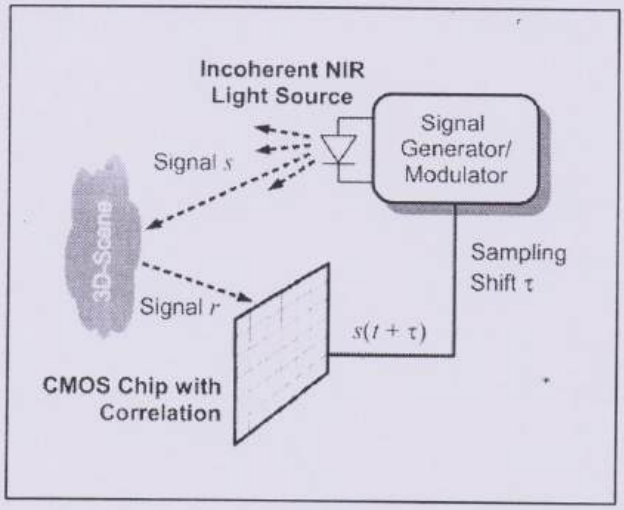


Fig.1: Time of Flight Technique [10]

It also calculates the time that is required for the light pulse to travel what is the object and reflect back. The accuracy depends upon the time required to travel. There are two types of techniques used in time of flight technique those are continuous-wave modulation and pulse modulation as shown in fig. 2.

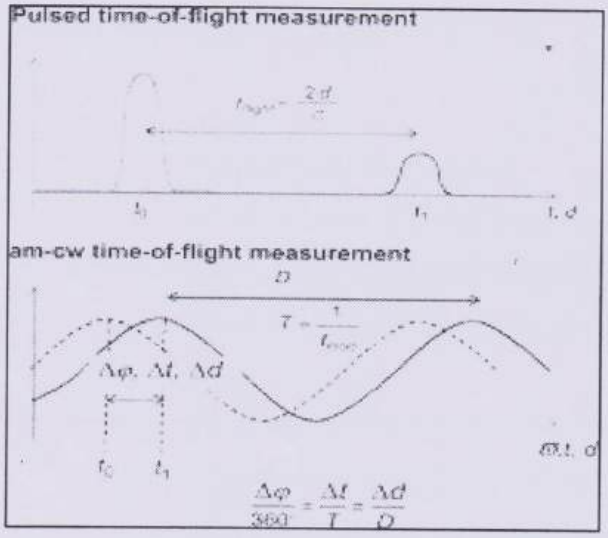


Fig.2: Pulsed Time of Flight and AM-CW Time of Flight Technique [2]

The pulse modulation technique produces very short light pulses. Thus, it requires more bandwidth as the rise time and fall time are very fast. The rise time and fall time are necessary because they as your accurate distance of the incoming light pulse. The four PMD sensors use the continuous wave modulation technique, this type of technique does not require any fast rise and fall times[4,5]. Therefore the bandwidth requirement is very less in continuous wave modulation technique and the light source is modulated before it gets transmitted on the target object. Therefore the modulated signal and received optical signal are correlated together. 5672

The correlation output results in phase and amplitude of the two signals. The phase difference that is obtained gives the distance between the camera and the target object. The correlation that takes places inside the processing circuitry has two signals of same frequencies. This type of modulation is known as homodyne modulation. The PMD-ToF [4] devices use the homodyne type of modulation technique. Thus, this modulation technique gives an advantage of requiring lesser bandwidth.

$$c(t) = (\frac{a}{2}) \times \cos(\Phi + \omega t) \quad \text{.....(3)}$$

The phase difference and the amplitude from the correlation signals are extracted by using the four free shifting techniques this technique require samplingthe correlation function at four different intervals. Considering the 4-phase shifting technique, the correlation signal is sampled at ωt0=0°, ωt1=90°, ωt2=180° and ωt3=270°. Thus, substituting the values in expression for c (t), we get:

$$c(t_0) = (\frac{a}{2}) \times \cos(\Phi) \quad \text{.....(4)}$$

$$c(t_1) = -(\frac{a}{2}) \times \sin(\Phi) \quad \text{.....(5)}$$

$$c(t_2) = -(\frac{a}{2}) \times \cos(\Phi) \quad \text{.....(6)}$$

$$c(t_3) = (\frac{a}{2}) \times \sin(\Phi) \quad \text{.....(7)}$$

$$a = \frac{\sqrt{[r(\tau_3) - r(\tau_1)]^2 + [r(\tau_0) - r(\tau_2)]^2}}{2} \quad (8)$$

Thus, the amplitude is given as:

$$\Phi = \tan^{-1}\left(\frac{r(\tau_3) - r(\tau_1)}{r(\tau_0) - r(\tau_2)}\right) \quad (9)$$

The phase signal is given as:

Measurement of Signal Amplitude and Phase

The operation of PMD sensor transmission of the modulated light signal and reflection of the modulated light from the object [9]. Thus, received

The distance is calculated as:

$$D = \frac{c \times \Phi}{4 \pi f_{mod}} \quad (10)$$

Optical light signal is correlated with the modulation signal. Thus the correlation of the two signals results in phase difference between the modulated light signal and the received optical signal. The phase difference that is obtained corresponds to the distance between the sensor and the targeted object. As shown in the figure 3, the phase shifting technique isinvolves four phase shift.

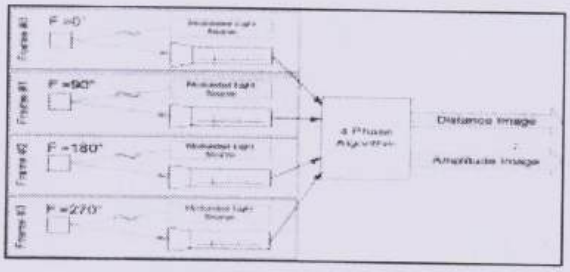


Fig.3: Four Phase Shifting Algorithm [7]

The measurement of the distance amplitude and phase signals is calculated using the four phase shifting algorithm. Assume that a signal travels at the speed of light and it reflects back to the camera with the phase shift of Φ. The modulation signal is given as s(t) and the received signal as r(t) with modulation amplitude as 'a' and phase shift 'Φ'.

$$s(t) = \cos(\omega t) \quad (1)$$

$$r(t) = 1 + (a^* \cos(\omega t + \emptyset)) \quad (2)$$

The resultant correlation is given as:

The maximum distance is given as Φ=2π.Therefore

for a given modulating frequency the distance will be fixed as the correlation takes place in homodyne mode. The range obtained from 0 to dmax is called asunambiguous range.

Working Principle of PMD Sensor

The structure of sensor is based on thestandard CMOS technology. The figure 4 below shows the working mechanism of PMD sensor.

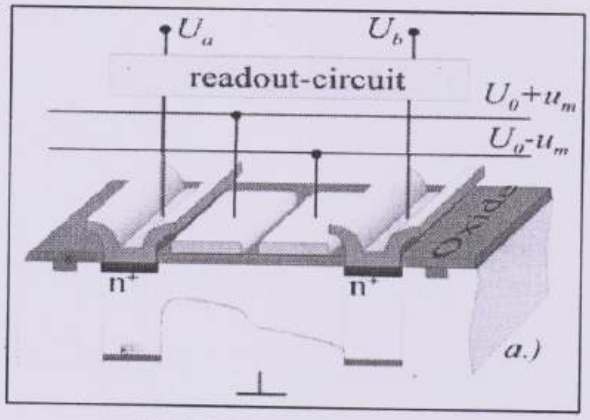


Fig.4: PMD Structure [12]

The PMD sensor consists of two modulating signals namely (Uo + Um) and (Uo – Um). The two modulating signals form a polysilicon gate which is isolated from the p-type substrate by an oxide layer. This whole structure forms of MOScapacitor. The two modulating signals are always out of phase with each other. Therefore the whole area forms a optical zone of the PMD sensor for receiving other modulated signals. Modulating signal, are two reverse biased diodes which have common anode on the ground potential. These form charge wells in the PMD sensor. Charge wells are used for collecting the charges that are generated when the light signal falls on the cell. These diodes are also called as read out diodes. The readout diodes are used in measuring the charge that gets accumulatedin the charge wells. The Ua and Ub terminals are the output terminals of the PMD sensors. As shown in figure 5, when light incidents on the optical sensitive zone electron-hole pairs get generated. Depending upon the modulation signal applied, there is a potential voltage generated does the electrons move either to the left or the right end of the charge wells. The readout diodes provide the charge accumulated in the corresponding charge wells. The sum of the channel data gives the total photocurrent corresponding to the optical intensity while the difference of the output signal gives the correlation product of the reflected optical signal and the input signal.

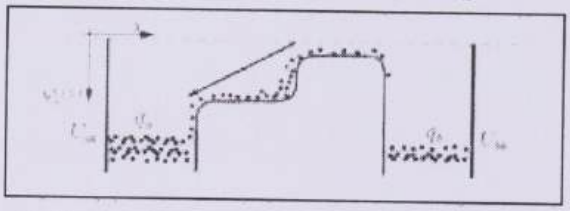


Fig.5: Charge Accumulation in PMD Sensor[6]

The time that is required for the channel data to accumulate in the charge wells is called as the integration time. In one integration time, there are many cycles of the modulating signal as the modulating signal is of high frequency. At every interval of the integration time, various effects are seen at the output of the PMD sensor of different value.

The performance of the PMD sensor increases with increase in the integration time. This region is called as the operating region [6]. If the charges start to saturate in the PMD cell, then the integration time goes out of the operating region thereby affecting the output of the PMD sensor. Thus, the output begins to degrade.

Wiggling Error

The artifacts that occur in PMD processing circuitry occur due to the variation in the integration time. As the integration time varies, as soon as the light is incident on the target object and is reflected back there is some noise addition which makes the captured scene full of errors. Thus, the PMD sensor cannot capture the image depth at proper proportion. The main objective is to capture the height, width and the depth of the target scene. But, variation in integration time results in unavailability of depth information. This is called as wiggling error. The wiggling error majorly occurs because the input signal that the processing circuitry has to process is not a pure signal. The signal is included with some noise which results in some distortions. Also, the correlation of the reflected signal and the modulated input signal is does not produce a distance output with maximum distance of $\Phi=2\pi$. Therefore, ideally the distance obtained must be equal to 6.18 or d_{max} which is not the practical case. Therefore, the values of distance and phase do not match to the ideal values. This results in addition of wavy component in the correlation signal which is called as wiggling.

(i) Correction of wiggling error

The wiggling error occurs due to the occurrence of sine like component in the correlation signal output. Also some offset is present between which is nothing but the maximum distance value. Due to this additional noise like components get added to make the signal more unstable.

This problem focuses on two possible solutions mainly the offset difference and the application of regression algorithm. If the offset value is subtracted from the correlation output signal then the signal shows errors due to non-mapping of the distance component to dmax. Regression is one another solution that results into observation of continuous value errors. Regression is a useful solution which gives results for all continuously varying values. Various types of regression algorithms like linear regression, multiple linear regression, polynomial regression, stepwise regression, logarithmic regression etc. Every of this algorithm has various advantages and disadvantages which vary according to the application. Out of all this application viz the 3D camera and the occurrence of wiggling error can be rectified using the linear regression algorithm. The following section depicts the results.

Results and Discussion

There are three different types of inputs applied as input modulated signal to the processing circuitry. As shown in figure 7, 8 and 9 respectively. The input modulated signals are sine wave, rectangular wave and charging-wave.



Fig.6: Input Sine Wave



Fig.7: Input Rectangular Wave

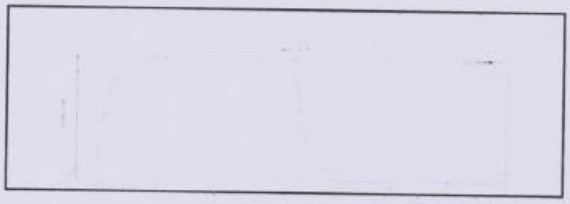


Fig.8: Input Charging Wave

The final correlation outputs for the three input waves result into phase and distance signals which are shown in figure 10, 11 and 12 respectively. These output signals depict the phase values and the distance between the target scene and the capturing device.

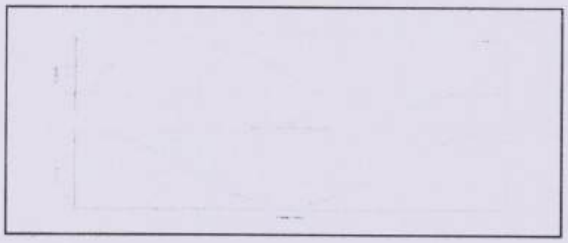


Fig.9: Output Correlation Signal for Sine Wave



Fig.10: Output Correlation Signal for Rectangular Wave

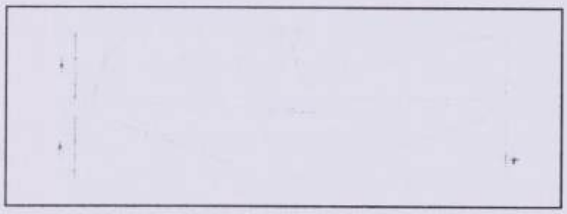


Fig.11: Output Correlation Signal for Charging Wave

Thus, it is observed that practically there cannot be a pure sine or a rectangular wave applied. There will be some noise component that gets added to the input signal. Thus the input is considered as the charging wave and the further processing is done. The wiggling error for charging wave input is as shown in figure 13.

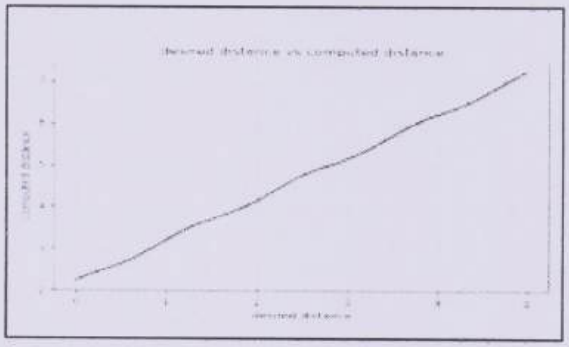


Fig.12: Wiggling Error in Distance Output

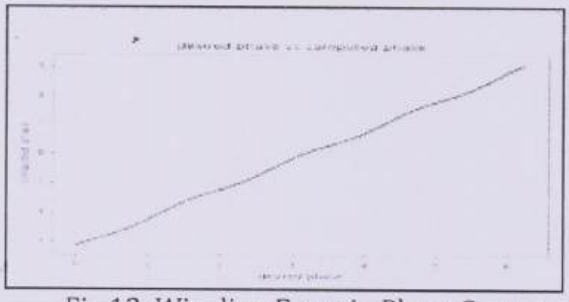


Fig.13: Wiggling Error in Phase Output

The offset subtracted from the two waves are as shown in figure 14, 15.

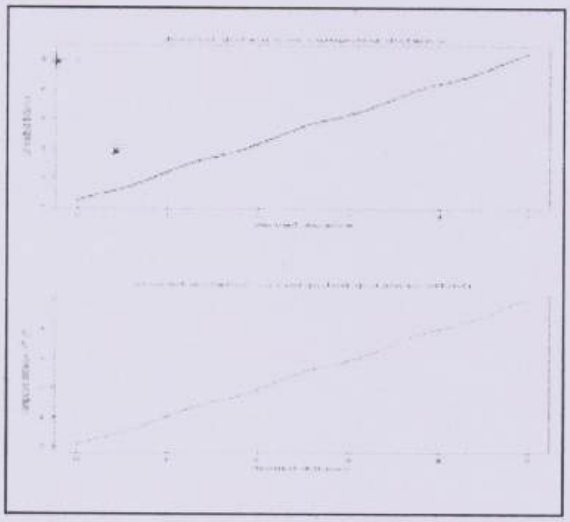


Fig.14: Offset in Distance Output

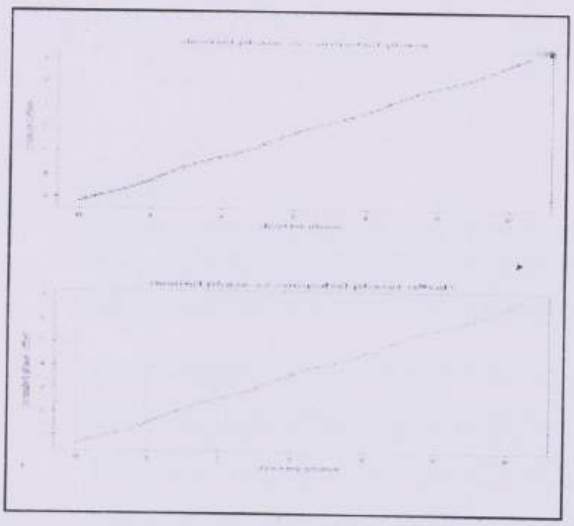


Fig.15: Offset in Phase Output

An application of regression technique is to get best possible output for the phase and distance and it is shown in figure 16.

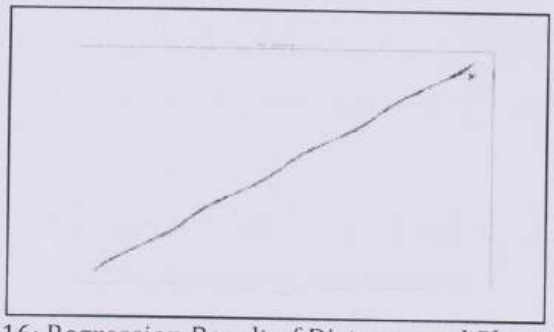


Fig.16: Regression Result of Distance and Phase

The regression results conclude that the best fit line passes through all the possible values of distance and phase and provides a linear solution to correction of error. Thus, using regression the error is seen increasing and also the points on the best fit line depict the values that has to be obtained from the correlation output results.

Conclusion

Images captured using 2D cameras faces lack of detailing and geometrical aspects in the form of height and width or length and width. Whereas the principle of 3D imaging produces an add-on effect on the captured 2D images in the form of stereoscopies illusions. This paper describes the structure of time of flight sensor and working principle of 3D camera. The working methodology of the modulated input signal and the reflected signals using regression method is proved by using mathematical calculations. The wiggling error that occurs in the 3D camera is removed by using distance and phase calculations by giving two probable solutions i.e. the offset difference and the application of regression algorithm. The final results that are obtained proven to be error free solution to the occurring artifacts in the 3D camera. The results are verified and meet the expectations.

References

[1] Meng Xua, Youchen Wangb, Bin Xuc, Jun Zhangc, Jian Renb, Stefan Poslada, Pengfei Xuc,*, "A Critical Analysis of Image-based Camera Pose Estimation Techniques" , Journal of Elsevier, January 19, 2022.

[2] R. Lange, S. Böhmer, B. Buxbaum, CMOS-based optical time-of-flight 3D imaging and ranging, Daniel Durini, High Performance Silicon Imaging (Second Edition), Woodhead Publishing, 2020

[3] Jiang, Y., Karpf, S. & Jalali, B., " Time-stretch LiDAR as a spectrally scanned time-of-flight ranging camera" , Nat. Photonics 14, 14–18 (2020).

[4] Yuzhen niu, yini zhong, wenzhong guo, yiqing shi, and peikun chen , "2D and 3D Image Quality Assessment: A Survey of Metrics and Challenges" , IEEE Access, January 4, 2019.

[5] Shuochen Su, Felix Heide, Gordon Wetzstein, Wolfgang Heidrich; Proceedings of the IEEE Conference on Computer Vision and Pattern Recognition (CVPR), (2018).

[6] Vandenberghe, S., Mikhaylova, E., D'Hoe, E. et al.,"Recent developments in time-of-flight PET". National Library of Medicine, Phys 3, 3 (2016).

[7] Chincholkar, Y. D. and Sachin Bangadkar. "A Review of ToF PMD Camera.", International Journal of Advanced Research in Electrical, Electronics and Instrumentation Energy (2015)

[8] S.Hussmann,T.Edeler , " Pseudo Four-Phase-shift Algorithm for Performance Enhancement of 3D-TOF Vision Systems" , IEEE Transcations on Instrumentation and Measurement., 59(5):1175 - 1181, June 2010.

[9] E. Charbon, "Introduction to time-of-flight

imaging",IEEE, pp. 610-613, 2012

[10] Marvin Lindner, Ingo Schiller, Andreas Kolb, Reinhard Koch, Time-of-Flight sensor calibration for accurate range sensing, Computer Vision and Image Understanding, Volume 114, Issue 12, (2010).

[11] Hahne, Uwe and Marc Alexa. "Depth Imaging by Combining Time-of-Flight and On-Demand Stereo." Lecture Notes in Computer Science book series (LNIP,volume 5742) (2009).

[12] Lindner, Marvin & Kolb, Andreas. Compensation of Motion Artifacts for Time-of-Flight Cameras. Lect. Notes Comput. Sci.. 5742. (2009).

[13] Lange, Robert Tjarko, "3D time-of-flight distance measurement with custom solid-state image sensors in CMOS/CCD-technology.", Computer Science' 13 November (2006).

[14] Ringbeck, Dr.-Ing. Thorsten. "A 3 D Time of flight camera for object detection.", computer science,(2007).

[15] Ringbeck, Thorsten & T, Möller & B, Hagebeuker. (2007). Multidimensional measurement by using 3-D PMD sensors. Advances in Radio Science - Kleinheubacher Berichte. 5. 10.5194/ars-5-135-2007.

Sources

ISSN | Enter ISSN or ISSNs | Find sources

ISSN: [illegible] x [illegible] x

Improved Citescore

We have updated the CiteScore methodology to ensure a more robust, stable and comprehensive metric which provides an indication of research impact, earlier. The updated methodology will be applied to the calculation of CiteScore, as well as retrospectively for all previous CiteScore years (i.e. 2019, 2017, 2016...). The previous CiteScore values have been removed and are no longer available. View CiteScore methodology >

Filter refine list

Clear filters

Display options

- Display only Open Access journals

Counts for 4-year timeframe

- No minimum selected
- Minimum citations
- Minimum documents

Citescore highest quantile

1 result

Download Scopus Sources list | Learn more about Scopus Source list

All

View metrics for year: 2021

	Source title	Citescore	Highest percentile	Citations 2018-21	Documents 2018-21	% Cited
1	NeuroQuantology	1.3	22% 1408205 Atomic and Molecular Physics, and Optics	1,044	781	47

Top of page

Type here to search

Rainfall ^ ENG 10:47 AM 26-11-2022

Source details

NeuroQuantology

Scopus coverage years: from 2007 to Present

Publisher: Anka Publishers

ISSN: 1303-5150

Subject area: Physics and Astronomy: Atomic and Molecular Physics, and Optics | Neuroscience: Cognitive Neuroscience | Neuroscience: Developmental Neuroscience

Source type: Journal

View all documents > | Set document alert | Save to source list | Source Homepage

CiteScore 2021
1.3

SJR 2021
0.285

SNIP 2021
1.038

Note: CiteScore rank & trend | Scopus content coverage

Improved CiteScore methodology

CiteScore 2021 counts the citations received in 2018-2021 to articles, reviews, conference papers, book chapters and data papers published in 2018-2021, and divides this by the number of publications published in 2018-2021. Learn more >

CiteScore 2021

1.3 = 1,044 Citations 2018 - 2021 / 781 Documents 2018 - 2021

Calculated on 05 May, 2022

CiteScoreTracker 2022

2.0 = 849 Citations to date / 419 Documents to date

Last updated on 05 November, 2022 • Updated monthly

CiteScore rank 2021

Category	Rank	Percentile
Physics and Astronomy: Atomic and Molecular Physics, and Optics	#160/205	22nd
Neuroscience: Cognitive Neuroscience	#85/107	21st

View CiteScore methodology > | CiteScore FAQ > | Add CiteScore to your site

e-ISSN 2320 –7876 www.ijfans.org
Vol.11,S Iss 1, 2022
© 2012 IJFANS. All Rights Reserved UGC CARE Listed (Group -I) Journal

Research paper

AWS Big Data Analytics And Management For Cyber Security.

Prof. Leena B Chaudhari
Assistant Professor, Bharati Vidyapeeths College of Engineering,
Lavale, Pune, MH, India.
leenapc23@gmail.com

Prof. (Dr.) Reena Singh
MES's, Pillai HOC College of Engineering &Technology,
Rasayani Taluka Panvel, Dist, Navi Mumbai, Maharashtra 410207, India.
dr.rsingh2014@gmail.com

Prof. (Dr.) B.K. Sarkar
MES's, Geh Research, Panvel, Dist, Navi Mumbai, Maharashtra 410207, India.
dr.bksarkar2003@yahoo.in

ABSTRACT

Setting: Enormous Information Network safety Investigation is progressively turning into a significant area of exploration and practice pointed toward safeguarding organizations, PCs, and information from unapproved access by breaking down security occasion information utilizing huge information devices and advancements. While a plenty of Huge Information Network protection Scientific Frameworks have been accounted for in the writing, there is an absence of a precise and complete survey of the writing according to a design viewpoint. Objective: This paper reports a precise survey pointed toward recognizing the most often revealed quality credits and design strategies for Large Information Network safety Logical Frameworks. Strategy: We utilized Orderly Writing Survey (SLR) technique for evaluating 74 essential examinations chose utilizing distinct rules. Results: Our discoveries are twofold: (I) recognizable proof of 12 most often detailed quality credits and the support for their importance for Enormous Information Online protection Scientific Frameworks; and (ii) ID and codification of 17 structural strategies for tending to the quality ascribes that are usually connected with Large Information Network safety Logical frameworks. The distinguished strategies incorporate six execution strategies, four exactness strategies, two versatility strategies, three dependability strategies, and one security and ease of use strategy each. End: Our discoveries have uncovered that (a) in spite of the meaning of interoperability, modifiability, versatility, over-simplification, secrecy, and protection affirmation, these quality credits need unequivocal structural help in the writing (b) observational examination is expected to assess the effect of systematized compositional strategies (c) a fair plan of exploration exertion ought to be contributed to investigate the compromises and conditions among the recognized strategies (d) there is a general absence of successful coordinated effort among the scholarly world and industry for supporting the field of Large Information Network safety Scientific Frameworks and (e) more exploration is expected on the near investigation among huge information handling structures (i.e., Hadoop, Flash, and Tempest) when utilized for Large Information Network protection Logical Frameworks.

e-ISSN 2320 –7876 www.ijfans.org
Vol.11,S Iss 1, 2022

© 2012 IJFANS. All Rights Reserved UGC CARE Listed (Group -I) Journal

Keywords: Big Data, Cybersecurity, Quality Attribute, Architectural Tactic.

Introduction

Network protection is a bunch of instruments, practices, and rules that can be utilized to safeguard PC organizations, programming projects, and information from assault, harm, or unapproved access [1]. Network protection is basic according to two viewpoints: 1) we live in a general public that is carefully hyper-associated for social commitment, organizations, schooling, medical services, and numerous different parts of regular day to day existences; 2) the rising reliance on digitalization propels the progression of danger scene where minor and major (e.g., High level Steady Dangers (Able)) network protection assaults are getting more coordinated and modern step by step.

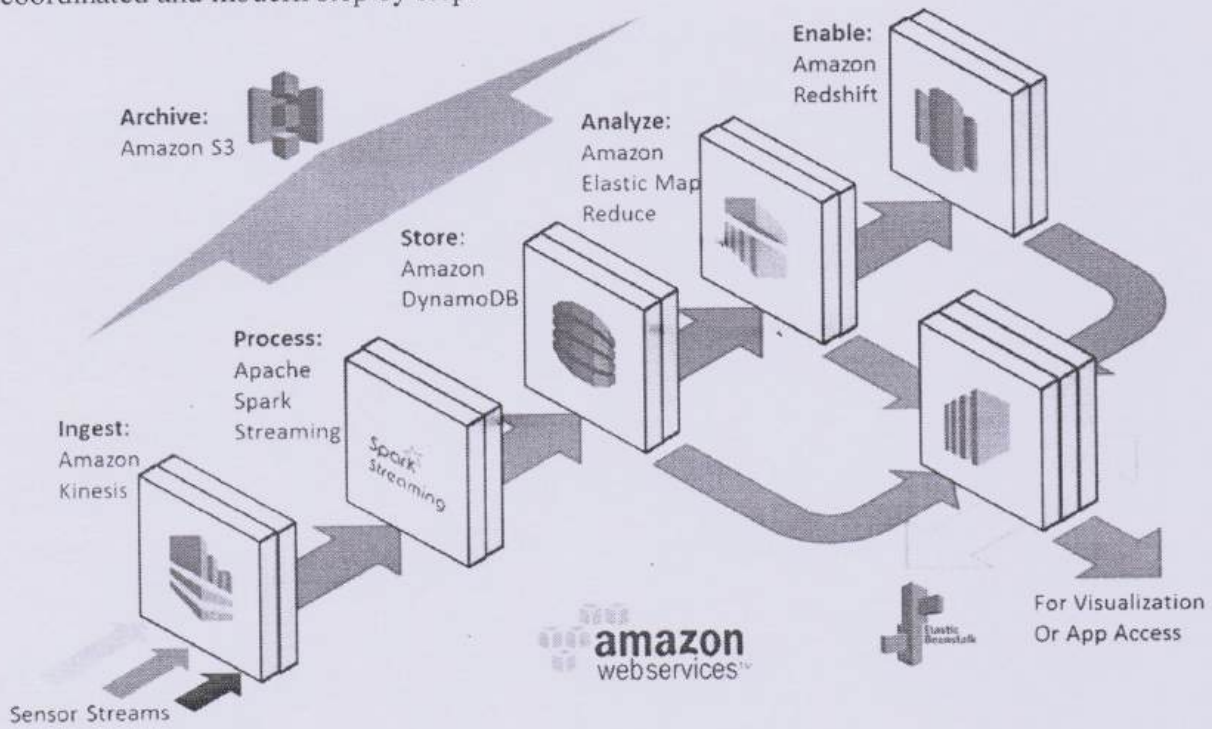


FIG.1: AWS Big data analytics and management for Cyber Security Flow Chart.

As per a new report [2], there can be on normal 27.4% more digital assaults for an association in 2017 contrasted with 2016. The speeding up digital assaults are very unfavorable and costing associations on normal $11.7 million every year. The tireless ascent in the fruitful execution of digital assaults and its boundless impacts show that the conventional online protection devices and practices can't adapt to the refined danger scene. Cardenas et al. [3] report the explanations behind such deficiency of customary network protection that incorporate (I) holding a lot of information (ii) examining unstructured information (iii) overseeing enormous information distribution centers (iv) answering progressively and (v) distinguishing Progressed Determined Dangers (Well-suited). To address these constraints, Cardenas et al. [4] propose an advancement model for network safety that empowers the fuse of enormous information devices and innovations. There exist many such apparatuses and advancements and are proven and factual in the scholarly writing [5]. A portion of the conspicuous enormous information instruments incorporate Hadoop, Flash, Tempest, Flume, HBase, Hive, Kafka, Cassandra, and Mahout. It has been proposed in [4] that huge

information devices and advances would change online protection examination by empowering associations to (I) gather a lot of safety related heterogeneous information from different sources like Ullah, F., and Babar, M.A (2018) 'Building Strategies for Large Information Network protection Scientific Frameworks:'

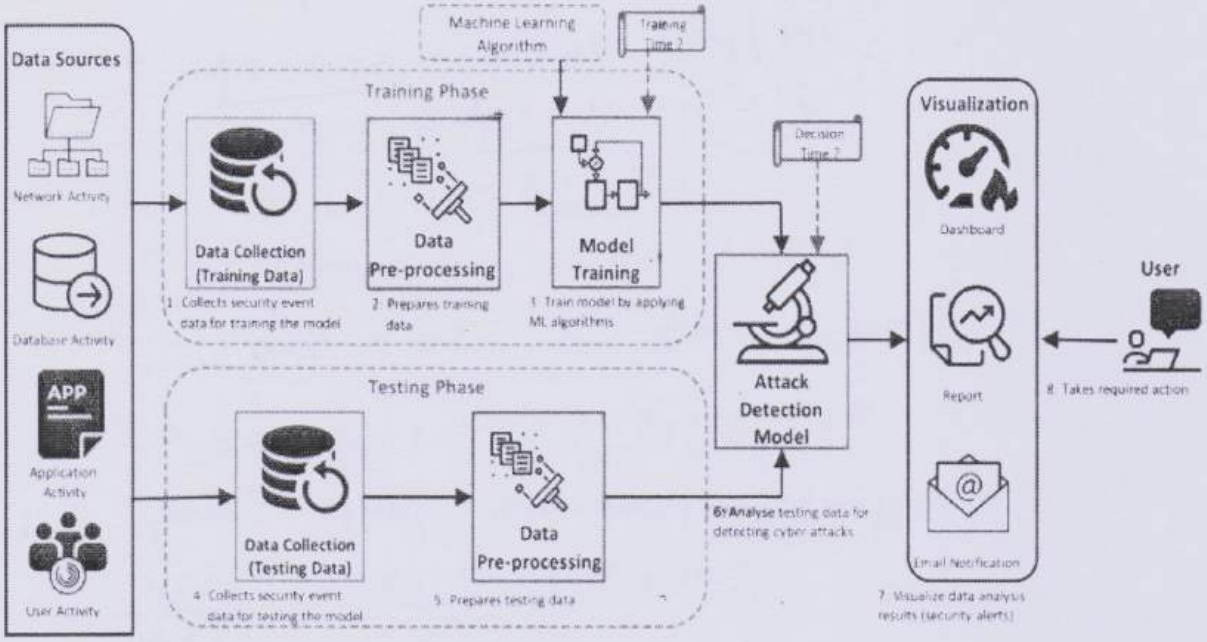


FIG.2: AWS Big data analytics and management for Cyber Security Process.

A Survey' 2 organizations, data sets, and applications (ii) perform profound security investigation at ongoing and (iii) give a merged perspective on the security-related data. This blend of online protection arrangements and enormous information devices has brought forth the term 'Huge Information Network safety Insightful frameworks', which alludes to frameworks that gather enormous measure of safety occasion information from various sources and break down it involving large information apparatuses and advancements for recognizing assaults either through assault design coordinating or distinguishing inconsistencies. Security occasions are substances of data that contain important understanding relevant to the network protection of an association. The sources from which security occasion information is gathered incorporate, yet not restricted to, network traffic information, firewall logs, web logs, framework logs, switch access logs, data set admittance logs, and application logs.

Research methodology

We utilized Precise Writing Audit (SLR) [14] technique for directing this survey. A SLR is focused on efficiently distinguishing and choosing pertinent examinations to be evaluated on a specific point and thoroughly breaking down and integrating the separated information from the checked on investigations to answer a bunch of exploration questions. We adhered to the SLR rules announced in [14]. The fundamental parts of our audit convention were: (I) research questions; (ii) search methodology; (iii) consideration and prohibition measures; (iv) concentrate on determination; and (v) information extraction and union techniques. These parts are examined in the accompanying subsections.

Search terms

We planned the hunt string as per the rules gave in [14]. Our hunt string comprised of two sections - security and large information handling structures. We additionally consolidated the equivalents and the terms connected with the fundamental two terms. We concluded the pursuit string(s) subsequent to guaranteeing that the pilot look through utilizing the hunt terms were returning the realized papers connected with our survey.

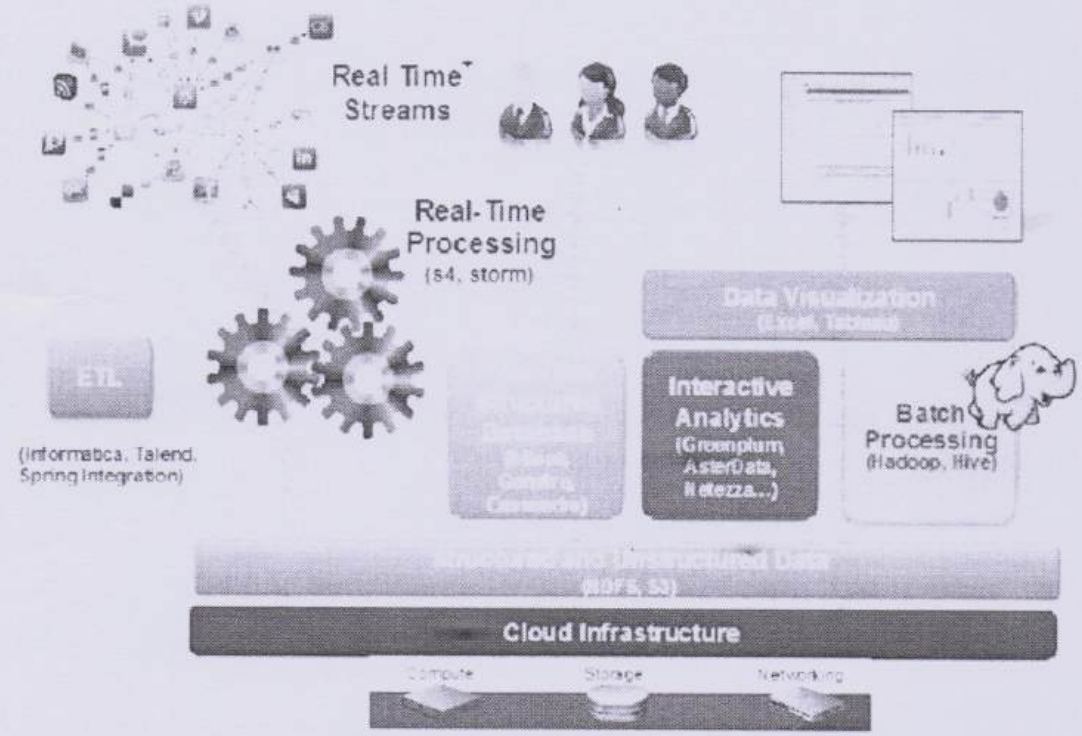


FIG.3: AWS Big data analytics and management for Cyber Security Data Set

The pursuit terms in the string were coordinated exclusively with the title, conceptual, and catchphrases of the papers in the computerized data sets (with the exception of Springer Connection which doesn't permit to confine the hunt to explicit pieces of a paper). We observed that few of the recovered papers were focussed on working on the security of huge information and its relating advances (rather than utilizing enormous information and comparing innovations for security is the focal point of this SLR), nonetheless, we sifted through those papers during the incorporation and avoidance stage.

Data sources

As recently referenced, we looked through six computerized data sets, which are displayed in Table 2. The IEEE Xplore and Science Direct don't uphold the execution of an inquiry with in excess of 15 terms. We needed to part our inquiry into two sections to make it run on IEEE Xplore and Science Direct. Aside from Springer Connection, we ran our question on different data sets to match the terms just in title, conceptual, and watchwords. We have proactively referenced that Springer Connection doesn't uphold look through in the particular pieces of a paper [8]. The impediment of Springer Connection constrained us to either confine our hunt just to the title of a paper or apply the inquiry string to the entire text of every one of the possibly significant papers. While the previous brought about an extremely low number of

© 2012 IJFANS. All Rights Reserved

papers, the later returned a seriously huge number of possibly significant papers (8483 altogether). To resolve this issue, we followed the system embraced in [8]. As indicated by this methodology, we inspected just the initial 1000 papers out of 8483 brought papers back. We declare that Scopus is a supplement to Springer Connection as it files countless diaries and gathering papers in programming and software engineering [9, 2]. We didn't utilize Google researcher because of its low accuracy of the outcomes and the inclination of returning countless unessential papers Information amalgamation.

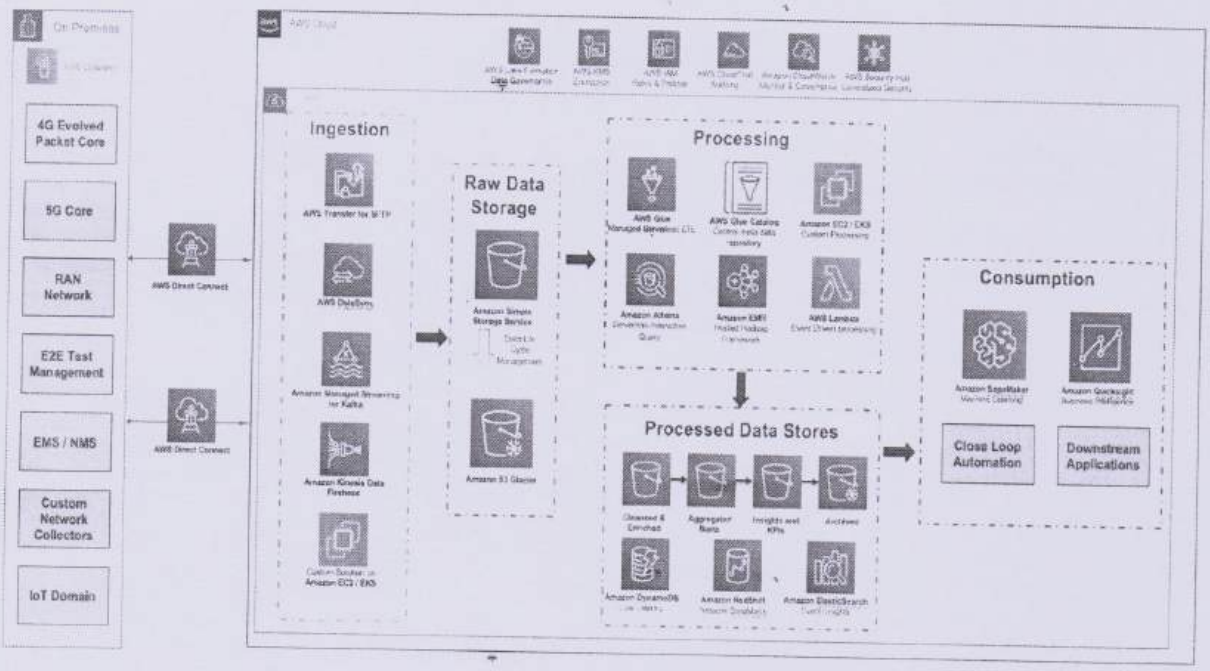


FIG.4: AWS Big data analytics and management for Cyber Security Complete Data Set.

We extricated three kinds of information - segment information, quality credits, and structural strategies. We dissected the segment information utilizing clear insights. The aftereffects of our examination of the segment information have been introduced in Area 3. We broke down the information things D11 (quality credits), D12 (reasoning for quality ascribes) and D13 (design strategies) utilizing topical examination technique [2, 3], which is a generally utilized subjective information investigation strategy. We followed the six-step cycle of topical investigation for blending the separated information. The cycle comprises of these means: (I) Acclimating with the information: The information extricated from the papers and kept in the succeed accounting sheet was all around read to get an

comprehension of the quality credits basic for security examination and the engineering strategies for accomplishing the accentuated quality ascribes; (ii) Creating starting codes: In the wake of acquiring the comprehension, starting codes were allocated to the reasoning for explicit quality ascribes and the building strategies; (iii) Looking for subjects: The at first created topics were dissected to allot explicit subjects to the reasoning recognized for every quality characteristic and the design strategies distinguished from different papers; (iv) Checking on subjects: The topics doled out to the reasoning and structural strategies were contrasted with one another with conclude which subjects should be consolidated or dropped;

© 2012 IJFANS. All Rights Reserved

(v) Characterizing and naming subjects: The names of the topics were audited, and subjects were renamed any place required; (vi) Delivering report: The aftereffects of the examination were accounted for as quality ascribes (Area 4) and compositional strategies for security examination. It is vital to make reference to that the design strategies are not revealed in that frame of mind in the essential examinations. Subsequently, we needed to counsel other scholarly sources connected with each distinguished strategy for social event the information expected to report the strategies as per the predefined layout announced in Area 5. For instance, concentrates on [S30] and [S45] integrate Information Cut Off strategy and show how this strategy can assist with accomplishing a decent presentation. To report it as indicated by the planned format, we should counsel other scholastic sources (i.e., [4-6]) to accumulate the necessary insights concerning Information Cut Off.

ML algorithm optimization Introduction.

The ML Calculation Improvement strategy is found in every one of the papers as all of the security scientific frameworks influence some sort of AI (ML) calculation for breaking down the security occasion information. The goal of this strategy is to feature the job of calculations in working on the presentation of a framework and give a few rules to choosing the calculation that is most effective with regards to computational intricacy. Inspiration. The two most significant elements connected with the presentation of a security logical framework are the kind of information and the utilized ML calculation [5]. Various ML calculations are accessible that can be utilized in a security logical framework. These ML calculations range from managed learning (e.g., Strategic Relapse, Backing Vector Machine, Guileless Bayes, Arbitrary Woodland, and Choice Trees) to solo learning calculations.

Result polling and optimized notification Introduction.

Result Surveying and Improved Notice strategy is tracked down in Include Me In [S56]. This strategy enhances the deferral caused due to a predefined time span for taking care of the outcomes from the mapper hubs into the minimizer hubs inside an equal handling security insightful framework. This strategy guarantees that when values inside the mapper hubs change to an adequate degree (set by the administrator), the mapper hub tells the minimizer hub and as needs be forward the refreshed outcomes to the minimizer hub. Inspiration. MapReduce is an equal handling system that is generally taken on in a conveyed arrangement [5]. This structure comprises of two stages - Guide and Lessen. In the Guide stage, highlights got from the organization traffic guides to a key and a worth through numerous mapper hubs. For instance, a key-esteem pair (s, d) may address bombed association endeavors from a source address's' to an objective location's'. In the Diminish stage, the keyvalue matches created by mapper hubs are taken care of into various minimizer hubs for producing results. The produced results are considered in contrast to a predicate edge through a trigger and on the off chance that the outcomes surpass a particular cutoff, an alarm is created that sign towards a potential digital assault.

Conclusion

Propelled by the developing meaning of enormous information scientific frameworks for network safety, it is critical to methodically assemble and thoroughly dissect and integrate the

© 2012 IJFANS. All Rights Reserved

writing on building techniques utilized for planning such frameworks. Considering there was a general absence of an outline of building procedures for large information network protection logical frameworks, we have led a deliberate writing survey of enormous information network safety scientific frameworks according to an engineering point of view. In view of the survey of 74 pertinent papers, we have recognized and made sense of 12 quality credits as basic for a major information online protection logical framework. Besides, we have likewise recognized and classified 17 compositional strategies for supporting the necessary characteristics (i.e., execution, exactness, versatility, unwavering quality, security, and convenience) in a major information network safety scientific framework. The consequences of this SLR can have a few ramifications both for scientists and experts. For specialists, our SLR have distinguished various regions for future exploration. The segment discoveries are of possible incentive for scientists to shape their future exploration bearings. For instance, it is very apparent that the consolidation of enormous information apparatuses and advancements in security examination is noticing a vertical development. Additionally, along the course of years, flash is getting more famous when contrasted with Hadoop. Considering that significant quality credits, for example, interoperability, modifiability, versatility, over-simplification, covertness and protection confirmation need building support, we attest that specialists need to investigate different choices for growing such a structural help. Different regions for potential exploration incorporate exact assessment of the detailed engineering strategies, tradeoff and reliance examination among the strategies, and relative examination among large information handling structures (e.g., Hadoop, Flash, and Tempest) when utilized in a major information cycB insecurity logical framework. For specialists, the recognizable proof of can be utilized as a most significant reference in planning enormous information digital quality credits and a list of building strategies security logical frameworks. non- - func Given that the elicitation of the useful necessities (e.g., protection, flexibility, versatility and so on) is a difficult errand, specialists can profit from our revealing of significant quality credits upheld by subjective and quantitative thinking to lay out non tional prerequisites for their large information network safety examination frameworks. It is worth focusing on that this SLR is an initial move towards directing programming designers and computer programmers to proficiently draftsman security insightful frameworks. For concretizing the exact proof, group of information and emerging experts' trust through we intend to lay out a trial arrangement of circulated figuring supplemented by enormous information instruments and advances for thorough observational assessment of the classified curve textural strategies. The exploratory plan will intend to research the tradeoffs and conditions among the strategies. We are additionally excited to put our future endeavors in creating robotization support for starting up these strategies, which will decrease the designers' work and speedup the improvement cycle. Similarly of computerization, we expect to research the refactoring of existing framework. We likewise plan to additional security scientific frameworks to help the consolidation of our strategies in the work with specialists by fostering a collection of information on qualities and shortcoming of large information devices and advancements utilized in security examination. Such a group of information will assist experts with choosing instruments and innovations as indicated by their sp ecific prerequisites

© 2012 IJFANS. All Rights Reserved

References

1. Craigen, D., N. Diakun-Thibault, and R. Purse, Defining cybersecurity. Technology Innovation Management Review, 2022. 4(10).
2. Accenture, Cost of Cyber Crime Study. Available at https://www.accenture.com/t20170926T072837Z__w__/usen/_acnmedia/PDF-61/Accenture-2017-CostCyberCrimeStudy.pdf. 2017.
3. Cardenas, A.A., P.K. Manadhata, and S.P. Rajan, Big data analytics for security. IEEE Security & Privacy, 2021. 11(6): p. 74-76.
4. Cárdenas, A.A., P.K. Manadhata, and S. Rajan, Big data analytics for security intelligence. Available at https://downloads.cloudsecurityalliance.org/initiatives/bdwg/Big_Data_Analytics_for_Security_Intelligence.pdf. University of Texas at Dallas@ Cloud Security Alliance, 2013: p. 1-22.
5. Chen, C.P. and C.-Y. Zhang, Data-intensive applications, challenges, techniques and technologies: A survey on Big Data. Information Sciences, 2019. 275: p. 314-347.
6. Verma, R., et al., Security analytics: essential data analytics knowledge for cybersecurity professionals and students. IEEE Security & Privacy, 2015. 13(6): p. 60-65.
7. Otero, C.E. and A. Peter, Research directions for engineering big data analytics software. IEEE Intelligent Systems, 2021. 30(1): p. 13-19.
8. Madhavji, N.H., A. Miranskyy, and K. Kontogiannis. Big picture of big data software engineering: with example research challenges. in Big Data Software Engineering (BIGDSE), 2015 IEEE/ACM 1st International Workshop on. 2019. IEEE.
9. Bass, L., P.C. Clements, and R. Kazman, Software architecture in practice. Addison-Wesley, 2012. 3rd ed.
10. Lewis, G. and P. Lago, Architectural tactics for cyber-foraging: Results of a systematic literature review. Journal of Systems and Software, 2020. 107: p. 158-186.
11. Procaccianti, G., P. Lago, and S. Bevini, A systematic literature review on energy efficiency in cloud software architectures. Sustainable Computing: Informatics and Systems, 2015. 7: p. 2-10.
12. Garcés, L., et al., Quality attributes and quality models for ambient assisted living software systems: A systematic mapping. Information and Software Technology, 2017. 82: p. 121-138.
13. Mahdavi-Hezavehi, S., et al., A systematic literature review on methods that handle multiple quality attributes in architecture-based self-adaptive systems. Information and Software Technology, 2017.
14. Kitchenhand, B. and S. Charters, Guidelines for performing systematic literature reviews in software engineering, in Technical report, Ver. 2.3 EBSE Technical Report. EBSE. 2007, sn.
15. Zhang, H., M.A. Babar, and P. Tell, Identifying relevant studies in software engineering. Information and Software Technology, 2021. 53(6): p. 625-637.

© 2012 IJFANS. All Rights Reserved

16. Wohlen, C. Guidelines for snowballing in systematic literature studies and a replication in software engineering. in Proceedings of the 18th international conference on evaluation and assessment in software engineering. 2014. ACM.

ugccare.unipune.ac.in/Apps1/User/WebA/SearchList

SAVITRIBAI PHULE PUNE UNIVERSITY

UGC-CARE List

Home

UGC

Search

UGC-CARE List

You searched for "**International Journal of Food and Nutritional Sciences**" Total Journals : 1

Search:

Sr.No.	Journal Title	Publisher	ISSN	E-ISSN	UGC-CARE coverage years	Details
1	International Journal of Food and Nutritional Sciences	Global E smart Technologies	2319-1775	2320-7876	from January-2021 to January-2023	Discontinued from Jan 2023

Showing 1 to 1 of 1 entries

Previous 1 Next

Copyright © 2023 Savitribai Phule Pune University. All rights reserved. | Disclaimer

Macromolecular Symposia

www.ms-journal.de

Contemporary and Looming Applications of Carbon Nanotubes

Nidhi Jain and Akanksha Negi*

Molding the future with the use of new technology is utmost important for the progress of human race. Nanotechnologies are the emerging field. Carbon nanotubes (CNTs) are the widely known substances used mostly in all types of the application such as catalysts, absorbents for water treatment, photocatalysis. Various methods of synthesis of CNTs are known, but in this paper, as a case study, green process synthesis has been discussed in CNTs. Different six stages in the life cycle of CNTs have been discussed in the paper that relates to different risk factors in the field. Synchronization of science and technology is important for usage of the materials. This paper provides more brief holistic view of the state of the CNTs at various fields. The attention of this study is also on the toxicity, bioaccumulation, and safety concerns as well as the remedial capabilities

1. Introduction

Nanotechnology is an exclusive technology, which attracts attention towards science, industries, and even in daily life of common people. CNTs (carbon nanotubes) are the key component of nanotechnology. Y. Ando produced the first CNT, which was reported by Iijima. Scientists found that nanotechnology has many applications. Over the years, a large number of efforts, energy, and money are globally charged in CNT projects. The skill of CNT production depends on the utilization of the preliminary specialization for some groups of material like source of carbons, catalyst, and evidence in any specific experiment.[1]

The global energy demand is increasing day by day. Continuous use of the fossil fuels made replenish and there is constant need of the alternative fuels, which provide low CO_2 and particulate emissions. One of the most promising solutions for this problem is use of biomass. This biomass has been generated by electricity/heat or through gasification. This study proposes the production of biomass in the form of miscanthus × giganteus by synthesizing AC and CNTs.[2–6]

CNTs are cylinders made up of the rolled sheets of graphene (lattice). With its various unique and interesting properties, CNTs are regarded as the core of research for the scientists, in advancements of nanotechnology. They are classified into SWCNTs and MWCNTs that is single-walled CNTs and multi-walled CNTs, respectively, based on the number of sidewalls present and their spatial way of alignment. The diametric length of the both the nanotubes are 0.8-2.0 and 5.0-20.0 nm, respectively. Various properties of CNTs and graphene have been discussed in Table 1.[7] CNTs are also used for the electrode materials for the capacitor. Owing to large surface area of CNTs are coupled with the thinner layer electrolyte, electrode and as the potential of the capacitor to reserve larger densities of energy.[8] Some of the properties of CNTs, based on the classification with comparative study of graphene, have been discussed in **Table 1** and **Figure 1**. Carbon nanoparticles and CNTs are also used as a catalyst, sensor manufacturing, photo-catalysis, food science, environmental applications.

2. CNT Application as a Catalyst

CNT can be used as a catalyst in many ways. CNTs can be combined with the different metals such as Fe, Co, Cr, Ti, Mn, Ni, Cu, Zn, Mo, Pd, Rh, Ag, Cd, Au, Hg, Pt, and also used as a catalyst. These catalysts are very useful. However, if the catalyst is formed by different types of adsorptions, i.e., physical and chemical, sometimes they are unstable and if CNTs tend to release significant amount of the metal in the environment and make it toxic. At the same time, metal have their own properties, which influence the parental properties of the CNTs and in turn affect the properties of the composite materials.

There is always a health risk, biocompatibility, and toxicity issues involved with it. Some CNTs have direct effect on the bacterial cell and it broke the bacterial cell. Example CNT-Ag-TiO_2-CNT photo-degradation and catalytic wet air oxidation also releases CNTs in the environment. The degraded product release in the environment might have bad effect in the environment. So, utmost care is needed to take to enhance the usage of CNT. This usage of CNT may lead to the treatment of waste water.

N. Jain
Department of Engineering Science
Bharati Vidyapeeth's College of Engineering
Pune 412115, India
E-mail: nidhijain1704@gmail.com
A. Negi
Department of Computer Engineering
Bharati Vidyapeeth's College of Engineering
Pune 412115, India

The ORCID identification number(s) for the author(s) of this article can be found under https://doi.org/10.1002/masy.202100387

DOI: 10.1002/masy.202100387

© 2023 Wiley-VCH GmbH

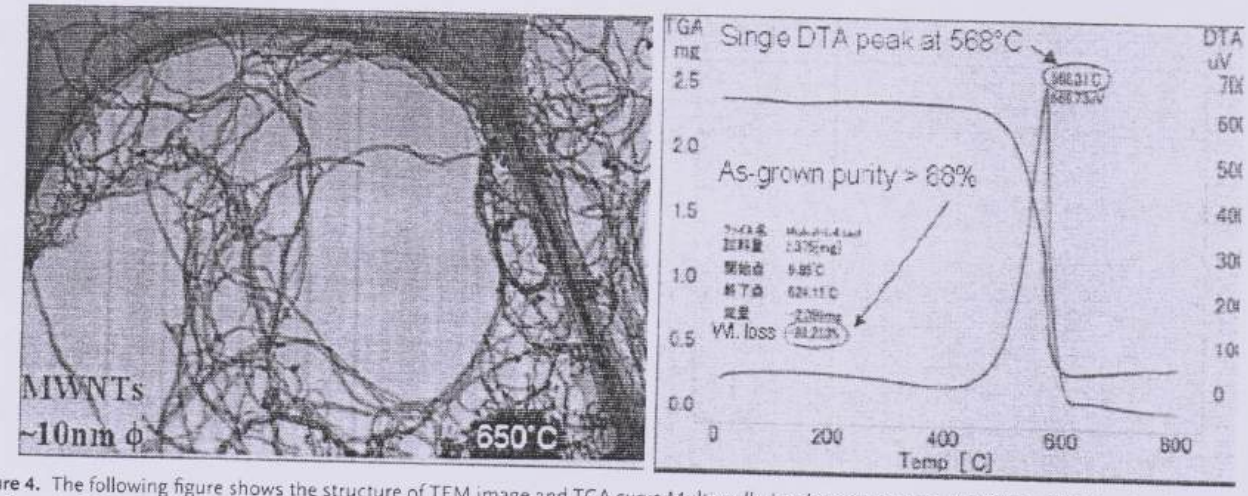


Figure 4. The following figure shows the structure of TEM image and TGA curve Multi-walled carbon nanotubes (MWCNTs)[29] (Reprinted with permission from Ref. [29]. Copyright 2007 IOP Publishing).

0.3 g Fe-Co- saturated zeolite that was supported on approx 655°C, is repeatedly carried out.

To define what the green chemistry means in implementation, 12 principles of green chemistry were developed by the United States Environmental Protection Agency and are used as protocols to gauge this camphor-based CNT synthesis.

From this evaluation, we see that to a great extent, the camphor-based CNT synthesis method abides by all the protocols given by the green chemistry. That concludes that our camphor can be an outstanding CNT precursor, just not only in terms of simplicity of fabrication and elevated purity, but also in terms of application prospects and growth management. It is eco-friendly and time saver.[30,31]

9. Nanotube Bioaccumulation by Lumbriculus Variegatus

Contentious carbon-wall structure, with width less than 100 nm are subject of great research for their potential revolution and are known as carbon nanotubes,[32] it is a hollow cylinder form of carbon atoms in sp^2-hybridization which are bonded in a hexagonal lattice. Single-Wall Carbon Nanotubes (SWCNTs) are one-layer allotropes of carbon with low diametric range. Whereas, Multi-wall Carbon Nanotubes (MWCNTs) consist of nested SWCNTs, with much larger diameters. Researches and numerous studies have revealed that these can enter cells[33] and cause toxic damages in them.[34]

A big task in the study of nanotube behaviors is the absence of technique to measure these nanotubes in environmental or biological medium. One approach that has successfully been used to quantify carbon nanotubes in cells of rabbits is known as spectrofluorimetry.[35]

There is a wide variation within the depuration behaviors and uptake of CNTs in *Lumbriculus variegatus* since the uptake can take place via three different routes: overlying water, pore waters and sediments ingestion. The size of CNTs might contribute other factors for poor absorption by *L. variagetus*. The low uptake was also speculated as an outcome of nominal desorption due to larger molecules blocking cellular uptake. Mention of cellular uptake of SWNTs and MWNTs has been established in many researches[36] but the extent to which they can penetrate the tissues of organism is still unknown. Their uncanny behavior gives rise to many ongoing researches on the different purposes they can serve, in bioaccumulation and food chain transfer, as concentrators, durable sources and much more.[37]

10. The Toxic Truth of CNTs in Purification of Water: A Perspective View

All types of CNT are toxic as they are able to modify the shape, size and composition. The CNT fibers (> 20μm) are engulfed by the macrophage which leads to harmful effects. It was found that size of the CNT plays a major role in increasing the toxicity. CNTs with superior diameters and longer length have higher toxicity than shorter ones. The dimensions of CNT can be supervised during the synthesis. Let us understand the toxicity of the CNT through its life cycle.

CNTs life cycle can give a comprehensive overview which can be meticulously monitored to decrease the toxicity of the product. 1. Initial stage of CNT manufacturing: The manufacturing of CNT is accomplished in a closed furnace without any interference of oxygen and that is why the exposure to CNTs is low. 2. Manufacturing of interim product: In the second stage there is a production of master batches and CNT- dispersed solutions in this case the powder handling take place. So, the exposure is less. 3. Manufacturing of the product: In the third stage there is a production of the CNT product and here the direct handling of second stage product. In this stage there is the release of the CNT in air takes place. 4. Processing of the product: In the third stage. The formed product is processed by physical and thermal stress formed by the CNT product.5. Use of CNT products by the consumers: In this stage there is the use of the product by the consumers and exposure in this case increases. 6. The recycling or disposal of the products based on CNTs: This is the final stage of the product and here disposal and recycling take place.[38,39]

Without nano safety rules, the durable suitability of CNTs for purification of water is controversial. Ongoing possibility measurement of CNTs is darkened by unpredictability. Advanced possibilities related with carbon nanotubes are differed by their physical properties. Although, risk of designs approximates are

© 2023 Wiley-VCH GmbH

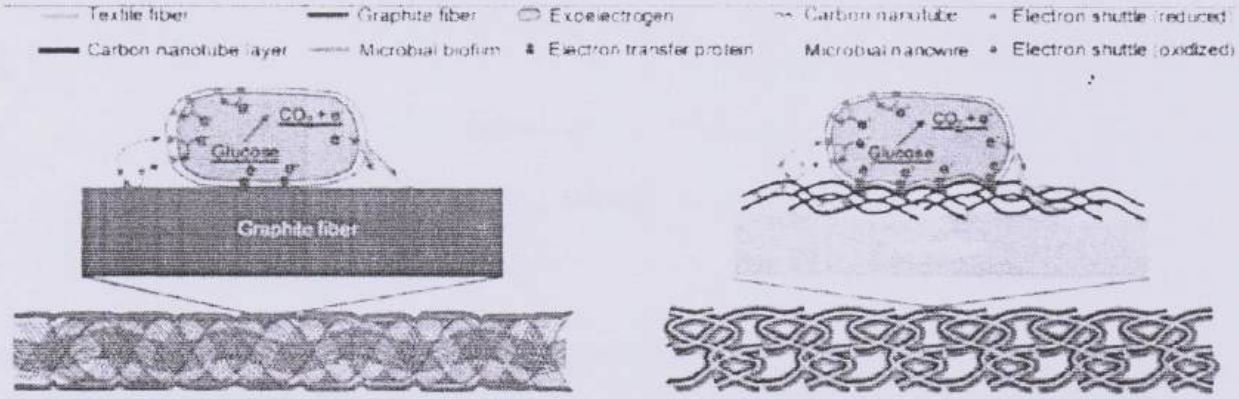


Figure 7. The figure illustrates in the left hand side carbon cloth anode and right hand side CNT-textile anode in which electrode configuration and electron-transfer mechanisms was shown[50] (Reprinted with permission from Ref. [50]. Copyright 2015 Premier Publisher).

like physical, chemical and electrical and it also has a numerous number of applications in different engineering fields. CNTs has a great name in maintainable green and environment friendly technologies such as renewable energy technologies, air pollution monitoring, super capacitors and green nano-technologies, waste water treatment and biotechnologies. CNT is used in different types of storage of energy, i.e., solar energy and hydrogen energy. CNT have been applied to adsorb several kinds of contaminants from water. There is a lack of description of physical and chemical properties of CNT related to adsorptive capacity and interference of other component in the gas mixture. CNT is also used as electrode material in microbial fuel cell. CNT have a great future as a good substance for application in several important fields.[47–48]

Microbial Fuel Cell (MFC) is an eco-friendly technique for the handling of wastewater with self-reliant electricity generation, utilizing pathogens. To CNTs having high surface to volume ratio, high conductivity can be a good anode material. Carbon nanotubes have cellular toxicity that leads to the additive inhabitation and demise of cells. Also, it can't be used directly. CNTs are used for the expansion of the specific surface area of the electrode and also for increasing the efficiency of charge transfer.[49]

A 3-D structure was accomplished by evenly coating CNTs. A three-dimensional CNTs anode displays the firm connection with microbial film and ease of electron transfer from electrogenic to conductor rod surface, therefore declining the resistance of charge transfer and increasing the performance of Microbial Fuel Cell. Electrons are accepted in the form of oxygen in cathode of MFC which is the most suitable terminal electron acceptor. Though poor reduction reaction of oxygen under similar operation condition decreases the performance of MFCs. CNT have a good interaction with redox active center of redox protein inside pathogens in cathode due to their shape and size, which leads to the transfer of electron and increase in the oxygen reduction reaction. It is also a magnificent ally for oxygen-reduction-reaction electro-catalyst such as magnesium dioxide. The extraordinary and adjustable electrical as well as structural properties make CNTs favorable in working as the upcoming MFC electrodes.

CNT has engulfed almost all the fields of environmental and other different engineering areas. CNT has also been proved as the most useful and effective material in different applications. It has a wide research scope in its synthesis with cost cutting, and yet different applications in the field of engineering are known to come. CNT has deciphered different complicated processes, depletion in materials and resources and also increased its efficiency. Other than this appealing feature, production cost and health impacts are important concern factors that are to be discussed to bring out solution by research. In few years, we can expect that the nanomaterial will rule the technological development.[50] The various concerns about the CNTs physicochemical properties in water purification technologies which lead to toxicity.[51–59]

13. Conclusion

The researchers and scientist have claimed that carbon nanotubes (CNTs) are the mainly useful materials for various applications. CNTs are novel one-dimensional macromolecules with exceptional properties. Several studies have been conducted on CNTs and found that CNTs are good catalysts enhanced Catalytic properties better absorbent water treatment, acting effectively in photocatalysis equilibrium. CNTs can be synthesized by the green process. Different six stages in the life cycle of CNTs have been discussed in the paper which relates to different risk factors in the field. From the review we found that CNTs have varied applications but the risk is also associated with the CNTs usage. The risk usage due to the change in the functionality, breakage and leakage can be further area for consideration. The researcher can set some guidelines for usage of CNTs at various fields which further enhanced revolutionized and improve the existing technologies.

Author Contributions

All persons who meet authorship criteria are listed as authors, and all authors certify that they have participated sufficiently in the work to take public responsibility for the content, including participation in the concept, design, analysis, writing, or revision of the manuscript. Furthermore, each author certifies that this material or similar material has not been and will not be submitted to or published in any other publication before its appearance in the Macromolecular Symposia.

© 2023 Wiley-VCH GmbH

Source details

Macromolecular Symposia

Formerly known as: Makromolekulare Chemie. Macromolecular Symposia
Scopus coverage years: from 1994 to Present
Publisher: Wiley-Blackwell
ISSN: 1022-1360 E-ISSN: 1521-3900
Subject area: Materials Science: Polymers and Plastics | Materials Science: Materials Chemistry | Physics and Astronomy: Condensed Matter Physics | Chemistry: Organic Chemistry
Source type: Journal

CiteScore 2022
1.5

SJR 2022
0.226

SNIP 2022
0.333

Save to source list Source Homepage

CiteScore | CiteScore rank & trend | Scopus content coverage

Improved CiteScore methodology

CiteScore 2022 counts the citations received in 2019-2022 to articles, reviews, conference papers, book chapters and data papers published in 2019-2022, and divides this by the number of publications published in 2019-2022. Learn more >

CiteScore 2022

1.5 = 1,155 Citations 2019 - 2022 / 783 Documents 2019 - 2022

Calculated on 05 May, 2023

CiteScoreTracker 2023

1.5 = 1,222 Citations to date / 836 Documents to date

Last updated on 09 December, 2023 • Updated monthly

CiteScore rank 2022

Category	Rank	Percentile
Materials Science Polymers and Plastics	#120/163	26th
Materials Science Materials Chemistry	#227/306	25th

Advances in Water Science
2022; 33(4)
ISSN: 1001-6791

AWS 水科学进展
Advances in Water Science

Crime Rate Prediction using Cyber Security and Artificial Intelligent

Dr. Aarti Amod Agarkar*[1], Dr. Manisha Ajaykumar Dudhedia[2], Prof. Swati G. Gawhale[3] & Dr. Uday Chandrakant Patkar[4]

*[1]Associate Professor, Department of Computer Engineering, Marathwada Mitra Mandal's College of Engineering, Pune, India Affiliated to Savitribai Phule Pune University, Pune, India
[2]Assistant Professor, Department of Electronics and Telecommunication Engineering, Marathwada Mitra Mandal's College of Engineering, Pune, India Affiliated to Savitribai Phule Pune University, Pune, India
[3]Assistant Professor, Bharati Vidyapeeth's College of Engineering, Lavale, Pune
[4]HOD, Department of Computer Engineering, Bharati Vidyapeeth's College of Engineering Lavale Pune

Abstract: *In the advanced age, cybercrime is spreading its root generally. Web development has gone out to an aid as well as revile for those standing up to the issues of protection, public safety, social conventionality, IP privileges, kid security, battling, distinguishing, and indicting cybercrime. Consequently, there emerges a need to distinguish the cybercriminal. Cybercrime distinguishing proof uses dataset that is taken from CBS open dataset. For distinguishing the cybercriminal, support vector machine (SVM) in the SVM grouping and - closest neighbor (KNN) models is used for deciding the cybercrime data. The assessment of the exhibition is finished thinking about the accompanying measurements: genuine positive, misleading positive, genuine negative and bogus negative, deception rate, identification rate, exactness, review, accuracy, particularity, responsiveness, order rate, and Fowlkes-Mallows Scores. Assumption amplification (EM) estimation is used for assessing the introduction of the Gaussian blend model. The exhibition of classifier's show is likewise finished. Exactness is achieved in case of collection through SVM classifier as 89.89% in the directed strategy.*

Keywords: *Crime, Rate, Prediction, Cyber Security, Artificial Intelligent, Fowlkes-Mallows, support vector machine*

1. Introduction

Cybercrime includes endeavouring a criminal offense through PC and an organization wherein the PC can go about as an instrument, objective, or the two of them. Numerous unapproved PC empowered exercises occur by means of worldwide electronic organizations. The examination sorts cybercrime into the following:

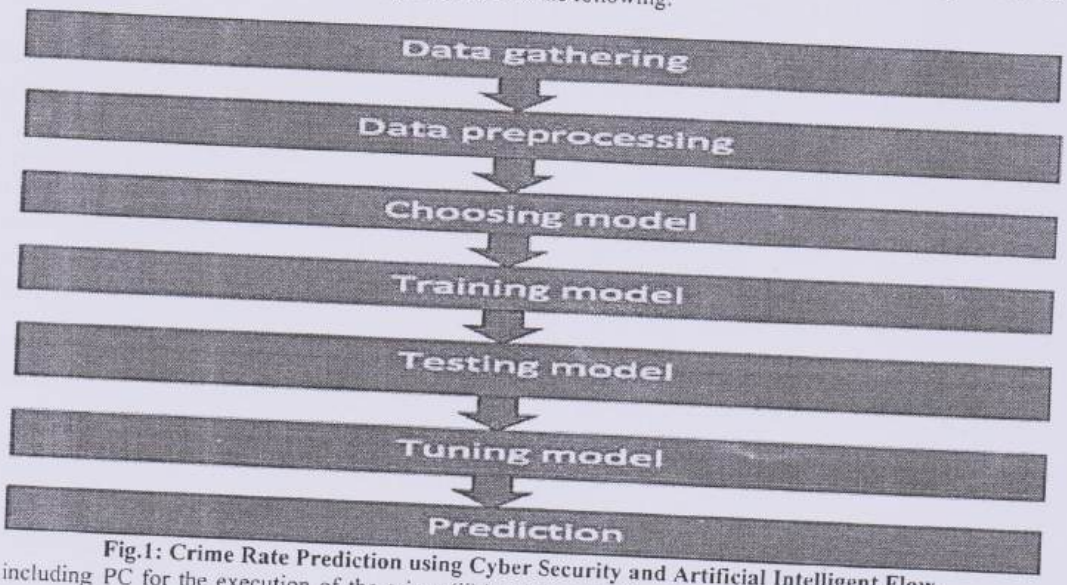


Fig.1: Crime Rate Prediction using Cyber Security and Artificial Intelligent Flow.

(i)A crime including PC for the execution of the crime (ii)A crime including PC for wrongdoing related data capacity and not really for the execution of the wrongdoing

Necessity of Detection of Cybercrime

Cybercrime has spread its foundations far on a worldwide scale and depicts an incredible risk towards event of either a lawbreaker or a fear monger movement. These dangers can influence both inside and outer security (military) without responding to single authority policing philosophies. There is loss of both individual and monetary information assuming that the cybercrime goes undetected.

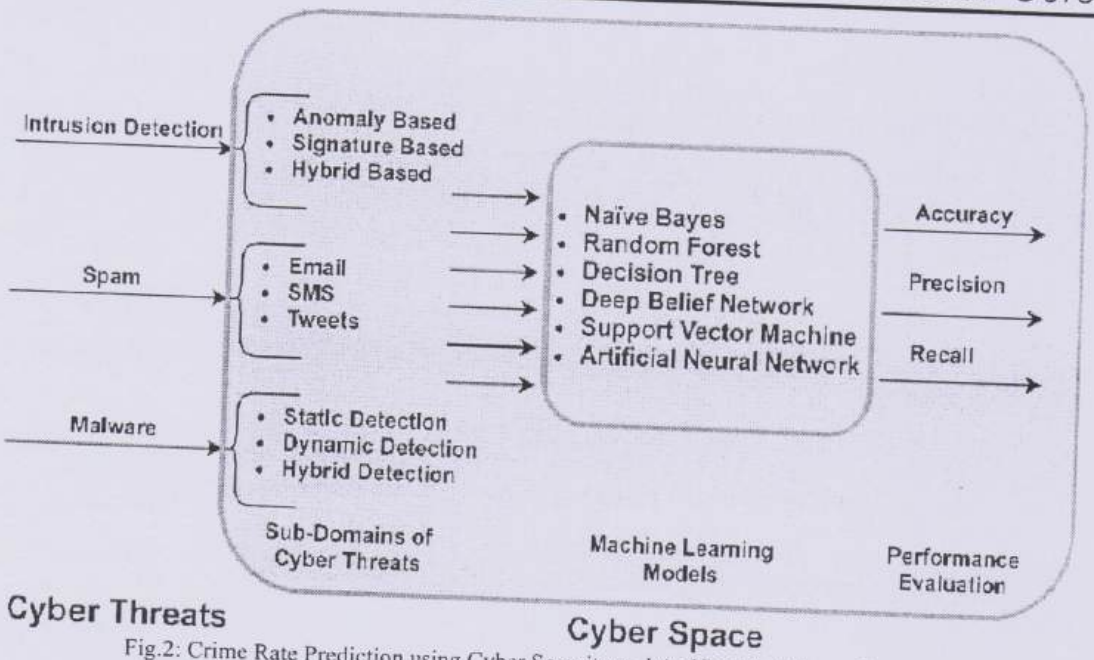


Fig.2: Crime Rate Prediction using Cyber Security and Artificial Intelligent Process

There have proactively been assaults on data framework and Internet providers. Online extortion and programmer assaults are just two cases of PC related wrongdoings that happen consistently. Cybercrime is said to have caused gigantic monetary harm. Malignant programming costs up to USD 17 billion in punitive fees in 2003 alone. As per a few evaluations, cybercrime pay outperformed USD 100 billion out of 2007, outperforming the unlawful medication exchange interestingly. In the US, around 60% of firms say that cybercrime is more exorbitant than actual wrongdoing. These figures show that shielding data infrastructures is so basic.

2. Research Methodology

SVM: is a regularization boundary that controls the compromise between the accomplishing a low preparation mistake and a low testing blunder that is the capacity to sum up your classifier to concealed information. Support vector machine: this investigation fragment uses the cybercrime distinguishing proof model through SVM for requesting the enlightening file recuperated from CBS data detail. In the SVM classifier preparing information, SVM classifier uses cybercrime revelation datasets through ML gadgets. In the exploration work, different clients are requested into wrongdoing client or authentic client.

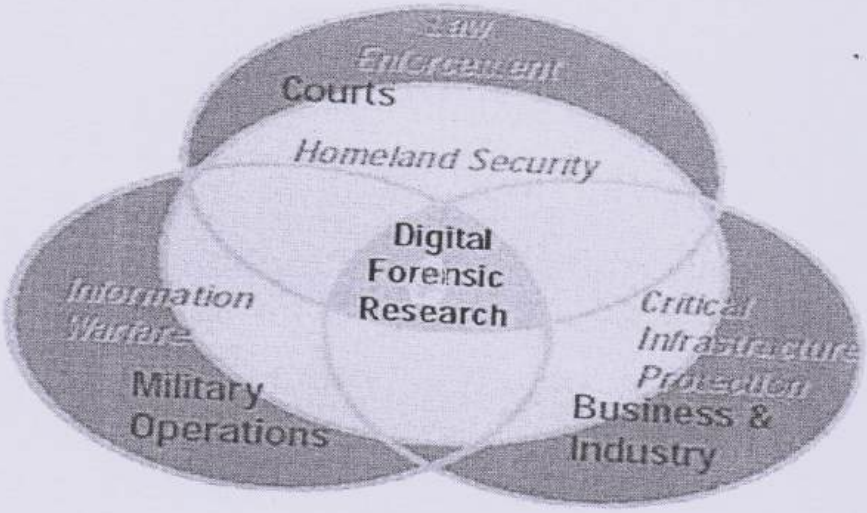


Fig.3: Crime Rate Prediction using Cyber Security and Artificial Intelligent Cycle

Performance of Different KNN Classification Learners

The KNN calculation portrays a nonparametric method utilized for performing grouping and relapse. Regardless, the information contains the - nearest preparing model in the trademark space. KNN calculation in KNN relapse is utilized to assess persistent factors. There is another calculation that uses a weighted normal of the k closest the marked models are requested by expanding distance. Neighbours go through the reverse of their distance. Following is the working of the calculation. Compute the Euclidean separation from the inquiry guide to the named models. Table 1 shows the KNN classifier with the few characterization stude: The quantities of qualities utilized were 25 executed for 1000 clients. The precision for medium KNN and cubic KNN with 88.7% and for optimizable KNN shown was 88.6%.

Comparison of SVM and KNN Classifier

Information order in KNN is based on distance metric however if there should be an occurrence of SVM, right preparation stage is required. SVM is of ideal sort; consequently, it is guaranteed that the isolated information would be isolated ideally displayed in Figure 2. Typically, KNN is utilized as multiclass classifiers; then again, the SVM isolates double information that being a piece of possibly one class. The methodology of one-up against one and one-versus everything is taken on for a multiclass SVM. In one-against one idea, SVMs are prepared, that is one SVM for each sets of classes. The example is taken care of that isn't known to the element, and a ultimate choice on the information type is made by greater part yield from the In general SVM yield. This approach is mostly utilized for multiclass arrangement. presents the exactness of classifiers.

Clearly, SVMs seem, by all accounts, to be computationally extreme, and when the information is prepared, the model can be utilized for anticipating classes despite the fact that new unlabeled information are experienced. However, in the event of KNN, each time another unlabeled information is experienced, the distance metric is registered.

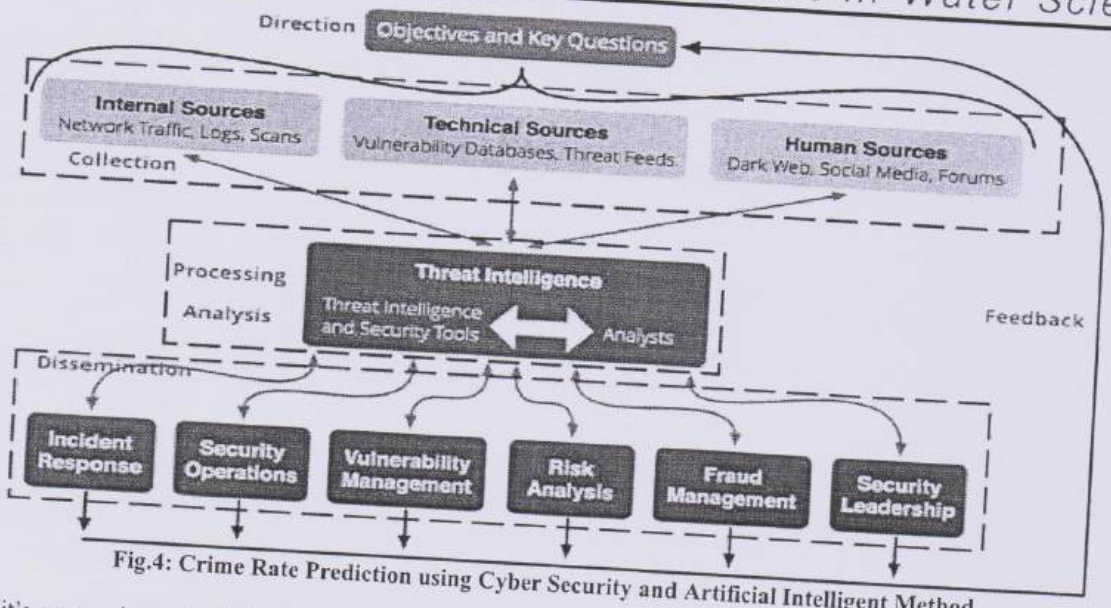


Fig.4: Crime Rate Prediction using Cyber Security and Artificial Intelligent Method

Thus, it's expected to fix just the boundary and pick distance metric that is adept for order in KNN what other place in SVMs is expected to pick the boundary (regularization term) alongside the piece boundaries on the off chance that the classes are directly indivisible. While looking at the precision of both the classifiers, SVMs portray ad lobbed exactness as opposed to KNN. Shows the Precision for the different arrangement students.

Network safety datasets: a large number of the scientists structure a store of different sorts of information according to their review perspective as well as giving this gathered information to local area vaults. The current segment portrays the predominant security based datasets through the strategies of ML and counterfeit savvy research.

Ecml-Pkdd 2007 dataset: The ECML-PKDD 2007 dataset was worked for the European Meeting on ML and Information Revelation in 2007. An information mining rivalry alluded to as ECML/PKDD Disclosure Challenge occurred related to the eighteenth European Gathering on AI (ECML). Table 4 portrays the characteristics of ECML/PKDD 2007. Depiction of dataset is utilizing extensible markup language (XML). All examples are communicated utilizing an exceptional id, and they include the three essential parts in particular: setting, class, and question.

Evaluation of Performance of Classifier

Proposed approach: utilization of honeypot and forestalling failing in remote organizations is completed in the accompanying way.

First stage: it includes general usefulness and social event of data connected with test system, fundamental honeypot capabilities, IDS, and so on. Besides, an examination design is done in this stage. second stage: this stage includes building an organization with IDS climate in NS2 test system. It attracts contrasts relating to the remote organization's presentation.

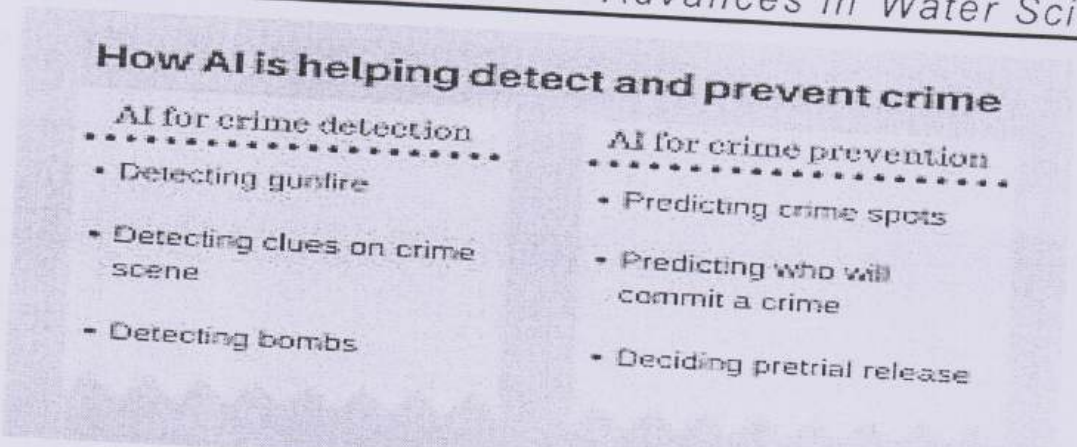


Fig.5: Crime Rate Prediction using Cyber Security and Artificial Intelligent

Third stage: the suggested conspire is utilized for honeypots for forestalling failing and achieving better checking techniques. Furthermore, a powerful honeypot strategy is consolidated collaborating with IDS for achieving high security in the remote organization. Soon after the firewall, honeypot is put, and the interruption discovery framework seriously synchronizes with honeypot and the sneaking around specialists as well. The sneaking around specialists will generally be a basic piece of most extreme organization exercises as it supports the method involved with separating and labeling. These specialists are constructed utilizing hinder type including traffic design data accessible for correspondence. Sneaking around specialist are executed in a style of guidance code that gets synchronized with honeypot. The specialists are set in such a way that the sifting system becomes powerful with by and large checking of dubious and sudden traffic. Observing is done at parcel and example level of the traffic. Recreation helps in observing and sifting of traffic for recognizing any interruption in the organization.

Review: the review metric figures the rate (an unaccounted for piece from the accuracy) from the genuine assault cases included by the classifier. Evidently, it is very much expected that the classifier has a high review esteem. The review metric is like the DR metric.

There is a perpetual expansion in the degree of organization based assaults since the gate crashers present a phony personality and subsequently escape from getting caught or captured. The issue of recognizing such digital hoodlums has become incredibly testing and complex since the interlopers conveys a progression of assaults by means of supposed the mediator has or alluded to as the venturing stones. This suggests that the assault from a specific source might cross through a progression of mediator has before really going after the person in question. Accordingly, the casualty stays ignorant regarding the beginning wellspring of the assault rather considers the last middle person has (or venturing stone) as the source from where the assault probably sent off. Consequently, it turns out to be profoundly critical that a successful and solid procedure is worked for the identification of the venturing stone assault to catch the assailants.

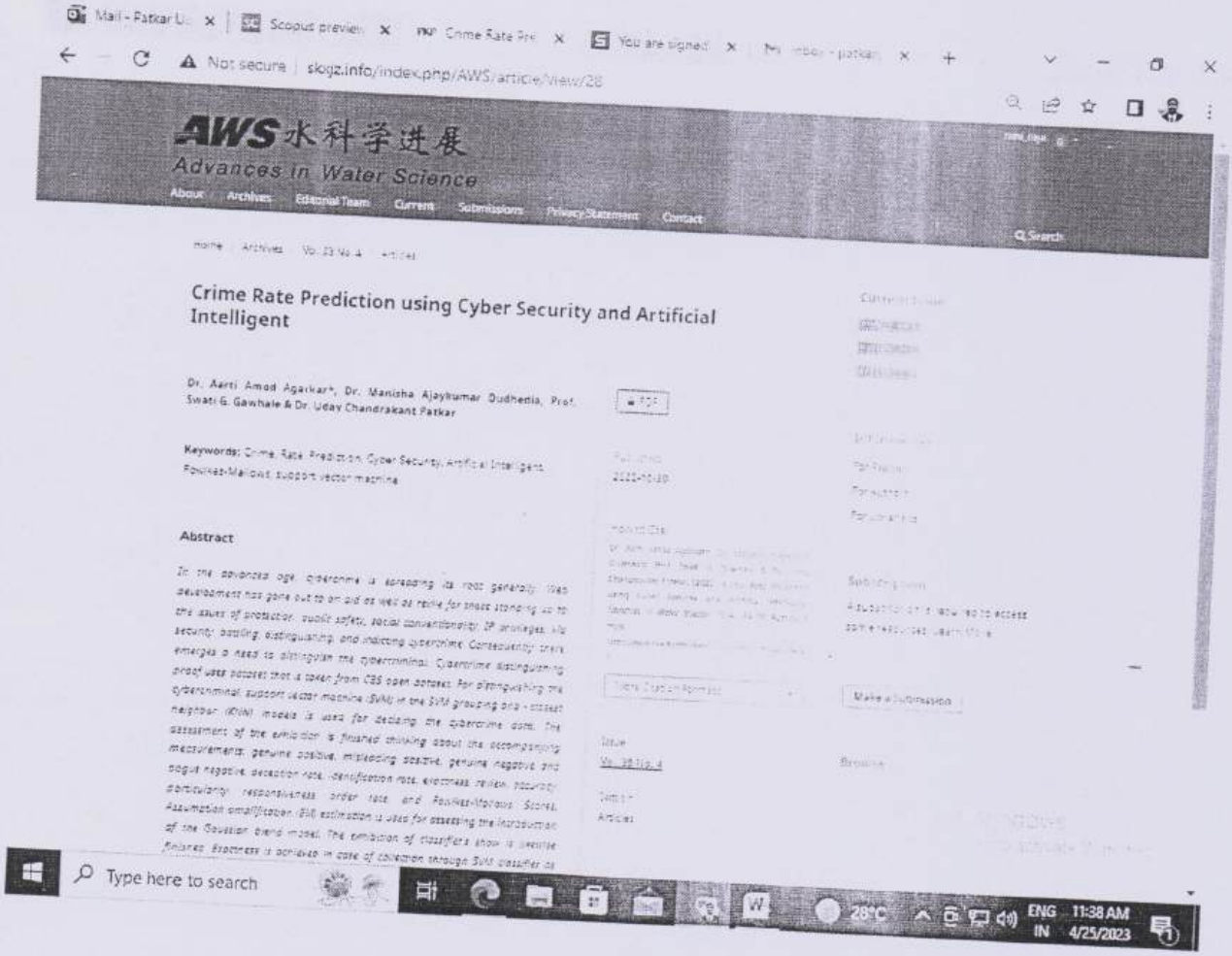
3. Conclusion

In the business world, man-made reasoning (simulated intelligence) and AI (ML) are habitually utilized. Truth be told, by 2020, 37% of organizations and associations will have integrated simulated intelligence into their frameworks and activities in some structure. Utilizing arrangements presented by these advancements, organizations can more readily foresee their clients' buy conduct, bringing about expanded pay. With the utilization of ML and man-made intelligence controlled devices, a few associations, for example, Amazon, which was esteemed at a trillion bucks in 2018, had the option to lay out exceptionally beneficial tasks. In this examination work, the client profile is utilized to recognize the cybercrime. Here, the fingerprints, motions, and different items are not utilized.

This examination work explains wrongdoing investigation, directed learning techniques integrating SVM, and KNN classifier and their correlation. The ascent in use of web has prompted the ascent in the presentation of crimes. It is an aid as well as a revile to the humankind including issues of security, public safety, social fairness, IP freedoms, kid insurance, battling, identifying, and indicting cybercrime. The assessment of the exhibition was performed thinking about the accompanying measurements: genuine positive, bogus positive, genuine negative and misleading negative, deception rate, discovery rate, exactness, review, accuracy, particularity, awareness, grouping rate, and Fowlkes Mallows Scores. The presentation investigation of SVM classifier as well as execution examination of ID of cybercriminal by utilizing group processing strategies was finished. It examined the reason for picking SVM, approach utilized in various procedures, assessment of calculation, time intricacy, and execution examination.

References

1. P. Duggal, Under Indian cyber law, even users can be prosecuted for posting content so it is best to exercise caution before uploading anything. Rand Corporation, New Delhi, 2021.
2. P. Fornacciari, M. Mordonini, A. Poggi, L. Sani, and M. Tomaiuolo, "A holistic system for troll detection on Twitter," Computers in Human Behavior, vol. 89, pp. 258–268, 2021.
3. A. A. Somwanshi and S. A. Joshi, "Implementation of honeypots for server security," International Research Journal of Engineering and Technology (IRJET), vol. 3, pp. 285–288, 2020.
4. R. D. Tale and B. P. Harne, "Deception detection method using independent component analysis of EEG signals," International Journal of Advanced Research in Electronics and Communication Engineering, vol. 4, pp. 1293–1298, 2020.
5. H. M. Alsafi, W. M. Abduallah, and A.-S. K. Pathan, IDPS: an integrated intrusion handling model for cloud, Networking and International Architecture, 2019.
6. M. Baykara and R. Das, "A novel honeypot based security approach for real-time intrusion detection and prevention systems," Journal of Information Security and Applications, vol. 41, pp. 103–116, 2018.
7. A. Khraisat, I. Gondal, and P. Vamplew, "An anomaly intrusion detection system using C5 decision tree classifier," in Trends and applications in knowledge discovery and data mining, pp. 149–155, Springer, 2019.
8. C. Modi, D. Patel, B. Borisaniya, H. Patel, A. Patel, and M. Rajarajan, "A survey of intrusion detection techniques in Cloud," Journal of Network and Computer Applications, vol. 36, no. 1, pp. 42–57, 2013.
9. R. K. Deka, K. P. Kalita, D. K. Bhattacharya, and J. K. Kalita, "Network defense: approaches, methods and techniques," Journal of Network and Computer Applications, vol. 57, pp. 71–84, 2015.
10. I. Butun, S. D. Morgera, and R. Sankar, "A survey of intrusion detection systems in wireless sensor networks," IEEE Communications Surveys & Tutorials, vol. 16, no. 1, pp. 266–282, 2014.


Mail - Patkar U...
Scopus preview
Crime Rate Pre
You are signed
Not secure
skqz.info/index.php/AWS/article/view/28
AWS水科学进展
Advances in Water Science
About
Archives
Editorial Team
Current
Submissions
Privacy Statement
Contact
Search
Crime Rate Prediction using Cyber Security and Artificial Intelligent
Dr. Aarti Amod Agarkar*, Dr. Manisha Ajaykumar Dudhedia, Prof. Swati G. Gawhale & Dr. Uday Chandrakant Patkar
Keywords: Crime Rate Prediction, Cyber Security, Artificial Intelligent, Fowlkes-Mallows, support vector machine
Abstract
Make a Submission
Vol. 34 No. 4
Articles
Type here to search
28°C
ENG
IN
11:38 AM
4/25/2023

Source details

Shuikexue Jinzhan/Advances in Water Science

Scopus coverage years: from 1998 to Present

Publisher: China Water Power Press

ISSN: 1001-6791

Subject area: Earth and Planetary Sciences: General Earth and Planetary Sciences

Source type: Journal

Save to source list Source Homepage

CiteScore 2022
3.1

SJR 2022
0.413

SNIP 2022
0.681

CiteScore | CiteScore rank & trend | Scopus content coverage

Improved CiteScore methodology

CiteScore 2022 counts the citations received in 2019-2022 to articles, reviews, conference papers, book chapters and data papers published in 2019-2022, and divides this by the number of publications published in 2019-2022. Learn more >

CiteScore 2022

3.1 = 963 Citations 2019 - 2022 / 315 Documents 2019 - 2022

Calculated on 05 May, 2023

CiteScoreTracker 2023

3.9 = 1,273 Citations to date / 326 Documents to date

Last updated on 05 December, 2023 • Updated monthly

CiteScore rank 2022

Category	Rank	Percentile
Earth and Planetary Sciences └ General Earth and Planetary Sciences	#73/192	62nd

View CiteScore methodology > CiteScore FAQ > Add CiteScore to your site

ISSN 2063-5346

Design of an ROV to find Dead Bodies Underwater

Dr. Uday Chandrakant Patkar[1] Prof. Megha Patil[2] Mr. Aditya Chandhoke[3] Mr. Abhijeet Jain[4]
Ms. Muskan Kumari[5] Mr. Namokar Jain [6] Dr. Shikha Bhardwaj[7] Dr. Uday Shankar Patil[8]
Bharati Vidyapeeth's College of Engineering, Lavale [1,2,7,8]
Student of Computer Engineering, Bharati Vidyapeeth's College of Engineering, Lavale, [3,4,5,6]

ABSTRACT - If we look at the current scenario of drowning in the world, we will be astonished to know that according to a WHO report, 650 people die every day, that is 26 per hour and as per the WHO'S 2021 Regional Status Report on Drowning in South-East Asia, nearly 48,000 drowning deaths were observed in India alone, of which 30% were children. To understand and address this problem on a local level, a system is needed to be designed to be better and more efficient at finding these bodies. To lower the danger of mortality brought on by unintentional drowning it is crucial to design a system that can detect and monitor persons in an underwater environment.

Hence, we present our solution of an underwater ROV (Remotely operated Vehicle) in which we will fit the camera to detect the human body in optimal time. For underwater operations, computer vision is one of the most important technologies. For an Underwater environment, weak lighting, and dissolved particles are tough for a pre-processing procedure, which is necessary for underwater vision. After the image pre-processing a Neural Network is proposed to perform the underwater body detection and classification, according to the characteristics of the underwater environment. The program will be used with an underwater robot, the results must be accurate and fast enough to help the robot achieve underwater working operation.

Keywords- Computer Vision, Image Processing, Classification, Neural Network, Deep Learning, Microcontroller.

ISSN 2063-5346

I. INTRODUCTION

Due to deep learning's scientific achievements over the last few years, classification and detection abilities have dramatically improved. To enhance the classification and detection capabilities, numerous novel strategies, and enhancements to already-existing algorithms have been put forth. Due to deep learning's scientific achievements over the last few years, classification and detection abilities have dramatically improved. To enhance the categorization and detection capabilities, numerous novel strategies and enhancements to already-existing algorithms have been put forth. Computer vision can be used to determine if an object is human or not. Unfortunately, marine ecosystems and underwater environments won't benefit greatly from conventional methods like Histogram Oriented Gradients (HOG) and Scale Invariant Feature Transform (SIFT) algorithms. This is because underwater environmental factors, such as distortions caused by water movement, changes in viewpoint, various lighting conditions, etc., have an impact on how underwater picture and video data are acquired.

II. LITERATURE REVIEW

A. Dr S. Nithya and team developed a remotely operated vehicle (ROV) that could work both on water and land for error rectifying purposes with the help of Raspberry Pi powered by micro-USB input. The paper's main consideration was making a combined technology for land and water rover by designing an ROV that could be operated by a host ship in water or humans on land. They focused on the vehicle's movement in all directions, adding sensors to sense faults and a camera to get live feed even if the sensors fail so that all the outputs can be seen on a computer screen attached to it. The developed vehicle is supposed to meet the requirement of finding errors in underwater HDVC transmission lines, oil leakage and ships or to find damage to structures of buildings and bridges.

B. Oscar Adrian Aguirre-Castro and his team developed an ROV of size 18.41 * 29.50 * 33.50 cm and weight of 15.64 kg to capture 800 * 640 pixels of images. The main aim of the paper was to get underwater video access by remote control communication in remote time via ethernet protocol. They used six motors governed through proportional, integrated, and derivative controllers. Motion control, 3D positioning, temperature capture and video capture are performed at the same time for Raspberry Pi 3 using a threading library for parallel computing. The interface was developed in Python. The device can be used up to 100 m in water. It can be used for surveillance, operations, maintenance, and measurements.

C. Divya SN, in her paper, developed an Alive Human body Detection system using BeagleBone Black. Its main aim is to detect burglars and intruders using various types of sensors. Here she has used a PIR sensor coupled with an ultrasonic and an IR sensor. It also has a temperature sensor for better detection capabilities. All the data from the sensors is collected and processed in the BeagleBone Black. It is also Wi-Fi enabled, so it can be accessed from anywhere. This

ISSN 2063-5346

solution targets home security, commercial shops, and natural calamities. We aim to pick up the concept of using Ultrasonic sensors from this paper.

D. In a thesis by Maowei Zheng and Wenjie Zhan, they have creatively explained the use of Deep Learning for finding human body parts in an underwater scene. It focuses on using different types of neural networks such as CNN, R-CNN, SSD and YOLO. In their thesis, they have compared the works of all three algorithms and even a combination of all. For the dataset, they have used web scraping and have manually labelled all of it. A total of 1960 images were fed to the neural network and the results were amazing. We aim to apply the same approach by using neural networks that are trained on our data for the project.

E. Underwater Human body detection by Ms Shyma Zaidi and her team talks more about how and what we are doing. They have tried to combine the technology of image processing, cloud computing and IoT. They are using IR to detect objects in the scene and then take a picture of the IR line that is broken. The snap is then sent to the cloud for processing and detecting if the body is human or not. Cloud processing is a part of MLops development and could be beneficial for our project so we will try and implement it.

F. In a paper from RIMLab and the team we found a novel algorithm for object detection in an underwater environment exploiting the multiscale graph-based segmentation. In this approach, it is independent of distortion, colour alteration and other peculiar effects that come with light and its propagation in water. Lighting underwater is a tough image to process as the light gets lesser and lesser the deeper, we go. This method has achieved precise and accurate detection. We too like their plan to implement this method and compare the results with the other methods we are using.

III. CONTENTS

A. MACHINE LEARNING MODEL

Machine learning is the branch of science that allows computers to learn without explicit programming. Machine learning is one of the most exciting technologies ever created. A mathematical representation of the results of the training process is known as a machine learning model. The study of various algorithms that may develop a model automatically through practice and historical data is known as machine learning. A machine learning model is like computer software that uses data or prior experience to identify patterns or behaviours. Our self-taught model will be a convolutional neural network (CNN) or recurrent neural network (Expected – We will opt for the one with higher efficiency).

B. BLENDER

A set of 3D computer graphics tools called Blender is available for free and is used to make

ISSN 2063-5346

animated movies, visual effects, artwork, 3D-printed models, motion graphics, interactive 3D

ISSN 2063-5346

applications, virtual reality, and, in the past, video games. 3D modelling, UV mapping, texturing, digital drawing, raster graphics editing, animation, match moving, rendering, and other features are available in Blender. We used this software to prototype and refactor our design until a streamlined design was approached. We are still open to altering the designs if something better is found.

Our prototype will look like this:

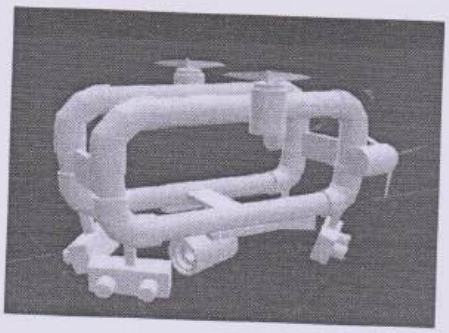


Figure 1 Model

C. MICROCONTROLLERS

An open-source development board called the Arduino Mega 2560 is built around the Atmega2560 AVR microcontroller. An 8-bit microcontroller, such as this one. It makes use of microchip technology ATmega16U2.

Programming for this board is possible using the wiring/processing language. The camera and the thruster are controlled by the Arduino on the ROV. The headlights may be turned on or off, and the camera modes can be changed via digital controls. It contains:

- 14 of the 54 digital input/output pins can be used as PWM outputs, while 16 of the pins are analogue.
- 4 UARTs (hardware serial ports)
- A 16Mhz crystal oscillator and a USB connection.
- A Reset Switch.

ISSN 2063-5346

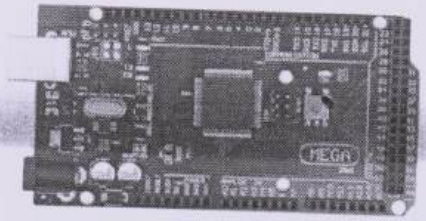


Figure 2 Microcontrollers

D. CAMERA

The ROV operator's primary source of visual information is the camera. These cameras are typically chosen because they are High Definition and work exceptionally well in low light. They are the main forward-facing camera utilised for driving the vehicle. The camera will capture all the information on the seabed and will show the detected object image to the user interface for verification of whether the detected object is a human body or not.

• TP-LINK 360° 3MP (2304 1296) will be used. Wi-Fi security camera with ultra-high definition and night vision.

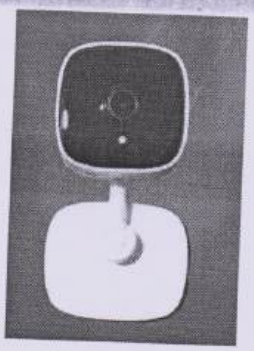


Figure 4 Camera

E. Lights

High-intensity LED strip lights will be used. Since water absorbs light, and while going deeper the water starts getting darker, it is important to use high-intensity gets in all directions to navigate our device wherever it is going in the right direction.

ISSN 2063-5346

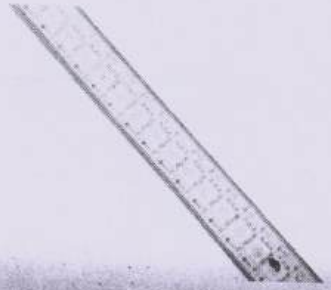


Figure 5 LED Lights

F. Pipes

PVC is a well-known and versatile thermoplastic that has long been used in plumbing applications for both residential and commercial structures as fittings and pipelines. Chlorinated polyvinyl chloride is a thermoplastic that belongs to the same family as PVC (CPVC). The skeletal structure of our prototype will be made from PVC pipes. We plan to use clear pipes to install lights for navigation.



Figure 6 Pipes

G. CAT-5 Cable

Category 5 cable is the name given to twisted pair cables used in computer networks (Cat 5). The cable standard supports most types of Ethernets over twisted pairs up to 2.5GBASE-T but is typically used for 1000BASE-T speeds. It offers the performance of up to 100 MHz, Through CAT-5, additional signals like phone and video are also delivered. Punch-down and modular connections are typically used to connect this cable. Thrusters will be controlled by these cables as they are strong enough and can control all the thrusters with a single wire.

ISSN 2063-5346



Figure 7 CAT-5 Cable

H. Water Pump

An electromechanical device known as a water pump increases water pressure so that it can be moved from one location to another. Modern water pumps are used worldwide to supply water for domestic, agricultural, industrial, and municipal applications. Here water pump will be modified into the thrusters that are required for our prototype. Their waterproof nature will be of great help to us.

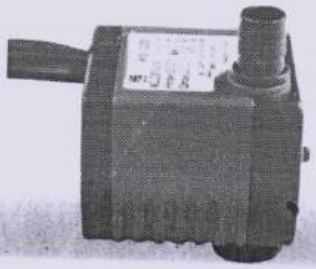


Figure 8 Pump

IV. METHODOLOGY

The working process of ROV is:

An underwater human body detection system allows the user to identify the human body or any other object in the water. It involves the technology of Image processing and Object Detection. This will be done by making an underwater drone. The drone will be made of PVC pipes and connected through silicon glue for waterproofing. The role of PVC pipe in ROV is that it can handle water very well and is corrosion resistant. Cameras, microcontrollers and LEDs are attached to drones for object or human-body detection. The drone will be dropped into the water. The Arduino on the ROV is used to operate the camera and thruster. Digital controls can be used to switch the camera modes and turn on or off the lights. The camera will capture all the information on the seabed and be able to detect if a human is found or not. As soon as a human is found it will notify the user about the same so that further action can be taken. CAT-5 cable wire is waterproof,

it is utilised for wiring. There will be high-intensity LED strip lighting applied. Since light is absorbed by water and the water becomes darker as one descends, it is crucial to utilise high-intensity lighting.

V. CONCLUSION

In this research, CNN and RNN algorithms are identified as suitable deep learning algorithms and they are trained with a dataset containing humans in various underwater scenarios, aiming to detect and track human bodies in an underwater environment which can save a lot of time while searching dead bodies. On the other hand, metrics like training time, and detection speed are necessary if other researchers are reproducing similar work, as these will help them to gain knowledge about the time required to train the algorithms as well as the speed of detecting required entities or objects. CNN algorithm can be given preference over RNN if the speed of detection is more important. But because this aims to solve a real-world problem, it can be concluded that RCNN is the algorithm of choice to effectively detect and track humans underwater.

VI. REFERENCES

[1] *Fenglei Han, Jingzheng Yao, Haitao Zhu, Chunhui Wang, "Underwater Image Processing and Object Detection Based on Deep CNN Method", Journal of Sensors, vol. 2020, Article ID 6707328.*

[2] *Sai Nishant Mattupalli Venkata "Detection and Tracking of Humans in an Underwater Environment Using Deep Learning Algorithms" Thesis no: MCS-20YY-NN 06 2019.*

[3] *Divya SN "Alive Human Body Detection System using Beaglebone Black" ISSN – 2455-0620 Volume - 2, Issue - 9, Sept – 2016.*

[4] *Nguyen, Duc Thanh, "Human detection from images and videos", Doctor of Philosophy thesis, School of Computer Science and Software Engineering, University of Wollongong, 2012.*

[5] *Karthik C, Keerthan HM, Preetam Londe, Samraj M, Ms Shyma Zaidi "Under Water Human Body Detection" (ISSN: 0973-7383) Volume 11 • Issue 1 pp. 532-539 Jan 2019 - June 2019.*

[6] *Paulo Drews Jr, Vinicius Kuhn, Sebastião Gomes "Tracking System for Underwater Inspection Using Computer Vision" 2012 International Conference on Offshore and Marine Technology: Science and Innovation.*

[7] *Shakil Ahmed, Md. Fazle Rabbi Khan, Md. Farhan Anjum Labib, AZM Ehtesham Chowdhury " An Observation of Vision-Based Underwater Object Detection and Tracking" (ICETCE-2020), 07-08 February 2020, (IEEE Conference Record 48199.*

[8] *Fabjan Kallasi, Dario Lodi Rizzini, Fabio Oleari, Jacopo Aleotti "Computer Vision in Underwater Environments: a Multiscale Graph Segmentation Approach" 978-1-4799-87368/15/2015 IEEE.*

ISSN 2063-5346

[9] Yoav Y. Schechner, Nir Karpel "Clear Underwater Vision" Proceedings of the 2004 IEEE Computer Society Conference on Computer Vision and Pattern Recognition (CVPR'04) 1063-6919/04/2004 IEEE.

[10] Supakit Kriangkhajorn "Underwater Computer Vision of the ZEABUS AUV" 2019 First International Symposium on Instrumentation, Control, Artificial Intelligence, and Robotics (ICA-SYMP)

[11] Mohd Shahrieel Mohd Aras, Muhamad Khairi Aripin, Hairol Nizam Mohd Shah, Marian Sulaiman, Alias Khamis, Mohd Bazli Bahar, Mohamad Haniff Harun "Underwater Obstacle Detection System Design using Sonar Sensor" International Journal of Recent Technology and Engineering (IJRTE) ISSN: 2277-3878, Volume-7, Issue-5S4, February 2019.

[12] Oscar Adrian Aguirre-Castro, Everardo Inzunza-González, Enrique Efrén GarciaGuerrero, Esteban Tlelo-Cuautle 2, Oscar Roberto López-Bonilla, Jesús Everardo, Olguín-Tiznado, José Ricardo CárdenasValdez "Design and Construction of an ROV for Underwater Exploration" Sensors 2019, 19, 5387; doi:10.3390/s19245387.

[13] Shagun Agarwal, Tanuj Jhunjhunwala, NT Saikiran, Prabhu Rajagopal "Demonstration of control and inspection by circumferentially guided ultrasonic waves using novel Remotely Operated Underwater Vehicle" ISSS Journal of Micro and Smart Systems · October 2018 DOI: 10.1007/s41683-018-0031-5

[14] Dr S. Nithya, Kanishk Yashvardhan, Suryansh Pravin Katiyar, Subham Kumar Singh "Land And Underwater Rover Using Raspberry Pi" e-ISSN: 2395-0056, p-ISSN: 2395-0072

Author Search Sources Create account Sign in

Source details

Feedback > Compare sources >

European Chemical Bulletin

Open Access

Scopus coverage years: from 2017 to Present

Publisher: Deuton-X Ltd.

E-ISSN: 2063-5346

Subject area: Chemistry: General Chemistry

Source type: Journal

Source Homepage

CiteScore 2021
0.8

SJR 2021
0.139

SNIP 2021
0.187

CiteScore | CiteScore rank & trend | Scopus content coverage

Improved CiteScore methodology

CiteScore 2021 counts the citations received in 2018-2021 to articles, reviews, conference papers, book chapters and data papers published in 2018-2021, and divides this by the number of publications published in 2018-2021. Learn more >

CiteScore 2021

0.8 = 182 Citations 2018 - 2021 / 217 Documents 2018 - 2021

Calculated on 05 May, 2022

CiteScoreTracker 2022

1.6 = 499 Citations to date / 313 Documents to date

Last updated on 26 April, 2023 • Updated monthly

Section A-Research paper

ECO-FRIENDLY ELECTRICITY GENERATION VIA GYM EQUIPMENTS

R.N. Patil[a], Jyoti Dhanke[b*], Hrishikesh Bhavar[c], Sifan Momin[d], Harshal Patil[e], Akshay Redekar[f], Avinash Dadge[g], Narayan Phadatare[h], Prajakta Pawar[i]

[a]Principal and Prof., Department of Mechanical Engineering, Bharati Vidyapeeth's College of Engineering, Lavale, Pune 412115, Maharashtra, India,

[b,i]Asst. Prof., Department of Engineering Science, Bharati Vidyapeeth's College of Engineering, Lavale, Pune 412115, Maharashtra, India, Corresponding Author jyotidhanke@gmail.com,

[c,d,e,f,g]Students, Department of Computer Engineering, Bharati Vidyapeeth's College of Engineering, Lavale 412115, Pune, Maharashtra, India

[h]Asst. Prof., Bharati Vidyapeeth Deemed to be University, College of Engineering, Pune 411043, Maharashtra, India,

Abstract:

The majority of recently developed technologies are fully dependent on electricity to function properly, hence the need for energy is rising daily. The development of humans has been greatly influenced by energy. The scientific community is turning its attention to renewable energy sources because conventional energy sources like coal, natural gas, and fossil fuels are finally running out. This study proposes a theoretical model of the Energy Generating Gyms System (EGGS), which will contribute its share to the renewable energy industry. People in today's society are concerned about their health and use gym equipment to practise activities that will help them reach their desired level of fitness. In a gym, numerous machines are physically operated by users exerting effort on the devices. The concept behind smart EGGS is that human energy used on gym equipment should be transformed into electrical energy. Smart EGGS will produce clean, sustainable, and renewable electrical energy. According to research for smart EGGS, people are also a source of renewable energy, and the chemical energy they possess can be turned into electrical energy [1]. EGGS will be tremendously helpful for nations who are suffering from severe energy difficulties. The combined output of all the gym equipment will provide the necessary quantity of electrical energy for the equipment. It is possible to resell extra electrical energy to a utility [2].

Key Words:

EGGS, Renewable energy, smart grid, EGGM, Gymnasium, Lat Pull down machine, DC motor, Prime Mover, unidirectional Pulley, Generator, Inverter.

1. Introduction:

The environment we live in is undergoing substantial change, and technology is becoming one of the main forces behind societal and economic advancement. Information technology (IT) has advanced quickly over the world, changing not just how people think but also how they behave. Since electricity is

used to power almost all modern technology, its share of the primary energy supply is growing more quickly than electricity.

In the present world, everyone is highly concerned about their health, thus they all join gyms to raise their level of fitness and burn calories. It is conceivable to build equipment for gyms that can transform the energy people consume during exercise into electrical energy_[3]. Producing energy-generating gym equipment for cardio charge and lightning is The Great Outdoor Gym (TGO) enterprise in the United Kingdom (UK). The Cardio Charger is a piece of mobile phone charging equipment. Sir George Monoux College, Trafalgar Square, and the Green Heart in Hull City all have green energy-generating exercise equipment installed by TGO. The Cross Trainer, Recumbent Bike, Spinning Bike, and Hand Bike have all been upgraded by TGO to green energy gym equipment, which generates an average of 50 to 100 watts per piece of equipment depending on the user's fitness level and offers a cardiovascular exercise. In 2015, there was 9,384 metric ton oil equivalents (MTOE) consumed globally as final fuel, and by 2040, that number will rise to 10706 MTOE. From 23.4 trillion kilowatt hours (kWh) in 2015 to 34.0 trillion kWh in 2040, the global net power generation grows by 45 %. Fossil fuels continue to be the primary source of energy in the world, accounting for 32.9% of all energy use, according to the World Energy Council. The possibility for renewable energy sources will be increased by the EGGS concept, which will generate electricity from the machinery in a gym's moving parts.

The best source for creating environmentally friendly, renewable energy is sunlight. To meet the energy needs of contemporary society, there are numerous techniques to collect and use solar energy. In nature, photosynthesis is the process.

by which solar energy enters and permeates the food web and food chain. Plant leaves, green algae, and other creatures like cyanobacteria naturally employ a process called photosynthesis to transform light energy into chemical energy that may then be released and used as an energy source by those organisms to power their activities. Carbohydrates like sugars, which are created from CO2 and water, are used to store the chemical energy that has been transformed. In addition to producing fuel, photosynthesis also produces oxygen as a byproduct. The advantages of simulating photosynthesis can be beneficial to all life on Earth in two ways. In this natural cycle, there are producers and energy converters.

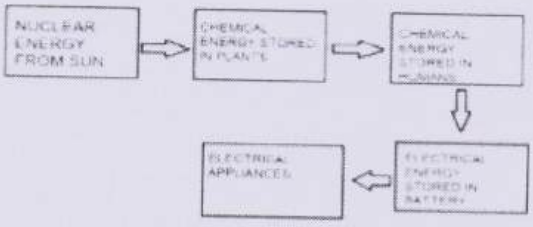


Fig -1: Human body converts solar nuclear energy into electrical energy.

Food (glucose) is produced using water and sunlight, consumed by people, and the chemical energy of this food is transformed into mechanical energy for use in practical work. With the use of EGGS, this mechanical energy can subsequently be transformed into electrical energy. The sequential steps of turning solar nuclear energy into electrical energy are shown in Fig. 1. The definition of energy is the capacity for work, and the human body is incredibly rich in energy, which powers daily tasks [4].

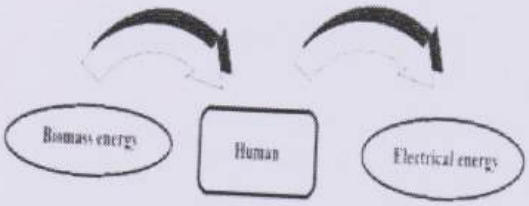


Fig -2: Human as a transducer

2. Proposed work

The graph of energy demand is rising daily, and scientists are looking into new technologies and energy sources to meet this demand. In this essay, we will talk about a technique for using human energy. As illustrated in Fig. 3, the proposed method considers humans to be a machine or devices for converting biomass energy into electrical energy. A transducer is a device that changes one type of energy into another type of energy. Man consumes calories from food and uses them for work, but if his diet is out of balance, too many extra calories will be stored as fat in his adipose tissues, giving him a chubby appearance. People attend gyms where they engage in various forms of exercise like running, weightlifting, and muscle building in order to maintain a healthy appearance and level of fitness. For example, cable preacher curls, close grip bar curls, barbell curls, and dumbbell lifting are some biceps exercises that can be performed on specific machines. Barbell bench presses, flat bench dumbbell presses, low inclined barbell presses, seated machine presses, and others are chest exercises. Cables and pulleys are used in the construction of several of the cardiovascular devices seen in gym equipment. The main focus of this research is on these machines since they can help capture energy. As energy consumption rises daily, it is essential to develop new methods and strategies for producing energy in constrained spaces, such as a house or a gym.

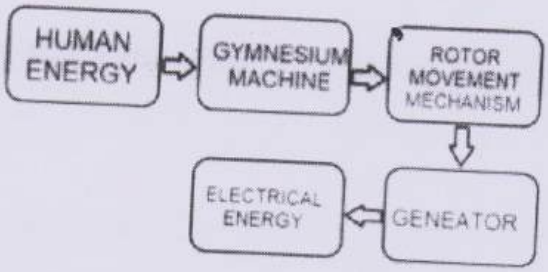


Fig-3: conversion of human energy into electrical energy

People exert effort on machines and use energy to work while exercising in a gym. The authors of this suggested work offer a theoretical method that will allow for the energy harvesting of specific gym equipment. The fundamental concept behind the research is to capture electrical energy from the moving components of gym equipment [5].

2.1 Installation of low RPM generator

A generator produces voltage by revolving at a slow speed while having a large winding.

By including rotor movement mechanisms in the generators, gym equipment can be connected to generators.

2.1.1 Generator components

Rotor/Armature: The generator's rotating armature has wires wound on it. Every time the gym's machine is used, the armature of the Low RPM generator rotates.

Stator: The stator is the stationary component of a generator and is formed of a permanent magnet or an electromagnet wound around a stator coil.

2.1.2 Bidirectional to Unidirectional Gear (BUG) PRIME MOVER:

it is simply a gear system that takes input rotation of both directions, but the output will be in a single and same direction either the input is anticlockwise or clockwise rotation. It contains three pulleys which are connected in the following way.

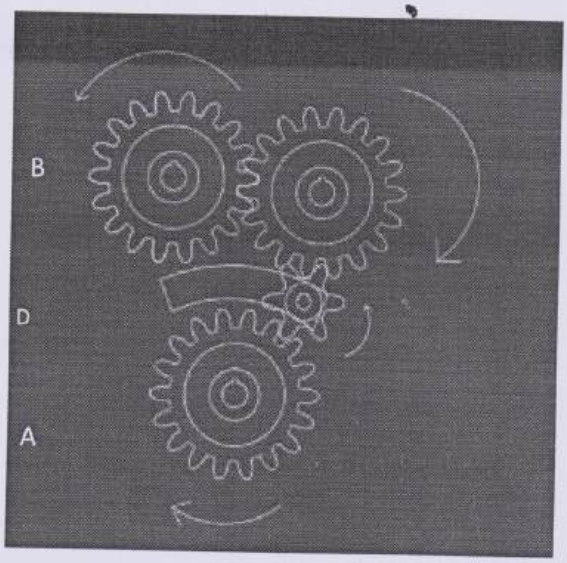


Fig-4: bidirectional to unidirectional gear system

2.1.3 Connection of BUG and generator

The pulley of the gym equipment is connected to pulley A of the gear system (BUG) and the generator is connected on another side of the gear to either pulley B or pulley C. Pulley B and pulley C rotates opposite to each other, but their rotation is unaffected by the direction of rotation of pulley A.

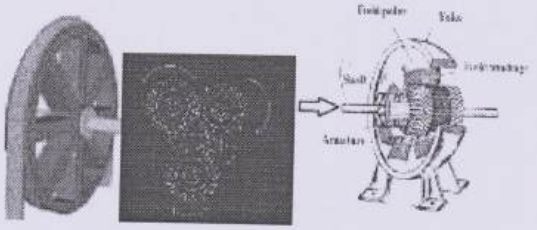


Fig-5: Connection of pulley and generator

2.1.4 Machine rotation of the armature

The grip of the recoil cord will be hooked to the gym equipment, and the rotor movement mechanism will be attached to the generator's shaft. Every time a gym machine is used, the recoil rope on the generator shaft winds and unwinds. When a cord is released, the spring's restoring force causes it to the wind once more. Only clockwise or anticlockwise rotation is made by the generator's armature.

2.1.5 Generator

An electric generator is a device that converts mechanical energy to electrical energy in electricity generation. A three-phase 750W, 220V, 50Hz permanent magnet alternator is used to generate electricity from kinetic energy. Around 2500-3000 RPMs the output current begins reach to its maximum potential [6].

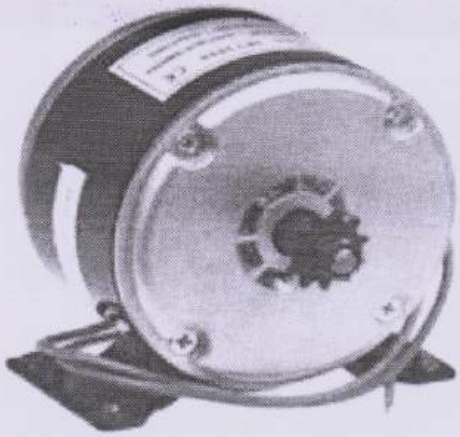


Fig-6: Generator

2.1.6 Recoil spring

Recoil spring is a mechanism that stores energy while rotating and gives out energy by rotating in opposite direction.

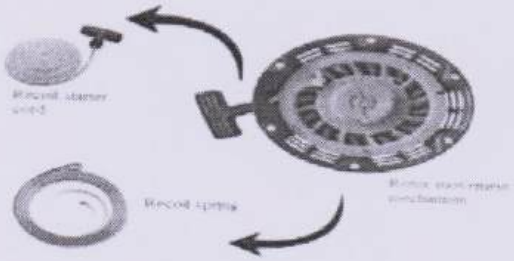


Fig-7: Recoil spring

2.1.7 BATTERY

The battery is the most important to provid power for the alternator rotor and the storage purpose of generated power. An electric battery is an advice consisting of one or more electrochemical cells which will convert stored chemical energy into electrical energy. A positive terminal, or cathode, and a negative terminal, or anode, are found in each cell. Electrolytes allow ions to move between the electrodes and terminals, which allows current to effuse of the battery to perform work Battery we used is 12V, 10 Ah rating [6].

2.1.8 Inverter circuit & step-up transformer

The inverter converts DC voltage to AC voltage and a step-up transformer is a type of transformer that stepped up the AC voltage. In this system, the inverter circuit converts 12V DC to 15V AC. Step-up Transformer makes the voltage to 250 V AC from 15 V AC [6].

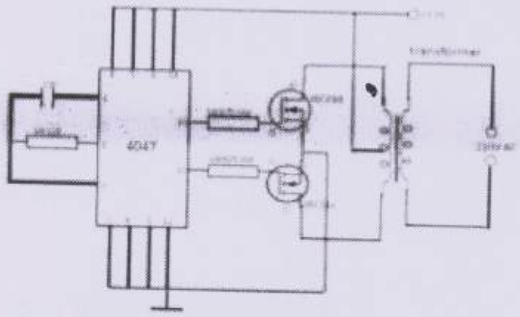


Fig-8: Inverter circuit & step-up transformer

2.2 Energy generating gymnasium machines (EGGM)

1) Lat pull down machine

Latissimus Dorsi, the name of the muscle, is abbreviated as "Lat" in English. Latissimus dorsi muscle development is the goal of the late pull-down machine.

The only components of a pull-down machine are pulleys and metallic cables. The user applies force to the cable's opposite end, which is coupled to an adjustable weight, to lift the weight. Depending on the type of activity, the cable may be dragged up or down. A multipurpose machine used to strengthen the biceps, triceps, shoulders, and legs, the working principle of the lat pull-down machine is shown in Fig. 9. The generator should connect to each stable pulley with the help of BUG and all the generators should be connected in a parallel way to the rectifier. This maintains the voltage constant and adds the current [7].

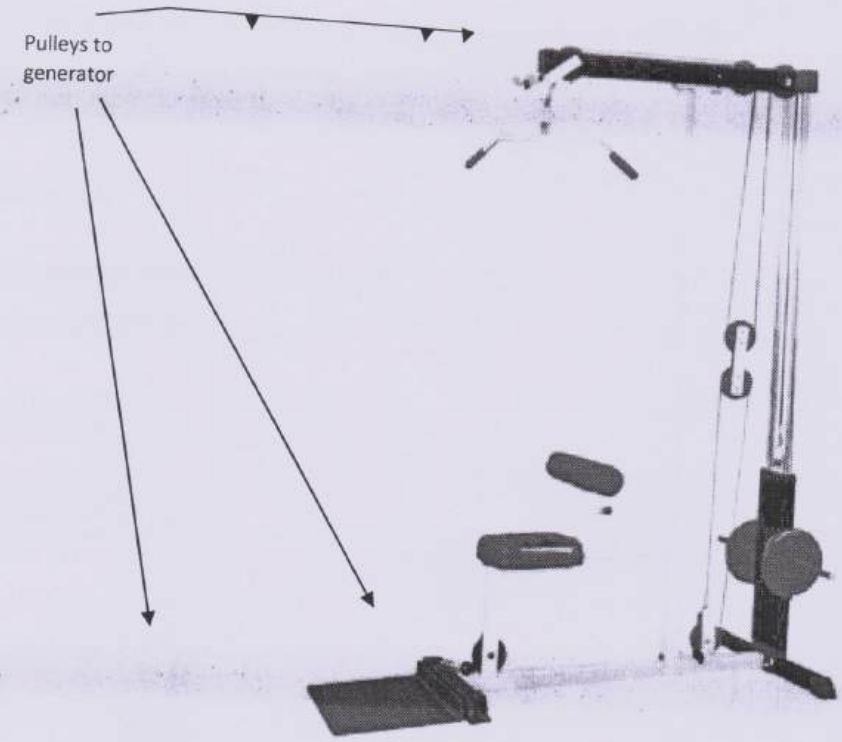


Fig-9: Lat pull down machine.

2) Butter fly

It goes by the name "butterfly arms" and is typically a standalone apparatus in a gym. The butterfly machine provides good exercise for the shoulders and chest. The purpose of the operation is to build up the chest muscles.

Operation: While seated, place your hands or forearms on the longboards. After pulling your arms together, open up your chest to release the tension.

Slowly revert to the starting position. By adding a low RPM generator, as shown in Fig. 10, it is feasible to transform the butterfly machine into an energy-generating device.

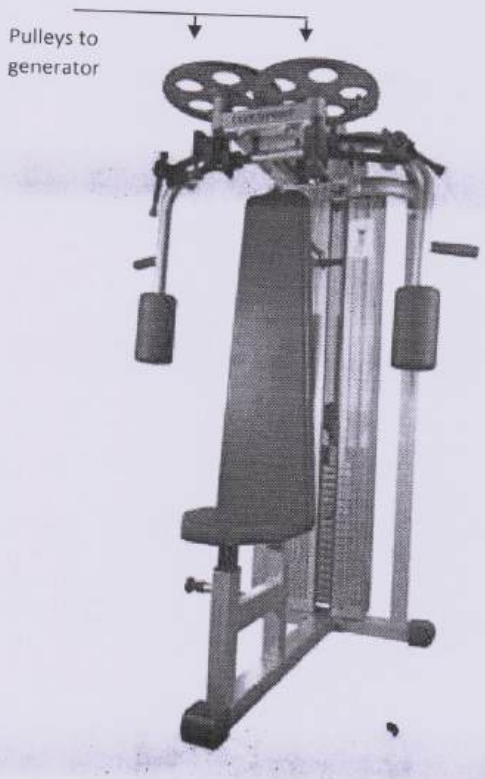


Fig-10: Butterfly gym equipment

3) Leg press machine

The leg press is a well-liked and straightforward exercise that can assist develop important leg muscles.

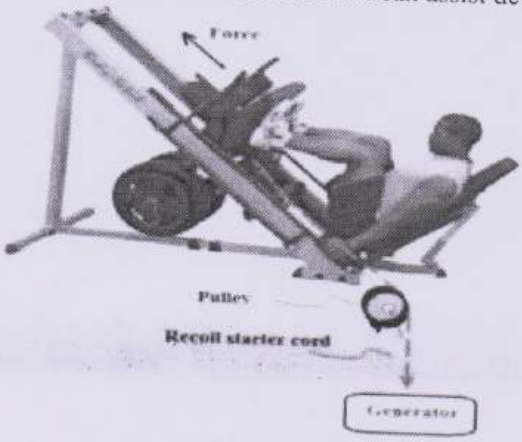


Fig-11: Leg press machine

The user sits on the machine with his head and back resting pleasantly against the padded support. Legs should form an angle of 90 degrees at the knees when feet are placed on the footplate, with heels kept flat. Knees should not be bent inward or outward and should be in line with the feet. When pressing, be sure to

maintain this alignment and refrain from raising your bottom off the seat. For a comfortable position, the seat is mobile. These offer assistance during the motion and aid in maintaining the proper alignment of your head and spine. A typical error that will ruin one's form is placing the hands on the knees. By adding a pulley, a recoil rope, and a generator in the machine's basement, as shown in Fig. 11, a leg press machine can also be turned into an energy-generating device. Every time a machine is turned on, the recoil rope over the pulley rotates the generator's armature.

4) Leg curls extension machines

A Leg curl machine is used to work out the muscles in the back or posterior of the leg, primarily the hamstrings. The leg extension machine makes the legs straighten against load resistance and thus works the muscles on the front or anterior of the leg called the quadriceps.

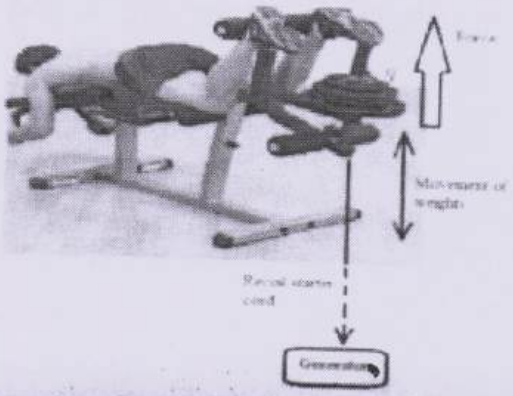


Fig-12: Leg curl machine

Quads: When we utilize the leg extension machine, the quadriceps muscles are engaged. The rectus femoris, vastus lateralis, vastus medialis, and vastus intermedius are the muscles that make up this group. The rectus femoris is the muscle that is most active during a leg extension exercise. The vastus medialis then contracts at the motion's conclusion when your knee is almost straight. Targeting the quadriceps muscle in the legs, the leg extension is a weight-resistance exercise.

Hamstrings: The muscles in the back of the thigh contract when using a leg curl machine to bend the knee. The biceps femoris, semimembranosus, and semitendinosus are the three muscles that make up the hamstrings. The biceps femoris is the largest of the three.

Calves: The gastrocnemius and the soleus are the two muscles that make up the calf; however, the gastrocnemius, which is the most superficial, is the one that is used most frequently during leg curls. When utilizing either of the leg curl machines, it spans the back of the knee and supports the hamstrings. Utilizing a device known as the Leg Extension Machine, the exercise is performed.

5) Stationary bicycle

A stationary bicycle, commonly referred to as an exercise bike or a spinning bike, is a basic device composed of a saddle, pedals, wheels, chain, and possibly handlebars mounted on the frame of a bicycle. The stationary bicycle's rider rotates the pedals, which causes the wheel to spin. Less body fat should be seen in riders after regular riding machine training. The front tire of a stationary bicycle is connected to a generator in such a way that the coils of wire within the generator rotate between the poles of the magnets [7]. By coupling the generator's shaft to the spinning wheel, which causes the generator's armature to

rotate, a stationary bicycle can produce energy. This process is shown in Fig. 13. Due to the load on the generator in this design, more force will be required to spin the bicycle's wheel. In comparison to a leg extension machine, the generator's load will feel like a weight that the rider must lift. Battery packs are then used to store the electrical energy (power packs). A stationary bike is another energy-producing workout equipment (EGGM) [4] [6].

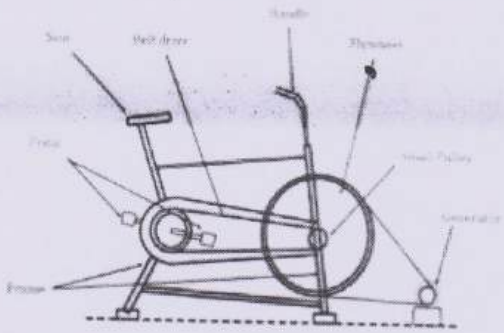


Fig-13: Stationary bicycle

3. SCOPE OF EGGS

In developing nations where young people are becoming more health concerned, the idea of an energy-generating gym system has a lot of potentials. The EGGM system will be able to cover a fair part of a single gym building's electrical needs.

Customers can use microgrids to return excess electricity from distributed energy sources (DES) to the utility under the emerging smart grid system for power distribution in the twenty-first century (MG). The reliability of the system is increased by MG, which is a compact collection of interconnected power generating and control technologies that can function either as part of or apart from a central grid. These systems can be more adaptable than conventional grids by enabling the incorporation of distributed generation (DG), such as wind and solar. As a foundational element for a potential low-voltage distribution system, the MG concept was first put forth in 2002. It was built on the concept of combining many micro sources (Renewables) and loads into a single distinct entity that, from the perspective of the overhead power system, might be understood as a single dispatchable prosumer [8]. The two main distinctions between an MG and a regular power plant are that MGs have a much smaller capacity compared to big conventional power plants and that electricity produced at distribution voltage can be directly fed into the utility distribution network. An MG's technological attributes make it ideal for distributing electricity to rural sections of a nation when access to the national grid system is either complicated by topology, harsh weather conditions, or artificial interruptions [9]. The fundamental benefit of an MG from a grid perspective is that it is regarded as a controllable entity inside the power system [9] [10]. From the perspective of the users, MG is advantageous for locally satisfying their electrical and heating needs and can deliver uninterruptible power, enhance local dependability, lower feeder losses, and provide local voltage support [9]. To run the AC appliances, direct current (D.C.) must first be converted into alternating current (A.C.) using an inverter as mentioned in 2.1 installation of the rpm generator [4].

4. MODELLING & ANALYSIS

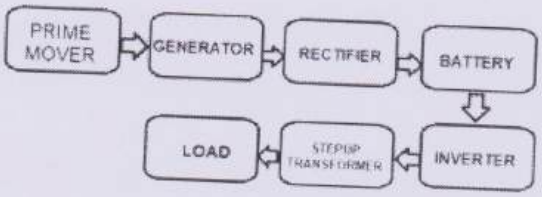


Fig-14: Block diagram of the proposed system.

i. For Stationary bicycle:

The alternator reaches its Maximum Potential at 25003000 RPM let's assume 30 rpm avg. speed of the pedal, so,

Alternator pulley speed (N) = 30 rpm × 5 × 3 × 3 × (3 / 2) × (4 / 3) = 2700 RPM

But coupling belt loss is 4.22% and gear loss is 7%. Subtracting coupling belt losses and gear losses we get 2400 RPM. That's enough to get average potential from the alternator. Normally, a gymnasium consumed 1000 units per month approximately. So,

Load demand (1000/30) /24 = 1.34 kWh.

The average number of members per day at the gym is about 200. The avg. number of members per day pedal the bike is about 60.

Pedalling time per mankind is about 20 minutes. So, the daily pedalling time per gym is 1200 minutes.

The output avg. current, I = 4.5A The output average voltage, V = 15V The average output power,

P = V× I = 15×4.5 = 67.5Watts.

A gym may capture 1.35 kWh of energy each day from this output power. This is enough energy to keep the lights on during load shedding or other maintenance.

EFFICIENCY: The force on the alternator shaft is 6.2 N. Alternator shaft diameter is 0.0254 m So, Torque (T) = F r sinθ = 0.1574 N-m Now, Power = Torque × Speed (rpm)/9.5488 = 39.56 watt

The mechanical input power is 39.56 watts. The obtained output power is 67.5 watt.

Overall efficiency = (output power / input power) × 100% = 58.62%

When all losses are subtracted from the total efficiency of the system, it equals 58.62 percent [6].

ii. For other equipments:

Similarly, we can generate electricity from other gym equipments via above mentioned setups.

5. APPLICATIONS

This project helps to lower the demand for energy. The electricity produced by this initiative will run the lightbulbs, tubes, laptop and mobile phone chargers, among many other things. This technology will assist in the requirement because certain areas are struggling with a lack of electricity. This project also benefits mountainous regions where access to electricity is challenging.

6. AKNOWLEDGEMENT

Prof. Dr. Jyoti Dhanke, Assistant professor, Department of engineering science, Bharati Vidyapeeth College of Engineering, Lavale, Pune, our internal guide and helper has worked very hard to help us mould our ideas and knowledge to match the project requirements. She has helped us complete every project milestone, stood by us when a project fails, and bolstered our confidence when a project succeeds.

7. CONCLUSION

By modelling each gym machine as an EGGM, this paper addressed the evolution of gym equipment. Although speculative, this discovery is a crucial first step toward a new method of producing energy with the help of people. Local DG of electricity through RES integration is the answer to the depletion of energy resources. Humans are regarded as a RES in the proposed research because EGGM would be powered by human labour. And the pulley will make this process easier as it takes input in both directions and gives single unidirectional output.

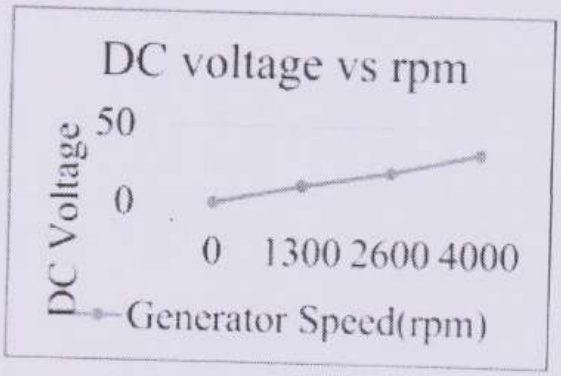


Fig-15: Graph of voltage vs rpm

AUTHORS CONTRIBUTIONS

Dr. Jyoti Dhanke: Supervision.

Hrishikesh Bhavar: Writing articles, Writing- original draft.

Sifan Momin: Concepts

Harshal Patil: Data gathering

Akshay redekar: Validation

Dr. R. N. Patil, Avinash Dadge, Dr. Narayan Phadatare, Prof. P. Pawar : Visualizations.

DECLARATION OF COMPETING INTEREST

The authors declare that they have no known competing financial interests or personal relationships that could have appeared to influence the work reported in this paper.

REFERENCES

[1] M. Musharraf, F. Iqbal and I. Saleem, "Energy Generating Gymnasiums Machines for Renewable, Sustainable and Green energy," *International Research Journal of Engineering and Technology (IRJET),* vol. 05, no. 12, pp. 153-160, 2018.

[2] M. Kumar and Dr. G. S. Mundada, "Energy Harvesting from Gym Equipments," *International Journal of Innovative Research in Electrical, Electronics, Instrumentation and Control Engineering,* vol. 5, no. 7, pp. 127-131, 2017.

[3] R. Strzelecki, M. Jarnut and G. Benysek, "Exercise bike powered electric generator for fitness club appliances," *2007 European Conference on Power Electronics and Applications,* 2008.

[4] K. Omprakash and T. B. Gottawala, "ELECTRICITY GENERATION THOUGHT GYM EQUIPMENT (GYM CYCLE)," *International Research Journal of Modernization in Engineering Technology and Science,* vol. 04, no. 02, pp. 1547-1552, 2022.

[5] C. Iwendi and G.-G. Wang, "Combined power generation and electricity storage device using deep learning and internet of things technologies," *ScienceDirect-Elsevier,* vol. 8, pp. 5016-5025, 2022.

[6] M. S. Borchate, A. Gaikwad, A. Jadhav and P. Dhage, "Design of Treadmill to Generate Electricity by using Mechanical Energy," *International Conference on Ideas, Impact and Innovation in Mechanical Engineering (ICIIIME),* vol. 5, no. 6, pp. 498-505, 2017.

[7] V. S. Bonde, B. V. Khatake, D. V. Zambare, V. D. Patel and N. V. Kadam, "Electric Power Generation from Gym Equipment with Polarity Checker and Changer Circuit. International Journal for Scientific Research & Development," *International Journal for Scientific Research & Development,* vol. 5, no. 2, pp. 992-995, 2017.

[8] T. Dragičević, X. Lu, J. C. Vasquez and J. M. Guerrero, "DC Microgrids—Part II: A Review of Power Architectures, Applications, and Standardization Issues," *IEEE,* vol. 31, no. 05, pp. 3528-3549, 2016.

[9] S. Chowdhury and P. Crossley, Microgrids and active distribution networks [electronic resource], London : Institution of Engineering and Technology, c2009, 2009.

[10] A. Rai, A. Mishra, A. S. Idreeshi, R. Yadav and K. Kumar, "An Innovative Technique of Electricity Generation and Use of Washing Machine by Treadmill," *International Journal for Research in Applied Science & Engineering Technology (IJRASET),* vol. 9, no. 6, pp. 209-2013, 2021.

Skip to main content

Author Search Sources Create account Sign in

Source details

Feedback > Compare sources >

European Chemical Bulletin

Open Access

Scopus coverage years: from 2017 to Present

Publisher: Deuton-X Ltd.

E-ISSN: 2063-5346

Subject area: Chemistry: General Chemistry

Source type: Journal

Save to source list Source Homepage

CiteScore 2021
0.8

SJR 2021
0.139

SNIP 2021
0.187

CiteScore CiteScore rank & trend Scopus content coverage

Improved CiteScore methodology

CiteScore 2021 counts the citations received in 2018-2021 to articles, reviews, conference papers, book chapters and data papers published in 2018-2021, and divides this by the number of publications published in 2018-2021. Learn more >

CiteScore 2021

0.8 = 182 Citations 2018 - 2021 / 217 Documents 2018 - 2021

Calculated on 05 May, 2022

CiteScoreTracker 2022

1.6 = 499 Citations to date / 313 Documents to date

Last updated on 04 April, 2023 • Updated monthly

JCST Journal of Data Acquisition and Processing
ISSN: 1004-9037
https://sicjycl.cn/
DOI: 10.5281/zenodo.7766259

ENHANCEMENT OF GRINDING PROCESS USING MOLYBDENUM DISULPHIDE AS A LUBRICANT BASED ON THE TAGUCHI METHOD

Dr. R. N. Patil[1,a *], Dr. J. A. Dhanke [2,b], Dr. Gurusharan Kaur[3,c], Prof. Atish Mane[4,d]

[1,2,4]Bharati Vidyapeeth's College of Engineering, Lavale, Pune, MH, India.

[3]Sagar Institute of Research and Technology, Bhopal, MP, India

[a]rnpatil1@gmail.com , [b]jyotidhanke@gmail.com, [c]kgurusharan@gmail.com, [d]mane.atish@bharatividyapeeth.edu

Abstract: Grinding is one of the most popularly used surface finishing process characterized by excellent process capabilities in terms of surface finish and material removal rate. It has wide applications in manufacturing industry as it can handle a wide variety of workpiece materials and forms. However it needs very high specific energy and gives rise to very high temperature, which results into high residual stresses, micro cracks and burn. To reduce these ill effects normally coolants are employed, which reduce the friction and provides effective cooling of work wheel interface. Conventional applications of coolants are many times ineffective due to inaccessibility of the fluid to grinding zone and film boiling. Many of the conventional coolants pose health hazard and support the green house effect. This paper deals with the use of solid lubricant, Molybdenum Disulphide carried in the proper medium to grinding zone and reducing the friction and hence eliminating the thermal ill effects on the grinding process. Results show that the grinding force, grinding energy and the surface roughness decreases with the help of the use of Molybdenum Disulphide compared with dry grinding and grinding with the conventional coolants.

Keywords: Coolant; Lubricant; Molybdenum Disulphide; Taguchi method.

I. INTRODUCTION

Grinding is the process of material removal in the form of small chips by mechanical action of abrasive particles bonded together in grinding wheel. It is basically a finishing process employed for producing close dimensional and geometrically accuracies and smooth surface finish. However in some applications, the grinding process is applied for higher material removal rates and is also referred as abrasive machining [1]. It is distinguished from many other machining processes on aspects like tool geometry, large contact area and high friction between tool and workpiece and high specific energy requirement. The high specific energy consumed during the grinding process results into heat. Major portion of heat is transferred to workpiece [2]. The severe heat input affects the workpiece quality. It may induce thermal damage such as burn, surface and subsurface cracks, metallurgical phase transformations, residual tensile stresses and dimensional distortions and many more ill effects [3-5]. To control the ill effects of heat generated during the grinding process at the cutting zone and ensure the quality of the workpiece, coolants are employed. Grinding fluids are introduced

into grinding operations to reduce and transfer heat during grinding, lubricate during chip formation, wash the grinding wheel of loose chip and swarf, chemically aid the grinding action or machine maintenance. Grinding fluids of five different categories are used popularly. These are petroleum base and mineral base cutting oils, water soluble oils, synthetic fluids, semi synthetic fluids, water plus additives, including rust inhibitors, water treatments (for examples, softeners), and defoaming agents. Several researchers have carried out research on the coolant type, its composition and supply characteristics [6]. However, during grinding operation coolants are relatively inaccessible to the grinding arc. Therefore, often it is ineffective in reducing the grinding zone temperature, but only provides bulk cooling of the work piece. The stiff boundary layer forming around the rotating grinding wheel also inhibits the access of the fluid to the grinding zone [7, 8]. Conventional coolants lose their cooling properties upon film boiling and that the film boiling temperature of these coolants are lower which affects the effectiveness of grinding fluid [9]. However, flooded coolant operation allows effective removal of grinding swarf, which is needed in grinding. Conventional grinding fluids are a source of environmental hazards and increasingly strict regulations are coming up with regard to their use and disposal [10]. The cost of these fluids is also high. As an alternate to conventional fluids several other coolants/ lubricants are tried. Some efforts have been carried out with the help of solid lubricants as a substitute which has shown substantial improvement in the process [11]. Further these factors prompted investigations on the use of biodegradable coolants, minimum quantity coolant and coolant free grinding [12]. But any attempt to minimize or avoid the coolant can be dealt with only by the substitution of the functions normally met by the coolants by some other means. Grinding employing cryogenic cooling by liquid nitrogen and minimum Quantity Lubrication (MQL) by ester oil supplied in the form of spot jet or spray mist are the alternative approaches towards this end. The effect of graphite nanoplatelets in solid lubrication grinding are also studied which gives effective way of improving the process [13]. The results are very encouraging but the required amount of nanomaterial significantly increases the overall cost.

The objective of the present investigation is to employ molybdenum disulphide, which is a high temperature solid lubricant, as a means to reduce the heat generated at the grinding zone and study the process performance. An experimental set-up is designed and built for comparative performance analysis of molybdenum disulphide assisted grinding with dry and conventional flooded coolant grinding.

II. EXPERIMENTAL SETUP

An experimental set up is designed and fabricated to ensure proper delivery of the solid lubricant with the carrier to the grinding zone. This is devised with the help of dead weight loaded cylinder. The mix of molybdenum disulphide and the carrier oil is introduced into the cylinder. Constant pressure is maintained on this mix with help of a piston which is in turn loaded by the dead weight mounted on the piston rod as shown in Fig. 1. The flow of mix is controlled with the help of the flow control valve. The mix is impinged on the grinding zone through a nozzle with an opening of 1mm * 25 mm. The width of the opening corresponds to the width of grinding wheel. The mix is first delivered to the soft rubber wheel, which is free to rotate and is maintained in constant contact with the grinding wheel. The paste is eventually

transferred to the grinding wheel and then to the grinding zone to serve as a lubricant in the grinding zone.

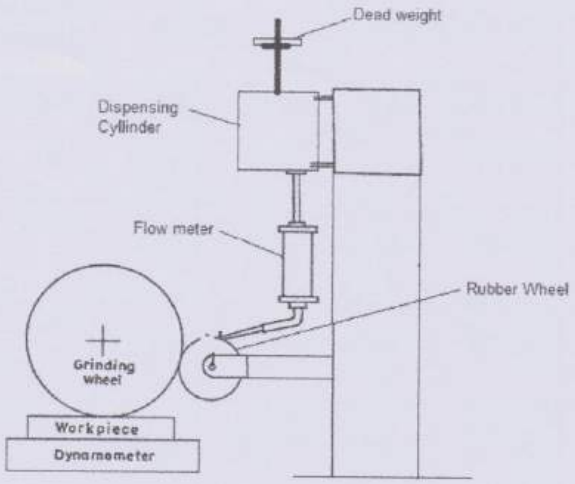


Fig. 1. Schematic diagram of Experimental set up.

2.1 Primary Experimentation

The grinding operation is carried out on horizontal reciprocating table surface grinding machine. The test specimen of size 100 mm*50 mm*10 mm thickness is used for the experimentation. Grinding is carried out along the length of the workpiece.

The ultimate effect in which industry is primarily interested is the quality of surface finish obtained through the process and the amount of energy consumed for the process. Hence for primary investigations following factors are kept constant. The details of which are provided in Table 1.

Primary experimentation is carried out on alloy steel AISI 4140 to observe the effect of uses of solid lubricants on the process. The results of experimentation are tabulated in Table 2.

Table 1. Factors kept constant in grinding.

Factor	Details
Workpiece material	Alloy steel AISI 4140
Grinding machine	Horizontal spindle surface grinding, machine, PMT make, Model SG 42, 5.5 kw
Grinding Wheel	A60L5V10, Diameter 300 mm, width 25 mm.
Wheel velocity	30m/min
Table feed rate	10m/min
Dressing conditions	With single point diamond dresser, 1 carat, in dry condition.

Table 2. Observations for preliminary experimentation.

Depth of Cut (µm)	Dry Grinding		Wet Grinding		Molybdenum disulphide	
	Force (N)	Ra (µm)	Force (N)	Ra (µm)	Force (N)	Ra (µm)
10	434.42	0.46	403.16	0.46	257.21	0.43
20	506.82	0.47	470.35	0.47	300.08	0.44
30	579.21	0.47	537.54	0.47	342.95	0.44
40	651.62	0.47	604.73	0.47	385.82	0.44
50	724.02	0.47	671.93	0.47	428.68	0.44

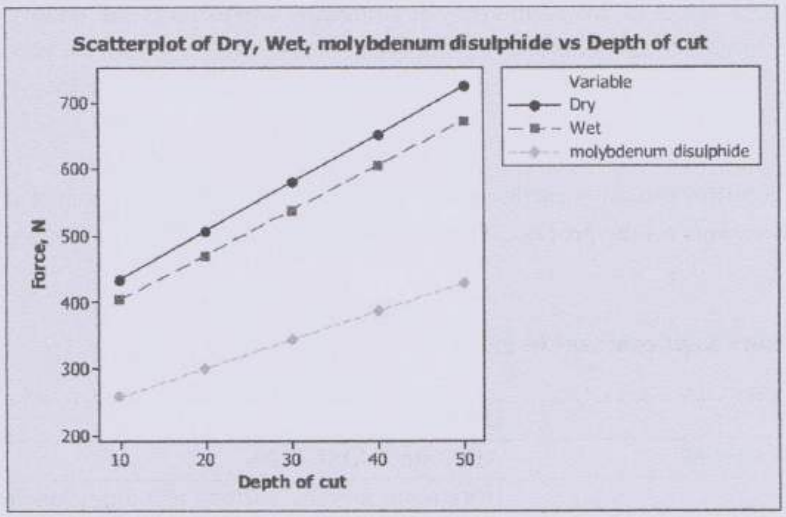


Fig. 2. Effect of coolants on force under varying depths of cut

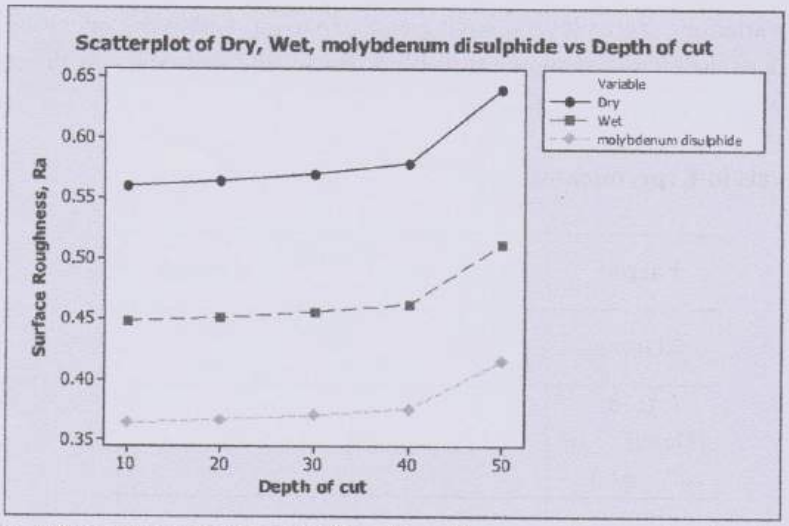


Fig. 3. Effect of coolants on Surface Roughness under varying depths of cut

2.2 Taguchi methods for design of experiments

Taguchi methods of experimental design provide a simple, efficient and systematic approach for the optimization of experimental designs for performance quality and cost. It has been proved successful to many manufacturing situations. The traditional experimental design procedures focus on the average product or process performance characteristics. But the Taguchi method concentrates on the effect of variation on the product or process quality characteristics rather than on its averages. That is, the Taguchi's approach makes the product or process performance insensitive (robust) to variation to uncontrolled or noise factors. Taguchi recommends that this can be done by the proper design of parameters during the 'parameter design' phase of off-line quality control. He designed certain standard orthogonal arrays (OAs) by which simultaneous and independent evaluation of two or more parameters for their ability to affect the variability of a particular product or process characteristic can be done in a minimum number of tests. Subsequently, decision is made for the optimum combination of these parameters.

The following objectives are fixed for the study:

(i) Find out the effect of use of molybdenum disulphide on force required for grinding and surface roughness obtained, and

(ii) Conduct a comparative study of the applications to various alloy steels.

The surface roughness (Ra) of the ground piece and the force required (F) are taken as the quality characteristics of the process. The surface finish is a direct process result and is measured by a Mitutoyo surftest. For force measurements a dynamometer is used, which recorded the two components of force. The resultant force is worked out and is considered as a single response.

The operating conditions such as speed and feed are held constant during the experimentation. However, infeed rate, workpiece material and flow rate of the lubricant is

considered for variation. Three levels, having equal spacing, within the operating range are selected for each of the factors as shown in Table 3. By selecting three levels the curvature or the non-linearity effects could be studied.

Table 3. Levels in Experimentation

Factor	Level 1	Level 2	Level 3
Material	AISI 4140	AISI 4310	AISI 52100
Infeed (Depth of cut), (μm)	10	30	50
Flow Rate, (mm^3/min)	20	40	60

Table 4 shows the experimental layout of an L_{27} 0rthogonal array consisting of three control factors and three levels according to Taguchi's suggestion. The numbers in each column indicate the levels for the specific factors and from the L_{27} orthogonal array 27 experiments are required to examine the total manufacturing parameters. The L_{27} orthogonal Array which meets this requirement is selected.

Table 4. L_{27} Orthogonal array.

Trial	Material	In feed (μm)	Flow Rate (mm^3/min)
1	1	1	1
2	1	1	1
3	1	1	1
4	1	2	2
5	1	2	2
6	1	2	2
7	1	3	3
8	1	3	3
9	1	3	3
10	2	1	2
11	2	1	2
12	2	1	2
13	2	2	3
14	2	2	3
15	2	2	3

16	2	3	1
17	2	3	1
18	2	3	1
19	3	1	3
20	3	1	3
21	3	1	3
22	3	2	1
23	3	2	1
24	3	2	1
25	3	3	2
26	3	3	2
27	3	3	2

2.3 Experimentation

By choosing the L_{27} orthogonal array the issue of repeating the tests is sorted out, as the array itself recommends the repetitions. This helps to obtain more reliable information from the statistical analysis of the experiment. Quality characteristics, i.e. surface roughness (Ra) in μm and force (F) in N are noted by the measurement systems. For having consistent results with Ra, pieces are ground giving seven sets of upward and downward spark out passes. The sample data obtained for the quality characteristics, i.e. surface roughness (Ra in μm) and force in N in the molybdenum disulphide assisted grinding is shown in Table 5. It is observed that there is considerable consistency in the obtained data and it is reliable for statistical analysis.

Table 5. Sample data for force and surface roughness in molybdenum disulphide assisted grinding.

Trial	Force (N)	Surface roughness (μm)
1	302.6	0.43
2	311.96	0.44
3	316.71	0.46
4	306.64	0.43
5	311.31	0.44
6	320.94	0.46
7	342.95	0.43
8	353.56	0.44
9	358.94	0.46
10	308.17	0.47
11	312.87	0.48
12	322.54	0.51
13	367.64	0.48

14	379.01	0.49
15	384.78	0.52
16	675.81	0.5
17	686.1	0.51
18	707.32	0.54
19	323.92	0.48
20	333.94	0.49
21	339.02	0.52
22	635.14	0.5
23	644.82	0.51
24	664.76	0.54
25	603.38	0.5
26	622.04	0.51
27	631.51	0.54

2.4. Analysis of the data

2.4.1. Evaluation of S/N ratios

Taguchi suggests the transformation of the repetition data in a trial into a consolidated single value called the S/N ratio. Here, the term 'signal' represents the desirable value (mean) and the 'noise' represents the undesirable value (standard deviation). So the S/N ratio represents the amount of variation present in the quality characteristic. Depending upon the objective of quality characteristic there can be various types of S/N ratios. Here the desirable objectives, the force required for the grinding operation and the surface roughness should be lower. Hence the lower-the-better type S/N ratio, as given below is applied for transforming the observed data:

$$Z = -\log_{10} \{\text{sum } (y^{**}2)/n\}$$

Where Z is the S/N ratio for the lower-the-better case, y is the measured quality characteristic for the i^{th} repetition, and n the number of repetitions in a trial. The S/N ratios, standard deviation and mean for grinding force for molybdenum disulphide assisted grinding for various alloy steels, the varying flow rates and infeed rates are calculated from the observed data and tabulated in Table 6.

Table 6. Calculated S/N ratio, Standard deviation and Mean for the experimentation.

Trial	S/N Ratio	Standard Deviation	Mean
1	-49.8406	7.1794	310.423
2	*	*	*
3	*	*	*
4	-49.9114	7.292	312.963
5	*	*	*

6	*	*	*
7	-50.9279	8.1363	351.817
8	*	*	*
9	*	*	*
1	-49.9547	7.3268	314.527
1	*	*	*
1	*	*	*
1	-51.5317	8.7211	377.143
1	*	*	*
1	*	*	*
1	-56.7753	16.0678	689.743
1	*	*	*
1	*	*	*
1	-50.432	7.6835	332.293
2	*	*	*
2	*	*	*
2	-56.2363	15.1033	648.24
2	*	*	*
2	*	*	*
2	-55.835	14.313	618.977
2	*	*	*
2	*	*	*

From the calculated values of signal to noise ratio, the values are obtained for the various levels of the factors and tabulated in Table 7.

Table 7 Signal to Noise Ratio: Smaller the better.

Level	Material	In feed (µm)	Flow rate (mm^3/min)
1	-50.23	-50.08	-54.28
2	-52.75	-52.56	-51.90
3	-54.17	-54.51	-50.96
Delta	3.94	4.44	3.32
Rank	2	1	3

The main effect plot (the data means) for the calculated S/N ratio is calculated and presented graphically as shown in the Fig. 4. The highest S/N ratio always yields the optimum quality with minimum variance. Therefore, the level with a higher value determines the optimum level of each factor. For the experimentation carried out the best results would be obtained for AISI4140, the workpiece material, infeed rate of 10 µm, and flow rate of 60mm^3/min.

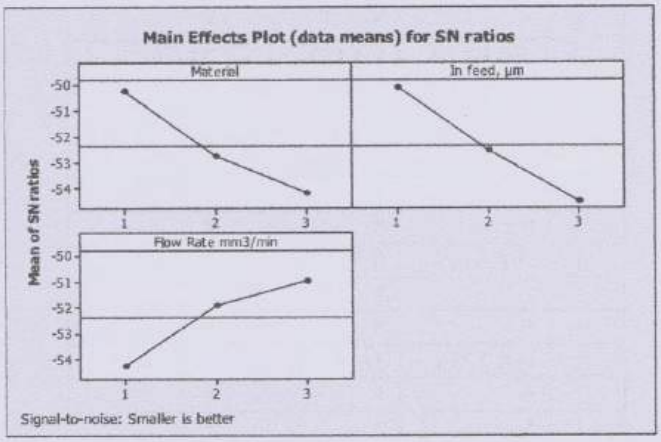


Fig 4. Main Effects Plot (data means) for SN rations (Signal to Noise: Smaller is better) for Molybdenum Disulphide.

From the calculated values of means, the values are obtained for the various levels of the factors and tabulated in Table 8 and the same is represented graphically in the Fig. 5

Table 8 Response Table for Means

Level	Material	In feed, µm	Flow rate, mm^3/min
1	325.1	319.1	549.5
2	460.5	446.1	415.5
3	533.2	553.5	353.8
Delta	208.1	234.4	195.7
Rank	2	1	3

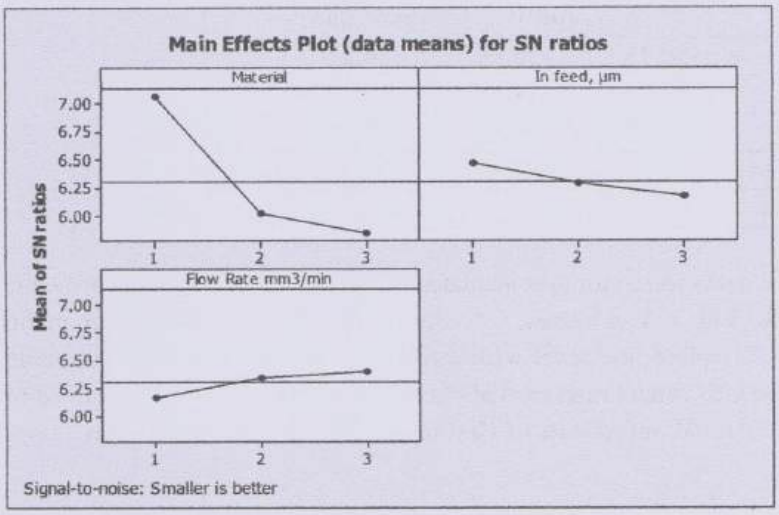


Fig.5 Main Effects Plot (data means) for Means

2.4.2 The regression Analysis

Taguchi technique can be used for the prediction of the full factorial design. The regression equation from full factorial prediction is

$$F = 371 + 0.181\ \tau s + 5.86\ d - 4.89\ f$$

Where, F is the grinding force in Newton, τs is the shear stress of workpiece material in MPa, d is the infeed in micrometers and f is flow rate in mm^3/min

Table 9 Regression Table

Predictor	Coefficient	Standard Error Coefficient	T	P
Constant	371.30	40.62	9.14	0.000
Shear stress	0.18117	0.03123	5.80	0.000
Infeed	5.8608	0.7161	8.18	0.000
Flow rate	-4.8929	0.7161	-6.83	0.000

S = 60.7615 R-Sq = 86.5% R-Sq(adj) = 84.7%

2.4.3. Analysis of Variance

ANOVA is a computational technique to estimate quantitatively the relative contribution which each controlled parameter makes on the overall measured response and is expressed as a percentage. Thus information about how significant the effect of each controlled parameter is on the experimental results can be obtained. The total variation in response is decomposed into variation due to various controlled factors and their interactions and due to the error involved in the experimentation. The ANOVA can be done with the raw data or with the S/N data. The ANOVA based on the raw data signifies the factors which affect the average response rather than reducing the variation. But ANOVA based on the S/N data takes into account both these aspects and so it is used here. Since it is a saturated design where all columns are assigned with the factors, the variations due to error are estimated by pooling the estimates of the factors having least variance. This also helped in determining the Fisher test (F-test) factor for finding out the confidence level of the results. The ANOVA is done for all the quality characteristics under study.

Table 10. ANOVA Table

Source	Degrees of Freedom	Sum of Squares	MS	F Value	P Value
Regression	3	543954	181318	49.11	0.000
Residual Error	23	84915	3692		
Total	26	628869			

Source	Degrees of Freedom	Seq. Sum of Squares
Shear Stress	1	628869
Infeed	1	124268
Flow Rate	1	172375

III. Interpreted Graphs For Force As A Quality Characteristic:

On the basis of the interpreted results of force required for grinding operation with the help of molybdenum disulphide as solid lubricant for the materials selected, AISI 4140, AISI 4340 and AISI 52100 are given in Fig.6 to Fig. 8.

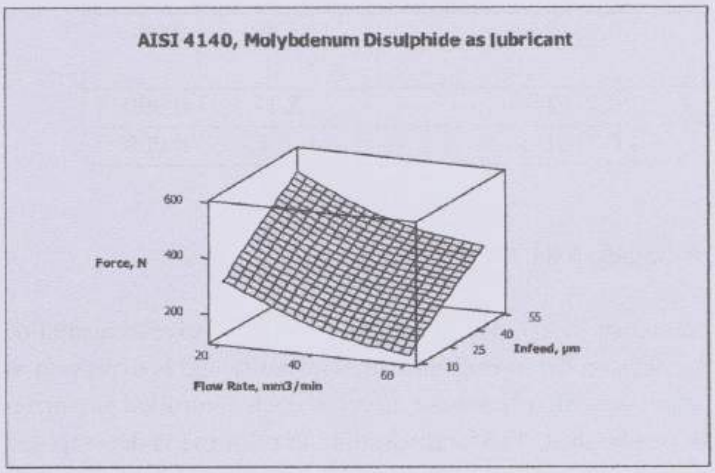


Fig. 6. AISI 4140, Molybdenum Disulphide as lubricant

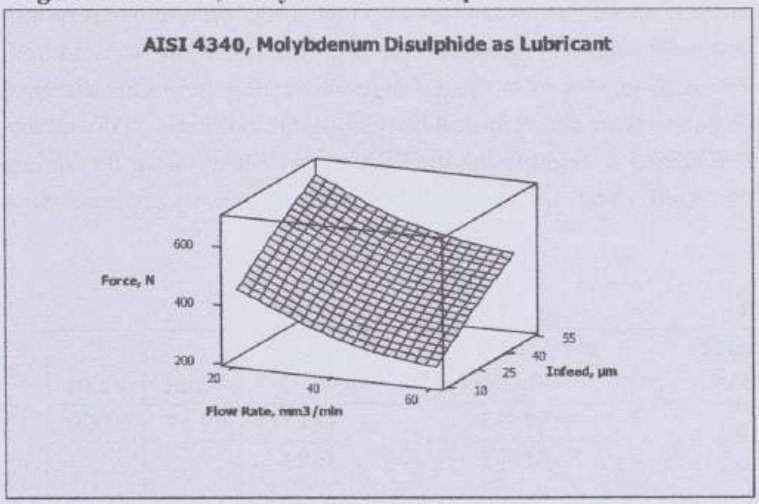


Fig. 7. AISI 4340, Molybdenum Disulphide as lubricant

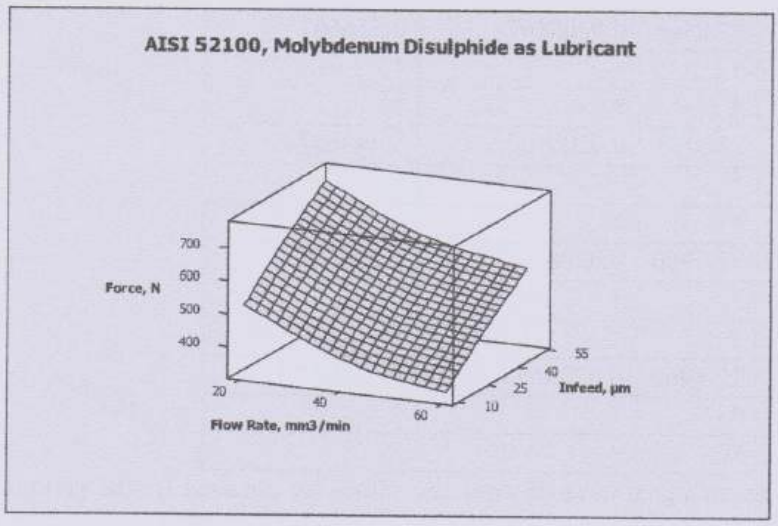


Fig. 8. AISI 52100, Molybdenum Disulphide as lubricant

IV. Analysis for Surface Roughness

On the similar lines of the force, Taguchi analysis is done for surface roughness obtained in the molybdenum disulphide assisted grinding process. The S/N ratios, standard deviation and mean for surface roughness for molybdenum disulphide assisted grinding for various alloy steels, the varying flow rates and infeed rates are calculated from the observed data are tabulated in Table 11.

Table 11. Calculated S/ N ratio, Standard deviation and Mean.

Trial	S/N Ratio	Standard Deviation	Mean
1	29.2548	0.0152753	0.443333
2	*	*	*
3	*	*	*
4	29.2548	0.0152753	0.443333
5	*	*	*
6	*	*	*
7	29.2548	0.0152753	0.443333
8	*	*	*
9	*	*	*
10	27.3764	0.0208167	0.486667
11	*	*	*
12	*	*	*
13	27.5531	0.0208167	0.496667
14	*	*	*
15	*	*	*

16	27.8960	0.0208167	0.516667
17	*	*	*
18	*	*	*
19	27.5531	0.0208167	0.496667
20	*	*	*
21	*	*	*
22	27.8960	0.0208167	0.516667
23	*	*	*
24	*	*	*
25	27.8960	0.0208167	0.516667
26	*	*	*
27	*	*	*

From the calculated values of signal to noise ratio, the values are obtained for the various levels of the factors and tabulated in Table 12.

Table 12. Signal to Noise Ratios Smaller is better

Level	Material	In feed (µm)	Flow rate (mm^3/min)
1	7.062	6.462	6.175
2	6.018	6.289	6.348
3	5.845	6.175	6.403
Delta	1.217	0.287	0.228
Rank	1	2	3

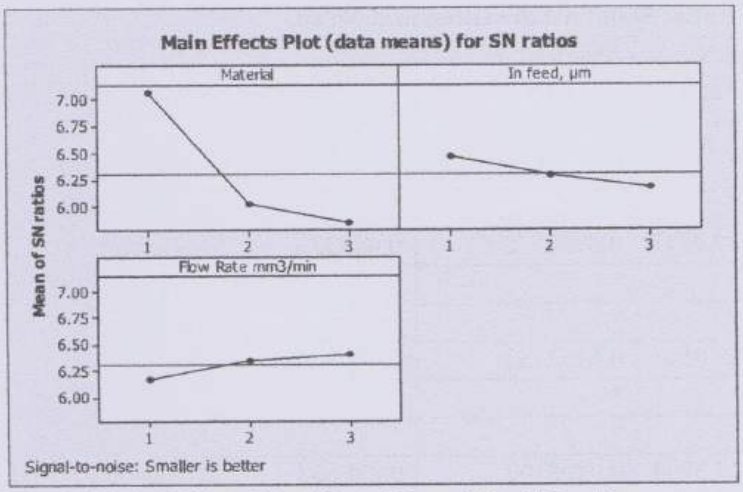


Fig. 9. Main Effects Plot (Data Means) for SN ratios

The main effect plot (the data means) for the calculated S/N ratio is calculated and presented graphically as shown in the Fig. 9. The highest S/N ratio always yields the optimum quality with minimum variance. Therefore, the level with a higher value determines the optimum level of each factor. For the experimentation carried out the best results would be obtained for AISI 52100, the workpiece material, infeed rate of 10 µm, and flow rate of 60mm^3/min.

From the calculated values of means, the values are obtained for the various levels of the factors and tabulated in Table 13 and the same is represented graphically in the Fig. 10.

Table 13 Response Table for Means

Level	Material	In feed (µm)	Flow rate (mm^3/min)
1	0.4433	0.4756	0.4922
2	0.5000	0.4856	0.4822
3	0.5100	0.4922	0.4789
Delta	0.0667	0.0167	0.0133
Rank	1	2	3

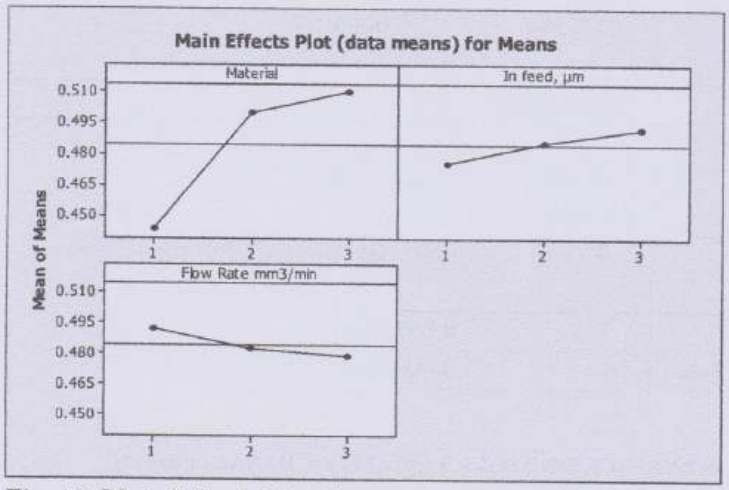


Fig. 10. Main Effects Plot (data means) for Means

4.1 The regression Analysis

Taguchi technique can be used for the prediction of the full factorial design. The regression equation from full factorial prediction is

$$Ra = 0.461 + 0.000050\ \tau s + 0.000417\ d - 0.000333\ f$$

Where, Ra is the grinding force in Newton, τs is the shear stress of workpiece material in MPa, d is the infeed in micrometers and f is flow rate in mm^3/min

Table 14. Regression Table

Predictor	Coefficient	Standard Error Coefficient	T	P
Constant	0.46089	0.01640	28.11	0.000
Shear stress	0.00005012	0.00001261	3.98	0.001

Infeed	0.0004167	0.00003931	10.60	0.000
Flow rate	-0.00033334	0.0002891	-1.15	0.261

S = 0.00333589 R-Sq = 92.5% R-Sq(adj) = 91.5%

4.2 Analysis of variance

ANOVA, the analysis of variance is carried out and the results are included in Table 15.

Table 15 ANOVA table

Source	Degrees of Freedom	Sum of Squares	MS	F Value	P Value
Regression	3	0.0115608	0.0038536	6.40	0.003
Residual Error	23	0138394	0.0006017		
Total	26	0.0254002			

Source	Degrees of Freedom	Seq. Sum of Squares
Shear Stress	1	0095108
Infeed	1	0.0012500
Flow Rate	1	0.0008000

V. INTERPRETED GRAPHS FOR SURFACE FINISH AS A QUALITY CHARACTERISTIC

On the basis of the interpreted results of surface roughness obtained in grinding operation with the help of molybdenum disulphide as solid lubricant for the materials selected, AISI 4140, AISI 4340 and AISI 52100 are given in Fig. 11 to Fig. 13.

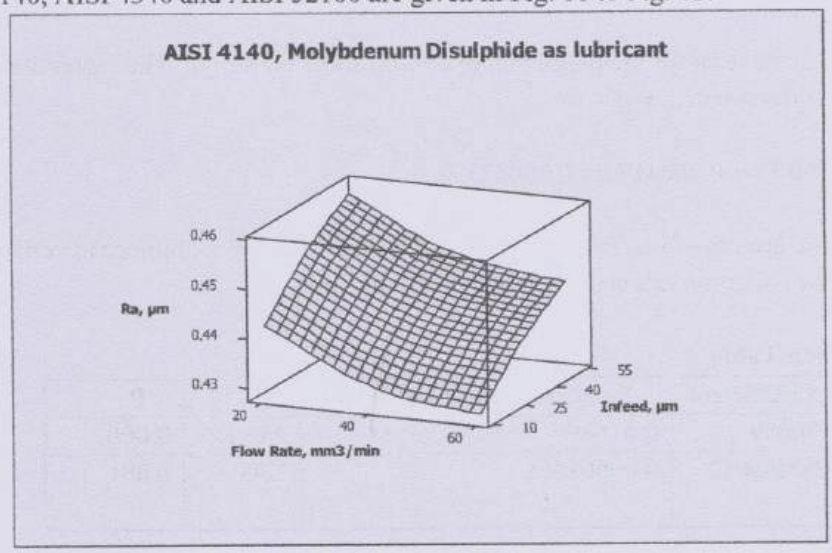


Fig.11. AISI 4140, Molybdenum disulphide as lubricant

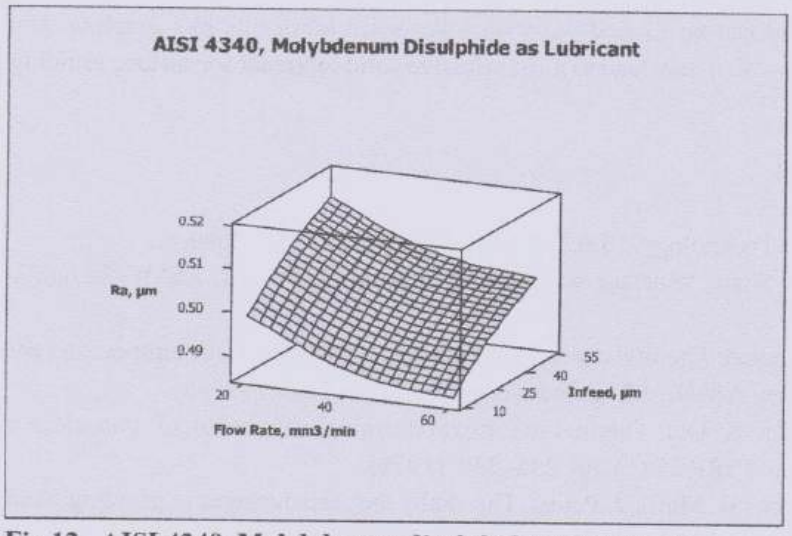


Fig.12. AISI 4340, Molybdenum disulphide as lubricant

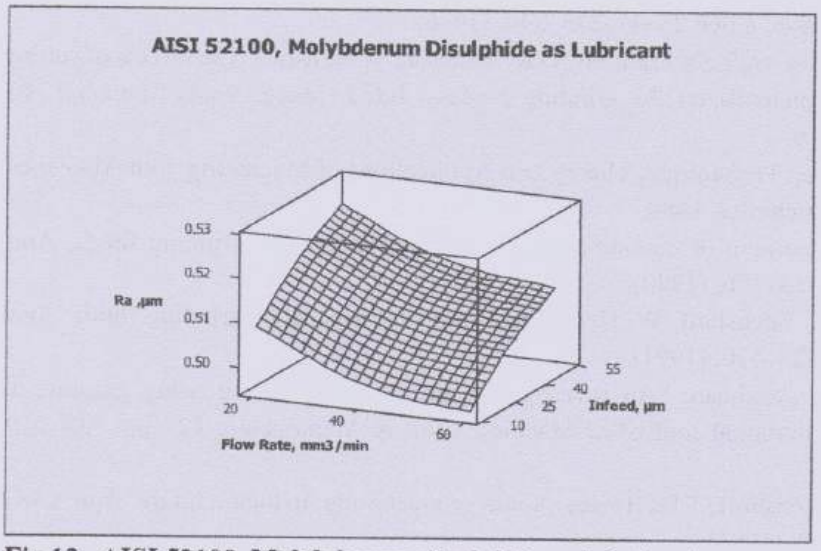


Fig.13. AISI 52100, Molybdenum disulphide as lubricant

VI. CONCLUSIONS

The experimental setup developed for the application of molybdenum disulphide as a means to reduce the heat generated in the grinding zone has been investigated for improving the surface finish and reducing the cutting forces involved in the process. The Taguchi method of experimental design is used for the investigations.

When compared with the dry grinding and grinding with the conventional coolants, molybdenum disulphide gives considerably reduces the force required for grinding operation

and the surface finished improved. Hence the effective role of molybdenum disulphide as a lubricant was evident from the improvement of output parameters.

Similar experimentation can be carried out with other solid lubricants like graphite, zinc phosphate and boric acid, which may lead to most effective solid lubricant for surface grinding.

VII. REFERENCES

1. H.M.T., "Production Technology," Tata McGraw Hill, pp.250-251, 2009.
2. J.O. Outwater, M.C. Shaw, "Surface temperature in grinding," Trans. ASME 74 pp.73–86, (1952).
3. S. Malkin, R. B Anderson, Thermal aspects of grinding — part II, surface temperature and workpiece burn, Trans. ASME, J.Eng. Indust. 96 , pp.1184–1191, (1974)
4. Y. Nakano, H. Uchida, K. Ota, Thermal deformations and profile errors of workpiece in surface grinding, Ann. CIRP 25 (1), pp. 235–240, (1976).
5. R. Snoys, K.U. Leuven, M. Maris, J. Peters, Thermally induced damages in grinding, Ann. CIRP 27 (2), pp.571–581, (1978).
6. Y. Nakano, H. Uchida, K. Ota, Thermal deformations and profile errors of workpiece in surface grinding, Ann. CIRP 25 (1) ,235–240, (1976).
7. S. Ebbrel, N.H. Wooley, Y.D. Tridimas, D.R. Allanson, W.B. Rowe, The effects of cutting fluid application methods on the grinding process, Int. J. Mach. Tools Manufact. 40, pp.209–223, (2000).
8. S. Malkin, Grinding Technology, Theory and Applications of Machining with Abrasives, Ellis Harwood, Chichester, 1989.
9. T.D. Howes, Assessment of cooling and lubricating properties of grinding fluids, Ann. CIRP 39 (1), pp. 313–316, (1990).
10. T.D. Howes, H.K. Toenshoff, W. Heur, Environmental aspects of grinding fluids, Ann. CIRP 40 (2), pp. 623–630, (1991).
11. S. Shaji, V. Radhakrishnan, "An investigation on surface grinding using graphite as lubricant," International Journal of Machine Tools & Manufacture 42 ,pp. 733–740, (2002).
12. I. Inasaki, H.K. Toenshoff, T.D. Howes, Abrasive machining in thethe future, Ann. CIRP 42 (2) pp.,723–732, (1993)
13. MatthewAlberts, KyriakiKalaitzidou, ShreyesMelkote, "An investigation of graphite nanoplatelets as lubricant in grinding," International Journal of Machine Tools & Manufacture, 49, pp.966–970, (2009).

12

Source details

Feedback > Compare sources >

Shu Ju Cai Ji Yu Chu Li/Journal of Data Acquisition and Processing

Scopus coverage years: from 2001 to Present

Publisher: Nanjing University of Aeronautics an Astronautics

ISSN: 1004-9037

Subject area: Computer Science: Signal Processing | Computer Science: Software

Source type: Journal

Save to source list | Source Homepage

CiteScore 2022
0.7

SJR 2022
0.140

SNIP 2022
0.221

CiteScore | CiteScore rank & trend | Scopus content coverage

Improved CiteScore methodology

CiteScore 2022 counts the citations received in 2019-2022 to articles, reviews, conference papers, book chapters and data papers published in 2019-2022, and divides this by the number of publications published in 2019-2022. Learn more >

CiteScore 2022

0.7 = 302 Citations 2019 - 2022 / 434 Documents 2019 - 2022

Calculated on 05 May, 2023

CiteScoreTracker 2023

0.8 = 329 Citations to date / 434 Documents to date

Last updated on 05 December, 2023 • Updated monthly

CiteScore rank 2022

Category	Rank	Percentile
Computer Science — Signal Processing	#110/122	10th
Computer Science — Software	#389/404	3rd

Journal of Data Acquisition and Processing
ISSN: 1004-9037
https://sjcjycl.cn/
DOI: 10.5281/zenodo.7766345

ENHANCEMENT OF GRINDING PROCESS USING ZINC PHOSPHATE AS A LUBRICANT

Dr. R. N. Patil[1,a] *, Dr. J. A. Dhanke [2,b] and Prof. Y. V. Kadam[3,c]
[1,2,3]Bharati Vidyapeeth's College of Engineering, Lavale, Pune, India.
arnpatil1@gmail.com , bjyotidhanke@gmail.com, yogesh.kadam@bharatividyapeeth.edu

Abstract
Grinding is one of the most popularly used surface finishing process characterized by excellent process capabilities in terms of surface finish and material removal rate. It has wide applications in manufacturing industry as it can handle a wide variety of workpiece materials and forms. However it needs very high specific energy and gives rise to very high temperature, which results into high residual stresses, micro cracks and burn. To reduce these ill effects normally coolants are employed, which reduce the friction and provides effective cooling of work wheel interface. Conventional applications of coolants are many times ineffective due to inaccessibility of the fluid to grinding zone and film boiling. Many of the conventional coolants pose health hazard and support the green house effect. This paper deals with the use of solid lubricant, Zinc Phosphate carried in the proper medium to grinding zone and reducing the friction and hence eliminating the thermal ill effects on the grinding process. Results show that the grinding force, grinding energy and the surface roughness decreases with the help of the use of Zinc Phosphate compared with dry grinding and grinding with the conventional coolants.
Keywords – Coolant, Zinc Phosphate , Grinding, Lubricant, Taguchi method.

1. Introduction

Grinding is the process of material removal in the form of small chips by mechanical action of abrasive particles bonded together in grinding wheel. It is basically a finishing process employed for producing close dimensional and geometrically accuracies and smooth surface finish. However in some applications, the grinding process is applied for higher material removal rates and is also referred as abrasive machining [1]. It is distinguished from many other machining processes on aspects like tool geometry, large contact area and high friction between tool and workpiece and high specific energy requirement. The high specific energy consumed during the grinding process results into heat. Major portion of heat is transferred to workpiece [2]. The severe heat input affects the workpiece quality. It may induce thermal damage such as burn, surface and subsurface cracks, metallurgical phase transformations, residual tensile stresses and dimensional distortions and many more ill effects [3-5]. To control the ill effects of heat generated during the grinding process at the cutting zone and ensure the quality of the workpiece, coolants are employed. Grinding fluids are introduced into grinding operations to reduce and transfer heat during grinding, lubricate during chip formation, wash the grinding wheel of loose chip and swarf, chemically aid the grinding action or machine maintenance. Grinding fluids of five different categories are used popularly. These are petroleum base and mineral base cutting oils, water soluble oils, synthetic fluids, semi synthetic

fluids, water plus additives, including rust inhibitors, water treatments (for examples, softeners), and defoaming agents.

Several researchers have carried out research on the coolant type, its composition and supply characteristics [6]. However, during grinding operation coolants are relatively inaccessible to the grinding arc. Therefore, often it is ineffective in reducing the grinding zone temperature, but only provides bulk cooling of the work piece. The stiff boundary layer forming around the rotating grinding wheel also inhibits the access of the fluid to the grinding zone [7, 8]. Conventional coolants lose their cooling properties upon film boiling and that the film boiling temperature of these coolants are lower which affects the effectiveness of grinding fluid [9]. However, flooded coolant operation allows effective removal of grinding swarf, which is needed in grinding. Conventional grinding fluids are a source of environmental hazards and increasingly strict regulations are coming up with regard to their use and disposal [10]. The cost of these fluids is also high. As an alternate to conventional fluids several other coolants/ lubricants are tried. Some efforts have been carried out with the help of solid lubricants as a substitute which has shown substantial improvement in the process [11]. Further these factors prompted investigations on the use of biodegradable coolants, minimum quantity coolant and coolant free grinding [12]. But any attempt to minimize or avoid the coolant can be dealt with only by the substitution of the functions normally met by the coolants by some other means. Grinding employing cryogenic cooling by liquid nitrogen and minimum Quantity Lubrication (MQL) by ester oil supplied in the form of spot jet or spray mist are the alternative approaches towards this end. The effect of graphite nanoplatelets in solid lubrication grinding are also studied which gives effective way of improving the process [13]. The results are very encouraging but the required amount of nanomaterial significantly increases the overall cost.

The objective of the present investigation is to employ Zinc Phosphate, which is a high temperature solid lubricant, as a means to reduce the heat generated at the grinding zone and study the process performance. An experimental set-up is designed and built for comparative performance analysis of Zinc Phosphate assisted grinding with dry and conventional flooded coolant grinding.

2. Experimental Setup

An experimental set up is designed and fabricated to ensure proper delivery of the solid lubricant with the carrier to the grinding zone. This is devised with the help of dead weight loaded cylinder. The mix of Zinc Phosphate and the carrier oil is introduced into the cylinder. Constant pressure is maintained on this mix with help of a piston which is in turn loaded by the dead weight mounted on the piston rod as shown in Fig. 1. The flow of mix is controlled with the help of the flow control valve. The mix is impinged on the grinding zone through a nozzle with an opening of 1mm * 25 mm. The width of the opening corresponds to the width of grinding wheel. The mix is first delivered to the soft rubber wheel, which is free to rotate and is maintained in constant contact with the grinding wheel. The paste is eventually transferred to the grinding wheel and then to the grinding zone to serve as a lubricant in the grinding zone.

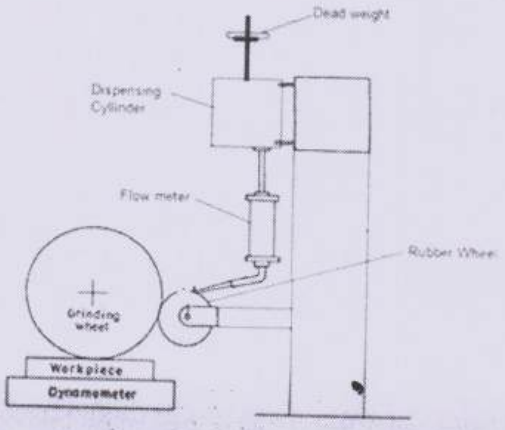


Fig. 1. Schematic diagram of Experimental set up.

2.1 Primary Experimentation

The grinding operation is carried out on horizontal reciprocating table surface grinding machine. The test specimen of size 100 mm* 50 mm* 10 mm thickness is used for the experimentation. Grinding is carried out along the length of the workpiece.

The ultimate effect in which industry is primarily interested is the quality of surface finish obtained through the process and the amount of energy consumed for the process. Hence for primary investigations following factors are kept constant. The details of which are provided in Table 1.

Primary experimentation is carried out on alloy steel AISI 4140 to observe the effect of uses of solid lubricants on the process. The results of experimentation are tabulated in Table 2.

Table 1. Factors kept constant in grinding.

Factor	Details
Workpiece material	Alloy steel AISI 4140
Grinding machine	Horizontal spindle surface grinding, machine, PMT make, Model SG 42, 5.5 kw
Grinding Wheel	A60L5V10, Diameter 300 mm, width 25 mm.
Wheel velocity	30m/min
Table feed rate	10m/min
Dressing conditions	With single point diamond dresser, 1 carat, in dry condition.

Table 2. Observations for preliminary experimentation

Depth of Cut,μ ↓	Dry Grinding		Wet Grinding		Zinc Phosphate	
	Force, N	Ra, μ	Force, N	Ra, μ	Force, N	Ra, μ
10	434.42	0.46	403.16	0.46	228.77	0.41
20	506.82	0.47	470.35	0.47	266.90	0.41
30	579.21	0.47	537.54	0.47	305.03	0.42
40	651.62	0.47	604.73	0.47	343.16	0.42
50	724.02	0.47	671.93	0.47	381.28	0.42

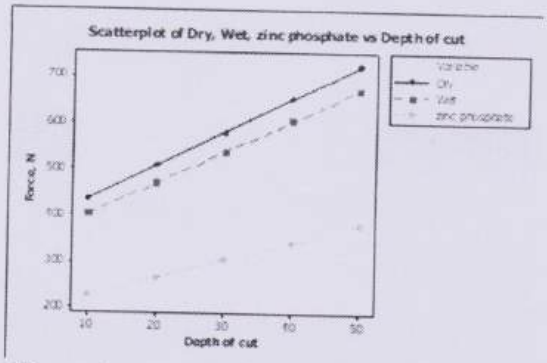


Fig. 2. Effect of coolants on force under varying depths of cut

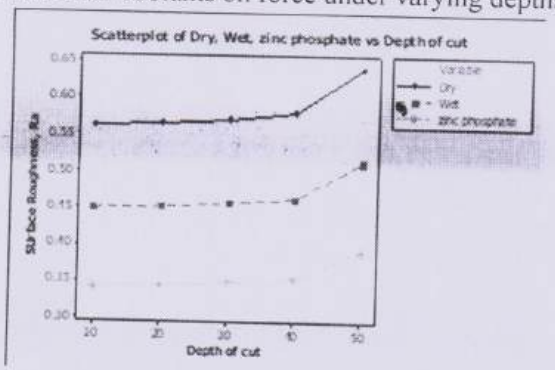


Fig. 3. Surface roughness for AISI 4140 using different coolants.

Results show that the grinding force, grinding energy and the surface roughness decreases with the help of the use of Zinc Phosphate compared with dry grinding and grinding with the conventional coolants.

2.2 Taguchi methods for design of experiments

Taguchi methods of experimental design provide a simple, efficient and systematic approach for the optimization of experimental designs for performance quality and cost. It has been proved successful to many manufacturing situations. The traditional experimental design procedures focus on the average product or process performance characteristics. But the Taguchi method concentrates on the effect of variation on the product or process quality characteristics rather than on its averages. That is, the Taguchi's approach makes the product or process performance insensitive (robust) to variation to uncontrolled or noise factors. Taguchi recommends that this can be done by the proper design of parameters during the 'parameter design' phase of off-line quality control. He designed certain standard orthogonal arrays (OAs) by which simultaneous and independent evaluation of two or more parameters for their ability to affect the variability of a particular product or process characteristic can be done in a minimum number of tests. Subsequently, decision is made for the optimum combination of these parameters.

The following objectives are fixed for the study:

(i) Find out the effect of use of Zinc Phosphate on force required for grinding and surface roughness obtained, and

(ii) Conduct a comparative study of the applications to various alloy steels.

The surface roughness (Ra) of the ground piece and the force required (F) are taken as the quality characteristics of the process. The surface finish is a direct process result and is measured by a Mitutoyo surftest. For force measurements a dynamometer is used, which recorded the two components of force. The resultant force is worked out and is considered as a single response.

The operating conditions such as speed and feed are held constant during the experimentation. However, infeed rate, workpiece material and flow rate of the lubricant is considered for variation. Three levels, having equal spacing, within the operating range are selected for each of the factors as shown in Table 3. By selecting three levels the curvature or the non-linearity effects could be studied.

Table 3. Levels in Experimentation

Factor	Level 1	Level 2	Level 3
Material	AISI 4140	AISI 4310	AISI 52100
Infeed (Depth of cut), (μm)	10	30	50
Flow Rate, (mm^3/min)	20	40	60

Table 4 shows the experimental layout of an L_{27} 0rthogonal array consisting of three control factors and three levels according to Taguchi's suggestion. The numbers in each column indicate the levels for the specific factors and from the L_{27} orthogonal array 27 experiments are required to examine the total manufacturing parameters. The L_{27} orthogonal Array which meets this requirement is selected.

Table 4. L_{27} Orthogonal array.

Trial	Material	In feed (μm)	Flow Rate (mm^3/min)
1	1	1	1
2	1	1	1
3	1	1	1
4	1	2	2
5	1	2	2
6	1	2	2
7	1	3	3
8	1	3	3
9	1	3	3
10	2	1	2
11	2	1	2
12	2	1	2
13	2	2	3
14	2	2	3

15	2	2	3
16	2	3	1
17	2	3	1
18	2	3	1
19	3	1	3
20	3	1	3
21	3	1	3
22	3	2	1
23	3	2	1
24	3	2	1
25	3	3	2
26	3	3	2
27	3	3	2

2.3 Experimentation

By choosing the L_{27} orthogonal array the issue of repeating the tests is sorted out, as the array itself recommends the repetitions. This helps to obtain more reliable information from the statistical analysis of the experiment. Quality characteristics, i.e. surface roughness (Ra) in μm and force (F) in N are noted by the measurement systems. For having consistent results with Ra, pieces are ground giving seven sets of upward and downward spark out passes.

The sample data obtained for the quality characteristics, i.e. surface roughness (Ra in μm) and force in N in the Zinc Phosphate assisted grinding is shown in Table 5. It is observed that there is considerable consistency in the obtained data and it is reliable for statistical analysis.

Table 5. Sample data for force and surface roughness in Zinc Phosphate assisted grinding.

Trial	Force (N)	Surface roughness (μm)
1	235.32	0.41
2	242.60	0.42
3	246.30	0.44
4	238.45	0.41
5	242.08	0.42
6	249.57	0.44
7	266.69	0.41
8	274.94	0.42
9	279.12	0.44
10	239.64	0.40
11	243.29	0.41
12	250.81	0.43
13	285.89	0.41
14	294.73	0.42
15	299.22	0.44
16	525.54	0.42
17	533.55	0.43

18	550.04	0.45
19	251.89	0.40
20	259.68	0.41
21	263.63	0.43
22	493.91	0.42
23	501.43	0.43
24	516.94	0.45
25	469.22	0.42
26	483.73	0.43
27	491.10	0.45

2.4. Analysis of the data

2.4.1. Evaluation of S/N ratios

Taguchi suggests the transformation of the repetition data in a trial into a consolidated single value called the S/N ratio. Here, the term 'signal' represents the desirable value (mean) and the 'noise' represents the undesirable value (standard deviation). So the S/N ratio represents the amount of variation present in the quality characteristic. Depending upon the objective of quality characteristic there can be various types of S/N ratios. Here the desirable objectives, the force required for the grinding operation and the surface roughness should be lower. Hence the lower-the-better type S/N ratio, as given below is applied for transforming the observed data:

$$Z = -\log_{10} \{\text{sum } (y^{**}2)/n\}$$

Where Z is the S/N ratio for the lower-the-better case, y is the measured quality characteristic for the ith repetition, and n the number of repetitions in a trial. The S/N ratios, standard deviation and mean for grinding force for Zinc Phosphate assisted grinding for various alloy steels, the varying flow rates and infeed rates are calculated from the observed data and tabulated in Table 6.

Table 6. Calculated S/N ratio, Standard deviation and Mean for the experimentation.

Trial	S/N Ratio	Standard Deviation	Mean
1	-47.6565	5.5864	241.407
2	*	*	*
3	*	*	*
4	-47.7268	5.6706	243.367
5	*	*	*
6	*	*	*
7	-48.7433	6.3251	273.583
8	*	*	*
9	*	*	*
10	-47.7700	5.6956	244.580
11	*	*	*
12	*	*	*
13	-49.3472	6.7823	293.280

14	*	*	*
15	*	*	*
16	-54.5910	12.4922	536.377
17	*	*	*
18	*	*	*
19	-48.2474	5.9738	258.400
20	*	*	*
21	*	*	*
22	-54.0518	11.7437	504.093
23	*	*	*
24	*	*	*
25	-53.6508	11.1325	481.350
26	*	*	*
27	*	*	*

From the calculated values of signal to noise ratio, the values are obtained for the various levels of the factors and tabulated in Table 7.

Table 7. Signal to Noise Ratios Smaller is better

Level	Material	In feed, µm	Flow rate mm^3/min
1	-48.04	-47.89	-52.10
2	-50.57	-50.38	-49.72
3	-51.98	-52.33	-48.78
Delta	3.94	4.44	3.32
Rank	2	1	3

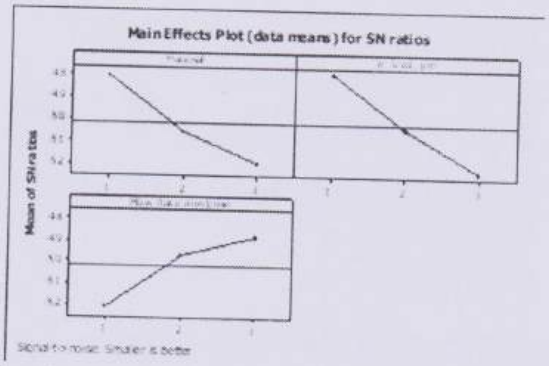


Fig. 4. Main Effects Plot (data means) for SN rations (Signal to Noise: Smaller is better) for Zinc Phosphate.

The main effect plot (the data means) for the calculated S/N ratio is calculated and presented graphically as shown in the Fig. 4. The highest S/N ratio always yields the optimum quality with minimum variance. Therefore, the level with a higher value determines the optimum level of each factor. For the experimentation carried out the best results would be obtained for AISI4140, the workpiece material, infeed rate of 10 µm, and flow rate of 60mm3/min.

From the calculated values of means, the values are obtained for the various levels of the factors and tabulated in Table 8 and the same is represented graphically in the Fig. 5

Table 8 Response Table for Means

Level	Material	In feed, µm	Flow rate mm^3/min
1	252.8	248.1	427.3
2	358.1	346.9	323.1
3	414.6	430.4	275.1
Delta	161.8	430.4	152.2
Rank	2	1	3

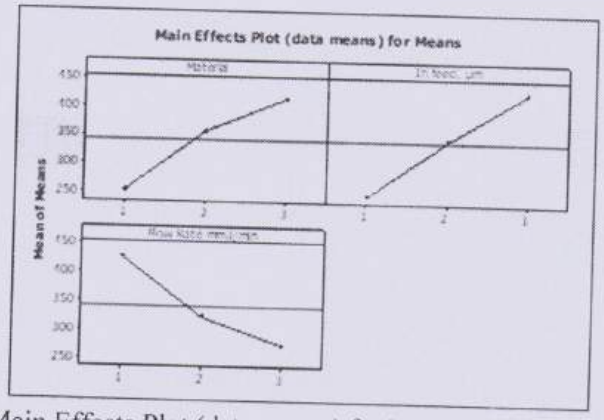


Fig. 5. Main Effects Plot (data means) for Means for Zinc Phosphate.

2.4.2 The regression Analysis

Taguchi technique can be used for the prediction of the full factorial design. The regression equation from full factorial prediction is

$$F = 289 + 0.141\ \tau s + 4.56\ d - 3.81\ f$$

Where, F is the grinding force in Newton, τs is the shear stress of workpiece material in MPa, d is the infeed in micrometers and f is flow rate in mm3/min
The regression equation is

Table 8. Regression Table

Predictor	Coefficient	Standard Error Coefficient	T	P
Constant	288.74	31.58	9.14	0.000
τs, MPa	0.14089	0.02428	5.80	0.000
d, µm	4.5577	0.5568	8.18	0.000
F, mm^3/min	-3.8051	0.5568	-6.83	0.000

S = 47.2500 R-Sq = 86.5% R-Sq(adj) = 84.7%

2.4.3. Analysis of Variance

ANOVA is a computational technique to estimate quantitatively the relative contribution which each controlled parameter makes on the overall measured response and is expressed as a percentage. Thus information about how significant the effect of each controlled parameter is on the experimental results can be obtained. The total variation in response is decomposed into variation due to various controlled factors and their interactions and due to the error involved in the experimentation. The ANOVA can be done with the raw data or with the S/N data. The ANOVA based on the raw data signifies the factors which affect the average response rather than reducing the variation. But ANOVA based on the S/N data takes into account both these aspects and so it is used here. Since it is a saturated design where all columns are assigned with the factors, the variations due to error are estimated by pooling the estimates of the factors having least variance. This also helped in determining the Fisher test (F-test) factor for finding out the confidence level of the results. The ANOVA is done for all the quality characteristics under study.

Table 9. ANOVA Table

Source	Degrees of Freedom	Sum of Squares	MS	F Value	P Value
Regression	3	328960	109653	49.12	0.000
Residual Error	23	51349	2233		
Total	26	380309			

Source	Degrees of Freedom	Seq. Sum of Squares
Shear Stress	1	75150
Infeed	1	149563
Flow Rate	1	104248

3. Interpreted Graphs For Force As A Quality Characteristic:

On the basis of the interpreted results of force required for grinding operation with the help of Zinc Phosphate as solid lubricant for the materials selected, AISI 4140, AISI 4340 and AISI 52100 are given in Fig.6 to Fig. 8.

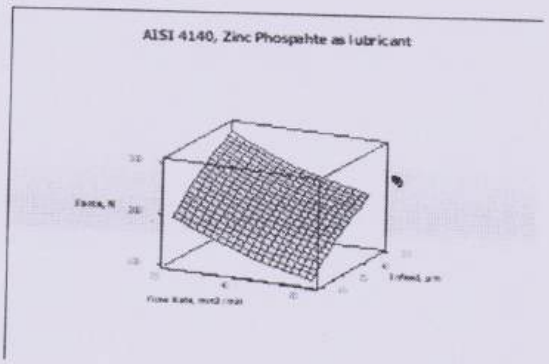


Fig. 6. AISI 4140, Zinc Phosphate as lubricant

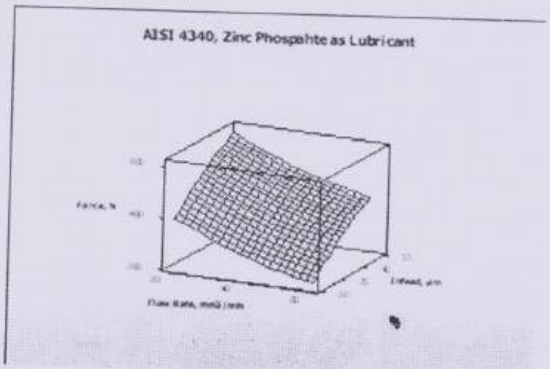


Fig. 7. AISI 4340, Zinc Phosphate as lubricant

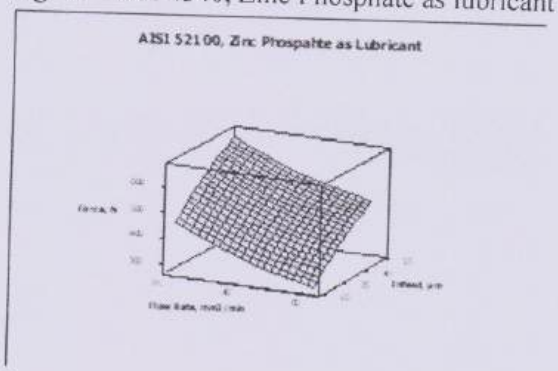


Fig. 8. AISI 52100, Zinc Phosphate as lubricant

4. Analysis for Surface Roughness

On the similar lines of the force, Taguchi analysis is done for surface roughness obtained in the Zinc Phosphate assisted grinding process. The S/N ratios, standard deviation and mean for surface roughness for Zinc Phosphate assisted grinding for various alloy steels, the varying flow rates and infeed rates are calculated from the observed data are tabulated in Table 10.

Table 10. Calculated S/ N ratio, Standard deviation and Mean..

Trial	S/N Ratio	Standard Deviation	Mean
1	7.46258	0.0152753	0.423333
2	*	*	*
3	*	*	*
4	7.46258	0.0152753	0.423333

5	*	*	*
6	*	*	*
7	7.46258	0.0152753	0.423333
8	*	*	*
9	*	*	*
10	7.67004	0.0152753	0.413333
11	*	*	*
12	*	*	*
13	7.46258	0.0152753	0.423333
14	*	*	*
15	*	*	*
16	7.25996	0.0152753	0.433333
17	*	*	*
18	*	*	*
19	7.67004	0.0152753	0.413333
20	*	*	*
21	*	*	*
22	7.25996	0.0152753	0.433333
23	*	*	*
24	*	*	*
25	7.25996	0.0152753	0.433333
26	*	*	*
27	*	*	*

From the calculated values of signal to noise ratio, the values are obtained for the various levels of the factors and tabulated in Table 11.

Table 11. Signal to Noise Ratios Smaller is better

Level	Material	In feed (µm)	Flow rate (mm^3/min)
1	7.463	7.601	7.328
2	7.464	7.395	7.464
3	7.397	7.328	7.532
Delta	0.068	0.273	0.204
Rank	3	1	2

The main effect plot (the data means) for the calculated S/N ratio is calculated and presented graphically as shown in the Fig. 9. The highest S/N ratio always yields the optimum quality with minimum variance. Therefore, the level with a higher value determines the optimum level of each factor. For the experimentation carried out the best results would be obtained for AISI 52100, the workpiece material, infeed rate of 10 µm, and flow rate of 60mm3/min.

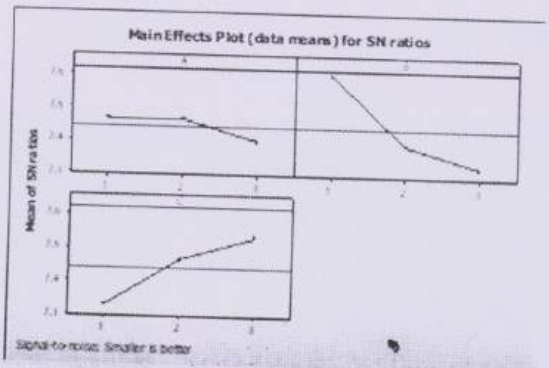


Fig. 9. Main Effects Plot (data means) for SN rations (Signal to Noise: Smaller is better) for Zinc Phosphate

From the calculated values of means, the values are obtained for the various levels of the factors and tabulated in Table 12 and the same is represented graphically in the Fig. 10.

Table 12 Response Table for Means

Level	Material	In feed (μm)	Flow rate (mm^3/min)
1	0.4233	0.4167	0.4300
2	0.4233	0.4267	0.4233
3	0.4267	0.4300	0.4200
Delta	0.0033	0.0133	0.0100
Rank	3	1	2

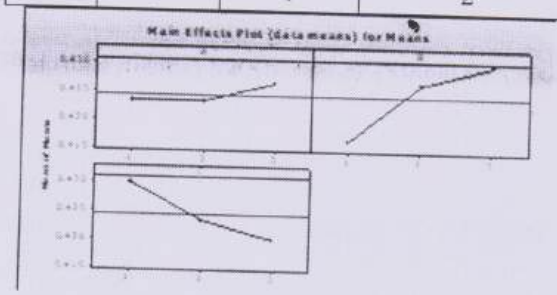


Fig. 10 Main Effects Plot (data means) for Means for Zinc Phosphate

4.1 The regression Analysis

Taguchi technique can be used for the prediction of the full factorial design. The regression equation from full factorial prediction is

$Ra = 0.428 - 0.000017\ \tau s + 0.000417\ d - 0.000333\ f$

Where, Ra is the grinding force in Newton, τs is the shear stress of workpiece material in MPa, d is the infeed in micrometers and f is flow rate in mm3/min

Table 13. Regression Table

Predictor	Coefficient	Standard Error Coefficient	T	P
Constant	0.422403	0.001273	331.87	0.000
Shear stress	0.0000041	0.00000098	4.29	0.000
Infeed	0.0003333	0.00002244	14.85	0.000
Flow rate	-0.000250	0.00002244	-11.14	0.000

S = 0.00190413 R-Sq = 94.0% R-Sq(adj) = 93.3%

4.2 Analysis of variance

ANOVA, the analysis of variance is carried out and the results are included in Table 14.

Table 14 ANOVA table

Source	Degrees of Freedom	Sum of Squares	MS	F Value	P Value
Regression	3	0.0013	0.00043	121.05	0.00
Residual Error	23	0.0000	0.00000		
Total	26	0.0014			

Source	Degrees of Freedom	Seq. Sum of Squares
Shear Stress	1	0.00006661
Infeed	1	0.00080001
Flow Rate	1	0.00045000

5. Interpreted Graphs For Surface finish As A Quality Characteristic

On the basis of the interpreted results of surface roughness obtained in grinding operation with the help of Zinc Phosphate as solid lubricant for the materials selected, AISI 4140, AISI 4340 and AISI 52100 are given in Fig. 11 to Fig. 13.

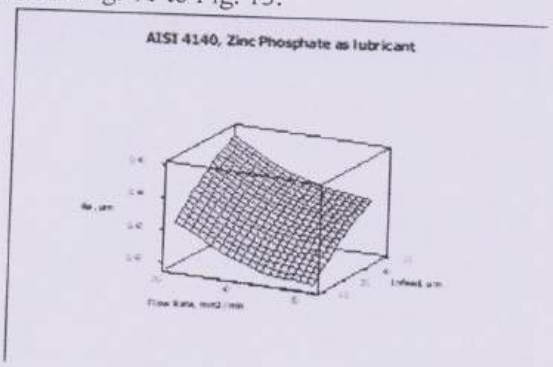


Fig. 11. AISI 4140, Zinc Phosphate as lubricant

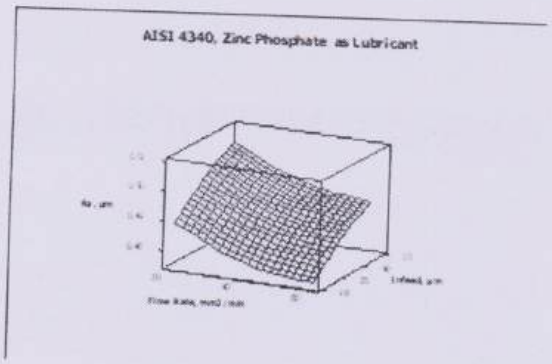


Fig. 12. AISI 4340, Zinc Phosphate as lubricant

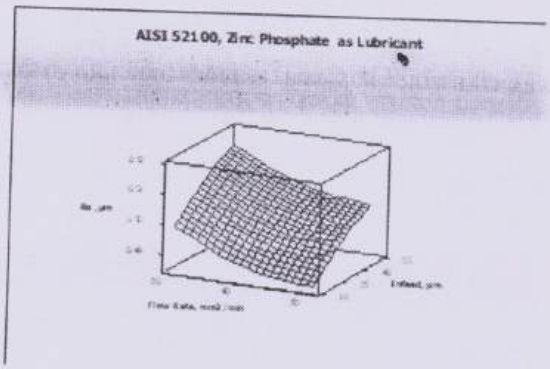


Fig. 13. AISI 52100, Zinc Phosphate as lubricant

6. Conclusions

The experimental setup developed for the application of Zinc Phosphate as a means to reduce the heat generated in the grinding zone has been investigated for improving the surface finish and reducing the cutting forces involved in the process. The Taguchi method of experimental design is used for the investigations. When compared with the dry grinding and grinding with the conventional coolants, Zinc Phosphate gives considerably reduces the force required for grinding operation and the surface finished improved. Hence the effective role of Zinc Phosphate as a lubricant was evident from the improvement of output parameters.

Similar experimentation can be carried out with other solid lubricants like molybdenum disulphide, graphite and boric acid, which may lead to most effective solid lubricant for surface grinding.

7. References

1. H.M.T., "Production Technology," Tata McGraw Hill, pp.250-251, 2009.
2. J.O. Outwater, M.C. Shaw, "Surface temperature in grinding," Trans. ASME 74 pp.73–86, (1952).
3. S. Malkin, R. B Anderson, Thermal aspects of grinding — part II, surface temperature and workpiece burn, Trans. ASME, J.Eng. Indust. 96 , pp.1184–1191, (1974)
4. Y. Nakano, H. Uchida, K. Ota, Thermal deformations and profile errors of workpiece in surface grinding, Ann. CIRP 25 (1), pp. 235–240, (1976).

5. R. Snoys, K.U. Leuven, M. Maris, J. Peters, Thermally induced damages in grinding, Ann. CIRP 27 (2), pp.571–581, (1978).
6. Y. Nakano, H. Uchida, K. Ota, Thermal deformations and profile errors of workpiece in surface grinding, Ann. CIRP 25 (1) ,235–240, (1976).
7. S. Ebbrel, N.H. Wooley, Y.D. Tridimas, D.R. Allanson, W.B. Rowe, The effects of cutting fluid application methods on the grinding process, Int. J. Mach. Tools Manufact. 40, pp.209–223, (2000).
8. S. Malkin, Grinding Technology, Theory and Applications of Machining with Abrasives, Ellis Harwood, Chichester, 1989.
9. T.D. Howes, Assessment of cooling and lubricating properties of grinding fluids, Ann. CIRP 39 (1), pp. 313–316, (1990).
10. T.D. Howes, H.K. Toenshoff, W. Heur, Environmental aspects of grinding fluids, Ann. CIRP 40 (2), pp. 623–630, (1991).
11. S. Shaji, V. Radhakrishnan, "An investigation on surface grinding using graphite as lubricant," International Journal of Machine Tools & Manufacture 42 ,pp. 733–740, (2002).
12. I. Inasaki, H.K. Toenshoff, T.D. Howes, Abrasive machining in thethe future, Ann. CIRP 42 (2) pp.,723–732, (1993)
13. MatthewAlberts, KyriakiKalaitzidou, ShreyesMelkote, "An investigation of graphite nanoplatelets as lubricant in grinding," International Journal of Machine Tools & Manufacture, 49, pp.966–970, (2009).

Source details

Feedback > Compare sources >

Shu Ju Cai Ji Yu Chu Li/Journal of Data Acquisition and Processing

Scopus coverage years: from 2001 to Present

Publisher: Nanjing University of Aeronautics an Astronautics

ISSN: 1004-9037

Subject area: Computer Science: Signal Processing | Computer Science: Software

Source type: Journal

View all documents | Set document alert | Save to source list | Source Homepage

CiteScore 2022
0.7

SJR 2022
0.140

SNIP 2022
0.221

CiteScore | CiteScore rank & trend | Scopus content coverage

Improved CiteScore methodology

CiteScore 2022 counts the citations received in 2019-2022 to articles, reviews, conference papers, book chapters and data papers published in 2019-2022, and divides this by the number of publications published in 2019-2022. Learn more >

CiteScore 2022

0.7 = 302 Citations 2019 - 2022 / 434 Documents 2019 - 2022

Calculated on 05 May, 2023

CiteScoreTracker 2023

0.8 = 329 Citations to date / 434 Documents to date

Last updated on 01 December, 2023 • Updated monthly

CiteScore rank 2022

Category	Rank	Percentile
Computer Science — Signal Processing	#110/122	10th
Computer Science — Software	#389/404	3rd

Journal of
Data Acquisition and Processing
ISSN: 1004-9037
https://sjcjycl.cn/
DOI: 10.5281/zenodo.7766255

ENHANCEMENT OF SURFACE GRINDING PROCESS USING GRAPHITE AS A LUBRICANT BASED ON THE TAGUCHI METHOD

Dr. R. N. Patil[1,a] *, Dr. J. A. Dhanke [2,b] and Dr. N. Tripathi[3,c]
[1,2,3]Bharati Vidyapeeth's College of Engineering, Lavale, Pune, M.H. India.
[3]Govt. PG Calculus Rajgarh M.P, India
arnpatil1@gmail.com , bjyotidhanke@gmail.com,ctripathin661@gmail.com

ABSTRACT
Grinding is one of the most popularly used surface finishing process characterized by excellent process capabilities in terms of surface finish and material removal rate. It has wide applications in manufacturing industry as it can handle a wide variety of workpiece materials and forms. However it needs very high specific energy and gives rise to very high temperature, which results into high residual stresses, micro cracks and burn. To reduce these ill effects normally coolants are employed, which reduce the friction and provides effective cooling of work wheel interface. Conventional applications of coolants are many times ineffective due to inaccessibility of the fluid to grinding zone and film boiling. Many of the conventional coolants pose health hazard and support the green house effect. This paper deals with the use of solid lubricant, graphite carried in the proper medium to grinding zone and reducing the friction and hence eliminating the thermal ill effects on the grinding process. Results show that the grinding force, grinding energy and the surface roughness decreases with the help of the use of graphite compared with dry grinding and grinding with the conventional coolants.

Keywords – Coolant, Graphite, Grinding, Lubricant, Taguchi method.

1. Introduction
Grinding is the process of material removal in the form of small chips by mechanical action of abrasive particles bonded together in grinding wheel. It is basically a finishing process employed for producing close dimensional and geometrically accuracies and smooth surface finish. However in some applications, the grinding process is applied for higher material removal rates and is also referred as abrasive machining [1]. It is distinguished from many other machining processes on aspects like tool geometry, large contact area and high friction between tool and workpiece and high specific energy requirement. The high specific energy consumed during the grinding process results into heat. Major portion of heat is transferred to workpiece [2]. The severe heat input affects the workpiece quality. It may induce thermal damage such as burn, surface and subsurface cracks, metallurgical phase transformations, residual tensile stresses and dimensional distortions and many more ill effects [3-5]. To control the ill effects of heat generated during the grinding process at the cutting zone and ensure the quality of the workpiece, coolants are employed. Grinding fluids are introduced into grinding operations to reduce and transfer heat during grinding, lubricate during chip formation, wash the grinding wheel of loose chip and swarf, chemically aid the grinding action or machine maintenance. Grinding fluids of five different categories are used popularly. These are petroleum base and mineral base cutting oils, water soluble oils, synthetic fluids, semi synthetic

fluids, water plus additives, including rust inhibitors, water treatments (for examples, softeners), and defoaming agents.

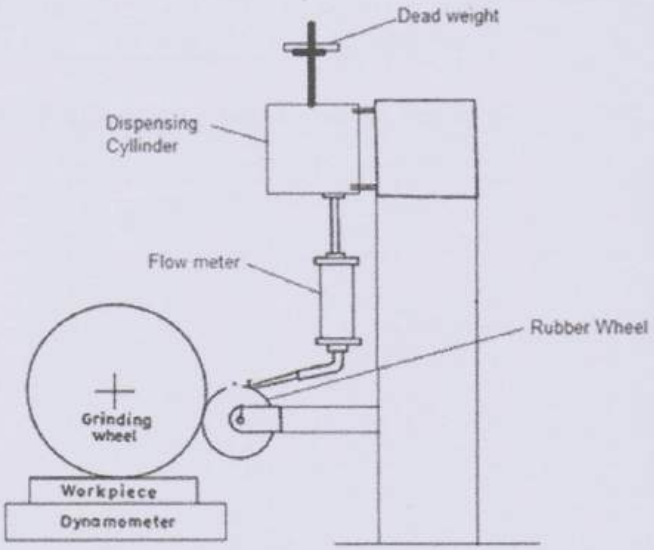
Several researchers have carried out research on the coolant type, its composition and supply characteristics [6]. However, during grinding operation coolants are relatively inaccessible to the grinding arc. Therefore, often it is ineffective in reducing the grinding zone temperature, but only provides bulk cooling of the work piece. The stiff boundary layer forming around the rotating grinding wheel also inhibits the access of the fluid to the grinding zone [7, 8]. Conventional coolants lose their cooling properties upon film boiling and that the film boiling temperature of these coolants are lower which affects the effectiveness of grinding fluid [9]. However, flooded coolant operation allows effective removal of grinding swarf, which is needed in grinding. Conventional grinding fluids are a source of environmental hazards and increasingly strict regulations are coming up with regard to their use and disposal [10]. The cost of these fluids is also high. As an alternate to conventional fluids several other coolants/ lubricants are tried. Some efforts have been carried out with the help of solid lubricants as a substitute which has shown substantial improvement in the process [11]. Further these factors prompted investigations on the use of biodegradable coolants, minimum quantity coolant and coolant free grinding [12]. But any attempt to minimize or avoid the coolant can be dealt with only by the substitution of the functions normally met by the coolants by some other means. Grinding employing cryogenic cooling by liquid nitrogen and minimum Quantity Lubrication (MQL) by ester oil supplied in the form of spot jet or spray mist are the alternative approaches towards this end. The effect of graphite nanoplatelets in solid lubrication grinding are also studied which gives effective way of improving the process [13]. The results are very encouraging but the required amount of nanomaterial significantly increases the overall cost.

The objective of the present investigation is to employ graphite, which is a high temperature solid lubricant, as a means to reduce the heat generated at the grinding zone and study the process performance. An experimental set-up is designed and built for comparative performance analysis of graphite assisted grinding with dry and conventional flooded coolant grinding.

2. Experimental Setup

An experimental set up is designed and fabricated to ensure proper delivery of the solid lubricant with the carrier to the grinding zone. This is devised with the help of dead weight loaded cylinder. The mix of graphite and the carrier oil is introduced into the cylinder. Constant pressure is maintained on this mix with help of a piston which is in turn loaded by the dead weight mounted on the piston rod as shown in Fig. 1. The flow of mix is controlled with the help of the flow control valve. The mix is impinged on the grinding zone through a nozzle with an opening of 1mm * 25 mm. The width of the opening corresponds to the width of grinding wheel. The mix is first delivered to the soft rubber wheel, which is free to rotate and is maintained in constant contact with the grinding wheel. The paste is eventually transferred to the grinding wheel and then to the grinding zone to serve as a lubricant in the grinding zone.

Fig. 1. Schematic diagram of Experimental set up.



2.1 Primary Experimentation

The grinding operation is carried out on horizontal reciprocating table surface grinding machine. The test specimen of size 100 mm* 50 mm * 10 mm thickness is used for the experimentation. Grinding is carried out along the length of the workpiece. The ultimate effect in which industry is primarily interested is the quality of surface finish obtained through the process and the amount of energy consumed for the process. Hence for primary investigations following factors are kept constant. The details of which are provided in Table 1.

Primary experimentation is carried out on alloy steel AISI 4140 to observe the effect of uses of solid lubricants on the process. The results of experimentation are tabulated in Table 2.

Table 1. Factors kept constant in grinding.

Factor	Details
Workpiece material	Alloy steel AISI 4140
Grinding machine	Horizontal spindle surface grinding, machine, PMT make, Model SG 42, 5.5 kw
Grinding Wheel	A60L5V10, Diameter 300 mm, width 25 mm.
Wheel velocity	30m/min
Table feed rate	10m/min
Dressing conditions	With single point diamond dresser, 1 carat, in dry condition.

Table 2. Observations for preliminary experimentation.

Depth of Cut (µm)	Dry Grinding		Wet Grinding		Graphite	
	Force (N)	Ra (µm)	Force (N)	Ra (µm)	Force (N)	Ra (µm)
10	434.42	0.56	403.16	0.46	312.53	0.44
20	506.82	0.57	470.35	0.47	364.62	0.45
30	579.21	0.57	537.54	0.47	416.70	0.45

40	651.62	0.64	604.73	0.47	468.79	0.45
50	724.02	0.56	671.93	0.47	520.88	0.45

Fig. 2. Effect of coolants on force under varying depths of cut.

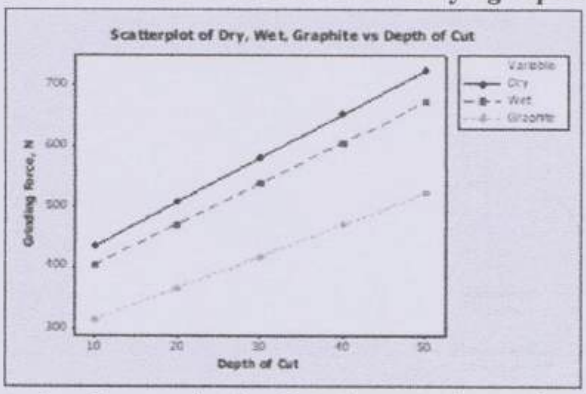
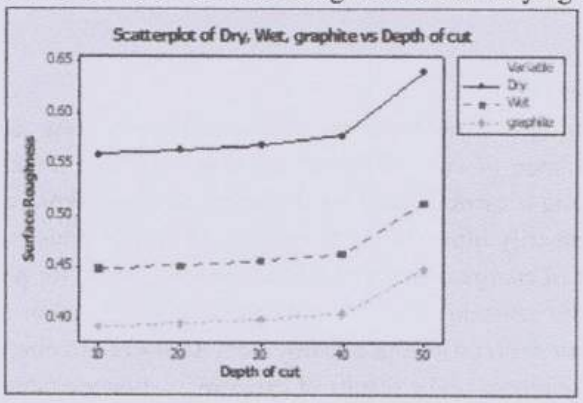


Fig. 3. Effect of coolants on Surface Roughness under varying depths of cut



Results show that the grinding force, grinding energy and the surface roughness decreases with the help of the use of graphite compared with dry grinding and grinding with the conventional coolants.

2.2 Taguchi methods for design of experiments

Taguchi methods of experimental design provide a simple, efficient and systematic approach for the optimization of experimental designs for performance quality and cost. It has been proved successful to many manufacturing situations. The traditional experimental design procedures focus on the average product or process performance characteristics. But the Taguchi method concentrates on the effect of variation on the product or process quality characteristics rather than on its averages. That is, the Taguchi's approach makes the product or process performance insensitive (robust) to variation to uncontrolled or noise factors. Taguchi recommends that this can be done by the proper design of parameters during the 'parameter design' phase of off-line quality control. He designed certain standard orthogonal arrays (OAs) by which simultaneous and independent evaluation of two or more parameters for their ability to affect the variability of a particular product or process characteristic can be done in a minimum number of tests. Subsequently, decision is made for the optimum combination of these parameters.

The following objectives are fixed for the study:

i. Find out the effect of use of graphite on force required for grinding and surface roughness obtained, and

ii. Conduct a comparative study of the applications to various alloy steels.

The surface roughness (Ra) of the ground piece and the force required (F) are taken as the quality characteristics of the process. The surface finish is a direct process result and is measured by a Mitutoyo surftest. For force measurements a dynamometer is used, which recorded the two components of force. The resultant force is worked out and is considered as a single response.

The operating conditions such as speed and feed are held constant during the experimentation. However, infeed rate, workpiece material and flow rate of the lubricant is considered for variation. Three levels, having equal spacing, within the operating range are selected for each of the factors as shown in Table 3. By selecting three levels the curvature or the non-linearity effects could be studied.

Table 3. Levels in Experimentation

Factor	Level 1	Level 2	Level 3
Material	AISI 4140	AISI 4310	AISI 52100
Infeed (Depth of cut), (μm)	10	30	50
Flow Rate, (mm^3/min)	20	40	60

Table 4 shows the experimental layout of an L_{27} 0rthogonal array consisting of three control factors and three levels according to Taguchi's suggestion. The numbers in each column indicate the levels for the specific factors and from the L_{27} orthogonal array $_{27}$ experiments are required to examine the total manufacturing parameters. The L_{27} orthogonal Array which meets this requirement is selected.

Table 4. L_{27} Orthogonal array.

Trial	Material	In feed (μm)	Flow Rate (mm^3/min)
1	1	1	1
2	1	1	1
3	1	1	1
4	1	2	2
5	1	2	2
6	1	2	2
7	1	3	3
8	1	3	3
9	1	3	3
10	2	1	2
11	2	1	2
12	2	1	2
13	2	2	3
14	2	2	3
15	2	2	3
16	2	3	1

17	2	3	1
18	2	3	1
19	3	1	3
20	3	1	3
21	3	1	3
22	3	2	1
23	3	2	1
24	3	2	1
25	3	3	2
26	3	3	2
27	3	3	2

2.3 Experimentation

By choosing the L27 orthogonal array the issue of repeating the tests is sorted out, as the array itself recommends the repetitions. This helps to obtain more reliable information from the statistical analysis of the experiment. Quality characteristics, i.e. surface roughness (Ra) in μm and force (F) in N are noted by the measurement systems. For having consistent results with Ra, pieces are ground giving seven sets of upward and downward spark out passes. The sample data obtained for the quality characteristics, i.e. surface roughness (Ra in μm) and force in N in the graphite assisted grinding is shown in Table 5. It is observed that there is considerable consistency in the obtained data and it is reliable for statistical analysis.

Table 5. Sample data for force and surface roughness in graphite assisted grinding.

Tria l	Force (N)	Surface roughness (μm)
1	367.68	0.44
2	356.65	0.43
3	362.16	0.41
4	372.58	0.44
5	366.99	0.43
6	361.40	0.41
7	416.70	0.44
8	404.20	0.43
9	410.45	0.41
10	374.44	0.42
11	368.82	0.41
12	363.21	0.39
13	446.71	0.43
14	433.31	0.42
15	440.01	0.40
16	821.15	0.45
17	808.83	0.44
18	796.52	0.42
19	393.59	0.41
20	381.78	0.40
21	387.69	0.38
22	771.74	0.43
23	760.16	0.42

24	748.59	0.40
25	733.15	0.43
26	711.16	0.42
27	722.15	0.40

2.4. Analysis of the data

2.4.1. Evaluation of S/N ratios

Taguchi suggests the transformation of the repetition data in a trial into a consolidated single value called the S/N ratio. Here, the term 'signal' represents the desirable value (mean) and the 'noise' represents the undesirable value (standard deviation). So the S/N ratio represents the amount of variation present in the quality characteristic. Depending upon the objective of quality characteristic there can be various types of S/N ratios. Here the desirable objectives, the force required for the grinding operation and the surface roughness should be lower. Hence the lower-the-better type S/N ratio, as given below is applied for transforming the observed data:

$$Z = -\log_{10} \{\text{sum } (y^{**}2)/n\}$$

Where Z is the S/N ratio for the lower-the-better case, y is the measured quality characteristic for the ith repetition, and n the number of repetitions in a trial. The S/N ratios, standard deviation and mean for grinding force for graphite assisted grinding for various alloy steels, the varying flow rates and infeed rates are calculated from the observed data and tabulated in Table 6.

Table 6. Calculated S/N ratio, Standard deviation and Mean for the experimentation.

Trial	S/N Ratio	Standard Deviation	Mean
1	-51.17	5.51	362.16
2	*	*	*
3	*	*	*
4	-51.29	5.59	366.99
5	*	*	*
6	*	*	*
7	-52.26	6.25	410.45
8	*	*	*
9	*	*	*
10	-51.33	5.61	368.82
11	*	*	*
12	*	*	*
13	-52.86	6.7	440.01
14	*	*	*
15	*	*	*
16	-58.15	12.31	808.83
17	*	*	*
18	*	*	*
19	-51.77	5.90	387.68
20	*	*	*
21	*	*	*
22	-57.61	11.575	760.16
23	*	*	*

24	*	*	*
25	-57.17	10.99	722.15
26	*	*	*
27	*	*	*

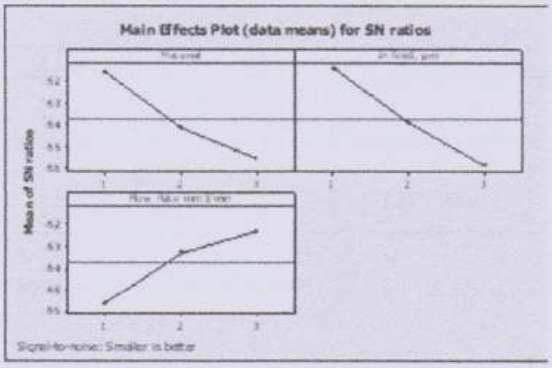
From the calculated values of signal to noise ratio, the values are obtained for the various levels of the factors and tabulated in Table 7.

Table 7 Signal to Noise Ratio: Smaller the better.

Level	Material	In feed (μm)	Flow rate (mm^3/min)
1	-51.58	-51.43	-55.65
2	-54.12	-53.93	-53.27
3	-55.52	-55.87	-52.30
Delta	3.94	4.44	3.35
Rank	2	1	3

The main effect plot (the data means) for the calculated S/N ratio is calculated and presented graphically as shown in the Fig. 4. The highest S/N ratio always yields the optimum quality with minimum variance. Therefore, the level with a higher value determines the optimum level of each factor. For the experimentation carried out the best results would be obtained for AISI4140, the workpiece material, infeed rate of 10 μm, and flow rate of 60mm3/min.

Fig.4. Main Effects Plot (Data Means) for SN ratios

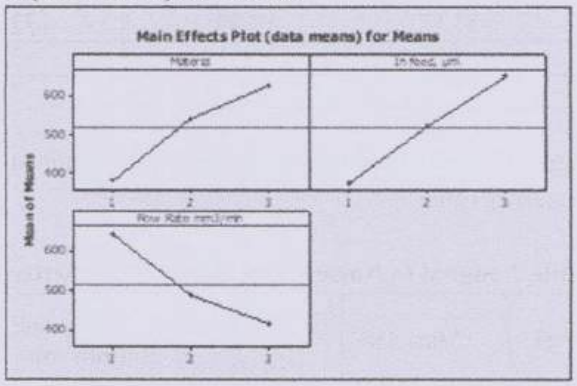


From the calculated values of means, the values are obtained for the various levels of the factors and tabulated in Table 8 and the same is represented graphically in the Fig. 5.

Table 8 Response Table for Means

Level	Material	In feed, μm	Flow rate mm^3/min
1	379.9	372.9	643.7
2	539.2	522.4	486.0
3	623.3	647.1	412.7
Delta	243.5	274.3	231.0
Rank	2	1	3

Fig.5 Main Effects Plot (data means) for Means



2.4.2 The regression Analysis

Taguchi technique can be used for the prediction of the full factorial design. The regression equation from full factorial prediction is

$$F = 437 + 0.211\ \tau s + 6.86\ d - 5.78\ f$$

Where, F is the grinding force in Newton, τs is the shear stress of workpiece material in MPa, d is the infeed in micrometers and f is flow rate in mm3/min

Table 9 Regression Table

Predictor	Coefficient	Standard Error Coefficient	T	P
Constant	436.58	47.81	9.13	0.000
Shear stress	0.21139	0.03676	5.75	0.000
Infeed	6.8564	0.8429	8.13	0.000
Flow rate	-5.7751	0.8429	-6.85	0.000

S = 71.5231 R-Sq = 86.4% R-Sq(adj) = 84.6%

2.4.3. Analysis of Variance

ANOVA is a computational technique to estimate quantitatively the relative contribution which each controlled parameter makes on the overall measured response and is expressed as a percentage. Thus information about how significant the effect of each controlled parameter is on the experimental results can be obtained. The total variation in response is decomposed into variation due to various controlled factors and their interactions and due to the error involved in the experimentation. The ANOVA can be done with the raw data or with the S/N data. The ANOVA based on the raw data signifies the factors which affect the average response rather than reducing the variation. But ANOVA based on the S/N data takes into account both these aspects and so it is used here. Since it is a saturated design where all columns are assigned with the factors, the variations due to error are estimated by pooling the estimates of the factors

having least variance. This also helped in determining the Fisher test (F-test) factor for finding out the confidence level of the results. The ANOVA is done for all the quality characteristics under study.

Table 10. ANOVA Table

Source	Degrees of Freedom	Sum of Squares	MS	F Value	P Value
Regression	3	747798	249266	48.73	0.000
Residual Error	23	117658	5116		
Total	26	865456			

Source	Degrees of Freedom	Seq. Sum of Squares
Shear Stress	1	169195
Infeed	1	338470
Flow Rate	1	240134

2. Interpreted Graphs For Force As A Quality Characteristic:

On the basis of the interpreted results of force required for grinding operation with the help of graphite as solid lubricant for the materials selected, AISI 4140, AISI 4340 and AISI 52100 are given in Fig.6 to Fig. 8.

Fig.6. AISI 4140, Graphite as lubricant

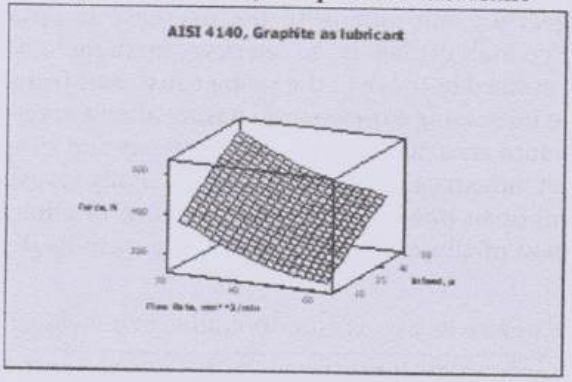


Fig. 7. AISI 4340, Graphite as lubricant

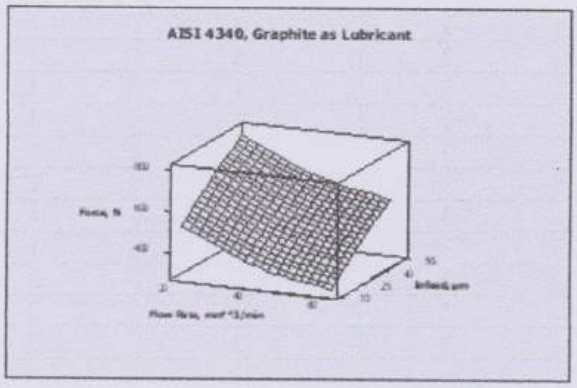
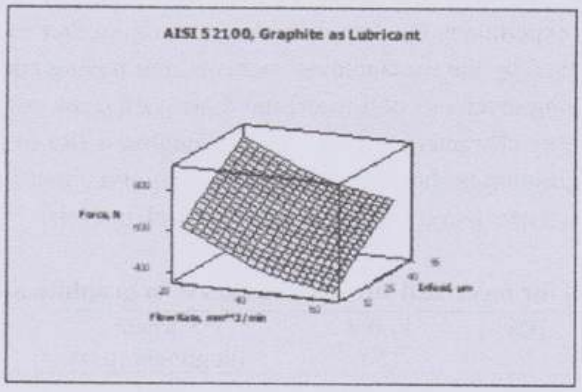


Fig. 8. AISI 52100, Graphite as lubricant



3. Analysis for Surface Roughness

On the similar lines of the force, Taguchi analysis is done for surface roughness obtained in the graphite assisted grinding process. The S/N ratios, standard deviation and mean for surface roughness for graphite assisted grinding for various alloy steels, the varying flow rates and infeed rates are calculated from the observed data are tabulated in Table 11.

Table 11. Calculated S/ N ratio, Standard deviation and Mean.

Trial	S/N Ratio	Standard Deviation	Mean
1	7.394	0.01527	0.426
2	*	*	*
3	*	*	*
4	7.394	0.0152	0.426
5	*	*	*
6	*	*	*
7	7.394	0.0152	0.426
8	*	*	*
9	*	*	*
10	7.811	0.0152	0.406

17	2	3	1
18	2	3	1
19	3	1	3
20	3	1	3
21	3	1	3
22	3	2	1
23	3	2	1
24	3	2	1
25	3	3	2
26	3	3	2
27	3	3	2

2.3 Experimentation

By choosing the L27 orthogonal array the issue of repeating the tests is sorted out, as the array itself recommends the repetitions. This helps to obtain more reliable information from the statistical analysis of the experiment. Quality characteristics, i.e. surface roughness (Ra) in μm and force (F) in N are noted by the measurement systems. For having consistent results with Ra, pieces are ground giving seven sets of upward and downward spark out passes. The sample data obtained for the quality characteristics, i.e. surface roughness (Ra in μm) and force in N in the graphite assisted grinding is shown in Table 5. It is observed that there is considerable consistency in the obtained data and it is reliable for statistical analysis.

Table 5. Sample data for force and surface roughness in graphite assisted grinding.

Tria l	Force (N)	Surface roughness (μm)
1	367.68	0.44
2	356.65	0.43
3	362.16	0.41
4	372.58	0.44
5	366.99	0.43
6	361.40	0.41
7	416.70	0.44
8	404.20	0.43
9	410.45	0.41
10	374.44	0.42
11	368.82	0.41
12	363.21	0.39
13	446.71	0.43
14	433.31	0.42
15	440.01	0.40
16	821.15	0.45
17	808.83	0.44
18	796.52	0.42
19	393.59	0.41
20	381.78	0.40
21	387.69	0.38
22	771.74	0.43
23	760.16	0.42

11	*	*	*
12	*	*	*
13	7.600	0.0152	0.416
14	*	*	*
15	*	*	*
16	7.193	0.0152	0.436
17	*	*	*
18	*	*	*
19	8.027	0.0152	0.396
20	*	*	*
21	*	*	*
22	7.600	0.0152	0.416
23	*	*	*
24	*	*	*
25	7.600	0.0152	0.416
26	*	*	*
27	*	*	*

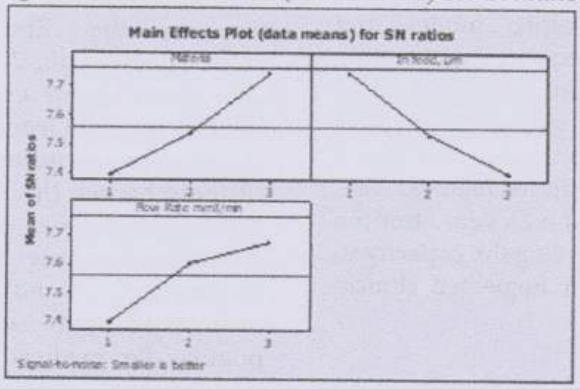
From the calculated values of signal to noise ratio, the values are obtained for the various levels of the factors and tabulated in Table 12.

Table 12. Signal to Noise Ratios Smaller is better

Level	Material	In feed (µm)	Flow rate (mm^3/min)
1	7.395	7.744	7.396
2	7.535	7.532	7.602
3	7.743	7.396	7.674
Delta	0.348	0.348	0.278
Rank	2	1	3

The main effect plot (the data means) for the calculated S/N ratio is calculated and presented graphically as shown in the Fig. 9. The highest S/N ratio always yields the optimum quality with minimum variance. Therefore, the level with a higher value determines the optimum level of each factor. For the experimentation carried out the best results would be obtained for AISI 52100, the workpiece material, infeed rate of 10 µm, and flow rate of 60mm3/min.

Fig. 9. Main Effects Plot (Data Means) for SN ratios



segment gives the general construction of this proposal and a part wise separation of the items.

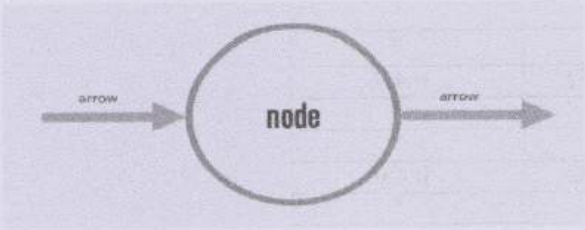


Figure 1. Elements of the map

Motivation

My advantage in plan for medical services began in the third year of my modern plan Lone wolf's program at the Public Organization of Plan, India. With Gujarat being one of the main harbors of diabetic patients on the planet, I chose to chip away at a Diabetes the executives Framework for my fifth semester project that would assist with composing 1 and 2 Diabetes patients. By understanding the intricacies of the pathophysiology of Diabetes Mellitus, I became captivated by the most common way of planning a patient-focused arrangement utilizing wearable gadgets and the idea of Web of Things. The undertaking was additionally introduced as a paper at the India HCI meeting (Kumar, 2014). The test that accompanied taking care of true medical services issues energized me, and started another interest in plan.

After two years I got a chance to foster a careful gadget as a component of my graduation project. The organization that supported it was a beginning up creating developments for reasonable and open medical care in India, and this was one of their most memorable items. The task included fostering a careful tool stash from a temporary patent to the alpha model, and provided me with the active experience of testing and item improvement in a lean group comprising of a clinician, a planner, and a biomedical designer. The experience persuaded me that I needed to keep working in plan for medical care. The item proceeded to be sent off a year after the fact, supporting my trust in having the capacity to foster significant answers for neglected clinical necessities (InnAccel, 2017).

Background

Clinical gadgets adversely affect the climate. It is assessed that the medical care area in the US (US) contributes practically 10% of their complete ozone depleting substance discharges (Eckelman and Sherman, 2016). In the Unified Realm (UK), clinical instruments and hardware are liable for around 13% of the ozone depleting substance (GHG) emanations of the medical care area, surpassing 3.5 Mt-CO_2e each year (NHS Britain, 2018). As a matter of fact, Hawkes (2012) distinguished that close to 66% of the outflows created by the Public Wellbeing Administration (NHS) come from sources, for example, drugs, clinical gadgets and the production network, which are not straightforwardly constrained by the NHS. Around the world, how much waste made per emergency clinic patient each day goes from 0.44 kg in Mauritius to 8.4 kg in the US of America, with European nations having a tendency to be between those two limits (UK 3.3 kg, Germany 3.6 kg and France 3.3 kg) (Minoglou et al., 2017).

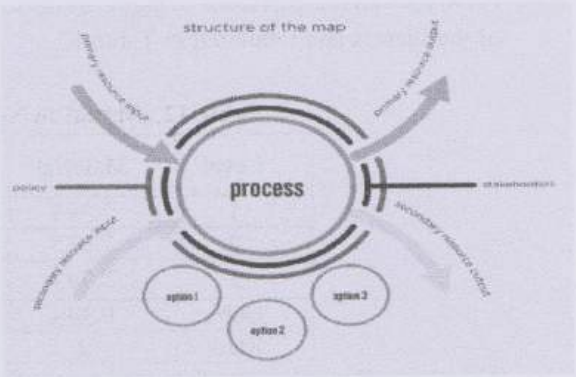


Figure 2: Structure of the map

The Challenges in existing Design Methods

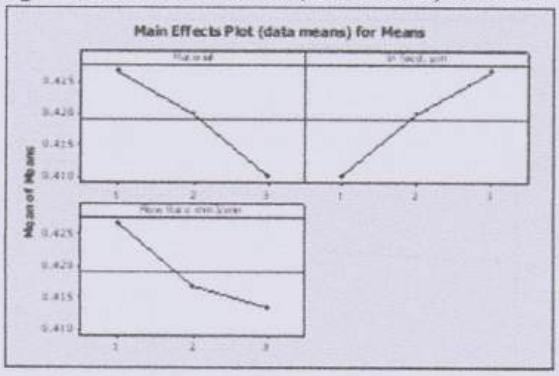
Past the advantages versus dangers of single-use and reusable gadgets, the basic for a less inefficient medical services framework in the UK lies in the Environmental Change Act (legislation.gov.uk, 2008), which commands the decrease of ozone depleting substance outflows by 80% by 2050 from the 1990 gauge. In view of the headway made such a long ways in lessening GHG discharges, the NHS is wealthy the expected GHG emanation decreases to be on course for the 80% decrease order (NHS Britain, 2018). With a rising populace, and expanding future rates, the NHS is ready to expect a critical expansion popular for medical care, which will build the requirement for clinical gadgets, and thus create

From the calculated values of means, the values are obtained for the various levels of the factors and tabulated in Table 13 and the same is represented graphically in the Fig. 10.

Table 13 Response Table for Means

Level	Material	In feed (μm)	Flow rate (mm^3/min)
1	0.4267	0.4100	0.4267
2	0.4200	0.4200	0.4167
3	0.4100	0.4267	0.4133
Delta	0.0167	0.0167	0.0133
Rank	1.5	1.5	3

Fig. 10. Main Effects Plot (data means) for Means



4.1 The regression Analysis

Taguchi technique can be used for the prediction of the full factorial design. The regression equation from full factorial prediction is

$$Ra = 0.428 - 0.000017\ \tau s + 0.000417\ d - 0.000333\ f$$

Where, Ra is the grinding force in Newton, τs is the shear stress of workpiece material in MPa, d is the infeed in micrometers and f is flow rate in mm3/min

Table 14. Regression Table

Predictor	Coefficient	Standard Error Coefficient	T	P
Constant	0.427995	0.002230	191.94	0.000
Shear stress	-0.00001700	0.00000171	-9.92	0.000
Infeed	0.00041666	0.00003931	10.60	0.000
Flow rate	-0.00033334	0.00003931	-8.48	0.000

S = 0.00333589 R-Sq = 92.5% R-Sq(adj) = 91.5%

40	651.62	0.64	604.73	0.47	468.79	0.45
50	724.02	0.56	671.93	0.47	520.88	0.45

Fig. 2. Effect of coolants on force under varying depths of cut.

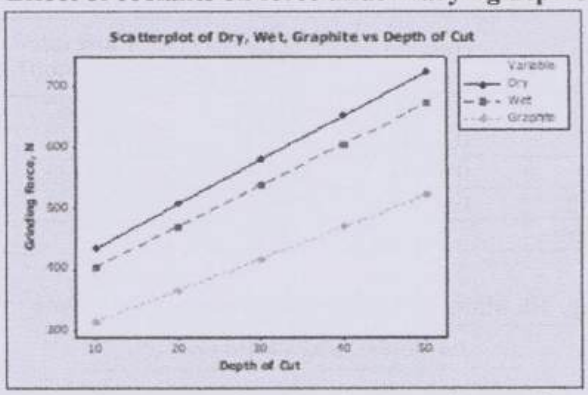
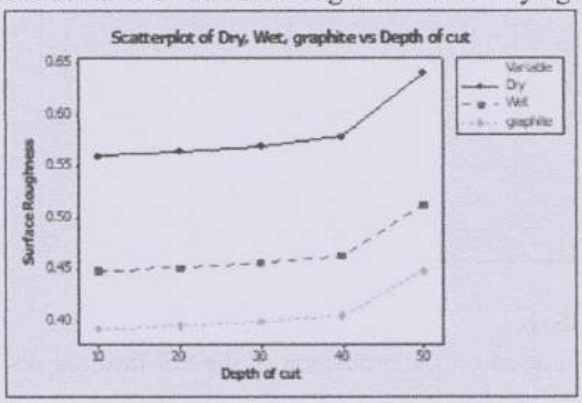


Fig. 3. Effect of coolants on Surface Roughness under varying depths of cut



Results show that the grinding force, grinding energy and the surface roughness decreases with the help of the use of graphite compared with dry grinding and grinding with the conventional coolants.

2.2 Taguchi methods for design of experiments

Taguchi methods of experimental design provide a simple, efficient and systematic approach for the optimization of experimental designs for performance quality and cost. It has been proved successful to many manufacturing situations. The traditional experimental design procedures focus on the average product or process performance characteristics. But the Taguchi method concentrates on the effect of variation on the product or process quality characteristics rather than on its averages. That is, the Taguchi's approach makes the product or process performance insensitive (robust) to variation to uncontrolled or noise factors. Taguchi recommends that this can be done by the proper design of parameters during the 'parameter design' phase of off-line quality control. He designed certain standard orthogonal arrays (OAs) by which simultaneous and independent evaluation of two or more parameters for their ability to affect the variability of a particular product or process characteristic can be done in a minimum number of tests. Subsequently, decision is made for the optimum combination of these parameters.

4.2 Analysis of variance

ANOVA, the analysis of variance is carried out and the results are included in Table 15.

Table 15 ANOVA table

Source	Degrees of Freedom	Sum of Squares	MS	F Value	P Value
Regression	3	0.0031	0.00104	94.18	0.000
Residual Error	23	0.00025	0.00001		
Total	26	0.00340			

Source	Degrees of Freedom	Seq. Sum of Squares
Shear Stress	1	0.0010940
Infeed	1	0.0012500
Flow Rate	1	0.0008000

5. Interpreted Graphs For Surface finish As A Quality Characteristic

On the basis of the interpreted results of surface roughness obtained in grinding operation with the help of graphite as solid lubricant for the materials selected, AISI 4140, AISI 4340 and AISI 52100 are given in Fig. 11 to Fig. 13.

Fig.11. AISI 4140, Graphite as lubricant

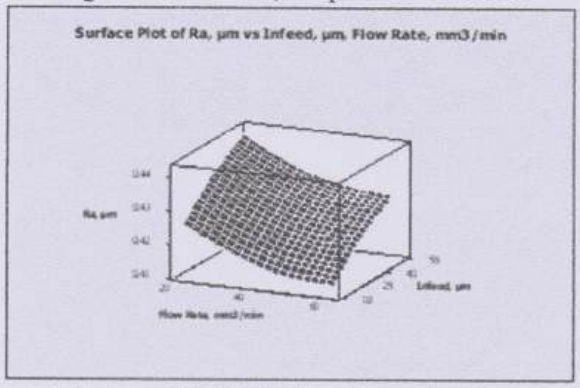


Fig.12. AISI 4340, Graphite as lubricant

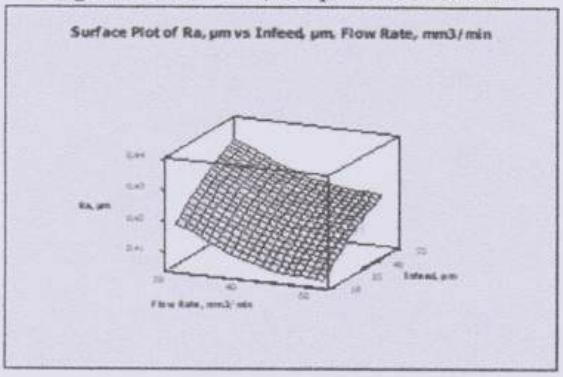
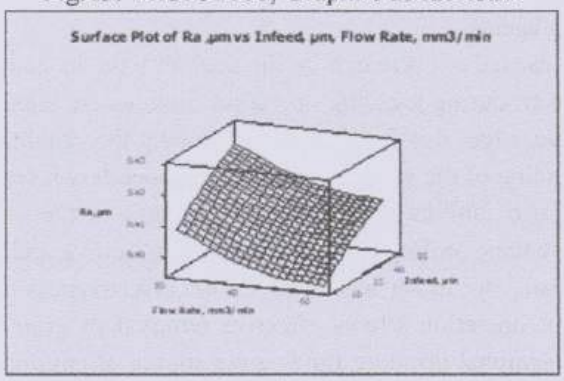


Fig.13. AISI 52100, Graphite as lubricant



6. Conclusions

The experimental setup developed for the application of graphite as a means to reduce the heat generated in the grinding zone has been investigated for improving the surface finish and reducing the cutting forces involved in the process. The Taguchi method of experimental design is used for the investigations. When compared with the dry grinding and grinding with the conventional coolants, graphite gives considerably reduces the force required for grinding operation and the surface finished improved. Hence the effective role of graphite as a lubricant was evident from the improvement of output parameters.

Similar experimentation can be carried out with other solid lubricants like molybdenum disulphide, zinc phosphate and boric acid, which may lead to most effective solid lubricant for surface grinding.

7. References

1. H.M.T., "Production Technology," Tata McGraw Hill, pp.250-251, 2009.
2. J.O. Outwater, M.C. Shaw, "Surface temperature in grinding," Trans. ASME 74 pp.73–86, (1952).
3. S. Malkin, R. B Anderson, Thermal aspects of grinding — part II, surface temperature and workpiece burn, Trans. ASME, J.Eng. Indust. 96 , pp.1184–1191, (1974)
4. Y. Nakano, H. Uchida, K. Ota, Thermal deformations and profile errors of workpiece in surface grinding, Ann. CIRP 25 (1), pp. 235–240, (1976).
5. R. Snoys, K.U. Leuven, M. Maris, J. Peters, Thermally induced damages in grinding, Ann. CIRP 27 (2), pp.571–581, (1978).
6. Y. Nakano, H. Uchida, K. Ota, Thermal deformations and profile errors of workpiece in surface grinding, Ann. CIRP 25 (1) ,235–240, (1976).
7. S. Ebbrel, N.H. Wooley, Y.D. Tridimas, D.R. Allanson, W.B. Rowe, The effects of cutting fluid application methods on the grinding process, Int. J. Mach. Tools Manufact. 40, pp.209–223, (2000).
8. S. Malkin, Grinding Technology, Theory and Applications of Machining with Abrasives, Ellis Harwood, Chichester, 1989.
9. T.D. Howes, Assessment of cooling and lubricating properties of grinding fluids, Ann. CIRP 39 (1), pp. 313–316, (1990).

Source details

Feedback > Compare sources >

Shu Ju Cai Ji Yu Chu Li/Journal of Data Acquisition and Processing

Scopus coverage years: from 2001 to Present

Publisher: Nanjing University of Aeronautics an Astronautics

ISSN: 1004-9037

Subject area: Computer Science: Signal Processing | Computer Science: Software

Source type: Journal

Save to source list | Source Homepage

CiteScore 2022
0.7

SJR 2022
0.140

SNIP 2022
0.221

CiteScore | CiteScore rank & trend | Scopus content coverage

Improved CiteScore methodology

CiteScore 2022 counts the citations received in 2019-2022 to articles, reviews, conference papers, book chapters and data papers published in 2019-2022, and divides this by the number of publications published in 2019-2022. Learn more >

CiteScore 2022

0.7 = 302 Citations 2019 - 2022 / 434 Documents 2019 - 2022

Calculated on 05 May, 2023

CiteScoreTracker 2023

0.8 = 329 Citations to date / 434 Documents to date

Last updated on 05 December, 2023 • Updated monthly

CiteScore rank 2022

Category	Rank	Percentile
Computer Science └ Signal Processing	#110/122	10th
Computer Science └ Software	#389/404	3rd

(16)

How to Cite:
Ganvir, N. N., & Yadav, D. (2022). Extract roi from mammogram images using morphological and k-means clustering. *International Journal of Health Sciences*, *6*(S5), 3040–3049. https://doi.org/10.53730/ijhs.v6nS5.9314

Extract roi from mammogram images using morphological and k-means clustering

Neha N. Ganvir
Associate Professor, Department of E & TC, BVCOEL, Pune
Email: ganvirneha@gmail.com

D.M. Yadav
Dean Director, G.H.Raisoni COE & M, Pune
Email: dineshyadav800@gmail.com

***Abstract*---**Cancer is leading cause of death in worldwide. Cancer cells damages all cells surrounded by it and hence covers the complete area of the body. Amongst women breast cancer is most common deadly disease as compared to men. In any type of cancer early-stage detection plays vital role as it can save the patient's life. If cancer is diagnosed early by using breast self-examination (BSE) and clinical breast examination (CBE), at 40-49 years of age, the survival rate of breast cancer reaches 100 per cent. New strategies named CAD (computer-assisted diagnosis) programs for early detection utilizing multiple mammogram datasets, such as mini-mias, DDSM, etc., CAD (Computer Aided Diagnosis) systems are mostly used for the second opinion for radiologists. Many researchers are already developing different CAD systems. Different databases are available for the researchers to study and detect the cancerous tumors. In this paper Mini-Mias database is used. Mammogram images are low contrast and may contain noise. Filtering or pre-processing is required to remove any noises present in the image, here Weiner filter is used. Two methodologies are compared here. First using morphological operated segmentation and second is by using k-means clustering algorithm. Both methodologies show segmented output of the image, but K-means clustering gives more accurate region of interest as compared to morphological. In this paper, pre-processing and segmentation is carried out. ROC output from K-Means clustering algorithm can be used to train any network to detect any cancerous tumor present in the images.

***Keywords*---**BSE, CBE, CAD, CT, DDSM (Digital Data Screening Mammography), GLCM, Mammograms, MRI, PET.

1. Introduction

Breast cancer is leading cause for women mortality. Every year new cases of cancer spreads the news in all over the world. It has been estimated 9.6 million death over the worldwide. A total of 1,806,590 new cancer cases and 606,520 deaths are expected in the US in 2020, which is about 4,950 new cases and more than 1,600 deaths each day. The numbers are reported in "Cancer Statistics, 2020. Post cancer survival for women with breast cancer was reported 60% for Indian women, as compared to 80% in the U.S. If breast cancer detected in early stage like stage 0 and 1 then it can be cure. Breast self-examination (BSE) is the first step to examine. If any lump node observed and it has been advised to immediate contact doctor. Women with age of 40 or more than this are advised to do this BSE and CBE (clinical breast examination). The main objective of medical image study is to useful information about the physiological processes by using external and internal sources of energy and to achieve this X-rays, magnetic resonance, nuclear medicine, or ultrasound are used. The most effective and economical breast imaging modality has been X-ray mammography due to its simplicity, portability and cost effectiveness low contrast image, an important source of radiological information for breast imaging is the presence and distribution of micro calcifications in the breast, this anatomical information can be obtained with high resolution technology using X-rays, As yet there is no comprehensive imaging modality for all radiological applications and needs, although the ability to computerize and analyze medical images provides a powerful means to assist physicians. Many tests are available now like Blood tests, such as a complete blood count, mammogram of the other breast to look for signs of cancer, Breast MRI, Bone scan, Computerized tomography (CT) scan, Positron emission tomography (PET) scan. In US, once the women crosse age of 40 it has been instructed to do CBE.100% recovery is possible if the patient is identified in early stage. In this, paper pre-processing and segmentations methods discussed.

2. Materials and Methods

It is a good idea to know how your breasts normally look and feel so you can notice any changes. Medical organizations have different recommendations for breast self-exams, though. A mammogram can show breast lumps up to 2 years before they can be felt. Different tests help determine if a lump may be cancer. Ones that are not cancerous tend to have different physical features than ones that are. Imaging tests such as mammograms and ultrasounds can often see the difference [5]. A digital mammogram hence very useful to detect cancer at early stage it uses special X-ray images to spot abnormal growths or changes in breast tissue. Many pre-processing techniques have been discussed and techniques included filtering is mentioned in [1], [2] with statics. Image pre-processing may have dramatic positive effects on the quality of feature extraction and the results of image analysis. Image pre-processing is analogous to the mathematical normalization of a data set, which is a common step in many feature descriptor methods [4]. Image used for processing is from mini-mias database. Mini-Mias has many types of images includes normal, benign, and malignant images with micro-calcified images. Microcalcifications are tiny bits of calcium deposited in breast typically size of 0.3mm to 1mm in scale [2]. Images

filtered using wiener filter. Weiner filter gives better results as compared to other filters and it has smooth response. If noise is present in the system, then it is additive white Gaussian noise (AWGN) then it is removed by using wiener filter. In a morphological operation, the value of each pixel in the output image is based on a comparison of the corresponding pixel in the input image with its neighbors. Separating the segmentation process into two parts creates its main interest: finding the markers is the intelligent part, since it requires an interpretation of the image, but the difficulty is counter well-adjusted by the fact that the resulting segmentation is largely independent of the exact shape or position of the markers. Moreover, the tedious part that is getting the contours is entirely automatic. The advantages of the method are good localization, invariance to lighting conditions, absence of parameters, high sensitivity as strongly or weakly compared objects are equally segmented [7].

The algorithm is composed of two passes preceded by a pre-processing step for simplifying small scale details of the image that might cause over-segmentation. In the first pass feature images at various scales are extracted and kept in respective level of morphological towers. In the second pass, potential features contributing to the formation of segments at various scales are detected. Finally, the algorithm traces the contours of all such contributing features at various scales [8]. When images are processed for pre-processing it may happen that noises or distortion may be added. The main goal of morphological operation is to remove this imperfection that mainly affects the shape and texture of images. Morphological operations can be very useful in image segmentation as the process directly deals with shape extraction in mammogram image. Morphology in context of image processing means description of shape and structure of the object in an image. Morphological operations work based on set theory and relied more on relative ordering of the pixel instead on their numerical significance [6]. Here, algorithm for morphological operation on mammogram image steps are as follows.

- Read the image.
- Detect the entire cell of an image.
- Binary Gradient Mask shows lines of high contrast in the image so dilate an image.
- Some holes are present in dilated image, fill those holes.
- Remove connected objects on border as the cell of interest has been successfully segmented, but it is not the only object that has been found.
- To make the segmented object look natural, smooth the object by eroding the image.
- Display the mask over the original image.
- Outlined the segmented Image.

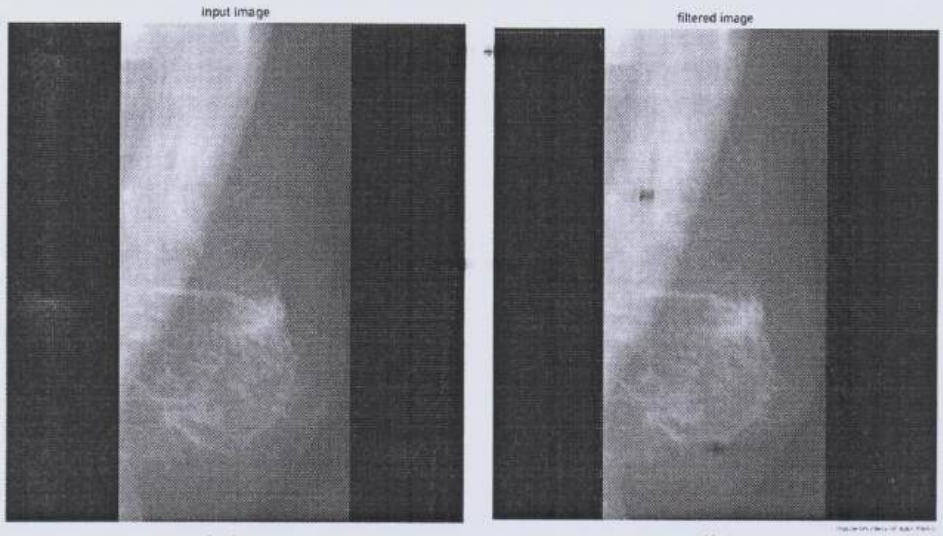
Step wise results are discussed in results and discussion section.
Second algorithm is segmentation by using K-means clustering algorithm. As segmentation stage is one of the most Significant steps since it affects the accuracy of the Feature Extraction & Classification. Rough k-means approach is used for segmentation of tumors from breast parenchyma. Pixel objects which belong to the tumor area are classified under smaller approximation, whereas objects which possibly belong to the same are considered as upper approximation. The difference of upper and lower approximation will result with

objects in the rough boundaries [9]. The K-means algorithm is an iterative technique that is used to partition an image into K clusters. In statistics and machine learning, k-means clustering is a method of cluster analysis which aims to partition and observations into k clusters in which each observation belongs to the cluster with the nearest mean. Algorithm states that pick K cluster centers, either randomly or based on some heuristic then assign each pixel in the image to the cluster that minimizes the distance between the pixel and the cluster center. Next step is to re-compute the cluster centers by averaging all the pixels in the cluster. Repeat last two steps until convergence is attained (e.g., no pixels change clusters) [10]. To segment the breast for grouping those pixels with similar tissue appearance according to certain number of clusters. The number of clusters were determined according to the number of bins in the image histogram [11], here histogram is used.

In this paper, Image is read from database. Then image masking is done which is pre-processing for k-means clustering algorithm. Once masking is over then image is ready for partition. As discussed, clusters analysis is done. Selecting K cluster centers which is calculating distance between the pixels in the clusters. The output of this discussed in results and discussion section.

3. Result and Discussion

In this Paper, two algorithms are discussed, and results are shown. First is by applying morphological operations and second is by using k-means clustering algorithm. Here Mini-Mias mammogram images have used. Normal and malignant image has been selected. Mammograms are low contrast images and has many artifacts like tags. Images should be preprocessed properly [1], [2].



(a) (b)

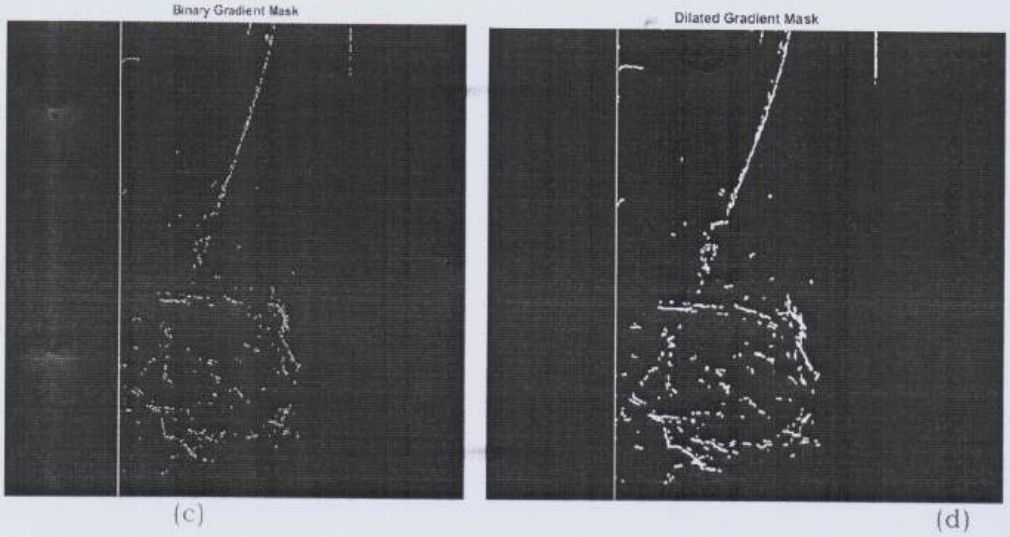
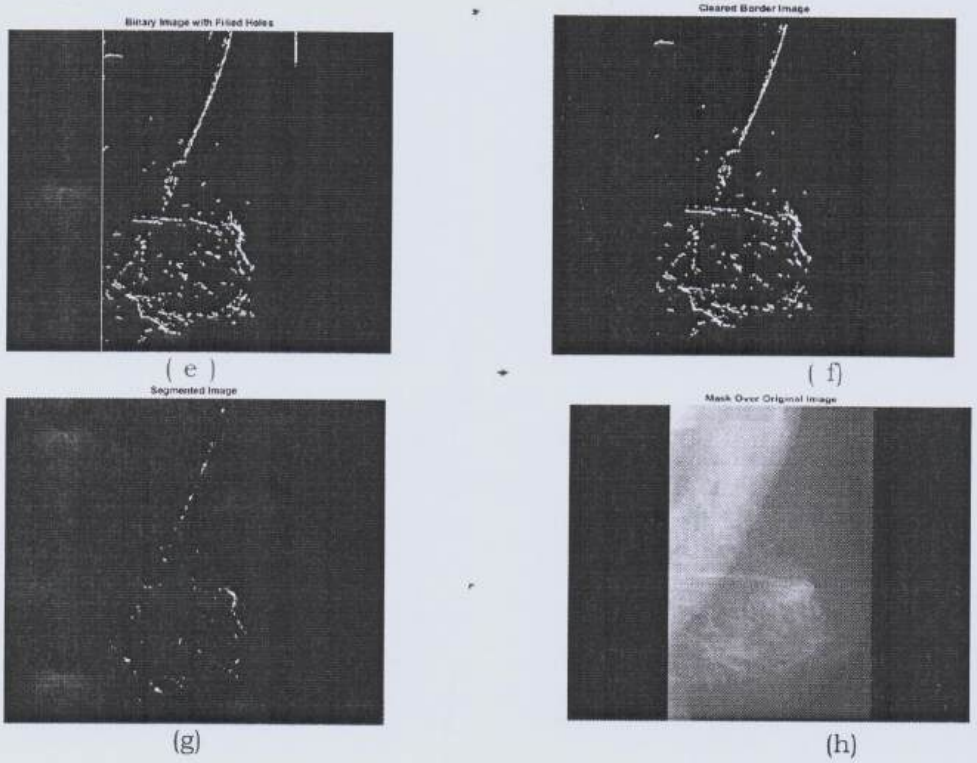
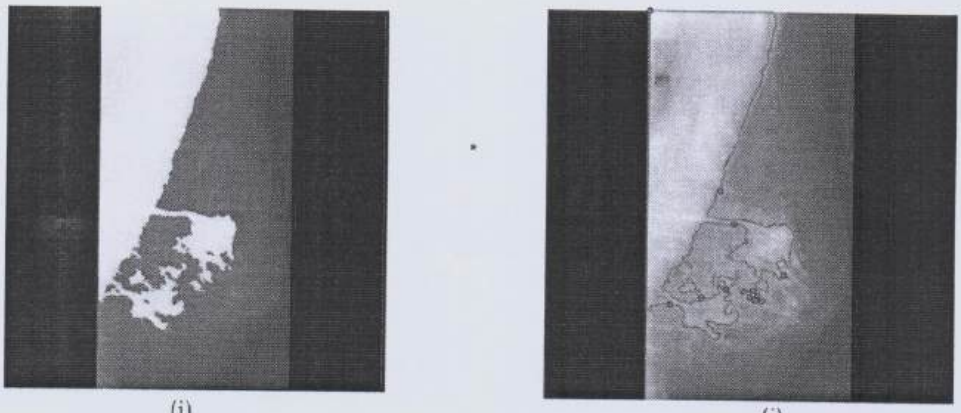


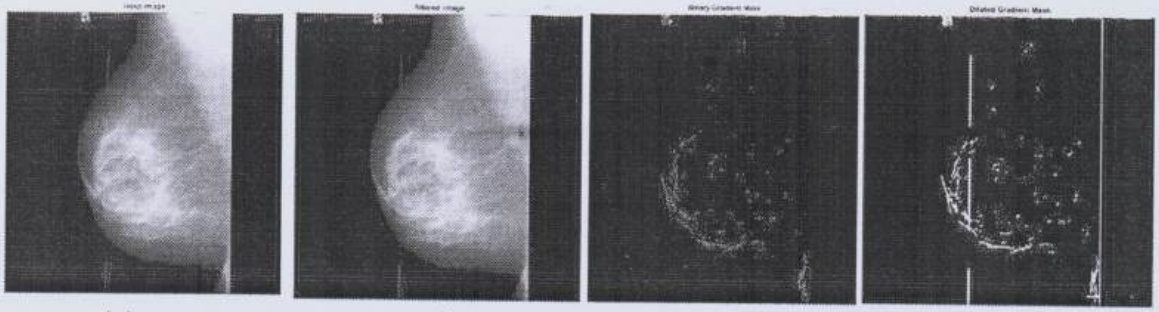
Figure 1: Mammogram Image (a) Input Mini-Mias Mammogram Image (b) Weiner filter Image (c)Binary Gradient Mask (d) Dilated gradient Mask Image.





(i) (j)

Figure 2: Mammogram Image (e) Binary Image filled with holes, (f) Cleared Border Image, (g) Segmented Image, (h) Pre-processing segmentation Mask. (i) Masked Image, (j) Locating Region of Interest Image using k-means clustering



(a) (b) (c) (d)

Figure 3: Mammogram Benign Image (a) Input Mini-Mias Mammogram Image (b) Weiner filter Image (c)Binary Gradient Mask (d) Dilated gradient Mask Image

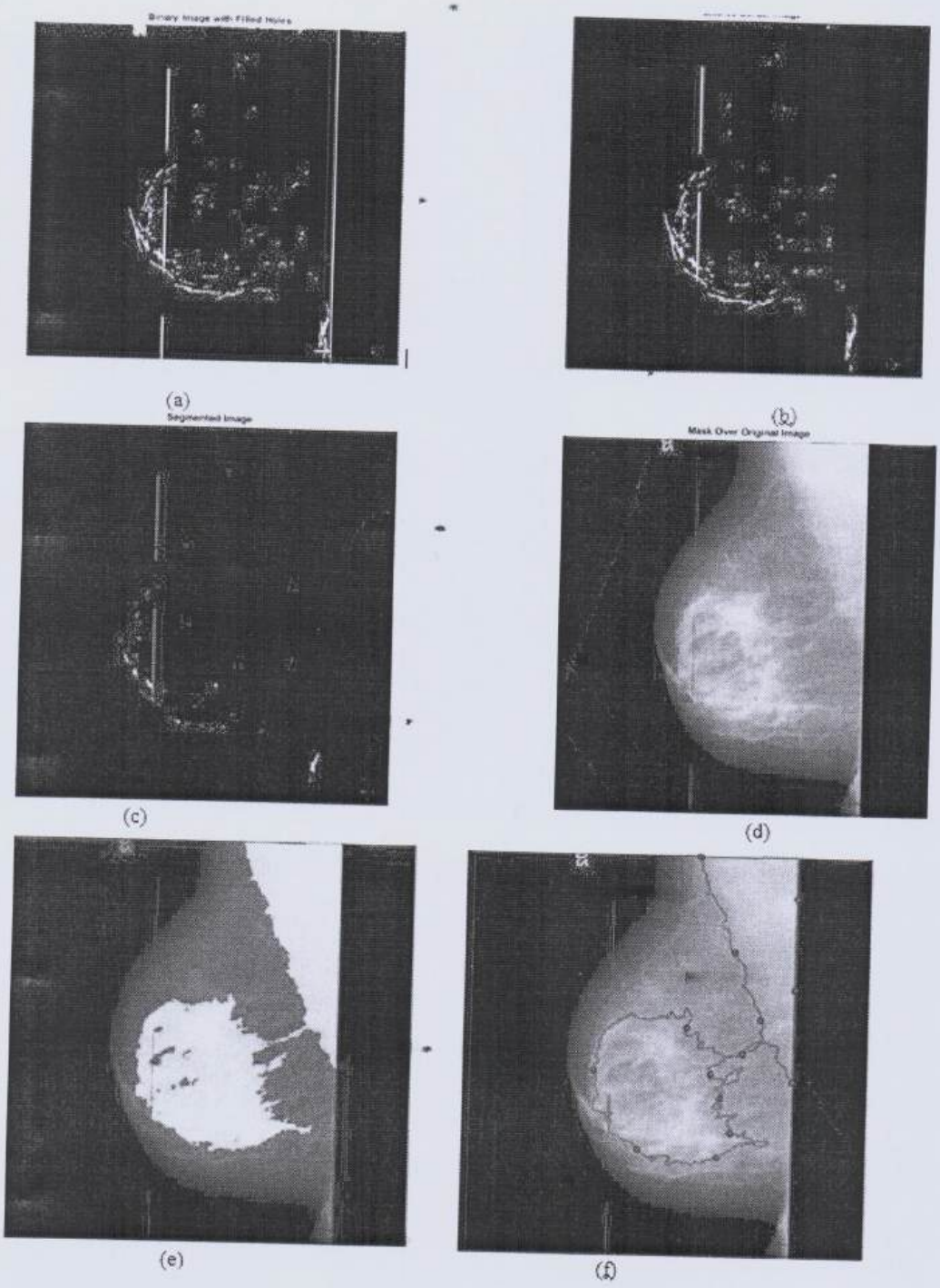


Figure 4: Mammogram Image (a) Binary Image filled with holes, (b) Cleared Border Image, (c)Segmented Image, (d) Pre-processing

segmentation Mask, (e) Masked Image, (f) Locating Region of Interest Image using k-means clustering.

Here, MATLAB platform is used for analyzing images. Figure 1 and 2 shows normal image from database, and figure 3 and 4 shows image outputs of malignant image from Mini-Mias database. Wiener filter has advantages of smooth filtering and maintaining aspect ratios of the image. Two types of segmented images have shown here first by performing morphological operations and second by using k-means clustering. Figure 1 and 2, fig 3 and 4 (a), (b), (c), (d) and (e), (f) and (g) shows morphological operated images. Figure 2, (h),(i) and (j) shows k-means clustering segmented images and figure 4 (d), (e) and (f) shows the same. Images are taken from Mini-Mias Database mathematical Morphology, dealing with geometrical features is a well-suited technique for segmentation purpose. Figure (a) shows mammogram image of normal and malignant image. This image is required to be processed; fig (b) shows Weiner filtered image. Selection of wiener filter is based on as per [1] as this image is again gone through morphological operations. The beauty of morphological operation is discussed in material and methods, detect a cell using edge detection and basic morphology. An object can be easily detected in an image if the object has sufficient contrast from the background. Figure (c) is used to detect the entire cell. A binary mask containing the segmented cell, calculate the gradient image and apply a threshold. Use edge and the Sobel operator to calculate the threshold value. Tune the threshold value and use edge again to obtain a binary mask that contains the segmented cell. Figure (d) is dilated image. The binary gradient mask shows lines of high contrast in the image. These lines do not quite delineate the outline of the object of interest. Compared to the original image, there are gaps in the lines surrounding the object in the gradient mask. Figure (e) shows binary image filled with holes, as the dilated gradient mask shows the outline of the cell quite nicely, but there are still holes in the interior of the cell. Figure (f) shows cleared border image as the cell of interest has been successfully segmented, but it is not the only object that has been found. Any objects that are connected to the border of the image can be removed. Finally, to make the segmented object look natural, smooth the object by eroding the image twice with a diamond structuring element, figure (g) shows segmented image after using morphological operation. Image can be visualized by masking the image as shown in figure (h). Second methodology is to segment the image using k-means clustering. It is discussed briefly in material and methods. Before processing to k-means clustering, the image should be pre-processed by using segmentation mask as shown in figure (i). After masking, segmentation is carried out with locating region of interest as shown in figure (j) in figure 2. It has been observed that as compared to morphological segmentation k-means clustering gives more properly segmented output and clearly identify region of interest. This region of interest can process further for extract useful features to detect images cancerous or not.

4. Conclusion

Cancer is deadly disease in worldwide. Breast cancer is most common death amongst women. It is very important to detect cancer in early stage. BSE and CBE are common technique to detect lumps or nodes in breast. In this paper, preprocessing segmentation technique with filter is discussed. Mini-Mias

database is used, normal and malignant images are used to perform different operations. Figure 1,2,3,4 shows different morphological operated images and figure (i) and (j) shows preprocessed k-means clustering used segmented images with highlighting region of interest. Mammograms are low contrast images and included marks, labels, and tags etc. Filtering is important to remove any noise present in the image. Weiner filter has smooth filtering performance and morphological operations are performed which works on the shapes of image. Outlined border is properly can observe from the results. Next methodology has been performed on mammogram images are k-means clustering segmentation. First partial stretching enhancement is applied to the image to improve the quality of the image before applying to K-means clustering algorithm. It is an unsupervised algorithm, and it is used to segment the interest area from the background. Figure shows region of interest from the mammogram image. K-means clustering gives best segmentation result as compared to morphological. This output of ROC can be processed further to extract different features to train any neural network to detect whether the image is cancerous or not.

5. References

[1] Neha N.Ganvir, D.M.Yadav, "*Filtering Method for Pre-processing Mammogram Images for Breast Cancer Detection*", International Journal of Engineering and Advanced Technology. ISSN: 2249 – 8958, Volume-9 Issue-1, (pp. 4222-4229),Oct 2019.

[2] Neha N.Ganvir, D.M.Yadav , "*Clustered Micro-Calcifications Extraction From Mammogram Images Using Cellular Automata Segmentation With Anisotropic Diffusion Filtering*" , International Journal of Scientific & Technology Research. ISSN 2277-8616, VOLUME 9, ISSUE 04, (pp. 1217-1221), April 2020.

[3] Marcotegui B., Meyer F. (1994), "*Morphological Segmentation of Image Sequences. In: Serra J., Soille P. (eds) Mathematical Morphology and Its Applications to Image Processing*". Computational Imaging and Vision, vol 2. Springer, Dordrecht. https://doi.org/10.1007/978-94-011-1040-2_14.

[4] Krig S. (2014), "*Image Pre-Processing. In: Computer Vision Metrics*". Apress, Berkeley, CA. https://doi.org/10.1007/978-1-4302-5930-5_2.

[5] https://www.webmd.com/breast-cancer/breast-cancer-detection.

[6] Srisha, Ravi & Khan, Am. (2013)., "*Morphological Operations for Image Processing : Understanding and its Applications*", Conference: National Conference on VLSI, Signal processing & Communications.

[7] Meyer F. (2005), "*Morphological segmentation revisited. In: Bilodeau M., Meyer F., Schmitt M. (eds) Space, Structure and Randomness*". Lecture Notes in Statistics, vol 183. Springer, New York, NY. https://doi.org/10.1007/0-387-29115-6_13.

[8] S. Mukhopadhyay and B. Chanda, "*Multiscale morphological segmentation of gray-scale images*," in *IEEE Transactions on Image Processing*, vol. 12, no. 5, pp. 533-549, May 2003, doi: 10.1109/TIP.2003.810757.

[9] Rinartha, K., & Suryasa, W. (2017). Comparative study for better result on query suggestion of article searching with MySQL pattern matching and Jaccard similarity. In *2017 5th International Conference on Cyber and IT Service Management (CITSM)* (pp. 1-4). IEEE.

[10] Bora V.B., Kothari A.G., Keskar A.G. (2012), " *Mammogram Segmentation Using Rough k-Means and Mass Lesion Classification with Artificial Neural Network*". In: Hassanien A.E., Salem AB.M., Ramadan R., Kim T. (eds) Advanced Machine Learning Technologies and Applications. AMLTA 2012. Communications in Computer and Information Science, vol 322. Springer, Berlin, Heidelberg. https://doi.org/10.1007/978-3-642-35326-0_7.

[11] Patel, Dr. Bhagwati & Sinha, Professor G. (2010), " *An Adaptive K-means Clustering Algorithm for Breast Image Segmentation*". International Journal of Computer Applications. 10. 10.5120/1467-1982.

[12] Shahine, Osama & Kelash, Hamdy & Faragallah, Osama & Attiya, Gamal. (2012). *"Breast Mass Detection in Mammograms using Modified K-means Clustering*". 10.13140/2.1.4115.4561.

Source details

Feedback > Compare sources >

International Journal of Health Sciences

Scopus coverage years: 2021
(coverage discontinued in Scopus)
Publisher: Universidad Tecnica de Manabi
ISSN: 2550-6978 E-ISSN: 2550-696X
Subject area: (Nursing: General Nursing) (Social Sciences: Education)
Source type: Journal

CiteScore 2021
2.0

SNIP 2021
0.138

Save to source list Source Homepage

CiteScore | CiteScore rank & trend | Scopus content coverage

Improved CiteScore methodology
CiteScore 2021 counts the citations received in 2018-2021 to articles, reviews, conference papers, book chapters and data papers published in 2018-2021, and divides this by the number of publications published in 2018-2021. Learn more >

CiteScore 2021

2.0 = 133 Citations 2018 - 2021
67 Documents 2018 - 2021

Calculated on 05 May, 2022

CiteScore rank 2021

Category	Rank	Percentile
Nursing └ General Nursing	#45/123	63rd
Social Sciences └ Education	#585/1406	58th

View CiteScore methodology > CiteScore FAQ > Add CiteScore to your site

Advances in Water Science
2022; 33(4)

ISSN: 1001-6791

AWS水科学进展
Advances in Water Science

Intelligent Face Detection using Machine Leaning

Dr. Aarti Amod Agarkar*[1], Dr. Manisha Ajaykumar Dudhedia[2], Prof. Lalita K. Wani[3] & Dr. Uday Chandrakant Patkar[4]

*[1]Associate Professor, Department of Computer Engineering, Marathwada Mitra Mandal's College of Engineering, Pune, India Affiliated to Savitribai Phule Pune University, Pune, India

[2]Assistant Professor, Department of Electronics and Telecommunication Engineering, Marathwada Mitra Mandal's College of Engineering, Pune, India Affiliated to Savitribai Phule Pune University, Pune, India

[3]Assistant Professor, Bharati Vidyapeeth's College of Engineering, Lavale, Pune

[4]HOD, Department of Computer Engineering, Bharati Vidyapeeth's College of Engineering Lavale Pune

Abstract: *This paper means to foster an AI and profound learning-based constant system for distinguishing and perceiving human countenances in shut circuit TV (CCTV) pictures. The conventional CCTV framework needs a human for all day, every day observing, which is expensive and lacking. The programmed acknowledgment arrangement of countenances in CCTV pictures with least human mediation and decreased cost can help numerous associations, like policing, the suspects, missing endlessly individuals entering a confined domain. Nonetheless, picture based acknowledgment has many issues, like scaling, turn, jumbled foundations, and variety in light force. This paper plans to foster a CCTV picture based human face acknowledgment framework involving various methods for include extraction and face acknowledgment. The proposed framework incorporates picture obtaining from CCTV, picture preprocessing, face discovery, limitation, extraction from the procured pictures, and acknowledgment. We utilize two element extraction calculations, head part examination (PCA) and convolutional brain organization (CNN). We use and look at the exhibition of the calculations K-closest neighbor (KNN), choice tree, arbitrary woods, and CNN. The acknowledgment is finished by applying these strategies to the dataset with more than 40K procured constant pictures at various settings like light level, pivot, and scaling for reenactment and execution assessment. At long last, we perceived faces with a base figuring time and a precision of over 90.8%.*

Keywords: Intelligent, Face, Detection, Machine Leaning, K-closest neighbor (KNN), CCTV picture

1. Introduction

The present associations face huge security challenges; they need a few uniquely prepared work force to accomplish the expected security. Notwithstanding, people commit errors that influence security. Shut circuit TV (CCTV) is right now utilized for different purposes in day to day existence. The advancement of video reconnaissance has changed straightforward inactive checking into a coordinated insightful control framework. Face recognition and its new applications for secure access control, monetary exchanges, and so on. Biometric frameworks (faces, palms, and fingerprints) have as of late acquired new significance. With progresses in microelectronics and vision frameworks, biometrics has become monetarily reasonable. Facial acknowledgment is a fundamental piece of biometrics.

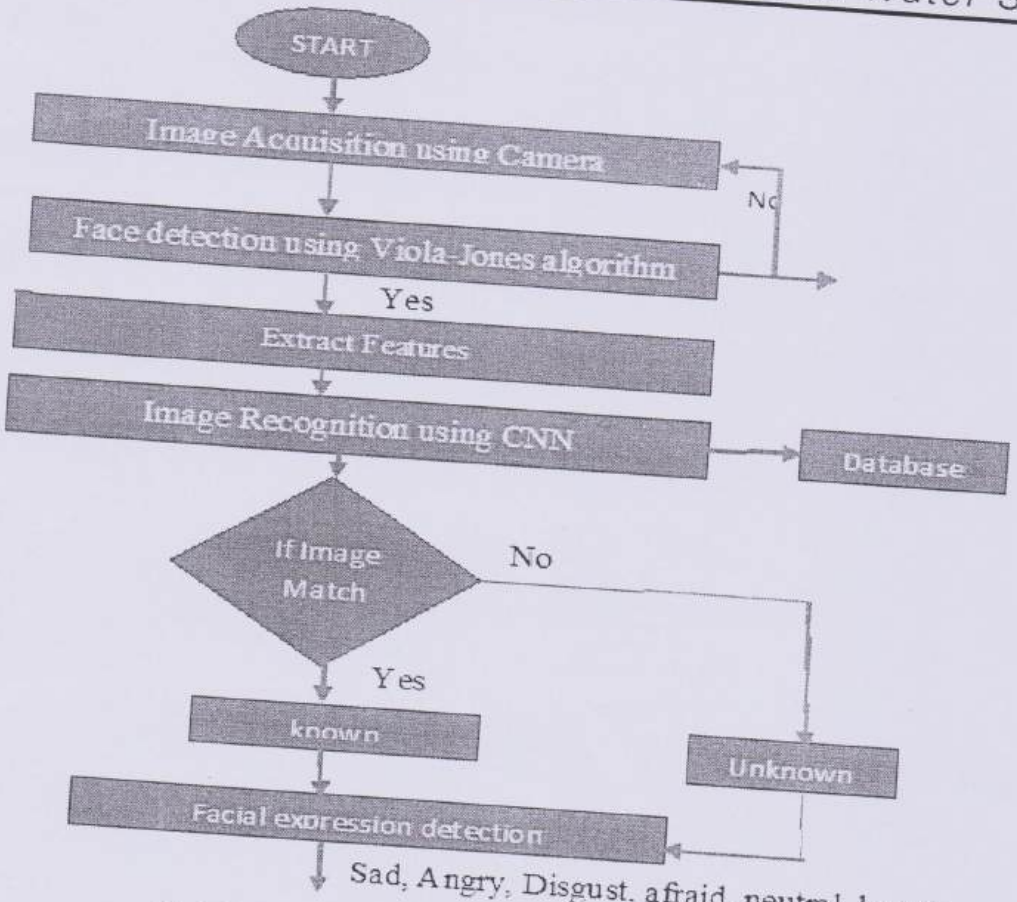


Fig.1: Intelligent Face Detection using Machine Leaning Flow

In biometrics, human essentials are planned to current information. The facial highlights are pulled out and carried out utilizing an effective calculation, and a few varieties are made to further develop the current calculation model. Face acknowledgment from the PC can be applied to various applied applications, including wrongdoing ID, security frameworks, and validation. A facial acknowledgment framework normally includes steps of face discovery where the essence of the information picture is distinguished, and afterward the picture interaction cleans the face picture for simple acknowledgment.

Geometric Methods for Face Detection

In the beginning phases of PC vision, analysts investigated numerous calculations that removed the picture qualities and used mathematical prerequisites to grasp the arrangements, everything being equal. This was somewhat because of extremely restricted computational assets. The decrease of data from the extraction of usefulness has made PC vision conceivable in the primary PCs [6, 7].

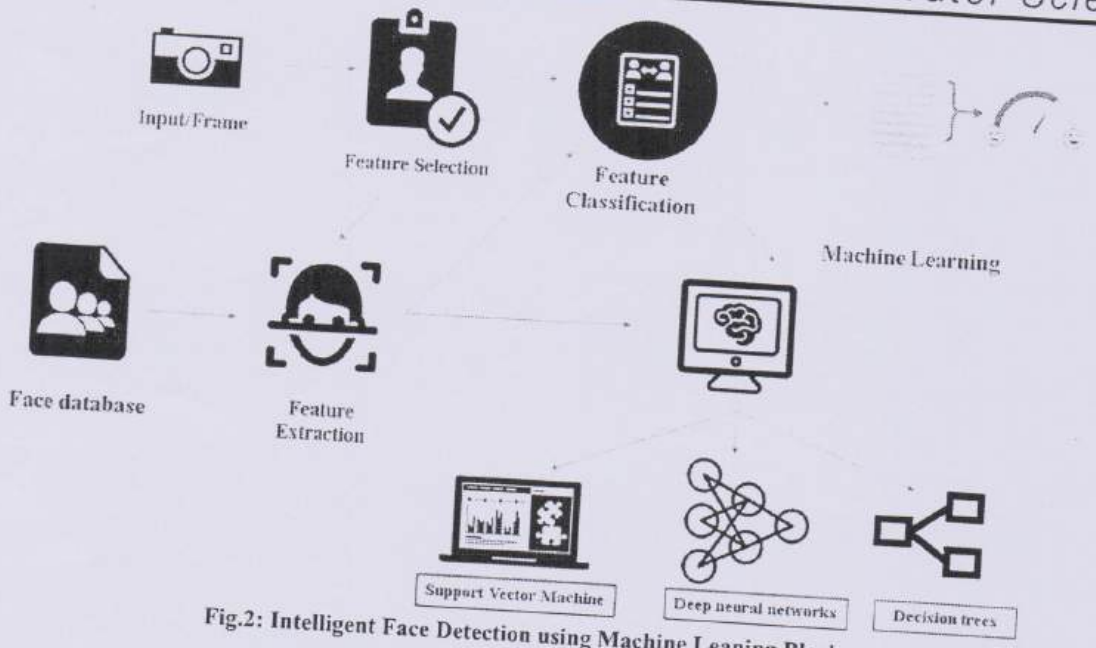


Fig.2: Intelligent Face Detection using Machine Leaning Block

Simple Templates

In the event that you are utilizing a skin-based strategy and one more skin tone is tracked down in the picture (like arms and hands), these calculations show misleading outcomes. Numerous specialists attempted to conquer this by utilizing basic models to incorporate outcomes from the variety matching of skin. These models have differed from certain ovals connected with the picture of the edge of the entry to the relationship models for the areas of skin tone and skin tone (like lips, hands, or eyes). In any case, these methods can upgrade the power of locators by variety, however with additionally the improvement of speed.

Face Recognition algorithms

Face acknowledgment is a strategy that has now achieved thought in AI and man-made brainpower. It assumes a fundamental part in numerous government backed retirement applications. There are many examinations and practices currently under research that can tackle the issue of face acknowledgment. Vivek and Guddeti [9] proposed joining feline multitude streamlining (CSO), molecule swarm advancement (PSO), and hereditary calculation (GA). This mixture strategy has enlivened numerous others to also work. Ali et al. consolidated SVM, higher-request ghostly (HOS), and irregular change (RT)

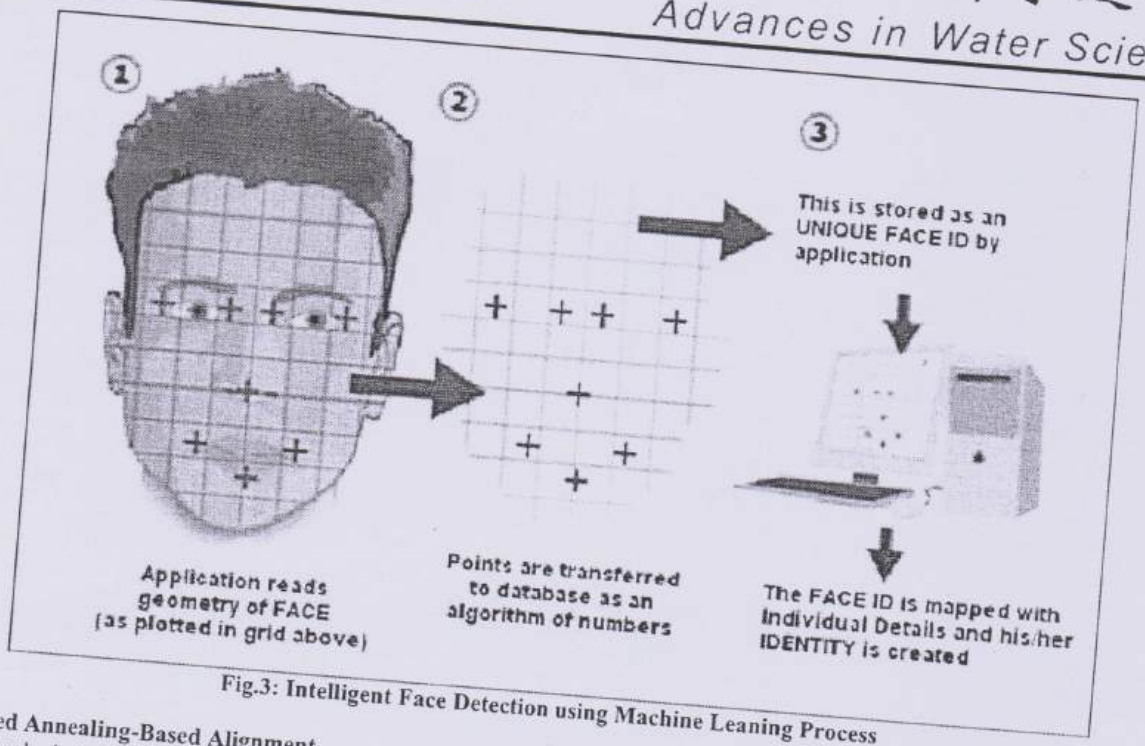


Fig.3: Intelligent Face Detection using Machine Leaning Process

Simulated Annealing-Based Alignment

It is a calculation in light of a stochastic cycle utilized for nearby examination [13]. The distinction between slope climbing and reenacted strengthening is that it can register a surprisingly more dreadful arrangement than the ongoing one in the cycle interaction. As reproduced toughening isn't limited by nearby minima, all things considered, you will track down an answer. Six boundaries are expected for reproduced tempering (in which three for each interpretation likewise the pivot referring to a 3D direction framework) which is utilized to characterize change grid which is utilized for an arrangement between two 3D countenances. This approach adjusts pictures of the face in three stages: (1) arrangement in beginning level, (2) arrangement in an estimated level, and (3) arrangement in the last level [14]. At first, the focal point of the two-sided mass is being adjusted.

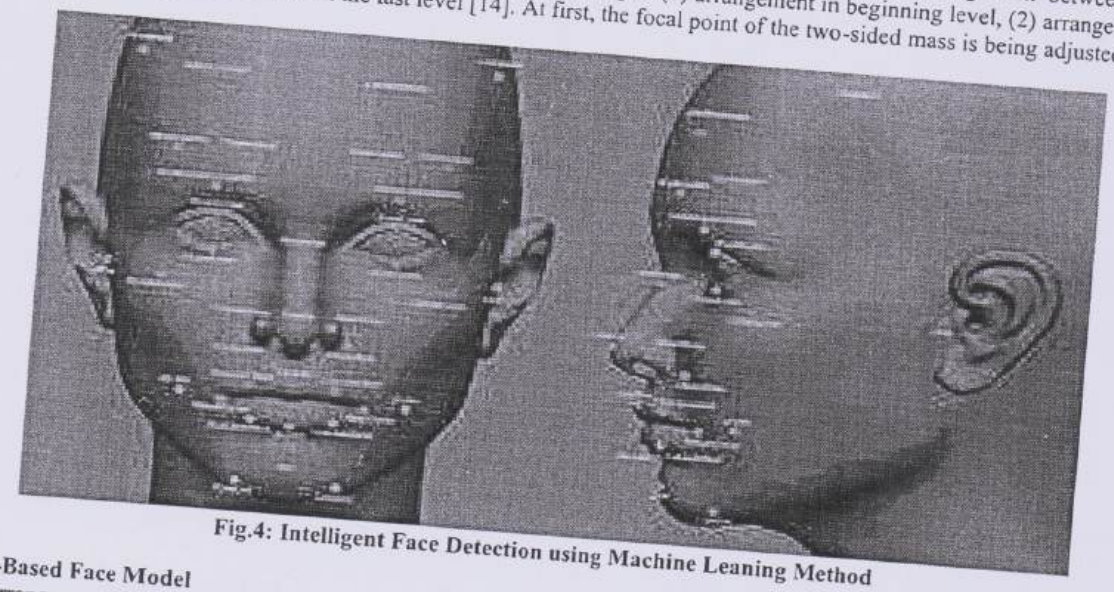


Fig.4: Intelligent Face Detection using Machine Leaning Method

Average-Based Face Model

This arrangement depends on the medium-based face model [15]. The reference, most importantly, focuses are on the face naturally or physically. Thusly, the normal of crucial directions determined, trailed by Procrustes assessment and changed achievement [16], are again interceded to get a face model. While in this strategy, the picture of the test face lines up with the

typical model utilizing an arrangement on the closest iterative point. A striking shortcoming of the arrangement in view of the medium face model is the low accuracy file [17] and part of the spatial material lost during the production of the medium face model.

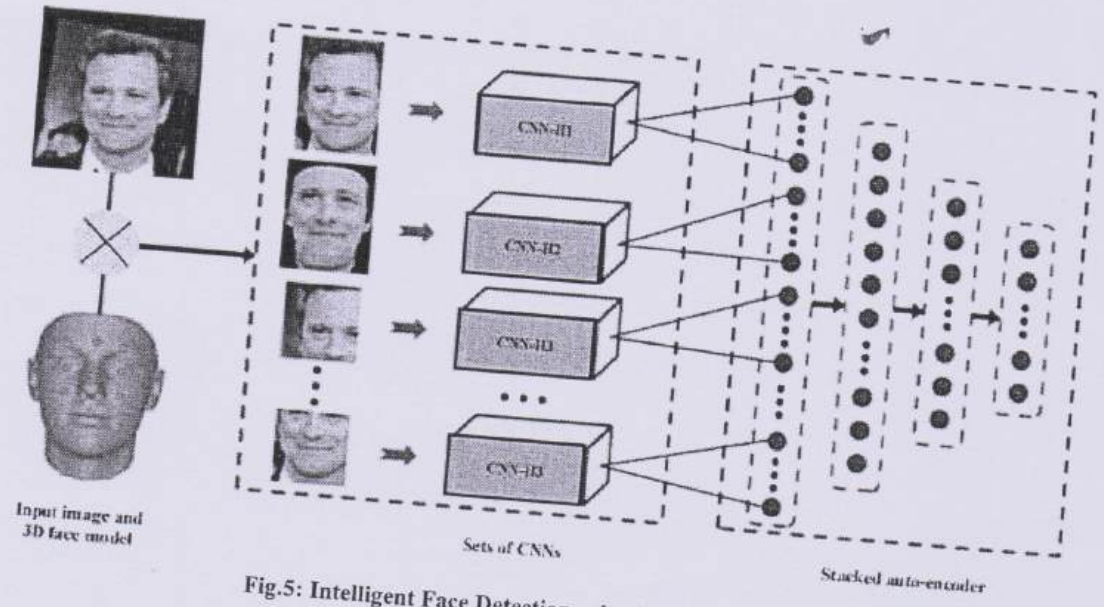


Fig.5: Intelligent Face Detection using Machine Leaning

The most vital phase in face acknowledgment is preprocessing. Pictures taken from a camera or progressively video observation arrangements might experience the ill effects of different debasements during the course of catch, change, transformation, or pressure [18]. For example, hazy, loud, and low-goal pictures influence the face acknowledgment process. Such issues might prompt huge difficulties in the face acknowledgment plan and decline its presentation.

2. Results

As in CNN, we should prepare our dataset. We have prepared our information in 5000 stages and got 95.7% precision with just 30 pictures for testing and 30 for preparing. with half information of preparing and testing. We prepared it in 4000 stages. In certain means, the preparation steps, the exactness expanded, and at certain places, it diminished, however toward the end, we have gotten a greatest precision of 95.67%, precision.

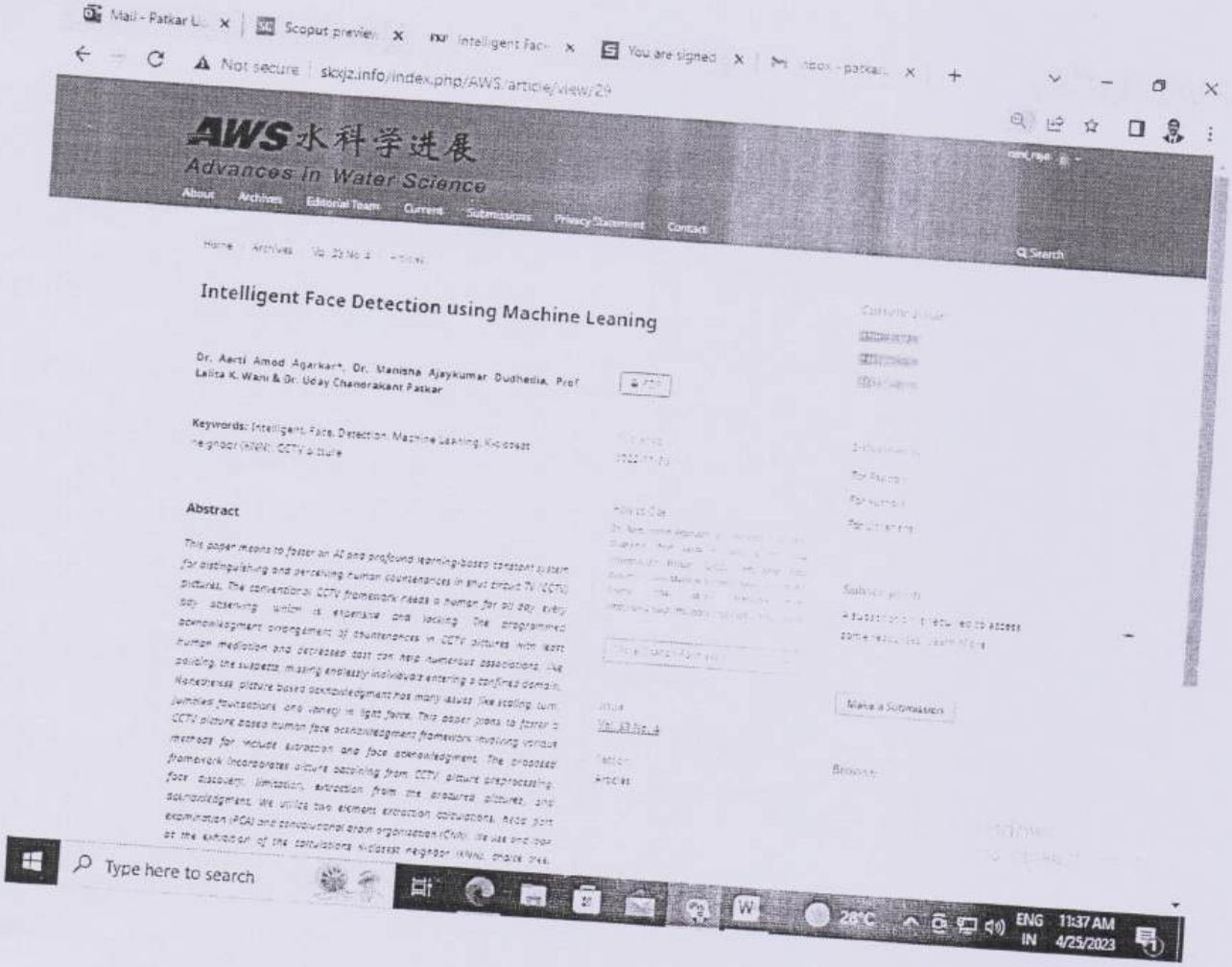
Presently we have gotten 95% precision in this segment, perhaps on the grounds that testing information is significantly less than preparing. Also, we have gotten this precision in 300 stages. Presently we have gotten 97.5% exactness in this segment, which might be on the grounds that testing information is substantially less than preparing information. Furthermore, we have prepared information in 5000 stages.

3. Conclusion

We have fostered a structure for programmed face acknowledgment in view of CCTV pictures utilizing different AI calculations in this work. One of the goals of this work is to gather in excess of 40,000 face pictures and contrast the presentation of calculations with get the most elevated acknowledgment exactness. We have carried out various calculations and have gotten high exactness for CNN. CNN is significantly more solid than PCA with DT, RF, and KNN. KNN is a sluggish calculation, and it really takes a look at every one of the occasions in the dataset for expectation while CNN perceives in next to no time from its model. The other explanation is that we have involved 41,320 pictures for 90 classes for PCA, and for CNN, we have utilized ten classes and 30 pictures for every class, and we got great exactness contrasted with PCA. We gathered in excess of 41,320 pictures. We will improve this framework by making it a total security framework. We perceive a solitary face from the picture; our following stage is to perceive different countenances in a live-real time video.

References

1. A. Deepali, A. Colburn, G. Faigin, L. Shapiro, and B. Mones, "Modeling stylized character expressions via deep learning," in Proceedings of the Asian Conference on Computer Vision, pp. 136–153, Springer, Taipei, Taiwan, November 2021.
2. S. T. Saste and S. M. Jagdale, "Emotion recognition from speech using MFCC and DWT for security system," in Proceedings of the International conference of Electronics, Communication and Aerospace Technology (ICECA), vol. 1, pp. 701–704, IEEE, Coimbatore, India, April 2020.
3. Recognition in human-computer interaction," IEEE Signal Processing Magazine, vol. 18, no. 1, pp. 32–80, 2021.
4. J. Edwards, H. J. Jackson, and P. E. Pattison, "Emotion recognition via facial expression and affective prosody in schizophrenia," Clinical Psychology Review, vol. 22, no. 6, pp. 789–832, 2012.
5. S. Umer, B. Chandra Dhara, and B. Chanda, "Face recognition using fusion of feature learning techniques," Measurement, vol. 146, 2019.
6. C. Lin and K.-C. Fan, "Human face detection using geometric triangle relationship," in Proceedings of the 15th International Conference on Pattern Recognition. ICPR-2000, vol. 2, pp. 941–944, IEEE, Barcelona, Spain, September 2000.
7. K. T. Talele and S. Kadam, "Face detection and geometric face normalization," in Proceedings of the TENCON 2009-2009 IEEE Region 10 Conference, pp. 1–6, IEEE, Singapore, January 2009.
8. J. Miao, W. Gao, Y. Chen, and J. Lu, "Gravity-center template based human face feature detection," in Proceedings of the Advances in Multimodal Interfaces - ICMI 2000, pp. 207–214, Springer, Beijing, China, October 2021.
9. T. V. Vivek and G. R. M. Reddy, "A hybrid bioinspired algorithm for facial emotion recognition using CSO-GA-PSO-SVM," in Proceedings of the 5th Int. Conf. Commun. Syst. Netw. Technol, pp. 472–477, Gwalior, India, April 2015.
10. H. Ali, M. Hariharan, S. Yaacob, and A. H. Adom, "Facial emotion recognition based on higher-order spectra using support vector machines," Journal of Medical Imaging and Health Informatics, vol. 5, no. 6, pp. 1272–1277, 2015.
11. P. J. Besl and N. D. McKay, "A method for registration of 3-d shapes," IEEE Transactions on Pattern Analysis and Machine Intelligence, vol. 14, no. 2, pp. 239–256, 1992.
12. X. Wang, Q. Ruan, Y. Jin, and G. An, "Three-dimensional face recognition under expression variation," EURASIP Journal on Image and Video Processing, vol. 6, pp. 281–289, 2014.
13. C. C. Queirolo, L. Silva, O. R. P. Bellon, and M. P. Segundo, "3d face recognition using simulated annealing and the surface interpenetration measure," IEEE Transactions on Pattern Analysis and Machine Intelligence, vol. 32, no. 2, pp. 206–219, 2021.


Not secure | skkjz.info/index.php/AWS/article/view/29
AWS水科学进展
Advances in Water Science
About Archives Editorial Team Current Submissions Privacy Statement Contact
Search
Intelligent Face Detection using Machine Leaning
Dr. Aarti Amod Agarkar, Dr. Manisha Ajaykumar Dudhedia, Prof Lalita K. Wani & Dr. Uday Chandrakant Patkar
Keywords: Intelligent, Face, Detection, Machine, Learning, K-closest neighbor (KNN), CCTV, picture
Abstract
This paper means to foster an AI and profound learning based constant system for distinguishing and perceiving human countenances in shut circuit TV (CCTV) pictures. The conventional CCTV framework needs a human for all day, every day observing, which is expensive and lacking. The programmed acknowledgment arrangement of countenances in CCTV pictures with next human mediation and decreased cost can help numerous associations, like policing, the subjects, missing excitedly individuals entering a confined domain. Nonetheless, picture based acknowledgment has many issues like scaling, turn, jumbles, foundations, and vibes in light force. This paper plans to foster a CCTV picture based human face acknowledgment framework involving various methods for include extraction and face acknowledgment. The proposed framework incorporates picture sampling from CCTV, picture preprocessing, face discovery, limitation, extraction from the procured pictures, and acknowledgment. We utilize two element extraction calculations, head part examination (PCA) and convolutional brain organization (CNN). We use and look at the execution of the convolutional K-closest neighbor (KNN) choice tree
Make a Submission
Type here to search
28°C
ENG IN 11:37 AM 4/25/2023

Source details

Feedback > Compare sources >

Shuikexue Jinzhan/Advances in Water Science

Scopus coverage years: from 1998 to Present

Publisher: China Water Power Press

ISSN: 1001-6791

Subject area: Earth and Planetary Sciences: General Earth and Planetary Sciences

Source type: Journal

Save to source list Source Homepage

CiteScore 2022
3.1

SJR 2022
0.413

SNIP 2022
0.681

CiteScore | CiteScore rank & trend | Scopus content coverage

Improved CiteScore methodology

CiteScore 2022 counts the citations received in 2019-2022 to articles, reviews, conference papers, book chapters and data papers published in 2019-2022, and divides this by the number of publications published in 2019-2022. Learn more >

CiteScore 2022

3.1 = 963 Citations 2019 - 2022 / 315 Documents 2019 - 2022

Calculated on 05 May, 2023

CiteScoreTracker 2023

3.9 = 1,273 Citations to date / 326 Documents to date

Last updated on 05 December, 2023 • Updated monthly

CiteScore rank 2022

Category	Rank	Percentile
Earth and Planetary Sciences └ General Earth and Planetary Sciences	#73/192	62nd

View CiteScore methodology > CiteScore FAQ > Add CiteScore to your site

Introduction to MERN Stack & Comparison with Previous Technologies

[1]Prof. Yogesh Kadam, [2]Akhil Goplani, [3]Shubit Mattoo, [4]Shashank Kumar Gupta, [5]Darshan Amrutkar, [6]Prof. Dr. Jyoti Dhanke

[1 to 5]Department of Computer Engineering, Bharati Vidyapeeth's College of Engineering, Lavale Pune, Maharashtra, India
Email: yogesh.kadam@bharatividyapeeth.edu
[6]Department of Engineering Science (Mathematics), Bharati Vidyapeeth's College of Engineering, Lavale Pune, Maharashtra, India

doi: 10.48047/ecb/2023.12.si4.1300

Abstract— The MERN stack is a popular technology stack used for developing web applications. It consists of MongoDB, Express.js, React, and Node.js. This paper discusses why the MERN stack is widely used and its advantages over previous technologies such as HTML, CSS, SQL, and NoSQL. The paper also provides a brief overview of the MERN stack components, their functionalities, and their role in developing web applications.

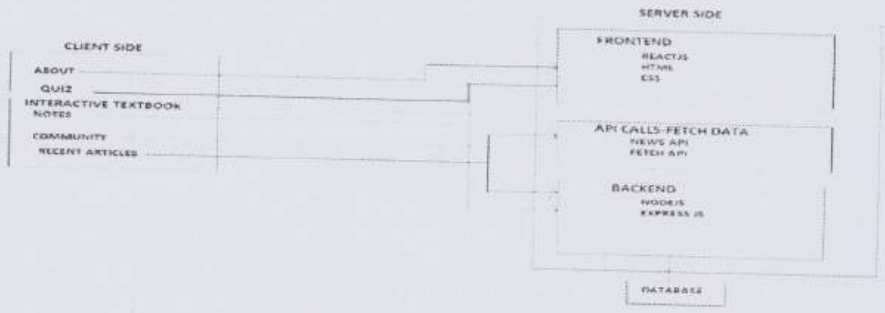
Keywords-MERN stack, MongoDB, Express.js, React, Node.js, web applications, HTML, CSS, SQL, NoSQL, front-end, back-end.

I. INTRODUCTION

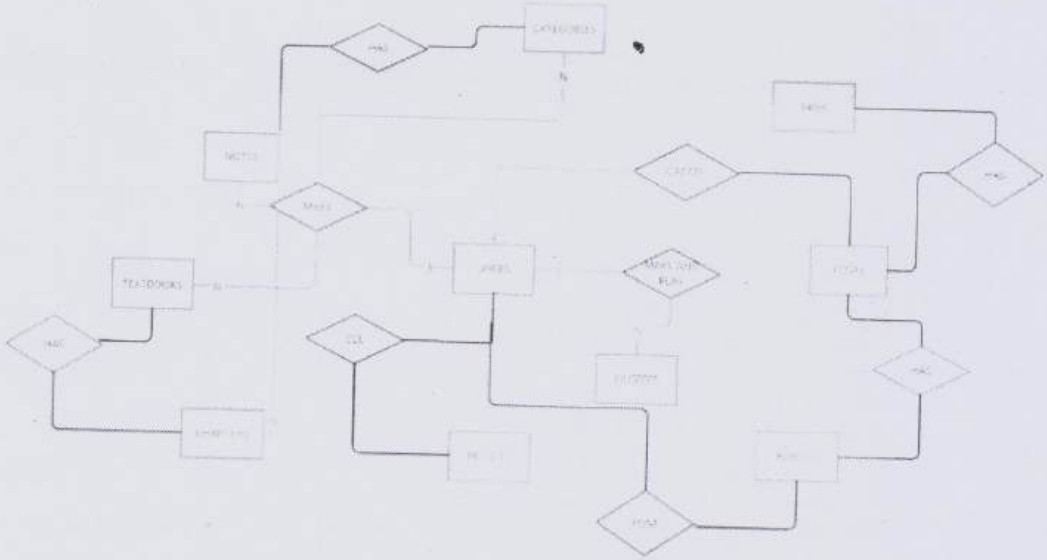
In recent years, the use of the MERN stack has become increasingly popular in web development. This technology stack consists of MongoDB, Express.js, React, and Node.js. Each component of the MERN stack has a specific function, and together they provide a full-stack development environment that allows developers to create web applications efficiently. In this paper, we will discuss why the MERN stack is widely used and its advantages over previous technologies such as HTML, CSS, SQL, and NoSQL. MongoDB is a popular NoSQL document-oriented database that stores data in flexible JSON-like documents, making it easy to scale and maintain.

Express.js is a lightweight and flexible Node.js web application framework that provides an easy-to-use API for building web applications. React is a JavaScript library for building user interfaces that allows developers to create reusable components and manage complex application states. Node.js is a powerful and efficient JavaScript runtime environment that allows developers to build scalable and high-performance server-side applications. Together, these technologies provide a full-stack JavaScript solution for building modern web applications. The MERN stack allows developers to leverage the power of JavaScript on both the client-side and server-side, providing a seamless and unified development experience. It is highly flexible and customizable, making it suitable for a wide range of applications, from small-scale prototypes to large-scale enterprise-level systems.

II. ARCHITECTURE



III. ER DIAGRAM



IV. WORKING

So here our project is to create an online system that provides interactive textbooks, notes and quizzes. Here in this project, we use MERN stack which stands for MongoDB, Express JS, React and Node JS. MongoDB which is a database used for storing the data of the user. Here, we have created the four schemas which are notes, interactive textbooks, login details and quizzes.

We have used MONGO DB because in SQL we can store only the data which is structured but in MongoDB we can store unstructured data as well. In our notes section, we can put various types of data like images, text, bold text which is unstructured that's why we have used MongoDB. Express JS is used for authentication and error handling. Errors like if for some reason the web page is not visible then which error have to show, the Express JS will handle this. Express js is used for making server-side applications with Node JS. Here we use the port 2000.
React JS which is used for making single web page applications. We make various components like ABOUT US , NOTES, WIDGETS, and many more. REACT uses virtual DOM so whenever is there any requirement to change the content that component will change so there is no need to refresh the page. We use memo to prevent the unnecessary rendering of the component. Suppose, there is a component named as useColour but suppose I have not used this component but this component renders every time so this will ultimately effects to cost and efficiency so to overcome this problem we use memo.

We use various types of hooks like useState, useContext, useRef, useEffect. useState is used for tracking the state of the properties. UseState will take two properties one is the variable and the other one is the function that updates the variable. UseEffect will be same as memo which is used to prevent the unnecessary re-rendering of the applications. UseEffect takes the two arguments first is function and second one is dependency. Dependency is like a array that decides how much times we have to render the application. Use context hook used together with use State to manage the state globally. In backend we have used hackerNEWS API, which is used to fetch the news with the help of the API. We use libraries like axioms and get method in which we pass the URL of that API. The data that is returned by get method in JSON format so we have to parse the JSON to extract the relevant data. To run the JavaScript on server we use node JS. JavaScript is synchronous single threaded language so to make the JavaScript asynchronous and multithreaded language we use node JS. Synchronous means one line will be executed at a time and execution takes place from top to bottom line by line.

Asynchronous means multiple functions can execute simultaneously like setTimeOut Function which takes the function and time as the argument so this the example of asynchronous JavaScript.

We have also import the functionality of like if the user wants to read their own articles means their favorite topic articles so they can search it in search bar and the screen will displays all the articles related to that topic. We have the quiz section in which we have to provide the question with four options and if there is any question like true false type then fill another two options with 0. After that the code will generate and we need to paste that code to start the quiz.

V. MERN STACK COMPONENTS

MongoDB is a NoSQL database that stores data in a document-oriented format. Express.js is a back-end web application framework that provides a set of tools for creating RESTful APIs. React is a front-end library that enables developers to create dynamic user interfaces. Node.js is a JavaScript runtime environment that allows developers to write server-side code in JavaScript.

Express.js is a popular web framework for Node.js that simplifies the process of building web applications. Here are some important points to keep in mind when working with Express.js:

1. Routing: Express.js provides an easy-to-use API for defining routes that respond to specific HTTP requests. This allows you to handle requests and return responses based on the requested URL, HTTP method, and other factors.

2. Middleware: Express.js allows you to use middleware functions to modify the request and response objects before they are processed by the route handler. This can be used for tasks such as authentication, logging, and error handling.

3. Template engines: Express.js supports a variety of template engines that allow you to render dynamic HTML pages based on data from the server. Some popular template engines supported by Express.js include EJS, Handlebars, and Pug.

4. Error handling: Express.js provides a built-in error handling mechanism that allows you to handle errors that occur during request processing. You can define error-handling middleware that will be called when an error occurs, allowing you to log the error, send an error response to the client, or take other actions.

5. Static files: Express.js provides a built-in middleware function for serving static files, such as HTML, CSS, and JavaScript files. This allows you to serve client-side assets directly from the server, without having to use a separate file server.

6. Security: Express.js provides a number of security features out of the box, such as CSRF protection, XSS protection, and content security policies. It also supports a variety of authentication and authorization strategies, such as session-based authentication, JSON Web Tokens (JWT), and OAuth.

VI. Advantages of the MERN Stack

1. One of the significant advantages of using the MERN stack is that it allows developers to use a single language, JavaScript, for both front-end and back-end development. This makes the development process more efficient and reduces the learning curve for developers who are already familiar with JavaScript.
2. Another advantage of the MERN stack is that it is based on open-source technologies, making it a cost-effective option for businesses and startups. The MERN stack also provides a flexible and scalable architecture that can be customized to meet the specific needs of Full-stack JavaScript.
3. The MERN stack uses JavaScript as the primary language for both server-side and client-side development, making it easy to build a consistent and seamless web application. This allows developers to use a single language and skillset to build an entire application, reducing the time and effort required for development.

4. The MERN stack is designed for rapid development, and it offers a wide range of tools and libraries that can speed up the development process. This allows developers to quickly build and deploy applications, reducing the time to market and allowing for faster iteration and feedback.

VII. COMPARISON OF HTML/CSS WITH REACT

React and HTML/CSS are both used for creating web applications, but they differ in several ways. One of the key differences is in their architecture. React is a component-based framework that allows developers to create reusable UI components, while HTML/CSS are markup and styling languages that define the structure and visual presentation of web pages, but do not provide a component-based architecture. Another difference is in the way they handle updates to the user interface. React uses a virtual DOM to efficiently update the UI, while HTML/CSS require a full-page refresh when changes are made. This makes React faster and more efficient, especially for complex web applications with many dynamic elements. React also has a steeper learning curve compared to HTML/CSS, as it requires knowledge of JavaScript and its syntax, as well as the React framework and its associated tools. However, React offers a streamlined development process by providing features such as hot module replacement, which allows developers to see changes in real-time without refreshing the page. It also has a large and active community that offers support, tutorials, and third-party libraries to enhance development.

In summary, React offers a component-based architecture, virtual DOM, efficient performance, and streamlined development process, while HTML/CSS provide markup and styling languages for defining the structure and presentation of web pages. The choice between React and HTML/CSS depends on the specific requirements of the application and the skill set of the development team.

VIII. COMPARISON OF SQL WITH MONGODB AND NOSQL

SQL and NoSQL are two different types of databases with different data models and storage structures. MongoDB is a popular NoSQL database. SQL databases use a structured data model, where data is organized in tables with rows and columns, and relationships are established between tables using foreign keys. This makes it easy to query data using SQL, a standardized language used to manage relational databases. On the other hand, NoSQL databases use a flexible data model, where data is stored in a variety of ways, such as key-value pairs, documents, or graphs. This allows for faster and more flexible queries, especially for large datasets with complex or changing structures.

When comparing SQL and NoSQL databases, some of the main differences include:

1. Data model: SQL databases have a structured data model with tables, while NoSQL databases have a flexible data model that can store data in various formats.
2. Scalability: NoSQL databases are typically more scalable than SQL databases, as they can be easily distributed across multiple servers.
3. Query language: SQL databases use SQL, a standardized language for querying relational databases, while NoSQL databases use a variety of query languages depending on the data model.
4. Transactions: SQL databases support ACID transactions, which ensure data consistency, while NoSQL databases typically sacrifice some level of consistency in favor of speed and scalability.

IX. WHEN COMPARING MONGODB WITH OTHER NOSQL DATABASES, SOME OF THE MAIN DIFFERENCE INCLUDES:

1. Data model: MongoDB stores data in BSON documents, which are similar to JSON documents, while other NoSQL databases may use different formats such as key-value pairs or graphs.

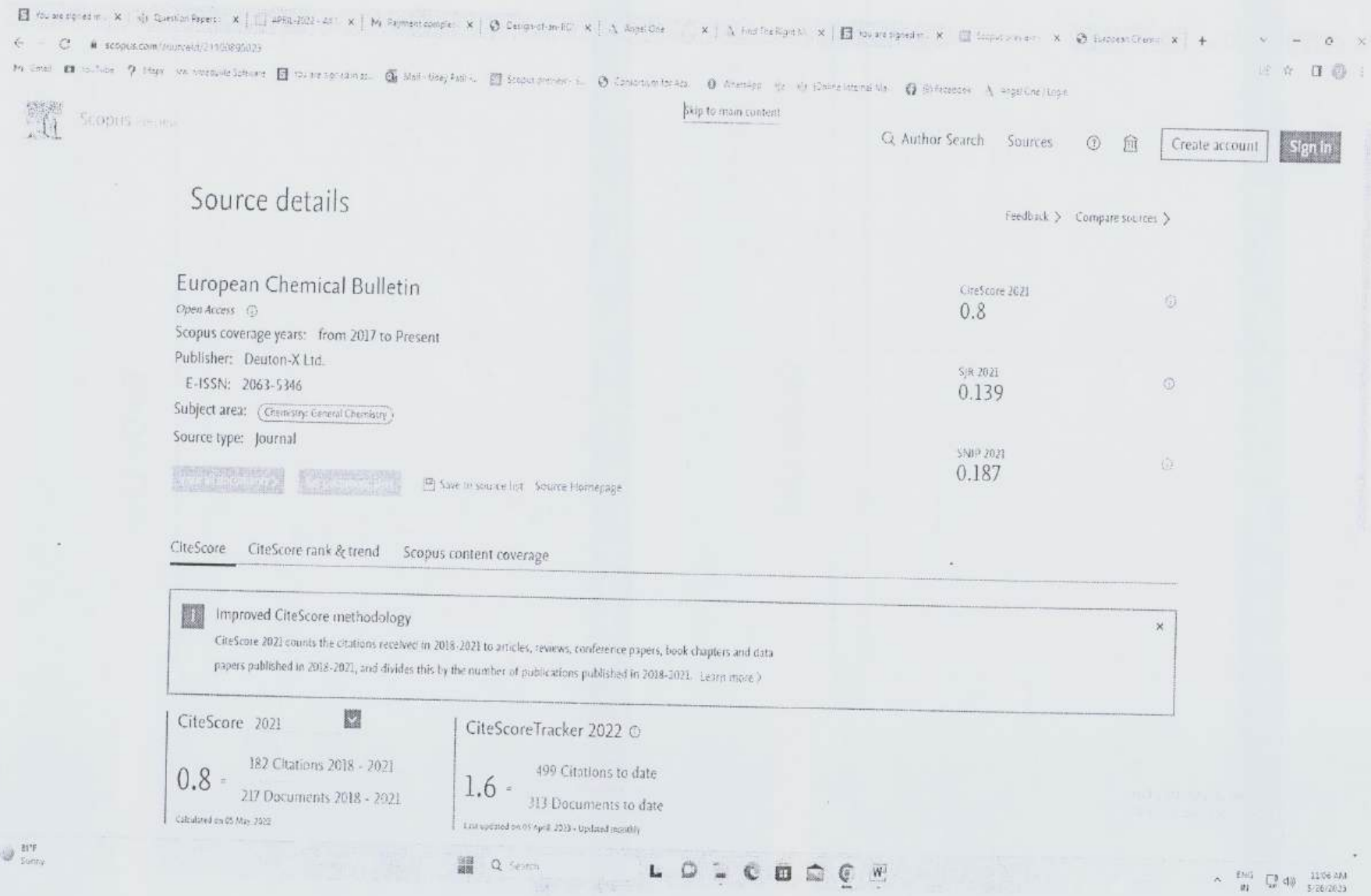
2. Query language: MongoDB uses a query language called MongoDB Query Language (MQL), which is similar to SQL in some ways, while other NoSQL databases may use different query languages.

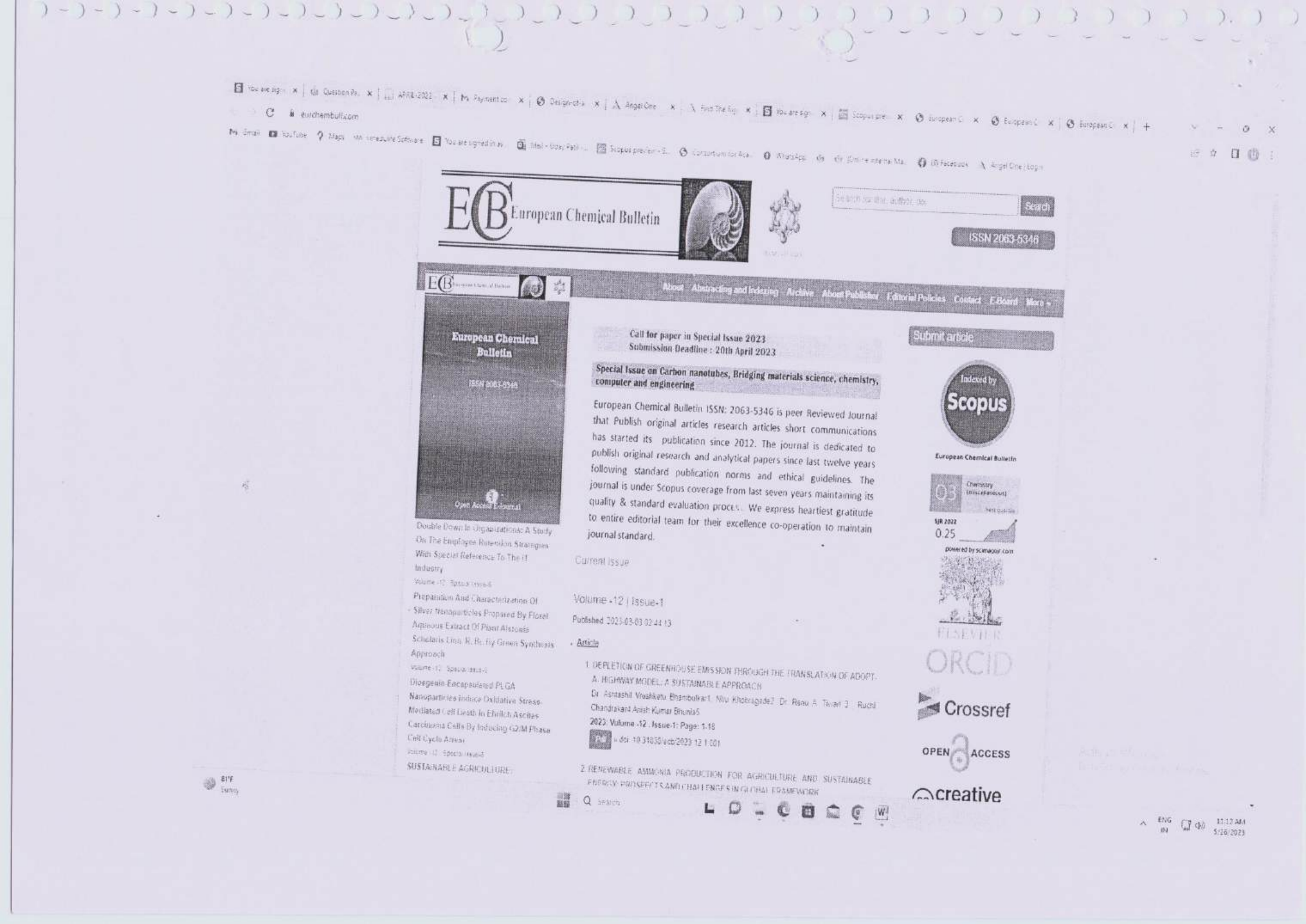
3. Indexing: MongoDB has a powerful indexing system that allows for fast queries, including geospatial queries, while other NoSQL databases may have more limited indexing options.

4. Schema flexibility: MongoDB allows for flexible schemas, which can be useful for storing unstructured or semi-structured data, while other NoSQL databases may have more rigid schemas.

X. REFERENCES

1. https://docs.mongodb.com/
2. https://expressjs.com/
3. https://www.freecodecamp.org/news/build-a-react-graphql-app-with-mongodb/
4. https://medium.com/crowdbotics/building-a-full-stack-mern-application-7a67039f2796
5. https://github.com/kevinfodness/mern-stack-boilerplate
6. Yogesh Baiskar, Priyas Paulzagade, Krutik Koradia, Pramod Ingole, Dhiraj Shirbhate, "MERN: A Full-Stack Development", International Journal for Research in Applied Science & Engineering Technology (IJRASET) ISSN: 2321-9653; IC Value: 45.98; SJ Impact Factor: 7.538 Volume 10 Issue I Jan 2022.
7. Sumangala A. Bafna, Pratiksha D. Dutonde, Shivani S. Mamidwar, Monali S. Korvate, Prof. Dhiraj Shirbhare, "Review on Study and Usage of MERN Stack for Web Development" International Journal for Research in Applied Science & Engineering Technology (IJRASET) ISSN: 2321-9653; IC Value: 45.98; SJ Impact Factor: 7.538 Volume 10 Issue II Feb 2022.
8. Dr. Santosh Kumar Shukla, Shivam Dubey, Tarun Rastogi, Nikita Srivastava, "Application using MERN Stack" International Journal for Modern Trends in Science and Technology, 8(06): 102-105, 2022.
9. Sourabh Mahadev Malewade, Archana Ekbote, "Performance Optimization using MERN stack on Web Application", International Journal of Engineering Research & Technology (IJERT) Vol. 10 Issue 06, June-2021.
10. Dr. Poornima Mehta, Harsh Kumar, Amit Sharma, "STUDY POINT WEBSITE USING MERN STACK", International Research Journal of Modernization in Engineering Technology and Science Volume:05/Issue:03/March-2023.


Skip to main content
Author Search
Sources
Create account
Sign in
Source details
Feedback
Compare sources
European Chemical Bulletin
Open Access
Scopus coverage years: from 2017 to Present
Publisher: Deuton-X Ltd.
E-ISSN: 2063-5346
Subject area: Chemistry: General Chemistry
Source type: Journal
Save to source list
Source Homepage
CiteScore 2021
0.8
SJR 2021
0.139
SNIP 2021
0.187
CiteScore
CiteScore rank & trend
Scopus content coverage
Improved CiteScore methodology
CiteScore 2021 counts the citations received in 2018-2021 to articles, reviews, conference papers, book chapters and data papers published in 2018-2021, and divides this by the number of publications published in 2018-2021. Learn more
CiteScore 2021
0.8 = 182 Citations 2018 - 2021 / 217 Documents 2018 - 2021
Calculated on 05 May 2022
CiteScoreTracker 2022
1.6 = 499 Citations to date / 313 Documents to date
Last updated on 05 April 2023 • Updated monthly



European Chemical Bulletin

ISSN 2063-5346

Search

About | Abstracting and Indexing | Archive | About Publisher | Editorial Policies | Contact | E-Board | More +

Submit article

European Chemical Bulletin

ISSN 2063-5346

Open Access E-Journal

Call for paper in Special Issue 2023
Submission Deadline : 20th April 2023

Special Issue on Carbon nanotubes, Bridging materials science, chemistry, computer and engineering

European Chemical Bulletin ISSN: 2063-5346 is peer Reviewed Journal that Publish original articles research articles short communications has started its publication since 2012. The journal is dedicated to publish original research and analytical papers since last twelve years following standard publication norms and ethical guidelines. The journal is under Scopus coverage from last seven years maintaining its quality & standard evaluation proces.. We express heartiest gratitude to entire editorial team for their excellence co-operation to maintain journal standard.

Current Issue

Volume -12 | Issue-1

Published 2023-03-03 02:44:13

- Article

1. DEPLETION OF GREENHOUSE EMISSION THROUGH THE TRANSLATION OF ADOPT-A- HIGHWAY MODEL: A SUSTAINABLE APPROACH
Dr. Ashtashil Vrushketu Bhambulkar1, Nitu Khobragade2, Dr. Rahul A. Tayade 3, Ruchi Chandrakant Anish Kumar Bhurila5
2023: Volume -12 , Issue-1: Page: 1-18
doi: 10.31838/ecb/2023.12.1.001

2. RENEWABLE AMMONIA PRODUCTION FOR AGRICULTURE AND SUSTAINABLE ENERGY PROSPECTS AND CHALLENGES IN GLOBAL FRAMEWORK

Double Down In Organizations: A Study On The Employee Retention Strategies With Special Reference To The IT Industry

Preparation And Characterization Of Silver Nanoparticles Prepared By Floral Aqueous Extract Of Plant Alstonia Scholaris Linn. R. Br. By Green Synthesis Approach

Diosgenin-Encapsulated PLGA Nanoparticles Induce Oxidative Stress-Mediated Cell Death In Ehrlich Ascites Carcinoma Cells By Inducing G2/M Phase Cell Cycle Arrest

SUSTAINABLE AGRICULTURE:

Indexed by Scopus

European Chemical Bulletin

Q3 Chemistry (miscellaneous)

SJR 2022 0.25

powered by scimagojr.com

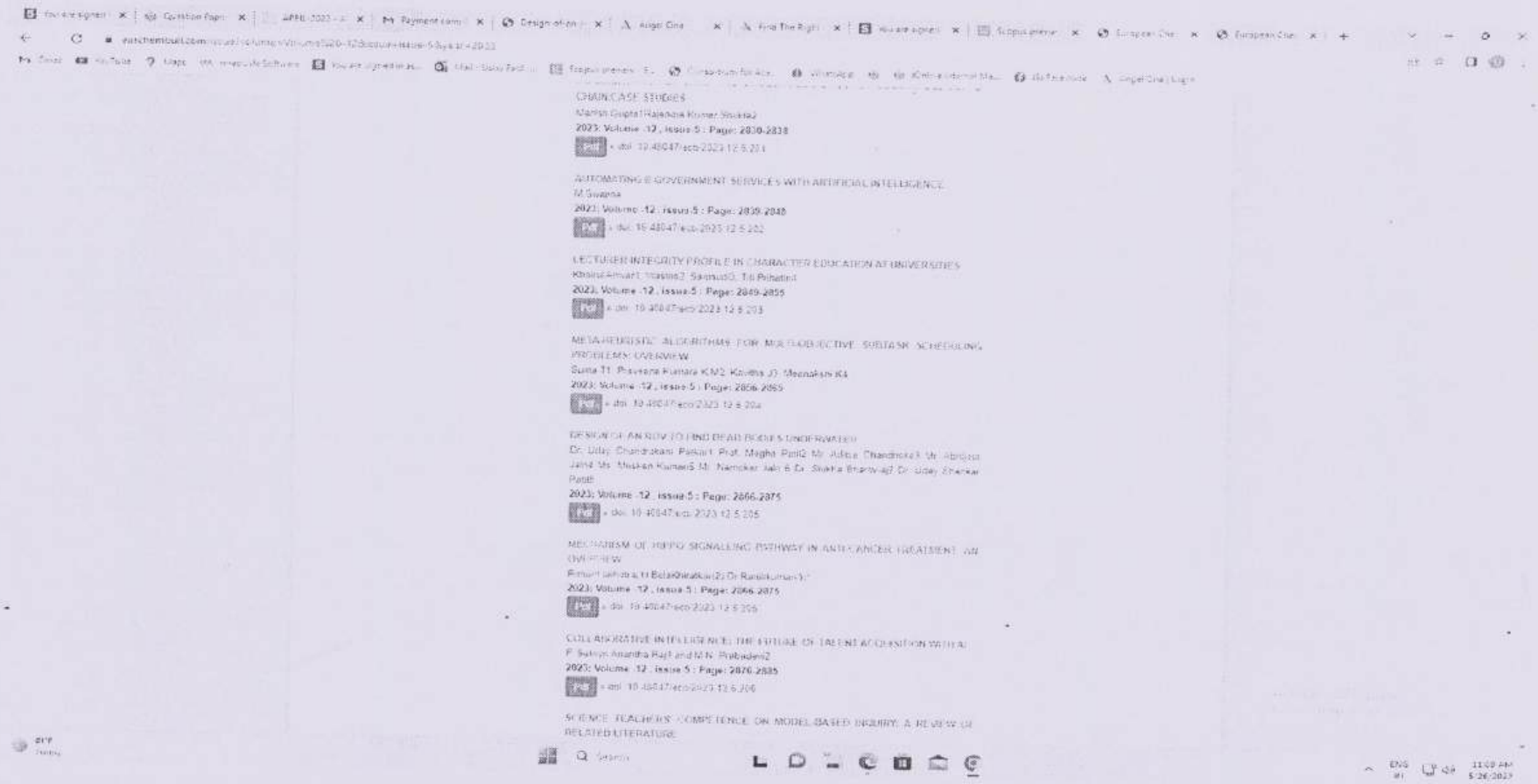
ELSEVIER

ORCID

Crossref

OPEN ACCESS

creative



1. Dr. Uday Chandrakant Patkar1 Prof. Megha Patil2 Mr. Aditya Chandhoke3 Mr. Abhijeet Jain4 Ms. Muskan Kumari5 Mr. Namokar Jain 6 Dr. Shikha Bhardwaj7 Dr. Uday Shankar Patil8
   2023;Volume-12,issue-5:Page:2866-2875
   »doi: 10.48047/ecb/2023.12.5.205

e-ISSN 2320 –7876 www.ijfans.org
Vol.11,S Iss 1, 2022
Research paper
© 2012 IJFANS. All Rights Reserved UGC CARE Listed (Group -I) Journal

Low Power VLSI Intelligent Circuits Design Methodologies

Prof. Lalita K. Wani
Assistant Professor, Bharati Vidyapeeth's College of Engineering,
Lavale, Pune, MH, India.
Lalita.wani@gmail.com

Prof. (Dr.) Reena Singh
MES's, Pillai HOC College of Engineering &Technology,
Rasayani Taluka Panvel, Dist, Navi Mumbai, Maharashtra 410207, India.
dr.rsingh2014@gmail.com

Prof. (Dr.) B.K. Sarkar
MES's, Geh Research, Panvel, Dist, Navi Mumbai, Maharashtra 410207, India.
dr.bksarkar2003@yahoo.in

Abstract:

Low power has arisen as a chief subject in this day and age of hardware ventures. Power dispersal has turned into a significant thought as execution and region for VLSI Chip plan. With contracting innovation lessening power utilization and over all power the board on chip are the vital moves underneath 100nm because of expanded intricacy. For some plans, streamlining of force is significant as timing because of the need to lessen bundle cost and expanded battery duration. For power the board spillage current additionally assumes a significant part in low power VLSI plans. Spillage current is turning into an undeniably significant part of the all out power dispersal of incorporated circuits. This paper portrays about the different procedures, strategies and power the executive's methods for low power circuits and frameworks. Future difficulties that should be met to plans low power superior execution circuits are additionally talked about.

Keywords: Power Dissipation, low power, process nodes, leakage current, power management.

INTRODUCTION

The benefit of using a mix of low-power parts related to low-control plan procedures is more significant now than any other time. Prerequisites for lower power utilization keep on expanding essentially as parts become battery-fueled, more modest and require greater usefulness. In the past the central issues for the VLSI fashioners was region, execution and cost. Power thought was the auxiliary concerned. Presently a day's power is the essential worried because of the surprising development and progress in the field of individualized computing gadgets and remote correspondence framework which request high velocity calculation and complex usefulness with low power utilization. The inspirations for lessening power utilization contrast application to application. In the class of miniature controlled battery worked convenient applications, for example, cells, the objective is to keep the battery

© 2012 IJFANS. All Rights Reserved

lifetime and weight sensible and bundling cost low. For superior execution convenient PCs, for example, PC the objective is to diminish the power scattering of the hardware piece of the framework to a point which is about portion of the complete power dispersal.

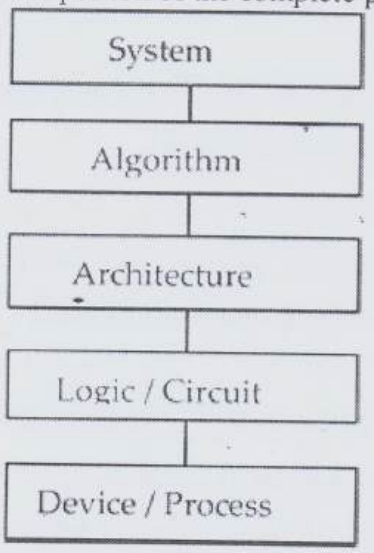


FIG.1: Low Power VLSI Intelligent Circuits Design Methodologies Flow Chart.

At last for the superior exhibition non battery worked framework, for example, workstations the general objective of force minimization is to diminish the framework cost while guaranteeing long haul gadget unwavering quality. For such elite execution frameworks, process innovation has driven capacity to the front to all variables in such plans. At process hubs under 100 nm innovation, power utilization because of spillage has joined exchanging movement as an essential power the board concern.

The upside of using a mix of low-power parts related to low-drive plan strategies is more significant now than any other time in recent memory. Necessities for lower power utilization keep on expanding altogether as parts become battery-controlled, more modest and require greater usefulness. In the past the main issues for the VLSI fashioners was region, execution and cost. Power thought was the optional concerned. Presently a day's power is the essential worried because of the noteworthy development and outcome in the field of individualized computing gadgets and remote correspondence framework which request high velocity calculation and complex usefulness with low power utilization.

© 2012 IJFANS. All Rights Reserved

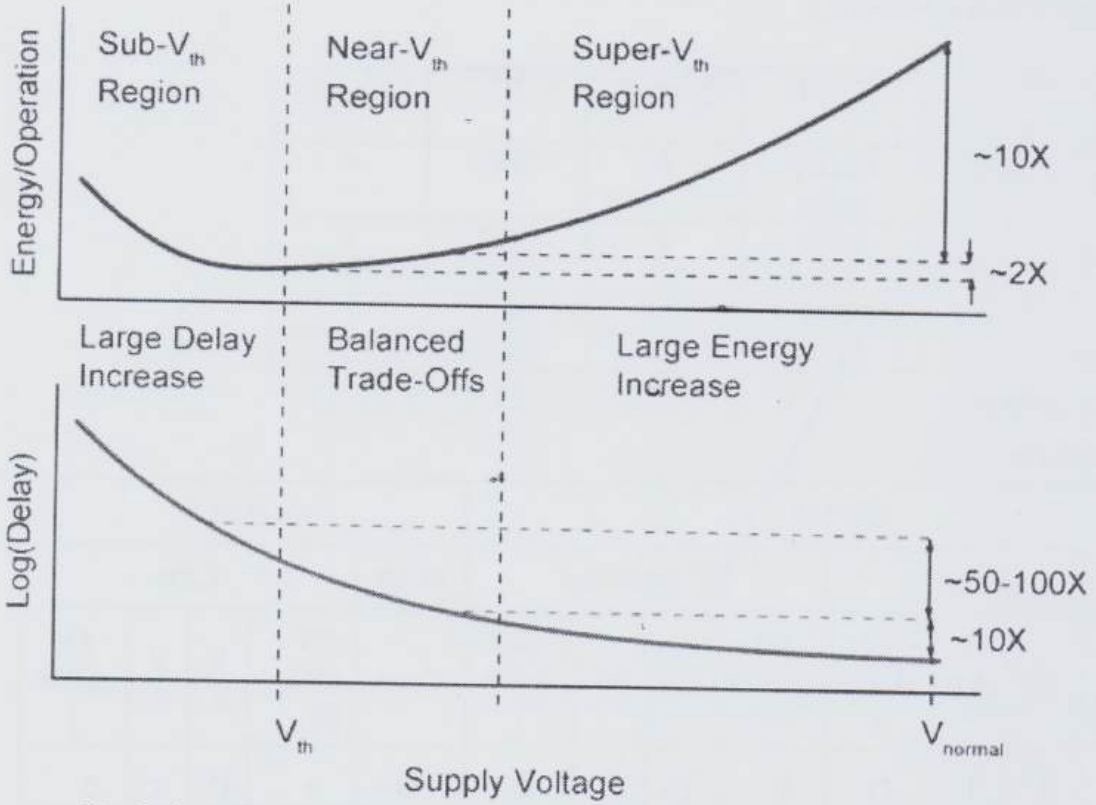


Fig.2: Low Power VLSI Intelligent Circuits Design Methodologies Graph.

The inspirations for diminishing power utilization contrast application to application. In the class of miniature fueled battery worked convenient applications, for example, phones, the objective is to keep the battery lifetime and weight sensible and bundling cost low. For superior execution convenient PCs, for example, PC the objective is to decrease the power dispersal of the hardware part of the framework to a point which is about portion of the complete power scattering. At last for the elite presentation non battery worked framework, for example, workstations the general objective of force minimization is to lessen the framework cost while guaranteeing long haul gadget dependability. For such elite execution frameworks, process innovation has driven capacity to the front to all elements in such plans. At process hubs under 100 nm innovation, power utilization because of spillage has joined exchanging action as an essential power the board concern.

Need for low power plan

Power dissemination is the primary requirement with regards to convey ability. Consequently, dealing with the framework's complete power consumption is fundamental. Limiting the general power utilization in such gadgets is fundamental since it is favourable to take advantage of the run time with least potential necessities on weight, battery duration and size owed to batteries. In this manner, in compact gadgets, 'the low power configuration is the most conclusive element to think while planning framework on chip. Typically, portable clients request extra elements and delayed battery duration at a lower cost. Practically 70% of clients search for longer talk time and backup time as key element for cell phones. One of the top administrator prerequisites in 4G is Power proficiency. Clients generally search for more

 © 2012 IJFANS. All Rights Reserved

modest, trim and effortless cell phones. This is the need of elevated degrees of silicon reconciliation in current cycles, yet modern cycles have naturally higher power extravagance. Thus, plan is vital in low power utilization gadgets.

Power demonstrating

Various power parts and their result should be recognized to diminish power utilization of specific circuit. Out of two power scattering types, the most extreme power dispersal connects with top immediate current and the subsequent kind is normal power dissemination. Because of electrical cable obstruction, top flow influences the commotion in supply voltage. This causes warming of gadget and thus brings about execution corruption. With a view on battery duration time, this typical power scattering turns out to be more significant. The three significant power dissemination parts are [1].

Plan boundary

The low power configuration work basically centers on assessing the unique power dispersal. Previously, the central issue of the originator was about region, speed and cost. The optional significance was accommodated power contemplations. As of late, power has become as the essential plan thought. A few variables add to this pattern like the development of individualized computing gadgets, for example, convenient work areas, sound and video-based interactive media items and remote correspondence frameworks which request high velocity calculation and complex usefulness with low power utilization [6]. So there is areas of strength for a for power utilization decrease to diminish bundling and cooling cost and further develop item dependability. At the point when the objective is a low power application, a power analyser/assessor positions the different plan viewpoints, in this manner helps in choosing the one that is possibly more compelling from the power outlook.

The Role of Technology Selection

Legitimate innovation determination is one of the vital parts of force the board [1]. The objective of every innovation headway is to further develop execution, thickness, and power utilization. The regular methodology in fostering another age of innovation is to apply consistent electric-field scaling. Process planners scale both the applied voltage and the oxide thickness to keep up with a similar electric field [13, 16].

e-ISSN 2320 –7876 www.ijfans.org
Vol.11,S Iss 1, 2022
© 2012 IJFANS. All Rights Reserved UGC CARE Listed (Group -I) Journal

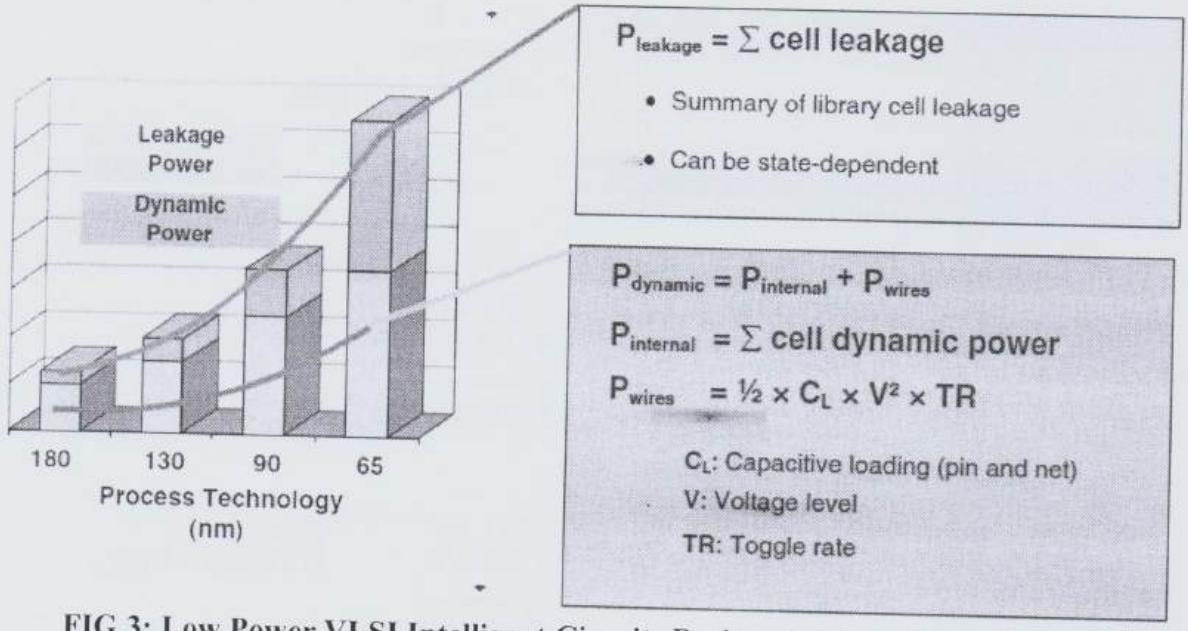


FIG.3: Low Power VLSI Intelligent Circuits Design Methodologies Process.

This approach decreases power by around half with each new innovation hub In any case, as the voltage gets more modest, the edge voltage likewise should downsize to meet the presentation focuses of that innovation.

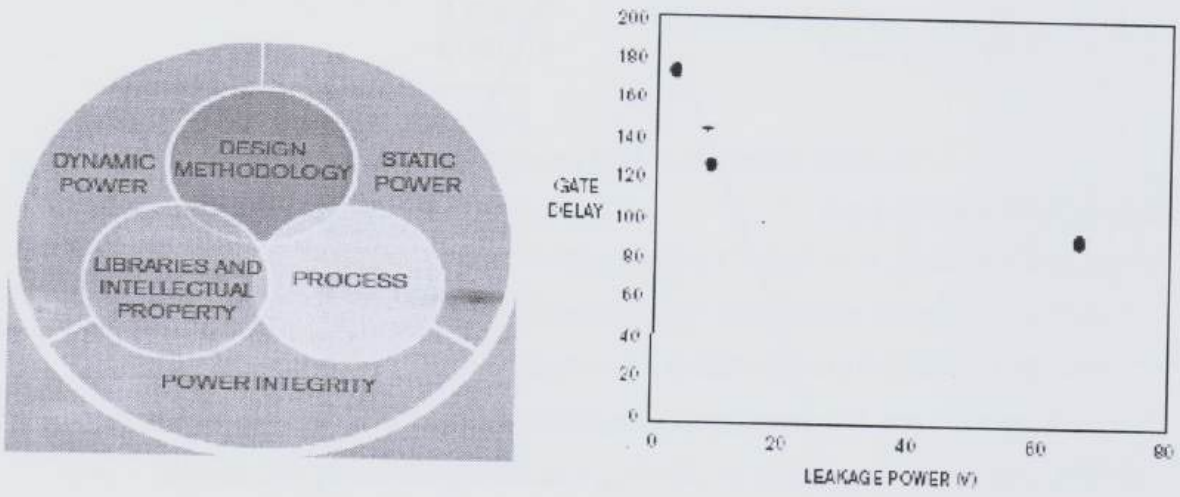


Fig.4: Low Power VLSI Intelligent Circuits Design Methodologies Cycle.

This scaling sadly builds the sub edge current and consequently the spillage power. To conquer this imperative, process designs never again apply steady field scaling for cycles of 65 nm or more modest; all things considered, they utilized a more summed up type of scaling. Since it is difficult to improve an innovation for both execution and spillage without a moment's delay, every innovation for the most part has two variations. One variation goes for the gold, and different goes for low spillage. The essential distinctions between the two are in the oxide thickness, supply voltage, and edge voltage.

Results

© 2012 IJFANS. All Rights Reserved

Analysts gaze at the plan of low power gadgets as they are administering the present hardware ventures. In VLSI circuits, power scattering is a basic plan boundary as it assumes a fundamental part in the presentation assessment of the battery worked gadgets especially utilized in biomedical applications. The diminishing in chip size and expansion in chip thickness and intricacy raise the trouble in planning better execution low power consuming framework on a chip. Further, in general power the executives on a chip is turning into a major test under 100 nm hub in light of its expanded plan intricacy. Moreover, spillage current likewise assumes an imperative part in Power the executives of low power VLSI gadgets. In sub-micron innovations, spillage and dynamic power utilization is turning into a fundamental plan boundary as it is scattering a significant part of the all out power utilization. To build the battery duration of convenient gadgets, spillage and dynamic power decrease is arising as an essential objective of the VLSI circuit plan. This paper gives an understanding about the different philosophies, methodologies and power the executive's strategies to be utilized for the plan of low power circuit based frameworks.

CONCLUSION

The requirement for lower power frameworks is being driven by many market portions. Sadly planning for low power adds one more aspect to the all-around complex plan issue and the plan must be streamlined for power as well as Execution and Region. All in all different issues and significant difficulties in regards to low power plans are:- 1 Innovation Scaling: It relates with the accompanying variables like: Capacitance per hub decreases by 30%, Electrical hubs increments by 2X, Kick the bucket size develops by 14% (Moore's Regulation), Supply Voltage diminishes by 15% and Recurrence Increments by 2X. To meet these issues moderately 2.7 X dynamic power will increment. 2 Spillage power: To satisfy recurrence need VT will be scaled which results high spillage power. A low voltage/low limit innovation and circuit configuration approach, focusing on supply voltage around 1V and working with decreased edges. 3 Unique power the executive's strategies, shifting inventory voltage and execution speed as per the action estimation. 4 Low power interconnect, utilizing advance innovation, diminished swing or movement approach. 5 Improvement of force cognizant strategies and devices for conduct blend, rationale combination and design enhancement. 6 Power saving strategies that reuse the sign energies utilizing the adiabatic exchanging chiefs rather them dispersing them as an intensity and promising in specific applications where speed can be exchanges for low power.

REFERENCES

[1] Michael Keating, David Flynn, Robert Aitken, Ala Gibsons and Kaijian Shi, "Low Power Methodology Manual for System on Chip Design", Springer Publications, New York, 2007.
[2] Creating Low-Power Digital Integrated Circuits the Implementation Phase, Cadence, 2007.
[3] Liu, Weidong, Xiaodong Jin, Xuemei Xi, James Chen, Min-Chie Jeng, Zhihong Liu, Yuhua Cheng, Kai Chen, Mansun Chan, Kelvin Hui, Jianhui Huang, Robert Tu, Ping K Ko, and Chenming Hu, BSIM3v3.3 MOSFET Model User's Manual, Department of Electrical Engineering and Computer Sciences, University of California-Berkeley, 2005.

© 2012 IJFANS. All Rights Reserved

[4] Glasser, Lance A, and Daniel W Dobberpuhl, TheDesign and Analysis of VLSI Circuits, Addison-Wesley Publishing Co, 1985.

[5] Shekar Borkar, "Design Challenges of Technology Scaling," IEEE Micro, July/August 1999, pg 23.

[6] T. Inukai, et.al, "Boosted Gate MOS (BGMOS): Device/Circuit Cooperation Scheme to Achieve Leakage Free Giga- Scale Integration," Proc. CICC 2000, pp.409- 412.

[7] F. Hamzaoglu and M. Stan, "Circuit-Level Techniques to Control Gate Leakage for sub 100nm CMOS," Proc. ISLPED, pp. 60-63, Aug. 2002.

[8] Y. Yeo, et.al, "Direct Tunneling Gate Leakage Current in Transistors with Ultrathin Silicon Nitride Gate Dielectric," IEEE Electron Devices Letters, vol.21, no.11, pp. 540-542, Nov.2000.

[9] S. Mutoh, et.al, "1-V Power Supply High-Speed Digital Circuit Technology with Multi-Threshold Voltage CMOS,"IEEE Journal of Solid State Circuits, vol. 30, no. 8, pp. 847-854, Aug. 1995.

[10] M. Alidina, j. Monterio, S. Devadas, A. Ghosh and M. Papaefthymiou. "Precomputation –based Sequential logic optimization for low power" In Proceedings of the 1994 International Workshop on Low Power Design, pages 57- 62, April 1994.

[11] Anand Iyer, "Demystify power gating and stop leakage cold", Cadence Design Systems, Inc.

[12] De-Shiuan Chiou, Shih-Hsin Chen, Chingwei Yeh, "Timing driven power gating", Proceedings of the 43rd annual conference on Design automation, ACM Special Interest Group on Design Automation, pp.121 - 124, 2006.

ugccare.unipune.ac.in/Apps1/User/WebA/SearchList

SAVITRIBAI PHULE PUNE UNIVERSITY

Home

UGC

Search

UGC-CARE List

UGC-CARE List

You searched for "**International Journal of Food and Nutritional Sciences**". Total Journals : 1

Search:

Sr.No.	Journal Title	Publisher	ISSN	E-ISSN	UGC-CARE coverage years	Details
1	International Journal of Food and Nutritional Sciences	Global E smart Technologies	2319-1775	2320-7876	from January-2021 to January- 2023	Discontinued from Jan 2023

Showing 1 to 1 of 1 entries

Previous 1 Next

Copyright © 2023 Savitribai Phule Pune University. All rights reserved. | Disclaimer

JCST Journal of Data Acquisition and Processing

ISSN: 1004-9037
https://sjcjycl.cn/
DOI: 10.5281/zenodo.7691383

A NEURAL NETWORK BASED MACHINE TRANSLATIONMODEL FOR ENGLISH TO AHIRANI LANGUAGE

Dr. Uday C. Patkar
Bharati Vidyapeeth's college of Engineering, lavale, Pune, (MS), India.
uday.patil@bharatividyapeeth.edu

Mrs. Pallavi Tekade
JSPM's rajarshi shahu College of Engineering, Pune, (MS), India.
tekade.pallavi@gmail.com

Mrs. N. S. Patil
Bharati Vidyapeeth (Deemed to be University) College of Engineering, Pune, 411043, India.
nspatil@bvucoep.edu.in

Dr. A. M. Pawar
Bharati Vidayapeeth's College of Engineering for Women, Pune (MS), India.
avinash.m.pawar@bharatividyapeeth.edu

Dr. Uday Patil
Bharati Vidyapeeth's college of Engineering, lavale, Pune, (MS), India.
uday.patil@bharatividyapeeth.edu

Mrs. Gauri Rao
Bharati Vidyapeeth (Deemed to be University) College of Engineering, Pune, 411043, India.
grrao@bvucoep.edu.in

Mrs. S. S. Patil
Bharati Vidyapeeth (Deemed to be University) College of Engineering, Pune, 411043, India.
sspatil@bvucoep.edu.in

Dr. K. D. Bamane
D Y Patil College of Engineering, Akurdi Pune (MS), India.
kdbamane@dypcoeakurdi.ac.in

ABSTRACT: Machine Translation is the process of converting one natural language into another through the use of computer-assisted translation. The fundamental goal is to bridge the linguistic gap that exists between two distinct languages speaking people, communities, or countries. India is a multilingual country, with different territorial languages spoken in different parts of the country. However, not all Indians are polyglots. There are 18 constitutional languages and ten widely used scripts in the world. The majority of the Indians, particularly the peasants in distant areas, do not understand, read,

or write English, making the use of an efficient language translator necessary and desirable. Machine translation systems that translate content from one language to another will contribute to the advancement of the enlightened civilization of Indians, regardless of their native tongue. Despite the fact that Marathi is the most widely spoken language in the state of Maharashtra, Ahirani is also extensively spoken. Taking advantage of the fact that English is a universal language and that Ahirani is the language spoken by the vast majority of Khandeshi people, we present a proposal for an English to Ahirani machine translation system using Recurrent neural networks (RNN).

***KEY WORDS**: Indian Languages, Machine Translation, Natural Language Processing, Lexical Analysis, Computational Linguistics, Rule Based Translation*

INTRODUCTION

Since 1940, machine translation has always been in the early stages of research and development. Machine translation has been on the rise since the 1940s and will continue to do so. Machine translation systems can be used to translate text or speech from one natural language to another. To translate a document or text from another commonly known language into your native language, you must use machine translation. You can overcome language barriers. NLP is a branch of computer science that seeks to fill this gap. Neural machine translation is conceptually simple, requiring only a rudimentary understanding of the domain. Large neural networks have been trained to generate very long word strings. Unlike regular machine translation systems, this model explicitly stores large phrase dictionaries and language models, making it more efficient. Georgetown University and IBM worked together and in 1965 he made the first deployment of the MT system. An important factor contributing to the importance of machine translation in multilingual societies is the social and political importance of translation in multilingual societies. Additionally, the concept of attention mechanisms is used.

Machine translation (MT) has difficulty dealing with the issue of translation discrepancies. Differences in translation can be defined by differences in grammar from one language to the next in its grammar. According to numerous studies, divergence occurs when sentences in one language (L1) are translated into sentences in another language (L2) in significantly different forms. Many different perspectives were considered, and various techniques were presented to address the problem. A system for identifying and resolving translation discrepancies is essential for machine translation systems to ensure that translations are accurate and reliable. Translators encounter translation discrepancies at various levels, and the degree of complexity of each translation discrepancy has a corresponding impact on the overall quality of the translation. Some types of translational differences are universal in the sense that they exist in all languages, while other types of translational differences are specific to Particular pairs of translated languages, as found in the literature. Therefore, to fully understand translation discrepancies, it is necessary to examine them from both an inter-language and a language-specific perspective. This research examines the translation language pair of English and Ahirani from the perspective of discovering language-specific differences. Due to the significant differences between English and the Ahirani dialect, this translation

language pair provides an excellent resource for exploring translation differences in machine translation.

These languages are also very syntactically, structurally, and sociocultural different from each other, and these differences need to be thoroughly investigated. The purpose of this work is to analyze some features of English and Ahirani grammar that may be related to translation discrepancies between Ahirani and English machine translations. We discuss the issue of syntactic and structural divergence in English-Ahirani machine translation, analyzing the same translation pair with back-translation to determine the nature of the divergence in each situation separately.

This paper examines language pairs in terms of Dorr's taxonomy of the problem of translation differences between English and Ahirani, which is the starting point for our investigation. Section 2 reviews the literature on the classification of translation discrepancies. This section describes various lexical-semantic and syntactic differences. Section 3 details how to implement a recurrent neural network for machine translation. Section 4 of the study is devoted to discussion of the results obtained, after which the work is completed.

REVIEW OF LITERATURE

Natural language processing is often performed when systems are deployed to manipulate or manipulate text or speech. As part of current research [1-5], a text-to-speech system was developed that synthesizes text by incorporating natural language processing (NLP) before proceeding to digital signal processing (DSP) to generate synthesized words. I was able to develop a simple but useful text-to-speech application that converts written text to speech and saves the result as an mp3 file.

Bridging the gap between linguistic scripts and languages for the deaf will have a positive impact on the promotion and growth of a closely domesticated population of civilians. Most of the literature on English text-to-speech mentions how difficult this is, but with limited success. If you're ever curious about text-to-speech conversion, researching the local language should give you results. In their study [6], they claim that this technique can be used to convert optional text to speech (2). In this case, instead of constructing a concatenated set of values from the actual language data, we convert directly from the registered language parameters. This algorithm also participates in a global comparison compared to another synthesizer commonly used for language learning purposes and responsible for most communication problems. A person who is not fluent in English can simply look at a grid of symbols enlarged on a computer screen to see how the content would be rendered in the original language if they were not fluent in English. This study presents data from 53 different languages and provides an opportunity to apply the results to a variety of other languages, thus providing a new research area. users can retrieve information in images based on their preferred language settings [7]. When we talk about Graphing, we are talking about the process of extracting text from images and translating the recovered text into multiple languages for viewing Google Speech API [Application Program Interface] and Tesseract OCR [Optical Character Recognition] were used in conjunction with each other. Therefore, travelers can spend their time relaxing by listening to audio in their preferred language, English. It is also accessible to people with visual impairments. This device is especially useful for those who want to read text in its original language.

Building on rule-based text-to-speech synthesis that has proven effective, this work combines natural phonetics and lexical formant approaches [8] to transform the final product into word and concatenated to the concatenation of phrases. Simulations show that in Marathi, the current system manages words, phrases, sentences and paragraphs better than the proposed approaches for better speech recognition. With 91% accuracy, the entire system can predict how long the process will take with 91% accuracy. Further efforts are needed to improve the accuracy of detecting stressed syllables and vocal strength.

To generate the output, the article breaks the text into its constituent parts and assembles them into speech. Voices are stored in a database and retrieved as needed. As a result, the considered work [9] used concatenated-input-based speech synthesis on the MATLAB 2010 platform, which is considered to have good and clear sound. It is widely used and gaining popularity as an aid for people with dyslexia and dyslexia, especially those with visual impairments. The software can be used for many other purposes, but its main purpose is to improve foreign language skills and pronunciation. These include reducing eye strain when reading (whether in paper or digital format), reducing document production costs through digital text printing, English translation, digital writing/editing, and enhancing listening comprehension.

Abstract: Translates simple English sentences into assertive Marathi sentences using rule-based techniques described in research [10]. Again, the algorithm accepts a simple sentence as input and once again outputs a phrase describing the output element or situation (lexeme). The tokenizer identifies each newly formed English letter and each letter found in the English dictionary according to a tokenizer (lexicon). If a lexical item has tokens associated with it, you can optionally access the morphological features associated with those tokens. Instead of extracting anything before finding a valid root, morphemes are classified based on features present in the word itself, saving time. Groups established in specific places provide information about how written sentences are grammatically correct. When using bottom-up parsing, syntax is verified by looking at the depth of parsing. In addition, this program's search dictionary is enriched with syntactic tokens (Marathi). This allows you to accurately identify the target language words in a sentence. If the required Marathi word cannot be found word by word and cannot be connected to the corresponding English word, then create a Marathi sentence with someone who can make an English translation of the text using the remaining words in the text. Topics covered in this article include the principles that form English sentences, and various ways of rearranging vocabulary and proofreading the intricacies of the language.

[11] The texts reviewed here show how the authors approved the Marathi language used in this study. We found two unique corpora in the original text. Each represents the author of the most frequently occurring term and an interpretation of the text based on patterns identified by us in the original text (his SMORDT sequential minimum optimality using statistical similarity models and rules transformation-based decision tree approach). To demonstrate that feature extraction is important for any model, we tested and validated the feature extraction method used in this experiment to demonstrate that it is. The proposed method has been tested over a long period of time, considering three main criteria: recall, accuracy and precision.

With the urbanization of civilization, the demand for clean air is increasing. Since it was first recorded, the technology has expanded the data volume, doubling his data volume

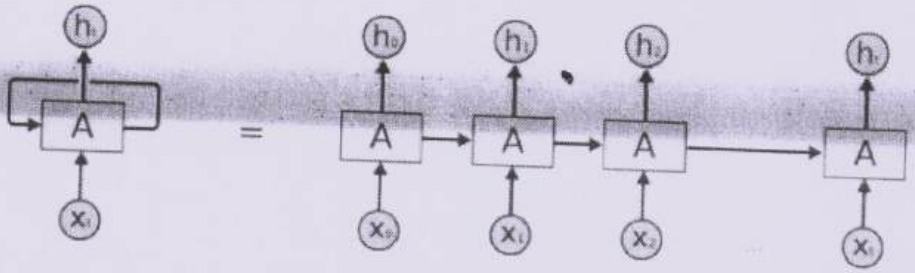
every two years since it was first released. As a result, computers are expected to acquire, analyze, interpret, and apply data with minimal human input, unlike previous methods. Many of these text segments in source code are difficult to interpret. However, some were included in "code mixing". Or "machine code-like" languages that are particularly hard to parse. This has already been done in this area and this work [12] is an active contributor and applying comparability to classify and evaluate these documents to classify and evaluate these documents into classes of learning systems (Bag of Words and Human Priors (NB, SVM)), Marathi and Hindi text translation documents (data We train and test a classification that examines the subjectivity of (using support vector machines and naive Bayes) to decide which classification method to use. On the other hand, the results of basic machine learning algorithms are often better than or often comparable to those of analytical approaches.

When writing sentences in Marathi, he can start each phrase with two words to clarify word breaks [13]. This is an option for those who speak the language. Marathi does not contain the beginning-of-sentence markers found in English, so it is difficult to distinguish between the beginning and the end of a sentence. To correctly determine the end of an order, a reliable system considers a large amount of information.

In particular translation apps [14-15] (tools to use language to complement English) translate Malayalam texts into their native languages and are used by language minorities who wish to engage with the culture and language of Kerala is intended for Machine translation and text-to-speech accuracy are improved by using various combined approaches that include both machine translation and text-to-speech. If Malayalam is the source language, the translation is completed using a grammar-based translation method that expands the English part, morphological analysis, and a Malayalam-Tamil-English dictionary. Individuals come from each of the translated Malayalam syllables and words and are distinct from each other (one in every). The syllable database contains large number of syllable recordings that have been created and recorded. The concatenation and synthesis of Malayalam words leads to the creation of synthesized words. In the first two iterations of Malayalam machine translation, the accuracy is 70%, increasing to 73% in three stages of unfolding. To ensure the accuracy of the speech output, the device should take advantage of naturalness and intelligibility characteristics .87% of the sentences are well formed during the grading process.

RNN FOR MACHINE TRANSLATION

RNN is a type of neural network with loops that can persist information across network steps. A loop tells the neural network to look at what happened in all previous words before deciding what the current word really means. RNNs can be thought of as copying and pasting the same network over and over again. Each new copy and paste adds slightly more information than the previous one. RNN applications differ greatly from traditional NN applications in that they do not have an output and input set as a concrete value; instead, they take sequences as input or output.



An unrolled recurrent neural network.

Figure1. An unrolled recurrent neural network

This issue can arise in any network that employs gradient-based optimization techniques. When back-propagation (calculating the gradients of loss with respect to the weights) is calculated, the gradients become extremely small as the back propagation algorithm moves through the network. As a result, the earlier layers learn much slower than the later ones. This reduces the effectiveness of RNNs because they are frequently unable to fully account for long sequences. An RNN becomes less and less effective as the gap between needed information grows larger.

An RNN also has different models that it can follow, this study follows a sequence-to-sequence model. Here the RNN receives an input sequence and outputs a sequence.

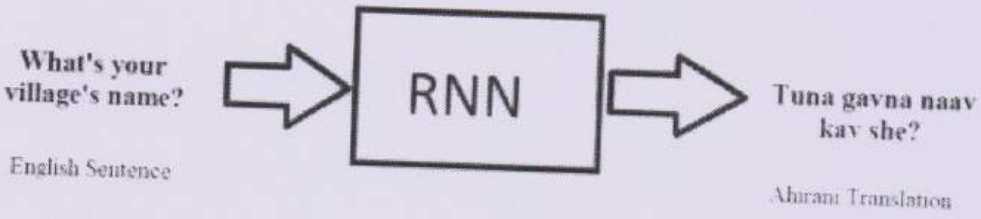


Figure 2. Machine Translation: an RNN reads a sentence in one language and then outputs it in another

The use of activation functions that do not cause vanishing gradients, such as the RNN reads a sentence in one language and outputs it in another problem. Long-Short Term Memory Networks are a better solution.

Setup of the RNN

Depending on your application, you may need to configure your RNN to handle inputs and outputs differently. As you can see below, this project uses many-to-many processes. The input is a sequence of English words and the output is a sequence of Japanese words (fourth from the left in the figure below).

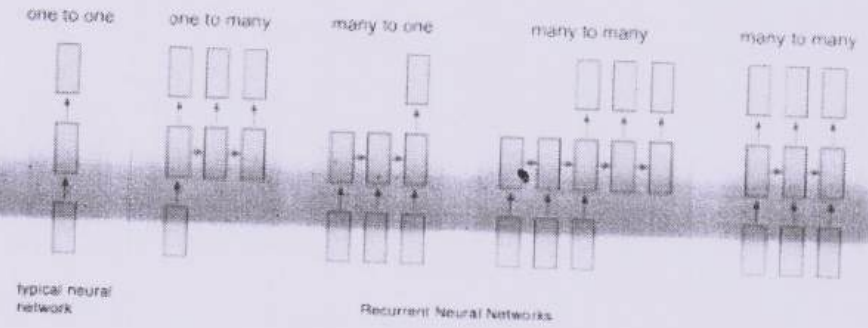


Figure 3. Recurrent Neural Network

The following section outlines various preprocessing and modeling steps. Here are the high-level steps:

- Preprocessing includes reading and inspecting data, cleaning, tokenizing, and padding.
- Modeling is the process of creating, training, and testing models.
- To be able to make predictions, we need to generate a specific translation from English to Ahirani and compare it with the ground truth translation.
- Continue to iterate on the model and experiment with different architectural configurations.

This study uses Keras for the frontend and Tensor Flow for the backend to achieve its goals. Using Keras on top of Tensor Flow is my preferred method as it has a simpler syntax and makes creating model layers more intuitive. The downside of Keras is that you lose the ability to make fine adjustments. This is a big advantage. However, this does not affect the model developed for this study.

PREPROCESSING

Load & Examine Data

Below is an example of data. The input is in English, and the output is a translation of the English text. The word count of the dataset indicates that the vocabulary of the dataset is relatively limited. This was designed specifically for this project.This allows the model to be trained in a reasonable amount of time.

Cleaning

No additional cleaning required at this time. Since the data has already been converted to lowercase and split, there are spaces between every word and punctuation as shown above.

Tokenization

Next, we need to tokenize the data. That is, it converts text to numbers. This allows the neural network to perform operations on the data it receives as input. Each word and punctuation mark is assigned a unique ID number for this project. Running to kenizer generates a word index, which is used to convert each sentence into vector form.

Padding

When entering a sequence of word IDs into a model, you must ensure that each sequence is the same size. Padding is applied to sequences shorter than the maximum length (that is, shorter than the longest sentence) to achieve this result.

Modeling

To understand the architecture of a RNN, we first need to look at it at a high level. As shown in the diagram above, there are several components of the model that you should be aware of:

Inputs-The input sequence enters the model word by word, with each time step represented by a different word. Each word is encoded as a single integer or as a one-hot encoded vector corresponding to the word in the lexical database of English records.

Layers for Embedding- Each word is converted into a vector by embedding. Vocabulary complexity affects the size of the vector representing the vocabulary. Iterative shift is a type of shift that occurs repeatedly (encoder). This means that the context from the previous time step word vector is applied to the current word vector. Layers that are dense (Decoder) Typical fully connected layers that are used to convert the encoded input into the correct translation sequence are depicted in the diagram.

Outputs- The output is returned as a series of integers or as a one-hot encoded vector that can be mapped to the French record vocabulary after processing.

Embedding

Embeddings should be used to achieve very simple semantic and syntactic word relationships. In particular each word is projected onto an n-dimensional space, giving us this result. Similar-sounding words occupy this space in a similarity search. The closer two words are, the more similar they are in meaning. And often the equation between both proverbs represents an interconnected network involving gender, prepositions, and even strategic ties.

Embedding large datasets from scratch requires a large amount of data and computation, making it infeasible for most people. To avoid having to train the embeddings from scratch, we typically use pre-trained embedding packages such as Glove or word2vec. Used in this way, embeddings can be viewed as a form of transfer learning. However, due to the limited vocabulary and few syntactical variations in this project's dataset, we use the Keras machine learning framework to train the embeddings themselves.

Encoder & Decoder

Our sequence-to-sequence model connects two recurrent networks: an encoder and a decoder, which are connected by a recurrent network. The encoder summarizes the input and stores it in a context variable, also known as a state variable. Afterwards, the decoding context is obtained, and the output sequence is generated.

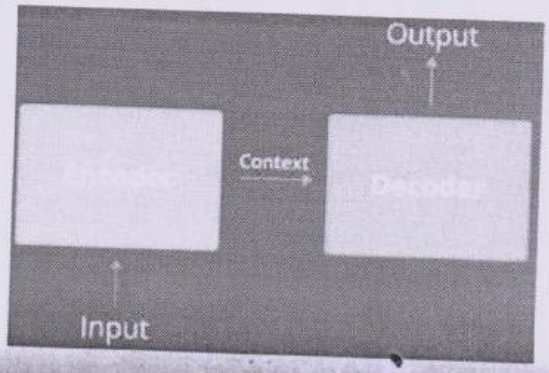


Figure 4. Encoder & Decoder

Due to the fact that both the encoder and decoder are recurrent, they both have loops that process each part of the sequence at a different time step. Unrolling the network to see what's going on at each time step is the most effective way to conceptualize this phenomenon.

To encode the entire input sequence, as shown in the following example, it takes four time steps. During each time step, the encoder "reads" the input word and applies a transformation to the hidden state of the input word. Then it moves on to the next time step with the hidden state in tow. Please remember that the hidden state is a representation of the relevant context that is passing through the network. The larger the hidden state, the greater the learning capacity of the model; however, the larger the hidden state also increases the computation requirements of the model.

The design of our suggested system is the same as that of the Moses SMT system, which allows us to compare the scores of the phrases in the phrase table obtained by the Moses SMT system. It is an RNN that progressively reads each symbol of an input sequence x, which is called the encoder. When the RNN reads a symbol, the hidden state of the RNN changes in accordance with the equation (1). Following the reading of the end of the sequence, the hidden state of the RNN is a summary c of the entire input sequence, as shown in the following figure. When the hidden state h is known, the proposed model's decoder is yet another RNN that has been trained to construct the output sequence by anticipating the next symbol yt when that state is known (t). The hidden state of the decoder at time t is calculated using the formula.

$$h_{(t)} = f(h_{(t-1)}, y_{t-1}, c)$$

And similarly, the conditional distribution of the next symbol is

$$P(y_t | y_{t-1}, y_{t-2}, \ldots, y_1, c) = g(h_{(t)}, y_{t-1}, c)$$

For given activation functions f and g (the latter must produce valid probabilities, e.g. with a SoftMax).

$$\max \frac{1}{N} \sum_{n=1}^{N} \log p\Theta(y_n | x_n)$$

The two components of the proposed RNN encoder-decoder are jointly trained to maximize the conditional log-likelihood.

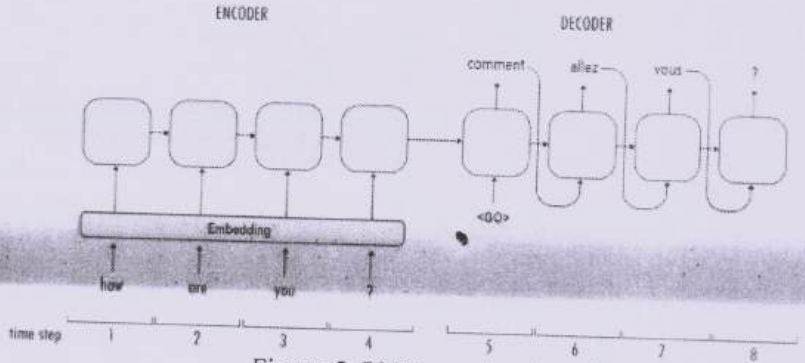


Figure 5. RNN encoder-decoder

Because the encoder and decoder are both recurrent, they both have loops that process every other part of the series at different time steps. To visualize this, we should unroll the network and examine what is happening at each time step.

Hidden Layer with Gated Recurrent Unit (GRU)

If you can choose which information from the hidden state is allowed to flow over the network, it's not desirable Maybe? Some information is more relevant than others, and some information should be removed entirely. The GRU, or Gated Repetition Unit, provides functionality similar to this. The Update Gate and Reset Gate are the only gates in the GRU and both are used together. A detailed explanation can be found in this essay by Simeon Kostadinov. In summary, the update gate (z) helps the model determine how much information is passed into the future from the previous time step. The reset gate (r), on the other hand, determines how much of the previous information is erased.

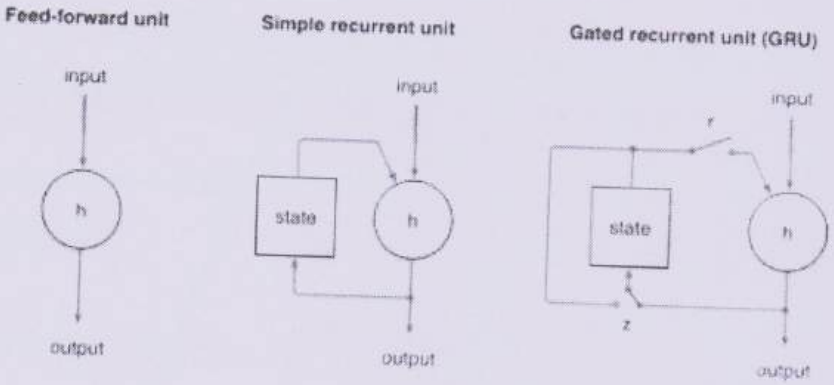


Figure 6. Gated Repetition Unit

RESULT ANALYSIS

Researchers Must Evaluate Their Research to Determine Success or Failure

This has its limitations, as most authors currently only assess their findings for precision and recall, or time lag and number of queries. Precision and recall can be just mathematical calculations, which can lead to unstructured research assessments. Therefore, there is a need to develop new parameters for evaluating research outcomes.

Using the Ahirani training corpus from the Ahirani dictionary (https://www.ahirani.in/en/books/ahirani-dictionary), consisting of parallel running source-target sentence pairs using English as the source language and the system was trained to work.

Commonly used in a variety of situations. Due to the limitations imposed on the corpus format by system training, data must be preprocessed prior to system training for a successful training session. Validation data, a subset of the training corpus containing 80% of the instances, is used to check the training convergence. The translation effectiveness of the trained and validated model was evaluated using a test corpus of approximately 1400 English sentences. Table 1 below shows the optimization parameters chosen for the implementation.

Table 1: RNN Algorithm Tunning Parameters

Number of Epochs	5
RNN Size	128
Batch Size	128
Epoch	2
Learning Rate	0.01
Encoding Embedding Size	128
Decoding Embedding Size	128
Keep Probability	0.8

Comparison of training and validation accuracy against number of epochs. Table 2 shows the Training and validation accuracy of RNN machine translation model of epochs. This analysis is also shown in figure 3.

Table 2: Number of Epoch Vs Training and Validation Accuracy

Epoch	Train Accuracy	Validation Accuracy
1	67.31	67.05
2	76.13	74.36
3	81.29	80.65
4	84.45	83.38
5	87.50	85.65

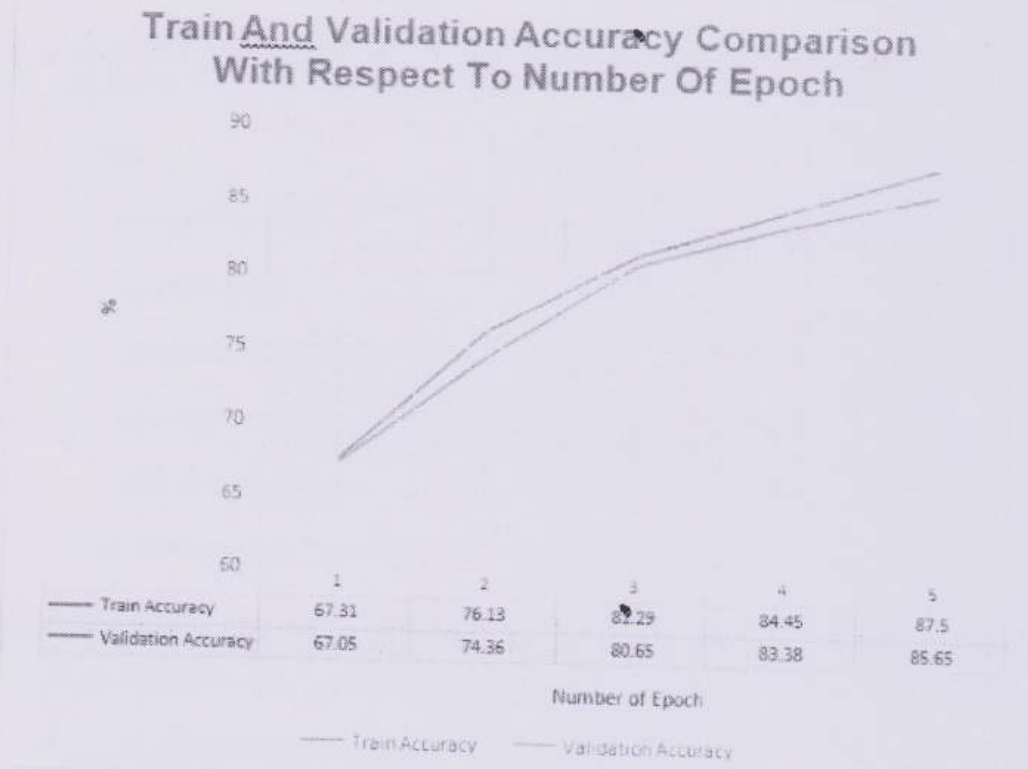


Figure 7. Training and Validation Accuracy for RNN Machine Translation Model

The losses occurred during the execution is shown in table 3 and represented in figure 4.

Table 3. Epochs Vs Training Losses

Epoch	Training Loss
1	0.4356
2	0.3316
3	0.2497
4	0.2070
5	0.1514

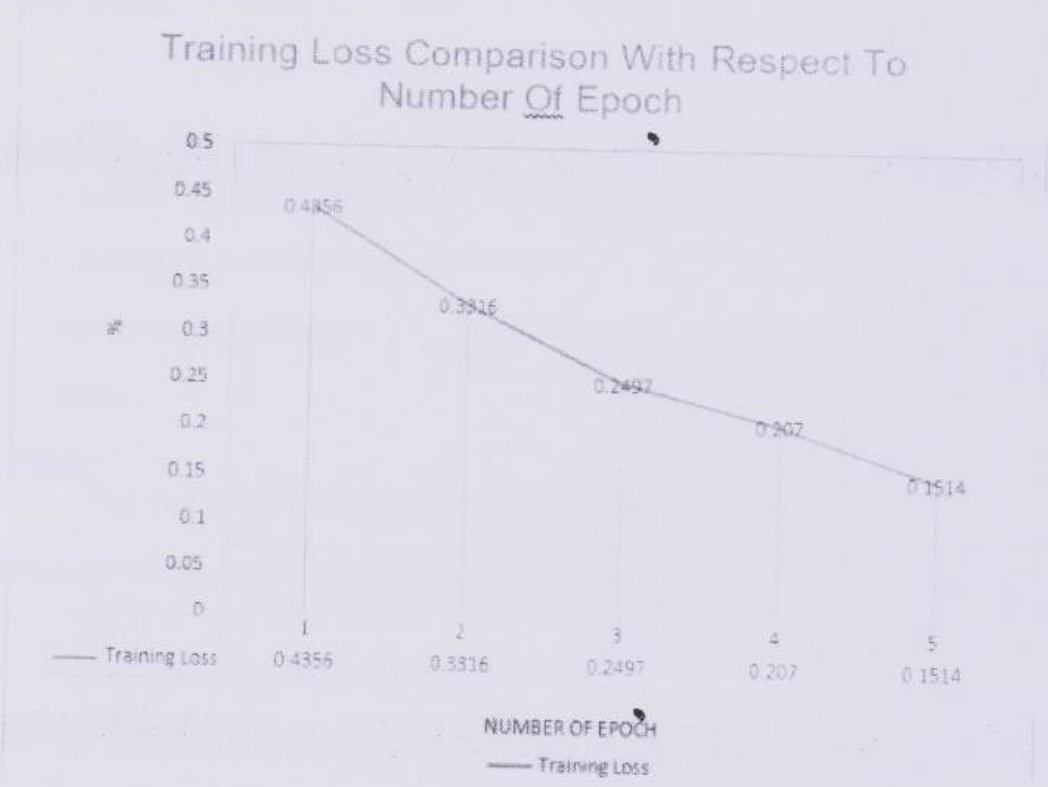


Figure 8. Training Losses for number of Epochs

CONCLUSION REMARKS

Network (RNN) system for predicting translations. Key benefits of using NMT in an Indic context include the ability to generate fluent translations, enhanced contextual analysis capabilities, and better performance than SMT systems. These are some of the main advantages that motivated us to study the use of NMT in the Indic context. In particular, the English-Ahirani pairing algorithm has been trained and tested by our team. Different experimental settings were also developed to investigate the relationship between translation efficiency of the English-Ahirani MT system and variations in the number of epochs, amount of training data, and test phrase length. After examining the predicted translations in detail, we came to the conclusion that the MT system produces fluent translations and performs better as the amount of training data and the length of the test phrases increase. Additionally, the translation performance against the epoch diagram helps determine whether the system training is converging.

The basic working concept of NMT is highly dependent on the size of the training corpus, so the number of training corpus instances should be increased for the training corpus to be effective. The attention mechanisms and scoring functions used to compute attention for each source state have the greatest impact on translation success. By changing the merit function, we can increase the interaction between the source state vector and the current hidden

state of the decoder. Moreover, a deeper understanding of the nature of the target language components helps improve the comprehensibility, relevance and fluency of translations.

Apart from that, skillful and thorough selection of settings for system parameters such as number of epochs, hidden layers and GPU can improve the overall quality of the translated text.

REFERENCES

1. Pramod Salunkhe, Mrunal Bewoor, Suhas Pati, Shashank Joshi, Aniket kadam, "Summarization and Hybrid Machine Translation System for English to Marathi: A Research Effort in Information Retriveal System (H-Machine Translation" ,Discovery The International journal (ISI thomas retuers indexed).2015.
2. Pramod Salunkhe , Mrunal Bewoor , Dr.Suhas Patil "A Research Work on English to Marathi Hybrid Translation System", (IJCSIT) International Journal of Computer Science and Information Technologies, Vol. 6 (3) 2015, 2557-2560.s
3. S. B. Kulkarni, P. D. Deshmukh "Linguistic Divergence Patterns in English to Marathi Translation International Journal of Computer Applications (09 75 8887) Volume 87 No.4, February 2014.
4. J. Ramanand, Akshay Ukey, Brahm Kiran Singh, Pushapak Bhattacharyya "Mapping and Structural Analysis of Multilingual Wordnets"
5. Bulletin of the IEEE Computer Society Technical Committee on Data Engineering.
6. Sreelekha.S, Raj Dabre, Pushpak Bhattacharyya "Comparison of SMT and RBMT, The Requirement of Hybridization for Marathi Hindi MT" [online pdf].
7. Amruta Godase, Sharvari Govilkar"Survey Of Machine Translation Development for Indian Regional Languages" International Journal of Modern Trends in Engineering and Research IJMTER- 2014.
8. M.L.Dhore & S.X.Dixit (2011) "English to Devnagari Translation for UI Labels of Commercial web based Interactive Applications, International Journal of Computer Applications (0975 – 8887) Volume 35 –No.10, December 2011.
9. Devika Pishartoy, Priya, Sayli Wandkar (2012) "Extending capabilities of English to Marathi machine Translator., IJCSI International Journal of Computer Science Issues, Vol. 9, Issue 3, No 3, May 2012.
10. Priyanka-choudhary "A approach for interlingua example based EM Translation, IJCSIT, 2015.
11. Abhay A, Anita G, Paurnima T, Prajakta G (2013), "Rule based English to Marathi translation of Assertive sentence International Journal of Modern Trends in Engineering and Research 2014.
12. Aniket Kadam, A.D. Dept. Inf. Tech., BVDUCOEP, Pune, India ; Joshi, S.D.; Medhane, S.P, "Question Answering Search engine short review and road-map to future QA Search Engine", Electrical, Electronics, Signals, Communication and Optimization (EESCO), 2015 , 10.1109/EESCO.2015.7253949.
13. Kadam Aniket, Prof.S.D.Joshi, prof.S.P.Medhane, "QAS" International Journal of Application or Innovation in Engineering & Management IJAIEM , Volume 3, Issue 5, May 2014 May 2015.
14. Kadam Aniket, Prof.S.D.Joshi, Prof.S.P.Medhane, "QAS" International Journal of

Application or Innovation in Engineering & Management IJAIEM , Volume 3, Issue 5, May 2014 May 2015.

15. Kadam Aniket, Prof.S.D.Joshi, Prof.S.P.Medhane "Search Engines to QAS:Explorative Analysis", International Journal of Application or Innovation in Engineering & Management IJAIEM , Volume 3, Issue 5, May 2014 May 2015 IJAIEM May 2015 .
16. Mishra, Sudha. "Heterogeneous Groups in Competition: Innovative Pedagogy for Teaching English as Second Language." International Journal of Educational Science and Research 4.2014 (2014): 1-6.
17. Jha, Sanjay Kumar. "Exploring the Causes of Sanskrit's Decline (A Pilot Study)." International Journal of Educational Science and Research (IJESR) 8 (2018): 165-172.
18. Kumar, Manoj, and Sanjay Kumar. "SPEECH AS TEXT FOR TEACHING: AN ANALYSIS OF LINGUISTIC AND STYLISTIC MANEUVERINGS OF STEVE JOBS" FAMOUS SPEECH STAY HUNGRY STAY FOOLISH AND EXERCISES FOR ENHANCING STUDENTS" LANGUAGE SKILLS." International Journal of English, and Literature (IJEL) 6.1 (2016): 47-58.

Source details

Feedback > Compare sources >

Shu Ju Cai Ji Yu Chu Li/Journal of Data Acquisition and Processing

Scopus coverage years: from 2001 to Present

Publisher: Nanjing University of Aeronautics an Astronautics

ISSN: 1004-9037

Subject area: Computer Science: Signal Processing | Computer Science: Software

Source type: Journal

Save to source list | Source Homepage

CiteScore 2022
0.7

SJR 2022
0.140

SNIP 2022
0.221

CiteScore | CiteScore rank & trend | Scopus content coverage

Improved CiteScore methodology

CiteScore 2022 counts the citations received in 2019-2022 to articles, reviews, conference papers, book chapters and data papers published in 2019-2022, and divides this by the number of publications published in 2019-2022. Learn more >

CiteScore 2022

0.7 = 302 Citations 2019 - 2022 / 434 Documents 2019 - 2022

Calculated on 05 May, 2023

CiteScoreTracker 2023

0.8 = 329 Citations to date / 434 Documents to date

Last updated on 05 December, 2023 • Updated monthly

CiteScore rank 2022

Category	Rank	Percentile
Computer Science: Signal Processing	#110/122	10th
Computer Science: Software	#389/404	3rd

View CiteScore methodology > | CiteScore FAQ > | Add CiteScore to your site

Int. J. Appl. Comput. Math (2022) 8:232
https://doi.org/10.1007/s40819-022-01436-9

ORIGINAL PAPER

Magnetohydrodynamic Radiative Simulations of Eyring–Powell Micropolar Fluid from an Isothermal Cone

Jyoti Atul Dhanke[1] · K. Thanesh Kumar[2] · Pudhari Srilatha[3] · Kurapati Swarnalatha[4] · P. Satish[5] · S. Abdul Gaffar[6]

Accepted: 25 July 2022
© The Author(s), under exclusive licence to Springer Nature India Private Limited 2022

Abstract
The magnetohydrodynamics thermal convection viscoelastic micropolar fluid from an isothermal cone is presented in this article. Greater temperature invokes radiation impacts that are studied by approximating Rosseland diffusion flux. To explain the non-Newtonian dynamics of the fluid, the Eyring–Powell viscoelastic model is employed that gives a great analogy for magnetic polymers. In order to simulate the polymer's microstructural and shearing features, the Eringen's micropolar Eyring–Powell fluid models are coupled. The Keller-Box scheme is used to solve the dimensionless couple conservation equations. Validation using previously published Newtonian solutions is also included. The fluctuations of velocity, angular velocity, temperature, concentration, skin friction, wall couple stress, heat and mass transfer rates are studied using graphical and tabulated findings. The computational modelling presented here have implications in hot polymer coating processes and industrial deposition procedures and they serve as a good reference for more generic computational fluid dynamics simulations.

Keywords Eyring–Powell fluid · Micropolar fluid · Vortex viscosity · Magnetohydrodynamics · Radiation · Wall couple stress · Angular velocity · Heat transfer rate

✉ S. Abdul Gaffar
abdulsgaffar0905@gmail.com

1 Department Engineering Science (Mathematics), SPPU, Bharati Vidyapeeth's College of Engineering, Lavale, Pune, Maharashtra 412115, India

2 Department of Mathematics, Hyderabad Institute of Technology and Management, Basuragadi, Hyderabad, Telangana 501401, India

3 Department of Mathematics, Institute of Aeronautical Engineering College, Dundigal, Hyderabad, Telangana 500043, India

4 Department of Chemistry, CH.S.D.ST. THERESAS College for Women, Eluru, West Godavari, Andhra Pradesh 534002, India

5 Department of Mathematics, Aditya Engineering College (A), Surampalem, Andhra Pradesh 533437, India

6 Department of Information Technology, Mathematics Section, University of Technology and Applied Sciences, Salalah, Oman

Published online: 24 August 2022

List of Symbols

A	Half angle of the cone
$r(x)$	Radius of the cone
B_0	Imposed magnetic field
B	Micropolar inertia density
C	Fluid concentration
C_1	Rheological fluid parameter
C_f	Skin friction coefficient
c_p	Specific heat [J/(K kg)]
D_m	Mass diffusivity
f	Dimensionless stream function
g_1	Gravitational acceleration (m/s^2)
g	Dimensionless angular velocity (micro-rotation)
Gr_x	Local Grashof number
j	Microinertial density
k_1	Vortex viscosity
k^*	The mean absorption coefficient
k	Thermal conductivity of the fluid [W/(m k)]
K	Eringen vortex viscosity parameter
M	Magnetic parameter
N	Microrotation velocity
Nu	Heat transfer coefficient
Pr	Prandtl number
q_r	Radiative heat flux
Sc	Schmidt number
Sh	Mass transfer coefficient
f_1	Body force per unit mass vector
l	Body couple per unit mass vector
P	Thermodynamic pressure
F	Radiation parameter
T	Fluid temperature
u, v	Dimensionless velocity components in X, Y directions (m/s^2)
V	Velocity vector
Wcs	Wall couple stress
x	Stream wise coordinate
y	Transverse coordinate

Greek Symbols

α	Thermal diffusivity (m^2/s)
β	Eyring–Powell fluid parameter
β_1	Coefficient of thermal expansion (ppm/°F)
δ	Local non-Newtonian parameter
θ	Dimensionless temperature
ε	Rheological fluid parameter
ϕ	Dimensionless concentration

η	Dimensionless radial coordinate
ν	Kinematic viscosity (Ns/m^2)
μ	Dynamic viscosity (Ns/m^2)
ρ	Fluid density (kg/m^3)
σ^*	The Stefan–Boltzmann constant ($W/m^2\ K^4$)
ξ	Dimensionless tangential coordinate
ψ	Dimensionless stream function
λ	Eringen second order viscosity coefficient
$\alpha^*, \beta^*, \gamma$	Spin gradient viscosity coefficients

Subscripts

w	Surface condition on cone
∞	Free stream conditions

Introduction

The simulations of polymeric thermal coating of non-Newtonian chemical is a great resource of chemical and process mechanical engineering. For these polymers with a number of various mathematical models, several distinct rheological properties characteristics can be modelled. Non-Newtonian micropolar fluids have received a lot of attention as the fluid characteristics with randomly distributed particles can't be fully described by Newtonian fluid theory. Because of the micromotions and local structure of the fluid elements, the micropolar fluid reveals tiny impacts. To fully describe the behavior of such fluids, the design and natural movement of distinct material particles are being analyzed. Micropolar fluids have micro constituents that rotate, affecting the flow's hydrodynamics, which is notably non-Newtonian. These microstructured fluids are classified as micro-orphic fluids, which are complicated fluids with non-symmetrical stress tensors. They can be used to study the behavior of novel lubricants, colloidal suspensions or polymers, crystallines, additive suspensions, chemical solutions, bodily fluids and turbulent shear flows, among other things. Various scholars used micropolar fluid in different areas of science and engineering over last few decades. The theory of micropolar fluid was developed by Eringen [1–3]. A unique feature of this fluid class is couple stress sustenance. Habib et al. [4] studied the magnetic and radiation impacts on double-diffusive flows of micopolar nanofluid through a permeable stretching surface with Gyrotactic microorganisms using RK 4th order technique. Yadav and Kumar [5] analytically studied the entropy generation in a rectangular conduit by a two phase · non-miscible Newtonian micropolar fluid. Ramesh et al. [6] presented the unsteady incompressible squeezing flows of Casson and micropolar nanofluid through parallel disks using RKF-45 technique. Hossam and Mahdy [7] analyzed the MHD micropolar hybrid nanofluid flows past a porous stretchy sheet using finite difference technique. Singh et al. [8] studied the impacts of internal heat generation/absorption, melting heat transfer and chemical reaction on micropolar stagnation point flow over a porous stretchy surface. Khader and Sharma [9] investigated the unsteady magnetized micropolar fluid through a stretching/shirking sheet with thermal radiation and non-uniform heat source/sink using fourth order predictor–corrector finite difference scheme. Beg et al. [10] explored the nonlinear, dissipative thermal

convection flows of micropolar fluid past a wedge using homotopy analysis method considering the viscous dissipation and heat sinking effects. The influences of Hall current, viscous and Joule electromagnetic dissipation on the non-isothermal micropolar fluid from a non-linear stretching/shrinking sheet was simulated by Beg et al. [11]. Hossam and Mahdy [12] examined the micropolar fluid flow behaviour of dust particles past a cone.

Since few decades, researchers have been making a significant contribution towards non-Newtonian fluids since these fluids are realistically vital in a wide range of research and manufacturing operations such as food processing, crude oil production, medicines and other industries. Unlike Newtonian fluids, which have a linear relationship between shear strain and stress, non-Newtonian fluids generally exhibit shear thinning or thickening behavior, as well as a yield stress on occasion. Due to the varied nature of fluid characteristics, the qualities of all non-Newtonian fluids cannot be encompassed in a single constitutive model, resulting in the creation of multiple non-Newtonian fluid models based on different physical attributes or rheology. These include Casson fluid model [13], Jeffery's fluid model [14], Maxwell fluid model [15], Tangent Hyperbolic fluid [16], Ostwald De-Wald power law fluid [17], Giesekus fluid [18], Reiner–Rivlin fluid [19], Sisko fliud [20], Carreau fluid [21], third grade fluid model [22]. The Eyring–Powell model [23], which is developed form the kinetic theory of liquids rather than empirical relations, is relatively simple yet useful non-Newtonian model among the various non-Newtonian fluids mentioned in the literature. This particular fluid model enables for the extraction of Newtonian behaviour as a special case for low and high shear stress circumstances. This model is a variant of the Powell model, which has similarly been demonstrated to have an exponential relationship between flow velocity and stress at intermediate stresses but a linear relationship at larger stresses. Recently, Khan et al. [24] investigated the laminar coating flow and heat transfer of Eyring–Powell micropolar fluid flows past an inverted isothermal cone with varying wall temperature. Haldar et al. [25] discussed the influences of thermal radiation on Eyring–Powell fluid moving over a power-law stretching surface when suction/blowing is present using the shooting technique. Abbas and Ahmed [26] used the Chebyshev spectral approach to investigate the Eyring–Powell steady flows across a multi-layered stretching porous sheet. Bilal and Samia [27] examined the consequences of heat generation and absorption on mixed convection Eyring–Powell fluid flows across a stratified stretching surface. They observed that increasing thermal stratification causes a decrease in fluid's velocity and temperature, while the heat generation has an opposite effect. Mustafa [28] presented the analytical solutions of Eyring–Powell model, which describes the rheology of fluid moving in a circular pipe. Deepak et al. [29] considered the mixed convective Eyring–Powell fluid flows past a vertical plate with variable velocity and temperature using homotopy analysis method. Taseer et al. [30] explored the 3D numerical simulation of Eyring–Powell nanofluid flows past a riga plate considering the influences of thermal radiation, velocity slip, convective heat transfers and Cattaneo-Christov heat flux model is used to analyse heat transport.

In the recent years, many physicists, mathematicians and biomedical researchers have shown their interest in magnetohydrodynamics (MHD) flow phenomena. Magnetohydrodynamics is the study of the magnetization of electrically conducting fluids. Electrodes, plasma, seawater and metal oxides are all examples of magnetic fluids. MHD can be used to stop bleeding in critical injuries, cancerous tumours, inflammations, hyperthermia ulceration, and growth of magnetic tracers [31]. Fatunmbi et al. [32] investigated the Darcy–Forchheimer flows of magneto reactive micropolar fluid through a nonlinear stretching surface considering the velocity, temperature and concentration slip effects. Singh et al. [33] studied the collective effects of heat source/sink and chemical reaction on slip flows of micropolar fluid through a permeable wedge in the presence of Hall and ionslip effects. Abbas et al. [34] studied the

effects of entropy generation and velocity slip on MHD incompressible peristaltic flow in diverging tube utilizing lubrication technique. Zakir et al. [35] presented the MHD convective flows of Williamson fluid past a stretching sheet and cylinder considering the effects of heat source, Joule and viscous heating using Keller-Box technique. Armaghani et al. [36] investigated the effects of heat source/sink on MHD mixed convection flow of hybrid nanofluid within L-shaped cavity. Their findings revealed that using the highest amount of sink power resulted in optimum thermal conductivity.

Radiation heat transfer is a mechanism for organizing warm-rate transfer in a variety of different ways with low convective heat transmission coefficient. Due to widespread applications in radiation therapy, glass production, polymer production, ceramic engineering, metal casting industry and other fields, several investigations have been conducted to investigate the effects of radiation on boundary layer flow with heat transfer characteristics. Sharma and Mishra [37] explored the natural convection stagnation point radiative flows of micropolar fluid across a stretched surface considering the effects of thermos-diffusion and heat source. Sreedevi and Reddy [38] investigated the laminar radiative MHD flows of Tiwari-Das nanofluid within a square cavity using finite difference technique considering the base fluid as Ethylene Glycol and TiO_2 as nanoparticles. Siddiqui et al. [39] examined the entropy generation of 3D Darcy–Forchheimer bioconvection Casson nanofluid between two stretchable rotating disks considering the effects of radiation and magnetic field using shooting technique. Waqas et al. [40] discussed the bioconvection flow of second-grade nanofluid over a stretched surface in the presence of microorganisms, melting heat transfer, activation and nonlinear thermal radiation, thermal and solutal Robin's conditions using bvp4c technique. Qasem et al. [41] presented the radiation effects on Ree-Eyring nanofluid flows between two stretchy spinning disks at varied stretching rates using RKF-45 scheme. Majeed et al. [42] investigated the unsteady radiative MHD flows of electrically conducting fluid comprising gyrotactic micro-organisms past a stretchy surface considering the velocity, thermal and concentrations slip effects.

To investigate the magnetohydrodynamics radiative flows of viscoelastic micropolar boundary layer flows past a vertical cone is considered in this article. The governing conservation equations are turned into dimensionless coupled partial differential boundary value problem with accompanying boundary conditions. Because the emergent model's nonlinearity precludes accurate solutions, an implicit finite difference Keller's Box method is used [43]. The Keller box results are validated using previous Newtonian research [44]. The current research may be used in dip coating, powder metallurgy, paper manufacturing, steel fabrication and deposition of metallic plates in cooling glasses and baths, etc. The computational modelling presented here have implications in hot polymer coating processes and industrial deposition procedures and they serve as a good reference for more generic computational fluid dynamics simulations.

Eyring–Powell Fluid Model

In the present study a subclass of non-Newtonian fluids known as the *Eyring–Powell fluid* is employed. The Cauchy stress tensor for Eyring–Powell fluids [45] takes the hyperbolic form:

$$\tau_{ij} = \mu \frac{\partial u_i}{\partial x_j} + \frac{1}{\beta_1} \sinh^{-1}\left(\frac{1}{C_1}\frac{\partial u_i}{\partial x_j}\right) \tag{1}$$

Considering the second-order approximation of the $sinh^{-1}$ function as:

$$\sinh^{-1}\left(\frac{1}{C_1}\frac{\partial u_i}{\partial x_j}\right) \approx \frac{1}{C_1}\frac{\partial u_i}{\partial x_j} - \frac{1}{6}\left(\frac{1}{C_1}\frac{\partial u_i}{\partial x_j}\right)^3, \left|\frac{1}{C_1}\frac{\partial u_i}{\partial x_j}\right| < 1. \tag{2}$$

Micropolar Constitutive Model

Simple microfluids are subdivided into micropolar fluids. The localized movements of the particles present in each of the volume elements i.e. microelements, influence the behavior and attributes of these fluids. Micropolar fluids are characterized by a microrotation vector and have volume elements holding hard particles that can spin around the volume element's center. The typical rigid body motion of the full volume element that defines Navier–Stokes fluids is supplemented by this local rotation of the particles. The classical continuum laws are thus supplemented in micropolar fluid mechanics by new equations that provide the microinertia conservation and the balances of initial stress moments that occur as a result of the study of fluid microstructure. As a result, classical continuum fluid dynamics theory is combined with novel kinematic variables (gyration tensor, microinertia moment tensor), as well as ideas of body moments, stress moments and microstress. The momentum field equations for micropolar fluids in generalized form can be stated following Bég et al. [46] as follows:

Conservation of Translational (Linear) Momentum

$$(\lambda + 2\mu + k)\nabla \times \nabla \cdot \mathbf{V} - (\mu + k)\nabla \times \nabla \times \mathbf{V} + k\nabla \times \mathbf{N} - \nabla P + \rho\,\mathbf{f}_1 = \rho\mathbf{V}' \tag{3}$$

Conservation of Angular Momentum (Micro-rotation)

$$(\alpha * + \beta * + \gamma)\nabla \times \nabla \cdot \mathbf{N} - \gamma\,\nabla \times \nabla \times \mathbf{N} + k\nabla \times \mathbf{V} - 2k\mathbf{N} + \rho\,\mathbf{l} = \rho j\mathrm{N}' \tag{4}$$

In the micropolar mode, we focus only on two independent kinematical vector fields, viz, the velocity vector field and the axial vector field that approximates the spin (micro-rotation) of the micropolar fluid particles, both of which are supposed to be rigid. It should be noted that in micropolar fluid theory, there are no external body forces in the case where the fluid has constant physical properties and the conservation equations for steady-state flow can be considerably reduced. Furthermore, when $k = \alpha^* = \beta^* = \gamma = l = \mathbf{f}_1 = 0$, the gyration vector vanishes and hence (4) vanishes. In this exceptional instance, (3) also simplifies to the traditional Navier–Stokes equation. The velocity vector V and the microrotation N dissociate in the case of zero vortex viscosity and the global motion is unchanged by the microroations (Fig. 1).

Mathematical Model

In an attempt to develop the mathematical model, we have considered a steady, laminar, 2-dimentional, incompressible flow of Eyring–Powell micropolar fluid past a vertical isothermal cone. A homogeneous external magnetic field B_0 is applied normal to the flow direction and the induced magnetic field is not taken into account due to a suitably low magnetic Reynolds number. The vertex of the cone is placed at the origin and the x-axis is measured along the slant surface of the cone and y axis is directed normal to the cone surface. The gravitational acceleration g, acts downwards. Due to low intensity of the magnetic field, the effects of hall

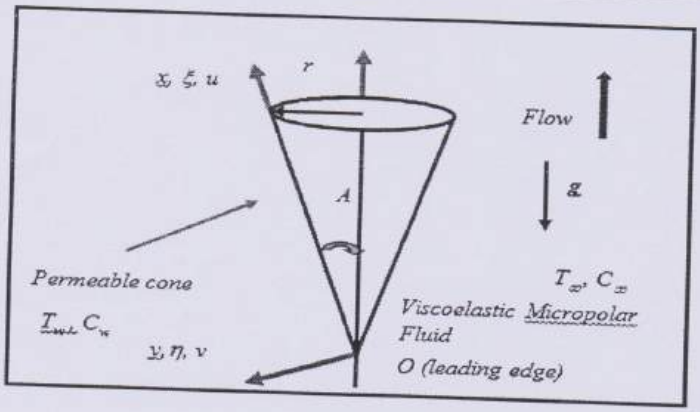


Fig. 1 Physical model and coordinate system

and ionslip current are also ignored. Because the flow is low and subsonic, Alfven waves are suppressed. The electron pressure (for poorly conducting fluids) and the thermos-electric pressure are also insignificant. The applied magnetic field is created by passing a continuous electric current parallel to the cone's longitudinal (z axis), where the cone edges terminate at ideal electrodes connected by a load. A radiative heat flux is considered that acts along the flow. We also assume that the Boussinesq approximation holds, i.e. the density variation in the momentum equation occurs solely in the buoyancy term. The temperature and concentration of both the Eyring–Powell Micropolar fluid and the cone are kept constant at first. They are elevated to a temperature $T_w > T_\infty$ and concentration $C_w > C_\infty$ equal to the fluid's ambient temperature and concentration, which remains constant. The equations for mass, momentum, angular momentum, energy and concentration, in line with Eyring and Powell [45] and Beg et al. [46] and introducing boundary layer approximations as follows:

$$\frac{\partial(ru)}{\partial x} + \frac{\partial(rv)}{\partial y} = 0 \tag{5}$$

$$u\frac{\partial u}{\partial x} + v\frac{\partial u}{\partial y} = \nu\left(1 + \frac{k}{\nu\rho} + \frac{1}{\nu\rho\beta C_1}\right)\frac{\partial^2 u}{\partial y^2} - \frac{1}{2\rho\beta C_1^3}\left(\frac{\partial u}{\partial y}\right)^2\frac{\partial^2 u}{\partial y^2} + g_1\left(\beta_1(T - T_\infty) + \beta_1^*(C - C_\infty)\right)\cos A + k_1\frac{\partial N}{\partial y} - \frac{\sigma B_0^2}{\rho}u \tag{6}$$

$$\rho j\left(u\frac{\partial N}{\partial x} + v\frac{\partial N}{\partial y}\right) = \gamma\frac{\partial^2 N}{\partial y^2} - k_1\left(2N + \frac{\partial u}{\partial y}\right) \tag{7}$$

$$u\frac{\partial T}{\partial x} + v\frac{\partial T}{\partial y} = \frac{k}{\rho c_p}\frac{\partial^2 T}{\partial y^2} - \frac{1}{\rho c_p}\frac{\partial q_r}{\partial y} \tag{8}$$

$$u\frac{\partial C}{\partial x} + v\frac{\partial C}{\partial y} = D_m\frac{\partial^2 C}{\partial y^2} \tag{9}$$

On the cone surface and in the freestream, the boundary conditions are:

$$\begin{aligned} &At \quad y = 0, \quad u = v = 0, \quad N = \frac{-1}{2}\frac{\partial u}{\partial y}, \quad T = T_w, \quad C = C_w \\ &As \quad y \to \infty, \quad u \to 0, \quad N \to 0, \quad T \to T_\infty, \quad C \to C_\infty \end{aligned} \tag{10}$$

The Rosseland approximation for the radiative heat flux q_r is given by [47, 48]:

$$q_r = -\frac{4\sigma^*}{3k^*}\frac{\partial T^4}{\partial y} \tag{11}$$

Implementing the Taylor series approximation for T^4 to express as a linear function of temperature we yield:

$$T^4 \cong 4T_\infty^3 T - 3T_\infty^4 \tag{12}$$

Using Eqs. (11) and (12) into Eq. (8), one can get:

$$u\frac{\partial T}{\partial x} + v\frac{\partial T}{\partial y} = \frac{k}{\rho c_p}\frac{\partial^2 T}{\partial y^2} - \frac{4}{3N}\frac{\partial}{\partial y}\left[\{1+(T_r-1)T\}^3\frac{\partial T}{\partial y}\right] \tag{13}$$

The stream function ψ is introduced as $ru = \frac{\partial \psi}{\partial y}$ and $rv = -\frac{\partial \psi}{\partial x}$ and hence the mass conservation equation is satisfied.

Introducing the dimensionless quantities as follows:

$$\xi = \frac{V_w x}{\nu}Gr_x^{-1/4}, \quad \eta = \frac{y}{x}Gr_x^{1/4}, \quad \psi = \nu r Gr_x^{1/4}\left(f+\frac{\xi}{2}\right), \quad \theta(\xi,\eta) = \frac{T-T_\infty}{T_w-T_\infty}$$
$$\phi(\xi,\eta) = \frac{C-C_\infty}{C_w-C_\infty}, \quad Gr_x = \frac{g\beta_1(T_w-T_\infty)x^3\cos A}{\nu^2}, \quad \gamma = \left(\mu+\frac{k}{2}\right)j \tag{14}$$

Equations (6), (7), (13) and (9) are thereby rendered into the following coupled nonlinear partial differential boundary layer equations:

$$(1+K+\varepsilon)f''' + \frac{7}{4}ff'' + \xi f'' - \frac{1}{2}(f')^2 - \varepsilon\delta(f'')^2 f''' + \theta + N\phi + Kg' - M\xi^2 f'$$
$$= \frac{\xi}{4}\left(f'\frac{\partial f'}{\partial \xi} - f''\frac{\partial f}{\partial \xi}\right) \tag{15}$$

$$\left(1+\frac{K}{2}\right)g'' + \frac{7}{4}fg' - \frac{1}{4}f'g + \xi g' - BK\xi^2(2g+f'') = \frac{\xi}{4}\left(f'\frac{\partial g}{\partial \xi} - g'\frac{\partial f}{\partial \xi}\right) \tag{16}$$

$$\frac{\theta''}{\Pr} + \frac{4}{3F}\left[(1+(T_r-1)\theta)^3\theta'\right] + \frac{7}{4}f\theta' + \xi\theta' = \frac{\xi}{4}\left(f'\frac{\partial \theta}{\partial \xi} - \theta'\frac{\partial f}{\partial \xi}\right) \tag{17}$$

$$\frac{\phi''}{Sc} + \frac{7}{4}f\phi' + \xi\phi' = \frac{\xi}{4}\left(f'\frac{\partial \phi}{\partial \xi} - \phi'\frac{\partial f}{\partial \xi}\right) \tag{18}$$

with

$$At \quad \eta = 0, \quad f = 0, \quad f' = 0, \quad g = \frac{1}{2}\frac{\partial^2 f}{\partial y^2}, \quad \theta = 1, \quad \phi = 1$$
$$As \quad \eta \to \infty, \quad f' \to 0, \quad g \to 0, \quad \theta \to 0, \quad \phi = 0 \tag{19}$$

Here

$$B = \frac{\nu^2}{jV_w}, \quad K = \frac{k}{\mu}, \quad \Pr = \frac{\nu}{\alpha}, \quad g = \frac{x^2 N}{\nu}\mathrm{Gr}_x^{-\frac{3}{4}}, \quad \varepsilon = \frac{1}{\mu\beta C}, \quad \delta = \frac{\nu^2}{2C^2x^4}\mathrm{Gr}_x^{\frac{3}{2}}, \quad \mathrm{Sc} = \frac{\nu}{D_m}$$
$$M = \frac{\mu\sigma B_0^2}{\rho^2 V_w^2}, \quad F = \frac{k\,k*}{4\sigma * T_\infty^3}$$

Table 1 Comparison values of $f''(\xi, 0)$ and $-\theta'(\xi, 0)$ for various values of Pr with $\varepsilon = F = M = \delta = K = B = 0$, for only isothermal, solid cone case selected from Hossain and Paul [21]

Pr	$f''(\xi, 0)$		$-\theta'(\xi, 0)$	
	Hossain and Paul [21]	Present	Hossain and Paul [21]	Present
0.001	1.5135	1.1536	0.0245	0.0244
0.01	1.3249	1.3248	0.0751	0.0750
0.1	1.0962	1.0960	0.2116	0.2115
1	0.7697	0.7698	0.5111	0.5112
10	0.4877	0.4878	1.0342	1.0341
100	0.2895	0.2894	1.9230	1.9229
1000	0.1661	0.1660	3.4700	3.4701

The *skin-friction coefficient* (C_f) *(shear stress at the cone surface), Wall Couple Stress (Wcs), Nusselt number (Nu) (heat transfer rate)* and *Sherwood number* (*Sh*) (*mass transfer rate*) are defined using the following expressions.

$$\mathrm{Gr}_x^{-\frac{3}{4}} C_f = \left(1 + \frac{K}{2} + \varepsilon\right) f''(\xi, 0) - \frac{\delta}{3}\varepsilon\left(f''(\xi, 0)\right)^3 \tag{20}$$

$$M_w = g'(\xi, 0) \tag{21}$$

$$\mathrm{Nu} = -\left(1 + \frac{4}{3F}\{1 + (T_r - 1)\theta\}^3\right)\theta'(\xi, 0) \tag{22}$$

$$\mathrm{Sh} = -\phi'(\xi, 0). \tag{23}$$

Keller Box Implicit Scheme Solution and Validation

The dimensionless Eqs. (15) to (18) combined with boundary conditions Eq. (19) form 9th order nonlinear coupled boundary value problem. The Keller's implicit finite differences technique [43] that converges quickly with 2nd order precision and is much more effective and frequent than other numerical techniques is used to solve Eqs. (15) to (19). Many studies [49–51] have supported this approach. This technique enhances precision on explicit or semi-implicit schemes and uses adaptable stepping in a completely implicit approach. At each level, this technique quantization is perfectly coupled and simulates the dynamics of parabolic models. The discrete calculus used by this technique is unlike any other numerical techniques. Comparison with prior Newtonian computations was done to verify the present code. The numerical results of heat transfer rate Nu, for various values of Pr are shown in Table 1.

Numerical Analysis

The tables and graphs representations of the solutions obtained in this study are provided in this section. Tables 2 and 3 illustrates results of skin friction (C_f), wall couple stress (Wcs),

Table 2 Values of Cf, Wcs, Nu and Sh for different values of ε, δ, M, F, and K

ε	δ	M	F	K	$\xi = 1$				$\xi = 2$				$\xi = 3$			
					Cf	Wcs	Nu	Sh	Cf	Wcs	Nu	Sh	Cf	Wcs	Nu	Sh
0					0.6418	0.2357	4.4400	0.7119	0.3791	0.4857	8.6105	1.2437	0.2481	0.7761	12.8089	1.8298
0.8					0.6493	0.2496	4.4353	0.7045	0.3837	0.5101	8.6104	1.2419	0.2517	0.8053	12.8086	1.8291
1.6					0.6555	0.2618	4.4318	0.6980	0.3880	0.5308	8.6103	1.2404	0.2553	0.8301	12.8081	1.8286
2.5					0.6596	0.2703	4.4299	0.6933	0.3912	0.5453	8.6102	1.2393	0.2581	0.8473	12.8074	1.8285
3.5					0.6635	0.2788	4.4282	0.6887	0.3946	0.5598	8.6101	1.2383	0.2613	0.8644	12.8067	1.8583
	0				0.6449	0.2413	4.4380	0.7089	0.3809	0.4957	8.6105	1.2430	0.2534	0.8179	12.8058	1.8292
	10				0.6444	0.2410	4.4380	0.7090	0.3807	0.4953	8.6103	1.2430	0.2495	0.7881	12.8065	1.8293
	20				0.6438	0.2407	4.4381	0.7092	0.3804	0.4949	8.6100	1.2429	0.2494	0.7877	12.8068	1.8294
	40				0.6427	0.2399	4.4381	0.7095	0.3801	0.4942	8.6097	1.2429	0.2492	0.7874	12.8070	1.8296
	50				0.6422	0.2395	4.4387	0.7096	0.3799	0.4938	8.6094	1.2429	0.2587	0.7865	13.2326	1.8896
		0			0.6982	0.2304	4.4420	0.7165	0.4757	0.4439	8.6131	1.2498	0.3393	0.7120	12.8088	1.8336
		2			0.4712	0.2755	4.4266	0.6866	0.2118	0.5747	8.6049	1.2324	0.1123	0.8837	12.8019	1.8219
		5			0.3398	0.2983	4.4196	0.6736	0.1165	0.6098	8.6034	1.2305	0.0355	0.9253	12.7990	1.8209
		8			0.2706	0.3088	4.4169	0.6689	0.0691	0.6246	8.6018	1.2267	− 0.0028	0.9430	12.7981	1.8145
		11			0.2251	0.3151	4.4161	0.6679	0.0385	0.6335	8.6016	1.2263	− 0.0276	0.9536	12.7974	1.8141
			0		0.5366	0.2525	7.3775	0.7020	0.3004	0.5211	14.3512	1.2399	0.1893	0.8184	21.3496	1.8276
			0.5		0.6151	0.2474	4.4359	0.7048	0.3430	0.5151	8.6093	1.2406	0.2180	0.8123	12.8061	1.8279
			1		0.6862	0.2413	3.1865	0.7080	0.3835	0.5072	6.1501	1.2414	0.2456	0.8042	9.1447	1.8284
			1.5		0.7508	0.2345	2.4977	0.7116	0.4222	0.4978	4.7854	1.2423	0.2719	0.7947	7.1115	1.8289

heat transfer rate (Nu) and mass transfer rate (Sh) at the cone surface.

Table 2 depicts the values of C_f, *Wcs, Nu and Sh* for increasing values of ε, δ, M, F and K along with ξ. The skin friction and wall couple stress are enhanced with increasing ε values while the and mass transfer rates are reduced. By def., the viscosity and rheological parameters are inversely proportional to the Rheological fluid parameter, ε. Hence a considerable change in the Eyring–Powell fluid parameter is evident when these parameters are changed. A rise in the local non-Newtonian parameter δ, causes the contrary pattern. The slight reduction in *Cf* and *Wcs* are observed when δ is greatly increased whereas Nu and Sh increase marginally. An increase in magnetic parameter M, clearly reduces skin friction, Nusselt number and Sherwood number while the wall couple stress is enhanced. An increase in radiation parameter enhances both *Cf* and Sh while it reduces both *Wcs* and *Nu*. An increase in K, increases C_f, and *Wcs* but decreases *Nu* and *Sh*. As a result of the increased vortex viscosity effect, the flow elevated, and the rotation of the micro-elements is promoted. Greatly micropolar polymer improves boundary layer flow properties in terms of linear and angular momentum as well as reducing heat transfer rate to the wall, which helps to cool the cone surface. This is important in controlling temperature in polymeric spraying processes because excessive heat transfer rate at the wall can cause flaws, thermal damage, de-bonding, etc.

Table 3 displays the impacts of *B, N Pr* and *Sc* on C_f, *Wcs*, *Nu* and *Sh* along with variations in ξ. A strong reduction in *Cf* and *Sh* is seen with a rise in Pr values while Wcs and Nu increase sharply. The ratio of momentum to energy diffusions represents the Prandtl number. If $Pr >$ 1, then the fluid's momentum diffusion rate surpasses the heat diffusion rate. Fluids having high *Pr* also have high viscosities and as *Pr* rises, the viscous resistance decreases.

Figures 2 and 3 shows how velocity (f') and angular velocity (g) distributions change as the Eyring–*Powell fluid parameter,* ε is increased. The velocity distributions usually develops a linear shape as ε rises, and hence reduces boundary layer thickens and velocity gradient. A similar trend is observed in case of angular velocity. Greater values of fluid parameter ε produces greater viscous forces, which are accountable for velocity's resistive tendency.

Figures 4, 5 and 6 displays the influences of magnetic parameter M, on velocity (f'), angular

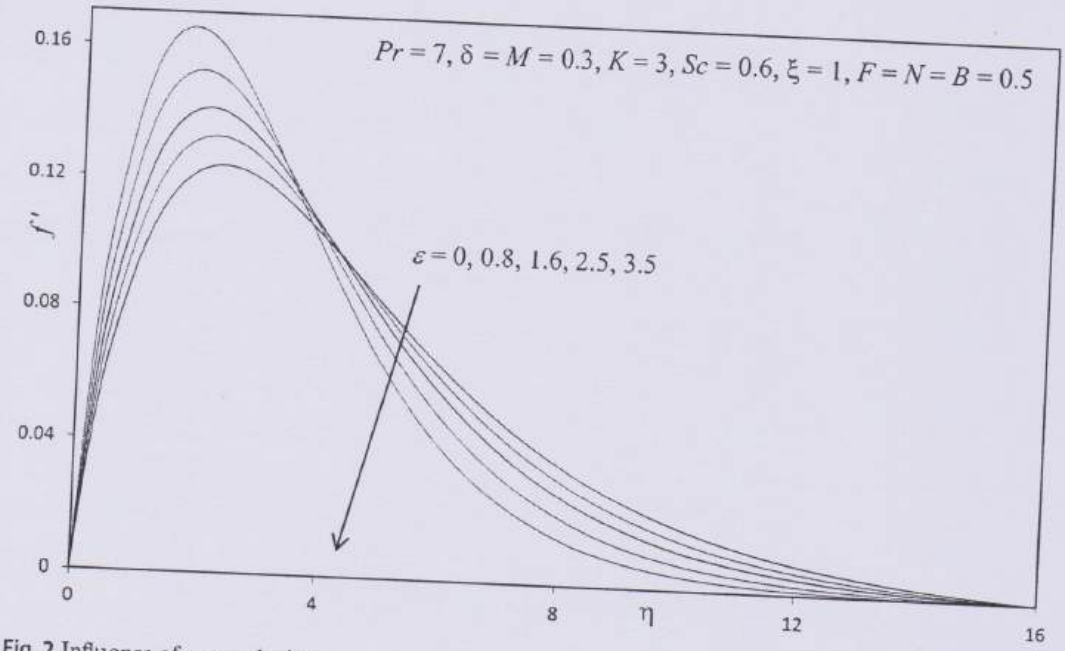


Fig. 2 Influence of ε on velocity

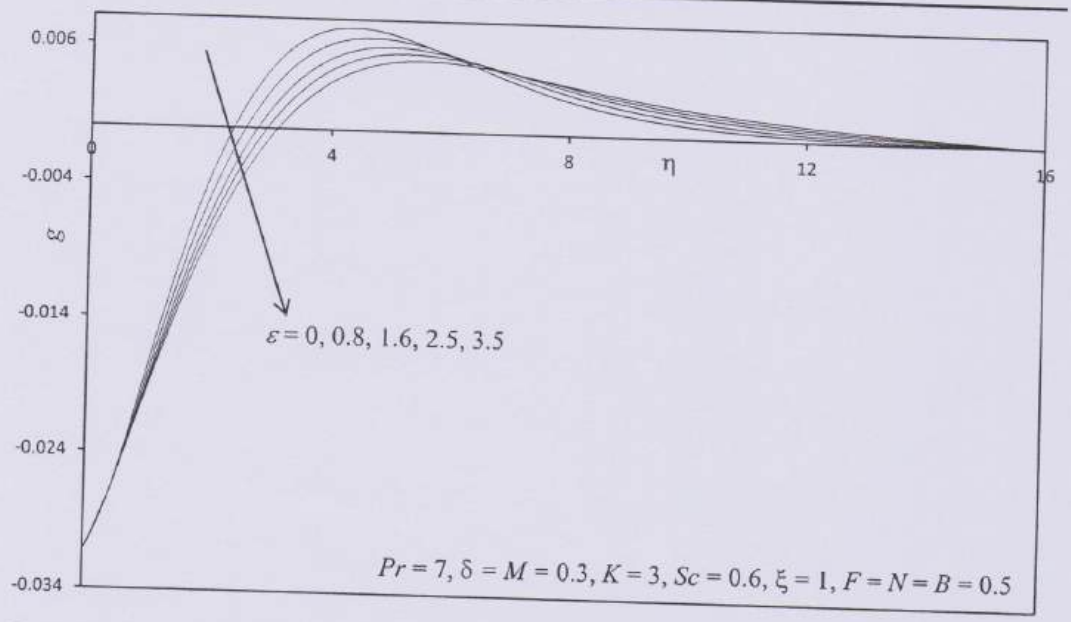


Fig. 3 Influence of ε on angular velocity

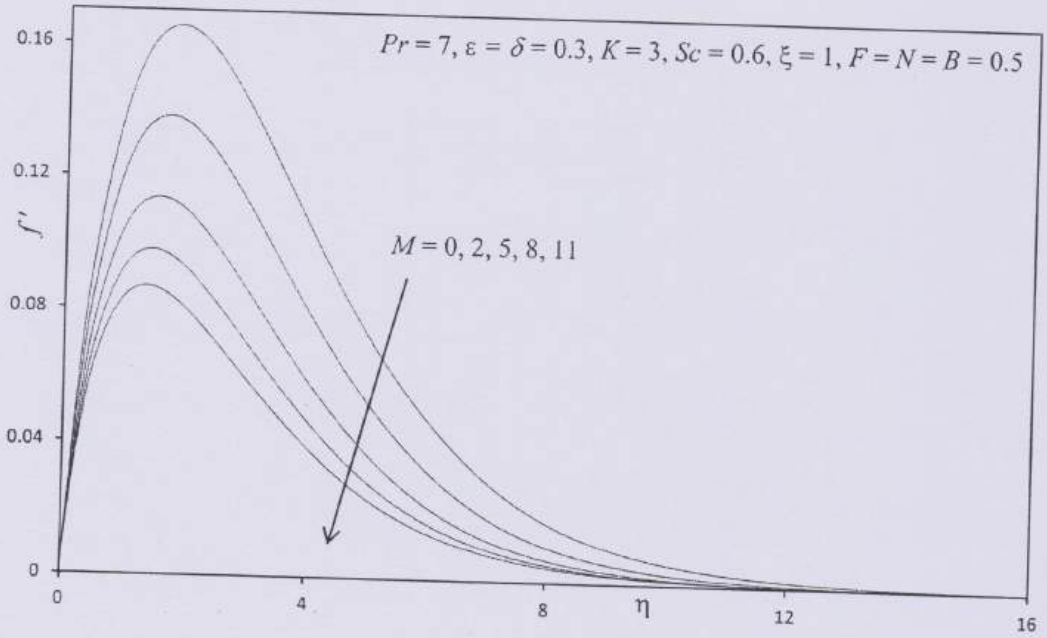


Fig. 4 Influence of M on velocity

velocity i.e. micro-rotation (g) and concentration (ϕ). As M increases, the velocity profiles and the corresponding boundary layer thickness decrease. Physically, the magnetic field has a retarding impact on free convection and increasing values of M causes a resisting force that slows down the fluid. Hence the increasing M values causes the velocity to decrease in the boundary layer. Likewise, a rise in magnetic parameter causes the angular velocity to decrease dramatically. However the effect is more localized at the cone surface and gradually declines moving away from the surface. And a significant increase in concentration distributions is

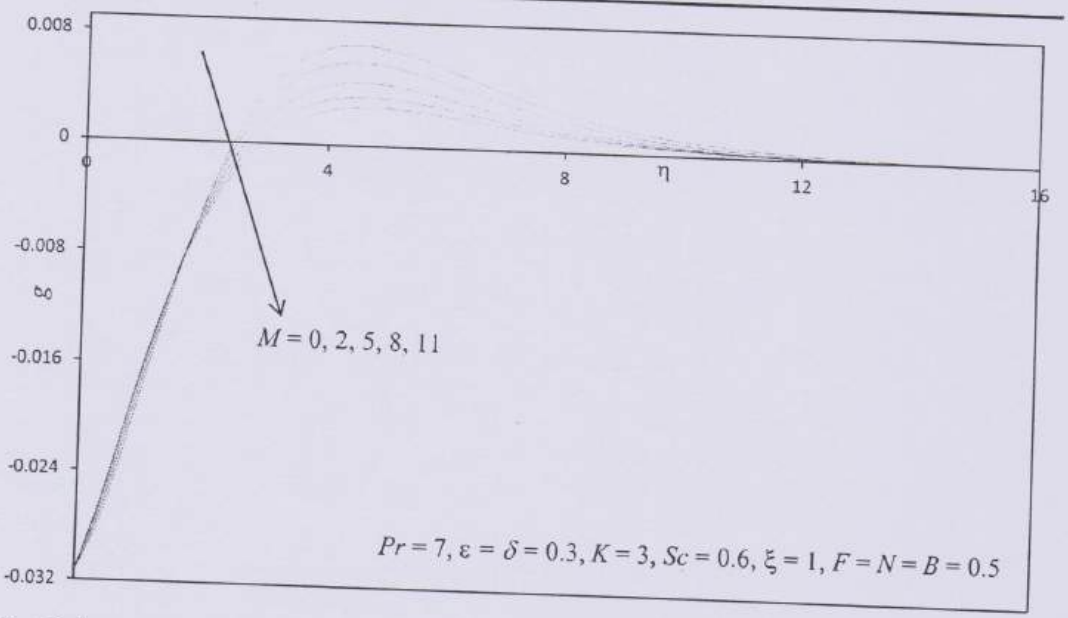


Fig. 5 Influence of M on angular velocity

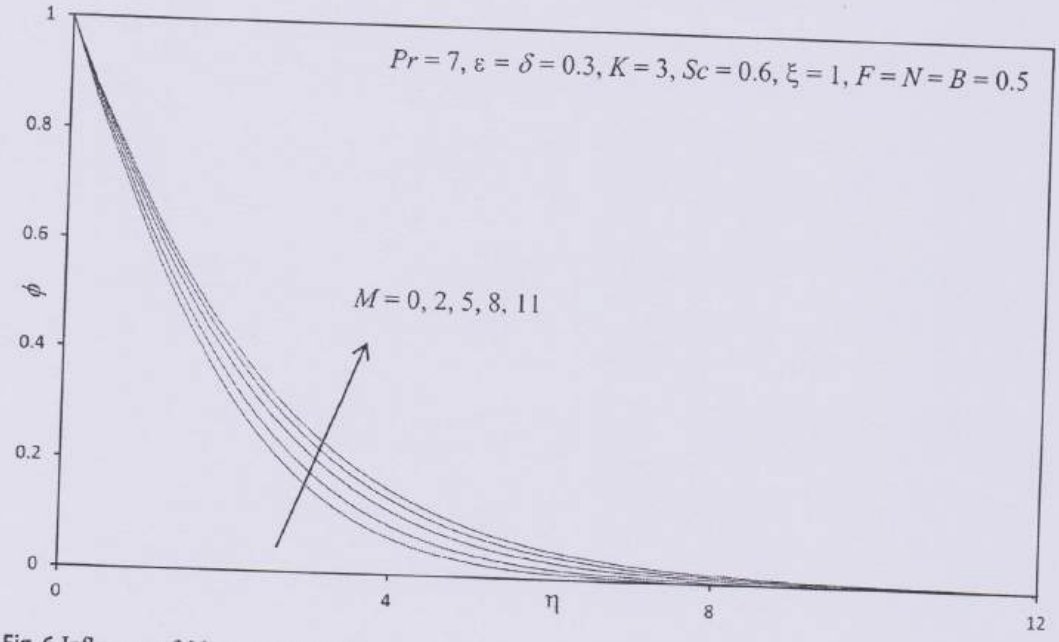


Fig. 6 Influence of M on concentration

seen with increasing M values. As the magnetic field is applied to an electrically conducting fluid, a resistive Lorentz force is created, that operates against the fluid flow. Nevertheless, the fluid velocity is maximum when $M = 0$. As the magnetic waves permeates fluid, particles vibrate at a greater frequency, boosting their kinetic energy. Because the kinetic energy is directly proportional to temperature, a rise in kinetic energy leads to rise in temperature [52].

Figures 7, 8 and 9 illustrates the distributions of velocity (f'), angular velocity i.e. micro-rotation (g) and temperature (θ) for *radiation parameter*, F. The radiation parameter specifies the proportion of heat transfer from thermal radiation to thermal conduction. If $F > 1$, thermal

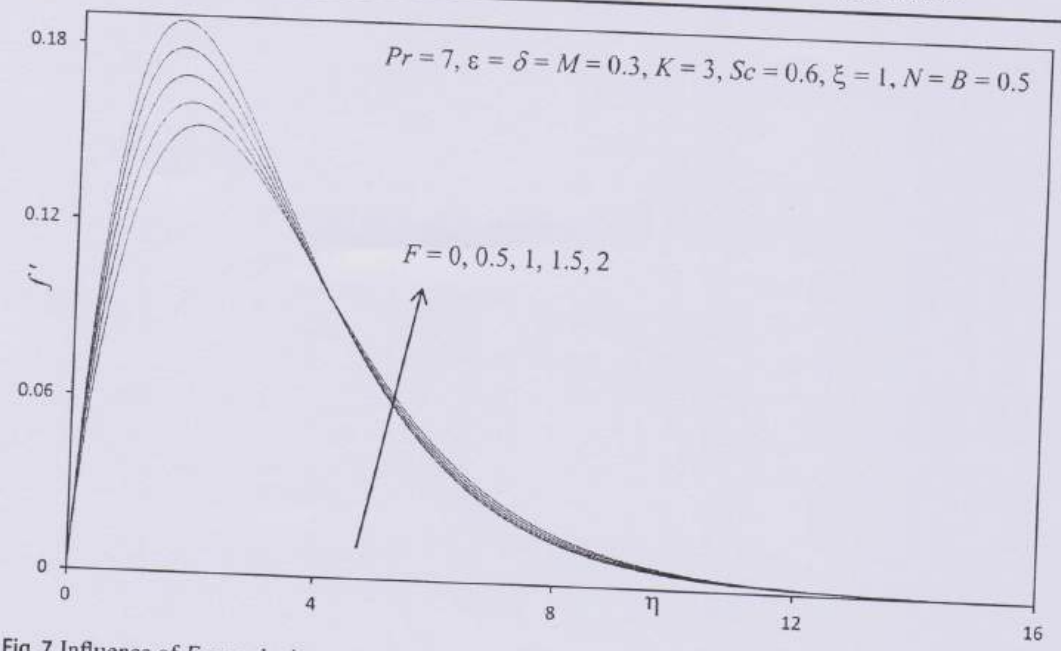


Fig. 7 Influence of F on velocity

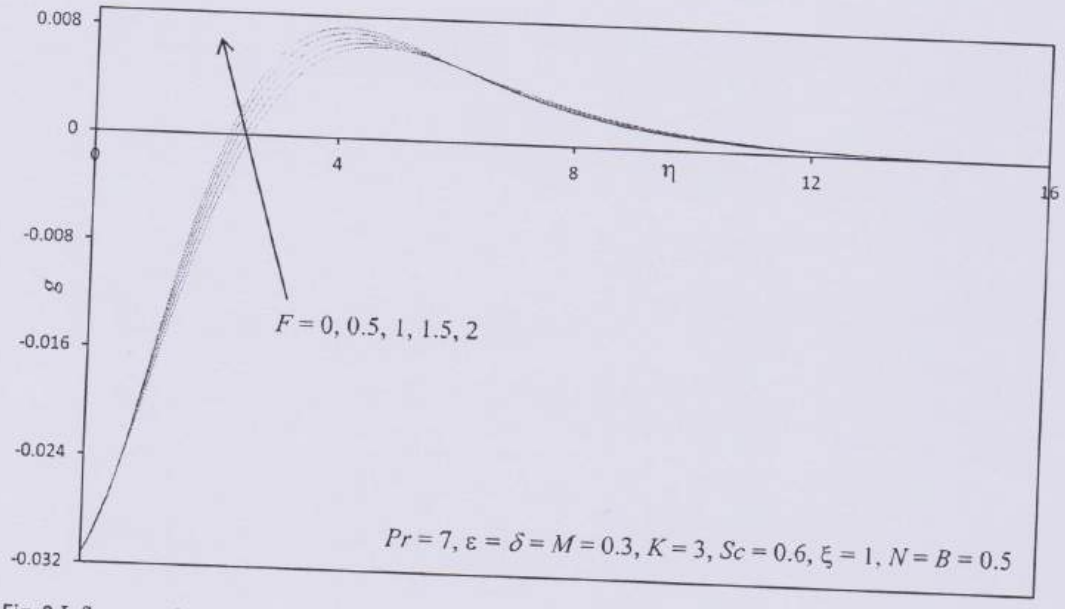


Fig. 8 Influence of F on angular velocity

radiation takes precedence over thermal conduction, if $F < 1$, thermal conduction takes precedence and if $F = 1$, the effects of thermal conduction and radiation are identical. With rising F values, the velocity, angular velocity and temperature distributions accelerates dramatically. Thermal radiation, which emits in the form of electromagnetic waves, is fully dependent on environment temperature. Hence thermal radiation is a function of temperature.

Figures 10, 11 and 12 depicts the effects of vortex viscosity parameter K on the velocity, angular velocity and concentration distributions. From the graphs it is clear that the non-Newtonian micropolar fluid stream-wise velocity ranges from 0 near the wall to maximum

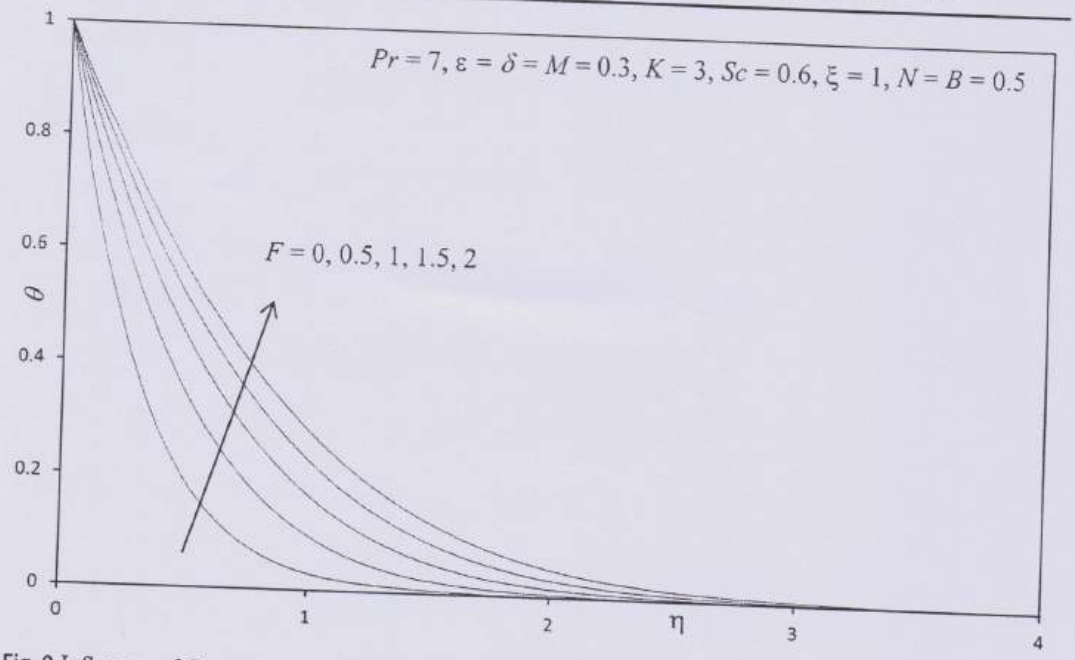


Fig. 9 Influence of F on temperature

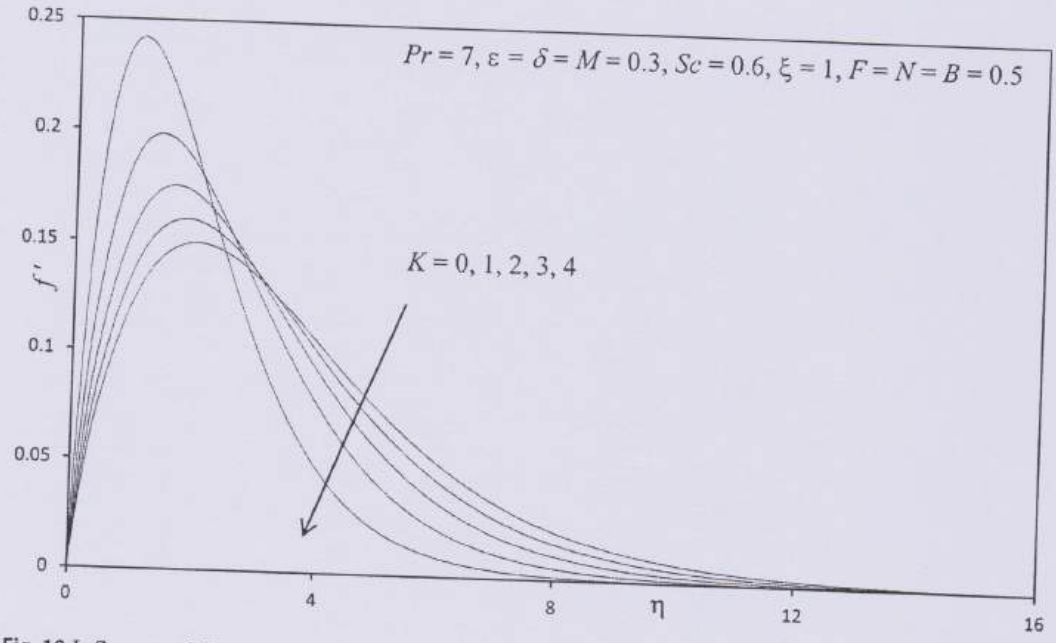


Fig. 10 Influence of K on velocity

and then fades away when the transverse coordinate is raised. Mircropolarity is ignored when $K = 0$, and the equation reduces to Newtonian form. The velocity is maximum at $K = 0$ and reduces as K increases. Both micropolar and Newtonian dynamic viscosities are identical if $K = 1$. The parameter K has a significant influence on all flow parameters. By increasing the vortex viscosity, the angular velocity and concentration distributions are enhanced. The hydrodynamic, thermal and concentration boundary layers are increased and the thicknesses of rotational boundary layer and fluid rotation are decreased. This really is due to the grater

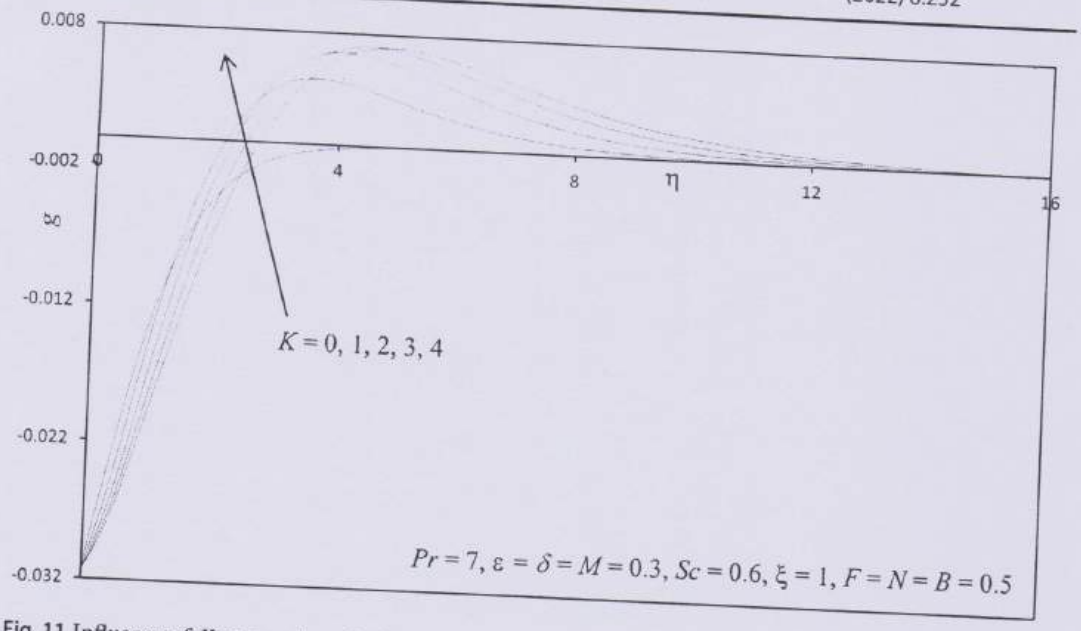


Fig. 11 Influence of K on angular velocity

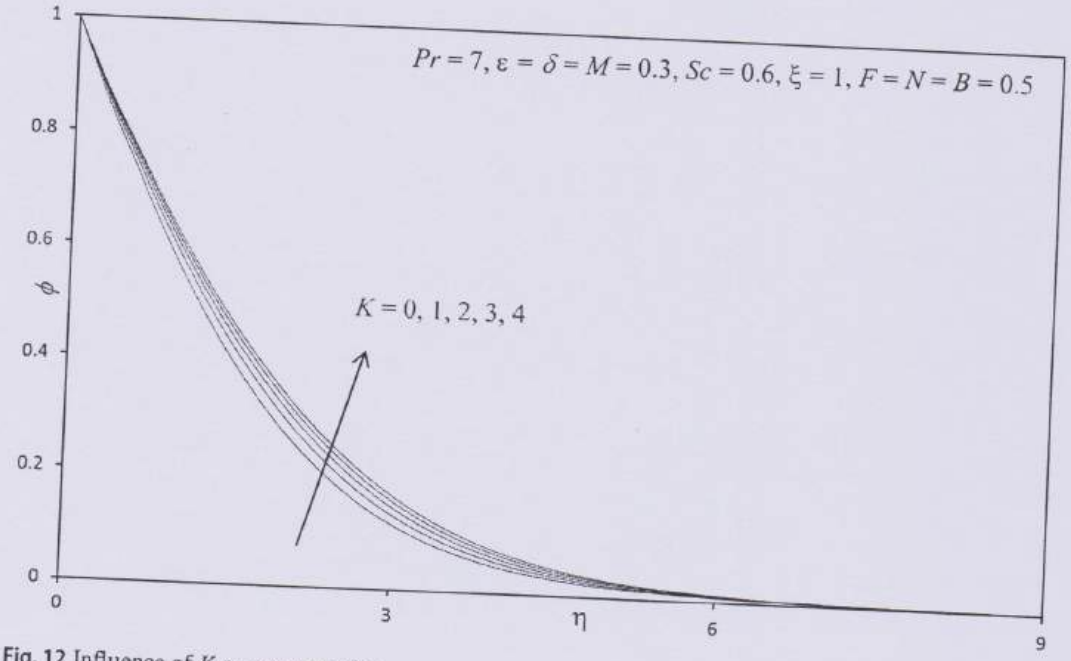


Fig. 12 Influence of K on concentration

mixing of fluid layers caused by the extra shear stress imposed. In contrast to the traditional behavior in flat plate boundary layer flows, a substantial reduction in the primary flow is achieved.

Figure 13 illustrates that as B increases, the angular velocity of micro-elements increases significantly.

Figures 14, 15 and 16 illustrates the profiles for velocity (f'), angular velocity (g) and concentration (ϕ) distributions for variations in *buoyancy ratio parameter* (N). The velocity and angular velocity increase markedly with an increase in N values while concentration is

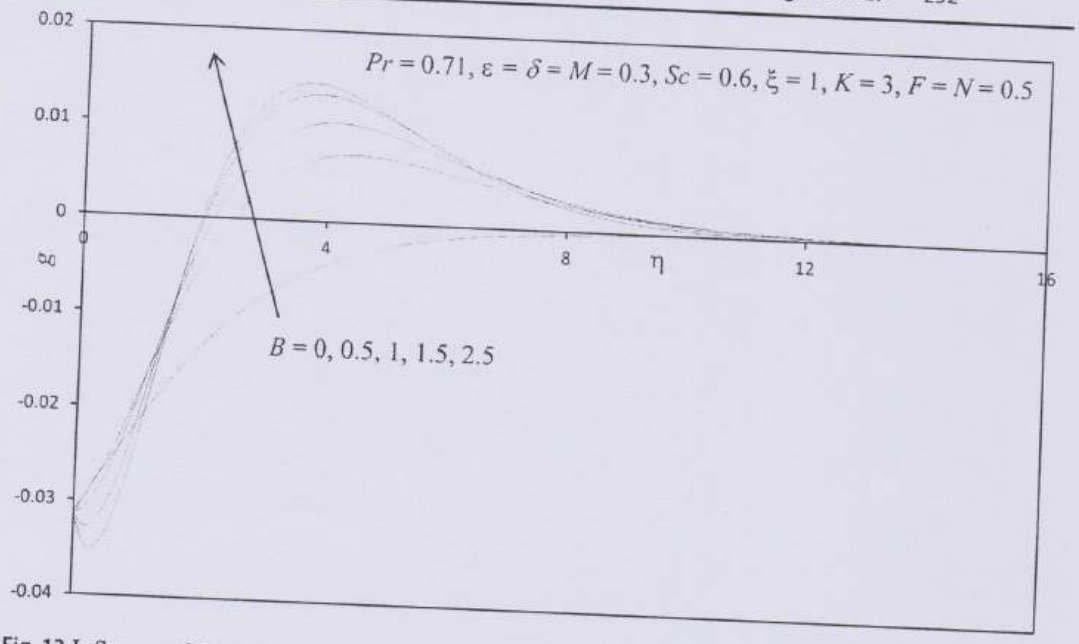


Fig. 13 Influence of B on angular velocity

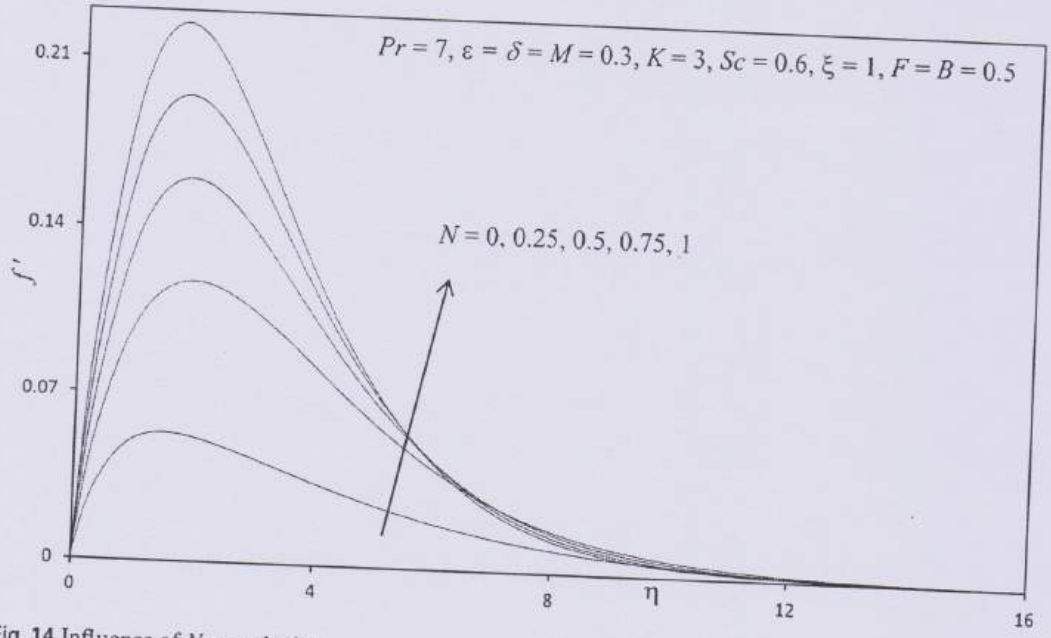


Fig. 14 Influence of N on velocity

depressed. If $N < 1$, the concentration buoyancy force is smaller than the thermal buoyancy force and vice versa if $N > 1$. And if $N = 1$, both buoyancy forces are identical.

Figures 17, 18, 19 and 20 depicts the influences of local non-Newtonian parameter δ on skin friction, wall couple stress, Nusselt number and Sherwood number. A rise in the local non-Newtonian parameter δ, causes the contrary pattern. The slight reduction in Cf and Wcs are observed when δ is greatly increased whereas Nu and Sh increase marginally. As a result, the flow accelerates rapidly down the cone surface, far away from the lower stagnation point. By Def, δ is inversely proportional to the kinematics viscosity (ν) and hence provides a

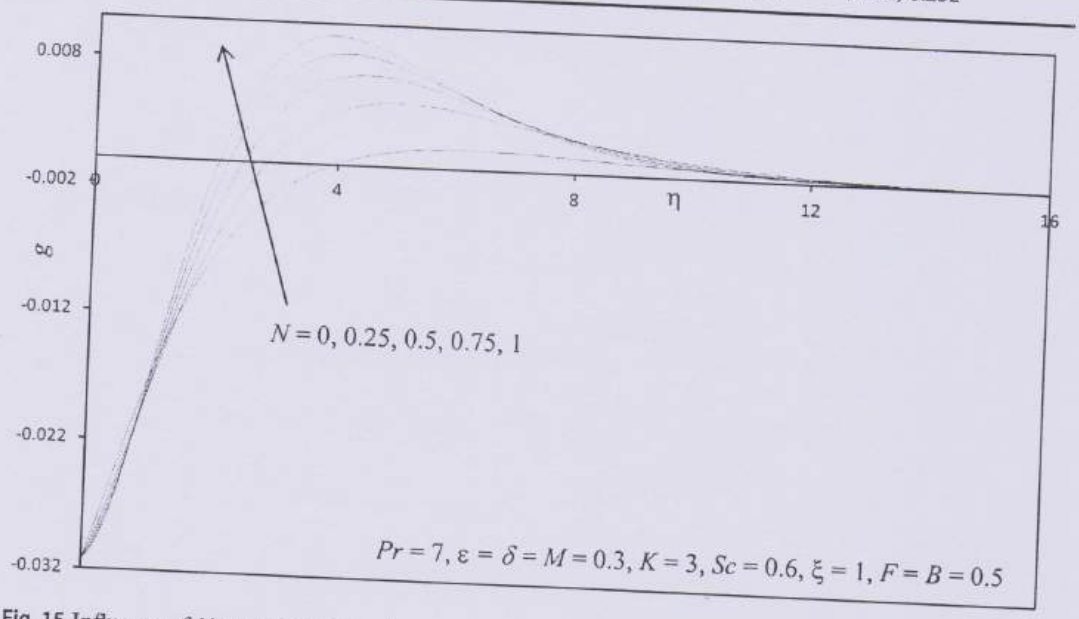


Fig. 15 Influence of N on angular velocity

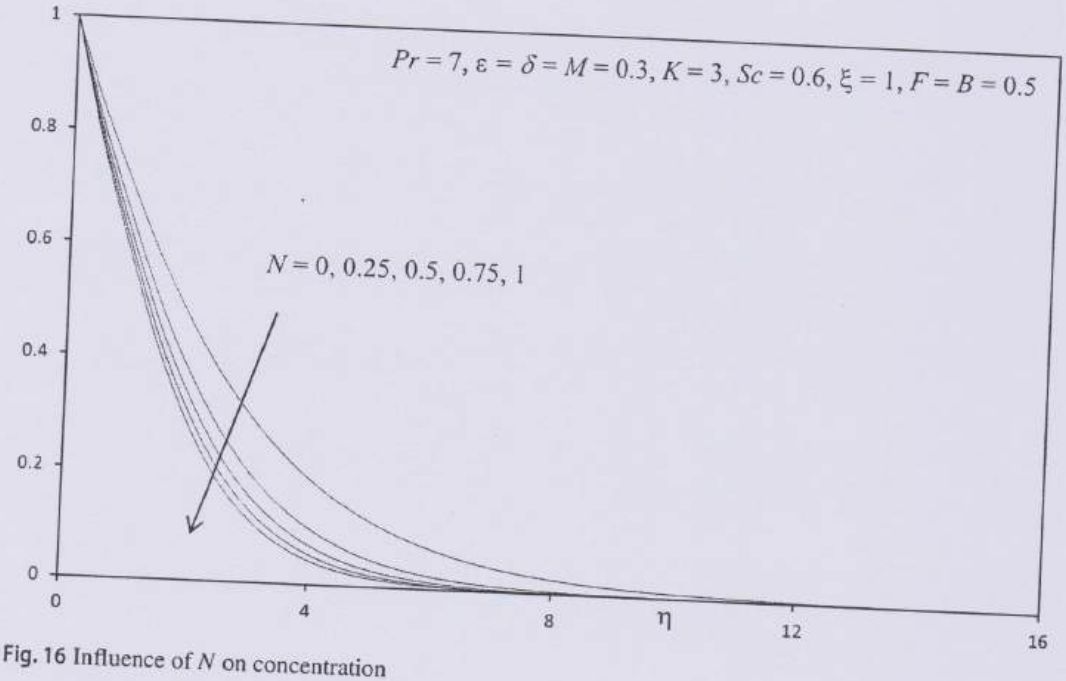


Fig. 16 Influence of N on concentration

substantial resistance to the flow, resulting in a slowdown in shear stresses. In contrast, δ is directly proportional to Grashof number implies that the thermal buoyancy forces rise as δ increases, resulting in a boost in heat transfer by convection from the cone surface.

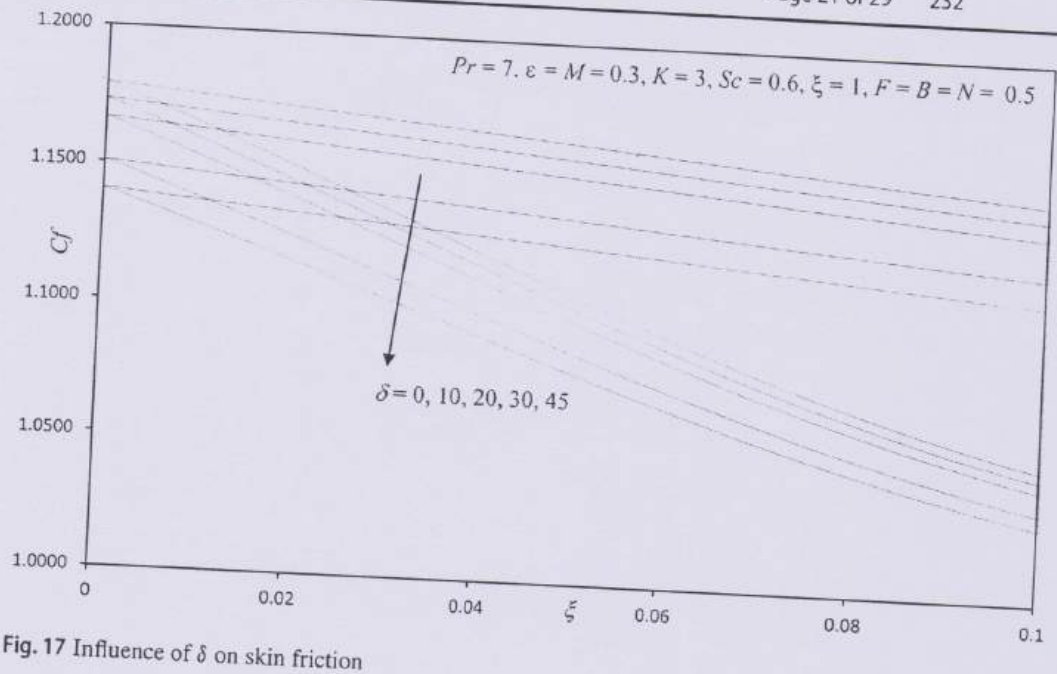


Fig. 17 Influence of δ on skin friction

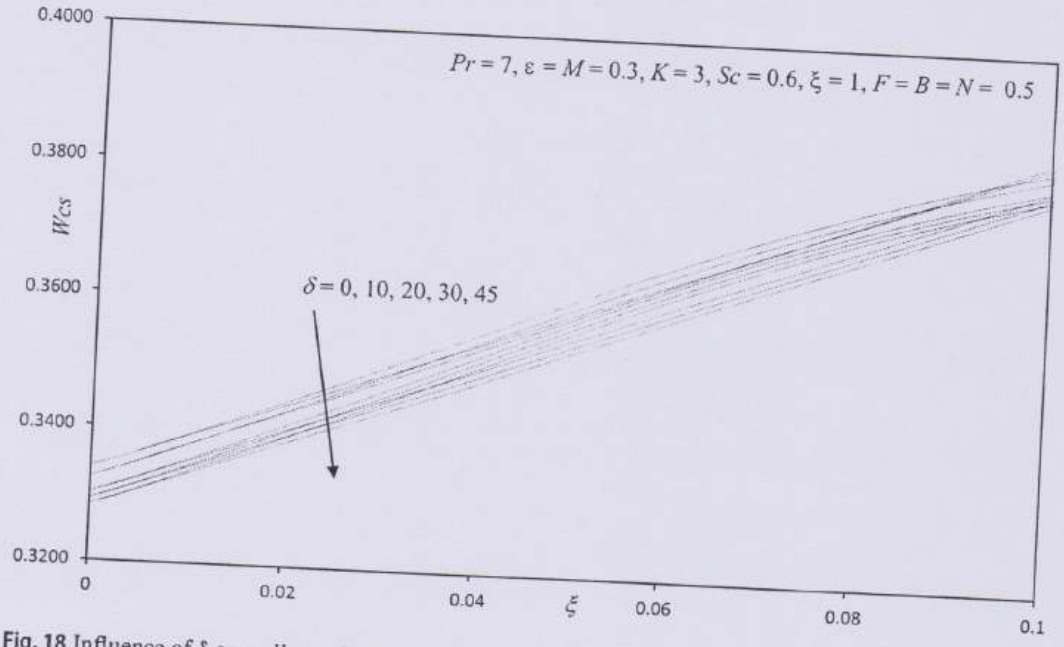


Fig. 18 Influence of δ on wall couple stress

Conclusions

The flow and heat transfer of two-dimensional, steady, laminar, incompressible flows of Eyring–Powell micropolar fluid past an inverted isothermal cone have been explored mathematically in this paper as a model for thermal coating polymer processes in the presence of thermal radiation and magnetic field. The wall and free stream boundary conditions, as well as the governing conservation equations are turned into a non-dimensional boundary value problem using non-similar quantities. The numerical analysis is done using the implicit

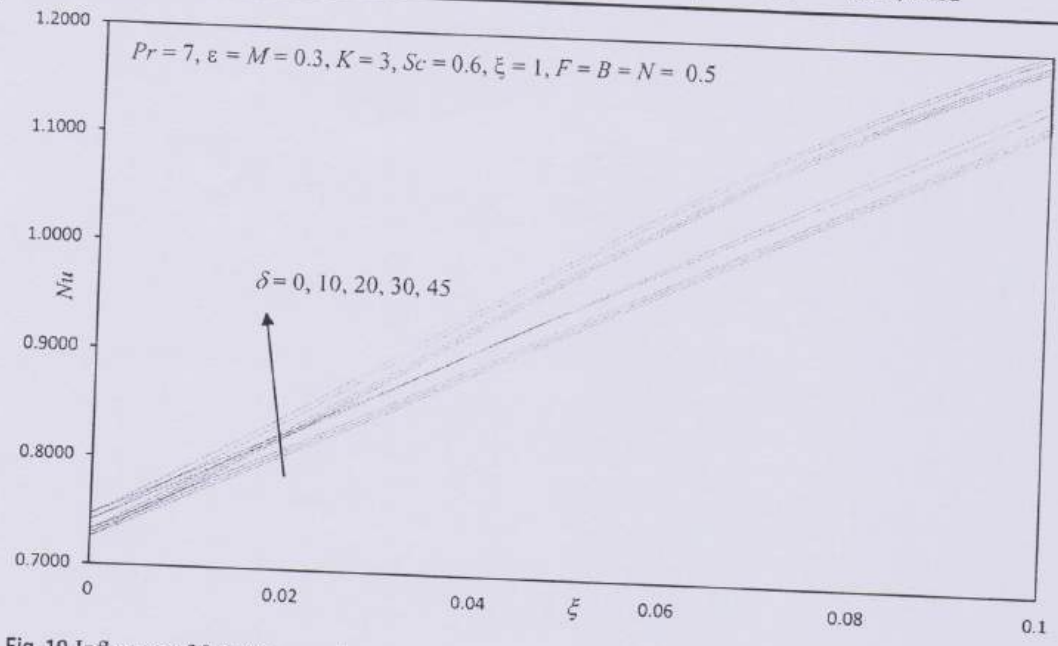


Fig. 19 Influence of δ on Sherwood numer

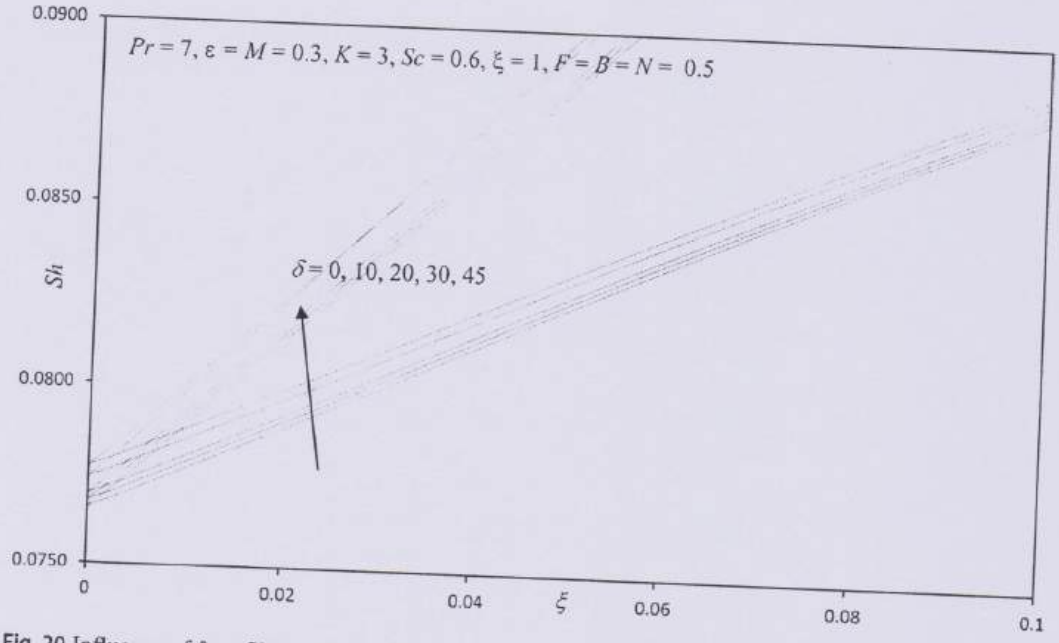


Fig. 20 Influence of δ on Sherwood numer

Keller-Box finite difference method. Validation is carried out using previously published Newtonian solution. The fluctuations of fluid velocity, micro-rotation (angular velocity), temperature, concentration, skin friction, heat and mass transfer rate are studied using graphically and tabular findings. The calculations have revealed that:

1. As the Eyring–Powell parameter, ε, rises velocity and angular velocity decreases and skin friction has increased by 3.38%.

2. A significant reduction in velocity and angular velocity is seen with a rise in M values while concentration increases and the heat and mass transfer rates are reduced by 058% and 6.78% respectively.
3. A rise in F values correspond to a significant rise in velocity, angular velocity and temperature.
4. Increasing K values significantly enhances concentration and micro-rotations but reduce velocity and the skin friction has increased by 1.127%.
5. Increasing buoyancy parameter increases velocity and angular velocity while reduces concentration.

Because the numerical code can solve nonlinear boundary layer equations quickly, it has a lot of potential for modelling transport events in non-Newtonian fluids. It is now being used to explore viscoplastic fluids in curved geometrical systems, which also reflect various chemical engineering working fluids. This article can be expanded to include the unsteady non-Newtonian fluid flows.

Funding The authors have not disclosed any funding.

Data Availability A data availability statement is mandatory for publication in this journal. Please confirm that this statement is accurate, or provide an alternative.

Declarations

Competing interests The authors have not disclosed any competing interests.

Appendix A: Keller Box Numerical Details

The Keller Box Scheme comprises four stages:

1. Decomposition of the Nth order partial differential equation system to N first order equations.
2. Finite difference discretization.
3. Quasilinearization of non-linear Keller algebraic equations and finally.
4. Block-tridiagonal elimination solution of the linearized Keller algebraic equations.

The algebraic details for the present problem are provided in "Appendix A". A typical mesh is given in Fig. 21 below.

Stage 1: Decomposition of Nth Order Partial Differential Equation System to N First Order Equations

Equations (15) to (18) subject to the boundary conditions (19) are first cast as a multiple system of first order differential equations. New dependent variables are introduced:

$$u(x, y) = f', \ v(x, y) = f'', \ s(x, y) = \theta, \ t(x, y) = \theta', \ z(x, y) = \phi, \ m(x, y) = \phi' \tag{24}$$

These denote the variables for velocity, temperature and concentration respectively. Now Eqs. (15) to (18) are solved as a set of fifth order simultaneous differential equations:

$$f' = u \tag{25}$$

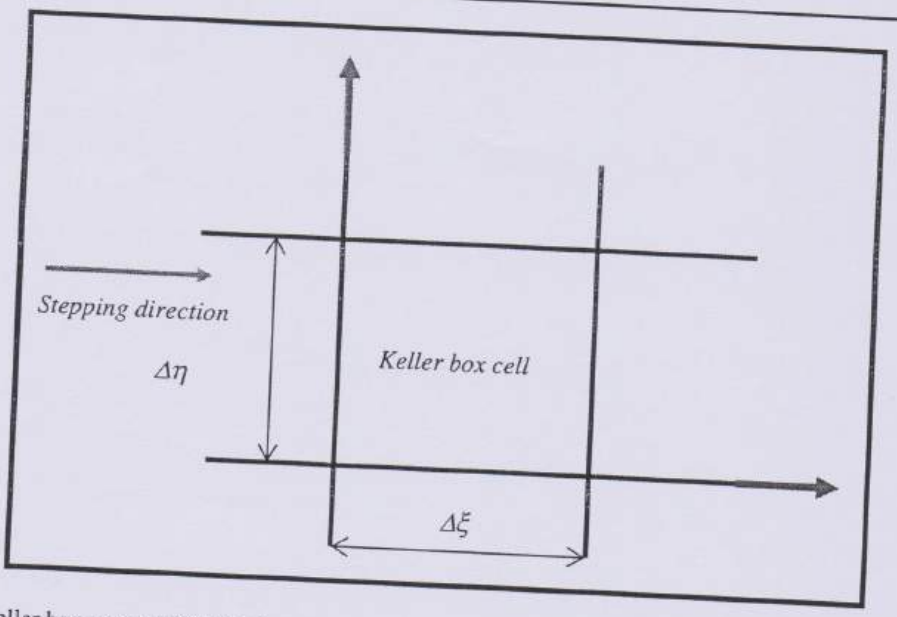


Fig. 21 Keller box computational cell

$$u' = v \tag{26}$$

$$g' = p \tag{27}$$

$$s' = t \tag{28}$$

$$z' = m \tag{29}$$

$$(1 + K + \varepsilon)v' + \frac{7}{4}fv + \xi v - \frac{1}{2}(u)^2 - \varepsilon\delta(v)^2 v' + s + Nz + Kp - M\xi^2 u = \frac{\xi}{4}\left(u\frac{\partial u}{\partial \xi} - v\frac{\partial f}{\partial \xi}\right) \tag{30}$$

$$\left(1 + \frac{K}{2}\right)p' + \frac{7}{4}fp - \frac{1}{4}ug + \xi p - BK\xi^2(2g + v) = \frac{\xi}{4}\left(u\frac{\partial g}{\partial \xi} - p\frac{\partial f}{\partial \xi}\right) \tag{31}$$

$$\frac{t'}{\mathrm{Pr}}\left(1 + \frac{4}{3F}\right) + \frac{7}{4}ft + \xi t = \frac{\xi}{4}\left(u\frac{\partial s}{\partial \xi} - t\frac{\partial f}{\partial \xi}\right) \tag{32}$$

$$\frac{m'}{Sc} + \frac{7}{4}fm + \xi m = \frac{\xi}{4}\left(u\frac{\partial \phi}{\partial \xi} - m\frac{\partial f}{\partial \xi}\right) \tag{33}$$

where primes denote differentiation with respect to the variable, η. In terms of the dependent variables, the boundary conditions assume the form:

$$\begin{aligned} &At \quad \eta = 0, \quad f = 0, \quad v = 0, \quad g = \frac{1}{2}\frac{\partial^2 f}{\partial y^2}, \quad s = 1, \quad z = 1 \\ &As \quad \eta \to \infty, \quad v \to 0, \quad g \to 0, \quad s \to 0, \quad z = 0. \end{aligned} \tag{34}$$

Stage 2: Finite Difference Discretization

A two dimensional computational grid is imposed on the ξ–η plane as depicted in Fig. 20. The stepping process is defined by:

$$\begin{aligned} &\eta_0 = 0, \quad \eta_i = \eta_{i-1} + h_j, \quad j = 1, 2, \ldots, J, \quad \eta_J \equiv \eta_\infty \\ &\xi^0 = 0, \quad \xi^n = \xi^{n-1} + k_n, \quad n = 1, 2, \ldots, N \end{aligned} \tag{35}$$

where k_n and $h_j$denote the step distances in the ξ and η directions respectively. If g_j^n denotes the value of any variable at (η_j, ξ^n), then the variables and derivatives of Eqs. (25) to (33) at $(\eta_{j-1/2}, \xi^{n-1/2})$ are replaced by:

$$g_{j-1/2}^{n-1/2} = \frac{1}{4}\left[g_j^n + g_{j-1}^n + g_j^{n-1} + g_{j-1}^{n-1}\right] \tag{36}$$

$$\left(\frac{\partial g}{\partial \eta}\right)_{j-1/2}^{n-1/2} = \frac{1}{2h_j}\left[g_j^n - g_{j-1}^n + g_j^{n-1} - g_{j-1}^{n-1}\right] \tag{37}$$

$$\left(\frac{\partial g}{\partial \xi}\right)_{j-1/2}^{n-1/2} = \frac{1}{2k^n}\left[g_j^n - g_{j-1}^n + g_j^{n-1} - g_{j-1}^{n-1}\right] \tag{38}$$

The resulting finite-difference approximation of Eqs. (16) to (20) for the mid-point $(\eta_{j-1/2}, \xi^n)$, take the form:

$$h_j^{-1}\left(f_j^n - f_{j-1}^n\right) = u_{j-1/2}^n \tag{39}$$

$$h_j^{-1}\left(u_j^n - u_{j-1}^n\right) = v_{j-1/2}^n \tag{40}$$

$$h_j^{-1}\left(g_j^n - g_{j-1}^n\right) = p_{j-1/2}^n \tag{41}$$

$$h_j^{-1}\left(s_j^n - s_{j-1}^n\right) = t_{j-1/2}^n \tag{42}$$

$$h_j^{-1}\left(z_j^n - z_{j-1}^n\right) = m_{j-1/2}^n \tag{43}$$

$$\begin{aligned} &(1 + K + \varepsilon)\left(v_j - v_{j-1}\right) + \frac{7+\alpha}{4}\frac{h_j}{4}\left(f_j + f_{j-1}\right)\left(v_j + v_{j-1}\right) \\ &+ \xi\frac{h_j}{2}\left(v_j + v_{j-1}\right) - \left(\frac{1}{2} + \frac{\alpha}{4}\right)\frac{h_j}{4}\left(u_j + u_{j-1}\right)^2 \\ &- \varepsilon\delta\left(v_j + v_{j-1}\right)^2\left(v_j - v_{j-1}\right) + \frac{h_j}{2}\left(s_j + s_{j-1}\right) + N\frac{h_j}{2}\left(z_j + z_{j-1}\right) \\ &+ K\frac{h_j}{2}\left(p_j + p_{j-1}\right) - M\xi^2\frac{h_j}{2}\left(u_j + u_{j-1}\right) = [R_1]_{j-/12}^{n-1} \end{aligned} \tag{44}$$

$$\begin{aligned} &\left(1 + \frac{K}{2}\right)(p_j - p_{j-1}) + \frac{7+\alpha}{4}(f_j + f_{j-1})(p_j + p_{j-1}) + \xi(p_j + p_{j-1}) \\ &- \frac{1+\alpha}{4}(u_j + u_{j-1})(g_j + g_{j-1}) - BK\xi^2(2(g_j + g_{j-1}) + (v_j + v_{j-1})) + \frac{\alpha}{4}g_{j-1/2}^{n-1}(g_j + g_{j-1}) \\ &- \frac{\alpha}{4}f_{j-1/2}^{n-1}(f_j + f_{j-1}) = [R_2]_{j-/12}^{n-1} \end{aligned} \tag{45}$$

$$\frac{1}{\mathrm{Pr}}\left(1 + \frac{4}{3F}\right)(t_j - t_{j-1}) + \frac{7+\alpha}{4}(f_j + f_{j-1})(t_j + t_{j-1}) + \xi(t_j + t_{j-1})$$

$$-\frac{\alpha}{4}(u_j+u_{j-1})(s_j+s_{j-1})+\frac{\alpha}{4}s^{n-1}_{j-1/2}(u_j+u_{j-1})$$
$$-\frac{\alpha}{4}u^{n-1}_{j-1/2}(f_j+f_{j-1})=[R_3]^{n-1}_{j-/12} \tag{46}$$

$$\frac{1}{Sc}(m_j-m_{j-1})+\frac{7+\alpha}{4}(f_j+f_{j-1})(m_j+m_{j-1})+\xi(m_j+\tilde{m}_{j-1})$$
$$-\frac{\alpha}{4}(u_j+u_{j-1})(z_j+z_{j-1})+\frac{\alpha}{4}z^{n-1}_{j-1/2}(u_j+u_{j-1})-\frac{\alpha}{4}u^{n-1}_{j-1/2}(z_j+z_{j-1})$$
$$-\frac{\alpha}{4}f^{n-1}_{j-1/2}(m_j+m_{j-1})+\frac{\alpha}{4}m^{n-1}_{j-1/2}(f_j+f_{j-1})=[R_4]^{n-1}_{j-/12} \tag{47}$$

where the following notation applies:

$$\alpha=\frac{\xi^{n-1/2}}{k^n} \tag{48}$$

$$[R_1]^{n-1}_{j-1/2}=-h_j\Bigg[(1+K+\varepsilon)(v')^{n-1}_{j-1/2}+\left(\frac{7-\alpha}{4}\right)(fv)^{n-1}_{j-1/2}+\xi v^{n-1}_{j-1/2}$$
$$-\left(\frac{1}{2}-\frac{\alpha}{4}\right)\left(u^{n-1}_{j-1/2}\right)^2-\varepsilon\delta\left(v^2\right)^{n-1}_{j-1/2}(v')^{n-1}_{j-1/2}+s^{n-1}_{j-1/2}$$
$$+Nz^{n-1}_{j-1/2}+Kp^{n-1}_{j-1/2}-M\xi^2u^{n-1}_{j-1/2}\Bigg] \tag{49}$$

$$[R_2]^{n-1}_{j-1/2}=-h_j\Bigg[\left(1+\frac{K}{2}\right)(p')^{n-1}_{j-1/2}+\left(\frac{7-\alpha}{4}\right)(fp)^{n-1}_{j-1/2}+\xi p^{n-1}_{j-1/2}$$
$$-\left(\frac{1-\alpha}{4}\right)(gu)^{n-1}_{j-1/2}-KB\xi^2\left(2g^{n-1}_{j-1/2}+v^{n-1}_{j-1/2}\right)\Bigg] \tag{50}$$

$$[R_3]^{n-1}_{j-1/2}=-h_j\left[\frac{1}{\mathrm{Pr}}\left(1+\frac{4}{3F}\right)(t')^{n-1}_{j-1/2}+\frac{(7-\alpha)}{4}(ft)^{n-1}_{j-1/2}+\xi t^{n-1}_{j-1/2}+\frac{\alpha}{4}(us)^{n-1}_{j-1/2}\right] \tag{51}$$

$$[R_4]^{n-1}_{j-1/2}=-h_j\left[\frac{1}{Sc}(m')^{n-1}_{j-1/2}+\frac{(7-\alpha)}{4}(fm)^{n-1}_{j-1/2}+\xi m^{n-1}_{j-1/2}+\frac{\alpha}{4}(uz)^{n-1}_{j-1/2}\right] \tag{52}$$

The boundary conditions are:

$$f^n_0=u^n_0=0,\quad g^n_0=1,\quad s^n_0=1,\quad m^n_0=1,\quad u^n_J=0,\quad v^n_J=0,\quad s^n_J=0,\quad m^n_J=0. \tag{53}$$

Step 3: Quasilinearization of Non-linear Keller Algebraic Equations

Assuming f^{n-1}_j, u^{n-1}_j, v^{n-1}_j, s^{n-1}_j, t^{n-1}_j to be known for $0\le j\le J$, then Eqs. (39) to (47) constitute a system of $5J+5$ equations for the solution of $5J+5$ unknowns f^n_j, u^n_j, v^n_j, s^n_j, t^n_j, $j=0, 1, 2\ldots, J$. This *non-linear* system of algebraic equations is *linearized* by means of Newton's method as explained in [22, 43].

Step 4: Block-Tridiagonal Elimination of Linear Keller Algebraic Equations

The linearized system is solved by the *block-elimination* method owing to its *block-tridiagonal* structure. The block-tridiagonal structure generated consists of *block matrices*. The complete linearized system is formulated as a *block matrix system*, where each element in the coefficient matrix is a matrix itself, and this system is solved using the efficient Keller-box method. The numerical results are strongly influenced by the number of mesh points in both directions. After some trials in the η-direction (radial coordinate) a larger number of mesh points are selected whereas in the ξ-direction (tangential coordinate) significantly less mesh points are necessary. η_{max} has been set at 16 and this constitutes an adequately large value at which the prescribed boundary conditions are satisfied. ξ_{max} is set at 3.0 for the simulations. *Mesh independence* has been comfortably attained in the simulations. The numerical algorithm is executed in MATLAB on a PC. The method demonstrates excellent stability, convergence and consistency, as elaborated by Keller [43].

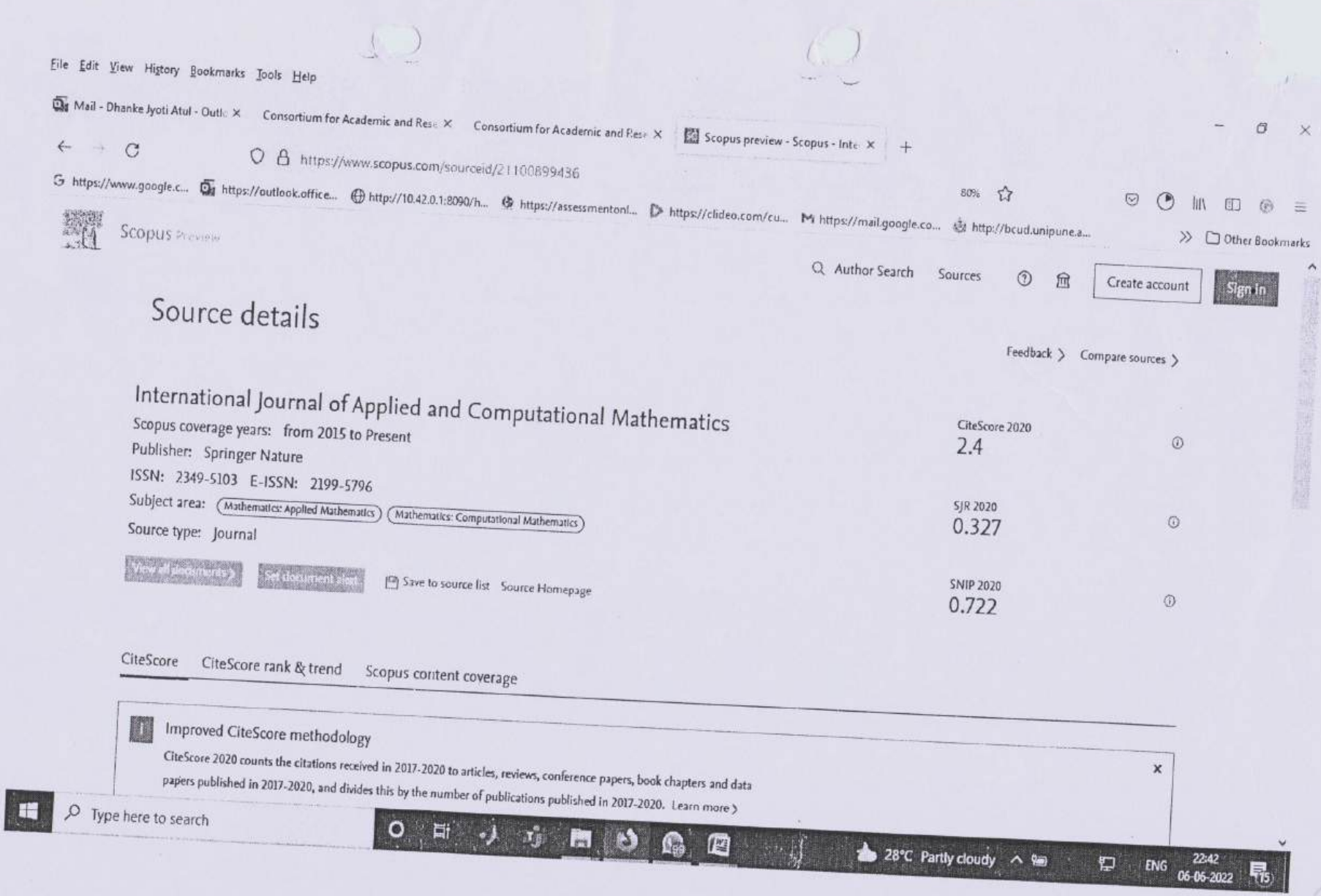
References

1. Eringen, A.C.: Simple microfluids. Int. J. Eng. Sci. **2**, 205–217 (1964)
2. Eringen, A.C.: Theory of micropolar fluids. J. Math. Mech. **16**, 1–18 (1966)
3. Eringen, A.C.: Micro-continuum Field Theories- II: Fluent Media. Springer, Berlin (2001)
4. Habib, D., Abdal, S., Ali, R., Baleanu, D., Siddique, I.: On bioconvection and mass transpiration of micropolar nanofluid dynamics due to an extending surface in existence of thermal radiations. Case Stud. Thermal Eng. **27**, 101239 (2021)
5. Yadav, P.K., Kumar, A.: An inclined magnetic field effect on entropy production of non-miscible Newtonian and micropolar fluid in a rectangular conduit. Int. Commun. Heat Mass Transf. **124**, 105266 (2021)
6. Ramesh, G.K., Roopa, G.S., Rauf, A., Shehzad, S.A., Abbasi, F.M.: Time-dependent squeezing flow of Casson-micropolar nanofluid with injection/suction and slip effects. Int. Commun. Heat Mass Transf. **126**, 105470 (2021)
7. Nabwey, H.A., Mahdy, A.: Transient flow of micropolar dusty hybrid nanofluid loaded with Fe304-Ag nanoparticles through a porous stretching sheet. Results Phys. **21**, 103777 (2021)
8. Singh, K., Pandey, A.K., Kumar, M.: Numerical solution of micropolar fluid flow via stretchable surface with chemical reaction and melting heat transfer using Keller-Box method. Propuls. Power Res. **10**(2), 194–207 (2021)
9. Khader, M.M., Sharma, R.P.: Evaluating the unsteady MHD micropolar fluid flow past stretching/shirking sheet with heat source and thermal radiation: implementing fourth order predictor-corrector FDM. Math. Comput. Simul. **181**, 333–350 (2021)
10. Bég, O.A., Vasu, B., Ray, A.K., Beg, T.A., Kadir, A., Leonard, H.J., Gorla, R.S.R.: Homotopy simulation of dissipative micropolar flow and heat transfer from a two-dimensional body with heat sink effect: applications in polymer coating. Chem. Biochem. Eng. Q. **34**(4), 257–275 (2020)
11. Anwar Beg, O., Ferdows, M., Enamul Karim, M., Maruf Hasan, M., Bég, T.A., Shamshuddin, M.D., Kadir, A.: Computation of non-isothermal thermo-convective micropolar fluid dynamics in a hall MHD generator system with non-linear distending wall. Int. J. Appl. Comput. Math **6**, 42 (2020). https://doi.org/10.1007/s40819-020-0792-y
12. Nabwey, A., Mahdy, A.: Numerical approach of micropolar dust-particles natural convection fluid flow due to a permeable cone with nonlinear temperature. Alex. Eng. J. **60**, 1739–1749 (2021)
13. Sarala Devi, T., Venkata Lakshmi, C., Venkatadri, K., Suryanarayana Reddy, M.: Influence of enternal magnetic wire on natural convection of non-Newtonian fluid in a square cavity. Partial Differ. Equ. Appl. Math. **4**, 100041 (2021)
14. Ge-JiLe, Hu., Nazeer, M., Hussain, F., et al.: Two-phase flow of MHD Jeffery fluid with the suspension of tiny metallic particles incorporated with viscous dissipation and porous medium. Adv. Mech. Eng. **3**(3), 1–15 (2021). https://doi.org/10.1177/16878140211005960
15. Olabode, J.O., Idown, A.S., Akolade, M.T., Titiloye, E.O.: Unsteady flow analysis of Maxwell fluid with temperature dependent variable properties and quadratic thermo-solutal convection influence. Partial Differ. Equ. Appl. Math. **4**, 100078 (2021)

39. Siddiqui, B.K., Batool, S., Malik, M.Y., Mahmood ul Hassan, Q., Alqahtani, A.S.: Darcy Forchheimer bioconvection flow of Casson nanofluid due to a rotating and stretchingdisk together with thermal radiation and entropy generation. Case Stud. Therm. Eng. (2021). https://doi.org/10.1016/j.csite.2021.101201
40. Waqas, H., Khan, S.A., Farooq, U., Khan, I., Alotaibi, H., Khan, A.: Melting phenomenon of non-linear radiative generalized second grade nanoliquid. Case Stud. Therm. Eng. **26**, 101011 (2021). https://doi.org/10.1016/j.csite.2021.101011
41. Al-Mdalla, Q.M., et al.: Ree-Eyring fluid flow of Cu-water nanofluid between infinite spinning disks with an effect of thermal radiation. Ain Shams Eng. J. (2021). https://doi.org/10.1016/j.asej.2020.12.016
42. Majeed, A., Zeeshan, A., Amin, N., Ijaz, N., Saeed, T.: Thermal analysis of radiative bioconvection magnetohydrodynamic flow comprising gyrotactic microorganism with activation energy. J. Therm. Anal. Calorim. **143**, 2545–2556 (2021)
43. Keller, H.B.: Numerical methods in boundary-layer theory. Ann. Rev. Fluid Mech. **10**, 417–433 (1978). https://doi.org/10.1146/annurev.fl.10.010178.002221
44. Hossain, M.A., Paul, S.C.: Free convection from a vertical permeable circular cone with non-uniform surface temperature. Acta Mech. **151**, 103–114 (2001)
45. Powell, R.E., Eyring, H.: Mechanism for relaxation theory of viscosity. Nature **154**, 427–428 (1944)
46. Beg, O.A., Bhargava, R., Rashidi, M.M.: Numerical Simulation in Micropolar Fluid Dynamics. Lambert, Saarbrucken
47. Gorla, R.S.R.: Radiative effect on conjugate forced convection in a laminar wall jet along a flat plate. In: Encyclopedia Fluid Mechanics, Suppl. 3: Advances in Flows Dynamics, Gulf Publishing, Texas, USA (1993)
48. Bég, O., Anwar, J., Zueco, S.K., et al.: Unsteady magnetohydrodynamic heat transfer in a semi-infinite porous medium with thermal radiation flux: analytical and numerical study. Adv. Numer. Anal. **2011**, 1–17 (2011)
49. Vedavathi, N., Dharmaiah, G., Abdul Gaffar, S., Venkatadri, K.: Entropy analysis of nanofluid magnetohydrodynamic convection flow past an inclined surface: a numerical review. Heat Transf. J. **50**(6), 5996–6021 (2021)
50. Vedavathi, N., Dharmaiah, G., Abdul Gaffar, S., Venkatadri, K.: Entropy analysis of magnetohydrodynamic nanofluid transport from an inverted cone: Buongiorno's model. Heat Transf. J. **50**(4), 3119–3153 (2021). https://doi.org/10.1002/htj.22021
51. Ramesh Reddy, P., Abdul Gaffar, S., Anwar Beg, O., Hidayathulla Khan, B.M.: Hall and ionslip effects on nanofluid transport from a vertical surface: Buongiorno's model. ZAMM (2021). https://doi.org/10.1002/zamm.202000174
52. Khan, N.M., Abidi, A., Khan, I., Alotaibi, F., Alghtani, A.H., Aljohani, M.A.: Dynamics of radiative Eyring–Powell MHD nanofluid containing gyrotactic microorganisms exposed to surface suction and viscosity variation. Case Stud. Therm. Eng. **28**, 101659 (2021)

Publisher's Note Springer Nature remains neutral with regard to jurisdictional claims in published maps and institutional affiliations.

Springer Nature or its licensor holds exclusive rights to this article under a publishing agreement with the author(s) or other rightsholder(s); author self-archiving of the accepted manuscript version of this article is solely governed by the terms of such publishing agreement and applicable law.


File Edit View History Bookmarks Tools Help
Mail - Dhanke Jyoti Atul - Outlc
Consortium for Academic and Rese
Consortium for Academic and Rese
Scopus preview - Scopus - Inte
https://www.scopus.com/sourceid/21100899436
https://www.google.c...
https://outlook.office...
http://10.42.0.1:8090/h...
https://assessmentonl...
https://clideo.com/cu...
https://mail.google.co...
http://bcud.unipune.a...
Other Bookmarks
80%
Scopus Preview
Author Search
Sources
Create account
Sign In
Source details
Feedback
Compare sources
International Journal of Applied and Computational Mathematics
Scopus coverage years: from 2015 to Present
Publisher: Springer Nature
ISSN: 2349-5103 E-ISSN: 2199-5796
Subject area: Mathematics: Applied Mathematics
Mathematics: Computational Mathematics
Source type: Journal
Save to source list
Source Homepage
CiteScore 2020
2.4
SJR 2020
0.327
SNIP 2020
0.722
CiteScore
CiteScore rank & trend
Scopus content coverage
Improved CiteScore methodology
CiteScore 2020 counts the citations received in 2017-2020 to articles, reviews, conference papers, book chapters and data papers published in 2017-2020, and divides this by the number of publications published in 2017-2020.
Learn more
Type here to search
28°C Partly cloudy
ENG
22:42
06-06-2022

International Journal of Engineering Trends and Technology
ISSN: 2231–5381 / https://doi.org/10.14445/22315381/IJETT-V71I5P218

Volume 71 Issue 5, 175-181, May 2023
© 2023 Seventh Sense Research Group®

Original Article

Mathematical Modelling of Response Parameters During Ultrasonic Assisted Electro-Discharge Machining Process

Atish Mane[1], Pradeep.V.Jadhav[2], Shankar Kadam[3], Jyoti Dhanke[4], Prashant Kadam[5], Amruta Pasarkar[6]

[1]*Department of Mechanical Engineering, Bharati Vidyapeeth Deemed University, College of Engineering, Pune, India*
[2]*Department Mechanical Engineering, Bharati Vidyapeeth Deemed University, College of Engineering, Pune, Maharashtra, India*
[1,3,4,5,6]*Bharati Vidyapeeth College of Engineering, Lavale Pune, Maharashtra, India*

[1]*Corresponding Author : mane.atish@bharatividyapeeth.edu*

Received: 07 January 2023 Revised: 18 April 2023 Accepted: 11 May 2023 Published: 25 May 2023

Abstract *- Choosing the optimum production conditions is one of the most important aspects of the Electric Discharge Machining operation because they affect critical variables such as roughness and rate of metal removal. Because this advanced material presents manufacturing issues if formed by standard methods, machining of Ni-Ti alloys is often attempted utilizing unconventional techniques for manufacturing, particularly EDM. In this work, shape memory alloy (NiTi) with ultrasonic vibration was used in the experiment. The work explains an effort to apply a low-frequency vibration on a shape memory alloy (NiTi) workpiece during the EDM process. Electrolytic copper tools on a die-sink discharge machine are utilized in the experiment to perform EDM on NiTi alloy. In the current work, a model for roughness and rate of metal removal during ultrasonic-aided electro-discharge machining (USA-EDM) of NiTi shape memory alloy using Buckingham's Pi-theorem has been attempted. The test finding shows that altering key dimensionless π parameters had a considerable impact on the values of roughness (SR) and rate of metal removal. Roughness (SR) and rate of metal removal (MRR) values predicted by the model created using Buckingham pi theorem and dimensions analysis are close to experimental findings.*

Keywords *- Ultrasonic Assisted Electro-Discharge Machine (USA-EDM), Roughness (SR), Rate of Metal Removal (MRR), Shape Memory Alloy (NiTi), Buckingham pi Theorem.*

1. Introduction

Electrically conductive materials, regardless of hardness, like metals, graphite, metallic alloys, and even some ceramic conductive materials, can be machined utilizing the widely used advanced manufacturing technology known as electrical discharge machining (EDM). It is commonly employed to manufacture surgical, automotive, aerospace, and mold and die components [1]. In this method, the workpiece and electrode repeatedly discharge electrically to remove material from the workpiece. In a gas or a dielectric liquid, this electric sparking process occurs. Small Viscosity, the strength of the dielectric high, efficient cooling, and flushing capacity are some of the desirable characteristics of an ideal dielectric [2]. E. Aliakbari et al. [4] discovered the optimal rotating process parameter setting and concluded from this study that current, on-time of pulse, the rotational speed of electrode, and electrode morphologies have the greatest impact on MRR, EWR, and SR as input parameters. They discovered the optimal rotating process parameter setting and concluded from this study that current, pulse on time, electrode rotational speed, and electrode morphologies have the greatest impact on MRR, EWR, and SR as input parameters. Cut width and depth are the factors that have the biggest impact on rough machining; according to Bala Murugan Gopalsamy et al. [6], cutting speed is the most significant element in final machining. Minhat et al. [7] provided the beginning, ignition, and discharge phases as the foundation for their mathematical model of EDM pulses. The model, however, was unable to identify the EDM profiles accurately, and the mathematical equations did not match the profiles in all stages. Bains et al. [9], and Ravindranath et. al.[10], used dimensional analysis and considered thermo-mechanical parameters to construct a mathematical model for Metal removal rate and surface roughness. Dimensional evaluation is a method where the most influential variables defining actual phenomena are chosen to formulate dimensionally correct equations. In dimensional analysis, mathematical models are created using algebraic equations [12]. The first and most crucial step in the dimensional analysis is to determine the variables that may have an impact on the outcome. The three types of variables are dependent, independent, and extraneous. It is possible to use response

This is an open access article under the CC BY-NC-ND license (http://creativecommons.org/licenses/by-nc-nd/4.0/)

surface methodology (RSM) to build an empirical model that predicts the roughness and rate of metal removal. The RSM model was only constrained by the settings for the machine. As a result, a dimensional model is created that considers both thermos physical and machine setup characteristics [14.16]. The current study solves the Multi-Response Optimization issue by applying an ideal parametric collection of input variables like on Time, off Time, and Voltage [19]. This study examines the influence of Cu, the nanopowder, on electrical current-discharge machining (EDM) on the difficult-to-cut material Titanium matrix composite (TMCs). The final result demonstrated that Cu nanopowder influences both response parameters. MRR of the machining process improves with greater volume quantity, but TWR increases as well due to the inclusion of Cu nanopowder. The significance of the experiment is explained by the ANOVA result [20]. The appropriate specifications assure that the turned product has a high surface quality. According to a review of the literature, there is little information available on the effect of the copper electrode on NiTi material utilizing RSM. It was also discovered that the majority of research published was restricted to a certain range of process parameters that create responses in the finish, semi-finish, or roughing regions. In this paper, mathematical models for linking the SR and MRR were established. The Buckingham Pi theorem is employed in the current work to try to create a link between process variables, thermal-mechanical features, and performance indicators. The goal is to create a mathematical model that can estimate the rate of metal removal (MRR) during ultrasonic EDM while varying process parameters like gap current, on-time of the pulse, off-time of the pulse, voltage, electrical conductivity of workpiece, and electrical conductivity of tool electrode during the experiments, electric discharge machining of Ni-Ti alloy was conducted.

1.1. Experimental Setup

The die sinks EDM equipment was used for testing, as illustrated in Fig 1. The tool was chosen to be copper, which serves as the cathode, and the workpiece was chosen to be a shape memory alloy (NiTi), which acts as an anode. For machining, 20 x 20 x 15 mm shape memory alloy plates were chosen. The low-frequency vibration generator was linked to a workpiece controlling the frequency and amplitude. The component was vibrated with low-frequency and low-frequency fluctuations.

1.1.1. Duty cycle (τ)

It is a proportion of the overall cycle time to the on-time. The on-time is divided by the entire cycle duration to calculate this.

$$\tau = T_{on} / (T_{on} + T_{off}) \qquad (1)$$

1.2. Design of Experiments

Experiment planning was carried out in this study using the central composite rotatable design (CCRD) of the response surface method (RSM). To accomplish the desired objectives/goals, also known as responses, the influential parameters (also known as factors) were changed within a specific range. Some settings remained constant throughout the experiment.



Fig. 1 USA-EDM setup

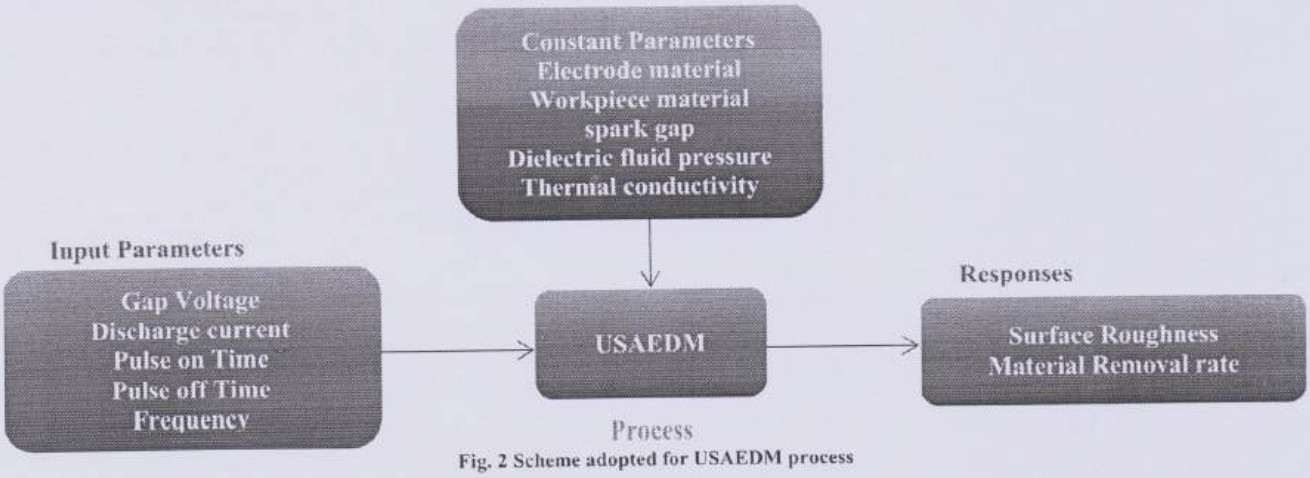


Fig. 2 Scheme adopted for USAEDM process

Fig. 2. shows the process parameters selected for USAEDM of shape memory alloy to achieve the desired response roughness of surface and rate of metal removal rate.

1.3. Factorial Design

Tests were created using the design of experiments. In this investigation, five input parameters with five levels each were used.

After conducting an experimental analysis, The findings were utilized to build a model using mathematics with various parametric combinations. Buckingham's theorem, a dimensional analysis, was applied to investigate the link between the SR, MRR, and machining variables. The projected SR and MRR determined with a model of mathematics were then compared to the experimental findings to test the design. [18].

Dimensional analysis is a strategy for formulating dimensionally correct equations by selecting the most relevant variables describing actual events. Algebraic equations are used to develop mathematical models in dimensional analysis. The first and most important stage in dimensional analysis is identifying the variables that may influence the outcome. Variables are classified into three types: dependent, independent, and superfluous. Response surface methodology (RSM) can be used to create an empirical model that predicts roughness and metal removal rate. The RSM model was only limited by the machine settings. As a result, a dimensional model is produced that takes into account both thermophysical and machine setup parameters.

1.4. Buckingham's 'π' Theorem

A mathematical strategy called the Buckingham Pi Theorem enables the development of a relationship for a quantity of interest between the model and the actual scenario [20]. The operational connection between the process variables and roughness and metal removal rate is determined in this work utilizing the dimensional analysis Buckingham Pi theorem. Selecting repeating and non-repeating variables is necessary before building the model using the Pi theorem.

Table 1. Machine parameters and their related variation levels

EDM Parameter	Unit	Level1	Level2	Level3	Level4	Level5
Gap Voltage	V	25	45	65	85	105
Discharge current	A	10	15	20	25	30
Pulse On Time	us	30	45	60	75	90
Pulse Off Time	us	6	8	10	12	14
Frequency	Hz	200	250	300	350	400

Fundamental dimensions and repeating variables both have an equal number of instances. Therefore, the following criteria were used to identify six recurring parameters.

1. Because SR and MRR are dependent variables, it could not be the recurring responses.
2. The recurring variable must have geometric, flow, or fluid qualities.
3. A dimensionless group should not be formed by each repeating variable.
4. The essential dimensions of a recurring parameter should be the same.
5. The dimensions of two recurring variables must not be the same. The suggested model may express the mass rate of material removal (MRR) and roughness of the surface rate in terms of the other parameters given in Eqs. (2) and (3). 'f' reflects the relationship between input variables and empirically determined response parameters.

Table 2. Parameters with associated dimensions, symbols, and measurement systems

Sr. No	Parameters	Symbol	Unit	Dimension
1	Material removal Rate	MRR	g/min	$M\,T^{-1}$
2	Roughness of Surface	Ra	µm	L
3	On-Time pulse	Ton	µs	T
4	Off-Time pulse	Toff	µs	T
5	Electrical resistivity	R	µ Ω-m	$ML^3T^{-3}I^{-2}$
6	Frequency	F	Hz	T^{-1}
7	Material Density	ρ	g/cm3	$M\,L^{-3}$
8	on time Ultrasonic	UT_{on}	µs	T
9	off time Ultrasonic	UT_{off}	µs	T
10	Specific heat	CP	J/goC	$L^2\,T^{-2}\,\Theta^{-1}$
11	Duty Cycle	DC		1
12	Voltage	V	V	$ML^2T^{-3}I^{-1}$
13	Current	I	A	I
14	The amplitude of Ultrasonic Vibration	A	µm	L
15	Material Conductivity	Mc	S/m	$M^{-1}L^{-3}\,T\,Q^2$
16	conductivity of Thermal	K	W/m-K	$M\,L\,T^{-3}\,\Theta^{-1}$
17	Flushing pressure	F_p	Kg/cm^2	$M\,L^{-2}$

$$MRR = f(\text{Ton, Toff, R, F, } \rho, T_{on}, UT_{off}, \text{CP, DC, V, I, A, Mc, K, } F_p) \quad (2)$$

$$Ra = f(\text{Ton, Toff, R, F, } \rho, \text{Ton, UToff, CP, DC, V, I, A, Mc, K, Fp}) \quad (3)$$

A Dimensional model for MRR and Ra is developed using a total of 17 variables, as shown in

The fundamental variables in the present instance are mass (M), length (L), time (T), temperature (θ) and, current (I), charge (Q). As a result, the total number of factors is seventeen, and the basic dimensions are six, seventeen, and six. n =17 and r = 6; thus, the, Π = n – r = 11. The current investigation, Π Terms

$\Pi_{R1} = MRR\,[V]^a[A]^b[M_c]^c[F_p]^d[k]^e[I]^f$

$\Pi_{R1} = [M\,T^{-1}]\,[ML^2T^{-3}I^{-1}]^a\,[L]^b\,[M^{-1}L^{-3}\,TQ^2]^c\,[M\,L^{-2}]^d[M\,L\,T^{-3}\,\Theta^{-1}]^e[I]^f$

$\Pi_{R1} = \frac{MRR_g}{V^{1/3}A^{2/3}Fp^{2/3}I^{1/3}}$

$\Pi_{R2} = SR\,[V]^a[A]^b[M_c]^c[F_p]^d[k]^e[I]^f$

$\Pi_{R2} = \frac{S_R}{A}$

$\Pi_3 = T_{on}[V]^a[A]^b[M_c]^c[F_p]^d[k]^e[I]^f$

$\Pi_3 = \frac{T_{on}I^{1/3}V^{1/3}A^{4/3}}{F_p^{1/3}}$

$\Pi_4 = T_{off}[V]^a[A]^b[M_c]^c[F_p]^d[k]^e[I]^f$

$\Pi_4 = \frac{T_{off}I^{1/3}V^{1/3}A^{4/3}}{F_p^{1/3}}$

$\Pi_5 = R\,[V]^a[A]^b[M_c]^c[F_p]^d[k]^e[I]^f$

$\Pi_5 = \frac{RI}{VA}$

$\Pi_6 = F[V]^a[A]^b\,[M_c]^c\,[F_p]^d\,[k]^e\,[I]^f$

$\Pi_6 = \frac{F\,A^{4/3}Fp^{1/3}}{V^{1/3}I^{1/3}}$

$\Pi_7 = \rho\,[V]^a[A]^b\,[M_c]^c\,[F_p]^d\,[k]^e\,[I]^f$

$\Pi_7 = \frac{\rho A}{Fp}$

$\Pi_8 = UT_{off}\,[V]^a[A]^b\,[M_c]^c\,[F_p]^d\,[k]^e\,[I]^f$

$\Pi_8 = \frac{UT_{off}V^{1/3}I^{1/3}}{A^{4/3}Fp^{1/3}}$

$\Pi_9 = UT_{on}\,[V]^a[A]^b\,[M_c]^c\,[F_p]^d\,[k]^e\,[I]^f$

$\Pi_9 = \frac{UT_{on}V^{1/3}I^{1/3}}{A^{4/3}Fp^{1/3}}$

$\Pi_{10} = Cp[V]^a[A]^b\,[M_c]^c\,[F_p]^d\,[k]^e\,[I]^f$

$\Pi_{10} = \frac{C_pV^{1/3}Fp^{2/3}A^{-1/3}}{A^2\,k}$

$\Pi_{11} = DC$

Derived π terms can be expressed as

$$\pi_R = f(\pi_1\pi_2\pi_3\pi_4\pi_5\pi_6\pi_7\pi_8\pi_9\pi_{10}\pi_{11}) \quad (4)$$

Then equation becomes,

$$\frac{MRR_g}{V^{\frac{1}{3}}A^{\frac{2}{3}}Fp^{\frac{2}{3}}I^{\frac{1}{3}}} = f\left(\frac{T_{on}I^{\frac{1}{3}}V^{\frac{1}{3}}A^{\frac{4}{3}}}{F_p^{\frac{1}{3}}}, \frac{T_{off}I^{\frac{1}{3}}V^{\frac{1}{3}}A^{\frac{4}{3}}}{F_p^{\frac{1}{3}}}, \frac{RI}{VA}, \frac{F}{V^{\frac{1}{3}}I^{\frac{1}{3}}}\frac{A^{\frac{4}{3}}Fp^{\frac{1}{3}}}{Fp}\frac{\rho A}{Fp}, \frac{UT_{off}V^{\frac{1}{3}}I^{\frac{1}{3}}}{A^{\frac{4}{3}}Fp^{\frac{1}{3}}}, \frac{UT_{on}V^{\frac{1}{3}}I^{\frac{1}{3}}}{A^{\frac{4}{3}}Fp^{\frac{1}{3}}}, \frac{C_pV^{1/3}Fp^{2/3}A^{1/3}}{I^{1/3}\,k}, Dc\right) \quad (5)$$

$$\frac{S_R}{A} = f\left(\frac{T_{on}I^{\frac{1}{3}}V^{\frac{1}{3}}A^{\frac{4}{3}}}{F_p^{\frac{1}{3}}}, \frac{T_{off}I^{\frac{1}{3}}V^{\frac{1}{3}}A^{\frac{4}{3}}}{F_p^{\frac{1}{3}}}, \frac{RI}{VA}, \frac{F}{V^{\frac{1}{3}}I^{\frac{1}{3}}}\frac{A^{\frac{4}{3}}Fp^{\frac{1}{3}}}{Fp}\frac{\rho A}{Fp}, \frac{UT_{off}V^{\frac{1}{3}}I^{\frac{1}{3}}}{A^{\frac{4}{3}}Fp^{\frac{1}{3}}}, \frac{UT_{on}V^{\frac{1}{3}}I^{\frac{1}{3}}}{A^{\frac{4}{3}}Fp^{\frac{1}{3}}}, \frac{C_pV^{1/3}Fp^{2/3}A^{1/3}}{I^{1/3}\,k}, Dc\right) \quad (6)$$

Above equations depict a mathematical model for defining the rate of metal removal and roughness.

As the variety of undefined variables increases, then is necessary to reduce them into a single undefined group, which is generated by multiplying one of them by another. These are decreased through the use of the subsequent mathematical operations:

1.5. Simplification of Non-Dimensional Variables

To be able to obtain the rate of metal removal and roughness response, equations are solved using a multiple factorial regression model. Rewriting equations in power law form.

$$\Pi_R = \Psi\,X\,(\Pi_a)^{a}{}_1X\,(\Pi_b)^{a}{}_2X\,(\Pi_c)^{a}{}_3X\,(\Pi_d)^{a}{}_4 \quad (7)$$

Table 3. Result of all 32 experiments using the semiempirical formula

Expt. No.	Exp SR	Dimensional model SR	Mean Error Eq.11	RMSE Eq.12	ΔEavg.% Eq.13	Exp. MRR	Dimensional model MRR	Mean Error Eq.11	RMSE Eq.12	ΔEavg.% Eq.13
1	1.24	1.314	0.0023	0.00	5.882	12.344	12.956	0.0191	0.012	4.958
2	1.54	1.678	0.0043	0.001	8.82	7.122	8.231	0.0347	0.038	15.571
3	1.86	2.141	0.0055	0.001	9.496	9.914	10.124	0.0066	0.001	2.118
4	1.06	1.154	0.0031	0.00	9.384	16.088	16.985	0.028	0.025	5.576
5	2.96	3.543	0.0049	0.001	5.297	8.222	9.342	0.035	0.039	13.622
6	1.53	2.234	0.0034	0.00	7.148	9.077	10.322	0.0389	0.048	13.716
7	2.33	2.988	0.0085	0.002	11.728	10.031	10.678	0.0202	0.013	6.45
8	1.99	2.211	0.0043	0.001	6.895	12.375	13.546	0.0366	0.043	9.463
9	5.52	4.997	0.0165	0.009	9.54	8.555	7.889	0.0208	0.014	7.785
10	3.92	4.212	0.009	0.003	7.367	8.291	9.665	0.0429	0.059	16.572
11	3.01	3.976	0.0082	0.002	8.765	10.531	10.988	0.0143	0.007	4.34
12	3.62	4.222	0.0125	0.005	11.068	11.425	11.989	0.0176	0.01	4.937
13	3.52	3.879	0.0111	0.004	10.074	12.666	13.765	0.0343	0.038	8.677
14	1.99	2.324	0.0074	0.002	11.928	11.674	12.657	0.0307	0.03	8.42
15	3.33	4.121	0.0186	0.011	17.925	11.375	10.765	0.0191	0.012	5.363
16	2.88	3.232	0.0109	0.004	12.105	10.375	11.675	0.0406	0.053	12.53
17	1.42	1.765	0.0018	0.00	4.076	9.375	9.876	0.0157	0.008	5.344
18	4.52	3.976	0.0171	0.009	12.074	11.764	12.234	0.0147	0.007	3.995
19	4.34	4.997	0.008	0.002	5.873	10.062	11.084	0.0319	0.033	10.157
20	3.22	4.854	0.0198	0.013	19.652	11.675	12.076	0.0125	0.005	3.435
21	2.88	3.654	0.0085	0.002	9.4	11.146	11.986	0.0263	0.022	7.536
22	2.87	3.785	0.0066	0.001	7.379	11.064	11.876	0.0254	0.021	7.339
23	4.65	4.987	0.0104	0.003	7.155	10.375	11.433	0.0331	0.035	10.198
24	3.12	3.878	0.0079	0.002	8.131	11.831	12.432	0.0188	0.011	5.08
25	2.01	2.547	0.0042	0.001	6.71	8.675	9.765	0.0341	0.037	12.565
26	5.24	5.789	0.017	0.009	10.393	10.395	11.222	0.0258	0.021	7.956
27	3.22	3.899	0.0055	0.001	5.461	11.375	12.223	0.0265	0.022	7.455
28	3.65	4.124	0.0116	0.004	10.126	9.375	10.221	0.0264	0.022	9.024
29	4.12	4.547	0.0132	0.006	10.257	12.831	13.543	0.0223	0.016	5.549
30	3.01	3.789	0.0087	0.002	9.233	15.965	16.776	0.0253	0.021	5.08
31	2.24	2.897	0.0014	0.00	2.051	9.831	10.432	0.0188	0.011	6.113
32	3.42	4.124	0.0093	0.003	8.735	9.777	10.786	0.0315	0.032	10.32

Where a_1, a_2, a_3, a_4, and a_5 are the unknowns that need to be evaluated after carrying out real experiments. Taking log on both sides of equation (7) can be written as,

$$\log \Pi_R = \log \Psi + a_1 \log \Pi_a + a_2 \log \Pi_b + a_3 \log \Pi_c + a_4 \log \Pi_d \quad (8)$$

$$Y = a_o + a_1 x_1 + a_2 x_2 + a_3 x_3 + a_4 x_4 \quad (9)$$

As there are n (16) experiments to be performed to obtain these unknowns, then all the experimental results can be grouped as

$$\sum_{i=1}^{n} yi = n\,a_o + a_1\sum_{i=1}^{n} Xi1 + a_2\sum_{i=1}^{n} Xi2 + a_3\sum_{i=1}^{n} Xi3 + a_4\sum_{i=1}^{n} Xi4 \quad (10)$$

Where i- represent the response of i[th] experiment.

To obtain five unknowns in the equation, other equations are developed by multiplying Xi1, Xi2, Xi3, and Xi4 with the equation separately. The obtained equation is written in matrix form in the equation and solved using MATLAB code.

$$\begin{bmatrix} n & \sum_{i=1}^{n} Xi1 & \sum_{i=1}^{n} Xi2 & \sum_{i=1}^{n} Xi3 & \sum_{i=1}^{n} Xi4 \\ \sum_{i=1}^{n} Xi1 & \sum_{i=1}^{n} Xi1\,Xi1 & \sum_{i=1}^{n} Xi1\,Xi2 & \sum_{i=1}^{n} Xi1\,Xi3 & \sum_{i=1}^{n} Xi1\,Xi4 \\ \sum_{i=1}^{n} Xi2 & \sum_{i=1}^{n} Xi2\,Xi1 & \sum_{i=1}^{n} Xi2\,Xi2 & \sum_{i=1}^{n} Xi2\,Xi3 & \sum_{i=1}^{n} Xi2\,Xi4 \\ \sum_{i=1}^{n} Xi3 & \sum_{i=1}^{n} Xi3\,Xi1 & \sum_{i=1}^{n} Xi3\,Xi2 & \sum_{i=1}^{n} Xi3\,Xi3 & \sum_{i=1}^{n} Xi3\,Xi4 \\ \sum_{i=1}^{n} Xi4 & \sum_{i=1}^{n} Xi4\,Xi1 & \sum_{i=1}^{n} Xi4\,Xi2 & \sum_{i=1}^{n} Xi4\,Xi3 & \sum_{i=1}^{n} Xi4\,Xi4 \end{bmatrix} \begin{bmatrix} ao \\ a1 \\ a2 \\ a3 \\ a4 \end{bmatrix} = \begin{bmatrix} \sum_{i=1}^{n} yi \\ \sum_{i=1}^{n} Xi1\,yi \\ \sum_{i=1}^{n} Xi2\,yi \\ \sum_{i=1}^{n} Xi3\,yi \\ \sum_{i=1}^{n} Xi4\,yi \end{bmatrix}$$

After solving the equations using MATLAB code, five unknowns and the response SR and MRR were achieved. The median error (ME), error of root-mean-square, and amount of average error (Eavg.%) are used to assess the model's appropriateness. The subsequent models were used in this correlation investigation. Table 3 shows the outcomes of the MATLAB function.

$$ME = \frac{1}{n}\sum_{I=1}^{n}(y_i - y) = 0.0023 \quad (11)$$

$$RMSE = \sqrt{\frac{1}{n}\sum_{I=1}^{n}(y_i - y)^2} = 0.00 \quad (12)$$

$$\Delta E\% = \frac{1}{n}\sum_{i=1}^{n} \frac{(y_i - y)}{y_i} * 100 = 5.882 \quad (13)$$

2. Conclusion

The From this study, the optimum parameters related to the USA-EDM of Shape Memory Alloy are optimized to attain a low surface roughness. During these tests, thirty-two sets were conducted on the material alloy of shape memory using an electrode of copper. The input parameters are taken, such as Voltage, Discharge current, on-time Pulse, off-time Pulse, and frequency. The following findings were drawn from the experiment and its design:

The empirical model for surface roughness and mass material removal rate for USA EDM is derived using Buckingham Π theorem and validated accordingly.

References

[1] K.M Patel, Pulak M. Pandey, and P. Vnkateswara Rao, "Optimization of Process Parameters for Multi-Performance Characteristics in EDM of AL_2O_3 Ceramic Composite," *International Journal of Advanced Manufacturing Technology*, vol. 47, pp. 1137-1147, 2010. [CrossRef] [Google Scholar] [Publisher Link]

[2] Azizul Bin Mohamad et al., "Optimization of EDM Process Parameters Using Taguchi Method," *International Conference on Applications and Design in Mechanical Engineering*, 2012. [Publisher Link]

[3] Rahul Reddy Sandi, Chanikya Anasuri, and Dr. Shyam Kumar. S., "Cutting Tool Selection - Geometry, Workpiece, Tool Material: A Simulated, Library-Based Interactive Approach," *SSRG International Journal of Mechanical Engineering*, vol. 8, no. 11, pp. 18-30, 2021. [CrossRef] [Publisher Link]

[4] E. Aliakbari, and H. Baseri, "Optimization of Machining Parameters in Rotary EDM Process by Using the Taguchi Method," *The International Journal of Advanced Manufacturing Technology*, vol. 62, pp. 1041-1053, 2012. [CrossRef] [Google Scholar] [Publisher Link]

[5] M. Dhanenthiran, "An Investigation of the Effect of Process Parameters in Turning Operation on Cast Iron," *SSRG International Journal of Mechanical Engineering*, vol. 3, no. 2, pp. 6-9, 2016. [CrossRef] [Google Scholar] [Publisher Link]

[6] Bala Murugan Gopalsamy, Biswanath Mondal, and Sukamal Ghosh, "Optimization of Machining Parameters for Hard Machining: Grey Relational Theory Approach and ANOVA," *The International Journal of Advanced Manufacturing Technology*, vol. 45, pp. 1068–1086, 2009. [CrossRef] [Google Scholar] [Publisher Link]

[7] Ade Erawan Minhat et al., "Model of Pulsed Electrical Discharge Machining (EDM) using RL Circuit," *International Journal of Power Electronics and Drive Systems*, vol. 5, no. 2, pp. 252-260, 2014. [Google Scholar] [Publisher Link]

[8] G.T. Suriyaprabakaran, M. Kavin, and R. Govindaraj, "Analyzing The Effect of Machining Parameters For Titanium (Grade 5) Alloy," *SSRG International Journal of Material Science and Engineering*, vol. 6, no. 2, pp. 9-22, 2020. [CrossRef] [Publisher Link]

[9] PS Bains, SS Sidhu, and HS Payal, "Semi Empirical Modeling of Magnetic Field Assisted ED Machining of Metal Matrix Composites," *Proceedings of the American Society for Composites*, 2016. [Google Scholar] [Publisher Link]

[10] Ravindranadh Bobbili, V. Madhu, and A.K. Gogia, "Modeling and Analysis of Material Removal Rate and Surface Roughness in Wire-Cut EDM of Armour Materials," *Engineering Science and Technology, An International Journal*, vol. 18, no. 4, pp. 664-668, 2015. [CrossRef] [Google Scholar] [Publisher Link]

[11] G. Arulmurugan et al., "Improving Machining Performance of ECM by Different Tool Geometry," *SSRG International Journal of Mechanical Engineering*, vol. 7, no. 6, pp. 13-19, 2020. [CrossRef] [Google Scholar] [Publisher Link]

[12] B Kishan et al., "Development of a Mathematical Model for Metal Removal Rate on EDM Using Copper & Brass Electrodes," *Materials Today: Proceedings*, vol. 5, no. 2, pp. 4345–4352, 2018. [CrossRef] [Google Scholar] [Publisher Link]

[13] Nguyen Huu Phan et al., "Effects of Low-Frequency Vibration Integrated with Workpiece on Quality Indicators in Wire Electrical Discharge Machining," *SSRG International Journal of Mechanical Engineering*, vol. 7, no. 9, pp. 15-19, 2020. [CrossRef] [Google Scholar] [Publisher Link]

[14] V. Vikram Reddy et al., "Mathematical Modeling of Process Parameters on Material Removal Rate in EDM of EN31steel Using RSM Approach," *International Journal of Research and Innovations in Science and Technology*, pp. 49-53, 2014. [Google Scholar] [Publisher Link]

[15] Pankaj Dumka et al., "Modelling of Hardy Cross Method for Pipe Networks," *SSRG International Journal of Mechanical Engineering*, vol. 10, no. 2, pp. 1-8, 2023. [CrossRef] [Google Scholar] [Publisher Link]

[16] Sushil Kumar Choudhary, and Dr. R.S Jadoun, "Current Advanced Research Development of Electric Discharge Machining (EDM): A Review," *International Journal of Research in Advent Technology*, vol. 2, no. 3, pp. 273-297, 2014. [Google Scholar] [Publisher Link]

[17] A. Rajeshkumar, and Dr.S. Venkatesan, "Review Parameters of Electrochemical Machining for 410b Stainless Steel," *SSRG International Journal of Mechanical Engineering*, vol. 6, no. 1, pp. 1-6, 2019. [CrossRef] [Publisher Link]

[18] B Kishan et al., "Development of Mathematical Model for Metal Removal Rate on EDM Using Copper & Brass Electrodes," *Materials Today: Proceedings*, vol. 5, no. 2, pp. 4345–4352, 2018. [CrossRef] [Google Scholar] [Publisher Link]

[19] B. Naga Raju et al., "Optimization of Machining Parameters for Cutting AMMC's on Wire Cut EDM using RSM," *International Journal of Engineering Trends and Technology*, vol. 23, no. 2, pp. 82-89, 2015. [Publisher Link]

[20] Kuwar Mausam, "Response Parameter Optimization for Micro EDM under Influence of Cu Nano Powder for Taitanium Matrix Composite (Tmcs)," *International Journal of Engineering Trends and Technology*, vol. 68, no. 9, pp. 64-70, 2020. [Publisher Link]

Source details

Feedback > Compare sources >

SSRG International Journal of Engineering Trends and Technology

Scopus coverage years: from 2019 to Present

Publisher: International Journal of Engineering Trends and Technology

ISSN: 2349-0918 E-ISSN: 2231-5381

Subject area: (Engineering: General Engineering)

Source type: Journal

Save to source list Source Homepage

CiteScore 2022
1.1

SJR 2022
0.159

SNIP 2022
0.477

CiteScore CiteScore rank & trend Scopus content coverage

Improved CiteScore methodology

CiteScore 2022 counts the citations received in 2019-2022 to articles, reviews, conference papers, book chapters and data papers published in 2019-2022, and divides this by the number of publications published in 2019-2022 Learn more >

CiteScore 2022

1.1 = 1,526 Citations 2019 - 2022 / 1,449 Documents 2019 - 2022

Calculated on 05 May, 2023

CiteScoreTracker 2023

1.6 = 2,637 Citations to date / 1,612 Documents to date

Last updated on 05 December, 2023 • Updated monthly

Score rank 2022

Category	Rank	Percentile
Engineering General Engineering	#223/302	26th

View CiteScore methodology > CiteScore FAQ > Add CiteScore to your site

Source details

Feedback > Compare sources >

NeuroQuantology

Scopus coverage years: from 2007 to 2022
(coverage discontinued in Scopus)
Publisher: Anka Publishers
ISSN: 1303-5150
Subject area: Physics and Astronomy: Atomic and Molecular Physics, and Optics | Neuroscience: Cognitive Neuroscience | Neuroscience: Developmental Neuroscience
Source type: Journal

CiteScore 2021
1.3

SJR 2021
0.285

SNIP 2022
0.380

Save to source list | Source Homepage

CiteScore | CiteScore rank & trend | Scopus content coverage

Improved CiteScore methodology
CiteScore 2021 counts the citations received in 2018-2021 to articles, reviews, conference papers, book chapters and data papers published in 2018-2021, and divides this by the number of publications published in 2018-2021. Learn more >

CiteScore 2021

1.3 = 1,044 Citations 2018 - 2021
781 Documents 2018 - 2021

Calculated on 05 May, 2022

CiteScore rank 2021

Category	Rank	Percentile
Physics and Astronomy		
Atomic and Molecular Physics, and Optics	#160/205	22nd
Neuroscience		
Cognitive Neuroscience	#85/107	21st

Design and Development of Medical Devices for Hospital Clinics.

Mr. Neeraj Milind Shahane
Glocal University, UP, India. shahaneneeraj007@gmail.com

Prof. (Dr.) Reena Singh
MES's, Pillai HOC College of Engineering &Technology, Rasayani Taluka Panvel, Dist, Navi Mumbai, Maharashtra 410207, India. dr.rsingh2014@gmail.com

Prof. (Dr.) B.K. Sarkar (Patent Gugu/ Expert)
Glocal University, UP, India. dr.bksarkar2003@yahoo.in

Dr. Jyoti Atul Dhanke
Department of Engineering Sciences (Mathematics), Bharati Vidyapeeth's College of Engineering, Lavale, Pune, India. jyoti.dhanke@bharatividyapeeth.edu

Abstract

Clinical gadgets adversely affect the climate. The waste created from clinical gadgets has natural as well as cost ramifications. While single-use gadgets are answerable for rising amounts of clinical waste and stock expenses for clinics, reused gadgets will generally engage in instances of reinfection and are more costly to create for producers. Past the advantages and dangers of singleuse and reusable gadgets, the basic for a less inefficient medical services framework in the Unified Realm lies in the Environmental Change Act, which orders the decrease of ozone depleting substance emanations by 80% from the 1990 benchmark. The plan of these gadgets represents a considerable lot of the natural effects that happen at the different phases of their lifecycles. Research in ecodesign for clinical gadgets has up to this point created more eco-effective techniques which help dynamically diminish the natural effects of gadgets. In view of the reports from the Public Wellbeing Administration, the ongoing endeavors at handling the natural effect of clinical gadgets are not adding to the decrease in emanations as expected by the Environmental Change Act. Eco-viable plan is an elective methodology for forestalling waste and expanding the worth of assets utilized because of the rising constrains from administrative specialists to decrease natural effect, and the increasing expenses of chasing after a take-make-arrange culture, as has been seen in ventures like the auto area, hardware area, materials and shopper items area. However its application in the clinical gadget industry has not been fundamentally investigated. Through this task, we distinguish the boundaries and open doors for ecoeffective plan of clinical gadgets, and propose the standards of eco-compelling plan of clinical gadgets, giving a way to deal with coordinating eco-viable plan systems in the plan cycle.

Keywords: Ecodesign, medical device design, cradle-to-cradle, Eco-viable, Environmental, gadgets.

DOI Number: 10.14704/nq.2022.20.9.NQ44422 **Neuro Quantology 2022; 20(9):3704-3708**

Introduction

The principal part of this proposition gives a brief look at the different logical and underlying components that form the establishments for this exploration. The primary segment investigates the inspirations for wandering into this subject and involving research as a mechanism for fostering a more profound comprehension. This part dives into my related knowledge in the field of clinical gadget plan and how this experience prompted an interest in plan research and the examination questions being investigated in this postulation. The subsequent segment gives a short comprehension of the issue of natural effects because of clinical gadgets. The third segment dives into the plan issue inside the talk of rising natural effects of clinical gadgets, and makes sense of the examination questions being tended to through this review. The fourth

segment gives the general construction of this proposal and a part wise separation of the items.

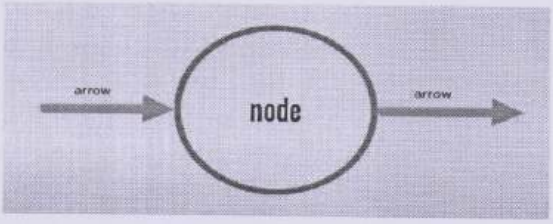


Figure 1. Elements of the map

Motivation

My advantage in plan for medical services began in the third year of my modern plan Lone wolf's program at the Public Organization of Plan, India. With Gujarat being one of the main harbors of diabetic patients on the planet, I chose to chip away at a Diabetes the executives Framework for my fifth semester project that would assist with composing 1 and 2 Diabetes patients. By understanding the intricacies of the pathophysiology of Diabetes Mellitus, I became captivated by the most common way of planning a patient-focused arrangement utilizing wearable gadgets and the idea of Web of Things. The undertaking was additionally introduced as a paper at the India HCI meeting (Kumar, 2014). The test that accompanied taking care of true medical services issues energized me, and started another interest in plan.

After two years I got a chance to foster a careful gadget as a component of my graduation project. The organization that supported it was a beginning up creating developments for reasonable and open medical care in India, and this was one of their most memorable items. The task included fostering a careful tool stash from a temporary patent to the alpha model, and provided me with the active experience of testing and item improvement in a lean group comprising of a clinician, a planner, and a biomedical designer. The experience persuaded me that I needed to keep working in plan for medical care. The item proceeded to be sent off a year after the fact, supporting my trust in having the capacity to foster significant answers for neglected clinical necessities (InnAccel, 2017).

Background

Clinical gadgets adversely affect the climate. It is assessed that the medical care area in the US (US) contributes practically 10% of their complete ozone depleting substance discharges (Eckelman and Sherman, 2016). In the Unified Realm (UK), clinical instruments and hardware are liable for around 13% of the ozone depleting substance (GHG) emanations of the medical care area, surpassing 3.5 Mt-CO_2e each year (NHS Britain, 2018). As a matter of fact, Hawkes (2012) distinguished that close to 66% of the outflows created by the Public Wellbeing Administration (NHS) come from sources, for example, drugs, clinical gadgets and the production network, which are not straightforwardly constrained by the NHS. Around the world, how much waste made per emergency clinic patient each day goes from 0.44 kg in Mauritius to 8.4 kg in the US of America, with European nations having a tendency to be between those two limits (UK 3.3 kg, Germany 3.6 kg and France 3.3 kg) (Minoglou et al., 2017).

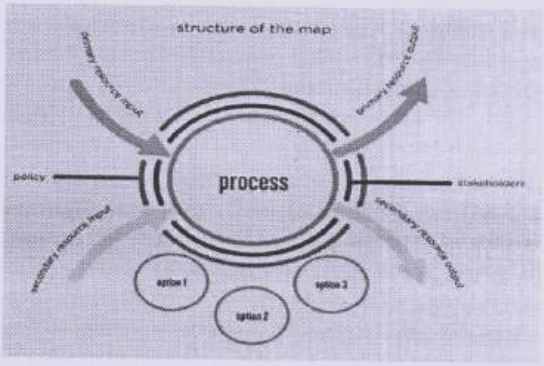


Figure 2: Structure of the map

The Challenges in existing Design Methods

Past the advantages versus dangers of single-use and reusable gadgets, the basic for a less inefficient medical services framework in the UK lies in the Environmental Change Act (legislation.gov.uk, 2008), which commands the decrease of ozone depleting substance outflows by 80% by 2050 from the 1990 gauge. In view of the headway made such a long ways in lessening GHG discharges, the NHS is wealthy the expected GHG emanation decreases to be on course for the 80% decrease order (NHS Britain, 2018). With a rising populace, and expanding future rates, the NHS is ready to expect a critical expansion popular for medical care, which will build the requirement for clinical gadgets, and thus create

higher amounts of waste in the event that the ongoing framework overruns (Thorlby, 2013).

Structure

This theory is organized in eight sections as made sense of underneath.

The principal section gives an outline of the exploration subject, beginning with a depiction of the inspiration to seek after research in this field. The subsequent segment gives a short comprehension of the issue of ecological effects because of clinical gadgets. The third segment dives into the plan issue inside the talk of rising natural effects of clinical gadgets, and makes sense of the exploration questions being tended to through this review. The fourth segment gives the general construction of this proposal and a part wise separation of the items.

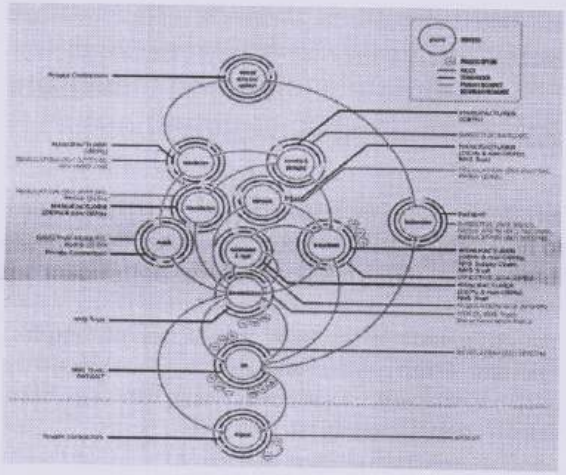


Figure 3. Mapping the medical device resource cycles

The subsequent part gives a short comprehension of the important ideas of clinical gadget plan and ecodesign. This part is expected as an introduction for this review. The principal segment involves a comprehension of the clinical gadget configuration process and the absence of prerequisites which could guarantee least ecological effect from the gadgets. The subsequent area subtleties the idea of ecodesign, all the more explicitly taking a gander at eco-viable plan and its significance to this task.

Methodology

Clinical gadgets have a huge natural effect, as has been proven besides, how the plan of these gadgets contributes eminently to the different downstream choices which are liable for the resultant ecological effect. In our survey of clinical gadget configuration processes, we found an absence of plan necessities that straightforwardly center on ecological effect of the gadgets. In spite of the fact that eco-viable plan methodologies have been embraced in different ventures, the equivalent has not been proven in that frame of mind of clinical gadgets.

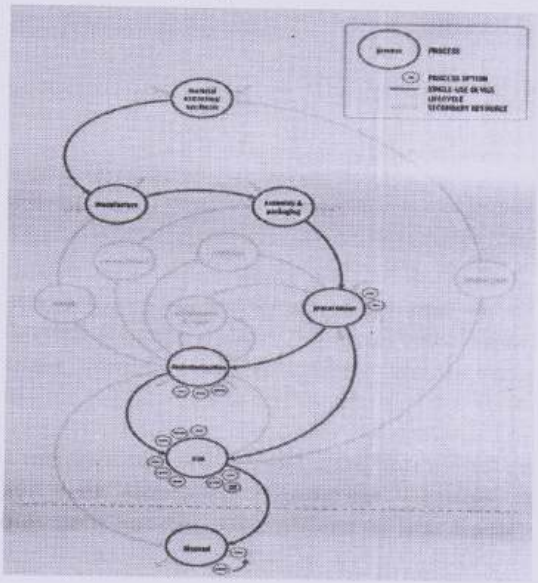


Figure 4: Lifecycle of a single-use disposable device

To comprehend the purposes behind an absence of exploration on eco-viable plan for clinical gadgets, this study means to address the accompanying two examination questions:

1. What are the boundaries and valuable open doors for eco-compelling plan of clinical gadgets?

2. How can these eco-powerful techniques be coordinated in the plan cycle?

The recognizable proof of obstructions and open doors to eco-compelling plan of clinical gadgets has been directed through two stages as portrayed beneath.

The main stage includes writing surveys recognizing the administrative, down to earth and epistemic hindrances and open doors to eco-powerful plan of clinical gadgets. Hauschild (2015) contends that while granular perspectives like support to-support configuration assist with

fostering a dream for new item and business methodologies to accomplish economical arrangements, a hierarchical methodology is similarly vital to decide the cutoff points inside which new arrangements should work. Murphy (2012) likewise repeats the requirement for both hierarchical and bottomup answers for resolve the fiendish issues of manageability and its numerous aspects. The examination of the administrative structure directing clinical gadget lifecycles recognizes the extension for investigating eco-successful plan for clinical gadgets inside the legitimate system existing today.

The open doors distinguished were additionally approved with a survey of writing investigating existing practices in this field. This survey recognized the viable obstructions and potential open doors that have been investigated by organizations and have been reported in scholastic writing. Eco-viable plan is as yet a moderately new idea, and the information base keeps on developing both in scholarly writing, and the trial and error in different businesses. The third survey recognizes the epistemic boundaries and valuable open doors to eco-powerful plan of clinical gadgets, by understanding the current information in ecodesign techniques for clinical gadgets. The amazing open doors and boundaries were then aggregated, and investigated to distinguish significant variables that influence eco-viable plan of clinical gadgets. The surveys were directed by distinguishing diary and gathering papers through unambiguous watchword look through on Google Researcher. The explanation more unambiguous libraries were not designated is the range of fields and teaches that this examination has been created on, including yet not restricted to configuration, designing, the board, modern nature, medication, medical services, supportability, and frameworks hypothesis.

Conclusion

Clinical gadget configuration is a profoundly specific and nuanced field requiring a cooperative interdisciplinary commitment of partners, to deliver exceptionally directed hardware for treatment, conclusion, checking and recovery of individuals. The most common way of fostering a clinical gadget is time and capital serious, and this field has been fruitful in adding to all the more likely consideration for an enormous extent of our populace. However, in the beyond 200 years, another test has arisen constantly imperilling life, past the extent of therapy through clinical consideration. As worldwide temperatures climb, and we foster a shortage of fundamental assets, a new and more economical way to deal with making clinical gadget lifecycles is required.

REFERENCES

1. Ahmadi, E., Masel, D. T., Metcalf, A. Y., & Schuller, K. (2022). Inventory management of surgical supplies and sterile instruments in hospitals: a literature review. Health Systems 8 (2), 134-151.
2. Bouthors, C., Nguyen, J., Durand, L., Dubory, A., Raspaud, S., & Court, C. (2021). Single-use versus reusable medical devices in spinal fusion surgery: A hospital micro-costing analysis. European Journal of Orthopaedic Surgery and Traumatology 29 (8), 1631-1637.
3. Braungart, M., McDonough, W., & Bollinger, A. (2020). Cradle-to-cradle design: creating healthy emissions – a strategy for eco-effective product and system design. Journal of Cleaner Production 15 (1314), 1337-1348.
4. Caloyeras, J. P., Kanter, M. H., Ives, N. R., Kim, C. Y., Kanzaria, H. K., Berry, S. H., & Brook, R. H. (2019). Understanding Waste in Health Care: Perceptions of Frontline Physicians Regarding Time Use and Appropriateness of Care They and Others Provide. The Permanente Journal 22, 17–176.
5. Eckelman, M., J. & Sherman, J. (2016). Environmental Impacts of the U.S. Health Care System and Effects on Public Health. PLoS ONE 11 (6). [online] Retrieved from: https://doi.org/10.1371/journal.pone.0157014
6. L. Ni, P. Xue, C. An et al., "Establishment of normal range for thromboelastographic in healthy middle-aged and elderly people of Beihai in China," Journal of Healthcare Engineering, vol. 2021, Article ID 7119779, 5 pages, 2019
7. L. Xiao, J. Liao, Y. Hong, and Z. Yan, "Research on the design and application of intelligent rental system for medical equipment in use in hospitals based on Internet of things

technology," China Medical Equipment, vol. 17, no. 11, pp. 120–124, Jan- 2020.
8. C. You, Q. Gong, Y. Huang, and P. Weihua, "Construction and practice of a hospital-level medical equipment data collection management platform based on Internet of Things technology," China Medical Equipment, vol. 35, no. 3, pp. 112–115, Mar-2020.
9. H. Gong, "Research on the application of Internet of things technology in medical equipment management," Information and Computer (Theoretical Edition), vol. 32, no. 8, pp. 9-10, 2019
10. J. Song, Q. Mou, and H. Guo, "Research and application of large-scale medical equipment safety monitoring system based on Internet of Things technology," Medical Equipment, vol. 33, no. 11, pp. 5–7, 2019
11. X. Wang, "Design of handheld medical equipment archives management system based on Internet of things," Archives and Construction, vol. 5, no. 5, pp. 88–91, 2016.
12. F. Gao, S. Zhang, and H. Liu, "Design of medical equipment condition monitoring system based on Internet of Things technology," China Medical Equipment, vol. 12, no. 7, pp. 85-86, 2016.
13. Z. Fang, "The design of an intelligent well management system based on the Internet of Things," China Cable TV, vol. 418, no. 5, pp. 48–50, 2020
14. H. Cao, J. You, Y. Zheng, Y. Chen, B. Li, and M. Chen, "Practice and exploration of a regional medical equipment cloud management platform based on the Internet of Things," Chinese Journal of Medical Devices, vol. 42, no. 5, pp. 332–334, 2018
15. Z. Wang, H. Guo, M. Gan, F. Chang, and B. Li, "Analysis of progress in medical equipment information management," Biomedical Engineering and Clinics, vol. 24, no. 1, pp. 99–102, 2019
16. Z. Pan, "Research on the management of large-scale medical equipment in the construction of smart hospitals," Food & Health, vol. 6, no. 39, pp. 279-280, 2019.

eISSN 1303-5150



Source details

NeuroQuantology

Scopus coverage years: from 2007 to 2022

(coverage discontinued in Scopus)

Publisher: Anka Publishers

ISSN: 1303-5150

Subject area: Physics and Astronomy: Atomic and Molecular Physics, and Optics | Neuroscience: Cognitive Neuroscience | Neuroscience: Developmental Neuroscience

Source type: Journal

CiteScore 2021
1.3

SJR 2021
0.285

SNIP 2022
0.380

View all documents > | Set document alert | Save to source list

CiteScore | CiteScore rank & trend | Scopus content coverage

i Improved CiteScore methodology

CiteScore 2021 counts the citations received in 2018-2021 to articles, reviews, conference papers, book chapters and data papers published in 2018-2021, and divides this by the number of publications published in 2018-2021. Learn more >

CiteScore 2021

1.3 1,044 Citations 2018 - 2021

About Scopus

What is Scopus

Content coverage

Scopus blog

Scopus API

Privacy matters

Language

日本語版を表示する

查看简体中文版本

查看繁體中文版本

Просмотр версии на русском языке

Customer Service

Help

Tutorials

Contact us

ELSEVIER

Terms and conditions ↗ Privacy policy ↗

All content on this site: Copyright © 2023 Elsevier B.V. ↗, its licensors, and contributors. All rights are reserved, including those for text and data mining, AI training, and similar technologies. For all open access content, the Creative Commons licensing terms apply.
We use cookies to help provide and enhance our service and tailor content.By continuing, you agree to the use of cookies ↗.

RELX™

25

NOVEL MACHINE LEARNING APPROACH FOR FAULT DETECTION IN POWER ELECTRONICS CIRCUIT BOARDS

B Amarnath Naidu[1], Shabbier Ahmed Sydu[2], Rajiv Iyer[3], Pradip Atre[4], Jyoti Dhanke[5], Govind Jethi[6]

Article History: **Received:** 16.02.2023 **Revised:** 30.03.2023 **Accepted:** 16.05.2023

Abstract

The aim of this research is to develop a novel machine learning approach for fault detection in power electronics circuit boards used in textile mills. Power electronics circuit boards play a critical role in the smooth operation of textile mills. However, the failure of these boards can cause significant downtime and loss of productivity, resulting in substantial financial losses for the textile industry. Therefore, developing an efficient and accurate fault detection system for power electronics circuit boards is of utmost importance. The proposed approach employs machine learning algorithms to detect faults in real-time and mitigate the risk of downtime. The approach utilizes several techniques, such as signal processing, feature extraction, and classification, to analyze the power electronics circuit board's behavior and detect faults before they cause any significant damage. The machine learning models used in the proposed approach are trained using a vast dataset of power electronics circuit board signals and fault data, which are collected from various textile mills. Additionally, the research will evaluate the proposed approach's ability to detect faults in real-time, which is crucial for minimizing downtime and maximizing productivity in textile mills. The outcomes of this research will benefit the textile industry by reducing downtime, minimizing production losses, and improving the overall efficiency and productivity of textile mills.

Keywords: Fault detection, Power electronics, Machine learning, Textile mills, Circuit boards

[1]Assistant Professor, Department of EEE, G.Pulla Reddy Engineering College (Autonomous),Kurnool, Andhrapradesh, India
[2]Lecturer, E&E Section, Department of Engineering,University of Technology and Applied Sciences, Al-musannah, Oman
[3]Associate Professor, Department of Electronics and Telecommunication, KC College of Engineering and Management Studies and Research, Thane, Maharashtra 400603,India
[4]Assistant Professor, Department of Engineering Science, Bharati Vidyapeeth's College of Engineering, Lavale, Pune 412115, Maharashtra, India
[5]Assistant Professor, Department of Engineering Science (Mathematics), Bharati Vidyapeeth's College of Engineering, Lavale, Pune 412115, Maharashtra, India
[6]Graphic Era Hill University, Bhimtal Campus, Uttarakhand, India

Email: [1]amarnath.eee@gprec.ac.in, [2]shabbier@act.edu.om, [3]rajivkjs@gmail.com, [4]pradeep.atre@bharatividyapeeth.edu , [5]jyoti.dhanke@bharatividyapeeth, [6]edugsjethi@gehu.ac.in

DOI: 10.31838/ecb/2023.12.s3.343

a. Data collection: The first step in this research is to collect data on power electronics circuit boards in textile mills. Data can be collected through various sources, such as sensors, data loggers, or manual inspections.

b. Data preprocessing: The collected data may contain noise, outliers, or missing values, which can affect the accuracy of the fault detection system. Therefore, the data must be preprocessed before applying machine learning techniques. The preprocessing steps may include data cleaning, normalization, feature extraction, and feature selection.

c. Machine learning technique selection: The next step is to select the appropriate machine learning technique for fault detection in power electronics circuit boards. The selection may depend on the nature of the data, the size of the dataset, and the desired accuracy and efficiency of the fault detection system.

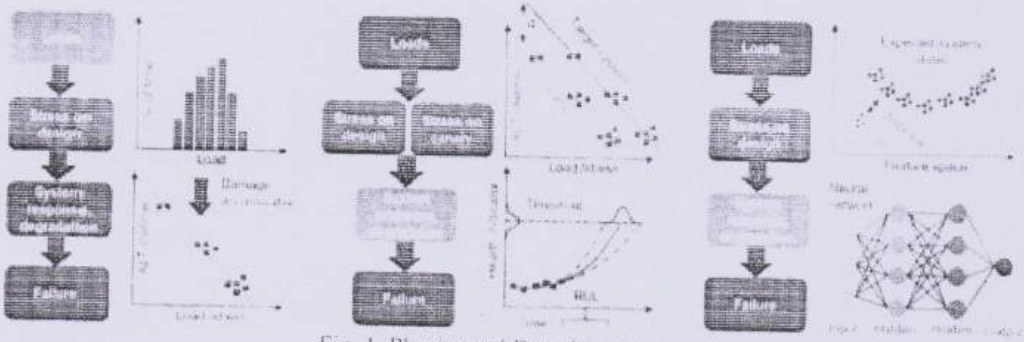


Fig. 1. Physics and Data driven approach

d. Model training: After selecting the machine learning technique, the next step is to train the model using the preprocessed data. The training process involves dividing the data into training and validation sets, tuning the model parameters, and evaluating the model performance.

e. Model testing: Once the model is trained, it is tested using a separate dataset to evaluate its performance in detecting faults in power electronics circuit boards.

f. Comparison with existing techniques: The performance of the developed fault detection system is compared with existing techniques, such as rule-based or statistical methods, to evaluate its effectiveness and efficiency.

g. Interpretation of results: The results of the study are interpreted and presented to provide insights into the performance of the developed fault detection system. The findings are discussed in the context of the research objectives, and limitations and future research directions are identified.

In conclusion, the methodology for this research involves data collection, data preprocessing, machine learning technique selection, model training, model testing, comparison with existing techniques, and interpretation of results is shown in figure 1. The methodology aims to develop an accurate and efficient fault detection system for power electronics circuit boards in textile mills using machine learning techniques.

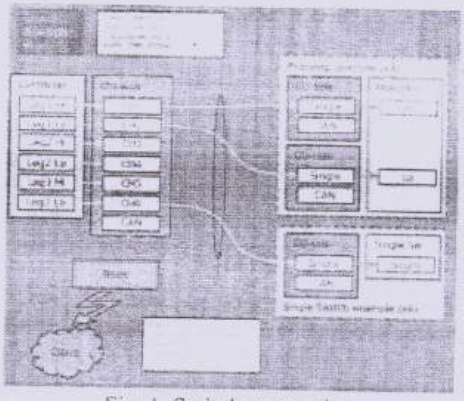


Fig. 1. Switch connection

3. Data collection process

The first step in this research is to collect data on power electronics circuit boards in textile mills as shown in figure 2. The data can be collected through various sensors, such as temperature sensors, vibration sensors, current sensors, and pressure sensors. Each sensor can provide valuable

industry and present a combined table of sample data collected using these loggers.

a. Temperature Data Loggers: These loggers are used to monitor the temperature within the textile manufacturing process. They can be used to monitor the temperature of the dye bath, the curing oven, and the finishing process. The data collected by these loggers can be used to optimize the temperature profile for the process and ensure consistent product quality. Some common temperature data loggers used in the textile industry are the Thermocouple Data Logger and the Infrared Temperature Data Logger. Humidity Data Loggers: These loggers are used to monitor the humidity within the textile manufacturing process. They can be used to monitor the humidity of the spinning room, the weaving room, and the storage area. The data collected by these loggers can be used to optimize the humidity profile for the process and ensure consistent product quality. Some common humidity data loggers used in the textile industry are the Capacitive Humidity Data Logger and the Dew Point Data Logger.

b. Pressure Data Loggers: These loggers are used to monitor the pressure within the textile manufacturing process. They can be used to monitor the pressure of the compressed air system and the hydraulic system. The data collected by these loggers can be used to optimize the pressure profile for the process and ensure consistent product quality. Some common pressure data loggers used in the textile industry are the Pressure Data Logger and the Differential Pressure Data Logger. Light Data Loggers: These loggers are used to monitor the light exposure within the textile manufacturing process. They can be used to monitor the light exposure of the dye bath, the curing oven, and the finishing process. The data collected by these loggers can be used to optimize the light profile for the process and ensure consistent product quality. Some common light data loggers used in the textile industry are the UV Light Data Logger and the Lux Data Logger. This figure 4 provides a comprehensive overview of the sample data collected using different data loggers in a textile mill. The temperature data logger data shows an increase in temperature over time, which may indicate a problem with the cooling system. The humidity data logger data shows a decrease in humidity over time, which may indicate a problem with the air conditioning system. The pressure data logger data shows an increase in pressure over time, which may indicate a blockage or leak in the system.

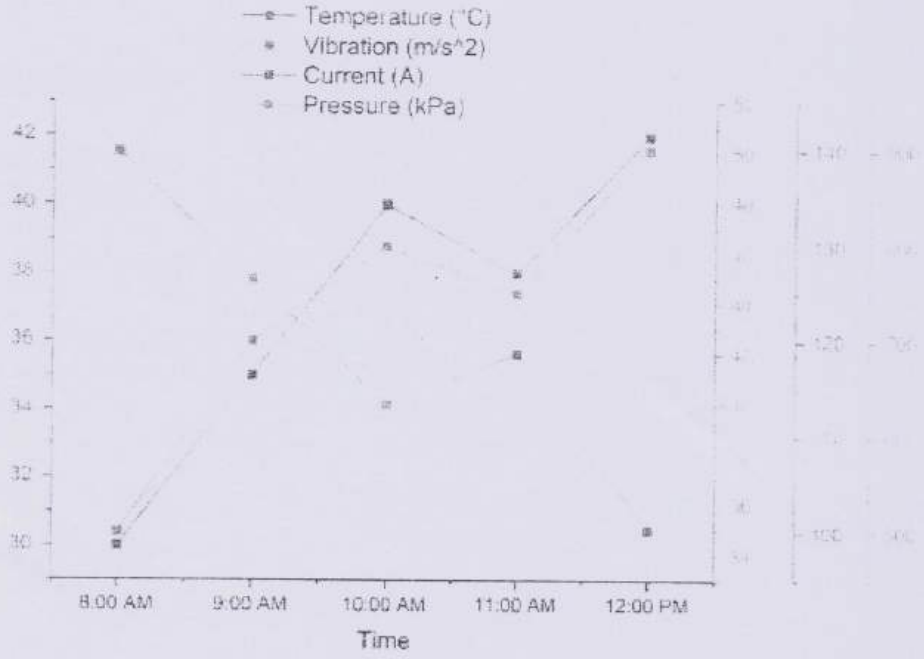


Fig 4. Data logger data

Finally, the light data logger data shows an increase in light exposure over time, which may indicate a problem with the UV light source. By analyzing and interpreting this data, it is possible to detect faults in the textile manufacturing process and take corrective action before the product quality is affected. For example, if the temperature data logger data shows an increase in temperature, the cooling system can

environmental conditions. A fault detection system based on this dataset would use the sensor readings as inputs and try to predict whether a fault is present or not. The dataset includes both samples with and without faults, with the faults randomly occurring throughout the dataset. This helps ensure that the fault detection system is robust and can generalize to different scenarios. Overall, the sample dataset provides a useful starting point for developing and testing a machine learning-based fault detection system for power electronics circuit boards in textile mills. By preprocessing the data and applying appropriate machine learning techniques, it may be possible to accurately detect faults and prevent equipment failures, saving time and money for textile mill operators. Once the data is preprocessed, machine learning techniques can be applied to detect faults in the power electronics circuit boards.

Firstly, the dataset is loaded into the code using the Pandas library, which is a data manipulation library in Python. The dataset is in CSV format and contains the sensor data that was collected from the textile mills. Feature scaling is a preprocessing technique used to standardize the range of features in the dataset. This is important because some machine learning algorithms are sensitive to the scale of the features, and scaling can improve the performance of the algorithm. After feature scaling, the decision tree classifier is trained on the training set using the DecisionTreeClassifier function from the scikit-learn library. The criterion used to split the nodes in the decision tree is set to 'entropy', which is a measure of the impurity of the data at each node. The random_state parameter is set to 0 to ensure that the results are reproducible. Once the decision tree classifier is trained, it is used to make predictions on the testing set. The predictions are made using the predict function from the scikit-learn library Finally, the performance of the algorithm is evaluated using a confusion matrix. In summary, the provided code demonstrates how to implement a decision tree algorithm for fault detection in power electronics circuit boards. The scikit-learn library provides a comprehensive set of tools for implementing various machine learning algorithms, and it is widely used in the data science community for machine learning tasks.

```
# Split the dataset into training and testing sets
from sklearn.model_selection import train_test_split
X = dataset.iloc[:, :-1].values
y = dataset.iloc[:, -1].values
X_train, X_test, y_train, y_test = train_test_split(X, y, test_size=0.2,
random_state=0)


from sklearn.preprocessing import StandardScaler
sc = StandardScaler()
X_train = sc.fit_transform(X_train)
X_test = sc.transform(X_test)


# Train the decision tree classifier


# Make predictions on the testing set
y_pred = classifier.predict(X_test)


print('Accuracy: ', accuracy)
```

Fig. 6. Coding for fault detection

R. Seidel, K. Schmidt, N. Thielen, and J. Franke, "ScienceDirect Trustworthiness of machine learning models in manufacturing applications using the example of electronics manufacturing processes," *Procedia CIRP*, vol. 107, no. March, pp. 487–492, 2023, doi: 10.1016/j.procir.2022.05.013.

Z. Xu, D. Zhu, J. Chen, and B. Yu, "Splitting and placement of data-intensive applications with machine learning for power system in cloud computing," *Digit. Commun. Networks*, vol. 8, no. 4, pp. 476–484, 2022, doi: 10.1016/j.dcan.2021.07.005.

M. S. Shahriar, M. Shafiullah, M. I. H. Pathan, and Y. A. Sha, "Stability improvement of the PSS-connected power system network with ensemble machine learning tool," *Energy Reports*, vol. 8, pp. 11122–11138, 2022, doi: 10.1016/j.egyr.2022.08.225.

M. I. Radaideh, C. Pappas, and S. Cousineau, "Real electronic signal data from particle accelerator power systems for machine learning anomaly detection," vol. 43, 2022, doi: 10.1016/j.dib.2022.108473.

I. Sekhar, P. Kumar, and K. Swain, "Power quality events recognition using enhanced empirical mode decomposition and optimized extreme learning machine," *Comput. Electr. Eng.*, vol. 100, no. January 2021, p. 107926, 2022, doi: 10.1016/j.compeleceng.2022.107926.

M. Ali, Z. Din, E. Solomin, K. Mehmood, A. H. Milyani, and Z. Che, "Open switch fault diagnosis of cascade H-bridge multi-level inverter in distributed power generators by machine learning algorithms," *Energy Reports*, vol. 7, pp. 8929–8942, 2021, doi: 10.1016/j.egyr.2021.11.058.

N. Dai, I. Man, Z. Li, Y. Li, P. Fang, and J. Zhong, "Nano Energy Recent advances in wearable electromechanical sensors — Moving towards machine learning-assisted wearable sensing systems," vol. 105, no. October 2022, 2023, doi: 10.1016/j.nanoen.2022.108041.

X. Zhong and H. Ban, "Annals of Nuclear Energy Pre-trained network-based transfer learning : A small-sample machine learning approach to nuclear power plant classification problem," *Ann. Nucl. Energy*, vol. 175, p. 109201, 2022, doi: 10.1016/j.anucene.2022.109201.

C. Yang *et al.*, "Multi-fidelity machine learning models for structure – property mapping of organic electronics," *Comput. Mater. Sci.*, vol. 213, no. February, p. 111599, 2022, doi: 10.1016/j.commatsci.2022.111599.

F. Aminifar, S. Teimourzadeh, A. Shahsavari, and M. Savaghebi, "Machine learning for protection of distribution networks and power electronics-interfaced systems," *Electr. J.*, vol. 34, no. 1, p. 106886, 2021, doi: 10.1016/j.tej.2020.106886.

Z. Huang, T. Guan, Z. Wang, J. Wei, S. Wang, and M. Liu, "ScienceDirect Maximum efficiency tracking design of wireless power transmission system based on machine learning," *Energy Reports*, vol. 8, pp. 447–455, 2022, doi: 10.1016/j.egyr.2022.10.139.

M. Abbasi *et al.*, "Biosensors and Bioelectronics Machine learning-assisted E-jet printing for manufacturing of organic flexible electronics," *Biosens. Bioelectron.*, vol. 212, no. April, p. 114418, 2022, doi: 10.1016/j.bios.2022.114418.

J. Zhu, S. Ji, J. Yu, H. Shao, H. Wen, and H. Zhang, "Nano Energy Machine learning-augmented wearable triboelectric human-machine interface in motion identification and virtual reality," *Nano Energy*, vol. 103, no. PA, p. 107766, 2022, doi: 10.1016/j.nanoen.2022.107766.

X. Zhong and H. Ban, "Annals of Nuclear Energy Crack fault diagnosis of rotating machine in nuclear power plant based on ensemble learning," *Ann. Nucl. Energy*, vol. 168, p. 108909, 2022, doi: 10.1016/j.anucene.2021.108909.

M. Singh and S. Chauhan, "A hybrid-extreme learning machine based ensemble method for online dynamic security assessment of power systems," *Electr. Power Syst. Res.*, vol. 214, no. PB, p. 108923, 2023, doi: 10.1016/j.epsr.2022.108923.

S. Sahoo and C. Lo, "Smart manufacturing powered by recent technological advancements : A review," *J. Manuf. Syst.*, vol. 64, no. January, pp. 236–250, 2022, doi: 10.1016/j.jmsy.2022.06.008.

A. Distinct and E. Method, "Subject Index of Volume 32," vol. 32, 2021, doi: 10.1016/S0921-8831(21)00603-8.

A. Co and B. California, "textile," pp. 355–364, doi: 10.1016/B978-0-08-101937-5.00026-9.

N. This, "No Title," pp. 508–510, doi: 10.1016/B978-0-12-809597-3.09001-5.

V. Azamfirei, F. Psaromiatis, and Y. Lagrosen, "Application of automation for in-line quality inspection , a zero-defect manufacturing approach," vol. 67, no. December 2022, pp. 1–22, 2023.

N. Abbreviations, "No Title," doi: 10.1016/B978-0-08-096532-1.18001-X.

Skip to main content

Author Search Sources Create account Sign in

Source details

Feedback > Compare sources >

European Chemical Bulletin

Open Access

Scopus coverage years: from 2017 to Present

Publisher: Deuton-X Ltd.

E-ISSN: 2063-5346

Subject area: Chemistry: General Chemistry

Source type: Journal

Save to source list Source homepage

CiteScore 2021
0.8

SJR 2021
0.139

SNIP 2021
0.187

CiteScore CiteScore rank & trend Scopus content coverage

Improved CiteScore methodology

CiteScore 2021 counts the citations received in 2018-2021 to articles, reviews, conference papers, book chapters and data papers published in 2018-2021, and divides this by the number of publications published in 2018-2021. Learn more >

CiteScore 2021

0.8 = 182 Citations 2018 - 2021 / 217 Documents 2018 - 2021

Calculated on 05 May 2022

CiteScoreTracker 2022

1.6 = 499 Citations to date / 313 Documents to date

Last updated on 11 April 2023 • Updated monthly

Original Article

Novel Management Trends Using Iot In Indian Automotive Spares Manufacturing Industries

Dr. Jnaneshwar Pai Maroor[1*], Dr.Neelam Labhade-Kumar[2], Sarika khandelwal[3], Bhola Khan[4], Parinita J Chate[5], E. Fantin Irudaya Raj[6]

Department of Humanities,NMAM Institute of Technology-Affiliated to NITTE (Deemed to be University)[1*]

Department of Electronics & Telecommunication, Shree ramchandra college of engineering, wagholi pune[2]

Department of Computer science & Engg., G H Raisoni College of Engineering Nagpur,India[3]

Department of Economics, Yobe State University, Damaturu, Nigeria[4]

Department of Computer Engineering, Bharati Vidyapeeth's College Of Engineering Lavale,Pune[5]

Department of Electrical and Electronics Engineering,
Dr. Sivanthi Aditanar College of Engineering, Tiruchendur, India[6]
jnan_pai@nitte.edu.in[1*], neelam.labhade@gmail.com[2], sarikakhandelwal@gmail.com[3], bholaakhan1512@gmail.com[4], parinitachate@gmail.com[5], fantinraj@gmail.com[6]
DOI: 10.47750/pnr.2022.13.S09.606

Abstract

The development of smart manufacturing systems is being driven by a variety of diverse needs for the dependability of equipment and the prediction of quality. In order to accomplish this objective through the use of machine learning, a wide range of approaches are being investigated. The management and protection of one's company's data presents yet another challenging aspect of doing business. In order to cope with fraudulent datasets, machine learning and internet of things technologies were utilised. These technologies were used to protect system transactions and manage a dataset. Because of this, we were able to find solutions to the problems that we had previously discussed. The gathered information was organised and examined with the help of big data techniques. The Internet of Things system was constructed using the Hyperledger Fabric platform, which is a private computer network. In addition, a hybrid prediction strategy was utilised for the defect diagnostic as well as the defect forecasting. The latest machine learning techniques were utilised in order to model the complexity of the environment and estimate the genuine positive ratio of the quality control system. The quality control of the system was evaluated using these pieces of data.

Keywords: Machine learning, IOT, PBFT, Smart Industrial, Security, and Quality Control.

I. INTRODUCTION

IOT technologies, physics, and cyber capabilities have been integrated into smart production setups so that the benefits of these setups can be realised to their full potential [1]. The overall system has been given a great deal of attention to detail in order to make it more adaptable and compatible. In order to encourage the use of cyber-physical systems, tools, and procedures in smart factories and make decision-making easier in the 4th generation of manufacturing, the German government came up with the name "Industry 4.0." [2] The enhanced speed, volume, and variety of data that

big data provides are utilised by smart manufacturing. When big data technologies are utilised, analyses become more accurate, and it becomes simpler to generate predictions [3, 4]. It is essential for businesses to have the features that have been outlined above, but the costs and other particulars can change depending on the provider as well as the configuration of the system. As a consequence of this, it is possible that the capacity of certain businesses can be increased by researching the overlap that exists between other industries.

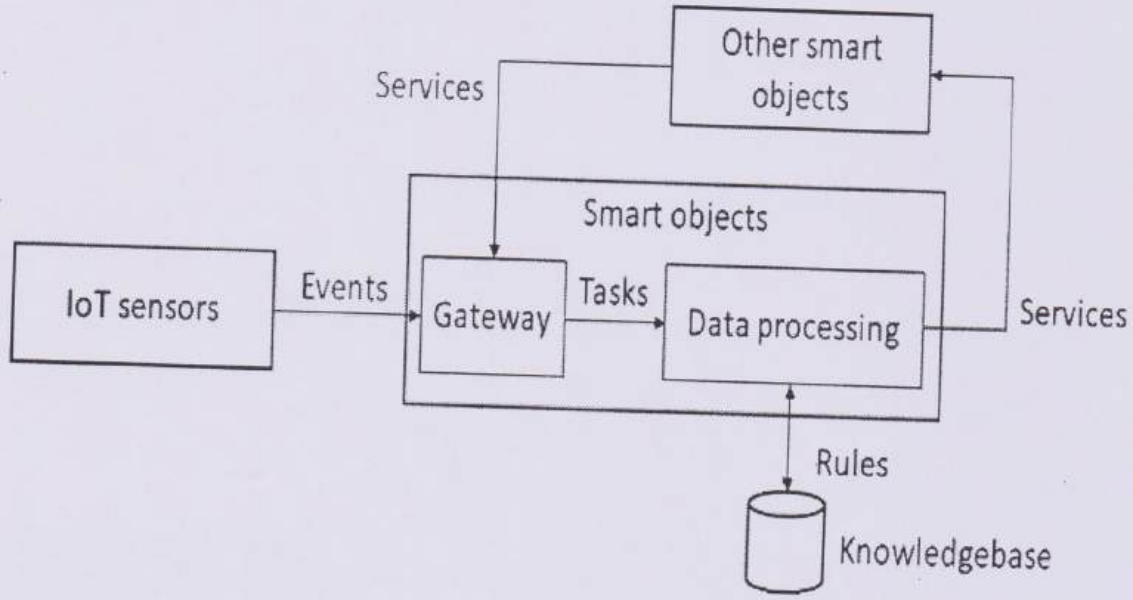


Figure 1. General Block diagram of Machine Learning with IOT for Smart Industrail

In recent times, there has been a lot of focus placed on the proliferation and use of IOT technologies in the financial services industry [5]. The typical applications of the Internet of Things are dependent on networks that contain smart contracts in order to transfer assets and exchange data. This technology is thought to be beneficial to a variety of different areas, including the corporate world and the manufacturing sector. The fundamental objective of the smart manufacturing initiative that is part of Industry 4.0 is to define the relationships between the many production facilities, retail locations, and other organisations that are involved [6]. This process will have an effect on both the automation and the operational optimization. Because of this, it is capable of greater adaptability, safety, and cost-effectiveness, in addition to increased productivity and profitability. Despite the fact that Industry 4.0 has a great deal of potential, its implementation has been hampered by a number of challenges that are specific to the manufacturing industry. The most prevalent sources of problems include information sharing across several devices, networking, and other similar activities [7]. The comprehensive procedure is shown in Figure 1. In this particular instance, both the business procedures of the manufacturer and those of the distributor are taken into consideration. The internal and external layers are the two components of the IOT system that have been presented for the manufacturer's transaction that are considered to be the most crucial. The manager will begin by making contact with the many parties involved in the production of the product, including the suppliers, manufacturers, and distributors. This is done in order to maintain quality control and reduce the number of errors that occur during production. The steps involved in the production of intelligent contracts have already been described. The information that is held in a given layer of the Internet of Things (IOT) can be accessed from that layer. The key point of emphasis that is placed on this layer is the decision that the producer makes on the manner in which their products are sold. After decrypting the data stored in the private layer, the author shares it with the rest of the participants. The dataset is encrypted in the same fashion using both the public key and the private key. There is no way to establish a direct connection between the public layer or the encrypted file and the private key. The transaction step of this method receives the vast majority of the attention and focus of the public layer. The first stage in managing and validating the transactions dataset is data mining, which you can read

more about here. The transaction is checked for legitimacy once the data have been inserted into the sequence structure of the IOT.

The following are this paper's key contributions:

- Monitoring in real-time based on IoT ambient sensors.
- Using IOT to reduce decision-latency. making's
- Making use of IOT and machine intelligence to protect decentralized, open transactions.
- The enhancement of the manufacturing network through use of smart contracts.
- Predictive assessment relies on the manufacturing system's fault diagnosis.
- Managing the huge industrial dataset using big data approaches.

The remaining sections of the essay are organized as follows: The practical literature evaluation of the most recent industrial and technical processes is presented in Section II. The suggested manufacturing approach architecture is shown in Section III. The results and discussion are presented in Section IV, and we wrap up this study in Section V.

II. LITERATURE SURVEY

This section covers information on smart manufacturing and outlines some current business problems that the scientific community has been oblivious to.

In the second decade of the twenty-first century, there was a substantial improvement made in both the field of next-generation analytics and business development. Because of breakthroughs in manufacturing techniques, brand-new devices like the FinFET [8] and the shift from 2D to 3D device design have been realisable. These modifications were required due to the fact that the devices are becoming progressively more difficult to use. During the second phase, new market trends encouraged the development of electronics that were more compact, quicker, and required less power. The technology that enables these devices to communicate with one another is referred to as the Internet of Things, or IoT for short (IoT). When it comes to connecting to the internet at a home or business, the process works like this. The process of collecting and analysing data from a wide variety of sources, including customer feedback, production data, information about the firm itself, requests, and so on, has enabled smart manufacturing to significantly improve decision-making. Manufacturers have profited from the feedback of customers and other stakeholders at various stages of product development in order to improve the quality, design, and other elements of their products. The analysis of customer preferences and product deficiencies in real time using big data is a significant tool that organisations can use to improve the products and services they offer. Because of this, data-driven advertising is a more effective instrument than conventional advertising when it comes to anticipating what products should be manufactured.

Big data technologies such as NoSQL MongoDB, Apache Kafka, and Apache Storm can be utilised to process and store the data that is produced by the manufacturing industry. Using the scalable messaging infrastructure provided by Apache Kafka, it is feasible to design applications that run in real time. The system's primary benefits include its swiftness, its capacity for expansion, and its adaptability in the face of error. Several research came to the conclusion that the utilisation of data collected by sensors connected to the Internet of Things (IoT) was advantageous in a variety of fields, including healthcare. The first time it was used in medical practise was in the year [13]. The sensor data collected from the patients is stored in Apache Kafka and MongoDB by the system that has been suggested. A method called Apache Kafka was applied to the process of developing an online parking system in [14].

The Internet of Things (IoT) has brought about revolutionary changes in the areas of data security, data transit, fault tolerance, and transparency [15]. The distributed ledger is an integral part of the process that is being carried out here. The Internet of Things places a premium on safety while retaining a high degree of adaptability, decentralisation, and openness. This is one of the most distinguishing characteristics of IOTs. Bitcoin [16] was the first cryptocurrency to make this technology accessible to the general public; since then, researchers have worked to make it more practical in a wide range of industries and applications. Internet of Things (IOT) applications can be found in a variety of fields, including cryptocurrency [22], agriculture [17], education [18], healthcare [19], economics [20], and transportation [21]. According to the authors of [23], the Internet of Things has the potential to be utilised to control and track agricultural supply networks. The key objectives of this system are the management of the supply chain and the localization of products. The Internet of Things-based agricultural supply chain makes use of Hyperledger Fabric and Ethereum, which are both independent IoT network platforms. There are considerable differences in both the manner in which transactions are carried out and the amount of time required to finish them. Utilizing this technique will allow you to keep your data protected from harm. According to the information presented in [25], using a network that consists of interconnected devices can be a risk-free means to obtain data. The utilisation of IOT technology, which enables digital information to be transmitted without consent and controls the timestamp dataset that connects the services and the system, is the essential component to accomplishing this objective. To put this plan into action, you will need to obtain the necessary permissions.

Cloud manufacturing is a relatively new method of producing goods that can be adapted to meet the specific requirements of the end user. Under the proposed paradigm, distributed resource management and cyber-physical manufacturing will each be managed as a separate service. Due to the centralised nature of the cloud's architecture, there are problems with both trust and security [26]. In the manufacturing industry in [27], both public and private networks were utilised in the capacity of cloud service providers. A public Internet of Things was utilised by the provider of the service (IoT). At the level of the workshop, a private IOT was utilised. The level of the machine was utilised so that the data could be acquired. According to [28], the absence of a moderator does not prevent a cloud-based IOT network from being able to contribute to the establishment of confidence in the network. The manufacturers expressed a wish to share some information, but the model that is now being proposed is unable to accomplish this goal. Because of this, there was an inefficiency and a decrease in the quality of the service that was provided [28].

The goal of the manufacturing sector is to create an intelligent manufacturing environment that allows for the possibility of machine learning by utilising new technologies such as the internet of things (IoT), big data, and others. The system of advanced manufacturing contains a wide variety of sensors, each of which is capable of collecting data in a different manner. The sensor data comes from a wide array of objects, pieces of equipment, activities, and sensors located throughout the environment. The primary focuses of this section [29] are conducting an analysis on a significant volume of data and making judgments in real time. They are able to identify patterns, learn on their own from the datasets provided, and carry out a broad variety of other operations. Learning by machine (ML) and artificial intelligence (AI) both [30] It is possible to enhance the product's quality while simultaneously accelerating production using a number of different tools and approaches. The following paragraphs will explain only two of the numerous applications where machine learning and artificial intelligence (AI) can be of assistance: forecasting production and performing routine maintenance. In predictive maintenance, data are used to construct systems that are capable of identifying potential issues before they manifest themselves. It is possible to monitor the productivity cycle over a period of time by analysing the data for patterns over time and then basing production estimates on those patterns. With the help of machine learning, it is feasible to obtain reliable outcomes from quality control inspection applications without the participation of humans beings (ML). The same holds true for people who operate in the manufacturing industry, as they are required to reach a consensus on the standards and procedures that will be used for freely interacting with one another. [31]'s approach to the manufacturing system has put a key emphasis on providing high levels of customer satisfaction. If artificial intelligence and information communication are combined, a factory may be able to be customised based on self-perception and intelligent decision-making in order to improve the quality of its production.

III. PROPOSED METHODOLOGY

The planned system's intricate architecture is covered in this section. The suggested system's design, which is predicated on IOT-based quality control, is depicted in Figure 2. The suggested system is composed of four primary layers: a business layer with multiple services, a distributed database layer, and IoT sensor layer, and a smart contract layer. Distribute the ledger for evaluating quality, assets, logistics, other transaction data safely using machine learning as well as IOT technologies. In the system described, the specified smart contract offers intelligence, privacy protection, including automation, and IoT sensors extract real-time data. The pre-processing and data analysis performed throughout this procedure uses machine learning modules.

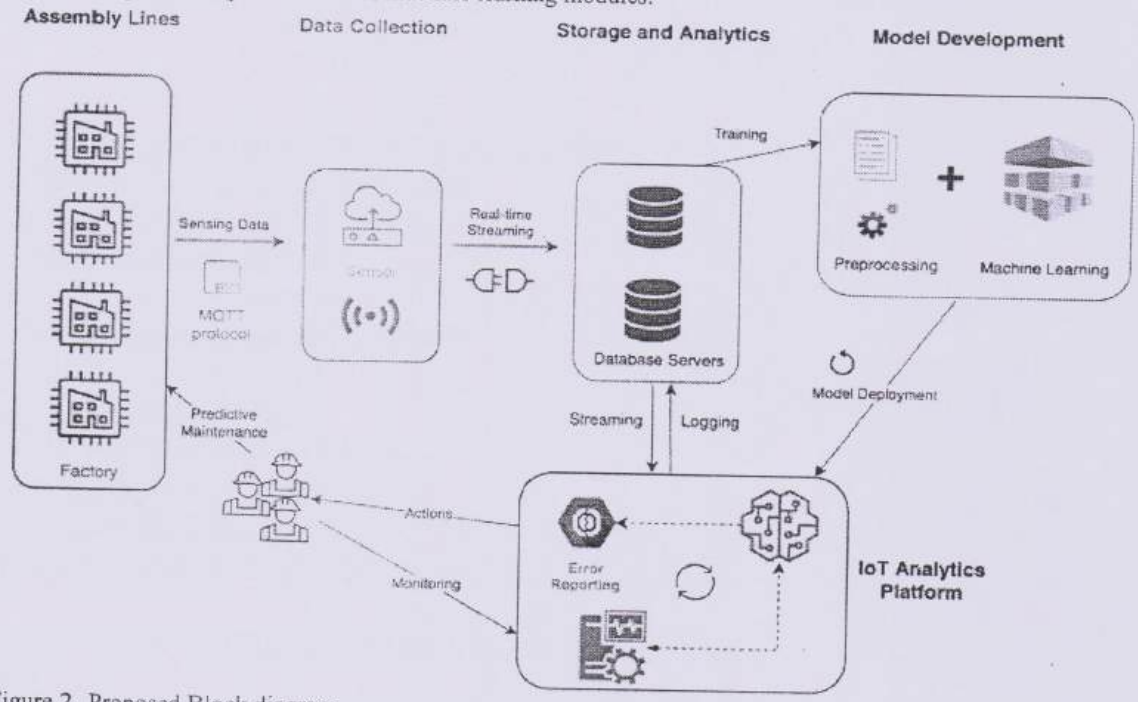


Figure 2. Proposed Block diagram

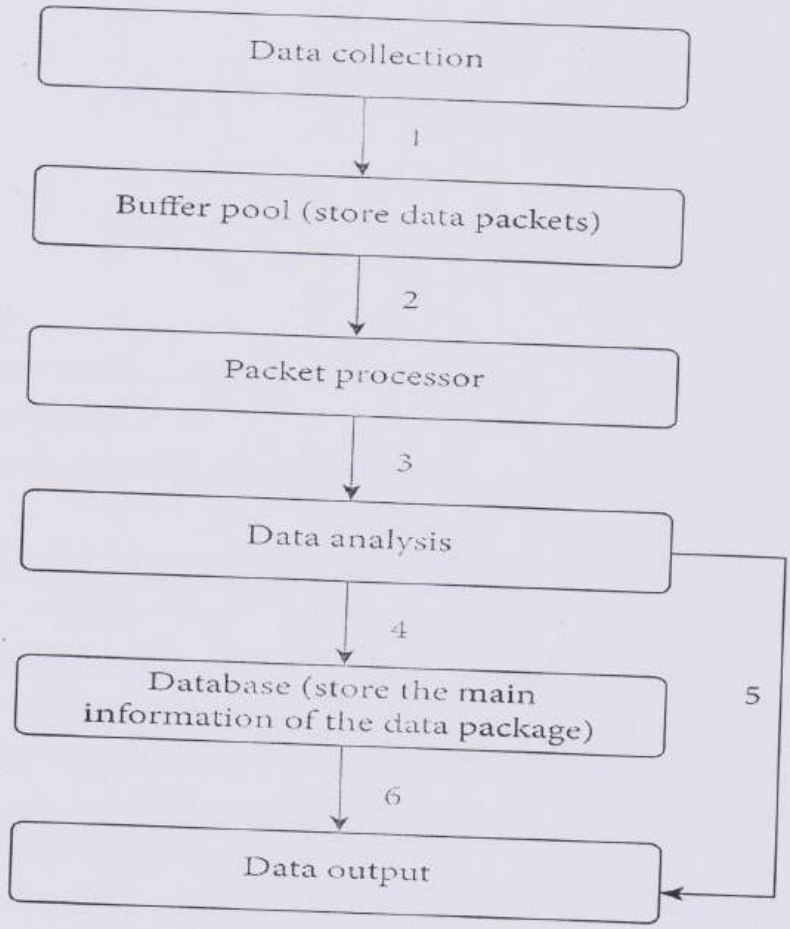


Figure 3. Flowchart of Proposed methodology

In order to keep track of the logistics and position data pertaining to the items, the sensor layer, which is the initial layer, uses GPS. Through the use of the Internet of Things, transactions, asset quality, and asset location can all be monitored. Barcodes can be utilised in processes where there are not many data points and accuracy criteria are not necessary because the prices of IOT are so high. In addition to sensors that measure temperature and humidity, a variety of other sensors may also be utilised in order to collect necessary data. The distributed ledger layer makes up the second tier of the Internet of Things (IOT) stack. This layer includes transactions, resources, logistics, and high-quality data as its components. Every one of these parties, including the manufacturer, the distributor, the retailer, and the owner of the banking institution that services the retailer, possesses a copy of this information. This information is utilised for the purposes of quality control and making certain that the system is operating effectively. The third layer of the supply chain is called a smart contract, and it is responsible for the collection and sharing of data. Digital identities are frequently used to set limits on who can access private information in the interest of keeping that information secure. This strategy is required to be applied whenever competitive businesses within a supply chain share confidential information with one another. The business layer incorporates each and every one of the numerous business procedures in addition to itself. In addition to this, IOT might be responsible for managing and monitoring the quality and support contracts.

3.1. Real time Quality Control

The Internet of Things (IoT) is becoming an increasingly valuable technology as the number of businesses and sectors that exist in the globe continues to grow. When organisations communicate their datasets both within and outside of

the plant, security concerns might arise, particularly in relation to machines, networks, participants, components, commodities, and logistics. The manufacturer has the ability to choose the optimal solution while minimising the drawbacks of IOT technology by providing challenges, opportunities, and industry knowledge. This ability is what determines the optimal position for IoT in each organisation, and it depends on the manufacturer's ability to identify its needs and issues. In order for the IOT technology to perform effectively across the entirety of the production process, it must at all times be understandable and trustworthy. For the purpose of achieving more transparency in the management of assets, it is essential to make use of standards, maintain quality standards, regulate firm identifiers, monitor supply chains, and track assets. The utilisation of smart contracts results in providers, manufacturers, and other relevant parties receiving notifications regarding the quality of both the real-time data processing and the product quality. The technology may be able to supply smart contracts to a wide variety of vendors by utilising digital IDs. Every component possesses both a one-of-a-kind digital identity and an identification number that is exclusive to the Internet of Things. In addition, a manufacturer is unable to read this data, which ensures that it will not be shared with other suppliers who offer similar services. Through the use of smart contracts, it is conceivable that manufacturers will be able to control the monitoring equipment.

3.2. Predictive Analysis Based on Machine Learning

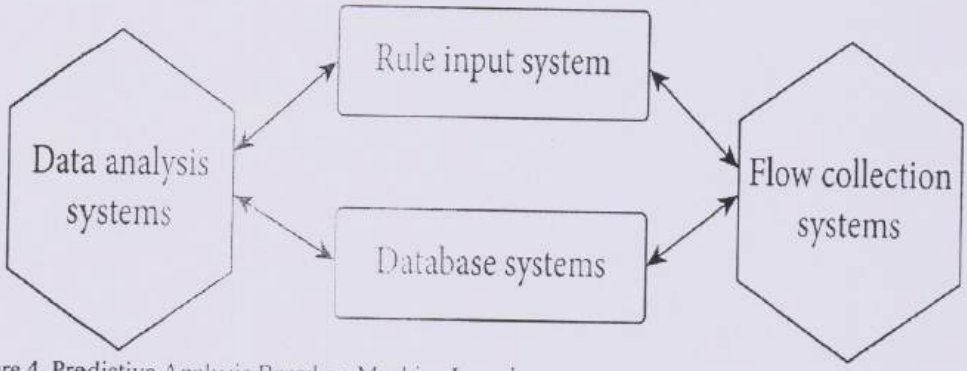


Figure 4. Predictive Analysis Based on Machine Learning

In the course of the last few decades, machine learning has been put to use in various industrial processes in order to foretell the future and make decision-making easier. In order for data extraction to be as efficient as it possibly can be, it needs to be able to recognise new patterns and forecasts, in addition to other pertinent data points. It is now possible to make decisions much more quickly than in the past. The method of production is directly affected in some way by each and every one of the things that have been brought up in this discussion. The major purpose of machine learning is to provide the industrial sector with a fresh point of view, which is why this field is so important. The stage of data preparation is an essential component of machine learning since it enables the user to extract the relevant information, investigate the structure, pick samples, and decide on a course of action. When it comes to the extraction and utilisation of data, it is also necessary to take into account changes in both the conditions and the tasks at hand. Only via careful data preparation and transfer is it possible to improve the overall quality of a dataset. Creating a training dataset is the first step that must be taken before deciding on the machine learning algorithm to use. When a model is chosen, the necessary parameters become available for selection. In the following stage, the overall performance will reach its conclusion. Evaluation and validation of the model's performance can be accomplished by a variety of methods, including cross validation, variable sensitivity analysis, modelling stability analysis, and others. After the dataset has been modelled and the performance has been validated, we then utilise the many ways to data analysis in order to improve our methodology. Clustering and supervision are two examples of analytical procedures, together with defect detection and diagnosis, terms of the specific, and quality. Using the fault diagnostic, any defects discovered during testing can have their causes thoroughly probed. It is possible that the fundamental cause of the problem is located within the process itself or a single sensor, according to the approach taken to diagnose faults. Following the completion of the clearing of the fault diagnosis output, the performance evaluation report is then

generated. Methods of soft sensing or prediction can be utilised in order to perform an evaluation of the operation's core performance. The predictive data models have the ability to extract and supplement the online prediction process based on the link between the components that are shared by both models. On the screen will be provided a real-time prediction output that is based on regression and prediction models.

3.2.1. Practical Byzantine Fault Tolerance Algorithm (PBFT)

Because of using the model, it is possible to obtain the income function of the attacker, as well as the income function of the intrusion prevention system, in order to build its attack and defence strategies. Additionally, it is possible to obtain the income matrix in order to obtain the Nash balance of the model based on the desired function [32]. The construction of a practical Proactive fault technique involves the combination of four tuples. Changing Equation (1) into the following equation, which represents the model RRDM through appropriate representations of the and as the revenue function of an attacker with an intrusion detection system, which represents the total number of games, is how the Byzantine fault-tolerant method (RRDM) is described.

$$R_{RDM} = (a, d; A_a, A_d; U_a(A_a), U_d(A_d), T) \quad (1)$$

Create a formula-based assault plan and defense strategy suit (1). These are the phrases.

$$S_a = (S_N, S_M, S_P, S_A) \quad (2)$$

$$S_d = (S_C, S_R, S_W, S_D) \quad (3)$$

S N, S M, S P, S A, and And in the formula stand for normal, attack, aberrant, and preattack action strategies. The letters S C, S R, S W, and S D stand for continuing execution, suggested execution, alarm, as well as protective action, respectively.

$$S_{ad} = (s_a, s_d | s_a \in S_a, s_d \in S_d) \quad (4)$$

Expressed the action strategy of both sides of the bureau.

3.3. Implementation of Proposed Methodology in Smart Manufactures

In this section, we will provide an analysis of the results as well as an application of the integrated methodology that was proposed. The procedures and instruments that were utilised during the execution are detailed in Table 2, along with the essential preparation steps. Ubuntu Linux 18.04.1 LTS and an Intel(R) Core(TM) i7-8700 running at 3.20 GHz were the operating systems and processors that were used to implement and carry out the strategy, respectively. The docker engine must be version 18.06.1-ce, and the suitable docker composer version was 1.13.0. The IOT environment requires both of these versions. IoT technology based on Hyperledger Fabric V1.2 was utilised, together with 32 gigabytes of primary memory. Composer REST Server, a well-known CLI (command line interface) tool, was used to deploy composers when working with the Composer-Playground integrated development environment (IDE) platform. TensorFlow was utilised as the programming language for the platform.

In order to implement the predictive analysis using this method, the scikit-learn module that is part of the PBFT model as well as the programming language Python were utilised. The fundamental algorithm of PBFT, PBFT, can be of significant assistance in the analysis of non-linear and numerical datasets. As a direct consequence of utilising this method, the overfitting issue will not arise. The process of making a forecast can be broken down into three steps. In this first section, we will discuss the best practises for data collection in an industrial environment. After going through the second stage of processing, the data are then prepared to be used in the stages of manufacturing that come after them. In conclusion, the PBFT prediction algorithm is applied in order to evaluate and foresee the quality of the suggested system when it is implemented in a production setting. The seven key activities that comprise the data

preprocessing segment include feature engineering, data transformation, feature comparison, dataset normalisation, feature selection, dataset division into training and test sets, and the implementation of the PBFT algorithm. Each of these activities is a part of the feature selection process.

IV. RESULTS AND DISCUSSION

Accuracy is a statistical measure that indicates how successfully a system recognises or ignores a binary classifier. The accuracy of this procedure was evaluated with the help of Equation 5, which was applied. The terms "true positive," "true negative," "false positive," and "false negative" are represented by the letters "Xa," "Xb," "Ya," and "Yb," respectively. A strong indicator of a solid performance is high accuracy on the hit. The outcomes of various machine learning algorithms are compared in Table 1, which illustrates how the suggested method stacks up against its competitors. The hardware and software specifications are listed in Table 2.

$$\text{Accuracy} = \frac{X_a + X_b}{X_a + X_b + Y_a + Y_b} \quad (5)$$

Equation (6) assesses this procedure's recall. The ideal indicator for choosing a model is the recall, which displays the genuine positive proportion that was properly detected.

$$\text{Recall} = \frac{X_a}{X_a + Y_b} \quad (6)$$

Equation (7) assesses the accuracy in light of the determined accurate and positive values. Similar to that, it calculates the expense of false-positive scenarios.

$$\text{Precision} = \frac{X_a}{X_a + Y_a} \quad (7)$$

Table 1. Comparable results of machine learning algorithms

Model	Training (s)	Prediction (s)	Accuracy (%)
Logistic Regression [34]	2.187	1.881	60.40
Naive Bayes [34]	1.484	1.682	68.50
KNN [35]	1.412	1.518	80.20
XGBoost [36]	1.219	1.312	91.73
Proposed PBFT	1.115	1.112	99.16

Table 2. Experimental environment

Tool's	Component's	Specification's
Hardware	CPU	Intel(R) Core (TM) i7-6500U @2.60 GHz
	Memory	8 GB RAM
Software	Operating software	Window 10
	Simulation Software	Pycharm 2019.2 (Python 3.8)

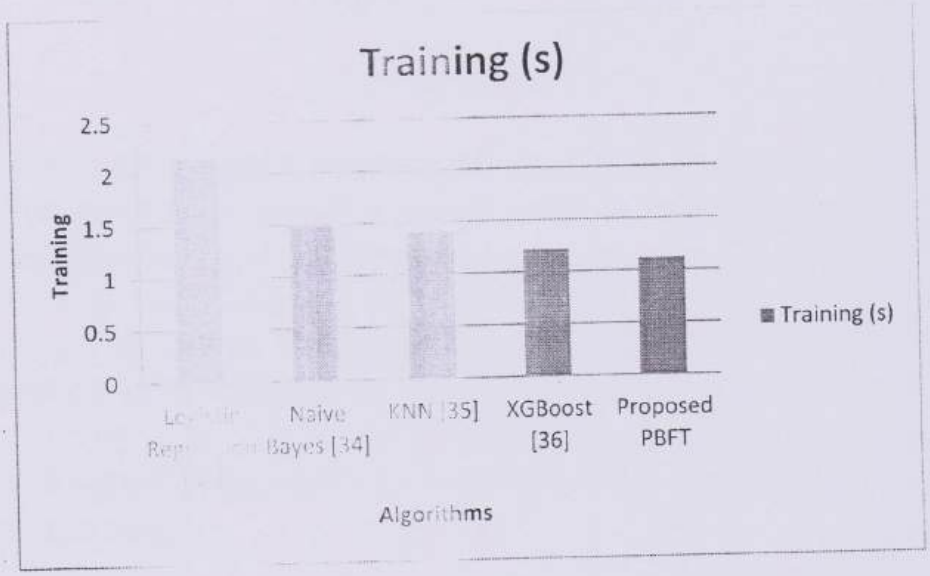


Figure 5. Comparative results of machine learning algorithms for Training (s)

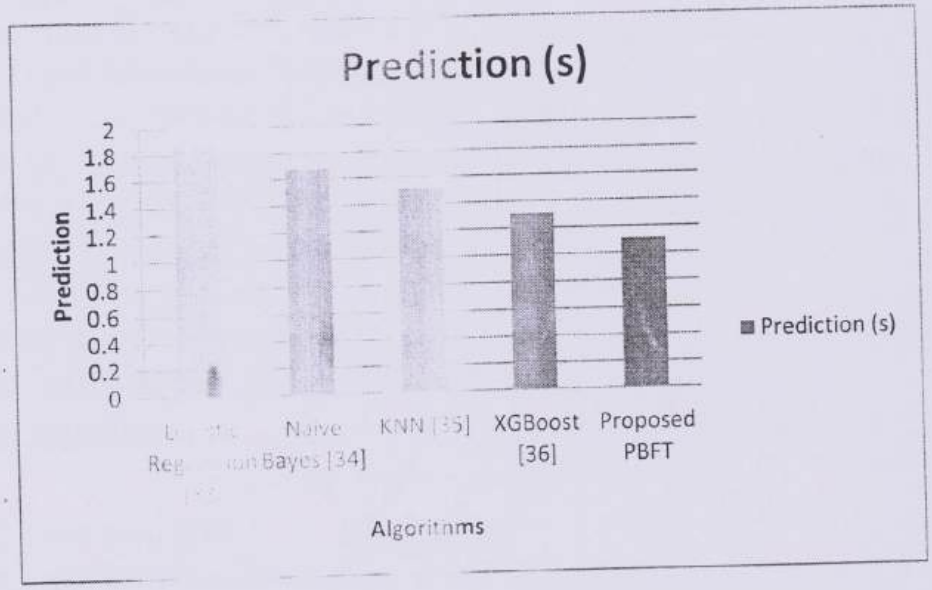


Figure 6. Comparative results of machine learning algorithms for Prediction (s)

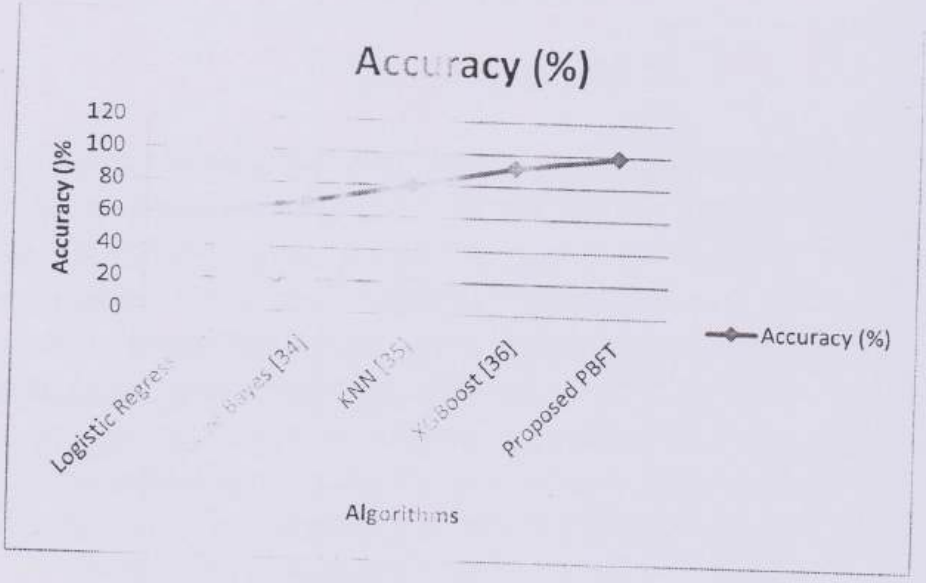


Figure 7. Comp[illegible] results of machine learning algorithms for Accuracy (%)

The smart manufacturing sector using machine learning plus IOT is presented. The outcomes of machine learning techniques for training, predictions, and accuracy are shown in figures 5, 6, and 7. The manufacturer may add, edit, and remove product information in the intelligent production management system over the IOT network. In order to enter new information, the manufacturer must complete the online form as well as all IOT network entries. Users may update their data on the IoT network in a similar way by sending a preferred method through the user interface.The suggested system's transaction history gateway for the IOT network is shown in Figure 4. The transaction history so all of the actions taken on this site are connected to the transactions offered. Dates, timings, entry kinds, participants, and activities are all recorded in the data. Similar to that, the network's transacted file system details are also given.

V. CONCL[illegible]

The purpose of this project was to investigate a number of different machine learning and internet of things-based approaches to multistage quality control. The correctness of the categorization was used as a criteria for doing the data validation. A comparison of PBFT with other machine learning approaches reveals that the complicated correlations derived from the data can be utilised to do an evaluation of the data set's overall quality. The solution that was provided was successful in enhancing the environmental quality of smart manufacturing processes and obtaining desirable results because it made use of an Internet of Things (IoT) and machine learning (ML). With the assistance of this technology, businesses and manufacturers can make their environments of work more trustworthy and secure. By extending the scale of the network, we will be able to test and evaluate the operation of the system in increasingly complex industrial scenarios with high precision, machine learning models, and other types of applications.

REFERENCES

1. Moyne, J.; Iskandar, J. Big data analytics for smart manufacturing: Case studies in semiconductor manufacturing. Processes 2017, 5, 39.
2. Shah, D.; Wang, J.; He, Q.P. An Internet-of-Things Enabled Smart Manufacturing Testbed. IFAC Pap. 2019, 52, 562–567.
3. Lee, J.; Kao, H.-A.; Yang, S. Service innovation and smart analytics for industry 4.0 and big data environment. Procedia Cirp 2014, 16, 3–8.
4. Thoben, K.D.; Wiesner, S.; Wuest, T. "Industrie 4.0" and smart manufacturing-a review of research issues and application examples. Int. J. Autom. Technol. 2017, 11, 4–16.
5. Rossmann, Marion, and Khadikar, Patrice De Franc, Laurent Perea, Ralph Schneider-Maul, Jerome Buvat, and Aritra Ghosh. "Smart Factories: How can manufacturers realize the potential of digital industrial revolution." Capgemini. com (2017).

6. Trade, G. (2[illegible] ("INSDUSTRIAL SMART MANUFACTURING FOR THE FUTURE"..
7. Galvin, P.; B[illegible]nur, R.; Lavera[illegible]r-industry spillovers through DIY laboratories: Entrepreneurship and innovation in the global bio[illegible]echnol. Forecast. Soc. Chang. 2020, 160, 120235
8. Lu, Y.; Xu, [illegible]. Smart manufacturing process and system automation–a critical review of the standards and envisioned scenarios. J. [illegible] 2020, 56, 312–[illegible]
9. Alizadeh, M.; [illegible] K.; Scheben, O. A Survey of Secure Internet of Things in Relation to Blockchain. J. Internet Serv. Inf. Secur. 2020, 3.
10. Ferdous, M.S.; [illegible]ury, M.J.M.; Hoque, M.A.; Colman, A. Blockchain Consensus Algorithms: A Survey; IEEE: New York, NY, USA, 2020.
11. Gorkhali, A.; [illegible]otha, A. Blockchain: A literature review. J. Manag. Anal. 2020, 7, 321–343.
12. Chiarini, A.; [illegible] W.; Grando, A. Industry 4.0 strategies and technological developments. An exploratory research from Italian manufacturi[illegible]s. Prod. Plan. Control 2020, 31, 1385–1398.
13. Romero, D.; [illegible] Thiesch, M. The Operator 4.0: Towards Socially Sustainable Factories of the Future; Elsevier: Amsterdam, The Netherlands, [illegible]
14. Oliveira, R.N.; [illegible]; [illegible]; C. Soft Error Impact on FinFET and CMOS XOR Logic Gates. J. Integr. Circuits Syst. 2020, 15, 1–12.
15. Yudhistyra, W.; [illegible]; E.M.; Ramgrattanaboorn, I.s.; Ratanavaraha, V. Using Big Data Analytics for Decision Making: Analyzing Customer Be[illegible]ing Association Rule Mining in a Gold, Silver, and Precious Metal Trading Company in Indonesia. Int. J. Data Sci. 2020, 1, [illegible]
16. Hoefflinger, [illegible]; International Roadmap for Devices and Systems, Rebooting Computing, S3S. In NANO-CHIPS 2030; Springer: Cham, Switz[illegible], pp. 9–17.
17. Moon, S.; B[illegible]ser, B.; Seibelmann, [illegible] Virtual learning for workers in robot deployed construction sites. In Advances in Informatics a[illegible]ring in Civil and Construction Engineering: Springer: Berlin/Heidelberg, Germany, 2019; pp. 889–895.
18. Alpaydin, E. [illegible]troduction to machine learning (2nd ed.). Cambridge, MA: MIT Press.
19. Ren, S.; Zhan[illegible]; Sakao, T.; Huisingh, D.; Almeida, C.M. A comprehensive review of big data analytics throughout product lifecycle to [illegible]ainable smart manufacturing: A framework, challenges and future research directions. J. Clean. Prod. 2019, 210, 1343–1365.
20. Brunato, M.; [illegible] R. (2005). Statistical learning theory for location fingerprinting in wireless LANs. Computer Networks, 47, 825–845. doi:10.1[illegible]omnet.2004.09.004
21. Burbidge, R.; [illegible]; Buxton, B., & Hodgkin, S. (2001). Drug design by machine learning: Support vector machines for pharmaceutic[illegible]analysis. Computers & Chemistry, 26, 5–14.
22. Çaydaş, U.; [illegible] (2010). Support vector machines models for surface roughness prediction in CNC turning of AISI 304 austenitic stainless steel. [illegible] Intelligent Manufacturing, 23, 639–650. doi:10.1007/s10845-010-0415-2
23. Loechner, J.; [illegible] Today's Data Created in Two Years; The Center for Media Research: Reston, VA, USA, 2016. 22. Lawlor, B.; Lynch, R.; M[illegible]; M.; Walsh, P. Field2Cloud genes: Using Apache Kafka as a bioinformatic data repository. GigaScience 2018, 7, giy036.
24. Alfian, G.; [illegible]; Ijaz, M.F.; Syafrudin, M.A.; Fitriyani, N.L.; Rhee, J. A personalized healthcare monitoring system for diabetic pati[illegible]ing BLE-based sensors and real-time data processing. Sensors 2018, 18, 2183.
25. Ji, Z.; Ganch[illegible]ssana, M.; Zhao, F.; Wang, X. A cloud-based car parking middleware for IoT-based smart cities: Design and implementat[illegible]ns. 2014, 14, 22372–22393.
26. Parliament, E[illegible]ustry 4.0. 2016 http://www.europarl.europa.eu/RegData/etudes/STUD/2016/570007.
27. Nakamoto, S.[illegible]; Peer-to-Peer Electronic Cash System; Technical Report; Manubot; Satoshi Nakamoto Institute: Tokyo, Japan, 2019.
28. Lin, Y.P.; P[illegible]; Anthony, J.; Mukhlis, H.; Liao, S.W.; Chou, C.F.; Ho, Y.F. Blockchain: The evolutionary next step for ICT e-agriculture. [illegible] 2017, 4, 50.
29. Chen, G.; [illegible]; Chen, N.S. Exploring blockchain technology and its potential applications for education. Smart Learn. Environ. [illegible]
30. Rabah, [illegible]pportunities [illegible]chain powered healthcare systems: A review. Mara Res. J. Med. Health Sci. 2017, 1, 45–52.
31. Jamil, F.; Iqb[illegible]; Amin, R.; Kim, D. Adaptive thermal-aware routing protocol for wireless body area network. Electronics 2019, 8, 47.
32. Jamil, F.; Ahm[illegible]; Iqbal, N.; Kim, D.H. Towards a Remote Monitoring of Patient Vital Signs Based on IoT-Based Blockchain Integrity Man[illegible]ent Platforms in Smart Hospitals. Sensors 2020, 20, 2195.
33. Jamil, F.; Kim[illegible] Improving Accuracy of the Alpha–Beta Filter Algorithm Using an ANN-Based Learning Mechanism in Indoor Navigation S[illegible]. Sensors 2019, 19, 3946.
34. Jamil, F.; Iqb[illegible]; Ahmad, S.; Kim, D.H. Toward Accurate Position Estimation Using Learning to Prediction Algorithm in Indoor Navigation. S[illegible]. 2020, 20, 4410.
35. Ahmad, S.; [illegible]; Gudoyberdiev, A.; Kim, D. Accident risk prediction and avoidance in intelligent semi-autonomous vehicles based on [illegible] and driver biological behaviours. J. Intell. Fuzzy Syst. 2020, 38, 4591–4601.
36. Jamil, F.; Kim[illegible]; Efficient Mechanism for Electronic Charging using Blockchain in Smart Vehicle. Korea 2019, 30, 31. 36. Jamil, F.; Hang, L.; Kim[illegible]; A medical blockchain model for drug supply chain integrity management in a smart hospital. Electronics 2019, 8, 505.

37. K... Secure Transa... Management Using Blockchain as a Service Software for the Internet of Things. In Soft... IoT, Big Data, Cloud, and Mobile Computing; Springer: Berlin/Heidelberg, Germany, 2021; pp. 117–128.
38. Sh... A Procedure for Tracing Supply Chains for Perishable Food Based on Blockchain, Machine Learning and Fuzz... 2021, 10, 41.

Source details

ournal of Pharmaceutical Negative Results

Scopus coverage years: from 2010 to 2011, from 2013 to Present
Publisher: Wolters Kluwer Health
SSN: 0976-9234 E-ISSN: 2229-7723
Subject area: Pharmacology, Toxicology and Pharmaceutics: Pharmaceutical Science
Pharmacology, Toxicology and Pharmaceutics: Pharmacology
Pharmacology, Toxicology and Pharmaceutics: Drug Discovery
Source type: Journal

CiteScore 2021
1.0

SJR 2021
0.128

SNIP 2021
0.162

View all documents > | Set document alert | Save to source list

Ci ore | CiteScore rank & trend | Scopus content coverage

Improved CiteScore methodology

CiteScore 2021 counts the citations received in 2018-2021 to articles, reviews, conference papers, book chapters and data papers published in 2018-2021, and divides this by the number of publications published in 2018-2021. Learn more >

CiteScore 2021

1.0 = 45 Citations 2018 - 2021 / 43 Documents 2018 - 2021

C. d on 05 May, 2022

CiteScoreTracker 2022

1.4 = 84 Citations to date / 62 Documents to date

Last updated on 05 November, 2022 • Updated monthly

CiteScore rank 2021

C. y	Rank	Percentile
Pharmacology, To. ology and P. aceutics — Pharmaceutical Science	#110/171	35th
Pharmacology, Toxicology and Pharmaceutics	#235/303	22nd

View CiteScore methodology > | CiteScore FAQ > | Add CiteScore to your site

About Scopus

What is Scopus

Content coverage

Scopus blog

Scopus API

Privacy matters

Language

日本語版を表示する

查看简体中文版本

查看繁體中文版本

Просмотр версии на русском языке

Customer Service

Help

Tutorials

Contact us

ELSEVIER

Terms and conditions ↗ Privacy policy ↗

Copyright © Elsevier B.V ↗. All rights reserved. Scopus® is a registered trademark of Elsevier B.V.

We use cookies to help provide and enhance our service and tailor content. By continuing, you agree to the use of cookies ↗.

RELX

ResearchGate

See discussions, stats, and author profiles for this publication at: https://www.researchgate.net/publication/371461833

Power Transmission Performance Optimization: Intelligent Approach Needed

Article in European Chemical Bulletin · June 2023

DOI: 10.56042/ecb/2023.12.v4.582

CITATIONS
0

READS
22

6 authors, including:



Sanket Pawar
Bharati Vidyapeeth Deemed University
14 PUBLICATIONS **10** CITATIONS
SEE PROFILE



Avinash Ingole
Bharati Vidyapeeth College of Engineering Lavale Pune
15 PUBLICATIONS **33** CITATIONS
SEE PROFILE



Pratima Kadam
Bharati Vidyapeeth`s College Of Engineering,Lavale,Pune
4 PUBLICATIONS **0** CITATIONS
SEE PROFILE



Yogesh Vasant Kadam
Bharati Vidyapeeth's College of Engineering, Lavale, Pune.
23 PUBLICATIONS **10** CITATIONS
SEE PROFILE

Power Transmission Performance Optimization: Intelligent Approach Needed !

[1]Sanket S. Pawar, [2]Avinash M. Ingole, [3]Pratima M. Kadam, [4]Yogesh V. Kadam, [5]Pradeep P. Atre, [6]Jyoti A. Dhanke,

[1to6]Assistant Professor (Bharati Vidyapeeth's College of Engineering, Lavale, Pune 412115, India)

Abstract—Continuous non interrupted Power Supply is blood line for super growth of country. Power Transmission system with transform at core and play vital role. Safeguarding Transformer against faulty high frequency current using optimized intelligent design approach is needed. Existing Techniques are static approach based which are based on specific hardware components like relay switch, current manipulation techniques. This Technique fails at point of time due to lack of dynamic nature to predict failures and take preventive measures. This Article focuses on power transmission problems, existing techniques to handle them and area of problem that requires focus measures to taken.

Keywords—power Transmission, Transformer protection, intelligent systems

DOI: 10.48047/ecb/2023.12.si4.982

1. INTRODUCTION

A power Transform is heart of power system and safeguarding it failures is important. Post failure treatment of transformer is time consuming and costly. Most of cases an overhead transmission system is likely to fail due to impulse voltage. line surge generated at end which would be 2x 3x time of rated system voltage would definitely cause transformer failure and complete system breakdown.

Applying insulation enforces failure safety but it cannot be applied compared to ratio of insulation to earth. This leads to partial flash winding with high breakdown changes [1]. Non detection of failure in such cases destroys actual failure point which remains un detection. This use case urges requirement of intelligent systems which would log in failure points as first priority and safeguard system by taking preventing failure measures.

The fundamental power frequency measure based on differential protection principle to avoid power system failure proves reliable to operation. Secondary current vs primary current comparison assists in failure prediction. Although this techniques fails for star connected winding with earth faults non detected. Such problems have made power transmission system complex and failure prone [2]. This is especially true if there is a sizable resistance present in the neutral connection to lower the earth fault current's intensity. The restricted earth fault protection must therefore be used. The complexity of the transformer protection is unquestionably increased by this. Additionally, due to the high transformation ratio between the turns in the short-circuit and the rest of the winding, a short circuit involving only a few turns of the winding will result in a significant increase in fault current in the short-circuit loop but a negligible decrease in terminal current. Partial discharge, which is high frequency in nature and has little impact on terminal current, is produced by a possible problem such deteriorating winding insulation. Thus, it is clear that measuring fault-generated transients has benefits. Additionally, despite being generally quite good, the current differential approach is vulnerable to erroneous tripping on the transitory magnetizing inrush current that flows when the transformer is turned on. Since this current only runs through the transformer's energized winding, the protection system interprets it as an internal fault condition. Any power transformer protection solution must consider the impact of magnetizing inrush current because this impact may result in relay malfunction [3]. The harmonic restraint relay is the most popular method for avoiding erroneous trips during energization [4]. The inrush differs from an internal fault current so far as its waveform comprises a high percentage of harmonics. The basis for the harmonic restraint is the One of the main drawbacks of these techniques is the slowness.

I. LITERATURE SURVEY

An electrical device called a transformer modifies voltage and stream in the power system by starting at one level and advancing steadily up to the strongest without changing or repeating. The power imbalance between the circuits is unaffected by a typical little blip that happens concurrently. The protection of huge power transformers is a critical issue while moving the power system. The defensive system has components that can identify the presence of a problem, show its location and class, identify any further odd defects, like working conditions, and start the process of opening circuit breakers to disconnect the affected parts of the power system. Due to the power transformer's inrush current being abundant in the second symphonically section and preventing unnecessary excursion, differential reasoning is used in a significant portion of the calculation for the location of the shortcoming in the computerized differential protection of the power transformer. The protection of huge power transformers is a critical issue while moving the power system. The defensive system has components that can identify the presence of a problem, show its location and class, identify any further odd defects, like working conditions, and start the process of opening circuit breakers to disconnect the affected parts of the power system. Due to the power transformer's inrush current being abundant in the second symphonically section and preventing unnecessary excursion, differential reasoning is used in a significant portion of the calculation for the location of the shortcoming in the computerized differential protection of the power transformer. The calculation window is quite narrow, and DFT simply records data for recurrence analysis—it doesn't offer time-domain information. Although DFT anticipated being an intermittent signal, inrush current and shortfall flows are not fixed signs. Artificial brain organizations (ANN) have been widely used in the field of power system protection since around 1994, especially since this issue is a subclass of example waveform recognition. In particular, design identification, image processing, load estimation, power quality analysis, and information pressure were some of the areas where ANNs were most frequently applied. The key advantages of ANN technology over conventional approach are intrinsic capacity to produce sensible decisions and non-algorithmic equal circulated engineering for data management. S.B. Vasutinsky offers a system for organizing the configuration of power transformers that takes into account all fundamental limitations, monitors transient occurrences in transformers, and more. The book includes similar information on transformer configuration.

Geromel, Luiz H., and Souza, Carlos R. offer a distinctive power transformer plan technique using inventive architectures. The method used in this paper enables the employment of artificial brain associations for a few discrete intervals of the layout. The arrangement framework-focused epic distributed logy is a vital instrument for working on the projects as well as for efficiently reducing the need for their execution. The function of the transformer arrangement, according to Pavlos S. Georgilakis, Marina A. Tsili, and Athanasius T. Safaris, is to economically utilize the material that is readily available to achieve lower cost, lower weight, smaller size, and better working performance for the many different parts of the transformer. The focus of the transformer plan optimization approach presented in this research is on the layout of the transformer to satisfy the stated with the base cost.

Budgetary restrictions on the design of power transformers are demonstrated by T.H. Putman. The numerical analysis illustrates the relationship between size, misfortunes, reactance's, and power yield in the case of a perfect transformer design. This essay isn't a guide on how to build power transformers efficiently given the constraints. Jabr claims that the design difficulty requires limiting the total mass of the wire and centre material while making sure that the various design limitations and transformer assessments are taken into account. This article describes the application of GP design, a sort of mathematical programming, to resolve design issues. The challenge of design optimization with a limited number of variables is addressed by GP, which guarantees that the solution is globally optimal.

The availability of PCs in research centres has expanded the educational options accessible for power design, claim Farrukh Shahzad and M.H. Shwehdi. With this tool, lab teachers may quickly and online answer students' questions while simultaneously demonstrating and explaining the transformer design concept on the screen. The students can learn more by utilizing the programme and talking to other students about their thoughts and queries. The understudies' creative instinct has significantly improved

by emphasizing on understanding of core transformer design ideas rather than mathematical analysis and computer programming. Paul H. Odessey claims that by combining conventional transformer design techniques with the incredible speed and logical variety of a modem PC, our understanding of the transformer design methodology has improved. This is anticipated in part because the PC can do a number of time-consuming and repetitive computations in a logical and progressive manner, resulting in a design that satisfies all information requirements. A few experimental relationships are employed as a suitable place to start when summarizing design techniques and handling alterations that emerge from them.

II. PROBLEM STATEMENT

A. *Design Optimization of Transformers*

Transformer design optimization relies on reducing or improving a goal capability that is constrained by a few imperatives. The most frequently utilized target capabilities among the numerous goal efforts are reducing absolute mass, lowering the cost of dynamic parts, lowering the cost of fundamental materials, lowering the cost of assembly, lowering the cost of having everything, or raising transformer evaluated power. High-end PCs have considerably reduced the cost of PC hardware, which has given computer programmers the chance to automate support for the transformer design process. A computer was used to design the main transformer in 1955. Transformer Design Programming bundle offered a user-friendly environment, while Jabr employed mathematical programming design to limit the total mass of transformers. For perception and transformer design. Judd and Kressler proposed a system that calculates the anticipated centre first, and then determines the benefits of electrical and seductive borders that raise the VA limit or lower misfortune. It was shown how to optimize a transformer's design while taking into account five constraints: excitation current, impedance, proficiency, no heap losses, and all losses, as well as four goals: total cost of ownership, mass, all out losses, and material cost. The best centre decision to minimize centre and winding errors was determined using a design model that accounts for high recurrence skin and closeness affects and shows the impact of the required number of turns on the value variety of the transformer.

B. *Transform design optimization Artifical Intelligence*

Transformer design optimization is a challenging subject that has been tackled using a variety of artificial intelligence techniques. The application of various artificial intelligence methods by

This section provides an illustration of scientists responding to TDO concerns.

1. *GA(Genetic Algorithms)*

Hereditary algorithms (GAs) are based on Darwin's principle of the survival of the fittest.
Numerous disciplines, including science, business, and design, have made extensive use of hereditary algorithms for optimization. While proving the viability of applying GAs to complicated issues, created the fundamental GA notions. Their broad applicability, ease of use, and global viewpoint are what largely fuel their prosperity. Transformer development costs as well as operation costs have been decreased through the usage of gases. The design of the cooling architecture for appropriation transformers has also been optimized using GAs. The GA-based modelling technique has produced a developing computer model that advised on the boundary distinguishing proof of the power transformer. For toroidal central transformers or cast-pitch type appropriation transformers execution optimization, hereditary methods have also been applied. Hereditary calculations and reenacted tempering were used to create the best design for a rectifier power transformer, proving the effectiveness of GA as a technique for doing so. Georgilakis combined restricted component hereditary algorithms with an outside elitism method to solve the transformer cost minimization problem. an automatic transfer switch.

2. *ANN (Artificial Neural Network)*

Computational model research that is motivated by structural beliefs and presumptions .Concern exists in the subject of artificial brain organization over the structure and functionality of naturally existing brain cell arrangements in the human mind. The majority of the time, they serve as examples for addressing Issues with computation, mathematics, and design. The nature of wound center conveyance transformers was studied using developmental programming and brain networks. Artificial Brain Organizations (ANN) were used to predict the desirable transformer centre attributes and center misfortune, with a particular emphasis on reducing the iron misfortunes of gathered transformers, while the use of neural networks (NN) to estimate transformer costs at the design stage was also suggested. In order to evaluate load profiles for all types of clients, the utility didn't need to perform calculations. Assessment of iron misfortunes under unequal stockpile situation utilizing brain networks was explored to show how to minimize iron misfortunes. Transformer oil's brain network model .The developed NN model was employed on ten different operational transformers of the realized breakdown voltage of transformer oil in the administration life ID procedure. It was suggested that, in view of astounding recognized open repeated brain organization, one employ the methodology to demonstrate a power transformer with non-linearity.

3. SI(Swarm Intelligence)

Swarm intelligence is the study of computing architectures through group intelligence.

Collective intelligence emerges as a result of the interactions between large groups of uniform specialists. Fish schools, avian flocks, and underground bug provinces

all accounted for in the models. The two main sub-fields of the worldview are Molecule Multitude Optimization (PSO) and Insect Settlement Optimization (ACO), which both investigate probabilistic algorithms animated by coaching, jogging, or grouping. Swarm intelligence algorithms are thought of as flexible methods and are frequently applied to search and optimization issues.

Scientists have recently expressed an increasing interest in using swarm intelligence algorithms to address TDO issues. The appropriate primary winding turn count was determined using ACO to lower the transformer's cost, and the size of the transformer tap setting was increased in the power transmission organization to improve voltage security. ACO has also been used to select the right transformer size to deliver an approximation of the load. The practical use rate of sheet material for feeding the centre regions of power transformers rose due to the adoption of ideal resistance design issues for the construction of power transformers. PSO calculation is just slightly superior to the other two approaches when comparing transformer cost computation using PSO, GA, and normal methods.

4. EA(Evolutionary Algorithm)

When an optimization problem only has one objective, single objective optimization is the method used to identify the best configuration. But when there are several goals involved in an optimization problem, multi objective optimization is the process of finding at least one optimal configuration.

Numerous verified optimization and research tasks have multiple goals. Multi-objective optimization strategies utilizing developmental algorithms have grown in popularity as more and more arrangements are managed in each age. This property has significant advantages for the use of developing algorithms to multi-objective optimization issues. The differential calculation development approach based on shortened gamma likelihood circulation capability was demonstrated, while the unlimited population size transformative multi-objective optimization calculation approach combined with turbulent groupings was used to combine the benefits of unrestricted population size and transformative multi-objective optimization for the transformer design optimization process. Multi-objective design optimization of high recurrence transformers was examined while taking into account boosting productivity and decreasing expenses using molecular swarm optimization. Multi-objective developmental optimization was also employed to estimate transformer design details with the greatest degree of accuracy. In an effort to boost efficiency while lowering costs for a 500 kVA transformer, it

was suggested to apply bacterial scavenging calculations to construct a multi-objective ideal transformer design. The authors recognize that the area of multi-objective ideal transformer design is still in its infancy and that multi-objective optimization methods like Vector Assessed Hereditary methods (VEGA), Weight Based

III. CONCLUSION

The essential design optimization techniques for power transformers have been tried.
The significant covers a wide range of mathematics and designing approaches. Selected distributions from the world's diaries, the numerous distributions show that this is a field that has been extensively investigated. The approach and the advancement of the transformers are developing together. More complicated transformer models and brand-new effects of the optimization hypothesis are taken into consideration by the original transformer optimization processes. Both the transformer models and optimization viewpoints have experienced significant change. These models are common in that they resolve the dynamic part borders by their dynamic parts and ignore the impact of the protection framework. Future study will focus on analyzing how the protection framework will impact this broad non-straight optimization issue. Regarding the application of artificial intelligence design optimization approaches, Power transformers are the costly and crucial elements of electrical power systems.

In order to handle the contradictory and complex requirements of power transformer security plans, computer-based intelligence approaches will be deployed. The evaluation of cutting-edge power transformer affirmation plans then uses the computer-based intelligence methodologies listed below:
ANN-based strategies include the WNN approach, ANN approach, ANNEPS approach, PSO-arranged ANN approach, and PSO-arranged WNN approach. Fuzzy reasoning-based philosophies include ANFIS, the Fluffy reasoning methodology, the Consolidated ANFIS with wavelet changes approach, and the Joined Fluffy reasoning with wavelet changes approach. Improved activity speed, precision, and consistency; assurance of safety; excellent adaptability; thorough self-observing and checking office. Thus, it is assumed that the AI applications are the ones that power transformer assurance programmers should use. A optimized power transmission system capable to prevent failure by taking preventive measure is essential. This Research problem can be solved with artificial Intelligence Techniques based System design approach.

ACKNOWLEDGMENTS

I acknowledge science Thanks to all above authors for their guidance and individual contribution.

REFERENCES

[1] Bishop M.T., Mendis S.R., Witte J. F. and Myers P. (2019). "Device Miscoordination", IEEE industry applications magazine, pp. 32 to 37.
[2] Bo Z., Weller G. & Lomas T. (2012). "A New Technique foe Transformer Protection Based on Transient Detection", IEEE Trans. on Power Delivery , Vol. 15, pp. 870-875.
[3] Dalstein T., Kulicke B., (2015)Neural network approach to fault classification for high speed protective relaying. IEEE Transactions on Power Delivery, Vol.10, No.2, pp.1002- 1009.
[4] Del Vecchio, R. M., Poulin, B., Feghali, P. T., Shah, D. M., Ahuja, (2013) "Transformer Design Principles: With Applications to Core-Form Power Transformers", 2nd ed., CRC Press, Hoboken, USA.
[5] E.I. Amoiralis, M.A. Tsili, A.G. Kladas, (2019)"Transformer Design and Optimization: A Literature Survey", IEEE Transactions on Power Delivery, Vol. 24, No.4, pp 2019-2024, 2019
[6] E.I. Amoiralis, P.S. Georgilakis, M.A. Tsili, A.G. Kladas & A.T. Souflaris (2015) "A complete software package for transformer design optimization and economic evaluation analysis". Materials Science Forum, Trans Tech Publications, Switzerland, Vol. 670, pp 535-546.
[7] IEEE Standard Terminology for Power and Distribution Transformers, IEEE Std. C. 57.12.80-2012

Source details

European Chemical Bulletin

Open Access

Scopus coverage years: from 2017 to 2022

(coverage discontinued in Scopus)

Publisher: Deuton-X Ltd.

E-ISSN: 2063-5346

Subject area: Chemistry: General Chemistry

Source type: Journal

CiteScore 2022
1.6

SJR 2022
0.247

SNIP 2022
0.471

View all documents > | Set document alert | Save to source list

CiteScore | CiteScore rank & trend | Scopus content coverage

Improved CiteScore methodology

CiteScore 2022 counts the citations received in 2019-2022 to articles, reviews, conference papers, book chapters and data papers published in 2019-2022, and divides this by the number of publications published in 2019-2022. Learn more >

CiteScore 2022

1.6 = 509 Citations 2019 - 2022

Research on Engineering Structures & Materials

journal homepage: http://www.jresm.org

Research Group



Process parameter improvement for NITi's electrical discharge machining (EDM) process utilizing the TOPSIS approach

Atish Mane, Pradeep V. Jadhav

Online Publication Date: 10 Dec 2022
URL: http://www.jresm.org/archive/resm2022.510ma0826.html
DOI: http://dx.doi.org/10.17515/resm2022.510ma0826

Journal Abbreviation: *Res. Eng. Struct. Mater.*

To cite this article

Mane A, Jadhav PV. Process parameter improvement for NITi's electrical discharge machining (EDM) process utilizing the TOPSIS approach. *Res. Eng. Struct. Mater.*, 2023; 9(1): 83-94.

Disclaimer

All the opinions and statements expressed in the papers are on the responsibility of author(s) and are not to be regarded as those of the journal of Research on Engineering Structures and Materials (RESM) organization or related parties. The publishers make no warranty, explicit or implied, or make any representation with respect to the contents of any article will be complete or accurate or up to date. The accuracy of any instructions, equations, or other information should be independently verified. The publisher and related parties shall not be liable for any loss, actions, claims, proceedings, demand or costs or damages whatsoever or howsoever caused arising directly or indirectly in connection with use of the information given in the journal or related means.

Published articles are freely available to users under the terms of Creative Commons Attribution - NonCommercial 4.0 International Public License, as currently displayed at here (the "CC BY - NC").

Research on Engineering Structures & Materials
journal homepage: http://www.jresm.org
MIM Research Group

Research Article

Process parameter improvement for NITi's electrical discharge machining (EDM) process utilizing the TOPSIS approach

Atish Mane*[a], Pradeep V. Jadhav[b]

Mechanical Eng. Bharati Vidyapeeth Deemed University, College of Engineering, Pune, Maharashtra, India

Article Info

Article history:

Received 26 Aug 2022
Revised 30 Oct 2022
Accepted 6 Dec 2022

Keywords:

Electro discharge Machine (EDM); Shape memory alloy; Surface roughness (R_a); Material removal rate (MRR); TOPSIS

Abstract

The current work focuses on finding the ideal set of Electro Discharge Machine (EDM) process variables for machining Shape memory alloy (NiTi). NiTi alloy is a significant class of smart material with several unique properties. There are numerous uses for NiTi in the security, marine, biomedical, and aerospace industries. NiTi is particularly difficult to cut using conventional machining methods due to its hardness; nevertheless, the material can be removed using an electric discharge machining technique. The experiments were carried out using Taguchi's L27 orthogonal array. A Multi-criteria decision-making (MCDM) technique known as TOPSIS is used to optimize the response performance variables of material removal rate (MRR) and surface roughness (SR). TOPSIS combines multiple objectives into a single objective and provides the optimum set of parameters, From the optimization results, the optimal combination of process parameters is obtained at Voltage=30V, Discharge Current= 20A, Ton=35µs, Toff=8µs. Confirmatory experiments show a satisfactory improvement of preference values utilizing TOPSIS in the EDM experimental and initial settings of 1.82.

© 2023 MIM Research Group. All rights reserved.

1. Introduction

According to the state of research, shape memory alloy (SMA) development is proceeding successfully. SMA demand is on the rise for a wide range of engineering components. When used as a binary alloy, nickel and titanium have different element weight percentages in the SMA [1]. Smart materials in the NiTi class have special qualities like super elasticity, high strength, biocompatibility, etc. In the fields of defense, aerospace, and medicine, NiTi alloy is widely applied. This alloy is difficult to machine using traditional machining techniques because it has unique qualities and applications. Instead, this alloy is machined using non-conventional techniques such as electric discharge machining (EDM) [2]. By generating controlled sparks between an electrode with a specific form and an electrically conductive workpiece, electrical discharge machining (EDM), a popular technique for shaping conductive materials, can be utilized to remove material [3]. Sushil Kumar Choudhary et al. examine the research that was done on die-sinking EDM, water-in EDM, dry EDM, and powdered mixed electric discharge machining from inspection through development. He noted that the main advancement in research had improved tool wear and metal removal rate [4]. Azizul Bin Mohamad et al., optimization of EDM parameters process and response parameters using Taguchi method. They observed that pulse on time and discharge current were most effective on the Surface and also duty factor as least influencing the machining process quality [5]. K.M Patel et al. investigated the effect of process parameters on surface quality. They investigated that the most significant factor is discharge current which affects surface quality. Surface roughness increases with an

*Corresponding author: mane.atish@bharatividyapeeth.edu
[a] orcid.org/0000-0002-4549-8004; [b] orcid.org/0000-0002-7167-2387
DOI: http://dx.doi.org/10.17515/resm2022.510ma0826

increase in discharge current and also affects the metal removal rate [6]. Singh Balbir et al. investigate the process of alloying AA 6061/ SiCp using Cu-W powder metallurgy electrodes in EDM. They investigated the effects of peak current, gap voltage, pulse off time, and pulse on time on response parameters metal removal rate, electrode wear, and surface roughness. They analyze that using powder metallurgy improves the surface quality [7].E. Aliakbari et al. found the ideal rotary process parameter setting and deduced from this experiment that the most influential input parameters on MRR, EWR, and SR are current, pulse on time, electrode rotational speed, and electrode shapes [8].Bala Murugan Gopalsamy et al, noticed that the parameters that have the most influence on rough machining are the cut width and depth. The most important factor in finish machining is cutting speed [9]. Ho and Newman presented a review of the electrical discharge machining process and discussed the parameters that are contributing to machining efficiency. EDM process involves many process parameters which can be broadly classified into two categories such as electrical and non-electrical process parameters. They stated that empirical modeling can be better described in the EDM process as it is stochastic in nature [10]. Mr. L.G. Machado et al. give a review on the medical applications of shape memory alloys. The aim of this review paper is to explain the most exciting uses of SMA in the biomedical field and to provide a brief overview of its thermomechanical behavior. These include surgical tools and uses for the heart and joints [11]. Multiple performance characteristic issues require the modeling and optimization of the EDM process. Kasdekar, D. K. et. al. suggested a TOPSIS, Simple Additive Weighting (SAW) method based on entropy to address the multi-performance parameter optimization issue in EDM [12]. Tripathy, S. et. al. assessed the efficiency of improving several performance variables for powder-mixed EDM of H-11 die steel using the copper electrode by combining the Taguchi technique with TOPSIS and grey relational analysis [13]. Vaddi, V. R. et. al. worked on using TOPSIS and the Taguchi technique to optimize EDM machining parameters for titanium alloys (Ti-6Al-4V), taking into account various performance concerns. All of the results demonstrated TOPSIS's ability to address a variety of concrete EDM-related challenges using the Taguchi approach. This technique reduced a multi-performance problem to a single equivalent objective problem [14]. Phan Huu Nguyen et. al. adjusts the process parameters for milling titanium alloy specimens with tungsten carbide. To determine improved process variables including voltage, capacitance, and electrode rotating speed, the Taguchi-TOPSIS approach was applied. To assess the depth of machining, overcut, and tool wear rate, voltage, capacitance, and electrode rotational speed were taken into account. The investigation revealed that the best settings can result in better surface polish and greater machining precision [15].M Somasundaram et. al. carries out studies to mill AZ31 alloy using EDM to optimize process parameters by combining multi-attribute optimization and Taguchi methodologies. In this work, multiple-response optimization was accomplished using Multi-Criteria Decision Making (MCDM) approaches such as the TOPSIS methodology and Grey Relational Analysis (GRA). Due of TOPSIS' flexibility in determining how much weight to give the response based on the need, researchers came to the conclusion that it is the best method for solving real-time multi-criteria problems. With GRA, which has a constant value for all response variables, it is not conceivable. [16].

The current study's objective is to maximize the material removal rate and minimize surface roughness during the machining of NiTi alloy by optimizing the electric discharge machining process parameter. Surface roughness (SR) and material removal rate (MRR) were the output parameters, and pulse current, voltage, gap, and pulse on-off time were the input parameters.

2. Design of Experiment

2.1 Experimental Setup

An EDM machine (Valpak) was used in this study to conduct experiments shown in Fig. 1. An electrode was a rectangular, pure copper plate that measured 40 mm by 40 mm by 20 mm. A moving dielectric fluid, kerosene, kept the workpiece and electrode apart. Shape memory alloy (NiTi) was used as the workpiece's material. For experimentation, shape memory alloy pates with dimensions of 25 mm by 40 mm by 15 mm were used. As a workpiece, NiTi shape memory alloy has been utilized in orthopedics to fix fractured bones.

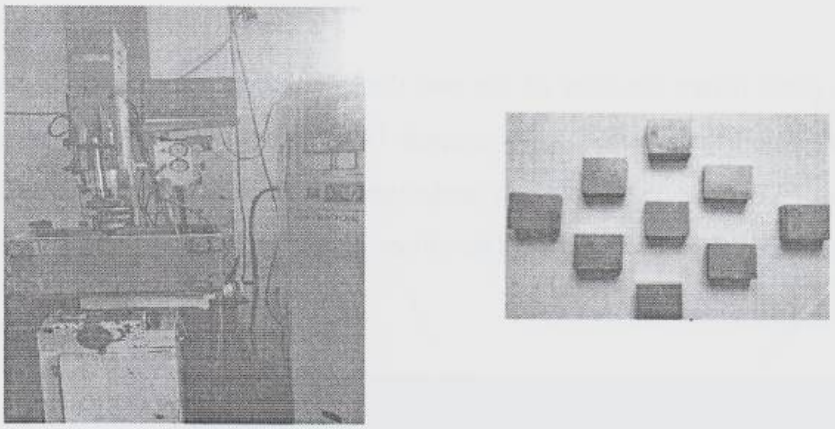


Fig. 1 EDM setup and Machined plates (Ni-Ti Alloy)

Placing the electrode in the ram hold and fixing it in place. To maintain a very small gap of 50 μm between the electrode tip and the surface of the workpiece, its height was automatically adjusted by the machine with respect to the workpiece. keeping the workpiece in place on the machine's work table's magnetic chuck. Flushing the dielectric fluid up to the height where the electrode sparking region is totally submerged, flooding the volume (work tank) around the workpiece. Perform the machining operation for the specified amount of time. It is possible to see intermittent sparking through the dielectric fluid. Small craters are generated as a result of a high number of current discharges that all contribute to the removal of material from the workpiece. The workpiece is removed from the device and its surface roughness (SR) is checked with Taylor-Hobson Surf Com equipment. The readings are noted down.

2.2. Selection of an orthogonal array

Machining experiments for determining the optimal machining parameters were carried out by setting: For each experiment the combinations of the 4 input parameters viz. Gap Voltage(V) in the range of 25V to 100V, Discharge Current (A) in the range of 10A to 20A, Pulse on-time (Ton) in the range of 35 μs to 100 μs, pulse off-time (Toff) in the range of 5 μs to 39 μs, all having 3 levels (Table 1)

The total degree of freedom when there are three independent variables, each with three levels, is nine. As a result, the chosen orthogonal array must include at least 9 experiments. This condition is satisfied by an L_9 orthogonal. Three levels and four factors were chosen for this investigation. An orthogonal array L_{27} was chosen for this experiment [18].

Table 1. Initial EDM Parameter

EDM Parameters	Unit	Level-1	Level-2	Level-3
Gap Voltage	V	25	30	100
Discharge current	A	10	15	20
Pulse On Time	µs	35	50	100
Pulse Off Time	µs	5	8	9

2.3. Conducting the Experiment

After choosing the orthogonal array, the experiments are carried out using the level combinations. The execution of all the experiments is required. L_{27} orthogonal array was used since there were four components and three levels in this investigation [23].

Table 2. Orthogonal Array of Experimental Combination

Test	Gap Voltage	Discharge current	Pulse On Time	Pulse Off Time
1	25	10	35	5
2	25	10	35	8
3	25	10	35	9
4	30	15	50	5
5	30	15	50	8
6	30	15	50	9
7	100	20	100	5
8	100	20	100	8
9	100	20	100	9
10	25	15	100	5
11	25	15	100	8
12	25	15	100	9
13	30	20	35	5
14	30	20	35	8
15	30	20	35	9
16	100	10	50	5
17	100	10	50	8
18	100	10	50	9
19	25	20	50	5
20	25	20	50	8
21	25	20	50	9
22	30	10	100	5
23	30	10	100	8
24	30	10	100	9
25	100	15	35	5
26	100	15	35	8
27	100	15	35	9

2.4. Machining Performance Measure

Surface Roughness Measurement-

The parameter Ra, which is the most frequently used, was chosen for this study from a variety of surface finish characteristics, including roughness average (R_a), root-mean-square (rms) roughness (R_q), and maximum peak-to-valley roughness (R_y or R_{max}). The experiments were carried out with various Gap voltage, Discharge current, Pulse on-time, and Pulse on-time settings (Table 2). The Taylor-Hobson Surf Com equipment was used to measure the specimens' surface roughness.

Material Removal Measurement-

Machining was executed using a fixed time and the MRR was measured by determining the weight difference of the workpiece before and after machining. The MRR measured in cubic millimeters per minute, was obtained using Eq. (1).

$$MRR = \frac{(W_1 - W_2)}{\rho_w\, t} * 10^3 \quad (1)$$

Where W_1 and W_2 are the work piece weight before and after machining, respectively, ρ_w is the density of the NiTi, SMA, and t is the machining time (min).

3. Result in Analysis

Minitab TM 18 tool is employed for data analysis. Two response parameters from the result in table 3 are selected for study in order to determine the best combination that can produce a high-quality machined surface finish. 27 experiments were carried out in accordance with the L_{27} orthogonal array, with the findings for surface roughness and metal removal rate displayed in table 3.

Table 3. Result Table

Test	Gap Voltage	Discharge current	Pulse On Time	Pulse Off Time	Surface roughness	MRR (mm^3/min)
1	25	10	35	5	5.31	7.375
2	25	10	35	8	5.35	6.146
3	25	10	35	9	5.55	6.914
4	30	15	50	5	6.25	6.062
5	30	15	50	8	6.15	6.056
6	30	15	50	9	6.44	6.062
7	100	20	100	5	6.01	6.062
8	100	20	100	8	5.9	7.375
9	100	20	100	9	6.26	7.375
10	25	15	100	5	6.52	6.291
11	25	15	100	8	6.32	5.531
12	25	15	100	9	6.82	4.425
13	30	20	35	5	4.62	7.375
14	30	20	35	8	4.52	8.749
15	30	20	35	9	5.12	7.375
16	100	10	50	5	5.01	7.375
17	100	10	50	8	5.24	7.375
18	100	10	50	9	5.44	6.914
19	25	20	50	5	6.11	6.062
20	25	20	50	8	5.96	7.375

21	25	20	50	9	5.34	6.146
22	30	10	100	5	5.12	6.062
23	30	10	100	8	5.05	7.375
24	30	10	100	9	5.37	5.531
25	100	15	35	5	5.2	7.375
26	100	15	35	8	5.18	7.375
27	100	15	35	9	5.34	7.375

4. Optimization Using Technique for Order of Preference (TOPSIS) & Results

A technique for multi-criteria decision analysis is called TOPSIS (Technique for Order of Preference by Similarity to Ideal Solution). By determining weights for each criterion, normalizing scores for each criterion, and calculating the geometric distance between each alternative and the ideal alternative, which is the alternative with the best score for each criterion, this compensatory aggregation method compares a set of alternatives. The criteria are assumed to be monotonically growing or decreasing by TOPSIS [14,15].

The steps involved in multi-objective optimization are [16]:

Step 1. Determine the objective and identify the pertinent evaluation criteria.

Step 2. Construct a decision matrix based on all the information available for the criteria. Each row of the decision matrix is allocated to one alternative and each column to one criterion. Therefore, an element, x_{ij} of the decision matrix shows the performance of i^{th} alternative with respect to j^{th} criterion.

Step 3. Obtain the normalized decision matrix, r_{ij} using the following equation:

$$r_{i_j} = \frac{x_{i_j}}{\sqrt{\sum_{i=1}^{m} x^2_{i_j}}} \tag{2}$$

Step 4. Construct the weighted normalized decision matrix.

$$v_{i_j} = r_{i_j} \times w_j \tag{3}$$

Step 5. Determine the Positive ideal Row (IDR) that one with the largest observed value for each column.

$$\text{IDR} = (\max v_{i1}, \max v_{i2}, \ldots\ldots, \max v_{in}) = (v_1^+, v_2^+, \ldots\ldots, v_n^+) \tag{4}$$

Similarly, the Negative-ideal Row (NDR) that one with the smallest value for each column.

$$\text{NDR} = (\min v_{i1}, \min v_{i2}, \ldots\ldots, \min v_{in}) = (v_1^-, v_2^-, \ldots\ldots, v_n^-) \tag{5}$$

Step 6. Measure the distance, d_i^+ for i= 1,2, 3,.....,m, of each alternative from the positive ideal one.

$$S_i+ = [\sum_{j=1}^{n} \left(v_{i_j} - v_j^+ \right)^2]^2 \qquad \text{for i= 1,2, 3,.....,m.} \tag{6}$$

Similarly, Measure the distance, d_i^- for i= 1,2, 3,.....,m, of each alternative from the negative ideal one.

$$S_i- = [\sum_{j=1}^{n} \left(v_{i_j} - v_j^- \right)^2]^2 \qquad \text{for i= 1,2, 3,.....,m.} \tag{7}$$

Step 7. Calculate the relative closeness of alternatives to ideal solution by computing what is known as Composite Index (CI).

$$P_i = \frac{d_i^-}{d_i^+ + d_i^-} \tag{8}$$

Step 8. A set of alternatives is arranged in descending order, according to P_i value, indicating the most preferred and the least preferred solutions.

The normalized decision matrix for the provided data is shown in Table 4. Table 6 illustrates the Weighted Decision matrix, respective Euclidian distances, degree of closeness, and ranks for a set of input parameters whereas Table 5 displays the weighting applied to each output response variable. These are all taken from an excel spreadsheet that was created.

Table 4. Normalized Decision Matrix

Experimental Result		Normalized Output	
Surface roughness	MRR (mm^3/min)	Surface roughness	. MRR (mm^3/min)
5.31	7.375	0.1811	0.1376
5.35	6.146	0.1825	0.1147
5.55	6.914	0.1893	0.129
6.25	6.062	0.2132	0.1131
6.15	6.056	0.2098	0.113
6.44	6.062	0.2197	0.1131
6.01	6.062	0.205	0.1131
5.9	7.375	0.2012	0.1376
6.26	7.375	0.2135	0.1376
6.52	6.291	0.2224	0.1174
6.32	5.531	0.2156	0.1032
6.82	4.425	0.2326	0.0826
4.62	7.375	0.1576	0.1376
4.52	8.749	0.1542	0.1632
5.12	7.375	0.1746	0.1376
5.01	7.375	0.1709	0.1376
5.24	7.375	0.1832	0.1376
5.44	6.914	0.1856	0.129
6.11	6.062	0.2084	0.1131
5.96	7.375	0.2033	0.1376
5.34	6.146	0.1821	0.1147
5.12	6.062	0.1746	0.1131
5.05	7.375	0.1723	0.1376
5.37	5.531	0.1787	0.1032
5.2	7.375	0.1774	0.1376
5.18	7.375	0.1767	0.1376
5.34	7.375	0.1821	0.1376

The normalized decision matrix has been formed as shown in Table 4.

Table 5. Considered weightage of output response

Output Response	R_a	MRR
Weightage	0.5	0.5

Table 6. Weighted normalized decision matrix, Euclidian Distance & Relative Closeness

Weighted Normalized Output					
Surface roughness	MRR (mm^3/min)	S_i+	S_i-	P_i	Rank
0.0906	0.0688	0.0186	0.0376	0.6691	8
0.0913	0.0574	0.0281	0.0297	0.5145	17
0.0947	0.0645	0.0245	0.0317	0.5636	12
0.1066	0.0566	0.0387	0.0181	0.319	23
0.1049	0.0565	0.0375	0.019	0.3366	22
0.1099	0.0566	0.0413	0.0166	0.2868	25
0.1025	0.0566	0.0356	0.0206	0.3663	20
0.1006	0.0688	0.0268	0.0317	0.5419	14
0.1068	0.0688	0.0324	0.0291	0.4735	18
0.1112	0.0587	0.0411	0.0181	0.3062	24
0.1078	0.0516	0.0429	0.0134	0.2373	26
0.1163	0.0413	0.0562	0	0.0002	27
0.0788	0.0688	0.0129	0.0465	0.7827	2
0.0771	0.0816	0	0.0562	0.9997	1
0.0873	0.0688	0.0164	0.04	0.7094	5
0.0855	0.0688	0.0153	0.0413	0.7294	3
0.0916	0.0688	0.0194	0.037	0.6564	10
0.0928	0.0645	0.0232	0.033	0.5872	11
0.1042	0.0566	0.0369	0.0195	0.346	21
0.1017	0.0688	0.0277	0.0311	0.5288	15
0.0911	0.0574	0.028	0.0299	0.5168	16
0.0873	0.0566	0.027	0.0328	0.5484	13
0.0862	0.0688	0.0157	0.0408	0.7218	4
0.0894	0.0516	0.0324	0.0288	0.4705	19
0.0887	0.0688	0.0173	0.039	0.6927	7
0.0884	0.0688	0.0171	0.0392	0.6964	6
0.0911	0.0688	0.019	0.0373	0.6628	9

The closest and farthest points from the ideal solutions, or the Euclidian distance (S+&S-), are determined. The P_i value, or degree of proximity to the best solution, is calculated from these Euclidean distances, and the highest P_i value is indicated as the first ranking, while the lowest P_i value is marked as the final rank or the 27th rank. Table 7 lists the P_i values,

Euclidian distances, Weighted Normalized Decision Matrix, and the corresponding rank assigned to each set of input parameters based on the P_i values.

Table 7. Summarized TOPSIS table ranking the set of input parameters

Test	Gap Voltage	Discharge current	Pulse On Time	Pulse Off Time	SR	MRR	S_i+	S_i-	P_i	Rank
1	25	10	35	5	5.31	7.3746	0.0186	0.0376	0.6691	8
2	25	10	35	8	5.35	6.1455	0.0281	0.0297	0.5145	17
3	25	10	35	9	5.55	6.9137	0.0245	0.0317	0.5636	12
4	30	15	50	5	6.25	11.0619	0.0387	0.0181	0.319	23
5	30	15	50	8	6.15	10.0563	0.0375	0.019	0.3366	22
6	30	15	50	9	6.44	11.0619	0.0413	0.0166	0.2868	25
7	100	20	100	5	6.01	11.0619	0.0356	0.0206	0.3663	20
8	100	20	100	8	5.9	7.3746	0.0268	0.0317	0.5419	14
9	100	20	100	9	6.26	7.3746	0.0324	0.0291	0.4735	18
10	25	15	100	5	6.52	12.2911	0.0411	0.0181	0.3062	24
11	25	15	100	8	6.32	5.531	0.0429	0.0134	0.2373	26
12	25	15	100	9	6.82	4.4248	0.0562	0	0.0002	27
13	30	20	35	5	4.62	7.3746	0.0129	0.0465	0.7827	2
14	30	20	35	8	4.52	14.7493	0	0.0562	0.9997	1
15	30	20	35	9	5.12	7.3746	0.0164	0.04	0.7094	5
16	100	10	50	5	5.01	7.3746	0.0153	0.0413	0.7294	3
17	100	10	50	8	5.24	7.3746	0.0194	0.037	0.6564	10
18	100	10	50	9	5.44	6.9137	0.0232	0.033	0.5872	11
19	25	20	50	5	6.11	11.0619	0.0369	0.0195	0.346	21
20	25	20	50	8	5.96	7.3746	0.0277	0.0311	0.5288	15
21	25	20	50	9	5.34	6.1455	0.028	0.0299	0.5168	16
22	30	10	100	5	5.12	11.0619	0.027	0.0328	0.5484	13
23	30	10	100	8	5.05	7.3746	0.0157	0.0408	0.7218	4
24	30	10	100	9	5.37	5.531	0.0324	0.0288	0.4705	19
25	100	15	35	5	5.2	7.3746	0.0173	0.039	0.6927	7
26	100	15	35	8	5.18	7.3746	0.0171	0.0392	0.6964	6
27	100	15	35	9	5.34	7.3746	0.019	0.0373	0.6628	9

From Table 7, Based on the relative closeness, we understand that Exp. 14 shows the best set of input parameters while Exp. 12 shows the worst results. The optimal input parameters for the combined EDM machining are shown in Table 8.

Table 8. The optimized set of input parameters (Weightage 0.5-0.5)

Gap Voltage	Discharge current	Pulse on Time	Pulse off Time
30	20	35	8

Confirmation Test:

The confirmation experiment is the last stage in the design of the experiment process's initial iteration. The verification experiment's purpose is to confirm the findings of the TOPSIS analysis phase. It is carried out by adjusting the process parameters to Voltage=30V, Discharge Current= 20A, Ton=35μs, Toff=8μs, as the optimum level and the actual surface roughness obtained is 6.34 μm to 4.52 μm and metal removal rate as 12.75 mm^3/min to 14.75 mm^3/min. Surface roughness and metal removal rate improvement shows that the accuracy of outcomes is increased by the TOPSIS multi-decision-making optimal design.

5. Conclusion

This study helped determine the ideal Shape Memory Alloy Electro Discharge Machine (EDM) parameters to optimize for low surface roughness (SR) and maximize metal removal rate (MRR). In these investigations, 27 sets of tests were carried out utilizing a copper electrode and an L_{27} Taguchi orthogonal array on shape memory alloy. Voltage, Discharge current, Pulse on time, and Pulse off time are some of the input parameters used. From the experiment and design of the experiment, the following conclusions were made; The many objectives are combined by Optimization using the Technique for order of preference (TOPSIS) into a single objective, and the optimum set of parameters, i.e., R_a & MRR, is provided. Table 6 lists the outcomes of the best solutions for both positive and negative ideal solutions. In Table 7, the output performances are sorted according to their proximity coefficient values. The largest MRR and the least amount of surface roughness are closer with the highest proximity coefficient value. By averaging the experiment data, the average proximity coefficient value for MRR and R_a is determined for levels 1-3. The shape memory alloy's MRR and Ra are determined in large part by the EDM machining parameters; among the parameters chosen, a larger current could produce enough discharge energy to melt and evaporate the reinforcement and matrix material. For the ideal good outcome, higher MRR and lower R_a are preferable. The results of the experiment show that voltage and discharge current have more effects. From the experiment, we get poor outcomes while keeping parameters set as Voltage=25V, Discharge Current= 15A, Ton=100μs, Toff=9 μs and best outcomes keeping parameters set as Voltage=30V, Discharge Current= 20A, Ton=35μs, Toff=8μs. Each performance is given a weight factor of 0.5. The optimum results obtained by the TOPSIS method for 0.5-0.5 weightage are as optimum surface roughness is 4.52 μm and metal removal rate as 14.75 mm^3/min by a combination of input parameters as Voltage=30V, Discharge Current= 20A, Ton=35μs, Toff=8μs. Confirmatory experiments show a satisfactory improvement of preference values utilizing TOPSIS in the EDM experimental and initial settings of 1.82.

References

[1]. Adam KM, Winowlin JJT, Samuel RKPS, Mashinini P. Machinability of Shape Memory Alloy Using Electro Spark Erosion Process. Research square. 2021: 1-13,

[2] Sabouni HR, Daneshmand S. Investigation of the parameter of EDM process performed on smart NiTi alloy using graphite tool. Life Sci. J. 2012, 9 (4), 504-510.

[3] Saeed D. Optimization of Electrical Discharge Machining Parameters for Niti Shape Memory Alloy by Using the Taguchi Method. Journal of Marine Science and Technology,2014, 22(4):506-512.

[4] Sushil K C, Jadoun RS , Current Advanced Research Development of Electric Discharge Machining (EDM): A Review, International Journal of Research in Advent Technology, 2014: 273-297.

[5] Azizul BM, Arshad NS, Gulam AQ, Zahid AK, Saini VK. Optimization of EDM process parameters using Taguchi method. International Conference on Applications and Design in Mechanical Engineering,2012.
[6] Patel KM, Pandey PM, Rao PV. Optimisation of process parameters for multi-performance characteristics in EDM of Al2O3 ceramic composite. Int J Adv Manuf Technol. 2010 Apr;47(9-12):1137-47. https://doi.org/10.1007/s00170-009-2249-7
[7] Singh B, Kumar J, Kumar S. Optimization and surface modification in electrical discharge machining of AA 6061/SiCp composite using Cu–W electrode. Proceedings of the Institution of Mechanical Engineers, Part L: Journal of Materials: Design and Applications. 2017 Apr;231(3):332-48. https://doi.org/10.1177/1464420715596544
[8] Aliakbari E, Baseri H. Optimization of machining parameters in rotary EDM process by using the Taguchi method. Int J Adv Manuf Technol. 2012 Oct;62(9-12):1041-53. https://doi.org/10.1007/s00170-011-3862-9
[9] Gopalsamy BM, Mondal B, Ghosh S. Optimisation of machining parameters for hard machining: grey relational theory approach and ANOVA. Int J Adv Manuf Technol. 2009 Dec;45(11-12):1068-86. https://doi.org/10.1007/s00170-009-2054-3
[10] Ho K, Newman S. State of the art electrical discharge machining (EDM). International Journal of Machine Tools and Manufacture. 2003 Oct;43(13):1287-300. https://doi.org/10.1016/S0890-6955(03)00162-7
[11] Machado L, Savi M. Medical applications of shape memory alloys. Braz J Med Biol Res. 2003 Jun;36(6):683-91. https://doi.org/10.1590/S0100-879X2003000600001
[12] Kasdekar DK. MADM Approach for Optimization of Multiple Responses in EDM of En-353 Steel. IJAST. 2015 Aug 31;83:59-70. https://doi.org/10.14257/ijast.2015.83.06
[13] Tripathy S, Tripathy D. Multi-attribute optimization of machining process parameters in powder mixed electro-discharge machining using TOPSIS and grey relational analysis. Engineering Science and Technology, an International Journal. 2016 Mar;19(1):62-70. https://doi.org/10.1016/j.jestch.2015.07.01
[14] Vaddi VR, Ch SR, Bushaboina SK, Banka H. Application of TOPSIS with Taguchi Method for Multi-Attribute Optimization of Machining Parameters in EDM. SAE Tech. Pap. Ser. 2018. https://doi.org/10.4271/2018-28-0033
[15] NGUYEN PH, T M, Pham DV, Shirguppikar S, Nguyen TN, Nguyen TC, et al. Multi-objective optimization of micro EDM using TOPSIS method with Tungsten carbide electrode. Sādhanā. 2022 Sep;47(3):1-12 https://doi.org/10.1007/s12046-022-01900-8
[16] Somasundaram M, Kumar JP. Multi response optimization of EDM process parameters for biodegradable AZ31 magnesium alloy using TOPSIS and grey relational analysis. Sādhanā. 2022 Sep;47(3):1-14 https://doi.org/10.1007/s12046-022-01908-0
[17] Mohd Abbas N, Solomon DG, Fuad Bahari M. A review on current research trends in electrical discharge machining (EDM). International Journal of Machine Tools and Manufacture. 2007 Jun;47(7-8):1214-28. https://doi.org/10.1016/j.ijmachtools.2006.08.026
[18] Mane AB, Jadhav P. Optimization of Response Parameters of Electrical Discharge Machine Using Shape Memory Alloy. International Journal of Mechanical Engineering. 2021; 6(3): 86- 91.
[19] Singh S. Optimization of machining characteristics in electric discharge machining of 6061Al/Al2O3p/20P composites by grey relational analysis. Int J Adv Manuf Technol. 2012 Dec;63(9-12):1191-202. https://doi.org/10.1007/s00170-012-3984-8
[20] Bansiddhi A, Sargeant T, Stupp S, Dunand D. Porous NiTi for bone implants: A review. Acta Biomaterialia. 2008 Jul;4(4):773-82. https://doi.org/10.1016/j.actbio.2008.02.009
[21] Mohd Jani J, Leary M, Subic A, Gibson MA. A review of shape memory alloy research, applications and opportunities. Materials & Design (1980-2015). 2014 Apr;56:1078-113. https://doi.org/10.1016/j.matdes.2013.11.084

[22] Markopoulos AP, Pressas IS, Manolakos DE. A Review On The Machining Of Nickel-Titanium Shape Memory Alloys, Rev.Adv. Mater. Sci. 2015; 42: 28-35.
[23] Mane AB, Jadhav P, Bilgi DS. Enhancement of Surface Finish of Shape Memory Alloy Using Electrical Discharge Machine, Annals of R.S.C.B., ISSN: 1583-6258, 2021; 25(5) 5224- 5232.
[24] Liu X, Shang H, Xu S, Wang Z, Zhang C, Fu Q. Patellar Shape-Memory Fixator for the Treatment of Comminuted Fractures of the Inferior Pole of the Patella. J of Materi Eng and Perform. 2011 Jul;20(4-5):623-8. https://doi.org/10.1007/s11665-011-9862-y
[25] Auricchio F, Boatti E, Conti M, SMA Biomedical Applications, Shape Memory Alloy Engineering,2015, ISBN 978-0-08-099920-3.
[26] Shashikant, Roy A K , Effect of optimization of various machine process parameters on surface roughness in EDM for an EN19 material using Surface Response Methodology, Procedia Materials Science, 2014; 5:1702 - 1709. https://doi.org/10.1016/j.mspro.2014.07.359
[27] Janardhan M. Multi-response optimization of EDM performance characteristics using response surface methodology and desirability function, ARPN Journal of Engineering and Applied Sciences, 2014,2635- 2649.
[28] Balasubramanian P, Senthilvelan T. Optimization of Machining Parameters in EDM Process Using Cast and Sintered Copper Electrodes. Procedia Materials Science. 2014;6:1292-302. https://doi.org/10.1016/j.mspro.2014.07.108
[29] Goyal P. Enhancement of MRR in EDM by Composite Material Electrode on Die Steel, International Journal of Science, Engineering and Technology Research, 2014; 2640-2643.
[30] Saeed D, Ehsan FK, Ali ALN, Vahid M. Optimization of Electrical Discharge Machining parameters for NITI shape memory alloy using Taguchi Method, Journal of Marine Science and Technology, 2014; 22(4):506-512.
[31] Esmail A, Saeed Da, Ali A L N, Vahid M., Analysis and Modeling of Electro Discharge Machining Input Parameters of Nitinol Shape Memory Alloy by De-ionized Water and Copper Tools, Int. J. Electrochem. Sci., 2014; 9: 2934 - 2943.
[32] Alidoosti A, Ghafari-Nazari A, Moztarzadeh F, Jalali N, Moztarzadeh S, Mozafari M. Electrical discharge machining characteristics of nickel–titanium shape memory alloy based on full factorial design. Journal of Intelligent Material Systems and Structures. 2013 Sep;24(13):1546-56. https://doi.org/10.1177/1045389X13476147
[33] Perveen A, Jahan MP. An Experimental Study on the Effect of Operating Parameters during the Micro-Electro-Discharge Machining of Ni-Based Alloy, International Journal of Materials and Metallurgical Engineering. 2016, 10(11): 1381-1387

Source details

Feedback > Compare sources >

Research on Engineering Structures and Materials

Scopus coverage years: from 2019 to Present

Publisher: MIM Research Group

ISSN: 2148-9807 E-ISSN: 2149-4088

Subject area: Engineering: Engineering (miscellaneous) Engineering: Mechanical Engineering Engineering: Mechanics of Materials Engineering: Civil and Structural Engineering

Source type: Journal

Save to source list Source Homepage

CiteScore 2022
1.5

SJR 2022
0.191

SNIP 2022
0.403

CiteScore CiteScore rank & trend Scopus content coverage

Improved CiteScore methodology

CiteScore 2022 counts the citations received in 2019-2022 to articles, reviews, conference papers, book chapters and data papers published in 2019-2022, and divides this by the number of publications published in 2019-2022. Learn more >

CiteScore 2022

1.5 = 231 Citations 2019 - 2022
198 Documents 2019 - 2022

Calculated on 05 May, 2023

CiteScoreTracker 2023

1.6 = 304 Citations to date
187 Documents to date

Last updated on 05 December, 2023 • Updated monthly

CiteScore rank 2022

Category	Rank	Percentile
Engineering — Engineering (miscellaneous)	#94/151	38th
Engineering — Mechanical Engineering	#436/631	30th
Engineering — Mechanics of Materials	#282/391	27th

ResearchGate

See discussions, stats, and author profiles for this publication at: https://www.researchgate.net/publication/371491960

Recognition of Vehicle number Plate for collection of toll Section A-Research paper Recognition of Vehicle number Plate for collection of toll

Article · June 2023

CITATIONS
0

READS
193

10 authors, including:



Uday Patil
Bharati Vidyapeeth Deemed University
25 PUBLICATIONS 3 CITATIONS
SEE PROFILE



Swapnil Mane
Bharati Vidyapeeth University
8 PUBLICATIONS 0 CITATIONS
SEE PROFILE



Ajinkya Suresh Hasabe
Bharati Vidyapeeth University
2 PUBLICATIONS 0 CITATIONS
SEE PROFILE



Shikha Bhardwaj Shrivas
bharati vidyapeeth college of engineering lavale
12 PUBLICATIONS 7 CITATIONS
SEE PROFILE

Recognition of Vehicle number Plate for collection of toll

Dr. Uday Shankar Patil[1]

Mr. SwapnilChandrakant Mane[2]

Mr. NeerajArun Gangurde[3]

Mr. Ajinkya Suresh Hasabe[4]

Mr. ShrikantRamchandra Sutar[5]

Mr. SagarArvind Kale[6]

Dr. Shikha Bhardwaj[7]

Dr. UdayChandrakant Patkar[8]

BharatiVidyapeeth's College of Engineering, Lavale [1,2,3,4,5,6,7,8]

Abstract-To design a real time application this will recognize the license plates automatically of vehicles. The proposed. License plate recognition (LPR) system is one kind of an intelligent transport system and is of considerable interest because of its potential applications in highway electronic toll collection and traffic monitoring systems. The purpose of this paper is to develop a real time application which recognizes license plates from vehicles. The image is given as input once the license plate is detected; its digits are recognized, display. In this system the yolov5 architecture is used to detect the licénse plate while tesseract is used to recognize the number plate.

Keywords—Number plate recognition, ALPR, YoLO, tesseract, computer vision.

I. Introduction

Automatic License Plate Recognition (ALPR) is also known as License Plate Recognition or License Plate Recognition. It uses image processing techniques to extract and recognize license plate information from images or video frames. The extracted information can be used in various applications such as electronic payment gateway systems, parking payment systems, road monitoring systems, and traffic control systems [1-3]. In real-world applications, ALPR researchers have to deal with a variety of challenges, such as license plate type, font, license plate color and font, license plate location, and environmental conditions such as lighting, weather, and objects. I have. License plates become difficult to recognize and recognize [4]. License plate formats tend to vary by country, as follows: B. Different Colors, Languages, and Fonts. Some plates have a different colored border than the background surrounding the plate and some have a plain background, indirectly adding challenges in capturing and recognizing car plates will occur. Variations in environmental conditions such as lighting and image background also affect the license plate recognition rate [5]. The ALPR system can be divided into his four main phases: image capture, license plate localization, segmentation and character recognition. Figure 1 shows the overall flow chart of the ALPR system. To achieve high accuracy in license plate recognition, the image quality must be high. Several factors can affect image quality. This includes the type of camera used, the resolution of the camera, the lighting and orientation of the camera used to capture the input image. Automatic Number Plate Recognition (ANPR) is widely known, but we know it is not used because it uses old technology, but an application that uses the same technology to manage visitors in a residential area We propose to develop a GPU-centric algorithm. To train the system, we use GPU-centric algorithms such as YOLO to address various challenges faced in using ANPR in countries such as India. To do. India faces challenges such as the cameras in use are mainly used for surveillance purposes and not for training and testing deep learning models. The second challenge is that license plate sizes and letter patterns vary from vehicle to vehicle and are highly complex.

The main purpose of this project is to detect a license plate from a video provided by a camera. An efficient algorithm is developed to detect a license plate in various luminance conditions. This algorithm extracts the license plate data from an image and provides it as an input to the stage of Car License Plate Recognition. Extracted image of the number plate can be seen on monitor. The scope of this project is to detect the license plate from the given image and observe the output on monitor. This project can work as a base for future improvements in the field of image processing, especially in license plate extraction and plate number recognition.

In this system, the Yolo v5 is used for detection of number plate and tesseract is used for the recognition of the number plate.

II. Literature Survey

ParidiSwaroop et al. [4] present a comparison of applications and methods using template matching. Templates are primarily sub-parts of objects that match completely different objects. The template matching technique is flexible and generally easy to use, making it one of the most popular object localization strategies. Template matching is performed in many areas such as image processing, signal processing, video compression, and pattern recognition. The following template matching techniques are used: Naive template matching, image correlation matching, sum of absolute differences, sum of squared differences. Lucky Kodwani et al. [5] present a fully functional vehicle detection, tracking, and license plate recognition system. It consists of vehicle recognition, license plate recognition and character recognition modules. Here, foreground estimation is first performed by a Gaussian mixture model, and then a real-time and robust license plate extraction method based on block variance techniques is proposed. License plate extraction is a key step in license plate recognition for automated transportation systems. The extracted license plate is split into individual characters using a region-based approach. The detection scheme combines adaptive iterative thresholding and template matching algorithms. Riazul Islam et al.[6] show a successful method for identifying vehicle license plates. The proposed technique is based on morphological manipulations based on various structural elements to maximally exclude regions of no interest and improve object regions. The system was tested using a database of license plates and simulation results show a significant improvement over other conventional systems. Muhammad Tahir Qadri et al. [7] provide an efficient automated licensed vehicle identification system based on vehicle registration numbers. The system has been implemented at the entrance of security checkpoints in highly restricted areas such as military areas, or in areas around high-level government agencies. Congress, Supreme Court, etc. The developed system first recognizes the vehicle and then captures an image of the vehicle. Vehicle license plate regions are extracted using image segmentation within the image. Optical character recognition technology is used for character recognition. The data obtained is used to obtain specific information such as vehicle owner, registration location, address, etc., compared to records in the database. AniruddhPuranic et al. [8] shows that India's urban areas are becoming more and more prosperous, necessitating car ownership. This has led to an unexpected civil society problem: traffic control and vehicle identification. Automatic Number Plate Recognition (ANPR) systems play a key role in solving these problems, from parking permits to city traffic monitoring to car theft tracking. Numerous ANPR systems based on different methodologies are currently available. In this article, we'll review different techniques and how to use them. The ANPR system was implemented using template matching and its accuracy was found to be 80% 8% of India's number. Byeong-Gil Han et al. [9] presents a new method for recognizing automatic license plates in real-time with high-definition video. Extensive research on license plate recognition has been conducted since his 1970s, but the proposed approaches derived from such research have difficulty processing high-resolution images in real time. Here we propose a new cascade structure that is the fastest available classifier by most efficiently rejecting false positives. Additionally, we train a classifier with core patterns for different license plate types to improve both the computational load and accuracy of license plate recognition. To demonstrate its superiority, we compare our approach with other state-of-the-art approaches. Additionally, we collected 20,000 images of him, including license plates from real traffic scenes, for a comprehensive experiment. The results show that the proposed approach significantly reduces computational load compared to other state-of-the-art approaches with comparable performance accuracy. NighatNaaz Ansari [10] Recognition of characters on license plates is proposed. A method used to recognize characters from a license plate based on template matching. In this method, the license plate image is first taken as input, then preprocessing steps such as grayscale image transformation, dilation, erosion, and convolution are performed to remove noise from the input image. Each letter on the license plate is then segmented. Segmentation is based on connected components. Next, after clipping, a template is applied to the clipped characters to recognize the characters. Matching is based on correlation between the extracted characters and templates in the database. In the final step, the numbers and letters recognized from the input image are displayed in a text file. The car plate is displayed in various types of character styles in one or two columns, varying in size, spacing, and number of characters. With such variability, even locating or detecting these plates becomes a time-consuming process. In existing systems, foreground estimation is performed by Gaussian mixture models, and a real-time and robust method for extracting license plates based on block-variance techniques is proposed. License plate extraction is a key step in license plate recognition for automated transportation systems. The extracted license plate is split into individual characters using a region-based approach. The detection scheme combines adaptive iterative thresholding and template matching algorithms.

III. PROPOSED SYSTEM

The block diagram of the proposed system is shown in Fig.1. The system consists of number plate detection and number plate recognition.

A. Number Plate Detection

The primary purpose of license plate recognition is to store information from the vehicle related to license plate characters. So you can use this information to track your vehicle. Yolo V5 architecture is used to recognize license plates in the scene. YOLOv5 is a family of composite scaling object detection models trained on the COCO dataset. It includes simple functionality for Test Time Augmentation (TTA), model assembly, hyperparameter development, and export to ONNX, CoreML, and TFLite. YOLOv5 has four models, s, m, l and x, each with different detection accuracy and performance. A YOLOv5 implementation can be found at https://github.com/ultralytics/yolov5. This work uses YOLOv5 to classify each digit of a license plate number.

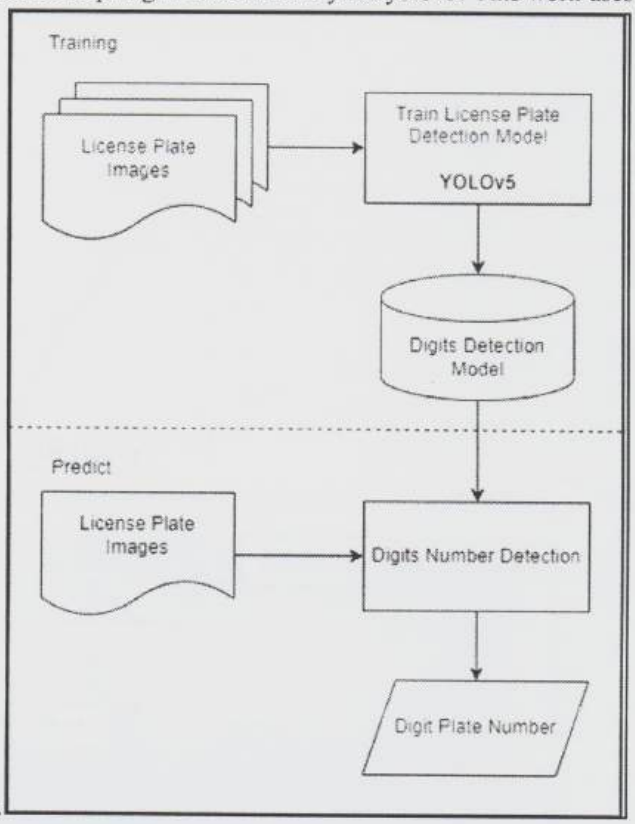


Fig. 1. Fig.1. Block diagram of the proposed system

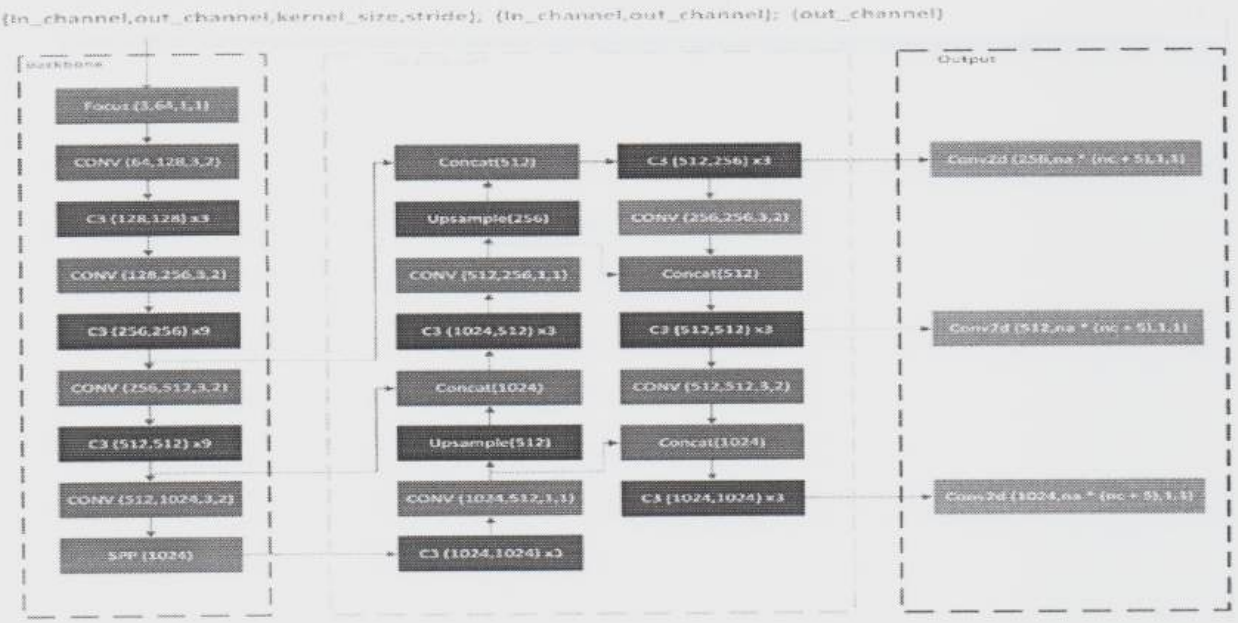


Fig. 2. Model Structure Overview of YOLOv5

We used data from Open Images V6 vehicle images with license plates. Open Images is a platform that provides various image datasets. In this work, we used an image dataset of the vehicle registration number class. The total data used to train the license plate recognition model in YOLOv4 was 3368. A total of 3000 images were used as training data and 368 images were used as test/validation data.



Figure 3. Dataset

example About 100 license plate images were randomly collected from real traffic conditions, Google Video, parking lots in Pune, Delhi and Haryana with different but imperfect lighting conditions. Please note that the data does not include all types of additional license plate accessories. B. Acrylic housing and all possible camera orientations. B. Includes slope and angle. A standard license plate in India begins with two alphabetic characters indicating the region in which the vehicle is registered, followed by two digits indicating the RTO passage, followed by two alphabetic characters of the current series, then 0001 to 9999. followed by four numbers up to . Data from up to 100 collected license plate images are labeled for each character object contained in each image. Image annotation is done using the annotation library. The architecture of yolo v5 is shown in Figure 2.

- Backbone

The main purpose of backbone is to extract the essential features of the input image. YOLOv4 used CSPDarknet53 as its backbone. The Cross Stage Partial (CSP) [5] architecture is derived from the DenseNet [8] architecture by taking the previous input and concatenating it with the current input before moving to the dense layer.Neck

A key role of the neck is to collect feature maps from different stages. YOLOv4 uses SPP (Spatial Pyramid Pooling) blocks to generate fixed-size features regardless of the size of the out-feature map [6], and PaNet to aggregate parameters from different backbone layers. [7].

- Head

For a one-stage detector, the key role of the head is to perform dense prediction. A dense prediction is a final prediction consisting of a vector containing the predicted bounding box coordinates, the confidence value, and the label of the prediction. As shown in Figure 2, YOLOv5 has a similar model architecture to YOLOv4. YOLOv5 is almost identical to YOLOv4 except for framework and configuration. YOLOv5 is based on the PyTorch framework and uses .yaml files for configuration. For the digit detection model, I trained his YOLOv5 model using the transfer learning

method. You trained a model to classify each letter object in a license plate image. We trained the model on 330 license plate images and validated the trained model on 111 images to calculate the mAP value.

- Inference

We use the License Plate Detection model and the Digit Recognition model that previously trained in our License Plate Recognition System as follows: First, the system will receive a vehicle image as an input. Then, the image will be processed by the License Plate Detection model. The model detected and cropped the plate number object.

The cropped image will be processed by the Digit Recognition model. The model classified all the characters in the cropped image and returned a sequence of digit plate numbers.

- Digit Recognition with YOLOv5

As the results show, as a result of the YOLOv5 transfer learning model, using the existing dataset, the digit recognition model achieved F1 score values of 80-83% with an accuracy value of 82.11% and a recall value of 81.97%. can be generated. Also, this model can achieve 84% mAP at 50% IoU threshold. The total detection time required for this model is 13.5 ms. A digit recognition model using YOLOv5 shows satisfactory results even with a small data set.

B. Number Plate Recognition

Text recognition is the process of recognizing text from scenarios by understanding and analyzing the underlying patterns. Also known as Optical Character Recognition (OCR). It can also be used for a variety of applications, such as reading documents, searching for information, and identifying products from shelves. OCR can be trained or used as a pretrained model. His pre-trained OCR model is used. This very important process forms the final stage of the ANPR process. Here the Tesseract OCR engine is applied to the recognized disc to recognize alphanumeric characters on the disc. The Tesseract engine used is trained to increase the accuracy of the recognition process. For training, we created an image of the characters to be recognized using the expected font, and created a dictionary of possible combinations of characters (area code, suffix, license plate) on a license plate. The output of this stage is a text representing the vehicle number.

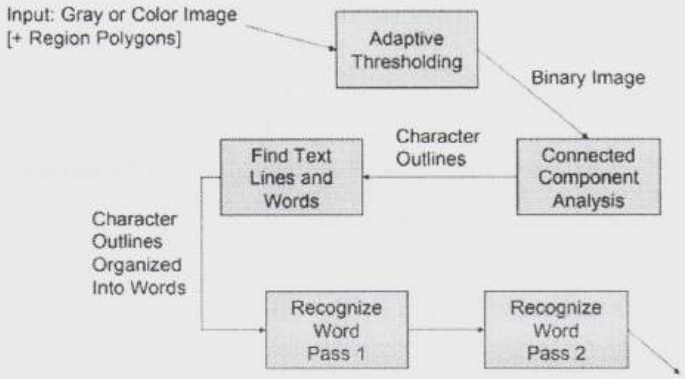


Fig. 3. Processes involved in tesseract-based character recognition

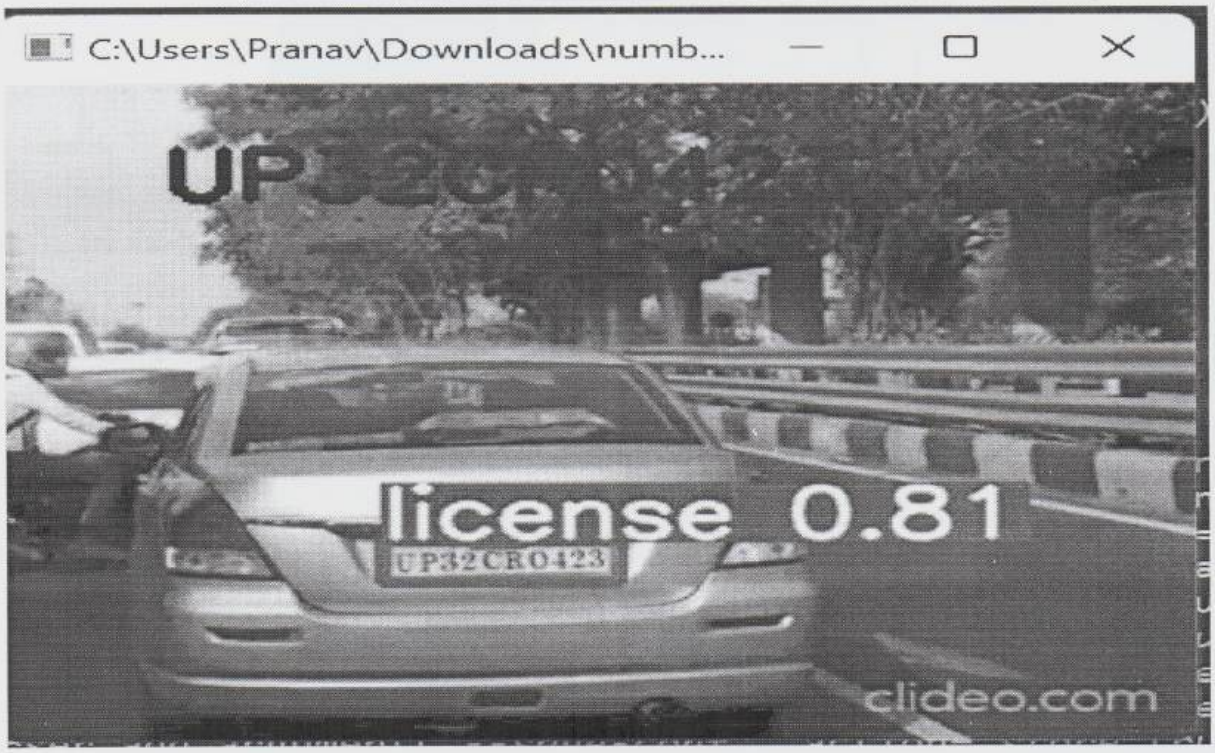
- In the next step, letter outlines are extracted from words. Text recognition starts as a two-pass procedure. In the first pass, word recognition is performed using static classification. Each word is fully passed to the adaptive classifier in the form of training data. A second pass is run over the page using a new adaptive classification model that does not exhaustively inspect words to re-examine modules. • Many of the processes involved in implementing the methods presented are summarized here. • First, a collection of training images is provided. • The next step is to get a series of data points from the available annotated images. The data points are then converted to a .csvfile.Then, the records are generated in TensorFlow. In the next stage, a training model is created using Faster R-CNN with Inception V2 method.
- Upon the completion of training model, new input images are provided to the system as shown in the figure.
- When new input images are provided, the Faster RCNN model detects the number plate at first instance correctly.
- Then, the text is recognized with the help of PyTesseract.
- Finally, the text in the vehicle number plate is identified correctly.

IV. RESULTS

The proposed system is implemented for license plate recognition in a real-time environment. License plate recognition uses Yolo V5 architecture and license plate recognition uses Tesseract. The results of the proposed system are shown below.



. 5.





V. Conclusion

ALPR applications are becoming increasingly complex in the context of India with tremendous exponential growth in the automobile, motorcycle and automotive industries. ALPR applications such as automatic toll collection, automatic charging systems in parking lots, managed vehicles in parking lots, and traffic monitoring have brought new research challenges to his ALPR in a newer dimension. We developed an automatic license plate recognition software by taking input from a live video feed. Character segmentation is implemented on the extracted license plates. Finally, we'll use the Tesseract engine to recognize license plates. The proposed system shows promising results in license plate recognition and recognition. The proposed system implementation can be extended to recognize multiple vehicle license plates in a single frame. Develop easy-to-use Android applications for traffic monitoring and management systems. Also, for higher accuracy, character recognition can be performed using various deep learning algorithms. With GPU you can get more performance in terms of computation time.

References

[1] M. Fang, C. Liang, and X. Zhao, "A method based on rough set and SOFM neural network for the car's plate character recognition, " in Intelligent Control and Automation, WCICA 2004, Fifth World Congress on, 5, 2004, 4037-4040. IEEE.

[2] N. A. Jusoh, J. M. Zain, and T. A. A. Kadir, "Enhancing Thinning Method for Malaysian Car Plates Recognition, "in Innovative Computing, Information and Control, ICICIC'07, Second International Conference on IEEE, 2007, 378-378. IEEE.

[3] E. R. Lee, P. K. Kim, and H. J. Kim, "Automatic recognition of a car license plate using color image Processing, " in Image Processing, ICIP-94., IEEE International Conference, 2, 1994, 301-305.

[4] Paridhi Swaroop, Neelam Sharma, "An Overview of Various Template Matching Methodologies in Image Processing", International Journal of Computer Applications (0975 – 8887) Volume 153 – No 10, November 2016

[5] Lucky Kodwani & Sukadev Meher "Automatic License Plate Recognition in Real Time Videos using Visual Surveillance Techniques ",ISSN (PRINT): 2320 – 8945, Volume -1, Issue -6, 2013

[6] Riazul Islam, Kazi Fatima Sharif and Satyen Biswas, "Automatic Vehicle Number Plate Recognition Using Structured Elements", IEEE Conference on Systems, Process and Control December 2015, pp 44-48.

[7] Muhammad Tahir Qadri, Muhammad Asif "Automatic Number Plate Recognition System for Vehicle Identification using Optical Character Recognition" IEEE 2009

[8] Aniruddh Puranic, Deepak K. T, Umadevi V "Vehicle Number Plate Recognition System: A Literature Review and Implementation using Template Matching" International Journal of Computer Applications (0975 – 8887) Volume 134 – No.1, January 2016

[9] Byung-Gil Han, Jong Taek Lee, Kil-Taek Lim, and Yunsu Chung "Real-Time License Plate Detection in High Resolution Videos Using Fastest Available Cascade Classifier and Core Patterns" ETRI Journal, Volume 37, Number 2, April 2015

[10] Nighat Naaz Ansari, Ajay Kumar Singh "License Number Plate Recognition using Template Matching" International Journal of Computer Trends and Technology (IJCTT) – Volume 35 Number 4- May 2016.

[11] M. M. Shidore, S. P. Narote," Number Plate Recognition for Indian Vehicles" IJCSNS International Journal of Computer Science and Network Security, VOL.11 No.2, Feb. 2011

Author Search Sources Create account

Source details

Feedback > Compare sources >

European Chemical Bulletin

Open Access

Scopus coverage years: from 2017 to Present

Publisher: Deuton-X Ltd.

E-ISSN: 2063-5346

Subject area: Chemistry: General Chemistry

Source type: Journal

Source Homepage

CiteScore 2021
0.8

SJR 2021
0.139

SNIP 2021
0.187

CiteScore | CiteScore rank & trend | Scopus content coverage

Improved CiteScore methodology

CiteScore 2021 counts the citations received in 2018-2021 to articles, reviews, conference papers, book chapters and data papers published in 2018-2021, and divides this by the number of publications published in 2018-2021. Learn more >

CiteScore 2021

0.8 = 182 Citations 2018 - 2021 / 217 Documents 2018 - 2021

Calculated on 05 May 2022

CiteScoreTracker 2022

1.6 = 499 Citations to date / 313 Documents to date

Last updated on 11 April 2023 - Updated monthly

Review One: Drowsiness Sensing System & Pothole Identification Technique For Monitoring Roads

Prof. Sanket S.Pawar[1] Miss. Sanyogita Paimode[2], Miss. Divya Raut[3], Miss. Shraddha Shirole[4], Mrs. Sandhya Sawalkar[5], Dr. Dhanke Jyoti[6]
Bharati Vidyapeeth's College of Engineering, Lavale, Pune

doi: 10.48047/ecb/2023.12.si4.1191

Abstract:

One of the major problems in developing countries is monitoring the road and traffic condition. Potholes on the road can affect the large proportion of society either directly or indirectly. Getting the pothole fixed, informing the authorities and asking them to take action is very time consuming. Implementing a system that involves citizens in the process of detecting pothole is what is being envisioned. many image processing techniques were proposed to inspect pavement defect for improving accuracy and efficiency for the onsite inspection by the humans but it gives you unacceptable stability. Therefore, an application of convolutional neural network is used for pothole detection using digital images in this study. This paper concludes earlier pothole detection methods that have been developed and suggest a cost-effective solution to detect the potholes on the roads and provides timely alerts to drivers to avoid critical problem that causes numerous car accidents annually is driver fatigue. Due to incapacity of driver to halt or minimize the impact accidents caused by driver's sleepiness are much more inclined to result in fatalities or severe accidents. this paper focuses on accident detection and avoidance system which detect accidents and alerts the driver by buzzer. It calculates the eye open ratio by using eye blinking algorithm.

Keywords:

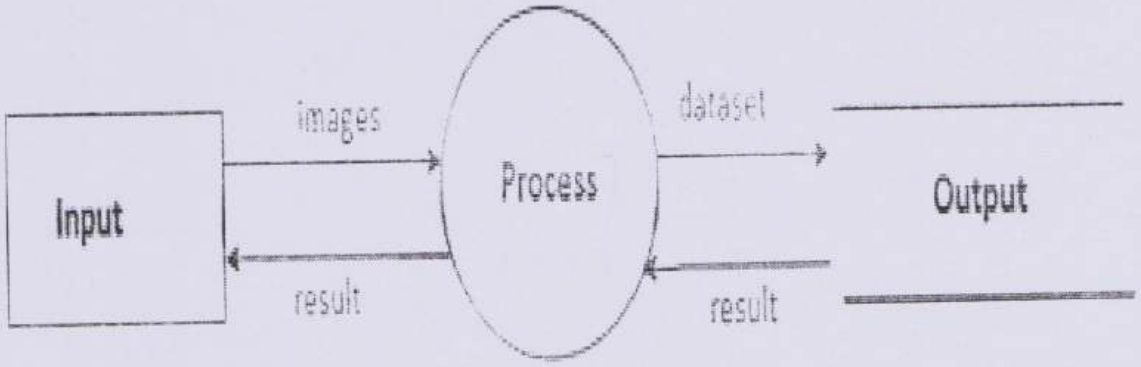
Convolutional Neural Network, Image processing, pothole detection, drowsiness detection

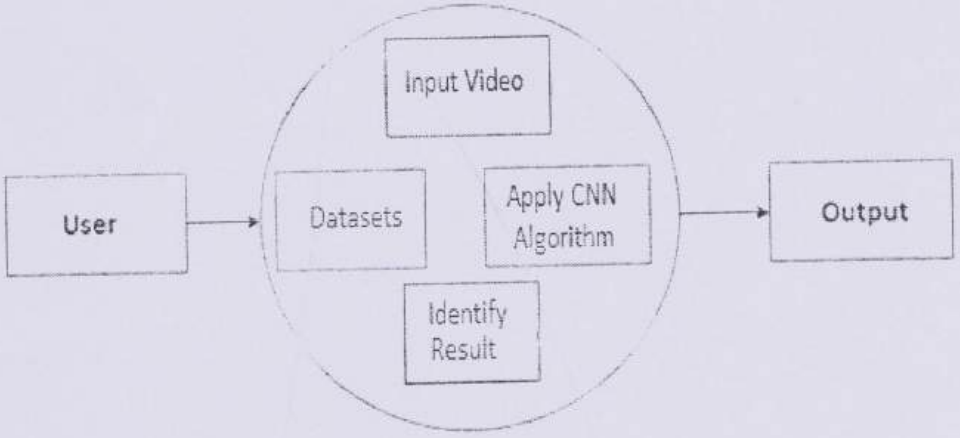
Introduction:

Road accidents occur due to multiple causes such as over speeding, use of mobile phones, drunken driving, vehicular condition, poor light condition, fault of driver, overtaking. In the context of population, India is ranked second with fast growing economy and it is known to have wide network of roads. Roads are prime means of transportation in India today. They carry almost 90 percent of country's passenger traffic and 65 percent of its freight [1]. however most of the roads in India are small and crowded with poor surface quality and road maintenance needs are not sufficiently met. Although technology has been widely used in many industries, it has not been widely adopted by industries, in the field of road infrastructure and repairs. By using right technology, it has potential to greatly improve the efficiency and effectiveness of pothole repair work, improving safety of roads. However, many municipalities are still using the old-age methods of cement to fix potholes.

According, to study it can be seen that sleepiness is a major cause for accidents, especially automated accidents. WHO statistics show that 1.2 million people worldwide die every year due to road crashes, accidents, 50 million people are injured and more than 4000 people die daily from road traffic injuries [2]. Activities such as driving a car, handling heavy machinery, monitoring a nuclear plant are activities that require visual reaction times; these can be affected by drowsiness. According to Peru's statistics indicate that in 2007 there were 3510 details due to traffic accidents and 49,857 injuries, most of them due to tiredness of the drivers [3].

Level 0 DFD:





Convolutional Neural Network

This Algorithm is very much popular and it is most widely used algorithm in image recognition problems. Few examples are:

Face Recognition: To recognize faces using convolutional neural network and you can design face recognition based attendance system or you can have even criminal identification using facial recognition system.

Emotion Recognition: so you can recognize emotions based on dataset available with you and again you can use CNN algorithm to recognize emotions. now based on emotions you can detect the depression of particular person and you can avoid suicides and other consequences.

CNN image classification takes an input image, process it and classify under certain categories. This mainly works on images. Types of images such as black and white (binary images), grey level (8 bit), color (24 bit/RGB) can be suitable for convolutional neural network but as it is deep learning algorithm even it is much advanced than the traditional machine learning algorithm.

IMAGE PROCESSING

Image processing is process of transforming an image into a digital form and executing certain operations to extract some meaningful information from it. This system treats all images as 2D signals by applying certain pre-set signal processing methods. It is an essential pre-processing systems in numerous applications such as face recognition, object detection and image compression. Such pre-processing can improve the performance of a model. Exploiting Images for example, Adding or removing objects to images is another application, particularly in the entertainment industry.

Image processing can be used for improving quality, remove undesired objects or creating new images. Image processing is broad and complex field with many different algorithms and techniques that can be used to gain different results

Types of Image processing:

Visualization- Find objects that are not visible in the image.

Recognition- Distinguish or detect objects in the image.

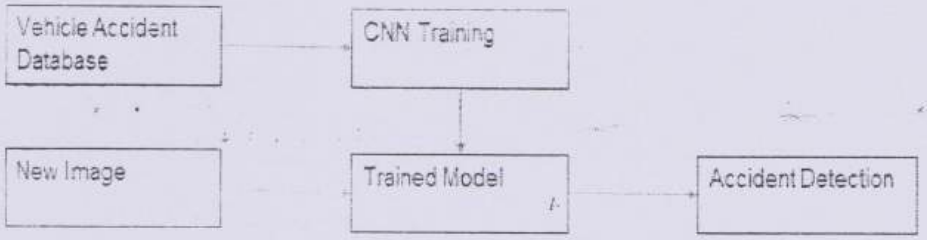
Sharpening and restoration- Create an enhanced image from the original image.

Pattern Recognition- Measure the various patterns around the objects in the image.

Retrieval - Browse and search images from a large database of digital images that are similar to the original image.

POTHOLE DETECTION

Pothole detection is main part of any automated driving system. previous works defined pothole as oval shaped area in the road surface that has different texture than road surface. The main Objective of this system is to identify potholes through deep learning approach. This system is used to automate task of detecting potholes and helps to understand whether the pothole is ahead or not. This system uses the object detection algorithm to detect the potholes and alerts by the buzzer.



System Architecture:

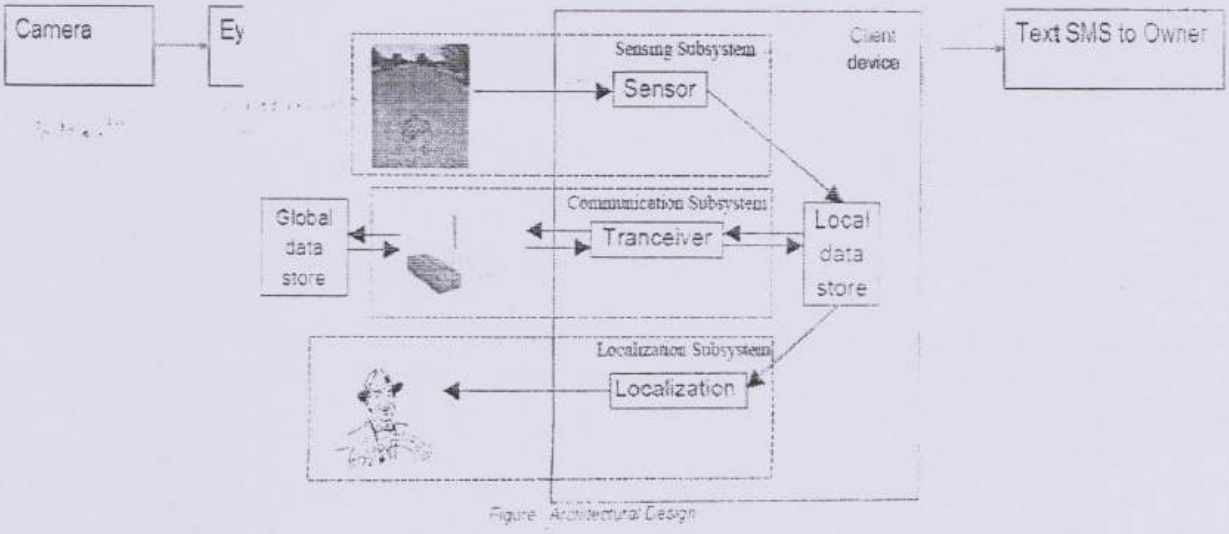


Figure Architectural Design

DROWSINESS DETECTION

Nowadays the driver safety in the car is one of the most wanted System to avoid accidents. For enhancing the safety. We are detecting the eye blink of the driver and estimating the driver status. In this system we are detecting the eye status of the driver to detect the whether the driver drowsy or not so to avoid situation like accidents. Firstly, camera as sensor captures the eye of the driver then it calculates eye aspect ratio using the eye blink detection algorithm and it results that if eye of the driver remains closed continuously and if the threshold value is below 0.35 then the driver is alerted by the buzzer sound and also sends the message of the driver status to respected owner via SMS.

Conclusion:

We studied a machine-learning algorithm for prediction of road quality. A unified model and convolutional neural network for object detection is implemented. The deep learning model is trained with pothole images to modify and predict potholes and drowsiness detection. A deformable parts model or CNN model can be trained with images to predict potholes but comparatively CNN eye blinking performs better in predicting potholes and produces promising results in time, speed and accuracy when compared. better training data could

improve the performance model. This model can be packed with flasks as an API and integrated with a mobile application to report potholes to the government which will reduce the communication gap between the government and its citizens. This model can also be used in real-time to predict pothole which implemented in autonomous vehicles so that it can prevent or execute a strategy to reduce discomfort to the passengers. The road sense application is an attempt to provide its users with better knowledge about the routes of their transportation. With further work in this field. It is possible for this project to play a proactive part in improving road conditions. Overall in this paper, we propose to upgrade the road type detection algorithm through detecting other road anomalies and trying other machine learning classifiers.

References:

[1] R. Madli, S. Hebbar, P. Pattar, and V. Golla, "Automatic detection and notification of potholes and humps on roads to aid drivers," IEEE Sensors Journal, vol. 15, no. 8, pp. 4313–4318, 2015.

[2] W. H. Organization. (2015) Global status report on road safety. [Online]. Available: http://www.who.int/violence_injury_prevention/road_safety_status/2015/en/pdf

[3] S. S. Pawar, A. Manepatil, A. Kadam and P. Jagtap, "Keyword search in information retrieval and relational database system: Two class view," 2016 International Conference on Electrical, Electronics, and Optimization Techniques (ICEEOT), Chennai, India, 2016, pp. 4534-4540, doi: 10.1109/ICEEOT.2016.7755576.

[4] Natalia I Vargas-Cuentas, Avid Roman-Gonzalez. Facial Image Processing for Sleepiness Estimation. 2nd International Conference on Bio-engineering for Smart Technologies, Aug 2017, Paris, France. ffhal-01637809f

Skip to main content

Author Search Sources Create account Sign in

Source details

Feedback > Compare sources >

European Chemical Bulletin

Open Access

Scopus coverage years: from 2017 to Present

Publisher: Deuton-X Ltd.

E-ISSN: 2063-5346

Subject area: Chemistry: General Chemistry

Source type: Journal

Save to source list Source Homepage

CiteScore 2021
0.8

SJR 2021
0.139

SNIP 2021
0.187

CiteScore CiteScore rank & trend Scopus content coverage

Improved CiteScore methodology

CiteScore 2021 counts the citations received in 2018-2021 to articles, reviews, conference papers, book chapters and data papers published in 2018-2021, and divides this by the number of publications published in 2018-2021. Learn more >

CiteScore 2021

0.8 = 182 Citations 2018 - 2021 / 217 Documents 2018 - 2021

Calculated on 05 May, 2022

CiteScoreTracker 2022

1.6 = 499 Citations to date / 313 Documents to date

Last updated on 05 April, 2023 • Updated monthly

e-ISSN 2320 –7876 www.ijfans.org
Vol.11,S Iss 1, 2022
Research paper © 2012 IJFANS. All Rights Reserved UGC CARE Listed (Group -I) Journal

Signature Verification And Alert Using AI And Machine Learning

Prof. Swati G. Gawhale
Assistant Professor, Bharati Vidyapeeth's College of Engineering,
Lavale, Pune, MH, India.
gawhaleswati@gmail.com

Prof. (Dr.) Reena Singh
MES's, Pillai HOC College of Engineering &Technology,
Rasayani Taluka Panvel, Dist, Navi Mumbai, Maharashtra 410207, India.
dr.rsingh2014@gmail.com

Prof. (Dr.) B.K. Sarkar
MES's, Geh Research, Panvel, Dist, Navi Mumbai, Maharashtra 410207, India.
dr.bksarkar2003@yahoo.in

Abstract.

Signature confirmation is a typical errand in measurable report examination. It is one of deciding if an addressed mark matches realized signature tests. From the perspective of mechanizing the errand it tends to be seen as one that includes AI from a populace of marks. There are two sorts of figuring out how to be achieved. In the first, the preparation set comprises of genuines and imitations from an overall public. In the subsequent there are veritable marks in a given case. The two learning assignments are called individual autonomous (or general) learning and individual reliant (or exceptional) learning. General gaining is from a populace of real and manufactured marks of a few people, where the distinctions among genuines and phonies across all people are learnt. The general learning model permits an addressed mark to be contrasted with a solitary real signature. In exceptional learning, an individual's mark is gained from different examples of just that individual's mark where inside individual likenesses are learnt. At the point when an adequate number of tests are accessible, unique learning performs better compared to general learning (5.06% higher exactness). With exceptional learning, confirmation precision increments with the quantity of tests. An intelligent programming execution of mark confirmation including both the learning and execution stages is portrayed.

Keywords: machine learning, forensic signature examination, biometrics, signature verification, digital document processing.

Introduction

The most widely recognized task in the field of measurable archive examination [1-5] is that of validating marks. The issue most often brought to a record inspector is the issue connecting with the genuineness of a mark: Does this addressed mark (Q) match the known, genuine marks (K) of this subject [6] A measurable report analyst otherwise called an

addressed record (QD) analyst involves long periods of preparing in looking at marks in settling on a choice in the event that work.

The preparation of a report inspector includes long periods of gaining from marks that are both certifiable and fashioned. In the event that work, models are generally just accessible for certified marks of a specific individual, from which the qualities of the veritable mark are learnt. Calculations for visual mark check are viewed as in this paper. The exhibition errand of mark check is one of deciding if an addressed mark is certifiable or not. The picture of an addressed mark is matched against different pictures of known marks.

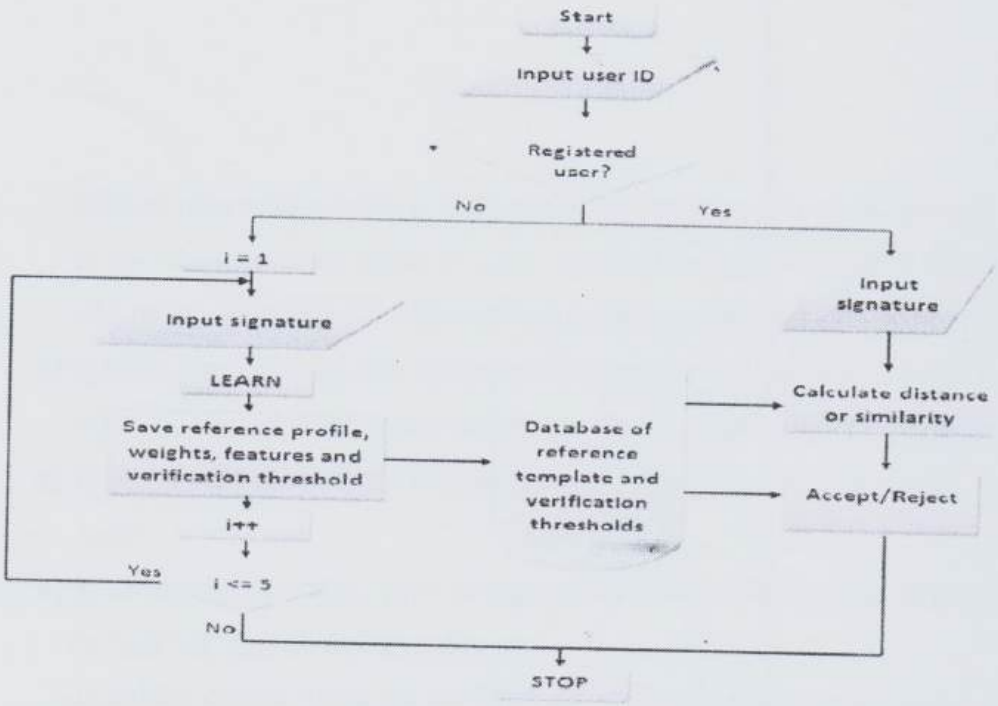


Fig.1: Signature verification and alert using AI and Machine Learning Flow Chart.

Visual mark confirmation is normally planned as an AI task. A program is said to display AI capacity in playing out an errand in the event that it can gain from models, work on as the quantity of models increment, and so forth [7]. Resembling the learning undertakings of the human addressed report analyst, the AI errands can be expressed as broad realizing (which is individual autonomous) or unique realizing (which is individual ward) [8].

On account of general gaining the objective is to gain from a huge populace of real and manufactured signature tests. The emphasis is on separating between real authentic contrasts and veritable imitation contrasts. The learning issue is expressed as learning a two-class order issue where the information comprises of the contrast between a couples of marks. The check task is performed by looking at the addressed mark against each known mark. The general learning issue can be seen as one where learning happens with close to misses as counter-models [9].

© 2012 IJFANS. All Rights Reserved

Feature Extraction and Similarity Computation Signatures are relied upon for identification

Because of the way that every individual creates interesting propensities for pen development which effectively address their mark. In this manner at the core of any programmed signature confirmation framework are two calculations: one for removing highlights and the other for deciding the likenesses of two marks in light of the elements. Highlights are components that catch the uniqueness.

In the QD writing such components are named segregating components or components of correlation. A given individual's examples can have a (potentially factor) number of components and the mix of components have more prominent separating power. Ahumandocument inspector utilizes a diagram of basic qualities [6]. Such components are ticks, perfection of bends, and perfection of strain changes, situation, development and dividing, top of composing, base of composing, angulation/incline, generally speaking tension, pressure change designs, gross structures, varieties, connective structures and microforms. Utilizing the natural attributes, for example, speed, extent, tension and not entirely settled.

Table 1. Examples of signatures given by two individuals and their thinned versions

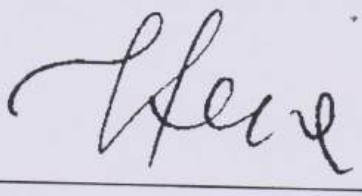
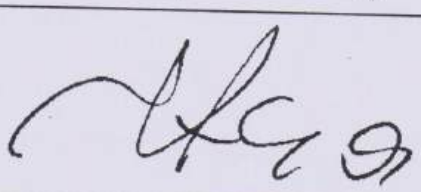
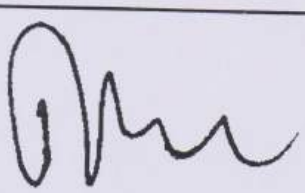
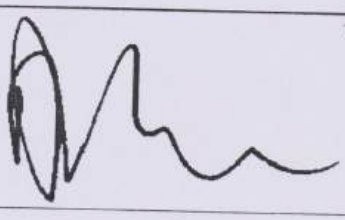
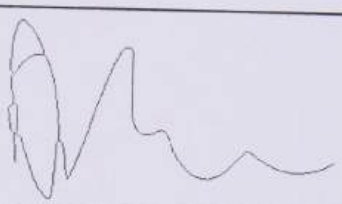
signature image	signature skeleton
	
	
	
	

Fig.2: Signature verification and alert using AI and Machine Learning Display

These thusly permit musicality and structure and their not entirely set in stone. Programmed signature check strategies depicted in the writing utilize an altogether unique arrangement of highlights. Some depend on picture surface, for example, wavelets while others center on math and geography of the mark picture. Sorts of highlights utilized for signature

© 2012 IJFANS. All Rights Reserved

confirmation are wavelet descriptors [17], projection appropriation capabilities [18, 14, 19], broadened shadow code [18] and mathematical elements [20].

Multiresolution Features

A semi multiresolution approach for highlights are the Inclination, Primary and Concavity, or GSC, highlights [21, 22]. Inclination highlights measure the neighbourhood scale qualities (got from the two-layered slope ofthe picture), primary elements measure the halfway scale ones (addressing strokes), and concavity can quantify the attributes over the size of entire picture (addressing concavities and geography). Following this way of thinking, three sorts of element maps are drawn and the comparing neighbourhood histograms of every phone is quantized into paired highlights. Illustration of a mark, which has a 4x8 framework forced on it for removing GSC highlights; lines and sections of the matrix are drawn in view of the dark pixel disseminations along the level and vertical bearings. Countless double highlights have been separated from these, which are worldwide word shape highlights [23]; there are 1024 pieces which are acquired by connecting 384 angle bits, 384 primary pieces and 256 concavity bits.

Image grid for signature matching

The GSC paired highlight vector relies on the lattice used to segment the picture one of which is displayed. The least complex one with equivalent cell size can be utilized for character acknowledgment. A more mind boggling straight matrix is gotten from two one-layered projection histograms got along even and vertical headings so the closer view pixel masses of cells are equivalent both section and line wise.

© 2012 IJFANS. All Rights Reserved

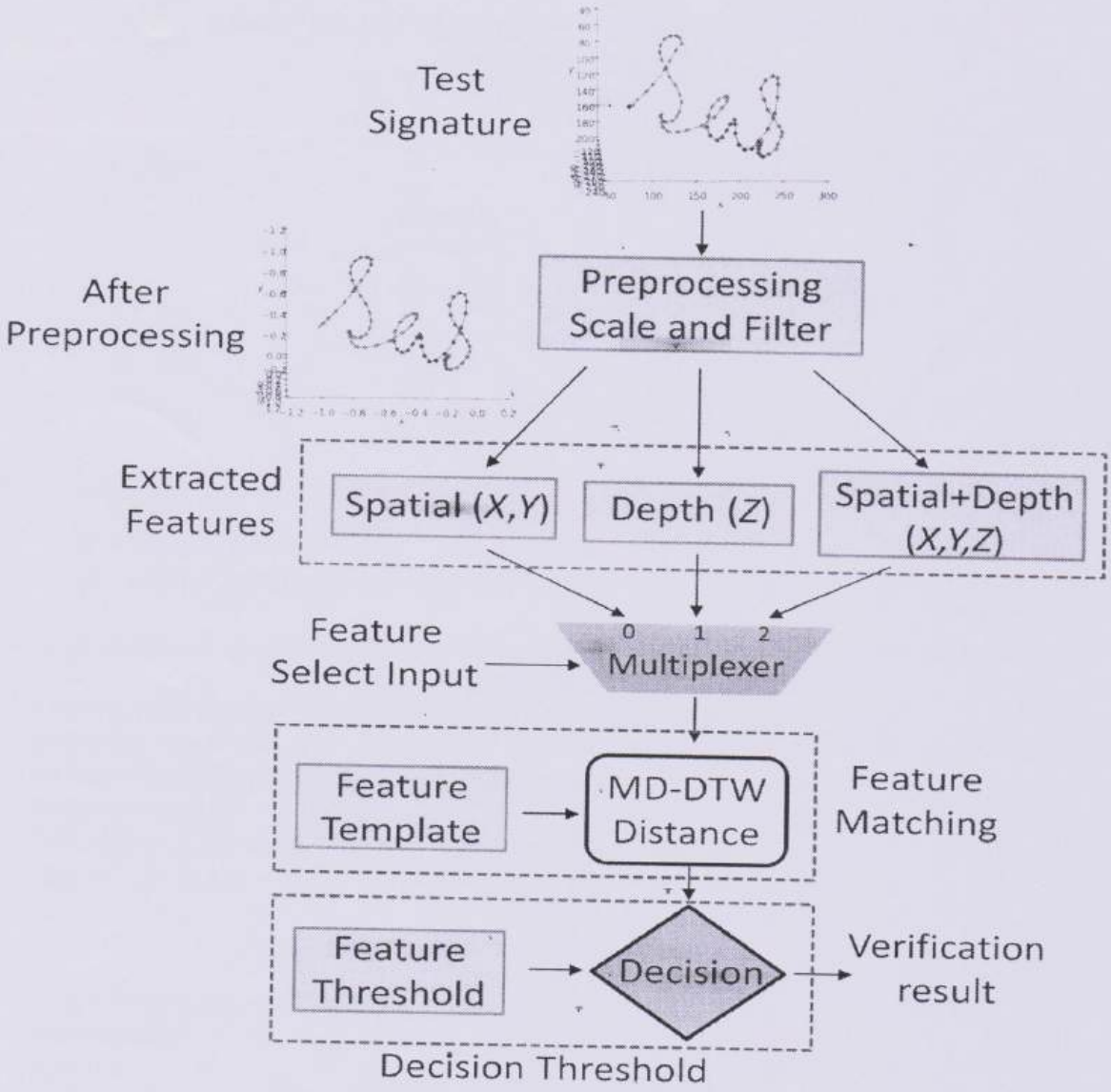


Fig.3: Signature verification and alert using AI and Machine Learning Block Diagram.

To accomplish great arrangement between signature pictures a non-straight examining framework ought to be applied. The issue of looking through a particular mathematical change or planning capability to match two firmly related pictures is an exemplary picture enrollment issue. Accordingly the age of non-straight framework comprises of two phases: point planning and change looking, which is additionally the overall arrangement of matching issue without earlier information on enrollment. In the primary stage, the extremas of strokes are marked as the milestones of marks, then, at that point, a suitable chart matching calculation is applied to match these two point sets. In light of the enlistment data got from the principal stage a mathematical change which limits a particular expense capability can be found. The non-straight network is normally the projection of the reference matrix by the planning capability.

© 2012 IJFANS. All Rights Reserved

Landmark mapping

Theextremasalong the strokes where the arch of shapes has nearby greatest record delegate data of individual composition. Subsequent to naming the extremas along the forms as milestones of pictures the Scott and Longuet-Higgins calculation [25] can be utilized to match the milestone sets of two pictures. In this calculation the two point sets are set at a similar surface and a vicinity framework G is developed to demonstrate their spatial relations, i.e., G = exp (−r2 ij/σ2), where rij is the Euclidean distance between focuses I and j. The matching network P is then developed to estimate a change framework which relates to a matching capability. Utilizing Scott and Longuet-Higgins calculation highlight point matching can be built between two point sets while gutting some awful matches.

Tests

Information base of disconnected marks was ready as a proving ground [13]. Every one of 55 people contributed 24 marks subsequently making 1320 real marks. Some were approached to produce three other journalists' marks, multiple times per subject, in this way making 1320 fabrications. One illustration of each of 55 genuines are displayed.

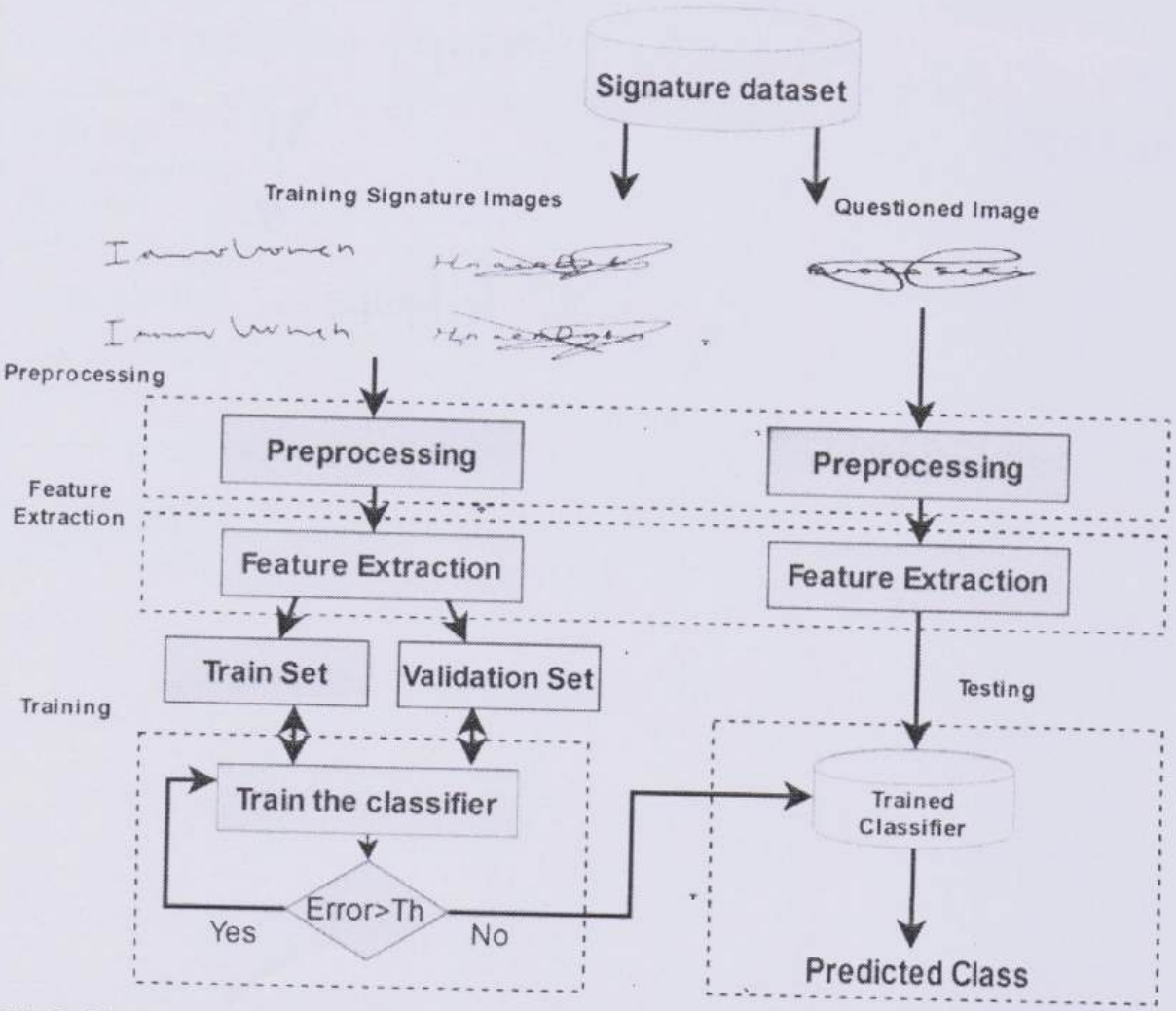


Fig.5: Signature verification and alert using AI and Machine Learning Block Diagram.

Ten instances of genuines of one subject (subject no. 21) and ten frauds of that subject are displayed. Every mark was checked at 300 dpi dim scale and binarized utilizing a dark scale histogram. Salt pepper commotion evacuation and inclination standardization were two stages engaged with picture preprocessing. The data set had 24 genuines and 24 imitations accessible for every essayist. For each experiment an essayist was picked and N veritable examples of that author's mark were utilized for learning. The leftover 24 – N real examples were utilized for testing. Likewise 24 produced marks of this essayist were utilized for testing. Two distinct mistake types can be characterized for any biometric individual distinguishing proof issue.

Summary and Discussion

Programmed signature check is an undertaking where AI can be utilized as a characteristic piece of the cycle. Two different AI draws near, one including genuines and fabrications in a general set and another including just genuines for a specific case were portrayed. The main methodology is practically equivalent to involving counterexamples with close to misses in the growing experience. The two methodologies include utilizing a comparability measure to register a distance between elements of two marks. Exceptional learning outflanks general advancing especially as the quantity of genuines increments.

General learning is helpful when the quantity of genuines is tiny (under four). A refined technique for removing highlights for marks was likewise examined which can additionally increment confirmation precision. An intuitive programming execution of mark check was depicted. Future work ought to think about consolidating the two sorts of figuring out how to further develop execution

Ref.

1. Osborn, A.: Questioned Documents. Nelson Hall Pub (1929)
2. Robertson, E.W.: Fundamentals of Document Examination. Nelson-Hall (1991)
3. Bradford, R.R., Bradford, R.: Introduction to Handwriting Examination and Identification. Nelson-Hall (1992)
4. Hilton, O.: Scientific Examination of Questioned Documents. CRC Press (1993)
5. 5. Huber, R., Headrick, A.: Handwriting Identification: Facts and Fundamentals. CRC Press (1999)
6. 6. Slyter, S.A.: Forensic Signature Examination. Charles C. Thomas Pub (1995)
7. Mitchell, T.M.: Machine Learning. McGraw-Hill (1997)
8. 8. Srihari, S.N., Xu, A., Kalera, M.K.: Learning strategies and classification methods for off-line signature verification. Proceedings of the Seventh International Workshop on Frontiers in Handwriting Recognition(IWHR), IEEE Computer Society Press (2004) 161–166
9. 9. Winston, P.: Learning structural descriptions from examples. In Winston, P., ed.: The Psychology of Computer Vision. McGraw-Hill (1975) 157–210
10. 10. Leclerc, F., Plamondon, R.: Automatic signature verification: the state of the art, 1989-1993. International Journal of Pattern Recognition and Artificial Intelligence 8 (1994) 643–660
11. Guo, J.K., Doorman, D., Rosen field, A.: Local correspondences for detecting random forgeries, Proceedings of the International Conference on Document Analysis and Recognition (1997) 319–323

© 2012 IJFANS. All Rights Reserved

12. Plamondon, R., Srihari, and S.N.: On-line and off-line handwriting recognition: A comprehensive survey. IEEE Transactions on Pattern Analysis and Machine Intelligence 22 (2000) 63–84
13. Kalra, M.K., Zhang, B., Srihari, and S.N.: Off-line signature verification and identification using distance statistics. International Journal of Pattern Recognition and Artificial Intelligence 18 (2004) 1339–1360
14. Fang, B., Leung, C.H., Tang, Y.Y., Tse, K.W., Kwok, P.C.K., Wong, Y.K.: Off-line signature verification by the tracking of feature and stroke positions. Pattern Recognition 36 (2003) 91–101
15. rehire, S.N., Cha, S., Arora, H., Lee, S.: Individuality of handwriting. Journal of Forensic Sciences (2002) 856–872
16. Srinivasan, H., Beal, M., Srihari, S.N.: Machine learning approaches for person verification and identification. Volume 5778. Proceedings of SPIE: Sensors, and Command, Control, Communications, and Intelligence Technologies for Homeland Security (2005) 574–586
17. Deng, P.S., Liao, H.Y., Ho, C., Tyan, and H.R.: Wavelet-base off-line handwritten signature verification. Computer Vision Image Understanding 76 (1999) 173–190
18. Sabourin, R.: Off-line signature verification: Recent advances and perspectives. BSDIA (1997) 84–98
19. Coetzer, J., B.M.Herbst, du Preez, J.: Off-line signature verification using the discrete radon transform and a hidden markov model. Journal on Applied Signal Processing 4 (2004) 559–571
20. Ferrer, M.A., Alonso, J.B., Travieso, C.M.: Off-line geometric parameters for automatic signature verification using fixed-point arithmetic. IEEE Transactions on Pattern Analysis and Machine Intelligence 27 (2005) 993–997
21. Srikantan, G., Lam, S., Srihari, S.: Gradient based contour encoding for character recognition. Pattern Recognition 7 (1996) 1147–1160
22. Zhang, B., Srihari, S.N.: Analysis of handwriting individuality using handwritten words, Proceedings of the Seventh International Conference on Document Analysis and Recognition, IEEE Computer Society Press (2003) 1142–1146
23. Zhang, B., Srihari, S.N., Huang, C.: Word image retrieval using binary features. In Smith, E.H.B., Hu, J., Allan, J., eds.: SPIE. Volume 5296. (2004) 45–53
24. Zhang, B., Srihari, S.: Properties of binary vector dissimilarity measures. Cary, North Carolina (September, 2003)
25. Scott, G.L., Longuett-Higgins, H.: An algorithm for associating the features of 2 images. Proceedings of the Royal Society of London Series B (Biological) 244 (1991) 21–26
26. Bookstein, F.L.: Principal warps: Thin-plate splines and the decomposition of deformations. IEEE Trans. Pattern Analysis and Machine Intelligence 11 (1989) 567–585
27. Press, W.H., Flannery, B.P., Teukolsky, S.A., Vetterling, W.T.: Numerical Recipes in C: The Art of Scientific Computing. Cambridge University Press (1992) 28. Srihari, S.N., Zhang, B., Tomai, C., Lee, S., Shi, Z., Shin, Y.C.: A system for handwriting matching and recognition, Proc. Symposium on Document Image Understanding Technology (2003) 67–75

ugccare.unipune.ac.in/Apps1/User/WebA/SearchList

SAVITRIBAI PHULE PUNE UNIVERSITY

Home

UGC

Search

UGC-CARE List

UGC-CARE List

You searched for "**International Journal of Food and Nutritional Sciences**" Total Journals: 1

Search:

Sr.No.	Journal Title	Publisher	ISSN	E-ISSN	UGC-CARE coverage years	Details
1	International Journal of Food and Nutritional Sciences	Global E smart Technologies	2319-1775	2320-7876	from January-2021 to January- 2023	Discontinued from Jan 2023

Showing 1 to 1 of 1 entries

Previous 1 Next

Copyright © 2023 Savitribai Phule Pune University. All rights reserved. | Disclaimer

Contents lists available at ScienceDirect

Materials Today: Proceedings

journal homepage: www.elsevier.com/locate/matpr

Smart materials – A state-of-the-art-review

Nidhi Jain *, Shubham Nandu Ovhal, Vaibhav Patil, Kaveti Nani Kartik

Department of Engineering Science, BharatiVidyapeeth College of Engineering, Lavale, Pune 412 115, India

ARTICLE INFO

Article history:
Available online xxxx

Keywords:
Smart materials
Aerogel
Self-healing polymers
Titanium foams

ABSTRACT

This paper focuses on smart materials which are of many types. Three of the Smart materials mentioned in the paper have multiple use and have potential to improve prevailing technology and enhance new functionality of the product in various fields like aerospace, chemical engineering, construction, electrical equipment, water purification, and biomedicine The three magical materials are aerogel, self-healing polymers, titanium foams etc. have wide applications and unique properties. As Smart materials are responsive to the external stimuli. These materials are alive materials which have a lot of similarity in the functioning of the human body. The paper focus on three different types of smart materials. The first materials discussed in the paper are Aerogel, different types of aerogels, preparation conditions-construction, characterization of aerogels etc. Aerogel has ultimately unlimited potential, and applications in human life. The second material is open-pore titanium foams. The tensile strength and yield asset of the foams were discovered to span the property lies between chancellors and cortex bone. And have biological implant fixation Third material is Self-healing polymers which can be repaired themselves. These materials do not need any manual interaction. The presents review paper focused on the study of self-healing polymer and their applications as well as its advantages and disadvantages.
© 2023 Elsevier Ltd. All rights reserved.
Selection and peer-review under responsibility of the International Conference on Future Trends in Materials and Mechanical Engineering.

1. Introduction

Diverse varieties of Smart materials have been seen in the new-fangled expanse of technologies. These materials have the ability to acceptable in the surrounding they have the ability to modify their forms and dimensions, mechanical properties to fit in the environment to response the physical changes As we have seen that from the oldest time, human has always tried to enhance the life by making the adjustment in the surrounding environment. As we see that in today's innovative world everything is becoming advanced in order to fulfill the human requirements and out of these, nanomaterial is one of the most developing fields. Nanomaterials have a lot of applications in every field such as medical, electronic devices, sunscreens, lasers displays and so on. And these properties and applications motivate us to study about smart and to make the contribution in the enhancement of human life and make some research work in this field. In order to do so, we have chosen three nanomaterials which work as a smart material and by using features and properties of these materials they will always help in the betterment of the human life.

Materials are generally as considered as dead materials, but smart materials are alive as they respond to the stimuli of the environment. They are not only used for structure construction but also used as active materials. The external environment and stimuli may be of several types like stress, strain, heat light, etc.

Different types of the smart materials are available such as self-healing polymer, shape memory polymers piezoelectric, aerogels, Titanium Foams, magnetostrictive, optical fibers, electro rheological and magneto rheological fluids, multifunctional nanocomposites.

These smart materials are nicely placed in different arrangements- honeycombs, changeable-stiffness tubes, corrugated structures for providing structural stability and unique properties Smart materials implement their activities in ways they are:

1. Self-actuating—these material or system takes out from the environment than after being stimulated provides output of light, heat, and displacement [3].
2. Self-sensing—when there is a change in the environment and also there in reaction to changes in the environment, the material or system produce electric or magnetic signals or undergo strain which actually describe the environment

* Corresponding author.
E-mail address: nidhi.jain@bharatividyapeeth.edu (N. Jain).

https://doi.org/10.1016/j.matpr.2023.03.226
2214-7853/© 2023 Elsevier Ltd. All rights reserved.
Selection and peer-review under responsibility of the International Conference on Future Trends in Materials and Mechanical Engineering.

Please cite this article as: N. Jain, S. Nandu Ovhal, V. Patil et al., Smart materials – A state-of-the-art-review, Materials Today: Proceedings, https://doi.org/10.1016/j.matpr.2023.03.226

3. Self-adaptive material or system could modify its geometry adapt to the environment

Smart materials working is similar to human and it is depicted in Fig. 2. As human gets information from the environment in the same way smart materials obtain acquire information from the environment through sensing and produces chemical or physical effect for decision making control by brain. And in the last implement actions through the movable structure or tentacles attached to it (Fig. 1).

2. Aerogel

This paper focuses on aerogel which contains different types of aerogels, preparation conditions-construction, characterization of aerogels and physical properties of hydrophobic silica aerogel. The data describes utilization of aerogel as insulation materials. Aerogel is manufactured porous ultra-light material obtained from gel in which liquid form gel is exchanged with a gas. It gives very low density and low thermal conductivity to Aerogel. Sol-gel is a common method of preparation. The melting point of aerogel is 1200 °C and thermal conductivity is almost zero. It contains 99.8% air, so it is the smallest density solid material. Aerogel has ultimately unlimited potential, believing that they have many applications in human life. Using aerogel as insulating material is the best choice because it completely blocks the heat transfer by convection, radiation and conduction. This is due to air does not circulate in its structure. If we use carbon-based gel, then it offers high resistance to radiation transfer. Therefore, silica aerogel with carbon as nanostructure material is mostly used for thermal insulation. Due to its high price makes it less usable. But in future aerogel will become one of the most preferable and attractive smart material [1,2].

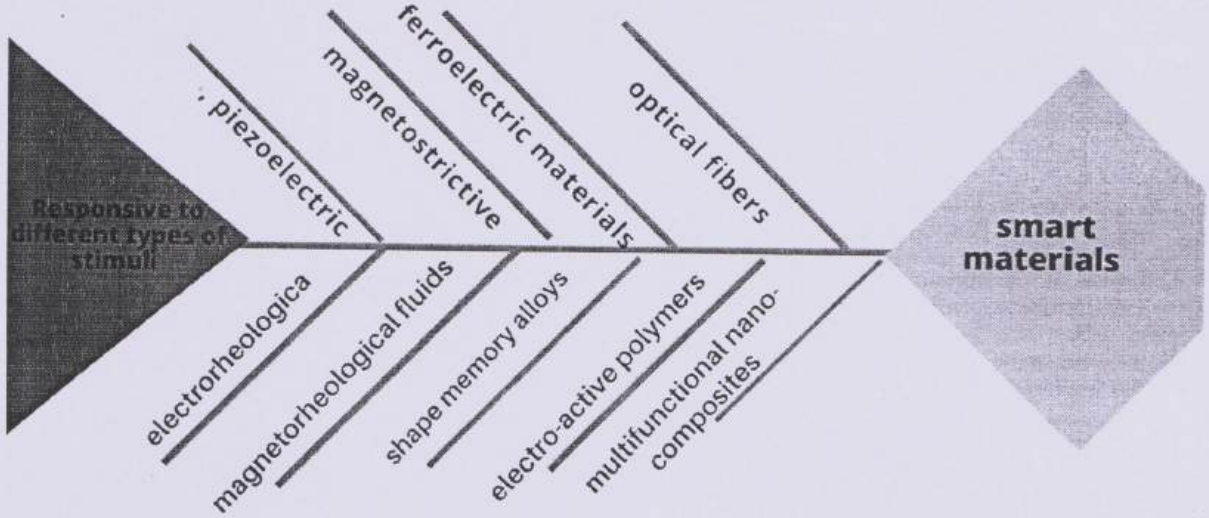
2.1. Aerogel as a material

Aerogel is a large concept which shows a group of materials that have been used in space travel from 1960s, but now a days it is used in wide range of industry [3]. Recently Eychmuler [4] defines: "Aerogel is a solid having meso- and micropores having diameter in few hundred nanometers and porosity is greater than 95% with gas dispersed phase." The special form of highly porous material having very low density (0.003–0.15 kg\m^3), low thermal conductivity, large surface areas (500–1000 m^2\g) and excellent transparency is known as aerogel (Silica aerogel) which can be obtained by exchanging liquid form gel with air. It is made up of nanosized particle which interconnect to form tridimensional network [4,5].

Due to its different properties, Aerogels are use in different industries. In building construction aerogel is used as thermal and acoustic material. It also used in large range of other domain such as, absorbents, nuclear waste storage, batteries and catalyst, etc. [6].

2.2. Aerogel preparation methods

Aerogel is prepared by two main technological strategies: super critical drying and subcritical drying technology, result in bulk



Ilustration of different types of smart materials

Fig. 1. The illustration of different types of smart materials.

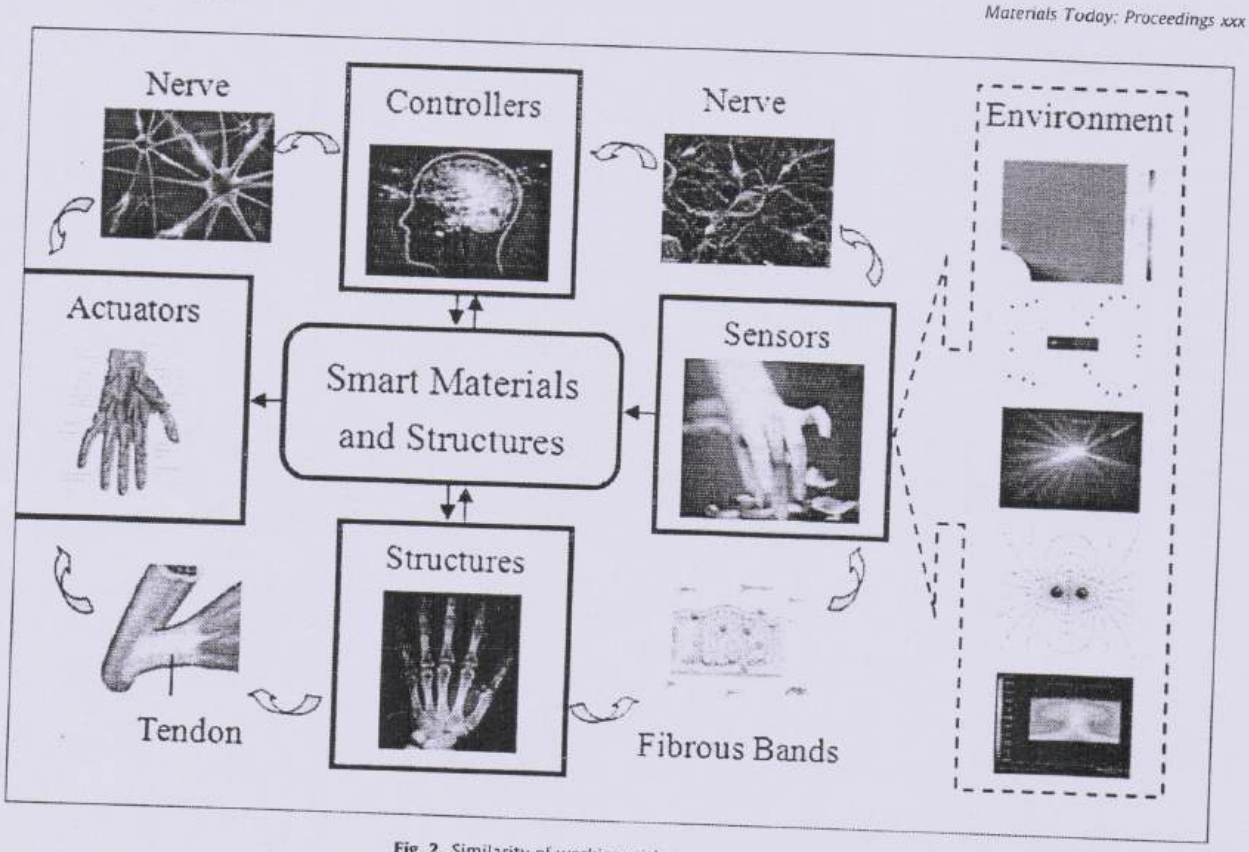


Fig. 2. Similarity of working with smart materials[8].

aerogels. Aerogels power or granules depends on preparation criteria [7].

2.3. Classification of aerogels

Aerogels are classified into five types such as silica, metal oxide organic, hybrid, carbon and composite aerogels [8]. Out of these all silica aerogel is the most useful and extensively investigated type.

2.3.1. Silica aerogels

Kistler, invented first time silica aerogel in 1931 which were made from inorganic precursors and containing SiO_2 chain with cross linked internal structure and large number of air porous [9].

Silica aerogels have wide range of applications in civil infrastructure field, with heat insulation of building, especially in those areas where optical transparency or translucency are necessary [9] and also used in solar collector and insulated building render as translucent heat insulator [10]. For increasing insulating properties silica aerogel can be used in combination with other material. E.g. foam concrete reinforced SiO_2 aerogel (FC-SA) material thus, the thermal conductivity of FC-SA measured low [11].

2.3.2. Metal oxide aerogels

The aerogels which are produce from oxides of transition metals such as aluminium oxide (Al_2O_3), titanium oxide (TiO_2), vanadium oxide (V_2O_5), chromium oxid (Cr_2O_3), iron oxide (Fe_2O_3) are known as metal oxide aerogels.

Metal oxide aerogels are mostly used for preparation of carbon nanotubes (CNT), as magnetic nanostructures, as energetic materials [12].

2.3.3. Organic and carbon aerogels

Monomeric or polymeric precursors e.g. melamine–formaldehyde, phenol-furfural cresol-formaldehyde, phenol melamine, etc. are used for preparation of organic aerogels. These aerogels are used for thermal and acoustic insulators, membrane for gas separation, catalyst support [13].

Carbon aerogels amorphous carbon material which are derivative of organic aerogels for this temperature should above 600 °C.-carbon aerogels are mainly used for electricity conduction.also used as thermal acoustic insulators, adsorbent and media for capacitive deionization and catalyst supports[14].

2.3.4. Hybrid and composite aerogel

To improve mechanical and physical properties such as thoughness, strength, and thermal conductivity of aerogel hybrid aerogel can be prepare. These aerogels are mostly prepared and contains organic and inorganic phases and nanoparticals in gel matrix [15].

2.4. Applications of aerogels

Building applications of aerogels: Aerogels have outstanding properties, like low thermal conductivity light weight and sound proof so, it can be used for variety of purpose. However, the cost of aerogel materials is high for many industries. So, the researcher continue to improve performance and reduce the cost of aerogel material. Granular aerogels highly used for commercial purpose, even it has low performance, because it is easy to produce cheaper Aerogel are mostly used for insulation purpose due their properties [16,17].

2.4.1. Aerogel applications in roofs, facades and windows

Now as we see aerogel applications in building which are widely used for daylighting goals. Kalwall company who offers highly insulated light transmitting product is one of the best example of high performance translucent building system. Thus, Fig. 4 shows aerogel use for rapid insulation from the outside skylight (Fig. 3a). Shows another application which is aerogel insulation

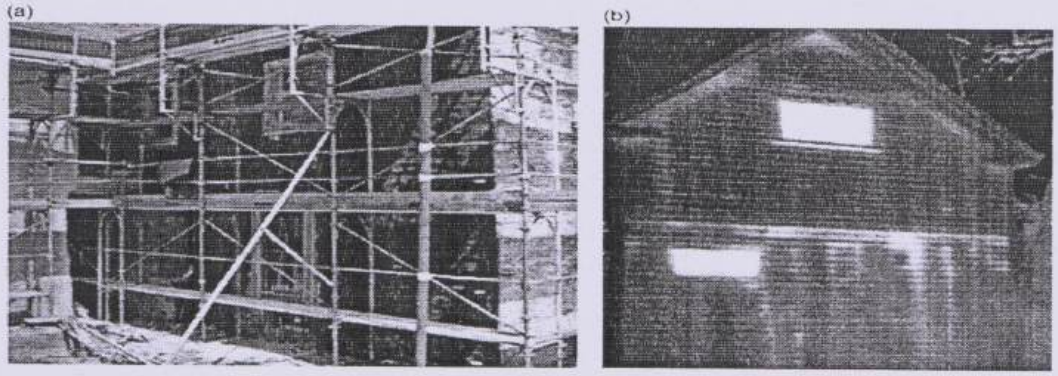


Fig. 3. a: Retrofitting of an old brick dwelling with Aspen aerogel insulation; b: Thermographic image of the building [56].

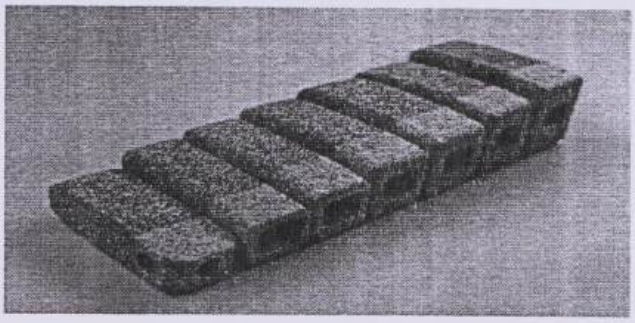


Fig. 4. Titanium foam implants for inter body fusion of the lumbar spine [50].

of an old brick building. In this thin layer of aerogel at the top floor use for insulation and not ground floor. The amount of heat loss from ground floor towards the top floor can be observed in thermographic image with thermal camera (Fig. 3b).

2.4.2. Aerogel application for sound insulation, fire delay and air purification

When aerogel is used as insulation plates their performance can be positively influenced by using the right binding material as it depends on the binder. The acoustic properties of cylindrical silica aerogel are invested by 'Gibiat et al.'. The sound velocity, for low ultrasonic frequencies, and the acoustical impedance in audible range is measured by them. Which founds, the low-density aerogel can show unexpected attenuation for frequency.i.e. It mostly depends on the geometry of the sample. Due to the chemical structure and their high melting point (12000C), aerogel can be used as non-flammable materials. To avoid spreading fire from one place to another aerogel is used inside the building [18].

2.5. Future research

For the future, there is mainly work on reducing the manufacturing cost if aerogel, development of aerogel as thermal insulation, Increasing use of aerogel as conventional materials [19]. Even the high cost of aerogel, they can be seen in a wide range of industries like textile industry [20], also it is used seen as thermal insulation for space launch application. If we reduced the cost, the usage of aerogel can be enhanced in our daily life in various forms.

This paper gives a brief overview of aerogel as a smart material with insulation material in civil domain, which considers both economic and technical performance of aerogel. This also focuses on application of aerogel in building construction such as roof, facades and windows, for sound insulation fire retardation, air purification and also the advantages of aerogel in electronic industries The aerogel is called as smart materials because of exceptional properties of aerogel and widespread applications in many industries [21].

3. Titanium foams

Titanium Foam is low density permeable material with plentiful applications. The describing characteristic of these foams is a very high porosity, typically 75–95% of the volume consisting of void spaces.

3.1. Mechanical properties of titanium foams

The space holder method is used to create open-pore titanium foams. The mechanical characteristics of titanium foams with porosities ranging from 50 to 80 percent are investigated. The tensile strength and yield strength of the foams are discovered to span the property range between chancellors and cortex bone. The dissected foams are anisotropic because of the utilization of nonspherical space holder particles which rework during the powder blend's compaction. The significance of biologic implant fixation was recognized more than 30 years ago. Many different types of porous coatings have been created and are now widely used in clinical settings to enhance bone apposition. In any case, the utilization of a permeable covering doesn't tackle the issue of mechanical befuddle between an embedded one and the bone. The generally utilized embed materials are a lot stiffer than the bone and may lead to a pressure protecting and nearby restoration of the bone. This impact can be kept away from by utilizing a material with bone-like solidness.

A recent review paper describes the manufacturing processes of porous metals for usage in biomedical application. During the previous decade, two forms of metallic foams have been developed as implant materials: tantalum foam which is created by thermal evaporation of tantalum onto an amorphous carbon skeleton, and nitinol foam [22], which is formed by combustion synthesis of a combination of titanium and nickel powder. These handling courses incorporate dispersion holding of agglomerated wires [23] solid state frothing by super plastic expansion [24] powder metallurgy utilizing space holders [25–28], dunking of removable polymer froth into a thyrotrophic slurry [29], foaming of a polymer cover stacked with titanium particles, and directional hardening of fluid titanium with dissolved gas [30]. The titanium foam seen here was created utilizing the powder metallurgical method and a space holding material [25–31]. The titanium foam's biological activity has been studied in vitro using human osteoblasts [31] and in vivo by implanting cylinders into the femurs of dogs [32]. Titanium foam is utilized in a first application as an intern body com-

bination gadget for the human lumbar spine (Fig. 4) where the incredible natural obsession properties of this material can be completely misused.

3.2. Macroscopic deformation band

As can be found in Fig. 6, titanium foams experienced diverse twisting modes up to the break point. Every prevailing twisting mode in each stage changes the state of foams on the large scale and micro scale, either forever or briefly. It is realized that twisting in cell edges of the froth in the direct versatile district is the prevailing component in open permeable constructions, and it doesn't change the example's shape for all time. The struts in the current study's produced foams had an hour-glass form (Fig. 5), thus material was concentrated at cell nodes and the thickness of the cell walls and edges was found to decrease from the cell node to the centre.

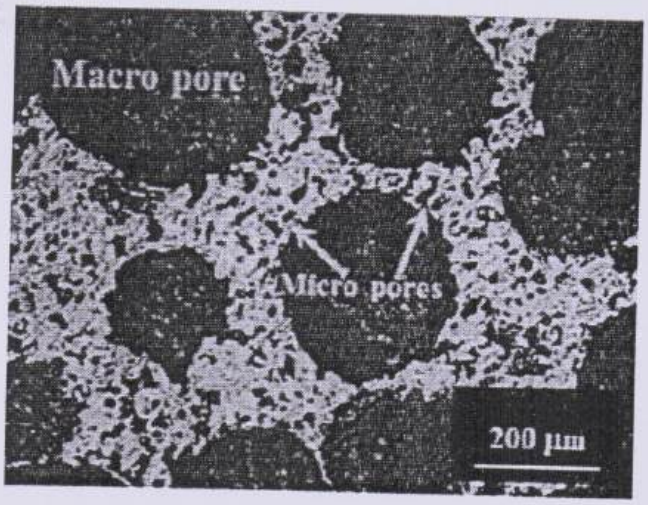


Fig. 5. Polished cross-sectional light microscope images of Ti foam with 55.9% porosity showing macro pores formed from Mg evaporation and micro porous cell walls [49].

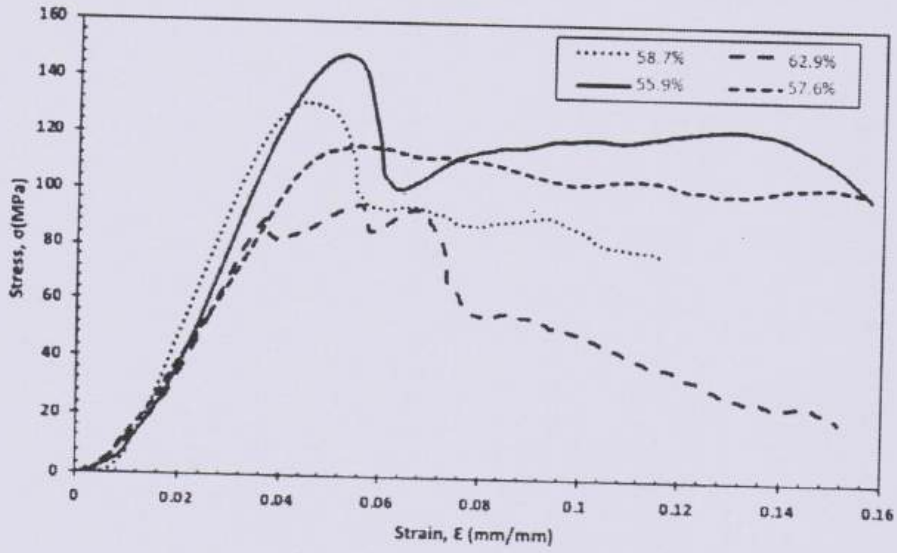
Furthermore, the struts were not completely dense and included micro pores left over from incomplete sintering. The lowest solid cross-sectional area, i.e., the region normal to the stress, is considered to dominate in the transmission of stress in minimum solid area (MSA) models. Mechanical models created for various foam constructions are simply customized MSA models at the moment. Properties and measurements of the struts or networks between the pores and the sintering level of the cell dividers assume a significant part in the mechanical properties since versatile and plastic disfigurement limits at those focuses.

Following the end of the linear elastic area in the current research, deformation bands perpendicular to the loading direction formed, resulting in plastic collapse of certain cells. This impact was accompanied by a rapid reduction in flow stress near the start of the plateau zone (Fig. 6).

3.3. Elasticity VS porosity curve

The modulus of elasticity of the titanium bunch tests with various porosity substance are introduced in Fig. 7. In the current examination, the versatile module were acquired from the inclines of the straight versatile areas subsequent to deducting the testing machine firmness. Thus, the modulus of elasticity for the first group of samples (55.9–62.9% porosity) were 3.1–4.5 GPA, 2.6–2.8 GPA for the second group of samples (65.6–69.9% porosity), and 1.2–1.65 GPA for the third group of samples (74.0–78.0% porosity). With decreasing porosity, the elastic modulus normally improved, with a maximum elastic modulus of 4 [34].

Similar to the change in elastic modulus VS porosity, the compressive strength (peak stress measured after the elastic zone) decreased with increasing porosity. However, the strength reduction above 60% porosity was very abrupt (Fig. 8). Albeit the examples in the principal bunch (55.9–62.9% porosity) had compressive qualities in the scope of cortical bone strength (100–230 MPA those in the third gathering (74.0–78.0% porosity) had qualities near that of cancellous bone 2–12 MPA [35]. In the meantime, the examples in the subsequent gathering (65.6–69.9%) showed compressive qualities between those of cortical and cancellous bone. It is obvious that by varying the porosity content, the



(a)

Fig 6. Compressive stress VS strain curve [49].

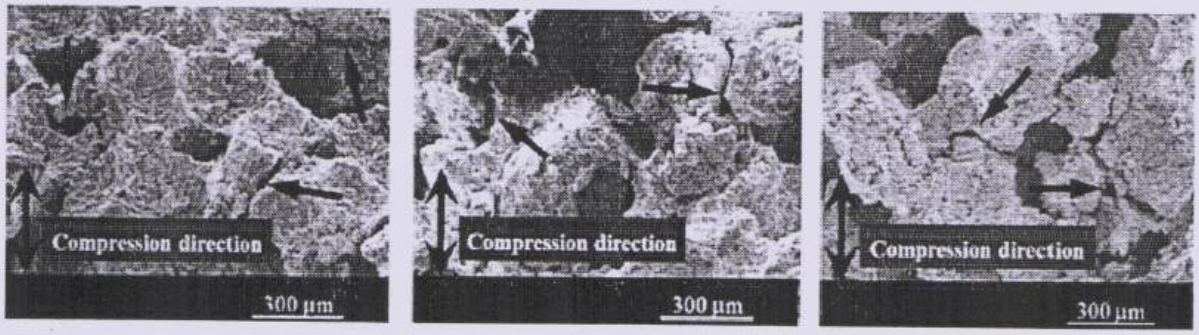


Fig. 7. Images of compressed porous Ti samples with different porosities at ×100 [49].

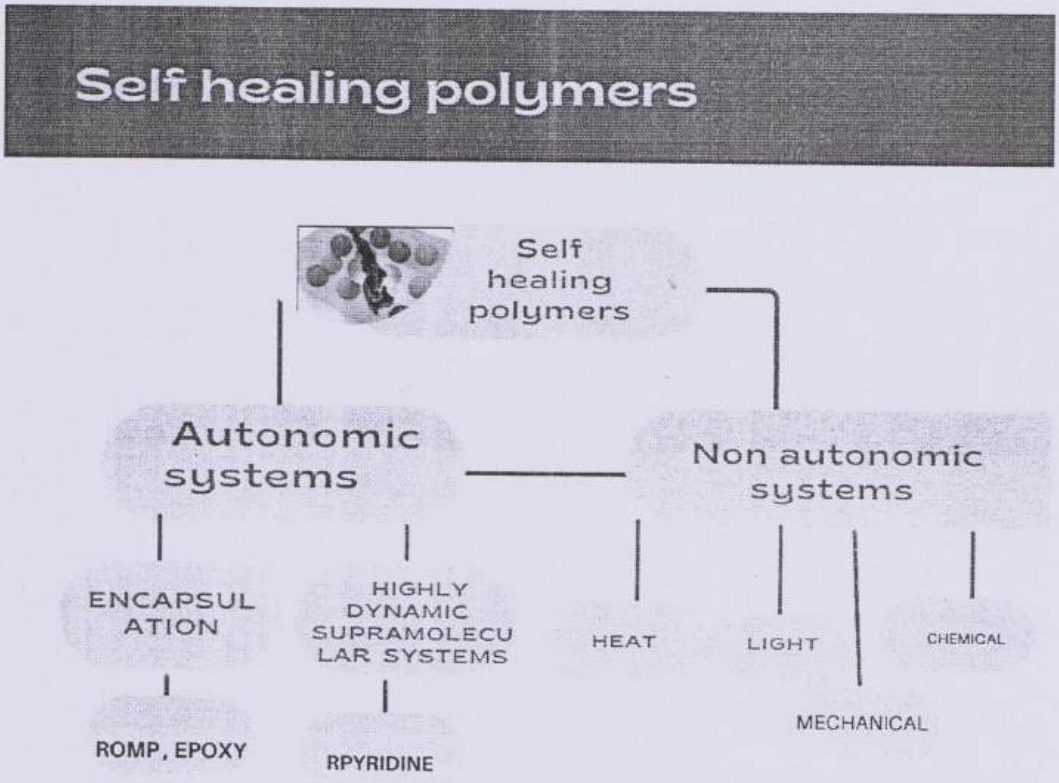


Fig. 8. a: Classification of materials on their self-healing polymers. b: Advantages of self-healing polymers.

mechanical characteristics of foams may be tuned to make them functionally more consistent with human bone [35].

The currently available bulk implant materials are stiffer than human bone, and hence fail to transmit the necessary amount of stress to the surrounding bone. Due to the restoration of the bone around the implant, this deficiency causes implant loosening. As a result, the development of implant materials with optimal combinations of compressive strength and low elastic modulus is required to minimize implant loosening, extend implant service life, and avoid surgical readjustment [32]. The modulus of elasticity human cortex is in the scope of 7–30 GPA, while that of human cancellous bone is under 5 GPA [35], and the compressive strength of human bone reaches from 2 to 230 MPA [35] The KIC (plane strain tensile strength) indices of cancellous and cortex bone have been reported to be 1.5 $MN/m^{3/2}$ and 3.5 $MN/m^{3/2}$, accordingly. As a result, the porosity composition, pore shape, and cell wall composition of the foams, as well as the intrinsic material characteristics of cell walls (i.e., purity), should be properly regulated in order to achieve tensile strength values near to the bone [35].

In the current examination, the space holder powder metallurgy method was utilized in blend with an Mg powder space holder to create biomimetic Ti frameworks with chose porosities (60%, 70%, and 80%). Each permeable framework showed a huge level of pore interconnectivity, which is positive for osseo integration and in-development of bone tissue. A porosity study also revealed that a suitable pore size range for facilitating osseo integration was obtained, as stated in earlier research Furthermore, the compressive strengths of the first group (55.9–62.9 percent porosity) and



(b).

Fig. 8 (*continued*)

the third group (74.0–78.0% porosity) samples were comparable to those of the human cortex and cancellous bone. Furthermore, all of the foam materials had modulus of elasticity comparable to cancellous bone [33,34].

4. Self-healing materials

Polymers have been used in our day-to-day life due to their various properties like light weight, availability,flexibility, light weight, tailoring, etc. Some materials have numerous importances in various fields such biomedical, environment etc. such as carbon nanotubes etc. There is low mechanical strength in them as compared to various materials. Research has shown that incorporation of nanomaterials significantly affects different properties of polymers including mechanical/physical properties in composite materials combination of polymer and nano-materials results in product which have excellent properties [51–55].

In the recent years many kinds of self- healing polymers are discovered Self- healing polymers are type of materials which can repair themselves when they are destructed. These materials do not need any manual interaction. The paper presents study of self-healing polymer and healing agents. It will also give information on various chemical processes employed while preparation of self-healing polymer and its advantages and disadvantages [36].

Synthetic self-healing polymers are new type of materials with have ability to self-heal itself just as self-healing quality that is observed in humans and many living organisms [37,38]. It is a required property for a sustaining life; it increases the lifetime of most living organisms [39-41]. Like many of the natural materials, research in synthetic self-healing polymer points on preparation of multifunctional materials that are able to recover their self fundamental properties like conductivity, corrosion resistance, conductivity, etc. after damage has been caused [42,43].

On the basis chemistry of self-healing polymer current we can categorize these materials into two classes [44].

(1) Autonomic self-healing materials
(2) Non autonomic self-healing materials

Autonomic self-healing materials are materials in which harnessed potential is released automatically and initiates repair to damaged part. It is exactly opposite in the case of non-autonomic healing materials [44].

Most among self-healing materials the polymer nano composites have superior characteristics like strength, cost, thermal stability, and low weight. These polymers are components in many applications to improve its durability and many other aspects. But here are some drawbacks where these materials lack macroscopic damage like very small cracks, surface stretches, etc. Presently the fields of self-healing polymer, nanocomposites, are rapidly emerging and new theories are being discovered [45].

4.1. Classification of self-healing materials: Extrinsic and Intrinsic:

Based on healing mechanism, these materials can be divided into two types namely intrinsic and extrinsic self- healing polymers. Extrinsic healing materials depend on external healing agent in the form of capsules or vascular networks [46]. The methods are most commonly used to prepare such materials (1) Microencapsulation and (2) Micro vascular network. The microencapsulation

Table 1
Comparison table describing key findings and other parameters of the three of the smart materials.

Parameters	Aerogel	Self-healing polymers	Titanium foams
Key findings	With large fraction of air (typically greater than 90%)embedded inside aerogel are self supported 3D dimensional networks structure [61]	Smart self-healing polymers have acknowledged much interest in few years, because of their ability to heal damaged material and at the same time retaining their original physico-chemical and mechanical properties [63]	Titanium Foam is low density permeable material with plentiful applications. The describing characteristic of these foams is a very high porosity, typically 75–95% of the volume consisting of void [68] spaces [60]
Smart materials	They are considered as magical materials because of enormously low densities and the ability of retaining nanoscale properties at the macroscale [61].	Self-healing polymers are a different class of smart materials which the capability to repair themselves without manual intervention of any kind [64].	The high strength, low weight ratio and outstanding corrosion resistance which are natural in titanium and its alloys [11]
Exceptional properties	They are having exceptional properties and called as the lightest solid porous material in the world, having three- dimensional (3D) network structure, extraordinary specific surface area, tremendously low density, and thermal conductivity [62].	The materials through different polymerization reactions and with exceptional mechanical, physical, rheological, thermal property are very nuch in demand [65,66].	Due to their high specific strength and exceptional corrosion resistance, titanium alloys have been widely used in engineering, namely in the aerospatiale, automotive and biomedical fields [69]
Polymers materials	The originator of aerogel are among organic polymers inorganic materials and polymeric hybrid materials [62].	Self-healing polymers have the capability to deal with any damage efficiently [65,66].	–
Prospect for its application	They are used in the fields of aerospace, chemical engineering, construction, electrical equipment, water purification, and biomedicine [62]	The self-healing polymers are multipurpose applications in space, biomedical, construction, automobiles, etc. [67]	Applications demanding high levels of reliable performance in surgery and medicine as well as in aerospace, automotive, and in major industries. These applications less cost-effective materials [70].

process has major drawbacks such as high cost of catalyst and the process occurs only once. So, to overcome the drawback many other ways are being found.

Intrinsic self-healing materials works on non-covalent chemistries or dynamic covalent chemistries [47]. The non-covalent chemistry approach uses π-π stacking, ligand– metal bonding, hydrogen bonding, or host–guest interaction stacking among other techniques. The reformation of chemical bonds in intrinsic materials is triggered by external stimuli including pH change, light, temperature, etc. Diels-Alder (DA) reactions are most frequently used to create self-healing polymers that utilize reversible bond formation [48] (Table 1).

5. Conclusion

Three of the Smart materials mentioned in the paper have multiple use and have potential to improve prevailing technology and enhance new functionality of the product in various fields like. aerospace, chemical engineering, construction, electrical equipment, water purification, and biomedicine First smart material Titanium foams due to the biological properties of the oxide underside [57] and the propensity to minimize the intrinsic elasticity and ductility to even more accurately reflect those demonstrated via skeletal remains. Titanium foams have an established track record for musculoskeletal biomedical implants also including spinal fusion. However, these foams' structure (such as pore interconnectivity) and multiphase flow characteristics are frequently poorly characterized, which may result in super performance. Researchers across several areas are focusing more on porous metals in general [59,60]. There is a chance of greatly broadening the application potential of porous Ti by tying recent advancements in foam properties characterization [58] to the enhancement of conventional, or new, Ti foam production pathways.

Crack formation in the synthesized nanocomposites is among very critical problems, comparable to that seen in polymer and polymer composite systems To resolve these problems, second smart materials both theoretical and experimental studies on self-healing of these polymer nanocomposites have been undertaken. In fact, the self- healing of polymer nanocomposites has remained largely unexplored, and it should provide new opportunities for development of high-performance multifunctional materials. In the following section, we will discuss the different theoretical and experimental aspects of self-healing of polymer nanocomposites.

Third the aerogel is recognised as a form of matter due to its distinctive properties and varied chemical composition. Aerogel research has had three major upsurges; the first two were sparked by a small number of recognizable technologies, whereas the third was inspired by a large number of novel technologies as we entered the twenty-first century. The study of aerogels is now advancing and growing. To ensure that this state of matter has a bright future, it is hoped that more and more researchers will concentrate on the creation of unique single-component aerogels, composite aerogel material design, and industrial application.

Three of the Smart materials help us to make our world a better place for living and these three are magical materials which enables us to adapt to dynamic changes by activating its functions.

Data availability

No data was used for the research described in the article.

Declaration of Competing Interest

The authors declare that they have no known competing financial interests or personal relationships that could have appeared to influence the work reported in this paper.

References

[1] N. Danchova, D. Paskalev, S. Gutzov, Bul. Chem. Commun. 50 (2018) 172–177.
[2] L. Melita, C. Croitoru, E3S Web of Conferences 111 (2019) 60–69.
[3] Y.J. Song, W.L. Wei, X.G. Qu, Adv. Mater. 23 (2011) 4215–4236.
[4] C. Ziegler et al., Angew. Chem. Int. Ed. 56 (43) (2017) 13200–13221.
[5] M. Antonietti, N. Fechler, T.-P. Fellinger, Chem. Mater. 26 (2013) 196–210.
[6] R. Baetens, B.P. Jelle, A. Gustavsen, Energ. Buildings 43 (4) (2011) 761–769.
[7] J. Sun, Q. Guan, Y. Liu, J. Leng, J. Intell. Mater. Syst. Struct. 6 (2016) 1–24.
[8] M. Karaaslan, J.F. Kadla, F. Ko, Lignin Based Aerogels (2016) 67–93.

[9] E. Cuce et al., Renew. Sustain. Energy Rev. 34 (2014) 273–299.
[10] M.J. Hanus, A.T. Harris, Prog. Mater Sci. 58 (7) (2013) 1056–1102.
[11] S. Liu et al., Energ. Buildings 177 (2018) 385–393.
[12] M.A. Aegerter, N. Leventis, M.M. Koebel, Aerogel Handbook ed. A.i. Sol-Gel and D.M.A. Technologies. 2011, New York: Springer New York.
[13] M. Karaaslan, J.F. Kadla, F. Ko, Lignin Based Aerogels (2016) 67–93.
[14] J. Biener et al., Energ. Environ. Sci. 4 (3) (2011) 656–667.
[15] Y. Liao et al., J. Sol- Gel Sci. Technol. 63 (3) (2012) 445–456.
[16] M. Dowson et al., Energ. Buildings 49 (2012) 173–187.
[17] J. Wernery et al., Energy Procedia 134 (2017) 490–498.
[18] T. Gao, B.P. Jelle, A. Gustavsen, Procedia Eng. 145 (2016) 723–728.
[19] S.B. Riffat, G. Qiu, Int. J. Low-Carbon Technol. 8 (1) (2012) 1–6.
[20] Y. Du, H.-E. Kim, Daily Clothing 21 (2019) 96–103.
[21] E. Lucchi et al., Build. Environ. 122 (2017) 258–268.
[22] K. Hoshijima, R.W. Nightingale, J.R. Yu, W.J. Richardson, K.D. Harper, H. Yamamoto, B.S. Myers, Spine 22 (1997) 1181–1188.
[23] N.G. Davis, J. Teisen, C. Schuh, D.C. Dunand, J. Mater. Res. 16 (2001) 1508–1519.
[24] M. Bram, C. Stiller, H.P. Buchkremer, D. Stoer, H. Baur, Adv. Eng. Mater. 2 (2000) 196–199.
[25] A. Laptev, M. Bram, H.P. Buchkremer, D. Stover, Powder Metal 47 (2004) 85–92.
[26] A. Laptev, O. Vyal, M. Bram, H.P. Buchkremer, D. Stover, 48 (2005) 358–364.
[27] C.E. Wen, Y. Yamada, K. Shimojima, H. Hosokawa, M. Mabuchi, J. Mater. Res. 17 (2002) 2633–2639.
[28] J.P. Li, de Groot K. Porous titanium with reticulate structure for orthopaedic implant, in: Lutjering G, Albrecht J, editors. Proceedings of 10th World Conference on Titanium. Weinheim: Wiley-VCH Verlag, 2003. Pp. 3157–3164.
[29] J.-P. St-Pierre, M. Gauthier, L.-P. Lefebvre, M. Tabrizian, Biomaterials 26 (2005) 7319–7328.
[30] H. Nakajima, T. Ikeda, S.K. Hyun, Fabrication of lotus-type porous metals and physical properties, in: J. Banhart, N.A. Fleck, A. Mortensen (Eds.), International Conference on Cellular Metals and Metal Foaming Technology, MIT-Verlag, Berlin, 2003, pp. 191–202.
[31] T. Matsushita, S. Fujibayashi, T. Kokubo, Modif. Charact. Prop 17 (2016) 111–130.
[32] X. Jian, C. Hao, G. Qiu, Y. Yang, X. Lyu, Mater. Des. 88 (2015) 132–137.
[33] S. Ahmad, A. Kassim, Fabrication of titanium foam by using compaction method, in: Proceedings of the 26th Regional Conference on Solid State Science & Technology 2011, Negeri Sembilan, Malaysia, 22–24 November2011.
[34] T. Kokubo, H.-M. Kim, M. Kawashita, Biomater 24 (2003) 2161–2175.
[35] S. Kashef, A. Asgari, T.B. Hilditch, W. Yan, V.K. Goel, P.D. Hodgson, Mater. Sci. Eng. A 527 (2010) 7689–7693.
[36] M. Ghidelli, M. Sebastiani, K.E. Johannas, G.M. Pharr, J. Am. Ceram. Soc. 100 (2017) 5731–5738.
[37] J.K. Pandey, H. Takagi, Int. J.Mod. Phys. B 25 (2011) 4216–4219, https://doi.org/10.1142/S0217979211066611.
[38] S.K. Ghosh, Self-Healing Materials: Fundamentals, Design Strategies, and Applications, in: Ghosh SK, editor. Self-Heal. Mater., Wiley-VCH Verlag GmbH & Co. KGaA; 2008, pp 1– 28.
[39] S.J. Kalista, in: Ghosh SK, editor. Self-Heal. Mater., Wiley-VCH Verlag GmbH & Co. KGaA; 2008, pp. 73–100.
[40] Y.C. Yuan, T. Yin, M.Z. Rong, M.Q. Zhang, ExpressPolym Lett. 2 (2008) 238–250.
[41] Y. Chen, A.M. Kushner, G.A. Williams, Z. Guan, Nat. Chem. 4 (2012) 467–472, https://doi.org/10.1038/nchem.1314.
[42] S. Billiet, X.K.D. Hillewaere, R.F.A. Teixeira, F.E. Du Prez, Macromol. Rapid Commun. 34 (2013) 290–309.
[43] S.D. Bergman, F. Wudl, J. Mater. Chem. 18 (2008) 41–62, https://doi.org/10.1039/B713953P.
[44] K.A. Williams, D.R. Dreyer, C.W. Bielawski, MRS Bull. 33 (2008) 759–765, https://doi.org/10.1557/mrs2008.162.
[45] A.C. Balazs, T. Emrick, T.P. Russell, Science 314 (2006) 1107–1110, https://doi.org/10.1126/science.1130557.
[46] S.C. Olugebefola, A.R. Hamilton, D.J. Fairfield, N.R. Sottos, Soft Matter 10 (2014) 544–548.
[47] Y. Bai, Y. Chen, Q. Wang, T. Wang, J. Mater. Chem. A 2 (2014) 9169–9177, https://doi.org/10.1039/c4ta00856a.
[48] S. van der Zwaag, Springer, Dordrecht, The Netherlands, 2007, pp. 2–9.
[49] C. Oktay, E. Ziya, Y. Bora, Substitute Mater. Met. 9 (2019) 340, https://doi.org/10.5390/met9030340.
[50] T. Imwinkel Ried, J. Biomed. Mater. Res. Part A 24 (2007) 964–970.
[51] N Jain, T. Seema, Mater. Today Proc. 2021 (in press). DOI: 10.1016/j.matpr.2021.01.895.
[52] N. Jain, N.J. Kanu, Mater. Today: Proc. 43 (2021) 2998–3005.
[53] N. Jain, E. Gupta, N.J. Kanu, Smart Sci. 10 (2021) 1–24, https://doi.org/10.1080/23080477.2021.1940752.
[54] N. Jain, R. Yevatikar, T.S. Raxamwar, Mater. Today Proc. 60 (2) (2022) 859–867.
[55] S. Tiwari, N. Jain, A. Agarwal, Int. J. Innov. Technol. Explor. Eng. 9 (2020) 6.
[56] B.P. Jelle, Aerogel Insulation for Building Applications, in The Sol- Gel Handbook.
[57] Y.T. Sul, C. Johansson, E. Byon, T. Albrektsson, Biomaterials 26 (2005) 6720–6730.
[58] R. Singh, P.D. Lee, T.C. Lindley, R.J. Dashwood, E. Ferrie, T. Imwinkelried, Acta Biomater. 5 (1) (2009) 477–487.
[59] J. Banhart, D. Weaire, Phys. Today 55 (7) (2002) 37–42.
[60] L.P. Lefebvre, J. Banhart, D.C. Dunand, Adv. Eng. Mater. 10 (9) (2008) 775–787.
[61] S.S. Kistler, Nature 127 (1931) 741.
[62] P.C. Je, M.T. Sultan, C.P. Selvan, S. Irulappasamy, F. Mustapha, A.A. Basri, S.N. Safri, J. Mater. Res. Technol. 9 (2020) 7370.
[63] N.N.F. Nik Md Noordin Kahar, A.F. Osman, E. Alosime, N. Arsat, N.A.M. Azman, A. Syamsir, Z. Itam, Z.A.A. Hamid, Polymer 13 (2021) 1194.
[64] E. Buslov, I. Komarov, V. Selivanov, V. Titov, N. Tovarnova, V. Feldstein, Acta Astronaut. 54 (2019) 163.
[65] I. Perrigon, A.M. Grande, Acta Astronaut. 177 (2020) 697.
[66] M.W. Lee, Polymer 12 (2020) 379.
[67] G. Megha, N.A. Satya, B. Nitu, J. Appl. Polym. Sci. 139 (2022) 52816.
[68] J.C. Li, D.C. Dunand, Acta Mater. (2011) 146–158.
[69] E.D. Spoerke et al., J. Biomed. Mater. Res. A 84A (2) (2008) 402–412.
[70] D.C. Dunand, Adv. Eng. Mater. 6 (6) (2004) 369–376.

Source details

Feedback > Compare sources >

Materials Today: Proceedings

Scopus coverage years: 2005, from 2014 to Present

E-ISSN: 2214-7853

Subject area: Materials Science: General Materials Science

Source type: Conference Proceeding

Save to source list Source Homepage

CiteScore 2022
3.2

SJR 2022
0.445

SNIP 2022
0.774

CiteScore CiteScore rank & trend Scopus content coverage

Improved CiteScore methodology

CiteScore 2022 counts the citations received in 2019-2022 to articles, reviews, conference papers, book chapters and data papers published in 2019-2022, and divides this by the number of publications published in 2019-2022. Learn more >

CiteScore 2022

3.2 = 80,455 Citations 2019 - 2022
24,871 Documents 2019 - 2022

Calculated on 05 May, 2023

CiteScoreTracker 2023

4.6 = 100,759 Citations to date
21,738 Documents to date

Last updated on 05 December, 2023 • Updated monthly

CiteScore rank 2022

Category	Rank	Percentile
Materials Science General Materials Science	#259/453	42nd

View CiteScore methodology > CiteScore FAQ > Add CiteScore to your site

THE SINGLE INJECTION CURRENT FLOW AN INSULATOR CONTAINING DISTRIBUTED DEEPTRAPS AROUND AN ENERGY OPERATING UNDER HIGH FIELD REGIME

DR.SHIKHABHARDWAJ SHRIVAS,DR. UDAY PATKAR,DR.UDAY PATIL,PROF.GAURI RAO, PROF. NETRA S PATIL, PROF.SNEHAL CHAUDHARY, PROF. SAMPAT P. MEDHANE
Bharati Vidyapeeth's College of Engineering,Lavale, Pune,
Bharati Vidyapeeth (Deemed to be University) College of Engineering, Pune

Abstract

The single injection current problems are studied widely from several decades.The modern concepts of energy band theory of solids are applied for such studies.The magnitude of current flow in insulator is drastically affected by the presence of distributed trapping states energetically located in the forbidden gap of the insulator. The injected current carriers are captured by the distributed trapping states for a trapping time which reduces the magnitude of the current flow significantly At low lower .The trapping of the free carriers by empty trapping states in insulator provides few additional transition regimes caused by the physical parameters characterizing the distributed trapping states. These transition regimes are not present in insulator in the insulator in the absence of trapping state .The high field mobility relationship is considered for the single injection current flow in insulator. In single crystals, the high field effects are observed at sufficiently high field strengths which give field dependent carrier mobility. The distribution of trapping states inside the insulator is observed in different forms of the trapping states in energy. The high field effects in single injection devices are obtained under high field conditions. Which give the fluctuations in the carrier velocity of electrons present in the conduction band of the insulator.

Keywords: Salami method, space charge limited, distributed trapping states, regional approximation, salami method, current voltage characteristics.

DOI Number: 10.14704/NQ.2022.20.16.NQ88028 NeuroQuantology2022;20(16):242-247

Introduction

The current injection technique is used for the studies of high field transport properties and thermal noise behavior of the insulating material. The results obtained in the regional approximation scheme are applied for the studies of thermal noise in the full variation of the applied voltage across the insulator .The salami method is applied for the thermal noise calculations in the complete range of injection levels of currents. The thermal noise is the main source of the noise in the injection devices and the present study gives the physical parameters to minimize the thermal noise. The different

thermal noise regimes are observed in the full span variation of the applied voltage across the insulator.

General Equations

Let us consider an insulator containing, the sufficient amount of distributed deep traps around a single energy level E_t.The general equations governing the current flow, poission's law and high field mobility relationship of the insulator with distributed deep traps are given by.

$$J = e\mu(E)n(x)E(x) \quad ..(1)$$

$$\frac{\in}{e}\frac{dE}{dx} = (n - n_0\ ) + (\ n_t - n_{t,0})$$

$$= (n - n_0\ ) + (\ p_{t,o} - p_t) ....(2)$$

Where

$P_t = N_T - n_t$, $P_{t,o}=N_t-n_{t,o}$...(3)

For, E>E_c , $\mu(E) = \mu_0 \sqrt{\frac{E_c}{E}}$ ....(4)

Where, J is the current density, e is the magnitude of electrical charge, $\mu(E)$ is the high field mobility of current carriers ,n is the concentration of free current carriers at position, € is the permittivity of the insulator.The equation (1) and (4) give the current flow equation of the present problem at high field as

$J = e\,\mu_o\, n(x)[E_c\, E(x)]^{\frac{1}{2}}$ .....(5)

The general equations characterizing the current injection problem mentioned above are subjected to a boundary condition for ohmic contact as.

E(0) =0 ..... (6)

Which is generally applied in most of the single injection current theories from several decades.

The full applied voltage across the insulator is defined by the equation given by .

$V = \int_0^L E(x)dx$....(7)

Which L is the device length.the current injection problem is described in terms of concentration of unoccupied trapping states $P_{t,o}$ given by the following equation as.

$P_{t,o} = \int_{\infty}^{F_o} N_E\, dE$.....(8)

Which is the value of $P_{t,o}$Electrically localized in the forbidden gap.

The concentration of injected trapped carriers at distance x is given by

$n_{ti}(x) = \left(n_t\,(x) - n_{t,o}\right) = \left[P_{t,o} - P_t(x)\right]$...(9)

Where the value of P_t and $P_{t,o}$ are unoccupied level corresponding to value n and n_o respectely .These are given by

$$p_t = (N_T - n_t)\ , \qquad P_{t,o} = \left(N_T - n_{t,o}\right) \ldots (10)$$

For the current injection in insulator such that N <<N_O.Therefore ,it is reasonable to consider $P_{t,o} \gg P_t$.

Regional Approximation Scheme.

At appropriate injection level of currents, the insulator is divided into three regions with the help of two imaginary transition planes $x_1$and x_2. The regions I and II are space –charge – limited and region-III is ohmic in nature. The imaginary transition planes are shifted towards anode with the increase of injection levels of currents. The general equation characterizing the current flow and poison's low for the three regions are given by .

eISSN1303-5150

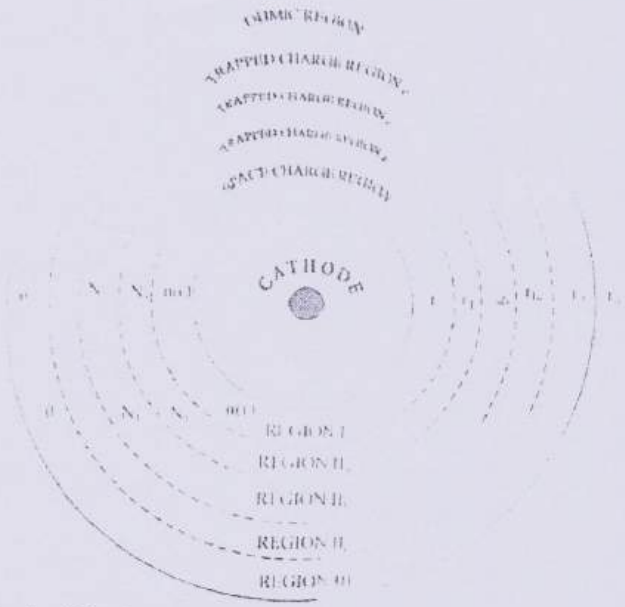


Fig A. Division of Spherical Diode into different regions by the regional approximation method

Region-I $(0 \leq x \leq x_1)$; $n(x) \gg n_t \gg n_0$
Perfect insulator region

$J = e\,\mu_o\, n(x)[E_c\, E(x)]^{\frac{1}{2}}$....(11)

$\frac{\epsilon}{e}\frac{dE}{dx} = n$...(12)

$N(x_1) = n_t(x_1) = P_{t,o}$...(13)

Region-II $(x_1 \leq x \leq x_2)$; $P_{t,o} \gg n(x) \gg n_0$
Trapped charge region

$J = e\,\mu_o\, n(x)[E_c\, E(x)]^{\frac{1}{2}}$....(14)

$\frac{\epsilon}{e}\frac{dE}{dx} = P_{t,o}$...(15)

$N(x_2) = n_0$...(16)

Region –III I $(x_2 \leq x \leq L)$; $n_0 \gg n(x)$
Ohmic Region

$J = e\,\mu_o\, n(x)[E_c\, E(x)]^{\frac{1}{2}}$....(17)

$\frac{\epsilon}{e}\frac{dE}{dx} = 0$...(18)

The continuity of the electric field strength at the two imaginary transition planes x_1 and x_2 is given by
$E(x_1^-) = E(x_1^+)$, $E(x_2^-) = E(x_2^+)$
Where the electric field strength at the two imaginary transition planes $E(x_1)$ and $E(x_2)$ ARE the values approaching from the left side of imaginary transition planes and the electric field strengths $E(x_1)$ and $E(x_2)$ are the values approaching to the transition planes x_1 and x_2 from the riht hand side.

Result Analysis :

The complete current –voltage –characteristic of the two sets of critical currents and critical voltages are defined by the following conditions as.

eISSN1303-5150

$$= \frac{3}{5}\left[\left(\frac{3J}{2 \in \mu_0 E_c^{-1/2}}\right)\right]^{2/3} x_1^{5/3}$$

$$= \frac{2\epsilon J^4}{5e^5\mu_0^4 \; P_{t,0}^5 E_c^2} \ldots (31)$$

The voltage developed across the region II is derived from the equations (7) , (23) ,(24) and (28) as

$$V_1 = \int_{x_1}^{x_2} E(x)dx$$

$$= \frac{eP_{t,0}}{2\epsilon}(x_2^2 - x_1^2) + \frac{J^2}{3e^2\mu_0^2 \; P_{t,0}^2 E_c}(x_2 - x_1)$$

$$= \frac{\epsilon J^4}{2e^5\mu_0^4 \; P_{t,0} E_c^2 n_0^4} \ldots (32)$$

The voltage across the region –III is derived from the equation (7) and (26) as

$V_1 = \int_{x_1}^{L} E(x)dx \ldots (33)$

The first critical voltage is observed at the first critical current J=$J_{cr,1}$ as

$V_{cr,1} = [V_1 + V_{II}]$At J=$J_{cr,1}$

$$= \frac{2\epsilon {J_{cr,1}}^4}{5e^5\mu_0^4 \; P_{t,0}^5 E_c^2} + \left[\int_{x_1}^{L} E(x)dx\right]_{At\, J=J_{cr,1}}$$

$$= \frac{eP_{t,0}\, L^2}{2\epsilon} \ldots (35)$$

where it is assumed that the concentration of unoccupied traps in thermal –equilibrium condition is significantly larger than the concentration of thermal free carriers ($P_{t,o} \gg n_0$)

The expression for the second critical voltage $V_{cr,2}$ is obtained at the current J=$J_{cr,2}$. The expression for the second critical voltage is evaluated from the equation (30) and (31) as

$$V_{cr,1} = \frac{2 \in {J_{cr,2}}^4}{5e^5\mu_0^4 \; P_{t,0}^5 E_c^2} L^2$$

$$= \frac{9eP_{t,0}}{10\epsilon} L^2$$

which depends greatly on the device length.

Discussion and Conclusions:

The present paper describes the theoretical description on the high field transport and thermal noise behavior of the steady State space-charge limited single injection current flow in insulated with distributed deep heaps. The regional approximation and salami methods are applied for the current flow and thermal noise generated inside the insulator, respectively. The application of the current injection mechanism and related features are considered and just similar to other complicated injection problems of this area of research. The general considerations of the problem are given below as :

a) The contribution of the diffusion current with compare to the drift current is negligibly small and present procedure.

b) The cathode is considered as infinite reservoir for the carriers injection in the insulator with the help of an injecting electrode end.

c) One of the electrical contact must be ohmic in nature.

These consideration are usually made by the several research workers who obtain the simplifying solutions in the injection problems.

The results are applicable to the thermal noise estimation of the insulator. The usual consideration of the simplified procedure is adopted to divide the complete current-voltage characteristic in to six situations with the help of two sets of critical points. The insulators are divided into three region of approximate injection level of currents with the help of two imaginary transition planes. These regions are obtained with the help of the regional approximation method. The transition planes are shifted towards anode with the increase of injection levels of currents. The region I is dominated by the injected space charge and the trapping effects are dominated in the region II. The ohmic conduction dominates in this region III.Therefore, the ohmic, trapping and space charge conduction mechanisms are considered in the entire insulator at high fields. All three types of conduction mechanism have different Poisson's law which is solved at high fields under the different boundary condition. The mathematical procedure shows that the length and location of the transition regimes in the complete current-voltage- characteristic depend on the various physical parameters.

References

1.Van der Ziel ,A., Noise in measurements, John Wiley,Inter-science ,New York (1976).
2. Wright,G.t., Proc.IEEE51, 1642 (1963).
3. Tredgold, R.H., Space Charge conduction in solids ,ElesvierPub.Co., Amsterdam (1966).
4.Trofimenkoff,F.N., Proc.IEEE53 1756 (1965).
5.Uishakas, Yu. K., Litov.Fiz.sbornik7 789 (1967).
6.Patrick, L., J. Appl.Phys.28 765 (1957).
7.Lampert, M.A. and Schilling ,R.B., RCA Report , PTR-2524 (1969) (unpublished).
8.Lanyon, H.P.D., Phys. Rev.130, 134 (1963).
9.Golder, J., Nicolet , M.A., and shumka ,A., Solid State Electronics 16 581 (1973).
10. Kao, K.C. AND Hwang , W., Electrical Transport in Solids , Pergamon Press , New York (1981).

eISSN1303-5150

Sources

ISSN | Enter ISSN or ISSNs | Find sources

ISSN: 1303 5150 ×

Improved Citescore

We have updated the CiteScore methodology to ensure a more robust, stable and comprehensive metric which provides an indication of research impact, earlier. The updated methodology will be applied to the calculation of CiteScore, as well as retroactively for all previous CiteScore years (ie. 2018, 2017, 2016...). The previous CiteScore values have been removed and are no longer available.

View CiteScore methodology. >

Filter refine list

Apply | Clear filters

...y options

- Display only Open Access journals
- ...hts for 4-year timeframe
- ...o minimum selected
- Minimum citations
- Minimum documents

Citescore highest quartile

- Show only titles in top 10 percent
- 1st quartile
- ...d quartile
- ...artile
- 4th quartile

ource type

- Journals
- Book Series
- C... ference Proceedings
- Tr... e Publications

...pply | Clear filters

1 result

Download Scopus Source List | Learn more about Scopus Source List

All | Export to Excel | Save to source list

View metrics for year: 2021

	Source title	CiteScore	Highest percentile	Citations 2018-21	Documents 2018-21	% Cited
1	NeuroQuantology	1.3	22% 160/205 Atomic and Molecular Physics, and Optics	1,044	781	47

Top of page

Source details

Feedback > Compare sources >

NeuroQuantology

Scopus coverage years: from 2007 to Present

Publisher: Anka Publishers

ISSN: 1303-5150

Subject area: Physics and Astronomy: Atomic and Molecular Physics, and Optics | Neuroscience: Cognitive Neuroscience | Neuroscience: Developmental Neuroscience

Source type: Journal

Save to source list | Source Homepage

CiteScore 2021
1.3

SJR 2021
0.285

SNIP 2021
1.038

CiteScore | CiteScore rank & trend | Scopus content coverage

Improved CiteScore methodology

CiteScore 2021 counts the citations received in 2018-2021 to articles, reviews, conference papers, book chapters and data papers published in 2018-2021, and divides this by the number of publications published in 2018-2021. Learn more >

CiteScore 2021

1.3 = 1,044 Citations 2018 - 2021 / 781 Documents 2018 - 2021

CiteScoreTracker 2022

2.0 = 849 Citations to date / 419 Documents to date

Type here to search

27°C Haze ENG 10:44 AM 28-11-2022

Hindawi
Computational Intelligence and Neuroscience
Volume 2022, Article ID 1359714, 9 pages
https://doi.org/10.1155/2022/1359714

Research Article

Recurrent Neural Model to Analyze the Effect of Physical Training and Treatment in Relation to Sports Injuries

Jyoti A. Dhanke,[1] Rajesh Kumar Maurya,[2] S. Navaneethan,[3] Dinesh Mavaluru,[4] Shibili Nuhmani,[5] Nilamadhab Mishra,[6] and Ellappan Venugopal[7]

[1]*Department of Science (Mathematics), Bharati Vidyapeeth's College of Engineering, Lavale, Pune 412115, India*
[2]*Department of Computer Applications, ABES Engineering College, Ghaziabad 201009, Uttar Pradesh, India*
[3]*Department of Electronics and Communication Engineering, Saveetha Engineering College, Chennai, Tamil Nadu, India*
[4]*Department of Information Technology, College of Computing and Informatics, Saudi Electronic University, Riyadh, Saudi Arabia*
[5]*Department of Physical Therapy, Imam Abdulrahman Bin Faisal University, Dammam 34212, Saudi Arabia*
[6]*School of Computing Science and Engineering, VIT Bhopal University, Madhya Pradesh 466114, India*
[7]*Department of Electronics and Communication Engineering, School of Electrical Engineering and Computing, Adama Science and Technology University, Adama, Ethiopia*

Correspondence should be addressed to Ellappan Venugopal; ellappan.venugopal@astu.edu.et

Received 9 July 2022; Revised 23 August 2022; Accepted 26 August 2022; Published 30 September 2022

Academic Editor: Amandeep Kaur

Copyright © 2022 Jyoti A. Dhanke et al. This is an open access article distributed under the Creative Commons Attribution License, which permits unrestricted use, distribution, and reproduction in any medium, provided the original work is properly cited.

Artificial intelligence has rapidly grown and has made the scenario that no field can function without it. Like every field, it also plays a vital role in the sports field nowadays. In certain sports, injuries happen very often due to heavy training and sudden speedy actions, especially in athletics and football. Here arises a need to analyze the effect of physical training in sportsperson by collecting data from their daily training. With the help of artificial intelligence, a recurrent neural model is developed to analyze the effect of physical training and treatment concerning sports injury. A Recurrent Neural Network (RNN) can be a subsection of Artificial Neural Networks (ANN) that uses the neural nodes connected in a temporal sequence. The temporal sequence is one of the essential terms in this research, which denotes a data sequence of events in a given timeframe. The recurrent neural model is an intelligent machine learning method that comprises a neural schema replicating humans. This neural schema studies the data it collects from the athletes/players and processes it by analyzing previous injuries. Sports injuries have to be analyzed because, in some cases, it becomes more dangerous to the sportsperson that they may even lose their career due to disability. Sometimes it may cause a massive loss to the club or company that hired the sportsperson for the sport. The prediction process can give the player rest until he recovers, thus becoming the safest approach in sports. Therefore, it is essential to analyze the sportsperson's track data to keep an eye on his health. In this research, RNN model is compared with the existing Support Vector Machine (SVM) in concerning to the effect of physical training and treatment for sports. The results show that the proposed model has achieved 99% accuracy, which is higher than the existing algorithm.

1. Introduction

A Recurrent Neural Network (RNN) model is a type of Artificial Neural Network (ANN) that aids in the system's dynamic behavior for a shorter duration. Additionally, the nodes in the networks are connected, which can construct a graph of directed or undirected categories over time. Athletes compete in a variety of events that require extreme fitness and stamina. Illness and aging produce anatomical and functional changes in the human body, putting senior people at risk of musculoskeletal and cardiovascular overload [1]. A substantial percentage of injuries (both acute and exceptional) are minor and can be treated with a bit of break from training and competition. The injuries of the

sportsperson have to be treated as soon as possible and as effectively as possible [2]. However, it is important to note that inactivity and immobility have a more significant influence on structures and functions in the old than in the younger. Most physically active seniors are selected because they have better health and physical capacity than sedentary individuals their age, increasing their physical capacity. They will, however, be impacted by some of the drawbacks of physical overloading, mainly because the aging body's capacity to respond to high levels of loading is impaired [3]. Acute injuries are prevalent in senior persons who participate in ball games, downhill skiing, and gymnastics, which involve a lot of coordination, reaction time, and balance. Muscle has been described as the most usually acutely damaged tissue among active senior athletes. The most prevalent type of injury is to the lower extremities [4].

2. Literature Review

The RNN approach is designed to capture temporal correlations and is more successful for sequential data than traditional neural networks (NNs). After competitions, athletes frequently engage in rigorous physical conditioning and specific skill training. Regular training sessions for athletes are typical of a greater intensity. Athletes' physical and emotional health are harmed by long-term, high-intensity exercise, which leads to sports injuries. An injured athlete could not achieve the expected result in the competition due to his inability to undergo high-intensity training [5]. Based on the relevance of neural networks for target recognition, they present a novel dual-level feature fusion neural network (NN) model for sports injury estimate. The proposed model improves effective discrimination by building a dual-fusion structure with a 1 : 1 convolution and linkage to overcome the problem of feature loss. According to the trials, the suggested model exhibited a classification accuracy of 97.0 percent, a sensitivity of 95.70 percent, and a specificity of 97.54 percent [6]. The proposed model outperforms all of the other models that were taken into account for this research. Using a neural network to build a sports match prediction model and anticipate the outcomes can provide a theoretical framework for practice, prediction, and analysis. Various data mining techniques examine these medical records [7].

The Recurrent Neural Network (RNN) is a reliable technique that has been extensively used in machine learning and bioinformatics. The research on injury classification and level identification of the spinal cord is done using CT scan images that have been segmented using adaptive thresholding methods. The disc is then localized using the sparse fuzzy C-means clustering technique once the segments have been created. The next stage recovers the connectivity characteristics, statistical features, image-level features, grid-level features, Histogram of Oriented Gradients (HOG), and Linear Gradient Pattern (LGP) from the localized disc. After that, a Deep Convolution Neural Network based on the Crow Search Rider Optimization approach is used to identify damage (CS-ROA-based DCNN). Once the occurrence of the injury has been identified, the proposed Deep Recurrent Neural Network (Deep RNN) is used to categorize the injury severity, and the procedure is terminated if there is no damage [8]. The damage level is determined by the injury detection classifier, which might be normal, wedge, concavity, or crush [9].

A vast body of research has paved the way to improvements in legislation and policies to lessen the incidence and impact of concussions during the previous decade. Young individuals who engage in high-risk activities like sports, on the other hand, commonly underreport concussions, while others may exaggerate reports for a variety of reasons. Such laws and legislation must function within a supportive social context to be effective. Therefore, understanding the culture around concussion is crucial to decreasing concussion and its consequences [10]. An automated deep neural network approach is performed to analyze public opinion on concussion concerns in sports. As a result, one of the project's objectives is to develop a viable method for analyzing and measuring the public's current attitude toward sports-related concussions by examining an extensive collection of public views and perspectives on the subject. Various stakeholders may use this method's data to measure public opinion and attitudes around concussions. This knowledge might aid in the successful implementation of concussion-reduction strategies. Continuous monitoring of lab data and high-dimensional vital signs is needed to detect and diagnose acute patient issues, whereas continuous monitoring has been a difficult task in the past [11]. Recurrent Neural Networks (RNNs), a type of deep learning model, have lately demonstrated their capacity to predict such events. In actuality, however, patient data are continually being added, and RNN does not have a feasible adaptation mechanism to integrate this new data and enhance accuracy. The suggested method relies on the previous projected output and its associated label to update the RNN's hidden state. The additional information offered by the predicted past production and label improved the model's performance. This model's regularization technique considers the model's label prediction errors and its input data estimate errors [12]. The regularization approach reduces the variance of the model and the time gap of the self-correcting mechanism. The proposed model is suitable for both classification and regression. The proposed models were evaluated using real-world, large-scale ICU datasets. This method includes historical timestamp prediction mistakes into the current timestamp forecast, allowing the model to "learn" from previous forecasts. A regularization technique took into account the model's estimating errors on the input data and its label prediction errors [13]. As a result, an intelligent system such as Recurrent Neural Networks (RNNs) is required to efficiently analyze, predict, and recognize sports injuries.

3. Motivation of the Work

Physical education is recognized as an essential component of health education as well as an ability to reflect of a school system. A sports leader is in charge of students' physical education and/or health training but also treatment.

Through student physical education classes at higher education institutions, this study suggested a technique for training but also treatment evaluation. The framework proposed by humans can improve the overall generalizability of the conventional BP network along with training time by integrating a neural network with the BP algorithm.

4. Proposed Model

Sport injuries can sometimes become more dangerous that it can cause disability to the sportsperson. This ends the career of the sportsperson and also causes big loss to the team who invested huge time and money on the particular player. Thus, a frequent monitor of their health is done periodically and the data are being recorded in a database. Each player/athlete has a separate kind of body health. In this scenario, one person's health data cannot be taken as a reference in treating other person beyond certain extent. Thus, the data of a player have to be compared and analyzed with his own dataset that was recorded previously. The data are collected and analyzed with the help of artificial neural networks. In this case, a Recurrent Neural Network (RNN) model has been used to analyze the effect of physical training and treatment in relation with sports injuries is depicted in the Figure 1.

The main phases involved in this method are as follows.

(1) Physical Training: The physical training plays an important part in the career of a sportsperson. Without training session, the fitness level to play the game is lost even by star sportsmen. But over indulgence in training can cause physical stress to the players, leading to sports injuries like muscle tear. Therefore, training has to be done in a manner that the occurrence of sports injury has also to be avoided by predicting it beforehand and taking leave for the session or sport until the completion of the healing process.

(2) Recurrent Neural Network: In order to predict the occurrence of a sports injury, an artificial neural network is assigned to accomplish the task. The ANN used here is Recurrent Neural Network (RNN), which analyzes the neural nodes with respect to the temporal sequence. The temporal sequence is a data collection method of collecting temporal data according to the sequence of happening in a given set of timeframe. These data are analyzed for predicting the sports injury.

(3) Analyze and Predict Sports Injury: There is a strong need in predicting the occurrence of sports injury to avoid the loses that occur in one or more ways. In Recurrent Neural Network (RNN), the outputs of all the neurons are connected to the inputs of the neurons. The Recurrent Neural Network is used as a computational device system in analyzing the data to produce computational data output, which can be used as a predictive measure to avoid sports injuries.

(4) Precaution Measures: With the help of the RNN output, the player is advised to take a break until complete healing process is done. This is also checked with the help of the medical support team and AI tools. Regarding AI tools used in the process, there are a number of AI sensors and biosensors that are already in use in the medical industry. Those biosensors are used to collect data in some cases. Thus, an intelligent RNN plays an important role in predicting the player's health to avoid sports injuries.

5. Proposed Work

The processing elements of such woman are x, which appear to be the analysis value of education physical quality education; the continental surface modules are x, and so are the extracted features i which appear to become the analysis significance of training physical quality education. Since the input image device transmits data directly to a frame node's center, the output of a input layer network equals a input; the information or data of a mid-layer access point seem to be the major contributors of an output node; and also the activation function alone has one network device, which also obtains the information of an intermediate layer access point but also produces an output its training but also treatment requirement evaluation effects.

Input data $m_i, i = \{1, 2, \ldots, x\}$, where x reflects training and treatment quality evaluation.

The equation (1) is represented by the input to the H middle of the specimen node.

$$H_j = \sum_{j=1}^{x} \varphi_{ij} m_i. \tag{1}$$

The result is as follows from the equation (2).

$$R_j = \sum_{j=1}^{x} \frac{1}{\left\{1 + \left[\left(\sum_{i=1}^{x} \varphi_i R_j\right)^{-1} - 1\right]^2\right\}'} = \sum_{j=1}^{x} \frac{1}{\left[\left(H_j^{-1} - 1\right)^2\right]}. \tag{2}$$

In which φ_j signifies the resilience from an input datatype ground station H_j^{-1} to a frame datatype center j *as well as* R_j signifies the data's factor, the i^{th} training as well as treatment quality evaluation index.

Node of input signal: There are only S nodes with in destination node (as shown in equation (3)), and also the information has been the high speed of the structure node's center point:

$$S = \sum_{j=1}^{x} \frac{1}{\left\{1 + \left[\left(\sum_{i=1}^{x} \varphi_i R_j\right)^{-1} - 1\right]^2\right\}^{2'}}. \tag{3}$$

The learning optimization technique is defined as even the mean score of such mean square sum $\sum_{i=1}^{x} \varphi_j R_j$ of such an error between such overall performances but also the measuring device value of G measurement techniques and the calculation is displayed in equation (4).

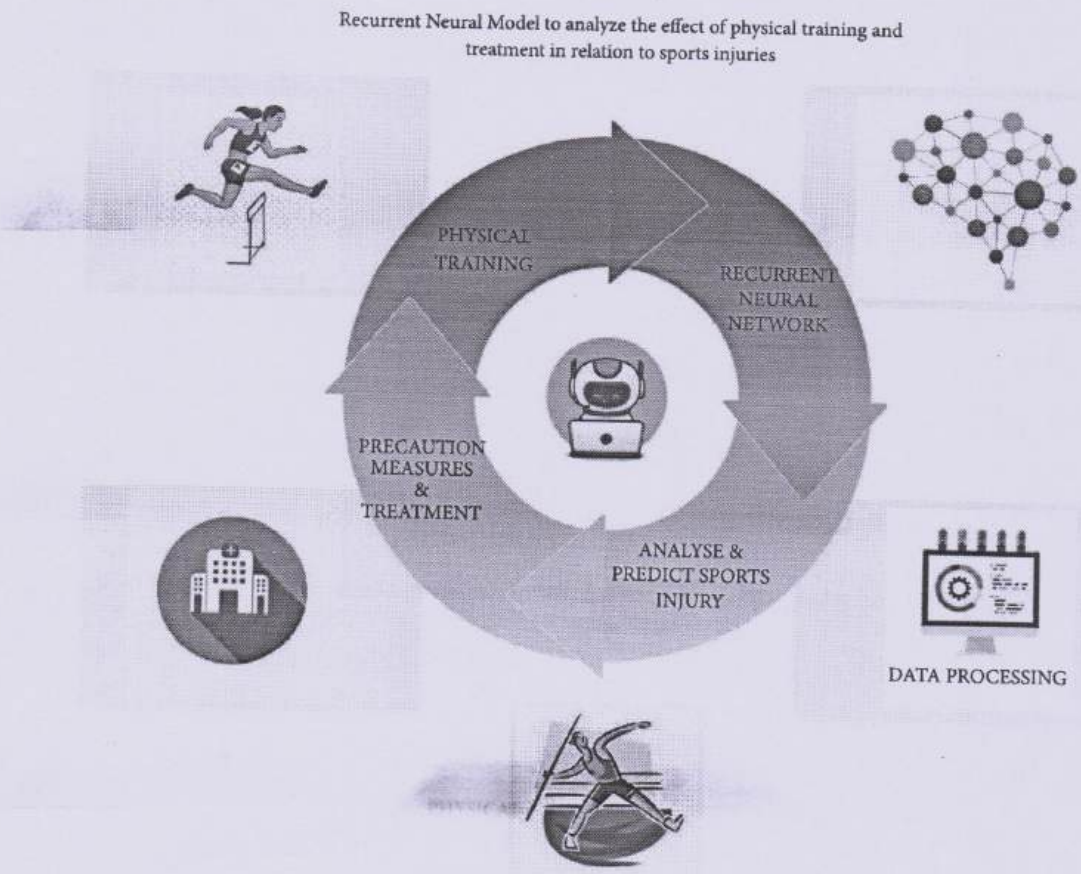


FIGURE 1: Proposed recurrent model for prediction and analysis of sports injuries.

$$G = \left(\frac{1}{M}\right) \sum_{m=1}^{m} [\underline{s} - s]^2 = \left(\frac{1}{M}\right) \sum_{m=1}^{m} G_j. \tag{4}$$

Despite the BP neural network evaluation process's modifying δG framework, the goal of network training and treatment is to minimize τ by modifying the network's authentication and authorization. The training algorithm technique δc_{ij} is being used to modify its delinking as in the following equation (5).

$$G_{ij} = \sum \left\{ \varphi_{ij} = -\tau \left(\frac{\delta G}{\delta c_{ij}} \right), \varphi_j = -\tau \left(\frac{\delta G}{\delta \varphi_{ij}} \right). \right. \tag{5}$$

Furthermore, for such a rate of learning, the $d_i \varphi_j R_j^2$ quantity of communication optimizing parameters here between the information data network and the medium layer wireless device is then shown in the equation (6).

$$\varphi_{ij} = d_i \varphi_j R_j^2 \left[1 - \sum_{i=1}^{x} \varphi_{ij} d_j \right] \omega_j. \tag{6}$$

The number of connection optimizing parameters is as in the following equation (7).

$$\varphi_i = \sum_{j=1}^{r} S^2 R_j \left[1 - \sum_{j=1}^{r} \varphi_j R_j \right] [\underline{s} - s]^2. \tag{7}$$

So, using this framework, its neural network's data transmission weight can also be described to use the $\sum_{j=1}^{r} \varphi_j R_j$ optimization technique of such a specific brain network and the imperfection between these overall performances, and also various sample values can be reduced. The framework will be in a higher optimization procedure, as shown in the equation (8), by using an optimized neural network.

$$(G) = \sum_{j=1}^{r} \int (\varphi_1, \ldots\ldots \varphi_n). \tag{8}$$

For which (G) seems to be the overall lack of accuracy of network training and $\varphi_1, \ldots\ldots, \varphi_x$ are the constant weights now since strong and secure numbering includes the weights of the network of input access to data points along with center layer access points and also the prediction models of concentrators and output node devices, and n represents the number of network weights. Among most of them, $\underline{s}$ and s are φ_1 variables which it represent its upper and lower bounds of change.

The optimization algorithm is a low capacity problem in the process of analytical algorithms. Because an individual's areas of interest are roughly equivalent to $\int(\varphi_1, \ldots\ldots, \varphi_x)$ ability, its representation of an optimization technique has a significant effect on genetic algorithms. Because of its close route planning friendship between both the $U-G$ optimization procedure and the optimization techniques, the $G<U$ strength training computational process described below equation (9) is being used.

$$\int_i = \sum_{i=1}\{U-G \quad G<U, 0 \quad G\geq U. \tag{9}$$

In which e represents the training optimization technique and G represents the sum of all $G\geq U$ in the current generation. The recommendations below are used by the M_r classification of genetic process parameters in order to accept responsibility for such $\int(U-G)/U \in [0, 0.6]$ efficiency of integration and also to eliminate excess integration caused by important evolutionary declassification.

$$M_r = \left\{2\left(\frac{\int_1 U-G \;\; G<U}{U}\right)\right\}, \frac{\int_1(U-G)}{U} \in [0, 0.5], \left[1-2\left(1-\left(\frac{\int_1 U-G \;\; G<U}{U}\right)^2\right)\right], \frac{\int_1(U-G)}{U} \in [0.5, 1]. \tag{10}$$

The min *and* d max technique is used for normalization handling $\int_1(U-G)/U \in [0.5, 1]$ since it is a successful implementation for processing information that can successfully retain its very own original definition while having caused no redundant data. The normalization equation (10) is to use this report for such input data.

The procedures of compacting a large variety of information into the field of view [0, 1] are known as normalization $\int_1(U-G)/U \in [0.5, 1]$. The solution to the normalization is given in the equation (11) and is as follows.

$$d' = \sum_{i=1}^{x} \frac{d-d_{\min}}{d_{\max}-d_{\min}}. \tag{11}$$

The standardization process σ entails converting the dataset's small and big outlier documentation into a discrete random variable with such an average overall value of 0 and then a confidence level of 1. The following equation (12) depicts the standardization process.

$$d' = \sum_{i=1}^{x} \frac{d-d_{\min}}{\sigma}. \tag{12}$$

Each data center is composed of three layers: input nodes, hidden nodes, and also convolution layers $\beta, \gamma,$ *and* α, also with weight training of each surface being and also including. It suggests that specific $\varphi_{y'y}q_{y'}^{t-1}$ information is managed to retain in RNN receptors after each cycle of data transmission. It must enter a $\varphi_y(q_{y'}^{t-1})$ next nerve cell as new information and effect the subsequent data output. The equation (13) for such corresponding input nodes, its original input of both the hidden units, and also the outcome variable to it of destination node at time step t is represented in the following: equations (14) and (15).

$$\beta_y^t = \sum_{i=1}^{M} \varphi_{iy}d_i^t + \sum_{y'}^{M} \varphi_{y'y}q_{y'}^{t-1}, \tag{13}$$

$$\alpha_{y'}^{t-1} = \varphi_y\left(q_{y'}^{t-1}\right), \tag{14}$$

$$\gamma_{y'}^{t-1} = \sum_{y=1}^{M} \varphi_{y0}q_{y'}^{t}. \tag{15}$$

As a result, by modeling differently in time-distance, this framework is enhanced much further, seeking to make this more distinctive than spatial transformation. The distributed probability, which gets to know to extract temporal features from streaming video using learning algorithm, is being used in the case as part of a hierarchy approach. As the introducing module, its own interpolation constricted machine effort in learning the hierarchy organization of the original data structure. The framework has become more difficult since it develops from highest to lowest level. The geographically but also temporally High Duplicate Network is named after a constant growth in interpretations.

Previously, the rapacious hierarchical model was used to train the Enlarged Deep Learning (Deep Belief Network (DBN)) model. Furthermore, each framework's input layers are informed at random, beginning with the lowest layer. The probability recognition of the hidden nodes is then reorganized, and understanding to some other layer is gained. This process was repeated indefinitely during training until all of the layers have been trained, since training the entire network might recover the hidden and exposed possibility representations of every particular part within the video.

6. Results and Discussion

The above graph having to learn optimization method is defined as the average score of these mean square $\sum_{i=1}^{x}\varphi_j R_j$ of such a mistake between such overall performance and the measuring handset value of G measurement methods. As in equation (4), Figure 2 depicts the physical education training and treatment performance of fourth- and eighth-grade students. The effectiveness of training and treatment is evaluated using a Recurrent Neural Network Model, a Support Vector Machine, and a Fuzzy Set Model based on hesitation. The computation is carried out by combining the

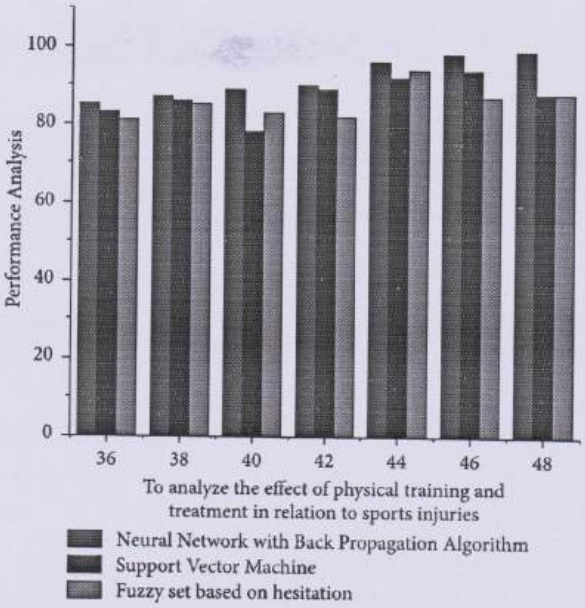


FIGURE 2: The computation accuracy of measurement weight results is compared.

TABLE 1: Analyze the effect of physical training and treatment on sports injuries using a result analysis. Precision in computing.

Effect of physical training and treatment in relation to sports	Recurrent Neural Network model (%)	Support Vector Machine (%)	Fuzzy set based on hesitation (%)
36	85	83	81
38	87	86	85
40	89	78	83
42	90	89	82
44	96	92	94
46	98	94	87
48	99	88	88

performance of the fourth- and eighth-grade students. The proposed algorithm, Recurrent Neural Network Model, has a lower percentile at the early stage of new technology. However, at a later stage, the algorithm was able to produce results that were comparable to the Support Vector Machine. The fuzzy model yields results that are indistinguishable from the Recurrent Neural Network Model and Support Vector Machine (SVM) algorithms. Such a comparative graph demonstrates how repeated training, treatment, and learning can improve the performance of students and teachers when using the Recurrent Neural Network Model. Table 1 shows that its Recurrent Neural Network Model provided small training accuracy than other algorithms for an average evaluation weight of 38. Furthermore, the accuracy rate of the Recurrent Neural Network Model is steadily improving compared to the other two algorithms with fluctuating results. Later on, the proposed algorithm achieved an accuracy of 99%, which is a minimum increase of nine percentage points over the Support Vector Machine and then a 18% increase over the Fuzzy set model.

The δG framework is being modified as part of the BP neural network evaluation process. The goal of capacity training, as well as treatment, seems to be to minimize τ by modifying Internet backbone authentication process. To adjust its delinking, the developer these skills technique δc_{ij} is used resemblance of performance measures with those of algorithms represent in Figure 3 also demonstrates that such built model performance when compared conventional algorithms, including such neural network models, through seeking to resolve activity recognition problems. The 98.55% training and treatment accuracy rate also confirms its high specificity. The convolutional neural network could capture the qualities of training (93.26%), training and treatment (95.47%), accuracy and loss of training (88.74%) analysis, optimize the required data, and improve the consistency of exercise physiology recognition simply by attempting to adjust the set of parameters. The neural network accuracy training and testing graph is capacity forecast in physical education training and treatment based on BP neural network.

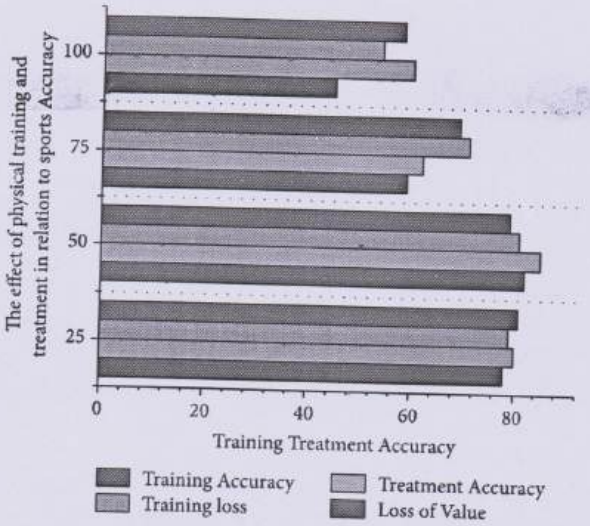


FIGURE 3: The effect of physical training and treatment on neural network accuracy but also loss in sports using the BP algorithm.

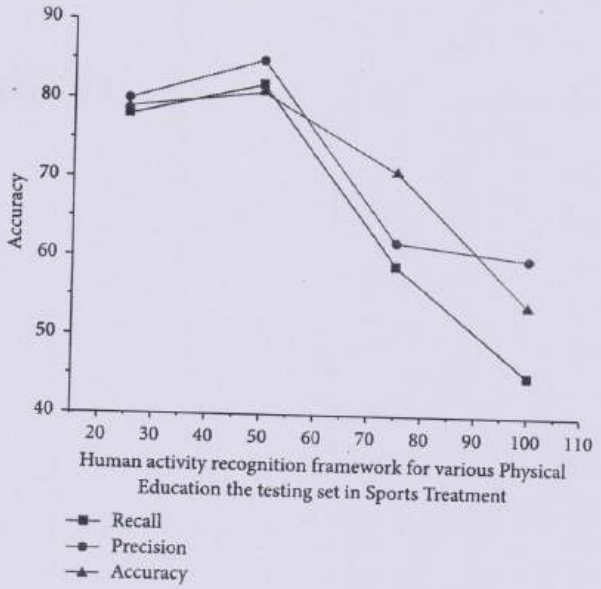


FIGURE 4: Performance evaluation of human activity recognition.

Moreover, with such a learning algorithm, the $d_i\varphi_j R_j^2$ quantity of communication optimization parameters between both the information data connection and the medium surface wireless device is shown in equation (6) elsewhere here represented in Figure 4; it also shows that trained human activity recognition framework appears to have an evaluation of overall accuracy of much more than 99.7%, precision of much more than 92.46 percent, recall frequency of many more than 89.72%, for the different topics; until training, the activity recognition framework for several Physical Education.

The isolation of visual medium, which includes higher rates of physical and also postures judgment in physical training and treatment, has been shown to continue providing educators with unbiased information about student movements, and thus, this recognition of educational body actions may provide legitimate input to improve training performance. Information from intelligent smart wearable sensors has been used to accurately determine human behavior, but the classification of constructions is a controversial subject. The experimental results (refer to Table 2) show that such a convolutional network-based activity recognition system could indeed accurately recognize human behavior with an accuracy of more than 98%. As a result of the Analysis for Multiple Physical Education assessment set in diverse physical education for precision (89%), recall (87%), and accuracy (99%), as well as the Human Sports Activity of precision (90%), recall (85%), and accuracy (98%).

The suggestions below are being used by the $M\ r$ categorization of genetic process variables to take accountability for such $\int_1 (U - G)/U \in [0, 0.6]$ integration efficiency and to remove unnecessary integration caused by significant evolutionary release of information. The evaluation process of physical education courses follows the training, treatment, and learning processes and the analysis is shown in Figure 5.

TABLE 2: Analysis for the result indifferent physical education the training set in sport treatment.

	Precision (%)	Recall (%)	Accuracy (%)
Various physical education	0.88	0.89	0.99
Human sports activity	0.91	0.86	0.97

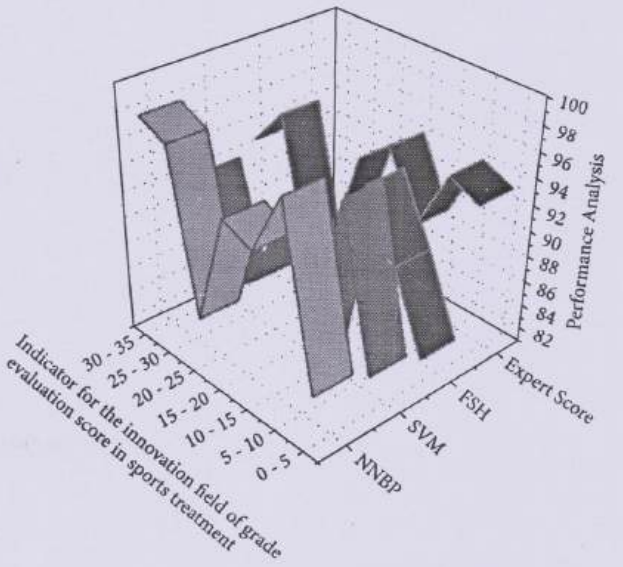


FIGURE 5: Analysis of evaluation score comparison results in sport training and treatment in physical education.

Table 3: Comparison result analysis for different algorithm in the effect of physical training and treatment in relation to sports injuries.

Effect of physical training and treatment	Recurrent Neural Network model (%)	Support Vector Machine (%)	Fuzzy set based on hesitation (%)	Expert score
0–5	85	84	83	93
5–10	98	96	89	94
10–15	93	83	94	89
15–20	94	93	86	94
20–25	85	86	85	92
25–30	97	84	96	84
30–35	98	92	93	82

When compared to expert evaluation, the proposed automatic evaluation via the Recurrent Neural Network model outperformed many assessments. The graph's peaks represent the evaluation value for the specific assessment for students in both grades. Table 3 shows the numerical representation. According to this table, the proposed Recurrent Neural Network model demonstrated fluctuating results during the learning process; however, it demonstrated consistent and increased performance at a later stage. Towards the final considered evaluation weight range of 30–35, the proposed system outperformed the existing Support Vector Machine, fuzzy set predicated on doubt, but also expert score by 6%, 5%, and 16%, respectively.

Figure 6 depicts the analysis of results performed on students of various grades again for physical education training, treatment, but also learning process. Students are encouraged to practice on a regular basis in order to be eligible for competitions in any sport. The graph above shows that the analysis is performed on people from four different categories, including normal people, majors, juniors, and seniors, using sports items, competition, and practice as parameters. All of the necessary equipment for practicing and participating in any specific sport is included in a sports item. In this study, it is assumed that the player has all of the necessary resources. Among some of the four categories of people, the average person with no prior experience was only able to achieve 16% in the competitions despite having access to all of the necessary resources. Individuals in the major, junior, but also senior categories, on the other hand, perform better by 23%, 35%, and 43%, respectively. Every data center is made up of three layers: input endpoints, hidden nodes, and convolution layers $\beta, \gamma, and\ \alpha$ with weight training of every surface included. It implies that specific $\varphi_{y'y} q_{y'}^{t-1}$ information is managed to maintain in RNN receptor sites after each data transmission cycle. It must enter the next neuron as new information and affect the subsequent data output.

The data in Figure 7 above demonstrate that training is required to participate in any sport, and learning them from a coach is also very important. The number of indicator or exercises increases with changes in this graph, as does the computing time or the players' duration of achievement. Initially, each person will devote the maximum amount of time to simple and short exercises. The duration of computation will be reduced as the players perform workouts and practices on a regular basis. It must enter the next neurone as new information as well as affect the subsequent

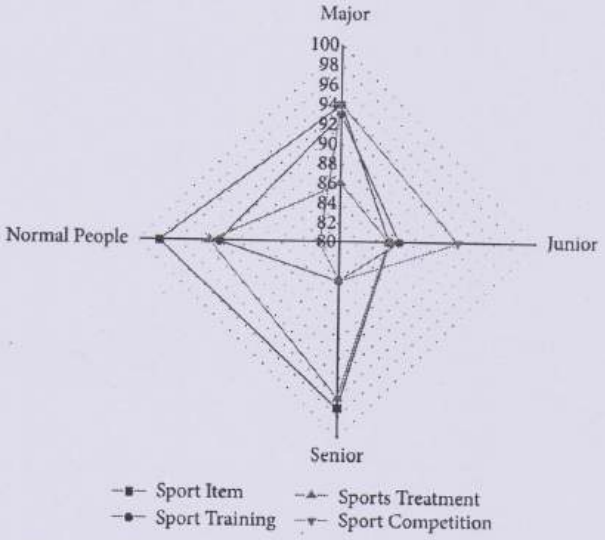


Figure 6: Analysis for result in the physical training and treatment.

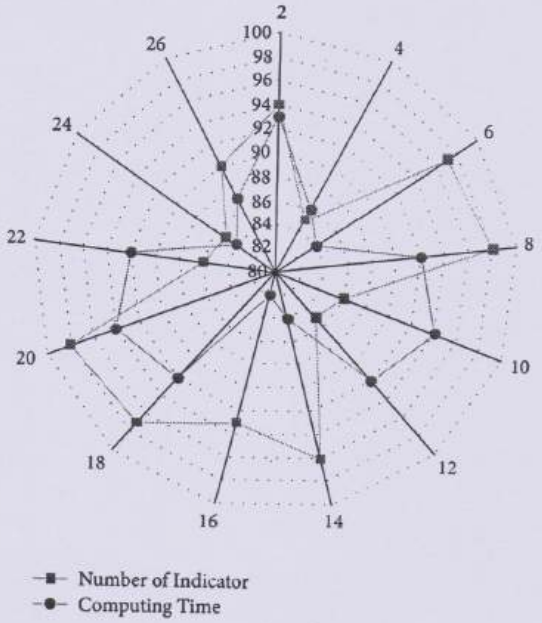


Figure 7: The thorough outcomes of sports training and treatment are critical.

data output. Figure 7 depicts the equations (13), for such corresponding input nodes, its original input of both hidden units, and the outcome variable to it of the destination node at time step t.

7. Conclusion

Injuries are most common among the sports persons during practice sessions and event participation. It is mandatory for them to recover from the injuries at the earliest and start a new beginning. In the technological development, physical training and treatment for the sports injuries can be monitored with the implementation of the intelligent system. This advancement in the technology aids the sports person and the coach to make regular updations on the status of improvement on the injuries concerning to the practice and treatment. In this research, Recurrent Neural Model is designed to perform frequent monitoring of the processes involved in sports injuries and predict the possibilities of injuries. The proposed model outperformed the existing Support Vector Machine, fuzzy set predicated on doubt, but also expert score by 6%, 5%, and 16%, respectively.

Data Availability

The data used to support the findings of the study can be obtained from the corresponding author upon request.

Conflicts of Interest

The authors declare that they have no conflicts of interest.

References

[1] L. Meng and E. Qiao, "Analysis and design of dual-feature fusion neural network for sports injury estimation model," *Neural Computing & Applications*, 2021.

[2] P. Chantamit-o-pas and M. Goyal, "Long short-term memory recurrent neural network for stroke prediction," in *Proceedings of the International Conference on Machine Learning and Data Mining in Pattern Recognition*, pp. 312–323, Springer, Cham, 2018, July.

[3] K. Tirdad, A. Dela Cruz, A. Sadeghian, and M. Cusimano, "A deep neural network approach for sentiment analysis of medically related texts: an analysis of tweets related to concussions in sports," *Brain Inf*, vol. 8, no. 1, p. 12, 2021.

[4] H. Du, Z. Pan, K. Y. Ngiam, F. Wang, P. Shum, and M. Feng, "Self-correcting recurrent neural network for acute Kidney injury prediction in critical Care," *Health Data Science*, vol. 2021, Article ID 9808426, 2021.

[5] M. Kallinen and A. Markku, "Aging, physical activity and sports injuries," *Sports Medicine*, vol. 20, no. 1, pp. 41–52, 1995.

[6] X. Wang and C. Jiang, "Computer-aided physical training sports injury risk simulation based on embedded image system," *Microprocessors and Microsystems*, vol. 83, Article ID 103975, 2021.

[7] A. Zadeh, D. Taylor, M. Bertsos, T. Tillman, N. Nosoudi, and S. Bruce, "Predicting sports injuries with wearable technology and data analysis," *Information Systems Frontiers*, vol. 23, no. 4, pp. 1023–1037, 2021.

[8] D. A. Dobrosielski, L. Sweeney, and P. J. Lisman, "The association between poor Sleep and the incidence of sport and physical training-related injuries in Adult athletic Populations: a Systematic Review," *Sports Medicine*, vol. 51, no. 4, pp. 777–793, 2021.

[9] S. Kozin, Z. Kozina, V. Korobeinik et al., "Neuro-muscular training for injury prevention of students-rock climbers studying in the specialty "Physical Education and Sports": a randomized study," *Journal of Physical Education & Sport*, vol. 21, 2021.

[10] S. Xianguo and W. Cong, "Research on the Application of artificial intelligence technology in physical training," in *Proceedings of the 2021 2nd International Conference on Big Data and Informatization Education*, pp. 261–264, ICBDIE, November 2021.

[11] D. Li, C. Yi, and Y. Gu, "Research on College physical education and sports training based on Virtual Reality technology," *Mathematical Problems in Engineering*, vol. 2021, pp. 1–8, 2021.

[12] N. Coleman, "Pediatric athlete development and Appropriate sports training," in *Common Pediatric Knee Injuries*, N. Coleman, Ed., Springer, Cham, 2021.

[13] O. V. Balberova, "Candidate genes and single-nucleotide gene variants associated with muscle and tendon injuries in cyclic sports athletes," *Personalized Psychiatry and Neurology*, vol. 1, no. 1, pp. 64–72, 2021.

Source details

Feedback > Compare sources >

Computational Intelligence and Neuroscience

Scopus coverage years: from 2007 to 2022

(coverage discontinued in Scopus)

Publisher: Hindawi

ISSN: 1687-5265 E-ISSN: 1687-5273

Subject area: Mathematics: General Mathematics | Computer Science: General Computer Science | Neuroscience: General Neuroscience

Source type: Journal

Save to source list

CiteScore 2021
3.9

SJR 2021
0.863

SNIP 2022
1.023

CiteScore | CiteScore rank & trend | Scopus content coverage

Improved CiteScore methodology

CiteScore 2021 counts the citations received in 2018-2021 to articles, reviews, conference papers, book chapters and data papers published in 2018-2021, and divides this by the number of publications published in 2018-2021. Learn more >

CiteScore 2021

3.9 = 4,319 Citations 2018 - 2021
1,113 Documents 2018 - 2021

Calculated on 05 May, 2022

Score rank 2021

Category	Rank	Percentile
Mathematics General Mathematics	#33/391	91st
Computer Science General Computer Science	#63/231	72nd
Neuroscience General Neuroscience	#66/112	41st

Hindawi
Computational Intelligence and Neuroscience
Volume 2022, Article ID 3564482, 11 pages
https://doi.org/10.1155/2022/3564482

Research Article

Smart Health Monitoring System with Wireless Networks to Detect Kidney Diseases

Jyoti Dhanke,[1] Naveen Rathee,[2] M.S. Vinmathi,[3] S. Janu Priya,[4] Shafiqul Abidin,[5] and Mikiale Tesfamariam[6]

[1]*Department of Engineering Science (Mathematics), Bharati Vidyapeeth's College of Engineering Lavale, Pune 412115, Maharashtra, India*
[2]*Department of Electronics and Communication Engineering, IIMT College of Engineering, Greater Noida 201310, Uttar Pradesh, India*
[3]*Department of CSE, Panimalar Engineering College, Bangalore Trunk Road, Nazarethpet, Poonamallee, Chennai 600123, Tamilnadu, India*
[4]*Department of Electronics and Communication Engineering, K. Ramakrishnan College of Engineering, Samayapuram, Tiruchirappalli, Tamilnadu 621112, India*
[5]*Department of Computer Science, Aligarh Muslim University, Aligarh 202002, Uttar Pradesh, India*
[6]*Department of Software Engineering, College of Computing and Informatics, Haramaya University, Dire Dawa, Ethiopia*

Correspondence should be addressed to Mikiale Tesfamariam; mikiale.tesfamariam@haramaya.edu.et

Received 20 August 2022; Accepted 5 September 2022; Published 8 October 2022

Academic Editor: Amandeep Kaur

Copyright © 2022 Jyoti Dhanke et al. This is an open access article distributed under the Creative Commons Attribution License, which permits unrestricted use, distribution, and reproduction in any medium, provided the original work is properly cited.

It is essential to change health services from a hospital to a patient-centric platform since medical costs are steadily growing and new illnesses are emerging on a worldwide scale. This study provides an optimal decision support system based on the cloud and Internet of Things (IoT) for identifying Chronic Kidney Disease (CKD) to provide patients with efficient remote healthcare services. To identify the presence of medical data for CKD, the proposed technique uses an algorithm named Improved Simulated Annealing-Root Mean Square -Logistic Regression (ISA-RMS-LR). The four subprocesses that make up the proposed model are a collection of data, preprocessing, feature selection, and classification. The incorporation of Simulated Annealing (SA) during Feature Selection (FS) enhances the ISA-RMS-LR model's classifier outputs. Using the CKD benchmark dataset, the ISA-RMS-LR model's efficacy has been verified. According to the experimental findings, the proposed ISA-RMS-LR model effectively classifies patients with CKD, with high sensitivity at 99.46%, accuracy at 99.26%, Specificity at 98%, *F*-score at 99.63%, and kappa value at 98.29%. The proposed system has many benefits including the fast transmission of medical data to the medical personnel, real-time tracking, and registration condition of the patient through a medical record. Potential enhancement of the performance measures the provider system's hospital capacity and monitoring of a significant number of patients with a concentrated average delay.

1. Introduction

An IoT is a key concept that focuses on the modeling and connecting of Internet-linked physical objects using the power of computer systems. Instead of using a certain number of high-powered such as computers, tablet devices, mobile phones, and so on [1, 2], the IoT is largely used for a range of applications using a large number of low-power devices. Such as wrist bands, refrigerators, and umbrellas. Combining IoT with Cloud Computing (CC) is beneficial when it comes to the creation of innovative approaches. An observation model has been built underneath the IoT integration and CC to monitor the state of patients and successfully gather the information, even in distant locations of greater assistance to medical professionals [3]. This model was created to watch the patient's condition. In several situations, the IoT technique is often kept with the assistance of the CC environment to improve efficacy in the

deployment of productive resources, data storage, and computational and processing capabilities [4].

The rate at which technological advancements occur is so rapid that almost anything may be connected over the World Wide Web [5]. The phrase IoT pertains to anything that is connected through the Internet. This term describes objects associated with the network and multiple objects connected to process information, and make decisions but also respond to the physical and virtual world [6]. IoT elements including cell phones, engines, sensors, and computing devices generate a significant quantity of data in real-time. The integration of cloud computing with the IoT is the greatest option. CC is indeed the fundamental virtual structure that can be utilized efficiently, and it encompasses many services like servers, networks, and storage [7]. Therefore, the combination of IoT and CC has substantial advantages and benefits in terms of algorithmic resource management, along with the existence and utilization of customizable resources and the usage of these resources as services [8]. There are a significant number of individuals throughout the globe who are afflicted with cardiovascular disease and diabetes may result in a stroke, heart, and kidney failure.

Blood pressure and heart rate sensors, together with an IoT-based cloud and Wi-Fi communications were used in the development of the system for monitoring the health of patients [9]. On the other hand, an actual electrocardiogram-based monitoring system is not included in the system. One such system has been proposed using an Arduino processor, the cloud, an ECG sensor, and a Raspberry [10]. Wi-Fi is used to make the connection to the Internet, and a cloud server receives the data, processes it, and then notifies the appropriate medical personnel in the event of an emergency [11]. It has been proposed that sensors equipment and a heartbeat Fitbit gadget are linked to the CPU through Bluetooth used to create a low-power health monitoring system. It is possible to use a Raspberry Pi as a server to store and process the vital signs of a patient in an emergency and send an alarm to the attending physician [12, 13]. CC is not supported on this system, and the user has a restricted range of motion to work within. Using temperature, pulse rate, ECG, and fall sensors and a Wi-Fi interface to transport the hospital's data to a cloud server, an IoT - based health system was built for real-time monitoring [14]. The system offers to monitor in real-time and makes a medical determination for the patient based on their current data and patient history. On the other hand, the system is not very precise when it comes to making judgments or, in the case of an emergency, alerting medical services [15]. The methods described in the aforementioned body of research provide several difficulties, including those about patient service area, the precision of decision-making, the database, warnings, real-time monitoring from any place, and the dimensions of the device [16].

2. Related Works

The purpose of developing and implementing smart watches wireless-based system for health monitoring that reads several vital parameters and then makes a selection based on a methodology that requested the server to contact the necessary person in the event of an emergency [17]. The system gathers information about the patient by employing several sensors and then transmits that information in real-time to a cloud server by way of an Arduino controller. The data is saved inside the cloud using an algorithm that was designed specifically to automatically monitor the health of the patients [18]. The system allows for a degree of adaptability for interaction between patients and the healthcare team using alerts, and it achieves a high level of precision in terms of decision-making [19]. When it comes to delivering medical treatment to a significant number of patients, healthcare institutions and caregivers face a variety of challenges that must be overcome. Because of the explosion in the use of contemporary biomedical sensors and IoT devices, an increasing number of sophisticated medical care and health monitoring systems have been created [20].

The majority of recent research has focused on the early identification of chronic disorders such as CKD, heart disease, and diabetes mellitus. In these studies, numerous factors that may influence chronic disease have been utilized. Despite this, the time complexity and performance of the illness prediction process continue to be significant issues [21]. This is even though all of the critical characteristics that are required for disease prediction are present. When attempting to diagnose CKD, the preliminary components often include a few influencing characteristics. These factors account for the long execution time and low precision of the prediction procedure. In addition to these qualities, however, additional symptoms such as insomnia, chest pain, nausea, and other indicators may also aid in the early diagnosis of probable CKD [22]. CKD stands for chronic kidney disease. Therefore, making use of the approach of feature selection may enhance the overall efficiency of CKD prediction made using a variety of classification strategies.

Then, we apply the important components derived from earlier research for CKD diagnosis in addition to the CKD severity level evaluation, which has not been explored before [23]. This was something that had not been done before. To evaluate the effectiveness of the categorization techniques that were put into practice, the samples needed for this study were taken from a selection of samples [24]. Also, in furthermore to the vital features that have been applied in recent research to predict CKD, several additional clinical symptoms are taken into consideration based on the proposed model [25]. These symptoms significantly contribute to the accuracy with which CKD and its severity degree can be predicted [26]. Therefore, to improve the implementation time and effectiveness of the testing and training process during the classification stage, we pertain to the influencing functionalities based on the clinical observations and experiences of physicians. The findings from earlier studies, provide three groups of crucial characteristics that have an impact on CKD [27]. In addition, if CKD is detected, this model can provide predictions on its subtype. The CKD level is the single most critical predictor in predicting CKD, although it has not been taken into account in any of the prior studies. The entire work done in the past was only devoted to making predictions about the presence of CKD, and the

samples were divided into two categories: healthy individuals and CKD patients.

The CC approach is more applicable for finding the basic linear function for NN to provide enough data training [28]. When a model is implemented, the classification procedure focuses on achieving the highest possible level of performance. To solve the problem that occurs in the Neural Network (NN)-CC technique's local optimum, modified techniques of NN-CC have indeed been developed and implemented. The main weights of the neuron connection are responsible for the operation of the NN, and the projected model makes use of the MCS scheme to bring down the overall Root Mean Square Error (RMSE) measurement which is calculated during the NN training process [29]. When contrasted with the NN-CS methodology, the obtained findings indicate that the NN-CC model has achieved an optimal level of function. The overall accuracy of CKD is brought down by the presence of missing values in a dataset. Because the conventional methods are executed during the data preparation stage, the data cleaning task is necessary to complete the work of filling in the missing data and getting rid of the scores that are not useful. It is anticipated that there will be a reevaluation technique used for all stages of CKD in which missing data have been calculated and inserted into the appropriate areas [30]. Even though conventional models are effective, a specialized illness detection system inside a healthcare dataset is still required to guarantee that CKD results are accurate. Within the context of this discussion, the FS task is seen as an essential component of the data categorization process.

This paper presents an ideal IoT and diagnosing chronic kidney disease (CKD) using a cloud-based decision support system, to deliver efficient virtual care to patients. The SA-oriented FS and Root Mean Square Propagation (RMSProp) driven Logistic Regression (LR) model termed ISA-RMS-LR is used by the proposed technique to identify the presence of CKD based on medical data. The proposed model has comprised a group of four different subprocesses, which include data collection, preprocessing, FS, and categorization. The incorporation of SA for FS contributes to the improvement of the classifier results generated by the ISA-RMS-LR model. Using a standard dataset for CKD, the validity of the ISA-RMS-LR model's predictive ability was investigated and confirmed. The results of the experiments suggest that the proposed ISA-RMS-LR model is superior to the methodologies that are being examined in terms of its ability to correctly diagnose and categorize CKD.

3. Proposed Model

Figure 1 shows the whole procedure for developing the proposed algorithm of the ISA-RMS-LR model. It depicts the data collecting process that occurs in a variety of ways. Following that, data preparation occurs, and this preprocessed data gets delivered into the ISA-FS model. The ISA-FS approach will choose the optimum subset of attributes, whereas the RMS-LR system will categories them.

In the first step, data is gathered via IoT devices that are connected to patients, a different benchmark healthcare dataset, individual health information, and a hospital administration server. The majority of the medical information provided by IoT devices linked to either a person is essential. A sensor attached to a person, for example, obtains accurate patient records at regular times [31]. CKD data were translated into an acceptable format in three processes. In the beginning, a format transforming operation is performed in which real data are transformed into a .csv file format. Several attribute values together in the dataset, like Absence, Present, and Yes or No, are simultaneously converted to numeric values such as 0 and 1. The median approach would then be used to complete a dataset's missing data.

Figure 2 depicts the general SA technique procedure. The physical aim is for molten material to cool at a minimum pace to assure the process of establishing thermal equilibrium at each temperature. When the temperature approaches absolute zero, the material achieves its ground state, which is composed of relatively low crystalline lattices. When a material solidifies at a temperature below its melting temperature, it forms an unsatisfactory framework that does not consume less energy [32]. In addition, Monte Carlo methods were used to predict the appearance of a material at a particular temperature. A little random disruption to the present state "I" of material with energy S_1 created the following state "n" with energy S_n. As long as S_n is below or equal to S_1, the condition may be considered current. Otherwise, the state has been spent with the following probability.

$$\mathrm{Exp}\left(\frac{(S_1 - S_n)}{(K_b T)}\right), \tag{1}$$

where T-current temperature; K_b-Boltzmann constant.

The Metropolis criteria are given the acceptance rule that was discussed, and the model was used in conjunction with the Metropolis criterion. A state of thermal equilibrium is reached by the material whenever it is heated to any degree because the temperature has indeed been progressively dropping.

$$P_T(X = 1) = \mathrm{Exp}\left(-\frac{S_1}{K_b T}\right)_n \sum_n \exp\ \frac{(-S_n)}{(K_b T)}, \tag{2}$$

where the sum of the energies of all possible states at temperature "T" serves as the denominator in equation (2).

3.1. Feature Selection Approach. To diagnose CKD, the proposed method uses the FS methodology. The success of the provided FS technique is contingent on the success of the ISA method which has seen widespread use for combinatorial optimizing tasks. It is presumed that the ISA model is one of the primary search approaches. This will allow the algorithm to find better ways to solve the problem. In this regard, the SA model has the quality of being able to achieve the best solution in contrast to the naive local search algorithm in every given set of conditions.

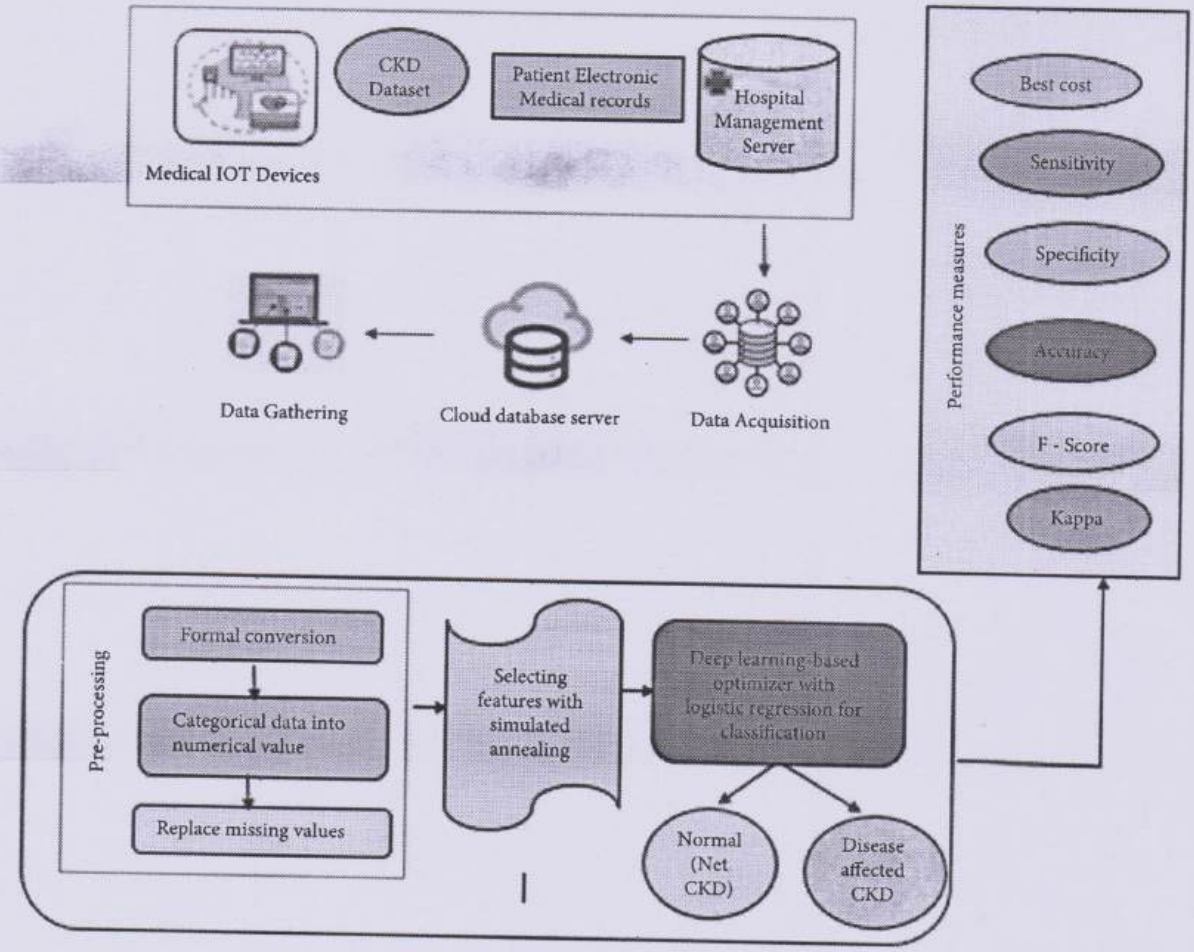


FIGURE 1: Proposed CKD system.

In most cases, it has been chosen in a completely arbitrary way because it has been a decision to be the best option. The use of the cost function allows for the estimation of the expense of an optimal state in a consecutive manner. When the temperature is unable to match the termination criterion, a solution that is adjacent to the most recent optimum solution is picked, and the cost is evaluated [33]. If the cost of a chosen adjacent solution is lower than or the same as the cost of the most recent optimum solution, then the most recent optimal solution may be swapped out for a new neighbor solution. An arbitrary function within the range has been chosen, even though the cost of nearby solutions is greater when contrasted with the cost of the present ideal solution (0, 1). When we attain this stage, the replacement of the optimum solution is initiated whenever the random value measured against is at its minimum $e = (\cos(Wn - \cos(e = \mathbf{W}_a))/T)$. After the temperature has been lowered using equation (3), the process is repeated as many times as necessary until the temperature satisfies the termination conditions.

3.2. RL-Based Classification Model. A classification task typically generates a presentation that is mapped with datasets of supplied classifications based on current data. Application of the deletion of required data content from a technique for determining the type of data. In the majority of instances, a variable has been required by the LR model for binary classification. This section defines LR approaches by focusing on two types of difficulties. This method's primary objective is to predict the existence of chronic kidney disease, which is typically confirmed using a binary classification methodology. In addition, LR approaches are often used to diagnose illnesses, identify multiple sclerosis, and classify health care data. The function of LR is to predict the presence or absence of CKD. Equation (3) demonstrates that the LR model is mostly reliant upon that linear regression technique:

$$\mathbf{R} = \alpha + \beta_1 \mathbf{i}_1 + \beta_2 \mathbf{i}_2 + \cdots + \beta_n \mathbf{i}_n. \quad (3)$$

Classification challenges are analogous to continuous-measurement-required linear regression problems. The

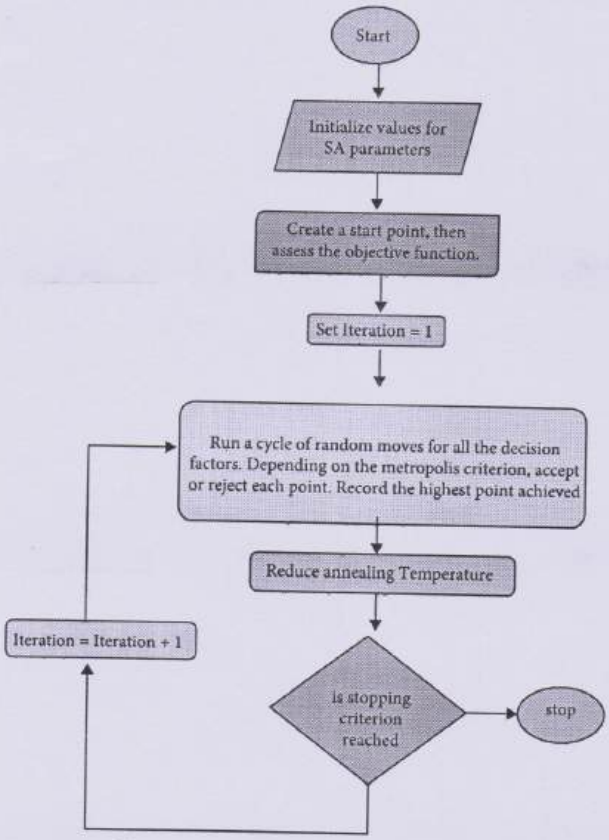


FIGURE 2: Simulated annealing model.

anticipated value of the categorization model falls between 0 and 1. The outcome is 1 if the numbers are above a specified threshold; otherwise, it is 0. Therefore, the LR parameter sequence falls inside the range [0, 1]. LR indicates that this level employs a sigmoid function. The entire linear model that detects the disease when such a sigmoid function has been applied is a feature.

$$\begin{aligned}
&\Pr(A = +1|B) \sim \beta.B \text{ and} \\
&\Pr(A = -1|B0 = 1 - \Pr(A = +1|Z), \\
&\downarrow\sigma(x) = \frac{1}{1+e^{-x}} \in [0,1], \\
&\Pr(A = +1|B) \sim \sigma(\beta.B) \text{ and,} \\
&\Pr(A = -1|B) = -\Pr(A = +1|B).
\end{aligned} \tag{4}$$

Classification is used at both the positive and the negative class levels here. Where "P" represents the existence of CKD, "Q" indicates the collection of eight elements' independent variables. Each regression model "Q" has a coefficient value represented by, which represents the weight. As determined by the LR model, these database values consist of weight values. It provides several linkages between Q and P for different weights. LR parameters may be altered to get an

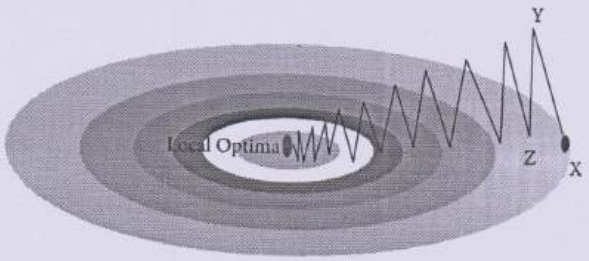


FIGURE 3: General RMSProp progress model.

optimal classification output. At this phase, the RMS model is utilized to choose the LR parameters.

The RMSProp model is based on the construction of such a weighted sum of grades, including such Gradient Descent (GD), using different progression parameters. Consider the scenario and evaluate a cost function made up of contours, with the red dot representing a local optimum. The very first iteration for GD begins at position 'A' and ends at point 'B;' Figure 3 shows the other end of an ellipse. The next phase of GD concludes at point 'C.' It reaches the optimum solution in ascending and descending dimensions faster than any prior iteration of GD. Although there is a greater learning value implementation, a lateral oscillation has a significant amplitude and decreases the GD while removing the higher learning value implementation. Vertical oscillations are caused by biases, but the horizontal motion is caused by weight. Vertical oscillation is reduced when the 'weights' are increased in value and the bias is adjusted. In backward propagation (BP), these parameters dW and db are utilized to modify W, whereas b is a fixed value.

$$\begin{aligned}
W &= W - \text{learningrate} * dW, \\
B &= B - \text{learningrate} * db.
\end{aligned} \tag{5}$$

RMSprop uses progressively average values of either a squared of dW and db rather than the nonepoch-dependent distribution of dW and db.

$$\begin{aligned}
SdW &= \beta * SdW + (1-\beta) * dW^2, \\
Sdb &= \beta * Sdb + (1-\beta) * db^2,
\end{aligned} \tag{6}$$

where β signifies an alternative hyperparameter that accepts the values 0 and 1, respectively. To compute the new weighted average, the weight from the average of previous values and the square of current values are assumed. In the factors updating process that follows the estimate of upper bound averages, SdW is quite small and Sdb is rather large.

$$\begin{aligned}
W &= W - \text{learning rate} * \frac{dW}{\sqrt{SdW}}, \\
b &= b - \text{learning rate} * \frac{dW}{\sqrt{Sdb}}.
\end{aligned} \tag{7}$$

Table 1: Dataset description.

Description	Value
Instances count	535
Features count	28
Class count	3
Percentage of positive samples	72.56%
Percentage of negative samples	37.52%
Data source	Own data from UCI data repository

Table 2: Analysis with CKD detection feature selection methodology results.

Methods	Best cost	Selected features
Proposed system	0.01054	7, 14,8,10,20,6,5,13,4,2,3
PSO-FS	0.03657	15,13,24,23,12,20,12,7,19,2,8,2,14,4, 1,5,18,17
GA-FS	0.03440	15,23,12,8,13,16,21,19,2,14,24,17,13, 5,3,9,3,20
PCA	0.04570	1,2,3,4,5,6,7,8,9,10,11,12,13,14,15, 16,17,18,19

3.3. Performance Validation. The effectiveness of the provided paradigm is validated by a comprehensive comparison with current practices. The proposed simulation was performed using MATLAB software. The number of Maximum iterations is set to 20, the Maximum Subiterations number is set to 5, and Initial Temp T0 is set to 10, with Temp. Reduction Speed alpha is set to 0.99. Table 1 depicts the dataset's overview and its accessible elements. The CKD dataset has a total of 400 occurrences with 24 characteristics. 250 occurrences are categorized as having chronic kidney disease (CKD), whereas the remaining 150 examples are designated as not having CKD.

4. Results and Discussion

The results of applying FS models to the CKD dataset are shown in Table 2, which can be found here. The optimum cost analysis of such SA-FS model that was supplied may be seen shown in Figure 4. With the best cost of 0.79, the table values proposed that perhaps the CFS model produced worse FS outcomes. In addition, it is shown that the best cost of the Principal Component Analysis technique is 0.04670, which is somewhat less than CFS but not significantly lower than competing models. The GA-FS and PSO-FS models have surpassed their predecessors and achieved almost equal best costs around 0.04640 and 0.04746, respectively. However, the proposed SA-FS model has selected just the thirteen qualities with the optimum cost, which is 0.01105. This lowest possible cost supplied by the SA-FS model ensured its greater performance in comparison to its predecessors.

Figure 5 depicts the various confusion matrices resulting from either the implementation of RMS-LR technology without FS at various epoch counts. The RMS-LR model has identified 182 cases as active and 150 instances as missing, as shown by the epoch count of 400. Likewise, for the epoch value of 800, the RMS-LR algorithm has categorized 117 cases as current and 150 occurrences as missing. Similarly, under the epoch value of 1200, the RMS-LR algorithm has identified 237 occurrences as present and 147 as missing. Concurrently, the RMS-LR algorithm has identified 242 cases as active and 146 occurrences as missing under the 2000 epoch count.

Figure 6 depicts several confusion matrices resulting from implementing ISA-RMS-LR using FS at varied epoch counts. Using such a different epoch count of 400 indicates that the ISA-RMS-LR method has identified 243 occurrences

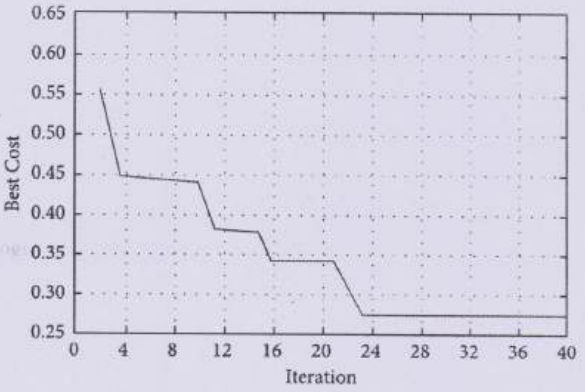


Figure 4: Comprehensive cost estimate of the ISA-FS technique.

as present and 145 instances as missing in a collection. Similarly, a count of 800 epochs demonstrates that the ISA-RMS-LR system classifies 243 cases as present and 145 instances as missing. By this, it is seen that, under the epoch count of 1600, the ISA-RMS-LR method has categorized 247 occurrences that were present and 146 instances were absent. The ISA-RMS-LR algorithm has categorized 246 cases as present and 146 instances are absent under the 2000 epoch count.

After evaluating the classifier results provided by an ISA-RMS-LR system under various epoch counts, it was determined that perhaps the ISA-RMS-LR model may provide the most precise classification performance when the epoch count is between 1600 and 2000. Figure 7 demonstrates that in this specific round, the ISA-RMS-LR algorithm classifies 247 cases as present and 146 instances as absent.

Figure 8 illustrates the accuracy of the RMS-LR and ISA-RMS-LR models concerning the 2000 epoch data. The ISA-RMS-LR produces more accuracy than the RMS-LR method. The precision of both proposed models increases as the number of epochs increases, reaching a peak at 2000 epochs. Figure 9 illustrates the loss curves for the RMS-LR with ISA-RMS-LR algorithms for varied numbers of 2000 epochs. It has been demonstrated that the ISA-RMS-LR model produces a lower loss rate than the RMSPO-LR model. The real loss of the proposed models starts to decrease as the number of epochs increases and becomes constant around 2000 epochs. The addition of an SA-based FS procedure dramatically reduces the loss graph, as seen.

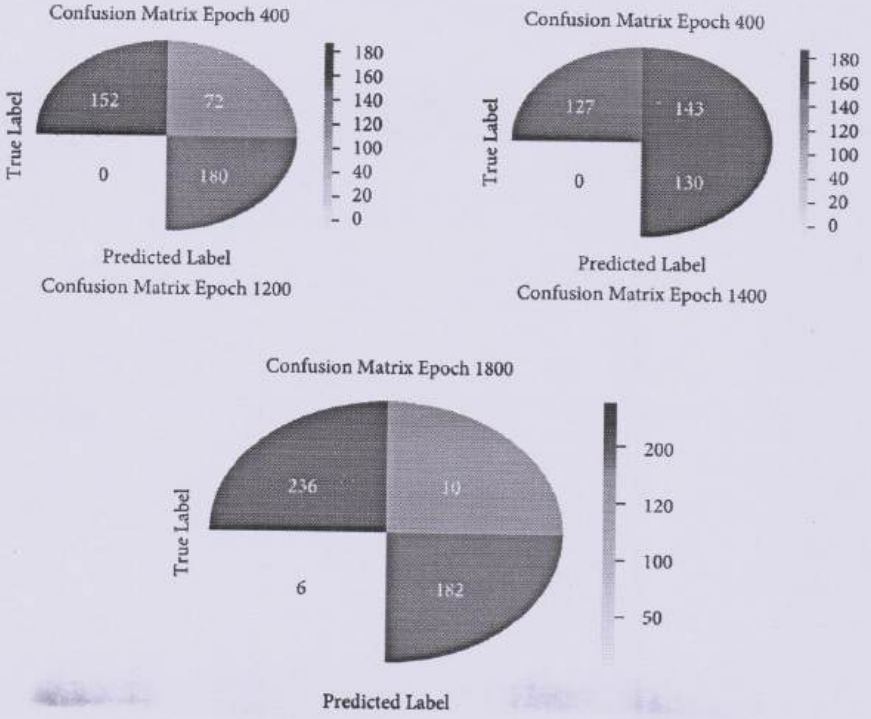


FIGURE 5: Confusion matrix for RMS-LR from 2000 Epoch FS.

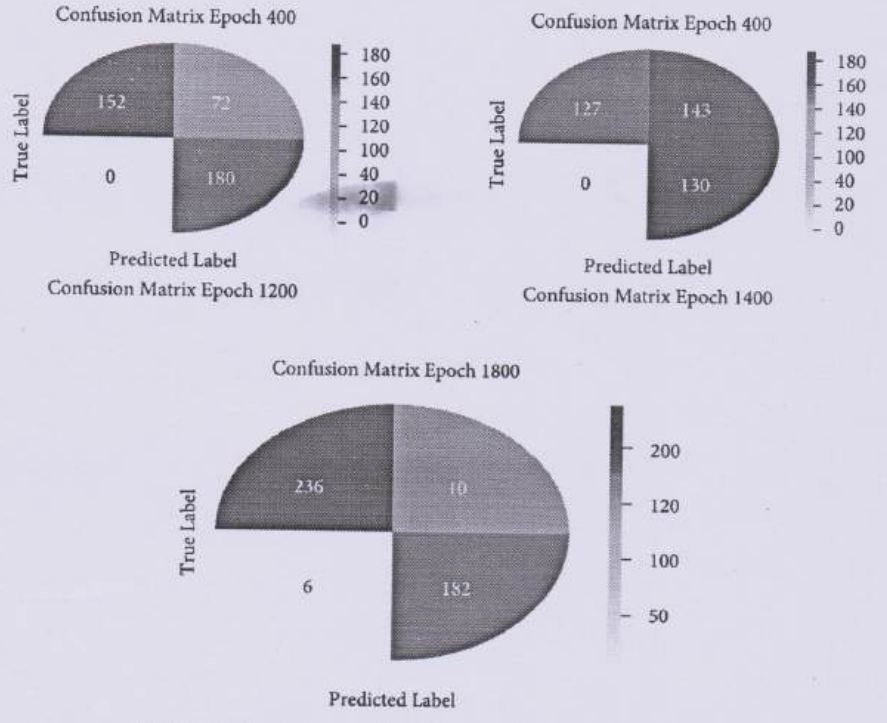


FIGURE 6: Confusion matrix of proposed system 2000 Epochs.

The outcomes of the ISA-RMS-LR model to those of current models for a variety of metrics compare in Table 3. Figure 10 presented a comparative examination of the sensitivity and specificity of the ISA-RSM-LR model's findings. In addition, it is discovered that the D-ACO yields successful outcomes with sensitivity and specificity values around 86.00% and 83.35%, respectively. Upon continuation, the DT model yields a somewhat tolerable performance

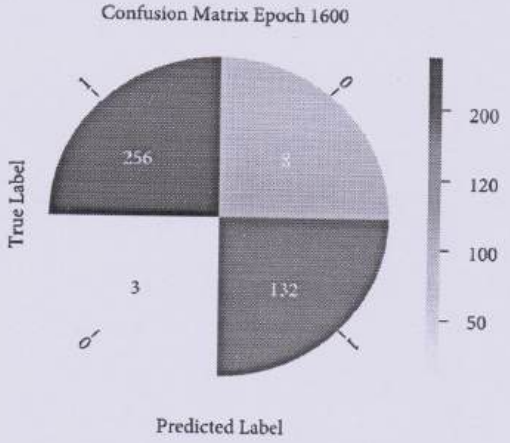
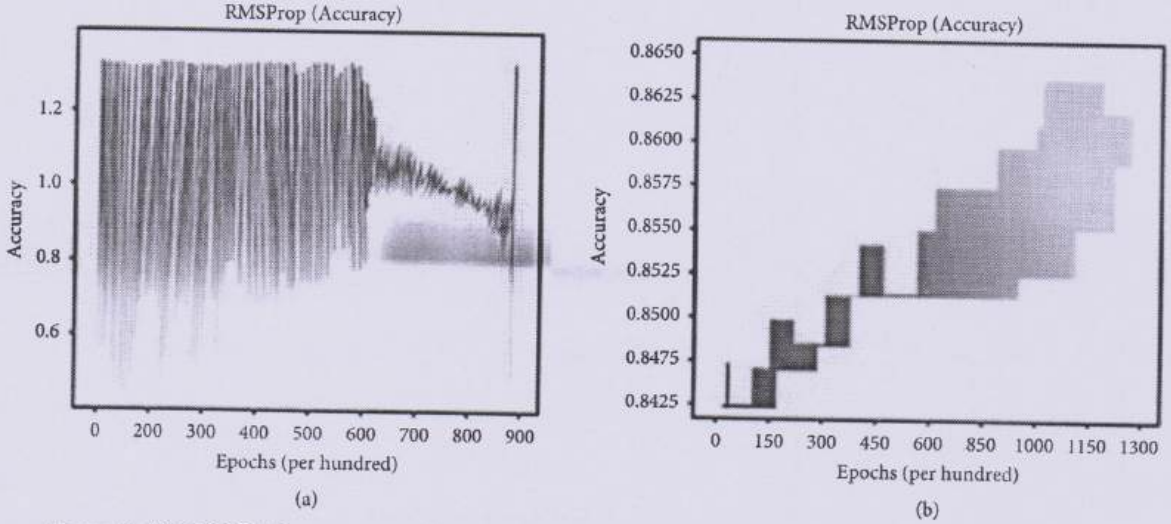
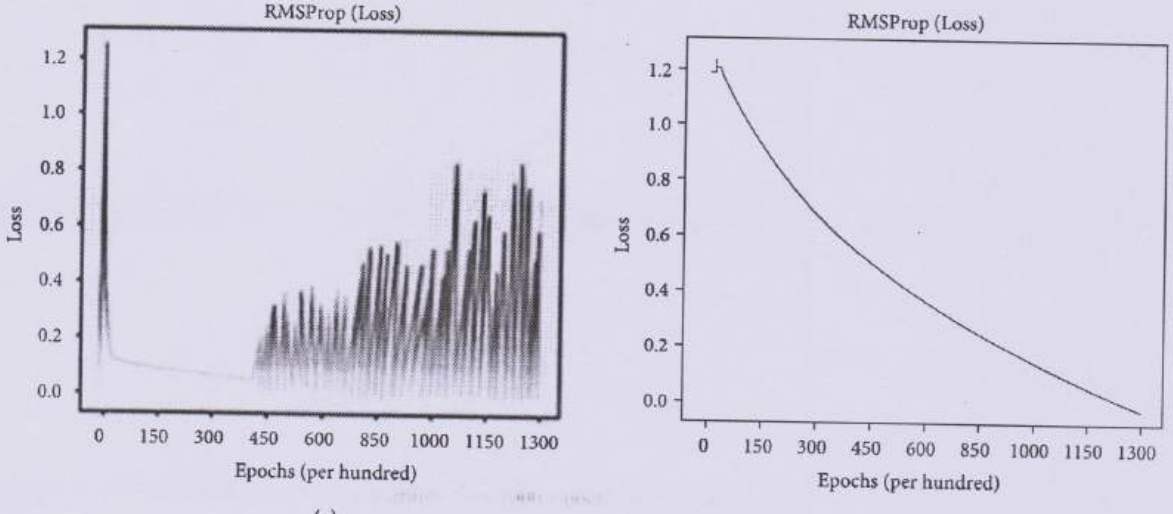


FIGURE 7: Confusion matrix for 1600th iteration.



(a) (b)

FIGURE 8: (a) RMSPO-LR accuracy graph with 2000 Epochs (b) ISA-RMS-LR accuracy graph with 2000 Epochs.



(a) (b)

FIGURE 9: (a) RMS-LR Loss Graph with 2000 Epochs (b) ISA-RMS-LR Loss Graph with 2000 Epochs value.

Table 3: Proposed Method using the Performance Evaluation of CKD.

Classifiers	Performance measures				
	Sensitivity (%)	Specificity (%)	Accuracy (%)	F-score (%)	Kappa (%)
ISA-RMS-LR	99.46	98	99.26	99.63	98.29
RMSPO-LR	98.35	94.86	97.09	97.59	93.63
FNC	85.69	85.88	85.75	86.64	88.88
D-ACO	86.00	83.35	85.00	86.03	89.34

Input: CKD dataset with training
Output: FS with weight: $\mathbf{W}_a$
Step 1: Initialize $\mathbf{W}_a \leftarrow$ NULL; $P \leftarrow 1000000$; $S \leftarrow 0.9$
Step 2: It produces an initial solution, $\mathbf{W}_1$;
Step 3: Assign $\mathbf{W}_a \leftarrow \mathbf{W}_1$;
Step 4: Calculate the initial solution cost as cost $(\mathbf{W}_a)$;
Step 5: While $(T > 0.001)$ do
{
Step 6: Choose a nearby arbitrary solution, $\mathbf{W}_n$ from $\mathbf{W}_a$ that has one bit varied from $\mathbf{W}_a$;
Step 7: If $(\text{cost}(\mathbf{W}_a) = \text{cost}(\mathbf{W}_n))$;
{
Assign $\mathbf{W}_a \leftarrow \mathbf{W}_n$;
}
else
{
Develop an arbitrary number "a" range between (0.1);
If $(a < e(\text{costt}(w_n) - \cos t(W_a)/T))$.
{
Assign $\mathbf{W}_a \leftarrow \mathbf{W}_n$; $T \leftarrow S \times T$
}
}
}

Algorithm 1: ISA-Based Feature Selection.

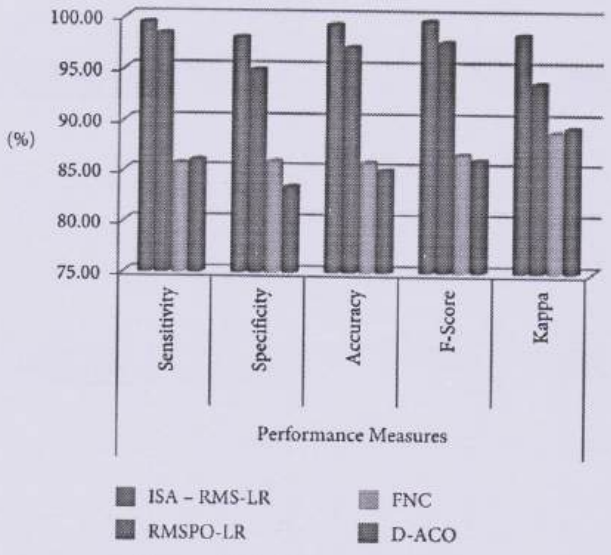


Figure 10: Performance measures.

using sensitivity and precision values of 91.38% and 88.28%, respectively. Similarly, the MLP model must achieve a classifier with sensitivity and precision values of around 93.30% and 93.86%, respectively. Simultaneously, the FNC model has shown consistent results, having sensitivity and accuracy values around 85.69% and 85.75%, respectively. The RMS-LR model has generated an effective classifier having sensitivity and accuracy values of around 98.35 percent and 97.09 percent, respectively. The maximal sensitivity and specificity values for the proposed ISA-RMS-LR models are 99.46% and 98%, respectively. In addition, it is shown that the LR has a significantly superior Kappa value of around 74.60%. In contrast, it is obvious that perhaps the XGBoost algorithm has achieved the same Kappa value at 75.42 percent. In addition, the PSO model beat current frameworks with a 68% higher Kappa value. In addition, ACO prefers to provide effective outcomes with a Kappa value of around 73.06%. However, with Kappa values of around 79.37%, the DT model produced slightly reasonable results. With Kappa values of 84.78 percent, the MLP model also achieves good classifier performance. Likewise, the FNC structure has shown consistency with a Kappa value of around 91.87 percent. Concurrently, it is obvious that the D-ACO approach produced a Kappa value that is even

higher, 88.33%. With both a Kappa value of 94.63 percent, the RMSPO-LR system is projected to provide competitive classification results. Therefore, the proposed ISA-RMS-LR method has produced results with a superior Kappa value of 93.26 percent. By evaluating the previous tables and graphs, it is determined that the RMSPO-LR model is a suitable medical diagnosis for CKD and may be utilized in real-time.

5. Conclusion

Using the ISA-RMS-LR model, this research assessed the optimal IoT and cloud-based decision support method for diagnosing CKD. Initially, the data collecting method captures the patient's information via medical devices. The gathered data are then preprocessed in preparation for future processing. The SA-FS method is then executed, and a subset of characteristics is provided to RMS-LR-based classifiers. The proposed classifier correctly identified the existence of CKD. The results of a detailed experimental investigation are verified using a benchmark dataset of CKD. The simulation results are reviewed for a range of epoch counts. According to the experimental findings, the proposed ISA-RMS-LR model effectively classifies patients with CKD, with high sensitivity at 99.46%, accuracy at 99.26%, Specificity at 98%, *F*-score at 99.63%, and kappa value at 98.29%. The obtained findings demonstrated the improved classification performance in comparison to the techniques evaluated. Clustering approaches may be used to enhance the performance of both the ISA-RMS-LR CKD diagnostic model as part of our future research. The framework intends to provide a complete patient history at home and around the world where the worldwide cloud server is frequently used, allowing the patient to easily access but also track health care providers from any location by logging through into platform, transferring past data, and accessing the web page data.

Data Availability

No data were used to support this study.

Conflicts of Interest

The authors declare that they have no conflicts of interest.

References

[1] B. Sumathy, S. Kavimullai, S. Shushmithaa, and S. S. Anusha, "Wearable non-invasive health monitoring device for elderly using IOT IOP conference series: materials science and engineering," *IOP Conference Series: Materials Science and Engineering*, vol. 1012, no. 1, Article ID 012011, 2021.

[2] Y. Xie, L. Lu, F. Gao et al., "Integration of artificial intelligence, blockchain, and wearable technology for chronic disease management: a new paradigm in smart healthcare," *Current Medical Science*, vol. 41, no. 6, pp. 1123–1133, 2021.

[3] G. Maniam, J. Sampe, R. Jaafar, and M. F. Ibrahim, "Smart monitoring system for chronic kidney disease patients based on fuzzy logic and IoT," *International Journal of Advanced Computer Science and Applications*, vol. 13, no. 2, 2022.

[4] H. Naz, R. Sharma, N. Sharma, and S. Ahuja, "IoT-inspired smart healthcare service for diagnosing remote patients with diabetes," in *Machine Learning for Edge Computing*, pp. 97–114, CRC Press, Boca Raton, FL, USA, 2022.

[5] S. Chitra and V. Jayalakshmi, "Analyze the medical threshold for chronic kidney diseases and cardio vascular diseases using internet of things," in *Proceedings of the 2021 4th International Conference on Computing And Communications Technologies (ICCCT)*, pp. 189–193, IEEE, Chennai, India, December 2021.

[6] S. Mishra, H. K. Thakkar, P. K. Mallick, P. Tiwari, and A. Alamri, "A sustainable IoHT based computationally intelligent healthcare monitoring system for lung cancer risk detection," *Sustainable Cities and Society*, vol. 72, Article ID 103079, 2021.

[7] L. T. Pugazhendhi, R. Kothandaraman, and B. Karnan, "Implementation of visual clustering strategy in self-organizing map for wear studies samples printed using FDM," *Traitement du Signal*, vol. 39, no. 2, pp. 531–539, 2022.

[8] P. Dileep and M. Thogaru, "Real time cloud computing based COVID-19 health monitoring system using IOT with integration of machine learning approach to create safety environment," *Annals of the Romanian Society for Cell Biology*, vol. 25, pp. 2076–2086, 2021.

[9] S. Maxwell and M. Grupac, "Virtual care technologies, wearable health monitoring sensors, and internet of medical things-based smart disease surveillance systems in the diagnosis and treatment of COVID-19 patients," *American Journal of Medical Research*, vol. 8, no. 2, pp. 118–131, 2021.

[10] J. Wang, Y. Wang, P. Pang, X. Jia, X. Yan, and Z. Lv, "Clinical analysis of the renal protective effect of GLP-1 on diabetic patients based on edge detection," *Journal of Healthcare Engineering*, vol. 2022, Article ID 6504006, 9 pages, 2022.

[11] R. Rajasekar and P. Sivakumar, "Swarm based intelligent transportation systems using internet of things in vehicular ad-HOC network," *Journal of Computational and Theoretical Nanoscience*, vol. 17, no. 12, pp. 5503–5508, 2020.

[12] R. P. Siguas, E. M. Solis, and H. M. Solis, "Design of a body temperature measurement system applied to health center personnel," *International Journal of Emerging Technology and Advanced Engineering*, vol. 12, no. 2, pp. 20–28, Article ID 22502459, 2022.

[13] R. P. Siguas, E. M. Solis, H. M. Solis, and L. M. Zamudio, "Non-invasive glucose meter system for monitoring diabetic patients using the photoplethysmographic signal," *International Journal of Emerging Technology and Advanced Engineering*, vol. 12, no. 6, pp. 14–19, Article ID 22502459, 2022.

[14] K. Sridharan and P. Sivakumar, "A systematic review on techniques of feature selection and classification for text mining," *International Journal of Business Information Systems*, vol. 28, no. 4, pp. 504–518, 2018.

[15] R. Perez-Siguas, E. Matta-Solis, H. Matta-Solis, and L. Matta-Zamudio, "Automated system for the classification of diabetic retinopathy," *International Journal of Emerging Technology and Advanced Engineering*, vol. 12, no. 6, pp. 40–46, 2022.

[16] T. P. Latchoumi, R. Swathi, P. Vidyasri, and K. Balamurugan, "Develop new algorithm to improve safety on WMSN in health disease monitoring," in *Proceedings of the 2022 International Mobile and Embedded Technology Conference (MECON)*, pp. 357–362, Noida, India, March 2022.

[17] F. Shafqat, M. N. A. Khan, and S. Shafqat, "SmartHealth: IoT-enabled context-aware 5G ambient cloud platform," in *IoT in Healthcare and Ambient Assisted Living*, pp. 43–67, Springer, Singapore, 2021.

[18] A. S. Albahri, J. K. Alwan, Z. K. Taha et al., "IoT-based telemedicine for disease prevention and health promotion:

state-of-the-Art," *Journal of Network and Computer Applications*, vol. 173, Article ID 102873, 2021.

[19] S. V. K. R. Rajeswari and V. Ponnusamy, "AI-Based IoT analytics on the cloud for diabetic data management system," in *Integrating AI in IoT Analytics on the Cloud for Healthcare Applications*, pp. 143–161, IGI Global, Pennsylvania, PA, USA, 2022.

[20] J. B. Awotunde, S. O. Folorunso, A. K. Bhoi, P. O. Adebayo, and M. F. Ijaz, "Disease diagnosis system for IoT-based wearable body sensors with machine learning algorithm," in *Hybrid Artificial Intelligence and IoT in Healthcare*, pp. 201–222, Springer, Singapore, 2021.

[21] J. Yarlagaddaa and M. Ramakrishna, "Fabrication and characterization of S glass hybrid composites for Tie rods of aircraft," *Materials Today Proceedings*, vol. 19, pp. 2622–2626, 2019.

[22] T. Bikku, K. S. Sree, J. Jarugula, and M. Sunkara, "A novel integrated IoT framework with classification approach for medical data analysis," in *Proceedings of the 2022 9th International Conference on Computing For Sustainable Global Development (INDIACom)*, pp. 710–715, IEEE, New Delhi, India, March 2022.

[23] K. Lakshmanan and S. Arumugam, "An efficient data science technique for IoT assisted healthcare monitoring system using cloud computing," *Concurrency and Computation: Practice and Experience*, vol. 34, no. 11, Article ID e6857, 2022.

[24] J. H. Majeed and Q. Aish, "A remote patient monitoring based on WBAN implementation with internet of thing and cloud server," *Bulletin of Electrical Engineering and Informatics*, vol. 10, no. 3, pp. 1640–1647, 2021.

[25] M. N. Alraja, H. Barhamgi, A. Rattrout, and M. Barhamgi, "An integrated framework for privacy protection in IoT—applied to smart healthcare," *Computers & Electrical Engineering*, vol. 91, Article ID 107060, 2021.

[26] J. Yarlagaddaa and R. Malkapuram, "Influence of MWCNTs on the mechanical properties of continuous carbon epoxy composites," *Revue des Composites et des Matériaux Avancés*, vol. 30, no. 1, pp. 35–41, 2020.

[27] A. Motwani, P. K. Shukla, and M. Pawar, "Novel framework based on deep learning and cloud analytics for smart patient monitoring and recommendation (SPMR)," *Journal of Ambient Intelligence and Humanized Computing*, pp. 1–16, 2021.

[28] R. K. Kher and D. M. Patel, "A comprehensive review on wearable health monitoring systems," *The Open Biomedical Engineering Journal*, vol. 15, no. 1, pp. 213–225, 2021.

[29] G. Geetha and K. M. Prasad, "The strategies to reduce healthcare costs and increase the quality of healthcare service delivery using hybrid technologies," in *Proceedings of the 2021 Asian Conference on Innovation in Technology (ASIANCON)*, pp. 1–7, IEEE, Pune, India, August 2021.

[30] M. Imran, U. Zaman, J. Imtiaz, J. Imtiaz, M. Fayaz, and J. Gwak, "Comprehensive survey of iot, machine learning, and blockchain for health care applications: a topical assessment for pandemic preparedness, challenges, and solutions," *Electronics*, vol. 10, no. 20, p. 2501, 2021.

[31] V. Ponnusamy, J. Christopher Clement, K. C. Sriharipriya, and S. Natarajan, "Smart healthcare technologies for massive internet of medical things," in *Efficient Data Handling for Massive Internet of Medical Things*, pp. 71–101, Springer, Cham, Switzerland, 2021.

[32] M. Haghi Kashani, M. Madanipour, M. Nikravan, P. Asghari, and E. Mahdipour, "A systematic review of IoT in healthcare: applications, techniques, and trends," *Journal of Network and Computer Applications*, vol. 192, Article ID 103164, 2021.

[33] G. Zhang and N. J. Navimipour, "A comprehensive and systematic review of the IoT-based medical management systems: applications, techniques, trends and open issues," *Sustainable Cities and Society*, vol. 82, Article ID 103914, 2022.

Source details

Feedback > Compare sources >

Computational Intelligence and Neuroscience

Scopus coverage years: from 2007 to 2022
(coverage discontinued in Scopus)
Publisher: Hindawi
ISSN: 1687-5265 E-ISSN: 1687-5273
Subject area: Mathematics: General Mathematics | Computer Science: General Computer Science | Neuroscience: General Neuroscience
Source type: Journal

View all documents > | Set document alert | Save to source list

CiteScore 2021
3.9

SJR 2021
0.863

SNIP 2022
1.023

CiteScore | CiteScore rank & trend | Scopus content coverage

Improved CiteScore methodology
CiteScore 2021 counts the citations received in 2018-2021 to articles, reviews, conference papers, book chapters and data papers published in 2018-2021, and divides this by the number of publications published in 2018-2021. Learn more >

CiteScore 2021

3.9 = 4,319 Citations 2018 - 2021
1,113 Documents 2018 - 2021

Calculated on 05 May, 2022

CiteScore rank 2021

Category	Rank	Percentile
Mathematics General Mathematics	#33/391	91st
Computer Science General Computer Science	#63/731	72nd
Neuroscience General Neuroscience	#66/112	41st

39

Contents lists available at ScienceDirect

Measurement: Sensors

journal homepage: www.sciencedirect.com/journal/measurement-sensors



Heterogeneous sensor data fusion acquisition model for medical applications

Jyoti Dhanke [a,*], M. Pradeepa [b], R. Karthik [c], Veeresh Rampur [d], I. Poonguzhali [e], Hemanand Chittapragada [f]

[a] Department of Engineering Science (Mathematics), Bharati Vidyapeeth's College of Engineering, Lavale, Pune, 412115, Maharashtra, India
[b] School of Information Technology and Engineering, Vellore Institute of Technology, Vellore, Tamil Nadu, 632 014, India
[c] School of Electronics and Communication Engineering, REVA University, Bangalore, India
[d] Dept of Electronics, Government First Grade College, Naubad, Bidar, 585401, Karnataka State, India
[e] Department of ECE, Panimalar Engineering College, Poonamallee, 600123, Tamilnadu, India
[f] Department of CSE, Sri Vasavi Engineering College, Tadepalligudem, 534101, Andhra Pradesh, India

ARTICLE INFO

Keywords:
Transfer learning idea
IoT-based electrocardiogram
Performance measures
Authentication
Fusion model

ABSTRACT

Electrocardiogram (ECG) and portable technologies with Internet of Things (IoT)-based biometric authentication have recently gained popularity. As a cutting-edge, potent technique utilized in numerous ways to increase authentication effectiveness over the past few decades, ECG-based biometric verification has garnered a lot of attention. However, a user's ECG signal may alter based on their health or physical condition, which would prevent verification. It should be vital to create a trustworthy method that takes into account unique ECG variations for verification to be successful. An effective and trustworthy ECG check technique is provided in this study. Using the concept of domain customization, this study presents a novel supervised learning platform. Data from many systems has been combined into a unique feature and given to a particular grader, like a Support Vector Machine (SVM), for verification. Cross-validation searches on two accessible data sets were used to assess how effective the proposed verification scheme was. The evaluation results show that the effectiveness of our suggested system achieved a verification prediction performance of 99.4% with a high level of quality & memory. The conclusions showed that the suggested strategy was well suitable for actual-time software to execute the task.

1. Introduction

Biometrics would be the quantitative assessment of an individual's distinctive physical and behavioral traits. It should be used to describe users being monitored or to regulate entry [1–3]. The fundamental principle of biometric authentication is that each person can be precisely classified according to their traits [4]. The biometric terms, which may refer to physical or behavioral objectivity, originate from the Greek words life and measure, respectively. Based on physiological or behavioral features, the two major categories of biometric identifiers were described in Ref. [5]. Consumer electronics, point-of-sale software, workplace, and public safety systems, and biometric authentication are increasingly common. Since no passwords or security codes need to be carried about, and biometric systems, that track a user's stride, could work without any direct experience with the individual being watched, the motivation behind biometric verification has been convenience as well as protection [6–8].

The biggest privacy concern about the use of biometrics was that the physical characteristics, retinal vascular drawings, and fingerprints have also been generally repaired and may not be modified. This sets them apart from non-standard variables like passwords and unique tokens that could be replaced if they were hacked, as was the case with the more than 20 million people whose fingerprints were stolen [9]. Office of Staff. The iris scanning authentication method was broken in 2015 by Jan Chrysler, popularly as "Starbug", a biostatistics study to the Chaos Computer Club. In 2017, Krissler also revealed the breaking of the scanner authentication mechanism. earlier studies have already demonstrated that Touch ID's fingerprint verification system was as unreliable by reproducing its clients' fingerprints from a high-resolution photograph [10]. The Samsung Galaxy S8 mobile phone uses an iris

* Corresponding author.
E-mail address: jyoti.dhanke@bharatividyapeeth.edu (J. Dhanke).

https://doi.org/10.1016/j.measen.2022.100552
Received 2 August 2022; Received in revised form 20 October 2022; Accepted 25 October 2022
Available online 26 October 2022
2665-9174/© 2022 The Authors. Published by Elsevier Ltd. This is an open access article under the CC BY-NC-ND license (http://creativecommons.org/licenses/by-nc-nd/4.0/).

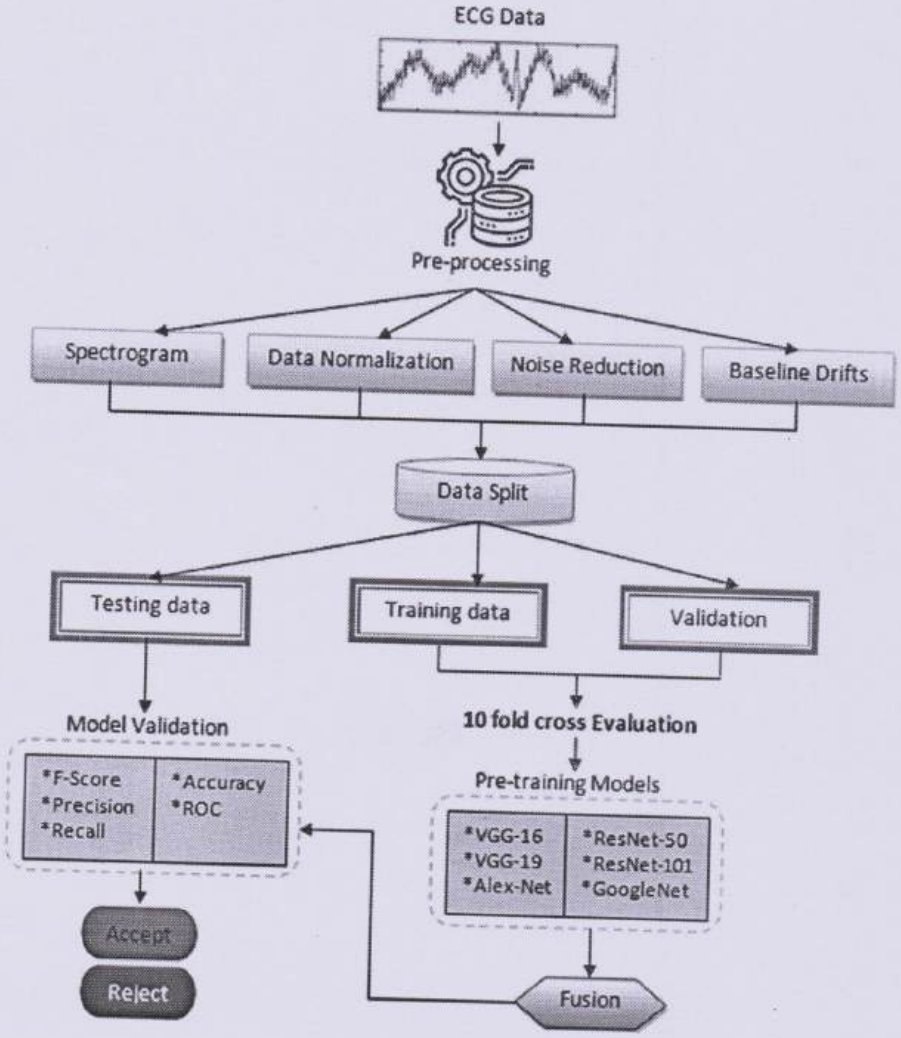


Fig. 1. The proposed verification program's block diagram.

scanner.

2. Related works

The ECG was made up of the electrical charge that the heart uses to beat. On the ECG, each component of the electric current's flow is identified by an alphabetical identifier. A heartbeat was initiated by a pulse or signal to the cardiac pacemaker [11]. This signal stimulates the two upper chambers of the heart [12]. The actuation of the atria is indicated by the P-wave. The lower cardiac chambers are then exposed to electrical charge [13]. At the ECG, the stimulation of the ventricles is represented by the QRS complex. The electrical flow then reverses course and returns to the ventricles.

They developed an ECG-based approach for identification and authentication applications, including & Gaussian Mixture Models, Support Vector Machines, and Multilayer Perceptrons, to categorization or Discrete Cosine Transform but also Haar transform for character recognition. They recorded a recognition precision of 94.9% and an identity verification error rate of 2.66%.SVM was used for categorization, and the typical spatial model technique was introduced for feature retrieval. They used a single chest-based lead of 200 participants in the PTB dataset to get the best detection accuracy of 98.92% with an EER of 0.08 [14–16]. an ECG-based verification technique that combines CNN with S-transformation.To power the CNN, they initially transformed the two-dimensional ECG signal and a one-dimensional picture. After that, they classified and extracted features using CNN [17]. The main findings were an accuracy of 96.63% and an EER of 5.68%. They performed an extensive from the ECG vector using a parallel system [18]. To apply this method more quickly, they separated the learner for categorization and employed the Adam optimizer. They obtained a 98.24% accuracy rate and a 2% EER. They extracted characteristics and categorized data using the deep learning method that was given [19]. They also increased the quantity of training data using data enhancement techniques. The proposed novel end-to-end algorithms for the segmentation and analysis of attributes; the first model utilized CNN and the second utilized ResNet with ResNet-Attention as its learning algorithm. They had a 99.27% accuracy rate.

2.1. IoT authentication system

We spoke about connecting the methodology developed to IoT devices as well as the latest technology to authenticate users using ECG signals. As more and more IoT gadgets enter the corporate, consumer, and corporate industries, including smart units, TVs, & thermostats as well as verification protocols, clinic equipment, and software applications, IoT became the hottest issue method. More gadgets could be now connected to the Network for communication and control [20–21]. In addition, new applications for portable technologies have been

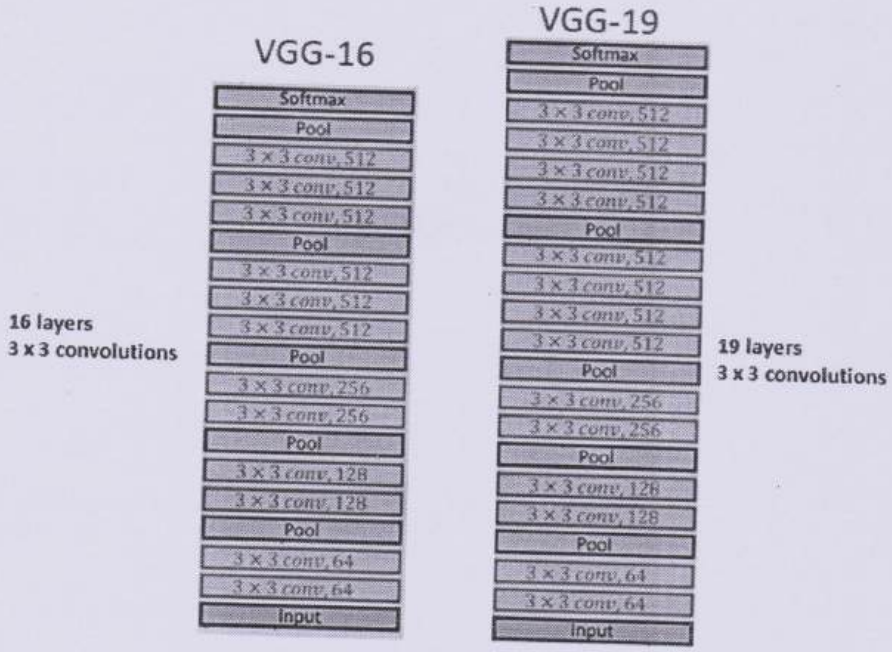


Fig. 2. The implementation of the pre-trained VGG-19 (Right) &VGG-16 (left).

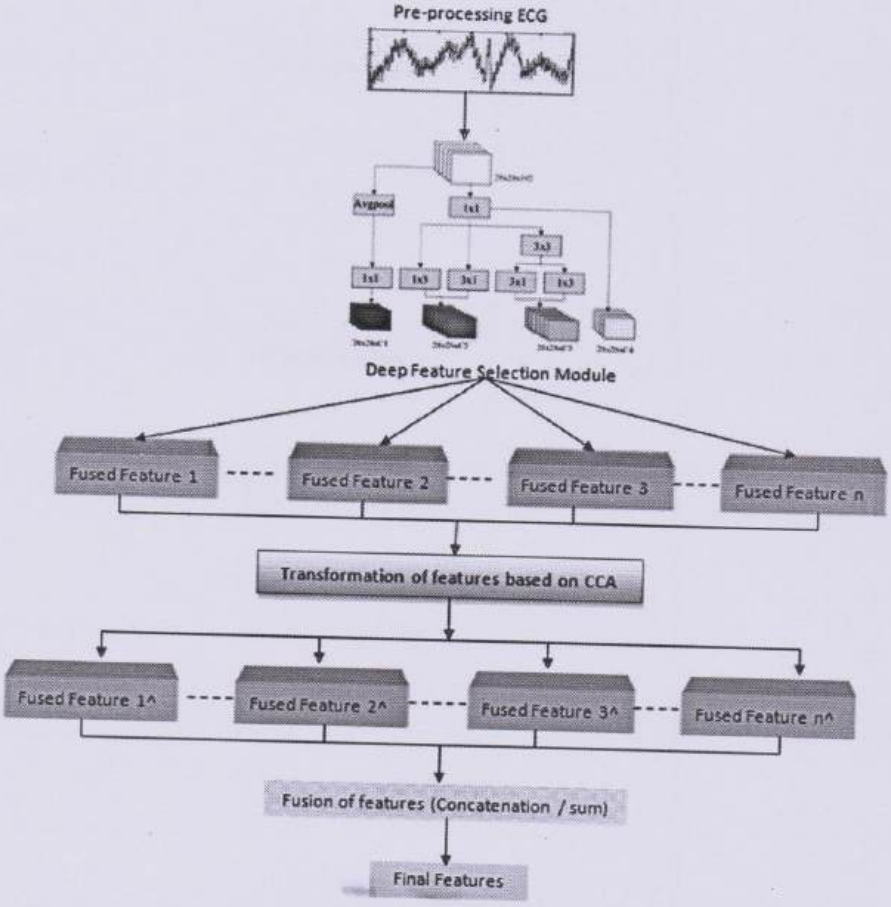


Fig. 3. Internal deep Fusion.

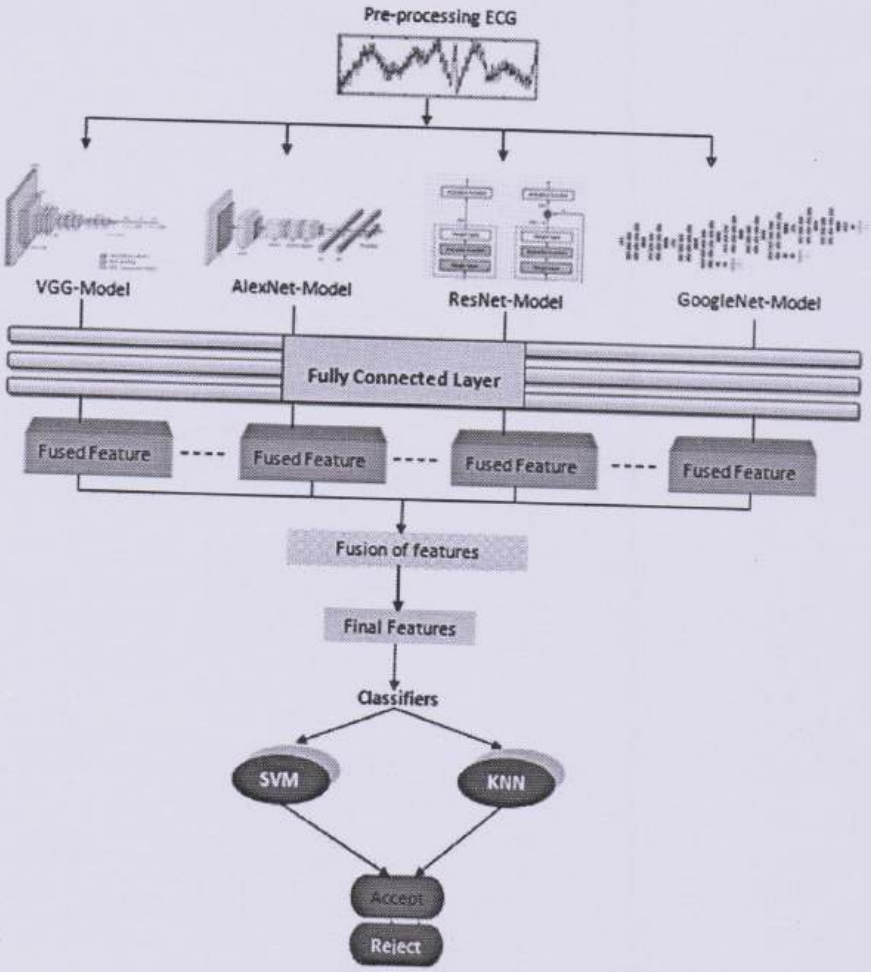


Fig. 4. The overall verification system after merging the attributes of each designer.

Table 1
Lists the attributes of the MWM-HIT program.

Conditions	Standing with exercise	Sitting	Standing	Supine	Sitting with exercise
# of records	100	100	100	100	100
Age range	22–60 years old				
Gender	66% Male and 34% Female from Total subjects of 100				

introduced that allow users to retrieve data from their devices. When these gadgets are combined with IoT, a variety of applications might be developed. Several IoT strategies could be used to use client information, particularly ECG signals, for biometric authentication. Nymi Band hash is signed by the server using the nonce server. Any random value generated by the server is suitable for this. The Nymi Band must be notified of this signature to confirm. A nonce provider & the RP decryption data were along with the signature.

3. Proposed method

The proposed ECG authentication process includes pre-processing, character recognition, feature reduction, and verification. We note that deep fusion approaches are widely used for a reliable ECG verification process [22] based on the debate in the research article. To do this, we proposed a fusion model that depends on machine learning that the deep features of the input ECG and uses it to get a reliable verification of these pulses. They begin this section to discuss the main elements of the proposed approach & the external fusion technique.

For good verification, it is necessary to have reliable pre-processing techniques. This basic step smoothes the ECG signal, lowers the

Table 2
Characteristics and algorithms of the training in a summary format.

Loss function	Categorical
Optimizer	Adam
Batch size	8
Epoch numbers	100

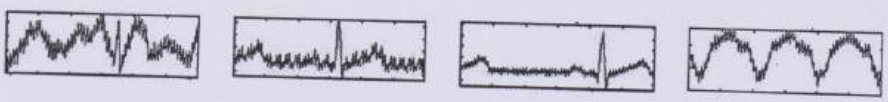


Fig. 5. Images of an ECG from the MWM-HIT data set.

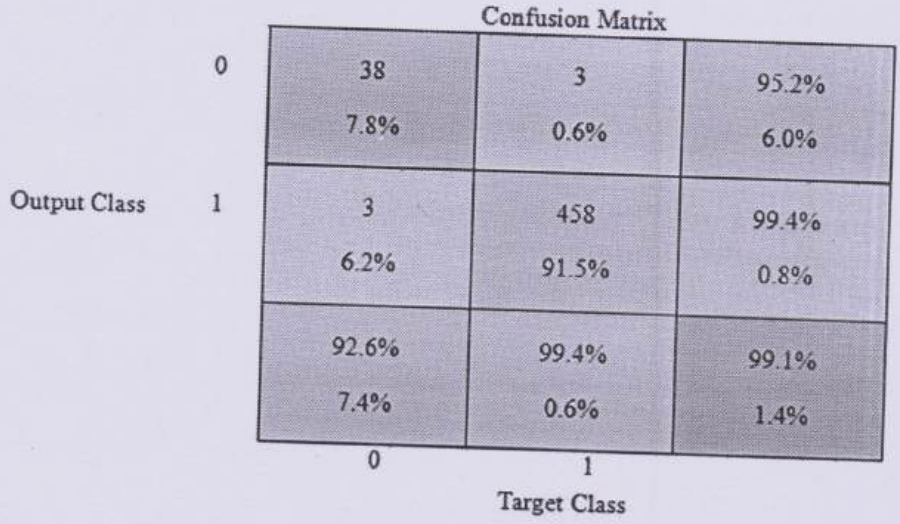


Fig. 6. Confusion matrix.

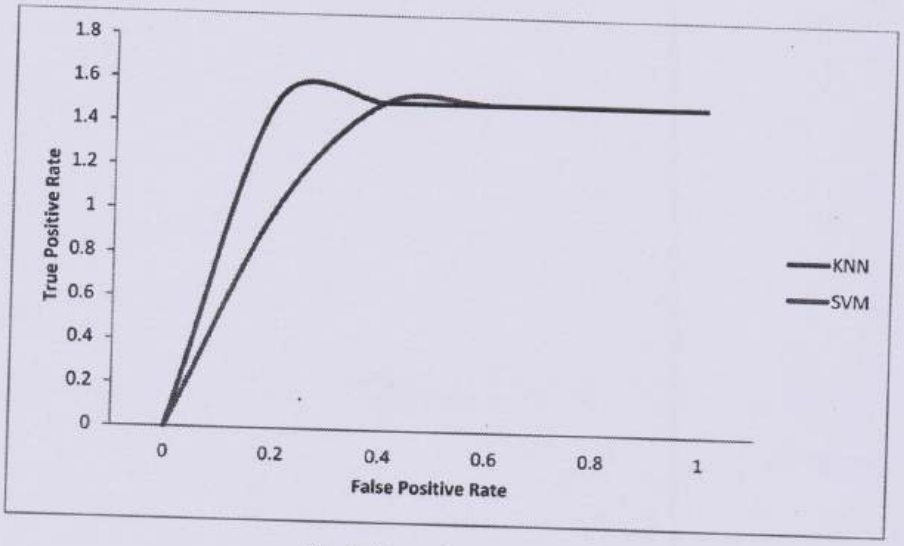


Fig. 7. Proposed system of ROC.

movement or removal of baseline drift, or removes distortion of input ECG signals [23]. The ECG promotion was ready for further computation after this preprocessing phase. It used a second-level less-pass Butterworth treatment to lessen the deformation of the input ECG signals. A signal would then be filtered using a five-order moving average. Lastly, they applied high pass filtering to lessen baseline wander and drift suppression. Without having to use a segmentation method, they were carried out on the whole ECG signal, which met the needs of a potential implementation. The 1-D ECG data were then transformed into a 2-D ECG spectrogram of a predetermined length of 224 × 224. Various pre-train designs are fed the results of the preprocessing phase.

The proposed method has helped to further speed up the rapidly evolving field of machine learning and, by extension, image categorization [24].In simple terms, transmission training allows us to benefit from an existing design that has been trained on a substantial amount of information for our purposes. As a result, creating a machine learning algorithm was reduced and because databases have undergone meticulous scrutiny could be confident in their dependability in Fig. 1.

ECG spectrogram of size 224x224, which has been processed via five sections of convolution stages for an entire 13 convolution operations, provides input to this framework, as seen in Fig. 2. These convolution layers use a very small filter (3 x 3) & padding. Following the block, a stride max pooling level was used (2, 2). The Softmax layer would then be fed three fully connected layers for categorization and ReLU stimulation.

3.1. Feature reduction stageand internal fusion

The method used for internal characteristics fusion of ECG used CCA was seen in Fig. 3. A new translation of these characteristics was generated using the CCA choosing the large characteristics of the framework. To represent each paradigm with a specific characteristic, they then combine these modified characteristics using inclusion or composition. Combining or concatenating all models to fuse them. We combine two useful attributes obtained from the ECG image with useful space in this fusion, which contains more detailed information than the input characteristics [25]. Following the use of this merge, the functionality extraction would include specific information to correctly describe the ECG image. As a result, this fusion is thought to be a reliable and effective method. Fig. 4 illustrates the end system after merging all previously different classifiers. The final characteristics were collected and transmitted to the appropriate algorithms (SVM or KNN).

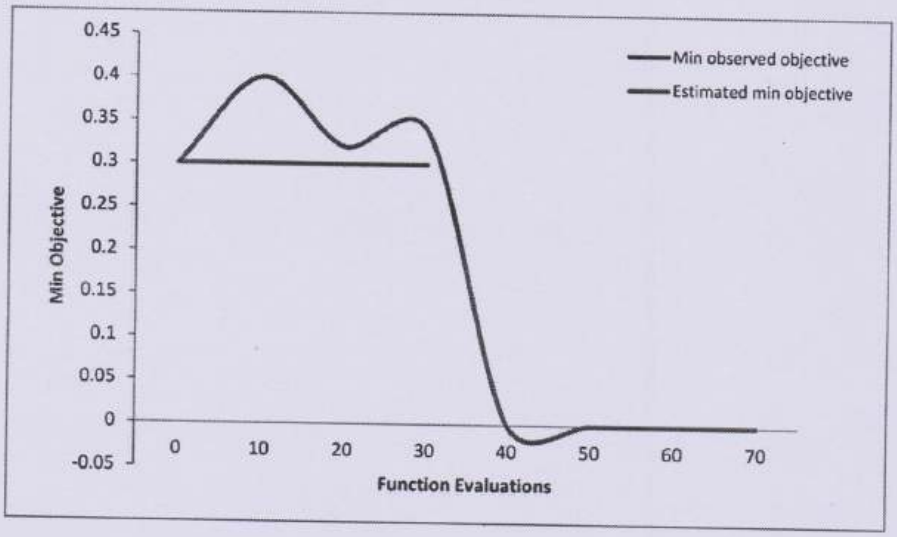


Fig. 8. Minimum goal and the quantity of computational power.

Table 3
The proposed system works when KNN and SVM.

Classifier	Accuracy(%)	Pre(%)	Rec(%)	F-score(%)
KNN	99	99.3	95	97.1
SVM	99.4	99.4	100	99.6

Researchers used five familiar categories at this stage, choosing the one with the highest level of verification validity. The following methods are used:

3.1.1. Support Vector Machine (SVM)

By locating a hyperplane that divides data into different domains, it should be a machine-learning approach that could be used for regression and classification issues. Linear SVMs for two-class issues and non-linear SVMs for several-class issues are the two primary SVM varieties.

3.1.1.1. CNN. It is one of the collective's supervised learning algorithms, and to use and consume for a short time, these are the simplest algorithms.

3.1.1.2. Random Forest. Random Forest creates potent & customizable neural network models. When there is a high percentage of missing information, accuracy has been maintained because it may be managing unbalanced information with missing data. The designer's size, however, should be larger than the amount of information to be assessed.

4. Results and discussion

We thoroughly assess & merged the effective accuracy of the experiment-tuned transmission training methods, namely, ResNet-50, GoogleNet, VGG-16, VGG-19, and Alex-NetResNet-101 utilized publicly available ECG databases to show the effectiveness of proposed methods of verifying the ECG signals. The investigations were conducted using the MATLAB 2019a program On an operating system Windows 10 Pro& an Intel Core i7 CUP and 16 GB of RAM. We used a tenfold cross-validation method to look at the proposed model.

10-s ECG recordings of 100 topics are available in this dataset. Each subject has five distinct samples, totaling 500 papers, each with a specific situation. The five states were sitting, standing, on their backs, sitting, and standing. To monitor, the Carewell ECG workstation was used. The collection device, the PCECG-500 A ECG data management program, the accompaniment device, & a PC were four components. At 1000 frames per second, samples have been digitally converted. The ECG of the patients is recorded using four sensors, similar to the arrangement for connections I, II, & III. The four components stand in for the right leg, right hand, left leg, and left hand. Table 1 displays the attributes of that data gathering. Fig. 5 shows the samples from the MWM-HIT data set.

4.1. Performance metrics

The proposed verification method was evaluated based on the F-score criterion. The program evaluation produced the following results. The first outcome would be the f-score & estimated period for the ECG verification scheme. The second result lists the FARs, FRRs, and Precision for the program. We use many pre-trained methods & implement them to ECG signals to obtain the feature information to examine the experimental findings of our approach on the aforementioned databases. Then, we choose the completely bound levels of each system to characterize these traits, as we combine levels within the internal system. To combine the selected depth functionality for each release, they use summation and conjunction procedures. The researchers used a linear SVM grader for verification because it was carried out in both datasets. Table 2 provides a summary of the variables and transactions used in model development. The proposed confusion matrix is shown in Fig. 6.

The ROC curve of the proposed verification program with the SVM and KNN algorithms is depicted in Fig. 7. From the previous ROC plot, it is clear that the SVM, which works better than the KNN classifier, was used by the proposed model for maximum reliability. The KNN could also be used for audit purposes because it is effective. As depicted in Fig. 8 in our situation, we could decrease tenfold cross-validation loss through automatic hyper-parameter modification. The highest confirmed and projected stains are found using 19 neighbors and as distance measurement, as shown in the figures and after assessing 30 operations. The proposed system works of KNN and SVM was shown in Table 3.

5. Conclusion

A deep transfer-based ECG verification system has been introduced in this research paper. The proposed technique has proven admirable for biometric identification under different circumstances of ECG signals. Two ECG databases, the MWM-HIT and PTB databases are used to assess the proposed methodology. When the efficiency of the program was compared to the effectiveness of existing ECG identification systems, it

functioned better. In addition, the process requires less time than earlier deep learning approaches because they have worked with pre-built designs and simply made minor adjustments to make them appropriate to our needs. The MWM-HIT dataset was used by the ECG authentication system to provide the correct recognition performance of 99.4%. The proposed method exhibited the highest verification performance compared to other deep learning-based ECG authentication systems. Real-time programs could be used with the proposed model as it is more robust and efficient. Researchers could attempt deep learning techniques in the future, including Long Short-Term Memory (LSTM).

CRediT authorship contribution statement

Jyoti Dhanke: Writing – original draft, Validation. **M. Pradeepa:** Data curation. **R. Karthik:** Writing – review & editing. **Veeresh Rampur:** Conceptualization, Writing – review & editing. **I. Poonguzhali:** Methodology. **Hamanand Chittapragada:** Supervision.

Declaration of competing interest

The authors declare that they have no known competing financial interests or personal relationships that could have appeared to influence the work reported in this paper.

Data availability

No data was used for the research described in the article.

References

[1] S. Qiu, H. Zhao, N. Jiang, Z. Wang, L. Liu, Y. An, G. Fortino, Multi-sensor information fusion based on machine learning for real applications in human activity recognition: state-of-the-art and research challenges, Inf. Fusion 80 (2022) 241–265.

[2] G. Muhammad, F. Alshehri, F. Karray, A. El Saddik, M. Alsulaiman, T.H. Falk, A comprehensive survey on multimodal medical signals fusion for smart healthcare systems, Inf. Fusion 76 (2021) 355–375.

[3] W.K. Ngai, H. Xie, D. Zou, K.L. Chou, Emotion recognition is based on convolutional neural networks and heterogeneous bio-signal data sources, Inf. Fusion 77 (2022) 107–117.

[4] P. Deeraj, G. Rohit, K.S. Abhishek, S.S. Subashka, A trah barrel suitable for both indoor and outdoor uses (A better way to clean your garbage), International Journal of Advanced Science and Technology 29 (5) (2020) 3103–3110.

[5] R.K. Vemuri, P.C.S. Reddy, P. Kumar, J. Ravi, S. Sharma, S. Ponnusamy, Deep learning based remote sensing technique for environmental parameter retrieval and data fusion from physical models, Arabian J. Geosci. 14 (13) (2021) 1–10.

[6] F. Hu, M. Huang, J. Sun, X. Zhang, J. Liu, An analysis model of diagnosis and treatment for COVID-19 pandemic based on medical information fusion, Inf. Fusion 73 (2021) 11–21.

[7] M.S. Minu, R. Aroul Canessane, S.S. Subashka Ramesh, Optimal Squeeze Net with Deep Neural Network-Based Arial Image Classification Model in Unmanned Aerial Vehicles.Traitement du Signal, vol. 39, 2022, pp. 275–281. 1.

[8] K.M. Boehm, P. Khosravi, R. Vanguri, J. Gao, S.P. Shah, Harnessing multimodal data integration to advance precision oncology, Nat. Rev. Cancer 22 (2) (2022) 114–126.

[9] P. Zhang, T. Li, G. Wang, C. Luo, H. Chen, J. Zhang, Z. Yu, Multi-source information fusion based on rough set theory: a review, Inf. Fusion 68 (2021) 85–117.

[10] W. Nsengiyumva, S. Zhong, M. Luo, Q. Zhang, J. Lin, Critical insights into the state-of-the-art NDE data fusion techniques for the inspection of structural systems. Struct. Control Health Monit. 29 (1) (2022), e2857.

[11] G. Soldi, D. Gaglione, N. Forti, L.M. Millefiori, P. Braca, S. Carniel, A. Farina, Space-based global maritime surveillance. Part II: artificial intelligence and data fusion techniques, IEEE Aero. Electron. Syst. Mag. 36 (9) (2021) 30–42.

[12] M. Monica, P. Sivakumar, S.J. Isac, K. Ranjitha, PMSG based WECS: control techniques, MPPT methods and control strategies for standalone battery integrated system. in: AIP Conference Proceedings, vol. 2405, AIP Publishing LLC, 2022, April. 040013.

[13] **T. Ragunthar, P. Ashok, N. Gopinath, M. Subashini, A strong reinforcement parallel implementation of k-means algorithm using message passing interface, Mater. Today Proc., Volume 46, 2021,Pp:3799-3802,** https://doi.org/10.1016/j.matpr.2021.02.032.

[14] G.N.R. Devi, S. Ponnusamy, J. Pandit, B. Buvaneswari, Development of medicinal industries in building A replica to the damaged human tissue for artificial organs with the application of micro-and nano technology (Mnt), J. Optoelectron. - Laser 41 (3) (2022) 79–83.

[15] I. Ullah, H.Y. Youn, Y.H. Han, Integration of type-2 fuzzy logic and Dempster–Shafer Theory for accurate inference of IoT-based health-care system. Future Generat. Comput. Syst. 124 (2021) 369–380.

[16] **A.P. Venkatesh, T.P. Latchoumi, S. Chezhian Babu, K. Balamurugan, S. Ganesan, M. Ruban, L. Mulugeta, Multiparametric optimization on influence of ethanol and biodiesel blends on nanocoated engine by full factorial design, J. Nanomater. 2022 (2022),** https://doi.org/10.1155/2022/5350122.

[17] A.M. Race, D. Sutton, G. Hamm, G. Maglennon, J.P. Morton, N. Strittmatter, J. Bunch, Deep learning-based annotation transfer between molecular imaging modalities: an automated workflow for multimodal data integration. Anal. Chem. 93 (6) (2021) 3061–3071.

[18] P. Ashok, J. Jayachandran, S. Sankara Gomathi, M. Jayaprakasan, Pest detection and identification by applying color histogram and contour detectionby Svm model, Int. J. Eng. Adv. Technol. 8 (3 Special Issue) (2019) 463–467.

[19] S. Wang, M.E. Celebi, Y.D. Zhang, X. Yu, S. Lu, X. Yao, I. Tyukin, Advances in data preprocessing for biomedical data fusion: an overview of the methods, challenges, and prospects, Inf. Fusion 76 (2021) 376–421.

[20] J. Fang, H. Hou, Z.M. Bi, D. Jin, L. Han, J. Yang, S. Dai, Data fusion in forecasting medical demands based on spectrum of post-earthquake diseases, Journal of Industrial Information Integration 24 (2021), 100235.

[21] D. Jagadish, P. Vinoth Kumar, P. Ashok, V. Hariharan, R. Moniraj, LMSDS: learning management system for deaf students in collaborative learning environment, Indian Journal of Science and Technology 9 (16) (2016), 92203.

[22] V.E. Cabrera, L. Fadul-Pacheco, Future of dairy farming from the Dairy Brain perspective: data integration, analytics, and applications, Int. Dairy J. 121 (2021), 105069.

[23] **P.R. Garikapati, K. Balamurugan, T.P. Latchoumi, G. Shankar, A quantitative study of small dataset machining by agglomerative hierarchical cluster and K-medoid, in: Emergent Converging Technologies and Biomedical Systems, Springer, Singapore, 2022, pp. 717–727,** https://doi.org/10.1007/978-981-16-8774-7_59.

[24] H. Nankani, S. Gupta, S. Singh, S.S. Subashka Ramesh, Detection analysis of various types of cancer by logistic regression using machine learning. Int. J. Eng. Adv. Technol. 9 (1) (2019) 99–104.

[25] S.K. Malchi, S. Kallam, F. Al-Turjman, R. Patan, A trust-based fuzzy neural network for smart data fusion in internet of things, Comput. Electr. Eng. 89 (2021), 106901.

Source details

Measurement: Sensors

Open Access

...us coverage years: from 2019 to 2024

...isher: Elsevier

E-ISSN: 2665-9174

Subject area: Engineering: Industrial and Manufacturing Engineering | Engineering: Electrical and Electronic Engineering | Engineering: Mechanics of Materials | Materials Science: Electronic, Optical and Magnetic Materials

Source type: Journal

CiteScore 2022
0.9

SJR 2022
0.215

SNIP 2022
0.390

Save to source list | Source Homepage

CiteScore | CiteScore rank & trend | Scopus content coverage

Improved CiteScore methodology

CiteScore 2022 counts the citations received in 2019-2022 to articles, reviews, conference papers, book chapters and data papers published in 2019-2022, and divides this by the number of publications published in 2019-2022. Learn more >

CiteScore 2022

...9 = 522 Citations 2019 - 2022
560 Documents 2019 - 2022

...alculated on 05 May, 2023

CiteScoreTracker 2023

2.3 = 2,064 Citations to date
887 Documents to date

Last updated on 05 December, 2023 • Updated monthly

CiteScore rank 2022

Category	Rank	Percentile
Engineering — Industrial and Manufacturing Engineering	#279/355	24th
Engineering — Electrical and Electronic Engineering	#623/738	15th

Journal of Data Acquisition and Processing
ISSN: 1004-9037
https://sicjycl.cn/
DOI: 10.5281/zenodo.7765986

ENHANCEMENT OF GRINDING PROCESS USING BORIC ACID AS SOLID LUBRICANT

Dr. R. N. Patil[1,a *], Dr. D. B. Jadhav[2,b] and Dr. J. A. Dhanke[3,c]

[1]Bharati Vidyapeeth's College of Engineering, Lavale, Pune, India.

[2]Bharati Vidyapeeth Deemed to be University College of Engineering, Pune, India.

[3]Bharati Vidyapeeth's College of Engineering, Lavale, Pune, India.

[a]rnpatil1@gmail.com , [b]dbjadhav@bvucoep.edu , [c]jyoti.dhanke@bharatividyapeeth.edu

Abstract.

The most commonly used technique grinding which is extensively applied for surface finishing that extracts unwanted parts of the material in the form of small pieces to attain required accuracy and precision. It has numerous uses in the manufacturing sector. Unfortunately, it demands a lot of energy and raises the temperature, which causes significant residual tensions, microscopic cracks, and burn. Coolants are typically used to mitigate these negative effects because they lower friction and effectively cool the work-wheel interface. Traditional coolant applications frequently fail because the fluid cannot reach the grinding zone and the film is boiling. Several conventional coolants are hazardous to health and contribute to the greenhouse effect. In order to reduce friction and, in turn, eliminate any negative thermal effects on the grinding process, this study discusses the use of solid lubricant, namely boric acid transported in the appropriate medium to the grinding zone. The demonstrative results shows that the important use of boric acid is to decrease the surface roughness, grinding force, and grinding energy, rather than to wettest grinding with standard cooling agents and dried grinding.

Keywords: Coolant, Boric acid, Grinding, Lubricant, Taguchi method.

Introduction

The displacement of spare and excess material separated as scrapes in small pieces in the grinding process. The act of grinding is the removal of material in the form of tiny chips with the use of an abrasive wheel and mechanical action of bound abrasive particles. It is essentially a finishing technique used to produce precise geometrical and dimensional surfaces with a smooth finish. Nonetheless, the grinding process is sometimes used for faster rates of material removal and is sometimes known as abrasive machining [1]. Aspects including tool geometry, a large contact area, significant friction between the tool and the workpiece, and a high specific energy requirement set it apart from many other machining processes. Heat is produced during the grinding process due to the high specific energy used. Heat is primarily conveyed to the workpiece [2]. The workpiece quality is impacted by the intense heat input. Burns, residual

tensile strains, outside texture as surface and subsurface cracks, metallurgical state variations, dimensional defects, and various other negative effects are examples of heat degradation that can occur [3-5]. The unfavorable results of heat produced are to be bound by using cooling agents. This process normally completed by grinding technique at the carving area that ensures the property of the workpiece. in grinding processes Grinding fluids are utilized to minimize and transfer heat, lubricate during chip produce, neat the grinding wheel of detached chips and cuttings, analytically support the grinding operation, or maintain the machine. There are five popular categories of grinding fluids.

These cutting oils include mineral or petroleum bases, are water soluble, contain additives including rust inhibitors, water treatments, and deformers, and are synthetic or semi-synthetic. Many studies on coolant type, content, and supply characteristics have been conducted [6]. Unfortunately, the grinding arc has rather limited access to coolants while grinding. As a result, it frequently just provides general cooling of the work piece and is unsuccessful at lowering the temperature of the grinding zone. The fluid can't enter the grinding zone because of the stiff boundary layer that is formed around the rotating grinding wheel [7, 8].

The efficiency of the grinding fluid is impacted by conventional coolants' loss of cooling qualities during film boiling and their lower film boiling temperature [9]. However, the elimination of grinding swarf, which is necessary for grinding, is made possible by flooded coolant operation. Traditional grinding fluids are a source of environmental risks, and usage and disposal guidelines are becoming more stringent [10]. These fluids are expensive as well. Several different coolants and lubricants are attempted as alternatives to conventional fluids. Solid lubricants have been used in certain efforts as a replacement and have demonstrated to significantly improve the technique [11]. Additionally, these elements sparked research on the usage of biodegradable cooling agents, minimal coolant amounts, and cooling agents free grinding [12].

Although, any experiment to reduce or destroy the cooling agents must be addressed by finding a different way to do the tasks that would typically be performed by the coolant. Other methods for achieving this goal include grinding with liquid nitrogen cryogenic cooling and minimum quantity lubrication (MQL) using ester oil provided as a spot jet or spray mist. In order to improve the process, the impact of graphite nanoplatelets in solid lubrication grinding is also investigated [13]. The results are quite positive, but the cost has been dramatically raised by the amount of nonmaterial needed. In order to boundary the heat produced at the grinding area and analyse the process functioning, the current research will use boric acid, a high temperature solid lubricant.

An experimental arrangement is constructed and fabricated for the design of comparing the effectiveness of boric acid-supported grinding with dry and standard flooded cooling liquid grinding.

Experimental Arrangement

To satisfy suitable carry of the solid lubricant and carrier to the grinding zone, an experimental setup is created. This was created using a cylinder that was loaded with dead weight. The cylinder is filled with the boric acid and carrier oil mixture. With the assist of a piston, which is in spin loaded by the dead weight connected on the piston rod as depicted in Figure 1, constant pressure is maintained on this mixture. The flow control valve is used to regulate the flow of the mixture.

Via a nozzle with a 1 mm * 25 mm aperture, the compound is impinged on the grinding zone. The size of the opening matches the size of the grinding wheel. The soft rubber wheel, which can freely move and is kept in continuous contact with the grinding wheel, receives the mix first. In the end, the paste is applied to the grinding wheel and consequently to the grinding area, where it works as a lubricant.

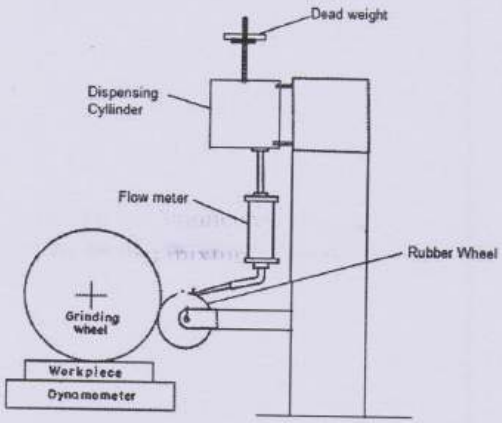


Fig. 1. Schematics Designs of Experimental Arrangement

Initial research and development

With a surface grinding machine with a horizontal reciprocating table, the grinding action is performed. For the experiment, a test specimen with the dimensions of 100 mm x 50 mm x 10 mm thick is used. Throughout the length of the workpiece, grinding is ended. The grade of surface conclude achieved using the process and the quantity of energy applied for the action are the final effects in which industry is particularly interested. Hence, the following factors are maintained constant during first investigations. This is described in further detail in below Chart 1.

Chart 1. Elements maintained constant in grinding.

Elements	Particulars
Workpiece substance	Compound steel AISI 4140

Grinding Device	Horizontal axle surface grinding, machine, PMT make, Model SG 42, 5.5 kw
Grinding Roll (Wheel)	A60L5V10, Diameter 300 millimetre, width 25 millimetre.
Roll (Wheel) velocity	30m per minute
Chart feed value	10m per minute
Dressing situation	With single point diamond dresser, 1 carat, in dry situation

AISI 4140 alloy steel is used for the initial experiments so that the effects of the use of solid lubricants on the process may be seen. Chart 2 lists the experimentation's findings.

Chart 2. Observations for preliminary experimentation.

Depth of Reduce (µm) ↓	Dry Grinding		Wet Grinding		Boric Acid	
	Force (N)	Ra (µ)	Force (N)	Ra (µ)	Force (N)	Ra (µ)
5	217.21	0.23	201.58	0.23	100.01	0.205
10	253.41	0.235	235.175	0.235	116.675	0.205
15	289.605	0.235	268.77	0.235	133.345	0.21
20	325.81	0.235	302.365	0.235	150.015	0.21

The plot of force vs cut depth is created to assess the forces under various cutting conditions. It shows that the force increases with cutting depth, but the amount depends on the type of coolant employed. It has been noted that employing solid lubricants results with two times of observations in less force being needed and better surface finish.

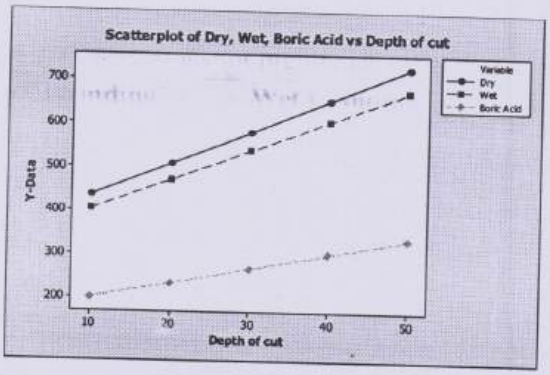


Fig. 2. Effect of coolants on force under varying depths of trim or cut

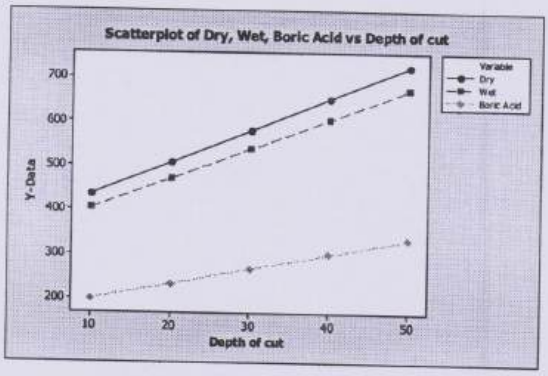


Fig. 3. Surface crudeness for AISI 4140 applying various cooling agents.

Extension of experiments using Taguchi methods

For the extension of experimental conceptions and drawings for functioning quality and cost, Taguchi methods of experimental design offer a straightforward, effective, and systematic approach. It has been proven effective in numerous manufacturing scenarios. The standard experimental design processes concentrate on the typical performance characteristics of the product or process. The Taguchi technique, however, focuses less on averages and more on the impact of variation on the quality features of the product or process. To put it another way, the Taguchi method renders the performance of the product or process insensitive (resistant) to change due to uncontrolled or noisy sources. This can be accomplished, according to Taguchi, by properly designing the parameters during the off-line quality control phase known as "parameter design." In order to evaluate two or more parameters simultaneously and independently for their capability to impact the irregularity of a precise product or process characteristic, he created a variety of standard orthogonal arrays (OAs).

The best possible combination of these parameters is then chosen. The study's fixed objectives are as follows: Research the impact of using boric acid on the amount of force needed to grind and the surface roughness that is produced, and compare the applications to different alloy steels.

The force needed (F) and the surface roughness (Ra) of the ground piece are used as the process's quality indicators. A Mitutoyo surftest is used to measure the surface finish, which is a direct process result. The two components of force were recorded by a dynamometer, which was used to measure force. The associated resultant force is measured and is taken into report as a individual reaction.

During the experiment, the working boundaries, containing speed and feed, are continued constant. Infeed rate, workpiece material, and lubricant flow rate are taken into account for variance. For each of the components, three levels with equal spacing are chosen within the working range, as shown in Chart 3.

Chart 3. Levels in Experimentation

Elements	Stage 1	Stage 2	Stage 3
Material	AISI 4140	AISI 4310	AISI 52100
Infeed (Depth of trim or cut), (μm)	5	15	25
Flow Rate, (mm^3/min)	10	20	30

The problem of repeating the tests is resolved by selecting the L27 orthogonal array because the array itself encourages the repetitions. This makes it easier to get more trustworthy information from the experiment's statistical analysis. The measurement systems record quality attributes such as force (F) in N and surface roughness (Ra) in m. Pieces are base giving seven groups of upward and downward spark out permits to have consistent outcomes with Ra.

The sampling data for surface roughness (Ra in m) and force (N) within the boric acid-assisted grinding method are displayed in Chart 4. The data gathered has a high degree of consistency, making it trustworthy for statistical analysis.

Chart 4. Observations and Analysis

Trial	Material	In feed (μm)	Flow Rate (mm^3/min)	Force (N)	Surface roughness (μm)	S/N Ratio	Std. Dev.	Mean
1	1	1	1	269.14	0.42	-48.822	6.3851	276.097
2	1	1	1	277.46	0.43	*	*	*
3	1	1	1	281.69	0.45	*	*	*
4	1	2	2	305.03	0.42	-49.865	7.2559	311.323
5	1	2	2	309.68	0.43	*	*	*
6	1	2	2	319.26	0.45	*	*	*
7	1	3	3	305.03	0.42	-49.910	7.2351	312.913
8	1	3	3	314.46	0.43	*	*	*
9	1	3	3	319.25	0.45	*	*	*
10	2	1	2	274.09	0.46	-48.936	6.5161	279.743
11	2	1	2	278.27	0.47	*	*	*
12	2	1	2	286.87	0.50	*	*	*
13	2	2	3	326.99	0.47	-50.513	7.7588	335.443
14	2	2	3	337.10	0.48	*	*	*
15	2	2	3	342.24	0.51	*	*	*
16	2	3	1	601.08	0.49	-55.757	14.292	613.477

17	2	3	1	610.24	0.50	*	*	*
18	2	3	1	629.11	0.53	*	*	*
19	3	1	3	288.10	0.47	-49.414	6.8335	295.547
20	3	1	3	297.01	0.48	*	*	*
21	3	1	3	301.53	0.51	*	*	*
22	3	2	1	564.91	0.49	-55.218	13.4306	576.560
23	3	2	1	573.52	0.50	*	*	*
24	3	2	1	591.25	0.53	*	*	*
25	3	3	2	536.67	0.49	-54.817	12.7298	550.540
26	3	3	2	553.26	0.50	*	*	*
27	3	3	2	561.69	0.53	*	*	*

Represented Plots for Force as A Prime Feature

On the groundwork of the represented findings of force essential for grinding process with the support of boric acid as solid lubricant for the materials chosen, AISI 4140, AISI 4340 and AISI 52100 are viewed in Fig.4 to Fig. 6.

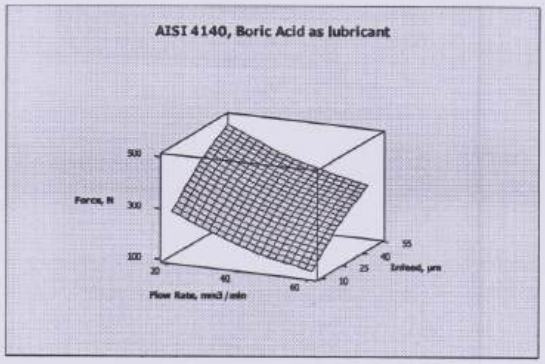


Fig. 4. Boric Acid as lubricant, AISI 4140

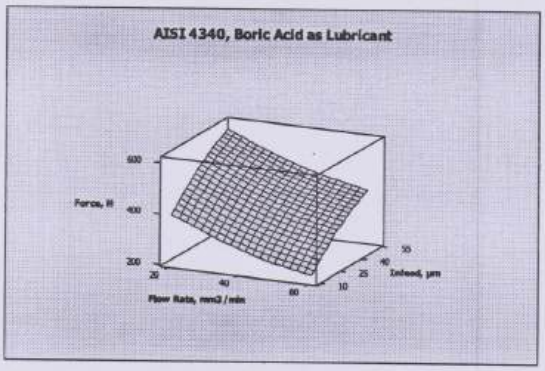


Fig. 5. Boric Acid as lubricant, AISI 4340

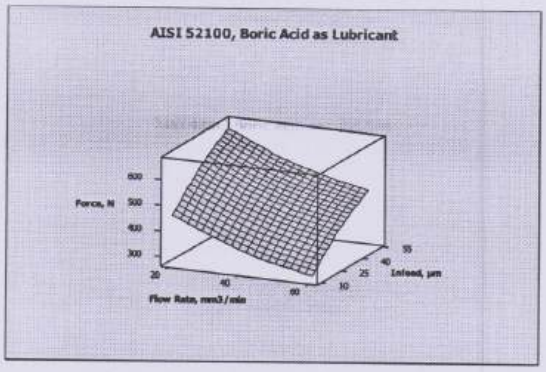


Fig. 6. Boric Acid as lubricant, AISI 52100

Study for Surface Crudeness and Roughness

In the same direction and in the same order of the force, Taguchi analysis is performed for surface roughness attained in the boric acid assisted grinding action. By the results of the represented findings of surface crudeness and roughness achieved in grinding process in consequence of boric acid as solid lubricant for the materials chosen, AISI 4140, AISI 4340 and AISI 52100 are provided in Fig.7 to Fig.9.

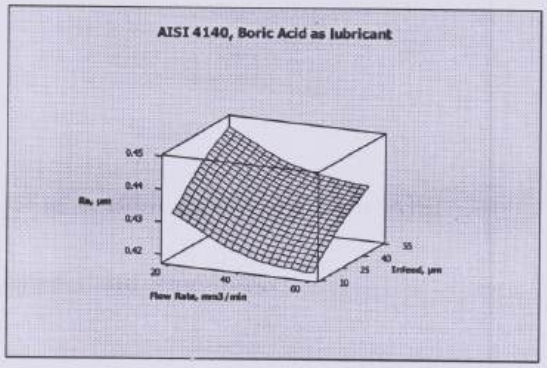


Fig. 7. Boric Acid as lubricant, AISI 4140

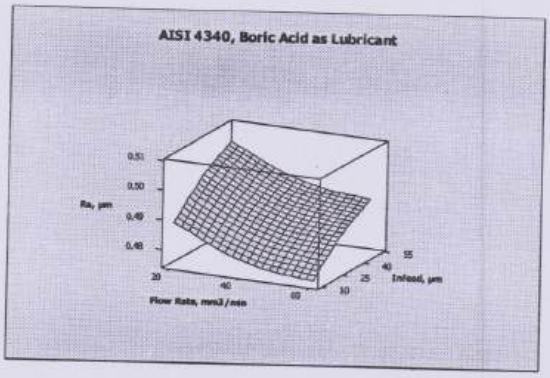


Fig. 8. Boric Acid as lubricant, AISI 4340

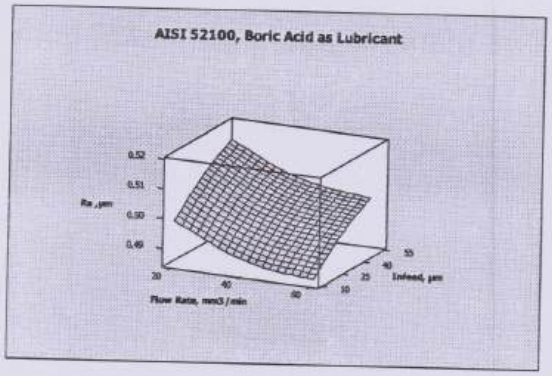


Fig.9. Boric Acid as lubricant, AISI 52100

Conclusions

The surface finish and cutting forces involved in the process have been enhanced using the experimental arrangement developed for the utilization of boric acid as a approach to decrease the heat produced in the grinding area. The research employ the Taguchi method of experimental design. Boric acid significantly reduces the force needed for grinding operations when compared to dry grinding and grinding with standard coolants, and the surface finish is also improved. Hence, the improvement in output metrics demonstrated the boric acid's beneficial role as a lubricant.

Other solid lubricants such as molybdenum disulphide, zinc phosphate, and graphite can be used in similar experiments, which may result in the most effective solid lubricant for surface grinding.

References

1. H.M.T., "Production Technology," Tata McGraw Hill, pp.250-251, 2009.
2. J.O. Outwater, M.C. Shaw, "Surface temperature in grinding," Trans. ASME 74 pp.73–86, (1952).
3. S. Malkin, R. B Anderson, Thermal aspects of grinding — part II, surface temperature and workpiece burn, Trans. ASME, J.Eng. Indust. 96 , pp.1184–1191, (1974)
4. Y. Nakano, H. Uchida, K. Ota, Thermal deformations and profile errors of workpiece in surface grinding, Ann. CIRP 25 (1), pp. 235–240, (1976).
5. R. Snoys, K.U. Leuven, M. Maris, J. Peters, Thermally induced damages in grinding, Ann. CIRP 27 (2), pp.571–581, (1978).
6. Y. Nakano, H. Uchida, K. Ota, Thermal deformations and profile errors of workpiece in surface grinding, Ann. CIRP 25 (1) ,235–240, (1976).
7. S. Ebbrel, N.H. Wooley, Y.D. Tridimas, D.R. Allanson, W.B. Rowe, The effects of cutting fluid application methods on the grinding process, Int. J. Mach. Tools Manufact. 40, pp.209–223, (2000).
8. S. Malkin, Grinding Technology, Theory and Applications of Machining with Abrasives, Ellis Harwood, Chichester, 1989.
9. T.D. Howes, Assessment of cooling and lubricating properties of grinding fluids, Ann. CIRP 39 (1), pp. 313–316, (1990).
10. T.D. Howes, H.K. Toenshoff, W. Heur, Environmental aspects of grinding fluids, Ann. CIRP 40 (2), pp. 623–630, (1991).
11. S. Shaji, V. Radhakrishnan, "An investigation on surface grinding using graphite as lubricant," International Journal of Machine Tools & Manufacture 42 ,pp. 733–740, (2002).
12. I. Inasaki, H.K. Toenshoff, T.D. Howes, Abrasive machining in thethe future, Ann. CIRP 42 (2) pp.,723–732, (1993)
13. MatthewAlberts, KyriakiKalaitzidou, ShreyesMelkote, "An investigation of graphite nanoplatelets as lubricant in grinding," International Journal of Machine Tools & Manufacture, 49, pp.966–970, (2009).

Author Sea

Source details

Feedback > Compare sources >

Shu Ju Cai Ji Yu Chu Li/Journal of Data Acquisition and Processing

Scopus coverage years: from 2001 to Present

Publisher: Nanjing University of Aeronautics an Astronautics

ISSN: 1004-9037

Subject area: Computer Science: Signal Processing | Computer Science: Software

Source type: Journal

Save to source list | Source Homepage

CiteScore 2022
0.7

SJR 2022
0.140

SNIP 2022
0.221

CiteScore | CiteScore rank & trend | Scopus content coverage

Improved CiteScore methodology

CiteScore 2022 counts the citations received in 2019-2022 to articles, reviews, conference papers, book chapters and data papers published in 2019-2022, and divides this by the number of publications published in 2019-2022. Learn more >

CiteScore 2022

0.7 = 302 Citations 2019 - 2022 / 434 Documents 2019 - 2022

Calculated on 05 May, 2023

CiteScoreTracker 2023

0.8 = 329 Citations to date / 434 Documents to date

Last updated on 05 December, 2023 • Updated monthly

CiteScore rank 2022

Category	Rank	Percentile
Computer Science — Signal Processing	#110/122	10th
Computer Science — Software	#389/404	3rd

View CiteScore methodology > | CiteScore FAQ > | Add CiteScore to your site



Smart Science

ISSN: (Print) (Online) Journal homepage: https://www.tandfonline.com/loi/tsma20

Plethora of Carbon Nanotubes Applications in Various Fields – A State-of-the-Art-Review

Nidhi Jain, Eva Gupta & Nand Jee Kanu

To cite this article: Nidhi Jain, Eva Gupta & Nand Jee Kanu (2021): Plethora of Carbon Nanotubes Applications in Various Fields – A State-of-the-Art-Review, Smart Science, DOI: 10.1080/23080477.2021.1940752

To link to this article: https://doi.org/10.1080/23080477.2021.1940752

Published online: 27 Jun 2021.

Submit your article to this journal

View related articles

View Crossmark data

Full Terms & Conditions of access and use can be found at
https://www.tandfonline.com/action/journalInformation?journalCode=tsma20

SMART SCIENCE
https://doi.org/10.1080/23080477.2021.1940752

Taylor & Francis
Taylor & Francis Group

Check for updates

Plethora of Carbon Nanotubes Applications in Various Fields – A State-of-the-Art-Review

Nidhi Jain [a], Eva Gupta [b,c] and Nand Jee Kanu [d,e]

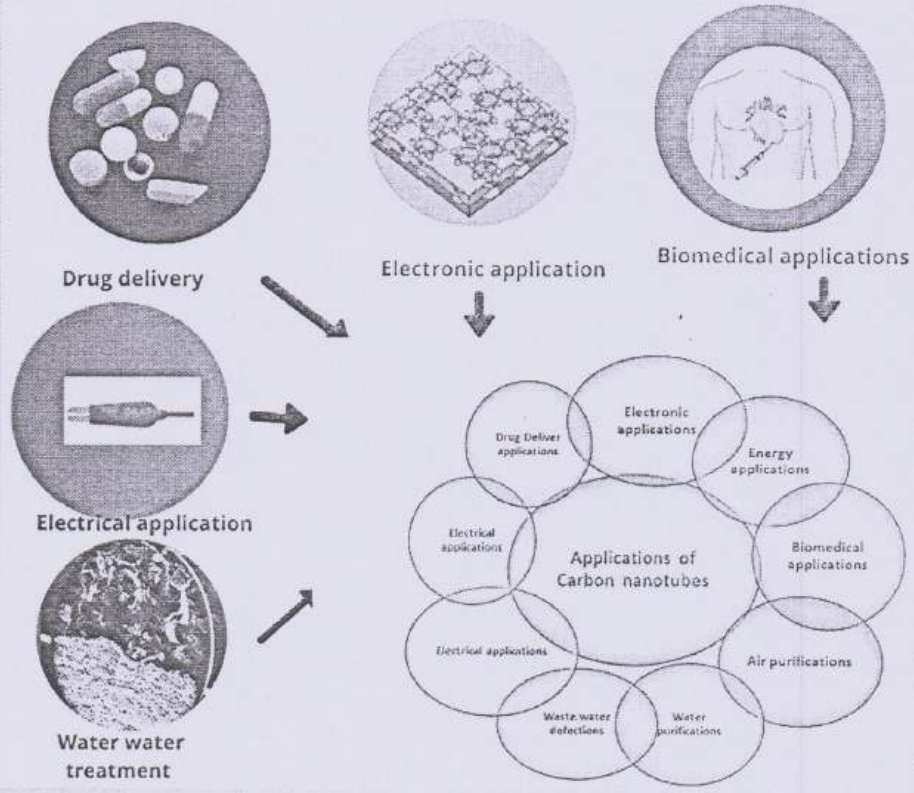
[a]Department of Engineering Science, Bharati Vidyapeeth College of Engineering, Lavale, Pune, India; [b]Department of Electrical Engineering, ASET, Amity University, Noida, India; [c]Department of Electrical Engineering, TSSM's Bhivrabai Sawant College of Engineering and Research, Pune, Maharashtra, India; [d]Department of Mechanical Engineering, S. V. National Institute of Technology, Surat, India; [e]Department of Mechanical Engineering, JSPM Narhe Technical Campus, Pune, India

ABSTRACT

Carbon nanotubes diverse applications have been discussed in the present study. Carbon nanotubes are a promising material in all façades of life, be it environment, electrical, electronics, biomedical energy, food technology applications, etc. Carbon nanotubes open new avenues to improve the environment, control pollution, and used in various fields. Increase in the population, urbanization and industrialization create several types of pollution. Carbon nanotubes solve various problems including environmental issues, pollution, bio-medicals, etc. It becomes an inevitable material for the present and future. In this review article, carbon nanotube applications to solve water purification, water disinfection, electrical and electronic applications, biomedical energy, or in-air purification have been discussed. A plethora of carbon nanotube applications in various fields have been discussed in articles covering the fields of water purification, biomedical applications in electrical/electronic applications, agricultural yields, etc. Eleven different case studies have been discussed in the paper and testimony of the use of CNTs in various fields was given by the patent trend.

ARTICLE HISTORY
Received 01 May 2021
Accepted 07 June 2021

KEYWORDS
Carbon nanotubes; nanotubes; nanomaterials; water purification; biomedical



CONTACT Nidhi Jain nidhijain1704@gmail.com Department of Engineering Science, Bharati Vidyapeeth College of Engineering, Lavale, Pune, 412115, India; Nand JeeKanu nandssm@gmail.com Department of Mechanical Engineering, Pune, India

© 2021 Nidhi Jain, Eva Gupta and Nand Jee Kanu

1. Introduction

Carbon nanotubes (CNTs) are constantly being used for environment protection. Single walled (SWCNTs) and multiwalled carbon nanotubes (MWCNTs) were used for the preponderance of nanoscale carbon production. A single sheet of graphene is used to synthesize single-walled carbon nanotubes, which have a cylindrical design. Under a transmission electron microscope, it appeared as two planes. Carbon nanotubes with several walls consisting of multiple layers of graphene arranged in a concentric shape all around the smallest nanotube. Pure water and air is the utmost important requirement for the survival of human beings. Water is being polluted day by day increase and over utilization of the resources. Air, which we breathe and exhaled, is continuously polluted because of the excess use of nonrenewable resources such as petrol and diesel, etc. Increase of demand of energy leads to industrialization and alternative resources. CNTs have astonishing physical, chemical, and electronic properties which act as cost effective in various applications. Reduction of waste disposal in the environment can be achieved by using carbon nanotubes as super capacitors which provide small size, high portability, maximum power density, long suitability, and high energy [1–5]. The hybrid materials manufactured by carbon nanotubes and carbon nanofibers in blend with inorganic (metal oxide) nanoparticles can be able to solve the maximum number of water treatment problems, helpful in preventing air pollution, and recycling of waste [6–10].

CNT sponges have high porosity and very low density and have haphazardly entangled three-dimensionally, which is used for removing oil from water [11–14]. Camphor is known as an environment-friendly hydrocarbon. High-purity carbon nanotubes (CNTs) can be produced from camphor hydrocarbons using the chemical vapor deposition method. The synthesis technique depicted here fully addresses the '12-principle' protocol of green chemistry [15–19].

Energy generation, which generally occurs through fossil fuels, has been recognized as the major issue for environmental degradation from global warming. Energy storage is also a hot issue for rapid growth in developing nations like India. Bio-medically, there is always a substantial demand of alternative materials for drug delivery, cancer treatment, biosensors, etc. To address these issues, carbon nanotubes act as a revolutionizing material for energy conversion and storage materials. And, it helps in reducing environment pollution in air and water media because of their exclusive structural, electronic, and mechanical properties [20–24].

Here, the authors can review the applications of carbon nanotubes to solve water purification, water disinfection, electrical and electronic applications,

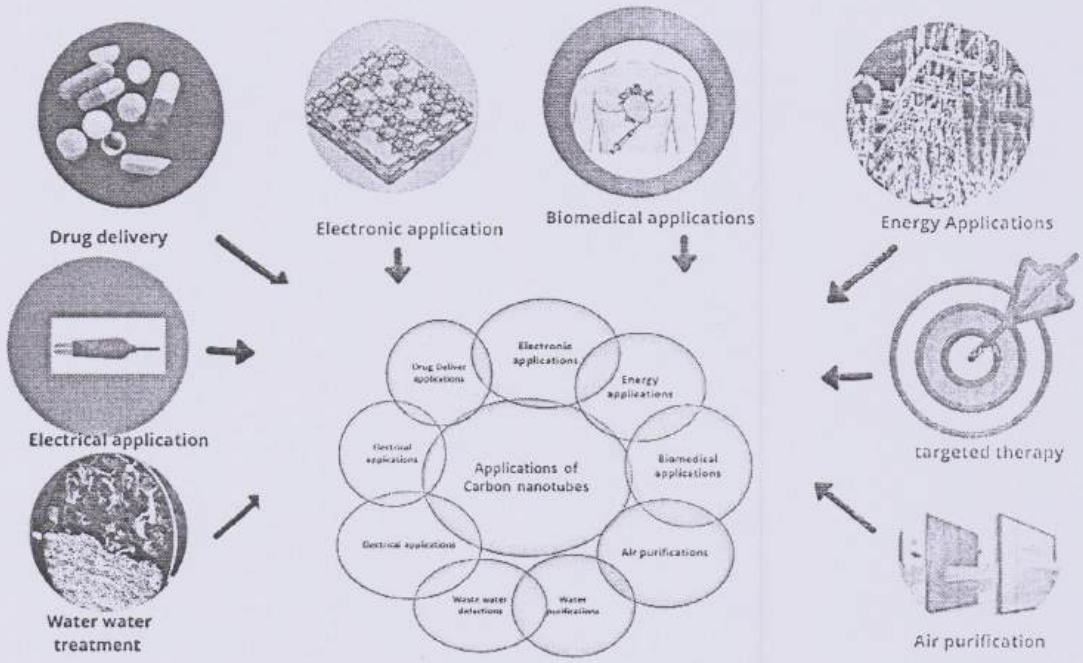


Figure 1. The various environmental applications of carbon nanotubes have been depicted in the figure, which includes water purification, waste water disinfection, electrical, electronic, energy, biomedical, and air purification.

future smart electronics, sensor tapes, and capacitors, and batteries, biomedical, energy, or in-air purification, etc. Figure 1 represents the various environmental applications of carbon nanotubes. Technology and equipment run by electricity is a vital issue in our daily life. Among a range of electrochemical energy storage Li–S batteries are a capable contender for quenching the thrust of energy for the next generation [25–35].

CNTs are used for delivering bio-fertilizers. When bio-fertilizer is delivered with the help of CNTs, the unique properties of its provided large surface area, superior reactivity, and smaller particle size help in the profound delivery of the bio-fertilizer inside the plant [36–40]. CNTs are used for delivering biofertilizer. CNTs facilitate nutrients delivery, which is helpful in humanizing their growth and yields [41–43].

Carbon nanotubes (CNTs), because of their distinctive 1D tubular structure and other inimitable properties such as electrical, thermal conductivity, surface area, etc. have been successfully used for improving the electrochemical characteristics of both the anode and cathode of Li-ion batteries. Various reviews are available in the literature which explains CNT-based composites are widely used for enrich energy conversion and storage capacities, and power density, capability, life cyclic, and protection of LIBs [44].

2. Carbon Nanotubes for Water Purification

Water is an important natural resource required for the existence of human beings. Human life cannot flourish without the availability of clean water. Water is a nonrenewable resource. Water contains different pollutants which makes it unfit for drinking water. Water is used in all scats of life. Different recent technologies are available for cleaning water is not as much effective. Carbon nanotubes are able to remove numerous types of pollutants in organic, inorganic, or biological materials. Lots of waste water is generated by the industry, which creates an ample range of landfills. Carbon nanotubes are able to clean industrial wastewater which in turn reduces landfills and protects our environment [45]. The carbon nanotubes based on specific nanotechnologies discussed in the paper solely focus on site remediation and some waste water treatment, for example: they have been recognized for their ability to absorb dioxins much more strongly than traditional activated carbon. They act as excellent adsorbents for the removal of numerous pollutants, including microorganisms from the drinking and water bodies present on earth. They have various magical and unique properties, which make it versatile such as excellent thermal stability, higher adsorption ability, broad range of pH, etc [45].

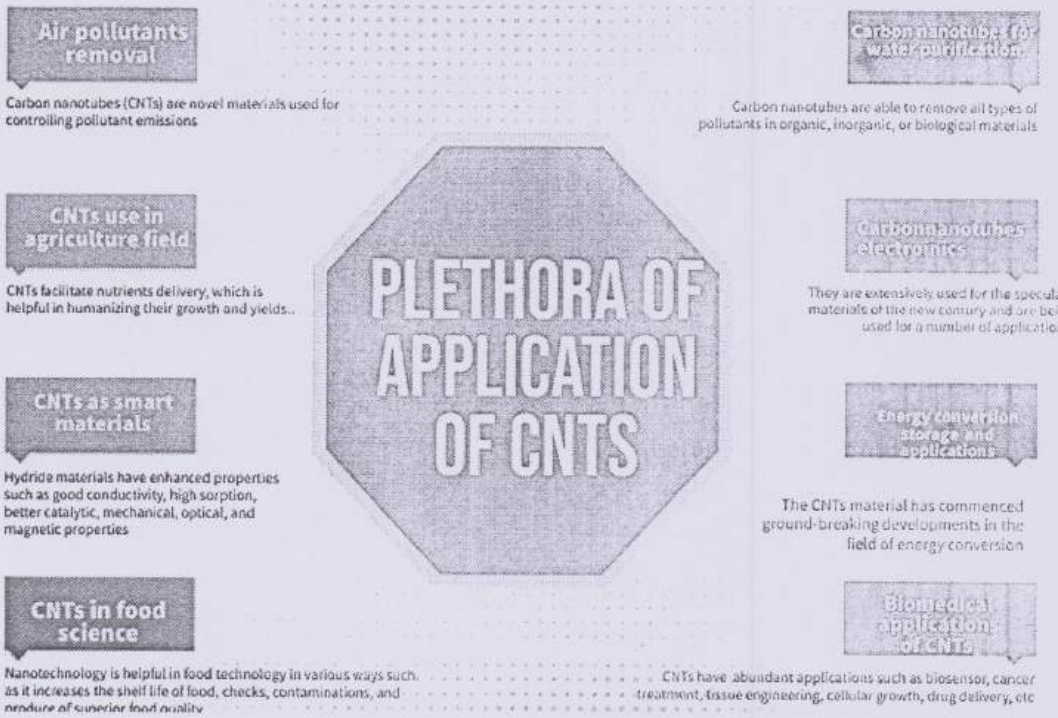


Figure 2. Plethora of applications of carbon nanotubes in various fields such as textile, biomedical, health care, food industry, electronics, environment, renewable energy, etc.

Carbon nanotubes have been utilized for the elimination of various harmful toxic substances from drinking and other wastewater, because of their well-defined structure and adjustable characteristics. Numerous researchers studied the strong exchanges between CNTs and heavy metal ions and with organic compounds. This is because of the surface functional groups and hydrophobic surface of CNT [46]. Modifications can be made in carbon nanotubes to improve its selectivity and removal of metals or ions from aqueous stream [47].

Functionalization of carbon nanotubes may also act as a promising option for the removal of water pollutants. Carbon nanotubes are used to remove several pollutants from water bodies which are harmful for the environment. Such compounds are organic in nature, pesticides, pharmaceuticals, antibiotics, and inorganic ions such as heavy metal ions [48].

Due to the structure and morphology of the carbon nanotube, it is useful for the adsorption of various organic and inorganic pollutants. They are far better than activated carbons in terms of their lesser equilibrium time, higher adsorption capacity and selectivity, and easier regeneration.

Nanocomposites such as magnetic polymer multiwall carbon nanotubes (MPMWCNTs) are formed by the combination of poly (1-glycidyl-3-methylimidazolium chloride) (an ionic liquid-based polyether) and ferroferric oxide. Such nanocomposite is very effective to remove various dyes such as orange II dye, sunset yellow dye, FCF, and amaranth dye from aqueous phase [49].

MPMWCNT is also effective in removing dye-containing wastewater because of high adsorption capacity, fast adsorption rate, and it separates from water if an external magnetic field is applied on it. The adsorption of ofloxacin (OFL) on carbon nanotubes (CNTs) has been reported by researchers and scientists by means of solubility, pH, and cosolvent effects [50] carbon nanotubes (CNTs) are cost-effective, simplistic, green, and extremely effective real/fruitful in water and wastewater treatment. Figure 2 illustrates the applications of carbon nanotubes in water purification.

Nano-structured TiO_2 are present in size, shape, and structure (particles, fibers, wires, rods, porous materials, and tubes all in nano dimensions). These morphologies are prepared and used in several applications [51]. Tubes of titanium dioxide have varied applications in the environmental field. After carbon nanotubes, TDN is the second most abundant. TDNs synthesized from the anodization of metal plates have substantial applications in water photo-electrolysis, hetero-junction, solar cells, gas sensing, and environmental purification [52,53], as they provide large surface area. Metal impurities in carbon nanotubes are accountable for the 'electrocatalysis' found at nanotube-modified electrodes. Metal inclusions may have a role in the reported 'electrocatalysis' linked to carbon nanotube-modified electrodes in some cases. Edge-plane pyrolytic graphite (EPPG) electrodes should be compared to carbon nanotube-modified electrodes in all electrochemical investigations. It will either reveal that edge-plane sites/defects are to blame, or it will imply that metal impurities may facilitate an electrochemical reaction.

The TDN provided is their inner diameter of approximately *101 nm* and an average length of around *3.5 μm*. Order structure of the TiO_2 film gives a unidirectional electrical channel and large surface area, which enhances photo-catalysis and photo-electrochemical applications [54,55].

Electrochemical oxidation of methyl orange degradation reported by Zhang can be possible effectively when combined with UV irradiation. Percentage will be *56.3%* in *90 minutes* where an initial dye concentration of 2×10^{-4} *M* [11]. TiO_2 nanotubes are used in electrocatalysis and act by electro-activating materials like noble metals (Ag, Au, Pd, Pt, and Ru) or metal oxides. TiO_2 is also used in electrochemistry because of semiconductive properties, longer stability [56]. Gold, silver, palladium, platinum, and Ruthenium nanoparticles (*3 nm*) loaded on TDN layers enhance TiO_2 PC properties [57].

3. Carbon Nanotubes in Electrical/Electronic Applications

Carbon nanotubes have the symmetry and unique electronic structure of graphene; nanotubes have a very high current carrying capacity. They are extensively used for speculate materials of the new century and are being used for a number of applications [58] ranging from automobiles to nanometer scale electronics. The electrical properties are useful for saving energy and in turn decrease the use of wood cutting and the use of traditional batteries by providing better electrical materials for future generations [59,60]. Carbon nanotubes provide small size, carbon-based nanoelectronics having high flexibility compared to conservative silicon electronics. Carbon nanotubes have unusual properties because of the low dimensionality [61]. Carbon nanotubes can be used to harness electronics devices, which is helpful in power saving, radiation, hardness, and reduced heat dissipation. Carbon nanotubes can be effectively used to relate the phenomena of photoconductivity, thermoelectricity, and superconductivity [61]. The basic conducting features of a graphene tubule are also known to be dependent on the type of wrapping

(chirality) and the diameter (usually, SWNTs possess diameters ranging from 0.4 nm to 2 nm). The CNTs replace traditional batteries such as electrochemical capacitors or super capacitors, which are not only given their miniature size, elevated power density, prolonged for a longer period of time, and high energy density, which decrease the waste disposal to the environment.

3.1. CNTs as Super Capacitors

Super capacitors consist of large surface area activated capacitors, which are having molecule-thin layer of electrolyte as dielectric [62]. The CNT is also used as an electrode material for the capacitor to augment the ability of the capacitor to store higher energy density because of the large surface area [63]. The CNTs possess high surface area, stability, and strong mechanical properties. The CNTs are not acting stronger candidates with low capacitance [64]. Therefore, CNTs, but also used actively in good specific capacitance transition metal oxides, for example, manganese oxide (MnO_2) and ruthenium oxide (RuO_2) [65,66]. The CNTs provide capacitances of approximately *5000 F* and energy densities up to *5 Wh/kg*, which is higher up to 10-fold higher than conventional capacitors, with only *0.5 Wh/kg* [67].

3.2 CNTs material has commenced revolutionary developments in the field of energy conversion, storage, and applications

Humanity is facing many issues out of top problems. Energy and environment both are in a prioritized list. Renewable sources of energy like oil, gas, and coal are fulfilling the need of energy until now, but they are depleted and exhausted because of the overuse. Pollution produced by these fossil fuels are numerous, because they increase greenhouse gases, global warming, and in turn is a major cause of natural disasters and environmental degradation. Industrial revolution, agricultural activities, metallurgical activities, and application of pesticides and herbicides require energy for sustainability.

Growth in any sector requires energy. Energy generated by conventional sources leads to pollution. Contamination of air, water, and soil leads to the depletion of our environmental quality. Quenching the requirement of energy for the protection of the environment is utmost important. Nanotechnology is now addressing the problem of energy by giving substituted products which are more efficient and have smaller dimensions showing new properties and behavior than bulk materials.

The CNTs have very distinctive structural properties and show unique electronic, chemical, and mechanical properties. The main culprit of global warming effects is fossil soil, which has been exploited for years. The CNTs based material has commenced ground-breaking developments in the field of energy conversion, which includes the development of solar cells, fuel cells. It also brings new developments in the field of energy storage such as hydrogen storage, lithium ion batteries, and electrochemical super capacitors, the hybrid nanocomposites of CNTs have also developed to save energy [58].

4. Carbon Nanotubes as Electrochemical And Electronic Biosensors

The carbon nanotubes used in biosensors are extremely successful and outstanding due to its exceptional properties such as fast electron transfer rate [68] and high electron transfer helping in good conductivity, better aspect ratio, elevated conductivity, good chemical stability and better sensitivity [69]. The basic requirement of biosensors is the control of biomolecules with its surface, which helps in the detection and signal transduction process. The CNTs improve electron transfer which is very useful in combining electrochemical and electronic biosensors [70,71]. Electrochemical biosensors developed on CNTs are used for distinguish nitric oxide and sensing epinephrine [72,73]. Several Scientists such as Bisker et al. 2016 [74] used the CNTs for detecting human blood proteins using 20 distinct SWCNT corona phases. The MWCNTs based device has been developed by Scientists Baldo et al. 2016 for detecting arginase-1. The SWCNTs are severed as operative optical probes in biomedicine due to their unique photophysical properties, good fluorescence emission in the NIR region, and photo stability [75].

5. Biomedical applications of CNTs in various fields

Medical field is mainly governed by good drug administration. Due to less selectivity and low half-life time, the drug cannot fulfill the real purpose of the treatment. To address the problem of multiplying the administration of drugs to fulfill the needs of the body, this leads to fatal issues. The CNTs are extensively used as nano carriers for drugs, gene delivery and cancer treatment and other biomedical applications. CNTs are extensively used and exploited in various biomedical applications such as biosensing, drug delivery, and cancer therapy. Presently, in this review we carefully reiterate the development of CNTs for biomedical applications [76].

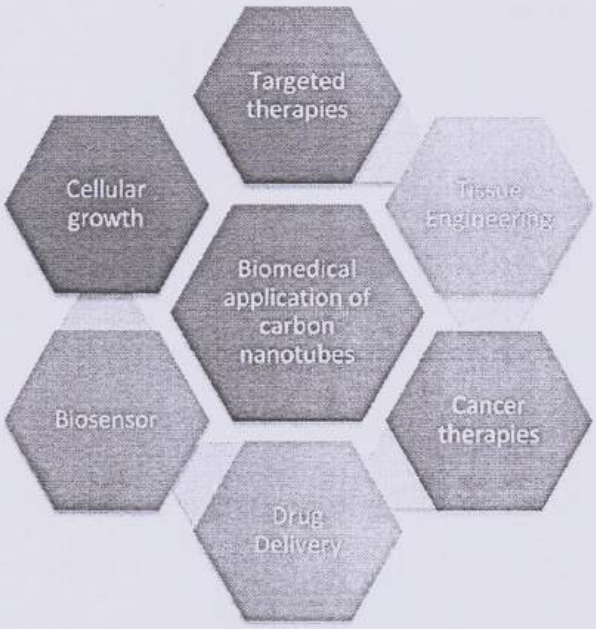


Figure 3. The figure represents the biomedical applications of CNTs such as targeted therapy, cellular growth, tissue engineering, cancer therapy, drug delivery, biosensors, etc.

CNT is used for targeted therapies such as drugs, gene delivery and cancer treatment and other biomedical applications. It has been seen that carbon nanotubes have numerous applications in various fields such as removal of water and air pollution, energy storage, semiconductors, food science, etc. However, the most important application is biomedical applications which safe the life of the human. Out of abundant applications such as biosensor, cancer treatment, tissue engineering, cellular growth, drug delivery, etc. Most significant is cardiovascular disease. India is considered as the hub for cardiovascular diseases. In 2016, the estimated dominance for cardiovascular diseases in India was approximate to be *54.5 million*. Every fourth death is caused by heart disease, out of which *>80%* heart disease is due to stroke [71].

5.1. Carbon Nanotubes for Drug Delivery and Cancer Therapy

CNT has gained attention in recent years because of its ability to attach to drug molecules via various types of bonding or functionalized CNTs and deliver drugs into living cells. Considerable attention was gained by CNTs because of noninvasive penetration across biological membranes [77,78]. CNTs act as a nano carrier in the last recent years, which shows exceptional cell transfection capabilities. Several researchers such as Liu et al. loaded the anticancer drug doxorubicin (DOX) with poly (ethylene glycol) (PEG) conjugated SWCNT which reaches to timorous tissue [79,80]. Some more examples are given which is covalently linked to MWCNT anticancer drug, 10-hydroxycamptothecin (HCPT) [81]. The CNTs are good in intracellular drug delivery and gene and protein delivery. Xu et al. also wrought magnetically directed nano carriers consuming a paramagnetic surfactant coating [82]. By seeing these examples, it can be concluded that CNTs are effectively used in drug delivery systems and act as nano carriers. Versatile properties of carbon nanotubes make it suitable for biomedical applications. They are used in delivering drugs for anticancer drugs, genes, and proteins [76]. SWCNTs are a kind of SP^2 hybridized carbon that looks a lot like fullerenes. The hexagonal composition of the structure is similar to that of graphite, forming six-atom carbon rings. MCNTs, on the other side, are made up of multiple tubes arranged in concentric rings in a cylindrical structure.

5.2. Potential Applications of CNTs in Tissue Engineering and Cellular Growth

Brain is a part of the body which to be delicately handled. Growth of the brain cell cannot be possible on any of the media. CNTs have been used as a promising material for neural signal transmission and it provides a good surface for cellular growth.

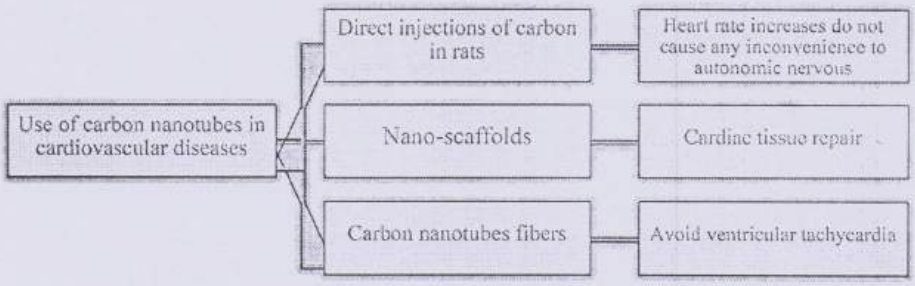


Figure 4. The figure represents the use of cardiovascular disease.

Several researches and scientists such as Mazzatenta et al. worked and concluded that SWCNTs stimulates brain circuit activity when SWCNTs and hippocampal cell combines [83]. Neurons would better grow on double walled carbon nanotubes (DWCNTs) because of the surface texture and good adsorption of culture medium than on SiO_2 surface, which helps in protein tolerating the growth of neuron networks [84]. Figure 3 represents the biomedical applications of CNTs.

5.3. Biomedical Importance of CNTs in Cardiovascular Diseases

Carbon nanotubes (CNTs) are novel materials which could save the world from cardiovascular diseases. It is widely used in various cardiovascular diseases. The nano-compatibility of the carbon nanotube proofs it as a novel candidate for future advance research in the field of medicine and biology.

Indeed, it is a fact that carbon nanotubes (CNTs) have a brilliant prospect in the field of revolutionary product research [85]. There are certain ways in which carbon nanotubes are used as they are represented schematically in Figure 4.

5.4. Cardiac Effects of MWCNTs by Direct Injection in the Rat's Body

The investigation of the cardiac effect of MWCNTs by direct injection has been seen in rats. When the CNTs are directly injected in rats, it was found through electrocardiogram (ECG) signals that the heart rate increases significantly. The CNTs do not cause any inconvenience to the autonomic nervous system (ANS), However scientists have to work with biocompatible nanotubes in the heart [85–89]. The CNTs have established that they have a strong ability to act as scaffolds to endorse cardiomyocyte propagation, maturation, and survival [41].

The CNTs fibers have the ability to transfer electrical signals to the myocardium. The CNTs provide electrical conductivity, strength, and flexibility to facilitate signals from blood vessels. They improve the conduction of ventricular and atrioventricular blood vessels. They provide uplifting solution to avoid ventricular tachycardia [42,43,90,91].

Furthermore, there is a constant need to check the biocompatibility of the CNTs inside the body. Many researchers are working hard in the field of materials-based improvements. They are facing many challenges to improve atrioventricular conduction (a pacemaker suffices), which is the main reason for the intramyocardial delay. Integration of the neuroscience surface modification is the need of the hour. In vivo reconstitution should be studied further for the biocompatibility of CNTs. However, the positive results of the CNTs based materials send new ray of light which is helpful in avoiding sudden death. After the survey of the literature, it is impossible to overlook CNTs based materials are having vivid applications in the biomedical field. CNTs can be used for practical applications on sensitive parts of the body [91]. Since, the development of biocompatibility of CNTs and surface improvement are required. Therefore, to preserve the balance in the structure of CNTs and modifying the CNTs to contemporary needs is still a challenging task. Moreover, it is likewise essential to improve the biocompatibility of CNTs while retaining natural properties. The review can also motivate researchers to explore improvements in various arenas of biomedical, environment, energy storage, semiconductors, food science, etc.

6. Air Pollutants Removal by Using Carbon Nanotube Filters

The impact of air pollution on human and other animals, plants living on earth is large. Greenhouse gases present in the environment make the mother earth hot. Greenhouse gases are the major reason for global warming. Greenhouse gases such as water vapor, carbon dioxide, methane, ozone, nitrous oxide, chlorofluorocarbons, etc. are the major contributors. In urban areas, diesel and gasoline fuels are mostly used as a nonrenewable source of energy, which is the major contributor of air pollution. Incomplete combustion of fuel emitted from automobiles and vehicles are the major contributor. Nitrogen oxides as NO combine with the ozone layer and deplete the ozone layer.

A volatile organic compound (VOCs) contains the organic compound benzene, which is very toxic for living organisms. Volatile organic compounds (VOCs) are generated by fuel combustion and incomplete combustion. Epidemiologic studies have reported that cardiopulmonary diseases and lung cancer are caused by air pollution. Daily increases in air pollution in cities, which are the major contributor of deaths [92]. Air purification is a subject of interest for environmentalists. They are looking for substitute technologies to overcome the conditions that happen seriously in human life and for the entire biosphere. Sorption process for storage and purification are used for decades. Carbon nanotubes (CNTs) are novel materials used for controlling pollutant emissions because of the unique chemical and physical properties. Carbon nanotubes (CNTs) are used as sorbents for controlling environment pollutions [93]. Carbon nanotubes (CNTs) are

developed on membrane support of diverse materials with pore sizes of around *10.5 mm*. CNTs are used to remove gases harmful and competence depends on diverse variants. Varied range of new filters has been developed using different materials such as metal or ceramic trusses. The CNTs based filters developed on Si/SiO_2 stainless steel or glass fiber show good filter efficiency for various particle sizes [94–96].

Various materials originated from carbon, for example, active carbon and carbon fiber, have extensively used in the gas sorption processes. In the current years, CNTs are extensively used for controlling pollutant emissions and they are acting as very good sorbent for environmental applications. Nanotube filter was efficaciously produced and exploited to remove bioaerosols and acted well with biological agents from the water for filtration [93,97–106].

7. Cases and Studies on the Toxicity Through CNT

Nano sized particles as being naturally present in the environment for millennia in the form of viruses, volcanic ash, and forest fire ash, etc. Human exposure to nano-sized particles leads to health-related problem. Industrial Revolution has increased the count of nano-sized particles noticeably. Polymer fumes, fumes produced by burning of metals, incinerators, or combustion engines. Nanoparticles are produced naturally as byproducts from these reactions. Growth of nanotechnology applications in various fields and exposure of nanoparticles to human and living beings is enviable. These exposures create several health-related issues in the living being. Health related should be taken care when there is use of nanomaterials such as CNTs.

7.1. Water soluble Carbon Nanotubes Increase Agricultural Yields

Agriculture sector is facing difficulties because of the lack of advanced technologies. Boost in agricultural production could be possible using nanotechnology-based applications. Nanotechnology is useful in controlling the delivery of nutrients which in turn increases the crop production. High-tech farming is supported by their direct and indirect applications of nanomaterials. When the plants are able to absorb a good amount of nutrients from the soil, the agricultural production is increased [107,108]. Studies had proved that CNTs play a supporting role in both in vitro and in vivo. Both types of CNTs such as MWCNTs and SWCNTs are useful in delivering nutrients to plants as they are able to cross the plant cell walls and reach cellular organelles. MWCNTs are shown to be much stronger than SWCNTs in experiments, Water solubility of CNTs is increased by chemical modification [109]. Chemical modification can be possible by introducing a variety of functional groups (covalently and non-covalently) on their outer surfaces. Some of the methods for the modifications in the gas phase are ozone-induced oxidation of CNTs; the second known methods are UV-ozone oxidative dielectric barrier discharge.

Internal translocation means a chromosome is transferred to another chromosome using CNTs. CNTs are used for delivering biofertilizer. When biofertilizer is delivered through CNTs, the unique properties of CNTs will provide large surface area, superior reactivity, and smaller particle size, which support the profound delivery of biofertilizer inside the plant [110]. The CNTs facilitate nutrients delivery, which is helpful in humanizing their growth and yields. When CNTs are administered at low concentrations, the positive response is shown by the plants. However, if the concentration of CNTs is more, then sometimes it causes damaging effects on plant growth. The CNTs effects on the surroundings should be investigated before extensive use in agriculture. Protection of plants should be on a priority base before large-scale use of CNTs is there [111].

7.2. Role of Carbon Nanotubes in Reducing Environmental Pollution

Carbon nanotubes (CNTs) play an imperative role in the removal of environmental pollutants. Protection of the environment and health is the major concern for scientists and environmentalists in the route of protecting the environment [1]. Nanotechnology has a broader perspective for protecting environmental health and sustainable development. The scientific data has been collected from various sources such as Google Scholar, Scopus, Elsevier, and PubMed and analyzed to evaluate the results. Out of the reviewed data, it was concluded that general methods of sewage treatment are not adequate to remove the environmental pollutants totally. The CNTs used adsorption methods are simple and require less energy consumption in comparison with conventional methods. It is extensively used in various applications such as drinking and sewage water treatment, and in removing pharmaceutical pollutants, in the treatment of leachate, in the removal of petroleum compounds, heavy metals, in dye removal, and in removing leachate contaminants [2,3].

With the increase in urbanization and population exploitation, there is a constant need for the protection of the environment for long-term survival of human beings. Controlling pollution generated by human

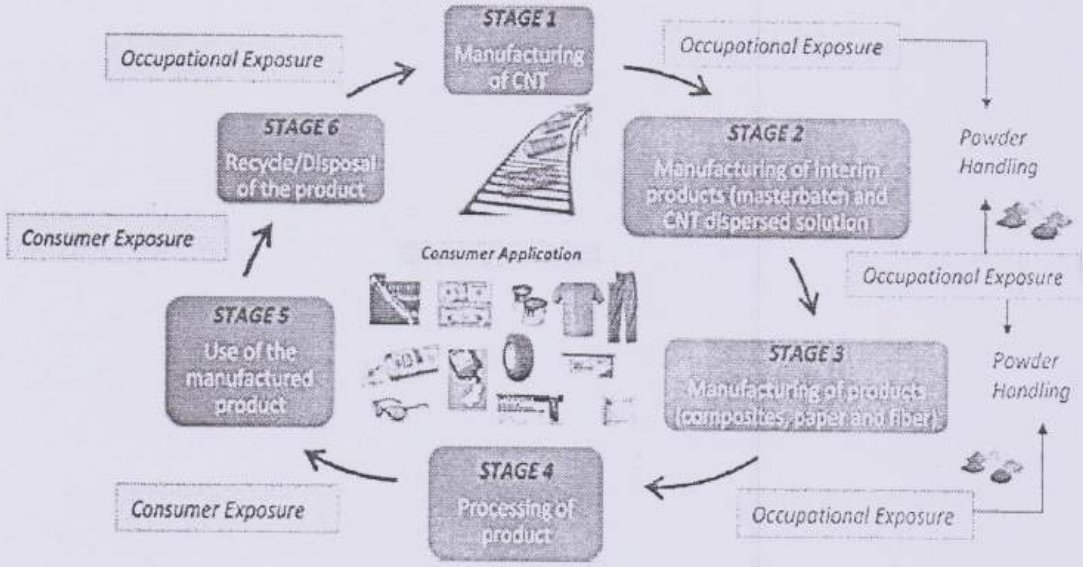


Figure 5. The life cycle of CNTs is related to risk assessment studies in which the first, second, third, and sixth are the stages of occupational exposure. The fourth and fifth stages come under consumer exposure (Reprinted with permission from Ref [11]. Copyright 2018 Springer Nature).

intervention is needed on the priority base. Easy, fast, high problem solving, cheap technologies are in demand. The research can be concluded as effective in establishing an impression that CNTs as effective adsorbents, have high prospective in removing pollutants which helps in sustainable development. It can be reused, recycled, and reduced consumption of fossil fuel. CNTs are painstaking eco-friendly materials which reduce carbon footprint in the environment [4,5].

7.3. The Toxic Effects of Carbon Nanotubes in Water Purification

The elongated-term use of carbon nanotubes (CNTs) for water purification requires nanosafety guidelines. Risk measurements decrease the toxic effects of CNTs. Different purification methods of waste water treatment by CNTs involve certain types of risk, which need to be studied through risk assessment of CNTs [11]. Scarcity of knowledge in terms of health risks associated with CNTs made scientists to design risk estimates. There should be universal CNT safety guidelines for analyzing the CNTs risk [12]. To narrow down the gaps, various new risk analysis routes and CNT-based water purification technologies have been developed to optimize the results. The CNTs safety clock has been designed to assess risk evaluation and organization. The CNTs safety guidelines have been designed by taking concerns about the diameter of CNTs, its length, aspect ratio, charge, hydrophobicity, functionality, etc. It helps in establishing CNTs actions in waste water treatment plants and consequent discharge into the environment [13].

In Figure 5, the life cycles of the CNTs, in brief has been discussed in six stages. The first, second, third, and sixth are the stages of occupational exposure. The fourth and fifth stages come under consumer exposure. The first stage in which the CNTs are manufactured occurs in a closed furnace without oxygen intrusion to avoid exposure to CNTs. The master batches and CNT-dispersed solutions are the intervening products that have been synthesized in the second stage. In the third is the product formation stage in which the handling of the CNTs will reduce. The fourth and fifth stage is the processing of products and final use of the product. And the last stage is disposal or recycling [14].

Many safety issues, risk assessment, and control measurements for E-CNT (Environmental CNTs) have been discussed in the research paper. With diverse applications, different types of risk are also a concern for the scientist. Application-specific risk assessment is utmost important in the case of nanomaterials such as CNTs. Risk associated with the use of nanomaterials creates a type of nano phobia among people. Scientists and researchers are working hard to remove such types of nano phobia by providing safe water facilities, conserving our environment.

The CNTs in water purification require proper handling, utilization, and discarding of nanomaterials in a more precise way. To address the safety challenges

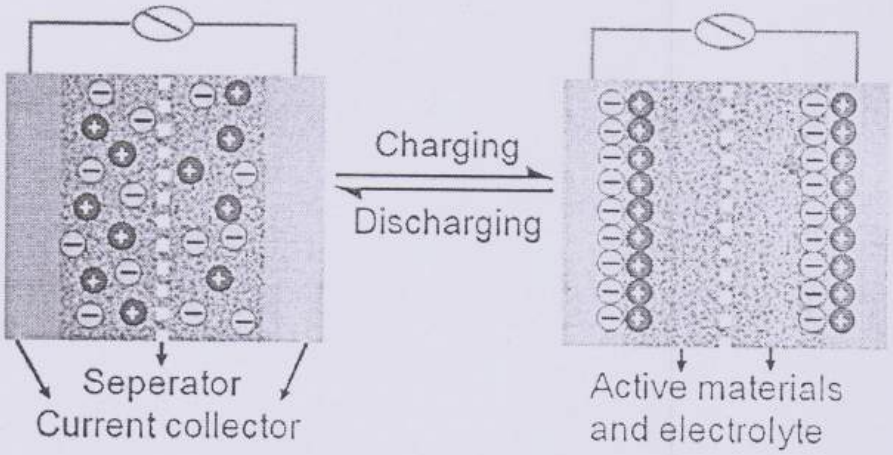


Figure 6. Schematic diagram of a super capacitor cell shown here is composed of high surface area activated capacitors with a very emaciated layer of electrolyte as dielectric. The CNTs act as superior electrode materials for capacitors (Reprinted with permission from Ref [115]. Copyright 2013 Elsevier).

associated with nanomaterials, there is a constant need of safety guidelines and regulatory frameworks. These safety guidelines and regulatory frameworks not only categorize and differentiate nanomaterials but also assess the impact on human health and the environment. Case-to-case study measures the profound risk assessment of nanomaterials' structure–property relationships. The assessment helps in fixing the universal safety guideline which accurately keeps an eye on the prospects of the CNTs [112].

7.4. An Insight into Sustainable Applications of Carbon Nanotubes in Protecting the Environment

In line with the sustainable environment and green technology perspectives, carbon nanotubes (CNTs) act as a promising material for recent developments. The CNTs, due to its distinctive properties, are set to be a benchmark in the field of pollution control and monitoring, waste management, composites, water treatment, biotechnology, super capacitors, renewable energy etc. and act as popularly known materials for decades. The CNTs have astonishing physical, chemical, and electronic properties which act as cost-effective in various applications. The potential hazards of these nano materials have been discussed in the review. CNTs are wonderful materials used in various environmental fields which come to know from the literature [113,114].

Reduction of waste disposal in the environment can be achieved by using the CNTs as super capacitors which provide small size, high portability, utmost power density, extended suitability, and elevated energy. Figure 6 shown here is composed of maximum surface area activated capacitors with a very emaciated layer of electrolyte as dielectric. The CNTs act as superior electrode materials for capacitors. Generally, the CNTs are coupled to a thinner layer of the electrode, increasing the capacity of the capacitor to accumulate higher energy density. The CNTs are placed in between the electrode and electrolyte. Vertical alignment of the CNTs increases the capacity of the super capacitor by increasing the surface area of the electrode. The CNTs alone are not suitable to use the electrode due to their little capacitance. However, CNTs combines with transition metal oxides to produce sustainable energy. The metal oxides are such as manganese oxide (MnO_2) and ruthenium oxide (RuO_2), etc. The energy density *(5 Wh/kg)* up to 10 folds increased using capacitors, with only around *1.0 Wh/kg* [115].

The green energy produced by clean combustion is the need of the hour. Biofuel cells created by biomass catalytic activity, photovoltaic devices formed from renewable sources such as solar, hydrogen fuel cells using hydrogen as feed produces energy without producing toxic gases to the atmosphere. These alternative energy producing devices prohibit the elevated demand for fossil fuel. On the other hand, these technologies are still required to cross many roads to fulfill growing energy demands. These technologies are on the emerging stage of development, practically needing more commercialization. The CNTs-based super capacitors produced superior power density bestowed as an

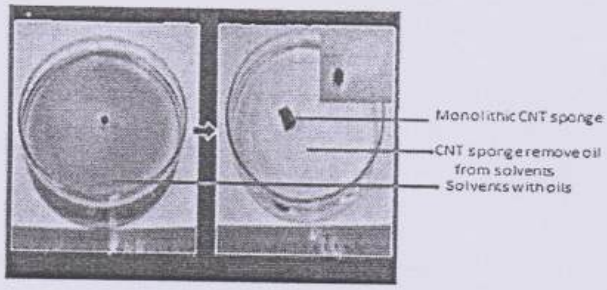


Figure 7. Application of CNT sponge in the cleanup of oil from water which shows a monolithic CNT sponge prepared by chemical vapor deposition via ferrocene as a precursor (Reprinted with permission from Ref [118]. Copyright 2015 Premier Publisher).

alternative fueling replacing traditional batteries. Super capacitors have high capacity and extended usage time that reduces the generation of waste in the environment. The involvement of CNTs as a nanocomposite design which is green in nature can fulfill the 3 R (reduction, reuse, and recycle) capability of raw materials. Low cost of CNTs also favors the usage of CNTs in various fields. Source reduction of CNTs should be avoided for safe human health hazards of CNTs [116,117]. It also demonstrates that MWCNTs perform even easier in corrosive environments. When used as a catalyst for fuel cells, MWCNTs exhibit lower loss or oxygen depletion than SWCNTs.

7.5. Environmental Applications of Carbon Nanotubes

Carbon nanotubes are the most studied materials in modern times. The CNTs have astonishing physical, electronic, and chemical properties, which creates an extensive diversity of applications. Here, the contribution of CNTs in various fields has been discussed, such as air pollution, water pollution, and safe renewable energy, developed energy, super capacitors, and green nanocomposites, etc [118]. It also works extensively in the field of biotechnology, providing sustainable environment and green technologies [119]. For deliberation of CNTs at a large scale, we need to discuss various aspects of charge and impending hazards. Based on the studies, it could be easily given the impression that CNTs have immense potential and are capable materials for large-scale application in various environmental fields [120].

Figure 7 shows a monolithic CNT sponge prepared by chemical vapor deposition via ferrocene as precursor. The CNTs sponges have elevated porosity and very little density and have haphazardly entangled three-dimensionally.

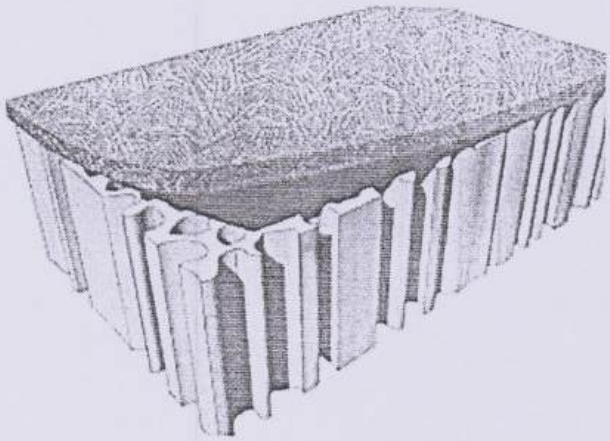


Figure 8. Hybrid filter for effective water purification in which a porous ceramic supports will provide the CNTs cross-linked filtration layer (Reprinted with permission from Ref [123]. Copyright 2008 American Chemical Society).

The CNTs sponge is useful in removing oil in large quantities, i.e., *80 to 180 times* their own weight, and can effectively be used in an extensive range of solvents and oils. The CNTs sponges have high floating-and-cleaning capability because of high hydrophobicity. Regeneration of CNTs sponge is easily possible by mechanical compression. Waste products could be easily burned in air without destroying the sponge structure [121].

The CNTs have been established as a large amount of practical and effectual material in diverse applications. It helps to create a simple process out of the complicated one which reduces the usage of material and resources which in turn decrease the exploitation of resources. Apart from this, the potential application of materials, health hazards, and production is also an area of concern. It covers all areas right from pollution control, environmental engineering, and biotechnology. It is very well said that nonmaterial would rule the world in technological development [122].

7.6. Future Applications of Carbon-Based Nanomaterials in Protecting the Natural Environment

Environmental challenges make human beings in search of new materials to solve their problems. Carbon-based nanomaterials are promising materials that address all challenges related to the environment [123]. The review touched out the arenas of environmental applications, such as water purification, membrane sorbents, environment sensors, and different modified filters for water and air purification, electronic materials which in turn helpful to save the renewable energy and prevent pollution [15]. In view of the unique physical, chemical, and

electronic properties of the CNTs, the present article fully explains the jest of future opportunities of nanomaterials' in protecting the environment.

Hybrid SWNTs ceramic filters have been developed and open new avenues in this field. They are having tapered diameter, large surface area, and good thermal resistance which combines the porous aggregate structure of SWNTs. In Figure 8, a porous ceramic support can provide the CNTs cross-linked filtration layer. These layers are highly permeable SWNTs filters demonstrated good efficiency in removing biological disease causing organisms from water. They are demonstrated elevated resistant to high temperatures and adequately durable for repeated reuse in water treatment applications [16].

Incorporation of green technology in product design and manufacturing is utmost important for saving our environment. Various opportunities for product design; regeneration for secondary applications has been explored. Nanomaterials which are used once could find it potential application in the form of 'Best out of waste' in various other fields like structural reinforcement or road construction. To minimize the disposal of nanomaterial's in the environment, certain types of strategies should be fixed. The multidisciplinary collaboration may act as a gift for future generations, which is possible by the joint effort of the product development engineer, environmental scientists, and toxicologists [17]. Several challenges act as barriers in this road for scaling up the technology from lab to industry. High price availability of nanomaterials is always a challenge in coming times. Waste management in the existing infrastructure system according to the present need is not sufficient to provide lodging for new nanomaterial's products. The risk of these new technologies is always a matter of concern for the scientist. Public awareness and concern about the risk of nanomaterials is also screwing up the minds of stake holders. Efforts are made to earn people approval and enhance the arena for nanomaterials, which is helpful in creating a conducive environment [18].

7.7. Life Cycle Assessment of Semiconductor Devices with Carbon Nanotubes

The use of carbon nanotubes (CNTs) in electronic applications is very much rampant due to its inimitable mechanical, thermal, and electrical properties. The environmental impact and health hazards of carbon nanotubes (CNTs) have been a concern with the increase in the commercialization of nanomaterials. There is should be short of the rate of information concerning the potential health hazards and environmental impact caused by the CNTs. The study of life sequence environmental impacts of CNT helps to evaluate the possible adverse effects caused by CNTs [19]. It enhances and motivates scientist researchers to develop

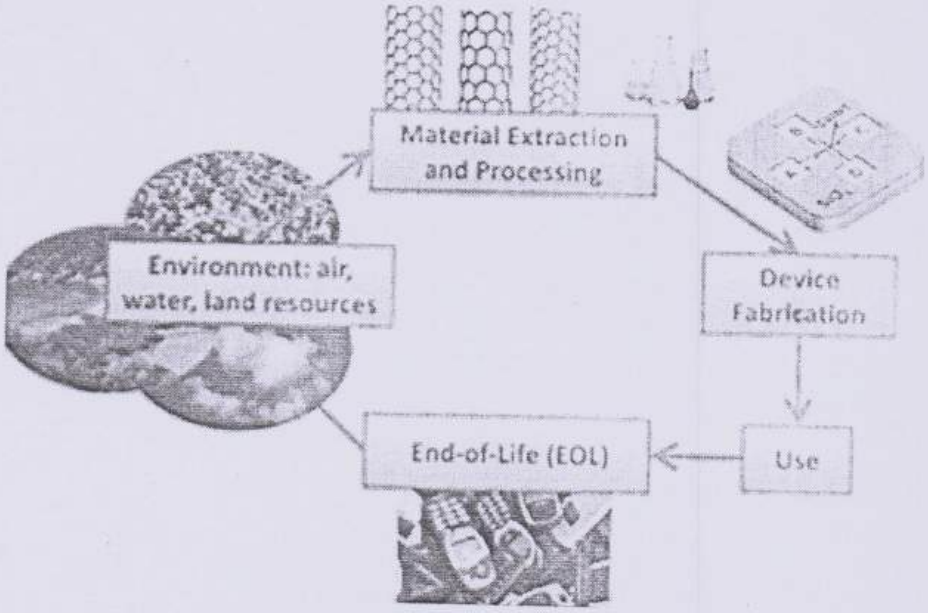


Figure 9. The figure shows life cycle assessment of semiconductor devices with carbon nanotubes. The present figure estimates the impending application of CNT switches to contemporary cellular phone flash memory (Reprinted with permission from Ref [10]. Copyright 2013 American Chemical Society).

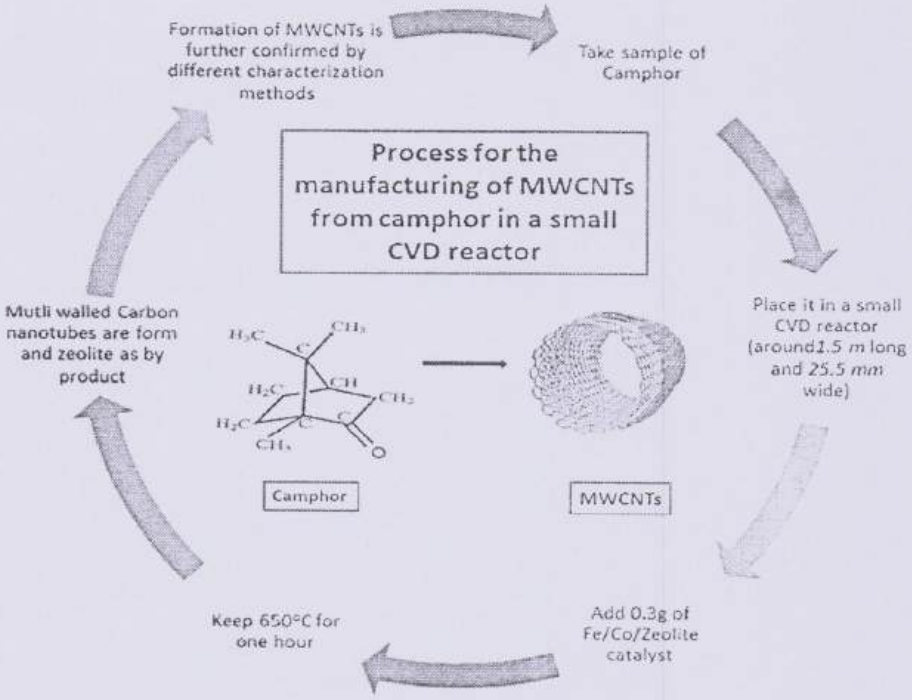


Figure 10. Step wise process for the manufacturing of MWCNTs from camphor in a small CVD reactor.

new products which minimize the adverse effects of CNTs.

The present Figure 9 estimates the impending purpose of CNT switches on contemporary cellular phone flash memory. Life cycle assessment (LCA) is an important tool to assess the environmental flow of nonvolatile bistable electromechanical CNT switches by studying the stages right from the beginning of fabrication application and end-of-life [20]. The study of the life cycle from first-order anticipated use of the CNTs product and end-of-life (EOL) stages indicates that there is a constant need of reducing the environmental burden at every stage.

The CNTs switch technology could be replaced by using NAND flash FGMOSFETs, which provides better improved results and in turn decreases the environment landfill and circumvents the release of CNTs. EOL (end-of-life) management of the CNTs switch designated in the separation and metallurgical processes used in the present day needs to be modified for proper release of the CNTs in the environment [21]. Lots of efforts need to be done at the modeling level to measure, control, and optimize the release of emissions from nanomaterials starting from the fabrication to the end of life level. There is always a need of qualifying each stage of the life cycle for better environment sustainability [22]. The fact is that CNTs technology is useful in reducing the energy expenditure and increasing usage in lots of applications. Knowledge of the life cycle will help scientists to start from the fabrication level through the development

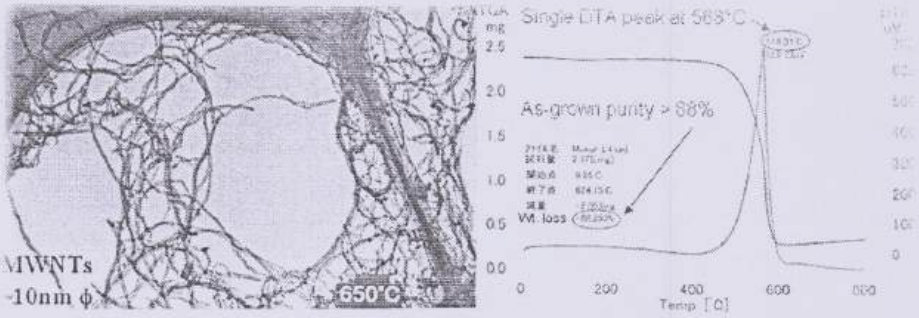


Figure 11.

stage until the final stage. The negative environmental impact is reduced by EOL management and brightens the future of CNTs-enabled technologies [23,24].

7.8. Potential Applications of Promising Carbon Nanotubes Prepared Using Organic Camphor

Environment friendly process is the need of the hour. Saving the environment is the paramount task for the human race. The synthesis technique depicted here fully addresses the '12-principle' practices of green chemistry. Camphor is known as an environment-friendly hydrocarbon. Elevated-purity carbon nanotubes (CNTs) can be produced from camphor hydrocarbons using a chemical vapor deposition method. The process can be accomplished in a small chemical vapor deposition (CVD) reactor (around *1.5 m* long and around *25.5 mm* wide). Approximately yield of *1.62 g* multiwalled carbon nanotubes (MWCNTs) of diameter *~10 nm* can be obtained by *3 g* camphor by optimizing the temperature of *650°C* at *1 h*. Generally, the camphor-to-CNTs manufacture efficiency is *50%*. However, optimizing the process efficiency would be increased up to *88%* [124].

Figure 10 clearly depicts the manufacturing of camphor in a small CVD reactor (around*1.5 m* long and *25.5 mm* wide). The process requires around *3.5 g* camphor which is vaporized at around 201°C under a tolerant argon flow of around *51 cm*. It is further pyrolyzed at around *0.35 g* Iron cobalt saturated zeolite support at around 655°C. The process can blow up the zeolite bed more than fifty times by volume, this leads to help in obtaining the yields of around *1.63 g* MWCNTs of diameter ~10 nm. The purity is further increased by *88%*, which is clearly demonstrated in the characterization process shown by transmission electron microscopy (TEM) images, and thermogravimetric analysis (TGA).

Figure 11 clearly demonstrates the characterization process with TEM (transmission electron microscopy) image and TGA (thermogravimetric analysis) curves of camphor and zeolite beads (Reprinted with permission from Ref [124]. Copyright 2007 IOP Publishing)

Nanotechnology opens all avenues and is widely used in all applications. As we all know that the carbon nanotubes (CNTs) are single-layer carbon atoms (graphene) and are rolled-up sheets in a cylindrical manner. Carbon nanotubes (CNTs) have incredible potential in nanotechnology and a gigantic amount of effort has been invested in producing CNTs worldwide [125–127]. The above technique fully is in line with the 12-principles of green chemistry. The described process is achieved and highly handled for all parameters of fabrication such as maximum yield and elevated purity growth control. It is the easiest process ever known which claims to produce high-quality CNTs by saving time, money, energy, and the environment [128].

7.9. Applications of Smart Materials Based on Carbon Nanotubes and Nanofibers

Industrial development requires a constant need for advanced materials for the advancement of science and technology. For fully filing with the ever-changing and increasing demand of better and advanced materials, the production of hybrid materials is a superior option.

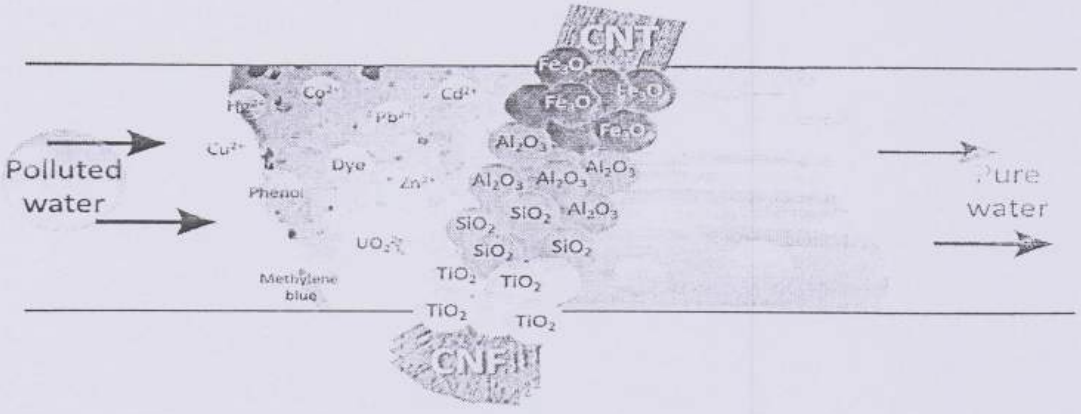


Figure 12. The figure depicts the application of hybrid materials in water purification. Hybrid materials are the synergy of two or more individual materials for the production of advanced materials (Reprinted with permission from Ref [129]. Copyright 2020 Frontiers in Chemistry).

Hybrid materials (HMs) are formed by combinations of different structural components which inherit some of their properties and functions [129]. After a combination of two or more different materials, the new material is structurally different from that of their constituent materials. Among many hybrid materials in the category of filamentous forms, hydride materials formed with carbon nanotubes and carbon nanofibers and some inorganic nanoparticles create a center of attention. Its structure and morphology, unique charge and energy transfer processes lead to synergistic effects. The review of these types of materials is useful in various ecological applications [130].

Figure 12 depicts the picture of the hybrid materials fabricated and utilized for environmental applications. The carbon nanofibers (CNFs), and carbon nanotubes (CNTs) and inorganic nanoparticles form a filamentous structure which render to a high specific surface area, unique properties better than the conventional nanomaterials.

Hybrid materials are the synergy of two or more individual materials for the production of advanced materials. It provides an additional degree of freedom which opens new avenues for the development of new materials. Hybrid materials have enhanced properties such as good conductivity, high sorption, better catalytic, mechanical, optical, and magnetic properties [131]. The hybrid materials manufactured by carbon nanotubes and carbon nanofibers in blend with inorganic (metal oxide) nanoparticles can be able to solve the maximum number of water treatment problems, helpful in preventing air pollution, and recycling of waste. These hydride materials act as proficient sorbents and help in photo catalysis which reduces the usage of materials. Environment electronic magnetic applications of hybrid materials could only be possible by developing enhanced compatibility among the materials used in making hybrids [132]. There is a need of development of novel protocols which proliferate new ideas for an inexpensive and trustworthy approach to the fabrication of advanced hybrid materials [133].

7.10. Diverse Applications, Present Trends, and Future Viewpoints of Nanotechnology in Food Science

Nanotechnology is a face-changing technology in various applications of food, medicine, and agriculture sectors [134]. Qualitative and quantitative production of healthier, safer food can be easily

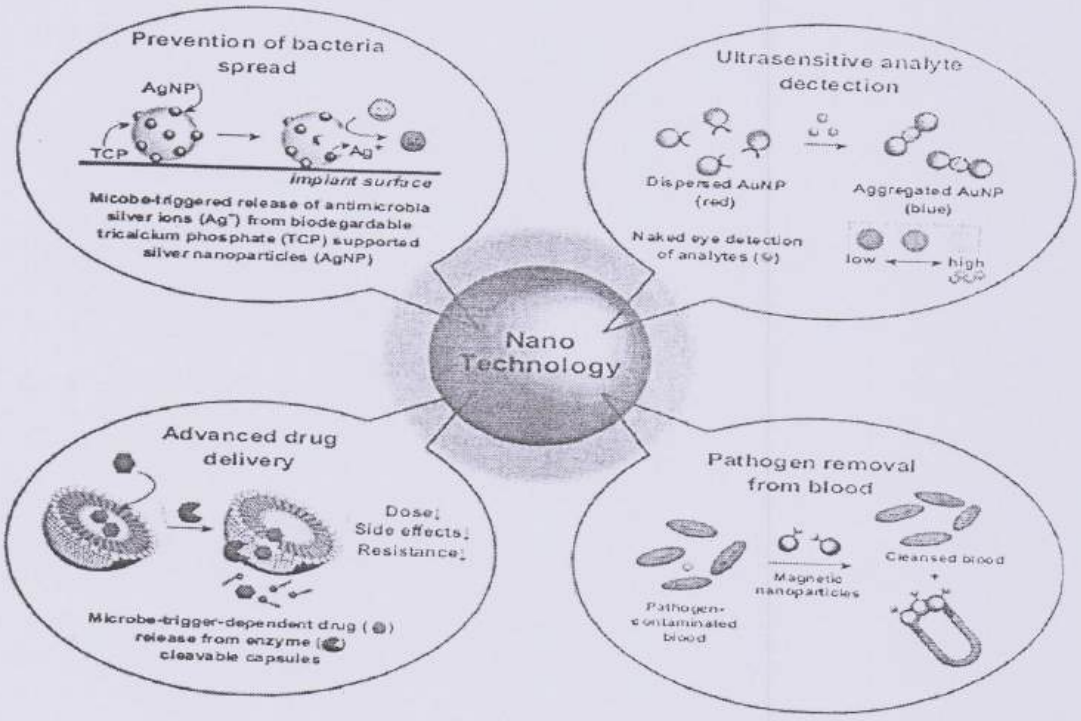


Figure 13. Nanotechnology-based solutions for the detection and prevention of microbial infections. In the figure, prevention of bacteria spread, ultrasensitiveanalyte advanced drug delivery, and pathogen removal from blood has been depicted (Reprinted with permission from Ref [134]. Copyright 2020 Springer Nature).

produced with the help of nanotechnology. Nanotechnology is helpful in food technology in various ways such as it increases the shelf life of food, checks, contamination, and produce of superior food quality. Better-quality food can be produced by nanotechnologies that are unpreserved or semipreserved in nature [135]. Conventional food technologies have certain voids which are easily filled by these nanotechnologies. Nanotechnologies are helpful in food technology in various arenas such as processing, packaging, security, and storage. It also helps in enhancing the esthetic look of the food. It increases the taste and consistency of food through inner modifications of particle size, surface charge, etc. Nanotechnology is also useful in food protection and conservation through advanced methods of food packaging, etc [136].

Nanotechnology is helpful in preventing, detecting, and treating bacterial infections. Various metallic nanoparticles are silver, gold are helpful in prevention, ultrasensitive detection, drug delivery, and pathogen removal from blood. Figure 13 clearly depicts the nanotechnology solutions usage at every stage in preventing disease drug delivery and detection.

Right from the food production, processing, storage, conversation, and packaging of food, nanotechnology plays a pivotal role [137]. Nanosensors help in detecting the stability of food, nutritional status, etc. Generally, food is biodegradable in nature, nanotechnologies raises the shelf life of food. Targeted deliverance of food bioactive compounds can be easily achieved by nanotechnology. Nanotechnology provides nano foods which are widely accepted by consumers. Uses of nanocolloidal particles in diverse branches of the food industry are prevalent. Sustainability and enhanced quality of foods can be achieved by colloidal particles in nanotechnology [138]. In a few countries, standard regulatory rules are implemented for the maximum use of nanotechnology in food products. Insufficient scientific investigations generate ambiguity among the producers as well as consumers and about the efficacy of nanosystems. Advancement of technologies like nanotechnology also creates a danger that it may come into the food chain through various sources of air, water, and earth. It can also damage DNA as well as cell death, etc. In vivo studies of nano foods in humans and animals may help in leading to certain conclusion. Scientists suggested that if nanotechnology is used in a regulated manner, it has been supporting and enhancing the quality of food which will benefit human health in the long run.

7.11. Conversation of Low Value Biomass with High Activated Carbon and Carbon Nanotubes

In the case study, carbon nanotubes were synthesized from low-value Miscanthus giganteus lignocellulosic biomass. The CNTs are synthesized from high-value materials out of low-value products. The characterization techniques such as XRD, SEM, FTIR, thermal analysis, TGA/DSC, and FTIR techniques were given here fully explained and provide testimony of the conversion of Miscanthus×giganteus lignocellulosic biomass into CNTs.

Universal energy requirement is accomplished by the constant use of fossil fuels. However, the use of fossil fuels replenishes our renewable resources at a very high speed. Certainly, there is a need for alternative fuels with low CO_2 and particulates to save our renewable resources and environment. The low biomass Miscanthus giganteus lignocellulosic has been converted into high-value materials such as activated carbon and carbon nanotubes. The

Miscanthus contains high alkali silicate content which generates a high amount of silica ash, emits NOx, SOx, and particulates [139]. The emissions related are spoiling our health, energy resources, and environment. An alternative approach has been tried here in which activated carbon has been synthesized by low biomass (Miscanthus giganteus). The formed activated carbon enhanced physical and chemical properties such as high surface area and pore volume of around $0.93\ cm^3g{-}1$.

Utilization of waste biomass into useful products is an illustration of a circular economy. Circular economy means using waste product in generating useful products which in turn reduces pressure on the environment, safe renewable energy, utilization of waste, hence constant supply of raw materials, motivating innovation, making better economic growth. Waste lignocellulosic biomass has been converted into high surface area activated carbon multiwalled carbon nanotubes. To get the desired result, activated carbon with a contact angle of around $\theta = 9.89°$ was mixed with nitrogen-based material and iron precursor. The synthesized materials were tested for heavy metal removal tests using a lead solution, 90% removal capacity has been seen after the first hour of testing. The material form may have a wide range of applications in the arena of wastewater treatment and other uses where activated carbon/carbon nanotubes are frequently used [140].

Table 1. Potential applications of CNTs in various fields.

Sr. No	Name of Material	Application in specific field	Roles	Reference
1	**Carbon nanotubes for water purification**	**Water purification**	Carbon nanotubes are able to remove all types of pollutants in organic, inorganic, or biological materials	[45]
2	**Carbon nanotubes in electrical/ electronic applications**	**Electrical/electronic applications**	Carbon nanotubes provide small size, carbon based nano-electronics having high flexibility compared to conservative silicon electronics. Carbon nanotubes have unusual properties because of the low dimensionality	[61]
3	**Carbon nanotubes in electrode materials**	**Electrode materials**	The CNT is also used as an electrode material for the capacitor to augment the ability of the capacitor to store higher energy density because of the large surface area	[63]
4	**Carbon nanotubes in energy conversion storage applications**	**Energy conversion storage applications**	The CNTs material has commenced ground-breaking developments in the field of energy conversion, which includes the development of solar cells, fuel cells, hydrogen storage, lithium ion batteries, and electrochemical super the capacitors.	[67]
5	**Carbon nanotubes as electrochemical and electronic biosensors**	**Electrochemical and electronic biosensors**	The CNTs improve electron transfer which is very useful in combining electrochemical and electronic biosensors	[70,71]
6	**CNT is used for targeted therapies such as drugs, gene delivery, and cancer treatment, other biomedical applications**	**Drugs, gene delivery and cancer treatment, other biomedical applications**	CNTs are effectively used in drug delivery systems and act as nano carriers. Versatile properties of carbon nanotubes make it suitable for biomedical applications. They are used in delivering drugs for anticancer drugs, genes, and proteins	[76]
7	**Carbon nanotube filters used in controlling air pollutants**	**Air pollutants**	Carbon nanotubes (CNTs) are novel materials used for controlling pollutant emissions because of the unique chemical and physical properties. Carbon nanotubes (CNTs) are used as sorbents for controlling environment pollutions	[93–96]
8	**Carbon nanotubes increase agricultural yields**	**Agricultural sector**	CNTs play a supporting role in both in vitro and in vivo. Both types of CNTs such as MWCNTs and SWCNTs are useful in delivering nutrients to plants as they are able to cross the plant cell walls and reach cellular organelles.	[97–99]
9	**Carbon nanotubes in reducing environmental pollution**	**Reducing environmental pollution**	CNTs are painstaking eco-friendly materials which reduce carbon footprint in the environment	[4,5]
10	**Environmental applications of carbon nanotubes sponge**	**CNTs sponge in the cleanup of oil from water**	The CNTs sponge is useful in removing oil in large quantities, i.e., *80* to *180* times their own weight, and can effectively be used in an extensive range of solvents and oils.	[110]
11	**Hybrid SWNTs ceramic filters has been developed and open new avenues in this field.**	**They are having tapered diameter, large surface area, and good thermal resistance which combines the porous aggregate structure of SWNTs.**	Efforts are made to earn people approval and enhance the arena nanomaterials, which is helpful in creating conducive environment	[112–184]
12	**Green carbon nanotubes**	**Carbon nanotubes prepared using organic camphor**	Elevated-purity carbon nanotubes (CNTs) can be produced from camphor hydrocarbons using chemical vapor deposition method	[113–115]
13	**Smart materials based on carbon nanotubes and nanofibers**	**Hybrid materials**	Hybrid materials (HMs) are formed by combinations of different structural components which inherit some of their properties and functions	[118]
14	**Nanotechnology in food science**	**Food Science**	Nanotechnology is also useful in food protection and conservation through advanced methods of food packaging, etc.	[125]
15	**Waste biomass into useful products with high activated carbon and carbon nanotubes**	**waste biomass into useful products with high activated carbon and carbon nanotubes**	Such CNTs have wide applications in the field of water adsorption applications, wastewater remediation, numerous industrial applications, for example, microelectronics, tissue engineering, composites, etc.	[128–132]

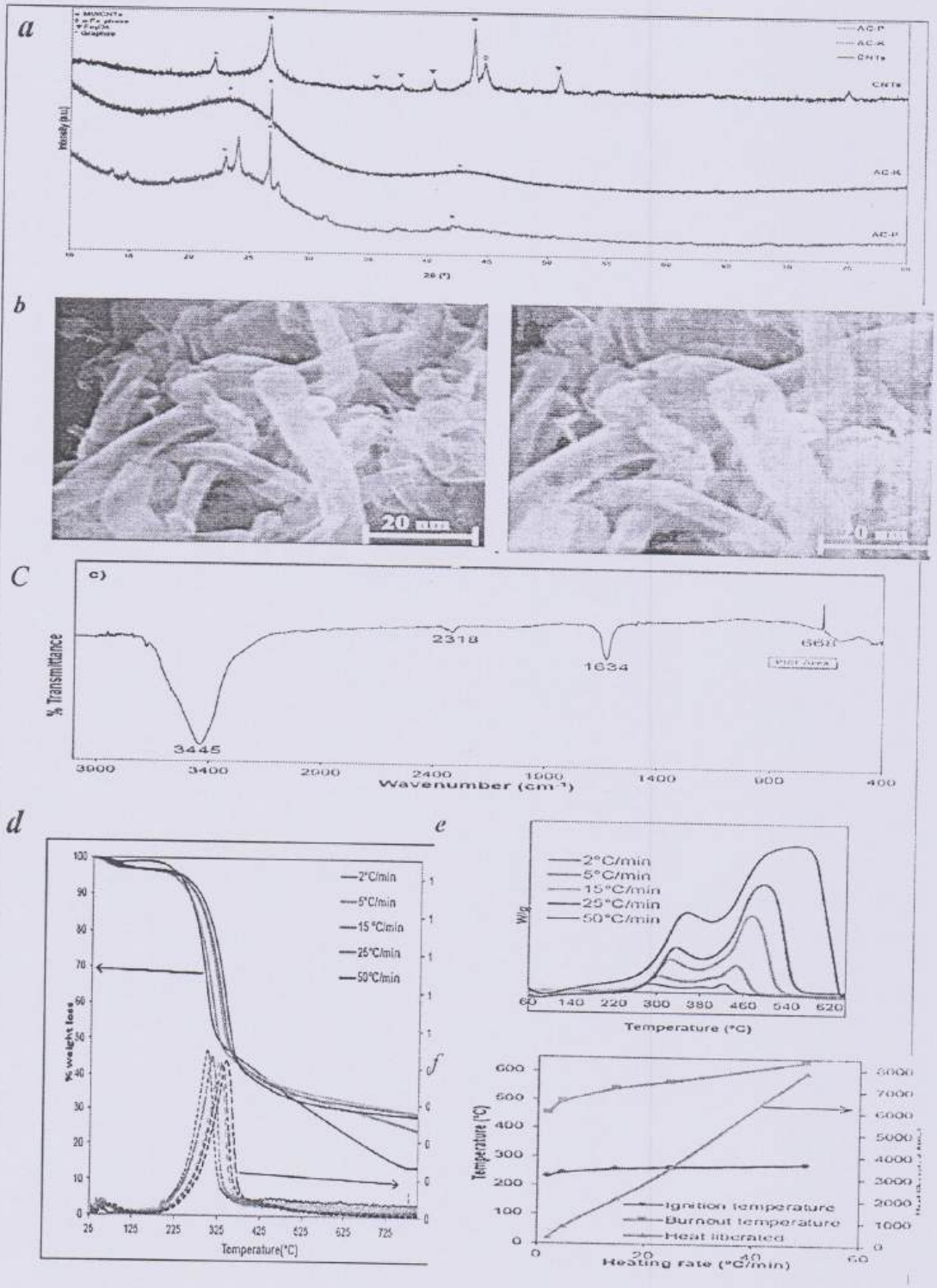


Figure 14. (a). The XRD diffractogram patterns of carbon nanotubes. (b). The SEM images of carbon nanotubes. (c) shows the FT-IR of the CNTs in the range of wave numbers of 400–4000 cm-1. (d) shows the thermal analysis under the N_2 atmosphere (e). The differential scanning calorimetry (DSC) curves with different heating rates under the N_2 atmosphere. (f) DSC curves with different heating rates under air atmosphere along with (g) the calculated ignition, burnout temperatures and heat liberated during the combustion (Reprinted with permission from Ref [139]. Copyright 2020 Springer Nature).

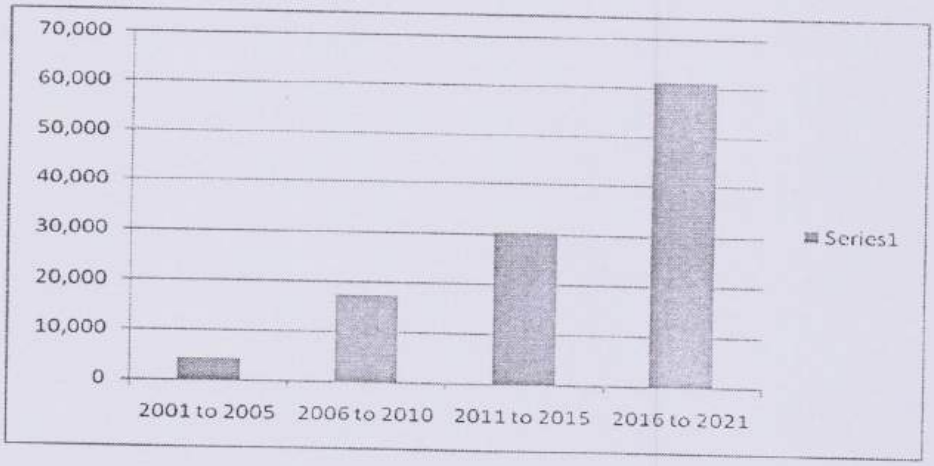


Figure 15. The trend of patents filed in the years [2001–2020].

7. Future Applications of CNTs

In this review article, the recent applications of CNTs in various fields, such as in water purification, water disinfection, electrical and electronic applications, biomedical energy, air purification, etc. have been discussed. They have given the 3 R (reduce, reuse, and recycle) concept. At the end, it is considered that the CNTs have been in use for decades for various applications. Nanomaterials, especially CNTs, act as an alternative material for future sustainable energy sources. The CNTs used in various applications serve as an excellent adsorbent, energy storage material, and energy transfer material. It can also be exploited in various applications of biomedical fields, such as biosensor, drug delivery, cancer treatment, etc. The CNTs are already commercially available and it is inevitable to escape from the application of CNTs. These technologies such as CNTs will hopefully open the gate to more successful and less costly toxicant technologies. As it can be seen, although, the success of these CNTs is reliant on a better understanding of their potential health impacts. The future application of CNTs have been discussed in Figure 15, which briefly portraits the trend of patents filed from 2001 to 2020. Summary of potential applications of CNTs in various fields are illustrated in Table 1 given below.

8. Conclusions

The material used in the future requires an extraordinary quality such as extraordinary mechanical, thermal, and chemical properties which can resist the adverse conditions of the environment as well as economical in use. The carbon nanotubes (CNTs) reinforced functionally graded composite material (FGCM) is a new generation material with uncharted potential and can be effectively used in various applications, such as aerospace, biomedical, industrial, and chemical applications. FGCM have numerous applications as its reinforced materials with the use of nanotechnology. Such types of materials are in demand and CNTs serve as an excellent candidate for future use [141,142].

To analysis the use of materials in the present and future, patent documents serve as a testimony of the materials. It helps to check the importance of the material in its current and future trends. It also serves as a source of data for use in innovation, technological change, and research and development. In the concluding paragraph, Figure 14 shows the trend of patents filed from 2001 to 2020. The data was collected from Derwent World Patents Index. The analysis not only proves that CNTs is an important material in the field of research and development but also provides a comprehensive picture of the CNTs innovation in the last 20 years [143–147].

Data Availability

The data that support the findings of this study are available from the corresponding author upon reasonable request.

Disclosure Of Potential Conflicts Of Interest

No potential conflict of interest was reported by the author(s).

ORCID

Nidhi Jain http://orcid.org/0000-0003-0964-9829

Eva Gupta http://orcid.org/0000-0002-6388-7791
Nand Jee Kanu http://orcid.org/0000-0003-3919-5098

Additional Information

The authors have not been funded in any way to carry out the research activities.

References

[1] Bahare D, Hamid RP, Mohammad MA, et al. A review of the performance of carbon nanotubes in reducing environmental pollution. J Environ Health Sustainable Dev. 2017;2(2):300.

[2] Li S, Gong Y, Yang Y, et al. Recyclable CNTs/Fe_3O_4 magnetic nanocomposites as adsorbents to remove bisphenol a from water and their regeneration. Chin J Chem Eng. 2015;260:231–239.

[3] Wang Q, Li. J, Chen C. "Removal of cobalt from aqueous solution by magnetic multiwalled carbon nanotube/iron oxide composites,". Chem Eng J. 2011;174 (1):126–133.

[4] Verlicchi P, Aukidy AM, Zambello E, Za. E Mbello. "Occurrence of pharmaceutical compounds in urban wastewater removal, mass load and environmental risk after a secondary treatment—a review,". Sci Total Environ. 2012;429:123–155.

[5] Augusto F, Carasek E, Silva RGC. New sorbents for extraction and microextraction techniques. J Chromatogr A. 2010;1217(16):2533–2542.

[6] Walser T, Demou E, Lang DJ, S. zellweg. "Prospective environmental life cycle assessment of nanosilver t-shirts,". Environ Sci Technol. 2011;45:4570–4578.

[7] Lee J, Mahendra S, Alvarez PJJ. Nanomaterials in the construction industry: a review of their applications and environmental health and safety considerations. ACS Nano. 2010;4(7):3580–3590.

[8] Klaine SJ, Alvarez PJJ, Batley GE, et al. Nanomaterials in the environment: behaviour, fate, bioavailability, and effects. Environ Toxicol Chem. 2008;27(9):1825–1851.

[9] Mudd GM. Global trends in gold mining: towards quantifying environmental and resource sustainability. Res Policy. 2007;32:42–56.

[10] Lindsay JD, Matthew JE, Ali H, et al. Environmental life cycle assessment of a carbon nanotube-enabled semiconductor device. Environ Sci Technol. 2013;28: 8471–8478.

[11] Rasel D, Bey FL, Finbarr M. The toxic truth about carbon nanotubes in water purification: a perspective view. Nanoscale Res Lett. 13:183.

[12] Kobayashi N, Izumi H, Morimoto Y. Review of toxicity studies of carbon nanotubes. J Occup Health. 2017;59 (5):394–407.

[13] Dong J, Ma Q. Myofibroblasts and lung fibrosis induced by carbon nanotube exposure. Part Fibre Toxicol. 2016;13(1):60.

[14] Wohlleben W, Brill S, Meier MW, et al. On the lifecycle of nanocomposites: comparing released fragments and their in-vivo hazards from three release mechanisms and four nanocomposites. Small. 2011;7 (16):2384–2395.

[15] Tong ZH, Bischoff M, Nies L, et al. Impact of fullerene (C-60) on a soil microbial community. Environ Sci Technol. 2007;41(8):2985–2991.

[16] Morones JR, Elechiguerra JL, Camacho A, et al. The bactericidal effect of silver nanoparticles. Nanotechnology. 2005;16(10):2346–2353.

[17] Lyon D, Brown DA, Alvarez PJJ. Implications and potential applications of bactericidal fullerene water suspensions: effect of nC60 concentration, exposure conditions, and shelf life. Water Sci Technol. 2008;57 (10):1533–1538.

[18] Shannon MA, Bohn PW, Elimelech M, et al. Science and technology for water purification in the coming decades. Nature. 2008;452(7185):301–310.

[19] Hischier R, Walser T. Life cycle assessment of engineered nano materials: state of the art and strategies to overcome existing gaps. Sci Total Environ. 2012;425:271–282.

[20] Wang F, Liu Y, Wei H, et al. Graphene induced growth of Sb2 WO6 nanosheets for high- performance pseudocapacitive lithium -ion storage. J Alloys Compd. 2020;839,155614.

[21] Wang F, Liu Y, Zhao Y. et al. Facile synthesis of two-dimensional porous MgCo2O4 nanosheets as anode for lithium-ion batteries. Appl Sci Basel. 2018;8, 22.

[22] Wang R, Cao X, Zhao D, et al. Wet-chemistry synthesis of Li4 Ti5 O12 as anode materials rendering high-rate Li-ion storage. Int. J. Energy Res. 2020;44 (6):4211–4223. .

[23] Wang G, Chen C, Chen Y, et al. Self-stabilized and strongly adhesive supramolecular polymer protective layer enables ultrahigh-rate and large-capacity lithium-metal anode. Angew Chem Int. 2020;59 (5):2055–2060. .

[24] Wang G, Lai Y, Zhang Z, et al. Enhanced rate capability and cycle stability of lithium-sulfur batteries with a bifunctional MCNT@PEGmodifiedseparator. J Mater Chem A. 2015;3(13):7139–7144.

[25] Wang J, Qin W, Zhu X, et al. Covalent organic frameworks(COF)/CNT nanocomposite for high performance and wide operating temperature lithium-sulfur batteries. Energy. 2020;199:117372.

[26] Zhang X, Lu W, Zhou G, et al. Understanding the mechanical and conductive properties of carbon nanotube fibers for smart electronics. Adv Mater. 2019;1902028.

[27] Pan K, Wang F, Wei S, et al. Low temperature solution synthesis and characterization of enhanced titanium dioxide photocatalyst on tailored mesoporous g-Al2O3 support. Compos Commun. 2020;19:82–89.

[28] Pan S, Yin Z, Cheng Q, et al. 2 /CNT as efficient polysulfide barrier to improve the performance of lithium -sulfur battery. J Alloys Compd. 2020;832:154947.

[29] Liu B, Wang S, Wu X, et al. Carbon nanotube/zirconia composite-coated separator for a high-performance rechargeable lithium-sulfur battery. AIP Advances. 2018;8(10):105315. .

[30] Wu N, Qiao XG, Shen JK, et al. Anatase inverse opal TiO2-x@N-doped C induced the dominant pseudocapacitive effect for durable and fast lithium/sodium storage. Electrochim Acta. 2019;299:540–548.
[31] Wu N, Shen J, Sun L, et al. HierarchicalN-doped graphene coated 1D cobalt oxide microrods for robust and fast lithium storage at elevated temperature. Electrochim Acta. 2019;310:70–77.
[32] Zhao X, Chen H, Kong F, et al. Fabrication, characteristics and applications of carbon materials with different morphologies and porous structures produced from wood liquefaction: a review. Chem Eng J. 2019;364:226–243.
[33] Ma J, Wei H, Liu Y, et al. Application of Co3O4-based materials in electrocatalytic hydrogen evolution reaction: a review. Int J Hydrogen Energy. 2020;45 (41):21205–21220. .
[34] Ma J, Wen J, Li Q, et al. Electrochemical polarization and corrosion behavior of Al-Zn-In based alloy in acidity and alkalinity solutions. Int J Hydrogen Energy. 2013;38(34):14896–14902.
[35] Wei H, Liu Y, Xi ZF, Wang, Xi. Ren, F. Tao, T. Li, G. Wang, F. Ren. "Application of CarbonNanotube-Based Materials asInterlayers in High-Performance Lithium-Sulfur Batteries: a Review,". Front Energy Res. 2020;8:585795.
[36] Pandey K, Mohamed HL, Victoria KH, et al. Effects of carbon-based nanomaterials on seed germination, biomass accumulation and salt stress response of bioenergy crops. PLoS One. 2018;13(8):e0202274.
[37] Georgakilas V, Perman JA, Tucek J, et al. Broad of carbon nanoallotropes: classification, chemistry, and applications of fullerenes, carbon dots, nanotubes, graphene, nanodiamonds, and combined superstructures. Chem Rev. 2015;115:4744–4822.
[38] Line C, Larue C, Flahaut E. Carbon nanotubes: impacts and behaviour in the terrestrial ecosystem - A review. Carbon. 2017;123:767–785. [GhoshM, Bhadra S, Adegoke A, et al. MWCNT uptake in Allium cepa root cells induces cytotoxic and genotoxic responses and results in DNA hyper-methylation. Mutat. Res. 015;774:49-58].
[39] Verma SK, Ashok KD, Saikat G, et al. Applications of carbon nanomaterials in the plant system: a perspective view on the pros and cons. Sci Total Environ. 2019;667:485–499.
[40] Viswanathan C, Z. Jian-Kang. "Epigenetic regulation of stress responses in plants,". Curr Opin Plant Biol. 2009;12:133–139.
[41] Martinelli V, Susanna B, Brisa P, et al. 3D Carbon nanotube-based composites for cardiac tissue engineering. ACS Appl Bio Mater. 2018;17: 1530–1537.
[42] McCauley, Vitale, YanIn JS, et al. Vivo Restoration of Myocardial Conduction With Carbon Nanotube Fibers. Circ Arrhythm Electrophysiol. 2019;12(8):72.
[43] Pok S, Vitale F, Eichmann SL, et al. Biocompatible carbon nanotube-chitosan scaffold matching the electrical conductivity of the heart. ACS Nano. 2014;8 (10):9822–9832.
[44] Liu X-M, Huang ZD, Oh SW, et al. Carbon nanotube (CNT)-based composites as electrode material for rechargeable Li-ion batteries: a review. Compos Sci Technol. 2012;72(2):121–144.
[45] Long RQ, Lane RT. Carbon nanotubes as superior sorbent for dioxin removal. J Am Chem Soc. 2001;123,(9):2058–2059.
[46] Ahmaruzzaman M. Adsorption of phenolic compounds on low-cost adsorbents: a review. Adv Colloid Interface Sci. 2008;143(1–2):48–67.
[47] Gupta VK, Saleh TA. Sorption of pollutants by porous carbon, carbon nanotubes and fullerene- An overview. Environ Sci Pollut Res. 2013;20(5):2828–2843.
[48] Brooks AJ, Lim HN, Kilduff JE. Adsorption uptake of synthetic organic chemicals by carbon nanotubes and activated carbons. Nanotechnology. 2012;23 (29):294008.
[49] Gao H, Kan T, Zhao S, et al. Removal of anionic azo dyes from aqueous solution by functional ionic liquid cross-linked polymer. J Hazard Mater. 2013;261:83–90.
[50] Peng F, Wang H, Yu H, et al. Preparation of aluminum foil-supported nano-sized ZnO thin films and its photocatalytic degradation to phenol under visible light irradiation. Mater. Res. Bull. 2006;41 (11):2123–2129.
[51] Chuangchote S, Jitputti J, Sagawa T, et al. Photocatalytic activity for hydrogen evolution of electrospun TiO_2 nanofibers. ACS Appl Mater Interfaces. 2009;1 (5):1140–1143.
[52] Zhang H, Quan X, Chen S, et al. Fabrication and characterization of silica/titania nanotubes composite membrane with photocatalytic capability. Environ. Sci. Technol. 2006;40,(19):6104–6109.
[53] Sun W, Yu Y, Pan H, et al. CdS quantum dots sensitized TiO_2 nanotube-array photoelectrodes. J Am Chem Soc. 2008;130(4):1124–1125.
[54] Liu Z, Zhang X, Nishimoto S, et al. Highly ordered TiO_2 nanotube arrays with controllable length for photoelectrocatalytic degradation of phenol. J Phys Chem C. 2008;112,:253–259.
[55] Zhang Z, Yuan Y, Shi G, et al. Photoelectrocatalytic activity of highly ordered TiO_2 nanotube arrays electrode for azo dye degradation. Environ. Sci. Technol. 2007;41(17):6259–6263.
[56] Macak J, Schmidt-Stein F, Schmuki P. Efficient oxygen reduction on layers of ordered TiO_2 nanotubes loaded with Au nanoparticles. Electrochem Commun. 2007;9 (7):1783–1787.
[57] Baughman RH, Zakhido VAA, de Heer WA. Schrodinger equation in the space with cylindrical geometric defect and possible application to multi-wall nanotubes. Science 2002;297, 787. https://arxiv.org/abs/1010.2913
[58] Li WZ, Wen JG, Ren ZF. Straight carbon nanotube Y junctions Appl. Phys Lett. 2001;79:1879.
[59] Vouris PA. Molecular electronics with carbon nanotubes. Chem. 2002;35:1026–1034.
[60] K elly MJ. Low-Dimensional Semiconductors. New York: Oxford University Press, Inc; 1995.
[61] Beckett P. Exploiting multiple functionality for nano-scale reconfigurable systems. 23(12):2013.

[62] Capek I. Dispersions, novel nanomaterial sensors and nanoconjugates based on carbon nanotubes. Adv Colloid Interface Sci. 2009;150(2):63–89.
[63] Hadjipaschalis I, Poullikkas A, Efthimiou V. Overview of current and future energy storage technologies for electric power applications. Renew Sust Energ Rev. 2009;13(6–7):1513–1522.
[64] Chou SL, Wang JZ, Chew SY, et al. Electrodeposition of MnO_2 nanowires on carbon nanotube paper as free-standing flexible electrode for supercapacitors. Electrochem commun. 2008;10, 1724-1727.
[65] Simon P, Gogotsi Y. Materials for electrochemical capacitors. Nat Mater. 2008;7(11):845.
[66] Lu J, Kumar B, Castro M, et al. Vapour sensing with conductive polymer nanocomposites (CPC): polycarbonate-carbon nanotubes transducers with hierarchical structure processed by spray layer by layer. Sens Actuators, B. 2009;140:451–460.
[67] Yan J, Fan Z, Wei T, et al. Carbon nanotube/MnO_2 composites synthesized by microwave-assisted method for supercapacitors with high power and energy densities. J Power Sources. 2009;194(2):1202–1207.
[68] Lin Y, Lu F, Tu Y, et al. Glucose biosensors based on carbon nanotube nanoelectrode ensembles. Nano Lett. 2004;4(2):191–195.
[69] Zhao Q, Gan Z, Zhuang Q. Electrochemical sensors based on carbon nanotubes. Electroanalysis. 2002;14 (23):1609–1613.
[70] Jacobs CB, Peairs MJ, Venton BJ. Review: carbon nanotube based electrochemical sensors for biomolecules. Anal. Chim. Acta. 2010;662(2):105–127.
[71] Yang N, Chen X, Ren T, et al. Carbon nanotube based biosensor. Sens Actuator, B. 2015;207:690–715.
[72] Ulissi ZW, Sen F, Gong X, et al. Spatiotemporal intracellular nitric oxide signaling captured using internalized, near-infrared fluorescent carbon nanotube nanosensors. Nano Lett. 2014;14(8):4887–4894.
[73] Mphuthi NG, Adekunle AS, Ebenso EE. Electrocatalytic oxidation of epinephrine and norepinephrine at metal oxide doped phthalocyanine/MWCNT composite sensor. Sci. Rep. 2016;6(1):26938.
[74] Bisker G, Dong J, Park HD, et al. Protein-targeted corona phase molecular recognition. Nat. Commun. 2016;7(1):10241.
[75] Baldo S, Buccheri S, Ballo A, et al. Carbon nanotube-based sensing devices for human Arginase-1 detection. Sens Bio-Sens Res. 2016;7:168–173.
[76] Adeli M, Soleyman R, Beiranvanda Z, et al. Carbon nanotubes in cancer therapy: a more precise look at the role of carbon nanotube-polymerinteractions. Chem Soc Rev. 2013;42(12):5231–5256.
[77] Chen J, Chen S, Zhao X, et al. Functionalized single-walled carbon nanotubes as rationally designed vehicles for tumor-targeted drug delivery. J Am Chem Soc. 2008;130(49):16778–16785.
[78] Panczyk T, Wolski P, Lajtar L. Coadsorption of doxorubicin and selected dyes on carbon nanotubes. Theoretical investigation of potential application as a pH-controlled drug delivery system. Langmuir. 2016;32 (19):4719–4728.
[79] Liu Z, Sun X, Nakayama-Ratchford N, et al. Supramolecular chemistry on water-soluble carbon nanotubes for drug loading and delivery. ACS Nano. 2007;1,(1):50–56.
[80] Liu Z, Fan AC, Rakhra K, et al. Supramolecular stacking of doxorubicin on carbon nanotubes for in vivo cancer therapy. Angew Chem. 2009;121(41):7804–7808.
[81] Wu W, Li R, Bian X, et al. Covalently combining carbon nanotubes with anticancer agent: preparation and antitumor activity. ACS Nano. 2009;3(9):2740–2750.
[82] Xu L, Feng L, Dong S, et al. Carbon nanotubes modified by a paramagnetic cationic surfactant for migration of DNA and proteins. Colloids Surf Physicochem Eng Asp. 2018;559:201–208.
[83] Mazzatenta A, Giugliano M, Campidelli S, et al. Interfacing neurons with carbon nanotubes: electrical signal transfer and synaptic stimulation in cultured brain circuits. J. Neurosci. 2007;27(26):6931–6936.
[84] Béduer A, Seichepine F, Flahaut E, et al. Elucidation of the role of carbon nanotube patterns on the development of cultured neuronal cells. Langmuir 2012;28 (50):17363–17371.
[85] Hosseinpour M, Azimirad V, Alimohammadi M, et al. The cardiac effects of carbon nanotubes in rat Bio-Impacts. 2016;6:79–84.
[86] Es'haghi F, Shahabi P, Frounchi J, et al. Investigation of ECG changes in absence epilepsy on WAG/Rij rats. Basic Clin Neurosci. 2015;6.:123–132.
[87] Ghamkhari NG, Shahabi P, Alipoor M, et al. Ethosuximide affects paired-pulse facilitation in somatosensory cortex of WAG\Rij rats as a model of absence seizure. Adv Pharm Bull. 2015;5,(4):483–489.
[88] Walvekar R, Siddiqui MK, Ong S, et al. Application of CNT nanofluids in a turbulent flow heat exchanger. J Exp Nanosci. 2016;11(1):1–17.
[89] Kayat J, Gajbhiye V, Tekade RK, et al. Pulmonary toxicity of carbon nanotubes: a systematic report. Nanomedicine. 2011;7(1):40–49.
[90] Greener ID, Sasano T, Wan X, et al. Connexin43 gene transfer reduces ventricular tachycardia susceptibility after myocardial infarction. J Am Coll Cardiol. 2012;60(12):1103–1110.
[91] da Cunha DN, Pereira VG, Favarato LS, et al. "Acute and chronic observations of complete atrioventricular block in rats,". Lab Anim. 2014;48(3):237–249.
[92] Daponte CA, Ordonez MJ, J.j G, et al. Relacion a corto plazo de la contaminacion atmosferica y la mortalidad en 13 ciudades espanolas. Medicina Clinica. 2003;121 (18):684–689.
[93] Cinke M, Li J, Charles W, et al. CO_2 Adsorption in single-walled carbon nanotubes. Chem Phys Lett. 2003;376(5–6):761–766.
[94] Qing. QL, Gao LL, Yu Z. Carbon nanotubes prepared from COon pre-reduced La2NiO4 perovskite precursor. Mater Res Bull. 2001;36(3–4):471–477.
[95] Park SJ, Lee DG. Performance improvement of micron-sized fibrous metal filters by direct growth of carbon nanotubes. Carbon. 2006;44(10):1930–1935.
[96] Park JH, Yoon KY, Na H, et al. Fabrication of a multiwalled carbon nanotube-deposited glass fiber air filter for the enhancement of nano andsubmicron aerosol particle filtration and additional antibacterial efficacy. In: Science of the total environment. Elsevier. Vol. 409. 2011. p. 4132–4138.

[97] Shohreh F, Masoud Vesali N, Mona C, et al. Improving CO2/CH4 adsorptive selectivity of carbon nanotubes by functionalization with nitrogen containing groups. Chem Eng Res Des. 2011;89(9):1669–1675.
[98] Somy A, Mehrnia MR, Delavari-Amrei H, et al. Adsorption of carbon dioxide using impregnated activated carbon promoted by zinc. Int J Greenhouse Gas Control. 2009;3(3):249–254.
[99] Budaeva AD, Zoltoev EV. "Porous structure and sorption properties of nitrogen-containing activated carbon,". *Fuel*. 2010;89:2623–2627.
[100] Thiruvenkatachari R, Su S, An H, et al. Post combustion CO2 capture by carbon fibre monolithic adsorbents. Prog Energy Combust Sci. 2009;35(5):438–455.
[101] Arrigo R, Havecker M, Wrabetz S, et al. Tuning the acid/base properties of nanocarbons by functionalization via amination. J Am Chem Soc. 2010;132 (28):9616–9630.
[102] Liang Q, Li Q, Gao L, et al. Carbon nanotubes prepared from CO on pre-reduced La2NiO4 perovskite precursor. Mater Res Bull. 2001;36(3–4):471–477.
[103] De Jong K, Geus J. Carbon nanofibers: catalytic Synthesis and Applications. Catal Rev Sci Eng. 2000;42(4):481–510.
[104] Nunes A, Al-Jamal K, Nakajima T, et al. Application of carbon nanotubes in neurology: clinical perspectives and toxicological risks. Arch Toxicol. 2012;86 (7):1009–1020.
[105] Ju-Nam Y, Lead JR. "Lead, Manufactured Nanoparticles: an Overview of their Chemistry, Interactions and Potential Environmental Implications,". SciTotal Environ. 2008;400(1–3):396–414.
[106] Shen Y, Bai J. A new kind CO2/CH4 separation material: open ended nitrogen doped carbon nanotubes formed by direct pyrolysis of metal organic frameworks. Chem Comm. 2010;46(8):1308–1310.
[107] Nadeem K, Jamal A, Abdul H, et al. Water soluble carbon nanotubes increase agricultural yields. J Biochem Biotech. 2020;3.
[108] Line C, Larue C, Flahaut E. Carbon nanotubes: impacts and behaviour in the terrestrial ecosystem - A review. Carbon. 2017;123:767–785.
[109] McGehee DL, Lahiani MH, Irin F, et al. Multiwalled carbon nanotubes dramatically affect the fruit metabolome of exposed tomato plants. ACS Appl Mater Interfaces. 2017;9(38):32430–32435.
[110] Adenuga AA, Truong L, Tanguay RL, et al. Preparation of water soluble carbon nanotubes and assessment of their biological activity in embryonic zebrafish. Int J Biomed Nanosci Nanotechnol. 2013;3 (1/2):38–51.
[111] Pereira A, Grillo R, Mello NF, et al. Application of poly (epsilon-caprolactone) nanoparticles containing atrazine herbicide as an alternative technique to control weeds and reduce damage to the environment. J Hazard Mater. 2006;268:207–215.
[112] Girardello R, Tasselli S, Baranzini N, et al. "Effects of carbon nanotube environmental dispersion on an aquatic invertebrate," Hirudo medicinalis. PLoS One. 2015;10.
[113] Wei C, Dai L, Roy A, et al. Multifunctional chemical vapor sensors of aligned carbon nanotube and polymer composites. J Am Chem Soc. 2006;128(5):1412.
[114] Xu D, Tan X, Chen C, et al. Removal of Pb(II) from aqueous solution by oxidized multiwalled carbon nanotubes. J Hazard Mater. 2008;154(1–3):1–3.
[115] Chen T, Dai L. Carbon nanomaterials for high-performance supercapacitors. Mater Today. 2013;16(7–8):272–280.
[116] Simon P, Gogotsi Y. Materials for electrochemical capacitors. Nat Mater. 2010;7(11):845.
[117] Song L, Qiu Z. Crystallization behavior and thermal property of biodegradable poly(butylene succinate)/ functional multi-walled carbon nanotubes nanocomposite. Polym Degrad Stab. 2009;94(4):632.
[118] Attar S, Ranveer A. Carbon nanotubes and its environmental applications Journal of Environmental Science. Comput Sci Eng Technol. 2015;4:304–311.
[119] Mansoori GA, Bastami TR, Ahmadpour ZA. Environmental application of nanotechnology. Annu Rev Nano Res. 2008;2.
[120] Tianjia G, Maosheng Y. "Use of carbon nanotube filter in removing bioaerosols. J Aerosol Sci. 2010;41 (6):611–620.
[121] Pillai. Ramaiyan K. Applications of carbon nanotubes in polymer electrolyte membrane fuel cells. J Indian Inst Sci. 2009;89(4):425–436.
[122] Avouris P, Appenzeller J, Martel R, et al., "Carbon nanotube electronics," *Proceedings of the IEEE*. USA. vol. 9, pp.1772–1784, 2003
[123] Meagans SM, Elimelech M. Environmental applications of carbon-based nanomaterials. Environ Sci Technol. 2008;42(16):5843–5859.
[124] Kumar M, Ando Y, "Carbon nanotubes from camphor: an environment-friendly nanotechnology," *Journal of Physics: Conference Series*. Switzerland. vol. 61, pp. 643–646, 2007.
[125] Kumar M, Ando Y. A simple method of producing aligned carbon nanotubes from an unconventional precursor – camphor. Chem Phys Lett. 2003;374(5–6):521–526.
[126] Kumar M, Kakamu K, Okazaki T, et al. Field emission from camphor-pyrolyzed carbon nanotubes. Chem Phys Lett. 2004;385(3–4):161–165.
[127] Kumar M, Ando Y. Controlling the diameter distribution of carbon nanotubes grown from camphor on a zeolite support. Carbon. 2005;43(3):533–540.
[128] Kumar M, Ando Y. Single-wall and multi-wall carbon nanotubes from camphor - a botanical hydrocarbon. Diam Relat Mater. 2003;12(10–11):1845–1850.
[129] Navrotskaya AG, Aleksandrova DD, Krivoshapkina EF, et al. Hybrid materials based on carbon nanotubes and nanofibers for environmental applications. Front Chem. 2020;8:546.
[130] Ghiasvand A, Yazdankhah F, Paull B. Heating-Cooling and vacuum-assisted solid-phase microextraction (HCV-SPME) for efficient sampling of environmental pollutants in complex matrices. Chromatographia. 2020;83(4):531–540.
[131] Guo H, Jiang S, Wang C, et al. Carbonaceous nanofibers-titanium dioxide nanocomposites: synthesis

and use as a platform for removal of dye pollutants. J. Wuhan Univ. Technol. Mater. Sci. Ed. 2019;34 (2):303–307.

[132] Navrotskaya AG, Krivoshapkina EF, Perovskiy IA, et al. "Synthesis and properties of carbon–metal oxide nanomaterials,". J. Sol-Gel Sci. Technol. 2019;92(2):449–457.

[133] Wang B, Liu G, Ye B, et al. Novel CNT/PbBiO2 hybrid materials with enhanced broad spectrum photocatalytic activity toward ciprofloxacin (CIP) degradation. J Photochem Photobiol A:Chem. 2019;382:111901.

[134] Shivraj HN, Venkidasamy B, Dhivya S, et al. Nanotechnologies in food Science: applications, recent trends, and future perspectives. Nano-Micro Lett. 2020;12, 45;1-34.

[135] Bajpai VK, Kamle M, Shukla S, et al. Prospects of using nanotechnology for food preservation, safety, and security. J. Food Drug Anal. 2018;26(4):1201–1214.

[136] Yadav SK (2017) Realizing the Potential of Nanotechnology for Agriculture and Food Technology. J Tissue Sci Eng 8: 195. doi: 10.4172/ 2157-7552.1000195.

[137] He X, Deng H, Hwang H. The current application of nanotechnology in food and agriculture. J Food Drug Anal. 2019;27(1):1–21.

[138] Morris MA, Padmanabhan SC, Cruz-Romero MC, et al. Development of active, nanoparticle, antimicrobial technologies for muscle-based packaging applications. Meat Sci. 2017;132:163–178.

[139] Osman AI, Farrell C, Al -Muhtaseb AH, et al. The production and application of carbon nanomaterials from high alkali silicate herbaceous biomass. Sci Rep. 2020;10(1):2563.

[140] Suárez-Eiroa B, Fernández E, Méndez-Martínez G, et al. "Operational principles of circular economy for sustainable development: linking theory and practice. J Cleaner Prod. 2019;214:952–961.

[141] Udupal G, Rao SS, Gangadharan KV, "Future applications of carbon nanotube reinforced functionally graded composite materials," *IEEE-International Conference On Advances In Engineering, Science And Management (ICAESM –2012)*, India. vol. 30, 399, 2010.

[142] Jain N, Pasarkar A, Patil.: RN. Synthesis, characterization and parametric study for diameter of nanofiber of Chitosan, Azadirachta Indica leaves extract composite nanofibers. Test Eng Manage. 2020;82:13616–13626.

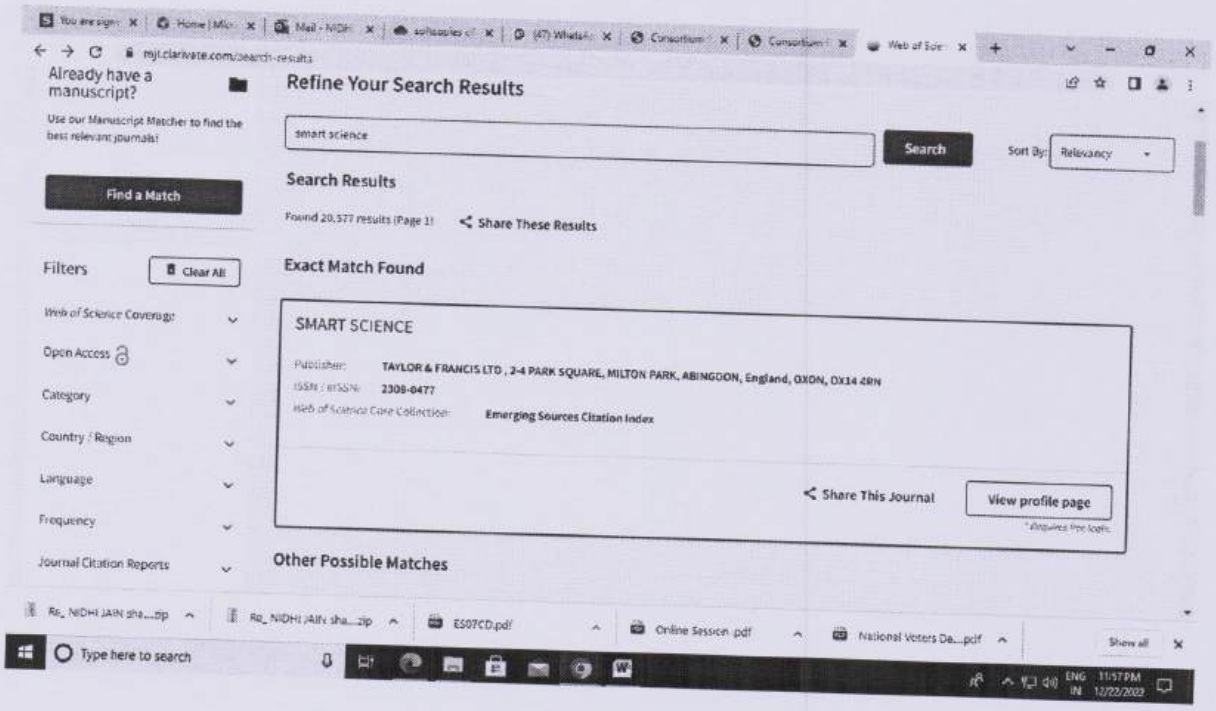
[143] Chang PL, Wu CC, Leu HJ. Using patent analyses to monitor the technological trends in an emerging field of technology: a case of carbon nanotube field emission display. Scientometrics. 2010;82(1):19.

[144] Choi C, Kim S, Park Y. A patent-based cross impact analysis for quantitative estimation of technological impact: the case of information and communication technology. Technol Forecasting Social Change. 2007;74(8):1296–1314.

[145] Nidhi J, Seema T. Biomedical application of carbon nanotubes (CNTs) in vulnerable parts of the body and its toxicity study: a state-of-the-art-review. Mater Today Proc. 2021;(In Press). DOI:10.1016/j.matpr.2021.01.895.

[146] Nidhi J. The potential application of carbon nanotubes in water Treatment: a state-of-the-art-review. Mater Today Proc. 2021;43(5):2998–3005.

[147] Achchhe L, Nand Jee K, "The nonlinear deflection response of CNT/nanoclay reinforced polymer hybrid composite plate under different loading conditions," *IOP Conference Series: Materials Science and Engineering*, India. vol. 814 (1), pp. 012033, 2020.


mjl.clarivate.com/search-results
Already have a manuscript?
Use our Manuscript Matcher to find the best relevant journals!
Find a Match
Refine Your Search Results
smart science
Search
Sort By: Relevancy
Search Results
Found 20,577 results (Page 1)
Share These Results
Filters
Clear All
Web of Science Coverage
Open Access
Category
Country / Region
Language
Frequency
Journal Citation Reports
Exact Match Found
SMART SCIENCE
Publisher: TAYLOR & FRANCIS LTD , 2-4 PARK SQUARE, MILTON PARK, ABINGDON, England, OXON, OX14 4RN
ISSN / eISSN: 2308-0477
Web of Science Core Collection: Emerging Sources Citation Index
Share This Journal
View profile page
Other Possible Matches
Type here to search
ENG
IN
11:57 PM
12/22/2023

Contents lists available at ScienceDirect

Materials Today: Proceedings

journal homepage: www.elsevier.com/locate/matpr

Comparative study of physico-chemical parameters and water quality index of river

Nidhi Jain [a], Rudrani Yevatikar [b], Tarul Sanjay Raxamwar [b]

[a] Department of Engineering Science, Bharati Vidyapeeth's College of Engineering, Lavale, Pune 412115, India
[b] Department of Civil Engineering, Bharati Vidyapeeth's College of Engineering Lavale, Pune 412115, India

ARTICLE INFO

Article history:
Received 29 August 2021
Accepted 29 September 2021
Available online xxxx

Keywords:
Physico Chemical Analysis
Water Quality
Water Pollution
Water Quality Index

ABSTRACT

The change in natural water quality is caused due to the diversity of human activities which is causing huge impact on the hydrologic cycle. The increasing pollution is impairing the use of the water which is creating hazards to the public health as well as the environment through toxicity and diseases. The water quality impact assessment has been undertaken to define the impact of pollution to the environment. The water quality analysis is very basic tool for determining water body condition. This study will help to analysis the water quality and better water resource management. The study is focused on the assessment of parameter of waste water affecting the quality of water and having hazardous effect. This will interprets the condition of the Mula Mutha river which can help the local authority of Pune city in taking the action and identification of sources of pollution and improving the water quality around the city. The data of 2013 to 2018 has been taken for the comparative study and Water quality index had been calculated to change caused in course of time.
Copyright © 2022 Elsevier Ltd. All rights reserved.
Selection and peer-review under responsibility of the scientific committee of the 4th Online International Conference on Science & Engineering of Material

1. Introduction

The increasing population on the earth is leading us to the urbanization. And it is adversely affecting both the surface water and ground water . Due to urbanization, the water demand is also increasing day by day. Increased demand leads to the decreased quality of water. It is well known that the water quality is very important for the survival of human race. The water in dams contain germs and dirt which is treated by the PMC. The treatment of water makes it safe and usable. The treatment mainly involves straining, chlorination, filtration and flocculation. The study area, Pune, is bestowed by three rivers which are Mula, Mutha and Pavana. Determining o the water quality of the study area is utmost (Table 1) important [1–5].

Since the growing industrial and domestic usage increased the demand of water which leads to the severe problem of the water pollution. The sources of water pollution are nearly increasing every day.With the increasing pollution the water related diseases are also increasing. Hence the assessment of the degree of water pollution is the need of the hour for survival of humans as well as other living beings. For any water body to function satisfyingly it must have the degree of purity. Hence for the increasing demand for water the concept of management of the quality of the water is becoming very important [6,7].

According to the uses of water from the water body we have 'Designated best use' developed by the Central Pollution Control Board (CPCB). In which the highest quality is known as its designated best value. The common quality attributes includes the Physical, biological, and chemical parameters. The water quality managers and the planners set water quality targets and design suitable restoration programs for different water bodies. For drinking water source without conventional treatments after disinfection the pH value should be in between 6.5 and 8.5, dissolved oxygen value should be 6 mg/l or more. The total coliforms organism MPN/100 ml shall be 500 or less and biological oxygen demand 5 days 20° C, 2 mg/l or less. For defining the quality of water WQI (water quality Index) is used [8–10].

2. Results

2.1. Study area of the review papers

Various location of the Pune city has been selected and data collections of the last five years has been done. The collected data has

https://doi.org/10.1016/j.matpr.2021.09.508
2214-7853/Copyright © 2022 Elsevier Ltd. All rights reserved.
Selection and peer-review under responsibility of the scientific committee of the 4th Online International Conference on Science & Engineering of Material

Please cite this article as: N. Jain, R. Yevatikar and Tarul Sanjay Raxamwar, Comparative study of physico-chemical parameters and water quality index of river, Materials Today: Proceedings, https://doi.org/10.1016/j.matpr.2021.09.508

Table 1
shows the sampling locations.

Sr. No.	Stations	Locations
1	Station 1 (G1)	Kivalegaon
2	Station 2(G2)	RavetPunavale bridge
3	Station 3(3):	Chinchwadgaon
4	Station 4(G4)	KalewadiPhata

been analyzed and comparative study has been carried out to know the changes in the water quality. The water quality Index studies also carried out to get the clear cut idea of the quality of water. The selected locations are.

2.2. Around Mula mutha river

Mula mutha river is the major source of Pune city which is located at 18°31'52.7" North 73°51'37.2" on Sahyadri range and western Ghats. Western margin of Deccan Plateau is 560 m (1837) above mean sea level. It is 7th most populated city in India and 2nd biggest city in Maharashtra. From last some years the city s converting to urban area by the growth of concrete jungle by decimating green jungle. Human activities like artificial lakes, dams, reservoir are also included for water utilization of Pune city.

2.2 Due to increased civilization of Pimpai -Chinchwad city industrialization has increased. Also the area flowing through Pimpri to Bopodi shows the large amount of human activities and water hyacinth on water body. The Pavana River originates from the Western Ghats, about 6 km South of Lonavala. Flowing eastwards initially, it becomes southbound and passes through the suburbs of Dehu, Chinchwad, Pimpri and Dapodi before it s confluence with the Mula river near Sangvi Fig. 1a and b showing the location in the map (Fig. 2).

3. Discussion

From the literature four locations have been selected to analyze the data. Selected sampling sites: total four sites were selected:

The highest pH value recorded at selected stations is 7.82 and average value 7.82. The maximum recorded value For DO, BOD, COD and hardness are 4.6, 6.25, 81 and 72,025 respectively [11–13]

In order to analyze water quality index and the water quality parameters in the year 2015 , stretch of the river, starting from Khadkawasla to Bund garden various station pointes selected are as illustrated in Table 2.

Maximum value of pH, DO, BOD, COD, Hardness and Turbidity recorded in Year 2015 are 8.4, 2.3, 51,58,112 and 21 respectively. Where as the average value recorded in 2015 for pH, DO, BOD, COD, Hardness and Turbidity are 7.325, 0.975, 29.875, 45.47, 76.12, 11 Respectively [14]

For study of Water parameters in year 2017 we have considered following sampling points in Table 3.

During the analysis of Year 2017 the maximum value of pH, DO, BOD, COD, Chloride and Hardness were recorded as 8.4, 2.3, 53, 102, 267 and 189 respectively. Whereas the average value for pH, BOD, COD, Chloride and hardness are 7.118, 1.08, 35.702, 83.6,169.6 and 102.116 respectively [15]

The physio chemical analysis water sample were taken from all the three rivers sampling locations were selected in such away to give a reasonable Comparison of water Quality in and around the Pune city. In year 2018 total 9 samples stations were considered (Table 4).

The respective maximum value of pH, DO, BOD, COD, Chloride, Hardness, Turbidity are 7.8, 6.56, 3.61, 5.6, 85.2, 292, 0.9. where as the average respective value of pH, DO, BOD, COD, Chloride, Hardness, Turbidity are7.322, 5.54, 2.68, 3.82, 43.388, 76 and 0.361 [16].

4. Materials and methods

Data have been collected from the literature and analysis to prepare a comparative chart. The study of Physico-Chemical parameters of water is utmost important and it contribute to the quality of water. The various physic chemical parameters are studied they are as follows. The data of 2013 to 2015 has been compiled in Table 5. The Fig. 3 shows the various sources of water pollution.

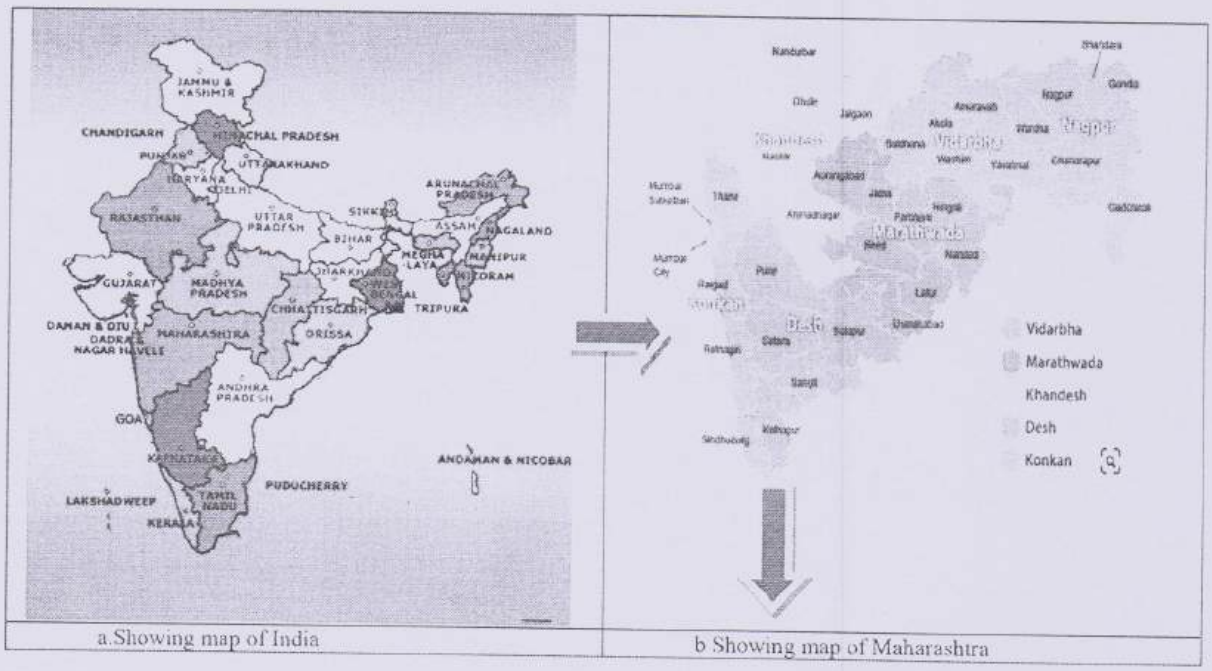


Fig. 1. (a) Showing map of India. (b) Showing map of Maharashtra.

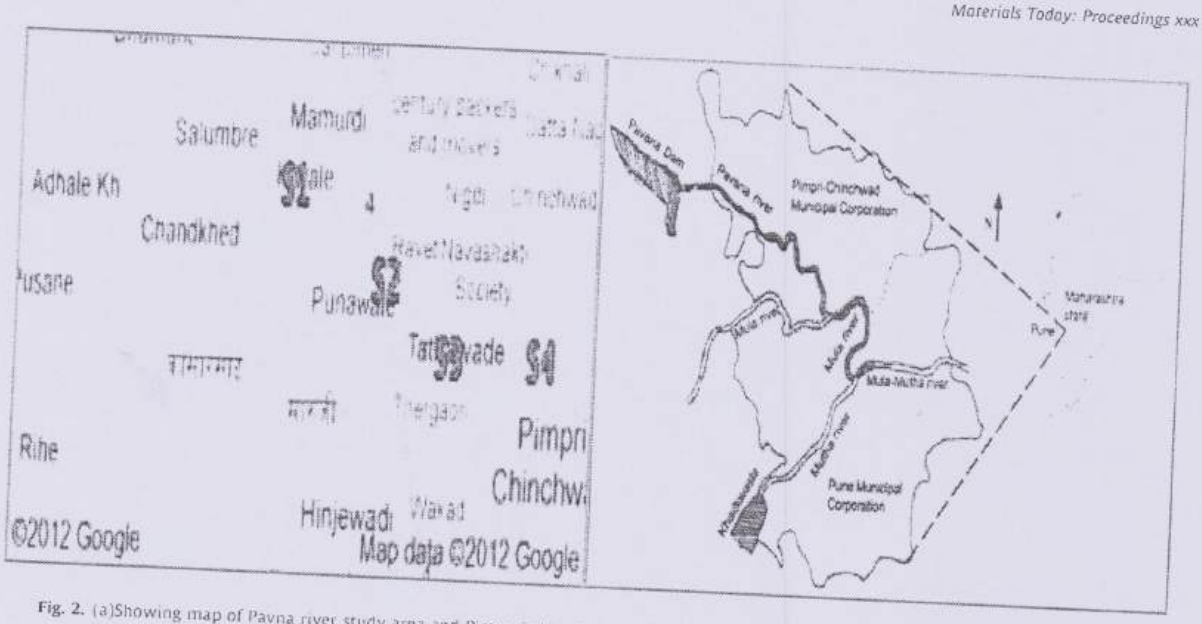


Fig. 2. (a)Showing map of Pavna river study area and Pimpari chinchwad, Pune. (b) Map of sampling locations. (c) All Sampling Locations.

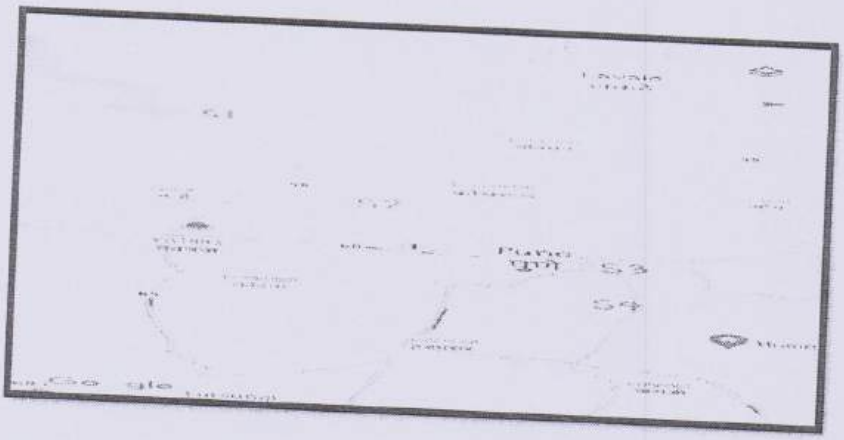


Fig. 2 (*continued*)

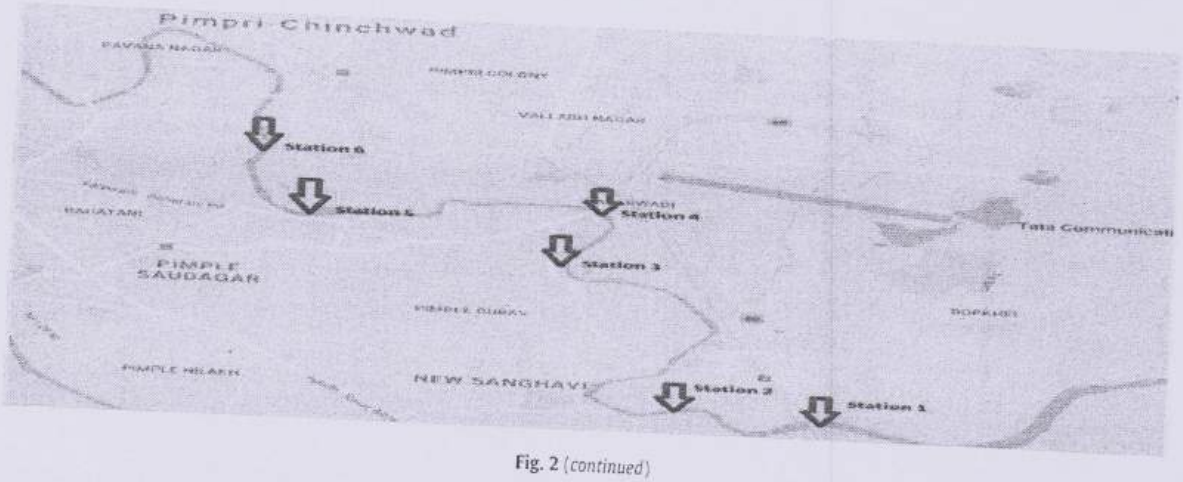


Fig. 2 (*continued*)

Table 2
Indicates the location from Khadkawasla to Bund garden various station pointes.

Sr. No.	Stations	Locations
1	Station 1 (S1)	Khadakwasala dam
2	Station 2(S2)	Vitthalwadi
3	Station 3(S3):	Sangamwadi
4	Station 4(S4)	Bund Garden

Table 3
Indicates the location from Khadkawasla to Wakad causeway various station pointes.

Sr. No.	Stations	Locations
1	Station 1 (S1)	khadakwasla
2	Station 2(S2)	Garware Causeway
3	Station 3(S3):	Holkar Bridge
4	Station 4(S4)	Wakad causeway

Table 4
Indicates the location from Panshet dam to Yerwada various station pointes.

Sr. No.	Stations	Locations
1	Station 1 (S1)	Panshet dam (Mutha river)
2	Station 2(S2)	Khadakwasalauprstrem(Mutha River)
3	Station 3(S3):	Khadakwasala downstream (Mutha River)
4	Station 4(S4)	Mulshi Dan (Mula River)
5.	Station 5(S5)	Paud (Mula river)
6.	Station 6(S6)	Pavanadam(Pavana river)
7.	Station 7(S7)	Bevadovthal (Pavana river)
8.	Station 8(S8)	Aundh (Mula river)
9.	Station 9(S9)	Yerwada (Mula-Mutha river)

4.1. pH

The pH value is determined by the pH meter. It was found that different water bodies have different pH scale. The lower pH value corresponds to the acidic water where as the higher pH values corresponds to the more basic water. The pH value of pure water is 7. It was studied by various researchers and when we see different standards given by WHO, ICMR, CPCB, BIS the required pH lies between 6.5 and 8.5. If the pH is less than 6.5, it is not good for human body. And if the pH is on the basic side like 8.5 then pH changes the taste of water more salty, which leads to several problems such as eye irritation and skin disorder etc. The rainwater is suitable for human consumption which has pH of 5.5–6. pH in the range 3.5–4.5 affects the aquatic life. The maximum level pH is seen in year 2013 and the minimum level in 2017. Fig. 4 shows pH value for various years. And Comparison is shown in it [17,18].

4.2. EC (Electrical conductivity) and (TDS) total dissolved Solids

These two water quality parameters are used to describe the salinity level. TDS is estimated from the Electrical conductivity assuming the dissolved solids are predominantly ionic species of low enough concentration. Pure water is actually a tremendous insulator as it is devoid of ionic content of the water and does not conduct electricity. Water that would be considered "pure" if it is condensed from steam would be distilled water or may be deionized water (used in laboratories). Electrical conductivity is the measure of dissolved mineral content in water..It is a useful tool to evaluate the purity of water [19].

4.3. Turbidity

Turbidity is the measure of the degree which losses the transparency of the water due to the presence of the suspended partials of water. Turbidity is considered as the good measure of the quality of the water. Extreme turbidity, or cloudiness, in drinking water is disagreeable, and may cause a serious health concern. Turbid water can provide food and shelter for pathogens. It should be removed on the immediate basis because turbidity can uphold regret of pathogens in the circulation system, leading to waterborne disease. High concentrations of particulate matter influence light penetration and efficiency, frivolous values, and habitat quality is affected by this. In water, where there is increased in sedimentation and siltation can harm to habitat areas for fish and other aquatic life. Particles increased the growth other pollutants, notably metals and bacteria. For this reason, turbidity is an indicator of potential pollution in a water body [20,21].

4.4. Alkalinity

It is the strength of buffer composed of weak acids and their conjugate bases. Alkalinity of water is definite as the ionic concentration, which can neutralize the hydrogen ions. Alkalinity in water is due to the existence of bicarbonates, carbonates and hydroxides of calcium, magnesium and sodium. Mineral salts of the water is estimated by Alkalinity value. The label of alkalinity should be maintained otherwise it will be harmful to human beings The Alkalinity is a major criterion for understand and controlling water treatment process [22,23].

4.5. Temperature

Temperature is most important parameter of the water quality because it exerts major influence on the biological activity and growth. It affects the dissolved oxygen level in the water. Temperature is also important because of its influence on water chemistry. The rate of chemical reactions generally increases at higher temperature. Water, particularly groundwater, with higher temperatures can dissolve more minerals from the rocks it is in and will therefore have a higher electrical conductivity. It is the opposite when considering a gas, such as oxygen, dissolved in the water. However warm stream water can affect the aquatic life. Warm water holds less dissolved oxygen than cool water, therefore it is not sufficent for the survival of different species of aquatic life. [24,25].

4.6. BOD

BOD is the empirical test to determine dissolved oxygen used by microorganism in biological process of metabolizing organic matter in water in a given water sample at certain temperature over a specific time period. The more organic matter present in the water the more is the value of BOD. The BOD value is most commonly articulated in milligrams of oxygen consumed per liter of sample during 5 days of incubation at 20 °C. BOD reduction is used as a measure of the efficiency of wastewater treatment plants. Biological oxygen demand (BOD) and Chemical oxygen demand (COD) analysis have similar type of function in that both measure the amount of organic compounds in water. COD analysis measure the organic matter which is chemically oxidized, rather than just levels of biologically oxidized organic matter [26,27]. Fig. 5 shows BOD value for various years.

4.7. DO

Dissolved oxygen is the oxygen that is dissolved in the water. It is one of the most important indicators of the water quality. DO is an essential parameter in water quality assessment and reflect the physical and biological processes prevailing in the water. The DO values indicate the degree of pollution (due to excess of decaying organic material) in water bodies. The disproportion in aquatic life

Table 5
The data of 2013 to 2015 has been compiled in table 5.

Parameters	PH	DO	BOD	COD	Hardness	Turbidity
			2013			
S1	7.34	2.63	5.62	74	356	121
S2	7.82	3.03	6.22	81	90	20
S3	7.75	4.6	6.25	70	261.2	100
S4	7.56	3.2	2.81	64	183.2	90
Min	7.34	2.63	2.81	64	90	27
Max	7.82	13.46	6.25	81	890.4	200
Average	7.6175	3.365	5.225	72.25	222.6	161
Parameters	PH	DO	BOD	COD	Hardness	Turbidity
S1	8.4	2.3	9.5	44	30.12	3
S2	6.71	0.8	28	39	83.96	21
S3	7.71	0.4	31	42	112.64	11
S4	6.48	0.4	51	58	77.76	9
Min	6.48	0.4	9.5	39	30.12	3
Max	8.4	2.3	51	58	112.64	21
Avg	7.325	0.975	29.875	45.75	76.12	11
Parameters	PH	DO	BOD	COD	Hardness	Turbidity
S1	8.4	2.3	9.51	44	33.12	5
S2	6.78	0.8	31	87	88.91	11
S3	7.73	0.7	32	89	113.32	21
S4	6.47	0.8	53	96	86.23	13
S5	6.21	0.8	53	102	189	20
Min	6.21	0.7	9.51	44	33.12	4
Max	8.4	2.3	53	102	189	18
Avg	7.118	1.08	35.702	83.6	102.116	
Parameters	PH	DO	BOD	COD	Hardness	Turbidity
			2018			
S1	7.2	6.56	2.13	3.2	32	0.05
S2	7	6.24	2.32	5.6	72	0.3
S3	7	6.13	2.41	4	44	0.4
S4	7.2	6.05	2.25	3.2	40	0.5
S5	7.5	5.43	2.93	5.6	36	0.3
S6	7.6	5.04	2.71	1.6	48	0.5
S7	7.4	5.61	2.41	0.8	44	0.2
S8	7.8	4.51	3.42	5.6	292	0.1
S9	7.2	4.32	3.61	4.8	25	0.9
Min	7	4.32	2.13	0.8	25	0.05
Max	7.8	6.56	3.61	5.6	292	0.9
avg	7.322222	5.543333	2.687778	3.822222	76	0.361111

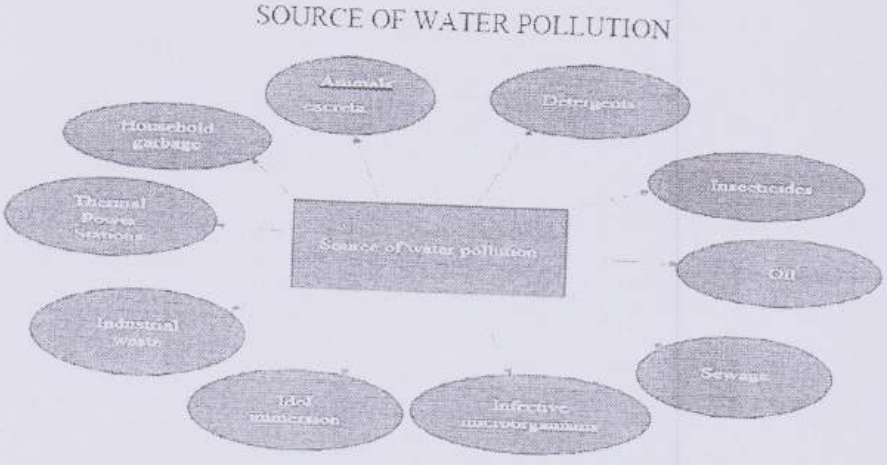


Fig. 3. Sources of water is illustrated in the figure [17].

is responsible for lowering the value of dissolved oxygen The increased value of dissolved oxygen can impart good aesthetic taste to drinking water. Depletion of dissolved oxygen in water supplies can persuade the microbial reduction of nitrate to nitrite and sulphate to sulphide resulting in foul smell. It can also cause an enlarge in the concentration of ferrous iron in solution, with consequent discoloration at the tap when the water is aerated [27].The given Fig. 6 shows DO value for various years.

4.8. COD

Chemical oxygen demand (COD) is defined as the amount of oxygen necessary by organic substances in water to oxidize them by use of the strong chemical oxidant. The analysis of COD values are extremely important for knowing the quality of water. In case of the BOD values determination is difficult due to the presence of toxins and micro-organisms. It was generally observed that, COD is



Fig. 4. shows pH value for various years.



Fig. 5. BOD value for Various years.

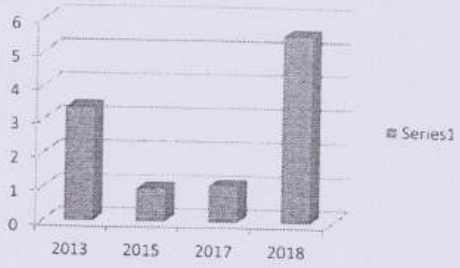


Fig. 6. DO value for various years.

more than the BOD values in the industrial areas. COD values are calculated on the basis of the efficiency of the treatment plants and also amount of discharge release from the industries, domestic waste generated at various kinds of water. Averge value of 10.0 mg/l which was proposed by WHO. COD (Chemical oxygen demand)is the measure of amount of oxygen that can be consumed by reactions in a solution. It is the measure of the wastewater quality. Organic matter contamination is studied in the form of

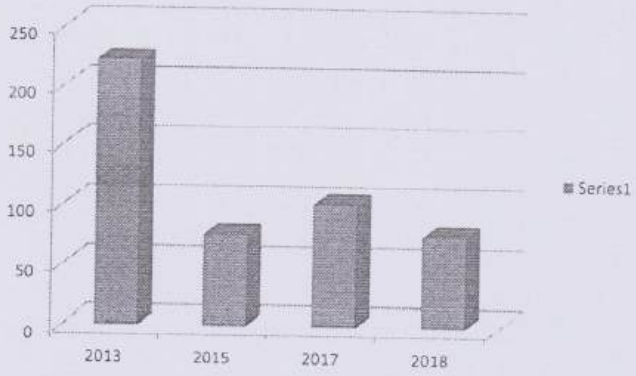


Fig. 7. COD values for various years.

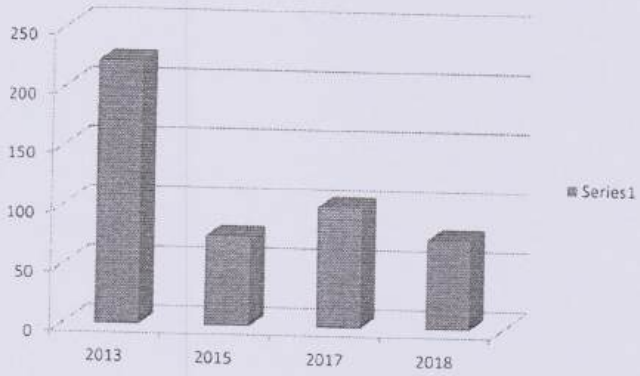


Fig. 8. Hardness comparision values for various years.

COD which is measured in mg/L. Chemical oxidation of the organic material is caused by dissolved oxygen in water. Environmental health of water bodies is measured by BOD and COD. They are commonly used in waste water treatment but rarely in general water treatment. (Milacron Marketing Co.). Fig. 7 shows COD value for various years [28–30].

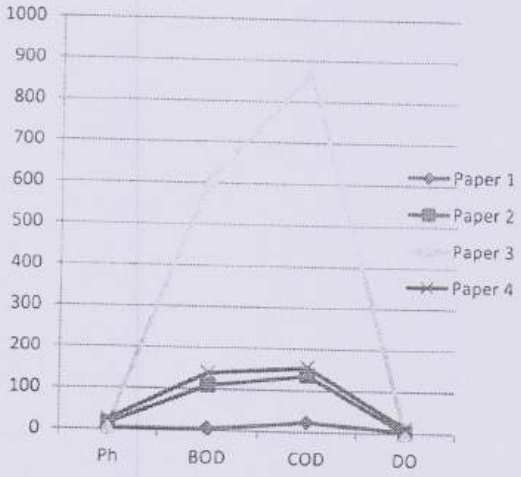


Fig. 9. Comparison of Various Parameters.

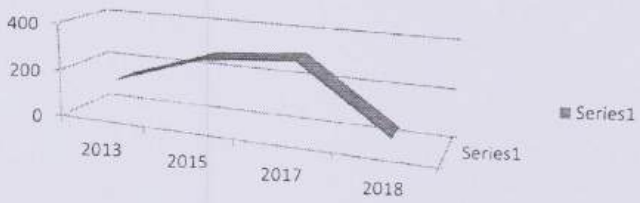


Fig. 10. Water Quality Index of 2013 to 2018.

Table 6
Range of water quality status.

WQI	Water Quality Status
0–25	**Excellent**
26–50	**Good**
51–75	**Poor**
76–100	**Very Poor**
Greater than 100	**Unfit for consumption**

Table 7
Water Quality Index2013.

YEAR 2013									
BIS Standards (Sn)	1/Sn	∑(1/Sn)	K=1/∑(1/Sn)	Wn=K/Sn	IDEAL VALUE(Vo)	MEAN CONC. VALUE (Vn)	Vn/Sn	Vn/Sn*100=Qn	WnQn
8.5	0.117647	0.3416471	2.926997245	0.3443526	7	7.6175	0.8825	88.25	30.38912
20	0.05	0.3416471	2.926997245	0.1463499	0	5.225	0.26125	26.125	3.82339
250	0.004	0.3416471	2.926997245	0.011708	0	72.25	0.289	28.9	0.338361
6	0.166667	0.3416471	2.926997245	0.4878329	7	3.635	2.365	236.5	115.3725
300	0.003333	0.3416471	2.926997245	0.0097567	0	222.6	0.742	74.2	0.723944
	0.341647			1					150.6473

WATER QUALITY INDEX = ∑WnQn/∑Wn
WATER QUALITY INDEX = 150.6472882

Table 8
Water Quality Index 2015.

YEAR 2015										
Parameters	BIS Standards (Sn)	1/SN	∑(1/Sn)	R=1/∑(1/∑Sn)	Wn=K/Sn	Ideal Value (Vo)	Mean Conc. Value(Vn)	Vn/Sn	Qn=Vn/Sn*100	WnQn
pH	8.5	0.117647	0.541647059	1.846220678	0.217202433	7	7.325	1.175	117.5	25.52129
DO	6	0.166667	0.541647059	1.846220678	0.307703446	7	0.975	5.025	502.5	154.621
BOD	20	0.05	0.541647059	1.846220678	0.092311034	0	29.875	1.49375	149.375	13.78896
COD	250	0.004	0.541647059	1.846220678	0.007384883	0	45.75	0.183	18.3	0.135143
HARDNESS	300	0.003333	0.541647059	1.846220678	0.006154069	0	76.12	0.253733	25.37333333	0.156149
TURBIDITY	5	0.2	0.541647059	1.846220678	0.369244136	0	11	2.2	220	81.23371
		0.541647			1					275.4562

WATER QUALITY INDEX = ∑WnQn/∑Wn
WATER QUALITY INDEX = 275.4562307

Table 9
Water Quality Index 2017.

YEAR 2017										
PARAMETERS	BIS Standards (Sn)	1/Sn	∑(1/Sn)	K=1/∑(1/Sn)	Wn=K/Sn	IDEAL VALUE(Vo)	MEAN CONC. VALUE (Vn)	Vn/Sn	Vn/Sn*100=Qn	WnQn
pH	8.5	0.117647	0.345647059	2.893124575	0.340367597	7	7.118	1.382	138.2	47.0388
DO	6	0.166667	0.345647059	2.893124575	0.482187429	7	1.08	4.92	492	237.2362
BOD	20	0.05	0.345647059	2.893124575	0.144656229	0	35.702	1.7851	178.51	25.82258
COD	250	0.004	0.345647059	2.893124575	0.011572498	0	83.6	0.3344	33.44	0.386984
CHLORIDE	250	0.004	0.345647059	2.893124575	0.011572498	0	169.6	0.6784	67.84	0.785078
HARDNESS	300	0.003333	0.345647059	2.893124575	0.009643749	0	102.116	0.34038667	34.03866667	0.32826
		0.345647			1					311.5979

WATER QUALITY INDEX = ∑WnQn/∑Wn

WATER QUALITY INDEX = 311.5979234

4.9. Total hardness

Total hardness of water samples were generally analyzed by using titration method with EDTA solution. Hardness of the water is defined as the property by which lathering of soap can be estimated. Hard water does not form good lather with soap. Hard water is not suitable even for industry as it creates major boiler problem. Permissible limit of Hardness for drinking water is given as 300 mg/l (IS:10500). Water is considered soft if the value of the TDS should have TDS 0–60 mg/l, it become moderately hard if it TDS lies in the range of 60–120 mg/l, hardness increase if the TDS lies in the range of 120–180 mg/l and water is defined as very hard if TDS lies between value of 180 mg/l and above. Comparative studies of data 2013 to 2018 have been done to know the quality of water in the study area. Maximum hardness we found in the year 2013 water samples and later on the hardness value start decreasing. The hardness of water have a major impact on the quality of ground water (Figs. 8 and 9) [31–34]. This has been compiled.

4.10. Water quality index

Water quality index (WQI) provide valuable information about the quality of water, this tool is helpful in determining and monitoring the quality of surface as well as ground water. WQI provide the value ranging from zero to hundred. Six parameters have been selected for developing the water quality index (Fig. 10) [35–40].

In the present study area the Water quality index has been calculated with the help of three steps. In the very first step, each of the Six parameters (PH, DO, COD, BOD, Hardness and turbidity) has been taken to know overall quality of water (Tables 6–10).

Table 10
Water Quality Index 2018.

YEAR 2018										
Parameters	BIS Standards (Sn)	1/SN	∑(1/Sn)	K=1/∑(1/∑Sn)	Wn=K/Sn	Ideal Value (Vo)	Mean Conc. Value(Vn)	Vn/Sn	Qn=Vn/Sn*100	WnQn
pH	8.5	0.117647	0.5456471	1.832686503	0.2156102	7	7.322	1.178	117.8	25.39887883
DO	6	0.166667	0.5456471	1.832686503	0.3054478	7	5.433	0.567	56.7	17.31888745
BOD	20	0.05	0.5456471	1.832686503	0.0916343	0	2.687	0.13435	13.435	1.231107158
COD	250	0.004	0.5456471	1.832686503	0.0073307	0	3.822	0.015288	1.5288	0.011207245
Chloride	250	0.004	0.5456471	1.832686503	0.0073307	0	43.388	0.173552	17.3552	0.127226563
Hardness	300	0.003333	0.5456471	1.832686503	0.006109	0	76	0.2533333	25.33333333	0.154760194
Turbidity	5	0.2	0.5456471	1.832686503	0.3665373	0	0.361	0.0722	7.22	2.64639931
		0.545647			1					46.88846675

WATER QUALITY INDEX = ∑WnQn/∑Wn
WATER QUALITY INDEX = 46.888467

The comparative study of the water quality Index has been done by the author over here. We have taken data of 2013, 2015, 2016, 2017 and analysed the water quality index. The WQI of 2013 was found to be 150.64. It was found that WQI of the study area was not good. In the similar manner WQI of 2015 has been calculated and found that 275.45 and whereas WQI of 2017 and 2018 was 311.59, 46.9 respectively [41–46].

While calculating the WQI the lowest index value indicated high-quality and the highest indicated deprived quality. After knowing the value, various standards have been considered such as the Bureau of Indian Standards permissible limits etc. It was found that some parameters have a better influence on water quality. The influence depends on the source and geographical location. The methods used for the calculations are WQI Formula This method has been extensively used by the variety of scientists and the calculation of WQI was made by using the following equation [1–57].

Step 1. Calculate the unit weight (Wa0 factors for each parameters by using formula

$$Wn = K/Sn$$

$$K = 1/(1/S1 + 1/S2 + 1/S3 + - - - - - - +1/Sn) = 1/\sum Sn$$

Sn = Standard desirable value of the nth parameters
On summation of all selected parameters unit weight factors, Wa = 1 (unity)

Step2. Calculate Sub-Index (Qn) value by using formula

$$Qn = |(Vn - Vo)|/|(Sn - Vo)| * 100$$

Where, Vn = mean concentration of the nth parameter
Sn = Standard desirable value of nth parameter
Vo = Actual value of parameter in pure water
(generally Vo = 0, for most parameters except pH and DO)
Hence, QpH = |(VpH-7)|/|(8.5–7)| *100

Step3. Combining step 1 and step 2, water quality index is calculated as follows
Over WQI= ∑WnQn/∑Wn

5. Conclusion

Based on the review carried out it is concluded that the water quality varies according to the civil and industrial effluents in the river. Increased water pollution is the biggest problem in all the rivers which is risking to both quality of human as well as aquatic life and the public life. There is constant need for proper treatment of water for the increasing load of pollution. Public awareness is necessary for the treatment of the sewage at household and the apartment level. Assessment of the current situation of water resources in the study area is necessary. The scientific quality and practicality of the assessment should be strengthened. The major reason behind the decreased water quality is the entrance of waste water from the industries, agriculture, and municipal wastewater in large quantity. The higher values of TDS and EC indicates the more pollution with higher free CO_2 . After studying various parameters and Calculating the Water Quality index it can be seen that the water of Mula Mutha river is very unfit for consumption. Hence the pollution level has increased tremendously. The treatment of river water is very much necessary for healthy and safe consumption of water. The water was most polluted in year 2017. The value of water Quality index between 26 and 50 is considered as good water for consumption.

From the analysis of the four papers we conclude following points:

1. The major reason behind the decreased water quality is the entrance of waste water from the industries, agriculture, municipal wastewater in large quantity.
2. The higher values of TDS and EC indicates the more pollution with higher free CO_2 .
3. The analysis shows the increasing pollution rate at Mula Mutha river as well as at the Pune.

Authors contribution statements

Nidhi Jain, Assistant Professor, Department of Engineering Science, Bharati Vidyapeeth College of Engineering, Pune-412115, has reviewed papers on above topic and compiled the work

Rudrani Yevatikar and Tarul Sanjay Raxamwar Engineering Students, Department of Civil Engineering, Bharati vidyapeeth college of Engineering Lavale, Pune-412115 has compiled the work.

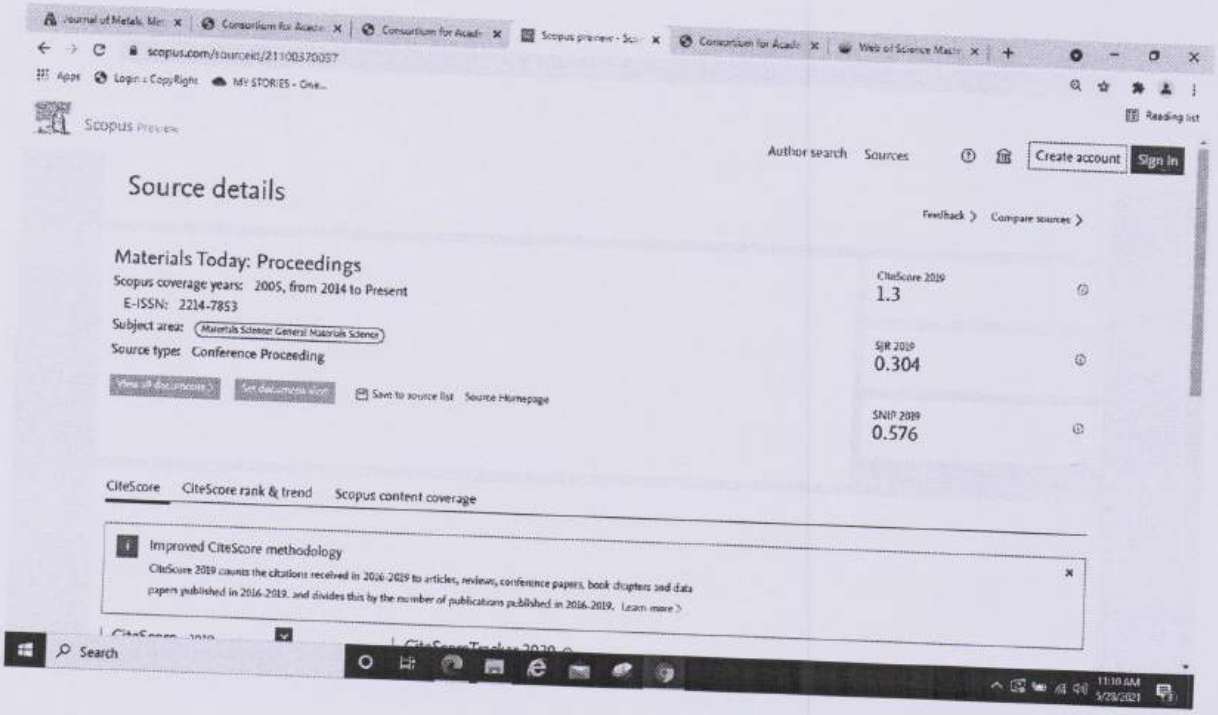
Declaration of Competing Interest

The authors declare that they have no known competing financial interests or personal relationships that could have appeared to influence the work reported in this paper.

Acknowledgements

All persons who have made substantial contributions to the work reported in the manuscript (e.g., technical help, writing and editing assistance, general support), but who do not meet the criteria for authorship, are named in the Acknowledgements and have given us their written permission to be named. If we have not included an Acknowledgements, then that indicates that we have not received substantial contributions from non-authors.

[1] ...idoo, S. ... ...iran A. D., International Journal of Environmental Research and Public Hea... 11 1 20... 249 270
[2] I.A.R. Al-A... , International Journal of Energy and Environment 9 4 2018 373 384
[3] V.S. Sale, International Advanced Research Journal in Science, Eng. Technol. 3 (2) (2007) 186–190.
[4] M. Kuitwin, P. Willems, A. El-Sadek, J. Berlamont, Int. J. River Management 1 2 (2003) 97–103.
[5] W.T. Jabbar, Master Thesis, Baghdad University, College of Science, 2013.
[6] M. Alam, Ecol. Ind. 95 (2018) 695–701.
[7] V. Golosov, V. Belyaev, Intern. Soil and Water Conservation Research 1 (2) (2013) 25–35.
[8] C. Dai, Y. Liu, T. Wang, Z. Li, Y. Zhou, Agric. Water Manag. 210 (2018) 41–48.
[9] G. Sofia, F. Ragazzi, P. Giandon, G.D. Fontana, P. Tarolli, Adv. Water Resour. 124 (2018) 120–138.
[10] I.A.R. Al-Ani, W.H.M.W. Mohtar, N.E.A. Basri, L.M. Sidek, KSCE J. Civ. Eng. 20 (7) (2016) 3045–3056.
[11] A.V. Mane, R.G. Pardeshi, V.R. Gore, R.L. Walave, S.S. Manjrekar, G.N. Sutar, Maharashtra J. Chem. Pharmac. Research 5 (8) (2013) 91–102.
[12] G.B. Hagan, F.G. Ofosu, E.K. Hayford, E.K. Osae, K. Oduro-Afriyie, Research J. Environ. Earth Sci. 3 (4) (2011) 385–392.
[13] NGBRA: National Ganga River Basin Authority (NGRBA), Draft, Environmental and Social Management
[14] Framework (ESMF), Volume I - Environmental and Social Analysis 2011 http://moef.nic.in/downloads/public-information
[15] P. Sahu, S. Karad, S. Chavan, S. Khandelwal, An Intern. J. 2 (2015) 2.
[16] Bureau of Indian Standards(BIS), Drinking Water–Specification is 10500: 2012; BIS: New Delhi, India, 2012
[17] M.V.S. Vaishnavi, Shelly Gupta, A Physico-Chem. Analy.J. Geo. Environ. Earth Sci. Intern. 16 (2) (2013) 1–11.
[18] R. Nayar, Intern. J. Eng. Resear. Technol. (IJERT) 9 (2020) 01.
[19] Shivasharanappa et al. JACPT. 3, 1 (2012)
[20] N. Gupta, S.M. Nafees, M.K. Jain, S. Kalpana, Rasayan J. review 4 (2) (2011) 686–692.
[21] M.A.M. Joarder, F. Raihan, J.B. Alam, S. Hasanuzzaman, Int. J. Environ. Res. 2 (3) (2008) 291–296.
[22] N. Jain, R. Shrivastava, Intern. J. Environ. Sci. Toxicol. Food Technol. (IOSR-JESTFT) 8 (6) (2014) 25–30.
[23] M.R. Mahananda, Intern. J. Resear. Review. Appl. Sci. 2 (3) (2010) 284–295.
[24] PV Rao, Textbook of Environmental Engineering, Eastern Economy Ed., Pretice-Hall Of India Private Limited, New Delhi, 2005, 3, 280.
[25] A.R. Thorvat et Al, International Journal of Advance Foundation and Research In Science & Engineering (IJAFRSE) 2 1 2015
[26] N. Jain, S. Saxena, R. Shrivastava, Pollution Research (2005) 149–153.
[27] P. Tyagi, D. Buddhi, R.L. Sawhney, R. Indian Kothari, J. Environ. Protection 23 (1) (2003) 1276–1282.
[28] A. Sharma et al., Multivariate Analysis Nat. Resources Research 5 (2013) 4.
[29] N. Saxena, A. Sharma, Intern. J. Appl. Environ. Sci. 12 (2) (2017) 359–370.
[30] K. Chouhan, A.K. Bansal, R.C. Chhipa, Rajasthan J. Drug Delivery, Therapeutics 4-A) (2019) 722–725.
[31] K. Chouhan, R.K. Yadav, P. Parashar, A.K. Bansal, R.C. Chhipa, Int J Innov Eng ch 11 (2) (2018) 35–42.
[32] R.K. Chauhan, A.K. Bansal, P.K. Parasha, R.C. Chhipa, Int J Eng App Managt Sci Parad 54 (4) (2019).
[33] R.K. Chauhan, A.K. Bansal, P.K. Parasha, R.C. Chhipa, Int J Innov Res Sci Eng Tech 8 (2) (2019).
[34] Singh & Hussian, India Cogent Eng. 3 (2016) 1177–2155.
[35] K. Srinivasamoorthy, S. Chidambaram, M.V. Prasanna, M. Vasanthavihar, A. John peter, P. Anandhan, J. Earth Sys. Sci. 117 (2008) 49–58.
[36] R.D. kangabam, S.D. Bhoominathan, S. Kanagaraj, M. Govindaraju, Appl Water Sci 7 (2017) 2907–2918.
[37] M. Rivera L., S. Salgado, V. BenavidesC., Coto-Campos J. Swinscoe, T. Water 9 2017 558
[38] Radu V.M., Ionescu, Deak G., Diacu E., Ivanov A.A. Zamfir S. Marcus M.I. Environ. Monit. Assess. 2020, 192, 135. [CrossRef]
[39] W. Duan.; He, B.; Chen, Y.; Zou, S.; Wang, Y.; Nover, D.; Chen,W.; Yang, G. PLoS ONE 13 (2018). e0188889. [CrossRef]
[40] M. Bora; D.C. Goswami, Appl. Water Sci. 7 (2017) 3125–3135. [CrossRef].
[41] D.S. Chandra, S. Asadi, M.V.S. Raju, Int. J. Civ. Eng. Technol. (IJCIET) 8 (2017) 1215–1222.
[42] I. Paun, National Research and Development Institute for Industrial Ecology, Bucharest, Romania, –402.
[43] T. Shweta, S. Bhavtosh, S. Prashant, D. Rajendra, Am. J. Water Resources 1 (3) (2013) 34–38.
[44] S.W. Al-Muqdadi, M.F. Omer, R. Abo, A. Naghshineh, J. Environ. Protection 7 (2016) 1096–1103.
[45] V. Kumar Swaroop, N.B. Singh, A. Verma, Intern. J. Civil Eng. Technol. 9 (8) (2018) 155–165.
[46] K. Sridhar, A. Lakshman, V. Sree Lakshmi, Intern. J. Civil Eng. Technol. 8 (4) (2017) 1614–2162.
[47] Gagan Matta, Avinash Kumar, K. Naik, A.K. Tiwari Pradeep, R. Bemdtsson, Taiwan Water Conservancy. 66 (1) (2018) 1–12.
[48] Matta, Gagan; Kumar, Avinash; Uniyal, D. P.;Singh, Prashant; Kumar, Amit; Dhingra, GulshanK.; Kumar, Ajendra; Naik, Pradeep K.and Shrivastva, Naresh Gopal, Int. J. for Env. Rehab. AndConser. 9(1) (2017) 187-204
[49] Matta, Gagan; Kumar, Avinash; Uniyal, D. P.;Singh, Prashant; Kumar, Amit; Dhingra, GulshanK.; Kumar, Ajendra; Naik, Pradeep K.and Shrivastva, Naresh Gopal Int. J. for Env. Rehab. AndConser. 9(1) (2017) 187-204
[50] Dipak Pati Jayesh, Vijay PatilKunal, BaravkarRushikesh, KotuleOnkar, Thakur Muskan, Jain Nidhi,Physico-chemical analysis of water - A Review. Journal Of Engineering Sciences 2020, 11(5)
[51] N. Jain, S. Shegaon, A. Goplani, S. Tiwari, S. Rutuja/amrutkar, J. Eng. Sci. 11 (2020) 5.
[52] N. Jain, M. Huzaif, Intern. J. Innovat. Technol. Explor. Eng. (IJITEE) 8 (2019) 12.
[53] N. Jain, intern. j. adv. Resear. (Published/November 3 (11) (2015) 916–920.
[54] N. Jain, Intern. J. innovat. Emerg. Resear. Eng. 4 (2017) 1.
[55] N. Jain, Intern. J. Scient. Research Eng. Technol. (IJSRET) 7 (2018) 1.
[56] N. Jain, R. Shrivastava, Int. J. Environ. des. Public Health 3 (8) (2014) 1–4.
[57] N. Jain, R. Shrivastava, Intern. J. Scientific Research 11 (2014).


scopus.com/sourceid/21100370057
Scopus Preview
Author search
Sources
Create account
Sign in
Source details
Feedback
Compare sources
Materials Today: Proceedings
Scopus coverage years: 2005, from 2014 to Present
E-ISSN: 2214-7853
Subject area: Materials Science: General Materials Science
Source type: Conference Proceeding
Save to source list
Source Homepage
CiteScore 2019
1.3
SJR 2019
0.304
SNIP 2019
0.576
CiteScore
CiteScore rank & trend
Scopus content coverage
Improved CiteScore methodology
CiteScore 2019 counts the citations received in 2016-2019 to articles, reviews, conference papers, book chapters and data papers published in 2016-2019, and divides this by the number of publications published in 2016-2019.
Learn more
Search

IJBPAS, November, Special Issue, 2021, 10(11): 1319-1330

ISSN: 2277–4998

International Journal of Biology, Pharmacy and Allied Sciences (IJBPAS)

'A Bridge Between Laboratory and Reader'

www.ijbpas.com

MICRO AND NANO-TECHNOLOGY (MNT) APPLICATIONS IN HEALTHCARE TO BUILD ARTIFICIAL ORGANS THAT REPLACE DAMAGED HUMAN TISSUE DUE TO RADIOACTIVITY

JYOTI A. DHANKE[1*], UMAMAHESWARI K[2], SOWMIYA S[3], VIGNESHWARAN.K[4], VINOTHINI.C[5] AND DHARMBIR SINGH[6]

1: Assistant Professor in Mathematics at Bharati Vidyapeeth's College of Engineering, Lavale, Pune, Maharashtra, India

2: Associate Professor, Department of Electronics and Communication, SRM TRP Engineering College, Tamil Nadu, India

3: UG Student, Final Year in Electrical and Electronics Engineering at KPR Institute of Engineering and Technology, Coimbatore, Tamilnadu, India

4: Assistant Professor in Electronics and Communication Engineering, K.Ramakrishnan College of Engineering, Samayapuram, Trichy, India

5: Assistant Professor in Physics at D.K.M College For Women, Vellore, Tamilnadu, India

6: Professor at Maharishi Markandeshwar University, Ambala-134007, Haryana, India

*Corresponding Author: Jyoti A. Dhanke; E Mail: jyoti.dhanke@bharatividyapeeth.edu

Received 26th July 2021; Revised 27th Aug. 2021; Accepted 1st Oct. 2021; Available online 1st Nov. 2021

https://doi.org/10.31032/IJBPAS/2021/10.11.1115

ABSTRACT

Advanced education plays a critical role in societal progress. Institutions of higher learning are common on a national level, although they are essentially fictional and creative. Those were essentially created consistent with previous findings from these institutions, as though they might be regarded near to concealed and impractical. As a result, the educational approach must be overhauled right now. Through the use of nanotechnology, as well as the method in which it is applied, is essential to educational change. The high technology semiconductor industry, which is at the heart of any and every single gadget, will have a

referred to as social property, and it eventually reflects on global civilization. As a result, financial competence, which functions as a social connection within a system of trade and a financial system of practices, confers a social position of power [4]. Financial competence is a concept used to explain variations in educational outcomes and academic achievement only within the education sector [5]. Student performance is divided into three categories: embodied cultural capital, which seems to be the combination of cultural behavior and endeavor inside a person and is made up of different understanding, information processing, and capacity.

The 2nd kind is institutionalized, which occurs when an organization acknowledges a person's social capital, typically on the order of academic qualifications, such as Graduate degree and Doctoral programs. Finally, objectification financial competence encompasses a multitude of commodities with a distinct cultural meaning [6]. When it comes to higher education, the profoundly internalized human diversity is particularly interested in instilling strong faith in its viability and demonstrating excitement for economic growth and development. As a result of the lower concentrations of intangible capitals, lesser education is regarded as critical to economic growth and development.

Secondary education should be a passionate conviction in achieving broader life objectives, as it satisfies wants and accomplishes its most identifiable utilitarian and hedonic life goals. Genuine career aspirations are also those that stem from and are influenced by one's self. Unmeasurable life goals are ambitions based on outside stimulation and encouragement for wealth, fame, and status [7]. University education as that an effective element in attaining trade and investment is primarily influenced by life objectives, whether big or little, at just the degree of intangible capitals. Students have little desire to achieve external life objectives via higher education; in fact, there is considerable opposition to it. The rising expenses and a load of postsecondary learning may aggravate this dilemma. As a result, education will regress rather than develop.

University education is placed in the "income range" as a result of this position, but it receives little scrutiny since governments' strategies and tactics focus their limited resources on boosting development and lowering crime rates. When evaluating educational ambitions from some kind of global viewpoint, they become a little

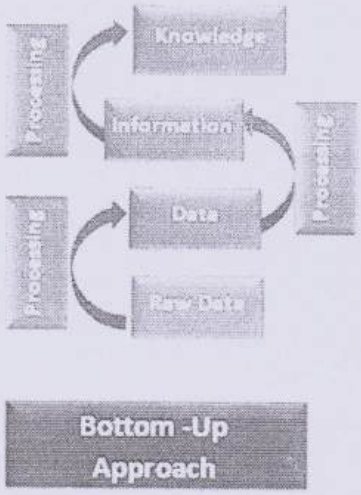


Figure 2: Bottom-up Education methodology architecture

The key factors that are monitored and gathered are raw data. This is also known as raw data, and it's transformed into the information collected that can then be examined and displayed using a variety of tools, graphics, and tables **[10]**. This will enable the data to be gathered while also making it more visible to the intended audience. This data must resolve one or more questions, and it may take whatsoever shape, size, or form **[11]**. Ultimately, the observation has the required information to make choices. As you've seen, facts, information, and understanding are all intertwined notions, but in the bottom-up method, each plays a distinct function **[12-17]**.

Concept and Methodological Approach

The scientific method for establishing the research center should indeed be based on the early education project management methodology, which assists business leaders in developing an effective vision for postsecondary learning at an improved infrastructure, which may be the primary objective at about the same moment as we seek to eliminate society's depressing picture of education, as can be seen in **Figure 3**. The above foundation's overall strategy is to reach the pinnacle of advanced communications, with an approach to teaching modern sophisticated technological theory; CMOS technology, which would also be connected with either the preparation and management of electronic components such as integrated circuits (IC) by the appropriate

The Mission of Micro and Nano Technology

Micro and Nano Technology's goal is to fully utilize this modern technology by contributing significantly to its development. The Institute of Micro-mission nanotechnologies is to properly use science and technology knowledge, such as Semiconductor and NEMS and MEMS advancements, to improve national capacities and create suitable development sectors. As a result, the institution aspires to contribute to the achievement of development objectives by increasing public awareness of the significance of science and technology in light of worldwide developments and national requirements. The institution will not be shielded or run in isolation from local, regional, or international stakeholders. Upon on alternative, the administration's personnel will start monitoring all improvements and changes that have taken place across the globe to establish a network with them to improve our local capabilities. It is essential to encourage clinical trials, as well as support growth and innovation, in particular concerning the commercialization of science and technology ideas in goods and businesses, which is dedicated to serving the development sectors. As a result of scientific and technical advancements, the nation will be well-represented on the world map.

Ideology and Tactic Avoid Radioactivity Signals

To comprehend how an institution such as Micro and Nano Technology is executed, one must first comprehend the benefits of things and then how message passing happens; to enable learning to take place, one must first comprehend the importance of education and just how message passing occurs. Furthermore, learning does not end with the acquisition of information; it can only be combined and used in the actual world. Generally essence, empowerment is a means that aids in the collection of information as well as the required values, opinions, qualifications, and capabilities. This must have been accomplished nearly so that this information may be used sensibly and realistically, rather than only theoretically. To throw light on this ideology, a methodology and attitude must be presented.

In consideration of the regulation of worldwide academic institutions, the methodology of this university is based primarily on combining two components of expertise, conceptual and experimental. As previously said, Nanostructures symbolizes an information world that will alter every area of humanity and international commerce, including architecture, materials, procedures, and uses. And that is exactly why MNT is searching for more than simply to combine

investors must be aware of current nanotechnology developments, as well as the applicability and value that nanostructures may bring to their businesses. Researchers may normalize the microscopic threshold though by learning nanomaterials architecture at the postgraduate level, as well as exposing nanostructures via the Micro and Nano Technique platform. This should assist customers, producers, and sellers in maximizing the benefits of new technologies while also emphasizing and safeguarding society from any drawbacks. The Department of Micro-Nanotechnology is working to create humans and machines "Tech Startups" for nanoparticles entrepreneurs in the long run. Those pursuing a genuine understanding of particular nano implementations on a local, regional, or worldwide level may come to our online or offline world. We'll accelerate the transition to us rather than experiencing the world.

Because there are so many components within this wide approach, the future is looking bright for nanostructures. Nanoscience, as a subset of genetic engineering, is a new area of scientific and technical possibilities that uses nanoparticle manufacturing techniques to the creation of biotic and abiotic research instruments. Scientists are discovering how to make new little nano gadgets to help people work more efficiently. They also apply innovative performance models and industrial applications in many areas of the business, including drones. The potential buyer in this area will discover a better set of organizational possibilities.

Nanotechnology in manufacturing industries in the form of nanoparticles, like petroleum products, wheat, and gemstones, are the main economic manufactured goods that have been genetically modified to the necessary accuracy. These nanoparticles are designed for use in a variety of industries, including manufacturing, cosmetics, meat packing, and health care. Whatever researchers believe concerning technological innovations is being altered by Micro and nanotechnology. Both as result, the nano-information sector has progressed into a global marketplace and financial instrument for nanotechnology. Even though machinery, computer systems, estate development, biomaterials, and physical objects integrate to deliver considerable potential in technological development, public safety, manufactured goods, tracking, renovation, agribusiness, and power generation, nano-computers and their operating systems, Micro and nano-robots, Quadcopter, Ornithopter, spy planes, and the finding was similar, biochemical, smart platforms will

[7] T. Kasser, R. Ryan, Further examining the American dream: Differential correlates of intrinsic and extrinsic goals, Personality and Social Psychology Bulletin, Vol. 3, issue: 22, PP. 280–287, 1996. DOI: doi.org/10.1177/0146167296223006

[8] Deepthi T, Balamurugan K, Uthayakumar M. Simulation and experimental analysis on cast metal runs behaviour rate at different gating models. International Journal of Engineering Systems Modelling and Simulation. 2021;12(2-3):156-64.

[9] S, Malkapuram R, Singaravel B. Performance analysis of micro textured cutting insert design parameters on machining of Al-MMC in turning process. International Journal of Lightweight Materials and Manufacture. 2021 Jun 1;4(2):210-7

[10] Garigipati RK, Malkapuram R. Characterization of novel composites from polybenzoxazine and granite powder. SN Applied Sciences. 2020 Sep;2(9):1-9.

[11] Yarlagaddaa J, Malkapuram R. Influence of carbon nanotubes/graphene nanoparticles on the mechanical and morphological properties of glass woven fabric epoxy composites. INCAS Bulletin. 2020 Oct 1;12(4):209-18.

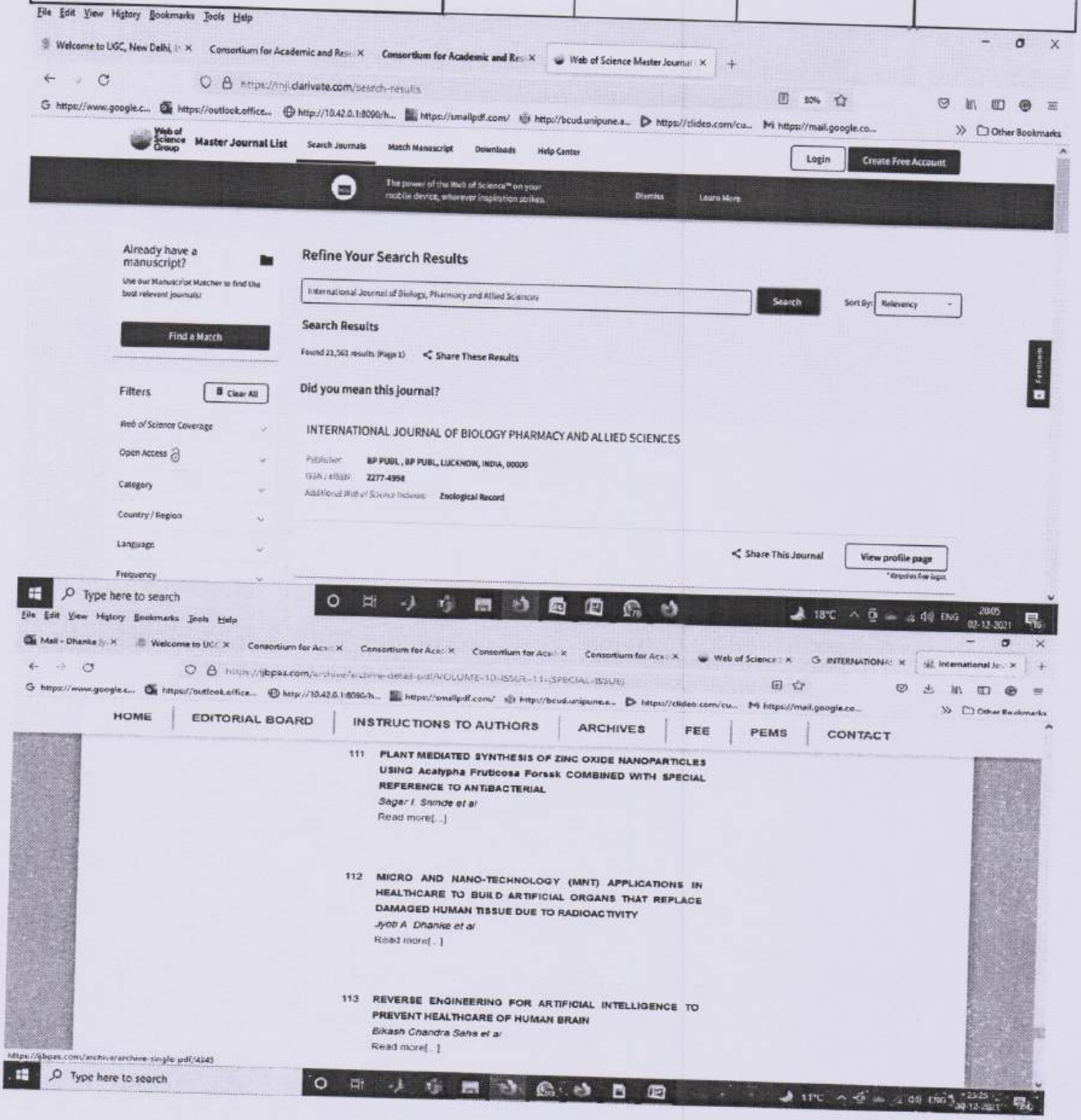
[12] Rama Krishna M, Tej Kumar KR, DurgaSukumar G. Antireflection nanocomposite coating on PV panel to improve power at maximum power point. Energy Sources, Part A: Recovery, Utilization, and Environmental Effects. 2018 Oct 18;40(20):2407-14.

[13] Yarlagaddaa J, Malkapuram R, Balamurugan K. Machining Studies on Various Ply Orientations of Glass Fiber Composite. InAdvances in Industrial Automation and Smart Manufacturing 2021 (pp. 753-769). Springer, Singapore.

[14] Ezhilarasi, T. P., Kumar, N. S., Latchoumi, T. P., & Balayesu, N. (2021). A Secure Data Sharing Using IDSS CP-ABE in Cloud Storage. In Advances in Industrial Automation and Smart Manufacturing (pp. 1073-1085). Springer, Singapore.

[15] Mishra, P., Jimmy, L., Ogunmola, G. A., Phu, T. V., Jayanthiladevi, A., & Latchoumi, T. P. (2020, December). Hydroponics cultivation using real time iot measurement system. In Journal of Physics: Conference

Title of paper	Name of journal	ISSN number	Link to website of the Journal	Is it listed in UGC Care list/Scopus/Web of Science/other, mention
MICRO AND NANO-TECHNOLOGY (MNT) APPLICATIONS IN HEALTHCARE TO BUILD ARTIFICIAL ORGANS THAT REPLACE DAMAGED HUMAN TISSUE DUE TO RADIOACTIVITY	Zoological Record	2277_4998 "VOLUME 10 ISSUE 11 (SPECIAL ISSUE)" : 110	https://ijbpas.com/archive/archive-single-pdf/4345	Web of Science

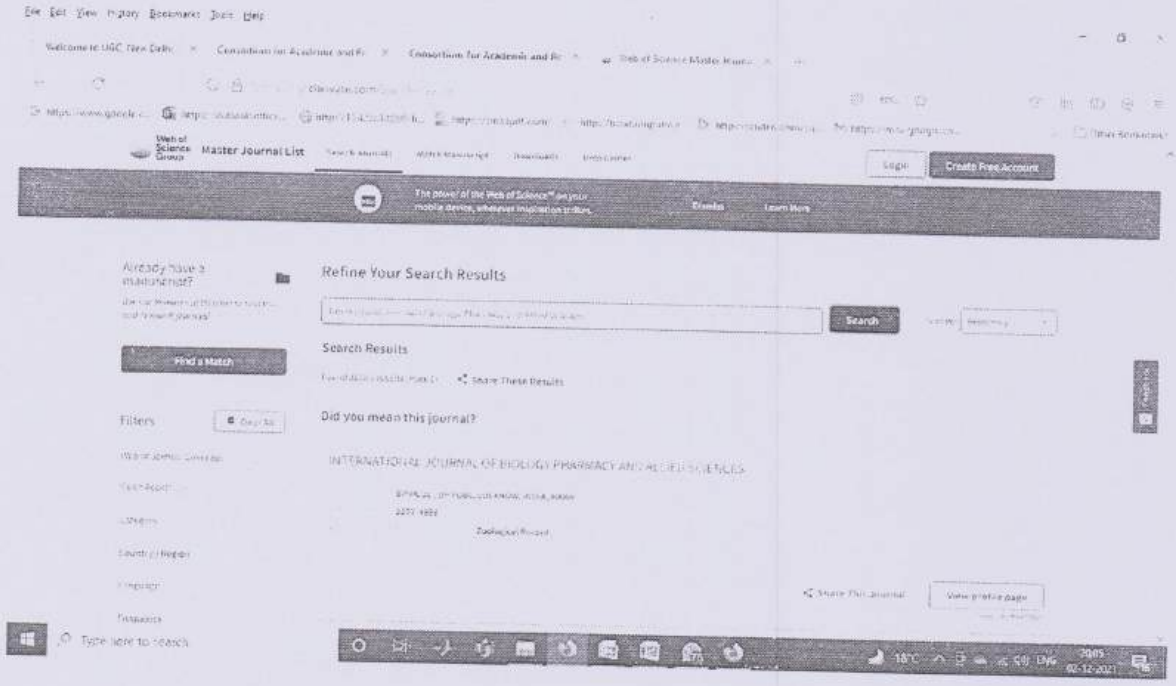


(15) Proof
Web of Science
Nov. 2021

Web of Science : Zoological Record
Publication date: 01/11/2021

Title : **MICRO AND NANO-TECHNOLOGY (MNT) APPLICATIONS IN HEALTHCARE TO BUILD ARTIFICIAL ORGANS THAT REPLACE DAMAGED HUMAN TISSUE DUE TO RADIOACTIVITY**

INTERNATIONAL JOURNAL OF BIOLOGY PHARMACY AND ALLIED SCIENCES



https://ugccare.unipune.ac.in/Apps1/User/WebA/CAREList

SAMRIDDHI
A Journal of Physical Sciences, Engineering and Technology
ISSN(P): 2229-7111
ISSN(O): 2454-5767

SEIZURE AND SLEEPING DISORDER DETECTION FROM EEG USING MACHINE LEARNING

Prof. Swati G. Gawhale
Assistant Professor, Bharati Vidyapeeth's College of Engineering, Lavale, Pune, MH, India, gawhaleswati@gmail.com

Prof. Lalita K. Wani
Assistant Professor, Bharati Vidyapeeth's College of Engineering, Lavale, Pune, MH, India, lalita.wani@gmail.com

Dr. Uday Chandrakant Patkar
HOD, Department of Computer Engineering, Bharati Vidyapeeth's College of Engineering Lavale Pune, MH, India, Email Patkarudayc@gmail.com

ABSTRACT

Our research Paper" Seizure and Sleeping Disorder Detection from EEG Using Machine Learning "is a Electroencephalogram (EEG) is quite possibly of the most useful asset that offer significant data connected with various anomalies in the human mind. One of these anomalies is the epileptic seizure. A system is proposed for distinguishing epileptic seizures from EEG signals recorded from ordinary and epileptic patients. The recommended approach is intended to consequently order the unusual sign from the typical one. This work expects to work on the precision of epileptic seizure location and diminish computational expenses. To address this, the proposed system utilizes the 54-DWT mother wavelets examination of EEG signals utilizing the Genetic calculation (GA) in mix with other four AI (ML) classifiers: Support Vector Machine (SVM), K-Nearest Neighbors (KNN), Artificial Neural Network (ANN), and Naive Bayes (NB). The exhibition of 14 distinct mixes of two-class epilepsy location is explored utilizing these four ML classifiers. The trial results show that the four classifiers produce tantamount outcomes for the got factual elements from the 54-DWT mother wavelets; nonetheless, the ANN classifier accomplished the best precision in many datasets blends, and it beat the other analyzed classifiers. The exactness was basically as high as conceivable in case1, case2, and case5, where it came to 100 percent. The most terrible exactness was acquired by cases 6, case 8, and case10, where their precision ranges somewhere in the range of 93.3% and 94.4%. The table shows that the exactness of the excess cases ranges somewhere in the range of 95% and 98.8 %. In NB classifier, the precision for the 14 blends of shows that the Naive Bayes calculation got the best outcomes in initial two cases, where the exactness arrives at up to 100 percent, however in the accompanying cases 3, 6, 8, the precision was low as conceivable where they didn't surpass 95%. Notwithstanding, in these cases, the precision was negligible, on the grounds that the highlights vector

SAMRIDDHI
A Journal of Physical Sciences, Engineering and Technology
ISSN(P): 2229-7111
ISSN(O): 2454-5767

coming about because of these cases in the elements extraction stage are less exact than the other cases as per the Euclidean distance.

KEYWORDS: Electroencephalogram (EEG), discrete wavelet transform (DWT), epilepsy, artificial neural network, k-nearest neighbor (k-NN), support vector machine (SVM),

INTRODUCTION

Epileptic seizures cause strange changes in the mind; accordingly, the identification of capricious epileptic seizures is executed generally by master clinicians. The specialists normally depend on visual perception of the EEG signals for distinguishing irregularities. This cycle is regularly time-consuming and inclined to human mistakes. Consequently, programmed determination of epileptic seizures is fundamental in the clinical climate, and there is a requirement for working on the computerized One of the most methods that are utilized for distinguishing the epileptic seizure is design acknowledgment, where the secret examples are separated from EEG.

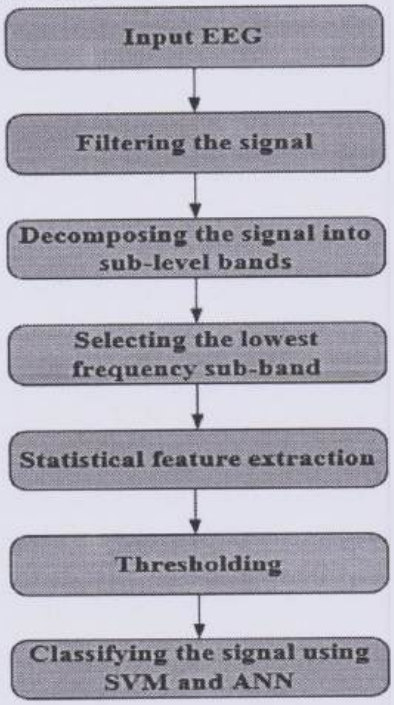


Fig.1: ECG Flow

Analysts have endeavored various highlights extraction strategies to remove the concealed examples from EEG signals like DWT, CWT, FT, DFT, IDFT, STFT, and FFT [2]-[6]. Also, various procedures, for example, Particle Swarm Optimization (PSO), Simulated Annealing (SA), Ant Colony Optimization (ACO) [7], and numerous different plans to choose the best elements were researched. In term of the arrangement strategies, different classifiers were analyzed by the analysts in particular help vector machines, choice tree, fake brain organization, k-closest neighbors (k-NN), credulous Bayes (NB), Gaussian blend.

In this paper, we expect to further develop the identification exactness for fourteen distinct mixes of datasets utilizing 54 DWT mother wavelets to remove a bunch of elements. These highlights incorporate Mean Absolute Value (MAV), Average Power (AVP), Standard Deviation (SD), Variance, Mean, Skewness, Shannon Entropy, Max, Min, Normalized SD, Kurtosis, and Energy [2]-[6]. The quantity of the determined highlights are then limited utilizing the hereditary calculation (GA) to choose the most pertinent elements. At long last, the chose qualities are concentrated on utilizing four classifiers to recognize the result as an epileptic seizure or not. The remainder of this paper is coordinated as follows: Section II presents the connected work, Section III presents the proposed include choice technique. The arrangement and analyses are examined in Section IV. Area V and VI examine the assessment procedure and the mathematical outcomes, separately. At last, Section VII contains ends and future work.

RELATED WORK

Numerous analysts stand out to EEG signals arrangement for epilepsy location. In this part, we survey a bunch of ongoing related works to epileptic seizure identification from EEG signals. The creators in [7] proposed another methodology in light of the 54-DWT mother wavelets partitioned into seven families to separate the EEG information into various sub-groups to extricate the factual elements. Then, at that point, a SVM classifier is utilized to sort the EEG signals in light of the extricated highlights. The exploratory outcomes show that the precision is mostly delicate to the degree of disintegration, and 40% of the redundancies were eliminated from the subsequent elements. The creators in [8] fundamentally depend on an examination of EEG announces utilizing discrete wavelet changes (DWT) to disintegrate the EEG information into various sub-groups, and afterward separate the measurable highlights. The got factual highlights from DWT are utilized to prepare the classifier. From that point onward, two classifiers are utilized to decide the signs in the event that they have epileptic or not. The two classifiers are KNN and Naive Bayes classifiers [18]. This examination estimates the exhibition of the 14 various blends of two class epilepsy recognition. That's what the exploratory outcomes characterized, for the location of epileptic seizure irregularity, the NB classifier accomplishes higher exactness for most mixes of the dataset with less calculation time, and the other classifier achieves better precision for only 4 informational indexes blend.

ARTIFICIAL NEURAL NETWORK (ANN)

ANN is a capability included neurons and loads. The neurons pass the info values through capabilities and result the outcomes, while the loads convey the qualities between neurons. The neurons can be arranged into three primary layers; input layers, stowed away layers, and result layers.

SAMRIDDHI
A Journal of Physical Sciences, Engineering and Technology
ISSN(P): 2229-7111
ISSN(O): 2454-5767

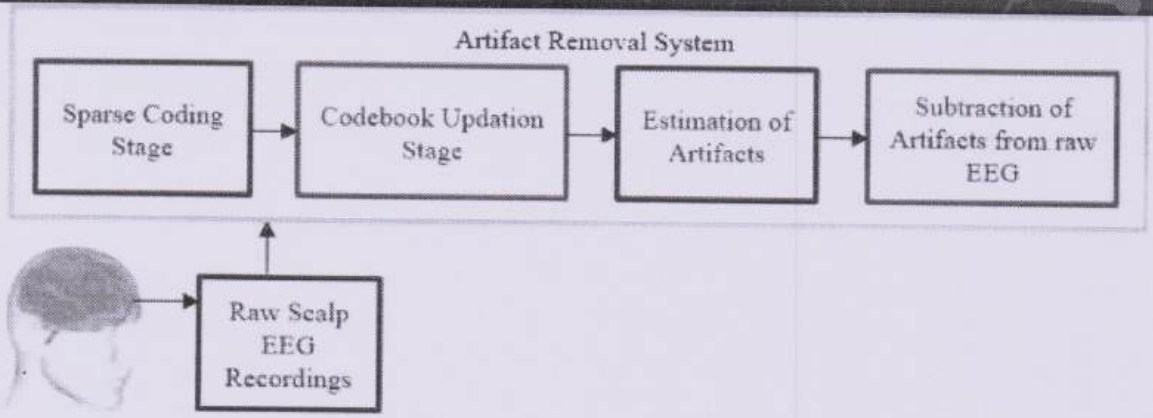


Fig.2: ARTIFICIAL NEURAL NETWORK (ANN)

The information layer contains different information units; the fundamental reason for the info layer is to address the data to be taken care of into the organization. The secret layers contain the secret units that depend on two factors: the first is the info units' exercises, and the subsequent one is the loads that are established on the associations among the information and the secret units.

NAIVE BAYES (NB) CLASSIFIER

The NB calculation manages elements and classes. It is thinking about a quick calculation that looks at all its preparation datasets, and it requires less information for grouping. NB is a probabilistic classifier, which depends absolutely on the advancing by thinking about that the elements are free given the class (Bayesian hypothesis), where each component of a specific class is free of different highlights. Freedom ordinarily is a horrendous suspicion. This calculation in light of the Bayesian hypothesis. For each occurrence, the relationship among each trait and the class are broke down in this classifier, to determine a restrictive likelihood for these connections.

SAMRIDDHI
A Journal of Physical Sciences, Engineering and Technology
ISSN(P): 2229-7111
ISSN(O): 2454-5767

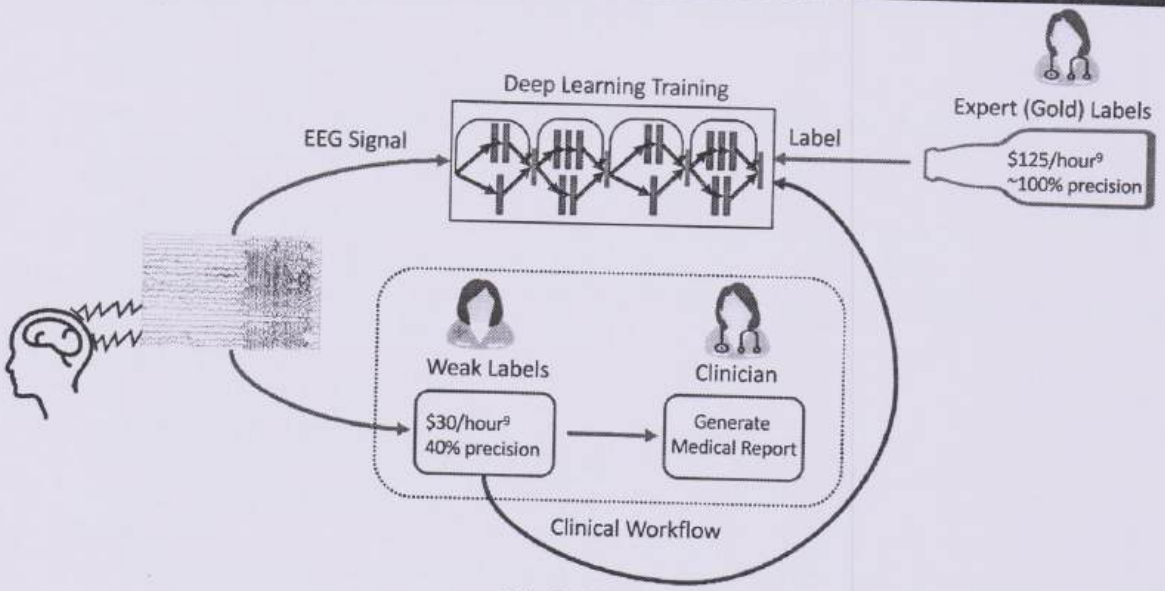


Fig.3: ECG Cycle.

From that point onward, the measurable elements are applied for the definite coefficients. In the following stage, the results (coefficients) of the low pass channel g[n] are passed to the high and low pass channels in a higher level; for each step, the recurrence goal is expanded, and the time goal is diminished. A similar cycle is rehashed until we arrive at an elevated degree of deterioration for each DWT wavelet. The component grid is a method for addressing the sign, and it is addressed when the wavelet coefficients have been delivered. The estimation coefficients and nitty gritty coefficients were used to frame the state of the component's lattice. These coefficients comprise the reach between 0.05 - 86 Hz of recurrence groups.

RESULTS AND DISCUSSION

The outcomes introduced here address the precision, particularity, and responsiveness of 14 dataset 'mixes, these outcomes address the assessment measurements that are created subsequent to applying the hereditary calculation. The examples in the local information are haphazardly partitioned into testing and preparing datasets: 70% for preparing, and 30% for testing. In this paper, 14 order mixes (preparing testing): (A-E), (B-E), (C-E), (D-E), (AB-E), (AC-E), (AD-E), (BC-E), (CD-E), (ABC-E), (ACD-E), (BCD-E), and (ABCDE). In all mixes, we utilized the dataset E as it is the only one treated as an epileptic seizure. These blends are utilized to recognize the epileptic sign from a typical sign. In this review, we led a correlation between classifiers for the ID of the epileptic sign. The reason for this study is to improve the recognition of anomaly exactness from EEG information.

ISSN(P): 2229-7111
ISSN(O): 2454-5767

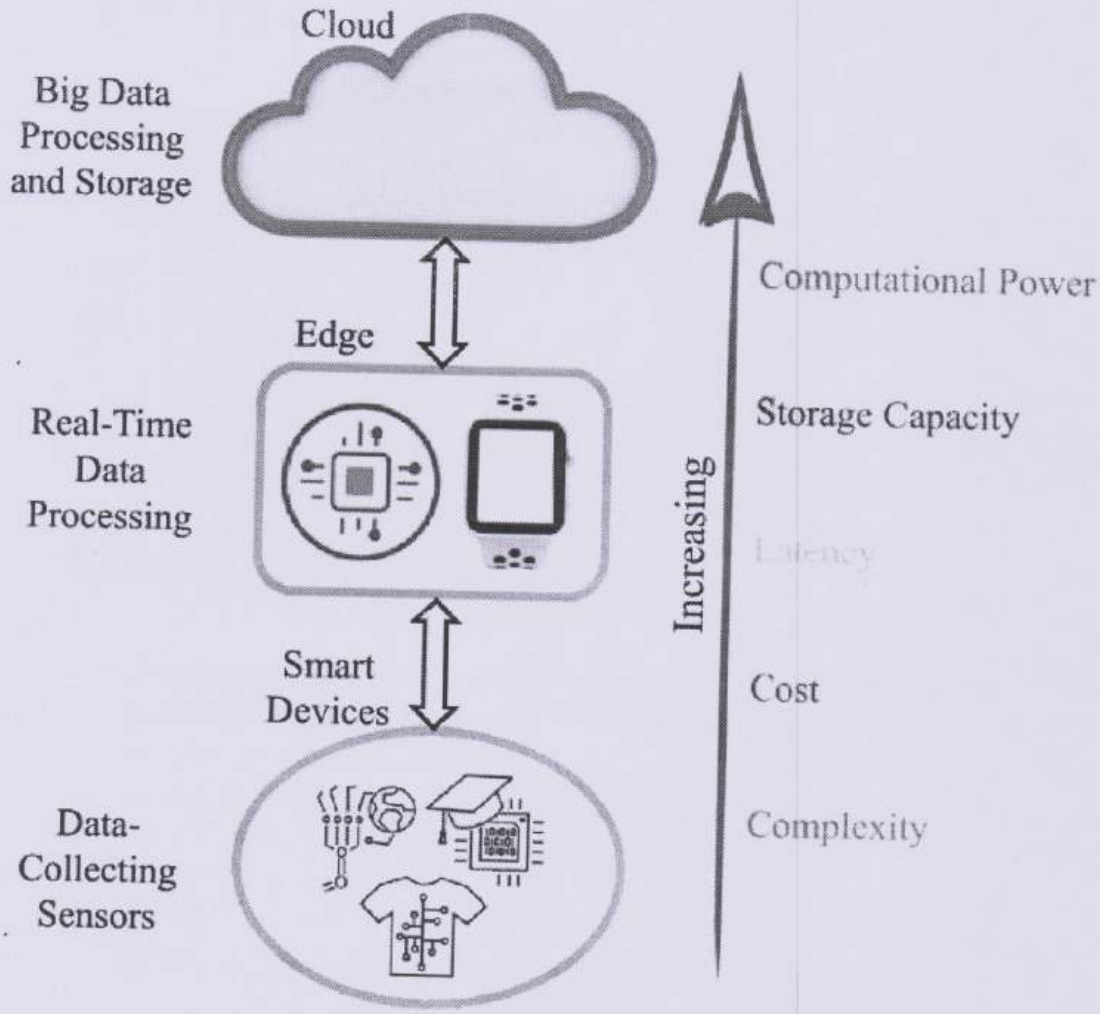


Fig.4: Real Time Processing

The exhibition of the four classifiers is contemplated with equivalent preparation and testing informational indexes. Table 2 shows the exhibition of four classifiers for the chose highlights from the hereditary calculation as per the exactness got from the SVM classifier. The precision was just about as high as conceivable in case1, case2, and case5, where it came to 100 percent. The most horrendously terrible exactness was acquired by cases 6, case 8, and case10, where their precision ranges somewhere in the range of 93.3% and 94.4%. The table shows that the precision of the leftover cases ranges somewhere in the range of 95% and 98.8 %. In NB classifier, the exactness for the 14 blends of shows that the Naive Bayes calculation got the best outcomes in initial two cases, where the precision arrives at up to 100 percent, yet in the accompanying cases 3, 6, 8, the precision was low as conceivable where they didn't surpass 95%. Nonetheless, in these cases, the exactness was negligible,

on the grounds that the elements vector coming about because of these cases in the highlights extraction stage are less precise than the other cases as per the Euclidean distance. The exactness in the leftover cases ranges somewhere in the range of 97.7% and 99.3% as far as precision utilizing the ANN classifier.

The exactness was the most incredible in case1, case2, and case5, because of the great precision of the highlights framework that seemed to shape these mixes, where the exactness arrives at up to 100 percent, as displayed in the table. The outcomes show that the accompanying cases: case3 and case10 showed less exactness than the other cases. Like different cases, the exactness goes from 96.6 % to 98.8%.In KNN classifier, the precision spans to 100 percent in four cases, which are case1, case2, case4, case5, the fundamental explanation for this results is the blend of elements that came about because of hereditary calculation have the most elevated exactness, while the exactness in both case6 and case 8 didn't surpass 95%, because of the low exactness of the arrangement of highlights that train this classifier.

REFERENCES

[1] L. Hussain, W. Aziz, A. S. Khan, A. Q. Abbasi, and S. Z. Hassan, ''Classification of electroencephalography (EEG) alcoholic and control subjects using machine learning ensemble methods,'' J. Multidisc. Eng. Sci. Technol., vol. 2, no. 1, pp. 126–131, Jan. 2021.

[2] A. Hamad, E. H. Houssein, A. E. Hassanien, and A. A. Fahmy, ''Feature extraction of epilepsy EEG using discrete wavelet transform,'' in Proc. 12th Int. Comput. Eng. Conf. (ICENCO), Dec. 2020, pp. 190–195.

[3] U. R. Acharya, S. Vinitha Sree, G. Swapna, R. J. Martis, and J. S. Suri, ''Automated EEG analysis of epilepsy: A review,'' Knowl.-Based Syst., vol. 45, pp. 147–165, Jun. 2020.

[4] P. Sarma, P. Tripathi, M. P. Sarma, and K. K. Sarma, ''Pre-processing and feature extraction techniques for EEGBCI applications-a review of recent research,'' ADBU J. Eng. Technol., vol. 5, no. 1, pp. 1–8, 2021.

[5] C. Umale, A. Vaidya, S. Shirude, and A. Raut, ''Feature extraction techniques and classification algorithms for EEG signals to detect human stress-a review,'' Int. J. Comput. Appl. Technol. Res., vol. 5, no. 1, pp. 8–14, Jan. 2021.

[6] K. Polat and S. Güneş, ''Artificial immune recognition system with fuzzy resource allocation mechanism classifier, principal component analysis and FFT method based new hybrid automated identification system for classification of EEG signals,'' Expert Syst. Appl., vol. 34, no. 3, pp. 2039–2048, Apr. 2018.

[7] O. Salem, A. Naseem, and A. Mehaoua, ''Epileptic seizure detection from eeg signal using discrete wavelet transform and ant colony classifier,'' in Proc. IEEE Int. Conf. Commun. (ICC), Jun. 2021, pp. 3529–3534.

[8] S. A. Aljawarneh, V. Radhakrishna, and A. Cheruvu, ''VRKSHA: A novel tree structure for time-profiled temporal association mining,'' in Neural Computing and Applications. Cham, Switzerland:

Springer, 2017, pp. 1–29. [Online]. Available: https://link.springer.com/article/ 10.1007%2Fs00521-018-3776-7

[9] S. A. Aljawarneh, R. Vangipuram, V. K. Puligadda, and J. Vinjamuri, ''G-SPAMINE: An approach to discover temporal association patterns and trends in Internet of Things,'' Future Gener. Comput. Syst., vol. 74, pp. 430–443, Sep. 2017.

ugccare.unipune.ac.in

UGC-CARE List

Journal Details

Journal Title (in English Language)	Samriddhi: A Journal of Physical Sciences, Engineering and Technology
Publication Language	English
Publisher	Institute of Technology, School of Management Sciences
ISSN	2229-7111
E-ISSN	2454-5767
Discipline	Science
Subject	Engineering (all)
Focus Subject	Genera
UGC-CARE coverage year	from J Present

Copyright © 2022 Savitribai Phule Pune University. All rights reserved. | Disclaimer

Engineering Failure Analysis 137 (2022) 106161



Contents lists available at ScienceDirect

Engineering Failure Analysis

journal homepage: www.elsevier.com/locate/engfailanal



Development on fatigue testing of hardfaced components in sodium cooled fast reactors



Amruta Pasarkar, S. Balaguru *

VIT Bhopal University, Sehore, Madhya Pradesh 466114, India

ARTICLE INFO

Keywords:
Ni-base alloy
Hardfacing
Cladding
Fatigue
Sodium Cooled Fast Reactor

ABSTRACT

Components in a nuclear reactor like Sodium Cooled Fast Reactor (SFR) are hardfaced with suitable coating material to avoid self-welding of components caused due to liquid metal coolant which acts as a metallic gum. Tensile stresses are observed at interface of base metal and coating due to difference in their coefficients of thermal expansion which leads to thermal fatigue failure at higher operating temperatures. This reduces the bonding strength between surfaces and also cause delamination of coating. Thus, selection of coating materials with good creep and fatigue life for achieving high breeding ratio and high fuel burn up is important. It is thus required to carry out design of SFR hardfaced components considering the fatigue parameters. This paper gives a review on need to study the fatigue characteristics of SFR components along with need for hardfacing of SFR components. This paper also reviews the fatigue testing methods and fatigue behaviour of various hardfaced materials like low carbon low nitrogen stainless steel (SS), low alloy steels, carbon steels, chromium enhanced steels, high strength steels etc. which are used as materials for different SFR component systems. Fatigue behaviour of cladded components for few other applications is also presented.

1. Introduction

Considering the electricity and energy requirement of India, there is a need to use nuclear energy to produce electricity. SFR is one of the fast breeder reactors developed for the proper utilization of these resources. A pressurized water reactor (PWR) can utilize uranium by only 1% but SFR can solve the problem of nuclear waste by using uranium resources by about 70% [1]. Fast-growing nuclear countries in the world have built today 21 sodium cooled fast reactors. Development of safe and robust SFR is a challenge as different domains like advanced materials, design, manufacturing technology etc. need to be rigorously studied [2,3].

Sodium cooled fast reactors have been a new concept over the light water reactors considering its thermal efficiency rise by approximate 40% achieved due to its higher core outlet temperature (~500 °C). It also has 5 times greater core power density. Sodium considered to be much effective heat transfer medium than water as it has a higher boiling temperature of 400 °C. One of the major challenges in design of materials for SFR is performance issues related to creep fatigue rupture of cladding at high burnup which is caused due to Fuel-Cladding Mechanical Interaction (FCMI) [4].

Loop type and Pool type are two SFR configurations. In loop type, intermediate heat exchanger (IHX) is located outside the reactor vessel while in Pool type the IHX is located in the reactor vessel and the primary sodium coolant is kept inside the vessel itself. A double walled piping is required outside the vessel for loop type SFR while larger reactor vessel leads to lesser primary pipe breakage or

* Corresponding author.
E-mail address: balaguruiitm@gmail.com (S. Balaguru).

https://doi.org/10.1016/j.engfailanal.2022.106161
Received 16 November 2021; Received in revised form 14 February 2022; Accepted 14 February 2022
Available online 17 February 2022
1350-6307/© 2022 Elsevier Ltd. All rights reserved.

Table 1
Requirements/Major issues for SFR component systems.

Sr. No.	Component system	Requirements/Functions	Major Issues
1.	Reactor core	Contains the nuclear fuel components and heat is generated by nuclear reactions.	• Core with zero sodium void Effect. • Design to avoid recriticality • design to sustain 500 °C outlet temperature. • Fuel-Cladding Mechanical Interaction.
2.	Core restrain system	• Controls horizontal movements of core assemblies from thermal expansion. • Maintains sufficient clearances to facilitate refuelling.	Design parameters include • Length and stiffness of lower adaptors • Number, location, and configuration of assembly • load pads • Rigidity of peripheral boundary
3.	Reactivity Control and Shutdown System	Brings the reactor from any operating conditions to cold state with the reactive assembly to be inoperative.	• Avoid the uncontrolled increase in core power • To check proper cooling of reactor core.
4.	Reactor Vessel (RV)	• Covers the core and primary heat transport components and is made of austenitic steels. • Placed at the bottom on the core support structure.	• Design to have highest level of reliability to prevent double leakage. • Provision should be provided to retain the coolant level and keep reactor core covered.
5	ReactorGuard vessel (RGV)	In case of seismic or thermal creep failure the guard vessel covers the reactor vessel.	• Design to have highest level of reliability to prevent double leakage. • Provision should be provided to retain the coolant level and keep reactor core covered.
5.	Heat Transport Systems	• Primary heat transfer system (PHTS)—cools the core. • Intermediate heat transfer system (IHTS)—transfers heat from the primary loop to the steam generator. • Both PHTS and IHTS are kept at low pressure since the boiling point of Na is significantly higher than normal operational temperatures.	• Sodium reacts with air and water and gives the need of leak proof system. • Use of double tubes, inert cells, or steel liners. • Opaqueness of sodium leads to maintenance challenges.
6	Energy conversion system (balance of plant)	Generate electricity with a turbine.	Components run at higher temperatures and should have higher energy conversion efficiency.

leakage in pool type SFR. The major component systems in SFR are reactor core, core restrain system, reactivity control and shutdown system, reactor and guard vessel, heat transport systems, energy conversion systems. Requirements and major issues related to these component systems are different and are addressed in Table 1.

Research on materials used for structural components of SFR is highly important for long shelf life at higher temperatures. The core components like cladding tube and hexagonal wrapper are mainly made of 15Cr15Ni2.5MoTi steel (alloy D9) or 304 and 316SS. Out of core components like the reactor vessel ,primary and secondary heat transfer systems are made of austenitic stainless steel 316 L(N) whereas, 9Cr1Mo (G91) ferritic steel is used for steam generator (SG) components [5]. G91 is used because of its low cycle fatigue resistance and high creep. It reduces the problem of sensitization seen in stainless steels. Low alloy steels are used mainly for SG Vessel Wall, turbine rotor, blades and carbon steels can be used for secondary piping [6]. Most of the components in a SFR are made of 316 LN SS due to its higher corrosion resistance and tensile strength property [7]. 316 LN SS is more vulnerable to self-welding at higher temperature and thus hardfacing is done for SFR components as a solution to avoid self-welding [8]. The material deposited is harder than that of substrate, thus the process is called as hardfacing [9]. It is done by methods like Plasma Transferred Arc (PTA), Shielded Metal Arc Welding (SMAW), Gas Tungsten Arc (GTA), Laser processing and High Velocity Oxygen Fuel coating (HVOF). The most used hardfacing materials are Ni based alloys, Co-based alloys and FE based alloys. Hardness of Ni based alloys is comparatively higher than that of Stellite i.e., Co-based alloys. As Ni-based alloys maintains its hardness at elevated temperatures, colmonoy5 which is Ni-Cr-B-Si alloy is usually used as cladding material for components in SFR [10]. Due to the difference in thermal expansion coefficient of the coating and base metal, thermal fatigue failure can occur at the surface which leads to delamination of coating.

Fatigue damage is found to be one of the major reasons for sudden breakdown of nuclear reactors. In Japan manufactured nuclear reactor Tsuruga-2 fatigue cracks were found in the connecting pipe due to coolant mixing at higher and lower temperatures. In BN 600 reactor, sodium coolant leakage was observed due to thermal fatigue caused by fluctuating mixing of hot and cold sodium. The IHX of BN-600 reactor showed fatigue damage on its shell joint [11]. Considering these examples, it is observed that design of nuclear reactors for fatigue damage is of utmost importance. Thus, research on materials with good creep and fatigue life for achieving high breeding ratio and high fuel burn up is of great need. Selection of reactor materials and coating needs to be done very critically considering the fatigue parameters for longer shelf life at higher temperature.

Hardfacing influences the fatigue and tensile properties of substrate [12]. Fatigue failure is an important factor that contribute to

Table 1
Requirements/Major issues for SFR component systems.

Sr. No.	Component system	Requirements/Functions	Major Issues
1.	Reactor core	Contains the nuclear fuel components and heat is generated by nuclear reactions.	• Core with zero sodium void Effect. • Design to avoid recriticality • design to sustain 500 °C outlet temperature. • Fuel-Cladding Mechanical Interaction.
2.	Core restrain system	• Controls horizontal movements of core assemblies from thermal expansion. • Maintains sufficient clearances to facilitate refuelling.	Design parameters include • Length and stiffness of lower adaptors • Number, location, and configuration of assembly • load pads • Rigidity of peripheral boundary
3.	Reactivity Control and Shutdown System	Brings the reactor from any operating conditions to cold state with the reactive assembly to be inoperative.	• Avoid the uncontrolled increase in core power • To check proper cooling of reactor core.
4.	Reactor Vessel (RV)	• Covers the core and primary heat transport components and is made of austenitic steels. • Placed at the bottom on the core support structure.	• Design to have highest level of reliability to prevent double leakage. • Provision should be provided to retain the coolant level and keep reactor core covered.
5	ReactorGuard vessel (RGV)	In case of seismic or thermal creep failure the guard vessel covers the reactor vessel.	• Design to have highest level of reliability to prevent double leakage. • Provision should be provided to retain the coolant level and keep reactor core covered.
5.	Heat Transport Systems	• Primary heat transfer system (PHTS)—cools the core. • Intermediate heat transfer system (IHTS)—transfers heat from the primary loop to the steam generator. • Both PHTS and IHTS are kept at low pressure since the boiling point of Na is significantly higher than normal operational temperatures.	• Sodium reacts with air and water and gives the need of leak proof system. • Use of double tubes, inert cells, or steel liners. • Opaqueness of sodium leads to maintenance challenges.
6	Energy conversion system (balance of plant)	Generate electricity with a turbine.	Components run at higher temperatures and should have higher energy conversion efficiency.

leakage in pool type SFR. The major component systems in SFR are reactor core, core restrain system, reactivity control and shutdown system, reactor and guard vessel, heat transport systems, energy conversion systems. Requirements and major issues related to these component systems are different and are addressed in Table 1.

Research on materials used for structural components of SFR is highly important for long shelf life at higher temperatures. The core components like cladding tube and hexagonal wrapper are mainly made of 15Cr15Ni2.5MoTi steel (alloy D9) or 304 and 316SS. Out of core components like the reactor vessel ,primary and secondary heat transfer systems are made of austenitic stainless steel 316 L(N) whereas, 9Cr1Mo (G91) ferritic steel is used for steam generator (SG) components [5]. G91 is used because of its low cycle fatigue resistance and high creep. It reduces the problem of sensitization seen in stainless steels. Low alloy steels are used mainly for SG Vessel Wall, turbine rotor, blades and carbon steels can be used for secondary piping [6]. Most of the components in a SFR are made of 316 LN SS due to its higher corrosion resistance and tensile strength property [7]. 316 LN SS is more vulnerable to self-welding at higher temperature and thus hardfacing is done for SFR components as a solution to avoid self-welding [8]. The material deposited is harder than that of substrate, thus the process is called as hardfacing [9]. It is done by methods like Plasma Transferred Arc (PTA), Shielded Metal Arc Welding (SMAW), Gas Tungsten Arc (GTA), Laser processing and High Velocity Oxygen Fuel coating (HVOF). The most used hardfacing materials are Ni based alloys, Co-based alloys and FE based alloys. Hardness of Ni based alloys is comparatively higher than that of Stellite i.e., Co-based alloys. As Ni-based alloys maintains its hardness at elevated temperatures, colmonoy5 which is Ni-Cr-B-Si alloy is usually used as cladding material for components in SFR [10]. Due to the difference in thermal expansion coefficient of the coating and base metal, thermal fatigue failure can occur at the surface which leads to delamination of coating.

Fatigue damage is found to be one of the major reasons for sudden breakdown of nuclear reactors. In Japan manufactured nuclear reactor Tsuruga-2 fatigue cracks were found in the connecting pipe due to coolant mixing at higher and lower temperatures. In BN 600 reactor, sodium coolant leakage was observed due to thermal fatigue caused by fluctuating mixing of hot and cold sodium. The IHX of BN-600 reactor showed fatigue damage on its shell joint [11]. Considering these examples, it is observed that design of nuclear reactors for fatigue damage is of utmost importance. Thus, research on materials with good creep and fatigue life for achieving high breeding ratio and high fuel burn up is of great need. Selection of reactor materials and coating needs to be done very critically considering the fatigue parameters for longer shelf life at higher temperature.

Hardfacing influences the fatigue and tensile properties of substrate [12]. Fatigue failure is an important factor that contribute to

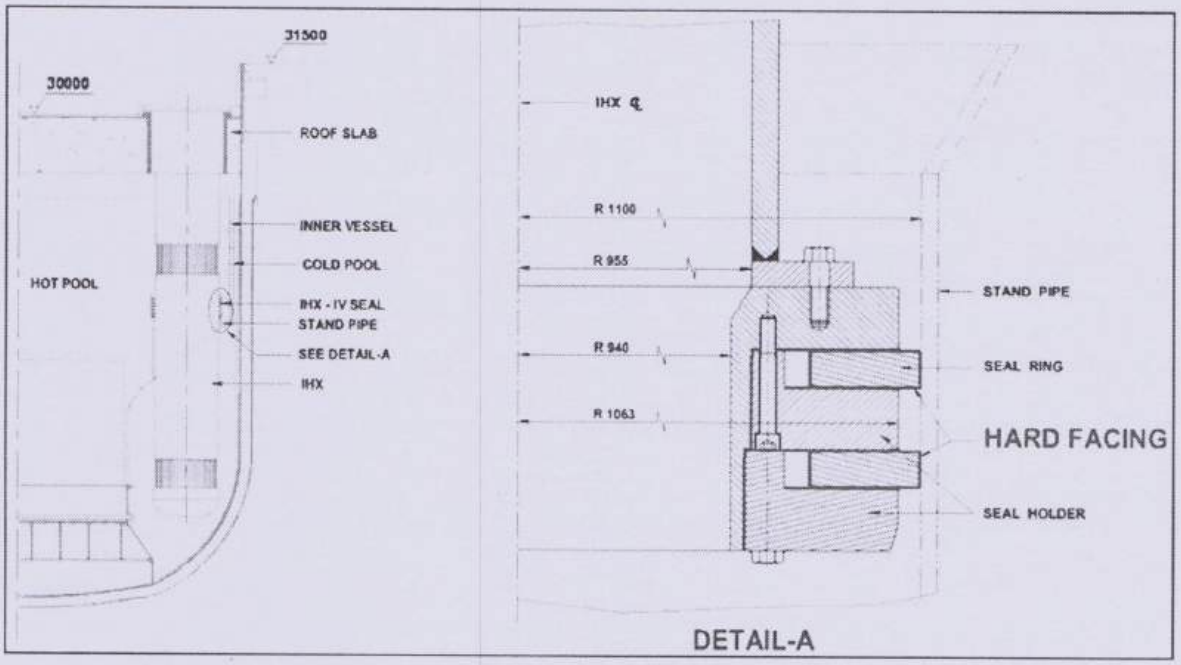


Fig. 3. Hardfaced seal assembly in nuclear reactor [25].

the material and its consequent decrease is due to reduced ductility of 316LN SS. Fig. 1 shows impact of nitrogen percentage on fatigue life of 316LN SS at different temperatures. It is observed that the fatigue crack opening is along slip bands and crack propagation is trans granular. Thus, the author concludes that,0.14 wt% of nitrogen is the best possible nitrogen content for 316LN SS for SFR components.

Baldev Raj et.al(2010) [14] performed low cycle fatigue tests for out of core components of SFR . The outcomes of low cycle fatigue tests show decline in fatigue life with decrease in strain rate for temperature of 773, 823 and 873 K. The decrease in fatigue life is because of dynamic strain ageing and cyclic hardening in the base metal. Also, the weld joint show metal of 316LN SS show lower fatigue life than base metal and weld metal shows higher fatigue life than base metal. Fig. 2 (a) shows the fatigue life at different temperatures with respect to strain rate and Fig. 2 (b) shows the strain life curve for base metal, weld joint and weld metal in out of core components.

Yukio Takahashi et.al (2008) [15] tested the specimen of 316FR stainless steel under creep fatigue conditions, using cruciform specimens for biaxial loading conditions. He studied the result of multiaxial stress on fatigue failure. The tests were taken for long time of 35,00 h and at temperatures of 550 °C and 600 °C. The creep fatigue life cycles decreased for increase in hold time for same strain range. Fatigue life of 316FR in sodium is longer as compared to air and it shows trans granular fracture mode for both the mediums [16]. Another work studied the effect of sodium on 304 and 316SS at 550 °C on low cycle fatigue behaviour [17]. Fatigue life of 316SS is greater in sodium than in the air whereas that of 304SS is approximately same for both environments. The fatigue life was also determined after thermally aging 304SS in 550 °C argon for 5000 h.The life of thermally aged material in sodium is more than the previous 304SS specimen. M.D.Mathew et.al [18] studied the effect of low cycle fatigue on SFR materials in air and sodium. The results show that the fatigue life in sodium is higher than in the air. Tai Asayama et.al [19,20] developed a fatigue testing model for Japan Sodium Cooled Fast Reactor (JSFR).They designed the SFR for 60 reactor years. They introduced new favourable materials for SFR i.e., 316FR and 9CrMo steel.

3. Importance of hardfacing in sodium cooled fast reactor components.

Use of liquid sodium SFR lead to removal of oxide film on the metal surfaces and open up the base metal surfaces. These components are in constant connection with each other and also have relative motion between them at the time of operation which causes higher contact stresses and results in self welding and fatigue loading at surfaces at higher temperatures. 316LN SS is more vulnerable to self-welding at higher temperature. Hardfacing is thus widely used for SFR components as a solution to avoid self-welding [21]. Indira Gandhi Centre for Atomic Research (IGCAR) has faced many challenges to design a robust material considering shielding wear and corrosion characteristics of materials at high temperatures. As Ni-based alloys maintains its hardness property at higher temperatures, colmonoy is used in nuclear reactor components for hardfacing [22]. Another challenge in hardfacing is to decide upon proper hardfacing process considering the dilution of base metals. PTA process is considered as most versatile process for hardfacing as width of dilution can be maintained at very lower range as 0.2 mm [23,24].

A work of [25] developed a procedure for hardfacing on the seal rings. The author said that the hardfacing on forged material seal

Table 2
Summary of papers referred for Laser Cladding Process.

Sources	Substrate/Reactor component system	Cladding Material	Type of Fatigue Specimen	Fatigue Tests Specifications	Significant Findings
[12]	X5CrNi18-10 (reactor core, fuel cladding) 42CrMo4(SG system)	Stellite 21	Round Specimen	Testing method: Four-Point Bending Fatigue testingFrequency: 66 ± 1 HzR Ratio: −1The tests were stopped after 10 million load cycles and this value was considered as endurance limit	The fatigue strength of the 42CrMo4 substrate specimens is considerably lower than steel X5CrNi18-10. X5CrNi18-10 specimen cracked at surface whereas crack initiation took place underneath the surface for 42CrMo4 specimens. Hardfacing of stellite 21 on 42CrMo4 and X5CrNi18-10 decreases fatigue strength.
[43]	316L SS(RV, RGV, PHTS)	Stellite 21	Round Specimen a. Cladding of Stellite 21 on SS b. Variation in composition across substrate/clad interface.	Testing method: Rotating-Bending fatigue testsAlternating Stress levels: 200–300 MPa	For both the conditions direct cladding and graded cladding, the fatigue failure initiated at the wrought SS portion of gauge area. All the specimens failed at similar number of loading cycles. Thus, the author says that the substrate SS part was the weakest area for fatigue crack to initiate. The ferrous zones showed plastic deformation and whereas cobalt zones showed brittle deformation.
[44]	X5CrNi18-10 (reactor core, fuel cladding) 42CrMo4(SG system)	Stellite 21	Round Specimen	Residual Stresses are found by Neutron Diffraction method	Residual stresses are important for the effect of fatigue properties after laser cladding.
[45]	S355-low alloy steel(SG Vessel Wall, turbine rotor, blades) 42CrMo4(SG system)	Co-base powder (Stellite 21) and Ni-base powder (Inconel 625)	Round Specimen	Testing method: Four-Point bending Fatigue testing	Fatigue failure depends on maximum stress concentrators caused due to macro load conditions and stress raisers at defects. Laser clad defects can be summarized into three types 0D-pores/ inclusions, 1D-clad waviness or 2D-planar cracks. To increase the fatigue life of laser cladded bars the stress concentrated areas should be avoided.
[47]	AISI 4130 steel (SG Vessel Wall, turbine rotor, blades)	Stellite 6 and Deloro 40G	Round Specimen	Testing method: Cantilever type rotary bending	The test results predicted that the coated specimens by stellite6 and Deloro 40G showed lower fatigue life as compared to unclad specimen. Due to lower tensile stresses in stellite 6, fatigue life is higher in these specimens for same load.
[48]	42CrMo4/S355 (SG Vessel Wall, turbine rotor, blades)	Inconel 625/ Stellite 21	Round Specimen	Testing method: Four-point bending testsTensile-Tensile Load: 75 to 160 kN. R Ratio: 0	Fatigue life of unclad S355 is higher than that of laser clad S355. The decrease in fatigue life for laser clad specimen is due to higher residual tensile stress and cladding defects. However, In625/42CrMo4 improved fatigue life at higher loads

(continued on next page)

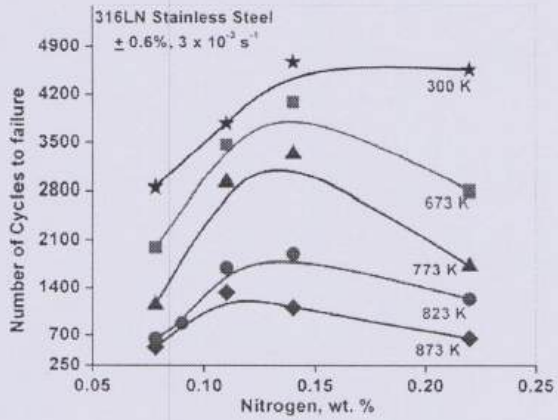


Fig. 1. Impact of nitrogen percentage on fatigue life of 316LN stainless steel at different temperatures [13].

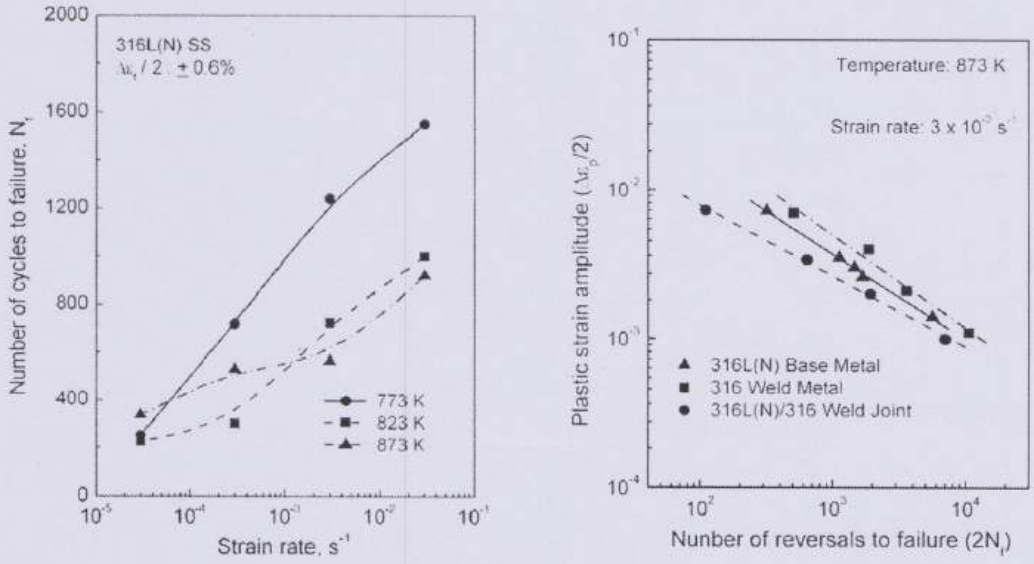


Fig. 2. (a) Fatigue life at different temperatures with respect to strain rate. (b) Strain life curve for base metal , weld joint and weld metal in out of core components [14].

80% of the mechanical losses. Most of the time many specimens need to be tested to generate the S-N curves which gives appropriate results about the fatigue behaviour. This paper gives an extensive understanding on three aspects, first, development of fatigue testing in sodium cooled fast reactor components, second, requirement of hardfacing for nuclear reactor components and third, the fatigue testing methods and fatigue behaviour of various hardfaced materials like low carbon low nitrogen SS, low alloy steels, carbon steels, chromium enhanced steels, high strength steels etc. which are used as materials for different SFR component systems. Fatigue behaviour of cladded components for few other applications is also presented. The review can give a depth idea on how to consider different methods for fatigue testing of hardfaced nuclear reactor components which can be helpful for future research. The hardfaced specimens are categorized into two types, rectangular and circular cross section according to ASTM standards. The type of fatigue test to be conducted depends on the specimen and its applications.

2. Development of fatigue testing in sodium cooled fast reactor components

In sodium cooled fast reactors, designed for 40 years of life, 316LN SS is preferably used for components operating at temperature above 700 K. For more robust behaviour of these components at higher temperature, low cycle fatigue tests are important to develop optimum material with optimum nitrogen percentage between 0.07 and 0.22 wt.%N. On this background, A.K. Bhaduri et.al (2015) [13] performed low cycle fatigue tests to study the effect of nitrogen percentage on fatigue behaviour of 316LN SS. The nitrogen ratio of 0.07 ,0.14 and 0.22 wt% was considered keeping all other parameters unchanged. The results showed that the fatigue life increases with increase in nitrogen ratio till 0.14 wt% beyond which it decreases. The increase in fatigue lifecycle is due to less slip localisation in

Table 2 (*continued*)

Sources	Substrate/Reactor component system	Cladding Material	Type of Fatigue Specimen	Fatigue Tests Specifications	Significant Findings
[57]	42CrMo4(SG system)	Stellite 21	Flat specimen	Testing Method- Cyclic Fatigue testing	and Lot 4 samples showed intergranular cracks. The fatigue strength for cladded specimen decreased than the uncladded specimen. Origins of cracks were seen at the cladded areas and at fillets on crankshaft.
[58]	AISI 4340(SG Vessel Wall, turbine rotor, blades)	AISI 4340and AerMet 100 steel powder	Flat specimenFour conditions were considered: AISI 4340 as-clad, AerMet 100, AISI 4340 as-clad (PCHT) and AerMet 100 (PCHT).	Testing method: Axial constant amplitude fatigue testing R ratio: 0.1 Frequency: 10 Hz	Use of Aermet100 clad layer improves fatigue properties of specimen as compared to as-clad AISI4340 steel. PCHT specimens shows increase in fatigue resistance and fatigue life as compared to without post heat treatment.
[59]	AISI 4340(SG Vessel Wall, turbine rotor, blades)	AISI 4340 Powder	Flat specimen	Testing method: Axial testingAlternating Stress levels: 290–650 MPaFrequency: 15 HzR Ratio: 0	Stress intensity factor and magnification factor is required to find out for predicting the fatigue crack growth. Finite element model was modelled for a range of crack depth and crack shape ratios. The predicted fatigue life was similar to experimental results.
[60]	AISI 4340 steels (SG Vessel Wall, turbine rotor, blades)	AISI 4340 steel powder	Flat specimenCategory I specimen is as-clad specimenCategory II specimen is a grooved specimen later filled with clad material Category III specimen is that the clad region is extended beyond the gage section of the fatigue test specimen.	Testing method: Axial testingR ratio: 0 Frequency: 15 Hz	There is decrease in fatigue strength for category I specimen as compared to substrate specimen. This reduction is due to large cracks initiating at the clad toe region. The fatigue strength for category II specimen is little closer to substrate specimen Fatigue failure occurred at clad material and groove intersection region. Fatigue strength of category III specimen is higher as compared to all other specimens.
[61]	EA4T steel -low alloy steel(SG Vessel Wall, turbine rotor, blades)	kf311 ferrous metal powder	Flat specimen	Testing method: Three-point bending testsApplied load- 4.8 kNFrequency: 10 HzR Ratio: 0.1	Thus, due to higher fracture strength and higher stress intensity factor threshold value, the fatigue crack growth rate is lower for cladded specimen than the base specimen. Thus, it is said that fatigue life is increased by laser cladding of kf311 ferrous metal powder.

4. Fatigue testing specimens

It is required to perform research to develop optimized materials of hardfaced reactor components considering the fatigue parameters. This review will give a critical understanding of methods for fatigue testing of hardfaced specimens which can be useful for researchers to design a methodology for robust testing of nuclear reactor components.

Broadly two fatigue testing specimens are prepared according to ASTM-E466. Cylindrical or flat dog bone specimens are generated for fatigue testing according to the applications and ASTM standards. A review is done in this study to identify various methods to

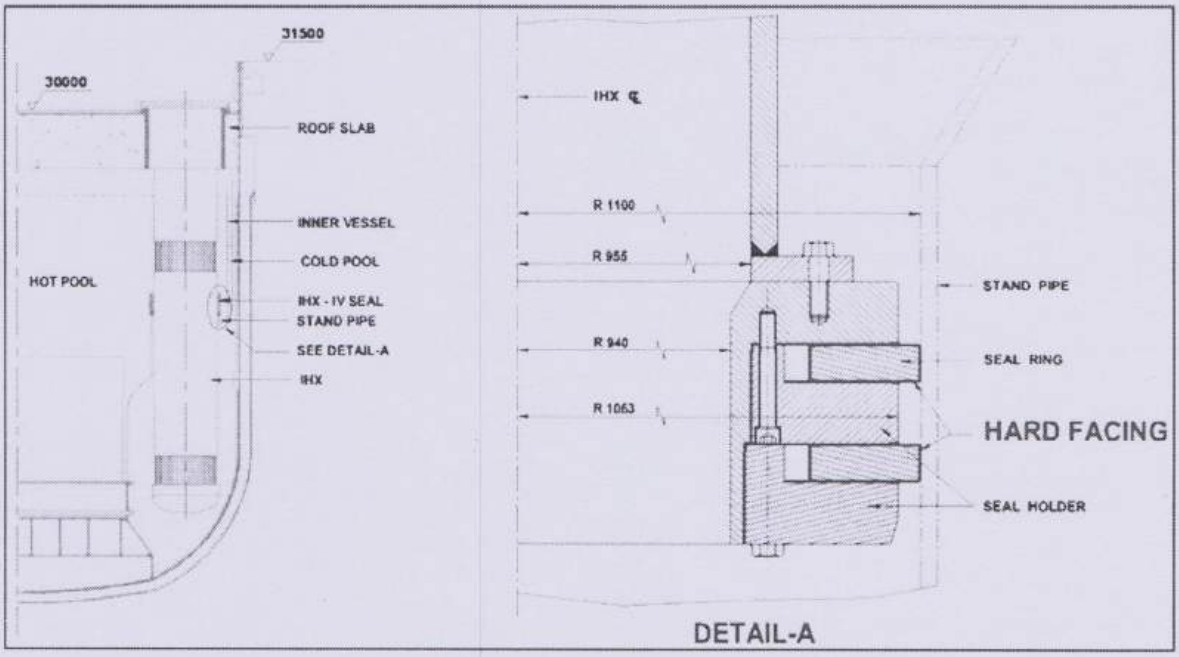


Fig. 3. Hardfaced seal assembly in nuclear reactor [25].

the material and its consequent decrease is due to reduced ductility of 316LN SS. Fig. 1 shows impact of nitrogen percentage on fatigue life of 316LN SS at different temperatures. It is observed that the fatigue crack opening is along slip bands and crack propagation is trans granular. Thus, the author concludes that,0.14 wt% of nitrogen is the best possible nitrogen content for 316LN SS for SFR components.

Baldev Raj et.al(2010) [14] performed low cycle fatigue tests for out of core components of SFR . The outcomes of low cycle fatigue tests show decline in fatigue life with decrease in strain rate for temperature of 773, 823 and 873 K. The decrease in fatigue life is because of dynamic strain ageing and cyclic hardening in the base metal. Also, the weld joint show metal of 316LN SS show lower fatigue life than base metal and weld metal shows higher fatigue life than base metal. Fig. 2 (a) shows the fatigue life at different temperatures with respect to strain rate and Fig. 2 (b) shows the strain life curve for base metal, weld joint and weld metal in out of core components.

Yukio Takahashi et.al (2008) [15] tested the specimen of 316FR stainless steel under creep fatigue conditions, using cruciform specimens for biaxial loading conditions. He studied the result of multiaxial stress on fatigue failure. The tests were taken for long time of 35,00 h and at temperatures of 550 °C and 600 °C. The creep fatigue life cycles decreased for increase in hold time for same strain range. Fatigue life of 316FR in sodium is longer as compared to air and it shows trans granular fracture mode for both the mediums [16]. Another work studied the effect of sodium on 304 and 316SS at 550 °C on low cycle fatigue behaviour [17]. Fatigue life of 316SS is greater in sodium than in the air whereas that of 304SS is approximately same for both environments. The fatigue life was also determined after thermally aging 304SS in 550 °C argon for 5000 h.The life of thermally aged material in sodium is more than the previous 304SS specimen. M.D.Mathew et.al [18] studied the effect of low cycle fatigue on SFR materials in air and sodium. The results show that the fatigue life in sodium is higher than in the air. Tai Asayama et.al [19,20] developed a fatigue testing model for Japan Sodium Cooled Fast Reactor (JSFR).They designed the SFR for 60 reactor years. They introduced new favourable materials for SFR i.e., 316FR and 9CrMo steel.

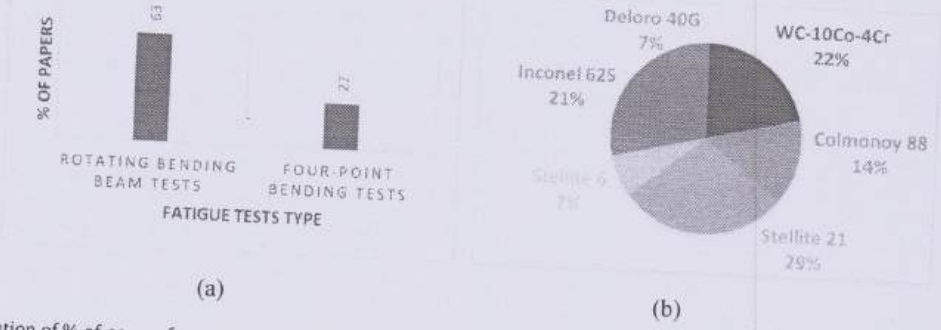
3. Importance of hardfacing in sodium cooled fast reactor components.

Use of liquid sodium SFR lead to removal of oxide film on the metal surfaces and open up the base metal surfaces. These components are in constant connection with each other and also have relative motion between them at the time of operation which causes higher contact stresses and results in self welding and fatigue loading at surfaces at higher temperatures. 316LN SS is more vulnerable to self-welding at higher temperature. Hardfacing is thus widely used for SFR components as a solution to avoid self-welding [21]. Indira Gandhi Centre for Atomic Research (IGCAR) has faced many challenges to design a robust material considering shielding wear and corrosion characteristics of materials at high temperatures. As Ni-based alloys maintains its hardness property at higher temperatures, colmonoy is used in nuclear reactor components for hardfacing [22]. Another challenge in hardfacing is to decide upon proper hardfacing process considering the dilution of base metals. PTA process is considered as most versatile process for hardfacing as width of dilution can be maintained at very lower range as 0.2 mm [23,24].

A work of [25] developed a procedure for hardfacing on the seal rings. The author said that the hardfacing on forged material seal

Table 4
Summary of papers referred for SMAW Process.

Sources	Substrate/ Reactor component system	Cladding Material	Type of Fatigue Specimen	Fatigue Tests Specifications	Significant Findings
[40]	Heat resistant cast steel (other applications)	Two filler materials i.e. soft filler material and heat resistant filler material	SMAW process	Testing method: Low cycle fatigue testing Testing temperatures: 750 and 920 °C Strain rate: 10^{-4} s^{-1}	The fatigue life of heat resistant cast steels is reduced due to welding. This can be attributed to presence of stress concentration close to interface with weld zone. For buttered samples the fatigue life reduced drastically because of tri axial stresses caused that leads to plastic strain of soft buttering layer that causes cracking.
[50]	304L SS (RV, RGV, PHTS)	Inconel 625	SMAW process specimens is prepared of 10% Inconel 625 and 15% Inconel 625, the remaining being the base	Testing method: Rotating-Bending fatigue tests Alternating Stress levels: 226.85 MPa.	Specimens comprising the higher clad content showed more fatigue strength than the specimen with lower clad content. The specimens with a 15% clad content showed higher fatigue strength than the specimens with 10% clad content. The substrate AISI 304L SS gives the least fatigue strength.



(a) (b)

Fig. 5. (a) Distribution of % of papers for rotating bending beam testing and four-point bending testing. (b) Distribution of % of papers on different cladding materials.

detect the fatigue behaviour and fatigue curve of hardfaced specimens of different types.

Most of the research on fatigue behaviour of hardfaced components till date is done to find out the fatigue properties of laser cladded specimens. Fig. 4 (a) shows the % of papers referred in this section for fatigue testing of specimens prepared by various cladding processes. The figures are generated considering the literature reviewed by the author in this section related to hardfacing and fatigue. Total 24 literature papers out of which 16 of laser cladding process, 6 of HVOF process and 2 of SMAW process are reviewed in this section. The other cladding process are not considered for review under this section. Fig. 4 (b) shows the % of papers referred in this section from 2001 to 2010 and 2011 to 2020. Table 2-4 shows the summary of papers referred for Laser cladding process, HVOF Thermal Spray process and SMAW process. The table specifies the substrate material and the reactor component system related to each substrate [6].

4.1. Fatigue testing of cylindrical hardfaced specimens

For the fatigue testing of cylindrical specimens, mostly rotating bending beam or four-point bending test is performed. The various technologies used for hardfacing in different literatures are Laser Cladding process, HVOF Process and SMAW process. From this. maximum paper reviewed have worked on laser cladding processed specimens. Total 11 number of papers are referred under this section of which 3 are of four point bending test and 8 are of rotating bending test. Fig. 5(a) shows the % of papers referred under this section for rotating bending beam testing and four-point bending testing. Fig. 5(b) shows % of papers referred under this section on different cladding materials.

C.J. Villalobos-Gutiérrez et al. (2008) [39] investigated the fatigue performance of AA6063T6 aluminium alloy coated with WC10Co4Cr by HVOF thermal spraying. Fatigue analysis using rotating beam machine was carried out in air and in 3% NaCl solution at stresses ranging from of 118–177 MPa and 50 Hz frequency. There is significant increase in fatigue resistance for coated specimen as compared to uncoated specimen. Rise in fatigue resistance (4300%) is more substantial at lower alternating stresses than maximum alternating stresses (540%). Also, in the NaCl solution, the rise in fatigue properties at low stresses is of around 1460%, whereas at higher stress it is of around 620%. Fatigue cracks initiated at the surface and then propagated towards the substrate.



Fig. 4. (a) Distribution of % of papers referred for fatigue testing of specimens under various cladding processes. (b) Distribution of % of papers referred from 2001 to 2010 and 2011 to 2020.

ring decreases amount of distortion. By controlling pre heat temperatures, deposition process, coating thickness and amount of deposition, a defect free and robust coating is possible on 316LN SS base metal. Hardfacing was done by using colmonoy 5 material which is a good substitute for cobalt-based alloys using PTA process. It is very challenging for deposition of colmonoy on 316LN SS due to different coefficient of thermal expansion which lead to residual stresses. Fig. 3 shows the seal assembly in nuclear reactor.

Sreedhar et al. (2015) [26] predicted that the corrosion resistance is increased for colmonoy 5 hardfaced on 316LN SS. Therefore, there are less chances of damage to the SFR hardfaced components. Kumar et al. (2017) [27] explored the wear behaviour of colmonoy alloy coatings on 316LN SS at higher temperatures. The hardfacing is done by GTA process. The results show that as contact increases, the wear rate increases. At high contact stress of 40 MPa, high damages were detected. In 1980 s, a study was conducted to find out preferrable coating materials for SFR components. The research said that the chromium carbide coatings with Inconel binder, Nickel aluminide surface coating materials and Tribaloy 700 which is cobalt free materials can be best used on 316 SS for SFR components. These coatings successfully reduced the self-welding and improved corrosion resistance during testing process in a higher temperature environment similar to SFR [28–30]. A research study proposed adding iron content in the tribaloy700 material during laser cladding of surfaces. Optimized amount of iron to be added is studied in this research. The addition of iron affects the wear property of material. Excessive iron leads to reduction in the wear resistant of tribaloy700 [31].

Zhang et al. (2010) [32] conducted laser cladding of colmonoy 6 material on 316 L stainless steel for nuclear applications. This increased the wear resistance of specimen by 53%. Author says that if the specimen is heated to 450 °C and then cooled gradually, cracking in the coating will be prevented. Use of Deloro 50 on 304 Stainless steel reduces wear at higher temperatures of around 200 °C and contact stress of 207 MPa. This is attributed to oxide layers formed at surfaces at higher temperatures. Research also says that Deloro 50 can be effectively used as hardfacing material in nuclear components [33]. Stellite 6 which is a Co-based alloy can also be used for hardfacing nuclear reactors flow control valves [34].

D. Kesavan et.al. (2010) [35] suggested that the environmental temperatures has a major effect on wear resistance of hardfaced components.316 LN stainless steel is coated with colmonoy 5 using PTA process. It was observed that at 873 °C highest wear resistance was attained. Also, hardness of coated specimen improved 2.5 times than base material due to formation of complex borides and carbides in coating.

Balaguru et. al. (2012) [36] developed a finite element model to find out the residual stresses in hardfaced circular grid plate of 304 SS cladded with colmonoy material. Mechanical and thermal analysis is done on the model using element birth and death technique. The tensile residual stresses are decreased by 12.3% as the welding speed increases. Whereas there is a substantial increase in compressive residual stress. The author suggest that substrate cladding interface will have good bonding at higher compressive residual stresses.

S. Balaguru et.al. (2016) [37] developed an elastoplastic model for measuring the residual stresses formed due to thermal cycling in sodium cooled fast reactors. Thermal cycling occurs in the SFR due to variations in the thermal expansions of coating and substrate material. Residual stresses are observed at three temperatures of 200 °C, 400 °C and 550 °C. The results show that in the circumferential direction, compressive residual stresses are formed in the coating and tensile residual stresses are formed at the base metal. In radial direction, compressive residual stress is formed in both coating and base metal. The computed numerical value of residual stress differs by 11 to 12 % from experimental value for both coating and base metal.

Balaguru et al. (2017) [38] tested specimen of 316 LN SS hardfaced with colmonoy material for its tensile properties at higher temperatures. Plasma transferred process was used for hardfacing. The substrate acts tensile load on the coating when specimen is subjected to higher temperatures. As the temperature increases, specimen becomes ductile at around 200 °C and material softening occurs. At 400 °C, the ultimate tensile strength of hardfaced specimen is measured 80% of that at the room temperature and at 550 °C it is measured 76% of that at the room temperature. Although there is reduction in the yield stress, it is more than the base metal at any operating temperatures. Thus, it can be concluded that the hardfacing with colmonoy on stainless steel is optimum considering the tensile properties at higher temperatures.

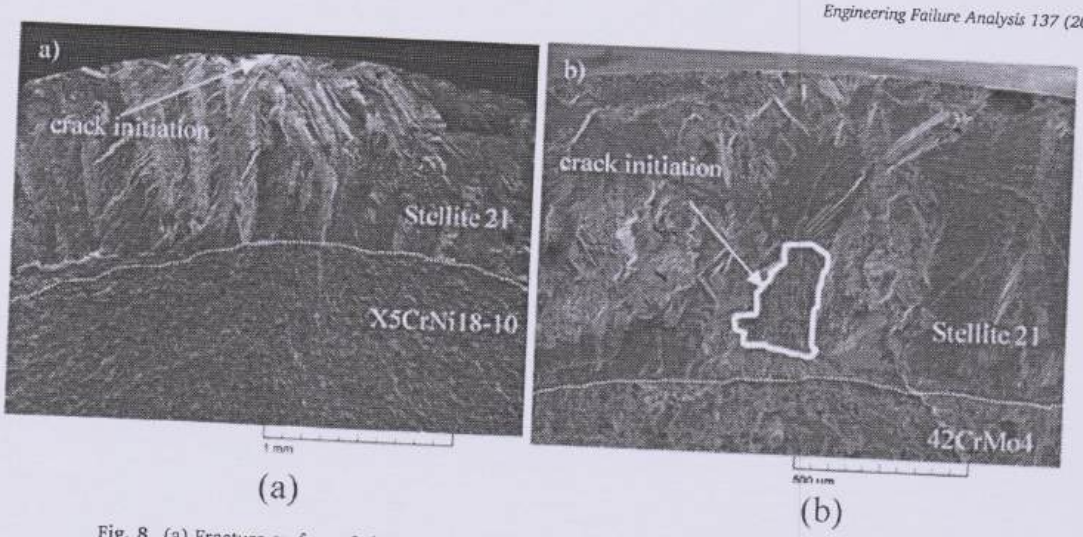


Fig. 8. (a) Fracture surface of cladded X5CrNi18-10. (b) Fracture surface of cladded 42CrMo4 [44].

deformation and whereas cobalt rich zones showed brittle deformation.

H. Koehler et al. (2012) [12] predicted the optimal process to find out the fatigue parameters and crack initiations. Stellite 21 is coated with laser cladding on two substrate material viz. austenitic steel and the hardened and tempered steel 42CrMo4. Specimens were prepared according to ASTM standards for four-point bending fatigue tests. Fatigue tests were performed at stress ratio −1 and 0 at frequency of f = 66 ± 1 Hz. The tests were suspended after 10 million load cycles and this value was considered as endurance limit. The experimental and FEA results predict that the fatigue limit of stellite 21 depends on core material. Concept of Local Fatigue Strength and Advanced Weakest-Link Concept was used to find out the residual stresses and results were compared. Fatigue strength of the 42CrMo4 substrate specimens is considerably lower than steel X5CrNi18-10. X5CrNi18-10 specimen cracked at surface whereas crack initiation took place underneath the surface for 42CrMo4 specimens.

Henry Köhler et al. (2012) [44] predicted the result of residual stress on fatigue life of cladded components. Four types of specimens were considered by the author viz. X5CrNi18-10 as substrate, X5CrNi18-10 substrate laser cladded with Stellite 21 and ground, 42CrMo4 substrate and 42CrMo4 substrate laser cladded with Stellite 21 and ground. Residual stress was found by neutron diffraction method and for the investigation round specimens were used. X5CrNi18-10 base material show high compressive residual stresses at the surface as compared to the core part as shown in Fig. 6(a). However, the cladded X5CrNi18-10 shows residual stress compressive in nature at the cladding interface as shown in Fig. 6(b). The 42CrMo4 base specimen show higher residual stress compressive in nature at the surface as shown in Fig. 7(a). However, the cladded 42CrMo4 specimen shows better tensile residual stresses at the cladding interface Fig. 7(b). These results also corelated with fatigue test results predicted in [5,24]. Cladded X5CrNi18-10 specimen cracked at the surfaces and cladded 42CrMo4 specimens cracked at cladding interface as shown in Fig. 8(a) and (b). Fatigue properties of cladded 42CrMo4 specimen decreases significantly and it shows that the residual stress after cladding plays an important role for change in fatigue properties.

M.M. Alam et al. (2013) [45] studied the fatigue failure of square and cylindrical cross section bars using four different fatigue loading conditions. Finite element analysis is used to carry out the results. Stellite 21 which is Co-base powder and Inconel 625 which is Ni-base powder were laser cladded on S355 steel bars and on 42CrMo4 steel respectively. Fatigue failure depends on maximum stress concentrators caused due to macro load conditions and stress raisers at defects. At wavy laser clad surface, notches raise the stress field at smaller notch radius and angles. Planar defects like lack of fusion and hot cracks are considered as crack initiators. To increase the fatigue life of laser clad bars the stress concentrators should be avoided.

J.G. La Barbera-Sosa et al. (2013) [46] carried out research to study the fatigue properties of SAE 4340 steel, coated with a 50% WC10Co4Cr/50% Colmonoy 88 by HVOF thermal spray. The authors considered the test at cyclic stress varying from 410 MPa to 470 MPa at frequency 50 Hz. The relationship of cycles to fatigue failure and alternating stress is described by Stromeyer equation and by Wöhler curve. The Wöhler curve shows that the coated specimen curve is below the steel substrate curve which means that there is fatigue limit debit of 33% and fatigue strength by 30% for coated specimen. If the curve is corrected for diameter, then the fatigue limit for coated specimen is decreased by 25%. Stress concentration at substrate coating interface and coating material properties lead to reduction in fatigue properties. Initiation of crack occurred at outer surface of coating and interface of substrate coating. Presence of alumina particles at the interface causes stress concentration and cracks at substrate coating interface.

Hutasoit et al. (2015) [47] did a research to test the fatigue behaviour of stellite6 and Deloro 40G alloys hardfaced on AISI4130 steel by laser cladding process. Fatigue specimens of Deloro 40 G alloy coating was prepared for coating thickness 1.82, 1.58 and 1.3 mm and fatigue specimens of Stellite 6 was prepared for coating thickness 1.46, 1.29 and 1.06 mm. Also uncoated substrate specimen was considered. Tests were carried out on cantilever type rotary bending machine for loads of 100, 150, 200 N. Load ratio considered is 1. The test results predicted that the coated specimens by stellite6 and Deloro 40G showed lower fatigue life as compared to unclad specimen. This is said to be because of occurrence of residual stress tensile in nature in coating area. Stellite 6 which is cobalt

Table 2
Summary of papers referred for Laser Cladding Process.

Sources	Substrate/Reactor component system	Cladding Material	Type of Fatigue Specimen	Fatigue Tests Specifications	Significant Findings
[12]	X5CrNi18-10 (reactor core, fuel cladding) 42CrMo4(SG system)	Stellite 21	Round Specimen	Testing method: Four-Point Bending Fatigue testingFrequency: 66 ± 1 HzR Ratio: −1The tests were stopped after 10 million load cycles and this value was considered as endurance limit	The fatigue strength of the 42CrMo4 substrate specimens is considerably lower than steel X5CrNi18-10. X5CrNi18-10 specimen cracked at surface whereas crack initiation took place underneath the surface for 42CrMo4 specimens. Hardfacing of stellite 21 on 42CrMo4 and X5CrNi18-10 decreases fatigue strength.
[43]	316L SS(RV, RGV, PHTS)	Stellite 21	Round Specimen a. Cladding of Stellite 21 on SS b. Variation in composition across substrate/clad interface.	Testing method: Rotating-Bending fatigue testsAlternating Stress levels: 200–300 MPa	For both the conditions direct cladding and graded cladding, the fatigue failure initiated at the wrought SS portion of gauge area. All the specimens failed at similar number of loading cycles. Thus, the author says that the substrate SS part was the weakest area for fatigue crack to initiate. The ferrous zones showed plastic deformation and whereas cobalt zones showed brittle deformation.
[44]	X5CrNi18-10 (reactor core, fuel cladding) 42CrMo4(SG system)	Stellite 21	Round Specimen	Residual Stresses are found by Neutron Diffraction method	Residual stresses are important for the effect of fatigue properties after laser cladding.
[45]	S355-low alloy steel(SG Vessel Wall, turbine rotor, blades) 42CrMo4(SG system)	Co-base powder (Stellite 21) and Ni-base powder (Inconel 625)	Round Specimen	Testing method: Four-Point bending Fatigue testing	Fatigue failure depends on maximum stress concentrators caused due to macro load conditions and stress raisers at defects. Laser clad defects can be summarized into three types 0D-pores/ inclusions, 1D-clad waviness or 2D-planar cracks. To increase the fatigue life of laser cladded bars the stress concentrated areas should be avoided.
[47]	AISI 4130 steel (SG Vessel Wall, turbine rotor, blades)	Stellite 6 and Deloro 40G	Round Specimen	Testing method: Cantilever type rotary bending	The test results predicted that the coated specimens by stellite6 and Deloro 40G showed lower fatigue life as compared to unclad specimen. Due to lower tensile stresses in stellite 6, fatigue life is higher in these specimens for same load.
[48]	42CrMo4/S355 (SG Vessel Wall, turbine rotor, blades)	Inconel 625/ Stellite 21	Round Specimen	Testing method: Four-point bending testsTensile-Tensile Load: 75 to 160 kN. R Ratio: 0	Fatigue life of unclad S355 is higher than that of laser clad S355. The decrease in fatigue life for laser clad specimen is due to higher residual tensile stress and cladding defects. However, In625/42CrMo4 improved fatigue life at higher loads

(continued on next page)

Table 2 (*continued*)

Sources	Substrate/Reactor component system	Cladding Material	Type of Fatigue Specimen	Fatigue Tests Specifications	Significant Findings
					and reduced at lower loads as compared to the substrate specimen. The residual stress was lower than the cladded defects were found cladding region of fractured surfaces.
[49]	AerMet100 Steel-High strength steel(Pump materials)	AerMet100 Powder	Round Specimen a. Substrate specimen without notch b. Substrate specimen with notch c. As-clad specimen d. As-clad + PHT	Testing method: Variable amplitude fatigue testStress Ratio: Between 0.1 and 0.7Maximum Alternating stress:1000 MPaFrequency: 5 Hz	Fatigue life improved for AerMet 100 as-clad in comparison to as-damaged specimen. This is attributed to the laser cladding that removed the stress concentration at the notch. The fatigue life of as-clad specimen is lower as compared to substrate specimen without a notch. Fracture initation took place from top surface of cladding which was of tearing topology. The fatigue life of PHT specimen did not show a substantial increase in fatigue life which is attributed to increase in hardness after PHT which causes brittleness.
[51]	Plain carbon Steel (Secondary Piping)	Co-Cr	Flat specimen	Testing method: Low cycle fatigue tests Mode: tensile– compression modeR ratio: −1	The fatigue tests revealed shorter life for cladded specimen as compared to substrate specimen. This shorter fatigue life is due to tensile residual stress. The experimental data showed the small scatter in the SN curve which predicts a very consistent and high-quality coating method.
[52]	Plain carbon steel (Secondary Piping)	Co-Cr	Flat specimen	Testing method: Low cycle fatigue testsMode: TensileStrain rate: 10^{-4} s^{-1}	The results show that there is very negligible difference of fatigue life for both the specimens with still higher fatigue life for higher hardness and thicker clad specimen.
[54]	AISI P20 (40 CrMnNiMo 8 6 4) and AISI H13(X 40 CrMoV 5 1) steel weld(SG system)		Flat specimen	Testing method: Axial test on Instron MachineR ratio: 0 and 0.4 Frequency: 25 Hz	Welded specimens for both P20 and H13 showed relatively lower fatigue strength as compared to plain specimens. Planar defects are seen normal to the crack surface which gives new surface for the crack initiation
[55]	AISI 4340(SG Vessel Wall, turbine rotor, blades)	75 wt% Cr powder and 25 wt% CrB2 powder mixed	Flat specimenThe specimens are dived into 3 samples according to the power of laser.	Testing method: high cycle fatigue on four-point bending test machine R ratio: 0.1 Frequency: 5 Hz Alternating Stress levels: 300 to 1600 MPa	The endurance limit of lot 2 samples was higher as compared to all other samples. Lot 4 samples showed poor performance due to unremoved coating which acted as stress concentrator. Lot 1 and Lot 2 samples showed trans granular crack propagation

(*continued on next page*)

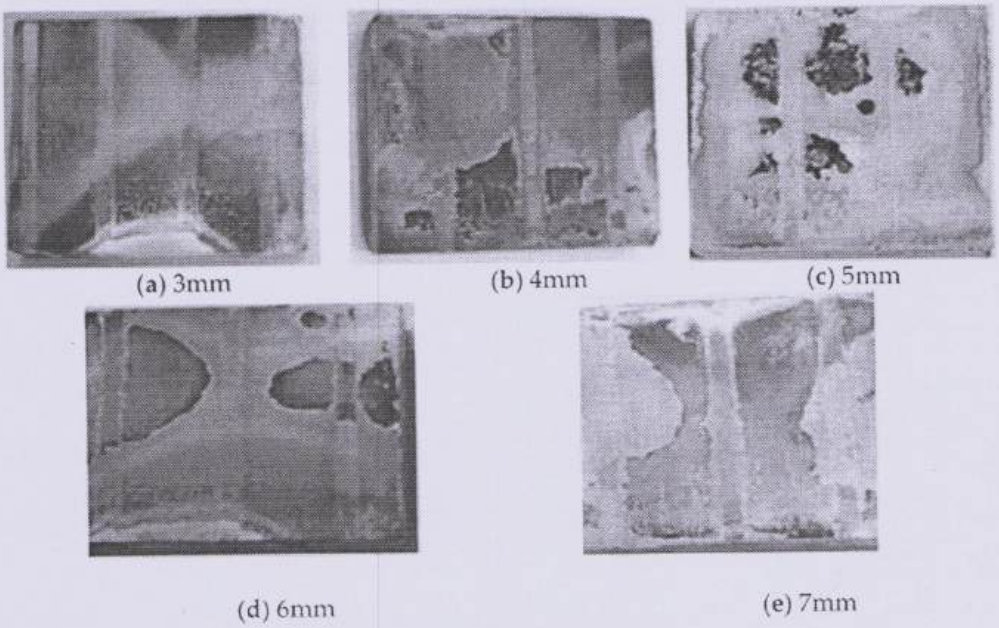


Fig. 11. Thermal fatigue on parallel structure [65].

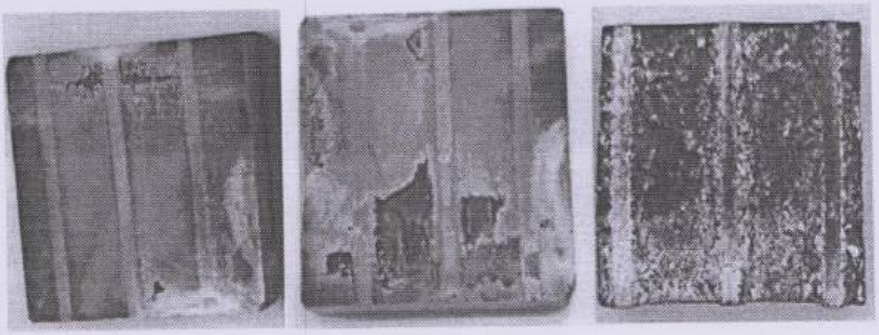


Fig. 12. Effect of thermal cycles on thermal fatigue.

MSS thus shows better fatigue properties than Stellite 6.

W.J. Wang et.al (2016) [64] studied the effect of use of lanthanum oxide on contact fatigue damage of wheel and rail specimen with Fe based alloy coating under oil lubrication condition. The Fe based alloy coating is done by laser cladding. It improves the fatigue resistance of rails. Use of lanthanum oxide is advantageous due to ease of application and improve the microstructure and grain boundary of cladding materials. There are many fatigue cracks seen for untreated specimens of wheel and rail. For specimens with cladding without lanthanum oxide layer, fatigue cracks are seen. Specimens with lanthanum oxide layer does not show any visible fatigue cracks. Use of 1.2% lanthanum oxide in Fe based alloy gives best fatigue dame resistance properties to the wheel and rail specimen under oil lubrication condition.

Fangping Yao et.al (2021) [65] prepared three different specimens of laser cladding which resembles bionic structures and these specimens were tested for thermal fatigue resistance. Laser cladding of NiWC25 was done on H13 steel base material. The effect of various bionic structures on the thermal-fatigue characteristics and cracks was studied by the authors. The bionic structures of laser cladding considered was first parallel structures which resemble 'canna', second, square structure which resembles 'nacre of the shell' and third, triangular structure which resembles 'wings of dragon fly'. To study the effect of spacing of parallel structures on thermal fatigue resistance, the specimens were heated to 800 °C and cooled till 20 °C in water. The specimens were subject to 300 cycles. The specimens with spacing of 3 to 7 mm was considered for test. The results as shown in Fig. 11 show that as the spacing increases more than 5 mm, the cracks increases and the crack propagation retarding ability of cladding layer reduces as spacing increases. The crack propagation is smaller if spacing is less than 5 mm. Thus, it is considered that 5 mm spacing is optimum value for the tests. Further tests were also conducted for varying cycles of 100, 300 and 1000 cycles to study the effect of thermal cycles on thermal fatigue. At 100

Table 2 (*continued*)

Sources	Substrate/Reactor component system	Cladding Material	Type of Fatigue Specimen	Fatigue Tests Specifications	Significant Findings
					and Lot 4 samples showed intergranular cracks.
[57]	42CrMo4(SG system)	Stellite 21	Flat specimen	Testing Method- Cyclic Fatigue testing	The fatigue strength for cladded specimen decreased than the uncladded specimen. Origins of cracks were seen at the cladded areas and at fillets on crankshaft.
[58]	AISI 4340(SG Vessel Wall, turbine rotor, blades)	AISI 4340and AerMet 100 steel powder	Flat specimenFour conditions were considered: AISI 4340 as-clad, AerMet 100, AISI 4340 as-clad (PCHT) and AerMet 100 (PCHT).	Testing method: Axial constant amplitude fatigue testing R ratio: 0.1 Frequency: 10 Hz	Use of Aermet100 clad layer improves fatigue properties of specimen as compared to as-clad AISI4340 steel. PCHT specimens shows increase in fatigue resistance and fatigue life as compared to without post heat treatment.
[59]	AISI 4340(SG Vessel Wall, turbine rotor, blades)	AISI 4340 Powder	Flat specimen	Testing method: Axial testingAlternating Stress levels: 290–650 MPaFrequency: 15 HzR Ratio: 0	Stress intensity factor and magnification factor is required to find out for predicting the fatigue crack growth. Finite element model was modelled for a range of crack depth and crack shape ratios. The predicted fatigue life was similar to experimental results.
[60]	AISI 4340 steels (SG Vessel Wall, turbine rotor, blades)	AISI 4340 steel powder	Flat specimenCategory I specimen is as-clad specimenCategory II specimen is a grooved specimen later filled with clad material Category III specimen is that the clad region is extended beyond the gage section of the fatigue test specimen.	Testing method: Axial testingR ratio: 0 Frequency: 15 Hz	There is decrease in fatigue strength for category I specimen as compared to substrate specimen. This reduction is due to large cracks initiating at the clad toe region. The fatigue strength for category II specimen is little closer to substrate specimen Fatigue failure occurred at clad material and groove intersection region. Fatigue strength of category III specimen is higher as compared to all other specimens.
[61]	EA4T steel -low alloy steel(SG Vessel Wall, turbine rotor, blades)	kf311 ferrous metal powder	Flat specimen	Testing method: Three-point bending testsApplied load- 4.8 kNFrequency: 10 HzR Ratio: 0.1	Thus, due to higher fracture strength and higher stress intensity factor threshold value, the fatigue crack growth rate is lower for cladded specimen than the base specimen. Thus, it is said that fatigue life is increased by laser cladding of kf311 ferrous metal powder.

4. Fatigue testing specimens

It is required to perform research to develop optimized materials of hardfaced reactor components considering the fatigue parameters. This review will give a critical understanding of methods for fatigue testing of hardfaced specimens which can be useful for researchers to design a methodology for robust testing of nuclear reactor components.

Broadly two fatigue testing specimens are prepared according to ASTM-E466. Cylindrical or flat dog bone specimens are generated for fatigue testing according to the applications and ASTM standards. A review is done in this study to identify various methods to

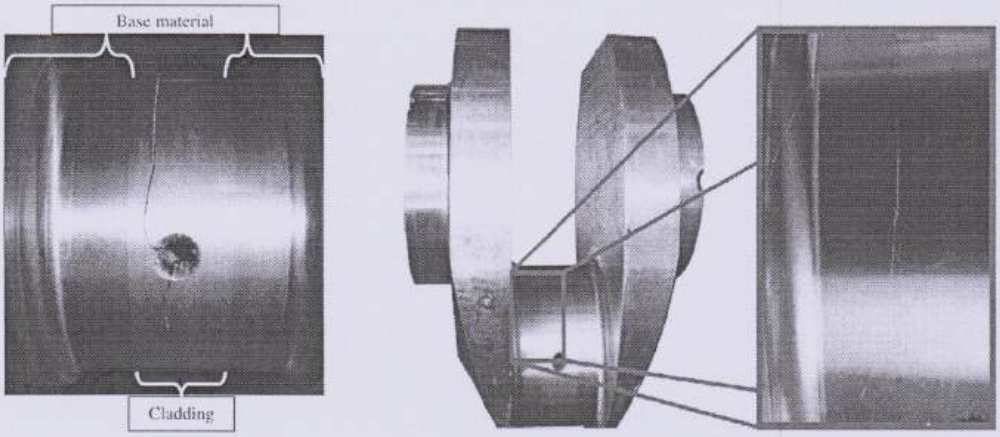


Fig. 10. (a) Fracture surface at oil bore (b) Fracture at fillet and at cladding interface [56].

substrates of identical geometry are considered having a slight variation of hardness and thickness. Thickness of plate 1 was 2 mm and plate 2 was 1. 6 mm.The hardness of HAZ is similar in both cases. Laser cladding of Co-Cr is done on substrate. Low cycle fatigue test was done for tensile mode at strain rate of $10^{-4}s^{-1}$. Coffin-Mansion calculations was also done to find out the fatigue life of specimens. The results show that there is very negligible difference of fatigue life for both the samples with still higher fatigue life for higher hardness and thicker clad specimen.

H.Y. Al-Fadhli et.al (2005) [53] did the fatigue experiment to find out the fatigue properties of welded and plain stainless-steel surfaces cladded with Inconel625 alloy material by HVOF process. Three specimens were considered for both types (a) surface coated, (b) surface coated and exposed to aqueous corrosion for period of 2 weeks and (c) surface coated and exposed to aqueous corrosion for period of 4 weeks. Axial fatigue testing was done on Instron 8501 machine for frequency of 20 Hz, stress ratio 0.1 and stress of 70% to 90% of ultimate tensile strength of base material. The tests showed that in both the cases of plain and welded stainless steels, the fatigue properties decreased as the time duration for corrosive environments increased. This is predicted to be due to lower bonding strength of coating at higher corrosive atmospheres. Both the welded and plain steels behave almost similarly in case of fatigue strength.

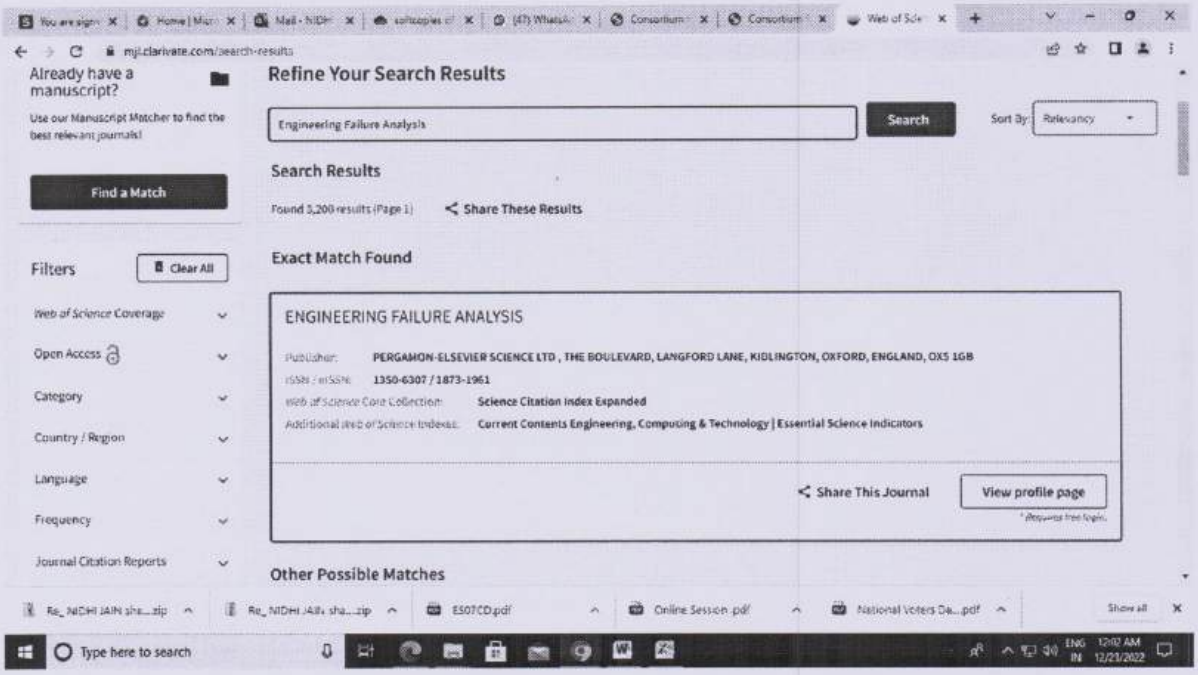
L.P. Borrego et.al (2007) [54] did the fatigue experiment to find out the fatigue properties of laser welded joints of two base materials AISI P20 steel and AISI H13 steel. These materials are used for mould production. Axial fatigue testing with constant amplitude loading was done on Instron machine for frequency of 25 Hz and stress ratio 0 and 0.4. Rectangular cross section plain specimens were prepared for fatigue testing and U notch was given to the weld specimens which was filled with laser welding deposits. Welded specimens for both P20 and H13 showed relatively lower fatigue strength as compared to plain specimens for $R = 0$. The decrease of fatigue strength can be predicted due to hardness, residual stress, filler material mechanical properties and welding defects. Planar defects are seen perpendicular to the fracture surface which gives new surface for the crack initiation.

R.L. McDaniels et al. (2008) [55] proposed study of effect of HAZ on fatigue behaviour of AISI4320 laser cladded steel. The specimens were tested for high cycle fatigue on four-point bend test machine. Lot1, Lot2 and Lot3 specimens were considered with laser power of 1750 W, 2000 W and 1400 W respectively and laser speed of 1500 mm/min. The test specimen was rectangular in shape. The specimens were tested at stress range of 300 to 1600 MPa under load control of stress ratio 0.1 and frequency of 5 Hz. The uncladded specimens were run at stress levels range from 1220 to1570 MPa as per ASTM standards. The endurance strength of as received samples was found to be 1144 MPa and for Lot1 samples was 1162 MPa. Endurance strength of Lot 2 samples was higher than as received and Lot 1 samples value for which was 1295 MPa. Lot 3 samples showed a poor performance of fatigue as compared to all other samples. The endurance strength for Lot 3 samples was 1050 MPa and it failed before they reach 10^4 cycles. The lower endurance strength of these specimens is due to stress concentration areas caused by unremoved coatings. There are inclusions and pores at coating substrate interface. These areas act as crack initiation areas. For lot 1 samples, the crack initiation took place at surface inclusions and crack propagation mode is trans granular. Both Lot1 and Lot2 specimens shows same fracture surface. The mode of crack propagation is trans granular, and there are no striations or intergranular fracture seen.

E.S. Puchi-Cabrera et al. (2010) [56] explored the fatigue behaviour of SAE 1045 steel substrate coated with colmonoy 88 alloy using high velocity oxygen fuel deposition (HVOF) spray technique. Fatigue test was performed at maximum stresses from 380 to 533 MPa at stress ratio 0.1. Tests were performed at three conditions uncoated, grit blasting, and grit blasting and coated. Fatigue strength and fatigue life were investigated through wohler curve and also by means of parametric relationship. It is observed that for grit blasting and grit blasting and coating the fatigue limit reduced by 11 to 13%. The fatigue curves are almost similar for grit blasting and grit blasting and coated specimens. This shows that the debit in fatigue properties grit blasting and coated specimens is also due to grit blasting done before coating. The fatigue cracks initiated at coating-surface interface and open surface of coating. These cracks can pass through entire coating thickness and caused delamination of coating.

Henry Koehler et.al. (2011) [57] found out the effect on fatigue properties due to laser cladding on marine crankshafts. The hot forged crankshaft of 42CrMo4 was cladded with Stellite 21. For fatigue analysis flat specimens were cut from crankshaft. IMAC

[12] H. Koehler, J. Schumacher, K. Schuischel, K. Partes, H. Bomas, F. Jablonski, F. Vollertsen, R. Kienzler, An approach to calculate fatigue properties of laser cladded components, Prod. Eng. Res. Devel. 6 (2) (2012) 137–148, https://doi.org/10.1007/s11740-012-0369-7.
[13] A.K. Bhaduri, K. Laha, Development of Improved Materials for Structural Components of Sodium-Cooled Fast Reactors, Procedia Eng. 130 (2015) 598–608, https://doi.org/10.1016/j.proeng.2015.12.276.
[14] B. Raj, B.K. Choudhary, A perspective on creep and fatigue issues in sodium cooled fast reactors, Trans. Indian Inst. Met. 63 (2-3) (2010) 75–84, https://doi.org/10.1007/s12666-010-0011-3.
[15] Y. Takahashi, H. Shibamoto, K. Inoue, Study on creep-fatigue life prediction methods for low-carbon, Nucl. Eng. Des. 238 (2008) 322–335, https://doi.org/10.1016/j.nucengdes.2006.09.017.
[16] S. Date, H. Ishikawa, T. Otani, Y. Takahashi, T. Nakazawa, Study on environmental effect on fatigue and creep-fatigue strength of 316FR stainless steel in sodium at elevated temperature, Nucl. Eng. Des. 238 (2) (2008) 353–367, https://doi.org/10.1016/j.nucengdes.2006.09.008.
[17] G.J. Zeman, D.L. Smith, Low cycle fatigue behavior of types 304 and 316 stainless steel tested in sodium at 550 degree C, Nucl Technol. 42 (1979) 82–89, https://doi.org/10.13182/NT79-A32164.
[18] M.D. Mathew, K. Laha, R. Sandhya, Creep and low cycle fatigue behaviour of fast reactor structural materials, Procedia Eng. 55 (2013) 17–26, https://doi.org/10.1016/j.proeng.2013.03.213.
[19] T. Asayama, S. Takaya, Y. Nagae, M. Ando, K. Tsukimori, Creep-fatigue evaluation methodologies and related issues for japan sodium cooled fast reactor (JSFR), Procedia Eng. 55 (2013) 309–313, https://doi.org/10.1016/j.proeng.2013.03.259.
[20] T. Wakai, M. Sukekawa, S. Date, T. Asayama, K. Aoto, S. Kubo, Development of high-chromium steel for the sodium-cooled fast reactor in Japan and creep-fatigue assessment of the steel, Int. J. Press. Vessel. Pip. 85 (6) (2008) 352–359, https://doi.org/10.1016/j.ijpvp.2007.11.011.
[21] E. Lemaire, M. Le Calvar, Evidence of tribocorrosion wear in pressurized water reactors, Wear. 249 (5-6) (2001) 338–344, https://doi.org/10.1016/S0043-1648(00)00544-5.
[22] A.K. Bhaduri, R. Indira, S.K. Albert, B.P.S. Rao, S.C. Jain, S. Asokkumar, Selection of hardfacing material for components of the Indian Prototype Fast Breeder Reactor, J. Nucl. Mater. 334 (2-3) (2004) 109–114, https://doi.org/10.1016/j.jnucmat.2004.05.005.
[23] K.G. Das CR, Albert SK, Bhaduri AK, Technology Development for Hardfacing of Large Components using Ni base Hardfacing Alloys, IGCAR Technol Mater. (2005) 170–171.
[24] B. Raj, Materials and manufacturing technologies for sodium cooled fast reactors and associated fuel cycle: Innovations and maturity, Energy Procedia. 7 (2011) 186–198, https://doi.org/10.1016/j.egypro.2011.06.025.
[25] P. Kumar, A. Pai, An overview of welding aspects and challenges during manufacture of Intermediate Heat Exchangers for 500MWe Prototype Fast Breeder Reactor, Procedia Eng. 86 (2014) 173–183, https://doi.org/10.1016/j.proeng.2014.11.026.
[26] B.K. Sreedhar, S.K. Albert, A.B. Pandit, Improving Cavitation Erosion Resistance Of Austenitic Stainless Steel In Liquid Sodium By Hardfacing – Comparison Of Ni And Co Based Deposits, Wear. 342-343 (2015) 92–99, https://doi.org/10.1016/j.wear.2015.08.009.
[27] H. Kumar, V. Ramakrishnan, S.K. Albert, A.K. Bhaduri, K.K. Ray, Friction and wear behaviour of Ni-Cr-B hardface coating on 316LN stainless steel in liquid sodium at elevated temperature, J. Nucl. Mater. 495 (2017) 431–437, https://doi.org/10.1016/j.jnucmat.2017.08.036.
[28] R.N. Johnson, Coatings for fast breeder reactor components, Thin Solid Films. 118 (1) (1984) 31–48, https://doi.org/10.1016/0040-6090(84)90104-4.
[29] R.N. Johnson, D.G. Farwick, Friction, wear and corrosion of laves-hardened nickel alloy hardsurfacing in sodium, Thin Solid Films. 53 (3) (1978) 365–373, https://doi.org/10.1016/0040-6090(78)90229-8.
[30] D.G. Farwick, R.N. Johnson, Wear and corrosion performance of metallurgical coatings in sodium, Thin Solid Films. 73 (1) (1980) 145–153, https://doi.org/10.1016/0040-6090(80)90341-7.
[31] H.M.P. Aubry, C. Blanc, I. Demirci, C. Gorny, Analysis of a Ni-Fe-Cr-Mo-Si hardfacing alloy manufactured by laser cladding : influence of the iron content on the wear resistance properties, Procedia CIRP. 74 (2018) 210–213, https://doi.org/10.1016/j.procir.2018.08.096.
[32] H. Zhang, Y. Shi, M. Kutsuna, G.J. Xu, Laser cladding of Colmonoy 6 powder on AISI316L austenitic stainless steel, Nucl. Eng. Des. 240 (10) (2010) 2691–2696, https://doi.org/10.1016/j.nucengdes.2010.05.040.
[33] S. Kim, J. Kim, Effects of temperature and contact stress on the sliding wear of Ni-base Deloro 50 hardfacing alloy, J. Nucl. Mater. 288 (2-3) (2001) 163–169, https://doi.org/10.1016/S0022-3115(00)00711-X.
[34] M.-W. Lee, Y.-K. Kim, Y.-M. Oh, Y. Kim, S.-H. Lee, H.-S. Hong, S.-J. Kim, Study on the cavitation erosion behavior of hardfacing alloys for nuclear power industry, Wear. 255 (1-6) (2003) 157–161, https://doi.org/10.1016/S0043-1648(03)00144-3.
[35] D. Kesavan, M. Kamaraj, The microstructure and high temperature wear performance of a nickel base hardfaced coating, Surf. Coatings Technol. 204 (24) (2010) 4034–4043, https://doi.org/10.1016/j.surfcoat.2010.05.022.
[36] S. Balaguru, S. Kumar, V. Murali, P. Chellapandi, Thermo mechanical analysis of SS304 circular grid plate hard faced with colmonoy, Appl. Mech. Mater. 229–231 (2012) 710–717, https://doi.org/10.4028/www.scientific.net/AMM.229-231.710.
[37] S. Balaguru, V. Murali, P. Chellapandi, Measurement of the Residual Stresses and Investigation of Their Effects on a Hardfaced Grid Plate due to Thermal Cycling in a Pool Type Sodium-Cooled Fast Reactor, Sci. Technol. Nucl. Install. 2016 (2016) 1–8, https://doi.org/10.1155/2016/8353256.
[38] S. Balaguru, V. Murali, P. Chellapandi, Effects of Different Operating Temperatures on the Tensile Properties of the Grid Plate Hardfaced with Colmonoy in a Pool Type Sodium Fast Reactor, Sci. Technol. Nucl. Install. 2017 (2017) 1–9, https://doi.org/10.1155/2017/5926105.
[39] C.J. Villalobos-Gutiérrez, G.E. Gedler-Chacón, J.G. La Barbera-Sosa, A. Piñeiro, M.H. Staia, J. Lesage, D. Chicot, G. Mesmacque, E.S. Puchi-Cabrera, Fatigue and corrosion fatigue behavior of an AA6063-T6 aluminum alloy coated with a WC – 10Co – 4Cr alloy deposited by HVOF thermal spraying, Surf. Coat. Technol. 202 (18) (2008) 4572–4577, https://doi.org/10.1016/j.surfcoat.2008.04.044.
[40] T. Branza, F. Deschaux-Beaume, V. Velay, P. Lours, A microstructural and low-cycle fatigue investigation of weld-repaired heat-resistant cast steels, J. Mater. Process. Technol. 209 (2) (2009) 944–953, https://doi.org/10.1016/j.jmatprotec.2008.03.002.
[41] W.A. González-Hermosilla, D. Chicot, J. Lesage, J.G. La Barbera-Sosa, I.C. Gruescu, M.H. Staia, E.S. Puchi-Cabrera, Effect of substrate roughness on the fatigue behavior of a SAE 1045 steel coated with a WC–10Co–4Cr cermet, deposited by HVOF thermal spray, Materials Science and Engineering: A 527 (24-25) (2010) 6551–6561.
[42] J.G. La Barbera-Sosa, Y.Y. Santana, C. Villalobos-Gutiérrez, S. Cabello-Sequera, M.H. Staia, E.S. Puchi-Cabrera, Effect of spray distance on the corrosion-fatigue behavior of a medium-carbon steel coated with a Colmonoy 88 alloy deposited by HVOF thermal spray, Surf. Coat. Technol. 205 (4) (2010) 1137–1144, https://doi.org/10.1016/j.surfcoat.2010.01.038.
[43] P. Ganesh, A. Moitra, P. Tiwari, S. Sathyanarayanan, H. Kumar, S.K. Rai, R. Kaul, C.P. Paul, R.C. Prasad, L.M. Kukreja, Fracture behavior of laser-clad joint of Stellite 21 on AISI 316L stainless steel, Mater. Sci. Eng. A. 527 (16-17) (2010) 3748–3756, https://doi.org/10.1016/j.msea.2010.03.017.
[44] H. Köhler, K. Partes, J.R. Kornmeier, F. Vollertsen, Residual Stresses in Steel Specimens Induced by Laser Cladding and their Effect on Fatigue Strength, Phys. Procedia. 39 (2012) 354–361, https://doi.org/10.1016/j.phpro.2012.10.048.
[45] M.M. Alam, A.F.H. Kaplan, J. Tuominen, P. Vuoristo, J. Miettinen, J. Poutala, J. Näkki, J. Junkala, T. Peltola, Z. Barsoum, Analysis of the stress raising action of flaws in laser clad deposits, Mater. Des. 46 (2013) 328–337, https://doi.org/10.1016/j.matdes.2012.10.010.
[46] J.G. La Barbera-sosa, Y.Y. Santana, D. Chicot, S. Decoopman, A. Jost, M.H. Staia, E.S.P., Details, J.G. La Barbera-sosa, Y.Y. Santana, D. Chicot, J. Lesage, Fatigue behavior of a structural steel coated with a WC – 10Co – 4Cr / Colmonoy 88 deposit by HVOF thermal spraying To cite this version : HAL Id : hal-01174230 Science Arts & Metiers (SAM), Surf. Coatings Technol. 220 (2013) 248–256.
[47] N. Hutasoit, V. Luzin, A. Blicblau, W. Yan, M. Brandt, R. Cottam, Fatigue life of laser clad hardfacing alloys on AISI 4130 steel under rotary bending fatigue test, Int. J. Fatigue. 72 (2015) 42–52, https://doi.org/10.1016/j.ijfatigue.2014.11.001.
[48] J. Tuominen, J. Näkki, J. Poutala, J. Miettinen, T. Peltola, P. Vuoristo, I. Rasehorn, M.M. Alam, Fatigue behavior of laser clad round steel bars Fatigue behavior of laser clad round steel bars, 012006 (2015). https://doi.org/10.2351/1.490335.
[49] J.M. Lourenço, S. Da Sun, K. Sharp, V. Luzin, A.N. Klein, C.H. Wang, M. Brandt, Fatigue and fracture behavior of laser clad repair of AerMet® 100 ultra-high strength steel, Int. J. Fatigue. 85 (2016) 18–30, https://doi.org/10.1016/j.ijfatigue.2015.11.021.


mjl.clarivate.com/search-results
Already have a manuscript?
Use our Manuscript Matcher to find the best relevant journals!
Find a Match
Refine Your Search Results
Engineering Failure Analysis
Search
Sort By: Relevancy
Search Results
Found 3,200 results (Page 1)
Share These Results
Filters
Clear All
Web of Science Coverage
Open Access
Category
Country / Region
Language
Frequency
Journal Citation Reports
Exact Match Found
ENGINEERING FAILURE ANALYSIS
Publisher: PERGAMON-ELSEVIER SCIENCE LTD , THE BOULEVARD, LANGFORD LANE, KIDLINGTON, OXFORD, ENGLAND, OX5 1GB
ISSN / eISSN: 1350-6307 / 1873-1961
Web of Science Core Collection: Science Citation Index Expanded
Additional Web of Science Indexes: Current Contents Engineering, Computing & Technology | Essential Science Indicators
Share This Journal
View profile page
Other Possible Matches
Re_ NIDHI JAIN sha....zip
Re_ NIDHI JAIN sha....zip
ES07CD.pdf
Online Session .pdf
National Voters Da....pdf
Show all
Type here to search
ENG IN
12:02 AM 12/23/2022

PalArch's Journal of Archaeology of Egypt / Egyptology

NUMERICAL STUDY OF TRANSFORMED MIGRATING CELLS IN TUMOR VASCULATURE GROWTH

Neeta D. Kankane[1] and Dhanke Jyoti Atul[2]

[1]*Former Professor, MIT-World Peace University, MAEER'S MIT, Pune, India*

[2]*Research Student, Department of Mathematics, Savitribai Phule Pune University, Pune, India*

Neeta D. Kankane and Dhanke Jyoti Atul: Numerical Study of Transformed Migrating Cells in Tumor Vasculature Growth -- Palarch's Journal of Archaeology of Egypt/Egyptology, ISSN 1567-214x

Keywords: Extracellular Matrix Fibronectin, Tumor Vasculature Growth, Endothelialization, Angiogenesis

ABSTRACT

A hybrid mathematical model is developed here to investigate angiogenesis. This model integrates the transformed migrating cells in tumor vasculature growth. This paper's primary purpose is to consolidate a view on the production of extracellular matrix fibronectin in the tumor vascular growth by the migration of the endothelial cells present in it. Migration of the endothelial cells is vital for forming new blood cells, angiogenesis, and endothelialization. For the advancement of migrating cells, the proceeding of angiogenesis by haptotaxis and further involving the extracellular matrix's degradation enables it.

INTRODUCTION

The integration of complex network of macromolecules that include various components that of, specialized proteins (fibrilin, elastin and fibronectin), protein (elastin and collagen), proteoglycans, glycoproteins and polysaccharides (hyaluronan) that have the distinct biomechanical, biochemical and physical properties. An important role is being played by the approach of extracellular matrix (ECM) to decipher these systems given by Ozbek *et al.* [1]. To safeguard the organ system's normal development, toughness, and physiology, the ECM dynamics are sturdily measured. When the disruption of such mechanisms occurs, the significant deregulation development of cancer is initiated, discovered by Lu P *et al.* [2]. In ECM, the fibronectin structure is that of a massive grid of extended fibrils that are branched out. The soluble fibronectins gathered (polymerized) and converted to fibrils that are insoluble of ECM thru a sturdily controlled, process that is dependent on cell being held toward the top or bottom rapidly studied by Magnusson and Mosher [3]. The stimulation of actin-dependent process is initiated by ligating the ECM of the fibronectin fibrils by cell receptors present on surface, along with actin-

dependent, cell spreading, growth and the migration promotes cell cohesion studied by Gui L. *et al.*, Hocking D.C. *et al.*, Sottile J. *et al.*, Robinson E.E. *et al.*, Salmenpera P. *et al.* [4-9]. For the vascularization to complete, the endothelial cells (EC) have to overcome the barrier that is the ECM. Consisting of the collagen fiber, interstitial tissue, fibronectin and fibronectin fibrils, and other components, the ECM is fibrous and monitors the capillary sprouts' growth. The origin of organ failure and damage to tissue architecture is caused due to the invasive tumor growth studied by A. Liotta *et al.* [10].

For the effective expansion and growth of solid tumors, the formation of blood vessels is vital. Cancer will remain in an undeveloped avascular state in the absence of a capillary network of the blood supply and removal of unused products. Tumor angiogenesis factor, i.e., TAF is known when the secretion of chemicals takes place in tumor to facilitate angiogenesis concept presented by J. Folkman and M. Klagsburn [11], that induces the surrounding endothelial cells to initialize migration towards the turnout into extracellular cells and also reduce its basal lamina, studied by Muthukkaruppan *et al.* [12]. To develop EC linkage to that of collagen is called fibronectin that was presented by Schor *et al.* [13], which is developed by the EC themselves. The hypotactic effect of fibronectin controls the retort towards the chemotactic effects of EC migration and tumor angiogenesis factor, studied by P. Monaghan et al., JC Bowersox *et al.*, [14,15].

MATHEMATICAL MODEL

Here in the paper, by taking into consideration the interaction between essential endothelial cells-extracellular matrix (ECM) through the inclusion of macromolecule fibronectin matrix, a mathematical model is presented. Based on Anderson and Chaplain' mathematical model [17], Jie Lyu's model [18], Anderson' model [19], and Chaplain' mathematical model [20], we improved and tweaked their model in respect to five aspects, namely being tumor cell density, ECM (Extracellular matrix) concentration, concentration of MDE (matrix degradative enzymes), concentration of tumor angiogenesis (TAF) and concentration of oxygen.

If $n(x,y,t)$ is tumor cell density, $f(x,y,t)$ is fibronectin concentration, $m(x,y,t)$ is concentration of matrix-degrading enzymes (MDE) and $c(x,y,t)$ is oxygen concentration, $a(x,y,t)$ is TAF concentration then the equations in the model take the form

$$\frac{\partial n}{\partial t} = D_n \nabla^2 n - \rho \nabla.(n \nabla f) - \beta_1 n \quad (1)$$

$$\frac{\partial f}{\partial t} = \beta_2 n - \gamma n f - \delta m f \quad (2)$$

$$\frac{\partial m}{\partial t} = D_m \nabla^2 m + \varepsilon n - \sigma m \quad (3)$$

$$\frac{\partial c}{\partial t} = D_c \nabla^2 c - \omega n - \emptyset c + \nu f \quad (4)$$

$$\frac{\partial a}{\partial t} = D_a \nabla^2 a + \beta_3 n - \varphi a \quad (5)$$

Where $D_n = 5 \times 10^{-6}$ is the diffusion constant of cells in the tumor, Where $D_n = 5 \times 10^{-6}$ being the MDEs diffusion coefficient, $D_c = 5 \times 10^{-4}$ is the constant for oxygen diffusion (on the outside of tumor) and $D_c = 2.5 \times 10^{-4}$ being the oxygen diffusion (on the inside of tumor). $D_a = 5 \times 10^{-6}$ is diffusion coefficient of TAFs, 1cm × 1cm is the area of simulation consistently distributed along 201 × 201 lattices. The space step is $\Delta x = \Delta y = 0.005$. Time step $\Delta t = 0.002$.

In order to restrict the ECM, tumor cells, oxygen and MDE within domain, on the grid a condition known as no-flux boundary condition is imposed. Early state assumed as 81 cells of the tumor gathered centrally, with 0 to 16h being the range of there age randomly, also the value for the concentration of ECM on individual grid point is at random between that of 0 and 1, with the concentration of MDE being fix at 0 in the whole of domain and that of oxygen concentration at 1, in the domain there is absence of vascular point. 35,000 steps is how much the simulation runs being equivalent to that of 1120h, Jie Lyu, *et al.* [18]. $\beta_1 = 3$ is cell loss parameter, Chaplain model [20]. $\beta_2 = 0.05$ is rate of production of fibronectin by migrating endothelial cells $\gamma = 0.1$ is fibronectin degradation by endothelial cells, A. Stephanou *et al.* [22]. $\delta = 50$ is degradation coefficients of ECMs, $\varepsilon = (3c + 0.7)\varepsilon_{std}$, here $\varepsilon_{std} = 1$ is MDEs rate of generation. $\sigma = 0$ being MDEs rate of decay. $\omega = (3c + 0.7)\,\omega_{std}$, here $\omega_{std} = 0.6$ is the rate by which tumor cells consume oxygen. $\emptyset = 0.05$ is natural rate of decay. $\rho = (3c + 0.7)\rho_{std}$,, here $\varepsilon_{std} = 0.0001$ is haptotaxis coefficients of tumor cells. $\beta_3 = 0, c > 0.4$, tumor cells do not secret TAFs and $\beta_3 = \beta_{std}, c \leq 0.4$, tumor cells secret TAFs, here $\beta_{std} = 0.025$ is TAFs rate of generation. $\varphi = 0.01$ is the rate of natural decay, Jie Lyu, *et al.* [18], $\nu = 0.5$ is the generation rate of oxygen, Anderson [19].

To estimate a row of cells of the tumor we also considered from Anderson model [17], Jie Lyu, *et al.* [18] and Anderson [19] and Chaplain model [20]. An early concentration feild of TAF of form, $a(x, y, 0) = e^{-(1-x)^2/\epsilon_1}, (x, y) \in [0,1] \times [0,1]$. The distribution of the early data is given in the form $n(x, y, 0) = e^{-x^2/\epsilon_3} sin^2(6\pi y),\ (x, y) \in [0,1] \times [0,1]$, positive parameter ϵ_3. The profile of initial concentration of the fibronectin is taken in order to give distribution in the ECM to have the form, $f(x, y, 0) = ke^{-x^2/\epsilon_2}, (x, y) \in [0,1] \times [0,1]$. Here $\epsilon_1, \epsilon_2, \epsilon_3$ are positive parameter. As for the boundary conditions, it is assumed zero-flux at the boundaries.

A finite difference scheme is being used in order to solve the above mentioned equations numerically of which the results are being shown in the text and diagrams. We introduced a model for coupled tumor development and angiogenesis. The model purposes the vessels to full scale, without delivering upscaled amounts such as microvascular thickness. Our calculations show that the model can be utilized to think about both avascular and vascular development. In the avascular case, that is, the point at which the tumor can't advance angiogenesis, our model predicts a gradually contracting, nearly lethargic tumor because of its absence of access to supplement. Be that as it may, in the vascular case, the model normally predicts the angiogenesis switch typically.

The paper's mathematical model presents cell movement related to fibronectin concentration, endothelial-cell density and tumor angiogenesis factor (TAF) concentration that reflects the contact inhibition of migration for the vascular growth of tumor cells. The use of parametric standards is done in order to present the system's numerical simulation. A form of distinct partial differential equation is being used in order to develop a random walk model that is bias, in turn enabling us to incorporate mitosis and locate discrete endothelial cells.

Discretization : Numerical Method And Implementation

Now it's all set to formulate a discrete model and derive the probability of movement in respect to an individual cell of the tumor. By taking in the use of Euler's finite difference approximation from Mitchell and Griffiths, 1980 [21], we discretize the equations (1) to (5). Which involves the guesstimate of two-dimensional domain in the on going way with time (t), grid with distinct points (h – mesh size) and distinct

augmentations (k – magnitude). Following is the complete discretized system. First we consider the tumor cell density,

$$n_{i,j}^{k+1} = n_{i,j}^{k}P_0 + n_{i+1,j}^{k}P_1 + n_{i-1,j}^{k}P_2 + n_{i,j+1}^{k}P_3 + n_{i,j-1}^{k}P_4$$

Where the coefficient P_0, that is in proportion with the probability of being static, has the coefficients P_1 to P_4 that is in proportion with the probability of it moving in directions like that of towards left, towards right, towards bottom and towards top respectively, having forms,

$$P_0 = 1 - \frac{4D_n\Delta t}{h^2} - \frac{\rho\Delta t}{h^2}\left(f_{i+1,j}^{k} + f_{i-1,j}^{k} + f_{i,j+1}^{k} + f_{i,j-1}^{k} - 4f_{i,j}^{k}\right) - \beta_1\Delta t$$

$$P_1 = \frac{D_n\Delta t}{h^2} - \frac{\rho\Delta t}{4h^2}\left(f_{i+1,j}^{k} - f_{i-1,j}^{k}\right)$$

$$P_2 = \frac{D_n\Delta t}{h^2} + \frac{\rho\Delta t}{4h^2}\left(f_{i+1,j}^{k} - f_{i-1,j}^{k}\right)$$

$$P_3 = \frac{D_n\Delta t}{h^2} - \frac{\rho\Delta t}{4h^2}\left(f_{i,j+1}^{k} - f_{i,j-1}^{k}\right)$$

$$P_4 = \frac{D_n\Delta t}{h^2} + \frac{\rho\Delta t}{4h^2}\left(f_{i,j+1}^{k} - f_{i,j-1}^{k}\right)$$

Where the subscripts along with superscripts specify location and time stages respectively, that is the positive parameters are $t = qk$, $y = jh$ *and* $x = ih$, where q, k, j, h *and* i are all parameters that are positive. For discrete technique, prevailing assumption taken is, of the five constants being P_0 to P_4 are proportionate with a probability that tumor cell is being static (P_0), or upwards (P_4), downward (P_3), or towards right (P_2), towards left (P_1). This shows us that the tumor cell is not biased in respect to any one direction and more or less remain immobile, similar to a random, impartial walk. It must be noted that as they interact with other tumor cells, the motion will be getting altered. The parameter values have been adopted from Anderson and Chaplain [17]. The domain is a square with length as 1.

$$f_{i,j}^{k+1} = f_{i,j}^{k} + \beta_2 n_{i,j}^{k}\Delta t - \gamma n_{i,j}^{k} f_{i,j}^{k}\Delta t - \delta m_{i,j}^{k} f_{i,j}^{k}\Delta t$$

$$m_{i,j}^{k+1} = m_{i,j}^{k} + \frac{D_m\Delta t}{h^2}\left(m_{i+1,j}^{k} + m_{i-1,j}^{k} + m_{i,j+1}^{k} + m_{i,j-1}^{k} - 4m_{i,j}^{k}\right) + \Delta t\left(\varepsilon_{i,j}^{k} n_{i,j}^{k} - \sigma m_{i,j}^{k}\right)$$

$$c_{i,j}^{k+1} = c_{i,j}^{k} + \frac{D_c\Delta t}{h^2}\left(c_{i+1,j}^{k} + c_{i-1,j}^{k} + c_{i,j+1}^{k} + c_{i,j-1}^{k} - 4c_{i,j}^{k}\right) - \Delta t\left(\omega_{i,j}^{k} n_{i,j}^{k} + \emptyset c_{i,j}^{k} - \nu f_{i,j}^{k}\right)$$

$$a_{i,j}^{k+1} = a_{i,j}^{k} + \frac{D_a\Delta t}{h^2}\left(a_{i+1,j}^{k} + a_{i-1,j}^{k} + a_{i,j+1}^{k} + a_{i,j-1}^{k} - 4a_{i,j}^{k}\right) + \left(\beta_3 n_{i,j}^{k} - \varphi a_{i,j}^{k}\right)\Delta t$$

NUMERICAL SIMULATION RESULTS

Figure 1 shows the relationship between survival cells and time. Figures 2 help us identify the growth in number of tumor cells and blood vessels with respect to time respectively.

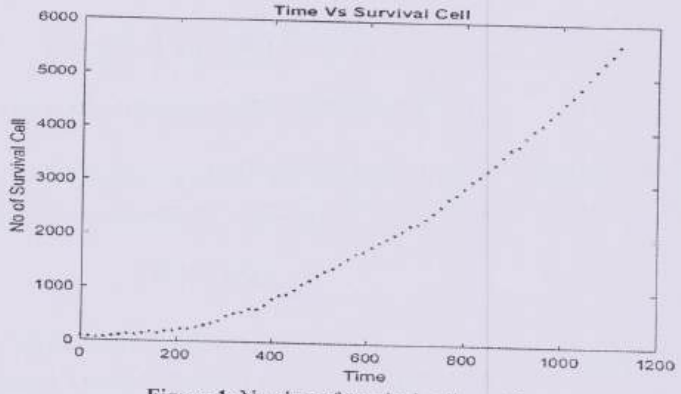


Figure 1: Number of survival cells vs. time

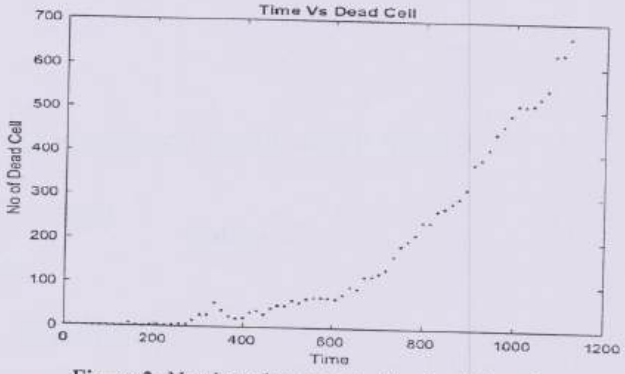


Figure 2: Number of tumor cells (dead cells) vs. time

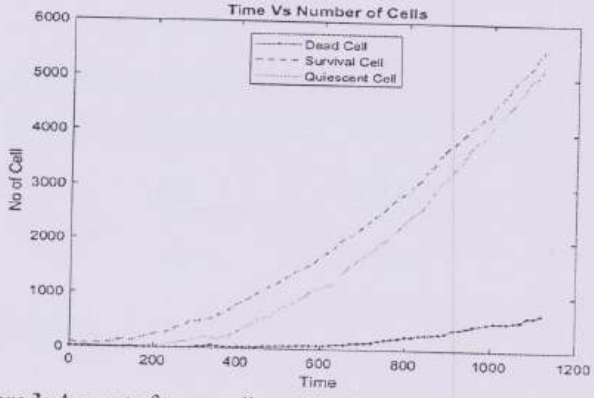


Figure 3: Amount of tumor cells and blood vessels with respect to time.

Figure 3 shows the amount of tumor cells and blood vessels with respect to time. At t = 200 to 450 dead cells are not present, only survival & quiescent cells are present

only. From t = 450, quiescent cells transferred into dead cells. This study indicates the formation of vascular network taking place gradually just as angiogenesis is introduced in the model when there is growth in tumor. In order for the tumor cells to grow in numbers there is a notable increase in the supply of oxygen, that helps the tumor in converting to a vascular stage from that of an avascular stage.

CONCLUSION

The study helps us find as to how the shift taking place in tumor microenvironment from its avascular phase to that of its vascular phase is related to increase in density points of the blood vessels starting from 0. An establishment of a new coupled model of angiogenesis and tumor growth is done. The use of this model through numerical simulation can be done in order to study the changes in the microenvironment of tumor, distribution of the concentration of oxygen, blood vessel development and to monitor the TAF concentration during the growth of tumor. The complicated process in tumor is that of angiogenesis. The mathematical model is developed here to investigate angiogenesis, which integrates the extracellular matrix fibronectin production in tumor growth. Researchers have found the involvement of a mechanism i.e., unclear gene expression modulation in regards to the tumor cells reaction to lack of acidic environment and oxygen. In order to activate the endothelial cells that is lined up on the wall of host blood vessel, TAFs are promoted and induced by the tumor cells.

REFERENCES

1. Ozbek S., Balasubramanian P.G., Chiquet-Ehrismann R., Tucker R.P., Adams J.C. The evolution of extracellular matrix. Mol. Biol. Cell. 2010;21:4300–4305. doi: 10.1091/mbc.E10-03-0251. [PMC free article] [PubMed] [CrossRef].
2. Lu P, Takai K, Weaver VM, et al. Extracellular matrix degradation and remodeling in development and disease. Cold Spring Harb Perspect Biol, 2011; 3. pii: a005058. [PMC free article] [PubMed].
3. Magnusson M. Mosher D.F. Fibronectin: structure, assembly, and cardiovascular implications. Arterioscler Thromb Vasc Biol. 1998;18:1363. [PubMed].
4. Gui L. Wojciechowski K. Gildner C.D. Nedelkovska H. Hocking D.C. (2006) Identification of the heparin-binding determinants within fibronectin repeat III1: role in cell spreading and growth. J Biol Chem., 281:34816. [PubMed].
5. Sottile J. Hocking D.C. Swiatek P.J. Fibronectin matrix assembly enhances adhesion-dependent cell growth. J Cell Sci. 1998;111:2933. [PubMed].
6. Hocking D.C. Chang C.H. Fibronectin polymerization regulates small airway epithelial cell migration. Am J Physiol Lung Cell Mol Physiol. 2003;285:L169. [PubMed].
7. Sottile J. Shi F. Rublyevska I. Chiang H.Y. Lust J. Chandler J. Fibronectin-dependent collagen I deposition modulates the cell response to fibronectin. Am J Physiol Cell Physiol. 2007;293:C1934. [PubMed].
8. Robinson E.E. Foty R.A. Corbett S.A. Fibronectin matrix assembly regulates alpha5beta1-mediated cell cohesion. Mol Biol Cell. 2004 : 15:973. [PMC free article] [PubMed].
9. Salmenpera P. Kankuri E. Bizik J. Siren V. Virtanen I. Takahashi S., et al. Formation and activation of fibroblast spheroids depend on fibronectin-integrin interaction. Exp Cell Res. 2008 : 314:3444. [PubMed].

Check whether you can access Scopus remotely through your institution

Source details

PalArch's Journal of Archaeology of Egypt/ Egyptology

Scopus coverage years: from 2012 to 2013, 2015, 2017, from 2019 to 2020

Publisher: PalArch Foundation

E-ISSN: 1567-214X

Subject area: Arts and Humanities: History | Arts and Humanities: Archeology (arts and humanities) | Social Sciences: Archeology

View all documents > | Save to source list

CiteScore 2019
0.2

SJR 2019
0.108

SNIP 2019
0.000

CiteScore | CiteScore rank & trend | Scopus content coverage

Improved CiteScore methodology

CiteScore 2019 counts the citations received in 2016-2019 to articles, reviews, conference papers, book chapters and data papers published in 2016-2019, and divides this by the number of publications published in 2016-2019. Learn more >

CiteScore 2019

$$0.2 = \frac{1 \text{ Citations 2016 - 2019}}{5 \text{ Documents 2016 - 2019}}$$

Calculated on 06 May, 2020

CiteScoreTracker 2020

$$0.3 = \frac{4 \text{ Citations to date}}{15 \text{ Documents to date}}$$

Last updated on 07 December, 2020 • Updated monthly

iteScore rank 2019

itegory	Rank	Percentile
ts and Humanities ...ory	#741/1259	40th
s and Humanities Archeology (arts and humanities)	#198/278	28th
ial Sciences	#191/263	27th

w CiteScore methodology > | CiteScore FAQ > | Add CiteScore to your site

Microprocessors and Microsystems 82 (2021) 103741

Contents lists available at ScienceDirect

Microprocessors and Microsystems

journal homepage: www.elsevier.com/locate/micpro

A machine learning based IoT for providing an intrusion detection system for security

Dhanke Jyoti Atul [a], R. Kamalraj [b], G. Ramesh [c], K. Sakthidasan Sankaran [d], Sudhir Sharma [e], Syed Khasim [f,*]

[a] Engineering Science (Mathematics), Bharati Vidyapeeth's College of Engineering, Lavale, Pune 412115, India
[b] MCA Department, School of CS &IT, Jain University, Bangalore, Karnataka, India
[c] Department of Computer Science and Engineering, Gokaraju Rangaraju Institute of Engineering & Technology, Hyderabad- 500090, Telangana State, India
[d] Department of Electronics and Communication Engineering, Hindustan Institute of Technology and Science, Chennai, India
[e] Computer Science & Engineering, Birla Institute of Applied Sciences, Bhimtal- Nainital (Uttarakhand) - 263136, India
[f] Computer Science & Engineering, Dr. Samuel George Institute of Engineering & Technology, Markapur, Andhra Pradesh, India

ARTICLE INFO

Keywords:
Cyber-physical system (CPS)
Energy-aware smart home
Machine Learning
IoT
Security

ABSTRACT

Digital communication is provided with an effective communication platform to share and transfer information. The emergence of the Cyber-Physical System (CPS) is a platform incorporated with electronic devices that enables the services through a digital platform. The considerable challenges of this system are security issues, abnormality, and service failure. Hence, the requirement of providing an effective system, which should be overcome these issues. This paper analyzes these problems and providing the paradigm in terms of enhanced communication paradigm, specifically propose Energy Aware Smart Home (EASH) framework. With this work, the problem in communication failures and types of network attacks are analyzed in EASH. With the utilization of the machine learning technique, the abnormality sources of the communication paradigm are differentiated. To evaluate the performance, we analyze the proposed work based on its accuracy, performance, and efficiency. Hence, we obtain better results especially the result shows an 85% accuracy rate. In the future, we try to enhance a high accuracy rate for further development.

Introduction

The advancement in modern technology enables effective communication to every field, in specific the Cyber-Physical System is a novel platform to provide a better platform to share and transfer information from one end to another via the different communicational channel. This technology enables advancement in communication transferring platforms; therefore, the development of the economy is reached a high destination. However, security and resiliency is still challenging and should be considered for security enhancement processes. The two considerable factors [1] of communication failure are security and component failures. The hackers or intruders enable malicious activity towards the CPS system; meanwhile, the development of it is tremendous and omnipresent in modern societies. Hence, security failure is a serious topic due to the abnormal behaviors of the system; however, the implications of these are not the same as other systems. Therefore, the development of new technology is to tackle these issues in terms of minimizing the attacks, providing security service, and protecting existing services by controlling abnormal behaviors. In this process, the parameter specification is the complex task of differentiation which needs the research on the CPS system based on its specific components [2-3], before incorporating with a holistic strategy. The modern world incorporated with tremendous development due to the emergence of technology. The technology growth provides huge benefits to the consumers; in specific, IoT is the platform for an effective communication process [4-5] that enables various devices for simplifying the difficulties in transferring information from source to source. However, the IoT has nowadays faced huge difficulties with the security issues are caused by component failures and malicious attack lead by attackers from outside. Lack of sensor nodes resources on the IoT, network complexity and communication available to the open wireless transmission is vulnerable to attack. The Intrusion Detection System (IDS) helps to identify the network of anomalies and take necessary measures to guarantee the security and dependability of the activity of IoT applications [6-7]. The

* Corresponding author.
E-mail address: khasim716@gmail.com (S. Khasim).

https://doi.org/10.1016/j.micpro.2020.103741
Received 7 November 2020; Received in revised form 18 December 2020; Accepted 22 December 2020
Available online 4 January 2021
0141-9331/© 2021 Elsevier B.V. All rights reserved.

objective of the work is to provide better development in the communication paradigm with IoT systems based on CPS in the field of Energy-Aware Smart Home System (EASH). In this system, the IoT system enables sensors or computer nodes that help to gage and communicate the consumption of energy in home electronic appliances. These measurement results are taken into the centralized node, which is acted as the coordinator node provide signals through the wireless medium or wired services. This coordinator node manages the entire result of the energy consumption rate in the house. Moreover, this result will be sent to the energy utility with the utilization of advanced metering infrastructure techniques. In this area, the process of communication between the consumer and the utility is being taken place. The utility is nothing but the Smart Grids to enable the consumer to determine their unit consumption in the home electricity. So, they can have control of their energy consumption in their house.

The integrity of the CPS is not stable due to sudden service failure caused by the components or the nodes. Therefore, the development of the fault diagnosing system is highly concentrated for maintaining its service and its abilities. The service failure is caused due to the nature of heterogeneity and wide service of the system. Moreover, an effective fault diagnosing system is required to overcome these issues. The conventional technique may not fulfill the necessity of providing high security to the system due to the complex and dynamic nature of the system [8][12]. The modern technique incorporates the sensor with an alarm facility is expected to provide better security than the traditional technique. Hence, the modern system enables machine learning techniques with IoT for fault diagnosing from its early stages. The machine learning technique can be provided with better results than human expertise provides. One of the machine learning technique is utilized for detecting the fault in the system is the Artificial Neural Network (ANN) technique with IoT. The most utilized Machine Leaning technique for predicting fault in the system is ANN, Radial Basis Function (RBF), and Support Vector Machine (SVM). However, various research is being utilized for enhancing the performance of the existing system, and high focus to reduce the fault with advanced technique. These days, CPS based research is being held for enabling effective fault diagnosing system in terms of detection, isolation, and recovery. The research should be focused on reducing the activities of malicious attacks of attackers, vulnerabilities in services, transmission problems between nodes, and control the packet growth which may lead to service breach. Hence, the appropriate system should require for mitigating these issues by utilizing machine learning with IoT based smart grid. Moreover, this research work should focus on cybersecurity and fault diagnosis. Therefore, the existing problem in EASH can be reduced in terms of detection mechanisms [9-11]. The abnormality of the system is identified from its early stage and takes an adequate step to reduce the existing problems of the system. Normal system behavior can be described by detecting anomalies in the condition assessment system or by using historical data used in intrusion detection mechanisms. Although the existing research is dedicated to the attack detection system, working with limited attacks and errors.

Literature review

In this section, we provide detailed information about various research articles are discussed based on this work

In this article, Yahya Al-Hadrami and FarrukhKhudairHussain [13] proposed a new technique to study existing datasets and their applications to IoT environments. Then, they introduced a framework for real-time data collection to create a dataset for IDS assessment and testing. The considerable advantages of the proposed dataset are that it consists of features explicitly designed for 6LoWPAN / RPL, which is the most commonly, used protocol in an IoT environment.

In this article, JunaidArshad et al. [14] have proposed one of the devices of limited intrusion detection energy of the energy structure which forms the basis of the ecosystem IoT. Given the ad hoc nature of these systems as well as emerging threats such as a complex botnet, they evaluate the feasibility of a mixture between the host (IoT devices) and advanced tools for effective intrusion detection while minimizing costs of energy consumption and communication. They implement the proposed framework with Contiki OS and conduct a rigorous evaluation of reciprocal evaluation yield potential. The results of the evaluation show that the proposed framework can reduce the burden of power and communications while enabling effective collaborative intrusion detection systems IoT.

In this article, Mr.Arafatour Rahman et al. [15] proposed a new technology based on the IDS system of the Internet of Things. Overcoming the limitations of IDS basis for resource-limited devices by providing two methods, semi-distributed and distributed, which combines high-performance feature extraction and selection with optimized resolution utilizing the potential of blurred edges. To transmit the processing work, they improve similar individual models of learning that correspond to a shared set of drive data. In the case of semi-distributed, the term advanced models are applied in parallel to select the features, followed by a single multilayer classification work in the fog. In distributed mode, the parallel model individually chooses the characteristics and classification of multilayer sensor after the output combined with coordinated edges final result. In light of a similar investigation of work while clarifying the mathematical outcomes and the rundown of proposed strategies, give SDI detection exactness comparable to senior centers, and shows the inherent barriers between accuracy and construction time.

In this paper, Wenjuan Li et al. [16] studied semi-supervised learning and designed DAS-CIDS by applying a disagreement-based semi-supervised learning algorithm to the CIDS system. During the evaluation, they examined DAS-CIDS performance using two datasets and real IoT network environments, both for detection performance and false-positive reduction. The experimental results showed that their approach was more effective than traditional supervised classifiers at detecting intruders and reducing false positives using unlabelled data.

In this article, Daming Li et al. [17] have proposed IoT extraction highlights and interruption recognition algorithms for the movement-based shrewd city in the learning model joins the profundity model of interruption location innovation with learning. As per the calculation of the accessible writing, a learning model demonstrating mapping relocation and information mining properties have been introduced in this article. In the test segment, KDD CUP 99 was picked as an assortment of trial information, and 10% of the information was utilized as preparing information. Simultaneously, the proposed calculation has been contrasted and existing algorithms. The outcomes indicated that the proposed calculation makes some shorter memories discovery and location productivity more prominent.

In this article, K.V.V.N.L SaiKiran et.al. [18] have proposed new work to build learning models of the machine proposed to identify network attacks IoT. In this model, they focused on the generation of the attack and the normal data IoT atmosphere [21]. A test bench was developed to imagine the environment Internet of Things based on MCUthe node ESP8266, DHT11 sensor, and the router or wireless connection [20]. The enemy structure was developed by a mobile structure that performed detective attacks and poisoning. The data collected by sensors such as humidity and temperature and the delivery spot, sent to the speak reflection platform and the wireless gateway was used [22]. In [1]the ordinary stage, the sensor esteems are obtained from the MCU node and shipped off think Speak server was put away and marked as expected information. At the time of the attack, the attacker could retrieve specific data with an enemy and modify system data that have been sent from the MCU server node and Think Speak. The media was performed man in the attack on the network based on ARP poisoning and entered data has been marked as training data.

Kelton AP da Costa et al. [19] proposed a new technique in which is based on rigorous, advanced literature on Internet-based machine learning techniques and intrusion detection for computer network

security [23]. Thus, the project focused on recent and in-depth searches for relevant articles on various intelligent methods and intrusion detection architectures applied to computer networks, with an emphasis on the Internet of Things and machine learning.

In the following table, we provide detailed information about techniques and their efficiency.

S. NO	Author	Technique	Accuracy	Objective
1	Al-Hadhrami, Yahya, and FarookhKhadeerHussain	6LoWPAN/RPL network, the most widely used protocol in the IoT environment.	98% accuracy it does not allow for real traffic evaluation	IoT-DDoS prevent three stages of attack related to IoT
2	Junaid Arshad	K-NN and K-Means	Minimize energy and communication overheads	To study the challenges in detecting intrusion for IoT
3	MdArafaturRahman	Dr., FAR, and TTBM	The accuracy is more than 90% rather to other	Detection rate(Dr.) is similar to the ratio of detected attacks
4	WeizhiMengWenjuan	DAS-CIDS and SSL algorithm	Provide better results than the other classifier	It is more effective in detecting and reduction of false alarm
5	Daming Li	SVM	The time and data clustering can be reduced effectively by the algorithm	An intrusion detection system (IDS) identifies the network troubleshooting
6	KVVNL SaiKiran	Decision tree and SVM	The data accuracy on the classifier model is 80%	IDS using the method to mention Man in Middle Attack on machine learning data (ML)
7	Kelton A.P. da Costa	the SVM method with CSOACNs	the accuracy rate of around 98%	CNN's have an excellent performance in image and high communication tasks

Proposed ML-based framework

In this section, the work provides a detailed description of the machine learning-based overall proposed model for the prediction of various attacks and faults. The previous study about the attacks on nodes shows that the attacks are identified is much harder due to the similar nature of normal nodes and malicious nodes in the communication channel. Here, the direct monitoring system is highly considered for overcoming the limitation of difficulties in diagnosing various attacks. Hence, a Machine learning-based diagnosing model is enabled to mitigate the attacks. This proposed work is incorporated with three levels, the first level deals with the normal, attack, and fault classes. The second level then manipulates different processing scenarios to create databases showing system functions in the default (normal), invalid (faulty), and attack classes. The third level is done with performance assessment datasets generated from a variety of supervised machine learning methods based on the classification process. This proposed model is based on the IoT-based CBS system for effective communication using effective machine learning techniques. To propose an effective technique using machine learning, different machine techniques are evaluated using different performance appraisal criteria here. Detailed information on the proposed machine learning diagnostic processes is shown in Fig. 1 below.

ML classification algorithms

In this section, we have analyzed several machine learning algorithms to evaluate them, focusing on the most relevant ones. Before discussing the particular algorithm, let's look at some machine learning algorithms most commonly used. Category classification algorithms are described briefly below.

A brief overview of ML classification approaches

A decision tree is a logical classification algorithm utilized by inductive logic to create a predictive model. Based classification model trees made the basis of classification of grades during training. A node in this tree is a function used for classification, and examples of each node root node are classified according to the attribute value.

They described ANN has three main aspects: its inputs, the activation function of different levels, The whole design and mass connected to each network level. the phase of learning, the input data adjustable weight of the network. These cases are constantly exposed on the Web so that networks learn from them. The widely used method for ANN is Multilayer Perceptron. Perceptrons are the node that calculates the number of weighted input and the value assigned to the output. If this amount is greater than the limit value, the output value is one, or else none. New Method for the algorithm classification was a Support Vector Machines and similar. The classifier of ANN aims to create over a plane

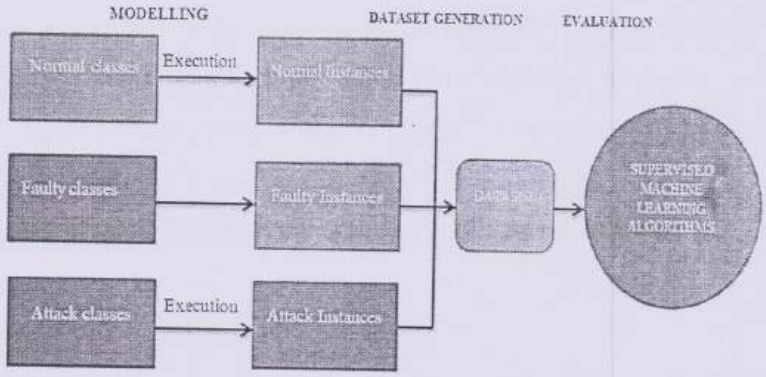


Fig. 1. shows the overall process of proposed work.

that split the categories of both data, maximize headroom, and thereby creating the possibility of a maximum distance between the aircraft and the presence of hyper. The method focuses to minimize generalization errors. Another category relates to statistical learning algorithms. Its main feature is a clear underlying probabilistic model that gives probability to any. The case to which he belongs. So the ultimate goal of these algorithms is to compute the probabilities of each presence in terms of its category. The general method to estimate the probability distribution using the image and predicted grade is the maximum entropy and discrete analysis.

Bayesian networks (BN) are considered a graphical model for the possible relationships between the groups of functions. This graphic model is a graph direct acyclic where nodes and edges elements of the relationship between the elements. Therefore, BN activities are based on the definition of the network structure and parameters and parameters of individual class learning. The encoding parameters are in the table for individual functions. The main features of the class are a slow learning process, because of the delay in the introduction of assessment. The nearest neighbor algorithm was the most common algorithm of this category, which can guess the presence of orders arranged by the nearby presence of previously evaluated. The advantage of this algorithm is a reduction in the time of training. For resolving the sample during qualifying they need the extension of time.

Selected classification algorithms

Select the algorithm to evaluate if it's executed by our comments on the described features of the data collection group. The indicate characteristics of the data set used are: (i) the static characteristics and (ii) nominal characteristics, the set of static data is not suitable for the use of e-learning algorithms. However, the algorithms are the same and used for two comparative tests and analyzed for simulation. Database created on a real-time data sample is larger than the data obtained from the simulation. Given the characteristics of our data set, we also use Evaluate the following supervisor classification algorithms:

J48: is a tree classification algorithm that utilizes a cut or uncut C4.5 decision tree as part of model training Classification. J48 enables a quick decision tree that addresses the subject with lost values and works well with nominal data sets.

Naive Bayes (NB): is a single Bayesian network (unidentified node) connected to the nodes which are the observed nodes. A strong case for this technique is that the network affiliates nodes are independent of the mother and the estimate was made in connection with the possible model for the characteristics of known order. Essential NB with fewer data and is therefore suitable for our data sets. Furthermore, as static data sets that are required category seems to be a reasonable option for the corrected mechanism

Multilayer perceptron (MLP)

This technique was the combination of Technical ANN is trained with the backpropagation algorithm (BP), which goals to identify the parameters (by weight) of a series of entries. An MNN comprises the biggest variables of units, which are considered the neurons. These are grouped into links containing entry-level information for output levels.

Multinomial logistic regression (MLG)

This technique was based on a classified superviser based on ANN techniques, which is developed while training where MLG of a ridge estimator is helping to classify instances. Particularly, this technique is very useful to deal with maximizing the likelihood estimator (MLE) in terms of peak estimator. With the detected value, the classifier can make the associate features to describe the instances with the corresponding target class.

Performance classes are utilized to produce values with the utilization of the WEKA tool). This is considered as a powerful tool of Introduction to science and industry

Selected algorithms execution parameters

Classification algorithms selected for team learning after the detailed test, a set of values of performance parameters based on their performance were selected. In particular, for each value of the parameter was selected, they focus on giving the best outcomes regarding precision, for the particular issue considered. To reproduce these experiments here, we provide all the performance parameters in Annex A were examined. This section of the appendix provides a detailed explanation of parameter execution for sorting algorithms selected.

Evaluation metrics

The prediction accuracy is highly essential for the evaluation process of a classifier. Dividing the dataset into training and testing is essential for the calculation of the accuracy based on prediction. Part of the training is considered in the development of the classification model, which is analyzed cases from the dataset. The second set is the testing phase, this is utilized for estimating the classifier performance. The results of prediction accuracy are considered into percentage calculation by calculation the total number of predictions. Then the performance of this technique is compared with other techniques by analyzing the results of prediction accuracy. As a result, with this result, the overall performance of the prediction process is measure easily. In this process, the entire datasets are divided into 75% data for the training phase and the remaining 25% data for the testing phase. The derived result will come after analyzing the sensitivity on training phase percentage divide on classification accuracy.

Here, the evaluation metrics are accuracy, kappa static value recall, and(k), precision. Initially, the observed precision is represented by (PO), measuring the accurate number for guess the global group of projections out classifier. The result was based on the percentage metric (%). In this process, dividing the datasets into two parts is vital to accuracy calculation. Then the next is Kappa Statistic Value, which is represented by κ and this is measured based on considering balancing data from the data sets and is the value is normal between 0 and 1. In this case, an imbalance is due to the huge amount of the body in normal data sets, since the normal behavior is that which is usually recorded. The evaluated value was mentioned below, where$p_e$is the

$$\text{Expected accuracy} : k = \frac{p_o - p_e}{1 - p_e}$$

Precision is a considerable performance metric, which is represented by calculating the true positive number divided by true positive added with the positives false number. Positives are false in cases where a design is mistakenly labeled as negative and is positive. reveal the data points with the results of our model is relevant.

The recall is represented by r_e, it is defined as the true positives number divided by the positives true plus number the false-negative number. Negatives false has been reported in which the model is negative when it is positive. Memory reveals can detect all matches in the dataset.

To clarify how expected accuracy (p_e), Observed Accuracy (p_o), Recall (r_e), and Precision (p_r) processed they use an actual model with both classes, as mentioned in Table 1. Quality, d is a true negative and

Table 1
Classification matrix example.

Predicted class / Actual class	Yes	No
Yes	a	b
No	c	d

Table 2
Sensitivity analysis matrix on training set percentage split on accuracy of the classification (Simulation).

Training set (%)	Classification algorithm (A)				
	J48	NB	MLP	MLG	AVERAGE
65	87.68	87.47	87.02	85.20	87.07
70	88.45	85.73	87.03	85.40	86.88
75	89.52	88.10	88.59	86.20	88.22
80	88.05	87.15	88.62	86.20	87.54

positive predictive mutually, and the b, values is a false negative and positive predictive respectively.

Calculation Precision (p_r) which is expected Accuracy (p_e), Accuracy observed (p_o), and Recall (r_e) given by the conditions attached to them:

$$\text{Precision} : pr = \frac{a}{a+c}$$

$$\text{Recall} : re = \frac{a}{a+c}$$

$$\text{Observed Accuracy} : p_o = \frac{a+d}{a+b+c+d}$$

$$\text{Expected Accuracy} : p_e = p_{ac} + p_{nc}$$

$$p_{ac} = \frac{a+b}{a+b+c+d}\frac{a+b}{a+b+c+d}$$

$$p_{nc} = \frac{c+d}{a+b+c+d}\frac{b+d}{a+b+c+d}$$

Simulation implementation & results

In the EASH system, the OPNET simulator tool is utilized for simulation purposes, where effective communication is executed by the ZigBee protocol. The star-topology can be built by using creating peripheral nodes with ZigBee End Devices (ZED) and creating a coordinating node with a ZigBee Coordinator (ZC). In our work, the peripheral nodes are acting as the monitoring tool in following the activities of specific appliances. The role of the coordinator node is for initializing the network and maintaining the incomings from the peripheral nodes. Once the initialization process is accomplished, the Scenario simulation node is configured to share measurements every minute.

Execution classes should be considered for an effective defect diagnosis process. These are normal class, faulty class, and attack class where normal represent N, faulty represent f, and attack represents A. Here, we discussed the faulty class, where F1 is caused by a failure that occurred due to the reason of functionality fault, F2 determined failure occurred by low energy, and the F3 occurred due to the reason of packet dropped failure. These failures are happening between the nodes in communication channels. Classes of attack are simulated by introducing an intermediate node of transformation between an edge node and the central coordinator. The attacker transmits packets received A1 (unchanged) from the sending node. SendtheA2 packets are discarded and payload packets A3 increases before being sent to the main coordinator. Then we exported all scenarios 25 network functions to create instances, every one of which is related to the execution class. Several organizations led to their data set. Then, 144 copies were made executing simulated scenarios. The sensitivity is measured by analyzing the size of the assembly and the accuracy of the training. They evaluated at 65%, 70%, 75%, and 80% of training data sets, developed to maintain a separation that should not replace our models and consider that the percentage of all of the training that has the highest accuracy average of (75%) of 88.22% Based on these observations, the correction is done by the percentage of the data trained, which leads to 25%, is used as the test data. For each machine learning algorithm considered, we reported accuracy, and kappa values were observed as a couple (in, k). Table 3 below provides a test case for the evaluation of the program in the experimental simulation: Case 1: normal attack (N over F3 F2 F1) case 2: normal every attack (N in connection with the A3 A2 A1), case 3: normal all attacks against all errors (N vs F3 F2 F1 A3 A2 A1).

More statistics for accuracy and recovery for the same algorithm and scoring choice presented by pairs (Table 4) (pr, Re) and the average yield at the end. They conclude that the solution is very trustful; since there are four relevant standards algorithms of accuracy over 86%. On average J48 algorithm accuracy and precision exceed other algorithms E Remember that the average is 0.906 and 0.886 respectively. Table 5 shows the results of the algorithm J48 and housing 1. AT appears in the algorithm cell cannot distinguish two categories according to the rows and columns of cells, and if the algorithm F cannot distinguish between the two categories. Does not differ for applying to the situations of the same class (in diagonal marked -). classifier J48 and 1 case, all cases were correctly classified, except in the case of failure low power (F1) which has been incorrectly classified as a case of packet loss error (F3) and vice versa. In the same way, we have built a table for each of the algorithms and the cases examined.

Testbed implementation & results

At the same as in the simulation environment, the test detection using real products. In this strategy, raspberry PI3 B more through Bluetooth includes CC2650 three label sensor for detecting, humidity values and temperature values (device nodes), MacBook collect and values are distributed and the working wire shark monitoring tool. For the constant test, the kind of anomalies executed by errors attacks is failures (F3) packet down and Low Energy fault (F1) for determining the class was (F) broken and (A2) sink Attack, modified communication (A3)to set the class attack of class (a). Class and ordinary situations are updated by node periphery (formed by RPI) to get sticky and the temperature of the sensor and then make a TCP packet with the estimate so that it can be sent to the coordinator node.

Dataset made by examining the TCP packet exported received by Ethereal Network Protocol Analyser. This is a packet exchange between the edge node and the node coordinator. Some example is stored as a value (CSV) eats only TCP communication having different values separated. Each package was analyzed with descriptive characteristics of the relative value related to the plan of classes inspected by us on the project. F1 fault is simulated with a single communication interfere with peripheral node to shut off the power. Package Dropped Failures (F3) was simulated by setting the limit to a package building process that shows the quality of the packages being developed.

This attack was carried out by using spoofing (poisoning) of the Address Resolution Protocol (ARP), which allows an attacker to change the ARP table in node communication by dispatching a (spoof) of ARP. The reason for this attack is to interface the attacker's MAC address to the IP address of another host. In our application, the MAC address restricting the attacker with a default door. This attack permits an attacker to follow the casings of information on network traffic to change or stop any development. An intercept the communication between the terminal and the central node, A2 simulated behavior, blocking all traffic on the network, and A3, and change the size of

Table 3
Observed Accuracy (po) & kappa value (k) evaluation matrix (Simulation Cases).

Case	Classification algorithm (A)			
	J48(p_o, k)	NB(p_o, k)	MLP(p_o, k)	MLG(p_o, k)
1	(82.76, 0.75)	(89.66, 0.89)	(80.00, 0.77)	(75.86, 0.69)
2	(100.0, 1.00)	(94.40, 0.86)	(94.40, 0.83)	(94.40, 0.79)
3	(86.11, 0.72)	(80.55, 0.85)	(91.67, 0.85)	(88.89, 0.82)
4	(89.62, 0.85)	(58.20, 0.67)	(88.69, 0.62)	(86.38, 0.75)

Table 4
Evaluation matrix (Simulation Cases)Recall (re)& Precision (pr).

Case	Classification algorithm (A) J48(pr, re)	NB(pr, re)	MLP(pr, re)	MLG(pr, re)
1	(0.837, 0.818)	(0.960, 0.891)	(0.703, 0.792)	(0.761, 0.749)
2	(1.000, 1.010)	(0.972, 0.948)	(0.972, 0.934)	(0.972, 0.934)
3	(0.880, 0.867)	(0.819, 0.800)	(0.935, 0.937)	(0.903, 0.879)
Average	(0.906, 0.899)	(0.917, 0.872)	(0.900, 0.875)	(0.879, 0.854)

Table 5
Differentiation results for J48 &(1) (Simulation Case).

	W_t^N	W_t^{F1}	W_t^{F2}	W_t^{F3}
W_t^n	–	T	T	T
W_t^{F1}	T	–	T	F
W_t^{F2}	T	T	–	T
W_t^{F3}	T	F	T	–

Table 6
Sensitivity analysis matrix on training set percentage split on accuracy of the classification (Testbed).

Training Set (%)	Classification algorithm (A) J48	NB	MLP	MLG	AVERAGE
65	89.15	89.22	92.24	87.79	89.65
70	89.20	89.10	92.33	86.72	89.44
75	89.54	89.48	92.66	87.43	89.83
80	88.24	89.12	92.42	86.71	89.12

Table 7
Observed Accuracy (po) & kappa value (k) evaluation matrix (Testbed Cases).

CASE	Classification algorithm (A) J48(p_o, k)	NB(p_o, k)	MLP(p_o, k)	MLG(p_o, k)
1	(96.36, 0.98)	(92.73, 0.80)	(98.18, 0.85)	(96.37, 0.98)
2	(95.83, 0.96)	(97.92, 0.91)	(97.91, 0.99)	(91.66, 0.88)
3	(76.71, 0.64)	(78.08, 0.72)	(82.19, 0.78)	(73.97, 0.69)
Average	(89.64, 0.89)	(89.58, 0.88)	(92.76, 0.89)	(87.33, 0.88)

Table 8
Precision (pr) & Recall (re) evaluation matrix (Testbed Cases).

Case	Classification algorithm (A) J48(pr, re)	NB(pr, re)	MLP(pr, re)	MLG(pr, re)
Case#1	(0.963, 0.954)	(0.929, 0.938)	(0.979, 0.988)	(0.963, 0.954)
Case#2	(0.974, 0.949)	(0.976, 0.965)	(0.973, 0.965)	(0.933, 0.928)
Case#3	(0.785, 0.759)	(0.804, 0.772)	(0.911, 0.833)	(0.715, 0.725)
Average	(0.907, 0.887)	(0.903, 0.885)	(0.954, 0.915)	(0.870, 0.862)

Table 9
Differentiation results for J48 &(1) (Test Bed Case).

	W_t^N	W_t^{F1}	W_t^{F3}
W_t^n	–	T	T
W_t^{F1}	T	–	F
W_t^{F3}	T	F	–

packets sent.

With the use of Wireshark, a total of twenty-four features of each message sent and configured if comma separated our data set was collected. Each instance is associated with a class of simulation run when a package has been conquered. The number of cases that we have to collect real-time data sets is 589. In the same way as in the case of a simulated environment data set, sensitivity analysis we are training size of the joint work of the classification accuracy. The same training rates were taken as 65%, 70%, 75%, and 80%. The training data provides that the average accuracy result is 89.94%. Here, we execute 75% dataset for training and 25% dataset for testing as similar to the process of simulation evaluation. Moreover, similar to the simulation environment, the same supervised machine learning algorithm is utilized for the evaluation matrix. The various results of our work are shown below based on different tables.

Classification results analysis

In this process of observation analysis of the results are classified and obtained it is distributed by using the structure of the previous section. This experiment is divided into two parts. The first part is handling to analyze the category of near to anomaly (malfunction, attack), and the second part of our analysis was based on data. The analysis is performed both in the set of experimental data (based on simulation and benchmarking). The experimental class explored for this analysis is common to two datasets. These are: electricity (F1), normal (N), packet error (F3), struck again (A2), and the attack on the third party message (A3).

This particular, in the initial stage of this investigation, we want to find categories of violations c according to these principles for a model intended to distinguish between a typical class and a single class extra-terrestrial. The clustered anomalies categories likewise refer to matches that require additional data (even the highlights shown) to effectively classify. The second aspect of the clip hopes to peek at the characterization performed by a particular algorithm (MLP) by placing the highlights in the records as evidenced by their meaning in the clustering. To do this, we evaluate position the salient features based on two regular positioning of pending plans: profit rate and gain information.

Similarity analysis of abnormality classes

In the initial segment of investigation, they concentrate on how to combine the class anomalies (errors and attacks) that can be characterized along these lines with the calculation because it highlights their basic share. The philosophy we have the following experiment. The proposed work is to establish a set of preparation consisted of typical and damaged examples Fi class like that. As recently saw, disability class regarded as F1 and F3 for the evaluation. Utilizing this preparation we set at the time of the train models utilizing the MLP. Assessment is done by utilizing the only offensive opportunity of A2 and A3. Models to establish their place of attack in the stock access classes for abnormal or normal characterized by prepared class are damaged.

Case ready circulated information on grouping the zone specified by the model is ready. The trial results were introduced in Fig. 1, in which the area is determined by the typical grouping, defects, and assault occasion. Blue (put in the figure below left) and red (inserted in the upper right image) sample (separated with a picture of 'x') structure of a typical classroom arrangement zone and damaged (resp.) in each situation. The cases marked with the "square" image shows how instances of the class indicated attacks. In that, in certain circumstances the incidence of assault named regular or as an example of the problem in both experimental settings, when it: (a) the incidence of attacks grouped under regular classes and can then be separated from the chance of disability in the two settings; or, for example (b) the attack was prepared under the class of problems and in this way a class attack cannot be separated from the class of problems. Finally long, contrastingly composed when cases of attacks in the two settings for certain situations, at that time we lead further tests to decide the highlights that may allow separation of classes.

Simulation and testbed

Model of NF1 (Figs. 4b, 2 a): they understand that both instances of the class assault (A3 and A2) for two datasets are marked in the order of the F1 problem. Furthermore, we reasoned that list they considered inadequate ability to separate the two classes of attacks F1. ModelsNF3 (Figs. 4d, 2 c): For this situation, they can understand that the incidence of assault class (A2 and A3) is arranged in various groupings more recreational zone and setting the testbed. In particular, the incidence of grade A3 and A2 are grouped below class shortcomings F3in the re-enactment and settings tested separately. By ratings more closely, it turns example A2 could not be separated for their TCP highlighting, for example, the sequence number (SEQ). Then again, the event A3 is not separated because of their highlights describes conditions around the world in the organization of our throughput and delay. So we reconsidered two situations to re-prepare their models with more or fewer highlights. *Re* NF3A2 ratings:Fig. 3 presents the results of the reassessment NF3 models to order A2 dataset example of reproduction by: (I) including SEQ highlight, (ii) eliminate the highlights world wide, and (iii) maintain just ten highlights the most critical. In each of the three analyzes, the results improved as A2 occurrences separated from F3 and grouped in a typical characterization of the region.

Re NF3A3 ratings: Fig. 4 shows the results of the re-prepare of the NF3 models for cases of A3 reservations dataset of test bed by including (i) delay highlight, Features (ii) Throughput, and (iii) Delay and throughput Features. By these studies, the results have not increased as events F3 separates A2 and are indicated for the control zone). As a result, highlighting additional may be considered to arrive at the separation between the classes (F3 and A3). The comparable test should perhaps more exploration arrangements similar to alternative clustering algorithms utilize either or include or omit dataset highlights.

Feature-based analysis

In this portion, they focus on the evaluation of the centrality of the highlights in terms of arrangements made for example the evaluation of their data set in two parameters, MLP is used for characterization algorithms. Before we venture into the results obtained, we provide an overview of the intended position of the elements used for the assessment and the way he leads. The positioning element of the map used is the information and gains Ratio. On the other hand, the position of the gigantic components by recording the quantity reduces the expected entropy classes. The number of classes is depending on the prices of entropy in the assessment was conducted. While holding, which positioned incentives of the two plans we register normally for every element and we have a normal sort of incentive to determine the five most important highlights of case assessment for the two datasets.

Case experimentally used for assessment were: (1): Normal (F3F1 vs N)Vs Every fault, Case (2): Every Attack Vs Normal(A2 A3vs N), (3): Every Attacks Vs Every mistake Vs Normal while five highlights removed by case basis and are recorded in Table 10. The dataset given their respective trademark and follow the line component ratings are presented in the manner in which the task of differentiation is done for cases of evaluation of the two datasets:

Simulated

Testbed

Case: 1 For recreation dataset occurrences, separation among ordinary and flawed classes is performed by zeroing in on highlights, for example, the traffic is generated, transmitted, and drop information, equally on the channel attributes such as delay in the network in general. Testbed for data set separation performed according to the time-sensitive highlights, for example, the general season of each frame and the full circle time, like the defer highlight of recreation dataset.

Case: 2 For example dataset reproduction, the separation between regular classes and the attack carried out on highlighting identified by the network node sends and receive with traffic generator.by separating the task and conclude the related time with testbed data set, for example, a full circle and the relative time, such as the number of edges, such as peak throughput datasets reproduction.

Case:3 For reproduction dataset examples, the separation performed over typical, assault, and the shortcoming classes are fundamentally performed by zeroing in on hub highlights, for example, the traffic created, bundles got, and drop. For dataset Testbed, the separation can be done by looking at the relevant time highlights, for example, the round trip time, time is relative, and the frame number, such as the traffic is generated peak recreation dataset.

Also, we realized that some of the traffic characteristics and feature significant delay and contribute to the task of differentiation in the same case and for the two data sets (Simulation Testbed). There is also a

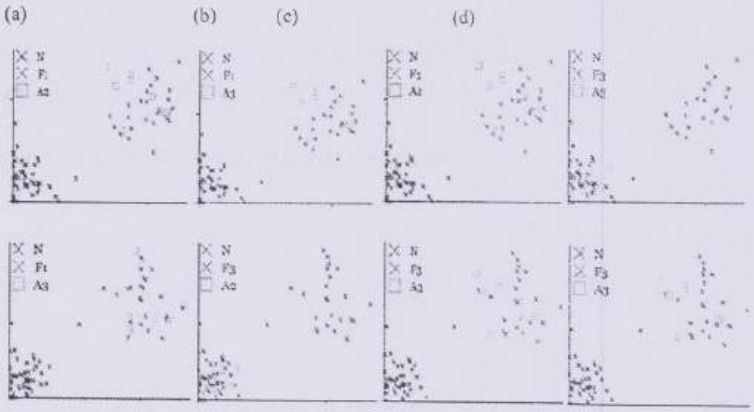


Fig.: 2. Simulation (first row) &Testbed (second row) Classification Areas for classifying attack instances on models trained with Normal and a Fault class.) Classifying A2 instances on N & F1 model (b) Classifying A3 instances on N & F1 model (c) Classifying A2 instances on N & F3 model (d) Classifying A3 instances on N & F3 model.

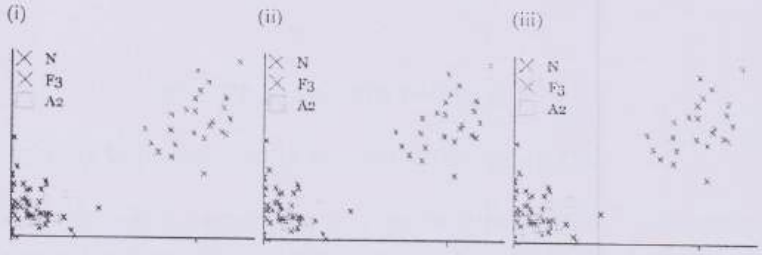


Fig. 3. Classification Results on re-evaluation of NF3 model (Simulation Dataset) Fig. 1c, with (i) SEQ feature addition (ii) Global Features Removal (iii) TOP 10 Features.

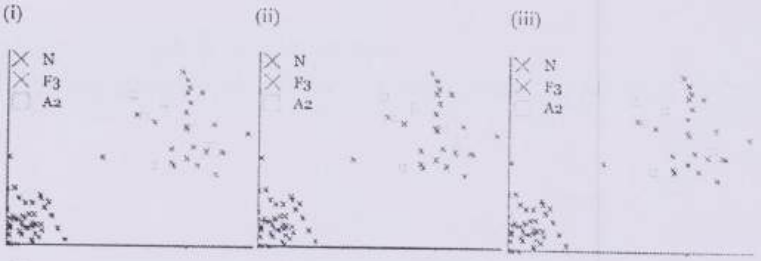


Fig. 4. Classification Results on revaluation of NF3 model (Testbed Dataset) Fig.d, (i) Delay (ii) Throughput (iii) Delay & Throughput.

Table 10
TOP 5 features per dataset case.

Simulation dataset (SD) Feature	Average value	Testbed Dataset (TD) Feature	Average balue
Case#1			
AC DATA SENT MAC	1	TCP ANALYSIS INITIAL RTT	0.8645
AC TRAFFIC DROPPED	0.90666	FRAME TIME RELATIVE	0.7855
AC TRAFFIC SENT APPL	0.90595	TCP TIME RELATIVE	0.7475
GLOBAL DELAY MAC	0.74395	TSVAL	0.644
GLOBAL E2EDELAY APPL	0.71975	TSECR	0.643
Case#2			
AC TRAFFIC SENT APPL	0.9075	TIME RELATIVE	0.86235
AC THROUGHPUT MAC	0.782	TCP ANALYSIS INITIAL RTT	0.75555
ESI DATA SENT MAC	0.762	TCP TIME RELATIVE	0.62855
ESI TRAFFIC RECEIVED APPL	0.792	FRAME NUMBER	0.59565
AC DATA RECEIVED MAC	0.79	TSVAL	0.52805
Case#3			
AC DATA SENT MAC	0.9976	TCP ANALYSIS INITIAL RTT	1.0442
ESI THROUGHPUT MAC	0.97535	FRAME TIME RELATIVE	0.8979
AC TRAFFIC SENT APPL	0.97515	TSVAL	0.8545
GLOBAL THROUGHPUT MAC	0.9382	TSECR	0.8439
AC TRAFFIC DROPPED	0.8248	FRAME NUMBER	0.8247

function, for example, traffic fell recreation and data set relative time in the dataset test, which is important for tax differentiation for a data set, but not in others. It is hoped that this trial as the state differs from the reproductive to the test. There is also counted as a fall in traffic simulation data sets and time on the set of test data, which is essential for the single dataset has different tax but not for all dataset. It is assumed that the different experimental imagination to the test. Finally, based on five functions to the case and set of data is mentioned in Table 10, reduction of measurement in the variation of both characteristics data sets is made to re-evaluate the performance of classification (MLP, J48, NB, MLG,) of algorithms, accurately observed by the terms. The four algorithms increased significantly with observed accuracy. The key case (Case # 3), enhanced the exactness of collection data imagination to 98% for every algorithm classification, whereas for a similar case the dataset tested increased to 87.0748% accuracy for J48 and MLP and NB MLG for 86.395%.

Conclusion

This article provides findings on the differentiation of labor between the anomalies affecting each system. Anomalies that are discussed in this paper may attack data or network attacks. The relationship between the type of anomaly and its impact on the system communication channel differentiation operator was studied and well-appointed. They are used for the approach based ML for classification of differentiation. The outcomes indicated the utilization of algorithms in the supervised machine learning was a positive methodology by separate between the harmed class and forceful with a serious extent of precision. The incorrect classification of cases with the same impact on the network and then analyzed, either in experimental settings (real-time simulation and testing), good for two classes of anomalies and characteristics examined. Our analysis shows that the ranking results can be further improved by adding or removing attributes from the dataset descriptive.

Declaration of Competing Interest

The authors declare that they have no known competing financial interests or personal relationships that could have appeared to influence the work reported in this paper.

References

[1] Alessio Netro, Matteo Flocco, Flavio Esposito, Guido Marchetto, An architecture for adaptive task planning in support of IoT-based machine learning applications for disaster scenarios, Comput. Commun. 160 (1 July 2020) 768–778.

[2] José Roldan, Juan Boubeta-Puig, Jose Luis Martinez, Guadalupe Ortiz, Integrating complex event processing and machine learning: an intelligent architecture for detecting IoT security attacks, Expert Syst. Appl. 149 (2020), 113251.

[3] Elhadj Benkhelifa, Thomas Welsh, Walaa Hamouda, A critical review of practices and challenges in intrusion detection systems for IoT: toward universal and resilient systems, IEEE Commun. Surv. Tutor. 20 (4) (2018) 3496–3509.

[4] Georgios Tertytchny, Nicolas Nicolaou, Maria K. Michael, Classifying network abnormalities into faults and attacks in IoT-based cyber-physical systems using machine learning, Microprocess. Microsyst. 77 (September 2020) 103121.

[5] Syeda Munira Thein, Hadis Karimipour, Petros Spachos, Machine learning-based solutions for the security of internet of Things (IoT): a survey, J. Netw. Comput. Appl. 161 (1 July 2020), 102630.

[6] Syed Rizvi, Ryan Pipetti, Nicholas McIntyre, Jonathan Todd, Ivonna Williams, the Threat model for securing the internet of things (IoT) network at device-level, Internet Things 11 (September 2020) 100240.

[7] Daming Li, Lianbing Deng, Wenlian Liu, Qinglina Su, Improving communication precision of IoT through behavior-based learning in a smart city environment, Future Generat. Comput. Syst. 108 (July 2020) 512–520.

[8] Francesco Meneghello, Matteo Calore, Daniel Zucchetto, Michele Polese, Andrea Zanella, IoT: internet of Threats? A survey of practical security vulnerabilities in real IoT devices, IEEE Internet Things J. 6 (5) (2019) 8182–8201.

[9] M.M. Rathore, A. Paul, W.-H. Hong, H. Seo, I. Awan, S. Saeed, Exploiting IoT and Big Data analytics: Defining Smart Digital City Using Real-Time Urban Data, 40, Sustainable Cities Soc, 2018, pp. 600–610.

[10] Lin Li, Real-time auxiliary data mining method for wireless communication mechanism optimization based on Internet of things system, Comput. Commun. 160 (1 July 2020) 323–341.

[11] Syed Rizvi, Ryan Pipetti, Nicholas McIntyre, Jonathan Todd, Ivonna Williams, the Threat model for securing the internet of things (IoT) network at device-level, Internet Things 11 (September 2020) 100240.

[12] Chaolong Zhang, Yigang He, Bolun Du, Lifen Yuan, Bing Li, Shanhe Jiang, Transformer fault diagnosis method using IoT based monitoring system and ensemble machine learning, Future Generat. Comput. Syst. 108 (July 2020) 533–545.

[13] Yahya Al-Hadhrami, Farookh Khadeer Hussain, Real-time dataset generation framework for intrusion detection systems in IoT, Future Generat. Comput. Syst. 108 (2020) 414–423.

[14] Junaid Arshad, Muhammad Ajmal Azad, Muhammad Mahboubi Abdeljaul, Khaled Salah, An intrusion detection framework for energy-constrained IoT devices, Mech. Syst. Signal. Process. 136 (2020), 106436.

[15] Md Arafatur Rahman, A. Taufiq Asyhari, L.S. Leong, G.B. Satrya, M. Hai Tao, M. F. Zolkipli, Scalable machine learning-based intrusion detection system for IoT-enabled smart cities, Sustain. Cities Soc. 61 (2020), 102324.

[16] Wenjuan Li, Weizhi Meng, Man Ho Au, Enhancing collaborative intrusion detection via disagreement-based semi-supervised learning in IoT environments, J. Netw. Comput. Appl. 161 (2020), 102631.

[17] Daming Li, Minhang Lei LianbingDeng, Haodong Wang, IoT data feature extraction and intrusion detection system for smart cities based on deep migration learning, Int J Inf Manage 49 (2019) 533–545.

[18] KVVNL Sai Kiran, R.N. Kamakshi Devisetty, N. Pavan Kalyan, K. MukundiniI, R. Karthi, Building an Intrusion Detection System for IoT Environment using Machine Learning Techniques, Procedia Comput. Sci. 171 (2020) 2372–2379.

[19] da Costa, A.P. Kelton, et al., Internet of Things: a survey on machine learning-based intrusion detection approaches, Comput. Netw. 151 (2019) 147–157.

[20] J. Lin, W. Yu, N. Zhang, X. Yang, H. Zhang, W. Zhao, A survey on the internet of things: architecture, enabling technologies, security, and privacy, and applications, IEEE Internet Things J 4 (5) (2017) 1125–1142.

[21] Y. Sahni, J. Cao, S. Zhang, L. Yang, Edge mesh: a new paradigm to enable distributed intelligence in the internet of things, IEEE Access 5 (2017) 16441–16458.

[22] Faiq Khalid, Syed Rafay Hasan, Osman Hasan, Muhammad Shafique, SIMCom: statistical sniffing of inter-module communications for runtime hardware trojan detection, Microprocess. Microsyst. 77 (2020), 103122.

[23] Georgios Tertytchny, Nicolas Nicolaou, Maria K. Michael, Classifying network abnormalities into faults and attacks in IoT-based cyber physical systems using machine learning, Microprocess. Microsyst. 77 (2020), 103121. ISSN 0141-9331.



Thanks, Jyoti Atul is currently working as a Faculty in the Department of Engineering Science (Mathematics) at Bharati Vidyapeeth's College of Engineering, affiliated with SPPU University, Lavale, Pune, Maharashtra, India. She is pursuing a Ph.D. in Mathematics. She has a total of 19 years of teaching and 6 years of research experience. She has over 4 research publications and 3 books to her credit, filed 5 patents, and Published 3 national patents in IP India Journal and 1 international patent in IP Australia. She contributed as a Resource Person for Development of Mathematics Practical Manual for *B.Sc.* B.Ed. held at NCERT. She has delivered a guest lecture on "Mathematical Software Awareness" to *M.Sc.* mathematics students and also she has delivered a keynote lecture on "Getting to Equal-Promoting Gender Equality through Human Development" in STTP. She is a member of the Board of Studies of Bharati Vidyapeeth (Deemed to be University). She is a member of seven professional bodies and an advisory member in two private Ltd companies. She has presented many research papers at national international conferences. She has organized an international online webinar on "Tracing of Curves", an online session on "NDLI USER AWARENESS" and many industrial visits.



Dr. R. Kamalraj received his Bachelor of Engineering in CSE in the year 2002 from Bharathiyar University. In the year 2009, he has completed his Master of Engineering in CSE from Anna University. After then, he received a Ph.D. degree from Anna University in the year 2017. He is having more than 15 years of experience in the teaching field. During that, he has presented many papers at National and International conferences and he published papers in International Journals also. He is a member of in 'Indian Society of Technical Education'. Currently, he is working as an Associate Professor in the School of CS & IT at Jain University, Bangalore, Karnataka, India.



Dr. G. Ramesh is currently working as an Associate Professor in the Department of Computer Science & Engineering, Gokaraju Rangaraju Institute of Engineering and Technology, Hyderabad. He received his B. Tech degree in information technology from RGMCET, Nandyal, Kurnool Dist. Andhra Pradesh and He received his M. Tech degree in Software Engineering from JNTUA College of Engineering, Anantapuramu, Andhra Pradesh, India, He received his pH. D from JNTUA, Anantapuramu, Andhra Pradesh, India. His-main research interest includes Software Engineering, Machine Learning, and Big Data. He is in teaching since 2008. He has published several papers in various international journals/ conferences. He is a life member of IAENG.



Dr.K.Sakthidasan Sankaran is an Associate Professor in the Department of Electronics and Communication Engineering at Hindustan Institute of Technology and Science, India. He received his B.E. degree from Anna University in 2005, M.Tech. Degree from SRM University in 2007 and Ph.D. Degree from Anna University in 2016. He is a Senior Member of IEEE and a member of various professional bodies. He is an active reviewer in Elsevier Journals and an editorial board member in various international Journals. His research interests include Image Processing, Wireless Networks, Cloud Computing, and Antenna Design. He has published more than 20 papers in Referred Journals and International Conferences. He has also published three books to his credit.



Mr. SUDHIR SHARMA, received a B.E. (IT), Masters of Engineering degree in Software engineering and currently pursuing a Ph.D. degree in Computer Science Engineering from Birla Institute of Technology, Mesra, Ranchi, India. His-paper has been selected for the Second Best Paper award from the NCCS-2019 in the LNE series Springer Nature, Singapore. His-research interest includes Machine learning, soft computing, and automata theory.



Dr.Syed Khasim, Obtained a Ph.D. degree in Computer Science & Engineering from Rayalaseema University, Kurnool, Andhra Pradesh, India. At present, working as a Professor in the Department of Computer Science & Engineering at Dr.Samuel George Institute of Engineering & Technology, Markapur, Andhra Pradesh, India. Having 16 years of experience in Teaching and Research. Published Various National and International Journals. His-research interests include Software Engineering, algorithm design, and analysis, the Internet of things, Machine learning & AI.

Source details

Microprocessors and Microsystems

Formerly known as: Microprocessors

Scopus coverage years: from 1978 to 2023

Publisher: Elsevier

ISSN: 0141-9331

Subject area: Computer Science: Computer Networks and Communications | Computer Science: Hardware and Architecture | Computer Science: Software | Computer Science: Artificial Intelligence

Source type: Journal

CiteScore 2022
4.9

SJR 2022
0.488

SNIP 2022
0.882

View all documents > | Set document alert | Save to source list

CiteScore | CiteScore rank & trend | Scopus content coverage

Improved CiteScore methodology

CiteScore 2022 counts the citations received in 2019-2022 to articles, reviews, conference papers, book chapters and data papers published in 2019-2022, and divides this by the number of publications published in 2019-2022. Learn more >

CiteScore 2022

4.9 = 6,017 Citations 2019 - 2022 / 1,239 Documents 2019 - 2022

Calculated on 05 May, 2023

CiteScoreTracker 2023

6.4 = 8,037 Citations to date / 1,253 Documents to date

Last updated on 05 December, 2023 • Updated monthly

CiteScore rank 2022

Category	Rank	Percentile
Computer Science — Computer Networks and Communications	#125/379	67th
Computer Science — Hardware and Architecture	#66/169	61st

View CiteScore methodology > | CiteScore FAQ > | Add CiteScore to your site

ARTICLE IN PRESS

Materials Today: Proceedings xxx (xxxx) xxx

Contents lists available at ScienceDirect

Materials Today: Proceedings

journal homepage: www.elsevier.com/locate/matpr

Numerical approach for avascular tumor growth with glucose and oxygen effect

Jyoti A. Dhanke [a,*], Neeta D. Kankane [b]

[a] SPPU, BVCOE, Lavale, India
[b] MIT-World Peace University, India

ARTICLE INFO

Article history:
Received 11 October 2020
Received in revised form 28 October 2020
Accepted 2 November 2020
Available online xxxx

Keywords:
Proliferation
Oxygen and glucose concentration
Finite difference method
Avascular tumor
Cell growth

ABSTRACT

Mathematical modelling and numerical approach can play a very vital role to express a mathematical formulation and explanation. The calculation of tumor cell growth and proliferation has been considered generally in early stage, both experimentally via the multicellular spheroid review, and theoretically using mathematical modeling formulation. Short oxygen levels in tumor cells may be a basic cause of uncontrollable avascular tumor progress in some cancers. In this numerical approach of this study for the development of tumor involving the effects of oxygen and glucose concentration together is analyzed on a mathematical model. Also, the new mathematical model implicates a different representation of cell development, which reproduces contact inhibition of migration and tumor cell growth. The mathematical model is solved numerically using finite difference scheme and further the magnitudes of parameters are analyzed.
© 2020 Elsevier Ltd. All rights reserved.
Selection and peer-review under responsibility of the scientific committee of the Emerging Trends in Materials Science, Technology and Engineering.

1. Introduction

For an avascular tumor growth a changed mathematical model, initially proposed by Sherratt and Chaplain [5] is examined. Details are provided by Araujo and McElwain [4] on the chronological sequence in which mathematical models were advanced for avascular tumor growth. The procedure of avascular tumor growth factor by assuming weak glucose and oxygen effect as an additional formulation of cell death adds to the understanding for further study. Tumor growth requires the carry of nutrients (for instance oxygen and glucose) from waste products to the neighboring tissue Mueller-Klieser W. *et al.* [6]. Tumors and multicellular tumor spheroids can expand gradients in oxygen concentration and glucose concentration.

The oxygen consumption rates as well as tumor cells' growth rates were measured by Casciari JJ *et al.* [1] at various glucose and oxygen concentrations. Peng Feng *et al.* [2] examined the result of apoptosis of proliferating cells and necrosis of quiescent cells. A mathematical model is produced and studied by Tindall *et al.* [3] accounting for diffusion of nutrient, patterns in cell cycling rates, the two different paths to cell death also active and inactive motion of the dead cell. In this paper we discussed a numerical study into the evolution of a tumor cell growth during proliferation involving the effects of oxygen and glucose concentration together is analyzed on a mathematical model. A reaction diffusion model includes avascular tumor growth model from a tumor image. Aim is to improvise the support system that permits studying the tumor microenvironment constraints like movements of proliferating cells, quiescent cells.

2. Mathematical model of tumor growth

To represent some aspects of avascular tumor growth many mathematical models were developed. Generally it is assumed that tumor to have a spherical shape and have been used in most studies. The structure has a necrotic core covered by quiescent ring and proliferating cells on the outermost layer was proposed by Mitchell Acland *et al.* [9].

Schematic illustration is shown by Keng-Cheng Ang [8] of a multicellular tumor spheroid figure Fig. 1.

Tumors contain necrotic regions, regions of cells that are in a quiescent state and regions where cells proliferate rapidly. The result of a cell to convert into proliferating or quiescent depends

* Corresponding author.
E-mail address: jyoti.dhanke@bharatividyapeeth.edu (J.A. Dhanke).

https://doi.org/10.1016/j.matpr.2020.11.033
2214-7853/© 2020 Elsevier Ltd. All rights reserved.
Selection and peer-review under responsibility of the scientific committee of the Emerging Trends in Materials Science, Technology and Engineering.

Please cite this article as: J.A. Dhanke and N.D. Kankane, Numerical approach for avascular tumor growth with glucose and oxygen effect, Materials Today: Proceedings, https://doi.org/10.1016/j.matpr.2020.11.033

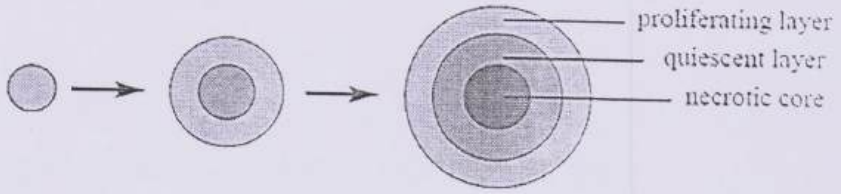


Fig. 1. Schematic illustration shown by Keng-Cheng Ang [8] of a multicellular tumor spheroid.

on oxygen and nutrient presence and on the availability of tumor necrosis factor, a substance generated by necrotic cells which inhibits growth of the tumor, as described by Wallace *et al.* [10].

This model depicts the cell densities which are represented by $n(x,t)$, $q(x,t)$ and $p(x,t)$ for the necrotic, quiescent and proliferating cells respectively, where x represents the spatial coordinate and t is time in a one-dimensional domain. It is seen that quiescent and proliferating cells are movable. Nevertheless, in a nearly closed-packed location like tumor spheroid, movement of cells can be controlled. In general cell flux considered as $-\frac{\partial}{\partial x}(p+q)$ of proliferating and quiescent populations. It is assumed that proliferating cells grow at a rate limiting to the total cell population, turning into quiescent at a rate depending on the concentration $c(x,t)$ of nutrients (glucose and oxygen) available and quiescent cells turn into necrotic at a rate dependent on $c(x,t)$.

The terms and their equations have been studied by Sherratt and Chaplain [5]; they are modified in more precise context of the expansion of structure surrounded by an avascular tumor with the effect of glucose and oxygen concentration. Further the following set of partial differential equations is produced.

$$\frac{\partial p}{\partial t}=\frac{\partial}{\partial x}\left(\frac{p}{p+q}\frac{\partial(p+q)}{\partial x}\right)+g_1(c)p(1-p-q-n)-f(c)p+g(c)q-h(c)p \tag{1}$$

$$\frac{\partial q}{\partial t}=\frac{\partial}{\partial x}\left(\frac{q}{p+q}\frac{\partial(p+q)}{\partial x}\right)+f(c)p-g(c)q-i(c)q \tag{2}$$

$$\frac{\partial n}{\partial t}=i(c)q+h(c)p \tag{3}$$

Here $c=C_{glu}+C_{oxy}$.

The concentration of glucose utilization decreases functioning into spheroid size and single exponential cells which are exposed to different concentrations of glucose at the time of measurement as

$$C_{glu}=\frac{\rho\mu^{\tau}}{\gamma+p}(1-\alpha(p+q+n)) \tag{4}$$

C_{glu} is glucose concentration studied by Freyer Jp [7].

$$C_{oxy}=\frac{c_0}{1+\gamma_1 p+\gamma_2 q}(1-\alpha(p+q+n)) \tag{5}$$

C_{oxy} is oxygen concentration is studied by M. A. J Chaplain and Sherratt, J. A. [5].

The functions $f(C)=K_p\left(1-\frac{C^{m_1}}{C_{crit1}^{m_1}+C^{m_1}}\right)$ is the rate of proliferating cells becoming quiescent, $i(C)=K_d\left(1-\frac{C^{m_1}}{C_{crit2}^{m_1}+C^{m_1}}\right)$ is the necrosis rate of quiescent cells, $g(C)=\frac{K_g C^{m_1}}{C_{crit1}^{m_1}+C^{m_1}}$ is the switching rate from quiescent cells reversing to proliferating cells, are adopted by Peng Feng [2].

3. Boundary conditions

Initial conditions at $t=0$, $q(x,0)=0$, $n(x,0)=0$, $c=1$, $p(x,0)=e^{-0.1x}$ and the density of proliferating cell decreases exponentially as x increases. As for the boundary conditions, it is assumed zero-flux at the boundaries. That is, $\frac{\partial p}{\partial x}=0, \frac{\partial n}{\partial x}=0$, at $x=0$ and as $x\to\infty$. The boundary conditions used at $x=0$ and $x=250$.

The system of equations (1) to (5) with boundary conditions is numerically solved by using the finite difference approximation method. The set of finite difference equations are obtained by using central differencing for space and forward differencing for time as follows.

$$p_i^{j+1}=p_i^j+\Delta t\left[u_i^j+g_1\left(c_i^j\right)p_i^j\left(1-p_i^j-q_i^j-n_i^j\right)-f\left(c_i^j\right)p_i^j+g\left(c_i^j\right)q_i^j-h\left(c_i^j\right)p_i^j\right]$$

$$q_i^{j+1}=q_i^j+\Delta t\left[v_i^j+f\left(c_i^j\right)p_i^j-g\left(c_i^j\right)q_i^j-i\left(c_i^j\right)q_i^j\right]$$

$$n_i^{j+1}=n_i^j+\Delta t\left[i\left(c_i^j\right)q_i^j+h\left(c_i^j\right)p\right]$$

$$C_{iglu}^j=\frac{\gamma\mu^{\tau}}{\gamma+p_i^j}\left[1-\alpha\left(p_i^j+q_i^j+n_i^j\right)\right]$$

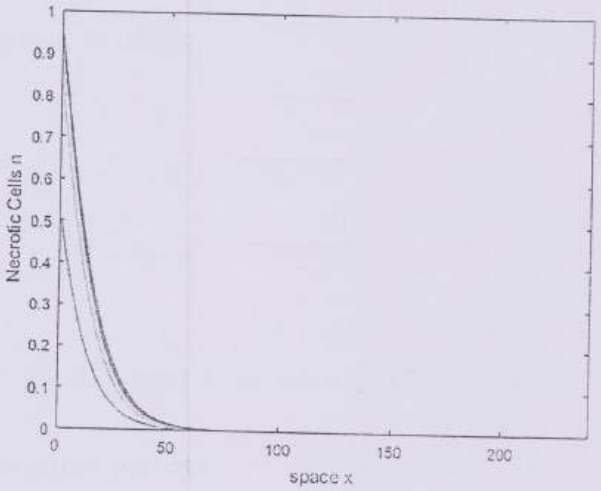


Fig. 2. (a) Without Glucose and Oxygen effect. (b) With Glucose and Oxygen effect. (c) Without Oxygen & with Glucose effect. (d) With Oxygen & without Glucose effect. 2(a), 2(b), 2(c), 2(d): Mathematical explanations of the model equations (1, 2, 3) as $\alpha=0.5, \beta=0.5, \gamma=10$ at $K_1=0.15$, $K_2=0.3$ and $p=e^{-0.1x}$. Cell densities of necrotic cells plotted as a function of space with no boundary conditions for n at time $t=0.2,\cdots,14$. With increasing time curves tend to move from left to right. The boundary conditions are considered at $x=0$ and $x=250$.

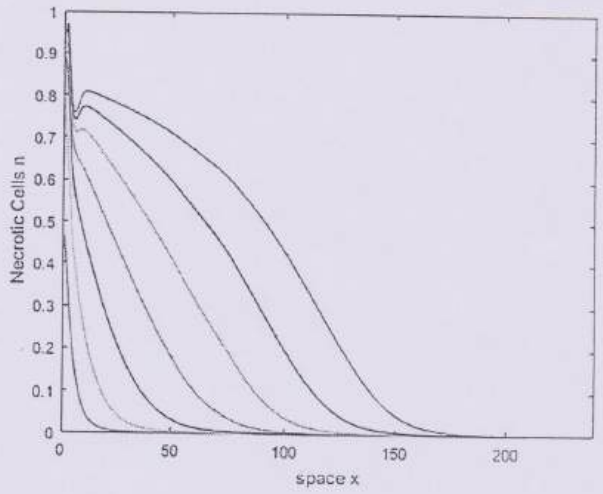


Fig. 2 (*continued*)

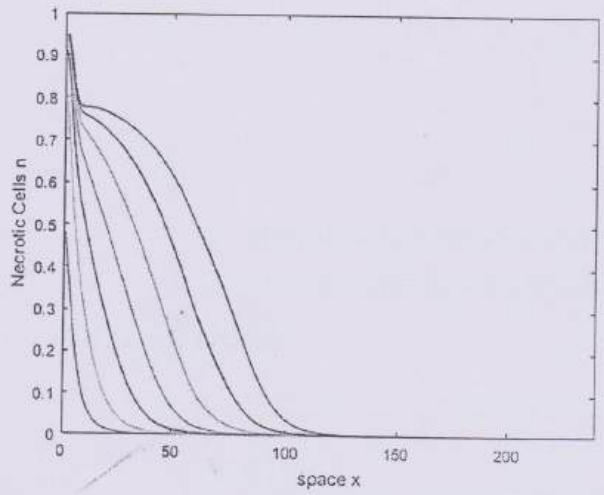


Fig. 2 (*continued*)

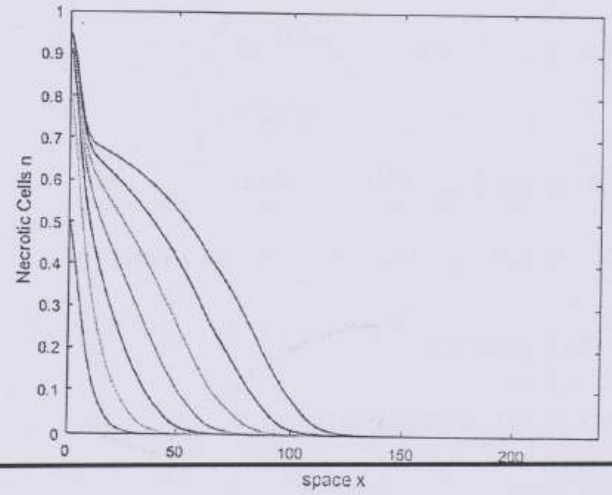


Fig. 2 (*continued*)

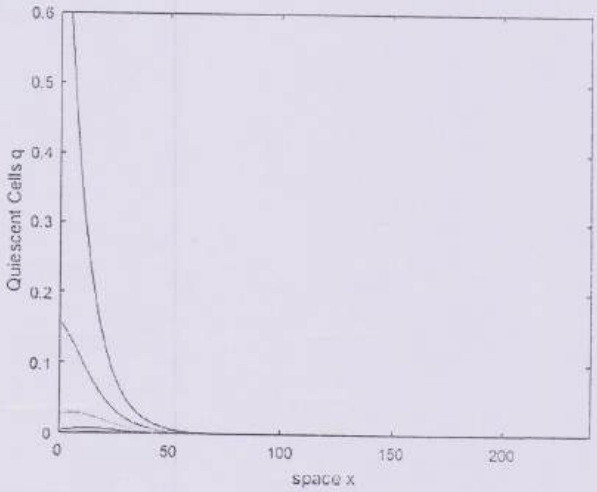


Fig. 3. (a) Without Glucose and Oxygen effect. (b) With Glucose and Oxygen effect. (c) Without Oxygen & with Glucose effect. (d) With Oxygen & without Glucose effect. 3(a), 3(b), 3(c), 3(d): Mathematical clarifications of the model equations (1, 2, 3) as $\alpha = 0.9$, $\beta = 0.5$, $\gamma = 10$ at $k_1 = 0.15$, $k_2 = 0.3$ and $p = e^{-0.1x}$. Cell densities of quiescent cells plotted as a function of space at some times $t = 0, 2, \cdots, 14$. With increasing time curves tend to move from left to right. The boundary conditions are considered at $x = 0$ and $x = 250$.

$$C^j_{ioxy} = \frac{c_0}{1 + \gamma_1 p^j_i + \gamma_2 q^j_i}\left[1 - \alpha\left(p^j_i + q^j_i + n^j_i\right)\right]$$

$$u^j_i = \frac{\left(p^j_{i+1} - p^j_{i-1}\right) r^j_i \left(r^j_{i+1} - r^j_{i-1}\right) + 4 p^j_i r^j_i \left(r^j_{i+1} - 2r^j_i + r^j_{i-1}\right) - p^j_i \left(r^j_{i+1} - r^j_{i-1}\right)^2}{4(\Delta x)^2 \left(r^j_i\right)^2}$$

$$v^j_i = \frac{\left(q^j_{i+1} - q^j_{i-1}\right) r^j_i \left(r^j_{i+1} - r^j_{i-1}\right) + 4 q^j_i r^j_i \left(r^j_{i+1} - 2r^j_i + r^j_{i-1}\right) - q^j_i \left(r^j_{i+1} - r^j_{i-1}\right)^2}{4(\Delta x)^2 \left(r^j_i\right)^2}$$

$$r^j_i = p^j_i + q^j_i$$

In the given finite difference equations the terms Δx and Δt are represented by space intervals and time steps respectively. The subscript and superscript for the dependent variables are present

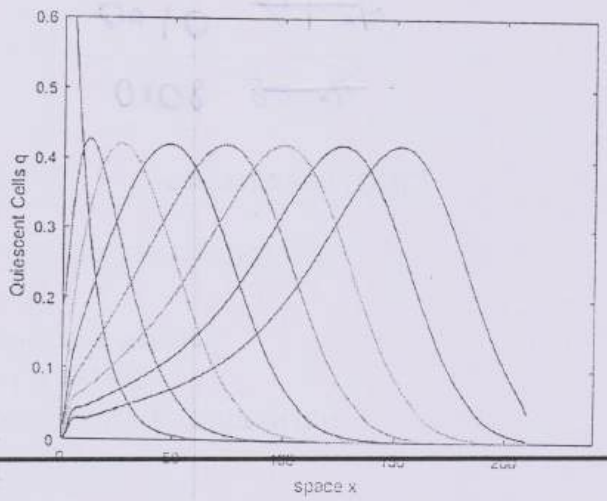


Fig. 3 (*continued*)

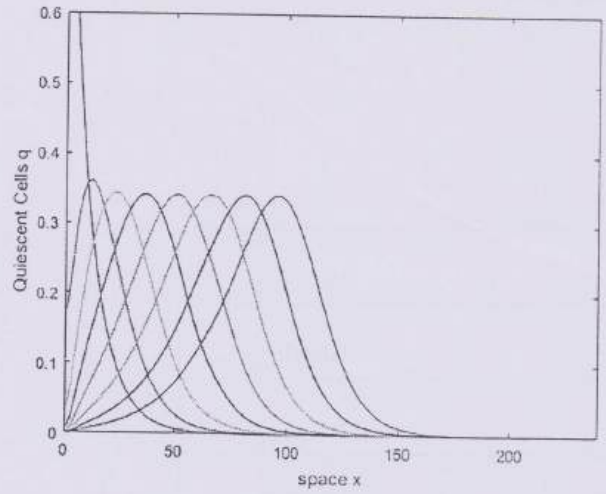


Fig. 3 (*continued*)

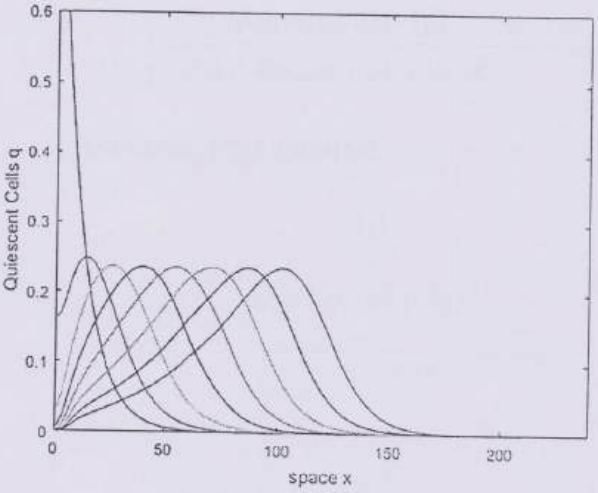


Fig. 3 (*continued*)

as space position x and time level t respectively. p_i^j refers to the density of the proliferating cells at the i^{th} space position and j^{th} time level. $\rho = 0.3 \times 10^2$ is constant parameter, $\mu = 0.47$ is constant parameter and we assumed $1 \leq \tau \leq 7$. $\alpha = 0.9$, $\gamma = 10$, dimensionless parameter, $\gamma_1 = \frac{k_2}{k_1} = 2$. positive parameter, $\gamma_2 = \frac{k_3}{k_1} = 0.4$, positive parameter, $c_o = 1$, $k_1 = 0.15$, oxygen degradation rate, $k_2 = 0.3$, oxygen consumption rate by proliferating cells, $k_3 = 0.06$, oxygen consumption rate by quiescent cells. For ease $\gamma_2 = (\frac{1}{5})\gamma_1$.

The oxygen is 0 for switching rate K_p. In the numerical simulations that follow, $K_p = 0.9$ as the standard value. $0 < K_d < 1$ is the maximum necrosis rate of quiescent cell, i.e. $K_d = 0.5$, K_q is switching rate as C is high. In the simulations that follow, here $K_q = 0.05$ as the standard value. Where $C_{crit1} = 0.5$ is the critical oxygen level proliferation, $C = 0.4$ critical oxygen level for necrosis, $m_1 = 3$, positive parameter which governs the sharpness of change $f(C)$ near the critical concentration and $h(C) = K_n$. as in [2] and $g_1(C) = \beta e^{\beta c}$ with $\beta = 0.5$ as in [5].

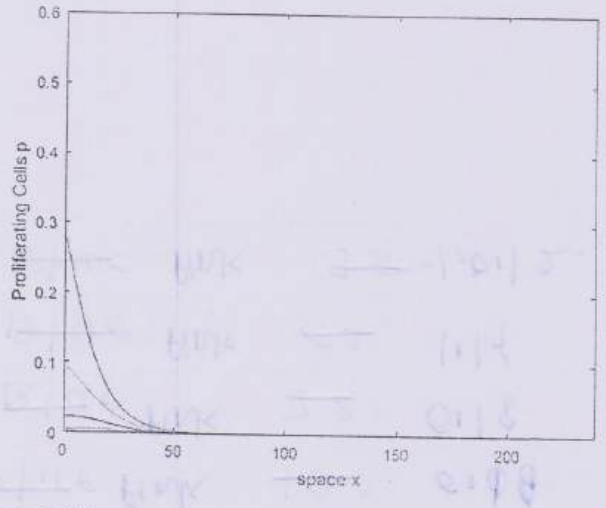


Fig. 4. (a) Without Glucose and Oxygen effect. (b) With Glucose and Oxygen effect. (c) Without Oxygen & with Glucose effect. (d) With Oxygen & without Glucose effect. 4(a), 4(b), 4(c), 4(d): Mathematical clarifications of the model equations (1, 2, 3) as $\alpha = 0.9$, $\beta = 0.5$, $\gamma = 10$ at $k_1 = 0.15$, $k_2 = 0.3$ and $p = e^{-0.1x}$. Cell densities of proliferating cells plotted as a function of space at some times $t = 0, 2, \cdots, 14$. With increasing time curves tend to move from left to right. The boundary conditions are considered at $x = 0$ and $x = 25$.

4. Graphical representation

Equations from (1) to (5) are solved with boundary conditions by using the finite difference schemes. Graphical simulations for the rate of transition from the quiescent cells'; glucose and oxygen consumption which take longer period were noted on MATLAB simulator. The graphical output for a mathematical model of avascular tumor depicts the variances in the growth of the tumor crowding of proliferating, quiescent and necrotic cells. Conveniently in the following graphs, line color represents cell density at various time t units,

$t = 14$(-), $t = 12$ (-), $t = 10$ (-), $t = 8$ (-), $t = 6$ (-), $t = 4$ (-), $t = 2$ (-).

Case 1: Fig. 2(a) demonstrates the result of without glucose and oxygen on necrotic cell density. Fig. 2(b) shows the result of both on necrotic cell density. Fig. 2(c) demonstrates the result of glucose without oxygen on necrotic cell density. Fig. 2(d) demonstrates the result of oxygen without glucose on necrotic cell density.

Case 2: Fig. 3(a) demonstrates the result of without glucose and oxygen on quiescent cells density. Fig. 3(b) demonstrates the result of both on quiescent cell density. Fig. 3(c) shows the result of glucose without oxygen on quiescent cell density. Fig. 3(d) demonstrates the result of oxygen without glucose on quiescent cell density.

Case 3: Fig. 4(a) demonstrates the result of without glucose and oxygen on proliferating cells density. Fig. 4(b) shows the result of both on proliferating cells density. Fig. 4(c) demonstrates the result of glucose without oxygen on proliferating cells density. Fig. 4(d) demonstrates the result of oxygen without glucose on proliferating cells density.

5. Visualizing tumor growth

In order to study the consequences of oxygen and glucose on the expansion of the avascular tumor, authors compared tumor cell thickness sketches at oxygen degradation rate at $k_1 = 0.15$ and oxygen consumption rate by proliferating cells $k_2 = 0.3$ at time $t = 4, 8, 14$. The growth pattern of tumor in tissue level is shown

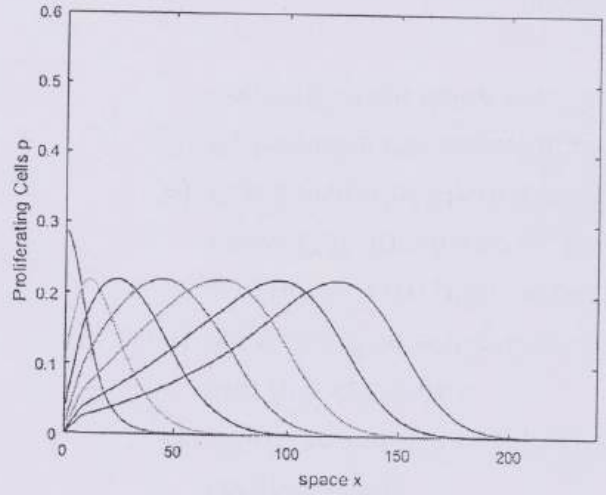


Fig. 4 (*continued*)

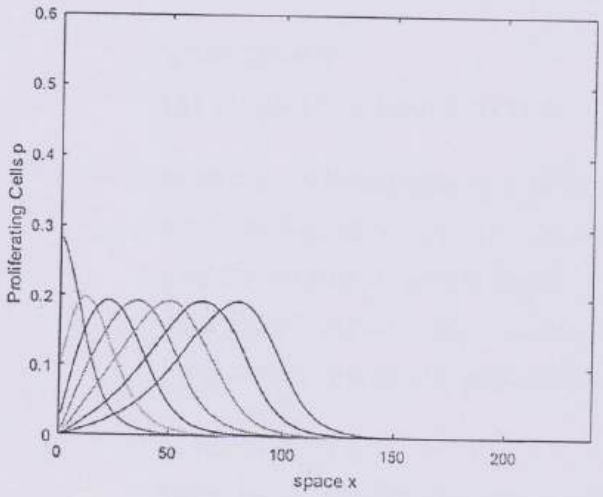


Fig. 4 (*continued*)

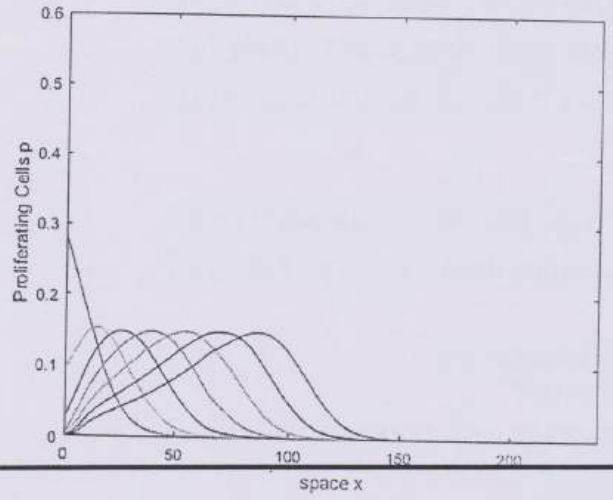


Fig. 4 (*continued*)

in image form. The series of snapshots generated is shown in Fig. 5 for $t = 4, 8, 14$.

The spreading of the tumor increases speedily as both glucose and oxygen present. At $t = 14$, the tumor radius is assumed to be small in size when both are absent, compared to when together present. The rate of degradation of glucose and oxygen increases, we observe reduction on necrotic region significantly.

The model is assumed to be 1D space by considering radial symmetry, although a figure can be generated of the cell distribution at any time$t$ in 2D or 3D space. At time t, the distribution of a cell type over the x space dimension is produced using this model. In this distribution, at any point $x = r$, cells could be distributed around

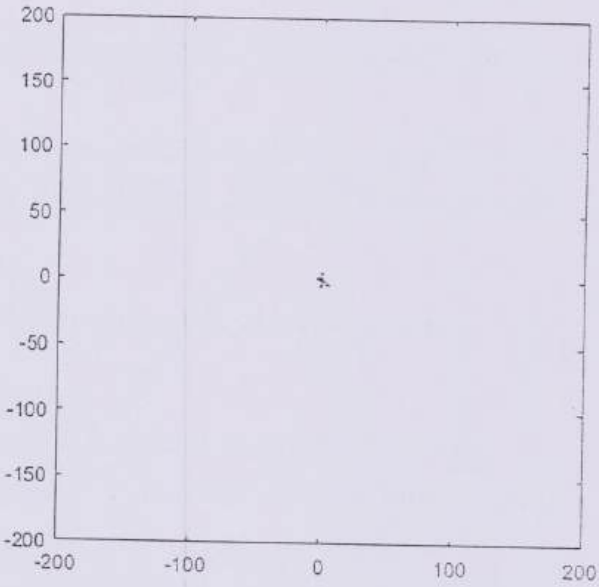


Fig. 5. Snapshots of simulated tumor growth at t = 4, 8, 16 units, with dots representing proliferating, quiescent and necrotic cells while studying the effect of glucose and oxygen respectively.

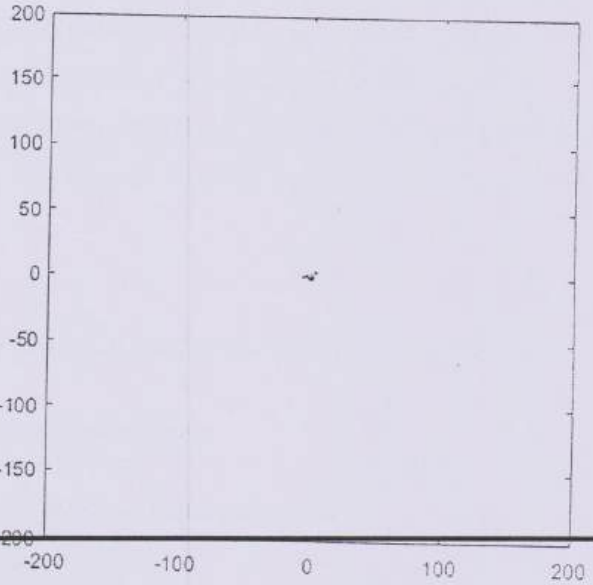


Fig. 5 (*continued*)

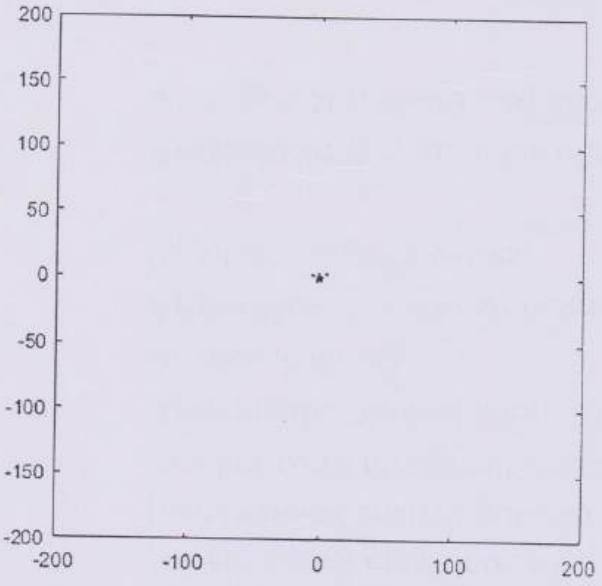


Fig. 5 (continued)

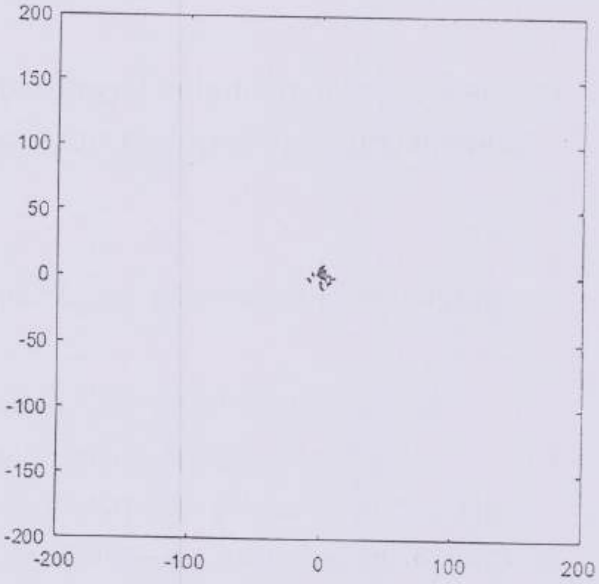


Fig. 5 (continued)

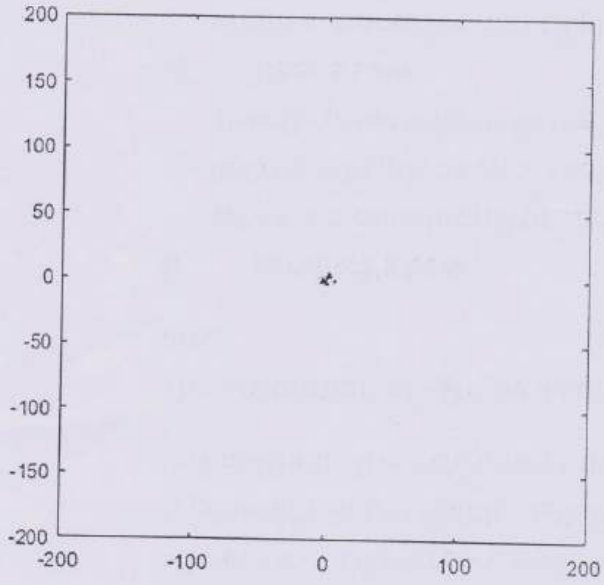


Fig. 5 (continued)

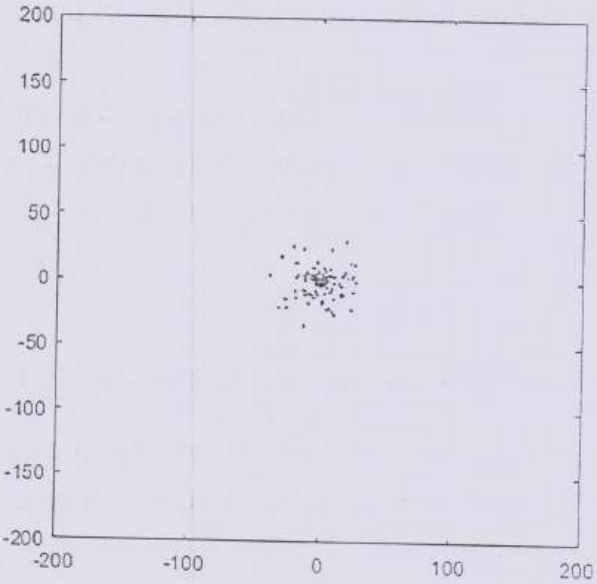


Fig. 5 (continued)

the circle having radius r. The number of proliferating cells at time $t = T$ and at position $x = r$ is assumed which is represented by $p(r, T)$. Cells are distributed along the boundary of the circle having radius r. It continuous for the complete range of values of x at different time intervals that shall produce a sequence of figures depicting the tumor development along with time.

6. Results and discussions

In this paper, we discussed numerical approach for the avascular growth of tumor that involves the various effects of oxygen and glucose concentration both having analyzed on a mathematical model. This model provides qualitative results that are further studied. By using a finite difference method the mathematical model is solved and the result is achieved on MATLAB. Results shown in the form of graphs and as a series of tumor pictures get improved in visualization. It is observed that as time rises the size of necrotic core grows and furthermore the amount of viable cells reduces in the presence of glucose and oxygen. Additional numerical results can be summarized as: (a) If the glucose degradation rate is high it decreases the range of necrotic section. (b) If the oxygen degradation rate is large expressively it reduces the range of necrotic section. (c) Rise in the critical oxygen concentration decreases the tumor growth rate.

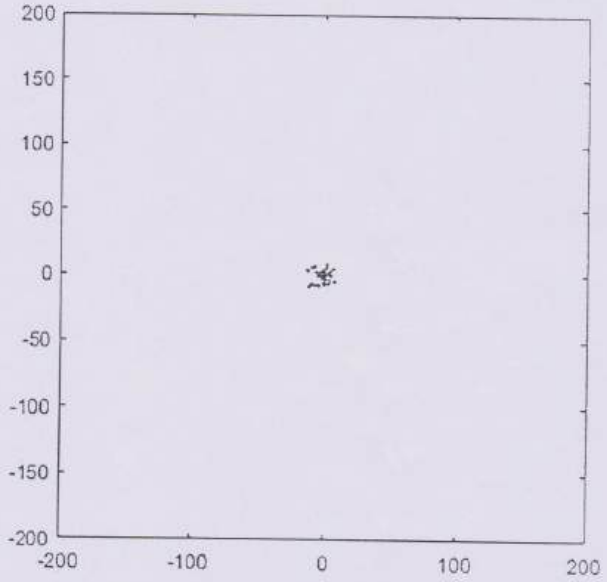


Fig. 5 (continued)

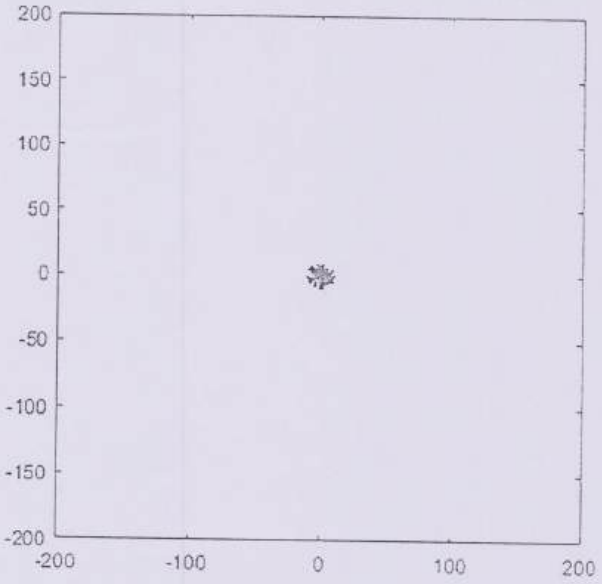


Fig. 5 (continued)

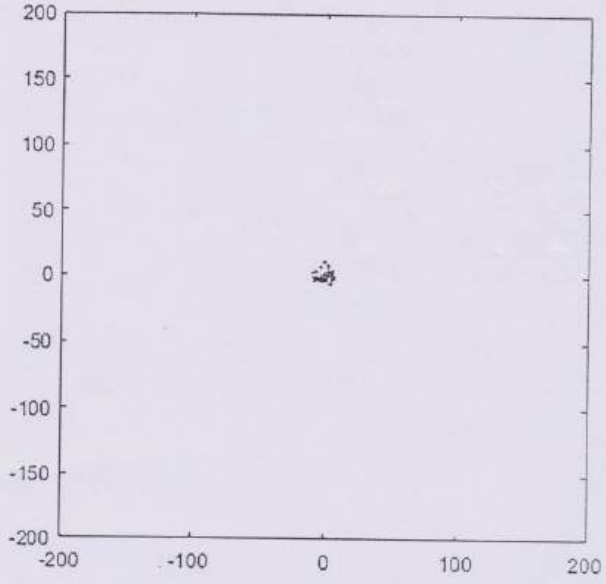


Fig. 5 (continued)

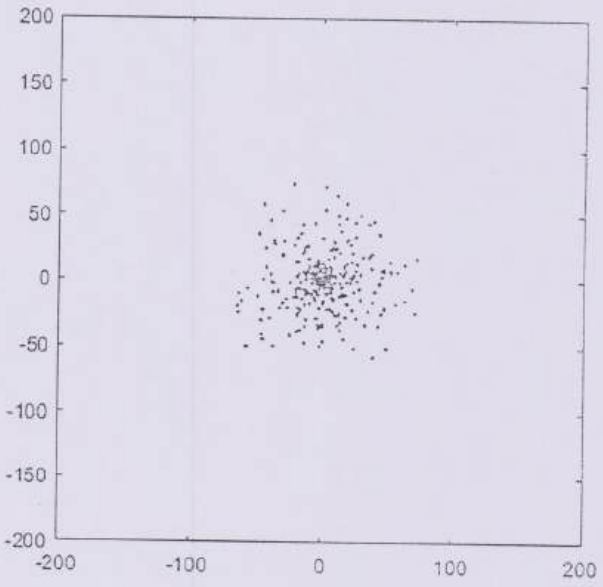


Fig. 5 (continued)

7. Conclusion

Complex formations of necrotic regions are seen to be scattered around the tumor core and are present in various regions in the proposed model. The mathematical model is solved with boundary conditions using a finite different scheme and executed on MATLAB. The results are obtained as graphs with the effect of glucose and oxygen and outcomes are presented as a series of tumor images for better visualization. A complete and multiscale cellular model of avascular tumor growth is developed in this proposed work.

The considered environmental parameters are oxygen and glucose concentrations for growth and inhibitory factors. Large degradation rate of oxygen and glucose expressively reduces the size of necrotic section. The model expects the existence states for cells within the microenvironment and proposes possible conditions for inhibitors and growth promoters and inhibitors which control cell-cycle. Proposed mathematical model that examines the effect of presence and absence of glucose and oxygen might help in the betterment of predictions of tumor growth.

Declaration of Competing Interest

The authors declare that they have no known competing financial interests or personal relationships that could have appeared to influence the work reported in this paper.

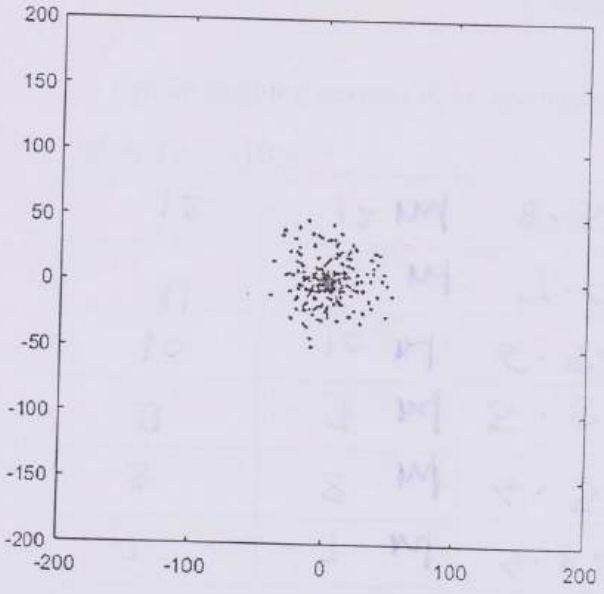


Fig. 5 (*continued*)

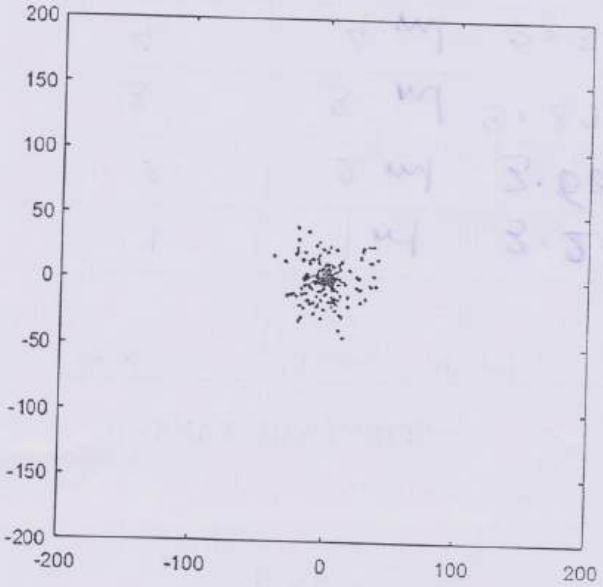


Fig. 5 (*continued*)

References

[1] J.J. Casciari, S.V. Sotirchos, R.M. Sutherland, Variations in tumor cell growth rates and metabolism with oxygen concentration, glucose concentration, and extracellular pH, J. Cell Physiol. 151 (1992) 386–394.
[2] Peng Feng, Zhewei Dai, Dorothy Wallace, On a 2D model of avascular tumor with weak allee effect, J. Appl. Math. (2019) 1–13.
[3] M.J. Tindall, C.P. Please, M.J. Peddie, Modelling the formation of necrotic regions in avascular tumours, Math. Biosci 211 (2008) 34–55.
[4] R.P. Araujo, D.L.S. Mcelwain, A history of the study of solid tumour growth: the contribution of mathematical modelling, Bull. Math. Biol. 66 (2004) 1039–1091.
[5] J.A. Sherratt, M.A.J. Chaplain, A new mathematical model for avascular tumour growth, J. Math. Biol. 43 (2001) 291–312.
[6] W. Mueller-Klieser, J.P. Freyer, R.M. Sutherland, Influence of glucose and oxygen supply conditions on the oxygenation of multicellular spheroids, Br. J. Cancer 53 (1986) 345–353.
[7] J.P. Freyer, R.M. Sutherland, A reduction in the in situ rates of oxygen and glucose consumption of cells in EMT6/Ro spheroids during growth, J. Cell Physiol. 124 (3) (1985) 516–524.
[8] A.N.G. Keng-Cheng, T.A.N. Liang-Soon, A numerical approach to modelling avascular tumour evolution with white noise, Austral. Mathematical Soc. 50 (2008) C569–C582.
[9] Mitchell Acland, Parul Mittal, Noor A. Lokman, Manuela Klingler-Hoffmann, Martin K. Oehler, Peter Hoffmann, Mass Spectrometry Analyses of Multicellular Tumor Spheroids, Proteomics Clin. Appl., 12 (3) (2018) e1700124.
[10] D.I. Wallace, X. Guo, Properties of tumor spheroid growth exhibited by simple mathematical models, Front. Oncol. 3 (51) (2013).

Source details

Materials Today: Proceedings

Scopus coverage years: 2005, from 2014 to 2023

E-ISSN: 2214-7853

Subject area:

Source type: Conference Proceeding

View all documents > | Set document alert | Save to source list

CiteScore 2022
3.2

SJR 2022
0.445

SNIP 2022
0.774

CiteScore | CiteScore rank & trend | Scopus content coverage

Improved CiteScore methodology

CiteScore 2024 counts the citations received in 2021-2024 to articles, reviews, conference papers, book chapters and data papers published in 2021-2024, and divides this by the number of publications published in 2021-2024. Learn more >

CiteScore rank

Category	Rank	Percentile

View CiteScore methodology > | CiteScore FAQ > | Add CiteScore to your site

ARTICLE IN PRESS

Materials Today: Proceedings xxx (xxxx) xxx

Contents lists available at ScienceDirect

Materials Today: Proceedings

journal homepage: www.elsevier.com/locate/matpr

The potential application of carbon nanotubes in water Treatment: A state-of-the-art-review

Nidhi Jain [a], Nand Jee Kanu [b,*]

[a] Department of Engineering Science, Bharati Vidyapeeth's College of Engineering, Pune 412115, India
[b] Department of Mechanical Engineering, S.V. National Institute of Technology, Surat 395007, India

ARTICLE INFO

Article history:
Available online xxxx

Keywords:
Carbon nanotubes
Water treatment
Water purification
Environment
Pollutants

ABSTRACT

Sustainability of the human race is dependent on the availability of clean water. Human race cannot be flourished without availability of clean water. Scientists and researchers are always in search of better and new technology for the treatment of waste water. Carbon Nanotubes has extensive range of applications in various fields of science and technology. Carbon Nanotubes nowadays are widely utilized for cleaning water. Carbon Nanotubes have emerged as a lucrative, effective and eco-friendly alternative in relation to that of existing water treatment facilities for the removal of various water pollutants. This review article comprehensively focuses on the major nanomaterials, how the single and double walled CNTs are acting differently. The highlighted features of the chapter covers CNTs as Sorbents, remediation of various pollutants organic and inorganic, factors effecting adsorption of organic molecule and inorganic molecules. It also postulates developments in the field to CNTs. To complement futures aspects have also been discussed. Attempts have been made to describe several aspects of water treatment using carbon nanotubes because of the immense importance of water quality.
© 2021 Elsevier Ltd. All rights reserved.
Selection and peer-review under responsibility of the scientific committee of the 7th International Conference of Advanced Materials Science and Technology 2019.

1. Introduction

Water is the major problem in the world especially in developing countries. According to the estimation of the World Bank. It has reported that about 40 percent of the populations are deprived from the clean water resources. The fresh water is the major problem in the developing countries. Due to the rapid urbanization and industrialization crisis of the fresh water is always there. Urbanization increases the demand of the water for construction and existence of the human resources. Population explosion leads to the over exploitation of the resources. Ubiquitous fresh water problems are prevalent and there is a constant need of the good water. Scientist and researcher are looking for purification method of waste water and saline water. Pollution of the water resources leads to water problem.

Clean and save water is important for human existence. In developing countries approximately 780 million people through the world are deprived from save fresh water facilities [1]. To solve this trouble numerous water purification expertise have been adapted, out of which carbon nanotube (CNT) based water treatment technologies is one of the leading and potential one. It is capable of purifying water from organic, inorganic and biological pollutants [2]. It has high surface area, lower in cost, greater reactivity, less chemical mass and less foot print on environment. The CNT used in research and purify water commercially. In past year 736 metric tons of CNTs were used for various energy and environmental applications [3]. It is made of hollow graphitic material consisting for grapheme layers. The structure helps in easy transport of water molecule and helps in water purification from water pollutants. CNT has enormous potential and adjustable nature for treatment of drinking water and other water bodies. Various studies have been reported in the literature about CNT that it contains surface functional groups, hydrophobic surface, heavy metal ions and organic compounds [4]. CNT is also used to remove metals or ions from aqueous streams [5]. For improving the properties of the carbon nanotubes functionalization is also used. Numerous pollutants have been removed by using CNT such as heavy metal ions, organic compounds, inorganic ions, pesticides, pharmaceuticals, antibiotics etc[6-14].

The morphology of the carbon nanotubes enhances the property as nano adsorbents, which is useful in achieving early

* Corresponding author.
E-mail address: nandssm@gmail.com (N. Jee Kanu).

https://doi.org/10.1016/j.matpr.2021.01.331
2214-7853/© 2021 Elsevier Ltd. All rights reserved.
Selection and peer-review under responsibility of the scientific committee of the 7th International Conference of Advanced Materials Science and Technology 2019.

Please cite this article as: N. Jain and N. Jee Kanu, The potential application of carbon nanotubes in water Treatment: A state-of-the-art-review, Materials Today: Proceedings, https://doi.org/10.1016/j.matpr.2021.01.331

equilibrium time, adsorption capacity and selectivity, and can be regenerated easily.

2. Nanomaterials for wastewater treatment

Nanomaterials such as activated Carbon, CNTs, graphene, Fe_3O_4, MnO_2, Co_3O_4, TiO_2, MgO, and ZnO, etc are predominately used for wastewater treatment [15]. They are available in all different forms such as particle nature, tube shaped and sheet forms [16]. Future prospect of these nanomaterials are very bright as they are extensively used in organic, inorganic heavy metals and dye removal.

3. Carbon nanotubes (CNTs)

3.1. Two types of CNTs nanotubes:

CNTs are the cylinder of graphite sheets mostly closed at the ends. They are imagined to be formed from graphite sheet, just like rolling of a paper into a cylinder. There are mostly two types of carbon nanotubes single walled carbon nanotubes (SWCNTs), and multiwalled carbon nanotubes (MWCNTs). Lot of work has been done on the adsorption capacity of SWCNTs, MWCNTs and hybrid CNTs (HCNTs).Out of the three single wall SWCNTs shows better adsorption capacity due to availability of higher surface area. It was reported in the literature that utmost adsorption capacities are around 9.99 and 9.97 mg g-1 of benzene and toluene respectively [17]. Reactive blue 29 (RB29) has been aloof by SWCNTs and result obtained is of 496 mg g-1[18].Researches and scientists find that carbon nanotubes have expressively higher sorption than the commercial activated carbon. The result of the sorption mechanisms showed the surface features, ion exchange process and electrochemical potential had played a major function in it [19].

4. CNTs/Functionalized CNTs as Sorbents

In search of the better material scientists are in search of quick solution for the treatment of water. Surface chemistry, morphology, chemical and physical interaction with organic and inorganic made CNT as most effective and preferred material for water remediation.CNT is now considered better material than most of the sorbent such as zeolite, clay, activated charcoal.

4.1. Organic pollutants

Organic compounds present in the water are engulfed by microorganisms, which decreases the oxygen content of the water during the decomposition process. This decreases oxygen in the water causes severe problem for the quality of the water bodies. Organic effluent from the industries also decreases oxygen contain of the water which in turn deteriorate the quality of water. Suspended solids present in effluents also obstruct the light penetrating the water which deteriorate the quality of river bed in absence of photosynthesis.

4.1.1. Organic compound present in water bodies

Adsorption of Organic molecule is mainly affected on the following factors: [2]

- Morphology and active sites of CNTs

The surface topography generally has large impact on the absorption capacity of nanomaterials. The rough surfaces have larger surface area than the smooth one. It was found that rough surfaces have greater absorption capacity in comparison of smooth pristine and graphitized Nanomaterials. It is around 31 and 29 mg/g, respectively. [20]

- Effect of pH on adsorption ionic potency and dispersion state of CNTs

Several scientists have done the comparative study of the effects of pH on controlling absorption Ghaedi et al [21] and they found that MWCNT higher adsorption capacity than activated carbon. MWCNT reaches the equilibrium at higher rate and as well as higher absorption capacity, physical forces and ionic interaction Example: MWCNT for removal of Eriochrome Cyanine R (ECR).

- Effect of temperature:

Absorption capacity of the CNT was studied by the scientists at different temperature. Methylene dye was removed using CNT from aqueous solution. It was found that absorption capacity increase as we increase the temperature. It is because the CNT is endothermic in nature which increase the absorption capacity [22].The highest results have been found at around 133 mg g − 1 at 310 K [23].

- Magnetic MWCNT:

Elimination of cationic dyes such as methylene blue (MB), Neutral red (NR), and gleaming cresyl blue (BCB) are studied by Gong et al. form watery solution by means of Magnetic MWCNT nanocomposite. And similar studies were done by Gaog et al [24]. For removing anionic azo dyes using same material and found that composite was very effective and separation process is easy using magnet. Many of the work were done on magnetic polymer MPMWCNT nanocomposite. The Nanocomposite which was composed of MWCNT, poly (1-glycidyl-3-methylimidazolium chloride) (ionic liquid-based polyether) and Ferro ferric oxide which is used to utilize for the absorption of orange II, sunset yellow FCF and amaranth dyes from Liquid phase (Gaoa et al., 2013[25].

4.2. Organic molecules and functional groups of CNTs

Hydrocarbon like hexane, benzene, and cyclohexane show good affinity with CNTS as surface of the CNTs is raw and hydrophobic over alcohols e.g., ethanol, 2-propanol).Several scientists studied the adsorption capacities and found in the order of toluene (greatest) > MEK > hexane > cyclohexane [26]. Scientist and researcher studied the absorption behavior of various organic compound such as aromatic (benzene), aromatic and heterocyclic (thiophene), and nonaromatic (cyclohexane) on CNT. Thiophene > benzene > cyclohexane shows best absorption[27].

- Nonpolar organic chemicals shows higher absorption capacity than polar

Absorption is governing factor in the removal of polar and non polar organic chemicals It was found that Nonpolar aliphatic < nonpolar aromatics < nitroaromatics. Nitro functional group shows highest absorption capacity. Sometimes functional group on the surface diminishes hydrophobicity, surges oxygen content, reductions precise surface area which resulted in reduction of adsorption of nonpolar hydrocarbons. [28].

- Hydrophobic interactions on the surface of CNTs, π-π interfaces, formation of hydrogen bonds, and action of electrostatic interactions, etc. are several mechanisms performing simultaneously [29].

Several mechanisms are working in this regard such Hydrophobic interactions on the surface of CNTs, π-π interfaces, formation of hydrogen bonds, and action of electrostatic interactions. These mechanism played important role in the removal process.

4.3. Inorganic pollutants

Heavy Metal Ions-Among the various heavy metals chromium lead and zinc causes grave problem to the surrounding.CNT can plays a significant role as absorbent in eliminating heavy metal ions from aqueous solution [30]. Sorption capacity has been improved by using HNO_3, NaOCl, and $KMnO_4$.

Researchers have studied on the adsorption of aqueous cadmium (II) onto tailored MWCNT. Lead sorption have been studied by several scientists and found that smaller and rich oxygen content favor adsorption ability [31].

Nickel and zinc removal from aqueous solution were testified by several scientists and researchers [32]. Pb(II), Cd(II) and Cr(VI) are show high sorption capacity on oxidized CNTs from water [33-35]. It was reported that multi-component sorption of metal ions were nicely done on CNT [70]. Absorption capacity on aqueous solution is also excellent for elimination of divalent metal ions [Cd (II), Cu(II), Ni(II), Pb(II), Zn(II)]. It has been proved that the CNTs have successful desorption of divalent metal ions and at the same time superior sorption capacity and it also helps in decreasing the environment pollution [36].

4.4. Problems in using CNTs as water purifications adsorbents

While using absorbent safety is utmost important criteria in water purification. When the pollutants are present at extremely high concentrations high concentration of CNT is required. CNT are present in different lengths, shapes, charges and about 50,000 types of CNTs are found in the market [37]. Some of them like pristine CNTs have generic impurities [38]. Recent search shows that there are certain problems in using CNT as absorbent such as, it increases metal contains and toxicity levels on living cells [39]. It was found that intake of pollutants for example humic acid and tannic acid (TA) alter the properties of CNT. A TEM image confirms that Carbon nanotubes become bulky in sizes after TA adsorption, which separate individual CNT from the bundle [40]. Surfactant intake onto the CNTs also leads to nanotubes release in water [41].This release of CNT from the WWTPs bundle may consumed by the microorganism which leads to sever problem in the environment. Inorganic pollutants which are metals such as Fe, Cd, Ni, As, Hg etc uptake by the CNTs shows superior reactivity and toxicity within the particle [42]. Biological absorbent especially microbes, are also changing the properties of CNT for example microbes convert hydrophobic pristine CNTs to hydrophilic ones, and some degraded C-CNTs into short CNT fragments[43]. In this way we can conclude that CNT is very harmful if its properties are changed after absorption. If should continuously monitor that CNT should not be cut, ground, sheered and ripped off after absorption.

But the exact quantity of the leakage of CNT is under study. There is the scarcity in the scientific data which powerfully determine the toxicity contain of the CNT. We are looking for the computational tools and effective model for the determination of the CNT toxicity. The advance technique helps us to determine the risk and consequence of the CNT at various places [44].

In the literature survey you can find that around 2 million tons of the human wastes are disposed in the water resources everyday and it was also found that 70% of the industrial waste is discarded untreated. Heavy metal pollution is also a major contributor of the pollution. It is difficult to remove the all the pollutant by conventional method. Carbon nanotubes are a material used for the treatment of the waste water and is considered as a effective and low cost technology. Carbon nanotubes have unique physical properties, chemical properties, electrical properties and also structural properties which enforce innovations to solve the water purification problem. Carbon nano-tubes are solving water problems by acting as sorbents, catalyst and membranes. Engineered nanomaterials (ENMs), are now a days frequently used which a source of the release of unused remains nanomaterials in the environment. During manufacturing the possibility of the release is quite often as in use, washing or disposal of the products. But at this point also the hazards of the nanomaterials are not reported as similar as bulk product. Because of this ambiguity the nanomaterials are considered as safe materials. When we see the broad spectrum of the nanomaterials we find that the nanomaterial seems to be safe for industry as very few problems are reported. Engineered nanomaterials (ENMs) are used in the water purification methods. Very good results have been obtained by these ENMs. CNT engineered nanomaterials (ENMs) are future is depended on the interfacial properties such as reactivity holding capacity etc. and also govern by water chemical properties such as pH, constituents present in the water and so on. It was found in various researches that the CNT sometimes leaked out during water purification, which in turns toxic for the further use[47]

Clean water, food and shelter are the three basic requirements of the human being for it's survival and existence. In developing countries excess of clean water is the rare commodity. Carbon nanotubes (CNTs) are coming as the emerging material for the purification of the water. It has the capability of removing varieties of pollutants from the water. Carbon nanotubes (CNTs) are known from its unique properties such as ample surface area, high chemical reactivity, low cost etc. But the risk associated with the carbon nanotubes is not clear. Huge amount of literature are present which gives the evidence of the use of carbon nanotubes in the variety of field such as sensors, membrane technology water purification, composites etc. It was found by the researches and scientist that there are the leakage of the Carbon nano-tubes (CNTs) at various sources while usage which create a bewilderment among the research community that we have to use it at various places or not. [45.46]It was found that there will be constant leakage of the CNTs that is given in percentages are 6.0 percentage leakage in waste water treatment plants (WWTPs),5.5% of CNTs waste ignition of the plants, soil (14.8%), air (1.4%) etc. This release of the Carbon nanotubes (CNTs) in the environment may leads to the various problems. The effects of the Carbon nanotubes (CNTs at environmental condition are a substance of concern for the scientist and researcher. The effects are not clear identified. From the literature we come to know that E-CNTs can be altered and can resist the biodegradation, toxic to terrestrial, aquatic animals. This evidence against CNT can create havoc for the usage of the CNT. But the economic suitability cannot allow CNT to be banned by the public [48,49].

5. Recent case studies

5.1. CNT membranes for water purification

This technology are extensively used in the treatment of water, some of the techniques like microfiltration, ultrafiltration, nanofiltration and reverse osmosis, etc are the known techniques for the water treatment systems. Some membranes are synthesized from the polymer to give better method of filtration application of the water. But the polymer based membranes have their disadvantage of chemical and mechanical stability. If the polymer have hydrophobic in nature and have the tendency to absorb organic

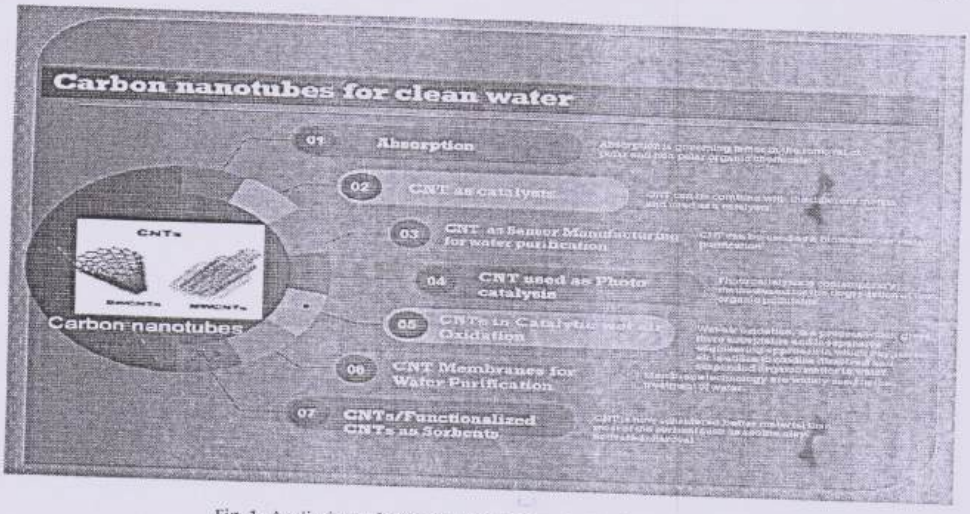


Fig. 1. Applicaions of CNTs in water treatment of various pollutants.

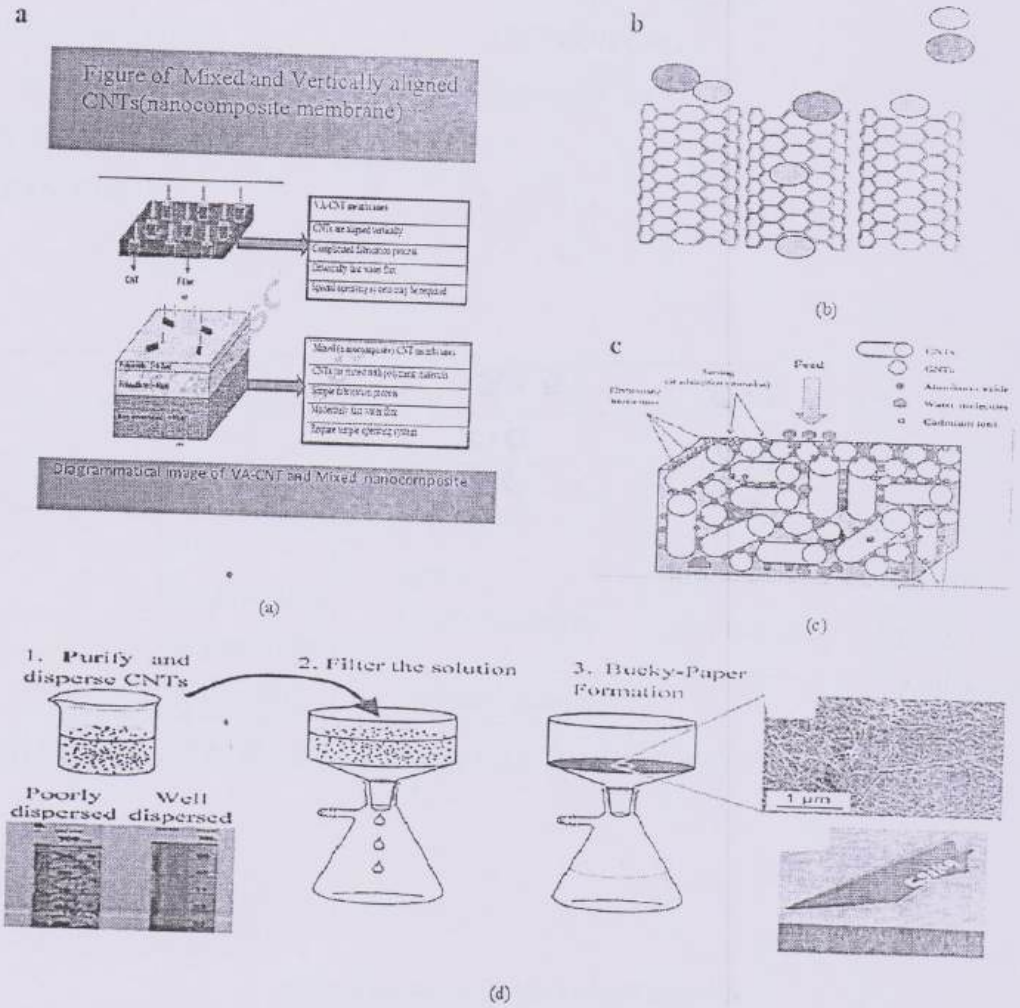


Fig. 2. (a) *CNTs* membranes could be distinguish depending upon the use of the application they are of two types; (b) Self-supporting CNT membranes; (c) mixed CNT membranes; (d) Bucky-paper CNT membrane. (Reprinted with permission from Ref. 56. Copyright 2010 MDPI).

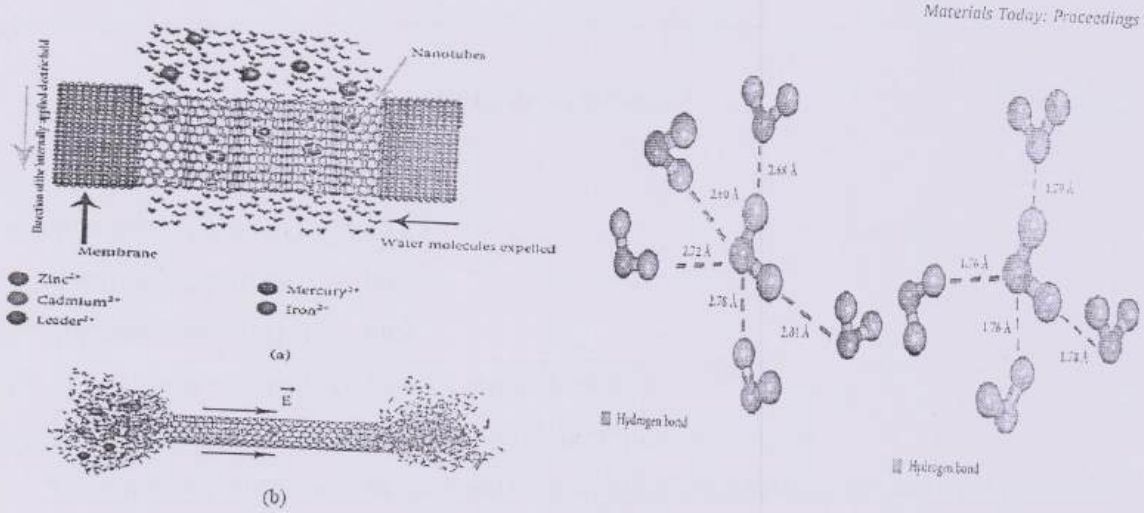


Fig. 3. Nano-filtering: (a) real model and (b) basic model for simulation under EF. (Reprinted with permission from Ref. 57. Copyright 2020 Hindawi).

foul ants than it stop filtration of organic, inorganic and biological substances.

CNTs outstanding properties have several merits like it has porosity of comparable size, unique surface chemistry, and sturdy antimicrobial activity. As the CNT has open new avenue in the filtration technique. It filters waste water in a very effective manner. Let us see the use of elevated water flux and electrical conductivity which severs as shows potential materials for filtration and separation.

CNTs membranes could be distinguish depending upon the use of the applications (Fig. 1) they are of two types (1) Self-supporting CNT membranes, and (2) Nanocomposite which is mixed CNT membranes. The Self-supporting CNT membranes are used in many applications such as desalination and water treatment and they are vertically aligned CNT (VACNT) membranes. In the VA-CNT membranes, CNTs are keeping at the vertical position as cylindrical pores which help to pass the fluid to between the CNTs bundles.

CNT membranes which is Bucky-paper are haphazardly arranged extremely huge porous 3D network (Fig. 2). All these membrane are very effective because of the surface and size of the nanotubes. After different studies it was found out that size is not only the criteria for the water purification factors such as the pH of the solution and also electrostatic interactions participate considerable factor The CNT membrane produces of a low stinking potential as compared RO and NF membranes which in un-turn reduces the cost and maintenance of the membrane. Low energy consumption takes place when CNT membrane is used during the flow of molecules. One more advantage of the CNTs is it does not require a high-pressure pump for the flow of molecules [50-55].

5.2. Nanotube and electric field are used for heavy metals nanofiltration by molecular dynamics

In the Fig. 3(a) computational modeling study is done examining the Molecular dynamics (MD) of Heavy metal filtration in water. The two medium is used to judge the effect of filtration they are CNTs and BNNT(boron nitride nanotubes) under constant electric field. The forces apply by the electric field act inside nanotubes which removes heavy metals from water leaving heavy metal inside the tube. The propelling electrical force is generated which push out water from the membrane and keep hold of ions. 100 ps time duration is required under constant temperature and pressure with electric fields around $10^{-8.5}$ to $10^{-1.5}$ au.

In the Fig. 4(a) and (b) illustrate the influence of external electrical charges on hydrogen bonds. The hydrogen bond under electric field show different behaviour than the without charge water because under the electric field the bonds are steady and happen in a shorter distance amidthe atoms demonstrated in Fig. 5.

The graph in the Fig. 5(a) and (b) clearly depicts the nanofiltration of heavy metal ions under the influence of electric field through CNT in Fig. 5(a) and boron nitride nanotubes (BNNT) in Fig. 5(b).The result showed that both the nanotubes are very efficient in removing heavy metal from the water. However the BNNT have better hydrophobicity and thermal conductivity. In present parameters the betters results are obtain for BNNT than CNTs [56-62].

5.3. Carbon nanotubes effect of shape and structure on desalination

The Fig. 6 depicts the effect of shape of CNTs on the water desalination efficiency. For conical CNT, the efficiency increases with the increase in the cone angle and when the solution is passes from the tip to the foot (Fig. 6(a)). The MD simulation results confirmed that the desalination efficiency increases with increase in

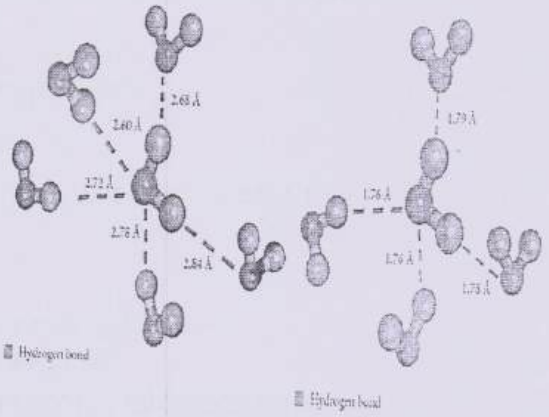


Fig. 4. Inter-atomic space of hydrogen bonds in water restricted without EF and beneath EF (Reprinted with permission from Ref. 57. Copyright 2020 Hindawi).

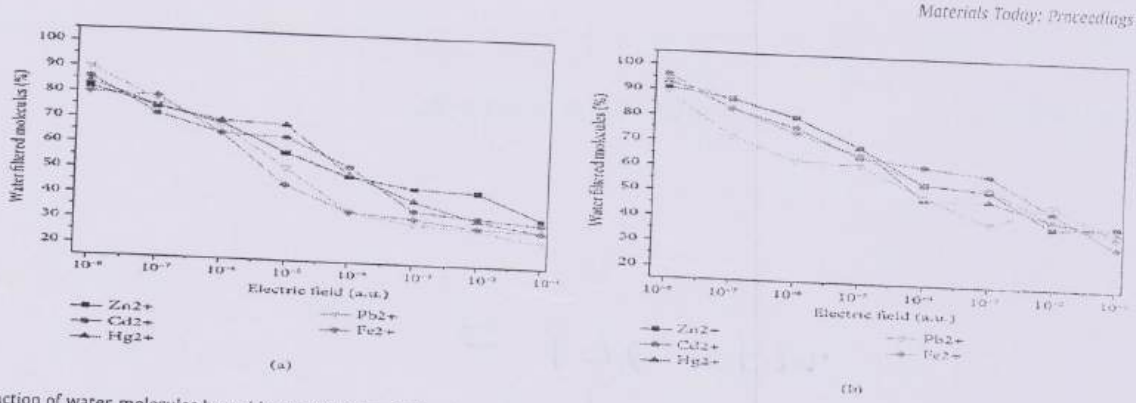


Fig. 5. Fraction of water molecules barred by NF (a) within CNT, and (b) Beneath EF inside BNNT. (Reprinted with permission from Ref. 57. Copyright 2020 Hindawi).

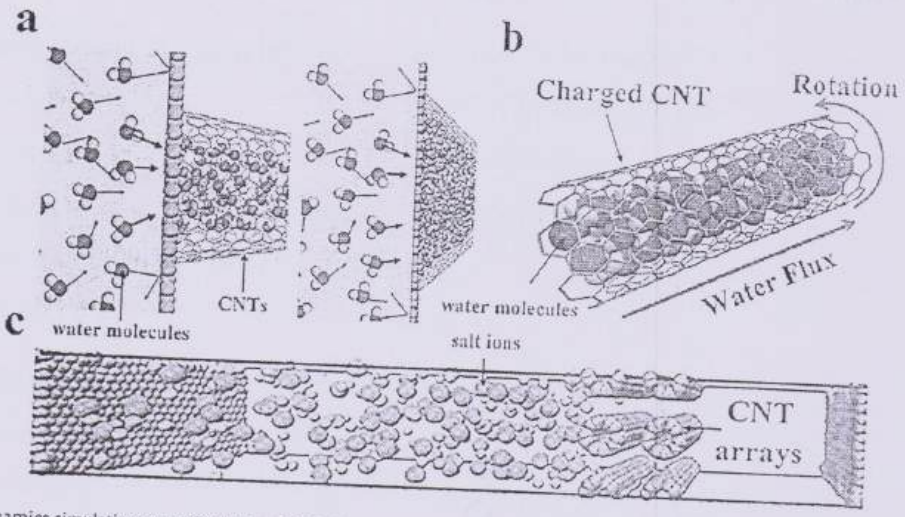


Fig. 6. (a)-(c) Molecular dynamics simulation water flow rate of CNTs. ((a) Reprinted with permission from Ref. 71. Copyright 2017 Elsevier; (b) Reprinted with permission from Ref. 72. Copyright 2017 ACS Publications; and (c) Reprinted with permission from Ref. 73. Copyright 2019 Elsevier).

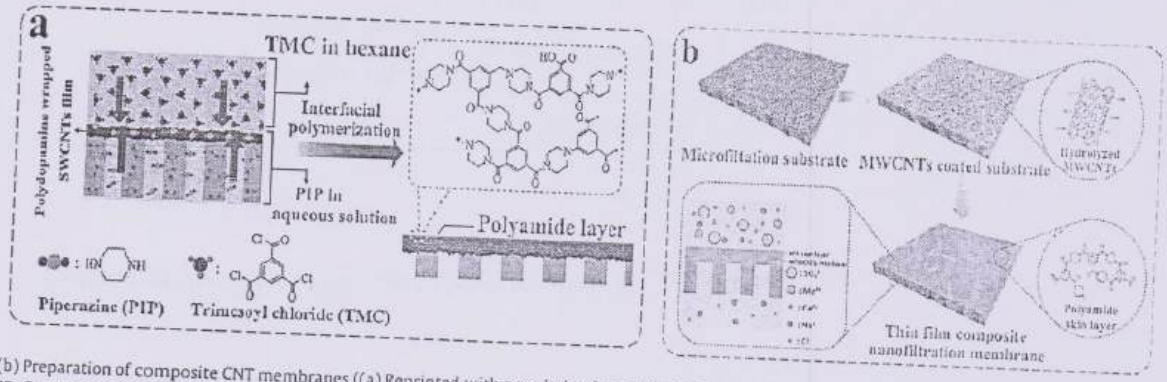


Fig.7. (a)-(b) Preparation of composite CNT membranes ((a) Reprinted with permission from Ref. 74. Copyright 2016 John Wiley and Sons; and (b) Reprinted with permission from Ref. 75. Copyright 2016 Elsevier).

the rotational speed of CNTs as the higher centrifugal force pushes water molecules away of the pores in the wall (Fig. 6(b)). Researchers have also studied another configuration containing a slit separated by horizontally stacked CNTs placed 1 nm apart. It was found from simulations that this configuration exhibits excellent desalination efficiency as compared to atomic-scale graphene slit membranes (Fig. 6(c)).

In the Fig. 7 decreases ion adsorption of chlorine because of the incorporation of MWCNTs which resist absorption of chlorine. The molecular dynamics exposed that high stability of MWCNT encumber the chlorination of the PA structure. The resistance of chlorine is seen because of high cross linking. When the crosslinking between the polymer and CNTs increased the results are good [63-74].

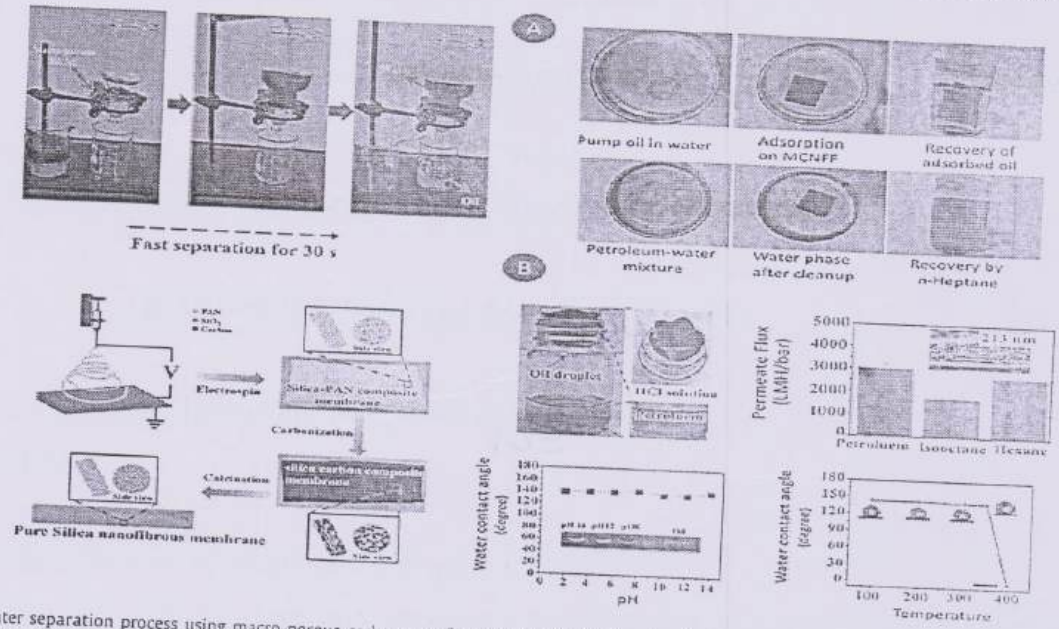


Fig. 8. (a) Oil–water separation process using macro-porous carbon nanofibers film (MCNFF) (Reprinted with permission from Ref. 76. Copyright 2014 Royal Society of Chemistry); and (b) The fabrication process (Reprinted with permission from Ref. 77. Copyright 2014 American Chemical Society).

5.4. Carbon-based polymer nanocomposite for separation of oily and water.

Amalgamation of carbon-based nanomaterials into polymeric membranes enhances the belongings of the materials such as hydrophobicity/hydrophilicity, and also other stability such as mechanical, thermal and chemical etc. The Fig. 8(a) and 8(b) clearly depict that oil or water could be easily removed from the oil–water mixture. In Fig. 8(a) oil separation can be seen and second recovery performance of MCNFF. In Fig. 8(b), fabrication process is illustrated [73-81].

6. Conclusion

Out the several technologies carbon nanotube (CNT) used water treatment are the mainly effective and reliable techniques as it provides of it's large surface area, good chemical reactivity, less in cost and requires less energy, fewer chemical mass and less foot print on the environment. The review article comprehensively focuses on the major nanomaterials, how the single and double walled nanotubes are acting differently. CNTs as Sorbents, remediation of various pollutants organic and inorganic, factors effecting adsorption of organic molecule and inorganic molecules are also discussed in this review article. It also postulates improvement in the field to CNTs. To complement futures aspects have also been discussed. Attempts have been made to describe several aspects of water treatment using carbon nanotubes because of the immense importance of water quality. Due to which researcher and scientist are working hard to exploit the carbon nanotube (CNT) based water treatment in more effective manner. Physicochemical and interesting properties of carbon nanotube (CNT) made it most reliable and effective technique for water purification. Preservation of environment is utmost important at this point of time. Day by day requirement of clean water is utmost important for life sustainability. Untreated water created major problems in the environment. Several water purification technologies have been explored. Presently known technique for water purification are adsorption, desalination, Chlorination, sedimentation, and distillation and most common ,filtration, biological processes such as slow sand filters chemical processes such as chlorination; and the use ultraviolet light from electromagnetic radiation. Among the research and development area carbon nanotubes open new area for exploration of new technology. These Carbon Nanotubes represent the development of a new area and process for the wastewater treatment. Carbon Nanotubes have high removal efficiency and cost-effectiveness.

Use of the nano-materials creates a nano-phobia among the scientist and research community. To avoid such nano phobia the handling, use and disposal of the material with proper care is important. The fate of the CNT in water technology is decided if the proper handling is taken place. At present very few methods are available which measure the toxicity and hazards of the CNT. There is always a need of the solid regularity guidelines which measure the potential risk of the CNT. These guidelines will deal with the challenges faced and also reckoned the impact on the human health and environment. Based on the structure and properties of the CNT nanomaterials structure–property associations risk assessment will help to understand CNT performance in WWTPs and their successive release in the environment. With the help of these guidelines worldwide safety guidelines will be prepared and which further help in estimating the CNT's future.

Declaration of Competing Interest

The authors declare that they have no known competing financial interests or personal relationships that could have appeared to influence the work reported in this paper.

References

[1] C. Sealy, Cleaning up water on the nanoscale, Nano Today, 8 (2013) 337–338.
[2] V.K.K. Upadhyayula, S.G. Deng, M.C. Mitchell, G.B. Smith, Science of The Total Environment, 408 (2009) 1–13.
[3] A.A. Keller, S. McFerran, A. Lazareva, S. Suh, J Nanopart Res, 6 (2013) 1–17.
[4] X. Ren, C. Chen, M. Nagatsu, X. Wang, Chemical Engineering Journal, 170 (2011) 395–410.
[5] O. Bakajin, A. Noy, F. Fornasiero, C.P. Grigoropoulus, J.K. Holt, J.B. In, S. Kim, H.G. Park, Elsevier Inc (2008), 77–93.
[6] A.J. Brooks, H.N. Lim, J.E. Kilduff, Nanotechnology, 39 (2012) 294008–294018.

ARTICLE IN PRESS

[7] H.Z. Chen, S.G. Yang, K. Yu, Y.M. Ju, C. Sun, The Journal of Physical Chemistry A 14 (2011) 3034–3041.
[8] H.H. Cho, B.A. Smith, J.D. Wnuk, D.H. Fairbrother, W.P. Ball, Environmental Science and Technology 42 (2008) 2899–2905.
[9] H.H. Cho, K. Wepasnick, B.A. Smith, F.K. Bangash, D.H. Fairbrother, W.P. Ball, Langmuir 26 (2010) 967–981.
[10] Y.J. Yao, B. He, F.F. Xu, X.F. Chen, Chemical Engineering Journal 170 (2011) 82–89.
[11] M.M. Rahman, S.A. Sime, M.A. Hossain, M. Shammi, M.K. Uddin, M.T. Sikder, M. Kurasaki, Arab. J. Sci. Eng. 42 (2017) 261–269.
[12] A.A. Farghali, H.A. AbdelTawab, S.A. AbdelMoaty, R. Khaled, J. Nanostruct. Chem. 7 (2017) 101–111.
[13] M.A. Salam, Journal of Molecular Liquids 233 (2017) 197–202.
[14] A.E. Chávez-Guajardo, J.C. Medina-Llamas, L. Maqueira, C.A.S. Andrade, K.C.B. Alves, P. Celso de Melo, Chemical Engineering Journal 281 (2015) 826–836.
[15] H.H. Abdel Ghafar, G.A.M. Ali, O.A. Fouad, S.A. Makhlouf, Desalin. Water Treat 53 (2015) 2980–2989.
[16] V. Gupta, O. Moradi, I. Tyagi, S. Agarwal, H. Sadegh, R. Shahryari-Ghoshekandi, A. Makhlouf, M. Goodarzi, A. Garshasbi, Crit. Rev. Environ. Sci. Technol. 46 (2016) 93–118.
[17] B. Bina, M. Amin, A. Rashidi, H. Pourzamani, Environ. Prot. 38 (2012) 3–25.
[18] K. Nadafi, A. Mesdaghinia, R. Nabizadeh, M. Younesian, M.J. Rad, Desalination Water Treat. 27 (2011) 237–242.
[19] Z. Gao, T.J. Bandosz, Z. Zhao, M. Han, J. Qiu, J. Hazard. Mater 167 (2009) 357–365.
[20] X. Peng, Y. Li, Z. Luan, Z. Di, H. Wang, B. Tian, Z. Jia, Chem. Phys. Lett. 376 (2003) 154–158.
[21] M. Ghaedi, A. Shokrollahi, H. Hossainian, S.N. Kokhdan, J. Chem. Eng. Data. 56 (2011) 3227–3235.
[22] Z. Huaiyu, L. Chunxiang, Z. Jiajun, L. Minghua, F. Shiyu, Trends, Carbohydr. Res. 2 (2010) 1–9.
[23] Z. Shahryari, A.S. Goharrizi, M. Azadi, Int. J. Water Resour. Environ. Eng. 2 (2010) 16–28.
[24] J. Gong, B. Wang, G. Zeng, C. Yang, C. Niu, Q. Niu, W. Zhou, Y. Liang, J. Hazard. Mater. 164 (2009) 1517–1722.
[25] H. Gaoa, S. Zhao, X. Cheng, X. Wang, L. Zheng, Chemical Engineering Journal 223 (2013) 84–90.
[26] S. Agnihotri, M.J. Rood, M. Rostam-Abadi, Carbon 43 (2005) 2379–2388.
[27] D. Crespo, R.T. Yang, Ind. Eng. Chem. Res. 45 (2006) 5524–5530.
[28] W.E.I. Chen, L.I.N. Duan, Environ. Sci. Technol. 41 (2007) 8295–8300.
[29] B. Pan, B. Xing, Environ. Sci. Technol. 42 (2008) 9005–9013.
[30] S. Srivastava, Mater. Lett. 4 (2013) 2–8.
[31] F. Yu, Y. Wu, J. Ma, C. Zhang, J. Environ. Sci. 25 (2013) 195–203.
[32] C. Lu, C. Liu, J. Chem. Technol. Biotechnol. 81 (2006) 1932–1940.
[33] Y.-H. Li, S. Wang, Z. Luan, J. Ding, C. Xu, D. Wu, Carbon 41 (2003) 1057–1062.
[34] Y.-H. Li, S. Wang, J. Wei, X. Zhang, C. Xu, Z. Luan, D. Wu, B. Wei, Chem. Phys. Lett. 357 (2002) 263–266.
[35] D. Robati, J. Nanostruct. Chem. 3 (2013) 1–6.
[36] G.P. Rao, C. Lu, F. Su, Sep. Purif. Technol. 58 (2007) 224–231.
[37] K S. Nanofrontiers: visions for the future of nanotechnology. Washington, DC: Contract No.: Report No. PEN 6. 2007
[38] R. Das, M.E. Ali, S.B.A. Hamid, M.S.M. Annuar, S. Ramakrishna, J. Nanomaterials (2014) 1–9.
[39] C. Wang, Z. Wei, M. Feng, L. Wang, Z. Wang, Environ Toxicol Chem. 33 (2014) 2522–2528.
[40] D. Lin, B. Xing, Environ Sci Technol. 42 (2008) 5917–5923.
[41] E. Heister, C. Lamprecht, V. Neves, C. Tilmaciu, L. Datas, E. Flahaut, B. Soula, P. Hinterdorfer, H.M. Coley, S.R.P. Silva, J. McFadden, ACS Nano. 4 (2010) 2615–2626.
[42] C.W. Lam, J.T. James, R. McCluskey, R.L. Hunter, Toxicol Sci. 77 (2004) 126–134.
[43] K. Zare, V.K. Gupta, O. Moradi, A.S.H. Makhlouf, M. Sillanpää, M.N. Nadagouda, H. Sadegh, R. Shahryari-ghoshekandi, A. Pal, Z.J. Wang, J. Nanostruct. Chem. 5 (2015) 227–236.
[44] A.A. Keller, S. McFerran, A. Lazareva, S. Suh, J Nanopart Res. 15 (2013) 1–17.
[45] C.W. Lam, J.T. James, R. McCluskey, S. Arepalli, R.L. Hunter, Crit Rev Toxicol. 36 (2006) 189–217.
[46] M. Mullins, F. Murphy, L. Baublyte, E.M. McAleer, Nat Nanotechnol. 8 (2013) 222–224.
[47] F. Murphy, M. Mullins, K. Hester, A. Gelwick, J.J. Scott-Fordsmand, T. Maynard, NatNanotechnol. 12 (2017) 717.
[48] F. Murphy, B. Sheehan, M. Mullins, H. Bouwmeester, H.J.P. Marvin, Y. Bouzembrak, A.L. Costa, R. Das, V. Stone, S.A.M. Tofail, Nanoscale Res Lett. 11 (2016) 1–8.
[49] L. Schlagenhauf, F. Nüesch, J. Wang, Fibers. 2 (2014) 2–5.
[50] C. Rizzuto, G. Pugliese, M.A. Bahattab, S.A. Aljlil, E. Drioli, E. Tocci, Sep. Purif. Technol. 193 (2018) 378–385.
[51] M.H.D.A. Farahani, V. Vatanpour, Sep. Purif. Technol. 197 (2018) 372–381.
[52] C. Thamaraiselvan, S. Lerman, K. Weinfeld-Cohen, C.G. Dosoretz, Sep. Purif. Technol. 202 (2018) 1–8.
[53] K.A. Tankus, L. Isaman, M. Stoilov, V. Freger, A.C.S. Appl. Nano Mater. 1 (2018) 2057–2061.
[54] W. Chen, S. Chen, T. Liang, Q. Zhang, Z. Fan, H. Yin, K.-W. Huang, X. Zhang, Z. Lai, P. Sheng, Nat. Nanotechnol. 13 (2018) 345–350.
[55] K. Sears, L. Dumee, J. Schutz, M. She, C. Huynh, S. Hawkins, M. Duke, S. Gray, Materials. 3 (2010) 127–149.
[56] T.S. Arouche, R.M.D.S. Cavaleiro, P.S.M. Tanoue, T.S.S. Pereira, T.A. Filho, A.M.D. J.C. Neto, Journal of Nanomaterials. 4063201 (2020) 1–12.
[57] D. Kaliannan, S. Palaninaicker, V. Palanivel, M.A. Mahadeo, B.N. Ravindra, S. Jae-Jin, Environmental Science and Pollution Research 26 (2019) 5305–5314.
[58] A. Singh, R. Kukreti, L. Saso, S. Kukreti, Molecules. 24 (2019) 1583–1590.
[59] K. Singh, S.A. Waziri, Journal of Materials and Environmental. Science. 2508 (2019) 657–667.
[60] J.N. Cruz, E.S. Moraes, R.P. Pantoja, T.S.S. Pereira, G.V.S. Mota, A.M.J.C. Neto, Journal of Nanoscience and Nanotechnology. 19 (2019) 5687–5691.
[61] J. Wei, M. Duan, Y. Li, A.S. Nwankwegu, Y. Ji, J. Zhang, Scientific Reports. 9 (2019) 13160.
[62] L. Zhang, L. Jia, J. Zhang, et al., Desalination. 464 (2019) 84–93.
[63] M.J. Shan, H. Kang, Z.W. Xu, N. Li, M.L. Jing, Y.L. Hu, K.Y. Teng, X.M. Qian, Shi J. Liu, J. Colloid Interface Sci. 548 (2019) 170–183.
[64] Y.B. Yang, X.D. Yang, L. Liang, Y.Y. Gao, H.Y. Cheng, X.M. Li, M.C. Zou, A.Y. Cao, R. Z. Ma, Q. Yuan, Science 364 (2019) 1057–1062.
[65] Z.Y. Wang, Z.X. Wang, S.H. Lin, H.L. Jin, S.J. Gao, Y.Z. Zhu, J. Jia, Nat. Commun. 9 (2018) 1–9.
[66] Y.M. Manawi, K. Wang, V. Kochkodan, D.J. Johnson, M.A. Atieh, M.K. Khraisheh, Membranes. 8 (2018) 106.
[67] J.A. Idarraga-Mora, A.S. Childress, P.S. Friedel, D.A. Ladner, A.M. Rao, S.M. Husson, Membranes. 8 (2018) 111.
[68] M. Alsuhybani, A. Alshahrani, A.S. Haidyrah, J. Chem. (2020) 1–9.
[69] K. Roy, A. Mukherjee, N.R. Maddela, S. Chakraborty, B. Shen, M. Li, D. Du, Y. Peng, F. Lu, L.C.G. Cruzatty, J. Environ. Eng. 8 (2020) 103572.
[70] W. Li, W. Wang, X. Zheng, Z.H. Dong, Y. Yan, J. Zhang, Comput. Mater. Sci. 136 (2017) 60–66.
[71] M. Khodabakhshi, A. Moosavi, J. Phys. Chem. C. 121 (2017) 23649–23654.
[72] E.Y.M. Ang, T.Y. Ng, J. Yeo, R. Lin, Z. Liu, K.R. Geethalakshmi, Journal of Membrane Science. 581 (2019) 383–392.
[73] Y. Zhu, W. Xie, S. Gao, F. Zhang, W. Zhang, Z. Liu, J. Jin, Small. (2016) 1–8.
[74] M.-B. Wu, Y. Lv, H.-C. Yang, L.-F. Liu, X. Zhang, Z.-K. Xu, Journal of Membrane Science. 515 (2016) 238–244.
[75] H. Liu, C.-Y. Cao, F.-F. Wei, P.-P. Huang, Y.-B. Sun, L. Jiang, W.-G. Song, Journal of Materials Chemistry A. 2 (2014) 3557.
[76] M.H. Tai, P. Gao, B.Y.L. Tan, D.D. Sun, J.O. Leckie, ACS Applied Materials and Interfaces. 6 (2014) 9393–9401.
[77] V. Santosh, J. Gopinath, P. VeeraBabu, A.V.S. Sainath, A.V.R. Reddy, Sep. Purif. Technol. 191 (2018) 134–143.
[78] J. Saththasivam, W. Yiming, K. Wang, J. Jin, Z. Liu, Sci. Rep. 3 (2018) 4–9.
[79] L. Zhang, K. Zha, C. Zhang, J. Gu, W. Zhang, Y. Huang, J. Mater. Chem. A. 6 (2018) 10217–10225.
[80] J. Gu, H. Guo, Y. Zhang, N. Zhao, J. Xiong Li, J. Colloid Interface Sci. 514 (2018) 386–395.
[81] V. Santosh, J. Gopinath, P. Veera, Sep. Purif. Technol. 191 (2018) 134–143.

Source details

Materials Today: Proceedings

Scopus coverage years: 2005, from 2014 to 2023

E-ISSN: 2214-7853

Subject area:

Source type: Conference Proceeding

View all documents > | Set document alert | Save to source list

CiteScore 2022
3.2

SJR 2022
0.445

SNIP 2022
0.774

CiteScore | CiteScore rank & trend | Scopus content coverage

Improved CiteScore methodology

CiteScore 2024 counts the citations received in 2021-2024 to articles, reviews, conference papers, book chapters and data papers published in 2021-2024, and divides this by the number of publications published in 2021-2024. Learn more >

CiteScore rank

Category	Rank	Percentile

View CiteScore methodology > | CiteScore FAQ > | Add CiteScore to your site

Materials Today: Proceedings xxx (xxxx) xxx

Contents lists available at ScienceDirect

Materials Today: Proceedings

journal homepage: www.elsevier.com/locate/matpr

Biomedical application of carbon nanotubes (CNTs) in vulnerable parts of the body and its toxicity study: A state-of-the-art-review

Nidhi Jain [a,*], Seema Tiwari [b]

[a] Department of Engineering Science, Bharati Vidyapeeth College of Engineering, Pune 412115, India
[b] Applied Science and General Engineering Department, Army Institute of Technology, Pune, India

ARTICLE INFO

Article history:
Received 31 December 2020
Received in revised form 16 January 2021
Accepted 27 January 2021
Available online xxxx

Keywords:
Carbon nanotubes
Drug delivery
Cancer
Nanocomposites
Hydrogels
Diagnostic
Tissue engineering
Toxicity

ABSTRACT

Carbon nanotubes are known for its distinctive, newer generation, unique materials for its appealing properties. They have excellent high surface area, high biocompatibility, and flexibility, electrical, mechanical and thermal properties which can be customized and functionalized on the basis of the materials. The use of such materials in biomedical field is on demand. The application of carbon nanotubes in biomedicines has been saving the lives of human race. When CNTs merged with organic materials developed better alternative in the field of biomedicines. In present review the applications of carbon nanotubes in biomedical field has been discussed with special references to sensitive area of the body. These diagnostic applications cover nervous tissue regeneration, neural scaffolds, Myocardial Conduction, and tissue engineering, cancer treatment etc. Toxicities of CNTs and factors effective to carbon nanotube applications were discussed in the review.
© 2021 Elsevier Ltd. All rights reserved.
Selection and peer-review under responsibility of the scientific committee of the 3rd International Conference on Materials, Manufacturing and Modelling.

1. Introduction

Increasing biomedical problems in humans leads to new materials. Carbon nanotubes are acting as good candidate for biomedical treatment. It has able to sever an alternative synthetic material which could combine with organic materials for better and improved results. As we all know that Carbon nanotubes (CNTs), are cylindrical in shape with C–C distance around *1.43 Å*, interlayer distance is around *3.45 Å*, and each carbon is having sp2 hybridization. As carbon nanotubes are already been used in various medical field but in this review CNTs use at very sensitive part of the body for diagnostic applications has been discussed such as nervous tissue regeneration, neural scaffolds, Myocardial conduction, and tissue engineering, cancer treatment etc [1–9].

Carbon Nanotubes are used in several other fields such as thermal conductivity devices, energy storage devices, conductive properties, adhesive, thermal materials, structural application etc. CNTs have appealing properties such as excellent high surface area, outstanding mechanical properties and light in weight, MWCNTs (Multi Walled Carbon Nanotubes) ability to bend, flexibility, and its strength measured by various scientists was around the value of 14.3 ± 0.9 GPa. It has aspect ratio covering high surface area, hollow from inside, hydrophobicity,high biocompatibility, good electrical and mechanical properties. Out of all allotropes of carbon, CNTs and Graphene are significant ones. CNT is thin film rolled as cylinder like 3D tube and Graphene is a 2D material in a single layer.CNT because of its rolled structure is able to act as carrier materials for drug delivery and act as superconductor. Important Physical and Mechanical Properties of Graphene and CNTs have been discussed in Table 1 [10].

Solubility of CNTs, both in organic and aqueous vehicles, can be customized and functionalized on the basis of the materials. CNTs are used because of the specific properties such as high Chemical reactivity, better surface are easily improved by using biomaterials. Biomaterials are developed through nano-materials like CNTs. Other nanomaterials used in this regards are graphene and graphene related materials etc. The biomolecules like nucleic acid, protein, and peptides interact with the CNTs through functionalize (chemically modify) and improve the properties of CNTs for biomedical application. Human cells are found to be grown on CNTs and they are nontoxic in nature. Carbon nanotubes (CNTs) possess remarkable distinct properties which make them good candidate in biomedical application such as good electronic

* Corresponding author.
E-mail address: nidhijain1704@gmail.com (N. Jain).

https://doi.org/10.1016/j.matpr.2021.01.895
2214-7853/© 2021 Elsevier Ltd. All rights reserved.
Selection and peer-review under responsibility of the scientific committee of the 3rd International Conference on Materials, Manufacturing and Modelling.

Please cite this article as: N. Jain and S. Tiwari, Biomedical application of carbon nanotubes (CNTs) in vulnerable parts of the body and its toxicity study: A state-of-the-art-review, Materials Today: Proceedings, https://doi.org/10.1016/j.matpr.2021.01.895

Table 1
Important Physical and Mechanical Properties of Graphene and CNTs.

Properties	Graphene	CNTs
Resistivity	Around 15–65 Ω-cm [16].	Individual SWNT, at room temperature, can be as low as 10–6 Ω cm – 1[19]
Thermal conductivity	Around 5.4 × 103 Wm-1 K-1 [16]	CNTs display longitudinal thermal conductivity of around 3000–6000 W/m K for a solitary nanotube at room temperature [20].
Elastic modulus/ Young's modulus	Elastic modulus around 0.6 – 1 Tpa [17].	Young's modulus was found to be for around 12 tubes and around 1.9 TPa, 0.45 TPa at lowest range and around 4.17 TPa for the highest[10],
Specific Surface area	Around 2635 m2 g – 1 [16]	A theoretical surface area was calculated around 1316 m2g – 1 [18].
Tensile strength	Around 135 GPa [16].	100–200 GPa range, among the highest in existing materials [17].
Structure	Graphene is a 2D material in a single layer [10].	CNT is thin film rolled as cylinder like 3D tube. [10].

properties, extremely penetrating capability on the cell membrane, elevated drug-loading and pH-dependent therapeutic use, reception capacities, thermal properties, huge surface area and trouble-free modification with molecules, which cause to be as useful material [11].

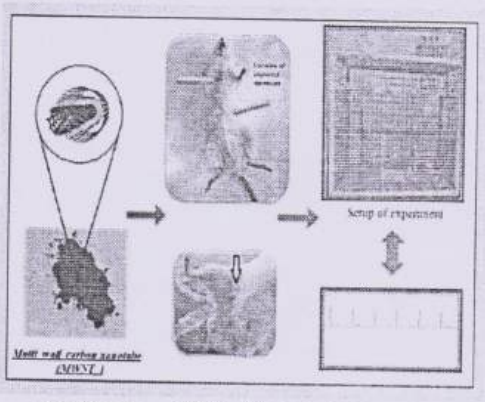
These properties gave them special edge in drug delivery mechanism and for pharmaceutical purposes. Researchers and scientist put forward that even life threatening disease cancer, tuberculosis, nervous tissue regeneration, neural scaffolds and myocardial conduction are easily treated using CNT-based drug delivery systems [12].The study of the toxicity of CNTs is an important factor as the usage of CNTs is significantly increased in drug delivery aspects [13]. Abundant data and reports have been invested to decide the nature of toxicity caused by CNTs in living systems, precisely in biomedical applications. Still there is lot of room for determining the toxicity of CNTs. Deficient toxicological studies and experimentations have not yet made clear picture about the real cause of toxicity in vitro as well as in vivo conditions. In the present review paper, various studies have been done to understand possible causes of toxicity due to various biological conditions [14–15].

The shape of SWCNTs (Single Walled Carbon Nanotubes) is hexagonal close-packed bundles with diameter ranges from 0.4 to 2 nm. They are in the form of single Graphene cylinder, whereas MWCNTs have several coaxial cylinders in which each Graphene sheet rolled together around the hollow core. The outer and inner diameter of MWCNTs ranges from 2 to 100 nm and 1 to 3 nm respectively, and their length is 0.2 to several meters. The chemical reactivity points of CNTs were tips and the sidewalls [21].

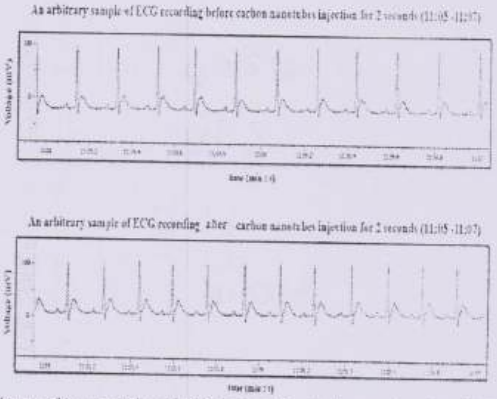
Carbon nanotube fibres are acting as important alternative for development of the biomedical application. Extraordinary properties of CNTs could be exploited to develop the biomedical application limiting their direct exposure. It was found out by the scientist that mechanical, thermal, electrical properties of hydrogel, fibres are improved when merged with CNTs. These embedded CNTs are very efficient drug delivery, scaffolds, tissue engineering materials etc. CNTs are novel material which is widely used in biomedical applications such as cardiovascular diseases. The nano-compatibility of the carbon nanotube proves it as a novel candidate for future advance research in the field of medicine and biology.

2. Direct injection of carbon nanotubes (CNTs)

The study of cardiac effect of MWCNTs on direct injection has been seen in rats. When carbon nanotubes are directly injected in the rats, it was found through Electrocardiogram (ECG) signals that the heart rate increases significantly. CNTs nano-tubes do not cause any inconvenience to autonomic nervous system (ANS). However scientist has to work on the biocompatible these nano-tubes on the heart.



Direct injection of CNT inside the body of the rat[1]



An random sample of ECG recording before and after CNT injection for 2 s, from 11:05 to 11:07 (min: s). (Top row) before CNT injection, (bottom row) after CNT injection[1]

Fig. 1. Direct injection of CNT inside the body of the rat[1].An random sample of ECG recording before and after CNT injection for 2 s, from 11:05 to 11:07 (min: s). (Top row) before CNT injection, (bottom row) after CNT injection[1]

From the Fig. 1a it was concluded from study that CNTs can be efficiently used in the biomedicine, pharmacology, and neurosciences Fig. 1b clearly illustrate the effects of MWCNTs on ECG signals on rat body before and after CNT injection.But there is constant need to check the biocompatibility of CNTs inside the body [22–25].

3. Nervous tissue regeneration using CNTs

Tissue regeneration is always a hot topic for the researcher and scientist. Nano-materials like carbon-nanotubes, fullerenes, carbon nano-fibers are coming as the suitable candidate for dealing such delicate issue in human body. Nano-materials and regenerative medicine are together acting as a strong candidate for repair and growth of damaged tissue in delicate organ such as nervous system. As Nervous system is dealing with significant functions of the body like memory, movement and control. Carbon nanotubes show inherent properties of good thermal, good mechanical and electrical properties which help them in growth, reconstruction, etc. Therapies like neurodegenerative and repair of spinal cord injuries involves nerve tissue engineering in which CNT interfaces helps in neuronal segregation, growth and network rebuilding [26–27].

3.1. Different CNTs based scaffolds for supporting neural cells

Fig. 1 In this figure Phosphate used glass microfiber (PGF) scaffold are shown with animated CNT Poly(l/d-lactic acid) (PLDLA) through electrospun Nanofibers. They are synthesised which is wrapped around the CNT-PGF substrate and are tested in a rat sciatic injury model. The developed model has shown superior neural interface, cell feasibility, and physicochemical integrity. The scaffolds implanted shows motor functions improvement in the muscle of the animal. [28].

Fig. 2 In this figure shown over here contains proteins silk fibroin (SF) combine with the carbon nanotubes have good mechanical properties used as nerve guide conduit (NGC), fibronectin with nanofibers (FN)helps in neuron development and relocation. FN merged with the SF/SWNTs NGCs tubes (conduits) helps in the growth and adhesion of U373 cell lines bioactivity. In rats when NGCs inserted in vivo, upto*10mm* sciatic nerve causes nerve regeneration after five weeks [29].

Fig. 3 In this figure manufacturing process is depicted where MWCNTs are combined in a poly(ethylene glycol) diacrylate (PEGDA) medium. 3D printing technologies is used for making scaffolds which help variation and progress of neural cells [30].

Fig. 4 Chitin-based composite hydrogels integrated MWCNTs: These hydrogel are hybrid type of hydrogel which consist of chitin nanofibers and carbon nanostructures. These hydrogel have good thermal stability, a improved hemocompatibility, good quality mechanical properties and shows slow biodegradability rates, and swelling ratio compared to control chitin hydrogels. In vitro assessment of Schwann cells show better and successful propagation of the neuronal cells with less cytotoxicity and neurotoxicity. CNTs act as good candidate as neuronal growth substrates and nerve regeneration [31].

CNTs toxicity acting as a roadblock for neuronal applications, come to know during the studies. To overcome the toxicity of CNTs nano-toxicological studies and alone with pharmacokinetic studies are required. We cannot bypass toxicity issues off CNTs while attaching it with the substrate. Carbon-based nano-materials (CBNs) have exposed great possibility when incorporated with nerve tissues. But extensive studies are still required to study the toxicity considering factors such as shape, size functional group attachment, release mechanism etc of Carbon nanotubes.

CNTs are integrated with devices like nerve conduits, various types of sensors, micro and nano- electromechanical systems (NEMS and MEMS) have open better avenue in nervous system function. Bio-compatibility and functionality of CNTs materials is also increased by advance manufacturing technologies like 3D printing. This advance manufacturing would help in better merging of CNTs with biological materials like proteins and biodegradable biopolymers which in turn help in nervous regeneration [32].

4. Tissue engineering utilizing CNT-Based hydrogels

The CNTs have unique and outstanding properties which fostered its use in the biomedical field. But the toxicity remains by the CNTs after when not properly excreted was studied in brief. Much work needed to be done. It was seen that free particles of the CNT are toxic depending upon their shape, size and structure. The use of hydrogel as safe(r)-by-design nano-composite widen the use of CNTs in biomedical application such tissue engineering, drug delivery and diagnostics [33].

Cell should have adhesion properties for making scaffolding materials. These scaffolding materials help in replacing dead tissues, treatment process etc. Scaffolding materials could act as suitable candidate for repair and maintenance of the cellular materials if they are able to address certain properties like cross-linked networks, good mechanically resistant properties, and biocompatible, good cell adhesion. Hydrogel prepared from biopolymer acts as chosen materials, which when merged with nanofillers like CNT augment the mechanical properties, electrical conductivity, etc. Several examples in the literature we can see in this regard like improvement in the tissue regeneration process through electroactive performance of cardiac or nervous improved tensile by adding of 1 wt% of SWCNT in an alginate scaffold, increase in growth, proliferation and maintenance etc. Improvement in the physical properties acting as a bon in cardiac application such as cardiomyocytes fitting or cardiac patches etc. Several scientist studied tensile and compressive modulus on the osteoblast multiplying in chitosan scaffold enclose crystalline hydroxyapatite, in thermosensitive chitosan hydrogels in surgeries like bone grafts, repair of spinal cord injury by filling gap, Nerve conduits for axon recovery were generated using injection moulding method using CNT/oligo (poly (ethylene glycol)fumarate) (OPF) nanocomposite could help axon recovery.See in Fig. 5(a) and (b)[34–35].Fig. 6

Scientist and researcher are working hard to increase in the biocompatibility of CNTs. CNT acts are promising materials in the biomedical field. CNTs could be combined with various organic compounds and metallic nano-particles to develop efficient scaffolds for nervous cells and tissues. They are acting as booster for cell growth and re-colonization in nervous cells. To overcome the toxicity of the CNTs biocompatible hydrogels with CNT are acting as substitute for harnessing the wonderful properties of the CNTs. The biocompatible hydrogels embedded with CNT restrict the risk of direct exposure and in turn increase its application in various avenues of nerve regeneration, tissue engineering, cell growth and proliferation. 3D structure of hydrogel broaden the applications, develop more flexibility in the field injectable tissues, biocompatible scaffolds etc. The unused remains of CNTs create a nuisance in the body. Hydrogel based nano-composite boundary their dispersal inside the organism widen the applications carbon nanoparticles for biomedical applications [36–46].

4.1. In vivo restoration of myocardial conduction with Carbon nanotube fibers

Carbon nanotube fibers (CNTfs) are used for the impaired myocardial conduction. The chest electrophysiology studies were

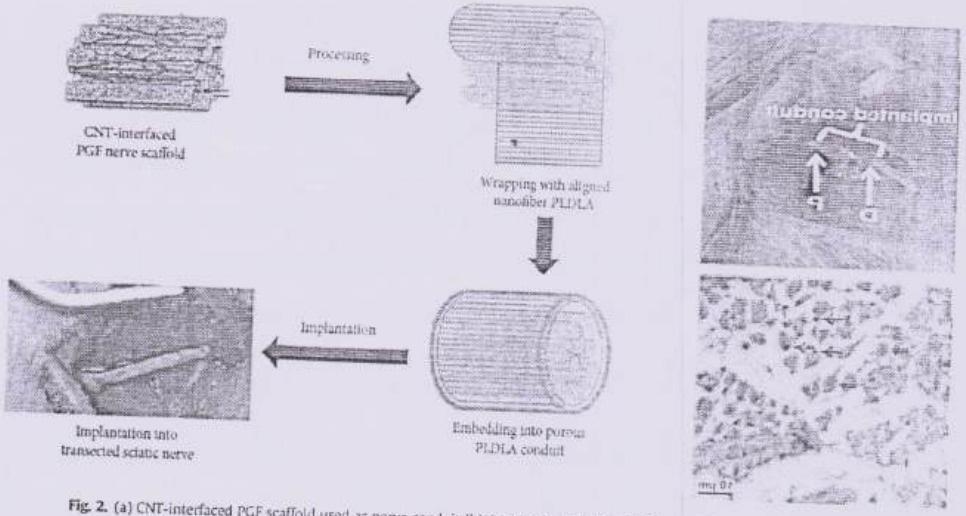


Fig. 2. (a) CNT-interfaced PGF scaffold used as nerve conduit (b) the implanted SF/SWNT/FN conduit in left sciatic nerve [31].

performed on various animals like sheep (around n = 4). It was found that there was enhancement in conduction velocity using CNTf. All the chronic cases recommencement of atrioventricular conduction. CNTfs used across epicardial scar shows betterment of the conduction. CNTs are able to restore electrical conduction providing persistence solution for the diseased myocardium. Researchers are trying to develop restorative solution to avoid ventricular tachycardia by improving ventricular and atrioventricular myocardial conduction.

Unique novel materials are used for disfigurement myocardium which can restore conduction velocity. In Ovine model it was proved that delayed conduction is caused by anatomic block (ie, radiofrequency-induced scar).Introduction of the conductive CNTf across the area of the block could decrease the myocardial conduction time. In rat vivo studies prove that CNTfs are compatible with heart implantation. It was found that nanoscale carbon nanotubes are toxic inside the body, but when CNT is used as CNTf bundles allows macroscopic/surgical manipulation. But still animal studies needed to be done prove that CNTf increases myocardial conduction. Primary study in the human model absent Atrio-ventricular conduction (pacing currents), but shows improvement in myocardial conduction. The increase in the pacing current is achieved by

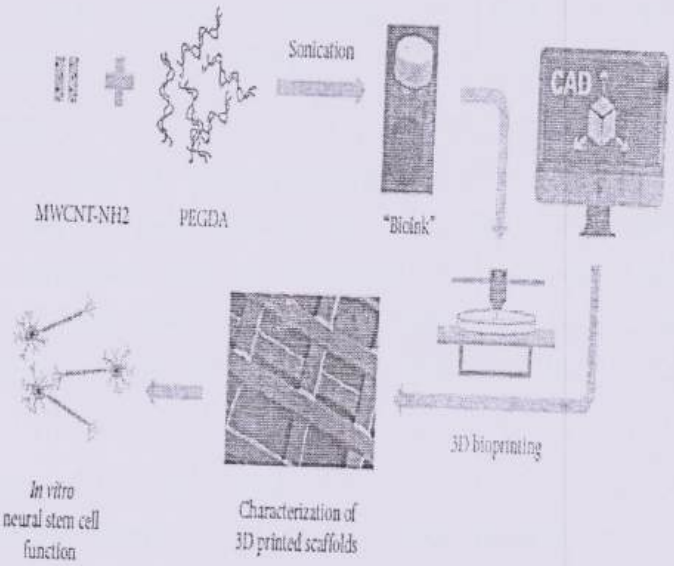


Fig. 3. In this figure manufacturing process is depicted where MWCNTs are incorporated in a poly (ethylene glycol) diacrylate (PEGDA) matrix for making scaffolds [31].

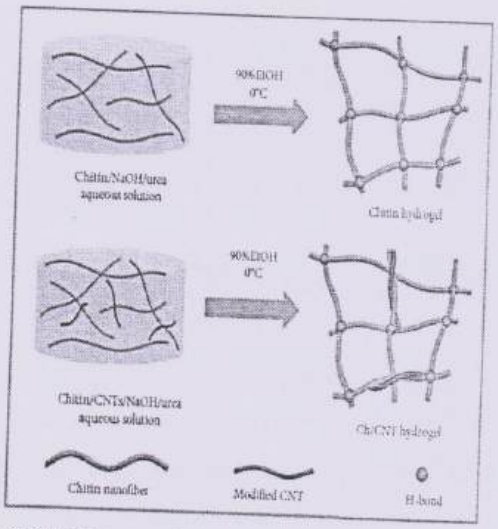


Fig. 4. Schematic representation of the synthesis process of chitin-MWCNT hydrogel hybrids [31].

surface improvement in the material. Surface modification helps in the integration of the synthetic materials with neural cells. More clinical studies are needed to define the suitability of the product. This is the first model which have provided evidences for the materials-based treatment in Renovation of Myocardial Conduction With Carbon Nanotube Fibers [47].

5. Use of CNTs in efficient cancer therapy

Tumor is caused by uncontrolled growth of the cells. Delivery of drug at specific site could be easily accomplished by the use of carbon-nanotubes substrate. CNTs have the advantage of compact nanosize and higher surface for efficient loading of the drugs. Major challenges faced by the anticancer drugs are toxic effect and site-specific delivery. GEM/HA-MWCNTs and GEM/HA-PEGMWCNTs are very effective drug for colon cancer. In the same way MWCNTs-COOH-CDDP formulation appreciably decline cell viability up-to 60% after 48 h as compared to MWCNT-COOH. DOX/MWCNTs is another drug which shows compared to free drug, which as pH-receptive system for delivering the drug and to lowering systemic toxicity [48–51]as represented in Fig. 7.

6. Toxicity of CNTs

Industrial exposure increases the toxicity of the CNTs on human body. The study of toxicity of CNTs on various organs of the body has been discussed in review paper. Toxicity is caused due to various routes of exposure such as oral inhalation, skin injection direct ingestion, etc. Once the CNTs is exposed to various organ of the body it causes severe problems in the body such as asthma, bronchitis, Emphysema at initial exposure and when the exposure is prolong and severe it causes lung cancer. It affects the other parts of the body such as digestive system, gastrointestinal tract (GIT) by causing diseases like Crohn's disease and colon cancer. At circulatory system it causes blood clotting and heart disease. CNT would mount up in liver and spleen also. We all know the toxicity of CNTs is reduced by shape, size, and composition, it also depends on the number of walls, chirality. Sometime the asbestos particles miss leaded as CNTs Figs. 8 and 9.

The shape of asbestos particles is light weight long, thin crystals which lead to toxicity [52–55].Sometimes CNTs are eliminated from the body through excretory system, but if it remains in the body at secondary organs. CNT excretion is governed by numerous parameters such as functionalization, scattering and extent. Shape and size are major factor which effect the excretion of the CNT could exit from the body via urinary. Smaller CNTs with low aspect ratio are macrophages can engulf MWNTs and finally drained by lymph vessels whereas when the size and aspect ratio is high that of CNTs it is difficult to be removed and it's collect in tissues, where they encourage carcinogenesis. If the solubility of CNTs is more than it's easily excreted from urine and avoid accumulation. CNT bundles could causes discomfort which leads to over reactivity and inflammation of the immune system leads to the development of cancer Shown in the Fig. 10.

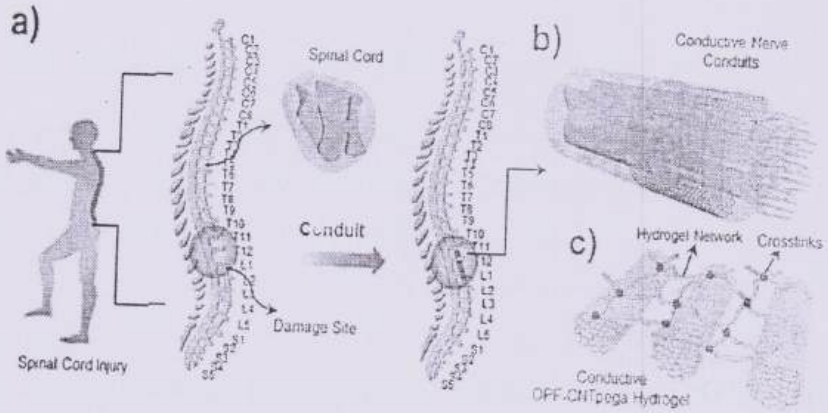


Fig. 5. (a) Figure illustrates the diagram of spinal cord in the human body. (b) Treatment of the spinal cord injury through Conductive nerve conduits (c) Representation of the conductive OPF-CNT pegahydrogel [32].

7. Conclusion

CNTs are good candidate in the biomedical treatment. Researchers and scientist are working hard to increase effective use in delicate organ of the body like nervous tissue regeneration, neural scaffolds, myocardial conduction, and tissue engineering, cancer treatment etc. There is a need to check the biocompatible with organic compounds, shape and size, aspect ratio of the CNTs for its proper and efficient output. From the past it was found that CNTs have been used in drug delivery system. Now CNTs as hydrogel, CNTs based scaffolds are developed for supporting neural cells, cardiac cell etc. The CNTs as hydrogels / fibres /scaffolds limit the exposure of the CNTs and increases efficiency for biomedical applications. CNTs could avoid solution to sudden death by providing alternative materials-based treatment. CNTs have massive prospective for clinical application, taking concern about the safety and toxicity. Considering the cytotoxicity of CNTS many parameters including shape, size, purity, production method and function-

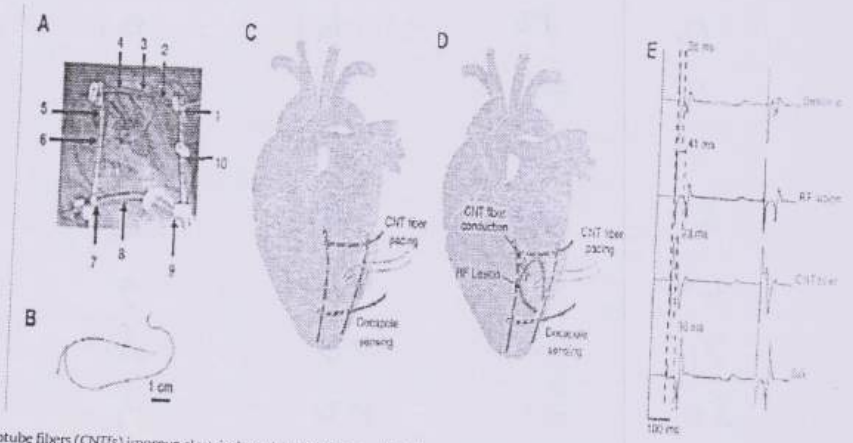


Fig. 6. Carbon nanotube fibers (CNTs) improve electrical conduction in myocardial tissue. Carbon nanotube fibers (CNTs) enhance electrical conduction in a severely scarred myocardial tissue. Picture (a) depicts the epicardially implanted of CNTF in a sheep heart. Picture (b) depicts CNTF tied onto 6–0 Prolene. Picture(c) and Picture (d) depicts decapolar sensing catheter setup after and before injury [56].

Unique novel materials are used for disfigurement myocardium which can restore conduction velocity. In Ovine

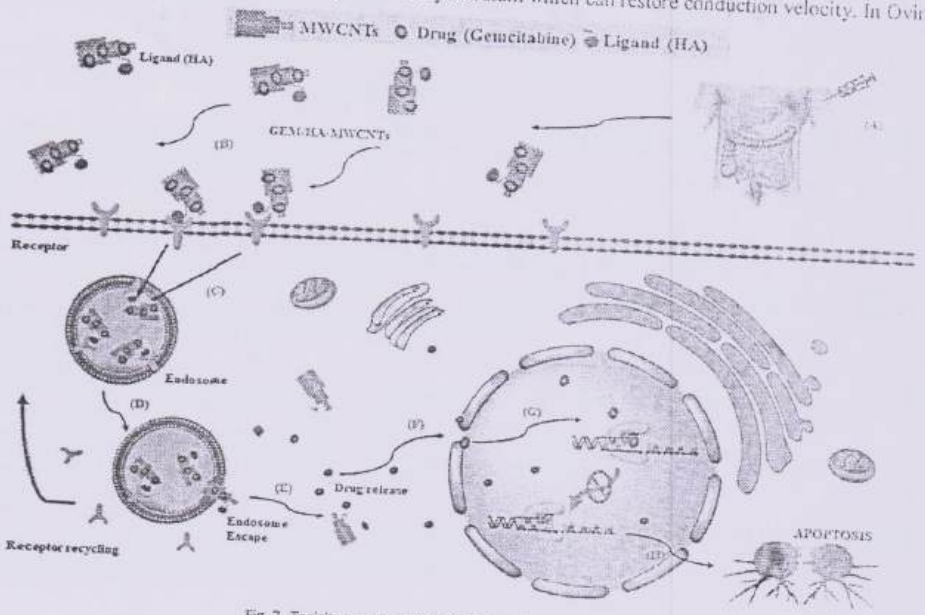


Fig. 7. Toxicity associated with CNTs on various organs [57].

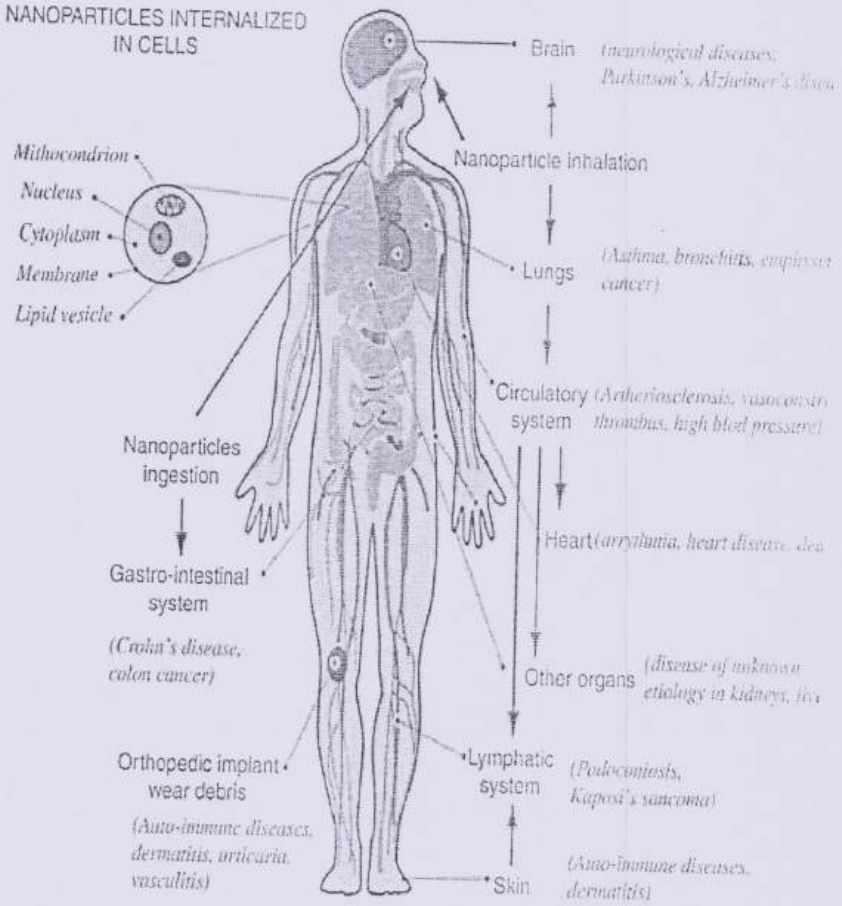


Fig. 8. Shows the toxic effect of CNTs on various parts of the body and also showcases the result of toxicity on various organs of the body. Reference No. [52].

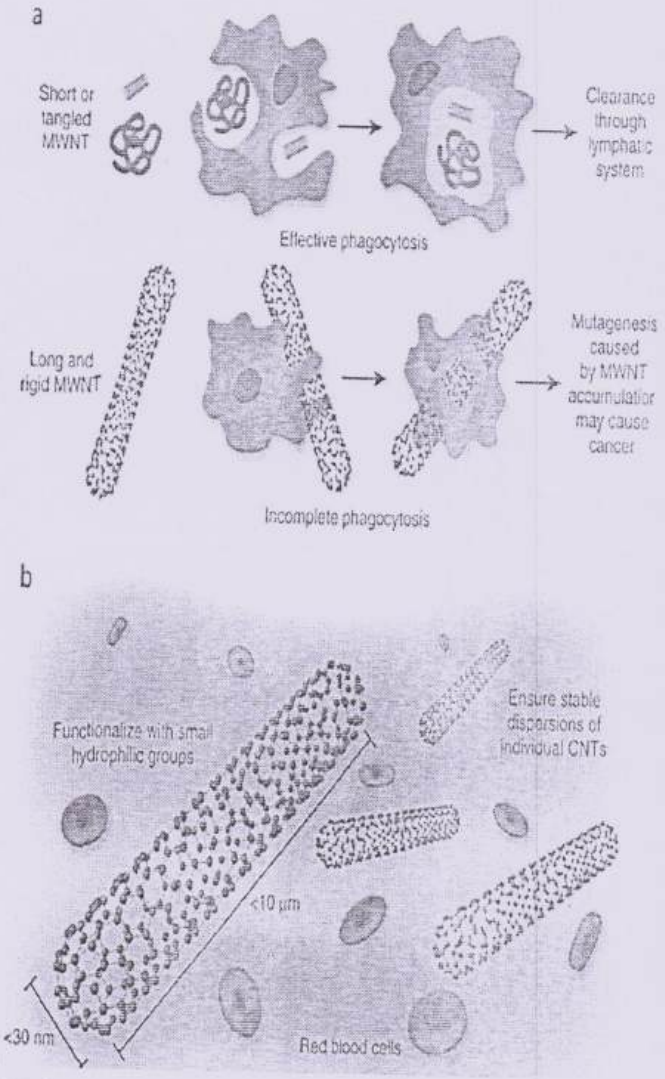


Fig. 9. The figure illustrates the significance of low aspect ratio and solubility of the CNTs. Reference No. [12].

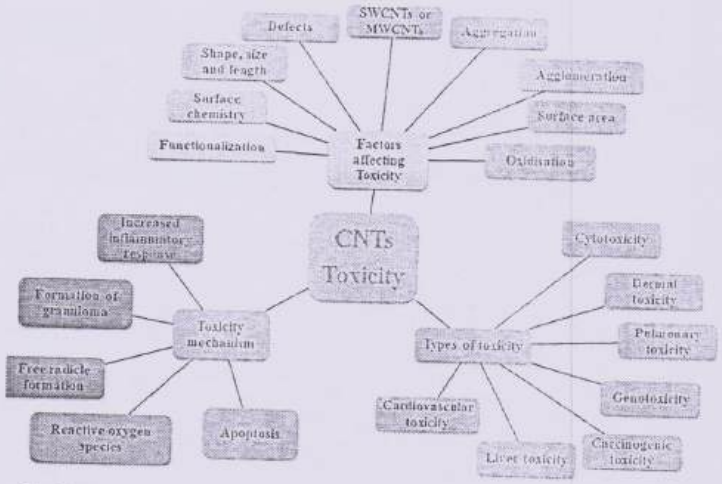


Fig. 10. Illustrate the CNT toxicity mechanism ,types and factores effecting the toxicity.Reference No.[57]

alisation are thoroughly studied.Further there is constant need for invivo studies to know different methods of administration. Whereas in-vitro studies have been useful in recognizing of CNT toxicity.

Declaration of Competing Interest

The authors declare that they have no known competing financial interests or personal relationships that could have appeared to influence the work reported in this paper.

Acknowledgements

All persons who have made substantial contributions to the work reported in the manuscript (e.g., technical help, writing and editing assistance, general support), but who do not meet the criteria for authorship, are named in the Acknowledgements and have given us their written permission to be named. If we have not included an Acknowledgements, then that indicates that we have not received substantial contributions from non-authors.

References

[1] M. Hosseinpour, M.A. Alimohammadi, P. Shahabi, M. Sadighi, N.G. Ghamkhari, Biolmpacts 6 (2) (2016) 79–84.
[2] Z. Huang et al., Carbon N Carbon 62 (2013) 127–134.
[3] Y. Y. Hui, et al., Carbon nanomaterials for biolmaging, bioanalysis,and therapy. New York: Wiley.
[4] A. Kassem, G.M. Ayoub, L. Malaeb, Science of the Total Environment 668 (2019) 566–576.
[5] J. Kaur, G.S. Gill, K. Jeet, S. Mohapatra, et al., Amsterdam: Elsevier,(2019) 113–135.
[6] D.W. Khang, et al., U.S. Patent, 9,981(2018) 042.
[7] S.K. Prajapati et al., European Polymer Journal 120 (2019) 109–191.
[8] S.K. Prajapati et al., International Journal of Biological Macromolecules 123 (2019) 691–703.
[9] V. Rathod et al., 20, 2(2019) 51.
[10] N. Tangboriboon, S.S. Mohapatra (Eds.), Nanocarriers for drug delivery. Elsevier, Amsterdam, 2019, pp. 451–467.
[11] J.P. Salvetat, J.M. Bonard, N.H. Thomson, A.J. Kulik, L. Forró, W. Benoit, L. Zuppiroli, Appl. Phys. A 69 (1999) 255–260.
[12] P. Sharma et al., Current Drug Delivery 13 (6) (2016) 796–817.
[13] J. Simon, E. Flahaut, M. Golzio, Materials 12 (2019) 624.
[14] D. Mohanta, S.Patnaik, S. Sood, N. Das, Journal of Pharmaceutical Analysis, 9 (2019) 293e300
[15] Y. Qu et al., Materials Science and Engineering 90 (2018) 764–780.
[16] H.G. Prashantha Kumar, M. Anthony Xavior, Procedia Engineering 97 (2014) 1033–1040.
[17] A. Peigney, C. Laurent, E. Flahaut, et al., Carbon, 39 (2001) 507–514.
[18] A. Takakura, K. Beppu, T. Nishihara, A. Fukui, T. Kozeki, T. Namazu, Y. Miyauchi, K. Itami, Nature communications 10 (2019) 3040.
[19] A. ka Lekawa-Raus, J. Patmore, L. Kurzepa, J. Bulmer, Advance functional materials, 24(2014), 3661–3682.
[20] Z. Han, A. Fina, Progress in Polymer Science 36 (7) (2011) 914–944.
[21] A.M. Asiri, A. Mohammad, eds. Applications of nanocomposite materials in drug delivery. Duxford, UK: Woodhead Publishing (2018)203–210.
[22] B.G.P. Singh, C. Baburao, V. Pispati, et al., International Journal of Research in Pharmacy and Chemistry 2 (2) (2012) 523–532.
[23] F. EsThaghi, P. Shahabi, J. Frounchi, M. Sadighi, H. Yousefi, Basic Clin Neurosci (2015) 123–32.
[24] N.G. Ghamkhari, P. Shahabi, M. Alipoor, P.F. Ghaderi, M. Asghari, A.M. Sadighi, Adv Pharm Bull 5(2015) 483–9. 10.15171/apb.2015.066.
[25] R. Waheliar, M.S. Siddiqui, S. Ong, A.F. Ismail, J Explanosens 1 1 (2016) 1–12.
[26] J. Kayat, V. Gajbhiye, R.K. Tekade, N.K. Jain, Nanomedicine 7 (2011) 40–49.
[27] C. Redondo-Gómez, R. Mora, D. Blanch-Bermúdez, C. Espinoza-Araya, D. Hidalgo-Barrantes, J. Vega-Baudrit, Advances in Polymer Technology Volume (2020) 16
[28] F. Mottaghitalab, M. Farokhi, A. Zamiby et al., 8 (2013) 9 Article ID e74417.
[29] H.-S. Ahn, J.-Y. Hwang, M.S. Kim, et al., Acta biomaterialia 13 (2015) 324–334.
[30] Y.S. Zhang, A. Khademhosseini, Advances in engineering hydrogels, Science 356 (2017) 6337.
[31] S.-J. Lee, W. Zhu, M. Nowicki et al., Journal of Neural Engineering 15, (2018) Article ID 016018
[32] A. Vashist, A. Kaushik, A. Vashist et al., Advanced Healthcare Materials, 7(2018) 9. Article ID 1701213.
[33] S. Wu, B. Duan, A. Liu, Y. Wang, Q. Ye, L. Zhang, Carbohydrate Polymers, 175 (2017) 830–840.
[34] J. Simon, E. Flahaut, M. Golzio, Materials 12 (4) (2019) 624.
[35] M. Srikanth, R. Annarufo, K. Cliff, L. Yan, ACS Omega 4 (2) (2019) 3044–3051.
[36] X. Liu, J.C. Kim, A.L. Miller, S.E. Waletzki, L. Lu, New J. Chem. 42 (2018) 17661.
[37] M. Shelhahelesiam, S.D. Wheeler, K.C. Dulle, M. Naveiras, A.J. Perales, P. Chen, Acta Biomater. 69 (2018) 107–119.
[38] A. Facciola, G. Visalli, S.L. Maestra, M. Coccaretti, F. D'Aleo, C. Minniti, G.S. Pellicano, A.D. Piero, Environ. Toxicol. Pharm. 65 (2019) 23–30.
[39] C. Wei, X. Dong, Y. Zhang, J. Liang, A. Yang, D. Zhu, T. Liu, D. Jiang, L. Wu, Sens. Actuators B Chem. 273 (2018) 264–275.
[40] R. Hindumathi, M. Jagannatham, P. Haridoss, C.P. Sharma, Nano Struct. Nano Objects 13 (2018) 39–45.
[41] K. Kuche, R. Maheshwari, V. Tambe, K.-K. Mak, H. Jogi, N. Kovel, M.R. Pichika, T. R. Kumar, Nanoscale 10 (2018) 8811–8827.
[42] E.Gaufrès, S.Marcet, V. Aymong, N.Y. Tang, W. Favron, A. Thouin, F. Allard, C. Rioux, D. Cottenye, N. M. Verhaegen, et al., 49(2018) 174–182.
[43] S. MansouriMajd, A. Salimi, Anal. Chim. Acta 1000 (2018) 273–282.
[44] P. Ramnani, Y. Gao, M. Ozsoz, A. Mulchandani, Anal. Chem. 86 (2014) 8004–8004.
[45] R. Pang, X.S. Tang, D. Li 14 (2018) 1800013.
[46] M. Mottaghi, B. Behnam, A. Saberkar, J. Cell. Physiol. 234 (2019) 249–259.

[47] Y. Zhou, Y. Fang, R.P. Ramasamy, Non-Covalent Functionalization of Carbon Nanotubes for Electrochemical Biosensor Development, Sensors 19 (2019) 392.
[48] D.M. Pedrotty, V. Kuzmenko, E. Karabulut, A.M. Sugrue, C. Livia, V.R. Vaidya, C.J. McLeod, S.J. Asirvatham, P. Gatenholm, S. Kapa, Three-dimensional printed biopatches with conductive ink facilitate cardiac conduction when applied to disrupted myocardium, Circ Arrhythm Electrophysiol. 12 (2019), https://doi.org/10.1161/CIRCEP.118.006920 e006920.
[49] A. Mihic, Z. Cui, J. Wu, C. Vlacic, Y. Miyagi, S.H. Li, S. Lu, H.W. Sung, R.D. Weisel, R.K. Li, A conductive polymer hydrogel supports cell electrical signaling and improves cardiac function after implantation into myocardial infarct, Circulation 132 (2015) 772–784.
[50] S. Pok, F. Vitale, S.L. Eichmann, O.M. Benavides, M. Pasquali, J.G. ACS Nano, 8 (2014)9822–9832.
[51] G. Xin, T. Yao, H. Sun, S.M. Scott, D. Shao, G. Wang, J. Lian 349(2015)1083–1087. Z. Xu, Y. Liu, X. Zhao, L. Peng, H. Sun, Y. Xu, X. Ren, C. Jin, P. Xu, M. Wang, et al. Adv Mater. 28(2016)6449–6456 10.1002/adma.201506842
[52] S.Y. Madani, A. Mandel, M. AlexanderA. Seifalian 4 (2013) 21–23.
[53] N. Lodhi, N.K. Mehra, M.K. Jain, J Drug Target 21 (1) (2013) 67–76.
[54] S.T. Yang, J. Luo, Q. Zhou, H. Wang Theranostics 2 (2012) 113–121.
[55] M. Luo, X. Deng, X. Shen, L. Dong, Y. Liu, J Nanosci Nanotechnol 13 (2013) 274–283.
[56] Y. Zhang, J. Deng, Y. Zhang, F. Guo, C. Li, Z. Zou, et al., J Mol Med (Berl) 91 (1) (2013) 117–128.
[57] S. K. Prajapati, A. Malaiya, P. Kesharwani, D. Soni, A. Jain (2020).

Source details

Materials Today: Proceedings

Scopus coverage years: 2005, from 2014 to 2023

E-ISSN: 2214-7853

Subject area:

Source type: Conference Proceeding

View all documents > | Set document alert | Save to source list

CiteScore 2022
3.2

SJR 2022
0.445

SNIP 2022
0.774

CiteScore | CiteScore rank & trend | Scopus content coverage

Improved CiteScore methodology

CiteScore 2024 counts the citations received in 2021-2024 to articles, reviews, conference papers, book chapters and data papers published in 2021-2024, and divides this by the number of publications published in 2021-2024. Learn more >

=

=

CiteScore rank

Category	Rank	Percentile

View CiteScore methodology > | CiteScore FAQ > | Add CiteScore to your site

European Journal of Molecular & Clinical Medicine
ISSN 2515-8260 Volume 07, Issue 02, 2020

Numerical Study of Tumor Growth : Tumor Development, Tumor Cells Movement and Cell–Matrix Interactions

[1]Neeta D. Kankane, [2]Dhanke Jyoti Atul
[1]Former Professor, MIT-World Peace University, MAEER'S MIT, Pune, India,
ndkankane@gmail.com
[2]Assistant Professor, SPPU, BVCOE, Lavale, India,
jyoti.dhanke@bharatividyapeeth.edu

ABSTRACT

In this paper we present a mathematical model of the tumor development, tumor cells movement and cell–matrix interactions. This model is considered tumor cells, concentration of oxygen, concentration of nutrient, changes in their microenvironment (tumor angiogenic factors (TAF), extracellular matrices (ECM)) and their matrix of blood vessels, expressed by a chain of discrete tips. With this mathematical model and the results of numerical simulation, the cell properties are closely individual-based cell interactions, can affecting the tumor shape, the tumor's final structure and also discussed which of these interactions is perhaps tumor cells are discrete. Also we described the procedure of tumor development and the changes in microenvironment from avascular to vascular phase, indicating that the matrix of blood vessels develops step by step as the tumor grows.

KEYWORDS: *mathematical model, tumor angiogenic factors, extracellular matrices, concentration of oxygen, concentration of nutrient.*

INTRODUCTION

Many previous models represent these as discrete layers, separated by moving boundaries. Here, we developed a new model, formulated in terms of densities of tumor cells, concentration of ECM, concentration of oxygen, concentration of nutrient, together with a nutrient and oxygen concentration.

Tumors can be regarded as one of the most significant causes of death among the human beings particularly that of malignant tumors, this Mathematical Oncology was tackled by

Anderson *et al.* [1], branch dealing with the research of tumor has gained consideration. Tumor growth is an intricate progression that involves synergy between the extracellular matrices and tumor cells with the inclusive of cell-cell interactions, & ultimately the proliferations and death of the tumor cells. A broadly used model amid the mathematical models dealing with tumor growth is termed as hybrid mathematical model that merges the concepts of discrete and continuous models. That deals with the chemical changes seen in tumors microenvironment on the basis reaction-diffusion equation was proposed by Jie Lyu *et al.* [2]. Since there are abundant of quantitative modeling methods, a surge in the successful implementation through theoretical tactics for cancer biology has been initiated subsequently by the last two decades was studied by Heiko Enderling *et al.* [3]. Other efforts in modeling angiogenesis include hybrid models that combine continuum and discrete approaches proposed by Vilanova G. *et al.* [4].

A particular enzyme by the name of matrix degrading enzymes (MDEs) is secreted by the tumor – cancer cells that help in making the ECM infective by degrading its functionality was studied by Linan Zhang *et al.* [5]. In regards of the hybrid model specific cell properties are taken into consideration at an individual level by the help of equation to help govern the cell migration, which is the discretized form of the partial differential equation. The parameters examined it the successful making of this model are production/degradation at the individual cell level, cell–cell adhesion, proliferation, death and mutation of cell at individual level while keeping the chemicals/ ECM at continuous levels was studied by Anderson *et al.* [6]. But we need to note that a few cell processes like that of cell–cell adhesion can be tough to model to that of the continuum level. To further more shed a light on angiogenesis, it is a process being carried out by the stimulus given external chemicals resulting in the formation of capillary sprout formation and a subsequent proliferation of cells near the tips of these sprout eventually completing the process. The focus to create such model is to scrutinize the corresponding influence of haptotaxis in ensuring the migration of endothelial cells, with also keeping in the mind to examine the formation of capillary network with or without the influence of endothelial cell, eventually creating a theoretical capillary network structure that's forms a model on the basis of sound physiological principles that are in line with the realistic parameter values as seen in vivo was studied by Anderson *et al.* [7]. In the other parts of the tumor there can be seen a variation in the cellular components of Tumor Microenvironment (TME) was studied by Quail *et al.* [8], also can be noticed in between tumors of a single person and in fact even in between patients was studied by Ansell *et al.* [9].

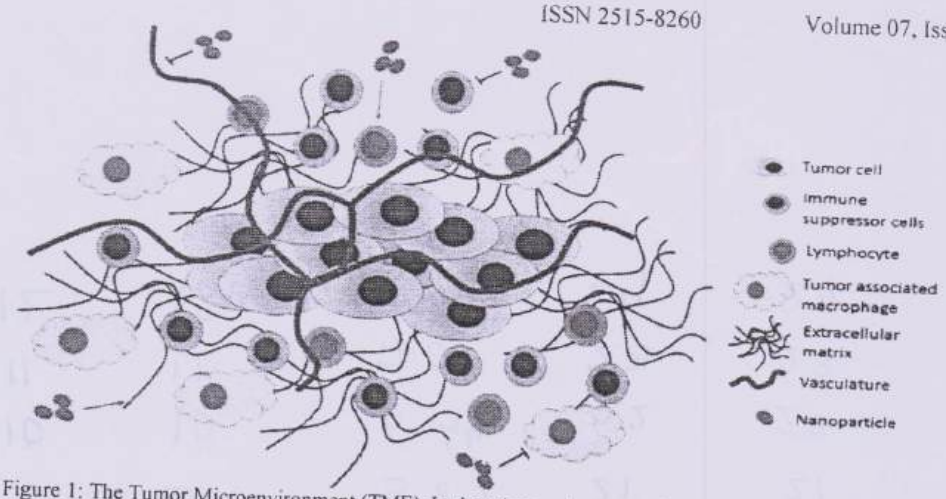


Figure 1: The Tumor Microenvironment (TME). In the microenvironment of TME there can be found the extracellular matrix (ECM), a variety of types of cells (stromal including immune and cancer cells) and myriad molecules like that of microRNAs, chemokines, cytokines and factors of growth as presented by Elizabeth L. Siegler *et al* [10].

Components of Tumor Microenvironment (TME) are shown in figure 1, aspects including vasculature, ECM, and immune cells, with a focus on modulating the immune response was described by Elizabeth L. Siegler *et al.* [10]. The idea in developing a mathematical model for tumor growth was inspired by the dependence of events taking place at different scales, and also to understand the interrelations among the cellular, subcellular, and tissue scales was studied by Deisboeck TS *et al.* [11]. Caleb M. Phillips, *et al.*, studied the growth and angiogenesis hybrid model to tumor growth [12]. The effects of tumor inhibitor factors (TIFs) on tumor angiogenesis and tumor angiogenesis factor (TAF) with also predicting its initiation of vascularization, a mathematical tool was presented by Maggelakis [13]. Anderson and Chaplain explained for the suppression of secondary tumors caused by the primary tumor put forward a one-dimensional mathematical model which in turn explains the angiogenic response of endothelial cells (ECs) on to a secondary tumor [14].

MATHEMATICAL MODEL OF TUMOR VASCULATURE GROWTH

We aim to showcase the in depth model to show the development needed to include the effects presented by the blood flow for vasculature tumor within its capillaries, also in line with the effects of oxygen concentration and nutrients. Based on Anderson and Chaplain' model [7], Heiko Enderling and M. A.J. Chaplain' model [3] and Jie Lyu's model [2], we modified and improved their model in five aspects i.e. density of tumor cells, concentration of extracellular matrix, nutrient concentration, oxygen concentration and concentration of tumor angiogenesis factor. This also aims to show the eventual increase in the number of blood

ISSN 2515-8260 Volume 07, Issue 02, 2020

vessels and tumor cells with time, respectively. The discrete points have been shown for the simulation results. It must be noted that a number of random factors have been taken into account to the model although keeping into consideration the number of blood points and tumor cells follow are persistent.

The logistic model is summarized the example of a per capita growth rate of tumor that is reliant on the tumor size which is relative to the host carry capacity was studied by McAneney H. *et al.* [15]. The balance of cell death and cell proliferation is actually a result of diffusion of nutrients and oxygen in the interior of the tumor at the time of vascular dormancy is presented by Holmgren L. *et al.* [16]. In context to this mathematical model to focus merely on the role of cancer cell migration in invasion, the cell proliferation studied by Anderson ARA *et al.* [17] in the later stages cancer cell proliferation was inducted into the separate version of model. Apart from this various other continumm were put forwarded studied by Chaplain and Lolas *et al.* [18] and Andasari *et al.* [19]. Scrutinizing in-depth detailed effects of degrading enzyems specially that of the urokinase plasminogen system is studied by Frieboes *et al.* [20]. Gerisch *et al.* has presented a Mathematical model of cancer cell invasion of tissue for Local and non-local models and the effect of adhesion [21].

In the system of partial differential equations being used to model for density of tumor cells $n(x,t)$, concentration of extracellular matrix $f(x,t)$, concentration of nutrients $u(x,t)$, oxygen concentration $c(x,t)$ and concentration of TAF $a(x,t)$ is as follows:

$$\frac{\partial n}{\partial t} = \underbrace{D_n \nabla^2 n}_{\text{Random Motility}} - \underbrace{\rho \nabla . (n \nabla f)}_{\text{Haptotaxis}} + \underbrace{\lambda n(1-n)}_{\text{Logistic Growth}} \quad (1)$$

$$\frac{\partial f}{\partial t} = \underbrace{-\mu u f}_{\text{Degradation}} + \underbrace{f(1-f)}_{\text{Logistic Growth}} \quad (2)$$

$$\frac{\partial u}{\partial t} = \underbrace{D_u \nabla^2 u}_{\text{Diffusion}} - \underbrace{\sigma u}_{\text{Decay}} \quad (3)$$

$$\frac{\partial c}{\partial t} = \underbrace{D_c \nabla^2 c}_{\text{Diffusion}} - \underbrace{\omega n}_{\text{Uptake}} - \underbrace{\emptyset c}_{\text{Decay}} \quad (4)$$

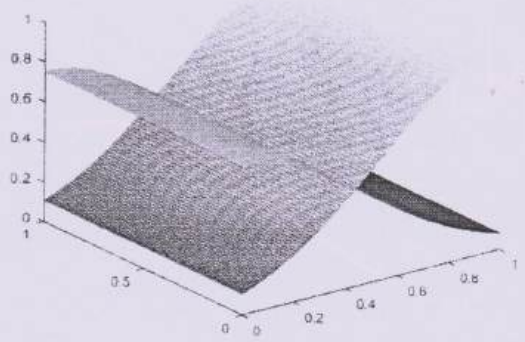


Figure 3. Initial fibronectin concentration and initial TAF concentration profiles for the two-dimensional simulations; The fibronectin initial concentration is highest near the parent vessel at $x = 0$.

To enable not just a qualitative but also quantitative comparison with *in vivo* experimental results a novel mathematical model will be developed that will be discrete model of tumor induced angiogenesis. The assumptions taken into consideration for the model will be based around the movement of an individual endothelial cell found at the tip of capillary sprouts which governs the motion of the entire sprout. The following discrete models can be taken as considered particular illustrations of a wider class of models that are referred broadly as cellular automata models, which in turn have been applicable to a widespread of problems in the various areas of applied mathematics.

Using the Euler finite difference approximation (Mitchell and Griffiths, 1980) [24], we discretize the equations (1) to (5)

$$\frac{\partial n}{\partial t} = \frac{n_{i,j}^{k+1} - n_{i,j}^{k}}{\Delta t}$$

$$D_n \nabla^2 n = D_n \left[\frac{n_{i+1,j}^{k} - 2n_{i,j}^{k} + n_{i-1,j}^{k}}{h^2} + \frac{n_{i,j+1}^{k} - 2n_{i,j}^{k} + n_{i,j-1}^{k}}{k^2} \right]$$

$$\nabla.(n\nabla f) = \frac{n_{i+1,j}^{k}}{4h^2}\left(f_{i+1,j}^{k} - f_{i-1,j}^{k}\right) - \frac{n_{i-1,j}^{k}}{4h^2}\left(f_{i+1,j}^{k} - f_{i-1,j}^{k}\right) + \frac{n_{i,j+1}^{k}}{4h^2}\left(f_{i,j+1}^{k} - f_{i,j-1}^{k}\right)$$

$$- \frac{n_{i,j-1}^{k}}{4h^2}\left(f_{i,j+1}^{k} - f_{i,j-1}^{k}\right) + \frac{n_{i,j}^{k}}{h^2}\left(f_{i+1,j}^{k} + f_{i-1,j}^{k} - 4f_{i,j}^{k} + f_{i,j+1}^{k} + f_{i,j-1}^{k}\right)$$

ISSN 2515-8260 Volume 07, Issue 02, 2020

being P_0 to P_4 are in proportion with the probability of tumor cell being static (P_0), or moving up (P_4), down (P_3), right (P_2) or left (P_1). Which shows us that in any one direction the tumor cell is not biased and is less (more) expected to be immobile approximating a random unbiased walk. It must be noted that as the interaction with other tumor cells, the motion will be get altered. The parameter values have been adopted from Anderson and Chaplain [7]. The domain is a square with length as 1 (non-dimensional).

With the yield of new cell, each of the cell is handed out an exclusive identification number (or also can be assigned in the beginning for the opening 50 cells). At each time step in the simulation primarily updating of all the positions of cells (by their identification number, i.e. larger the number will be, later will it be updated) and once this is done the updating of the individual-based process for all cells is done, e.g. mutation, death and proliferation. As a cause of this the cells do not get simultaneously updated or in a top-to-bottom, left-right manner but as per their identification number. For the update in migration part, the cells with smaller numbers are given a priority in the identification method (i.e. they get to move primarily) but since there is a widespread distribution of the cells over the tumor this method shall not produce any visible bias. The moment the cells have moved, the process of updating the individual-based process gets under way and done again for per cell identification number, but only now the cells get updated immediately after process occurs, e.g., proliferation, this shall evade any conflicts for space.

Simulation results for the discrete model

Figure 4 shows the tumor growth process during the time of simulation, where the proliferative cells are denoted by the blue area, where as yellow for quiescent cells and eventually for the dead cells its inside blue. Figure 5 intensifies the vascular network synchronization as the growth of tumor takes place. Figure 6 and 7 show the oxygen and TAF concentration at individual moment respectively.

The oxygen can be seen as sufficient within the simulated area during the early stages of the tumor growth, the tumor cells are small in number and cells have ample room for tumor proliferation. As a result of which proliferation cells are found in abundance than the others. Meanwhile TAF is secreted by the hypoxic cells, which includes the blood vessel point surrounding the tumor. Since there is limited distribution and concentration of TAF in the simulation area is at this point is depressed, to improve the oxygen environment the blood

ISSN 2515-8260 Volume 07, Issue 02, 2020

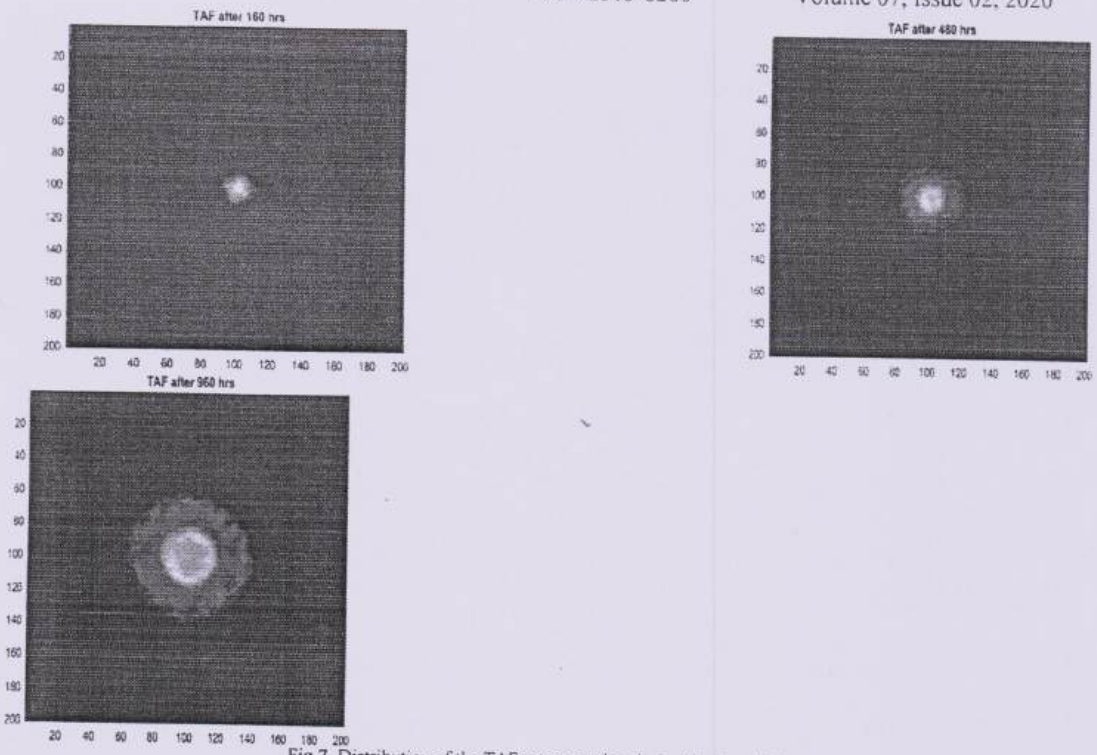


Fig 7. Distribution of the TAF concentration during the simulation.

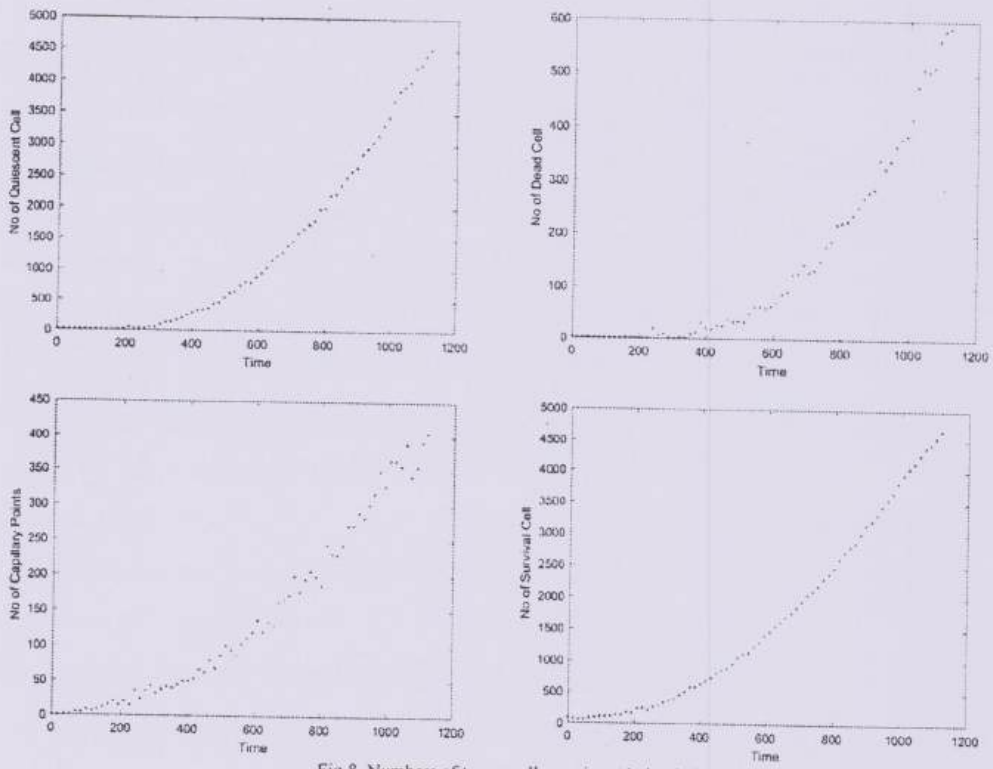


Fig 8. Numbers of tumor cells vs. time (4 simulations).

This study has added more linking features focusing on the early stage of tumor growth by taking the basis of coupled model of tumor growth, tumor angiogenesis and blood perfusion in preceding work.

CONCLUSIONS

The mathematical model has been developed complete interfacial framework for tumor cells movements, cell–matrix interactions and tumor vasculature growth. Subsequently this study introduces a new mathematical model and numerical simulation to visualize the changes in the tumor microenvironment, distribution of oxygen concentration, distribution of nutrient concentration, growth of blood vessels, concentration of extra cellular matrix (ECM) and concentration of tumor angiogenesis factor (TAF) during tumor growth. Additionally, numerical simulation provides simplification for tumor cells migration by secreting matrix-degrading enzymes which degrade the extra cellular matrix. Also this discretized form of the partial differential equations demonstrates the significance of interactions between extracellular matrix and endothelial cells. The presence of fibronectin in the extra cellular matrix and a haptotactic response from the endothelial cells arbitrates a vast variation of cellular interactions with the extracellular matrix and takes key role in cell movements, cell-matrix interaction and tumor vasculature growth. These results would create the impression to appear better haptotactic response for the formation of enough effectively-connected growth in tumor vasculature.

REFERENCES

[1] Anderson, A.R.A.; Maini, P.K. Mathematical oncology. *Bull. Math. Biol.* 2018, 80, 945–953. [CrossRef] [PubMed].

[2] Jie Lyu, *et. al.,* Coupled Hybrid Continuum-Discrete Model of Tumor Angiogenesis and Growth. *PLoS One.* 2016; 11.

[3] Heiko Enderling and M. A.J. Chaplain, Mathematical Modeling of Tumor Growth and Treatment, *Current Pharmaceutical Design*, 2014, 20, 1-7.

[4] Vilanova G, Colominas I, Gomez H. A mathematical model of tumour angiogenesis: growth, regression and regrowth. *J R Soc Interface.* 2017; 14. https://doi.org/10.1098/rsif.2016.0918 PMID: 28100829.

[5] Linan Zhang, *et. al.*, Computational analysis of the effects of matrix-degrading enzymes on cancer-cell invasion, *Journal of Applied Physics*, 2012, 112, 124704 (1 -7).

[6] Anderson ARA. A hybrid mathematical model of solid tumour invasion: the importance of

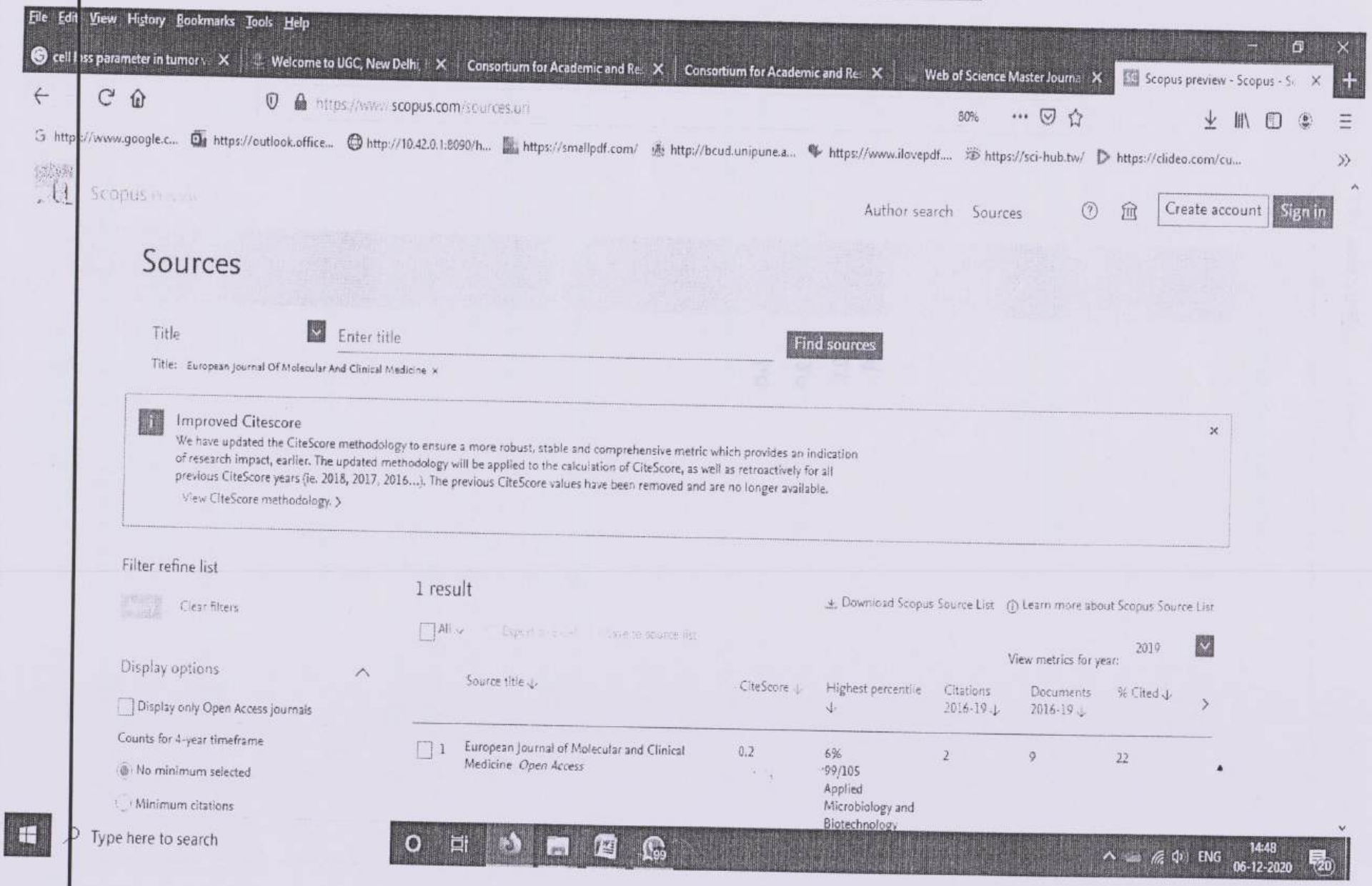
[21] Gerisch A, Chaplain MAJ. Mathematical modelling of cancer cell invasion of tissue: Local and non-local models and the effect of adhesion. *J Theoretical Biology* 2008; 250(4): 684-704.

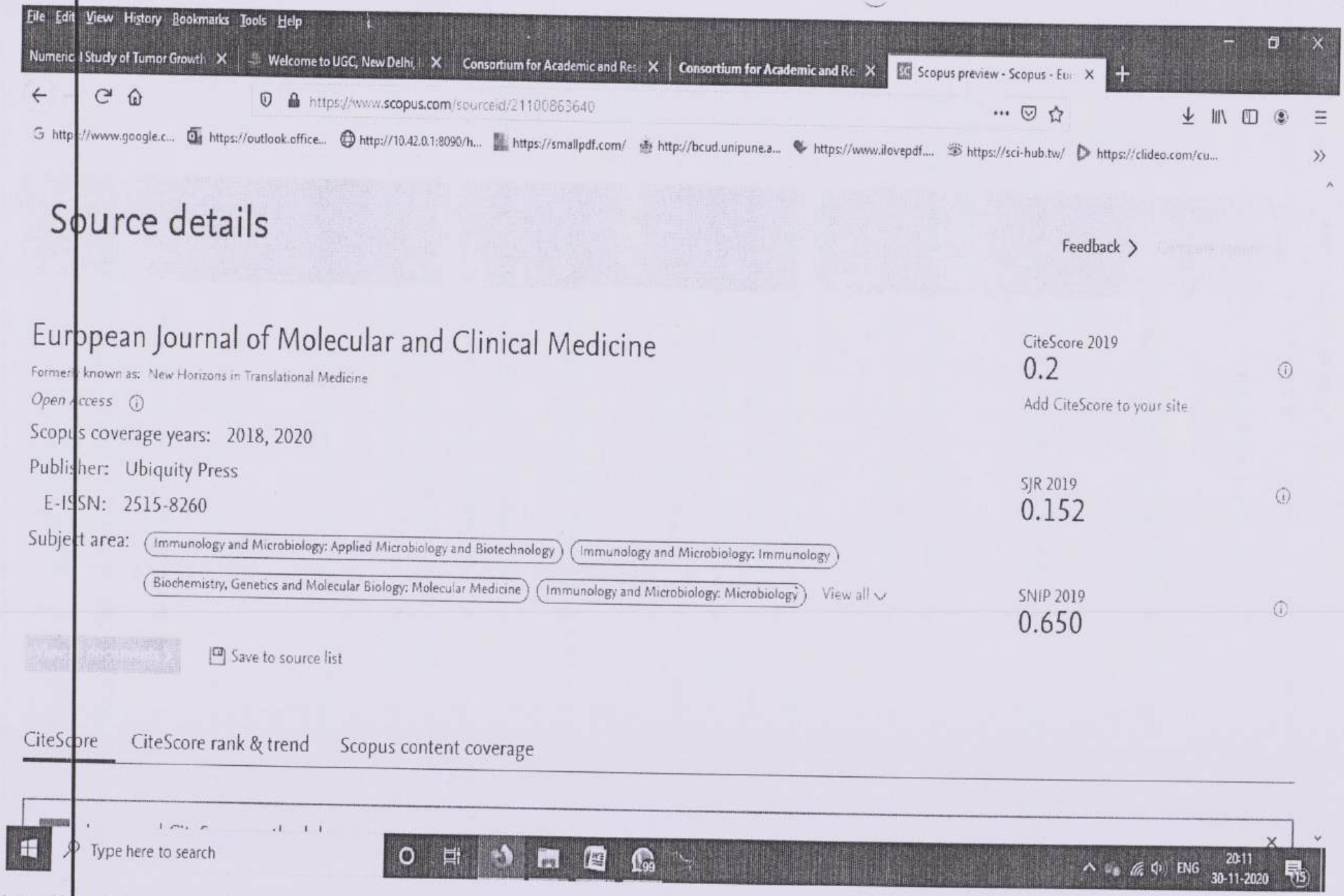
[22] Chaplain MAJ, Ganesh M, Graham IG. Spatio-temporal pattern formation on spherical surfaces: numerical simulation and application to solid tumour growth. J *Math Biol Springer-Verlag* 2001; 42(5): 387-423.

[23] Cai Y, Xu S, Wu J, Long Q. Coupled modelling of tumour angiogenesis, tumour growth and blood perfusion, *J Theor Biol.* 2011; 276: 90–101.

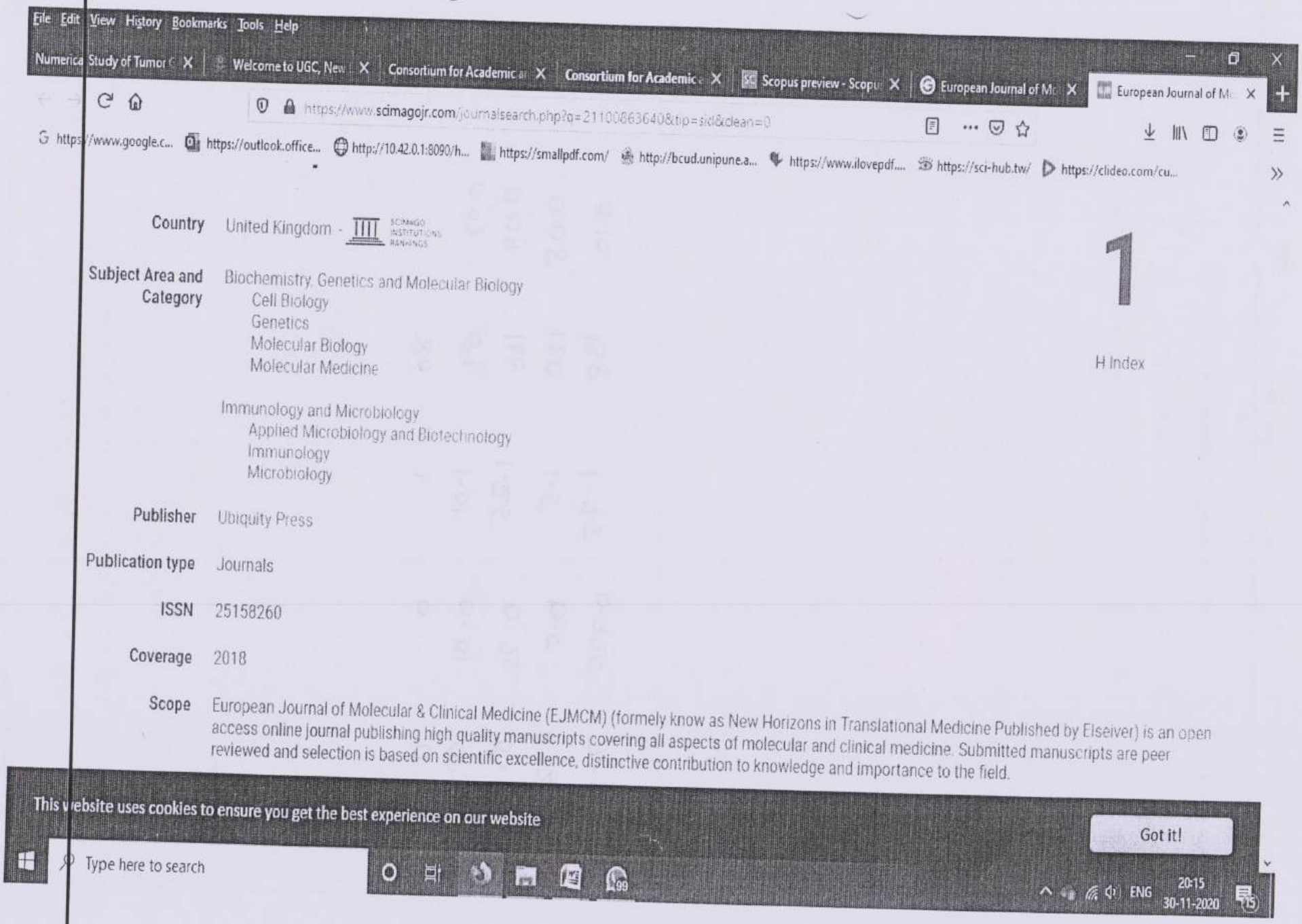
[24] Mitchell, A. R. and D. F. Griffiths, The Finite Difference Method in Partial Differential Equations, *Chichester: Wiley*, 1980.

European Journal of Molecular and Clinical Medicine





https://www.scimagojr.com/journalsearch.php?q=21100863640&tip=sid&clean=0


File Edit View History Bookmarks Tools Help
Numerical Study of Tumor G
Welcome to UGC, New
Consortium for Academic ar
Consortium for Academic
Scopus preview - Scopu
European Journal of Mo
European Journal of Mo
https://www.scimagojr.com/journalsearch.php?q=21100663640&tip=sid&clean=0
https://www.google.c...
https://outlook.office...
http://10.42.0.1:8090/h...
https://smallpdf.com/
http://bcud.unipune.a...
https://www.ilovepdf....
https://sci-hub.tw/
https://clideo.com/cu...
Country United Kingdom -
SCIMAGO INSTITUTIONS RANKINGS
1
H Index
Subject Area and Category
Biochemistry, Genetics and Molecular Biology
Cell Biology
Genetics
Molecular Biology
Molecular Medicine
Immunology and Microbiology
Applied Microbiology and Biotechnology
Immunology
Microbiology
Publisher Ubiquity Press
Publication type Journals
ISSN 25158260
Coverage 2018
Scope European Journal of Molecular & Clinical Medicine (EJMCM) (formely know as New Horizons in Translational Medicine Published by Elseiver) is an open access online journal publishing high quality manuscripts covering all aspects of molecular and clinical medicine. Submitted manuscripts are peer reviewed and selection is based on scientific excellence, distinctive contribution to knowledge and importance to the field.
This website uses cookies to ensure you get the best experience on our website
Got it!
Type here to search
ENG
20:15
30-11-2020

European Journal of Molecular & Clinical Medicine
ISSN 2515-8260 Volume 07, Issue 02, 2020

Biogas production from paper and pulp mill wastewater using Helical baffled bio-film reactor by methanogens

Dhanke JyotiAtul

Assistant Professor, Engineering Science (Mathematics), BharatiVidyapeeth's College of Engineering, Lavale, Pune, 412115, jyotidhanke@gmail.com

Abstract

In thisstudy,paper and pulp millwastewater (Chemical oxygen demand, COD is 2055 ± 5 mg/L) collected from secondary clarifier istreated by Anaerobic helical baffle biofilm sequential batch reactor (AnHBBSBR). To improve the performance of the reactor Carbon fiber (CF) is used.The helical shape baffle in the reactor provides the microorganisms to utilize organics available in the entire capacity of the reactor and enhance biogas production with COD removal. Reactor was operated in a continuous mode for anaerobic biodegradation of wastewater effluent for 140 days. Results show that COD is reduced from 2055 ± 5mg/l to 232 ± 5mg/lwith the efficiency of 86 ± 2.0 % and the highest methane production (564ml-CH_4/g) by the effect of selected methanogens in AnHBBSBR compared to a normal AnSBR methane yield (264 ml-CH_4/g). Thermogravimetric analysis showed better combustion value and absolute oxidation of anaerobic treated sludge at 500 °C, with 10.14 MJ kg^{-1} heating value.

Keywords: Anaerobic treatment, helical baffle biofilm sequential batch reactor, Carbon fibre, biogas energy, Thermogravimetric analysis

1.INTRODUCTION

Pulp and paper mill industries produce tremendous volume of organic wastes that could be changed to source of energy in the form of methane.The pulp and paper industry is a water consuming industry, that creates a various types of wastewater with different qualities, at different stages of paper making process [1].The sludge biomass comprises of wood strands (lignin, cellulose and hemicellulose), paper making fillers like kaolin and calcium carbonate, pitch, lignin secondary products and ash

A study of sequential anaerobic and aerobic treatment in two phases bioreactor for removal of color in the pulp and paper mill effluent with varying pH of the effluent and upsurge in biomass of microorganisms. [14].Based on the previous research work like anaerobic biofilm batch reactor (ABBR) and anaerobic baffled sequential batch reactor (ABSBR), in this present study an attempt have made to investigate the performance of AnHBBSBR for COD removal and biogas production. Further sludge particle size distribution was carry out to distinguish the sludge particle volume. Along with the thermogravimetric analysis is carried out to investigate the wastewater sludge characteristics.

2. MATERIAL AND METHODOLOGY

2.1. Sample water from paper mill plant

Wastewater collected from secondary clarifier of paper industry treatment plant and transported for laboratory study. Collected wastewater is stored at 4°C for further investigation. The characterization of wastewater carried out by standard method of examination of wastewater (APHA, 2005).

2.2. Culture isolationand identification

The methanogens are the bacterial culture which speedup or digest the organics to usable products this process is known as methanogenesis.The aggregates are mainly composed of methanogenic bacteria which accelerate acetate and H_2/CO_2 into methane. Temperature and pH ought to be kept up in the reach which is ideal for methanogenic microorganisms at 32to 50 °C and pH 6.5 to 7.5. The strain was continued utilizing potato dextrose agar (PDA) as medium, and cultivated for 6 days at 30°C to form the inoculants.The dimension of the microorganisms was approximately 2.5 μm.

2.3. Anaerobic Helical baffled Biofilm Sequencing Batch Reactor

The bench-scale AnHBBSBRreactor with 20 L (mixtures of substrate and inoculums) of working volumewere used in this study for treating pulp and paper mill wastewater. The reactor is made using

3. RESULTS AND DISCUSSION

Fig. 2 shows that sequential changes in the COD removal and fractional contribution by each stage of the reactor treating paper mill wastewater. The readings were monitored after 2 -3 days from the start of the anaerobic treatment. An early change was ascribed to technical issues with the peristaltic feed pump. From day 5, the reactor was fed with 100% paper mill wastewater with a microbe dosage of 55 ml/lit during the acclimatization period, the COD removal efficiency of the reactor system was around 84%. This indicated that there were no substantial reductions in the COD removal efficiency when the paper mill wastewater was present up to 90% of the feed. In addition, these results also indicated that there was not any substantial inhibitory effect to the methanogens when wastewater was introduced into the reactor system. It is observed from the figure that COD removal efficiency increases with increase in number of treatment days. The maximum COD removal efficiency of the developed AnHBBSER is 86 ±2%. The reactor shows continuous improvement in terms of COD removal when time was increased further. The average COD reduction efficiency was around 80%.

The effect of organic loading rate of biogas composition can be used as a direct indicator of the vitality of the anaerobic digester. Biogas production was scrutinized at all stages throughout the process of the reactor, particularly for the evaluation of methanogenic movement.Fig. 3. Shows the methane composition produced in each stage of the reactor system during the treatment of paper mill wastewater. The highest methane composition was produced in the earlier stage of the anaerobic treatment between (0-20 days) and the stable CH_4 production efficiency was observed after (40-50 days) of the treatment. From the biogas composition data, it can be concluded that, even high COD removal efficiency was observed during this period, the methane composition profile does not reflect the actual methane composition. This is probably due the problem of the gas measurement device. In actual fact, the methane composition should reflect the performance of the reactor system.

The flow and movement of the reactor content in the baffle region in AnHBBSBR was observed visually. It may be mentioned that mixing of AnHBBSBR reactor content (visual observation) was much better than that observed in AnSBR reactor. In AnHBBSBR, sludge biomass gets fluidized, and transfers through top end region of baffle and then moves on the other side of the baffle and gets deposited on the lower side of the baffle from where it gradually gets recirculated. There was some accretion of sludge biomass espied between lower end of the baffle and reactor wall which obviously indicated sludge biomass recirculation. Improved mixing in AnHBBSBR reactor improves the feasibility of contact of suspended particles in wastewater with sludge biomass, this possibly may lead to entrapment of suspended organics into sludge biomass. Biodegradable suspended organic substance existent in the wastewater should be effectually entrapped in sludge biomass in order to alter the organics into methane gas [15].

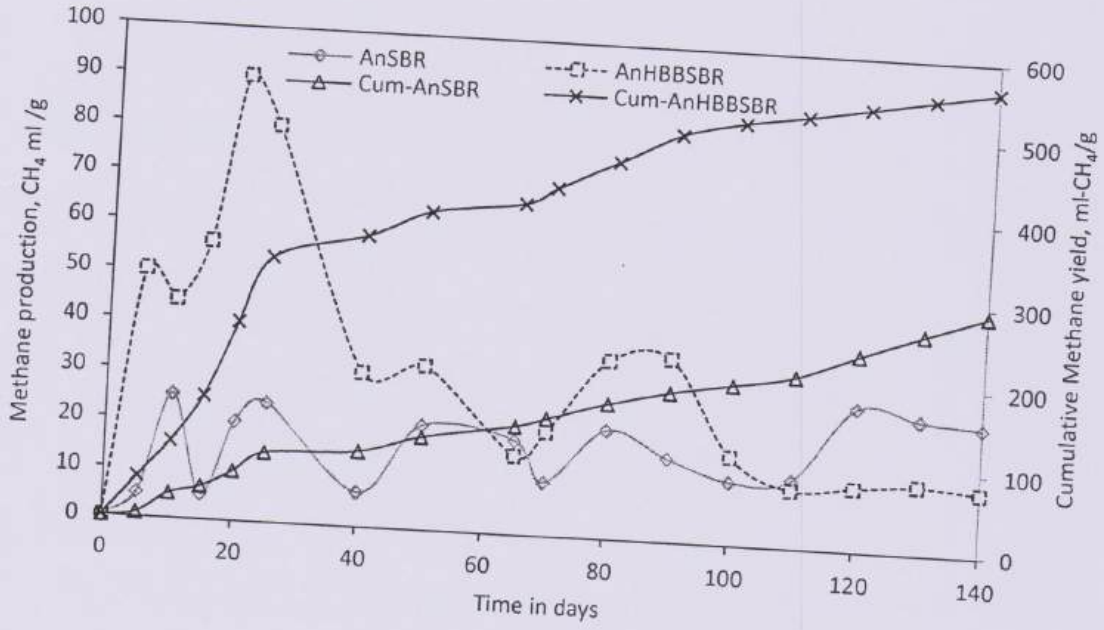


Fig. 2. Production of CH_4 (%) in AnSBR&AnHBBSBR

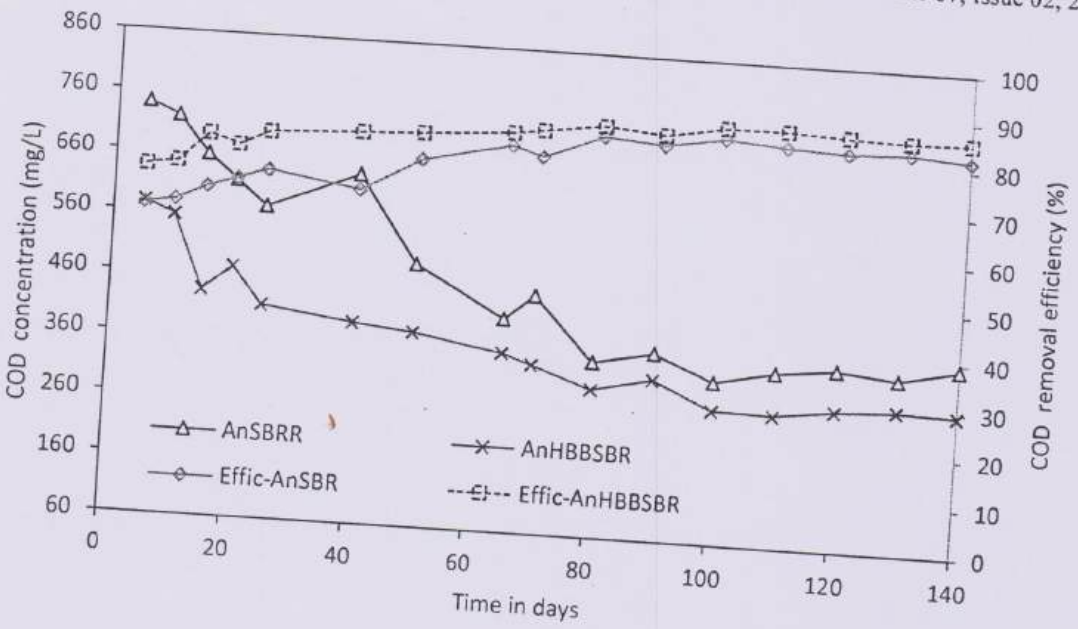


Fig. 3. COD removal efficiency

3.1. Particle size distribution

The 140 days of AnHBBSBR operated inoculum were deposited and dispersed on a glass slide and observed under a stereomicroscope (Metji- Stereo microscope, Chennai Metco Pvt. Ltd) equipped with a digital camera. Samples having 1000 mg of biomass were spread above petri dishes and a stereomicroscope captured the 2D particles shape. A 10 Petri dishes were required to evaluate the size distributions per sample, and with 10-30 pictures per Petri dish. In all petri dish, a minimum of 500 particles were totaled to confirm the depiction of size distributions with better statistical agreement. The images were focused to acquire a good description of the particle shapes. The mean anaerobic granule diameters were evaluated in samples from the inoculums and the biomass extracted at 10 days, 60 days and 140 days of AnHBBSBR operation as shown in Fig. 4. It is observed through particle size distribution analysis, the mean particle size get decrease and its density increases. This is because of pressure apply by the form of an AnHBBSBR operation along with sequential phases of feed; reaction; settling and discharge of the treated effluent. The augmented biomass density indications that was enough to uphold

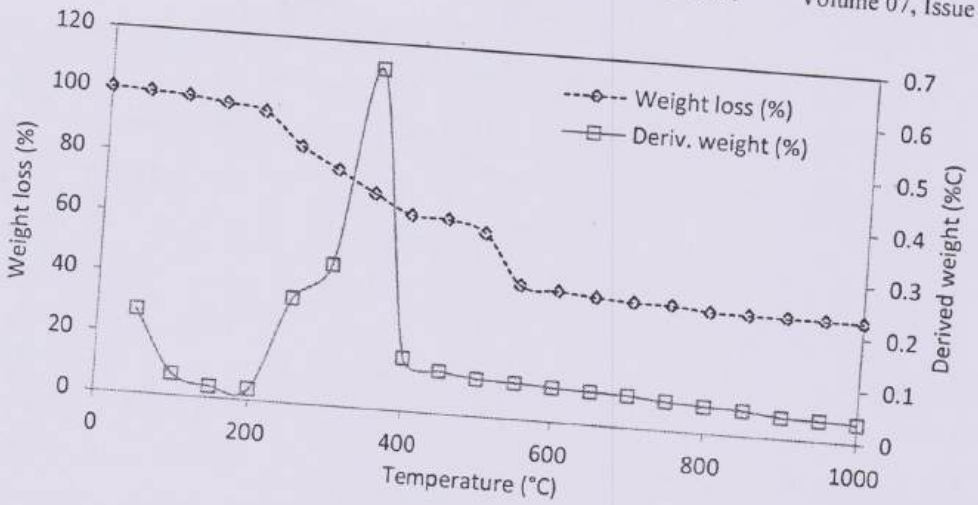


Fig. 5.Thermo gravimetric analysis of paper mill sludge

The active oxidation zone follows this initial zone from 200 to 500 °C with total degradation of 56.2% Subsequently, the sample weight decreased gradually with the total degradation of 4.5% up to 1000 °C. The residue left at 1000 °C is ash and is about 19.84% of the original sample weight. This sludge can be utilized for making blend fuel briquettes with other organics, that can be further used as a fuel in the furnaces. The ash content attained after its combustion can be merged with the cementitious mixture used in construction purposes, thus recuperating energy from the sludge biomass.

4. CONCLUSION

AAnHBBSBR shows the better performance over conventional anaerobic treatment process with the development of the mixing process by the implementation of helical baffle and carbon fibre layer. Better removal of COD and biogas production were observed on AnHBBSBR. Increases in microbe dosage and aeration time were found to induce a positive effect on effluent treatment efficiency. Results showed that COD is reduced from 2055 ± 5 mg/L to 232 ± 5 mg/L. Methane production (564 ml-CH_4/g) by the effect of selected methanogens in AnHBBSBR compared to a normal AnSBR methane yield (264 ml-CH_4/g). Thermo gravimetric analysis was performed for sludge it showed good combustion at characteristics and complete oxidation of the anaerobic treated sludge at 500 °C, with a heating value of

European Journal of Molecular & Clinical Medicine
ISSN 2515-8260 Volume 07, Issue 02, 2020

sequencing batch reactor/moving bed sequencing batch biofilm reactor. International Biodeterioration& Biodegradation, 71, 43-49 (2012)

11. Sethupathy A, Sivashanmugam P., Enhancing biomethane potential of pulp and paper sludge through disperser mediated polyhydroxyalkanoates. Energy Conversion and Management, 173:179–86 (2018).
12. Noori M,CataSaady, Daniel I. Masse.,High rate psychrophilic anaerobic digestion of high solids (35%) dairy manure in sequence batch reactor. Bioresource Technology, 186, 74–80 (2015)
13. Roberta Silva de Souza Santana, Andressa Adriane Pretti, Juliana Gaspar Moreno, Gustavo C esarDacanal, GiovanaTommaso, Rogers Ribeiro., Effect of biomass configuration on the behavior of pilot-scale anaerobic batch reactors treating dairy wastewater. International Biodeterioration& Biodegradation 106, 80-87 (2016)
14. Pratibha Singh, InduShekhar Thakur.,Colour removal of anaerobically treated pulp and paper mill effluent by microorganisms in two steps bioreactor. Bioresource Technology, 97, 218–223 (2006).
15. Lettinga, G and Hulshoff Pol LW., UASB process design for various type of wastewater, Water Science Technology. 24, pp. 87-106 (1991)

Source details

European Journal of Molecular and Clinical Medicine

Formerly known as: New Horizons in Translational Medicine

Scopus coverage years: 2018, 2020
(coverage discontinued in Scopus)

Publisher: EJMCM, International House

E-ISSN: 2515-8260

Subject area: Immunology and Microbiology: Applied Microbiology and Biotechnology | Immunology and Microbiology: Immunology | Biochemistry, Genetics and Molecular Biology: Molecular Medicine | Immunology and Microbiology: Microbiology | View all

Source type: Journal

CiteScore 2019
0.2

SJR 2019
0.152

SNIP 2022
0.000

View all documents > | Set document alert | Save to source list

CiteScore | CiteScore rank & trend | Scopus content coverage

i Improved CiteScore methodology
CiteScore 2019 counts the citations received in 2016-2019 to articles, reviews, conference papers, book chapters and data papers published in 2016-2019, and divides this by the number of publications published in 2016-2019. Learn more >

CiteScore 2019

$$0.2 = \frac{2 \text{ Citations 2016 - 2019}}{9 \text{ Documents 2016 - 2019}}$$

Calculated on 06 May, 2020

CiteScore rank 2019

Category	Rank	Percentile
Immunology and Microbiology └ Applied Microbiology and Biotechnology	#99/105	6th
Immunology and Microbiology └ Immunology	#192/200	4th

View CiteScore methodology > | CiteScore FAQ > | Add CiteScore to your site

https://doi.org/10.1051/e3sconf/202017003008

Analysis and Examination of Heart distress from ECG signal using Artificial Intelligence.

Leena B. Chaudhari[1]* *and Dhananjay E. Upasani*[2]
[1] Bharati Vidyapeeth's College of Engineering, Lavale, Pune, India.
[2] MIT School of Engineering, MIT ADT University, Pune, India.

Abstract: Health data analysis is usually based on a comparison of derived health measures to predefined thresholds. Symptoms can be observed if a value is above or below a threshold. Early detection of signs of heart failure allows the prediction of strokes of heart failure and can therefore prevent these. So identifying "accurate" criteria is the most important task. The accuracy of an experiment depends strongly on the accuracy of the criteria used. Congestive heart failure (CHF) occurs when the heart can not pump sufficient blood for a stable physiological condition. CHF usually occurs when the coronary artery blockage causes the heart tissue to become acidic. The data used to analyze data such as Linear Regression, Missing Enrollment Data, Search Signal, Clinical Data Protection Programs, and Early Adaptive Alarm. The proposed system involves models including server and data warehouse processing, pre-processing, extraction classification characterization in this paper. Classification of heart defects and prediction of heart failure by using applied classifier for hybridization, guideline for treating patients as a gym, level of stress management. In this article, the program tracks the heart disease patients, predicts atrial fibrillation and ventricular fibrillation, and alerts patients when the critical condition occurs.

1 Introduction

According to the World Health Organization (World Health Organization, 2016), chronic diseases such as coronary heart disease, cancer, chronic obstructive pulmonary disease and type 2 diabetes mellitus are the world's leading cause of death, accounting for around 60% of all deaths. Chronic diseases are due mainly to heart failure, currently the leading cause of death in most western countries. The American Heart Heart Association (AHA) 2016 Heart Disease and Stroke Statistics update estimated that 15.5 million people in the United States suffer from cardiovascular disease, a prevalence that is growing with age for both men and women [1]. Throughout Europe, the predominance of individuals describing heart problems for both sexes was 9.2 per cent over the last year [2]. Cardiovascular diseases are the main cause of death in Italy in particular, accounting for 44 per cent of all deaths. Cardiovascular disease passages in India grew from 1.3 million in each of 1990 to 2.8 million in 2016, and most of the passages were caused by heart disease.

Social insurance is a pending problem with worldwide difficulties[3]. The acute socio-economic situation confronting a significant portion of developed countries is generating greater pressure to find more cost-effective solutions to health and social care delivery. In addition, healthcare systems in developing countries face serious difficulties in providing care and assistance, primarily due to a lack of staff and resources.Over the last few years a few proposals have emerged as a part of the new period of human services. Drug 2.0, Wellness 2.0/3.0, ePatient, and eDoctor are usually dispersed examples of such terms, among other commonly established words such as eHealth, telehealth, or telemedicine. Likewise, frameworks might be utilized in a pervasive way and give consistent observing abilities.One of the major disadvantages of the up-to-date portable health monitoring tools from a technical perspective is the processing and storage capacities. Checking gadgets consist regularly of many sensors which measure physiological sizes and convert them into discernible machine data [4]. While some of these devices contain dedicated resources for processing the information, they are very sparse and limited. Although some of these devices contain dedicated information processing tools, they are very sparse and minimal. On the other hand, mobile devices are the perfect way to collect data from health monitoring systems, provide local processing capabilities or even provide access to cloud services (high-performance computing, large capacity storage, and data analytics) [5] . Through this, not only the data collected from the patient could be taken into account for their health assessment and treatment, but also the records of hundreds, thousands or even millions of patients, which might share similar needs and conditions [6].

Atrial fibrillation (AF) has been depicted by doctors as the commonest heart arrhythmia in clinical everyday

*Corresponding author: leenapc23@gmail.com

© The Authors, published by EDP Sciences. This is an open access article distributed under the terms of the Creative Commons Attribution License 4.0

https://doi.org/10.1051/e3sconf/202017003008

practice, with an expected predominance of 1.5%–2% of the overall public in the created world [7]. In excess of 6,000,000 individuals in Europe and 3,000,000 individuals in the USA experience the ill effects of this arrhythmia [7]. It is additionally expected that its predominance will twofold in the following 50 years [8] . Today, three distinct sorts of AF are clinically stratified relying upon the scene length. The arrhythmia would then be able to be grouped into paroxysmal AF (PAF), persevering or long-standing tenacious AF and, at long last, perpetual AF . Indeed, the nearness of AF is related with a five-crease danger of stroke and a three-overlay frequency of congestive cardiovascular breakdown, accordingly inciting that AF patients have double the danger of death than sound individuals of a similar age [7] . Inside this specific situation, an early discovery of AF may help with decreasing that hazard by reestablishing typical heart mood or by improving the blood stream with antithrombotic treatment. This early finding may likewise include prominent advantages for social insurance benefits the world over, in light of the fact that the high hospitalization paces of AF, just as its extensive weight on wellbeing assets could be fundamentally restricted . Cardiovascular sign from both surface and intracardiac accounts have been generally utilized in AF thinks about planning to comprehend the atrial electrical conduct to improve adequacy of interventional removal treatment, however the nearness of ventricular movement (VA) on these sign has hampered the investigation with probability of mutilated outcomes. It is imperative to think about atrial action (AA) without the impact of the VA to improve comprehension of AF beginning and support [9].

Ventricular fibrillation is the quick, disarranged, and offbeat withdrawal of ventricular muscle. Hoffa and Ludwig recommended in 1850 that the inconsistency of these developments is on the grounds that the individual anatomical components lose their interrelationship and quit contracting as one. In 1887, MacWilliam depicted "a condition of fibrillar compression comprised by a quick progression of in facilitated peristaltic constrictions, and in 1914, utilized the term ventricular fibrillation to portray what he thought about the reason for unexpected passing. Superficially electrocardiogram, ventricular fibrillation is portrayed by the nonappearance of unmistakably characterized QRS edifices. It frequently happens in patients with auxiliary heart variations from the norm. Be that as it may, in certain patients, show coronary illness is missing, and the reason for the arrhythmia can't be distinguished or must be learned by broad assessment (e.g., hereditary investigation). Incredible consideration has been given to ventricular fibrillation since it speaks to the last basic pathway for death in many patients who experience out-of-clinic heart failure, and its pace of repeat is about 30% in the primary year in effectively revived patients. Since the particular reasons for ventricular fibrillation are examined in different sections, this section gives a progressively broad outline of the clinical issue and its administration. Ventricular fibrillation (VF) is a significant reason for dismalness and abrupt passing (SD), yet it is one of the most troublesome arrhythmias to viably treat. The implantable cardioverter defibrillator (ICD) offers delayed endurance by ensuring against death because of arrhythmia and is the best quality level treatment for essential and auxiliary anticipation for in danger patients. Be that as it may, gadget implantation doesn't influence the fundamental substrate. Moreover, up to 20% of patients with an ICD experience repetitive scenes of VF or electrical tempests, bringing about numerous gadget treatments, which fall apart the nature of life1 as well as increment related mortality. Antiarrhythmic medications, for example, amiodarone, β-blockers, and lidocaine have been utilized forever undermining arrhythmias, including VF, yet their adequacy has not yet been exhibited on an enormous scale. In addition, they are related with different symptoms, which frequently exceed the questionable prognostic advantage.

2 Objectives of the Study

1. To develop system for individuals tormented by chronic diseases that modify the gathering, sharing and exchange of physiological knowledge, like pressure level, heart and respiration rate and cardiogram signals.
2. To predict heart disease strokes by police investigation connected symptoms.
3. To give notice the specialist and therefore the patient once a heart disease stroke has been foreseen.
4. To work out mechanically and update thresholds in keeping with recorded historical knowledge.
5. To test rules and compare the value to predefined threshold of each derived health indicator.
6. Updating threshold values according to requirement.
7. To do the review and save the original files, which can be accessed and sent to the medical specialist whenever the user wants.

3 Approach of the study

3.1 Quantitative approach

- Constant Mathematical Model: The consistent work could be a work whose esteem is the same for each input esteem.
- Step Function Mathematical Model: The constant perform may be a perform whose price is that the same for each input price.
- Average and Confidence Level Mathematical Model: A simple method to update thresholds that comes back to adding the average of p past data values to the confidence level of this average.
- Moving Average (MA): MA is one of the widely known technical indicators used for time series analysis. During its development, many variations and implementations

https://doi.org/10.1051/e3sconf/202017003008

have been proposed by researchers. Basic type of moving average is the Simple Moving Average (SMA).

3.2 Qualitative approach

- Allow physiological data, such as blood pressure, heart and respiration rate and ECG signals, to be recorded, transmitted, and exchanged.
- The audit report and the original files are saved, can be accessed and sent to the medical specialist whenever the user wants them to.

4 Architecture

In this design, the limit esteems are consequently processed by utilizing factual methodologies. The produced edges rely upon the patient state and his/her authentic estimations. The thought comprises of recognizing cardiovascular breakdown manifestations and thusly foreseeing basic circumstances (i.e.,strokes).

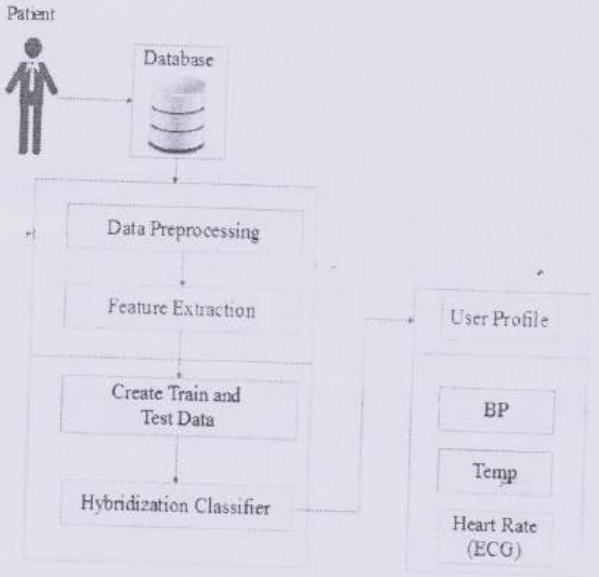


Fig. 1. Proposed System Architecture

1). Dataset: In this architectural study, the MIMIC II waveform database can be used. This is in line with the subgroup from the Psionet Benchmark, which is available online, and is collected from bed patient monitors in the adult and neonatal ICU (intensive care units).
2) First, the device stores data, such as CSV files, in a database. So, patient history is established.
3) Data is preprocessed in the preprocessing stage and the replacement values with threshold values or None are lackinga.
4) The machine performs the extraction process of the element once the preprocessing is completed. The values of the data function are determined using methods of main component analysis. The PCA's goal is to cut down on data and rate columns with a high impact point. This eliminated characteristics from this column after choosing heavily impacted columns such as weight, blood pressure, body temperature.
5) Then build the training and test files using extracted features and use implemented hybridization classifiers to perform classification. The system detects Ventricular Fibrillation and Atrial Fibrillation.
6) Finally, this program suggests care for patients such as Gym, the control of stress levels.

5 Scope

The program can be used to predict strokes that cause heart failure. By frequent monitoring along with support and suggestions it can be helpful for CHF patients. Patients with cardiovascular system disorders may measure their weight, blood pressure, activity, and other factors related to the health.

6 Advantages

1) Patients with heart disease are tracked by the machine.
2) Predicts ventricular and atrial fibrillation.
3) Warns patients when the situation is serious.
4) Automatically calculates and updates thresholds based on historical data collected.

7 Conclusion

Develop system for people suffering from chronic diseases. Rules are based on discussion with cardiologist and comparing extracted parameters with threshold. Feature values of data are calculated using the principal component analysis (PCA) techniques. Rules are based on discussion with cardiologist and comparing extracted parameters with threshold. This technique can be used to the prediction of Atrial Fibrillation and Ventricular Fibrillation.

References

1. Md Saiful Islam, Md Mahmudul Hasan, Xiaoyi Wang , Hayley D. Germack, and Md Noor-E-Alam, Healthcare 2018, 6, 54, (2018).
2. Afef Mdhaffar, Ismael Bouassida Rodriguez, Khalil Charfi, Leila Abid, and Bernd Freisleben, IEEE TRANSACTIONS ON NANOBIOSCIENCE, VOL. **16**, NO. 8, (2017)
3. Salvatore Naddeo, Laura Verde, Manolo Forastiere, Giuseppe De Pietro and Giovanna Sannino, SCITEPRESS Science and Technology Publications, (2017).
4. A. Dhillon, S. Majumdar, M. St Hilaire and A. El. Haraki, Conference: IEEE International Conference on Internet of Things, (2017).

https://doi.org/10.1051/e3sconf/202017003008

5. Sebastian D. Goodfellow, Andrew Goodwin, Robert Greer, Peter C. Laussen, Mjaye Mazwi, Danny Eytan, Computing in Cardiology 2017; VOL **44**
6. Francesco Nocera, Tommaso Di Noia, Marina Mongiello, Eugenio Di Sciascio, SEMAPRO 2016 : The Tenth International Conference on Advances in Semantic Processing, (2016).
7. A. Javari and M. Jalili, Knowledge Information System, volume-**44**, no.3, (2015).
8. Y. Rao, N. Zhang, and H. Zou,Knowledge Information System, volume. **44**, No. 3, PP. 663–688, (2015).
9. R. Pathak and V. Vaidehi, in Proc. 3rd Int. Conf. Eco-Friendly Comput. Commun. Syst. (ICECCS), pp. 61-66,(Dec. 2014).

Source details

E3S Web of Conferences

Open Access

Scopus coverage years: from 2013 to 2023

E-ISSN: 2267-1242

Subject area: Earth and Planetary Sciences: General Earth and Planetary Sciences | Environmental Science: General Environmental Science | Energy: General Energy

Source type: Conference Proceeding

View all documents > | Set document alert | Save to source list

CiteScore 2022
1.0

SJR 2022
0.182

SNIP 2022
0.213

CiteScore | CiteScore rank & trend | Scopus content coverage

Improved CiteScore methodology

CiteScore 2022 counts the citations received in 2019-2022 to articles, reviews, conference papers, book chapters and data papers published in 2019-2022, and divides this by the number of publications published in 2019-2022. Learn more >

CiteScore 2022

$$1.0 = \frac{27{,}581 \text{ Citations 2019 - 2022}}{28{,}843 \text{ Documents 2019 - 2022}}$$

Calculated on 05 May, 2023

CiteScoreTracker 2023

$$0.9 = \frac{29{,}063 \text{ Citations to date}}{32{,}004 \text{ Documents to date}}$$

Last updated on 05 December, 2023 • Updated monthly

CiteScore rank 2022

Category	Rank	Percentile
Earth and Planetary Sciences └ General Earth and Planetary Sciences	#143/192	25th
Environmental Science └ General	#176/227	22nd

View CiteScore methodology > | CiteScore FAQ > | Add CiteScore to your site

TEST Engineering & Management

January – February 2020
ISSN: 0193-4120 Page No. 13616 - 13626

Synthesis, characterization and parametric study for diameter of nano fiber of Chitosan, AzadirachtaIndica leaves extract composite

Nidhi Jain[1], Amruta Pasarkar[2], R.N. Patil[3]

[1]Department of Chemistry, BharatiVidyapeeth College of Engineering Lavale, Pune, India
[2,3]Department of Mechanical Engineering, BharatiVidyapeeth College of Engineering Lavale, Pune, India
[1] nidhijain1704@gmail.com, [2] amruta.pasarkar@bharatividyapeeth.edu,[3]rajendrakumar.patil@bharatividyapeeth.edu

Article Info
Volume 82
Page Number: 13616 - 13626
Publication Issue:
January-February 2020

Abstract

In the present examination, AzadirachtaIndica Leaf Powder and chitosan-based nanofibers are orchestrated utilizing electro-turning process. Acquired nanofibers are portrayed by FTIR, SEM and XRD considers. Chitosan can be acquired normally and are utilized in various fields, for example, biomedical, natural, tissue designing, body embed and so forth. AzadirachtaIndica leaves powder to have their fluctuated antimicrobial application. Both AzadirachtaIndica leaves and chitosan polymers were difficult to electro-spun, to create nanofibers yet we figure out how to do as such by utilizing extraordinary solvents like 90% acidic corrosive. It has found to diminish the surface strain making electrospinning practical. Parametric Study for distance across of Nanofibers is finished utilizing ANOVA table for every one of the three factors. Ends are produced using various plots like region chart, shape plot and so forth. These outcomes can be utilized in future for electro spinning of Nano fibers of explicit distance across

Article History
Article Received: *18 May 2019*
Revised: *14 July 2019*
Accepted: *22 December 2019*
Publication: *24 February 2020*

Keywords: *Electrospinning, Nanofiber, parametric study, Chitosan, AzadirachtaIndica, characterization*

I. METHODOLOGY

Nanofibers

Nanofiber has known for varied characteristics and distinctiveness in their properties such as surface area to volume ratio. Ithas very large and high porosity with very minute pore sizes that is why the nanofibers shows high potential materials for countless applications such asprotective clothing, wound dressings, bone tissue engineering, drug delivery etc. It is also used in the formation of filter for water purification and for sensing applicationsetc [1].

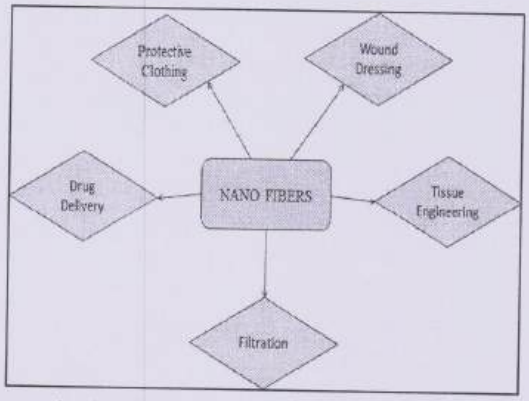


Figure 1: Applications of electrospunnanofibers in the biomedical field

Electro-spinning

Electrospinning is a technique for synthesis of nanofibers using electric field. Theelectrostatic force is used to "produce fine fibers from polymeric solution.Nanofibers Made out of this

January – February 2020
ISSN: 0193-4120 Page No. 13616 - 13626

electrospinninghave a nano distance across (inside the request for nanometers to micrometers). The electrospinningstrategy can combination nanofibers that have more noteworthy floor territory than that received from everyday turning process [2]. Electrospinning has giving a nanofiber which might be having higher porosity, excessive percentage of floor to quantity and specifically nanofibers are adaptable and can be formed into special styles and sizes [3].Electrospinning method makes use of high electric powered fieldwhich is applied to the bead of an answer or dissolve turning out from the top of a narrow. It calls for a Direct Current voltage supply within the scope of a few numerous kV in an effort to deliver electrostaticforces.Strong electrical lousy powers created by using this voltage supply beat the greater prone powers of floor pressure within the fluid bead to deliver electrospinningnanofibers. The electrostatic powers influencing the fluid reason the kingdom of the bead to alternate from adjusted meniscus to the Taylor cone, a wonder noticed due to the electrostatic aversions between comparative expenses in the fluid [4].When fluid arrives at the simple factor, the electric discipline turns into beats the floor stress of the fluid prompting the association launched out from the top of the Taylor cone.As the fly is going thru the air there may be a vanishing of the solvents which favors the development of the nanofibers.The ventilated chambers are applied to preserve a strategic distance from even negative discharges of sure polymers or dissolvable fumes duringthe spinning[5].- Electro turning method can be union nanofibers by using consolidating remedial professional within the fibers,this expands the appropriateness in medicate conveyance framework. The vast claims to fame of nanofibers explore within the biomedical area. Bioactive nature of the medication atoms" may be retainedby electro-turning strategy.

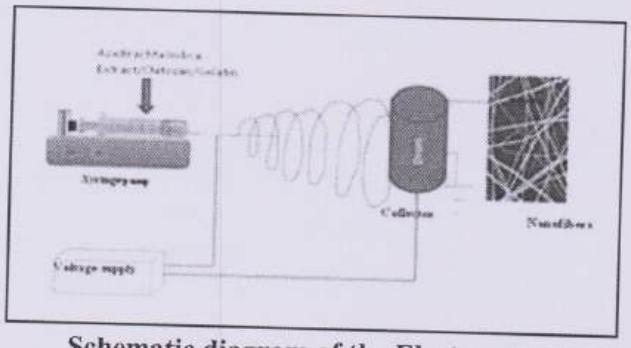
The arrival of meds at the harm can be doable increment and symptom may be decreased via utilizing electro-spun filaments regionally, which move approximately as a medicine transporter [6].

Restricted treatment by way of the medication is accelerated by way of Electro-spun strands. The debasement of the polymer filaments shows the arrival of the medication and can be appropriately overseen in tranquilize conveyance applicationselectro-spun strands

These filaments manage the medication and spare the drugs from the chemical substances and bacterial development. Right now, beneficial operators stay unaltered and secured until required on the website online of interest [7].

Tissue building is a board area requiring the joint and enormous data on medicine, science, designing and material technological know-how fields. Tissue culture is wherein we're utilizing the mixture of cells, substances, restorative experts and special biochemicals use and it offers recovery of tissues that have been demolished via illnesses, wounds or inherent defects[8].

The stringy section of ECM offers operational help and gadget-pushed uprightness to tissues which in turns bolster the form, recuperation, movement, and separation made of protein filaments, for instance, collagen, elastin, keratin, laminins, fibronectin and vitronectin. In this manner, ECM strands are possibly the most widespread section that's expected to take care during fake tissue regeneration[[9,10].



Schematic diagram of the Electro-spun nanofibers

Chitosan

Chitosan is a polymer obtained from chitin and which are now having large interest in the field of research and development [11]. Organic polymer chitosan has the spectrum of properties which are

TEST Engineering & Management

January – February 2020
ISSN: 0193-4120 Page No. 13616 - 13626

not only non-toxic, biocompatible, eco- friendly, bio-functional, and water loving. It is used in the field of various field of pharmaceutics, wastewater treatment, cosmetics industry agriculture, food science, and textiles industry as well as antimicrobial and antiviral material. In acidic conditions chitosan have very good activity.

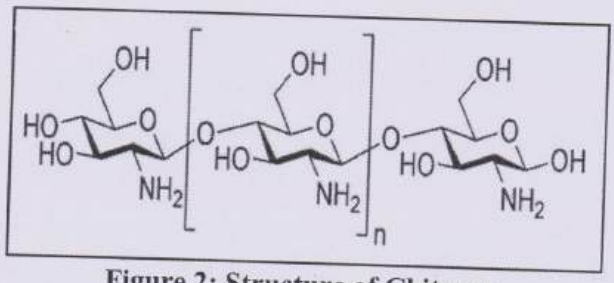


Figure 2: Structure of Chitosan

Gelatin is similar like collagen have naturally obtained easily as biopolymer. Gelatin is biocompatibility and biodegradability. It is abundantly found in animal tissue such as skin, muscle, and bone.

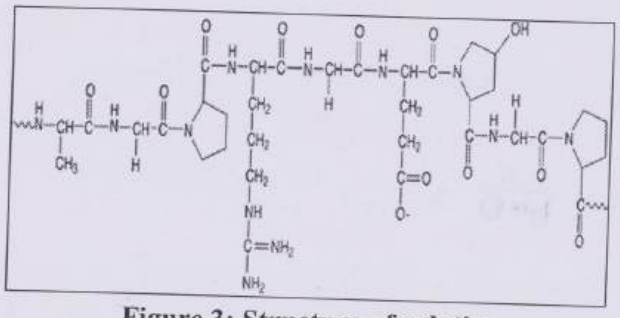
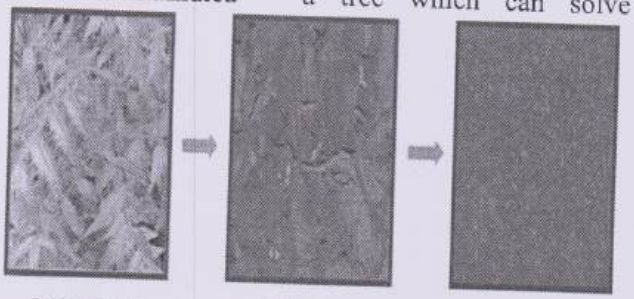


Figure 3: Structure of gelatin

AzadirachtaIndica

The Neem tree (AzadirachtaIndica) from ages (more than 2000 years) known in India and neighboring countries The AzadirachtaIndica always remains green, which generally cangrow up to the height of 15–20m and a trunk thickness of 1.5–3.5m.The plant is known for its fast-growing nature [28]. The significance of AzadirachtaIndica has been identified by the US National Academy of Sciences, resulting in a 1992 report entitled "AzadirachtaIndica – a tree which can solve



global problems". The AzadirachtaIndicatree survives any types of polluted environment such as cities having high pollution Index and village with low pollution [29]. Some of the most vigilant researchers are saying that AzadirachtaIndica deserves to be called a "wonder plant" because of its antifungal, antidiabetic, antibacterial, antiviral, contraceptive property.The main chemical component, present in various segments of the AzadirachtaIndica tree, consist of a few compounds belongs to the "triterpene", or more specifically "limonoid" group which is anatural product. The main components present in AzadirachtaIndica are azadirachtin, salannin, meliantriol, nimbinandnimbidin.

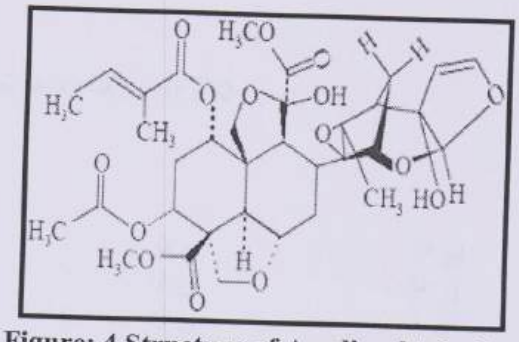


Figure: 4 Structure of AzadirachtaIndica

II. EXPERIMENT

Chitosan, Glacial Acetic Acid, Gelatin were precured of Sigma-Aldrich. Characterization of the nanofibers is done using FTIR, XRD, and SEM. FTIR was used to determine the functional group of AzadirachtaIndica Extract

XRD Chitosan/Gelatinnanofiber was used to determine the structure of nanofibers. The Surface

January – February 2020
ISSN: 0193-4120 Page No. 13616 - 13626

morphology of nanofibers was easily studied by means of SEM Image processing software which was used to measure the diameter of the nanofiber captured in the SEM micrograph.

AzadirachtaIndica extract solution was prepared by heating 10gm of leaves of AzadirachtaIndica in 100 ml of water. Heat the solution until the volume of the solution reduces to half. Filtered the final heated solution via filter paper. Final solution after filtration appears brown in color.

Nanofibers solution was prepared by taking 10ml of AzadirachtaIndica extract and 5 ml of 50% diluted Glacial Acetic Acid. Add 0.3g of Chitosan slowly into the above solution. Once the chitosan is completely dissolved then add 0.3g Gelatin. Keep the solution for 1 hour on the magnetic stirrer. The solution was obtained by blending Chitosan,

AzadirachtaIndica Extract, Glacial Acetic Acid, and gelatin solution. The prepared AzadirachtaIndica Extract/Chitosan/Gelatin solution was then filled into 12-mL plastic syringe. 0.4-mm needle was used at a high voltage of 15 kV, with a tip-at a distance of 14 cm, was applied to the solution and fiber collected on the plane collector

Table-1Chemical composition of AzadirachtaIndica

Table No.1	Compound	Amount	Compound	Amount
1	Moisture	59.4 %	Niacin Vitamin	1.40 mg/100g
2	Proteins	7.1 %	C Carotene	218 mg/100g
3	Fat	1.0 %	Calorific value	1998
4	Fiber	6.2 %	Glutamic acid	microgram/100g
5	Carbohydrates	22.9 %	Tyrosine	1290 kcal/kg
6	Minerals	3.4 %	Aspartic acid	73.30 mg/100g
7	Calcium	510	Alanine	31.50 mg/100g
8	Phosphorous	mg/100g	Proline	15.50 mg/100g
9	Iron	80 mg/100g	Glutamine	6.40 mg/100g
10	Thiamine	17 mg/100g		4.00 mg/100g
		0.04		1.0 g/100g
		mg/100g		

III. CHARACTERIZATION: FT- IR SPECTROSCOPY

TABLE NO.2	WAVE NUMBER (CM-1)		
S. NO.	**NLP (BEFORE)**	**NLP**	**BOND STRETCHING**
1	3284.88 IN CASE OF NLP	3269.45 IN CASE OF NLP	-O-H IN ALCOHOLS, ACID, PHENOLS AND –N-H IN AMINES AND AMIDES.
2	2924.18,2854.74 IN CASE OFNLP,	2918.40, 2852.81 IN CASE OF NLP	-C-H IN –CH3 AND CH2.
3	1722.49 IN CASE OF NLP	1658.84 IN CASE OF NLP	-C=O IN CARBONYL, CARBOXYL GROUPAND LACTONES.

TEST Engineering & Management

January – February 2020
ISSN: 0193-4120 Page No. 13616 - 13626

4	1649.19, 1612.54,1543.10, 1442.80 IN CASE OF NLP	1543.10 IN CASE OF NLP	-C=C- IN AROMATIC RINGS, -C=O IN HIGHLY CONJUGATED.
5	1319.35, 1039.67 IN CASE OF NLP	1317.43 IN CASE OF PLP	-C-O IN ALCOHOLS, PHENOLS,
6	879.57, 761.91, 638.46 IN CASE OF NLP AND ALP 789.62, 686.62, 630.74 IN CASE OF PLP	651.96 IN CASE OF PLP 883.43, 615.31 IN CASE OF ALP	-C-C- DEFORMATIONS AND OUT OF PLANE - C-H DEFORMATION IN AROMATICRINGS.

Table No. 2: Bands assigned to the surface functional

The FT- IR spectroscopy method was used to obtain the informationabout the types of the functional groups [30, 31]. The principle of IR spectroscopy is based on the fact that when the molecules vibrates at with specific frequencies associated with internal vibrations of groups of atoms. These frequencies occur in the IR region which is a part of the electromagnetic spectrum, i.e. ~ 200 to ~4000cm -1. A Fourier Transform Infrared (FT- IR)helpful in knowing the type of functional present

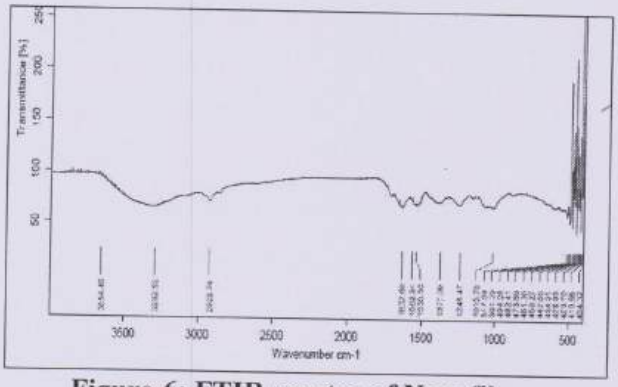


Figure-6: FTIR spectra of Nanofibers

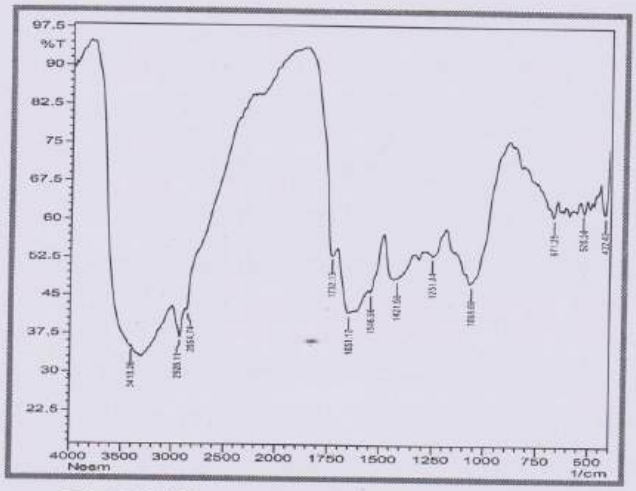


Fig.5 FTIR spectra of AzadirachtaIndica

The spectra change before and after formation of nanofibers can be visible in FTIR

IV. RESULTS AND DISCUSSIONS:

" BothAzadirachtaIndica leaves and chitosan polymers were found to be prepared extract and manage to produce nanofibers using special solvents 50% acetic acid which found to reduce the surface tension making electrospinning feasible. Electrospinning is shown potential applications in biomedical fields like tissue engineering scaffolds and wound healing capabilities."

FTIR spectra of NANOFIBERS

1) SEM Study of SurfaceTopography

Scanning Electron Microscopy (SEM) is a very important method to study the surface topography of a material in a solid state. SEM imaging gives better

January – February 2020
ISSN: 0193-4120 Page No. 13616 - 13626

results than optical microscopy because of enhanced resolution and depth.

AzadirachtaIndica. Leaf Powder as shown in figure 7., shows quite rough texture of surface of the particles with quite big vides throughout the surface. This indicates that particles are having some porosity.

Indica Leaves Powder



Figure 7: SEM image of the surface Azadirachta

SEM results of Nano fibers show the formation of the nanofiberswiththeAzadirachtaIndica Extract/Chitosan/Gelatin solution. The fibers are clearly visible in the image. The diameters of the nanofiberswerecalculated

The beads are more at this scale

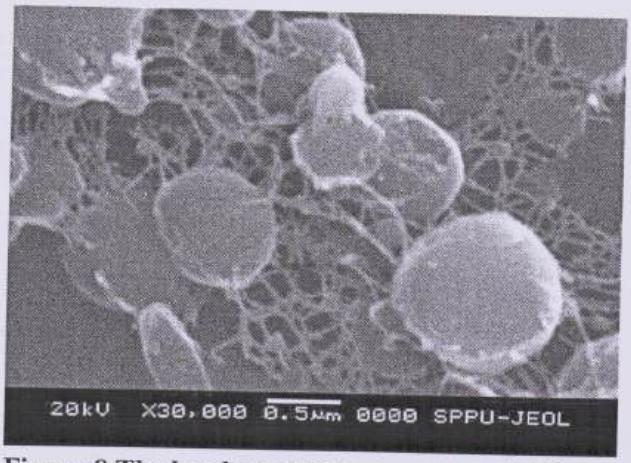


Figure-8 The beads and fibers are morevisible

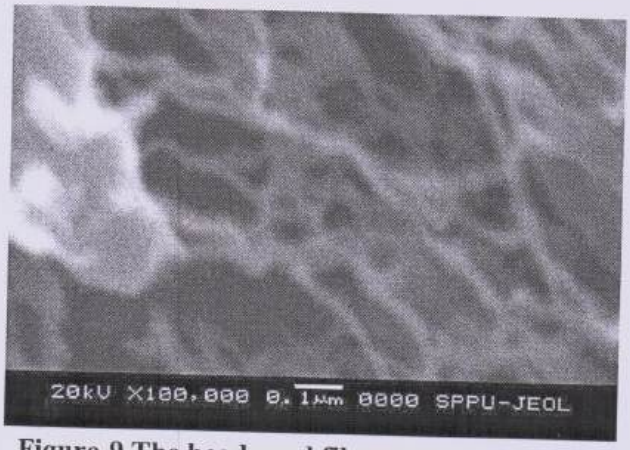
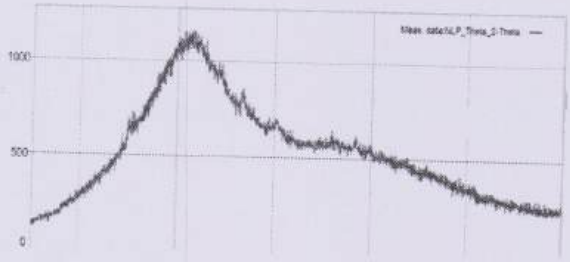


Figure-9 The beads and fibers are morevisible

to 80°, with a goniometric specification radius of 150 mm and Soller slit ±2.5° (divergence angle).

2)XRD

"Powder X-ray diffraction (PXRD) patterns were recorded using benchtop X-ray diffractometer (Model: RigakuMiniflex 600). The operating target voltage was 30 kV and the current were 15 MA. The radiations of Cu Kα were generated using X-ray generator and the β radiations were suppressed using Ni filter. The sample was powdered and scanned for 2θ ranges from 5° to 80°, with goniometer specification radius of 150 mm and roller slit ±2.5° (divergence angle)."



V. PARAMETRIC STUDY FOR DIAMETER OF NANOFIBER

Thefollowing factors are being selected for the experiment:

1. Distance(cm)
2. Flow Rate(ml/hr)
3. Voltage(kv)

TEST Engineering & Management

January – February 2020
ISSN: 0193-4120 Page No. 13616 - 13626

Number of Observation:

The experiment is designed .in the table No.3, there were three independent variables are varied at two levels i.e. low and high during experimentation. Hence the minimum numbersofobservation are 23 i.e.8.

Table No.3	Parameters	Nomenclature	Low (-1)	High(+1)
1	Distance	Cm	10	13
2	Flow Rate	Ml/hr	0.1	0.3
3	Voltage	KV	15	20

For the design of the experiment, the data is collected in Table No.4 through the experiments. In the synthesis of nanofiber by electrospinning method we have taken at two levels, one is higher and other is lower. The higher level abbreviated as '+1' and the lower abbreviated '-1' .The data table referred here combined as per the higher and lower levels.

VI. EXPERIMENTATION AND DATA COLLECTION

TableNo.4	Distance (cm)	Flow Rate(Ml/hr)	Voltage (Kv)
1.	-1	-1	-1
2.	1	-1	+1
3.	-1	+1	-1
4.	-1	+1	+1
5.	+1	-1	-1
6.	+1	-1	+1
7.	+1	+1	-1
8.	+1	+1	+1

Experimental Results [32]

Experimental Results are given in table No5

Table No.5	Experiment No.	Distance (cm) A	Flow Rate(Ml/hr) B	Voltage (Kv) C	Diameter (nm) X
1.	1.	-1(10)	-1(0.1)	-1(15)	40
2.	2.	-1(10)	-1(0.1)	+1(20)	35
3.	3.	-1(10)	+1(0.3)	-1(15)	70
4.	4.	-1(10)	+1(0.3)	+1(20)	55
5.	5.	+1(13)	-1(0.1)	-1(15)	35
6.	6.	+1(13)	-1(0.1)	+1(20)	32
7.	7.	+1(13)	+1(0.3)	-1(15)	35
8.	8.	+1(13)	+1(0.3)	+1(20)	32

VII. ANALYSIS OF EXPERIMENTS [33]

Mean square or variance (MS or V)

Variance is calculated for all the factors as well as interactions Analysis of Variance has been calculated in table No 6 for factors A, B, C.

Table No.6	Analysis of Variance				
Source	DF	Adj SS	Adj MS	F-Value	P-Value
A	1	544.5	544.5	6.02	0.07
B	1	312.5	312.5	3.45	0.137
C	1	84.5	84.5	0.93	0.389
Error	4	362	90.5		
Total	7	1303.5			

Analysis of Variance has been calculated in table No 7 for factors AB.

Table No.7	Analysis of Variance				
Source	DF	Adj SS	Adj MS	F-Value	P-Value
AB	3	1169.5	389.83	11.64	0.019
Error	4	134	33.5		
Total	7	1303.5			

Analysis of Variance has been calculated in table No 8 for factorsBC

Table No.8	Analysis of Variance				
Source	DF	Adj SS	Adj MS	F-Value	P-Value
BC	3	409.5	136.5	0.61	0.643
Error	4	894	223.5		
Total	7	1303.5			

Analysis of Variance has been calculated in table No 9 for factorsAC

Table No.9	Analysis of Variance				
Source	DF	Adj SS	Adj MS	F-Value	P-Value
AC	3	653.5	217.8	1.34	0.38
Error	4	650	162.5		
Total	7	1303.5			

MS = Sum of square / degree of freedom

Our experiments were a strong correlation between various operating conditions and diameters of

January – February 2020
ISSN: 0193-4120 Page No. 13616 - 13626

nanofibers, we found that increasing the voltage(C) and distance (A) led to reduce the diameter of the nanofibers. However, increased flow rate resulted in thicker fibers. In our experiments, the diameters of the nanofibers varied from 32 nm to 70 nm.

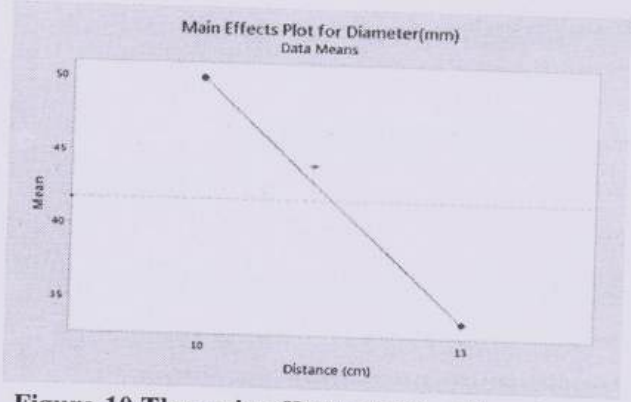


Figure-10 The main effects plot for diameter vs. distance

The main effects plot for diameter vs. distance shows that for distance of 10cm and 13cm mean diameter is 50 mm and 33.5mm respectively.

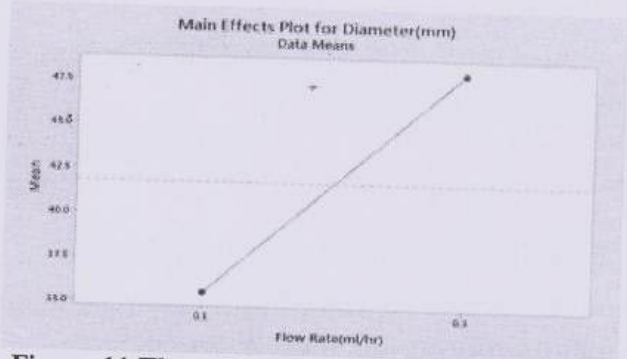


Figure-11 The main effects plot for diameter vs. flow rate

The main effects plot for diameter vs. flow rate shows that for flow rate of 0.1 ml/hr and 0.3ml/hr the mean diameter is 35.5 mm and 48mm respectively.

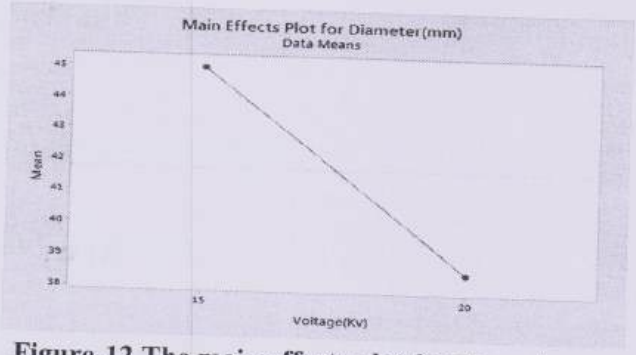


Figure-12 The main effects plot for diameter vs. voltage

The main effects plot for diameter vs. voltage shows that for voltage of 15Kv and 20Kv, the mean diameter is 45 mm and38.5 mm respectively.

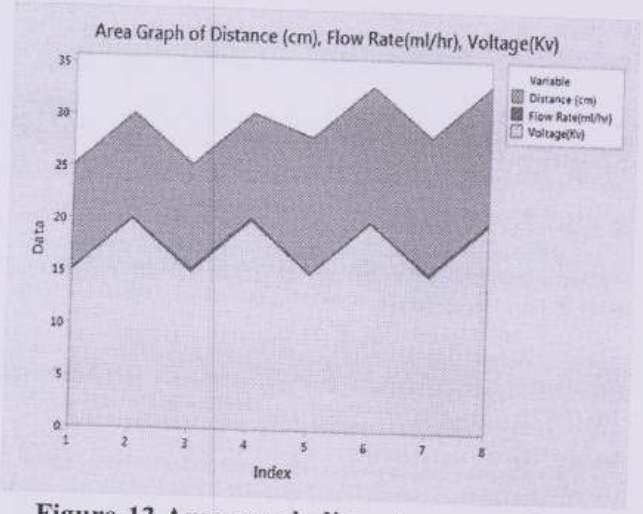


Figure-13 Area graph diameter across three variables

"The following area graph shows diameter across three variables distance, flow rate and voltage. Voltage contributes the most to the diameter from variables. Flow rate contribute least to the diameter.The highest values of diameter are in the upper left corner of the plot, which corresponds with low values of both voltage and distance.The lowest values of diameter are in the lower right corner of the plot, which corresponds with higher values of both Voltage and distance."

TEST Engineering & Management

January – February 2020
ISSN: 0193-4120 Page No. 13616 - 13626

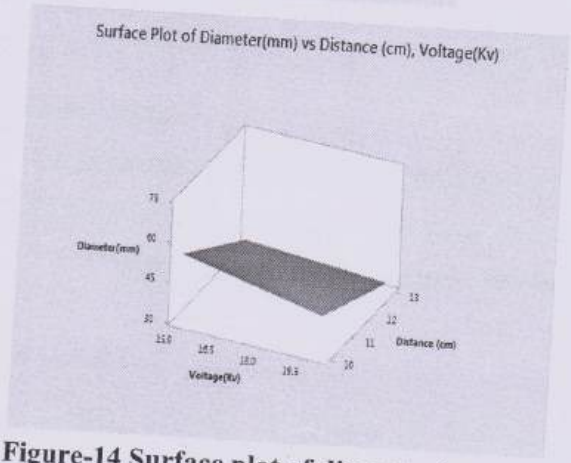


Figure-14 Surface plot of diameter (mm) vs. Distance (cm), Voltage (KV)

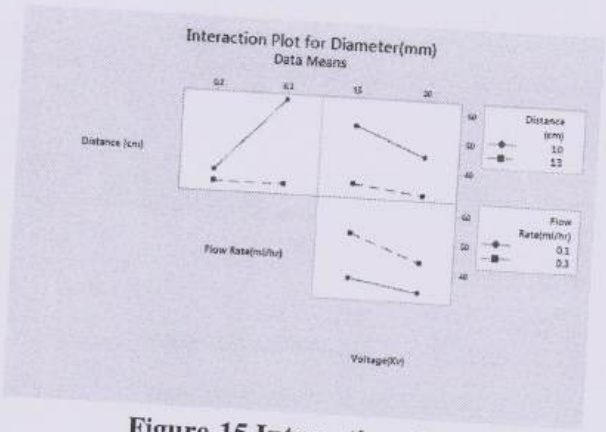


Figure-15 Interaction plot

In this connection plot regarded over heredoes no longer the parallellines.The first cooperation impact indicates that the connection between movement rate and width relies upon the estimation of separation. It indicates that for circulation rate zero.1ml/hr and 0.3ml/hr separation of 10cm is related with most expanded imply diameter.The second connection impact indicates that the connection among voltage and breadth is based upon the really worth ofdistance. It suggests that for voltage of 15 Kv and 20Kv, separation of 10cm is related with maximum noteworthy mean diameter.The 1/3 collaboration impact indicates that the relationship amongst voltage and distance across is predicated upon the estimation of flowrate. It suggests that for voltage of 15 Kv and 20Kv, circulate pace of zero.3ml/hr is associated with most expanded meandiameter.

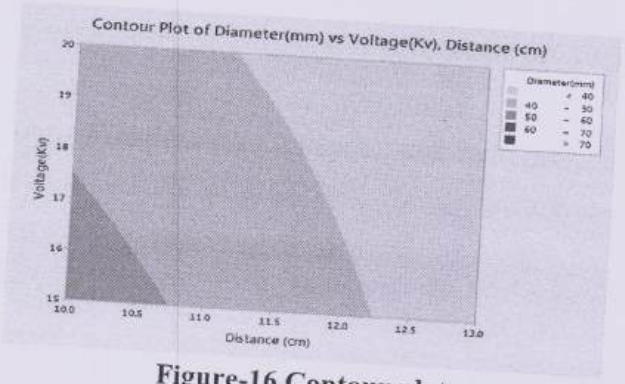


Figure-16 Contour plot

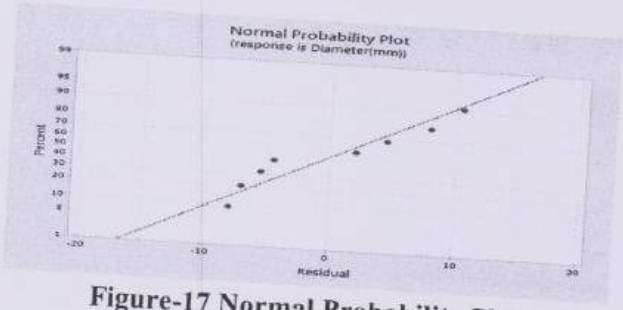


Figure-17 Normal Probability Plot

This contour plot shows the relationship between the distance and voltage settings used to get the response of diameter. Darker regions indicate higher diameters.

VIII. CONCLUSIONS

The AzadirachtaIndica Extract/Chitosan/Gelatinnanofiber wassuccessfullysynthesisbyelectrospinningmethod.There resultsof FTIR, XRD, and SEM display that AzadirachtaIndica Extract/Chitosan/Gelatinnanofiber is framed. SEM picture indicates the electro-spun came about in nanoscale distance throughout of the fiber. The combination of nanofibers can be successfully executed via way of electro-turning method at a voltage 15 to 20 kV, with a tip-authority separation of 10 to 13 cm. We located that increasing the voltage(C) and separation (A) caused lower the space across of the nanofibers. It became determined that the electrospinning of the ordinary filaments

January – February 2020
ISSN: 0193-4120 Page No. 13616 - 13626

werevery difficult thinking about that they will be for the maximum detail include high atomic loads, the form consist of the solid spine.These tendencies make the association gooey that is tough to electro-spum.Thisobstaclewastheformationofsmall dabs with the strands. Utilization of focused acidic corrosive as a dissolvable (ninety%) which was observed to decrease floor stress or combo of solvents a Nanofibers from AzadirachtaIndica Extract/Chitosan/Gelatin will be framed successfully utilizing solvents. Parametric Study for width of Nanofibers is finished using ANOVA table for every one of the three factors. Ends are produced the use of various plots like region chart, form plot and so on. These effects can be applied in future for electrospinning of nanofibers of specificdiameter.

Zone plot display that voltage contributes the most to the distance throughout from factors. Stream price contribute least to the dimensions. Surface plot show that maximum noteworthy estimations of breadth are inside the higher left corner of the plot, which relates with low estimations of every voltage and separation. This form plot suggests the relationship between the separation and voltage settings used to get the reaction of breadth. Darker districts monitor better breadths above 70mm.The principle influences plot and verbal exchange plots are plotted to get the advise width at numerous ranges of things.

REFERENCES

[1] M.Z. Elsabee, H.F. Naguib, and R.E. Morsi, Mater. Sci. Eng. C 32, 1711(2012).
[2] K. Garg and G.L. Bowlin, 1 (2011).-
[3] N. Bhardwaj and S.C. Kundu, 28, 325 (2010).
[4] HilalTurkogluSasmazel and OzanOzkan, "Advance in Electrospinning of Nanofibers and their Biomedical Applications", Current Tissue Engineering, Vol. 2, No. 2, 2013.
[5] P. V.Londhe, S.S.Chavan, P.N.Deshmukh, "Appraisal of Electro spun Nanofibers: A Parametric Study for Diameter of Nanofiber",2012.
[6] Nishath Khan, "Livelihoods of electrospunnanofibers within the biomedical locale", Studies with the helpful resource of Undergraduate Researchers at Guelph Vol. Five, No. 2, , sixty 3-seventy 3, 2012.
[7] Jian Fang, Xungai Wang and Tong Lin, "Rational Applications of ElectrospunNanofibers, Intech, Vol.6, 1030-1035.2010.
[8] Md. Mahabub Hasan, A.K.M. MashudAlam, "Use of electrospinning methodologies for the strategy for tissue engineeringscaffolds: A Review", European Scientific Journal May vol.10, No.15 1857 – 7881, 2014
[9] Yinxian Yu, Sha Hua, Mengkai Yang, Zeze Fu, SongsongTeng, KerunNiu, Qinghua Zhao and Chengqing Yi, "Creation andcharacterization of electrospinning/3-D printing bone tissue method starting degree", Issue 112, Page 110460 to 111631,2016.
[10] A. GholipourKanani, S. HajirBahrami, "Surveys on ElectrospunNanofibers Scaffold and Biomedical Applications", TrendsBiomater. Artif Organs, vol 24(2),ninety three-one hundred fifteen,2010
[11] K. Paipitak, T. Pornpra, P. Mongkontalang, W. Techitdheera, and W. Pecharapa, 8, one zero one (2011).
[12] X. Mi, K.S. Vijayaragavan, and C.L. Heldt, Carbohydr. Res. 387, 24(2014).
[13] Jayakumar, R.; Prabaharan, M.; Nair, S.V.; Tamura, H. Novel chitin and chitosan nanofibersinbiomedicalapplications. Biotechnol. Adv. 2010, 28, 142–one hundred fifty. [CrossRef] [PubMed]
[14] Torres-Giner, S.; Ocio, M.J.; Lagaron, J.M. Improvement of dynamic Antimicrobial fiber-based absolutely absolutelytruelychitosanpolysaccharide nanostructures using electrospinning. Eng. Life Sci. 2008, 8, 303–314. [CrossRef]
[15] Subramanian, A.; Vu, D.; Larsen, G.F.; Lin, H.Y. Readiness and assessment of the electrospun chitosan/PEO fibersforpotentialapplicationsincartilagetissuee ngineering.J. Biomater. Sci. Polym. Ed. 2005, 16, 861–873.[CrossRef] [PubMed]
[16] Rinaudo, M. Chitin and chitosan: Properties and obligations. Prog. Polym. Sci. 2006, 31, 603–632.[CrossRef]
[17] Younes, I.; Rinaudo, M. Chitin and chitosan accessibility from marine assets. Structure,

January – February 2020
ISSN: 0193-4120 Page No. 13616 - 13626

homes and projects. Blemish. Remedies 2015, thirteen, 1133–1174.[PubMed]

[18] Rujitanaroj, P.- O.; Pimpha, N.; Supaphol, P. Wound-dressing substances with antibacterial improvement from electrospun gelatin fiber mats containing silver nanoparticles. Polymer 2008, 40 nine, 4723–4732.

[19] Young, S.; Wong, M.; Tabata, Y.; Mikos, A.G. Gelatin as a movement vehicle for the supervised appearance of bioactive flotsam and jetsam. J. Control. Discharge 2005, 109, 256–274.

[20] Jongjareonrak, A.; Benjakul, S.; Visessanguan, W.; Prodpran, T.; Tanaka, M. Portrayal of consumable movies fromskin gelatin of brownstripe pink snapper and bigeyesnapper. Sustenance Hydrocoll. 2006, 20, 492–501.

[21] Huss, F.R.; Junker, J.P.; Johnson, H.; Kratz, G. Macroporousgelatine floats as way of life substrate, transplantation automobile, and biodegradable shape for guided repairing of sensitive tissues. In vivo examinations in revealed mice. J. Plast. Reconstr. Aesthet. Therapeutic shape 2007, 60, 543–555

[22] Vandervoort, J.; Ludwig, A. Course of motion and assessment of medication stacked gelatin nanoparticles for topical ophthalmic use. Eur. J. Pharm. Biopharm. 2004, fifty seven, 251–261.

[23] Tabata, Y.; Hijikata, S.; Ikada, Y. Improved vascularization and tissue granulation with the manual of great fibroblast development factor impregnated in gelatin hydrogels. J. Control. Discharge 1994, 31,189–199.

[24] Liu, T.- Y.; Hu, S.- H.; Liu, K.- H.; Liu, D.- M.;Chen, S.- Y. Blueprint and portrayal of magnificent connecting with hydrogels and its utilization for calm release.J. Magn. Magn. Mater. 2006, 304, e397–e399.

[25] Liu, J.; Meisner, D.; Kwong, E.; Wu, X.Y.; Johnston, M.R. A tale trans-lymphatic therapy conveyance structure: Implantable gelatin wipe impregnated with PLGA-paclitaxel microspheres. Biomaterials 2007, 28,3236–3244.

[26] Schmutterer, H., in: H. Schmutterer (Ed.).; The AzadirachtaIndica Tree, VCH, Weinheim.; 1995, pp. 1.

[27] Raju, K. R. T., Reddy, T. V., Gonda, C.,in:H. Schmutterer (Ed.).; The AzadirachtaIndica Tree, VCH, Weinheim.; 1995, pp. 86.536 - 550.

[28] Eid I., BrimaParvez, I. Haris.; Arsenic Removal from Drinking Water utilizing Different Biomaterials and Evaluation of a Phytotechnology Based Filter.; Int. Res. J. Condition Sci.; 2014, Vol. Three(7), pp 39-40 four.

[29] Elangovan, R., Pilip L. What's greater distinguished essential, Chandraraj K.; Biosorption of Chromium species through method for Aquatic Weeds: Kinetics and Mechanism investigates.; Journal of Hazardous Materials.; 2008, Vol. 152, pp100-112

[30] Maeur.; Surface topography of the AzadirachtaIndica Leaf Powder have develop to be considered withScanning

[31] C.R.Kothari "Examination Methodology"techniques and systems (2nd changed dispatch) New Age International Publishers

Published by: The Mattingley Publishing Co., Inc.

Source details

Test Engineering and Management

Scopus coverage years: from 1970 to 1971, from 1974 to 1979, from 1985 to 1989, from 1993 to 2020 (coverage discontinued in Scopus)

Publisher: Mattingley Publishing

ISSN: 0193-4120

Subject area: Business, Management and Accounting: General Business, Management and Accounting | Physics and Astronomy: Instrumentation | Engineering: Mechanical Engineering | Engineering: Mechanics of Materials

Source type: Trade Journal

CiteScore 2019
0.1

SJR 2019
0.101

SNIP 2022
0.071

View all documents > | Set document alert | Save to source list

CiteScore | CiteScore rank & trend | Scopus content coverage

i Improved CiteScore methodology

CiteScore 2019 counts the citations received in 2016-2019 to articles, reviews, conference papers, book chapters and data papers published in 2016-2019, and divides this by the number of publications published in 2016-2019. Learn more >

CiteScore 2019

$$0.1 = \frac{62 \text{ Citations } 2016 - 2019}{458 \text{ Documents } 2016 - 2019}$$

Calculated on 06 May, 2020

CiteScore rank 2019

Category	Rank	Percentile
Business, Management and Accounting └ General Business, Management and Accounting	#185/221	16th
Physics and Astronomy └ Instrumentation	#121/129	6th

View CiteScore methodology > | CiteScore FAQ > | Add CiteScore to your site

Mathematical and Experimental Approach for Removal of Fluoride, Arsenic, Lead by Non-Conventional (NLP, PLP, ALP) Absorbents

[1]Nidhi Jain and [2]Amruta Pasarkar
[1]Department of Applied Science and [2]Department of Mechanical Engineering Bharati Vidyapeeth's College of Engineering Lavale, Pune, India

Asia Pacific Journal of Multidisciplinary Research
Vol. 7 No.4, 71-77
November 2019
P-ISSN 2350-7756
E-ISSN 2350-8442
www.apjmr.com
CHED Recognized Journal
ASEAN Citation Index

Date Received: July 4, 2019; Date Revised: September 2, 2019

Abstract - *In the present study various types of leaves powder such as Neem Leaf Powder (NLP), Peepal Leaf Powder (PLP), Amla Leaf Powder (ALP) are used for the removal of fluoride, lead and arsenic from synthetic solutions. NLP, PLP, ALP leaves after experiments showed greater adsorption potential and strong affinity toward the ions. The experimental values regarding adsorption of different ions are extrapolated using MATLAB software to formulate corresponding quadratic equations. These equations can be used to interpolate the values of ions removal for any amount of adsorbent. The extrapolated values by MATLAB software helps, in theoretical calculations of the values without experiments, which in turn useful for the pilot project as well as to scale up the material at industrial level. The study of Adsorption kinetics clearly shows that the percentage removals of all three ions are increased by increasing adsorbent.*

Keywords: *Adsorption, experimental mathematical approach, leaves powders, Removal.*

INTRODUCTION

Water is a marvelous and unique substance which is essential for life. For the agronomist, water is necessary for food crops. Water is an important chemical compound as a cooling agent from engineering point of view. Water is a medium as well as climate factor for the biologist and meteorologist respectively. Its availability with good quality and adequate quantity is very important for human life and other purposes. In general, the quality of water is equally important as the quantity. Therefore, water quality is considered as an important factor to judge environment changes which are strongly associated with social and economic development

Water is a marvelous and unique substance which is essential for life. For the agronomist, water is necessary for food crops. Water is an important chemical compound as a cooling agent from engineering point of view. Water is a medium as well as climate factor for the biologist and meteorologist respectively. Its availability with good quality and adequate quantity is very important for human life and other purposes. In general, the quality of water is equally important as the quantity. Therefore, water quality is considered as an important factor to judge environment changes which are strongly associated with social and economic development [1].

Water is contaminated by several types of the contaminants such as organic, inorganic. The organic contaminates may be microorganism such as bacteria, protozoa and other types of virus and inorganic contaminates in the forms of different types of ions such as fluoride, Arsenic and lead.

1.1 FLUORIDE

Fluoride is naturally abundant from 0.065% to 0.09% by weight in the earth's crust. Fluoride ion is extremely reactive. It is the 13th most abundant element on earth. In halogen group of minerals and are natural constituents of the environment the fluorides are one of them. Fluorides are originated soil of the earth's crust by the solvent action of water on the rocks. Fluoride never encountered in nature as it the most electronegative of all chemical elements and is exit in element form. [2]. Geological sources are the main sources of fluoride contamination which is the main source of drinking water contamination. [3, 4]

Fluoride contamination is injurious to health when taken in excessive amount above permissible limits of 1.0 mg/L, it leads to causes mottling of teeth in mild

cases, dental or skeletal fluorosis involve chronic problems, neurological damage and bone damage are sever problems [5].

1.2 AARSENIC

Arsenic is very poisonous in nature and commonly referred to as king of poisons because it is powerful, prudent, odorless and tasteless; hence it can be easily camouflaged in food [6]. Arsenic is metalloid in nature mainly available in nature in local bedrocks. It comes into the soil through weathering of rocks and minerals, their leaching through anthropogenic sources. There are many source of Arsenic, inorganic arsenic sources are geological, while organic arsenic is found in abundance in marine life.

Surface water gets contaminated when geothermal fluids, rich in arsenic come in contact with it [7]. Arsenic may exist in different forms. The stability, solubility and toxicity of arsenic vary among its various forms. The inorganic forms of arsenic, namely arsenate and arsenite are more persistent and bio available; hence they are more hazardous as compared to their organic counterparts [3].

1.3 LEAD

Industrial water act has present and future hazards for the environment by producing pollutants such as heavy metal contamination. Heavy metal contamination act as most crucial pollutants in surface and ground water [8]. The industrial wastewater contains toxic metals are Cd, Zn, Pb and Ni. Nowadays, due to population explosion there is continuous increase in heavy metal emissions into the environment and it is essential to control them [9,10] Toxic elements like lead causes many serious disorders like, anemia, kidney disease, nervous disorders, and even death [11].

OBJECTIVES OF THE STUDY

The objective of the study is to extrapolate experimental values in theoretical calculations by using MATLAB software of all adsorption of different ions for removal process, such of the values which in turn useful for the pilot project as well as to scale up the material at industrial level.

MATERIALS AND METHODS

1.1. PREPARATION OF LEAF POWDER (NLP, PLP AND ALP):

The preparation of the adsorbent, NLP, PLP and ALP included the various steps such as:

Firstly, Green neem leaves were collected from tree and were brought to the laboratory in plastic bags. The leaves were washed repeatedly with water to remove dust and then dry at room temperature in a shade. The dried leaves were ground and sieved to 50. The washed powder was dried for several hours at room temperature; then the powder was preserved in glass bottles for use as an adsorbent.

1.2. PREPARATION OF IONS SOLUTION

In present study the removal of all selected ions by adsorption method was conducted in synthetic single ion solution. For this purpose, stock solution of desirable concentration for every ion was prepared. From this solution different standard solutions of 50 to 300 mg/L were prepared by dilution. 50 ml of each of these solutions was used in every experiment. All chemicals were used of A. R. Grade.

Effect of nature of adsorbent: The adsorption on all types of adsorbents was investigated. In each case a fixed amount (1.0 gm) was placed in a conical flask. An ion(s) solution was then added to each adsorbent followed by the pH adjustment by adding 0.01M NaOH of 0.1 m HCl. The flask was then capped and shaken for 1hr. at 30°C±2°C. This procedure was followed for all ions selected in the present investigation.

1.3. DETERMINATION METHODS OF IONS CONCENTRATION

Determination of Fluoride (F-) ion: JENWAY ion meter and a fluoride selective electrode (JENWAY ISE: 924305) equipped single junction calomel electrode was employed for the measurement of fluoride ion concentration.

Determination of Lead (Pb^{2+}) ion:

Atomic absorption spectrophotometer AA-6300 SHIMADZU was used for determination of lead. Lead Hollow Cathode Lamp at 283.3 nm and acetylene – air flame was used for this purpose.

Determination of Arsenic ($As^{3+/5+}$) ion:

The determination of arsenic in water samples was conducted by AAS with Flow Injection - Hydrides Generation (FI-HG) AAS system. AA-6300 SHIMADZU AAS, double beam atomic absorption spectrophotometer was also used for the determination of arsenic.

RESULTS AND DISCUSSION

1.4 Effect of Absorbent Doses On Fluoride

Experimental Procedure

The study shows effect of NLP, PLP and ALP dosage on removal of fluoride. At initial fluoride concentration of 5mg/L, pH 5.0, temperature30°± 2°C, contact time 2hr., shaking time 1hr, 0.2-1.0gm is used.

Before reaching equilibrium, the contact time was ended. Results are seen in table 1.0, 2.0, 3.0 and figure 1. Results shows that by increasing adsorbent dose, percentage of fluoride removal is increased. The highest adsorption in case of NLP is 79.49%, in case of PLP is 81.89% and 82.76% in case of ALP. The adsorption capacity for ALP > PLP > NLP. Similar results have been reported by Researchers. [11 and 12]

Table 1

Fluoride onto NLP				
Amount of fluoride adsorbed at varying adsorbent dosage. (Initial concentration: 5mg/L, Temperature: 30°C ± 2°C, pH: 5.0, Contact time: 2hr., Shaking time: 1hr.)				
S. No.	Amount of Adsorbent (w)	Equilibrium Concentration (C_e)	Adsorbed amount (q_e)	Removal (R)
	gm	mg/L	mg/g	%
1	0.2	3.17	9.19	36.73
2	0.4	2.96	5.09	40.76
3	0.6	2.28	4.53	54.47
4	0.8	1.90	3.88	61.93
5	1.0	1.02	3.98	79.49

Table 2. Fluoride onto PLP

Amount of fluoride adsorbed at varying adsorbent dosage (Initial concentration: 5mg/L, Temperature: 30°C ± 2°C, pH: 5.0 , Contact time: 2hr., Shaking time: 1hr.)

S. No.	Amount of Adsorbent(w)	Equilibrium Concentration (Ce)	Adsorbed amount(qe)	Removal (R)
	gm	mg/L	mg/g	%
1	0.2	3.07	9.68	38.71
2	0.4	2.89	5.27	42.13
3	0.6	2.18	4.71	56.50
4	0.8	1.79	4.01	64.28
5	1.0	0.90	4.09	81.89

Table 3. Fluoride onto ALP

Amount of fluoride adsorbed at varying adsorbent dosage (Initial concentration: 5mg/L, Temperature: 30°C ± 2°C, pH: 5.0 , Contact time: 2hr., Shaking time: 1hr.)

S. No.	Amount of Adsorbent (w)	Equilibrium Concentration (Ce)	Adsorbed amount (qe)	Removal (R)
	gm	mg/L	mg/g	%
1	0.2	2.97	10.18	40.71
2	0.4	2.59	6.04	48.37
3	0.6	2.17	4.72	56.64
4	0.8	1.53	4.33	69.29
5	1.0	0.87	4.13	82.76

Mathematical Formulation

The experimental values of NLP, PLP and ALP dosage on fluoride removal is extrapolated using MATLAB software to formulate corresponding quadratic equations relating to –

- Amount of Adsorbent (x) and Equilibrium Concentration (y)
- Amount of Adsorbent (x) and Adsorbed amount (y)
- Amount of Adsorbent (x) and Removal (y)

These equations can be used to interpolate the values of fluoride removal for any amount of adsorbent.

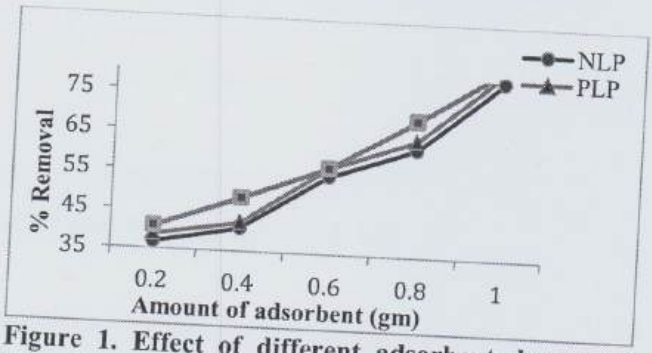


Figure 1. Effect of different adsorbent dosage on Fluoride removal by NLP, PLP and ALP

Table 4. Fluoride onto NLP

Amount of fluoride adsorbed at varying adsorbent dosage

S.S No.	Amount of Adsorbent (w) gm	Equilibrium Concentration (C_e) mg/L	Adsorbed amount (q_e) mg/g	Removal (R) %
Mathematical Equations		y=-1.85x*x-0.45*x+3.354	y=14.83x*x-23.62*x+12.97	y=37.16x*x+8.75*x+33.07
1	0.3	3.05	7.22	39.04
2	0.5	2.66	4.87	46.73
3	0.7	2.12	3.70	57.40
4	0.9	1.44	3.73	71.04

Table 5. Fluoride onto PLP

Amount of fluoride adsorbed at varying adsorbent dosage				
SNo.	Amount of Adsorbent (w) gm	Equilibrium Concentration (C_e) mg/L	Adsorbed amount (q_e) mg/g	Removal (R) %
Mathematical Equations		y=-1.96x*x-0.36*x+3.24	y=15.78x*x-25.16*x+13.70	y=38.91x*x+7.56*x+35.04
1	0.3	2.95	7.57	40.80
2	0.5	2.57	5.06	48.54
3	0.7	2.02	3.82	59.39
4	0.9	1.32	3.83	73.36

Table 6. Fluoride onto ALP

Amount of fluoride adsorbed at varying adsorbent dosage				
S. No.	Amount of Adsorbent (w) gm	Equilibrium Concentration (C_e) mg/L	Adsorbed amount (q_e) mg/g	Removal (R) %
Mathematical Equations		y=-1.39x*x-0.95*x+3.21	y=15.73x*x-25.78*x+14.42	y=28.57x*x+18.22*x+36.04
1	0.3	2.79	8.10	44.07
2	0.5	2.38	5.46	52.29
3	0.7	1.86	4.08	62.79
4	0.9	1.22	3.95	75.57

1.5 Effect of Absorbent Doses On Lead Experimental Procedure

The study shows effect of NLP, PLP, ALP dosage on removal of lead. At initial fluoride concentration of 0.1mg/L, pH 6.5, temperature 30°± 2°C, contact time 2hr., shaking time 1hr , 0.2-1.0gm is used. Before reaching equilibrium, the contact time was ended. Results are seen in table 7.0, 8.0, 9.0 and figure 2. Results shows that by increasing adsorbent dose, percentage of lead removal is increased. The highest adsorption in case of NLP is 85.2%; in case of PLP is 81.5% and 83.6% in case of ALP. There was no significant variation in % removal by all adsorbents. A similar result was observed with other adsorbent [13]

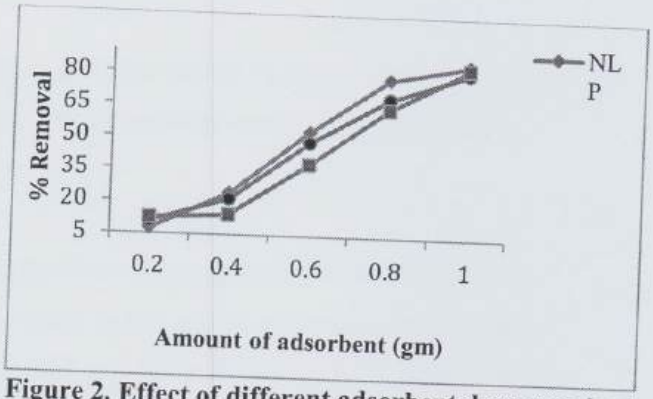


Figure 2. Effect of different adsorbent dosage on lead removal by NLP, PLP and ALP

Table 7. Lead onto NLP

Amount of lead adsorbed at varying adsorbent dosage (Initial concentration: 0.1mg/L, Temperature: 30°C ± 2°C, pH: 6.5 , Contact time: 2hr., haking time: 1hr.)				
S. No.	Amount of Adsorbent (w)	Equilibrium Conc(Ce)	Adsorbed amount(qe)	Removal(R)
	gm	mg/L	mg/g	%
1	0.2	0.09	0.03	7.4
2	0.4	0.08	0.02	24.1
3	0.6	0.04	0.89	53.2
4	0.8	0.02	0.09	78.1
5	1.0	0.01	0.09	85.2

Table 8. Lead onto PLP

Amount of lead adsorbed at varying adsorbent dosage (Initial concentration: 0.1mg/L, Temperature: 30°C ± 2°C, pH: 6.5 , Contact time: 2hr., Shaking time: 1hr.)				
S. No.	Amount ofAdsorbent (w)	EquilibriumConc(Ce)	Adsorbed amount (qe)	Removal (R)
units	gm	mg/L	mg/g	%
1	0.2	0.09	0.05	10.6
2	0.4	0.08	0.05	21.4
3	0.6	0.05	0.09	48.2
4	0.8	0.03	0.09	69.1
5	1.0	0.01	0.09	81.5

Table 9. Lead onto ALP

Amount of lead adsorbed at varying adsorbent dosage (Initial concentration: 0.1mg/L, Temperature: 30°C ± 2°C, pH: 6.5, Contact time: 2hr., Shaking time: 1hr.)				
S. No.	Amount of Adsorbent (w)	Equilibrium Concentration (Ce)	Adsorbed amount (qe)	Removal (R)
units	**gm**	**mg/L**	**mg/g**	**%**
1	0.2	0.09	0.07	12.4
2	0.4	0.09	0.04	14.2
3	0.6	0.07	0.07	38.1
4	0.8	0.03	0.09	64.3
5	1.0	0.01	0.09	83.6

Mathematical Formulation:

The experimental values of NLP, PLP and ALP dosage on lead removal is extrapolated using MATLAB software to formulate corresponding quadratic equations relating to –

- Amount of Adsorbent (x) and Equilibrium Concentration (y)
- Amount of Adsorbent (x) and Adsorbed amount (y)
- Amount of Adsorbent (x) and Removal (y)

These equations can be used to interpolate the values of lead removal for any amount of adsorbent.

Table 10. Lead onto NLP

Amount of lead adsorbed at varying adsorbent dosage				
S. No.	Amount of Adsorbent (w) gm	Equilibrium Concentration (C_e) mg/L	Adsorbed amount (q_e) mg/g	Removal (R) %
Mathematical Equations		**y=0.035x*x-0.15*x+0.12**	**y=-2.94x*x+3.63*x-0.65**	**y=-41.78x*x+154.94*x-24.98**
1	0.3	0.07	0.17	17.74
2	0.5	0.05	0.43	42.04
3	0.7	0.03	0.45	63.00
4	0.9	0.01	0.23	80.62

Table 11. Lead onto PLP

Amount of lead adsorbed at varying adsorbent dosage				
S. No.	Amount of Adsorbent (w) gm	Equilibrium Concentration (C_e) mg/L	Adsorbed amount (q_e) mg/g	Removal (R) %
Mathematical Equations		**y=-0.017x*x-0.083*x+0.11**	**y=-0.071x*x+0.14*x+0.018**	**y=-4.82x*x+100.53*x-12.04**
1	0.3	0.08	0.05	17.68
2	0.5	0.06	0.07	37.02
3	0.7	0.04	0.08	55.96
4	0.9	0.02	0.08	74.53

Table 12. Lead onto ALP

Amount of lead adsorbed at varying adsorbent dosage				
S. No.	Amount of Adsorbent (w) gm	Equilibrium Concentration (C_e) mg/L	Adsorbed amount (q_e) mg/g	Removal (R) %
Mathematical Equations		**y=-0.10x*x+0.018*x+0.094**	**y=0.089x*x-0.062*x+0.07**	**y=66.60x*x+16.32*x+3.42**
1	0.3	0.08	0.05	14.31
2	0.5	0.07	0.06	28.23
3.	0.7	0.05	0.07	47.47
4	0.9	0.03	0.08	72.05

1.6 Effect of Absorbent Doses On Arsenic

Experimental Procedure

The study shows effect of NLP, PLP, ALP dosage on removal of arsenic. At initial fluoride concentration of 0.1mg/L, pH 6.5, temperature30°± 2°C ,contact time 2hr., shaking time 1hr , 0.2-1.0gm is used. Before reaching equilibrium, the contact time was ended. Results are seen in table 13.0, 14.0, 15.0 and figure 3. Results shows that by increasing adsorbent dose, percentage of arsenic removal is increased. The highest adsorption in case of NLP is 82.1%, in case of PLP is 81.0% and 80.6% in case of ALP. There was no significant variation in % removal by all adsorbents. Further we concluded that increasing adsorption dosage provides more available active sites for fixed arsenic concentration. As compared to all used adsorbent dosage, the adsorption capacity for NLP was higher. Similar results were reported by [14].

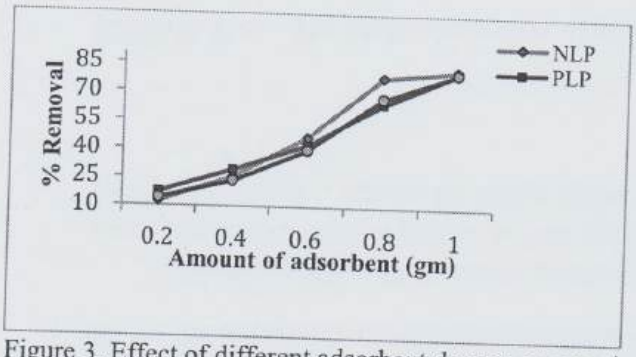


Figure 3. Effect of different adsorbent dosage on arsenic removal by NLP, PLP and ALP

Table 13

Arsenic onto NLP

Amount of arsenic adsorbed at varying adsorbent dosage

(Initial concentration: 0.1mg/L, Temperature: 30°C ± 2°C, pH: 6.5 , Contact time: 2hr., Shaking time: 1hr.)

S. No.	Amount of Adsorbent(w)	Equilibrium Concentration (Ce)	Adsorbed amount(qe)	Removal (R)
	gm	mg/L	mg/g	%
1	0.2	0.09	0.07	12.3
2	0.4	0.08	0.07	25.4
3	0.6	0.05	0.08	46.2
4	0.8	0.02	0.09	78.1
5	1.0	0.01	0.09	82.1

Table 14. Arsenic onto PLP

Amount of arsenic adsorbed at varying adsorbent dosage

(Initial concentration: 0.1mg/L, Temperature: 30°C ± 2°C, pH: 6.5, Contact time: 2hr., Shaking time: 1hr.)

S. No.	Amount of Adsorbent (w)	Equilibrium Concentration (Ce)	Adsorbed amount (qe)	Removal (R)
units	gm	mg/L	mg/g	%
1	0.2	0.01	0.09	17.3
2	0.4	0.02	0.08	29.1
3	0.6	0.04	0.08	42.2
4	0.8	0.07	0.09	64.1
5	1.0	0.01	0.09	81.0

Table 15. Arsenic onto ALP

Amount of arsenic adsorbed at varying adsorbent dosage

Initial concentration: 0.1mg/L, Temperature: 30°C ± 2°C, pH: 6.5, Contact time: 2hr., Shaking time: 1hr.)

S. No.	Amount of Adsorbent (w)	Equilibrium Concentration (Ce)	Adsorbed amount (qe)	Removal (R)
units	gm	mg/L	mg/g	%
1	0.2	0.09	0.01	14.1
2	0.4	0.08	0.02	23.4
3	0.6	0.07	0.03	39.7
4	0.8	0.03	0.07	67.2
5	1.0	0.01	0.09	80.6

Mathematical Formulation:

The experimental values of NLP, PLP and ALP dosage on arsenic removal is extrapolated using MATLAB

Software to formulate corresponding quadratic equations relating to –

- Amount of Adsorbent (x) and Equilibrium
- Concentration (y)
- Amount of Adsorbent (x) and Adsorbed amount (y)
- Amount of Adsorbent (x) and Removal (y)

These equations can be used to interpolate the values of arsenic removal for any amount of adsorbent.

Table 16. Arsenic onto NLP

Amount of arsenic adsorbed at varying adsorbent dosage

S. No.	Amount of Adsorbent (w) gm	Equilibrium Concentration(C_e) mg/L	Adsorbed amount (q_e) mg/g	Removal (R) %
Mathematical Equations		y=0.0x*x-0.11*x+0.11	y=0.00x*x+0.030*x+0.062	y=-12.67x*x+111.36*x-12.42
1	0.3	0.07	0.071	19.84
2	0.5	0.05	0.077	40.09
3	0.7	0.03	0.083	59.32
4	0.9	0.011	0.089	77.54

Table 17. Arsenic onto PLP

Amount of arsenic adsorbed at varying adsorbent dosage			
Amount of Adsorbent (w) gm	**Equilibrium Concentration (C_e) mg/L**	**Adsorbed amount(q_e) mg/g**	**Removal (R) %**
Mathematical Equations	y=-0.23x*x+0.30*x-0.05	y=0.053x*x-0.059*x+0.098	y=33.92x*x+40.48*x+7.52
0.3	0.01	0.08	22.71
0.5	0.04	0.08	36.24
0.7	0.04	0.08	52.48
0.9	0.03	0.08	71.43

Table 18. Arsenic onto ALP

Amount of arsenic adsorbed at varying adsorbent dosage				
SS. No.	**Amount of Adsorbent (w) gm**	**Equilibrium Concentration (C_e) mg/L**	**Adsorbed amount (q_e) mg/g**	**Removal (R) %**
Mathematical Equations		y=-0.089x*x+0.002*x+0.094	y=0.089x*x-0.002*x+0.006	y=34.64x*x+46.82*x+1.66
1	0.3	0.08	0.01	18.82
2	0.5	0.07	0.02	33.73
3	0.7	0.05	0.04	51.41
4	0.9	0.02	0.07	71.86

CONCLUSION AND RECOMMENDATION

NLP, PLP, ALP leaves after experiments showed greater adsorption area and strong affinity toward the ions. The experimental values of fluoride, arsenic and lead dosage on NLP, PLP and ALP removal is extrapolated using MATLAB software to formulate corresponding quadratic equations..These equations can be used to interpolate the values of ions removal for any amount of adsorbent. The extrapolated values by MATLAB software helps, in theoretically calculating the values without experiments, which in turn useful for the pilot project as well as to scale up the material at industrial level.

REFERENCES

[1] Darapu, Er. S. S. K., SudhakarEr. B., Krishna K. S. R., Rao P. V., and Sekhar M. C.; Determining Water Quality Index for the Evaluation of Water Quality of River. International Journal of Engineering Research and Applications (IJERA); **2011**, Vol. 1, Issue 2, pp.174-182.

[2] K., Brindha, R., Rajesh., R., Murugan., L., Elango.; Fluoride contamination in groundwater in parts of Nalgonda District, Andhra Pradesh, India.; Environ Monit Assess.; 2010, 10661–010–1348-0

[3] Gupta, S., Gupta, V.; Speciation and toxicity of arsenic: a human carcinogen. Res. J. Recent Sci.; 2013, Vol. 2, pp 45 – 53

[4] D.L.Ozsvath, Fluoride and environment health: a review, Rev. Environ. Sci. Biotechnol. 8 (2009) 59–79.

[5] S. L.Wang, C. H. Liu, M. K. Wang., Y. H. Chuang, P. N. Chiang; Arsenate adsorption by Mg/Al-NO3 layered double hydroxides with varying the Mg/Al ratio.; Appl. Clay Sci.; 2009, 43, 79–85.

[6] Hughes, M. F., Beck B. D., Chen Y., Lewis A.S., Thomas D. J.; Arsenic exposure and toxicology: a historical perspective.; Toxicol. Sci.; 2011, Vol. 123(2), pp 305 332.

[7] Garelick, H., Jones, H., Dybowska, A., Valsami-Jones, E.; Arsenic pollution sources. Rev. Environ. Contam. Toxicol.; 2008, Vol. 197, pp 17 60.

[8] Brinza L., Nygård C. A., Dring M. J., Gavrilescu M., & Benning L. G.; Cadmium tolerance and adsorption by the marine brown alga Fucusvesiculosus from the Irish Sea and the Bothnian Sea.; Bioresource Technology.; 2009, 100, pp 1727–1733.

[9] Mousavi H. Z., Hosseynifar A., Jahed V., Dehghani S. A. M.; Removal of Lead from aqueous Solution using waste Tire Rubber Ash as an Adsorbent.; Brazilian Journal of Chemical Engineering.; 2010, Vol. 27(01), pp. 79–87

[10] Maximous, N, George F., & Wan K.; Removal of Heavy Metals from Wastewater by Adsorption and Membrane Processes: a Comparative Study.; World Academy of Science, Engineering and Technology.; 2010, pp 64.

[11] Karthika, C., Vinnilamani N., Pattabhi S., & Sekar M.; Utilization of Sago Waste as an Adsorbent for the Removal of Pb (II) from Aqueous Solution: Kinetics and Isotherm Studies.; International Journal of Engineering Science and Technology.; 2010, Vol. 2 (6), pp 1867–1879.

[12] Karthikeyan, M., Elango, K. P.; Removal of fluoride from aqueous solution using graphite: A kinetic and thermodynamic study.; Ind. J.Chem. Technol.; 2008, Vol. 15, pp 525-532.

[13] Reddy, D. H. K., Seshaiah, K., Reddy, A. V. R., Rao, M. M., Wang, M. C.; Biosorption from aqueous solution by Moringa oleifera bark.; Equilibirum and Kinetic studies.; J. Hazard. Mater.; 2010, Vol. 174, pp 831- 838.

[14] Demarco, M. J., Sengupta, A. K., Greenleaf, J. E.; Arsenic removal using a polymeric / inorganic hybrid sorbent.; Water Res.; 2002, 37, pp 164-174.

COPYRIGHTS

Copyright of this article is retained by the author/s, with first publication rights granted to APJMR. This is an open-access article distributed under the terms and conditions of the Creative Commons Attribution license (http://creativecommons.org/licenses/by/4.

UGC-CARE List

You searched for "**2350-7756**". Total Journals : **1**

Search:

Sr.No.	Journal Title	Publisher	ISSN	E-ISSN	UGC-CARE coverage years	Details
1	Asia Pacific Journal of Multidisciplinary Research	Lyceum of The Philippines University	2350-7756	2350-8442	from June-2019 to February- 2020	Discontinued from Feb. 2020

Showing 1 to 1 of 1 entries

Previous 1 Next

Copyright © 2024 Savitribai Phule Pune University. All rights reserved. | Disclaimer

International Journal of Innovative Technology and Exploring Engineering (IJITEE)
ISSN: 2278-3075, Volume-8 Issue-12S2, October 2019

A Research Paper on Contamination of Water Due to Fluoride, Lead and Arsenic and its Removal Techniques

Nidhi Jain, Huzaif Umarsharif Mujawar

Abstract*— Due to undesirable changes in the physical, chemical and biological characteristics of air, water and soil people across the globe have been subjected to severe environmental catastrophes. With no signs of stabilization of population explosion, rapid industrialization, have polluted the essential resources beyond threshold In this changing scenario availability of quality water is an indispensable feature for preventing diseases and improving quality of life. It is of utmost importance to assimilate the details of different physico-chemical parameters viz. color, temperature, acidity, hardness, pH, sulphar and chloride content, DO, BOD, COD, alkalinity used for testing of water quality. Few metals viz. fluoride, lead and arsenic in their ionic form are of are major source of water contamination affecting the aquatic ecosystem and terrestrial life forms.

The paper addresses the effect of different adsorbents used for removal of fluoride, arsenic and lead.

Keywords: water, physic - chemical, hardness, fluoride, lead and arsenic contamination

I. INTRODUCTION

Water is a magical substance. It is both simple and complex in nature. A water molecule is composed of atoms of hydrogen and oxygen. H_20. The makeup of these building blocks produces a molecule with almost magical properties, which forms the basis for its wide variety of uses. Water is an essential element for sustenance of life on earth.. The excessive loss of water from human body leads to severe health complications sometimes turning fatal.

Water quality at a certain location and time based on. A water quality index (WQI) based on several quality parameters was developed by Scientist form National Sanitation Foundation (NSF) in 1970. The NSF WQI provides a standardized method for comparing the water quality of various water bodies.

Fluoride:

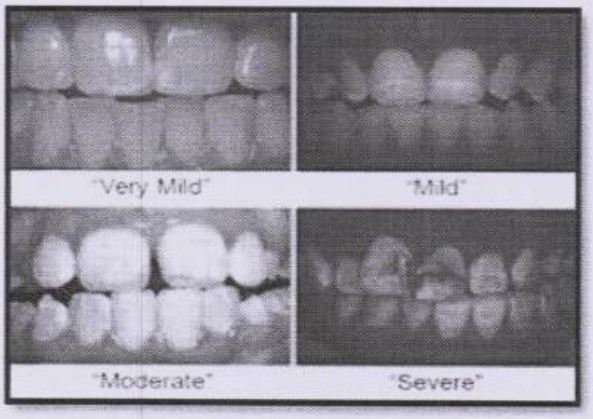
As per estimates the amount of fluoride found in earth crust is around 85 million tones and nearly 12 million tones are located in India. The principal sources of fluorine are drinking water, food derived from aquatic sources , cheese and tea. Fluoride is present in all forms of water and in particular higher concentrations is found in in ground.

Toxicity:

Skeletal and dental flurosis are caused by high fluoride level in drinking water which acts has critical health hazard of this century. It was estimated that 62 million people were found to be affected with varying degree of fluorosis in India such as dental, skeletal and non-skeletal form of fluorosis [Susheela, A. K, **2001**].

Two-edged sword is called as Fluoride It is beneficial for the human body as it is made up of 96% of fluoride in the form of bones and teeth. Mineralization of bones and formation of dental enamel fluoride plays important role.

If it is ingested in large quantity above daily requirement it cause through drinking water it causes dental and skeletal fluorosis [Park, K. **2011**].





There are two types of cation by which fluoride is associated one is water soluble monovalent cations such as NaF and KF . And second one is water in soluble with divalent cations such as CaF_2 and PbF_2

If we compare the toxicity of fluoride we find that

Fluoride is "more toxic than lead and less toxic than arsenic". [Jain, J. K.,Gupta, Nidhi, **2013**]

Revised Manuscript Received on 14 September, 2019.

Dr. Nidhi Jain, Department of Engineering Science, Bharati vidyapeeth college of engineering Lavale, Pune - 412115,Maharashtra, India. (Email: nidhijain1704@gmail.com)

Huzaif Umarsharif Mujawar, Department of Computer Engineering, Bharati vidyapeeth college of engineering Lavale, Pune-412115, Maharashtra, India. (Email: huzaifmujawar1998@gmail.com)

A RESEARCH PAPER ON CONTAMINATION OF WATER DUE TO FLUORIDE, LEAD AND ARSENIC AND ITS REMOVAL TECHNIQUES

According to WHO, 2006 guidelines fluoride is an essential mineral (WHO, 2006) which is beneficial when taken within permissible limits and also causes as well as various disorders such as skeletal fluorosis, brittle bones, cancer, infertility in women and Alzheimer syndrome [Dobaradaran, S. **2008,** Guo, X.,et al 2003, Mahvi, A, **2006**] .

Lead

Atmospheric lead concentrations of 50 pg /m3 have been found in remote areas. Levels of lead in soil range between 10 and 70 mg/kg and a mean level near roadways of 138 mg/kg have been reported. Present levels of lead in water rarely exceed a few micrograms/liter; the natural concentration of lead in surface water has been estimated to be 0.02 m g/liter [Gavaghan, Helen].

Lead is hazardous to mankind as well as for the environment because [Verstraeten, S.,2008].Generally lead is in elemental form, cannot be scale down into less dangerous material. Major health problems associated with neurological and physiological repercussions. Paint is the major source of lead ingestion. In US 38 million households used lead containing paints in 2002 and out of which significant lead based hazards are caused. [Tripathi, R. M., et al, 2001].,[Toscano, C., Guilarte, T.;2005.]

Toxicity:

Contaminated ground water has the major source of diseases by heavy metals ions such as lead etc. Plumbism is caused by lead toxicity. It can also be caused by inhaling contaminated air.

Large numbers health problems are caused by

Lead toxicity and its cause toxic effect on human body [Navas-Acien, A., 2007 etal.,Woodruff et al.,2008, Iqbal, S., etal.,2008] Some of the major problems caused by lead are blood disorders and Anaemia, Rapid deterioration of brain and the nervous system, Reduced fertility both in men and women, Failure of the kidney, Alzheimer disease.

In 2000, the allowable level of lead in drinking water was reduced from 0.6 ppm to 0.05ppm. However, no level of lead is considered to be actually safe today.

About 90 % of the lead body burden is stored in the bones and teeth of adults. The corresponding value for children is 70 %. Higher mobility of lead in children results from continuous growth and re/desorption of bone making children more susceptible to the adverse health effects of lead. Similar bone lead mobilization also occurs during pregnancy. [Barbosa, F.,etal.,2005] and elevated blood lead concentrations have been associated with reduced hemoglobin synthesis and red blood cell quantity [Tripathi, R. M., 2001]leading, in the worst case, to anaemia.

Parkinson's disease and amyotrophic lateral sclerosis are also major caused by Lead contamination. Lead effects enzyme production with heme which in turn spoil energy metabolism,

[Khan, A **2008**]. lead poisoning can be controlled by taking proper precautionary measures Environmental and domestic sources of Pb^2 [Robert,et al,2008].

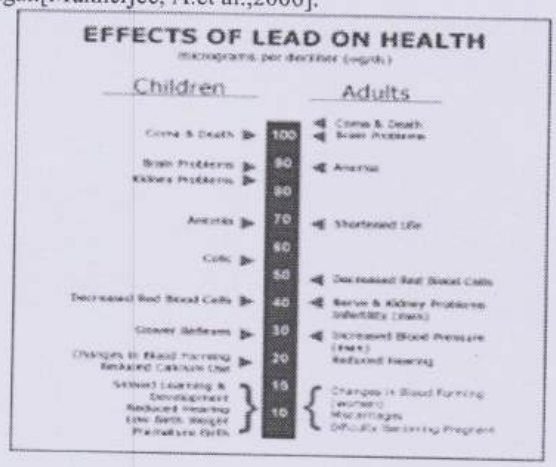
Arsenic

Arsenic (As3+/5+) is ubiquitous in nature and widely distributed in soils, sediments, water and atmosphere. Arsenic is a metalloid with atomic number 33 and atomic weight 74.9216 g/mol. In the terrestrial environment, concentration of as ranges from 1.5–3 mg kg−1and found as the 20th most plentiful element in earth's crust [Mahimairaja, S.,2005]. In seawater and human beings it is ranked the 14th and 12th element in abundance, respectively.

Arsenopyrite. is the most prevalent form of Arsenic, as arsenic is a metalloid which is ubiquitous as organic and inorganic in the ecosystem. The compounds like arsenite and arsenate that are the inorganic forms of arsenic tend to show higher rate of toxicity in humans than other natural counterparts.

The king of Poison is what Arsenic is Frequently referred to as it is discreet, accessible, unscented and leaves no taste: hence can go easily undetected in daily intake.

Inorganic source of arsenic is mainly geological where as that of organic if the marines. The first ever Arsenic poisoning dates back to July, 1983 in the region of West Bengal.[Mukherjee, A.et al.,2006].



The geothermal fluids that have abundance of arsenic tend to comtaminate the surface water when in contact. [Garelick, H et al., 2008]. The contribution to arsenic flux in the environment is mainly from the dissolution of the compound Aresenopyrite or the arsenic which is released from rocks or sediments. One of the main Atmospheric depletion due to arsenic is caused by the coal fired power generation plants or by burning vegetation and volcanism.

The Percentage of arsenic in earth's crust varies a lot, in the range of about 1 to 40 part to about a million parts of soil (ppm) with an average of about 3-4 ppm. However, the areas such as mining or smelting sites or the places where arsenic induced pesticides had been applied in the fields can show a lot higher levels of arsenic.

The Ground water carries a rich level of arsenic than that of surface water, and since the consumption of ground water is more in INDIA, it causes a wide range of toxicity. Ingestion of as little as 100 mg usually results in severe poisoning and 130 mg has proved to be fatal. All human beings are exposed to it in one form or other. However water and food constitutes major source of exposure to population [Datta, D. V., and Kaul, M. K,1976].. The stability, solubility and toxicity of arsenic depends on

the various forms that it is found in. The Persistent and bio available inorganic forms of arsenic, that are more hazards when compared to their organic [Gupta, S., Gupta, V.; **2013**].



Arsenic lesions on feet and arsenic poisoning in hand

The following figures illustrate the arsenic toxicity in various part of body. The accumulation of arsenic in tissues leads to health hazards [Vahter, M., Concha, G.2001].

Exposure to inorganic arsenic causes many adverse health effects, including cardiovascular, hepatic and renal disease in addition to cancer in kidney, liver, lungs, urinary bladder and skin [Puthenveedu et al.,2012]. Scientists have made sure to do all the necessary tests to prevent the public from the hazards of toxic chemicals and constantly in search of ways to cure the effected.

II. REVIEW OF LITERATURE

Review of fluoride levels in water.

There has been a huge increase of fluoride in ground waters in the leading developed and developing countries that includes India around 19 states are facing acute fluorosis problem[Mehto, A., Chakrapani, G. J.,2013]. Consumption of this fluoride rich water (>1.5 mg/l) is a major source of health hazards in Humans. [Puthenveedu et al., 2012].

The presence of floride can be detected unanimously in the world, ranging from water (higher concentration in ground water), mineral deposits, rocks, also can be found in products used in our daily lives i.e. toothpaste, drugs, cosmetics, chewing gums, mouthwashes and so on. When used in small proportions it has certain benefits as well as in preventing Dental problems when used in the concentration of below 1.0 ppm, anything above that is hazardous and harmful. According to the World Health Organization (WHO) and IS: 10500 have stated to keep the levels of fluoride form 1.0 to a max of 1.5 ppm in drinking water. [Thatte, C. D.1994, Subba, Rao, N et al 1997]. When exposed to higher levels of fluoride may lead to join pain, cancer and even partial paralysis. [Cantor, K. P.;1997] possibly raise the risk of some bone defoematiseThe main source of fluoride in this modern era are the excess use of fluoride based fertilizers or the coal that are fluoride infiltrated used in Thermal Power plants which play a major role in polluting the surrounding areas. A lot of reports related to this have been recorded, one such coming from North India. [Pathak, R. P.,2012].

A disease such as Fluorosis was first detected in India in the early 1930s in four states and by the year 1992 it was recorded to be found in as many as 177 districts across 19 states. [Waheped, S.,et al.,2009].

If we talk about the problem across the globe, as many as 200 million peoples in 25 nations are affected by health issues due to increase in the level of fluoride in drinking water. Countries like India and China are the ones who have been hit by this problem the most. As a matter of fact, in India the endemic fluorosis has affected a total of around 1 million alone and is said to have a major problem in more than half of the country, especially in the states of Rajasthan and Gujarat. [Rao, R. J., Naidu, M. G. C,1973.,Brunt, R. L. et al,2004].

There are serious problems faced in various countries because of rise in the presence of fluoride in drinking water, which is a source of major dental and skeleton related issues.. There have been reports in high concentrations of fluoride in ground water in more than 28 countries that carry both the developed as well as developing which also includes India, in which it is found in around 19 states.[Sharma, B. S.et al.,2011]. Levels of Fluoride that are above the prescribed limit (1.5mg/l) in the consuming water turns into a very hazardous drink that lead to dental fluorosis and skeleton fluorosis.

[Punita Parikh et al., 2013] a recent study was done to check the status of fluoride in ground water of Kheralu block of Mehasana district, Gujarat. It showed that, in around 43 villages i.e about more than 55 %, it is seen that the level of fluoride are in a range of 1 – 1.5 ppm out fo which around 16 villages had their levels checked and resulted in a level below 1 ppm while the 27 villages showed a level that exceeds the maximum level of around 1.5 ppm. The factors which have lead to this may be due to the reason of major loss of surface water and presence of semiarid climate along with sedimentary rock basin.

The other documents which are reviewed on fluoride contamination of water are Kataria et al 2008]. It states that the content of fluoride in the surface and ground water in the city of Bhopal salve et al,2008] have also been reported to have gone past the acceptable limit which also the same in that of kadi tehsil in the region of Mehsana in the state of Gujarat.

Review of literature on fluoride contamination reveals that the Gujarat, Rajasthan and Andhra Pradesh [Unicef state of art report 1999 FR & R'DF data bank] are the areas which have been the most affected by the fluorosis in which more than half of their districts i.e. 18 of 24 are highly prone to be hit by fluorisis, this is due to the high levels of fluoride in their waters. In north region of Gujarat, where districts like Mehsana, Patan and Banaskantha have been majorly effected, apart from other affected districts like Amreli, Ahemdabad Sabarkantha and Baroda.[Punita,et al.,2013] Banaskantha are affected by high fluoride concentrations. Mehsana, Patan, and [Kundu N. et al., 2001] have investigated that the geochemical raise of fluoride in the ground water that is in the area of Nayagarh district

of Orissa.. There study result shows that the composition of the hot spring water is very comparable to the other thermal waters of the world. Thermodynamic considerations show that more than 65% of the groundwater and hot spring water samples are oversaturated with calcite, and only four samples are oversaturated with fluorite. Fluoride concentration shows a positive relation to sodium, bicarbonate and pH, and a negative relation to calcium and magnesium in fluoride rich groundwater and hot spring water. Principal component analysis shows that the fluoride rich groundwater was produced due to a mixing of hot spring water with the surrounding groundwater.

Datta B.K. et al. [74] have reported that the Stable isotope (180) which investigates on the processes of controlling fluoride contamination of ground water. The reports showed that about 50% of the entire area is being affected by fluoride contamination and that the level of fluoride has gone beyond the required limit. The environs of brick kilns are found to have high levels of fluoride in their ground waters.

Review of removal of fluoride in water

A lot of research has been done in the field of removal of fluorine from drinking water by many researchers across the globe. The removal of fluorine is divided in two sections mainly dealing with Membrane and various adsorption methods. Techniques such as reverse osmosis, nano-filteration, electro-dialysis have been talked about under the first half. In adsorption, i.e. a very conventional technique which uses adsorbents like alumina/aluminum based materials along with clays and soil, material that are calcium based, also carbon based material and synthetic compounds are used. There are also reviews that have been done on the removal of fluoride from aqueous solution with the help of different type of zeolites such as reversed and modified, then certain ion exchange resins that are based on the cross-linked polystyrene.. Below are such developments which are being discussed.

Even though the use of membrane has fruitfully lowered down the levels of fluoride to the required levels, the surface adsorption still plays an eminent role in the research of defluoridation due to its great accessibility and low stress on the pocket. It is due to this reason that even when there are new techniques which are gaining popularity, researchers still prefer to explore in the greater depths to improve low-cost adsorbents so as to increase their overall effectiveness. [Biswas, K.et al.,2007].

[A. V. Jamode et al., 2004] came across a way in the form of very low-cost technique involving the use of adsorbents in the form of leaf. In this study of leafs such as that of neem (Azadirachta indica), pipal (Ficus religiosa) and khair (Acacia catechu wild) trees were used. It was found that when the fluoride ion concentration level is at its peak, in the effluent the level of fluoride ion bit by bit comes down to 0 mg/l keeping the conditions at 29 ± 0.5°C for a period of 180 min and the dose of adsorbent is kept at 10 g/l. there is an isotherm called Langmuir which a process adsorption which involves statistical and experimental data calculated from Isotherm equation.

[Mohammad Mehdi Mehrabani Ardekani et al , 2013] compared the following three in respect for fluoride removal from water by adsorption, they are Bagas, Modified Bagas and Chitson. The optimum or best possible set-up for these to work efficiently could be seen when the pH value is set at 7, a contact time of 60 min with the adsorbent dose fixed at 2 g/L The pH value of 7, contact time of 60 min and adsorbent dose of 2 g/L were determined as optimum conditions for all three adsorbents. Chitosan and Bagasse do not show great potential for removal of fluoride, whereas the modified bagas shows an enormous rate of about 90% of removal of fluoride in the same above mentioned conditions. Compounds like Langmuir and Freundlich isotherms also show moderately good correlation for account of required results, but the Langmuir model with the correlation value of 0/99 is superior. [Valencia-Leal S. A. et al., 2012.] The Maximum adsorption which was recorded is seemed to have occurred at pH5.0 to 8.0.at first the procees was found to be endothermic in nature. Later Langmuir and Freundlich isotherm models wear used to get the estimate data of the adsorption rate. To describe the kinetics related to fluoride adsorption in which the guava seeds are used, the pseudo-second order model is used. The Langmuir model is used to best describe the isotherm's experimental data that shows us the adsorption mechanism using guava seeds in the fluoride ions is chemisorptions when done on a homogeneous material.

[Veeraputhiran V. and Alagumuthu G. et al, 2011] studied the use of Phyllanthus Emblica as adsorbent for fluoride removal from the aqueous solution. The highest recorded adsorption capacity was found at neutral pH with 0.75g of the adsorbent dose used, the adsorption process was that of heterogeneous with percentage removal of fluoride recorded was 82.1% by Phyllanthus embilica.

[C. M. Vivek Vardhan and J. Karthikeyan ,2011]carried out different ways to remove the fluoride contamination from water by using a certain physic-chemical method for adsorption by using very cost effective materials like rice husk, use of certain chemicals like manganese sulphate and manganese chloride, Rice husk , etc.

It was seen that when rise husk is used at a constant weight of 6g/L, 83% of fluoride from a sample of 5mg/l fluoride solution in a span of 3 hours was removed. At and approximate rate of 92, 94 and 91 % respectively for removal of fluoride from a test solution of 5mg/l at a set dosage of 1000 mg/l by using Moringa oleifera seed extracts, Manganese Sulphate and Manganese Chloride. It was observed that when manganese sulphate, Manganese Chloride and MOE is used for fluoride removal, the best suited condition for the same is at a set pH of 6.0. [Mohan, S. V.et al.,2007].

A range of other adsorbents systems such as the activated ions like carbon, alumina and bauxite as well as the use of natural and synthetic zeolite and use of various other ion exchange resins for removal of fluoride contamination in water.

[Nigussie W. et al., 2007] have made a report in which they recorded a successful method of fluoride removal by the use of waste or residue left behind in the manufacturing of alum in industries, it was observed that in the initial phase the adsorption of fluoride was very rapid for around 5 min and as we move on it showed a gradual increase up until it reaches the equilibrium condition at around the 1 hour mark. As the adsorbent dosage was increased the efficiency could be seen to climb on to the higher side.the use of heat and surface neutralization could have no effect on raising the bar of efficiency in fluoride removal. There is seen a constant rate of removal observed when pH is kept at around 3-8 pH.

The adsorption data at ambient pH were well fitted to the Dubinin-Radushkevick (D-R) isotherm model with a capacity of 332.5mg/g of the adsorbent. The adsorption kinetic was found to follow a pseudo-second-order rate equation with an average rate constant of 2.25gm in (-1) mg (-1).

[Sarkar M. et al., 2006] have found a way of removal of fluoride, in that of Laterite. A variety of tests have been done on the different functionality ratios of that of Laterite for as to use as a removal agent. The areas such as thermodynamic parameters like free energy change, entropy of the process and enthalpy as well as the basic sorption isotherm were also investigated.

The extent of solute removal is determined by initial solute concentration, operational conditions, laterite dose, and solution pH. For a fixed set of experimental conditions, a model equation is developed from which the percent removal corresponding to each load of fluoride is determined. The elution of the retained fluoride was studied and the effectiveness of column operation was determined by the retention-elution cycles.

Lots of researcher had work on removal of fluoride by adsorption and adsorbent are as follows Pali Shahjee et al ,2013, Naba Kumar et al ,2012, Bhagyashree M et al,2012, Das Kumar et al 2011.

Review of lead contamination in water

Lead is well known non – biodegradable toxic metal in the environment and now it has become a global health issue [Gracia, R. C., et al ,2007, Mc Carthy et al,2006]. One of the earliest recorded diseases is that of the Lead poisoning. It has a major threat on the public health and safety measure, especially in that of the upcoming developing countries. If exposed to lead poisoning it was recorded certain hazards such as that of on the hematopoietic, renal, and reproductive and central nervous system mainly caused due to the increased levels of oxidative stress. [Flora,et al.,2012].

The reports that are collected have shown that there is a great interlink between chronic lead exposure to children and impaired cognitive skills, reduced IQ [Miranda, M.L, 2007], it is also seen that the chronic lead exposures towards adults have lead to the damage towards the problems mentioned above. [Shih, R. A., 2007].

Leaded crystal, cigarette smoke, lead solder used in canned foods produced outside the United States, children's toys, vinyl lunchboxes, contaminated candy imported from Mexico, and children's jewellery produced outside the United States have all been shown to contain significant amounts of lead.

In the year 1996 in the area of North Carolina it was surveyed that, around 75 percent of children were exposed to lead poisoning cases in a short period of six-month which includes the major contributor to this cause i.e. the lead dust from vinyl mini-blinds.[Norman, E. H. et al,1997].

The symptoms after being exposed to lead, were growth deficiency, lowered intelligence levels, loss in hearing and memory loss. After prolonged exposure to higher levels it may lead to a severe brain damage and even death [Cleveland,L. M.,2008]. This also leads to a reduced lifespan for the circulating erythrocytes by the increase in fragility of cell membranes. The total aftermath of this leads to anaemia.[Cornelis,R., 2005, Guidotti, T. L., 2008].

Literature survey showed that lead contamination in water, food and air is increased day by day. Recently we read in newspaper Maggie 2- minutes [Times of India 3-June 2015] noodles contains dangerously high levels of lead which causes an estimated 143,000 deaths a year worldwide. As per our various review of literature, the presence of lead in water in various cities is presented in table 2.1

Table No. 2.1	LEAD CONTENT IN WATER		
ALARMING	HIGH	MEDIUM	LOW
Kolkata	Delhi	Chennai	Bangalore
Kochi	Coimbatore	Ludhiana	Ahmadabad
Mumbai	Madurai	Surat	Hyderabad
Pune	Bhubaneswar	Ghaziabad	Indore
Nagpur		Jamshedpur	Bhopal
Nasik			Chandigarh
Guwahati			Lucknow
			Mangalore
			Mysore

In which about 41% sample of potable water were unfit for drinking **LEAD action news,2010**. The elevated levels of lead in blood of children 200 µg/L and in dogs it is 250 µg/L of Indian mega cities were reported. From 1970's to this decay though surface water and ground water. K. S. Patel has reported the lead environmental pollution in [Patel K. S., et al 2019.] Lead to be the toxic metal Kumar, K. S.,2008 with very little or no nutrient values, is abundant almost everywhere in the nature.

[Dooyema, C. A., **and their co-workers** 2012] have studied on the Outbreak of fatal childhood lead poisoning related to artisanal gold mining in northwestern Nigeria. Their goal was to determine the cause of the childhood lead poisoning outbreak, investigate risk factors for child mortality, and identify children < 5 years of age in need of emergency chelation therapy for lead poisoning.

Lead exposure to human being had been found worldwide. Documentation of lead poisoning from environmental sources and occupational setting in literature has been well mentioned some of them are Rajappa B.et al.,**2010**, K. Ravichandran et al., 2011

On the basis of review of literature on lead in ground water, we have concluded that the industrialization, anthropogenic activity and geochemical processes are main sources of lead in drinking water.

Review of lead removal in water.

The Water used in the industrial sector leads to a lot of potential dangers to the environment by the introduction of soil and water resource damaging contents in the form of heavy metals. These heavy metals hold a major role in what is known as the pollutants for the degradation of our natural resources. [Brinza L.,et al.,2009]

Thus there is greater need to treat and have a safe way to discharge this contaminated water. The important polluting contents are like that of Cd, Zn, Pb and Ni.

Nowadays, with a drastic increase in population, it is a high time to control the emission of such toxic materials in the environment.

[Mousavi H. Z., Hosseynifar A., Jahed V., 2010], [Maximous, N, George F., & Wan K.;,2010.] The lead exposure tends to have a serious effect on our health in the form of anaemia, nervous disorders, kidney disease and even death in major exposures.

[Kafia M. and Surchi Shareef ,2011] have found ways to use the agricultural waste as a substitute Low Cost Adsorbent for the removal of Pb. With the help of these five low-cost natural adsorbents which give us an efficiency rate of 85, 90, 100, 86 and 98 percentage respectively, these are chalf, rice husk, sesame, sun flower and residue of tea.

[Brooks Robert M., 2010] have observed the process in which to lower down the lead quantity from its aqueous solution by the use of AAM-PRB i.e. alkali ash material permeable reactive barrier which is a newly developed novel material with the help of fly ash alkali to remove lead (pb). The AAM-PRB were created with high permeability capabilities. The permeability ration must be high so for a barrier material around 10-2 cm/sec to 10-1 cm/sec. The AAM-PRB are formed from three sources with permeability in the range of 10-1 cm/sec and later crushed into pellets.

[Pandhare et al., 2013] have investigated the use of neem leaves with powdered activated carbon as adsorbents. They used methyl red & $K_2Cr_2O_7$ solution and to offer this biosorbent as local replacement for existing commercial adsorbent materials.

[Gupta S. S. and Bhattacharya K. G., 2005] Used the waste from the fertilizers to creat the activated carbon to remove, Pb (II) Hg (II), Cr(VI), and Cu (II). The time required for the formation of initial primary adsorption was between 1 to 2 hrs. The present saturation at break point is 79.2, 75.0, 66.6 and 64.3% for Pb^{2+}, Hg^{2+}, Cr^{6+}, and Cu^{2+} respectively.

[Pandhare Ghanshyam and their co-workers.2013]

Investigated and reported the removal of lead from a sample solution by the use of neem leave powder.

They prepared Neem Leaves Powder as an adsorbent using chemical activation process and the surface area measured. The adsorbent material adopted was found to be an efficient media for removal of Lead (II) ion with different parameter like Adsorbent dosages, Concentration and contact time etc. They were found that the metal uptake capacity (amount of removal) of lead (II) ion decreased but the adsorption capacity (percentage of removal) increased with the decrease in the concentration of Lead (II) in the initial sample solution. Correlation coefficient and isotherm constant was also calculated from isotherm studies with different parameter.

Nagpal Uma et al.,2010

Have reported and calculated the Equilibrium sorption for Pb^{2+} on three different samples of biomasses. These three are formed by the help of dried leaves of the following, Terminalia Catappa, Dalbergialatifolia and Ficus benghalensis . it was found that the total amount of Pb ions adsorbed increased as the concentration of the initial metal ion was increased. It was observed that equilibrium sorption capacity for 800 mg 1-1 for metal solution was 77.55, 59.35 and 19.35 mg g-1 respectivelyfor the three leaves mentioned above.

Lovell Agwaramgbo et al.,2013 Investigated the use of Solid Biomaterials like Charcol, Coffee, Tea, Fishbone and Caffeine for the removal of lead from its contaminated aqueous solutions.

The results observed were as follows from a sample solution of 1300 ppm of lead solution, Charcoal (100%) > Tea (97%) > Coffee Ground (88%) > Instant Coffee (83.5%) > Coffee Bean (82%) > Fishbone (76%) > Caffeine (1.3%). It was observed from these results that not all the biomaterials taken in investigation can absorb lead.

Review of arsenic contamination in water

One of the major sources of pollution concern comes from the suspensions of the bedrock/minerals and other anthropogenic activities e.g., the contaminated water coming in from mines, preservatives of wood, discharge from uncontrolled mining and metallurgical industries also the use of excessive agricultural chemicals are a major contributor to pollution. [Lacasa, E.et al,2011; Wang, S. L. et al,2009].

It leads to many health hazards such as carcinogenic effects on organs, cardiovascular and neurological effects, also effects are seen on the immune systems due to the continuous exposure to contaminated water. Major organizations around the globe like the European Union (EU), The United States (US), and The WHO have reported that a maximum value of 10 µg is what is acceptable level of contamination in water as in potable water [Chetia, M. et al,2011].

As in today's world the entire population across the globe depends on sources of ground water for their daily cooking and drinking purpose. An estimate of around 105 countries in which about >200 million people have come in contact with the Geogenic arsenic contamination of ground water

In the region of Ganga-Meghna-Brahmaputra, >100 million people have been in risk and threatened by the arsenic contaminated groundwater. In most of the arsenic hit Asian countries the level of contamination has gone past the max level of 10ppb to as high as 50ppb.

In India the arsenic contamination is a major issue and can be said to be among the top countries who have been effected by this contamination the most.

The Arsenic contaminated groundwater is being used for agricultural purpose which in turns pollutes the food we in take as a consumer.

In the reports that have been studied uptill now it can be firmly said that in India Logically the contamination levels in water should not be more than 5 ppb. It is also observed that the risk of being effected by cancer by the continuous consumption of highly arsenic contaminated water at 50 ppb and 1L/day is 1.3/100.[Smith, A. H.,2002].

One of the Asian countries that is severely effected by Arsenic contamination is Bangladesh. More than half of its ground water contains or is naturally contaminated by arsenic, where the contaminations leave have gone past 10 µg/L [Caussy, D., Priest N. D.,2008]

In the last few decades around 35-37 million people living in the country of Bangladesh have been exposed to the toxic levels from that of the contaminated water[Argos, M.et al.,2010], from the total of its popullion count of 164 Million. [PRB.,2010].

Van Halem, S. A. Bakker et al.,2009

According to their investigations it is reported that the arsenic contamination in water supply is a problem that is taken a global scale and hit even develoved countries like that of USA and China. In the European countries the countries manily hit are Serbia, Hungary and Italy where the arsenic related problems are mainly confined to at a great scale as of now in their groundwater.

[Chaurasia et al., 2012]

On their investigation on the Finger Print of Arsenic Contaminated Water in India, It was reported that the people have been hit by diseases such as that of ulcer, skin cancer pigmentation in skin various other skin hazards due to the exposure of continuous arsenic contaminated water.

A lot more measures have been started to take place or are being proposed to help analyses the arsenic situation in India, which will in turn help in establishing preventive measures and how should we the control the arsenic contamination in water

The review has resulted in finding out that the concentration of this contamination is increasing on a day to day basis which has indirect or direct effects on the lives of people living there.

Even more studies and analysis on the problem related to arsenic contamination can be found in literature [Roy, Madhumita et al.,2014,] **Sharma et al.,2013]**.

Singh Amrit Pal and their co-workers, 2004 have investigated the mechanisms pertaining to arsenic toxicity.

In their investications it was found that excessive exposure of such contaminated water has taken a huge toll on the health of people by opening up to the way to major diseases such as cardiovascular abnormalities, diabetes mellitus, neurotoxicity, and nephrotoxicity.

They founded that the chronic arsenic exposure is a cause of immense health distress as it accounts for the increased risk of various disorders such as cardiovascular abnormalities, diabetes mellitus, neurotoxicity, and nephrotoxicity. In addition, the exposure to arsenic has been suggested to affect the liver function and to induce hepatotoxicity. The present review addresses diverse mechanisms involved in the pathogenesis of arsenic-induced toxicity and end-organ damage.

Several other studies on contamination of arsenic are as follows: Mazumder Debendra Nath Guha [2010], Basu Atreyee **2015** etc.

Review of removal of arsenic in water

There are numbers of arsenic removal methods, which include coagulation followed by precipitation, membrane separation, anion exchange; etc. Arsenic pollution has emerged as a serious public health concern in Pakistan also. The use of low-cost adsorbent obtained from a environmentally friendly materials, has been investigated as a replacement for the current expensive methods of removing arsenic from solution. There are various other low-cost adsorbents which are more superior like that of carbons that is derived from agricultural waste, bio-sorbents, goethite and other commercial adsorbents including resins, gels, silica tested.

Many other systems have been taken into account for the removal of Arsenic like ion exchange, activated alumina, reverse osmosis, modified coagulation membrane filtration and enhanced lime softening.[Berg.M.,2006]

[Eid I., et al.,2014]

Have investigated ways for the arsenic removal with the help of certain plant-based biomaterials that can easily be found in the arsenic prone areas in the country of Bangladesh. They are the powdered roots of water Hyacinth (WH) which is best for removal of arsenic type (III) and type (V), other include that of banana-pseudo stem (BN), jute and sugar cane bagasse (SC).

Razzouki B. and their co-workers.,1993 Have founds ways to remove the arsenic type (III) and (V) with help of iron hydride.

have investigated on remove As (III) and As (V) using iron hydroxide. The study was performed with the effect of pH and its contact time (T) on the basis of Co precipitation-sorption of Arsenic (III) and Iron (III) Hydroxides. The result shows that the co-precipitation of arsenic (III) with Fe $(OH)_3$ was more dependent on the concentration of iron and H+ ions. Complexation in a monodentate area was more important than the bidentate throughout the pH range studied, but the bidentate complex has important role near pH 8.

[Ashraf Ali M. et al.] have been developed three $As^{3+/5+}$ removal technologies, these were: (i) removal system based on alum and iron coagulation; (ii) sorptive filtration using iron coated sand filter, and (iii) sorptive filtration using gravel bed containing iron sludge. Also two technologies, Based on laboratory performance, ferric chloride coagulation, and sorptive filtration through iron-coated sand, were selected for the development of household arsenic removal units.

[Mohapatra D. et al., 2008] have determined that As (V) removal from an aqueous medium by calcined refectory grade bauxite (CRB) as a function of solution pH, time, As (V) concentration and temp.

The residual value of the arsenic (V) was observed to have lowered from 2mg/L to about 0.01 mg/L in the range of pH kept around 4.0-7.0 by the use of 5gm/L of CRB in a time span of 3 hours. Contact time

III. CONCLUSION

Water is becoming a important factor for development and the quality of life in many countries. In arid areas it has even become a survival factor. There is need to have proper collection and treatment of waste and need to regulate the flow. Upon the various research done It can be concluded that the major source of pollution may have come from a natural path or/even manmade. The researchers have successfully found ways to lower down or remove the contamination of the compounds discussed i.e. F, Pd and $As^{3+/5+}$ from the waters, which in turn help in solving a variety of problems caused not only in India but worldwide as well.

REFERENCES

1. Argos, M., Kalra T., Rathouz P. J., Chen Y., Pierce B., Parvez F., Islam T., Ahmed A., Rakibuz-Zaman M., Hasan R., Sarwar G., Slavkovich V., Geen, A. V., Graziano, J., Ahsan H.; **Arsenic exposure from drinking water, and all-cause and chronic-disease mortalities inBangladesh (HEALS):A prospective cohort study**.; Lancet **2010**, Vol. 376, pp 252–258.
2. Ashraf, Ali, M., Badruzzaman, A. B. M., Jalil, M. A., Delwar Hossain, M., Hussainuzzaman, M. M., Badruzzaman, M., O. I., Mohammad, N. Akter.; Development of Low-cost Technologies for Removal of Arsenic from Groundwater.; pp 99-120.
3. Basu, Atreyee, Sen Parijat, Jha Ayan.; Environmental arsenic toxicity in West Bengal, India: A brief policy review.;Indian J Public Health.; 2015, 59, pp 295-298.
4. Berg, M., Luzi S., Trang P. T. K., Viet P. H.; Giger, W., Stuben D.; Arsenic removal from groundwater by household sand filters: Comparative field study, model calculations, and health benefits., Environ. Sci. Technol.; 2006, 40, 5567–5573.
5. Bhagyashree, M., Mamilwar, A., G., Bhole, A. M., Sudame.; International Journal of Engineering Research and Applications (IJERA).; 2012, Vol. 2(4), pp 334-338.
6. Brooks Robert M.; Bahadory Mozhgan, Tovia Fernando, Rostami Hossein.; Removal of Lead from Contaminated Water.; International Journal of Soil, Sediment and Water; 2010, Vol. 3: Iss. 2, pp 14.
7. Brunt, R. L., Vasak, J., Griffioen.; A report: Fluoride in groundwater: Probability of occurrence of excessive concentration on global scale.; International groundwater resources assessment centre.; 2004.
8. Biswas, K., Saha, S. K., Ghosh, U. C.; Adsorption of fluoride from aqueous solution by a synthetic iron(III)–aluminum(III) mixed oxide.; Ind. Eng. Chem. Res.; 2007, Vol. 46, pp 5346–5356.
9. Cantor, K. P.; Drinking water and cancer.; Cancer Causes Control.; 1997,8(3):292-308.
10. Caussy, D., Priest N. D.; Introduction to arsenic contamination and health risk assessment with special reference to Bangladesh.; Rev. Environ. Contamin. Toxicol.; 2008, Vol. 197, pp 1–15.
11. Chaurasia, Neha, Mishra, Amarnath, Pandey, S. K.; Finger Print of Arsenic Contaminated Water in India-A Review.; J. Forensic Res.; 2012,Vol. 3, pp 10.
12. Chetia, M., Goswamee R. L., Banerjee S., Chatterjee S., Singh L., Srivastava R. B., Sarma H.P.; Arsenic removal from water using calcined Mg-Al layered double hydroxide.; Clean Techn. Environ. Policy.; 2011, doi: 10.1007/s10098-011-0365-1.
13. Cleveland, L. M., Minter M. L., Cobb K. A., Scott A. A., German V. F.; Lead hazards for pregnant women and children: Part 1: immigrants and the poor shoulder most of the burden of lead exposure in this country. Part 1 of a two part article details how exposure happens, whom it affects, and the harm it can do.; Am J Nurs.; 2008, Vol. 108, pp 40–49.
14. Cornelis, R. Handbook of elemental speciation II: species in the environment, food, medicine & occupational health.; Wiley.; 2005.
15. C. M., Vivek, Vardhan, J., Karthikeyan.; Removal of fluoride from water using low-cost materials.; Fifteenth International Water Technology Conference.; IWTC-15; 2011, Alexandria, Egypt.
16. Das, Kumar Malay, Attar, J., Salim.; Comparative Study of Batch Adsorption of Fluoride Using Commercial and Natural Adsorbent.; Research Journal of Chemical Sciences.; 2011, Vol. 1(7), pp 68-75.
17. Dadwhal, M., Sahimi M., Tsotsis T. T.; Adsorption isotherms of arsenic on conditioned layered double hydroxides in the presence of various competing ions.; Ind. Eng. Chem. Res.; 2011, 50, 2220–2226.
18. Datta, D. V., Kaul, M. K.; Arsenic content in drinking water in villages of Northern India.; J. Assoc. Phy. Ind.; 1976, Vol. 24, pp 599-604..
19. Dooyema, C. A., Neri A., Lo Y. C., Durant J., Dargan P. I., Swarthout T., Biya O., Gidado S. O., Haladu S., Sani-Gwarzo N., Nguku P. M., Akpan H., Idris S., Bashir A. M. ,Brown M. J.; Outbreak of fatal childhood lead poisoning related to artisanal gold mining in northwestern Nigeria.; Environ Health Perspect.; 2012,Vol. 120(4), pp 601-7.
20. Eid I., Brima Parvez, I. Haris.; Arsenic Removal from Drinking Water using Different Biomaterials and Evaluation of a Phytotechnology Based Filter.;Int. Res. J. Environment Sci.; 2014, Vol. 3(7), pp 39-44.
21. Flora, Gagan, Gupta, Deepesh, Tiwari, Archana.; Toxicity of lead: A review with recent updates.; Interdiscip Toxicol.; 2012, Vol. 5(2), pp 47–58.
22. Garelick, H., Jones, H., Dybowska, A., Valsami-Jones, E.; Arsenic pollution sources. Rev. Environ.Contam. Toxicol.; 2008, Vol. 197, pp 17 60.
23. Gracia, R. C., Snodgrass, W. R.; Lead toxicity and chelation therapy.; Am.J. Health-System Pharm.; 2007, Vol. 64, pp 45-53.
24. Guidotti, T. L., Mc Namara J., Moses M. S.; The interpretation of trace element analysis in body fluids.; Indian J Med Res.; 2008, Vol.128, pp 524–532..
25. Gupta S. S.; Bhattacharya K. G.; Interaction of metal ions with Clays: I, A case study with Pb(II).; Appl. Clay Sci.; 2005, Vol. 30(3-4), pp 199-208.
26. Gupta, S., Gupta, V.; Speciation and toxicity of arsenic: a human carcinogen. Res. J. Recent Sci.; 2013, Vol. 2, pp 45 - 53.
27. Jamode, A., Sapkal, V.; Defluoridation of water using inexpensive adsorbents.; J. Indian Ins. Sci.; 2004, Vol. 84(5), pp 163-171.
28. Kataria, K. C., Bux, S., Namdeo, M.; study of fluoride content in ground water and surface water of Bhopal city.; I.J.E.P.; 2008, Vol. 29(5), pp 461-464.
29. Kafia, M., Shareef Surchi.; Agricultural Wastes as Low Cost Adsorbents for Pb Removal: Kinetics, Equilibrium and Thermodynamics.; International Journal of Chemistry.; 2011, Vol. 3(3), pp 103.
30. Kumar, K. S., Sajwan, K. S., Richardson, J. P., Kannan, K.; Contamination profile of heavy metals.; U.S.A.; Mar. Pollut. Bull.; 2008, Vol. 56, pp 136-149.
31. Kundu, N., Panigrahi, M., Tripathy, S., Munshi, S., Powell, M., Hart, B.; Geochemical appraisal of fluoride contamination of groundwater in the Nayagarh District of Orissa, India.; Environmental

Geology.; 2001, Vol. 41, pp 451-460.

32. Lacasa, E., Canizares, P., Saez, C., Fernandez, F. J., Rodrigo, M. A.; Removal of arsenic by iron and aluminium electrochemically assisted coagulation.; Separ. Purific. Technol.; 2011, Vol. 79, pp 15–19..
33. Lovell Agwaramgbo, Nichole Lathan, Shelby Edwards, ShaKayla Nunez.; Assessing Lead Removal from Contaminated Water Using Solid Biomaterials: Charcoal, Coffee, Tea, Fishbone, and Caffeine.; Journal of Environmental Protection; 2013, Vol. 4, pp741-745.
34. Maximous, N, George F., & Wan K.; Removal of Heavy Metals from Wastewater by Adsorption and Membrane Processes: a Comparative Study.; World Academy of Science, Engineering and Technology.; 2010, pp 64.
35. Mazumder, Debendra Nath Guha , Ghosh Aloke , Mazumder, Kunal Kanti , Ghosh,Nilima , Saha, Chandan , Mazumder, Rathindra Nath Guha.; Arsenic contamination of ground water and its health impact on population of district of Nadia, West Bengal, India.; 2010, Vol. 35(2), pp 331-338.
36. Mc Carthy, Hafner, H. R., Montzka, S. A.; Background concentration of 18 air toxics for North America.; J.Air Waste Manage. Assoc.; 2006, Vol. 56, pp 3-11.
37. Miranda, M. L., Dohyeong, K., Galeano, M. A., Paul, C. J., Hull, A. P., Morgan, S. P.; The Relationship between Early Child Hood Blood Lead Levels and Performance on End-of-Grade Tests.; Environmental Health Perspectives.; 2007, Vol. 115, pp 1242-1247.
38. Mohammad, Mehdi, Mehrabani, Ardekani, Roshanak, Rezaei, Kalantary, Sahand, Jorfi, Mohammad, Nurisepehr.; Comparison the Efficiency of Bagas, Modified Bagas and Chitosan for Fluoride Removal from Water by Adsorption.; Journal of Environmental Treatment Techniques.; 2013, Vol. 1(1), pp 1-7.
39. Mehto, A., Chakrapani, G. J.; Spatio-temporal variation in the hydrochemistry of Tawa River, Central India: Effect of natural and anthropogenic factors.; Environmental Monitoring and Assessment.; 2013, Vol. 185(12), pp 789-9802.
40. Mohan, S. V., Ramanaiah, S. V., Rajkumar, B., Sarma, P. N.; Removal of fluoride from aqueous phase by biosorption onto algal biosorbent Spirogyra Sp.-102: sorption mechanism elucidation.; J. Hazard. Mater.; 2007, Vol. 141, pp 465–474.
41. Mohapatra D., Mishra D.; Park K.; A laboratory scale study of arsenic(V) removal from aqueous medium using calcined bauxite ore.; J. Environ. Sci. (China).; 2008, Vol. 20(6), pp 683-9.
42. Mousavi H. Z., Hosseynifar A., Jahed V., Dehghani S. A. M.; Removal of Lead from aqueous Solution using waste Tire Rubber Ash as an Adsorbent.; Brazilian Journal of Chemical Engineering.; 2010, Vol. 27(01), pp. 79–87.
43. Naba, Kr. Mondal, Ria, Bhaumik, Arnab, Banerjee, Jayanta, Kr. Datta, Tanmoy, Baur.; A comparative study on the batch performance of fluoride adsorption by activated silica gel and activated rice husk ash.; International Journal of Environmental Sciences.; 2012,Vol. 2(3), ISSN 0976 – 4402.
44. Nagpal, Uma, M. K., Rezaei Hassan.; Equilibrium sorption studies for Cu2+ and Pb2+metal ions on three different biomasses.; Current World Environment.; 2010, Vol. 5(2), pp 243-251.
45. Nigussie, W., Zewge, F., Chandravanshi, B. S.; Removal of excess fluoride from water using waste residue from alum manufacturing process.;J Hazard Mater.; 2007, Vol.147(3), pp 954-63.
46. Norman, E. H., Hertz-Picciotto, I., Salmen, D. A., Ward, T. H.; Childhood lead poisoning and vinyl miniblind exposure.; Arch Pediatr Adolesc Med.; 1997, Vol. 151, pp 1033-1037.
47. Pali, Shahjee, B. J. Godboley, A. M. Sudame.; Removal of fluoride from aqueous solution by using low cost adsorbent.; International Journal of Innovative Research in Science, Engineering and Technology.; 2013, Vol. 2, pp 7.
48. Pandhare Ghanshyam, Trivedi Nikhilesh, Kanse Nitin, Dawande S.,D.; Synthesis of low cost adsorbent from azadirachta indica (neem) leaf powder.; International Journal of Advanced Engineering Research and Studies.; 2013,Vol. II(II), pp 29-31.
49. Park, K.; Park's Text Book of Preventive and Social Medicine. Ed 21.; Ba-narasisdas Bhanot Publishers, 1167. Premnagar, Jabalpur, India.; 2011, pp 577.
50. Pathak, R. P., Sharma, Pankaj, Vyas, Sameer, Mahure, N. V., Kumar, Rajeev, Murari Ratnam.; Detection of Fluoride Contamination in the Surface and Sub-Surface Water near Thermal Power Station.; International Journal of Engineering and Science.; 2012, Vol. 1, PP 44-47.
51. Punita, Parikh, Rahul, Parikh.; Current status of fluoride contamination in ground water of Kheralu block of Mehasana district, Gujarat.; International Journal of Environmental Sciences.; 2013, Vol. 3, pp 2199-2207.
52. Puthenveedu, Sadasivan, Pillai, Harikumar, Chonattu, Jaseela, Tharayil, Megha.; Defluoridation of water using biosorbents.; Natural Science.; 2012,Vol. 4(4), pp 245-251.
53. Rajappa, B., Manjappa S., Puttaiah E.T.; Monitoring of Heavy metal concentration in ground water of Hakinaka Taluk, India.; Cont. Engin.Sci.; 2010, Vol. 3(4), pp 183-190.
54. Rao, R. J., Naidu, M. G. C.; Geochemistry of high fluoride natural waters if Jaggaiahpalem, fluorosis endemic village near Visakhapatnam district, Andhra Pradesh.; Inst. Symposium on Recent researches and applications of Geochemistry, Patna, India.; 1973, pp 6.
55. Ravichandran K., Jayaprakash M.; Seasonal variation on physico chemical parameters and trace metal in ground water of an industrial area of North Chennai, India.; Ind. J.Sci. and Tech.; 2011, Vol. 4(6), pp 646-649.
56. Razzouki, B., S. EL Hajjaji, K. Azzaoui, A. Errich, A. Lamhamdi, M. Berrabah, L. L. Elansari.; Physicochemical study of arsenic removal using iron hydroxide.; J. Mater. Environ. Sci.; 2015, Vol.- 6 (5), pp 1444-1450.
57. Roy, Madhumita, Mukherjee, Apurba, Mukherjee, Sutapa, Biswas, Jaydip.; Arsenic: an alarming global concern.; Int.J.Curr.Microbiol.App.Sci.; 2014, Vol. 3(10), pp 34-47.
58. Salve, P. R., Maurya, A., Kumbhare, P. S., Ramteke, D. S., Wate, S. R.; Assessment of groundwater quality with respect to fluoride.; Bulletin of environmental contamination and toxicology.; 2008, Vol. 81(3), pp 289-293.
59. Sharma, B. S., Agrawal, Jyoti, Gupta, Anil, K.; Emerging Challenge: Fluoride Contamination in Groundwater in Agra District, Uttar Pradesh.; ASIAN J. EXP. BIOL. SCI.; 2011, Vol. 2(1), pp 131-134.
60. Sharma, S., Dixit, S., Jain, P., Shah, K. W., Vishwakarma, R.; Statistical evaluation of hydrobiological parameters of Narmada river at Hoshangabad city, India.; Env. Moni. and Asses.; 2008, Vol. 143 (1-3), pp 195- 202.
61. Shih, R. A. H. Hu, M. G. Weisskopf, B. S. Schwartz.; Cumulative Lead Dose and Cognitive Function in Adults. A Review of Studies that Measured both Blood Lead and Bone Lead.; Environmental Health Perspectives.; 2007, Vol. 115, pp 483-492.

62. Singh, Thakur Lokendra, Semil, Pradeep.; Removal Of Arsenic In Aqueous Solution By Low Cost Adsorbent: A Short Review.; International Journal of ChemTech Research.; 2013, Vol. 5(3), pp 1299-1308.
63. Smith, A. H., Lopipero P. A., Bates M. N., Steinmaus C. M.; Public health. Arsenic epidemiology and drinking water standards.; Science .; 2002 , Vol. 296, pp 2145-6.
64. Subba, Rao, N., Prakasa, Rao, J., Niranjan Babu, P., Chandra Rao P., Krishna, Rao G.; Hydrogeochemical zoning in crystalline terrain and its significance to water quality.; Jour.Geol. Soc. India.; 1997, Vol. 49(6), pp 715-719.
65. Susheela, A. K.; "Fluorosis: Indian scienario" A treatise on fluorosis. Fluoro-sis.; Research and Rural Development Foundation; New Delhi, India.; 2001.
66. Sarkar, M., Banerjee, A., Pramanick, P. P., Sarkar, A. R.; Use of laterite for the removal of fluoride from contaminated drinking water.; J Colloid Interface Sci.; 2006, Vol. 302(2), pp 432-41.
67. Thatte, C. D.; Matching of water supply with growing demands.; J. IWWA.; 1994, 26(2): pp 67-71.
68. Valencia-Leal, S. A., R., Cortés-Martinez, R., Alfaro-Cuevas-Villanueva.; Evaluation of Guava Seeds (Psidium Guajava) As a Low-Cost Biosorbent for the Removal of Fluoride from Aqueous Solutions.; International Journal of Engineering Research and Development.; 2012, Vol. 5(4), pp 69-76.
69. Veeraputhiran, V., Alagumuthu, G.; Treatment of High Fluoride Drinking Water Using Bioadsorbent.; Research Journal of Chemical Sciences.; 2011, Vol. 1(4), pp 49-54.
70. Waheped, S., Deshmukh, S. J., Attar, M. D., Waghmare.; "Investiga-tion on Sorption of Fluoride in Water Using Rice Husk as an AdsorbentNa-ture Environment and Pollution Technology".; An International Quarterly Scien-tific Journal.; 2009, Vol. 8(2), pp 217-223.
71. Wang, S. L., Liu C. H., Wang M. K., Chuang Y. H., Chiang P. N.; Arsenate adsorption by Mg/Al-NO3 layered double hydroxides with varying the Mg/Al ratio.; Appl. Clay Sci.; 2009, 43, 79–85.
72. Brinza L., Nygård C. A., Dring M. J., Gavrilescu M., & Benning L. G.; Cadmium tolerance and adsorption by the marine brown alga Fucus vesiculosus from the Irish Sea and the Bothnian Sea.; Bioresource Technology.; 2009, 100, pp 1727–1733.

Source details

International Journal of Innovative Technology and Exploring Engineering

Scopus coverage years: from 2018 to 2019
(coverage discontinued in Scopus)
Publisher: Blue Eyes Intelligence Engineering and Sciences Publication
E-ISSN: 2278-3075
Subject area: Engineering: Civil and Structural Engineering | Computer Science: General Computer Science | Engineering: Electrical and Electronic Engineering | Engineering: Mechanics of Materials
Source type: Journal

CiteScore 2019
0.6

SJR 2019
0.102

SNIP 2022
0.316

View all documents > | Set document alert | Save to source list

CiteScore | CiteScore rank & trend | Scopus content coverage

Improved CiteScore methodology
CiteScore 2019 counts the citations received in 2016-2019 to articles, reviews, conference papers, book chapters and data papers published in 2016-2019, and divides this by the number of publications published in 2016-2019. Learn more >

CiteScore 2019

$$0.6 = \frac{5{,}200 \text{ Citations 2016 - 2019}}{8{,}638 \text{ Documents 2016 - 2019}}$$

Calculated on 06 May, 2020

CiteScore rank 2019

Category	Rank	Percentile
Engineering └ Civil and Structural Engineering	#249/310	19th
Computer Science └ General Computer Science	#187/221	15th

View CiteScore methodology > | CiteScore FAQ > | Add CiteScore to your site

A review on synthesis, advantages and disadvantages of Nanofibers

[1] krushna Prakash Zamwar,[2]Shravani Tonge, [3] Janhavi Suresh Raut, [4] Payal Sadhu Parshive[5] Ruchita Rajesh Bharsakale,[6]Nidhi Jain*–

[1]Department of Engineering Science, Bharati Vidyapeeth College of Engineering Lavale, Pune-412115
Email: [1]krashuzamwar@gmail.com, [2]tongeshravani@gmail.com, [3]janhaviraut0@gmail.com, [4]payalparshive2017@gmail.com, [5]rrbhar2001@gmail.com, *nidhi.jain@bharatividyapeeth.edu

Abstract

This review paper aims to study the synthesis of nanofibers using Chitosan, Gelatin (which consists of a mixture of peptides and proteins produced by partial hydrolysis of collagen extracted from the skin, bones, and connective tissues of animals).. The nanofibres were fabricated through the electrospinning technique.The research paper discusses the detailed analysis of nanofibres with respect to our synthesized materials. It has proper description of the purpose of synthesizing, Advantages, and disadvantages of various methods in preparing Nanofibers, and it also covers brief description and application in various important fields of sciences by using nanofibers.

keywords:. Nanofibers Chitosan, Gelatin, electrospining

I.Introduction

Nano-fibre, can be defined in the terms by splitting into two parts namely "nano" and "fibre". The textile industry defines fibres as a filament natural or synthetic as cotton or nylon capable of being spun into yarn. A "fibre" is defined from a geometrical standpoint as a slender, elongated, threadlike object or structure [1]. The term "nano" is technically referred to the scale of billionth of the unit. Generally, nano-fibre is a term used for fibres with a diameter between 50 and 300 nano-meters [2].

Nanotechnology is the science concerned with the study of the phenomena and functions of matter within the dimensional range of 0.1 – 100 nm. A nano-meter abbreviated as nm, is a unit for length the measures on billionth of a meter [3-4] unusual and unique properties of nano-scale materials arise from their exhibited profile compared to macro materials. Novel properties exhibited by these materials investigated from their minute dimension which converted into unusual mechanical, thermal, biological, optical, magnetic and electrical properties [5].

Nano materials is currently under investigation in different fields such as self assembly and thin films, quantum dots, nano-fibres, nanorods, nanotubes, nanowires, nanocrystals and nanofoams[6]

Nano-fibre technology incorporated in different application area such as batteries and fuel cells, capacitors, transistors and diodes, system for energy transfer, composites for aerospace structures, drug delivery and tissue engineering.

Nano-fibre technology is a branch of nanotechnology whose primary objective is to create materials in the form of nano-scale fibres in order to achieve superior function. The unique combination of high specific surface area, flexibility and superior directional strength makes such fibres a preferred material for many application ranging from clothing to reinforcements for aerospace structure. The effect of fibre diameter on the performance and process ability of fibrous structures has long been recognized. Several scientists such as Professor Parallel Reneker almost a decade ago had popularized the electro-spinning technology [7].

Several methods have been developed to fabricate nano-fibres, such as templates [8-9] self-assembly[10-12], phase separation[13], melt-down[14] and electro-spinning[15-18]. Electro-spinning is currently the most promising technique to produce continues nano-fibres on a large scale and the fibre diameter can be adjusted from nano-meters to microns. Also, electro-spinning is a relatively easy and fast process to produce nano-fibres.

Although, the first patent on electro-spinning technique was published as early as in 1934. [19], this technique has not been well established until recent times [20-23]. Technically, electro-spinning is a process that uses a strong electric field to draw a polymer fluid into the filaments[24-27].

Although there are several alternative methods for generating fibres in a nanometre scale, nano matches the popularity of the electro-spinning technology due largely to the simplicity of the electro-spinning process. Electro-spinning can be carried out from polymer melt or solution. The structures and properties of the fibres produces by the electro-spinning process are then examined. Recognizing the enormous increase in specific fibre surface, bioactivity, electro-activity and enhancement of mechanical properties, numerous applications have been identified including filtration, biomedical energy storage, electronics and multifunctional structure composites.

Chitosan is a polysaccharide derived from chitin; Chitin is the second most abundant polysaccharide in the world, after cellulose. The presence of amino group in the Chitosan structure might be protonated. Providing solubility in diluted acidic aqueous solution, several remarkable properties of chitosan offered unique opportunities to the development of biomedical applications. Elucidation of Chitosan for medical and pharmaceutical interest has been done. The haemostatic activity of chitosan can also be related to the presence of positive charges on chitosan backbone. Due to its positive

Advantages and Disadvantages Of Various Methods In preparing Nanofibers Table No.1 [43]

charges, chitosan can also interact with the negative part of cell membrane, which can lead to reorganisation and an

S.	Technique	Advantages	Disadvantages
1.	Drawing	It produces single long nano-fibres.	It limits to viscoelastic material, depending on the orifice size of the extrusion mould which leads to difficulties in obtaining fibres of diameters less than 100nm.
2.	Template synthesis	It uses Nano- porous membrane as a template.	It cannot craft the long continuous nano fibers.
3.	Freeze drying	It is simple and cost effective.	Its uniform porosity cannot be maintained.
4.	Phase Separation	It controls the pore size and structures and the range of shapes and sizes.	Long continuous fibres cannot be produced due to its limitations which is limited to a very few polymers. The high cost of synthesis of biomaterials have limited their applications; engineered peptide nanofibers can be fragmented which are suspect-able to endocytosis.
5.	Self-		The long continuous fibres cannot be produced because of its limitation a very few polymers.
6.	Electrospi	Fibres are of diameter size, ranging from nanometre to the few microns ,which are relatively inexpensive technique and have high aspect ratio and have enhanced mechanical properties.	They undergo several difficulties in making a large volumeofscaffold.

opening of the tight junction proteins, explaining the permeation enhancing property of this polysaccharide.

The polycationic nature of Chitosan also allows explaining Chitosan analgesic effects. Now, to explain Chitosan biodegradability, it is important to remember that Chitosan is not only a polymer bearing amino groups, but also a polysaccharide, which consequently contains breakable glycosidic bonds. Chitosan is actually degraded in vivo by several proteases and mainly lysozyme, Chitosan is biocompatible, biodegradable and non-toxic, so that it can be used as medical application as antimicrobial and wound healing biomaterials. It is used as chelating agent due to its ability to bind with cholesterol, fats, proteins and metal ions [28].

Chitin and Chitosan nanofibers with (50-500nm diameter) are biocompatible and biodegradable, so they can used as haemostatic and wound healing material [29].

Synthesis:

Several techniques are used for the synthesis of nano-fibre that electrospining is the promising one. The advantages and disadvantages are discussed in the table no.1

Electrospinning :-

Nonwoven fibrous materials can be effortlessly and constructively made by using electrospinning technique. But for synthesising nanofibres, detailed study of electro-spinning parameters is very essential [30]. Highly precise manufacture of nanofibres can be done using process like self-assembly[31-34] whereas large volume manufacture is done using process like island-in-sea[35]. Due to its comparatively large manufacture rate and affordability, Electro-spinning technique has an edge over the other methods.

The apparatus usually consists of collector, spinneret and high power supply. The required potential is applied and maintained between the spinneret and collector [36-37]. And both of them are placed at a fixed distance.

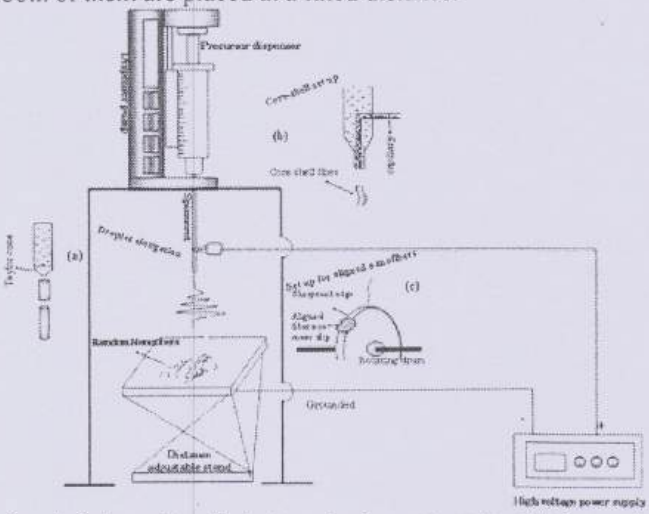


fig. 1 Schematic of electrospinning set up to obtain random nanofibers. (a) Enlarged view of formation of fiber starting from the Taylor cone. (b) Set up to obtain aligned nanofibers using rotating drum with sharp edge. (c) Set up to obtain core-shell nanostructures [38].

Electrospinning inherits attributes of both conventional solution dry spinning and electro spraying of fibers[39]. Nano fibers can be of two types : aligned and non-aligned. Usually non-aligned nano fibers can be formed using this set up but in order to form aligned nanofibers external set up like a circular rotating disc is used or electric field is optimised. Circumferentially oriented nano fibers are a consequence of spinning of cylindrical collector at high speed [40-42].

Applications

1. Filtration

Filters have been widely used in both households and industry for removing substances from air or liquid. Filters for environment protection are used to remove pollutants from air

er water. In military, they are used in uniform garments and isolating bags to decontaminate
aerosol dusts, bacteria and even virus, while maintaining permeability to moisture vapour for comfort. Respirator is another example that requires an efficient filtration function. Similar function is also needed for some fabrics used in the medical area. For a fiber-based filter, removal of particles is determined by different mechanisms. Large particles are blocked on the filter surface due to the sieve effect. Particles that are smaller than the surface-pores will penetrate into the filter, which could still be collected by the fibers, via either interception or impaction, or static electrical attraction. Also, very fine particles could be captured due to the Brownian motion effect. The filtration efficiency is normally influenced by the filter physical structure (fiber fineness, matrix structure, thickness, pore size, etc), fiber surface electronic properties, and its surface chemical characteristic (e.g.surface free energy). The particle collecting capability is also related to the size range of particles being collected. Besides the filtration efficiency, other properties such as pressure drop and flux resistance are also important factors to be evaluated for a filter media.

2. Recovery of metal ions and affinity membranes

Surface chemistry, incorporation of functional materials, and coating techniques are some of the methods which provide electrospun nanofibers a very good potential to be operational. These nanofibers would possibly be able to accumulate metal-ions or fine molecules from a solution. For instance, dye cibacron blue F3GA (CB) was surface functionalized with electrospun cellulose nanofibers, and further the electrospun membrane depicted a powerful affinity towards bovine serum albumin (BSA) [44]. A membrane was synthesized from electrospun polysulphone (PSU) fibers of the same affinity as BSA which was suface functionalized with toluidine blue O [45], another dye. In comparison to conventional microfibers, the two nanofiber-based affinity membrane exhibited higher flux and lower pressure drop. In extension to this, silk/keratin wool electrospun fibroin blend nanofibers have demonstrated to have an attribute to chelate absorb Cu(II) ions from H2O [46]. During an experiment, it was observed that if nanofiber membrane is surface coated with conducting polymer then , it gained the ability to accumulate teh gold ions from aqueous solution. The gold ions were eventually converted to elemental gold particles [47].

3. Wound healing

Wound healing is a native process of regenerating dermal and epidermal tissues. When an individual is wounded, a set of complex biochemical actions take place in a closely orchestrated cascade to repair the damage. Normally, body cannot heal a deep dermal injury. In full thickness burns or deep ulcers, there is no source of cells remaining for regeneration, except from the wound edges. As a result, complete re-epithelialization takes a long time and is complicated with scarring of the base[48]. Dressings for wound healing function to protect the wound, exude extra body fluids from the wound area, decontaminate the exogenous microorganism, improve the appearance and sometimes accelerate the healing process. For these functions, a wound dressing material should provide a physical barrier to a wound, but be permeable to moisture and oxygen. For a full thickness dermal injury, the adhesion and integration of an "artificial dermal layer" consisting of a 3D tissue scaffold with well cultured dermal fibroblasts will considerably assist the re-epithelialization. A study on using electrospun polyurethane membrane as wound dressing material revealed that the membrane effectively exuded fluid from the wound, without fluid accumulation under the membrane cover, and no wound desiccation occurred either[49]. Details about skin tissue engineering have been summarized already. In vivo wound healing of diabetic ulcers was investigated using electrospun block copolymer (PCL-PEG) and PCL. When the nanofibers were chemically modified with a recombinant human epidermal growth factor (rhEGF), the expression of keratinocyte-specific genes and EGF-receptor were enhanced[50]. Post-surgery tissue adhesion is a widely recognized problem for abdominal surgeries. It not only renders future operations more difficult but also causes other problems such as small bowel obstruction, female infertility, and chronic debilitating pain[51,52].

4. Reinforcement

Early studies on electrospun nanofibers also included reinforcement of polymers. As electrospun nanofiber mats have a large specific surface area and an irregular pore structure, mechanical interlocking among the nanofibers should occur. When a thin electrospun nylon-4,6 nanofiber mat was added to epoxy, the composite showed transparency to visible light, and both the stiffness and strength were increased considerably compared with the pure epoxy film[53]. Electrospun polybenzimidazole (PBI) nanofibers have been used as fillers to reinforce epoxy and rubber[54]. An epoxy containing 15 wt% electrospun PBI nanofibers was found to have higher fracture toughness and modulus than the one containing 17 wt% PBI whiskers. Also the Young's modulus and tear strength of styrene-butadiene rubber (SBR) containing the PBI nanofibers were higher than those of pure SBR. In addition, electrospun nylon PA 6 nanofibers were used to improve the mechanical properties of a BISGMA/TEGDMA dental restorative composite resins[55].

5. Release control

Controlled release is an efficient process of delivering drugs in medical therapy. It can balance the delivery kinetics, minimize the toxicity and side effects, and improve patient convenience[56]. In a controlled release system, the active substance is loaded into a carrier or materials science device first, and then releases at a predictable rate in vivo when administered by an injected or non-injected route. As a potential drug delivery carrier, electrospun nanofibers have exhibited many advantages. The drug loading is very easy to implement via electrospinning process, and the high applied voltage used in the electrospinning process had little influence

on the drug activity. The high specific surface area and short diffusion passage length give the nanofiber drug system higher overall release rate than the bulk material (e.g. film). The release profile can be finely controlled by modulation of nanofiber morphology, porosity and composition. Nanofibers for drug release systems mainly come from biodegradable polymers, such as PLA[57], PCL[58,59,60], poly(D-lactide)(PDLA)[61], PLLA[62—64], PLGA[65,66], and hydrophilic polymers, such as PVA[67-69], PEG[66,70] and PEO[71]. Non-biodegradable polymers, such as PEU[72], were also investigated.

Conclusion:

This review has covered the diverse applications of electrospun nanofibers. The review is by no means exhaustive, and new nanofibers and applications are emerging continuingly. . It has proper description of the purpose of synthesise, advantages and disadvantages of various methods in preparing Nanofibers and its also covers brief description and application in various important fields of sciences by using nanofibers. While the potential for nanofibers is enormous, there are also considerable challenges ahead. Most of the studies in this area have been conducted on fibers produced on very small scale, using a needle based system to electrospin nanofibers from a polymer solution. The fibers produced on the large scale equipment to ensure consistent fiber quality and address the environmental issues associated with solvent/solution based electro-spinning technology. Producing uniform fibers with an average diameter below 100 nm remains a challenge

References

[1] M. King, B. Zhu, and S. Tang, "Optimal path planning," *Mobile Robots*, vol. 8, no. 2, pp. 520-531, March 2001.

[2] H. Simpson, *Dumb Robots*, 3rd ed., Springfield: UOS Press, 2004, pp.6-9.

[3] M. King and B. Zhu, "Gaming strategies," in Path Planning to the West, vol. II, S. Tang and M. King, Eds. Xian: Jiaoda Press, 1998, pp. 158-176.

[4] B. Simpson, et al, "Title of paper goes here if known," unpublished.

[5] J.-G. Lu, "Title of paper with only the first word capitalized," *J. Name Stand. Abbrev.*, in press.

[6] Y. Yorozu, M. Hirano, K. Oka, and Y. Tagawa, "Electron spectroscopy studies on magneto-optical media and plastic substrate interface," *IEEE Translated J. Magn. Japan*, vol. 2, pp. 740-741, August 1987 [*Digest 9th Annual Conf. Magnetics Japan*, p. 301, 1982].

[7] M. Young, *The Technical Writer's Handbook*, Mill Valley, CA: University Science, 1989. Reference:-

[8] Ramakrishna, S., Fujihara, K., Teo W-E Lim, T.-C and ma, Z. An introduction to electrospinning and nano-fibers world scientific publishing Co. Pte Ltd, USA (2015)

[9] Hayewood, J.F. Polymeric Nanofibers fantasy or future; Technical Textile Technology, 1(1)(2002)

[10]Nalwa, H.S. Handbook of nanostructeral materials & nanotechnology, Academic press, San Diego (2000)

[11]KO, f.k and wan, Y. Introduction to nanofiber materials Cambridge university press, United Kingdom, (2014)

[12]Laurencin, C.T and Nair, L.S Polyphosphazene Nano-fibers for Biomedical Application prelimlinary studies, Nanoengineered Nanofibrous material series: Nato Science series II, mathematics, physics and chemistry 283-302 (2004)

[13]Krupk, R., Hennrich F., Lohneysen H.V. and Kappes M.M separation of metallic form semiconducting single walled carbon tubes science, 301 (5631), 344-347, (2003)

[14]Reneker, D. Hand chun, I., Nanotechnology, 7, 216, (1966)

[15]Li., H key, Hu. Y. Polymer nanofibers prepared by template melt extrusion, I Appl polym sci, 2006, 99(3): 1018-1023 [DOI]

[16]Ikegane M, Tajima K, nida T, template synthesis of polypyrrole nanofibers insulated within one-dimensional silicate channels: Hexagonal versus lamellar for recombination of polarons into bipolarons Angew Chem Int Edit, 2003, 42(19): 2154-2157 [DOI]

[17]Yang Z, XUB, Supermoleacular hydrogels based on biofunctional nanofibers to self-assembled small molecules. I mater chem, 2007, 17(23): 2385-2393 [DOI]

[18]Feng X, Yang G, XU Q, et al: self-assembly of polyangiline/Au composities: from nanotubes to nanofibers, macromol rapid comm, 2006, 27(1): 31

[19]Hong Y, Legge R L, Zhang S, et al. Effect of amino acid sequence and pH on nanofiber formation of self-assembling peptides EAK1,11 and EAK16-1V. Biomacromolecures, 2003, 4(5): 1433-1442 [DOI]

[20]Ma P X, Zhang R. Synthetic nano-scale fibrous extracellular matrix. Biomed Mater Res Part A, 1999, 46(1): 60—72 [DOI]

[21]Ellison C J, Phatak A, Giles D W, et al. Melt blown nanofibers: Fiber diameter distributions and onset of fiber breakup. Polymer, 2007, 48(20): 3306 —3316 [DOI]

[22]Teo W E, Ramakrishna S. A review on electrospinning design and nano- fibre assemblies. Nanotechnology, 2006,17(14): R89—R106 [DOI]

[23]Gu B K, Shin M K, Sohn K W, et al. Direct fabrication of twisted nal—, hers by electrospinning. Appl Phys Lett, 2007, 90(26):263902 [DOI]

[24]Panda P K, Ramakrishna S. Electrospinning of alumina nanofibers using different precursors. J Mater Sci, 2007, 42(6): 2189-2193 [DOI]

[25]Kim G, Kim W. Formation of oriented nanofibers using electrospin-ning. Appl Phys Lett, 2006, 88(23):233101 [DOI]

[26]Formhals A. Process and apparatus for preparing artificial threads. US Patent 1975504, 1934

[27]Doshi J, Reneker D H. Electrospinning process and applications of electrospun fibers. J Electrostat, 1995, 35(2-3): 151-160 [DOI]

[28]Srinivasan G, Reneker D H. Structure and morphology of small diameter electrospun aramide fibers. Polym Int, 1995, 36(2): 195-201 [DOI]

[29]Reneker D II, Chun I. Nanometer diameter fibres of polymers, produced by electrospinning. Nanrsechnology, 1996, 7(3): 216-223 [DOI]
[30]Jaeger R, Schonherr H, Vancso G J. Chain packing in electro-spun poly(ethylene oxide) visualized by atome force microscopy. Macro¬molecules, 1996, 29(23): 7634— 7636 [DOI]
[31]Yarin A L, Koombhongse S, Reneker D H. Bending instability in electro- spinning of nanofibers. J Appl Phys, 2001, 89(5): 3018-3026 [DOI]
[32]Li D, Xia Y. Electrospinning of nanofibers: Reinventing the wheel? Adv Mater, 2004, 16(14): 11 51 — 1170 [DOI]
[33]Subbiah T, Bhat G S, Tock R W, et al. Electrospinning of nanofibers. J Appl Polym Sci, 2005, 96(2): 557-569 [DOI]
[34]Greiner A, wendorff I H. Electrospinning: A fascinating method for the preparation of ultrathin fibers. Angew Chem Int Edit, 2007, 46(30): 5670-5703 [DOI]
[35]Bhardwaj, N. and S.C. Kundu, Electrospinning: a fascinating fiber fabrication technique. Biotechnology advances, 2010. 28(3): p. 325-347
[36]Lee, K.Y., et al., Electrospinning of polysaccharides for regenerative medicine. Advanced Drug Delivery Reviews, 2009. 61(12): p. 1020-1032
[37]Sajjad Haider , Waheed A. Al-Masry, Nausheen Bukhari, Muhammad Javid, First published:16 August 2010
[38]Huie, J. C., Smart Mater. Struct. (2003) 12, 264
[39]Faul, C. F. J., and Antonietti, M., Adv. Mater. (2003) 15, 673
[40]Whitesides, G. M., and Boncheva, M., Proc. Natl. Acad. Sci. USA (2002) 99, 4769
[41]Zhang, S., Biotechnol. Adv. (2002) 20, 321
[42]2. Pike, R. D., Superfine microfiber nonwoven web, US Patent 5,935,883, (1999)
[43]V. Thavasi , G. Singh and S. Ramakrishna DOI: 10.1039/B809074M (Review Article) Energy Environ. Sci., 2008, 1, 205-221
[44]V. Thavasi , G. Singh and S. Ramakrishna DOI: 10.1039/B809074M (Review Article) Energy Environ. Sci., 2008, 1, 205-221
[45]V. Thavasi , G. Singh and S. Ramakrishna DOI: 10.1039/B809074M (Review Article) Energy Environ. Sci., 2008, 1, 205-221
[46]Ziabicki, A. (1976) Fundamentals of fiber formation, John Wiley and Sons, London, ISBN 0-471-98220-2.
[47]M. B. Bazbouz and G. K. Stylios, J. Appl. Polym. Sci., 2008, 107, 3023–3032 CrossRef CAS .
[48]M. B. Bazbouz and G. K. Stylios, Eur. Polym. J., 2007, 44, 1–12 .
[49]J. A. Matthews, G. E. Wnek, D. G. Simpson and G. L. Bowlin, Biomacromolecules, 2002, 3, 232–238 CrossRef CAS.
[50]Electrospinning of collage nanofiber scaffolds for tissue repair and regeneration-Scientific Figure on Research Gate. Available from: https://www.researchgate.net/figure/1-Advantages-and-Disadvantages-of-Various-Methods-in-Preparing-Nanofibers_tbl1_314233145[accessed13Mar,2020]
[51]Ma Z, Kotaki M, Inai R, et al. Potential of nanofiber matrix as tissue-engineering scaffolds. Tissue Eng, 2005, 11(1-2): 101—109[DOI]
[52]Ma Z, Kotaki M, Ramakrishna S. Surface modified nonwoven polysulphone (PSU) fiber mesh by electrospinning: A novel affinity membrane. J Membrane Sci, 2006, 272(1-2): 179—187[DOI]
[53]Ki C S, Gang E H, Um I C, et al. Nanofibrous membrane of wool keratose/silk fibroin blend for heavy metal ion adsorption. J Membrane Sci, 2007, 302(1-2): 20—26[DOI]
[54]Wang H, Ding J, Lee B, et al. Polypyrrole-coated electrospun nanofibre membranes for recovery of Au(III) from aqueous solution. J Membrane Sci, 2007, 303(1-2): 119—125[DOI]
[55]Marler J J, Upton J, Langer R, et al. Transplantation of cells in matrixes for tissue regeneration. Adv Drug Deliver Rev, 1998, 33(1-2): 165—182[DOI]
[56]Khil M-s, Cha D-i, Kim H-y, et al. Electrospun nanofibrous polyurethane membrane as wound dressing. J Biomed Mater Res Part B: Appl Biomater, 2003, 67B(2): 675—679[DOI
[57]Choi J S, Leong K W, Yoo H S. In vivo wound healing of diabetic ulcers using electrospun nanofibers immobilized with human epidermal growth factor (EGF). Biomaterials, 2008, 29(5): 587—596[DOI]
[58]DeCherney A H, DiZerega G S. Clinical problem of intraperitoneal postsurgical adhesion formation following general surgery and the use of adhesion prevention barriers. Surg Clinics North Am, 1997, 77(3):671—688[DOI]
[59]Menzies D. Peritoneal adhesions. Incidence, cause, and prevention. Surg Ann, 1992, 24: 27—45
[60]Bergshoef M M, Vancso G J. Transparent nanocomposites with ultrathin, electrospun nylon-4,6 fiber reinforcement. Adv Mater, 1999, 11(16): 1362—1365[DOI]
[61]Kim J-S, Eneker D H. Mechanical properties of composites using ultrafine electrospun fibers. Polym Comp, 1999, 20(1): 124—131[DOI]
[62]Fong H. Electrospun nylon 6 nanofiber reinforced BIS-GMA/ TEGDMA dental restorative composite resins. Polymer, 2004, 45(7): 2427—2432[DOI]
[63]Yih T C, Al-Fandi M. Engineered nanoparticles as precise drug delivery systems. J Cell Biochem, 2006, 97(6): 1184—1190[DOI]
[64]Kenawy E-R, Bowlin G L, Mansfield K, et al. Release of tetracycline hydrochloride from electrospun poly(ethylene-co-vinylacetate), poly(lactic acid), and a blend. J Contr Rel, 2002, 81(1-2): 57—64[DOI]
[65]Zhang Y Z, Feng Y, Huang Z M, et al. Fabrication of porous electrospun nanofibres. Nanotechnology, 2006, 17(3): 901—908[DOI]
[66]Luong-Van E, Grondahl L, Chua K N, et al. Controlled release of heparin from poly(e-caprolactone) electrospun fibers. Biomaterials, 2006, 27(9): 2042—2050[DOI]

Issn No : 2347-3150

[67]Jiang H, Hu Y, Zhao P, et al. Modulation of protein release from biodegradable core-shell structured fibers prepared by coaxial electrospinning. J Biomed Mater Res Part B: Appl Biomater, 2006, 79B(1): 50—57[DOI]

[68]Zong X, Kim K, Fang D, et al. Structure and process relationship of electrospun bioabsorbable nanofiber membranes. Polymer, 2002, 43(16): 4403—4412[DOI]

[69]Zeng J, Xu X, Chen X, et al. Biodegradable electrospun fibers for drug delivery. J Contr Rel, 2003, 92(3): 227—231[DOI]

[70]Xu X, Yang L, Xu X, et al. Ultrafine medicated fibers electrospun from W/O emulsions. J Contr Rel, 2005, 108(1): 33—42[DOI]

[71]Qi H, Hu P, Xu J, et al. Encapsulation of drug reservoirs in fibers by emulsion electrospinning: morphology characterization and preliminary release assessment. Biomacromolecules, 2006, 7(8): 2327—2330[DOI]

[72] Luu Y K, Kim K, Hsiao B S, et al. Development of a nanostructured DNA delivery scaffold via electrospinning of PLGA and PLA-PEG block copolymers. J Contr Rel, 2003, 89(2): 341—353[DOI]

[73]Kim K, Luu Y K, Chang C, et al. Incorporation and controlled release of a hydrophilic antibiotic using poly(lactide-co-glycolide)-based electrospun nanofibrous scaffolds. J Contr Rel, 2004, 98(1): 47—56[DOI]

[74]Taepaiboon P, Rungsardthong U, Supaphol P. Drug-loaded electrospun mats of poly(vinyl alcohol) fibres and their release characteristics of four model drugs. Nanotechnology, 2006, 17(9): 2317—2329[DOI]

[75]Yang D, Li Y, Nie J. Preparation of gelatin/PVA nanofibers and their potential application in controlled release of drugs. Carbohydr Polym, 2007, 69(3): 538—543[DOI]

[76]Kenawy E-R, Abdel-Hay F I, El-Newehy M H, et al. Controlled release of ketoprofen from electrospun poly(vinyl alcohol) nanofibers. Mater Sci Eng A: Struct Mater Prop Microstruct Proc, 2007, A459(1-2): 390—396

[77]Jiang H, Fang D, Hsiao B, et al. Preparation and characterization of ibuprofen-loaded poly(lactide-co-glycolide)/poly(ethylene glycol)-gchitosan electrospun membranes. J Biomater Sci Polym Edit, 2004, 15(3): 279—296[DOI]

[78]Kim T G, Lee D S, Park T G. Controlled protein release from electrospun biodegradable fiber mesh composed of poly(e-caprolactone) and poly(ethylene oxide). Int J Pharm, 2007, 338(1-2): 276—283[DOI]

[79]Verreck G, Chun I, Rosenblatt J, et al. Incorporation of drugs in an amorphous state into electrospun nanofibers composed of a waterinsoluble, nonbiodegradable polymer. J Contr Rel, 2003, 92(3): 349—360[DOI]

[67]Jiang H, Hu Y, Zhao P, et al. Modulation of protein release from biodegradable core-shell structured fibers prepared by coaxial electrospinning. J Biomed Mater Res Part B: Appl Biomater, 2006, 79B(1): 50—57[DOI]
[68]Zong X, Kim K, Fang D, et al. Structure and process relationship of electrospun bioabsorbable nanofiber membranes. Polymer, 2002, 43(16): 4403—4412[DOI]
[69]Zeng J, Xu X, Chen X, et al. Biodegradable electrospun fibers for drug delivery. J Contr Rel, 2003, 92(3): 227—231[DOI]
[70]Xu X, Yang L, Xu X, et al. Ultrafine medicated fibers electrospun from W/O emulsions. J Contr Rel, 2005, 108(1): 33—42[DOI]
[71]Qi H, Hu P, Xu J, et al. Encapsulation of drug reservoirs in fibers by emulsion electrospinning: morphology characterization and preliminary release assessment. Biomacromolecules, 2006, 7(8): 2327—2330[DOI]
[72] Luu Y K, Kim K, Hsiao B S, et al. Development of a nanostructured DNA delivery scaffold via electrospinning of PLGA and PLA-PEG block copolymers. J Contr Rel, 2003, 89(2): 341—353[DOI]
[73]Kim K, Luu Y K, Chang C, et al. Incorporation and controlled release of a hydrophilic antibiotic using poly(lactide-co-glycolide)-based electrospun nanofibrous scaffolds. J Contr Rel, 2004, 98(1): 47—56[DOI]
[74]Taepaiboon P, Rungsardthong U, Supaphol P. Drug-loaded electrospun mats of poly(vinyl alcohol) fibres and their release characteristics of four model drugs. Nanotechnology, 2006, 17(9): 2317—2329[DOI]
[75]Yang D, Li Y, Nie J. Preparation of gelatin/PVA nanofibers and their potential application in controlled release of drugs. Carbohydr Polym, 2007, 69(3): 538—543[DOI]
[76]Kenawy E-R, Abdel-Hay F I, El-Newehy M H, et al. Controlled release of ketoprofen from electrospun poly(vinyl alcohol) nanofibers. Mater Sci Eng A: Struct Mater Prop Microstruct Proc, 2007, A459(1-2): 390—396
[77]Jiang H, Fang D, Hsiao B, et al. Preparation and characterization of ibuprofen-loaded poly(lactide-co-glycolide)/poly(ethylene glycol)-gchitosan electrospun membranes. J Biomater Sci Polym Edit, 2004, 15(3): 279—296[DOI]
[78]Kim T G, Lee D S, Park T G. Controlled protein release from electrospun biodegradable fiber mesh composed of poly(e-caprolactone) and poly(ethylene oxide). Int J Pharm, 2007, 338(1-2): 276—283[DOI]
[79]Verreck G, Chun I, Rosenblatt J, et al. Incorporation of drugs in an amorphous state into electrospun nanofibers composed of a waterinsoluble, nonbiodegradable polymer. J Contr Rel, 2003, 92(3): 349—360[DOI]

MUKt SHABd JOURNAL

Mukt Shabd Journal

UGC CARE GROUP - I JOURNAL

ISSN NO : 2347-3150 / web : www.shabdbooks.com / e-mail : submitmsj@gmail.com

Certificate ID : MSJ838

CERTIFICATE OF PUBLICATION

ज्ञान-विज्ञान विमुक्तये UGC APPROVED

IMPACT FACTORS 4.6

This is to certify that the paper entitled

"A review on synthesis, advantages and disadvantages of Nanofibers"

Authored by

Nidhi Jain, Assistant Professor

From

Bharati Vidyapeeth College of Engineering Lavale, Pune.

DOI : 10.37896/MSJ

crossref member

CROSSREF.ORG THE CITATION LINKING BACKBONE

Has been published in

MUKTH SHABD JOURNAL, VOLUME IX, ISSUE V, MAY - 2020

Sumit Ganguly
Editor-In-Chief
MSJ
www.shabdbooks.com

UGC-CARE List

You searched for "**Mukt Shabd**". Total Journals : 1

Search:

Sr.No.	Journal Title	Publisher	ISSN	E-ISSN	UGC-CARE coverage years	Details
1	Mukt Shabd (print only)	Shabd Publication	2347-3150	NA	from June-2019 to Present	View

Showing 1 to 1 of 1 entries

Previous 1 Next

Copyright © 2024 Savitribai Phule Pune University. All rights reserved. | Disclaimer

Journal Details

Journal Title (in English Language)	Mukt Shabd (print only) | (Current Table of Content)
Journal Title (in Regional Language)	मुक्त शब्द (print only)
Publication Language	Marathi
Publisher	Shabd Publication
ISSN	2347-3150
E-ISSN	NA
Discipline	Arts and Humanities
Subject	Arts and Humanities (all)
Focus Subject	Literature and Literary Theory
UGC-CARE coverage years	from June-2019 to Present

Copyright © 2024 Savitribai Phule Pune University. All rights reserved. | Disclaimer

International Journal of Mechanical Engineering and Technology (IJMET)
Volume 9, Issue 10, October 2018, pp. 1444–1460, Article ID: IJMET_09_10_148
Available online at http://www.iaeme.com/ijmet/issues.asp?JType=IJMET&VType=9&IType=10
ISSN Print: 0976-6340 and ISSN Online: 0976-6359

© IAEME Publication  **Scopus** Indexed

PRIORITIZATION OF GREEN SUPPLY CHAIN INDICATORS WITH ANALYTIC HIERARCHY PROCESS (AHP) MODEL

Mrs. A. S. Chavan
Research Scholar* Bharati Vidyapeeth (Deemed to be University) College of Engineering, Pune-Satara Road, Pune,

Dr. R. N. Patil
I/C Principal, Bharati Vidyapeeth's College of Engineering, Lavale Pune,

Dr. S T. Chavan
Professor,Maharashtra Institute of Technology, Kothrud, Pune

ABSTRACT

Purpose *Today the innovative tool used for enhancing the efficiency of Supply Chain Management is Green Supply Chain Management (GSCM). This paper, aims to identify and rank the major indicators and sub indicators that helps achieve successful implementation of Green Supply Chain Management (GSCM) in Indian manufacturing industry.*

Design/methodology/approach: *Analytic Hierarchy Process (AHP) is used to rank the indicators and sub indicators which have been identified through literature review and experts' opinions from industry and academicians.*

Findings: *The study categorizes the GSCM implementation strategies into main sixteen indicators and 116 sub indicators. Main indicators are Non-Members of Supply Chain, Top Management Perspective, Eco Product Design, Eco Procurement, Eco Manufacturing, Internal Environmental Management, Green Packaging, Eco Marketing and Communication, Eco Logistics Design, Environmental Performance, Operational Performance, Economic Performance, Performance of Human and Technological Resources, Performance of Vendor Management, Owners' Satisfaction and Customer Co-Operation. These identified indicators play an important role in greening the supply chain.*

Research limitations/implications: *Here we have used the opinion of the experts from academics and industry to compare pair-wise indicators.*

Practical implications: *The indicators and sub indicators are prioritised according to the importance of their applications. This prioritization further can be used to construct the Interpretive Structural Model (ISM) for cost and efficiency benefits in GSCM performances in Indian manufacturing industry.*

Keywords- Green Supply Chain Management, Sustainability and Manufacturing, and Analytical Hierarchical Process.

Cite this Article Mrs. A. S. Chavan, Dr. R. N. Patil and Dr. S T. Chavan, Prioritization of Green Supply Chain Indicators with Analytic Hierarchy Process (Ahp) Model, International Journal of Mechanical Engineering and Technology, 9(10), 2018, pp. 1444–1460.

http://www.iaeme.com/IJMET/issues.asp?JType=IJMET&VType=9&IType=10

1. INTRODUCTION

After the economic liberalization policies in 1991 the growth rate has been increased by 42.7%. As per National Manufacturing Policy (NMP) Government of India is planning to increase Gross Domestic Product (GDP) in the manufacturing sector from the current level of 16% to 25% by 2025. In order to achieve the target, country will have to study impact of environment which has been mentioned by Planning Commission in Twelfth Five Year Plan now called as NITI Aayog.

Greenhouse gas is alarmingly increasing as compared to developing countries like China, Japan and USA. The carbon dioxide (CO_2), concentration of India was from 280 ppm in 1750 to 406 ppm in early 2017, which is now a serious cause to save the environment.
Environmental Performance Index (EPI) Switzerland ranks first with EPI score as 87.42, France 2nd with 83.95, United Kingdom 6th with79.89, China 120th with 50.74 score, India ranked hundred and 177th with score 30.57 [Source: 2018 Yale Center for environmental law & policy].

The Global Green Economy Index (GGEI) measures both the green economic performance of 80 countries and how experts assess that performance. Sweden ranks first with green index score 77.61, Norway second 66.11, China sixty fourth rank with 41.77 score, India sixty eighth with score 40.43 (Source: The Global Green Economy Index 2016).

The Logistics Performance Index (LPI) also plays an important role as an indicator which is an interactive benchmarking tool created by the World Bank to help countries identify the challenges and opportunities they face in their performance based on trade logistics and what they can really do to enhance their performance. *India ranks 35th with score 3.42/5 amongst survey of 150 countries.*

2. GREEN SUPPLY CHAIN MANAGEMENT (GSCM):

Green Supply Chain Management (GSCM) in the manufacturing industry [02] is the answer to make whole supply chain more environment sustainable thus by integrating the traditional supply chain practices with environmental friendly practices. Green supply chain management is well defined as "the process of using environment friendly inputs and transforming these inputs into outputs that can be reclaimed and re-used at the end of their life cycle thus, creating a sustainable supply chain." Integrating environmental thinking into supply chain management, including product design, material sourcing and selection, manufacturing processes, delivery of the final product to the consumers, and end-of-life management of the product after its useful life plays a vital role in today's globalization world [19]. Zhu and Sarkis defined GSCM as has ranged from green purchasing to integrated supply chains starting from supplier, to manufacturer, to customer and reverse logistics, which is "closing the loop". Over the past few years, GSCM is playing an important role in the building of sound economic-environmental performances on various levels in business [37, 38].

3. LITERATURE REVIEW:

The major need of Green supply chain came into existence after the quality revolution in the year 1980s and the supply chain revolution in the year 1990s. To enrich the traditional supply chain, green supply chain came into existence and the literature begins with corporate environmental management, environmentally conscious manufacturing strategy . The work of the green supply chain commenced in the year 1989 and Kelle and Silver used for forecasting system, 1991, Navin- Chandra's used to minimize the product waste. Augmentation of deterioration of the surrounding environment has raised concerns amongst various researchers and academicians. Which results into increase in the publication of the articles in past few years related to GSCM [22, 24]. GSCM is meaningfully expressed as the addition of environmental thought in the business. Thus GSCM contributes as a useful measure so as to enhance the ecological performance of the enterprise and to reduce the environmental risks [46]. In a study, GSCM has also been related to human resource management so as to achieve organizational sustainability and actual sustainable supply chains. [29]. GSCM has created buyers an opportunities to have environment friendly product, which in return increase the performance of environmental economy [28].

Walton, Handfield and Melynyk have made a mark and claimed that "now a days strategic planning agendas and executive suites due to implementation of strong public mandates and government regulation [38]. Roy and Whelan developed a standardized model so as to reduce waste without harming the environment.

GSCM was identified as a competitive advantage to enhanced profit ratios [20]. Rao and Holt, claimed over improvement in efficiency of an organization. The competitive gains and ecological proficiency is also enhanced due to implementation of green factor in supply chain. Due to many environmental issues implementations of green supply chain management has observed higher risks[05]). But even many many researchers had worked with GSCM and has come up with good outcome with respect to environmental aspects.

Once the factors are selected now the need is to analyze the performance and inter-relations of these indicator's and sub-indicator's so that GSCM may be implemented in Manufacturing Industries. The effectiveness in the implementation of GSCM practices is incorporated by giving weightages to indicator's and sub-indicator. Therefore, the outcome of this study is to prepare the GSCM model in which interrelationships of the indicator's and sub-indicator's and their levels can be understand. The sub-indicator's are categorized depending on their priority weightage. However this study provides a statistical analysis of GSCM indicator's and sub-indicator by using pair wise comparison method of AHP.

Researchers have developed number of criteria, methods and models by taking into consideration the importance of role of Green factors in the functioning of supply chains. Usually GSCM problem involves more than one criterion and these criteria have differences with each other. So Multi Attribute Decision Making (MADM) techniques are implemented to solve the multi level problem. One of the MADM techniques is AHP.

Analytical Hierarchical Process (AHP): A multi attribute decision-making method thus prioritizes indicators when multiple criteria are involved and allows to structure complex problems in the form of a hierarchy, or a set of levels. This method incorporates qualitative and quantitative criteria. This hierarchy has three different levels, which include goals, criteria, and alternatives. AHP utilizes a ratio scale for human judgements; the alternatives weights reflect the relative importance of the criteria so as to achieve the goal of the hierarchy [07, 14, 16].

After the critical review and the suggestions from academic and industrial experts following indicators were selected for the implementation of GSCM.

AHP WEIGHTS AND RANKS						
			Relative weights using AHP	Global weights using AHP	RANK	References
NON-MEMBERS OF SUPPLY CHAIN						
1	Central government legalizations	CGL	2.192307	0.548077	1	Green et al. (1996) [8], Walton et al. (1998) [33], Beamon (1999) [03], Hall (2001) [9], Min and Galle (2001) [22]and Walker et al. (2008) [35]
2	State government legalizations	SGL	1.222941	0.305735	2	
3	Non government organizations	NGO	0.406295	0.101574	3	
4	International environment agreements	IEA	0.178457	0.044614	4	
Eigen Value: 4.2469 Consistency Ration: 0.08230 Consistency Index: 0.0914						
TOP MANAGEMENT PERSPECTIVE						
1	Organizational policies	OP	1.796699	0.449175	1	Dashore and Sohani (2013) [05], Walker et al(2008) [34], Zhu and Sarkis (2007)[41]
2	Commitment and initiatives	CI	1.074936	0.268734	2	
3	Technology Enhancement	TE	0.542909	0.135727	4	
4	Information technology Enhancement	IT	0.585456	0.146364	3	
Eigen Value: 4.2180, Consistency Ration: 0.7267, Consistency Index: 0.08074						
ECO PRODUCT DESIGN						
1	Product design with reuse, recycle, recovery of material, components parts	RRR	1.845074	0.255289	1	Zhu et al. (2004, 2005, 2007a,b, 2008a,b,c),[37-46] Hu and Hsu (2006)[12], Routroy (2009)[28] Walton (1998)[33], Beamon B.M (1999)[3], Lippmann S(2001)[16], Rao P (2009)[26], Green K(1996)[08], Azevedo S G(2011)[02], Eltayeb TK
2	Product design with reduce use of hazardous material	HM	1.846279	0.220096	2	
3	Product eco-design with feedback from customers.	ED	1.451094	0.166877	3	
4	Products are designed & developed for ease in dismantling & remanufacturing	PDR	0.954176	0.084522	5	

5	Product design with application of value engineering/analysis	VE	0.907285	0.159627	4	(2011)[06], Hervani AA (2005)[10] Rao P (2005)[27] Ali Diabat (2013) [01]
6	Product durability	PD	0.500293	0.049917	6	
7	Life cycle assessment of product with respect to environment impact and cost.	EIC	0.338855	0.032326	7	
8	Design the product according to 3S-Standardization, Specification and Simplification.	3S	0.157304	0.031345	8	
Eigen Value: 6.55, Consistency Ration: 0.11043, Consistency Index: 0.0890						
ECO PROCUREMENT						
1	Provision of education/assistance to suppliers on environmental matters in order to increase supply chain efficiency.	EDU	2.178366	0.363061	1	Rao P (2005)[27] Ali Diabat (2013) [01], Zhu and Sarkis (2006)[45], Zhu et al. (2005
2	Joint decision with our supplier to reduce overall impact of the product and logistics operations	PLO	1.079864	0.179977	2	
3	Provides design specification to suppliers that include environmental requirements for purchased item	SSEP	0.9694	0.161567	3	
4	Second-tier supplier's environmentally friendly	EFP	0.938708	0.156451	4	

	practice evaluation					
5	Procurements mainly from ISO14000 certified suppliers	ISO	0.593355	0.098893	5	
6	Work with other business functions to discuss and improve purchasing procedures.	PP	0.240404	0.040067	6	
Eigen Value: 6.55, Consistency Ration: 0.11043, Consistency Index: 0.0890						
ECO MANUFACTURING						
1	Selection of proper manufacturing process with environment considerations.	SMP	1.434363	0.179295	1	Zhu and Sarkis (2006)[45], Zhu et al. (2005, 2007a, 2008c)[40, 44, 43] and Rao and Holt (2005)[27]
2	Use of renewable sources of energy	RSE	1.273117	0.15914	4	
3	Consideration of environmental issues in the process of production planning and control	PPC	1.425514	0.178189	2	
4	Integrated environmental & efficiency criteria in manufacturing	IEE	1.185827	0.148228	5	
5	Avoid hazardous waste in manufacturing	MW	0.489149	0.061144	7	
6	Selection of optimized material handling system	MHS	0.572972	0.071621	6	
7	Selection of best method	SBM	0.298255	0.037282	8	
8	Implementation of tools to	WME	1.320804	0.1651	3	

	optimization of water, material and energy.					
Eigen Value: 8.72, Consistency Ration: 0.102, Consistency Index: 0.072						
INTERNAL ENVIRONMENTAL MANAGEMENT						
1	Green supply chain management policy implementation by senior managers	CSM	1.895652	0.210628	1	Zhu and Sarkis (2006))[45], Zhu et al. (2005, 2007a, 2008c)[40, 44, 43], Rao and Holt (2005)[27], Hu and Hsu (2006)[13], Vachon (2007)[31] and Holt and Ghobadian (2009)[11] Lippman (2001)[16], Eltayeb TK (2011)[06], Hervani AA (2005)[10], Rao P(2005)[27], Ali Diabat (2013)[01]
2	Implementation of total quality environmental management	TQE	1.471647	0.163516	3	
3	Promotion of quality circles	QC	1.600855	0.177873	2	
4	Implementation of ISO 14001 certification	14001	0.772299	0.085811	6	
5	Lean And Agile Manufacturing	LA	0.362149	0.040239	9	
6	Admire the competitors with respect implementation of GSCM.	AC	0.486503	0.054056	8	
7	Implementation of environment auditing program.	IAP	0.49853	0.055392	7	
8	Linkage policy of GSCM with economic, environmental and process performance.	EEPP	1.106325	0.122925	4	
9	GSCM support at all the levels of management	SLM	0.806041	0.08956	5	
Eigen Value: 9.89, Consistency Ration: 0.11125, Consistency Index: 0.0767						
GREEN PACKAGING						
1	Design packaging for refilling or recycling and use standardized packaging when applicable	SPA	2.328188	0.291023	1	Rao and Holt (2005)[27], Holt and Ghobadian (2009)[11], Paulraj (2009)[24],

2	Co-operation with customers for environmental packaging	CEP	1.48157	0.185196	2	and Vachon (2007)[31]
3	Re-organizing the packaging policy	ROPP	0.444673	0.055584	7	
4	Limit packaging to the necessary size	LPS	1.267923	0.15849	3	
5	Returnable recyclable packaging for in-house storage	RIP	0.939681	0.11746	4	
6	Use of recyclable material for packaging	RM	0.866073	0.108259	5	
7	Reduced cost of packaging	RCP	0.107215	0.013402	8	
8	Safety packaging system	SP	0.564677	0.070585	6	
Eigen Value: 8.626, Consistency Ration: 0.08857, Consistency Index: 0.0628						
MARKETING AND COMMUNICATION						
1	Marketing and communicating the product by using environmental information	MCEI	1.490216	0.186277	3	Green et al. (1996) [08] Mathiyazhagan et al. (2013a)[20], Mollenkopf et al. (2010)[23].
2	Exchange of information and departmental interaction regarding efficiency, performance and environment etc	EPE	0.307231	0.038404	8	
3	Protecting consumer rights and growth by assuring a clean and safe environment in which they can live	CSE	0.354422	0.044303	7	

4	Commitment from the organization to ensure the preservation of the natural environment	PNE	0.641155	0.080144	6	
5	Manufacturing of environmentally friendly products	EFP	1.207391	0.150924	4	
6	Improve their environmental performance by assisting the customers	EPC	1.493484	0.186686	2	
7	Requirement and activities of customer regarding environment should monitored	CEM	1.563718	0.195465	1	
8	Logo or label of environmental friendly product	ELFP	0.942381	0.117798	5	
Eigen Value: 8.72, Consistency Ration: 0.10285, Consistency Index: 0.0729						
ECO LOGISTICS DESIGN						
1	Application of Reverse logistics	RL	1.851503	0.2645	1	Lippman (2001)[16], Rao and Holt (2005)[27], Zhu et al. (2005)[40], Hu and Hsu (2006)[13], Vachon (2007)[31], and Routroy (2009)[28] Eltayeb TK (2011)[06], Hervani AA (2005)[10], Ali Diabat (2013)[01], Holt and Ghobadian (2009)[11] Mangla et al. (2013)[19], Rao and Holt
2	Recycled and reused of products/parts whose are identified in logistics system	RRLS	1.133339	0.161906	3	
3	Planning for recollecting used packaging material	PRPM	0.884587	0.12637	5	
4	Unit Load Logistics	ULL	0.113341	0.016192	7	
5	Material Handling System	MHS	0.554702	0.079243	6	
6	Green packing	GP	1.072966	0.153281	4	
7	Environment design of logistics management	ELM	1.389561	0.198509	2	

						(2005)[27], Rao (2002)[25].
Eigen Value: 7.69, Consistency Ration: 0.115, Consistency Index: 0.08712						
ENVIRONMENTAL PERFORMANCE						
1	Reuse of waste water	RWW	0.685123	0.097043	1	Rao and Holt (2005)[27], Holt and Ghobadian (2009)[11], Paulraj (2009)[24], and Gonzalez et al. (2008)[07], Bowen et al. (2001)[04], Mathiyazhagan et al. (2013a), (2014)[20, 21], Toke et al. (2012)[29].
2	Training to avoid environmental accidents	TEA	0.280189	0.039687	7	
3	Selling not required capital equipments.	RCE	0.676204	0.095779	5	
4	Try to avoid hazardous materials	THM	0.436734	0.06186	6	
5	Policy of using rejected material and recovery through scrap.	PRMS	1.9511	0.276359	2	
6	Try to avoid air emission	AE	1.942411	0.275128	3	
7	Selection of proper engineering tools to avoid solid waste	SW	1.088264	0.154144	4	
Eigen Value: 7.71, Consistency Ration: 0.1183, Consistency Index: 0.0896						
OPERATIONAL PERFORMANCE						
1	Optimize the inventory	OI	1.318803	0.16485	3	Madaan and Mangla (2015)[18] Mathiyazhagan et al. (2013a)[20], Dashore and Sohani (2013)[05], Walker et al(2008)[32].
2	Program to promote and track the reduction of waste	WR	0.801044	0.10013	5	
3	Maximized the use of capacity	MUC	0.711786	0.088973	6	
4	Promotion of environmental quality products	QP	0.822776	0.102847	4	
5	Delivery of goods on time	DOT	0.259871	0.032484	7	
6	Use of energy efficient equipments	UEEE	2.151491	0.268936	1	

7	Policy to reduce the pollution	PEP	0.1357	0.016962	8	
8	Practice 4R concept – reduce, reuse, recover & recycle	4R	1.79853	0.224816	2	
Eigen Value: 8.626, Consistency Ration: 0.08857, Consistency Index: 0.0628						
ECONOMIC PERFORMANCE						
1	Proper Energy consumption	EC	0.248487	0.035498	7	Zhu and Sarkis (2005) (2007)[40, 38], Ali Diabat (2013)[01], Mollenkopf et al. (2010)[23], Paulraj (2009)[24], Rao and Holt (2005)[27], Rao (2002)[25].
2	Design of Good Plant Layout	PL	2.151333	0.307333	1	
3	Reduced cost of material to be purchased	MP	0.282712	0.040387	6	
4	Design of Good MHS	MHS	0.713558	0.101937	5	
5	Selection of proper method	SPM	1.611552	0.230222	2	
6	Environmental cost evaluation wrt new technology and capital purchased	TC	0.95732	0.13676	4	
7	Environmental cost associated to customer wrt disposal and use of product	CDU	1.035038	0.147863	3	
Eigen Value: 7.71, Consistency Ration: 0.118, Consistency Index: 0.0896						
PERFORMANCE OF HUMAN AND TECHNOLOGICAL RESOURCES						
1	Selection of employee and Technology	SET	1.573696	0.262283	1	Dashore and Sohani (2013)[05], Walker et al(2008)[32], Bowen et al. (2001)[04], Mathiyazhagan et al. (2013a), (2014)[20, 21], Toke et al. (2012)[29].
2	Awareness of environmental issues	AEI	1.131586	0.188598	3	
3	Safety Methodologies	SM	0.64225	0.107042	5	
4	Implementation of new technology in consultation of experts	CNT	0.770031	0.128338	4	
5	Training of employee	TE	1.249474	0.208246	2	
6	Investment on Employee and Technology	IET	0.632963	0.105494	6	

Eigen Value: 6.61, Consistency Ration: 0. 122, Consistency Index: 0.09838						
PERFORMANCE OF VENDOR MANAGEMENT						
1	Selection of Environmental certified vendor	SEV	2.294482	0.458896	1	Vachon (2007)[31], Zhu et al. (2005, 2007a, 2008c)[40,44, 43], Paulraj (2009)[24], Zhu and Sarkis (2006)[45], Lippmann (1999)[17], Yuang and Kielkiewicz-Yuang (2001)[36], Klassen and Vachon (2003)[14], Lippman (2001)[16], Hu and Hsu (2006)[13], Vachon (2007)[31] and Holt and Ghobadian (2009)[11], Bowen et al. (2001)[04], Mathiyazhagan et al. [(2013a), (2014)][20, 21], Toke et al. (2012)[29].
2	Training of vendors	TV	1.236252	0.24725	2	
3	Response time to adapt	RTC	0.765258	0.153052	3	
4	Delivery in time	DT	0.272212	0.054442	5	
5	Awareness of environmental issues	AEI	0.431796	0.086359	4	
Eigen Value: 4.43, Consistency Ration: 0.1075, Consistency Index: 0.095						
OWNERS' SATISFACTION						
1	Achieved competitive leadership in the market through environmentall y friendly products.	EEP	2.553288	0.510658	1	Zhu Q, Sarkis J (2007)[38], Eltayeb TK (2011)[06], Lin RJ (2013)[15], Tseng ML, Chiu ASF (2013)[30], Zhu Q, Sarkis J (2004)[37], Vachon
2	Good reputation	GR	0.377725	0.075545	4	
3	More profits	MP	0.155767	0.031153	5	
4	Positive attitude for Business	PAB	1.28921	0.257842	2	

5	Confidence	C	0.62401	0.124802	3	(2007)[31], Rao P(2002)[06], Ali Diabat (2013)[01], Zhu and Sarkis (2006)[45], Zhu et al. (2005, 2007a,b, 2008a,b,c) [37-46], Green et al. (1996)[08] Mathiyazhagan et al. (2013a)[20], Mollenkopf et al. (2010)[23].
Eigen Value: 5.41,Consistency Ration: 0.1025, Consistency Index: 0.0915						
CUSTOMER CO-OPERATION						
1	Co-operation from customers for eco-design	ED	2.507103	0.501421	1	Vachon (2007)[31], Zhu et al. (2008a,b,c),[44,-46], Paulraj (2009)[24], Holt and Ghobadian (2009)[11], Klassen and Vachon (2003)[14], Zhu and Sarkis (2006)[45], Zhu et al. (2005, 2007a,b, 2008)[37-46], Eltayeb TK (2011)[06], Zhu Q, Sarkis J (2004)[37], Zhu Q, Sarkis J, Geng Y (2005)[40], Ali Diabat (2013)[01].
2	Co-operation from customers for Eco-procurement	GM	0.536964	0.107393	4	
3	Co-operation from customers for green manufacturing	GMI	0.713456	0.142691	3	
4	Co-operation from customers green logistics	GL	1.066578	0.213316	2	
5	Co-operation with customers for green marketing	EM	0.175898	0.03518	5	
Eigen Value: 5.39, Consistency Ration: 0.0975, Consistency Index: 0.0870						

Sample calculation for Analytical Hierarchical Process (AHP)

Central Government Legislations (CGL)	State Government Legislations (SGL)
Non-Government Organizations (NGO)	International Environment Agreements (IEA)

	CGL	SGL	NGO	IEA
CGL	1	3	5	9
SGL	0.33	1	5	7
NGO	0.2	0.2	1	3
IEA	0.11	0.14	0.33	1
Σ C	1.64	4.34	11.33	20

	CGL	SGL	NGO	IEA	SUM	Priority Vector (PV)	RANK
CGL	0.609756	0.691244	0.441306	0.45	2.192307	0.548077	1
SGL	0.20122	0.230415	0.441306	0.35	1.222941	0.305735	2
NGO	0.121951	0.046083	0.088261	0.15	0.406295	0.101574	3
IEA	0.067073	0.032258	0.029126	0.05	0.178457	0.044614	4
					= 4	1	

Eigen Value (λ_{max}) = $\Sigma C_i * (PV)_i$

Eigen Value (λ_{max}): 4.2469

Consistency Index (CI) = (λ_{max} - n) / (n-1)

Consistency Index: 0.0914

Consistency Ratio (CR) = CI/ RI

Consistency Ratio: 0.08230

4. CONCLUSION

- In this paper, a literature review was carried out to identify various strategies that help in implementation of GSCM practices in Indian manufacturing industry. After the detail discussion with experts from industry 16 main indicators and 103 sub-indicators were identified, categorized into four strategic dimensions based on their direct or indirect role in greening.
- This paper may add up GSCM practitioners to select suitable indicators to make a perfect fit with the environmental regulations and customers requirements. Further appropriate selection of main indicators and sub - indicators will enable the organizations to enjoy cost benefits as well as better brand image.
- Green Supply Chain is the only tool to enhance environmental performance i.e. environmental standards, resource consumption, reductions in air emissions and consumption of hazardous materials as mentioned in NITI AAYOG when compared with traditional supply chain.

- Analytical Hierarchical Process (AHP) had been used to develop inter-relationship of these indicator's and sub-indicator's. The sub-indicator is categorized depending on their priority weightage by using pair wise comparison method of AHP. Finally AHP prioritized 48 sub-indicators for large scale industries, 46 for medium scale industries and 31for small scale industries.

REFERENCES

[1] Ali Diabat , Roohollah Khodaverdi & Laya Olfat "An exploration of green supply chain practices and performances in an automotive industry" Int J Adv Manuf Technol (2013) 68:949–961 DOI 10.1007/s00170-013-4955-4970.

[2] Azevedo, S.G., Carvalho, H., & Machado, V.C., (2011) "The Influence of Green Practices on Supply Chain Performance: A Case Study Approach", Transportation Research Part E, Vol. 47, pp 850-871.

[3] Beamon B M. Designing the green supply chain. Logistics Information Management 1999;12(4):332–342.

[4] Bowen, F.E., Cousins, P.D., Lamming, R.C. and Faruk, A.C. The role of supply management capabilities in green supply. Production and Operations Management 2001, 10(2): 174-89.

[5] Dashore, K. and Sohani, N. Green Supply Chain Management - Barriers and Drivers: A Review. International Journal of Engineering Research and Technology 2013, 2(4): 2021-2030. [6]

[6] Eltayeb TK, Zailani S, Ramayah T (2011) Green supply chain initiatives among certified companies in Malaysia and environmental sustainability: investigating the outcomes. Resour Conserv Recycl 55:495–506.

[7] Gonzalez P, Sarkis J, Adenso-Diaz B. Environmental management system certification and its influence on corporate practices: evidence from the automotive industry. International Journal of Operations & Production Management 2008;28(11):1021–41.

[8] Green, K., Morton, B., & New, S. (1996). Purchasing and environmental management: interactions, policies and opportunities. Business Strategy and the Environment, 5(1), 188-197.

[9] Hall J. Environmental supply chain innovation. Greener Management International 2001;35:105–19

[10] Hervani, A.A., Helms, M.M. and Sarkis, J. Performance measurement for green supply chain management. Benchmarking: An international Journal 2005, 12(4): 330-353.

[11] Holt, D., and Ghobadian, A. An empirical study of green supply chain management practices amongst UK manufacturers. Journal of Manufacturing Technology Management 2009, 20(7): 933-956.

[12] Hsu, C.W., and Hu. A.H. Green Supply Chain Management in the Electronic Industry. International Journal of Science and Technology 2008, 5(2): 205-216.

[13] Hu AH, Hsu CW. Empirical study in the critical factors of green supply chain management (GSCM) practice in the Taiwanese electrical and electronics industries. In: Proceeding of 2006 IEEE international conference on management of innovation and technology, 21–23 June 2006; 2006. p. 853–7.

[14] Klassen RD, Vachon S. Collaboration and evaluation in the supply chain: the impact on plant-level environmental investment. Production & Operations Management 2003;12(3):336–52.

[15] Lin RJ (2013) Using fuzzy DEMATEL to evaluate the green supply chain management practices. Journal of Cleaner Production 40:32–39

[16] Lippman S. Supply chain environmental management. Environmental Quality Management 2001;11(2):11–4.

[17] Lippmann S. Supply chain environmental management: elements of success. Corporate Environmental Strategy 1999;6(2):175–82.

[18] Madaan, J., and Mangla, S. Decision Modeling Approach for Eco-Driven Flexible Green Supply Chain. In Systemic Flexibility and Business Agility. Springer India 2015, 343-346.

[19] Mangla, S., Madaan, J. and Chan F.T.S. Analysis of flexible decision strategies for sustainability-focused green product recovery system. International Journal of Production Research 2013, 51(11): 3443-3462.

[20] Mathiyazhagan, K., Govindan, K. and Noorul Haq, A. An ISM approach for the barrier analysis in implementing green supply chain management. Journal of Cleaner Production 2013a, 47: 283-297.

[21] Mathiyazhagan, K., Govindan, K. and Noorul Haq, A. Pressure analysis for green supply chain management implementation in Indian industries using analytic hierarchy process. International Journal of Production Research 2014, 52: 1-16.

[22] Min H, Galle WP. Green purchasing practices of US firms. International Journal of Operations & Production Management 2001;21(9):1222–38.

[23] Mollenkopf, D., Stolze, H., Tate, W.L. and Ueltschy, M. Green, lean, and global supply chains. International Journal of Physical Distribution and Logistics Management 2010, 40(1/2): 14-41.

[24] Paulraj, A. Environmental motivations: a classification scheme and its impact on environmental strategies and practices. Business Strategy and the Environment 2009, 18(7): 453-468.

[25] Rao P (2002) Greening the supply chain: a new initiative in South East Asia. Int J of Oper Prod Manag 22(6):632–655

[26] Rao P, Holt D, Ghobadian A. An empirical study of green supply chain management practices amongst UK manufacturers. Journal of Manufacturing Technology Management 2009;20(7):933–56.

[27] Rao, P., & Holt, D. (2005). "Do green supply chains lead to competitiveness and economic performance?", International Journal of Operations and Production Management, vol 25(9), pp 898-916.

[28] Routroy S. Antecedents and drivers for green supply chain management implementation in manufacturing environment. ICFAI Journal of Supply Chain Management 2009;6(1):20–35.

[29] Toke, L. K., Gupta, R. C, Dandekar M. An empirical study of green supply chain management in Indian perspective. International Journal of Applied Science and Engineering Research 2012,1(2): 372–83.

[30] Tseng ML, Chiu ASF (2013) Evaluating firm's green supply chain management in linguistic preferences. Journal of Cleaner Production 40:22–31

[31] Vachon S, Klassen RD (2007) Environmental management and manufacturing performance: the role of collaboration in the supply chain. Int J Prod Econ 111(2):299–315

[32] Walker H, Di Sisto L, McBain D. Drivers and barriers to environmental supply chain management practices: lessons from the public and private sectors. Journal of Purchasing and Supply Management 2008;14(1):69–85.

[33] Walton S, Handfield R, Melnyk S. The green supply chain: integrating suppliers into environmental management processes. International Journal of Purchasing and Materials Management 1998;3(2):2–11.

[34] Yuang A, Kielkiewicz-Yuang A. Sustainable supply network management. Corporate Environmental Management 2001;8(3):260–8

[35] Zhu Q, Sarkis J (2004) Relationships between operational practices and performance among early adopters of green supply chain management practices in Chinese manufacturing enterprises. J Oper Manag 22(3):265–289.

[36] Yuang A, Kielkiewicz-Yuang A. Sustainable supply network management. Corporate Environmental Management 2001;8(3):260–8.

[37] Zhu Q, Sarkis J (2004) Relationships between operational practices and performance among early adopters of green supply chain management practices in Chinese manufacturing enterprises. J Oper Manag 22(3):265–289

[38] Zhu Q, Sarkis J (2007) The moderating effects of institutional pressures on emergent green supply chain practices and performance.Int J of Production Research 45:4333–4355

[39] Zhu Q, Sarkis J, Cordeiro J, Lai KL (2008) Firm-level correlates of emergent green supply chain management practices in the Chinese context. Omega 36:577–591

[40] Zhu Q, Sarkis J, Geng Y. Green supply chain management in China: pressures, practices and performance. International Journal of Operations and Production Management 2005;25(5/6):449–69.

[41] Zhu Q, Sarkis J, Lai K (2007) Green supply chain management: pressures, practices and performance within Chinese automobile industry. J Clean Prod 15:1041–1052

[42] Zhu Q, Sarkis J, Lai K (2008) Green supply chain management implications for closing the loop. J Transp Res Part E 44:1–18

[43] Zhu Q, Sarkis J, Lai K. Confirmation of a measurement model for green supply chain management practices implementation. International Journal of Production Economics 2008c;111(2):261–73.

[44] Zhu Q, Sarkis J, Lai KH. Initiatives and outcomes of green supply chain management in China. Journal of Environmental Management 2007a;85(1):179–89.

[45] Zhu Q, Sarkis J. An inter-sectoral comparison of green supply chain management in China: drivers and practices. Journal of Cleaner Production 2006;14(5):472–86.

[46] Zhu, Q., and Sarkis, J. The moderating effects of institutional pressures on emergent green supply chain practices and performance. International Journal of Production

[47] Satya Mandal and Dr. Seema Sarkar Mondal. Analytic Hierarchy Process (AHP) Approach for Selection of Open Cast Coal Mine Project, International Journal of Industrial Engineering Research and Development, 7(2), 2016, pp. 01–13

[48] D. Teja Swaroop, D. Satish Chandra and SS. Asadi, Application of Safety and Risk Management Techniques in Construction using Analytic Hierarchy Process (AHP)- A Case Study, International Journal of Civil Engineering and Technology, 9(4), 2018, pp. 719–724.

Scopus Preview

Source details

Check whether you can access Scopus remotely through your institution

Maybe later | Check access

International Journal of Mechanical Engineering and Techno

Scopus coverage years: from 2016 to 2019
(coverage discontinued in Scopus)
Publisher: IAEME Publication
ISSN: 0976-6340 E-ISSN: 0976-6359
Subject area: Engineering: Industrial and Manufacturing Engineering | Engineering: Mechanical Engineering | Engineering: Mechanics of Materials
Source type: Journal

CiteScore 2017
1.2

SJR 2019
0.293

SNIP 2022
0.311

View all documents > | Set document alert | Save to source list

CiteScore | CiteScore rank & trend | Scopus content coverage

Improved CiteScore methodology

CiteScore 2017 counts the citations received in 2014-2017 to articles, reviews, conference papers, book chapters and data papers published in 2014-2017, and divides this by the number of publications published in 2014-2017. Learn more >

CiteScore 2017

$$1.2 = \frac{1{,}691 \text{ Citations 2014 - 2017}}{1{,}437 \text{ Documents 2014 - 2017}}$$

Calculated on 01 May, 2018

CiteScore rank 2017

Category	Rank	Percentile
Engineering — Industrial and Manufacturing Engineering	#143/328	56th
Engineering — Mechanical Engineering	#322/577	44th

View CiteScore methodology > | CiteScore FAQ > | Add CiteScore to your site

International Journal of Mechanical Engineering and Technology (IJMET)
Volume 9, Issue 13, December 2018, pp. 1264–1273, Article ID: IJMET_09_13_128
Available online at http://www.iaeme.com/ijmet/issues.asp?JType=IJMET&VType=9&IType=13
ISSN Print: 0976-6340 and ISSN Online: 0976-6359

© IAEME Publication  **Scopus** Indexed

RELATIVE RELIABILITY RISK INDEX FOR GREEN SUPPLY CHAIN MANAGEMENT

***Mrs. A. S. Chavan**
Research Scholar, Bharati Vidyapeeth (Deemed to be University)
College of Engineering, Pune-Satara Road, Pune,

Dr. R. N. Patil
I/C Principal, Bharati Vidyapeeth's College of Engineering, Lavale, Pune,

Dr. S T. Chavan
Professor, Maharashtra Institute of Technology, Kothrud, Pune

Mr. Nitin Kulkarni
Research Scholar, Sri Satya Sai University of Technology & Sciences, Sehore, M.P, India.

Dr. Sachin. S. Chavan
Professor, Bharati Vidyapeeth (Deemed to be University), College of Engineering, Pune-Satara Road, Pune,
*corresponding author

ABSTRACT

Green Supply Chain Management (GSCM) has become one of most promising tool in reducing environmental hazards of manufacturing industries. Selection of indicators and its implementation needs good decision making. The Aim of Relative Reliability Risk Index (R^3I) is to assess relatively the reliability of an industry wherein GSCM can be implemented and to screen out the ones that are judged to have unacceptable level of rank and hence risk. The relative measurement of indicators is done by Analytical Hierarchy method and weights are assigned through entropy method. Alternatives Functionality Graph is plotted to get to know the strength of each indicator. Relative Reliability Risk Index (R^3I) is calculated and results obtained from the case study are compared.

Key words: Reliability, Analytical Hierarchical Process (AHP), Relative Reliability Risk Index (R^3I). Alternative Functionality Graphs (AFGs), Green Supply Chain (GSCM)

Cite this Article: Mrs. A. S. Chavan, Dr. R. N. Patil, Dr. S T. Chavan, Mr. Nitin Kulkarni, Dr. Sachin. And S. Chavan, Relative Reliability Risk Index for Green Supply Chain Management, Journal of Mechanical Engineering and Technology, 9(13), 2018, pp. 1264–1273
http://www.iaeme.com/IJMET/issues.asp?JType=IJMET&VType=9&IType=13

1. INTRODUCTION

Green Supply Chain plays an important role in an industry and has direct impact on its efficiency and effectiveness. Many multi-criteria decision making methods are available to prioritize and rank the indicators identified by the researchers, but knowing the most important indicator and its depth may consume time for any new industry, so to get to know the rank of the indicators and thereafter its implementation may enhance the profit of any industry. Therefore it is projected to relatively assess the reliability of indicators for an industry. Since reliability is a very important criterion, it is proposed to evaluate reliability and obtain ratings and ordinal ranking. Performance is a measure of reliability and the functionality index which refers to the performance of an industry after the implementation of GSCM indicators and sub-indicators. Therefore a relative approach is followed in calculating R^3I using the Analytical Hierarchy Process. The idea of Alternative Functionality Graph (AFG) is introduced to enable an industry to look at the final outcome graphically and provide ease of making decisions.

2. LITERATURE

Selection of vendors with the different performance factors is done by many researchers since 1960, Dickson [1], Weber et al. [2], but the solutions involve high degree of uncertainties and fuzziness. Bellman and Zadeh [3] proposed Fuzzy set theory for problem modelling and solution, introduced fuzzy set theory in Multi Attribute Decision Making as an approach to effectively deal with the inherent impression, vagueness and subjectiveness of the human decision making process. AHP based strategic sourcing model is developed for effective vendor selection by Bindu et al. [4]. Vendor selection as mentioned in the perspective by Bindu et al. [5] is having a direct impact on the efficiency and responsiveness of the entire supply chain. Although many multi-criteria decision making methods, are available to select the final vendor from the set of available vendors, the data to calculate reliability of vendors may not be available, in case of new vendors. Therefore it is proposed to relatively assess the reliability of new alternative vendors and then screen out those that seem to have unacceptable level of rank. Performance is a measure of reliability and the functionality indication, as concluded by Weber et al. [2] refers to the performance of the vendor. Therefore a relative approach is followed in calculating R^3I using the Analytical Hierarchy Process.

Since 1960 many researchers worked on measuring the performance of GSCM and analysis of various criteria for its selection and implementation, Joseph Sarkis et al. [7]. In selection of various criteria from the main problem there exist a high degree of fuzziness and uncertainties, Stefan Seuring et.al.[8].

The selection and implementation of indicators and sub-indicators of Green supply chain Management for any industry should not only meet ecological requirements and in turn bring profit to any industry, but also help in fulfilling various criteria such as reduction in carbon footprint, reduction of scarp, and enhancing quality. It is needed to develop a systematic selection process for identifying and prioritizing important indicators and sub-indicators and to evaluate the tradeoffs between technical, economic and performance criteria, as brought out by Rao et al. [6]. The method should also reduce time in selection of various indicators, implementation of Green supply chain management (GSCM) practices and develop consensus decision making, A. S. Chavan et.al [14].

The Aim of introducing Relative Reliability Risk Index (R^3I) is to assess relatively the reliability of an industry wherein Green supply Chain management can be implemented and then to screen out the ones that are judged to have unacceptable level of rank and hence risk. Further therein to optimize the operations so as to gain benefits in terms of profit and reduction in carbon footprints and thus attain effective GSCM implementation. The objective of introducing R^3I is to

highlight the industries that are relatively stronger in terms of reliability. Table 1 shows the list of indicators and its abbreviations for R^3I.

3. METHODOLOGY

Seven industries are to be ranked with respect to seven indicators identified from multi-criteria decision making methods. The problem is to identify the best industry for the implementation of GSCM. The subjective assessments of the seven industries based on seven main indicators were the only available data from within but for new industry this data need to be captured progressively over a period of time and which will be subjective in nature. The subjective assessment of seven industries based on seven indicators as shown in Table 2. The methodology is used to decide the overall ranks of an industries alternative and validate the ranks with the qualitative and quantitative outcomes obtained from the case study.

Table 1 List of Indicators and abbreviations for R^3I [14]

Sr. No.	Indicators	Abbreviations
1	Consideration of environmental issues in the process of production planning and control (Six Sigma/process capability, Product Stewardship)	PPC
2	Consideration of environmental issue during selection of manufacturing process (Industrial engineering tools: 5S, Kaizen, Method Study, Work Measurement, Industrial Safety, Ergonomics)	SMP
3	People involvement initiative (Quality circle)	QC
4	Co-operation with customers for environmental packaging	CEP
5	Application of Reverse logistics	RE
6	Are you recovering your scrap through government certified agency?	RSRM
7	Selection of Employee and Technology	SET

Table 2. Subjective assessment of industries based on indicators

Sr. No.	Abbreviations	Green 1	Green 2	Green 3	Green 4	Green 5	Green 6	Green 7
1	PPC	8	7	6	7	6	5	7
2	SMP	8	6	5	8	7	5	7
3	QC	10	8	8	6	8	6	8
4	CEP	8	7	7	8	8	6	7
5	RE	8	8	6	7	6	6	7
6	RSRM	10	8	6	6	7	5	8
7	SET	9	8	7	7	6	6	8
Total		61	52	45	49	48	39	52
Rank		1	2	6	4	5	7	3

To calculate Relative Reliability Risk Index (R^3I) of the alternatives available, four tier method is used. The schematic representation of the various steps in four tier method is as shown in figure 1.

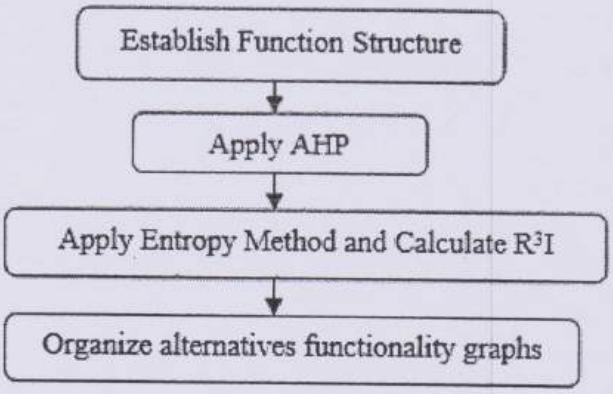


Figure 1. Methodology of Four Tier Method

The steps are as follows:

In **step 1**, the function structure i.e. Industry Evaluation attributes is established. Main objective is the selection of an industry forms the highest level of the hierarchy. The lower level is represented by seven main indicators of Green Supply Chain. The bottommost hierarchy is occupied by the seven industry alternatives available as shown in Figure No. 2.

In **step 2**, once the function structure is established, the Analytical Hierarchy Process developed by Saaty et al. [9-11], is applied so as to relatively rate the main indicators of the function structure as shown in figure 1. After the comparisons have been made, we obtain the priorities. Application of AHP is done using a Microsoft Excel to calculate consistency ratio. Any number of main indicators can be compared and a measure of inconsistencies during the comparisons is provided which gives a good measure of the relative ratings and provides a check whether the comparison should be performed again.

However, prioritization among the main criteria is optional. In the method proposed here, we calculate the priorities of the alternatives with respect to the objective. This is because the criteria those are available with us are the main indicators from the function structure. It would be inadvisable to compare the indicators that are basic to the system using the pair wise comparison matrix, because all the main indicators may seem to be equally important. Instead, we use entropy method to calculate the weights of the indicators available with us.

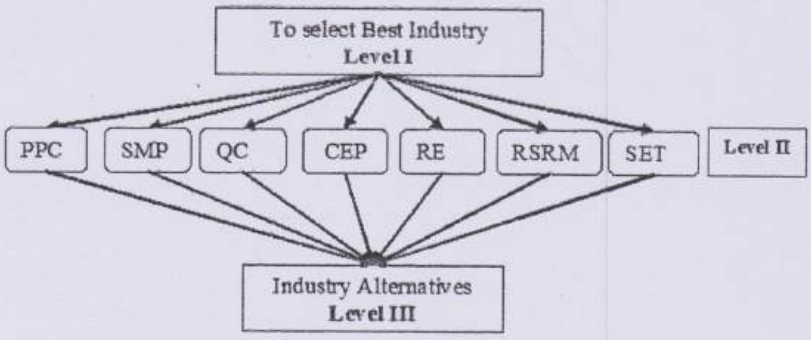


Figure 2. Structural Hierarchy for Industry Selection

Therefore after establishing the level structure, comparison matrices are formed and comparisons of lower level criteria are made with respect to the property at the upper level. There are seven industries alternative. The indicators on which the selection depends are seven i. e. Consideration of environmental issues in the process of production planning and control (Six Sigma/process capability, Product Stewardship) (PPC), Consideration of environmental issues during selection of Manufacturing process (Industrial engineering tools: 5S, Kaizen, Method

Study, Work Measurement, Industrial Safety, Ergonomics) (SMP), People involvement initiative (Quality circle) (QC), Co-operation with customers for environmental packaging (CEP,)Application of Reverse logistics (RE), Are you recovering your scrap through government certified agency? (RSRM), and Selection of Employee and Technology (SET) as shown in Table 1. We compare all the seven alternative industries with respect to each criterion at the level above it. There will be seven comparison matrices for these comparisons. The information on the priorities obtained for all the indicators is tabulated in the form of Decision Matrix as shown in Table 5.

In **step 3**, using these priorities, the Alternatives Functionality Graphs (AFGs) are drawn. AFG indicates the relative measure of functionality fulfilment with respect to each of the available alternatives.

In **step 4**, Using entropy method, weights are assigned to the functions. This method is preferred because it does not require the decision maker to affix the weight; instead weights are calculated using the information obtained from the decision matrix after applying AHP. It rules out any chance of prejudice or manipulation to assign weights by the decision maker. Even if the weights have already been assigned by the decision maker, they can be combined with the weights obtained using this method. The application of AHP leads to normalized priorities in the decision matrix, which are then used to extract information for input to the entropy method. The weights of seven main indicators are obtained. Using these weights, the R^3I of all the seven industry alternatives are calculated. Industry with highest R^3I ranks the best industry for the implementation of GSCM practices.

The steps for the developed methodology are as given below:

i. Decide the priorities among the seven industries based on each main function using Analytical Hierarchy Process (AHP).

AHP was developed in 1972 as a practical approach for solving relatively complex problems as depicted by Saaty [9-11]. It is used for multi criteria problems in a number of application domains. The general approach of AHP is to decompose the problem and make pair wise comparison of all the indicators at a given level with the related indicators in the level just above to which it belongs.

For the qualitative analysis for selection among industry alternatives, Pair wise comparisons for each criterion is done on a scale of relative importance, 1 reflecting equal weightage and 9 reflecting absolute importance shown by Saaty [6]. Here the AHP method is used to select the best industry wherein GSCM can be effectively implemented. We compare the seven industry alternative with respect to seven main indicators at the level above it. The sample comparison matrices for PPC are as shown in Table 4.

Table 3. Assessment Data of Industries based on Indicators

Performance Measure	PPC	SMP	QC	CEP	RE	RSRM	SET
GREEN 01	Excellent	Excellent	Superb	Excellent	Excellent	Superb	Superb
GREEN 02	Good	Fair	Excellent	Good	Excellent	Excellent	Excellent
GREEN 03	Fair	Poor	Excellent	Good	Fair	Fair	Good
GREEN 04	Good	Excellent	Fair	Excellent	Good	Fair	Good
GREEN 05	Fair	Good	Excellent	Excellent	Fair	Good	Fair
GREEN 06	Poor	Poor	Fair	Fair	Fair	Poor	Fair
GREEN 07	Good	Good	Super	Good	Good	Excellent	Excellent

ii. Form a Decision Matrix with the priorities obtained for seven main indicators for all the seven alternatives.

The comparison matrices are used to calculate the final priorities for the available alternatives. With each matrix, there is associated a consistency ratio (CR), which gives the measure of consistency in the comparisons made. CR should be less than or equal to 0.1 for the results to be acceptable, else the comparison should be undertaken again.

PPC: For assessing the 'PPC' aspect of all the seven industries, pairwise comparison weightages obtained by consensus of the experts, are entered in the (7 x 7) comparison matrix as shown in Table 4. After the AHP calculations, the functional priorities of all the seven industries are obtained which shows Industry Green 01 has obtained the highest ranking in the indicator PPC.

Table 4. Comparison Matrix for Industry Alternatives w. r. t. PPC

PPC	GREEN 01	GREEN 02	GREEN 03	GREEN 04	GREEN 05	GREEN 06	GREEN 07	Priority Function (PF)
GREEN 01	1	2	3	2	3	4	2	0.281
GREEN 02	1/2	1	2	1	2	3	2	0.180
GREEN 03	1/3	1/2	1	1/2	1	2	1/2	0.088
GREEN 04	1/2	1	2	1	2	3	1	0.161
GREEN 05	1/3	1/2	1	1/2	1	2	1/2	0.088
GREEN 06	1/4	1/3/	1/2	1/3	1/2	1	1/3	0.053
GREEN 07	1/2	1/2	2	1	2	3	1	0.149
Eigen Value: 7.098, Consistency Ratio: 0.0124, Consistency Index: 0.0164								

Similarly, Priority Function have been calculated for remaining indicators i.e SMP, QC, EP, RE, RSRM, and SET. A Decision Matrix is then attained by compiling the obtained functional priorities of all the seven industries on all the main criteria as shown in Table 5.

Table 5. Decision Matrix

Industry i = 1→7 / Criteria j = 1-7 ↓		A1	A2	A3	A4	A5	A6	A7
		GRE 01	**GRE 02**	**GRE 03**	**GRE 04**	**GRE 05**	**GRE 06**	**GRE 07**
V1	PPC	0.281	0.180	0.088	0.161	0.088	0.053	0.149
V2	SMP	0.248	0.088	0.053	0.248	0.147	0.092	0.122
V3	QC	0.273	0.151	0.151	0.050	0.166	0.052	0.158
V4	CEP	0.206	0.107	0.107	0.206	0.206	0.061	0.107
V5	RE	0.247	0.247	0.076	0.140	0.076	0.076	0.140
V6	RSRM	0.311	0.193	0.070	0.070	0.117	0.044	0.193
V7	SET	0.303	0.184	0.105	0.105	0.060	0.060	0.184

iii. Alternatives Functionality Graphs (AFG).

AFGs are graphs between the functional priorities calculated by AHP and the alternatives. This approach towards evaluating alternatives helps identify the strengths and weaknesses of all the alternatives, function wise. Unfortunately systematic methods are not always used in industries as stated by Chakraborty et. al. [12]. The AFG is shown in Figure 3. X axis represents seven number of industry alternatives.

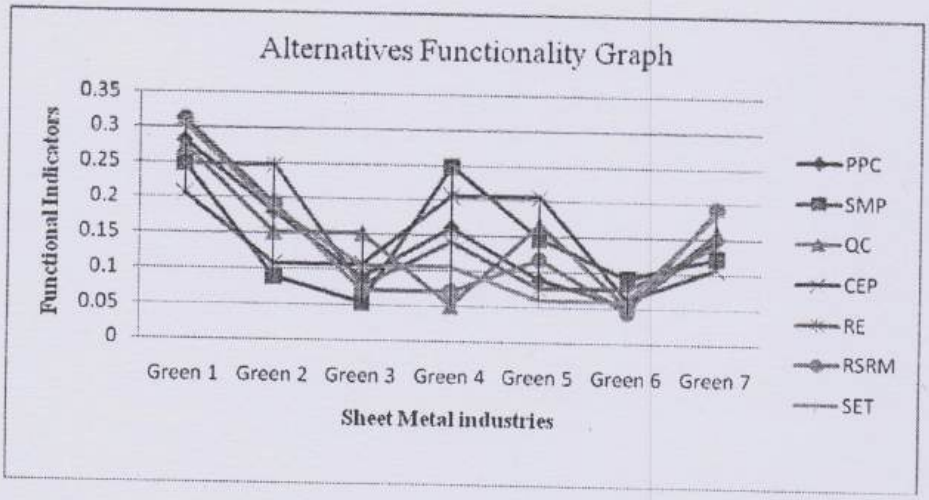


Figure 3. Alternatives Functionality Graph

iv. Entropy Method

After the application of AHP, the priority *I* Decision Matrix obtained is shown in Table 5. The weights for the seven indicators considered are calculated using the information from the decision matrix and the entropy method. The entropy method is Multi Attribute Decision Making Method, as stated by Hwang [13]. This method has been adopted as a part of calculating R^3I, because it may be inappropriate for a decision maker to compare indicators relatively from the function structure. The information contents of the normalized values of the attributes can be measured using entropy values. The entropy V_j of the set of normalized outcomes of attribute j is given by,

$$V_j = -\beta \sum_{i=1}^{n} (l_{ij}\ X\ In\ (l_{ij})) \text{ For all j (j = 1 to k represents attributes)} \quad 1$$

And (i = 1 to n represents alternatives)

I_{ij} = Normalized element of the Decision Matrix

$$\beta = \text{constant} = (1 \div \text{In (n)}) \quad 2$$

The smoothness (E_j) of a function j = ($1-V_j$) is calculated for all the seven functions. If there are no preferences available, the criteria weights are calculated using the equation,

$$W_j = (E_j \div (\sum_{j=1}^{k} E_j) \quad 3$$

Where, E_j = ($1-V_J$)

If the decision maker has the weights available beforehand i. e. W_e, then it can be combined with the weights calculated above, resulting in new weights that are W_{new}. The weights obtained after the application of the method are shown in the Table 13.

$$W_{new} = ((We \times W_j) \div (\sum_{j=1}^{k} (W_e \times W_j)) \quad 4$$

Table 6. Weights for the criteria as obtained by Entropy Method

Criteria	Weights Obtained (%) (W_j)
PPC	9.95 (W_1)
SMP	10.55 (W_2)
QC	10.56 (W_3)
CEP	6.77 (W_4)
RE	9.71 (W_5)
RSRM	15.49 (W_6)
SET	36.93 (W_7)

Normalization of Decision Matrix is not required since the sum of the priorities for any attributes j is 1. Having calculated the weights and priorities, we obtain R^3I, shown in Table 7 using the following equation.

$R^3I_i = \sum_{j=1}^{k}(l_{ij} \times W_j)$ for all i

5

Table 7. Results of R^3I Ranking

R^3I of Industries	R^3I Rating	RANK
Green 1	0.2809	1
Green 2	0.1721	2
Green 3	0.0945	6
Green 4	0.1246	4
Green 5	0.1034	5
Green 6	0.0609	7
Green 7	0.1631	3

SAMPLE CALCULATIONS:

Let l_{ij} = Normalized element of Decision matrix as shown in Table 5.

N = Number of alternative industries, there are seven industry alternatives. (i = 1 to n and n = 7).

K = Number of industry evaluation criteria. In this case there are seven criteria, viz. PPC, SMP, QC, CEP, RE, RSRM and SET. (j = 1 to k and k = 7).

Then, $$\beta = \frac{1}{\ln(n)} = \frac{1}{\ln(7)} = \frac{1}{\ln(n)9459} = 0.5139$$

Calculate Entropy of each criterion, V_j (j = 1-7) by the following formula,

$V_j = -\beta \sum_{i=1}^{n}(l_{ij}\, X\, In\, (l_{ij}))$ (j = 1 to k represents attributes)

(i = 1 to n represents alternatives)

Calculate Smoothness of each function, $E_j = 1 - V_j$ (j = 1 - 7)

$$\sum_{j=1}^{8} E_j = (E_1 + E_2 + E_3 + E_4 + E_5 + E_6 + E_7 + E_8)$$

= (0.0619+ 0.0656+ 0.0657+ 0.0421+ 0.0604+ 0.0963+ 0.2296)
=0.6216

Calculate the Weights for the indicator by using the following formula,

$W_j = (E_j \div (\sum_{j=1}^{k} E_j))$

Indicator	Weights Obtained (%) (W_j)
PPC	16.32
SMP	11.36
QC	14.9
CEP	8.9
RE	18.31
RSRM	10.28
SET	10.81

Calculate the Relative Reliability Risk Index (R^3I) for all the industries using the following formula,

$R^3I_i = \sum_{j=1}^{k}(l_{ij} \times W_j)$ for all i

By taking the values of l_{ij} from Table 6 and the corresponding weights W_j from Table 7, we calculate R^3I of each industry as shown below,

4. RESULTS

The results are as discussed. By arranging the above results in descending order, we get Table 8 Comparison between the industries ranking obtained by entropy method and Qualitative outcome and carbon footprints.

Table 8. Results of R^3I and comparison with Questionnaire and Carbon footprints

R^3I of Industries	Point Scale Questionnaire Outcome	Reduction in Carbon Foot prints (%)	R^3I Rating	RANK
Green 1	117	31.64	0.2809	1
Green 2	90	29.82	0.1721	2
Green 3	78	23.41	0.0945	6
Green 4	88	27.78	0.1246	4
Green 5	84	26.18	0.1034	5
Green 6	77	20.82	0.0609	7
Green 7	89	28.15	0.1631	3

5. CONCLUSION

R^3I thus used relative index reliabilities to compare the ranking obtained by questionnaire and Carbon footprint generation. The methodology involves application of the AHP to relatively compare the choices and the entropy method for obtaining the weights of the indicators considered. The ranks obtained by the industries observed to be same with all the methods.

REFERENCES

[1] Dickson, W., "An analysis of vendor selection systems and decisions", Journal of Purchasing, Vol. 2, 1966, pp. 5-17.

[2] Weber, C.A., Current, J.R., Benton, R, "Vendor Selection Criteria and Methods", European Journal of Operational Research, Vol.50 (2), 1991,pp.2-18.

[3] Zadeh, L.A., "Fuzzy sets, Information and Control", 1965, pp.338-353.

[4] Rupa Bindu, B. B. Ahuja., "AHP Based Strategic Sourcing – A Novel Integration for Vendor Selection", Proc. of the International conference on Issues and Challenges in Supply Chain Management, B.H.U., Varanasi, U.P. 2008.

[5] Rupa Bindu, Prashant More., "SCM in India- A Perspective", Proc. of the International Conference on Manufacturing and Management, Vellore, India, 2004.

[6] Rao, P. & Holt, D. (2005), "Do Green Supply Chains Lead to Competitiveness and Economic Performance", *International Journal of Operations & Production Management*, 25(9), pp. 898-916.

[7] Joseph Sarkis, Aref A. Hervani, Marilyn M. Helms, (2005), "Performance measurement for green supply chain management", *Benchmarking: An International Journal, Vol. 12 Issue*: 4, pp.330-353.

[8] Stefan Seuring, (2012), "A review of modelling approaches for sustainable supply chain management", *Decision Support Systems*, 54, pp. 1513–1520.

[9] T.L. Saaty, How to make a decision: the analytic hierarchy process, European Journal of Operational Research 48 (1) (1990) 9–26.

[10] Thomas L. Saaty, Yoram Wind, "Marketing Applications of the Analytical Hierarchy Process", JSTOR (Journal of scientific tools in operation research), Management Science, Vol. 26, No.7, July 1980, pp. 641-658.

[11] Thomas L. Saaty," Decision making for Leaders", 2001, Pittsburgh.

[12] Dr. Shankar Chakraborty and Dr. Diganta Taha., "A Supply Chain Management Module for Integrated functioning of a Manufacturing Organization", Manufacturing Technology Today, 2005, pp. 15-18.

[13] Hwang, C.L., Yoon, K., "Multiple Attributes Decision Making Methods and Applications", 1981, Springer Berlin, Heidelberg.

[14] A. S. Chavan, Dr. R. N. Patil and Dr. S T. Chavan, Prioritization of Green Supply Chain Indicators with Analytic Hierarchy Process (AHP) Model, International Journal of Mechanical Engineering and Technology, 9(10), 2018, pp. 1444–1460.

Scopus Preview

Check whether you can access Scopus remotely through your institution

Maybe later | Check access

Source details

International Journal of Mechanical Engineering and Techno

Scopus coverage years: from 2016 to 2019

(coverage discontinued in Scopus)

Publisher: IAEME Publication

ISSN: 0976-6340 E-ISSN: 0976-6359

Subject area: Engineering: Industrial and Manufacturing Engineering | Engineering: Mechanical Engineering | Engineering: Mechanics of Materials

Source type: Journal

CiteScore 2017
1.2

SJR 2019
0.293

SNIP 2022
0.311

View all documents > | Set document alert | Save to source list

CiteScore | CiteScore rank & trend | Scopus content coverage

Improved CiteScore methodology

CiteScore 2017 counts the citations received in 2014-2017 to articles, reviews, conference papers, book chapters and data papers published in 2014-2017, and divides this by the number of publications published in 2014-2017. Learn more >

CiteScore 2017

$$1.2 = \frac{1{,}691 \text{ Citations 2014 - 2017}}{1{,}437 \text{ Documents 2014 - 2017}}$$

Calculated on 01 May, 2018

CiteScore rank 2017

Category	Rank	Percentile
Engineering — Industrial and Manufacturing Engineering	#143/328	56th
Engineering — Mechanical Engineering	#322/577	44th

View CiteScore methodology > | CiteScore FAQ > | Add CiteScore to your site

International Journal of Mechanical Engineering and Technology (IJMET)
Volume 9, Issue 13, December 2018, pp. 284–292, Article ID: IJMET_09_13_031
Available online at http://www.iaeme.com/ijmet/issues.asp?JType=IJMET&VType=9&IType=13
ISSN Print: 0976-6340 and ISSN Online: 0976-6359

© IAEME Publication  Scopus Indexed

MODELLING AND SIMULATION OF THERMOCLINE STORAGE FOR SOLAR THERMAL POWER PLANT

Dr. R. N. Patil
Principal, Bharati Vidyapeeth College of Engineering, Lavale
Pune University, Pune, Maharashtra, India

Prof. Jadhav Sandhya Dilip
Research Scholar, Department of Mechanical Engineering,
Bharati Vidyapeeth Deemed University, Pune, Maharashtra, India

ABSTRACT

Storage of thermal energy increases the capacity factor of a solar plant. Thermocline storage tanks are preferred option of thermal energy storage in central receiver solar thermal power plant. It is difficult to conduct the experiment due to large size of storage tank. Code is developed using Visual Basic for studying performance of plant. Code is first validated from experiment data in available literature. The effect of inclusion of storage tank on electrical power generation is studied by simulation. Then simulation is done for thermocline tank with Molten salt Hitec XL and quartzite rocks as storage media. Heat exchange between molten salt and quartzite rock and their temperature profiles are studied.

Keywords: Central Receiver Solar Thermal Power Plant, Modelling and Simulation, Thermocline Storage Tank, Molten Salt.

Cite this Article: Dr. R. N. Patil and Prof. Jadhav Sandhya Dilip, Modelling and Simulation of Thermocline Storage For Solar Thermal Power Plant, International Journal of Mechanical Engineering and Technology, 9(13), 2018, pp. 284–292.
http://www.iaeme.com/ijmet/issues.asp?JType=IJMET&VType=9&IType=13

1. INTRODUCTION

In the present solar power generation technologies available, central receiver solar thermal power plant is the most efficient technology therefore development work is going in this field all over the world. In photovoltaic plants, energy storage is too costly and hence plant has less efficiency. In thermal power plants it is easy and cheaper to store thermal energy as compared to electrical energy in photovoltaic plants. In central receiver thermal plants, a large array of mirrors called heliostats receive the solar radiation and focus it on a large receiver placed on

the top of a tower. Heat transport flows through the tubes of receiver and absorbs thermal energy and delivers the thermal energy to power block.

The central receiver solar thermal power plant must satisfy the energy demand like any other power plant. The electrical energy of a central receiver solar thermal power plant is affected by the variation in weather. It is unavailable in night and every time a shadow is cast on collection area, the power output is either reduced or plant stops operating.

In order to cope with these fluctuations and to utilize the maximum solar radiation, excess thermal energy is produced during day time and stored for cloudy weather conditions or later use in night. Hence, solar thermal power plant can be operated in absence of solar radiation without burning fossil fuel. Similarly gap between the amount of solar radiation supplied by the sun and required electrical energy is reduced. All thermal power generated from the receiver is delivered to the thermal storage tank, provided the thermal storage tank can accept it(i.e. tank is not full).

The turbine operates, after a minimum amount of thermal energy required to run the turbine is accumulated in the storage tank. The extra thermal energy remains in the storage tank. This process continues till the availability of sunshine hours. The stored thermal energy is used to run the plant after the sunshine hours. The daily variation in solar radiation and electricity requirement profile decides the use of thermal storage system. The earliest storage system was incorporated in Solar One central receiver solar thermal pilot power plant (from 1982 to 1986).

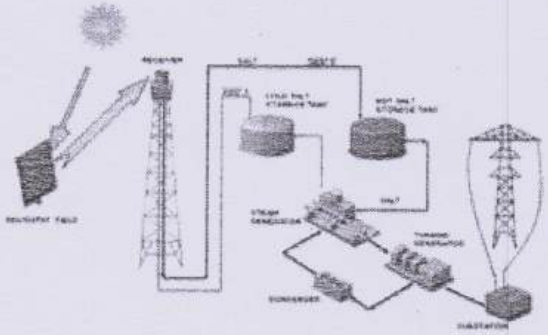


Fig.1 Central receiver solar thermal power plant

2. THERMAL ENERGY STORAGE

The most developed concept is the sensible heat storage concept due to its commercial use especially in chemical plants. Two options for thermal energy storage are available, namely two tank storage system and single tank thermocline system. Although the two-tank model for thermal storage has been more commonly adopted in CSP plant designs, the prominence of thermal storage with stratification in solar applications has prompted the development of a single tank plant model. The potential benefits of using a single tank with stratification are reduction in required total tank volume, reduced construction costs due to consolidation from two tanks to one, a simplified control scheme, reduced piping, and reduced pumping requirements. However, there are some considerable drawbacks with stratification. The average temperature of the tank approximates the thermal inventory of the tank. When the average temperature in the tank approaches the cold outlet temperature, the thermal storage is nearly fully discharged, and when the average temperature is near the hot outlet temperature, the opposite is true.

The cost of a thermal energy storage system mainly depends on the storage material used for storage of thermal energy, the heat exchanger for charging and discharging the system and the cost for the vessel or tank for the thermal energy storage system. The synthetic oils used for heat transport fluid are very expensive as well as have pressures at high temperatures, therefore molten salts namely, Hitec, Hitec XL, solar salts are preferred as fluid for high temperature thermal energy storage. Molten salts are stable up to higher temperature range of $450^0C - 550^0C$ with very low vapour pressure. Their operating temperatures are compatible with todays high pressure and high temperature steam turbines. Molten salts are efficient low cost medium to store thermal energy. It is non-flammable and non toxic. At present, molten salts are widely used in chemical and metal industries as a heat transport fluid. At high temperatures, the heat of fusion of molten salts is preferred. Many salts are being used because of their high mass and volumetric heat storage capabilities, their abudance in nature and their low cost per unit storage capability. By utilizing the heat of fusion (liquid-solid transition) of various salts, large amounts of thermal energy can be stored and subsequently released at nearly constant temperature.

3. THERMOCLINE STORAGE

The performance of thermocline system is of significant interest to future central receiver solar thermal power plants. The intent of this article is to review thermocline tank storage studies and also study temperature profile in the tank. It is difficult to conduct physical experiments due to large size of thermal energy storage tanks. Therefore, numerical solutions are preferred to study performance of thermal energy storage tanks. Kolb simulated a 1 MW_e Sagurao parabolic trough power plant with addition of 30 MWh_t thermocline tank and found that capacity factor of plant was increased by 23% to 42%. Van Lew used Schumann equations and proved that a small increase in thermal storage efficiency due to larger aspect ratios of tank height to diameter. This gain is due to improved forced convection between solid material and fluid. Increased fluid due to larger tank height increases the convection.

Molten salts are expensive, therefore molten salts are substituted partially by low cost storage solid materials, thus reducing the total cost of required storage material. Packed bed storage uses the tank filled with rocks, through which hot fluid is passed from top to bottom of the tank. The filler material used should have compatibility with molten salt (the heat transport fluid used in tank) and also high heat capacity. On a volumetric basis, the specific heat of the rock is about five percent larger than the specific heat of the nitrate salt. The rocks widely available are quartzite, taconite, marble and limestone. Out of these quartzite rock and silica sand can withstand high temperature molten salt without deterioration.

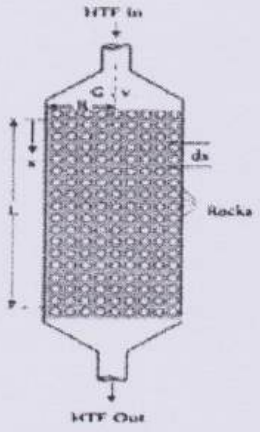


Fig.2 Packed bed storage tank

Table No 2. Temperature of hot fluid along axial distance of tank at time intervals during charging

Distance in m (from top of tank)	Temperature of hot fluid in tank in ^{0}C			
	60 min	120 min	180 min	240 min
0	550	550	550	550
3.44	464	533	548	548
6.88	363	475	547	548
10.32	285	352	517	547
13.75	270	283	419	533

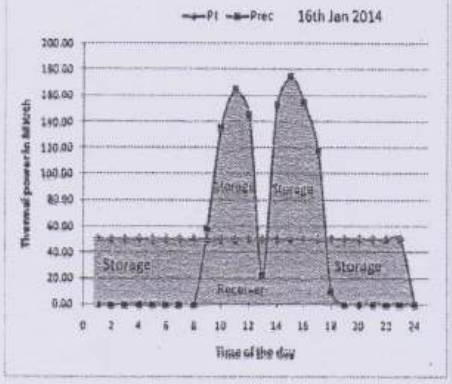


Fig. 4 Effect of storage of thermal energy in power generation on a cloudy day

At 0 minutes, temperature of solid is initial temperature i.e. 270^{0}C. As hot fluid is introduced from top of tank with mass flow of 125 kg/sec, it travels down the tank height.

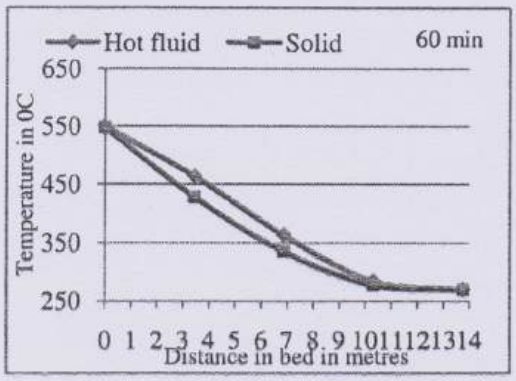


Fig. 5(a)

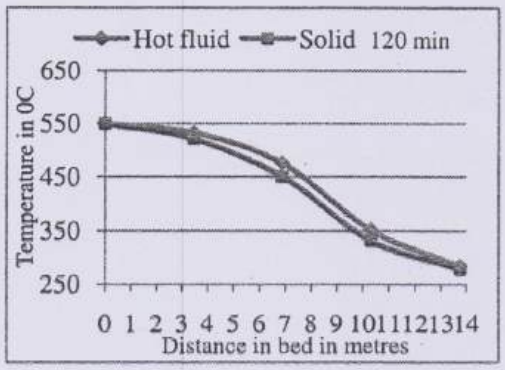


Fig. 5(b)

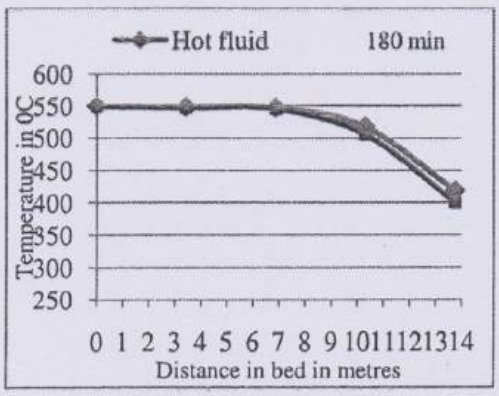


Fig. 5(c)

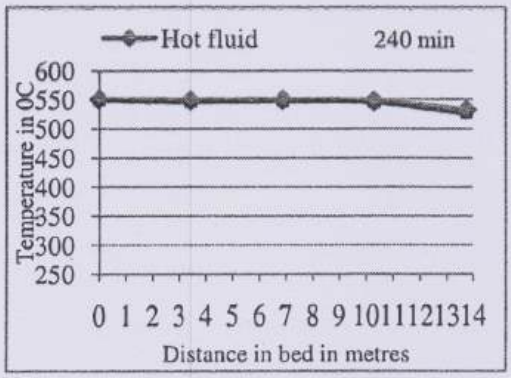


Fig. 5(d)

In Fig, 5(b), rise in temperature of solid can be observed. This increase in temperature of both continues till equilibrium occurs. The equilibrium reaches after 240 min, as shown in Fig. 5(d). Fig.No.6 shows the variation of temperature of solid bed with time, along the height of tank. It can be seen, that, after 150 minutes (1.5 hrs), temperature of hot fluid and solid become almost equal at a distance of 3.44m from top of tank. After 180 minutes (3 hrs), it reaches equilibrium till 6.88m, i.e. only till mid of tank, whereas it takes 210 minutes (3.5 hrs) to reach equilibrium at a distance of 10.32 m from top of tank as shown in Fig.No.5(d). It takes 240 min (4 hrs) for the temperature of solid and hot fluid to be equal at the bottom of tank, i.e. at 13.75 m.

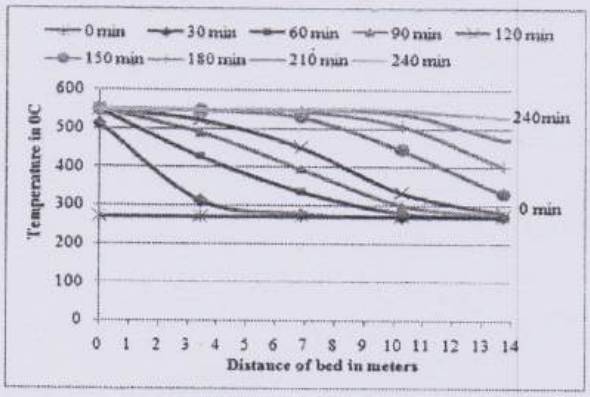


Fig. 6

7. CONCLUSION

The effect of thermal storage on plant performance is studied by the developed code. The storage system helps the plant to operate in intermittent cloudy weather conditions. Thermocline tank with Hitec XL as heat transport fluid and quartzite rock as solid bed material is studied. Thermal characteristics, including temperature profiles are explored and it is observed that it almost takes 4 hrs for the entire temperature in tank to reach 550^0C. The efficiency increases with tank height. However, it can be expensive in terms of storage material. The smaller size of rocks also increases efficiency as area of contact between Hitec XL and quartzite rock is increased. Comparing the different storage materials, it is observed that density of liquid sodium is very less; therefore volume of liquid sodium required is more as compared to other storage materials. Hitec XL is having the highest density, therefore volume required is least among all the storage materials. The use of storage of thermal energy reduces the cost of power generation.

REFERENCES

[1] Herrmann Ulf, David W. Kearney, Survey of Thermal Energy Storage for Parabolic Trough Power Plants, Journal of Solar Energy Engineering , Vol. 124, pp. 145-152, May 2002.

[2] L.J.Yebra, M. Berenguel, S. Dorando and M. Romero, Modelling and Simulation of Central Receiver Solar Thermal Power Plants in Proceedings of the 44th IEEE Conference on Decision and Control and the European Control Conference,Spain Dec 12-15, 2005.

[3] M. C. Stoddard, S. E. Faas, C. J. Chiang & J. A. Dirks, SOLERGY – A Computer Code for Calculating the Annual Energy from Central receiver Power Plants, Sandia Report, May 1987.

[4] Magal, B. S., 1994, Solar Power Engineering, Tata McGraw Hill Publishing Company Limited, Second Print.

[5] Manuel Romero, Reiner Buck & James E. Pacheco, An Update on Solar Central Receiver Systems, Projects, and Technologies, Journal of Solar Energy Engineering May 2002, Vol. 124, pp 98-108.

[6] Mary Jane Hale, Survey of Thermal Storage for Parabolic trough Power Plants, NREL, September 2000, NREL/SR-550-27925.

[7] Ortega, J., J. Burgaleta, M. Tellez, May 2008, Central Receiver System (CRS) Solar power plant using molten SALT as heat transfer fluid, Journal of Solar Energy Engineering, Vol. 130, No. 2

[8] S. P. Sukhatme, Solar Energy Principles of thermal collection and Storage, Second Edition, Tata McGraw-Hill, 1996

[9] Winter, C. J., R. L. Sizmann, L. L. Vant, - Hull (Eds.), Solar Power Plants – Fundamentals, Technology, Systems, Economics , 2005

[10] Wang K. Y., West R. E., Kreith and Lynn P., High-temperature Sensible-Heat Storage Options, Energy Vol. 10, No. 10, pp 1165-1175, 1985.

[11] www.nrel.gov/international/ra_india.html, May 2015.

Scopus Preview

Check whether you can access Scopus remotely through your institution

Maybe later | Check access

Source details

International Journal of Mechanical Engineering and Techno

Scopus coverage years: from 2016 to 2019
(coverage discontinued in Scopus)
Publisher: IAEME Publication
ISSN: 0976-6340 E-ISSN: 0976-6359
Subject area: Engineering: Industrial and Manufacturing Engineering | Engineering: Mechanical Engineering | Engineering: Mechanics of Materials
Source type: Journal

CiteScore 2017
1.2

SJR 2019
0.293

SNIP 2022
0.311

View all documents > | Set document alert | Save to source list

CiteScore | CiteScore rank & trend | Scopus content coverage

Improved CiteScore methodology

CiteScore 2017 counts the citations received in 2014-2017 to articles, reviews, conference papers, book chapters and data papers published in 2014-2017, and divides this by the number of publications published in 2014-2017. Learn more >

CiteScore 2017

$$1.2 = \frac{1{,}691 \text{ Citations 2014 - 2017}}{1{,}437 \text{ Documents 2014 - 2017}}$$

Calculated on 01 May, 2018

CiteScore rank 2017

Category	Rank	Percentile
Engineering — Industrial and Manufacturing Engineering	#143/328	56th
Engineering — Mechanical Engineering	#322/577	44th

View CiteScore methodology > | CiteScore FAQ > | Add CiteScore to your site